National Library
of Canada

Acquisitions and
Bibliographic Services Branch

395 Wellington Street
Ottawa, Ontario
K1A 0N4

Bibliothèque nationale
du Canada

Direction des acquisitions et
des services bibliographiques

395, rue Wellington
Ottawa (Ontario)
K1A 0N4

Your file Votre référence

Our file Notre référence

NOTICE

The quality of this microform is heavily dependent upon the quality of the original thesis submitted for microfilming. Every effort has been made to ensure the highest quality of reproduction possible.

If pages are missing, contact the university which granted the degree.

Some pages may have indistinct print especially if the original pages were typed with a poor typewriter ribbon or if the university sent us an inferior photocopy.

Reproduction in full or in part of this microform is governed by the Canadian Copyright Act, R.S.C. 1970, c. C-30, and subsequent amendments.

AVIS

La qualité de cette microforme dépend grandement de la qualité de la thèse soumise au microfilmage. Nous avons tout fait pour assurer une qualité supérieure de reproduction.

S'il manque des pages, veuillez communiquer avec l'université qui a conféré le grade.

La qualité d'impression de certaines pages peut laisser à désirer, surtout si les pages originales ont été dactylographiées à l'aide d'un ruban usé ou si l'université nous a fait parvenir une photocopie de qualité inférieure.

La reproduction, même partielle, de cette microforme est soumise à la Loi canadienne sur le droit d'auteur, SRC 1970, c. C-30, et ses amendements subséquents.

Canada

UNIVERSITY OF ALBERTA

SEDIMENTOLOGY, STRATIGRAPHY AND PETROGRAPHY OF THE MIDDLE TRIASSIC HALFWAY FORMATION, PEEJAY FIELD, NORTHEASTERN BRITISH COLUMBIA

BY

MARK LAURENCE CAPLAN

A thesis submitted to the Faculty of Graduate Studies and Research
in partial fulfillment of the requirements for the degree of MASTER OF SCIENCE.

DEPARTMENT OF GEOLOGY

Edmonton, Alberta
FALL 1992

National Library of Canada
Canadian Theses Service
Ottawa, Canada
K1A 0N4

Bibliothèque nationale du Canada
Service des thèses canadiennes

ISBN 0-315-77072-4

UNIVERSITY OF ALBERTA
RELEASE FORM

Name of Author: MARK LAURENCE CAPLAN

Title of Thesis: SEDIMENTOLOGY, STRATIGRAPHY AND PETROGRAPHY OF THE MIDDLE TRIASSIC HALFWAY FORMATION, PEEJAY FIELD, NORTHEASTERN BRITISH COLUMBIA.

Degree: MASTER OF SCIENCE

Year This Degree Granted: 1992

Permission is hereby granted to the University of Alberta Library to reproduce single copies of this thesis and to lend or sell such copies for private, scholarly or scientific research purposes only.

The author reserves all other publication and other rights in association with the copyright in the thesis, and except as hereinbefore provided neither the thesis nor any substantial portion thereof may be printed or otherwise reproduced in any material form whatever without the author's prior written permission.

M. Caplan

Mark Laurence Caplan

91, Kenton Lane,
Kenton,
Harrow,
Middlesex, HA3 8UJ
England,
United Kingdom.

Date: 30/9/92

UNIVERSITY OF ALBERTA

FACULTY OF GRADUATE STUDIES AND RESEARCH

The undersigned certify that they have read, and recommend to the Faculty of Graduate Studies and Research for acceptance, a thesis entitled Sedimentology, Stratigraphy and Petrography of the Middle Triassic Halfway Formation, Peejay Field, Northeastern British Columbia submitted by Mark Laurence Caplan in partial fulfillment of the requirements for the degree of Master of Science.

Dr. T. F. Moslow (Supervisor)

C R Stelck

Dr. C. Stelck

Philippe Erdmer

Dr. P. Erdmer

Dr. I. Campbell

Date: 29/9/92

ABSTRACT.

The Middle Triassic deposits within the Peejay field of northeastern British Columbia are composed of four coarsening-upward parasequences, forming a progradational parasequence set. Individual parasequences thicken to the east-northeast and become sandier. Conversely, they become thinner and more shaly toward the west-southwest, and amalgamate forming a condensed zone within the lower part of Doig Formation. Each parasequence contains deposits previously assigned to the lithostratigraphically defined Halfway and Doig formations. Within the Peejay field, chronostratigraphic correlation demonstrates the shortcomings of lithostratigraphy in terms of the depositional framework.

Middle Triassic deposits become thinner in a northeasterly direction due to early Carnian synsedimentary tilting, faulting and subsequent erosion. Reservoir lithofacies within the Peejay field were preserved within early Carnian north-south aligned grabens. Deposits situated above horst features or to the northeast of the study area experienced increased erosion, resulting in erosion of reservoir lithofacies, and heavy cementation. Genetically unrelated impermeable continental playa-lake deposits of the Charlie Lake Formation erosively overlie the Middle Triassic deposits, forming a seal rock. The hydrocarbon trapping style of the Peejay study area is both structural and stratigraphic.

The most proximal parasequence (Pa. 4) is composed of sublitharenite and litharenite tidal inlet channel fill deposits, composing 74% of the parasequence, truncating, reworking and replacing coarsening-upward prograding shoreface deposits. This is characteristic of a barrier island shoreline. Tidal inlet fills of parasequence 3 however, comprise only 16% of the shoreface deposits. This is more characteristic of a strandplain shoreline. The tidal inlet fills are characteristic of those found along modern wave-dominated shorelines. The inlet fills are oriented parallel to palaeodepositional strike (NNW-SSE), indicative of lateral migration processes. These inlet fills form the best reservoir quality deposits within the field. Arenaceous biodolomicrite tidal inlet fills are less abundant and of lower reservoir quality. Reservoir quality reduces as the Charlie Lake contact is approached due to diagenetic effects.

ACKNOWLEDGEMENTS

I would like to thank Unocal Canada Exploration Limited and Norcen Energy Resources Limited for their financial contributions. The waivering of core handling fees by the British Columbia Ministry of Energy, Mines and Petroleum Resources was greatly appreciated. Technical support from Doug Glass (Unocal) and Steve Glover (EMPR) were invaluable. I would also like to thank Western Atlas International Core Laboratories for the use of their microscopy equipment.

I would also like to thank Andrew Willis for his continual encouragement and review of the final manuscript. I am also grateful to Leon Halwa who helped draft the diagrams with me. Finally, I would especially like to thank my supervisor, Dr. T. F. Moslow, for his invaluable input into this study, and the sincerity and hospitality that both Tom and his wife (Maxine) gave on my arrival and subsequent stay in Canada.

TABLE OF CONTENTS.

LIST OF TABLES.

LIST OF FIGURES.

LIST OF PLATES

KEY

Lithology

- Sandstone
- Siltstone
- Shale
- Coquina
- Anhydrite Nodules
- ●▲● Conglomerate

Pa. 3	Parasequence Three
M.F.S.	Marine Flooding Surface
— —	Gradational Contact
——	Sharp Contact
〰	Erosional Contact

Sedimentary Structures

- Parallel-Lamination
- Hummocky Cross-Stratification
- Planar Cross-Bedding
- Trough Cross-Bedding
- Symmetrical Ripple Lamination
- Asymmetrical Ripple Lamination
- Biogenic Activity
- • • • Lithoclasts
- ■ Stromatolites
- Gastropods

☒	No Core (Information Derived from Geophysical Logs)
■	Perforated Interval

1.0.0. INTRODUCTION.

The purpose of this study is to determine the sedimentology, petrography and sequence stratigraphic framework of the upper-Middle Triassic Halfway Formation in the Peejay field of northeastern British Columbia (Figure 1). This study is intended to improve information derived from previous sedimentologic studies (Clark, 1961; Armitage, 1962; Barss *et al.*, 1964; Fulton, 1966; Mothersill, 1968; Chunta, 1969; Munroe and Moslow, 1990) and petrographical studies conducted within the study area (Sharma, 1969). There has been no attempt in the past to erect a sequence stratigraphic framework for the Peejay field. This study also aims at examining the Middle Triassic hydrocarbon trapping mechanism.

The Halfway Formation is a sandstone that subcrops within the Peace River area of northeastern British Columbia and western Alberta. It has been defined as the first appearance of a marine sandstone bed beneath the red beds of the Upper Triassic Charlie Lake Formation (Hunt and Ratcliffe, 1959) (Figure 2). The Halfway Formation was originally interpreted as a transgressive marine sandstone by Hunt and Ratcliffe (1959), Clark (1961), Armitage (1962) and Mothersill (1968) and has more recently been interpreted as a regressive marine sandstone by Barclay and Leckie (1986), Campbell and Horne (1986), Cant (1986), Munroe and Moslow (1990) and Willis (1992).

These Halfway regressive sandstones have previously been mapped lithostratigraphically as a single regressive sandstone sheet that covered the entire Western Canada Sedimentary Basin. It is highly unlikely that this sandstone sheet formed from one regressive event, since a large and continuous sediment source would be required, in order for the regressive sheet to cover the Western Canada Sedimentary Basin. Chronostratigraphically significant laterally continuous markers have been recognized within the Halfway shoreface sandstones (Wittenberg, 1992; Willis, 1992). These synchronous markers extend down into the Doig Formation distal basinal marine shales and siltstones. Hence, it is probable that the Halfway and Doig formations were formed coevally. It also appears that the Halfway sheet sandstone is composed of a series of genetically related discrete sandstone packages. Therefore, lithostratigraphic mapping would result in diachronous correlation and an inaccurate picture of the depositional

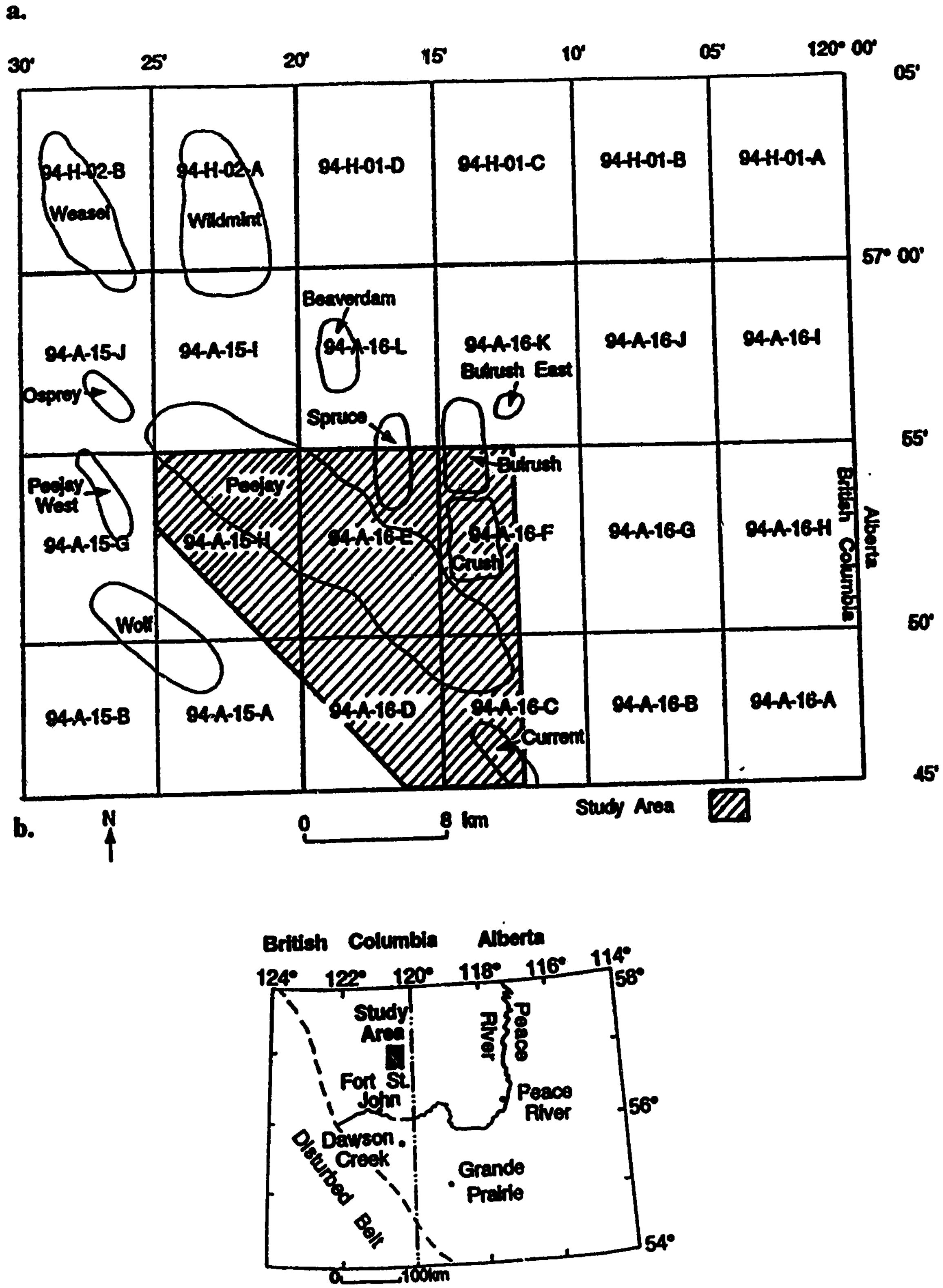

Figure 1. a: Location map of the Middle Triassic oil fields within and surrounding the study area. b: Location of the study area within northeastern British Columbia.

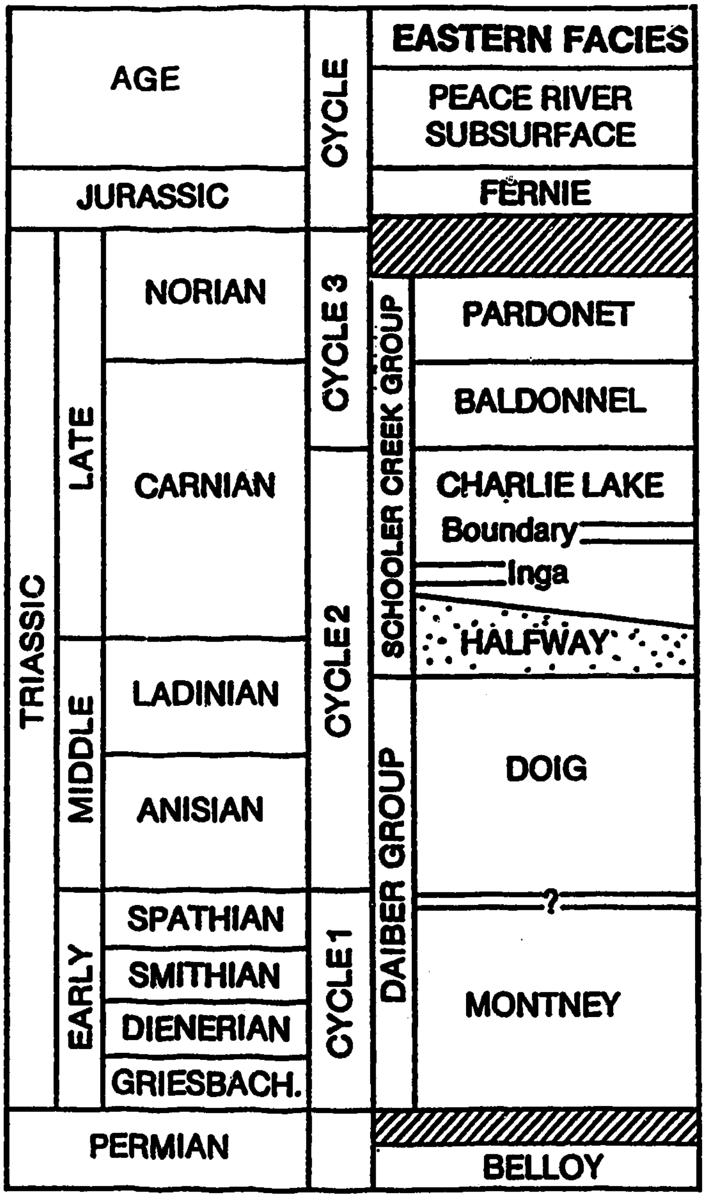

Figure 2. Middle Triassic subsurface stratigraphy of the Peace River area of the Western Canada Sedimentary Basin (after Podruski *et al.*, 1988; Willis, 1992).

framework of the Middle Triassic deposits, within the Western Canada Sedimentary Basin.

1.1.0. STUDY AREA.

The Peejay Field is located approximately 113.4 km (70 miles) north of Fort St. John in northeastern British Columbia (Figure 1). The study area extends 2.5 blocks (20km or 12.35miles) east to west and 2 blocks (16km or 9.88 miles) north to south, covering an area of 320 km^2 (198.2 miles^2), encompassing the Peejay, Crush, Bulrush, Spruce and Current fields (Figure 1). The well location coordinate scheme employed within this area is the National Topographic Series (N.T.S.). The Peejay field is 24 km (14.8 miles) long and 6km (3.7 miles) wide, covering an area of 144 km^2 (88.89 miles ^{2}). The study area contains approximately 340 wells. The majority of wells in the study area were drilled before the early 1970's. Consequently, the geophysical wire-line logs are mainly gamma-ray, sonic, spontaneous potential and resistivity, of low bed resolution.

1.2.0. OBJECTIVES.

The main objectives of this study are to:

1.) Process sedimentologically describe the 'Halfway' lithologies in wells from the Peejay field, in order to derive vertical lithofacies associations.

2.) Laterally correlate the vertical lithofacies associations in order to derive a three-dimensional depositional model.

3.) Determine the three-dimensional geometry, spatial distribution and orientation of the reservoir lithologies identified from core in order to improve enhanced recovery performance in the Peejay field. This may result in improved insight in discovering new reservoir pools and fields.

4.) Examine the petrography of the reservoir lithofacies, in order to determine the origin and quantitative extent of porosity in the Halfway Formation. This would provide a better understanding concerning the migratory behaviour of fluids through diagenetically altered homogeneous lithology.

5.) Construct a sequence stratigraphic framework for the Middle Triassic of the Peejay field, in order to gain a clearer insight into the chronostratigraphic as opposed to lithostratigraphic relationship of depositional packages. Models developed would be applicable to other Middle Triassic fields within northeastern British Columbia.

6.) Reconstruct the geological history of the Middle Triassic deposits within the study area, in order to explain the origin of the Halfway reservoir and the hydrocarbon trapping mechanism in the Peejay field.

1.3.0. MIDDLE TRIASSIC OIL AND GAS RESERVES.

The Middle Triassic plays of the Western Canada Sedimentary Basin hold $65x10^6m^3$ (409 million barrels) of recoverable oil from 169 pools, with $26x10^6m^3$ (164 million barrels) of potential reserves expected from at least 300 new pools (Podruski *et al.*, 1988). These amount to 4% of both the total Western Canada Sedimentary Basin oil reserves of $2.3x10^9m^3$ (14 billion barrels) and total undiscovered oil resources of $0.6x10^9m^3$ (4 billion barrels). This suggests that 30% of oil within the Western Canada Sedimentary Basin remains undiscovered (Barclay, 1988). Of the discovered initial reserves of the Western Canada Sedimentary Basin, five percent are from Triassic stratigraphic traps in the Peace River region. It is believed that the Triassic embayment was centred above the Peace River Arch, and that subsidence occurred during this time to produce the traps. Podruski *et al.* (1988) divided these traps into eleven Triassic plays within the Western Canada Sedimentary Basin.

The Milligan-Peejay play includes all pools and prospective sandstones of the 'discontinuous' phase of the Halfway Formation. Podruski *et al.* (1988) indicated that the isolated lows within the erosional Doig lows were infilled with Halfway deposits, and were sealed by the overlying evaporites of the Charlie Lake Formation. Pools within this play have porosities ranging from 8 to 28%, averaging at 15%, net pay from 0.8 to 5 metres, and permeability up to one Darcy. There are 35 discovered pools containing 44 x 10^6m^3 (368.7 mbbls) oil-in-place. Estimated remaining potential for this play has a median expectation value of 5 x 10^6m^3 (41.9 mbbls) oil-in-place from 15 new pools (Podruski *et al.*, 1988). Reservoir performance statistics for the oil and gas fields within the study area are shown in Table 1.

Field	Original Oil In Place Volume 10^3m^3 (10^6bbls)	Remaining Oil Reserves 10^3m^3 (10^6bbls)	Original Gas In Place Volume 10^6m^3 (tcf)	Remaining Gas Reserves 10^6m^3 (tcf)	Discovery Year
Bulrush	885 (7.42)	40.4 (0.339)	68 (1.93)	4.3 (0.122)	77
Crush	1580 (13.24)	58.6 (0.49)	164 (4.64)	8.1 (0.24)	67
Current	952 (8.00)	22.5 (0.19)	630 (17.84)	353.3 (10.00)	65
Current West	81 (0.68)	15.3 (0.13)	234 (6.63)	32.7 (0.93)	79
Peejay	28243 (236.78)	1237.8 (10.37)	2460 (69.66)	502.7 (14.23)	59
Peejay West	1050 (8.8)	2.4 (0.02)	547 (15.49)	174.7 (4.95)	62

Table 1. Halfway oil and gas reserves for fields within the study area, northeastern British Columbia (after E.M.P.R. Pool Reserves Report, 1991).

The field was discovered in 1959 by Sinclair Canada Oil Company with the drilling of the Sinclair Pacific Peejay d-39-E well. Many wells within the 'H' block of the Peejay field have been drilled as far as the base of the Halfway sands. Thus, correlation of Halfway stratigraphy, using phosphatic beds within the "Phosphate Zone" of the lower Doig Formation, was impossible. Deeper well penetration, however, occurs in the eastern part of the field, consequently, correlation of Halfway deposits was possible. The wells have been drilled, on average, between 0.35km (0.21 miles) and 0.75km (0.46 miles) apart, enabling relatively confident lateral lithofacies relationships between adjacent wells to be made.

The Peejay field contains a water leg downdip to the southwest, and a gas cap updip to the northeast (Rogan and Smith, 1965). Crude oil occurring within Halfway reservoirs of the Peejay field is 36° specific gravity, indicating that it is of relatively low density. The Peejay field was put under waterflood in 1964, in order to maintain the field pressure. Water was injected into a well at the southern edge of the field, pushing the oil updip. Wells in the northern part of the field were producing gas which lowered the reservoir pressure, this finally required the need for pumping equipment. The Peejay field is currently under a secondary enhanced recovery scheme, in the form of waterflooding.

Riediger *et al.* (1990) and Creaney and Allen (1990) demonstrated that the Montney and lower beds of the Doig Formation (within the "Phosphate Zone") are potential source rocks for the hydrocarbons trapped within most Halfway and some Charlie Lake reservoirs based on biomarker fingerprinting of reservoir-oil-to-source rock correlation. The Doig Formation within most of British Columbia is overmature, except at its northeastern subcrop edge, thus limiting the areal extent of exploration programmes.

1.4.0. METHODS.

This sub-surface project involved the manipulation and lateral correlation of 340 geophysical well-logs in the Peejay area. From these wells 4.7 kilometres (2.9 miles) of Middle Triassic Halfway deposits from 132 cored sequences, were chosen for detailed sedimentologic analysis (Figure 3; Table 2; Appendix A). The core was described at the British Columbia Ministry of Energy, Mines and Petroleum Resources core repository at Charlie Lake, during a three month period in the summer of 1990, two weeks in the winter of 1991, and three weeks in the summer of 1991.

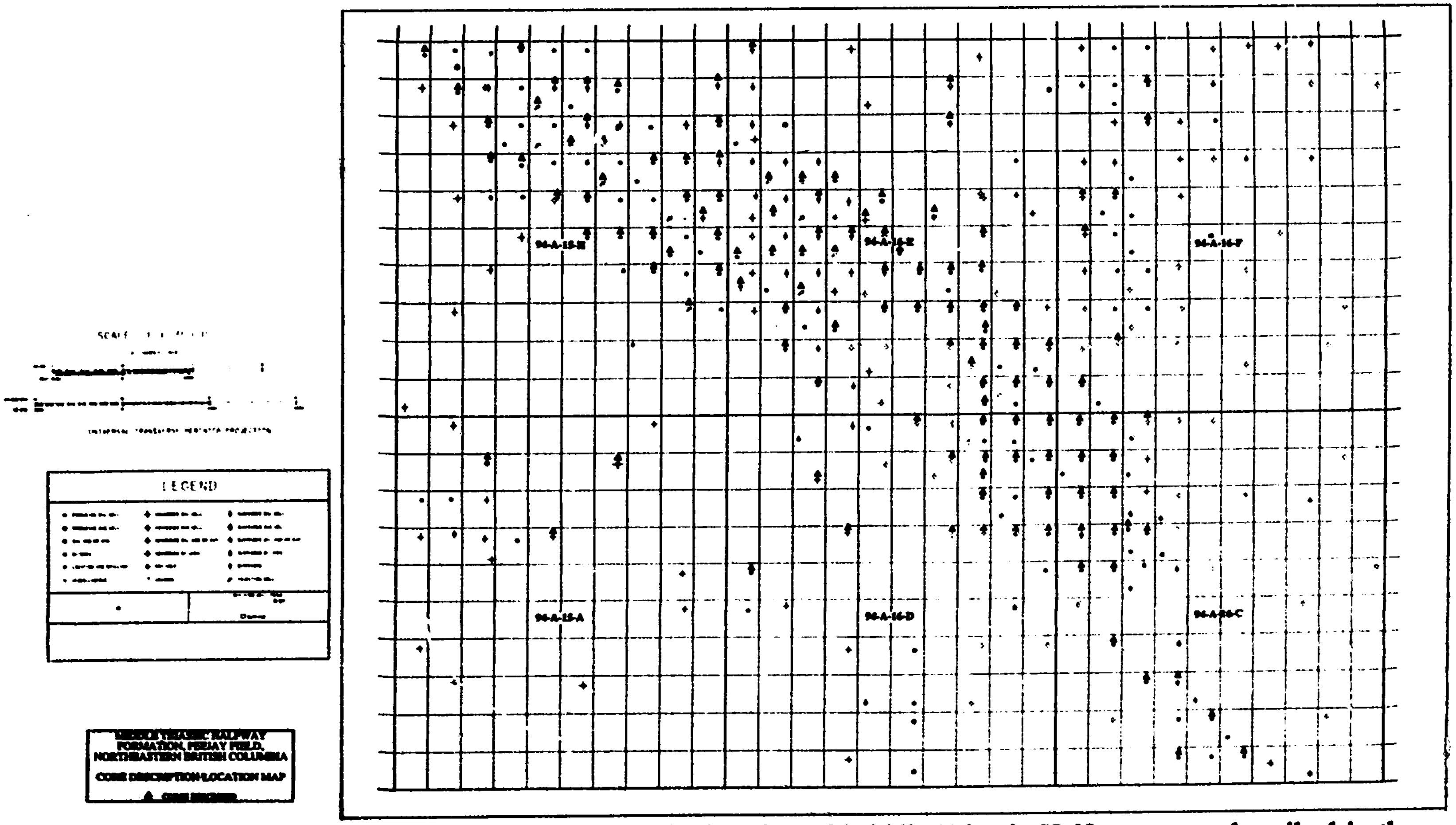

Figure 3. Map showing the location of Middle Triassic Halfway cores described in the study area.

d-066-A/94-A-15	d-089-H/94-A-15	d-073-D/94-A-16	d-036-E/94-A-16
d-084-A/94-A-15	d-095-H/94-A-15	d-081-D/94-A-16	b-038-E/94-A-16
d-088-A/94-A-15	d-097-H/94-A-15	d-082-D/94-A-16	b-040-E/94-A-16
d-022-H/94-A-15	d-100-H/94-A-15	a-083-D/94-A-16	d-043-E/94-A-16
d-031-H/94-A-15	d-033-I/94-A-15	d-083-D/94-A-16	b-045-E/94-A-16
d-033-H/94-A-15	d-013-J/94-A-15	d-084-D/94-A-16	d-046-E/94-A-16
d-041-H/94-A-15	d-018-B/94-A-16	a-088-D/94-A-16	b-047-E/94-A-16
b-042-H/94-A-15	d-005-C/94-A-16	d-091-D/94-A-16	d-047-E/94-A-16
d-043-H/94-A-15	d-007-C/94-A-16	d-092-D/94-A-16	b-048-E/94-A-16
d-044-H/94-A-15	d-016-C/94-A-16	d-093-D/94-A-16	d-048-E/94-A-16
d-045-H/94-A-15	d-027-C/94-A-16	d-095-D/94-A-16	b-049-E/94-A-16
b-051-H/94-A-15	d-028-C/94-A-16	d-001-E/94-A-16	b-050-E/94-A-16
d-051-H/94-A-15	d-039-C/94-A-16	d-002-E/94-A-16	b-054-E/94-A-16
d-052-H/94-A-15	d-059-C/94-A-16	a-003-E/94-A-16	b-056-E/94-A-16
d-055-H/94-A-15	d-060-C/94-A-16	d-003-E/94-A-16	d-056-E/94-A-16
d-056-H/94-A-15	c-068-C/94-A-16	d-008-E/94-A-16	d-058-E/94-A-16
d-061-H/94-A-15	d-068-C/94-A-16	d-011-E/94-A-16	b-059-E/94-A-16
d-062-H/94-A-15	d-069-C/94-A-16	d-012-E/94-A-16	b-067-E/94-A-16
d-063-H/94-A-15	d-070-C/94-A-16	b-013-E/94-A-16	b-068-E/94-A-16
b-064-H/94-A-15	d-079-C/94-A-16	d-013-E/94-A-16	b-069-E/94-A-16
d-067-H/94-A-15	d-080-C/94-A-16	d-014-E/94-A-16	d-069-E/94-A-16
d-068-H/94-A-15	d-089-C/94-A-16	d-019-E/94-A-16	d-074-E/94-A-16
d-071-H/94-A-15	d-090-C/94-A-16	d-022-E/94-A-16	d-084-E/94-A-16
b-074-H/94-A-15	d-098-C/94-A-16	a-023-E/94-A-16	d-100-E/94-A-16
b-075-H/94-A-15	d-099-C/94-A-16	d-023-E/94-A-16	d-010-F/94-A-16
d-075-H/94-A-15	d-100-C/94-A-16	d-024-E/94-A-16	d-019-F/94-A-16
d-077-H/94-A-15	d-060-D/94-A-16	d-025-E/94-A-16	d-050-F/94-A-16
d-078-H/94-A-15	d-061-D/94-A-16	d-026-E/94-A-16	d-059-F/94-A-16
d-081-H/94-A-15	d-062-D/94-A-16	b-027-E/94-A-16	d-060-F/94-A-16
d-084-H/94-A-15	d-063-D/94-A-16	d-029-E/94-A-16	d-078-F/94-A-16
d-085-H/94-A-15	d-064-D/94-A-16	d-033-E/94-A-16	d-088-F/94-A-16
b-086-H/94-A-15	d-067-D/94-A-16	d-034-E/94-A-16	d-038-K/94-A-16
d-086-H/94-A-15	d-071-D/94-A-16	d-035-E/94-A-16	a-027-L/94-A-16

Table 2. N.T.S. coordinates of Halfway core described within the study area.

1.4.1. Core Description.

Before sedimentologic analysis of the core could be undertaken it had to be examined for any signs of mishandling that could otherwise jeopardise sedimentologic interpretations using the criteria outlined by Siemers and Tillman (1981). Once this had been accomplished it was then possible to determine the amount of core loss, if any, that had occurred from each well. Unfortunately, core gamma-ray scans were not made available for core-to-log depth correlation adjustments. Depth corrections applied to the core depths were obtained instead, from the cross-correlation of core-to-down-hole gamma-ray logs. The identification of sedimentologic lithofacies from core were cross-correlated to the gamma-ray well-logs, so that signatures on the well-logs could be recognized. The correlation of this sedimentologic information to gamma-ray logs in which core was either not observed, or not cored, led to better sedimentologic coverage and correlation between wells. This enabled a better resolution depositional model to be constructed. Most of the core had been slabbed, making identification of sedimentary structures an easier task.

Colour photographs were obtained of slabbed and unslabbed pieces of core of sedimentologic interest. Most photographs were taken from lithological contacts, the contact between the Doig-Halfway-Charlie Lake Formations, and from every lithofacies identified. Colour photographs and slides were taken with a 35mm S.L.R. camera.

Samples of the core were also obtained, in order to carry out more detailed petrographical analysis. Samples were 2 to 3cms in length and 0.7cms average width. Samples were taken from each lithofacies, in order to provide petrographical descriptions and paragenetic interpretations. The latter enabled reservoir quality and fluid behaviour to be explained.

1.4.2. Lithofacies Description.

The term *facies* was introduced by Gressly (1838) who defined the facies as a body of rock with specific characteristics. The term lithofacies is used to describe the physical and chemical characteristics of a rock. This information was recorded on core-logging sheets, the vertical scale recorded mainly in feet since the well-logs were recorded in imperial units. Thus, a continuous vertical record of the sedimentologic information from the entire core was obtained. Vertical variation within and between each lithofacies were described, and the nature of lithological contacts was determined.

1.4.3. Process Sedimentology.

The process sedimentologic approach required an accurate recognition and delineation of lithofacies within the vertical and lateral sedimentary sequence. This approach attempts to interpret the hydrodynamic processes expected in the formation of the lithofacies by observing and interpreting the significance of physical, biological and chemical observations. For example, oscillatory current hydrodynamic processes can be inferred from the appearance of symmetrical ripples. In this way a predictive depositional model can be constructed. This model can then be compared to pre-existing similar depositional models.

1.5.0. PREVIOUS RESEARCH.

Triassic rocks in the Western Canada Sedimentary Basin were first studied in 1871 by A. R. C. Selwyn, of the Geological Survey of Canada, within the upper Peace River of the northeastern British Columbia Foothills. Later, Dawson (1879, 1887) and McConnell (1891) described Triassic strata from the Pine and Liard River valleys, respectively. McLearn published a series of papers between 1918 and 1947 determining the Triassic rock-stratigraphic terminology, fossil zonation, and time-stratigraphic subdivisions within the Foothills of northeastern British Columbia. This work was later summarized by McLearn and Kindle (1950) and McLearn (1953). McLearn (1921, 1950) first defined the "Schooler Creek Formation" which incorporated sediments of Middle and Upper Triassic age which crop out in the Peace River Foothills. Tozer (1961) used McLearn's terminology, but applied the term Toad, introduced by Kindle (1944), for strata in the Liard River area, close to the base of the Triassic section. The Toad Formation was also recognized at Mount Wright by McLearn (1946).

Hunt and Ratcliffe (1959) were the first to correlate the formations identified in outcrop by McLearn (1921) and McLearn and Kindle (1950) in the Foothills of northeastern British Columbia, to newly described and named subsurface formations within the Peace River area. They increased the status of the Schooler Creek Formation to Group level. The formations named and included within this Group are (in ascending order); Halfway, Charlie Lake, and Baldonnel. The Lower to Middle Triassic Toad and Grayling

Formations that were previously defined by McLearn and Kindle (1950) from the subsurface were grouped together as their log signatures were so similar. Fossils were rarely recovered from the subsurface, making correlations with the surface equivalent formations somewhat dubious. Armitage (1962) defined two new formations in the subsurface, these were the Montney and Doig which were positioned below the Schooler Creek Group; themselves collectively defining the Daiber Group. This subsurface terminology is still in active use today.

Colquhoun (1960) introduced rock-stratigraphic terminology, and mapped subsurface and surface rocks together, according to lithology and fauna. He introduced the terms, Mount Wright to include McLearn's 'Flagstones' and 'Dark siltstones', and Hart Pass (this term not being acceptable to the 1961 Code of Stratigraphic Nomenclature) for strata lying below. Colquhoun (1962) mapped and correlated the formations of the subsurface and surface outcrops, throughout northeastern British Columbia. He was able to correlate phosphate beds, of the subsurface Doig Formation, with those of the surface Mount Wright Formation.

Pelletier (1962, 1965) measured a number of Triassic sections from northeastern British Columbia in which, stratigraphy, source area, lithology, outcrop distribution, textural studies and palaeogeography of the Triassic Formations were described. He also interpreted the Liard Formation (equivalent to the Halfway Formation) as deposited on a shallow marine platform. Tozer (1967) produced a continuous biostratigraphic framework for the Triassic of Western Canada, defining 31 ammonite zones. Irish (1969) mapped out the Triassic of the Halfway River. He also stated that lithostratigraphic correlation between surface and subsurface formations was dubious due to the lack of sufficient fossils in the subsurface with which to correlate. He stated that in outcrop, correlation along depositional strike was possible for many miles but along depositional dip lithology varied within a few miles making regional lithostratigraphic correlations problematic.

There has been very little published material concerning the subsurface Halfway Formation from the Milligan-Peejay area of northeastern British Columbia, although Clark (1961), Armitage (1962), Barss *et al.* (1964) and Fulton (1966) concluded that the discontinuous Halfway was deposited in lows in Doig erosional surfaces. Mothersill (1968) studied core and well-logs, compiling size and statistical analysis of the sediment of the Halfway Formation and concluded that it was deposited as a transgressive sandsheet. Rogan and Smith (1964) documented and explained the waterflooding enhanced recovery technique that was to be applied to the Peejay field. Chunta (1969) and Sharma (1969) examined the sediments from the Halfway of the Peejay field, the former in regard to production performance, the latter in regard to paragenesis. Both authors state that the Halfway was overlain conformably by the Charlie Lake; the former stating that the Halfway unconformably overlies the Doig. Chunta (1969) also realized that waterflooding of the Peejay field lead to unexpected flow patterns, thus alluding to a more complex lithofacies arrangement than previously thought. More recent, detailed core studies have been undertaken within northeastern British Columbia, including the Peejay field by Munroe and Moslow (1990) who interpreted the Halfway as a prograding wave-dominated barrier island system punctuated by laterally migrating tidal inlets.

According to early research (Hunt and Ratcliffe, 1959; Clark, 1961; Armitage, 1962; Mothersill, 1968; and Sharma, 1969), tectonic uplift occurred at the end of Doig times, followed by an initial transgression of the Halfway sea (from the northwest) producing the Halfway sand. The Halfway sands were deposited as shore and beach sands, sourced from the northwest. This first transgressive phase that occurred in the Schooler Creek Group produced a series of sands known as the continuous Halfway. East of this zone, the Halfway sands formed a discontinuous series of sand lenses, interpreted as 'beach bars' (Mothersill, 1968) (Figure 4). During basinal subsidence, sandstones continued to be deposited in the west, while evaporites and siltstones were deposited in the east behind sandstone barriers. These barriers produced a restricted environment in which the evaporites formed.

As knowledge of sedimentology and stratigraphy increased, so interpretations of regional models of geological history from within the region also improved. Barss *et al.* (1964) and Pelletier (1965) reported that the Halfway was deposited as a regressive sandstone.

Clark (1961) described the primary sedimentary structures of the Halfway sandstone within the Milligan Creek oilfield, in order to devise an environmental interpretation. He

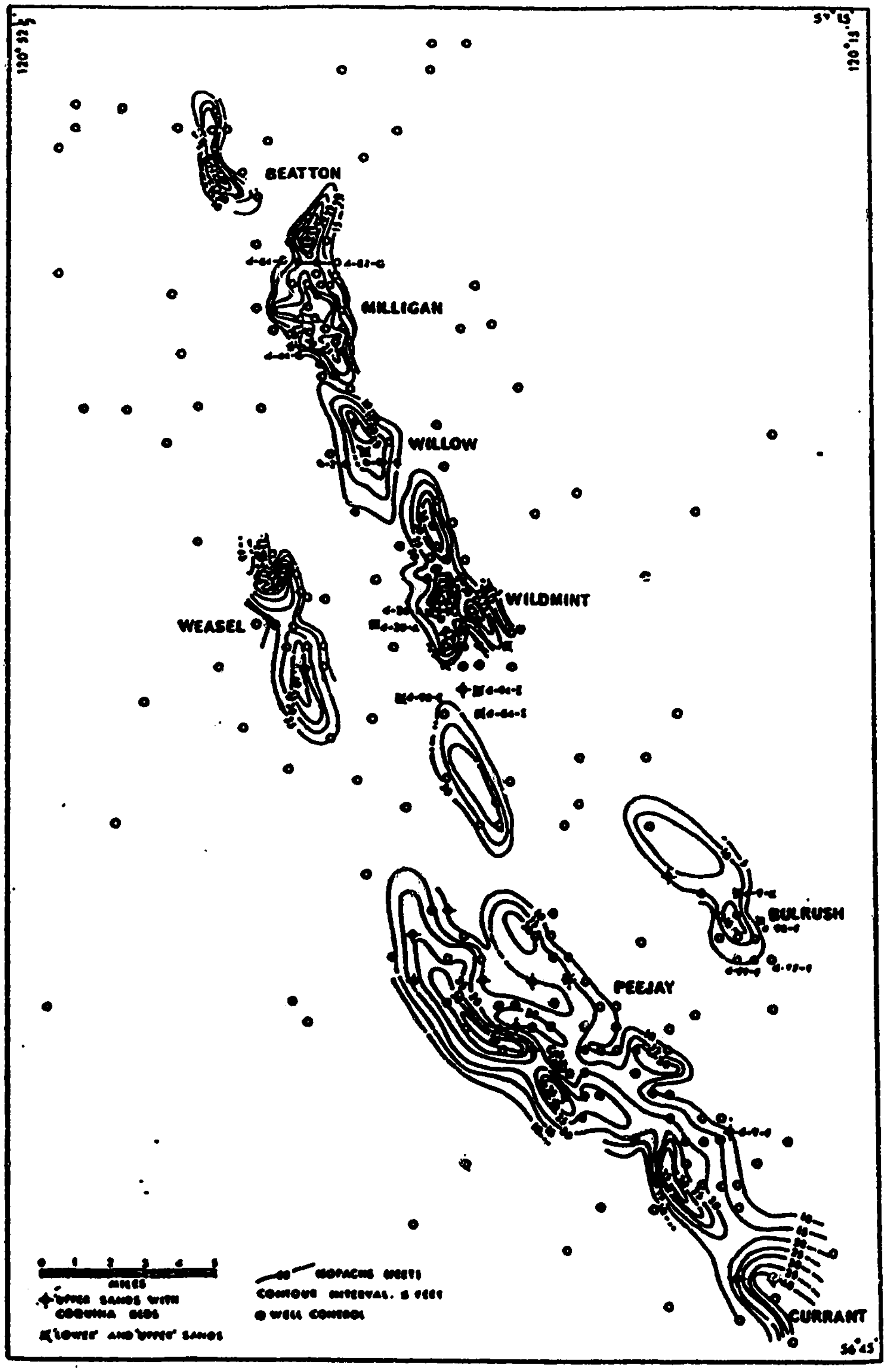

Figure 4. Isopach of Halfway Formation from the Milligan-Peejay area of northeastern British Columbia. The contours are closed indicating the isolated nature of sand pods from the 'discontinuous' Halfway (after Mothersill, 1968).

was the first to interpret the Halfway sandstones in this region as 'barrier bars'. Torrie (1973) also described the Milligan-Peejay reservoirs as shoreline sand bars, orientated parallel to coastline.

Numerous studies of the Triassic System within the Western Canada Sedimentary Basin by Torrie (1973), Gibson (1975), Cant (1986), Aukes and Webb (1986), Campbell and Horne (1986), Barclay and Leckie (1986), Leckie and Rosenthal (1987), Barclay (1988), among others, have been conducted. Gibson and Barclay (1989) and Gibson and Edwards (1990) have concluded that there were three major transgressive-regressive depositional cycles (of possible second-order Vail Cycles). These cycles were controlled by sediment supply, climate and relative sea level changes. The Lower Triassic (Griesbachian to Spathian) was the first transgressive phase, characterized by basal phosphates overlain by shales and silts of the Lower Montney. These were in turn overlain by regressive middle and upper Montney siltstones. Lower to middle Late Triassic sediments (Anisian to lower Carnian) represented a regressive cycle, with a basal phosphatic lag transgressing a hiatal surface, followed by an overall prograding barrier island shoreface sequence (Doig-Halfway-Charlie Lake formations). Upper Triassic (upper Carnian-Norian) began with a transgression of the Baldonnel and Pardonet carbonates, ending with a regression of the Bocock Formation.

Halton (1981), Horne *et al.* (1985), Cant (1986) and Campbell and Horne (1986) published their findings on the Halfway Formation of western Alberta, interpreting the Halfway as a prograding barrier island shoreline. Horne *et al.* (1985) were one of the first researchers to identify the presence of tidal inlet deposits within the Halfway as a mechanism to explain the erosional contact between the Halfway sands and the Doig interbedded sandstones and shales. Aukes and Webb (1986) were the first to describe and interpret the Middle Triassic as a series of prograding stacked shoreface successions. Their study concentrated on the Spirit River field (45 km east of the Wembley field, in west-central Alberta). The field was interpreted as an erosional remnant of a Doig barrier island, based on cross-sections hung on a Doig marker (Figure 5). Erosion occurred due to the progressively deeper incision and erosion (to the east) of a pre-Charlie Lake erosion surface (Figure 6). From their stratigraphic column, it becomes obvious that the Halfway-Doig lithostratigraphic nomenclature becomes weakened when this model is applied.

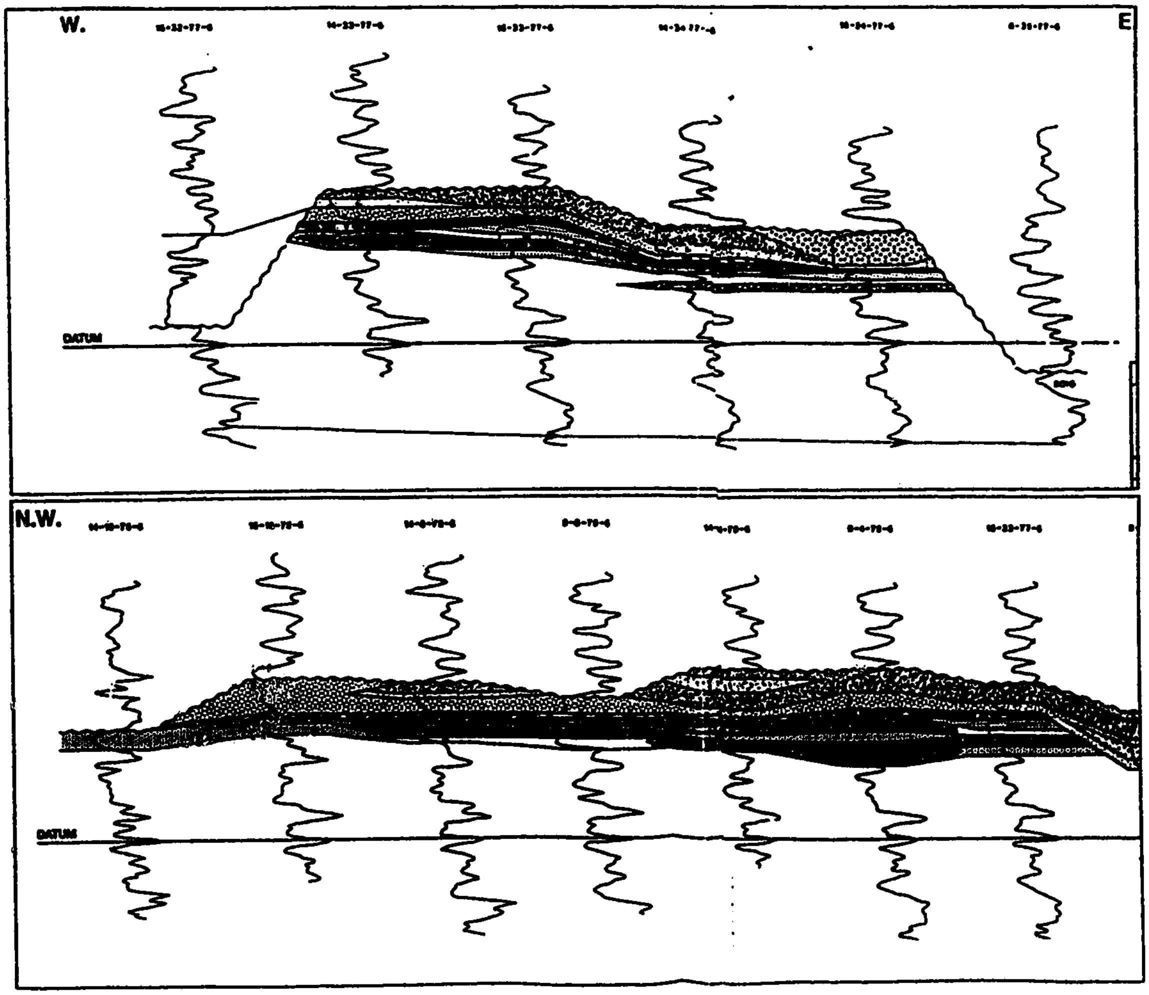

Figure 5. Chronostratigraphic cross-section showing the lithofacies relationships of the Doig Formation within the Spirit River field. The section is hung on a phosphatic bed within the lower Doig Formation. The Doig barrier island deposits have been preserved as an erosional remnant forming the Spirit River field (after Aukes and Webb, 1986).

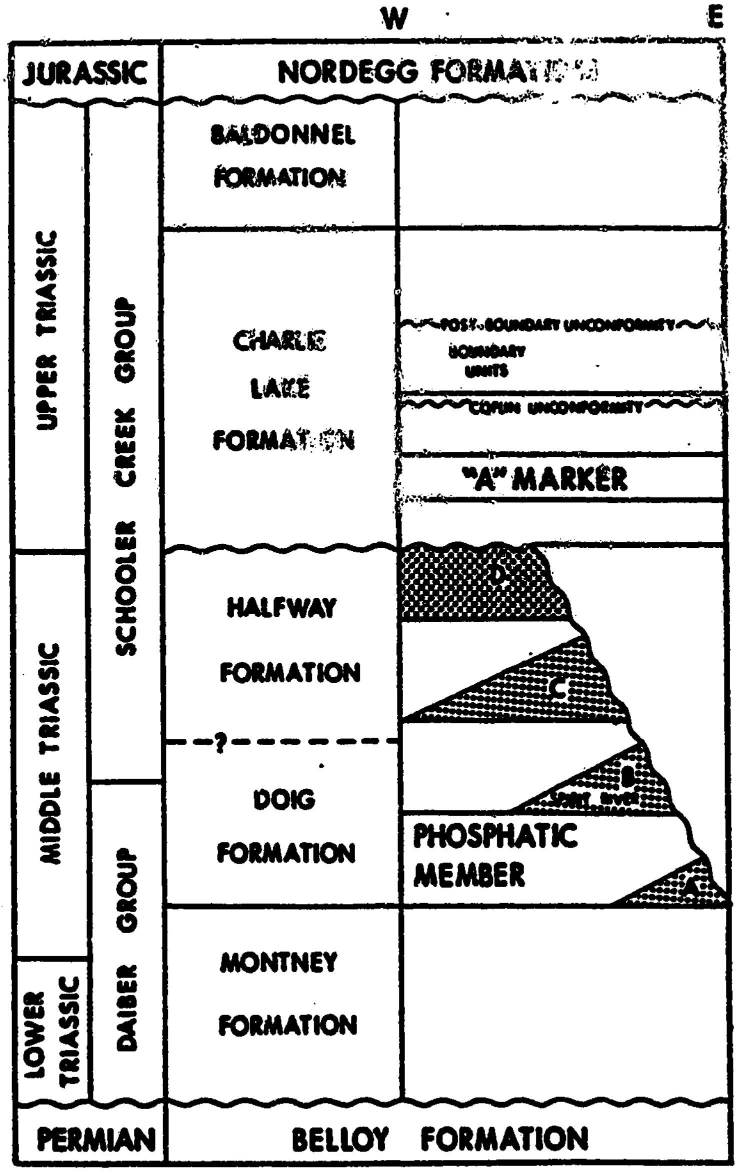

Figure 6. Stratigraphy of the Triassic in west-central Alberta. Note that the Halfway and Doig lithostratigraphic units have been made redundant, having been divided into 4 progradational sandstone parasequences, all of which have been truncated by a pre-Charlie Lake sub-regional unconformity forming erosional remnants (after Aukes and Webb, 1986). The Spirit River field occurs within parasequence B.

Origin of Halfway hydrocarbon reservoirs within Alberta have been documented by Campbell and Hassler (1989) and Campbell *et al.* (1989) as shown in Figure 7. They show six prograding shorelines successively overstepping one another in a southwesterly direction within the Doig Formation. Internally within the Doig is an unconformity, which explains the presence of Doig overthickened sandstone bodies, which were believed to represent estuarine channels, developed during a lowstand incision event. The Halfway overlies the Doig, bounded above and below by unconformity surfaces, suggesting that relative changes in sea-level have been frequent and large in magnitude. The Halfway is composed of two prograding shorelines, which are truncated by a pre-Charlie Lake unconformity. The degree of erosion increases to the northeast, where the pre-Charlie Lake unconformity has produced a series of roughly shoreline-parallel subcrop belts within the Halfway and Doig deposits. Intra-Charlie Lake unconformities can also be seen cutting down through the strata into the Halfway. Previous authors had identified the Halfway-Charlie Lake contact to be transitional, however, these reports suggested that there was a pre-Charlie Lake regionally extensive unconformity.

Cant (1986) stated that normal faults producing horst and graben features in the Doig, were formed by relaxation of the Peace River Arch. He also stated that the formations thin to the east, not by erosion between the deposition of each formation, but by sedimentary thinning and pinching out. He stated that synsedimentary tilting and subsidence occurred to the west, within the Western Canada Sedimentary Basin, with subsequent exposure and erosion occurring to the northeast at the margin of the basin during Doig times. Halfway deposits later onlapped this surface. Deep channels within the Doig had been identified as estuarine channels which were formed in response to a relative drop in sea level and backfilling during the successive transgression (Cant, 1986). He also suggested that the shales at the base of the Halfway cores within the Wembley field (which he interpreted as Doig) were deposited in non-typical marine conditions, as no bioturbation was displayed in core and pyrite nodules were apparent. These sediments were deposited in an anoxic shallow marine environment.

Podruski *et al.* (1988) identified eleven Halfway plays within the Western Canada Sedimentary Basin, providing estimates of the proven and potential reserves. Dudley *et al.* (1989) examined the effects that acidization had on Halfway mineralogy. Organic geochemical work has been applied to the hydrocarbons within the Halfway reservoirs, in

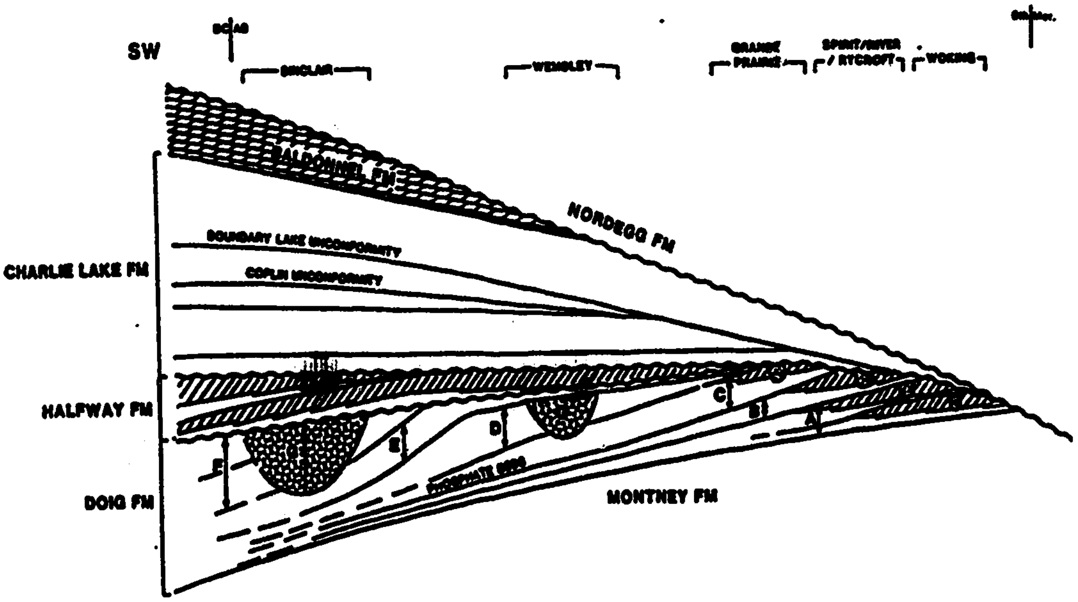

Figure 7. Schematic stratigraphic cross-section through the Triassic of central Alberta. The Doig Formation is composed of 4 westward prograding parasequences, the Halfway resting erosively ontop composed of 2 parasequences. Increased intensity of pre-Charlie Lake downcutting occurs to the east producing erosional remnants (after Campbell *et al.*, 1989).

order to obtain geochemical fingerprints. The fingerprints were used to correlate the hydrocarbons found in reservoirs with those in source rocks. Results suggest that the Halfway hydrocarbons were sourced from the lower Doig "Phosphate Zone" (Riediger *et al.*, 1990). O'Connell *et al.* (1990) and Barclay *et al.* (1990) described the subtle structural effects induced by development of the Dawson Creek Graben Complex on Triassic deposits within the Peace River Arch area of northwest Alberta and northeastern British Columbia. They documented that horst and graben structures, with displacements of up to 15 metres (49 feet) occurred within Triassic deposits.

Gibson (1975) summarized a series of papers that he had previously published on the Triassic sedimentology, stratigraphic correlation between subsurface and surface formations, and interpretation of depositional environments. Lithostratigraphic Triassic studies of the Peace River Arch region by Gibson and Barclay (1989) were concentrated in the Foothills of northeastern British Columbia, and recent subsurface summaries by Gibson and Edwards (1990) in the Interior Plains and Foothills.

Wittenberg (1992) identified a number of prograding shoreline successions, originally recognized by Aukes and Webb (1986) and Campbell *et al.* (1989). He interpreted these as individual parasequences, bounded above and below by basinal shales which he interpreted as condensed horizons, within west-central Alberta. These represented a relative increase in water depth associated with a transgression, and were termed marine flooding surfaces. He further deduced that the lithofacies within each parasequence varied from basinal shales and siltstones of the Doig Formation, coarsening-upward and in an easterly direction into shoreface sandstones of the Halfway Formation. Thus, he deduced that the Halfway and Doig lithostratigraphic formations were time-equivalent within each parasequence. He also documented that the Doig overthickened sandbodies were contemporaneous with the Doig deposits surrounding them, noting that the sandstones did not cut through phosphatic horizons. These sandstone bodies were formed by synsedimentary seafloor failures. This contrasts with the earlier theory of a later incision event produced by a fall in sea level as proposed by Campbell *et al.* (1989). Thus, Wittenberg did not interpret the Halfway as unconformably overlying the Doig Formation, or recognize an intra-Doig unconformity related to a lowstand incision event.

Willis (1992) examined a smaller area within west-central Alberta from the Wembley field. He identified 5 westward prograding parasequences which converged in a downdip direction into amalgamated phosphates, and diverged in an updip direction into shoreface deposits. The extreme updip termination of each parasequence was characterized by laterally extensive washover fans developed along depositional strike representative of barrier island retrogradation and associated with a transgression at the termination of every regressive parasequence. The washover sandstones proved to be the most productive reservoir element within the Wembley field. Tidal inlet deposits were of low reservoir quality due to the presence of abundant mud plugs and complex lithofacies relationships. These mud plugs occur at the top of tidal inlet sequences and represent abandonment. These inlet deposits were identified as forming on a prograding tide-dominated barrier island shoreline. He also concluded that the Halfway-Charlie Lake contact was conformable within this area due to the almost complete preservation of the entire coarsening-upward shoreface sequence. Willis (1992) again demonstrated that the lithostratigraphic nomenclature for the Middle Triassic cannot be applied as it does not reflect the true depositional framework of the deposits (Figure 8).

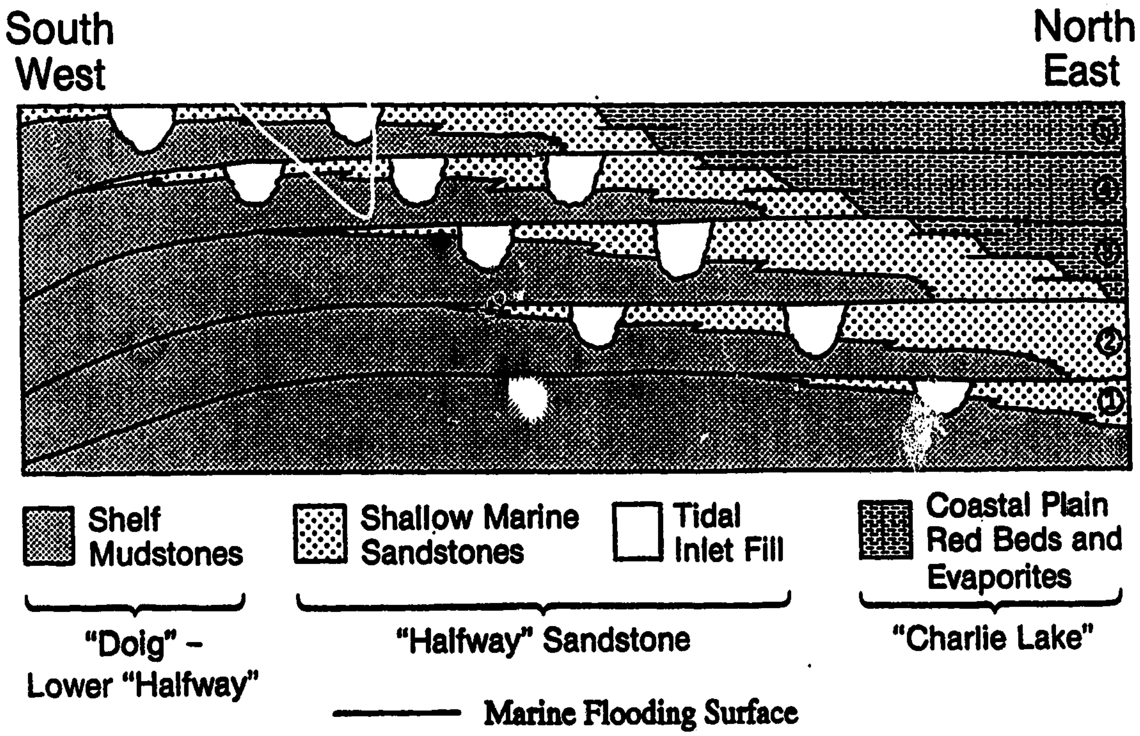

Figure 8. Schematic cross-section, within west-central Alberta, of Middle Triassic sequence stratigraphy showing how the Doig-Halfway-Charlie Lake formations are bound and related within each parasequence. Successively younger parasequences prograde to the southwest. producing a progradational parasequence set (after Willis, 1992).

2.0.0. REGIONAL STRATIGRAPHY.

2.1.0. INTRODUCTION.

The Triassic deposits of the Western Canada Sedimentary Basin spans the Early Griesbachian to Late Norian, encompassing 37 million years (208-245 ma). The Triassic rocks cover a restricted area extending between the eastern part of the Rocky Mountains eastward to the Sturgeon Lake field in northwestern Alberta, and from 54° N. Lat. to 59° N. Lat., an area of 142,000 km^2 (55,000 square $miles^2$). Thicknesses of the Triassic section range from zero, at the eastern erosional edge, thickening westward to more than 1200 metres (4000 feet) in the Foothills (Figure 9). A northwest-southeast structural strike with a shallow dip to the southwest effects the Triassic strata.

Triassic rocks rest unconformably on Carboniferous limestones or sandy cherts and dolomites of the Rocky Mountain Formation, and Permian cherts sourced from the Fantasque, Debolt, Belcourt, Belloy, and Mowitch formations. The Triassic strata are overlain unconformably by Jurassic shales of the Fernie Group (Nordegg Member) to the south, and Cretaceous shales in the north (McLearn, 1953; Hunt and Ratcliffe, 1959; Pelletier, 1962, 1965; Gibson, 1975). The subsurface and surface stratigraphic terminology employed for the Triassic within the Western Canada Sedimentary basin is shown in the stratigraphic column (Figure 10) and the schematic cross-section (Figure 11).

2.2.0. DAIBER GROUP.

The Toad-Grayling Formation, originally defined by Hunt and Ratcliffe (1959) in outcrop, was increased in status and termed the Daiber Group by Armitage (1962) (Figure 12). The Daiber Group varies in thickness from 610 metres (2000 feet) in the Foothills to zero at its eastern erosional edge. Toad-Grayling Formation is correlated with the lower beds of the Liard Formation ('Flagstones' unit). The Toad-Grayling Formation commenced deposition in early Lower Triassic times (Lower Scythian) and concluded by early Middle Triassic (Anisian age).

Armitage (1962) divided the Daiber Group into two subsurface formations; a lower argillaceous siltstone unit which grades down into grey shale known as the Montney

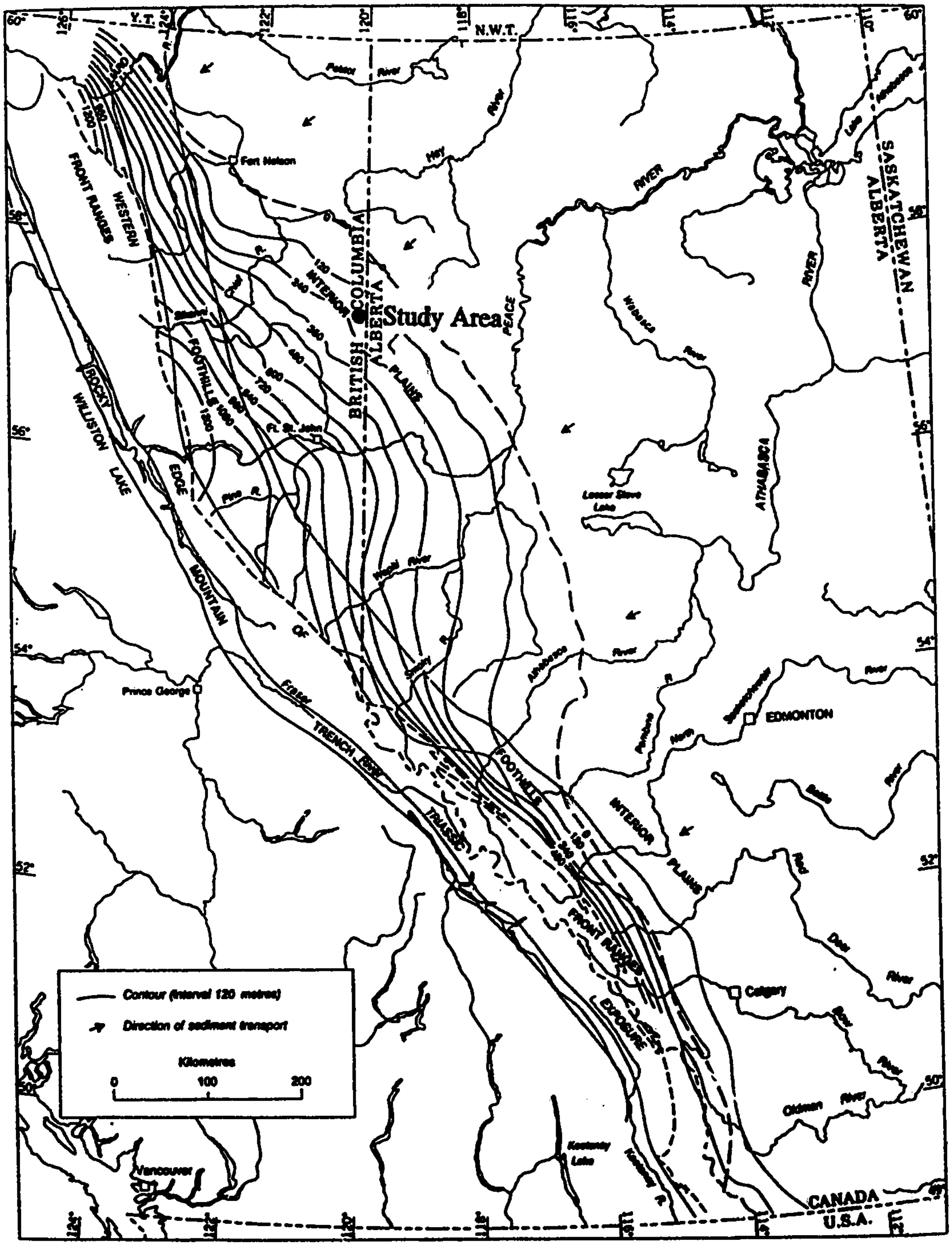

Figure 9. Plan showing the location of the study area, at which the Triassic isopach indicates a total thickness of 200 metres. Note the thickening from zero at the erosional edge to over 1200m at the Front Ranges to the west (after Barrs *et al.*, 1964; Gibson and Barclay, 1989).

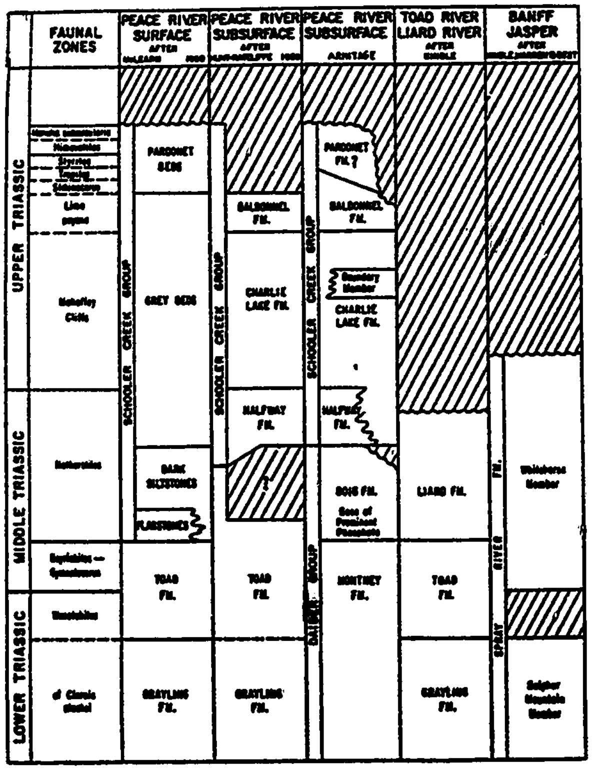

Figure 10. Stratigraphical correlation of surface and subsurface formations within the Western Canada Sedimentary Basin (after Armitage, 1962).

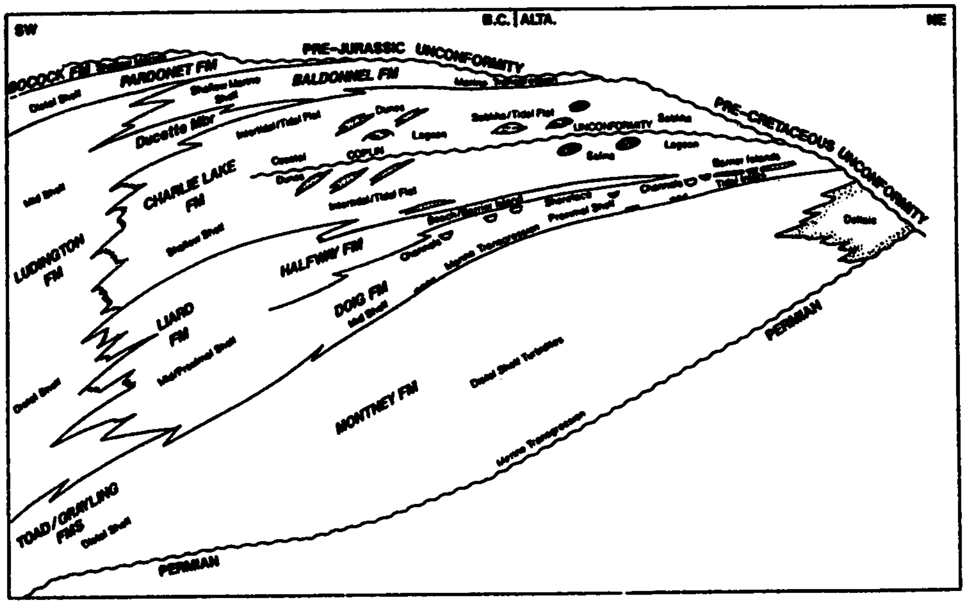

Figure 11. Schematic cross-section showing the relationships and depositional environments of Triassic formations between the subsurface Peace River area (NE) and the Foothills (SW) (after Gibson and Edwards, 1990).

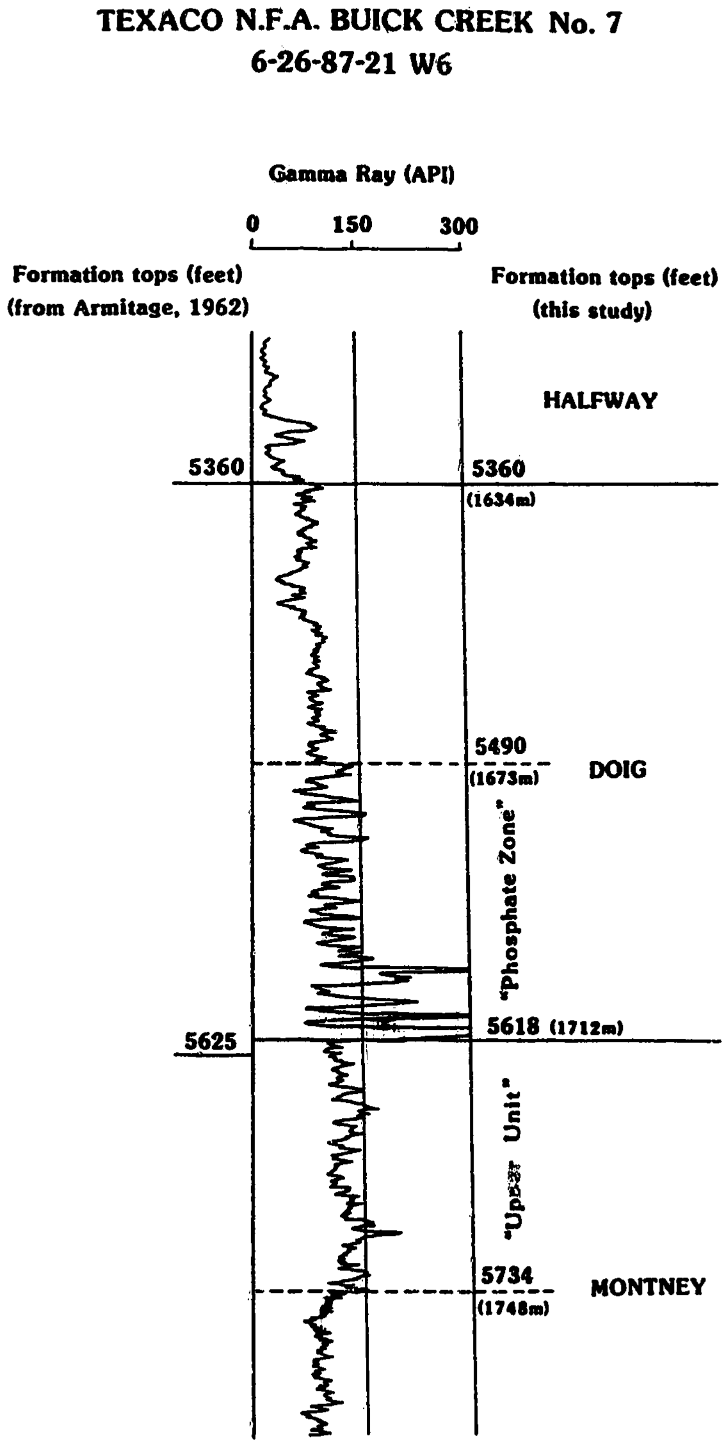

TEXACO N.F.A. BUICK CREEK No. 7
6-26-87-21 W6

Figure 12. Type well for the Daiber Group, showing the Doig and Montney subsurface formations (after Armitage, 1962; in Riediger *et al.*, 1990).

Formation and an upper dark grey bituminous siltstone unit known as the Doig Formation.

2.2.1. Montney Formation.

The Montney Formation grades from dark grey shales upward into dark grey, argillaceous siltstones and interbedded shales. The formation is over 457 metres (1500 feet) thick, and thins to an eastern erosional edge (Armitage, 1962). Sediment size increases to the east forming shoreline sandstones at its eastern extent (gas production from Sturgeon Lake field). Miall (1976) has identified four prograding cycles characterized by deltaic deposits in the eastern region. The top of the Montney Formation is represented by a phosphatic pebble conglomerate having formed in response to a major transgression, above which are prominent phosphatic shale beds (Armitage, 1962; Gibson and Barclay, 1989; Gibson and Edwards, 1990). The base of the Montney Formation is placed at the conglomerates of the Palaeozoic unconformable surface.

2.2.2. Doig Formation.

The Doig Formation is composed of dark grey, argillaceous, bituminous siltstones. The formation thins from 122 metres (400 feet) in the west, to zero at the eastern erosional edge. Gibson and Edwards (1990) state that the contact between the Halfway and Doig in the subsurface is erosional to the east and gradational to the west. The Doig is of Anisian to earliest Ladinian age based on the appearance of *Ussurites* (pers. comm. C. Stelck, 1992) found within the phosphate beds of the lowest part of the Doig Formation. The formation is correlatable with the upper Toad, Liard and 'Flagstones' formations (Kindle, 1944).

The base of the formation is characterized by a phosphatic conglomerate composed of fish scales and bone fragments (Wittenberg, 1992). Gibson and Barclay (1989) stated from limited palaeontological evidence that there is no significant hiatus between the top of the Montney and the base of the Doig; instead they are separated by a diastem. Phosphatic beds occurring at the base of the Doig, have been referred to as the 'Phosphate Zone' by Armitage (1962). A number of coarsening-upward prograding shoreface cycles have been interpreted above the 'Phosphate Zone' by Aukes and Webb (1986), Wittenberg (1992) and Willis (1992). Toward the top of the Doig Formation thick sand bodies occur. They have been interpreted as incised valley systems cut by a fall in sea-level (Campbell and Horne, 1986; Cant, 1986; Campbell and Hassler, 1989; Campbell *et al.*, 1989). Gibson and Edwards (1990) state that they could alternatively be formed from channels cut into the lower shoreface. Wittenberg and Moslow (1991), Munroe (1991) and Wittenberg (1992) have interpreted the sandstone bodies as forming in response to contemporaneous slope failure on a shelf.

2.3.0. SCHOOLER CREEK GROUP.

The Schooler Creek Group (spanning the Middle Ladinian to Upper Norian stages) increases in thickness from zero at its eastern subcrop erosional edge to 610 metres (2000 feet) in the Foothills. Hunt and Ratcliffe (1959) in their subsurface study, upgraded the status of the Schooler Creek Formation (originally proposed by McLearn, 1921) to Group level. The 'Flagstones', 'Dark siltstones', 'Grey beds' and Pardonet beds (McLearn and Kindle, 1950) have been assigned to the Schooler Creek Group. The 'Flagstones' and 'Dark Siltstones' have been correlated to the Liard Formation within the Liard River valley to the north, as described by Kindle (1944), based on similar occurrences of the ammonite fauna *Nathorstites*.

The Schooler Creek Group is divided into four formations: the basal sandstones known as the Halfway Formation; evaporites and anhydrites known as the Charlie Lake Formation; an extensive carbonate known as the Baldonnel Formation; and an argillaceous carbonate restricted to the eastern Foothills known as the Pardonet Formation (Hunt and Ratcliffe, 1959). The Group is overlain unconformably by the Lower Jurassic Fernie Group shales. Colquhoun (1962) reapplied the Schooler Creek Group to surface outcrops, the basal Halfway sandstones demarcating the lower limit of the Group. The Schooler Creek Group rests erosively in the east and gradationally in the west on the Toad and Grayling formations (Kindle, 1944) of Lower to Middle Triassic.

2.3.1. Halfway Formation.

The name 'Halfway' is taken from the Halfway River where the type section for the Halfway Formation was chosen (at the junction between the Halfway and Peace Rivers) due to the completeness of the core (Southern Production's well no. B-14-1, located in Lsd. 1, Sec. 12, T. 84, R. 23, W. 6th Mer.) (Hunt and Ratcliffe, 1959) (Figure 13). The formation thickens from zero at the subcrop edge in the east, to over 120 metres (400 feet) in the Foothills (Hunt and Ratcliffe, 1959). The lithology consists of marine, grey to light grey, fine- to medium-grained, calcareous to dolomitic quartz arenite, with minor amounts of grey to buff finely crystalline dolomite and dolomitic siltstones. Sediments in the eastern Peace River area lie disconformably on the Toad-Grayling Formation and are conformably overlain by the Charlie Lake Formation, while in the west both the upper and lower contacts are conformable and transitional. Campbell *et al.* (1989) state that there may be an unconformity in the eastern part of the Western Canada Sedimentary Basin which separates the Halfway from the Charlie Lake formations.

Hunt and Ratcliffe (1959) correlate the Halfway sediments with the lower grey, calcareous, fine sandstones of the 'Grey beds' (McLearn, 1940) and the Liard Formation (Kindle, 1944) due to the presence of *Lingula selwyni* (found by C.R. Stelck in cores from the Halfway Formation).

Clark (1961) described the Halfway Formation in the subsurface of the Milligan Creek oilfield in northeastern British Columbia as the first sandstone encountered below the Charlie Lake dolomites in core (Figure 14). The shales below the Halfway sandstone were assigned to the Toad-Grayling Formation. The top and bottom contacts are sharp and distinct. Specimens of the genera *Myophoria*, *Trigonia?*, *Lima* and *Spiriferina* (identified by C. R. Stelck) were found within a Milligan Creek core. Bed by bed correlation with the type core from Pacific Fort St, John No. 8 suggested that the Halfway was a diachronous formation. The top 6 to 20 feet of the formation represent shallowing conditions. Hunt and Ratcliffe (1959), Clark (1961) and Armitage (1962) interpreted the Halfway sands as basal transgressive sands producing a regional unconformity. Clark (1961) was the first to interpret the Halfway Formation as a "barrier sand bar" within the Milligan Creek area. Pelletier (1965) also stated that the Halfway sandstones were deposited during a regression, infilling the basin to the west. He also derived palaeocurrent transport directions toward the southwest.

Sedimentological studies carried out by Campbell and Horne (1986), Cant (1986), Munroe and Moslow (1990) and Willis (1992) indicate that sharp based Halfway sandstones found within the Wembley and Peejay fields, are tidal-inlet channel fills. These inlets eroded down into the offshore shales associated with the distal part of the same Halfway shoreface system. Indeed, many cores within the Wembley field have been interpreted as gradationally based, coarsening upward shoreface sequences (Campbell

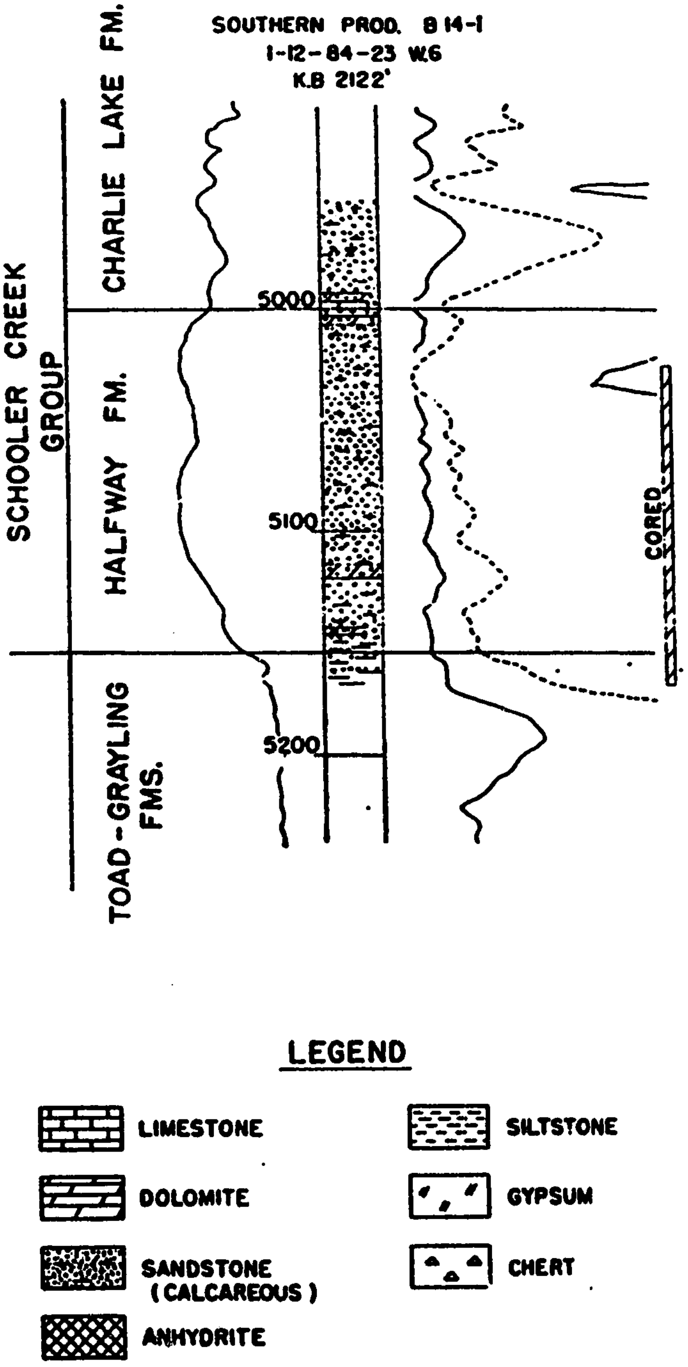

Figure 13. Type section of the Middle Triassic Halfway Formation. The Halfway is overlain by Charlie Lake evaporites and red beds, and overlies Toad-Grayling siltstones (after Hunt and Ratcliffe, 1959).

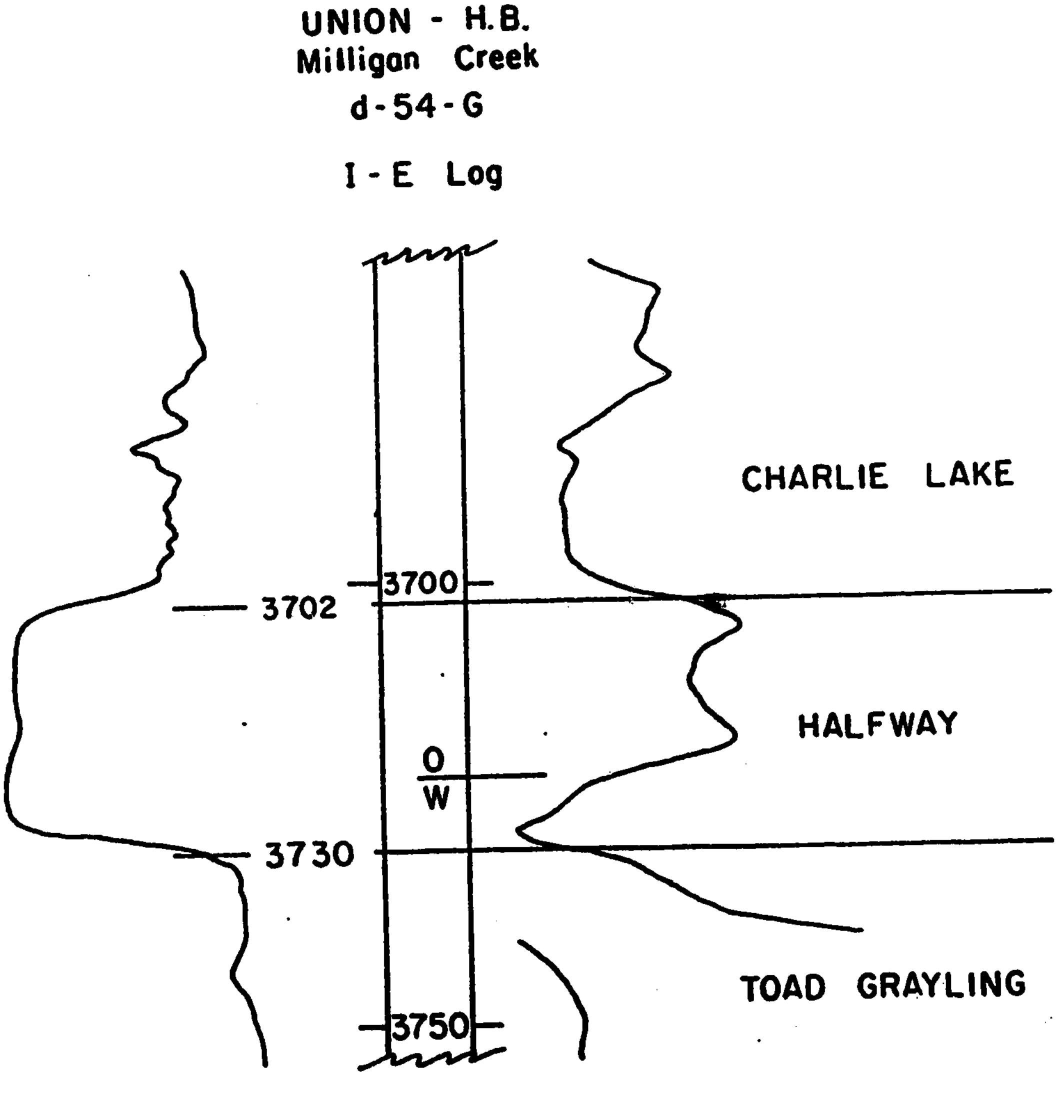

Figure 14. Typical induction log signature for the Halfway Formation in the Milligan Creek oilfield. The SP produces a pronounced and sharp response within the Halfway sandstone. The Halfway is overlain by Charlie Lake dolomitic claystones, and sharply overlies Toad-Grayling bituminous shales (after Clark, 1961).

and Horne, 1986). This would suggest that the shales, originally classed as Toad-Grayling and Doig, are in fact part of the Halfway Formation.

2.3.2. Charlie Lake Formation.

The Charlie Lake Formation, formally designated by Hunt and Ratcliffe (1959) consists of massive anhydrites, red dolomitic siltstones, microcrystalline to cryptocrystalline, buff to grey dolomites, interbedded anhydrites and minor amounts of halite. To the west, sandstones and limestones of similar lithology to the Halfway are intercalated with evaporites and few comminuted shell debris, making the lower contact of the Charlie Lake difficult to recognize (Hunt and Ratcliffe, 1959). For this reason, the lower contact has been termed gradational by (Colquhoun, 1962). In the east however, the contact is easier to distinguish. Pelletier (1962) indicated that a number of thin sand layers within dolomitic sediments yielded a palaeocurrent direction toward the southwest. The upper contact of the formation is conformable with the Baldonnel Formation. Thicknesses range from 0 to 427 metres (1,400 feet).

It has been tentative suggested that the Charlie Lake Formation be correlated with the Mahaffy Cliff fauna of the middle of the 'Grey beds' (McLearn, 1950), since the overlying Baldonnel Formation is equivalent to the *Lima poyana* zone of the upper Grey Beds, and the *Nathorstites* faunal zone of the lower Grey Beds has been correlated with the Halfway Formation. Lateral lithofacies variations, from west to east, produce difficulties for correlation purposes.

Hunt and Ratcliffe (1959), Armitage (1962), Barclay and Leckie (1986), Cant (1986), Campbell and Horne (1986), Gibson and Barclay, (1989) and Gibson and Edwards, (1990) have all documented that the Halfway (and equivalent formations) barrier island shoreline deposits grade into the Charlie Lake red beds, anhydrite nodules, algal mats, and dolomites interpreted as a sabkha setting forming behind a barrier island shoreline. Campbell *et al.* (1989) and Campbell and Hassler (1989) however, state that the contact is unconformable, with erosion into the underlying deposits increasing to the east. This is also confirmed by Aukes and Webb (1989) on a local scale, where Halfway deposits have been completely removed by early Carnian erosion.

3.0.0. DEPOSITIONAL SETTING.

3.1.0. SEDIMENT SOURCE.

McLearn (1953), Pelletier (1965) and Podruski *et al.* (1988) indicated a sediment source from the east and northeast due to palaeocurrent studies. Mothersill (1968), Gibson (1975), Campbell and Horne (1986) and others, indicate sediment supply was sourced from the north and northwest during Middle Triassic times, transported by longshore drift currents developed parallel to palaeocoastline (orientated northwest-southeast). Campbell and Horne (1986) suggested that the Middle Triassic coastline may have been supplied with sediment sourced from a Halfway age delta to the northwest, in northeastern British Columbia. The presence of a delta within northeastern British Columbia has not been confirmed in published reports, to date. The pre-Charlie Lake erosion surface, truncating Middle Triassic deposits in northeastern British Columbia, may have completely removed any evidence to support the existence of a delta.

The Middle Triassic sandstones are fine grained, and mineralogically and texturally mature, indicating multi-cyclic processes of derivation. They were derived from the Permian (Fantasque, Debolt, Belcourt, Belloy and Mowitch formations) and Carboniferous (Gibson and Barclay, 1989; Gibson and Edwards, 1990). These rocks had all been gently uplifted on the craton to the northeast (Podruski *et al.*, 1988; Gibson and Barclay, 1989; Gibson and Edwards, 1990). The fine grained nature of the Triassic clastics suggests that the cratonic source was a gentle low lying region, or alternatively a very remote region.

3.2.0. PALAEOLATITUDE.

Determinations of palaeolatitude during the Middle Triassic have been addressed in palaeomagnetic, palaeontologic and sedimentologic studies. Tozer (1982) identified marine fauna in the Middle Triassic of northeastern British Columbia, representative of a mid palaeolatitude faunal province. Using palaeomagnetic data, reconstructed by Irving (1977), the mid palaeolatitude fauna were placed at 40° north of the palaeoequator, during Triassic times, based on polar wondering curves. Habicht (1979), however, derived a palaeolatitude value for northeastern British Columbia during the Triassic of 26° north of the palaeoequator. Sedimentological information supports both values, in that algal laminites, sabkha deposits and red beds found within the Charlie Lake are consistent with those found today in warm (subtropical to tropical) arid climates at latitudes between 35° north and south of the equator (Campbell and Horne, 1986). Modern day equivalents of Charlie Lake anhydrites, however, form between 20° N and S of the equator (Habicht, 1979).

3.3.0. PALAEOCLIMATE.

Palaeoclimate of the Triassic was described and interpreted as warm (subtropical to tropical) arid by Habicht (1979) and Campbell and Horne (1986), based on the presence of algal-laminites, anhydrites and red beds. Gibson and Barclay (1989) document that the palaeoclimate was mid-temperate to subtropical in the Middle and Lower Triassic, but became more arid to hot subtropical toward the Late Triassic as evidenced by the appearance of evaporitic deposits.

Fauna also suggest that the temperature of oceanic water was cold until the Upper Triassic, since cold water fauna were identified by Tozer (1982) from northeastern British Columbia, during Middle Triassic times. The cold water, may however, have been produced by upwelling of deep, oxygen poor, nutrient rich, cold water, that flowed across the western continental shelf of the Pangaea Supercontinent during Middle Triassic times. Initiation of upwelling cells along modern day western continental shelves result from offshore blowing winds, transporting surface water in a seaward direction. The water is replaced with upwelling deep, nutrient rich, anoxic, cold water. The present day wind pattern, at low latitudes, approximately 26° north of the equator, is the Northeasterly Trade Wind Belt (located between 0° and 30° north of the equator, Chang, 1972). If the wind direction was similar during the Middle Triassic, then dominant winds would have blown across the arid continental interior, and offshore from the coastline into the Panthalassa Ocean, initiating the upwelling cells across the continental shelf, at palaeolatitudes of 26° (Habicht, 1979; Kristan-Tollmann and Tollmann, 1981). This is evidenced by the presence of phosphatic rich shale beds within the "Phosphatic Zone" of the Doig Formation, and the marine origin indicated by the type II kerogen extracted from phosphatic source rocks within the "Phosphate Zone" (Riediger *et al.*, 1990). Outcrops of aeolian cross-bedded deposits at Williston Lake in northeastern British Columbia, within the Charlie Lake Formation, also indicate the presence of easterly winds (Arnold, 1992 pers. comm.).

Campbell and Horne (1986), however, interpreted the dominant palaeowind direction as northwesterly, at a palaeolatitude of approximately 30° north of the palaeoequator. They derived this result from the assumption that modern wind belts have not changed much in position. They reconstructed the palaeocoastline within west-central Alberta to have been orientated northwest-southeast. Grain size plots from samples studied by Campbell and Horne (1986) along the Halfway shoreline, demonstrate that grain size decreases to the southeast, thus indicating that a longshore current flowing southeastward was initiated. It is not documented, however, whether or not the sand sized samples were collected from a time synchronous lithofacies, or if the samples were derived from a shoreline of consistent geological age.

There is a certain amount of risk in assuming that the Triassic wind and climatic belts were similar to those of the present day. It is possible that the climatic belts may have shifted latitudinal position in the past. It is unlikely that they have remained in the same position since the Triassic. They can be affected by continental drift, which controls latitude changes, mountain building, sea level changes, configuration and orientation of continental land masses, and the consequent changes in ocean current and wind patterns (Habicht, 1979). The widespread presence of a huge continental interior desert environment within Pangaea throughout the Triassic, would have reduced the geographical extent of the poles, (reducing temperature and pressure imbalances between the poles and equator) consequently effecting the ocean circulation patterns and wind patterns. It should be pointed out, however, that the Coriolis force may have imparted a constant effect on the wind belts and ocean circulation patterns, in that gross circulation patterns would have remained fairly constant.

3.4.0. PALAEOGEOGRAPHY.

Gibson and Barclay (1989) stated that the west coast of the Pangaea Supercontinent was a tectonically stable passive margin during the Triassic Period. There has been no cited evidence of autochthonous volcanic activity in the Western Canada Sedimentary Basin during the Triassic, except from Moslow (1992 pers. comm.) who has observed thick bentonitic beds within the Ring Border and Sturgeon Lake fields of Lower Triassic Montney Formation in northeastern British Columbia and Alberta. However, there is evidence to suggest that subduction of oceanic crust of Panthalassa under the Pangaea continental crust was occurring in Baja, California and Oregon during the Triassic

(Davies *et al.*, 1978; Monger and Irving, 1980; Monger *et al.*, 1982; Irving *et al.*, 1985; Mortimer, 1986; Blome and Nestell, 1991). Volcanic activity occurring in Oregon may have been responsible for the derivation of the bentonitic beds within the Western Canada Sedimentary Basin. In studying the palaeogeographical location of fauna in western Canada, Tozer (1982) determined that the interbedded volcanic and sedimentary Triassic rocks, west of the Rocky Mountain Cordillera were exotic or suspect terranes, occurring as volcanic islands (Figure 15). Warm water fauna containing corals found within these terranes, suggest that they were originally formed in low palaeolatitudes, approximately 3000km (plus or minus 1500km) to the south of the present location.

Podruski, *et al.* (1988); Gibson and Barclay (1989) and Gibson and Edwards (1990) identified three transgressive-regressive phases within the Triassic of northeastern British Columbia, which were interpreted as the result of relative sea level movements in response to changes in clastic influx supply and minor local tectonism associated with the Peace River Arch. Smaller order cycles are evidenced as closely related facies are repeated in vertical sequence. An alternative theory for the formation of the major cycles is from the break up of Pangaea, and the subsequent northward drifting and collision of exotic terranes on to the North American continent during Triassic times (Gibson and Barclay, 1989; Gibson and Edwards, 1990).

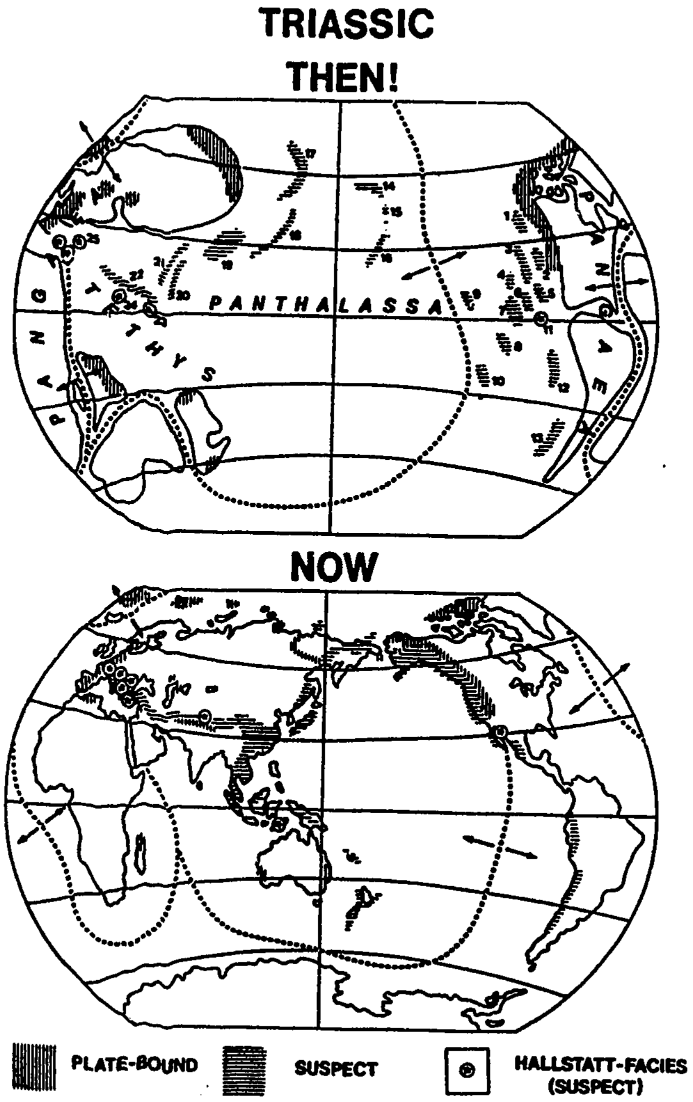

Figure 15. Palaeogeographical reconstruction of the Triassic showing the position of suspect terranes (based on their faunal characteristics) and plate bound fauna. The present day map shows that fauna of both types are juxtoposed on the western side of the North American continent. During Triassic times, suspect terranes were scattered throughout Panthalassa. as isolated volcanic islands. 1: Possible MPL volcanic terrane now in British Columbia border zone, 2: Quesnellia, 3: Stikinia, 4: Chulitna terranes, 5: Luning terrane, 6: Alexander terrane, 7: Wrangellia, 8: Shasta County, California, 9: Peninsular terrane, 10: Vizcaino terrane, 11: Mina el Antimonio, 12: Peru, 13: Chile, 14: Northern New Guinea, 15: New Caledonia, 16: New Zealand, 17: Northeast Siberia terranes, 18: Japan and Primor'ye, 19: Yangtze Platform, 20: Gandise-Hengduan terranes, 21: Qilian-Bayanhar terranes, 22: Northern Tethyan Himalaya, 23: Timor, 24: Kiogars, 25: Hallstatt occurrences of Mediterranean area (after Tozer, 1982).

4.0.0. LITHOFACIES DESCRIPTIONS AND INTERPRETATIONS.

The Middle Triassic deposits within the study area have been divided into thirteen lithofacies (Table 3). Each lithofacies has been separated by recognition of physical and biogenic sedimentary structures, texture, lithology, colour, cement, bedding contact nature and soft sediment deformation features. Hydrodynamic processes and the mechanisms responsible for their formation were reconstructed from lithofacies descriptions, from which environmental interpretations were derived. Where insufficient information was available, environmental interpretations were made using vertically adjacent lithofacies successions.

In some cases, deposits within the same lithofacies were interpreted as forming in separate environments, or within similar environments but due to different physical processes or mechanisms.

4.1.1. LITHOFACIES A. BIOCLASTIC LITHARENITE.

This lithofacies is spatially restricted within the study area. Where it does occur, it lies erosionally on Lithofacies C (offshore-transition), Lithofacies D (lower shoreface), Lithofacies E (lower shoreface), or Lithofacies F (upper shoreface), and is overlain sharply by either Lithofacies C (offshore-transition), Lithofacies D (lower shoreface), or Lithofacies E (lower shoreface). This lithofacies may be difficult to recognize in core, especially when it is bedded between two similar sandstone lithologies. The upper contact may be marked by a pyrite layer. Lithofacies A is very thin, ranging in thickness from 24 to 90 cms (0.8ft to 3 ft).

Lithofacies A is composed of dolomite cemented very-fine lower and rarely upper sand sized grains. Lithoclasts of black chert, phosphate and shale, are concentrated toward the top of the lithofacies. These lithoclasts are sub-angular, ranging in size from medium upper sand (common) to pebble (rare). Shell biomolds are also common toward the top of the lithofacies, and are associated with low concentrations of phosphatic shell fragments (e.g. d-082-D/94-A-16, 3870.2 feet to 3871 feet; d-027-C/94-A-16, 3916 to 3913 feet; Appendix A).

Lithofacies	Lithology	Physical Sedimentary Structures	Biogenic Sedimentary Structures	Bedding Style	Thickness	Environmental Interpretation
A	Bioclastic litharenite	None	None	Erosional base	0.2-0.9m (0.8-3 ft)	Transgressive lag
B	Black shale	Parallel-lamination and asymmetrical ripple cross-lam.	None	Normally graded siltstone 'pinstripe' lamination	0.3-9.8m (1-32 ft)	Offshore
C	Interlaminated shale, siltstone and sandstone	Parallel lamination, asymmetrical ripple cross-lam., H.C.S.	*Planolites,* *Palaeophycus* *Teichichnus* Escape traces	Normally graded, sharp based siltstone beds	0.3-6.4m (1-21ft)	Offshore-Transition
D	Interbedded sandstone, siltstone and shale	Convolute lamination, H.C.S., ripple laminatioa, parallel-lamination synaeresis cracks	*Planolites,* *Palaeophycus* *Teichichnus* Escape traces	Normally graded, sharp, loaded based beds. Biogenic activity destroys sedimentary structures	0.3-9.8m (1-32 ft)	Lower Shoreface
E	Thickly interbedded sandstone, siltstone and shale	H.C.S. asymmetrical and symmetrical ripple cross lam., parallel-lamination, synaeresis cracks	*Planolites* *Palaeophycus* *Teichichnus* *Cylindrichnus* *(?)Bergauer-ia* *Skolithos*	Normally graded, sharp based sandstone beds, fining up into wavy bedding	0.3-5.2m (1-17 ft)	Lower to Middle Shoreface
F	Sandstone	structureless, symmetrical ripple cross-lam., trough cross-bedding, parallel-lamination	*Skolithos*	thickly-bedded, structureless sharp-based shell-rich beds	1.5-3.3m (5-10.8 ft)	Upper Shoreface
G	Biodolomicrite (coquina)	Parallel-lamination, cross-bedding, imbrication	None	comminuted and whole shells, shale basal intraclasts	1.6-6.1m (5.1-20 ft)	Tempestites. Active Tidal Inlet Channel
H	Sublitharenite	Cross-bedding, Parallel-lamination, current and climbing wave ripple cross-lam.	None	Cross-bedded sets 3-17cms thick. Basal lithoclasts	1.1-11.0m (3.6-36ft)	(H1) Active Tidal Inlet Channel (H2) Spit Platform
I	Polymict conglomerate	Minor ripple cross-lam.	None	Poorly-sorted, polymict lithoclasts, matrix supported	0.3-1.5m (1-5ft)	(Halfway/Charlie Lake) erosional lag
J1	dolomite-anhydrite laminite	parallel-lamination	Crypt-algal laminite	crinkly parallel-lamination	2.5-13 cms (1-5 inch.)	Playa-Lake Margin

Lithofacies	Lithology	Physical Sedimentary Structures	Biogenic Sedimentary Structures	Bedding Style	Thickness	Environmental Interpretation
J2	shale and siltstone intraclasts, silty-shale matrix, anhydritic nodules	parallel-lamination, asymmetrical ripple cross-lam.	None	mud-chip intraclasts	(12.5-60cms 5inch.-2ft)	Playa-Lake Mudflats
J3	Interlaminated siltstone and shale, anhydritic nodules	parallel-lamination, current ripple cross-lam.	None (?)	sharp, loaded based normally graded siltstone	0.3-4.6 m (1-15ft)	Playa-Lake to Marginal Mudflats
K	Orange shale with shale intraclasts	Crude parallel-lamination	None	Sharp loaded based normally graded siltstone, shale intraclasts	>6.1m (>20ft)	Playa-Lake
L	Red shale	Crude parallel-lamination	None	Sharp loaded based normally graded siltstone, shale intraclasts	>7.3m (>24ft)	Continental Mudflats

Table 3. Lithofacies identified from the Halfway and Charlie Lake formations of the Peejay field.

In places, the upper contact is gradational, characterized by shale free sandstones grading into wavy-bedded sandstone and shale, and up into interlaminated siltstone and shale. By applying lithostratigraphic nomenclature used by Campbell and Horne (1986) from the Wembley Field, west-central Alberta, the deposits below Lithofacies A would have been grouped within the Doig Formation, while those above would have been assigned to the Halfway Formation.

4.1.2. ENVIRONMENTAL INTERPRETATION.

The erosional base of the lithofacies, sub-rounded lithoclasts, and medium upper to pebble grain size, all point to sediment reworking under high-energy conditions. Coarse grained and rare pebble material is concentrated within this lithofacies, forming a winnowed lag deposit. The top, however, abruptly or gradationally passes into finer grained sandstone, siltstone or shale, reflecting an abrupt or gradual decrease in energy level. This is attributed to an increase in water depth.

Lithofacies A is located at the top of a coarsening-upward package of lithofacies (lithofacies B, C, D and E), which have been interpreted as a shallowing-upward sequence. Above Lithofacies A are finer grained deposits, interpreted as forming in relatively deeper water, above which is another coarsening- and shallowing-upward sequence. Hence, Lithofacies A occurs above deposits formed within shallow water conditions, and below deposits formed in deeper water conditions. Thus, it would seem that a transgression had occurred between these two packages of sediment, recorded by the erosional lag represented by Lithofacies A. The erosional lag was formed by prolonged reworking and erosion of the shoreface by fairweather waves during a relative sea level rise, forming a ravinement surface (Nummedal and Swift, 1987). Hence, the transgressive lags occur above sandstones inferred to have formed in shallow palaeowater depths. They are not present above shales and siltstones with inferred deep palaeowater depths. As water depth increased with time, fairweather waves could no longer 'feel' the sea floor, thus low energy conditions returned, recorded by the presence of shales and siltstones, resulting from suspension deposition. For this reason, the lithofacies has been interpreted as a transgressive lag.

4.2.1. LITHOFACIES B. LAMINATED BLACK SHALE.

Lithofacies B passes up gradationally into overlying Lithofacies C, and overlies Lithofacies A or Lithofacies D, either abruptly or gradationally. Average thickness of the lithofacies is 2 metres (6.4 feet), with maximum thickness of 9.8 metres (32 feet) and minimum thickness of 0.3 metres (1 foot). Lithofacies B is characterized by monotonous black, parallel-laminated shale. Colour may vary from black to olive-green. The latter is restricted to the top of Lithofacies B, and is associated with the introduction of silty-shale. Shales located at the base of Lithofacies B are black in colour, and tend to produce high A.P.I. values on the gamma-ray curve. The high values may be caused by uranium bound within organic and phosphatic material within the shales.

There are occasional very thin laminae (maximum thickness of 1cm) of coarse silt sized, light grey, normally graded siltstones, located throughout the lithofacies. This has been referred to as 'pinstripe lamination' by Cant (1986). The frequency and thickness of these laminae increase up through the lithofacies, spaced at intervals of at least 9cm (3.6 inches) apart. These siltstones display sharp (sometimes erosional), loaded basal contacts and gradational tops. Convolute laminae may also be recognized at the base of each laminae, overlain by parallel-lamination, passing up into asymmetrical ripple stratification. Biogenic activity within the lithofacies, whether as body or trace fossils, is rare. In some cases micro-faults and oversteepened laminae occur.

The pinstripe siltstone laminae within this lithofacies are weakly to strongly cemented with calcite or dolomite. Pyrite cement is subordinate, occurring as interstitial and framboidal forms. Alternatively, it may form concentrated laminae within the siltstones. Euhedral anhydrite crystals in the form of swallow tail shapes, or hopper shapes, occur sparsely throughout the lithofacies (e.g. b-064-H/94-A-15). They tend to deform the shale laminae around them.

4.2.2. ENVIRONMENTAL INTERPRETATION.

The dominant lithology of Lithofacies B is shale. These particles were deposited from suspension in the water column. This process occurred in low energy, quiescent conditions, devoid of turbulence within the water column. Muds were deposited from suspension. The continual slow rate of deposition of hemi-pelagic material produced a muddy stratum on the sea floor. The lack of symmetrical ripple lamination, produced from oscillatory current processes, suggests deposition of sediments within the marine offshore bathymetric zone, as defined by Elliott (1986) (Figure 16). He defined this zone as that occurring below the influence of mean storm wave base, hence, there should be minimal evidence of sediment reworking by oscillatory storm-generated currents.

The continual slow rate of mud sedimentation within the offshore zone was interrupted by relatively catastrophic events, reflected by relatively rapid incursion and sedimentation of siltstone laminae within Lithofacies B. Loaded basal contacts and convoluted structures within the basal parts of siltstone laminae, suggest that these deposits were rapidly emplaced. Unidirectional currents reflecting upper flow regime hydrodynamic conditions, were responsible for the formation of the parallel-laminated structures within the basal parts of siltstone laminae. Asymmetrical (current) ripple lamination occurring above the parallel-laminated structures within the siltstone laminae, reflect deposition by weaker portions of the same waning unidirectional current. The ripples were formed by traction-bedload and saltation transportation processes. The gradational upper contact between the siltstones and shales reflects a gradual waning of the current and change in the mechanism of deposition. As the currents waned, coarser silts were removed from the water column; the clay particles remaining to settle out of suspension at slower settling rates from low velocity currents. The grain size of the siltstones suggested they were deposited in currents attaining maximum velocities of less than 60 cms/sec within the parallel-laminated portions of the siltstone, decreasing to less than 20 cms/second in the current rippled upper portions of the siltstone laminae (Harms *et al.*, 1982). Similar graded silt and sand beds have been found in water depths of 30 to 40 metres, ranging from 20 to 30 kilometres from the coastline (Hayes, 1967; Reineck and Singh, 1972).

The presence of current ripple lamination within the siltstone laminae of Lithofacies B, and the interpreted palaeocurrent strength of between 20 to 60 cms/sec, conflict with the observations and results of the model reported by Reineck and Singh (1972). They documented that laminated sands were produced by deposition of sand and silt from suspension clouds in still water or slowly moving water (current velocities of less than 20cms/sec.). The current ripple lamination identified within Lithofacies B was formed by a higher velocity unidirectional current. Symmetrical wave ripple lamination occurring within the silts reported by Reineck and Singh (1972), having forming due to the effects of storm waves, have not been observed within the siltstone laminae of Lithofacies B.

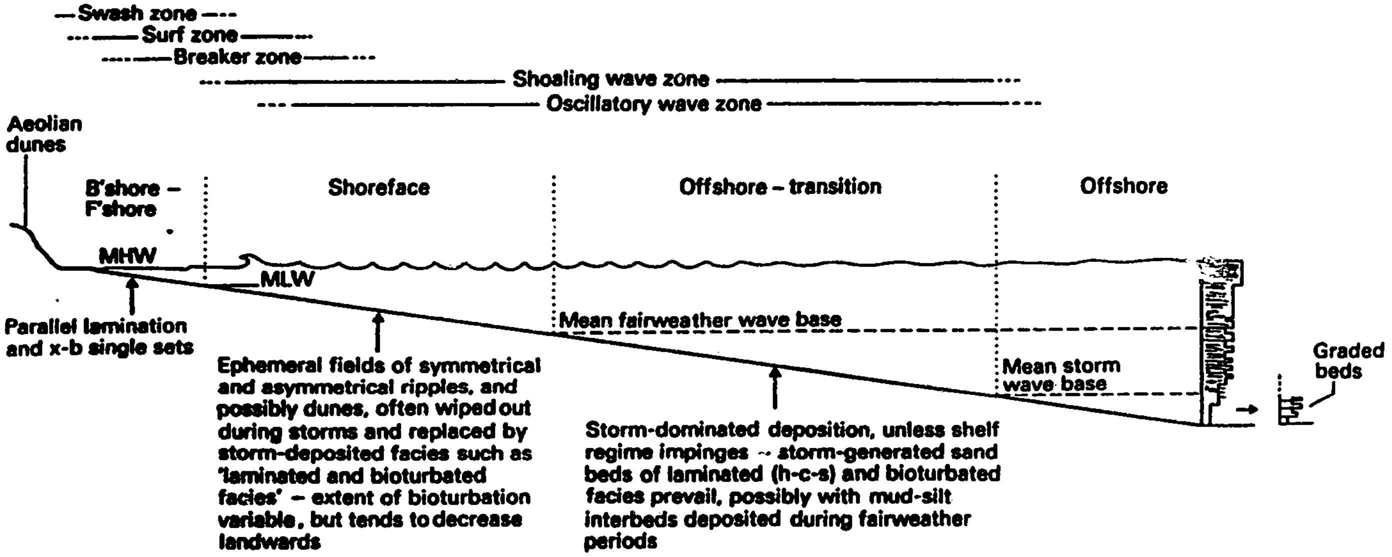

Figure 16. Bathymetric zones, processes and facies identified within the shoreface environment (after Elliott, 1986).

Sedimentological evidence displayed within Lithofacies B suggests that storm-generated geostrophic currents are a viable alternative mechanism for the formation of the graded siltstone layers. The structures produced by these geostrophic currents are more likely to be preserved below storm wave base, where reworking of the bottom sediment by storm waves is minimal. The dominant current below storm wave base is the shore-parallel unidirectional geostrophic steady to slowly varying current (Swift *et al.*, 1983, 1987; Duke *et al.*, 1991). Its formation and orientation of flow is controlled by the interaction of isobaric inequilibrium and the Coriolis force. Unfortunately, within the study area the core has not been oriented, therefore, it is not known whether the unidirectional current, responsible for the deposition of the graded siltstone beds, was directed normal to or parallel to the palaeoshoreline. Hunter and Clifton (1982), Mount (1982) and others, propose that similar storm-generated currents should have occurred in the past.

Modern geostrophic currents reported from modern continental shelves, generally attain unidirectional velocities of between 30 and 80 cms/sec (Swift and Nummedal, 1987). This corresponds more closely to the predicted palaeocurrent velocities and sedimentary structures from the siltstone laminae of Lithofacies B. Hart *et al.* (1990) have produced evidence from the rock record (Cretaceous Kaskapau, and Cardium formations of northwestern Alberta and British Columbia) that geostrophic currents can be preserved from the middle and inner shelf.

The shales of Lithofacies B have yielded information concerning the original palaeo-oceanic water chemistry, and oceanic cell patterns of the Middle Triassic ocean basin. The lack of biogenic activity, and the presence of pyrite nodules within the black shale reflect restricted, stagnant, oxygen poor (euxinic) basinal water conditions. Phosphatic beds, inferred from high gamma-ray readings in non-cored sections are characteristic of areas receiving low rates of sedimentation. The formation of phosphates involves a mechanism whereby an oceanic upwelling cell of deep (100-300 metres) cold, nutrient-rich, phosphorous-rich, oxygen poor, basinal water flows onto a shallow continental shelf stimulating phytoplanktonic blooms in water depths of less than 200 metres below sea level (Figure 17). This upwelling occurs today off the west coast of Africa (Diester-Haass and Schrader, 1979) and South and Central America (Figure 18). The phosphates are extracted by photosynthesis are returned to the ocean by excretion or by organic decay (Giresse, 1980).

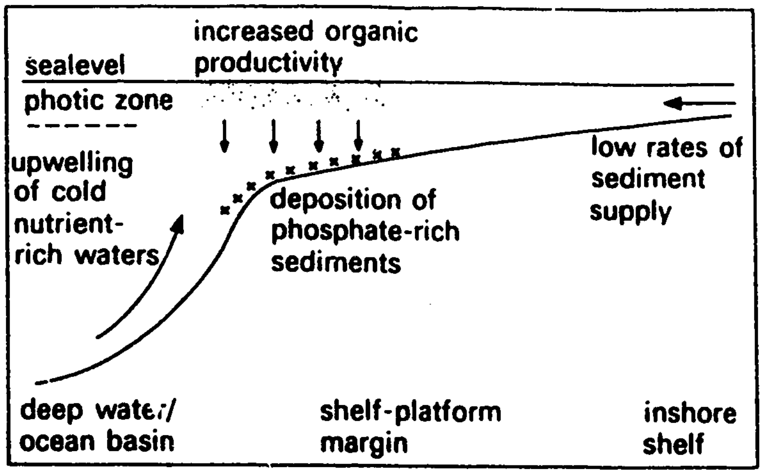

Figure 17. A current model explaining the formation of marine phosphates on continental shelves (after Tucker, 1991).

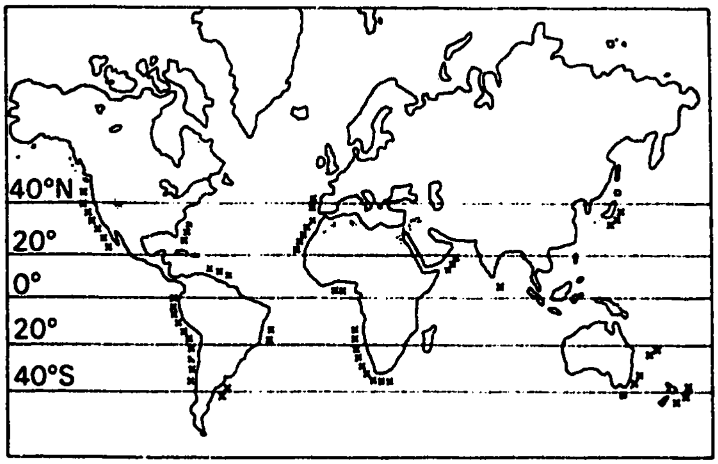

Figure 18. Distribution of modern marine phosphates (after Tucker, 1991).

Upon death, the phytoplankton settle out of suspension and decompose on the sea floor due to sulphate and iron reduction, releasing organic material and phosphorous.

Biochemical reactions due to organic decay lead to the consumption of total oxygen content of the bottom waters forming euxinic conditions. This resulted in anaerobic conditions, not only of the bottom waters, but also within the first few centimetres of sediment on the sea floor. This can explain the apparent lack of biogenic activity within the black shales of Lithofacies B. The phosphorous may be released into the water column during early diagenesis, or it may remain in the sediment and become highly concentrated (Sheldon, 1981). The phosphorous content of pore waters (released by the decay of organic material) is highest where the dissolved oxygen in the bottom waters is lowest, hence the abundance of phosphatic rich beds beneath oxygen poor upwelling deep oceanic waters.

It is interesting to note that phosphates today are formed at latitudes of less than 40° N. and S. within hot and arid climatic belts, associated with the Tradewind Belt located 30° north and south of the equator (Chang, 1972). These values are close to the predicted palaeolatitude value of the study area during the Middle Triassic (see Chapter 3). Further evidence in support of this model is the identification of a cold water fauna from Tozer's (1982) mid-palaeolatitude faunal suite. These fauna would have lived within the cold upwelling waters, on the continental shelf. Phosphate beds within the basal parts of Lithofacies B (inferred from gamma-ray geophysical well-logs) represent very slow rates of sedimentation, producing condensed sections within the distal offshore location.

The occurrence and association of authigenic anhydrite and pyrite within Lithofacies B may provide further clues as to the past geochemistry and hydrodynamic conditions of the bottom waters within the Middle Triassic basin. Siesser and Rogers (1976) documented the association of these two minerals in modern sediments from the southwest African continental slope, associated with the upwelling Benguela Current. Anaerobic bacteria reduced SO_4 dissolved in sea water produced H_2S. The H_2S reacted with iron minerals present within the sediment to produce FeS, additional elemental sulphur produced the pyrite mineral. The bottom waters were strongly reducing (low pH) and became saturated with calcium obtained by the dissolution of phytoplanktonic calcareous organisms. The lack of calcareous microfossils and the presence of phosphate in the shale of Lithofacies

B may reflect reducing conditions, and the dissolution of the material. Gypsum was precipitated once the product of the concentration of dissolved calcium and SO4 exceeded the gypsum solubility product. Similar theories have documented the authigenic growth of gypsum in deep sea sediments (Briskin and Schreiber, 1978; Muza and Wise, 1983).

4.3.1. LITHOFACIES C. LAMINATED SILTSTONE AND SHALE.

This lithofacies commonly passes gradationally up into Lithofacies D and gradationally down into Lithofacies B. It may also be erosionally overlain by lithofacies E, H or K. The average thickness of this lithofacies is 2.4 metres (8 feet), with maximum thickness of 6.4 metres (21 feet) and minimum thickness of 0.3 metres (1 foot). The dominant lithology is characterized by interbedded calcareous cemented siltstone and shale. The colour of the shale component changes from black to light green, toward the top of the lithofacies. Very -fine lower, brown sandstone is introduced toward the top of the lithofacies. Slightly asymmetrical rippled bedforms form on the top surface of the sandstone laminae. The quantity of siltstone to shale increases to ratios of 80:20 toward the top of the lithofacies. Biogenic activity correspondingly increases, commonly reworking the tops of sandstone beds and bases of overlying shale beds. It can, however, vary in intensity and quantity from 5% to 90%, in places destroying the primary physical sedimentary structures. The traces are dominantly horizontal in attitude.

The siltstone laminae commonly possess sharp bases that are loaded into underlying shale, the latter being flamed into the siltstone. Basal parts of siltstone beds exhibit convoluted lamination, passing up into undisturbed parallel-lamination (Plate 1). Siltstone laminae, devoid of shell fragments, may exhibit parallel-lamination that increase in dip upward, are sub-horizontal, and contain slight discordant surfaces. These are described as hummocky-cross-stratification structures (Harms *et al.*, 1975; Hamblin and Walker, 1979; Walker, 1979). Hummocky-cross-stratification forms dominantly in sediment sizes ranging from coarse silts to very-fine upper sands (Harms, 1975). These structures pass up into asymmetrical ripple laminated siltstone, passing into a zone of interlaminated siltstone and shale and starved ripple lamination (Plate 2), passing gradationally into increasingly burrowed shale (up to 40% burrowed), which include the following trace fossils; *Planolites*, *Palaeophycus* and *Teichichnus*. The shale laminae may display synaeresis cracks. The slightly asymmetrical loaded ripples may, alternatively become

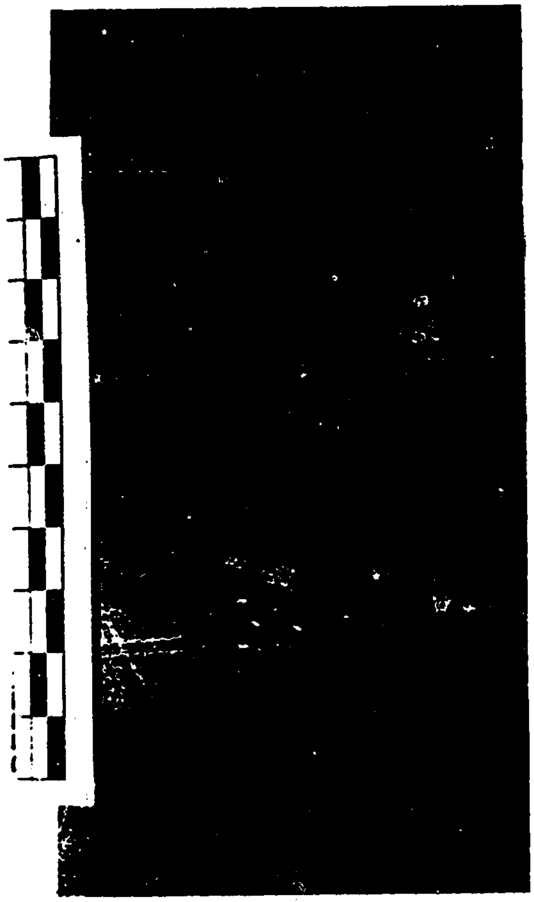

Plate 1. Thick bed of siltstone with basal convolute lamination passing up into parallel-lamination and into massive structures, and up into interlaminated siltstone and shale with *Planolites* trace fossils. Synsedimentary listric normal fault in sharp based interlaminated siltstone and shale bed. Taken from upper part of Lithofacies C. Well d-046-E/94-A-16, 3833.4 feet. (Scale bar in cms).

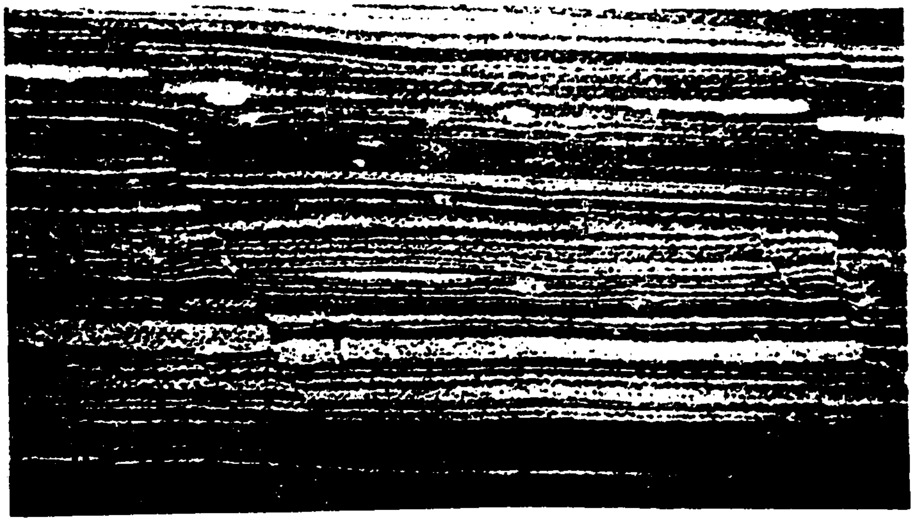

Plate 2. Interlaminated siltstone and shale. Siltstone laminae are not laterally continuous. This is starved ripple lamination. There are at least three parallel sets of normal micro-faults. Well d-043-E/94-A-16, 3823 feet, taken from top of Lithofacies C. (Scale bar in cms).

draped with shale. Internally, they display tangential ripple foreset laminae.

An alternative, but as common sequence of sedimentary structures within the siltstones are poorly developed parallel-laminations at the base passing up into slightly asymmetrical ripple laminated finer grained siltstones, the top rippled contact draped with shale. Siltstone beds increase in frequency and thickness from 4cms (1.6 inches) at the base of the lithofacies to over 20cms (8 inches) at the top. These siltstone laminae and beds are laterally continuous, but vary in thickness along the bed. This is due to the loaded base and occasional rippled top to the beds. Symmetrical ripples and wave ripple lamination become more common toward the top of the lithofacies.

In rare cases, delicate, comminuted shell fragments and whole shells are concentrated into thin sparse layers within the siltstone laminae. The base of these layers is sharp; the top of the bed grading up into background shale. The top of the siltstone and base of shale display biogenic activity. The silty layers are dark grey in colour, whereas the shale layers are black (although the colour may become beige to green toward the top). Some shell layers are up to 4cms (1.6 inches) thick (e.g. d-066-A/94-A-15 and d-005-C/94-A-16). Shell concentration is up to 30% of the sediment within an individual bed. The shell fragments are very thin and appear delicate, but are coarsely ribbed. The shells are aligned into crude parallel-laminations. They are calcareous in composition, and exhibit calcareous rods which project up above the surface of the shell. These internal structures are common to pseudopunctate or punctate brachiopods.

In some cases micro-faulting of the siltstone and shale laminae occur, some of this in the form of synsedimentary normal listric micro-growth faults (e.g. d-046-E/94-A-16; Plate 1). Laminae on the hanging wall, thicken and curve downward toward the fault plane.

Micro-faulting in the form of reverse faults also occurs (e.g. d-027-C/94-A-16 and d-043-E/94-A-16).

There are occasional tabular laths of anhydrite crystals developed within the shales (e.g. d-069-C/94-A-16 and d-012-E/94-A-16). They may deform the surrounding laminations. Disseminated pyrite nodules are common within both lithologies. Interstitial pyrite cement may be concentrated within the siltstone laminae. Calcite and dolomite cement occur mainly as intergranular pore filling cements within the lithofacies.

4. 3. 2. ENVIRONMENTAL INTERPRETATION.

Sharp based siltstone beds displaying parallel-laminated structures that pass up into hummocky-cross-stratification, in turn passing up into slightly asymmetrical rippled lamination, and finally up into interlaminated siltstones and shales that are burrowed, were deposited by storm-generated currents. Current velocities were relatively strong compared to background conditions. These currents waned with time. Physical hydrodynamic conditions responsible for the formation of this succession of sedimentary structures were complex, involving the combination of a high orbital velocity oscillatory and unidirectional components of flow.

Within Lithofacies C the basal parts of the siltstone laminae are parallel-laminated. These may have formed from high velocity orbital currents with negligible unidirectional velocity components (Duke, 1985, 1986; Duke, 1990; Arnott and Southard, 1990; Southard *et al.*, 1990; Duke *et al.*, 1991). As the former currents waned in strength (in relation to the unidirectional currents) with time, hummocky-cross-stratification was produced. The asymmetrical ripple lamination above the hummocky-cross-stratification was formed by the interaction of weaker oscillatory and relatively stronger unidirectional currents. They are termed genetically as combined-flow ripples. This sequence suggests that the siltstone beds were deposited under the influence of dominant strong oscillatory currents that waned with time. The unidirectional currents correspondingly became relatively more important. The oscillatory component resulted from the effects of storm waves impinging the sediment surface, whereas the unidirectional component resulted from geostrophic currents (Swift *et al.*, 1983). Eventually, the unidirectional current component also declined, sedimentation returning to suspension deposition of muds that were subsequently burrowed. These muds reflected background conditions. The low density of bioturbation and species types within this lithofacies is due to the restricted conditions experienced within the top layer of sediments, since the water column was still poorly oxygenated within this environmental zone.

The background sediments within Lithofacies C are represented by shale and siltstone laminae which are commonly parallel-laminated. These sedimentary structures were formed under lower flow regime conditions. Thick siltstone laminae and beds exhibiting hummocky-cross-stratification were formed by storm processes. These observations suggest that this lithofacies was deposited below the influence of mean fairweather wave base, but above the influence of mean storm wave base (see Figure 16). This bathymetric zone has been termed the offshore-transition zone by Elliott (1986). Toward the top of the lithofacies, however, oscillation ripple lamination within the background sediments become more common. The sedimentary structures displayed by this lithofacies are similar to those found within the present day transition facies (9.3 metres to 18.7 metres below mean sea level) from the high energy coastline transect of California (Howard and Reineck, 1981). Transects from the low energy coastline of Georgia, carried out by the same authors, indicate occurrences of the same environmental zone at depths of between 2 and 5 metres below mean sea level.

4.4.1. LITHOFACIES D. INTERBEDDED RIPPLED SANDSTONE, SILTSTONE AND SHALE.

This lithofacies passes down gradationally into Lithofacies C and gradationally up into Lithofacies E, or less commonly into lithofacies B or C. It may also be erosionally overlain by lithofacies E or H. Average thickness of Lithofacies D is 2 metres (6.4 feet), with maximum thickness of 9.8 metres (32 feet) and minimum thickness of 0.3 metres (1 foot). The dominant lithology is interbedded sandstone, siltstone and minor components of shale. The quantity, frequency, thickness and grain size of the sandstone component of the lithofacies increases uniformly upward approaching ratios of 80:20, sandstone:siltstone, within the upper regions. Sandstone beds thicken from an average of 1.5cms (0.6 inches) at the base of the lithofacies to greater than 10cms (4 inches) toward the top.

The sandstone is brown in colour, commonly dolomite cemented, and very-fine lower in grain size. The siltstone is beige to green in colour, coarse silt sized, and commonly dolomite cemented. Shale laminae are beige to green in colour and dolomite to calcite cemented. The shales contain *Planolites* trace fossils. Other traces of minor quantity are *Palaeophycus* and *Teichichnus*. The burrows are infilled with sand, sourced from the bed above. The diversity of trace fossil genera within the lithofacies is low. The quantity of burrowing increases upward, at times obliterating physical sedimentary structures (burrowing activity varying from 5% to over 90%) (Plate 3). In the latter situation, wisps

Plate 3. Intensely burrowed sandstone and shale in upper part of Lithofacies D. Well d-060-C/94-A-16, 3910 feet. (Scale in cms).

of shale within structureless sandstone are the only indication of heterogeneities in lithology. The burrows within this region of the lithofacies are oblique to horizontal in attitude, mud lined, and sand filled *Palaeophycus* traces. Synaeresis cracks developed within the calcareous cemented shale and silty shales are ubiquitous.

Common to this lithofacies are erosionally based, brown coloured, calcite to dolomite cemented, and very -fine lower to upper sand grain size sandstone beds. The basal parts of these sandstone beds may contain contorted and convoluted lamination (Plate 4). These pass upward from parallel-laminated structures into interlaminated sandstone (60%) and siltstone (40%) sedimentary structures, undulatory in geometry, with divergent laminae, and internal minor truncation surfaces (Plates 4, 5, 6). This structure is interpreted as hummocky-cross-stratification (Harms *et al.*, 1975, Hamblin and Walker, 1979; Walker, 1979). This passes up into ripple lamination, the upper surface of which is slightly asymmetrical in geometry (wavelength 4.5cms, amplitude 0.3cms). These pass gradationally or sharply up into burrowed green to beige shale. The top of the shale beds are truncated by the next sandstone bed. The sandstone bases are erosional or loaded onto the shales beneath, the latter commonly flamed into the former. Thickness of the sandstone beds varies laterally across the core due to loading and ripple bedforms. Unassociated with sharp based sandstone beds are very-fine lower sand sized sandstone beds demonstrating symmetrical ripples on the upper surface (wavelength 7.0cms, amplitude 0.5cms), and are draped with shale. Internally, sedimentary structures within these sandstone beds are rare (Plate 7). These sandstone beds become more common toward the top of the lithofacies. The sand sized grains are sub-angular, and moderately well-sorted.

Normal and reverse micro-faulting may occur forming small displacements in the order of 1-2cms. Some sandstone beds within the lithofacies are dominated with biogenic activity that has completely destroyed the physical sedimentary structures. The burrows, in places, are ovoid in cross-section (2mm x 4mm) and 1.5cms long, forming cylindrical shapes. They are infilled with calcite cemented very-fine lower sandstone. The burrows vary in attitude from horizontal through oblique to sub-vertical. They are unbranched. They are best preserved within well b-042-H/94-A-15.

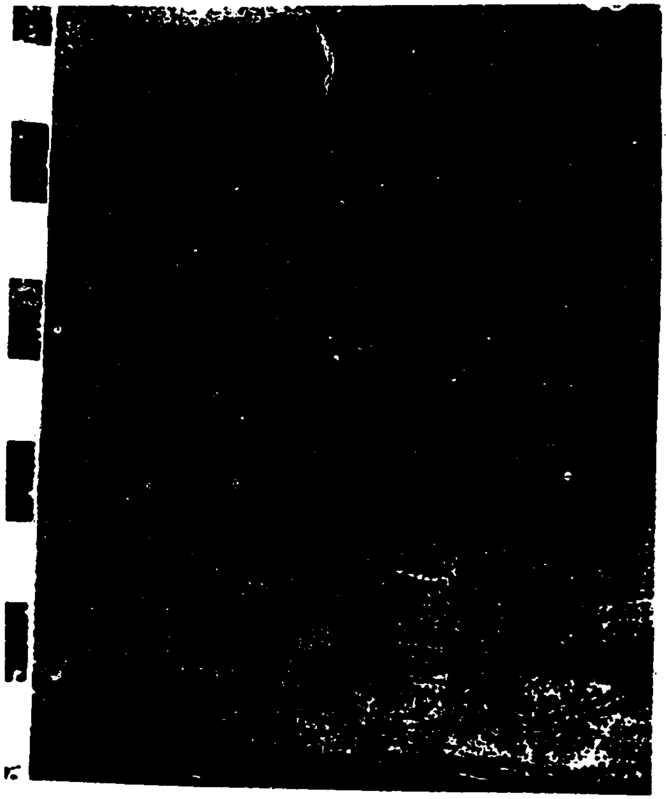

Plate 4. Sharp loaded based sandstone storm bed, with basal contorted lamination passing up into hummocky-cross-stratification, characterized by divergent laminae. Note the shale flaming into the basal sandstone. Close to top of Lithofacies D. Well d-097-H/94-A-15, 3838 feet. (Scale in cms).

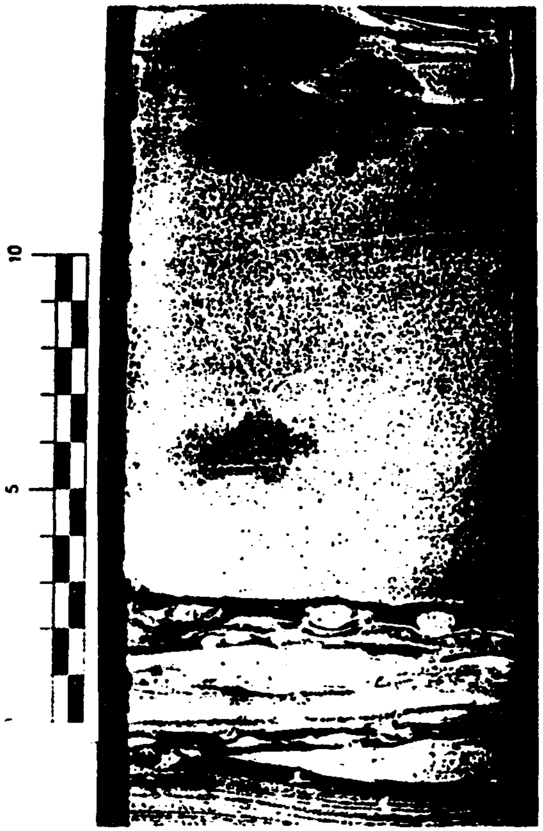

Plate 5. Sharp based storm-generated sandstone bed, characterized by hummocky-cross-stratification, passing up into starved loaded rippled lenticular- and wavy-bedded sandstone and shale. Sandstone sits abruptly on wavy-bedded rippled sandstone and *Planolites* burrowed shale, representative of background deposition. Close to the top of Lithofacies D. Well d-068-C/94-A-16, 3917 feet. (Scale in cms).

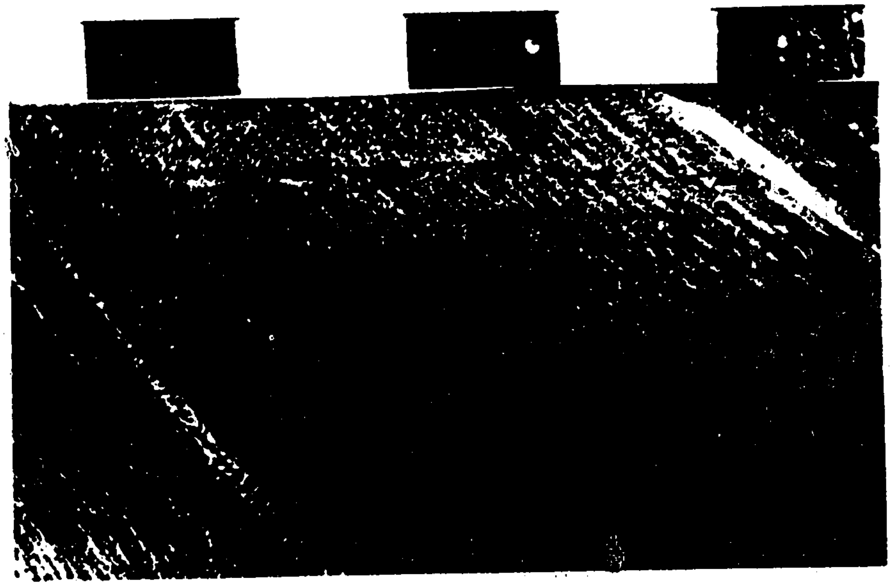

Plate 6. Close up illustrating convergent and divergent laminae characteristic of hummocky-cross-stratification. Well d-043-E/94-A-16, 3818.5 feet. (Scale in cms).

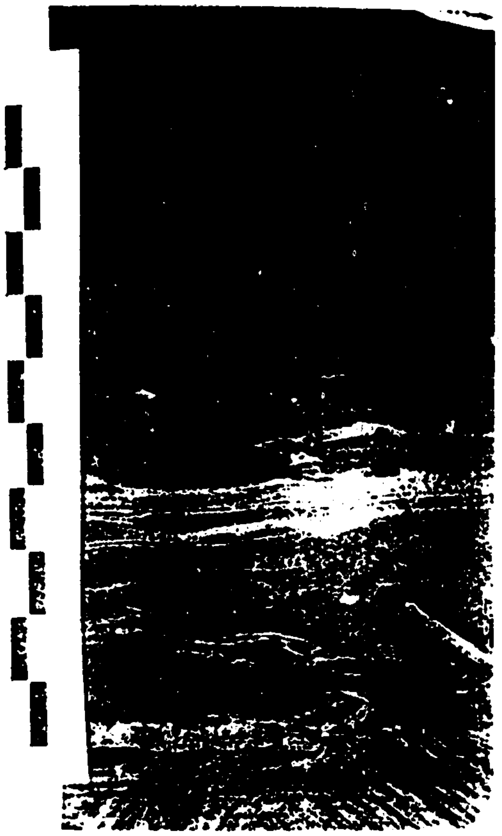

Plate 7. Burrowed flaser-bedded sandstone and shale. Asymmetrical ripple forms recognizable at top of sandstone bedding surfaces. Well d-013-E/94-A-16, 3855.3 feet. (Scale in cms).

The sandstones within this lithofacies are cemented with various proportions of calcite and dolomite. They occur as intergranular, pore rimming and poikilotopic cements. This reduces permeability and porosity to very low values. There are occasional anhydrite and pyrite nodules scattered throughout the lithofacies, the former becoming more common toward the top.

4.4.2. ENVIRONMENTAL INTERPRETATION.

The base of the sandstone beds is erosional, suggesting the rapid incursion of a high energy-level event. The parallel-laminated structures within the basal parts of the sandstone beds could have formed from dominantly high orbital velocity currents, producing strong oscillatory currents on the sea floor associated with storm-generated processes (Southard *et al.*, 1990; Arnott and Southard, 1990). The appearance of hummocky-cross-stratification above the parallel-laminations resulted from a slight weakening of oscillatory current velocities. As with the storm-generated beds of Lithofacies C, the storm-generated oscillatory currents reduced in magnitude as the storm migrated away from the area, consequently reducing wind-forcing effects. Thus, unidirectional geostrophic currents of low velocity became more dominant producing asymmetrical ripple lamination (Swift *et al.*, 1983). As energy conditions waned, mud fall-out from suspension, and wave ripple laminated sandstones reworked by fairweather oscillatory currents, were deposited. The thickness of these storm-generated deposits, the geometry of the ripples, and the grain size of the lithology indicates that Lithofacies D experienced more intense storm events than Lithofacies C, suggesting closer proximity to a palaeostrandline.

There are a number of models present in current literature to explain the emplacement of the erosional based sandstone beds. The mechanism, however, is storm-associated. It has been documented, by various researchers, that more proximally emplaced storm beds are formed by a combination of oscillatory and unidirectional currents (Walker, 1979; Morton, 1982; Swift *et al.*, 1983; Duke *et al.*, 1991).

These storm-generated beds occur frequently within this lithofacies with minimal beds of shale, siltstone or wave-ripple laminated sandstone preserved. Thus, background hydrodynamic processes were dominated by weak oscillatory currents produced by fairweather waves. This zone was therefore deposited above the influence of mean fairweather wave base. This bathymetric zone is defined as the lower shoreface (Elliott, 1986) (Figure 16).

An increase in the quantity of bioturbation within this lithofacies indicates a direct response to a more oxygenated, better circulated water column. Biogenic activity is found most commonly within the background sediments and at the top of storm-generated beds.

4.5.1. LITHOFACIES E. THICK INTERBEDDED SANDSTONE, SILTSTONE AND SHALE.

Lithofacies E grades down into Lithofacies D. It may pass gradationally up into Lithofacies F or, more commonly, is erosionally truncated by lithofacies G, H, I or J. Average thickness of the lithofacies is 2.4 metres (8 feet), with maximum thickness of 5.2 metres (17 feet) and minimum thickness of 0.3 metres (1 foot). Sandstone is the dominant lithology, ranging in grain size from lower to upper very-fine sand. The sandstone beds are calcareous cemented (commonly dolomitic) and are brown in colour. Dolomite cemented green to beige shale and siltstone are minor in quantity. The quantity of sandstone to shale increases up through the lithofacies. This trend is also reflected by the slight increase in grain size and increased bedding thickness characterised by the sandstones. The ratio of sandstone to shale within this lithofacies is 80:20 toward the top.

Imbricated lithoclasts of beige to green, dolomite cemented shale are common, and concentrated in layers. They range in size from 4cms x 1.5 cms to 7cms x 5cms. The lithoclasts are commonly broken up *in situ* and are angular to sub-rounded in shape, reflecting transportation over short distances. The lithoclasts may be tabular or more spherical in shape dominating particular laminae within the lithofacies. Matrix material is very-fine lower to very-fine upper sand sized, and is calcareous cemented. Some shale lithoclasts are slightly bent, indicating that they were semi-cohesive upon rip-up. Internally, some lithoclasts exhibit parallel-laminated structures with synaeresis cracks. Biomolds may also be concentrated within these lithoclastic layers. Above these lithoclasts are parallel-laminated, or upwardly divergent laminae representative of hummocky-cross-stratification within the sandstone. Load and flame structures characterise the basal sandstone-upper shale contact. These sandstone beds commonly truncate the top of shale beds (Plate 8). Asymmetrical rippled top surfaces of sandstone beds are draped with shale.

There are occasional vertical or oblique burrows, 1cm in diameter, outlined by a mud coating. This trace is *Skolithos* and occurs in association with layers of brecciated subrounded shale lithoclasts, with sharp, erosional bases to the beds. Sand infilled horizontal *Planolites* trace fossils are common within the shale laminae toward the top of these successions. There are occasional isolated laminae (2-3cms thick) of non-calcareous, uncemented olive-green shale with synaeresis cracks. In some cases, there are structureless vertical escape traces that penetrate parallel-laminated, sharp based, sandstone beds, curving the laminae downward, adjacent to the burrows. The burrows within this lithofacies are dominantly horizontal and are larger in size than those of Lithofacies D. Vertical traces, however, become more common.

In places, the lithofacies is composed of a series of wavy-bedded sandstone and shale beds; the former truncating the tops of the latter beds (Plates 9 and 10). The base of the sandstones are parallel-laminated, passing into ripple lamination. The top surface of the sandstone may be sharp and wavy, reflecting the geometry of ripples. These ripples are symmetrical, particularly toward the top of the lithofacies with typical dimensions of 3cms wavelength and 0.4cms amplitude. This passes up into shale that is burrowed by horizontal sand filled *Planolites, Teichichnus and Cylindrichnus* traces (MacEachern, 1992, pers. comm.). Synaeresis cracks are also common within these shale beds. Basal parts of the lithofacies are concentrated with asymmetrical ripple lamination. Small-scale trough-cross bedded structures become common toward the top of the lithofacies. These sandstones are sharp based and pass up into ripple cross-lamination and into background interlaminated siltstones and shales. Sand grains within these beds are sub-rounded to sub-angular and well-sorted.

Within this lithofacies are beds (20cms to 30cms thick) of coquina and bioclastic sandstone, usually structureless or parallel-laminated. They have sharp bases with high concentrations of beige to green coloured dolomite cemented sub-angular shale lithoclasts. The top of these beds grade back into parallel-laminated and asymmetrical ripple laminated sandstone and interlaminated shale. Lithoclasts may be orientated into parallel horizontal laminations, with a sandstone matrix. Some beds are normally graded.

Sandstone within this lithofacies is cemented by calcite or more commonly dolomite. The porosity is primary intergranular. Light hydrocarbons have stained the sandstone a dark

Plate 8. Sharp based, massive sandstone sits abruptly on wavy-bedded rippled sandstone and burrowed shale.
Taken from middle of Lithofacies E.
Well d-011-E/94-A-16, 3819.2 feet.
(Scale in cms).

Plate 9. Wavy-bedded sandstone and shale. Sharp based, rippled sandstone and burrowed shale. Shale contains abundant sandstone filled synaeresis cracks, and is burrowed by *Cylindrichnus* (Cy.), *Teichichnus* (Te.) and *Planolites* (*Pl.*) traces.Taken from lower to middle of Lithofacies E. Well d-010-F/94-A-16, 3856.2 feet.
(Scale in cms).

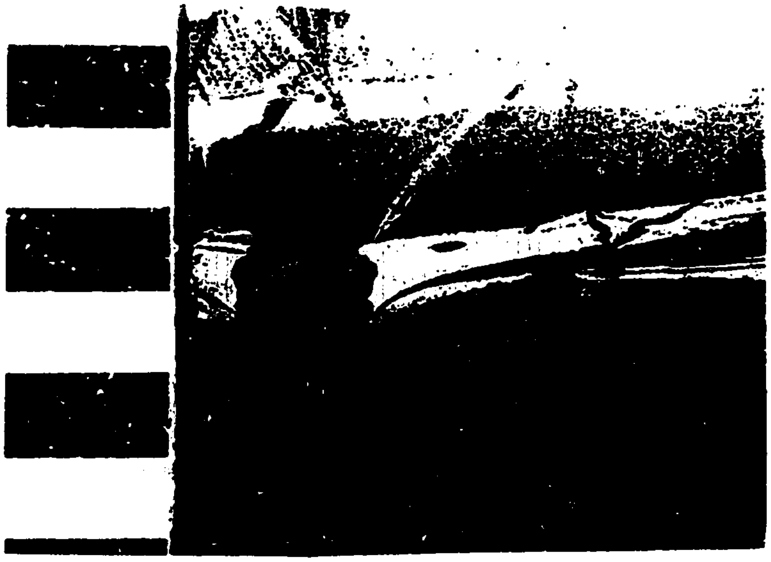

Plate 10. Wavy-bedded sandstone and shale. Sandstone is rippled and ripple laminated, and sharp based. Shale is burrowed by *Planolites* (Pl) and *Bergaueria* (?) (Be) traces (MacEachern, 1992, pers. comm.), with abundant synaeresis cracks infilled with sandstone, and truncated above by sandstone. Taken from middle of Lithofacies E. Well d-071-H/94-A-16, 3814 feet. (Scale in cms).

brown colour. Pyrite crystals occur throughout the lithofacies. Heavy hydrocarbons are present lining the pore walls producing a dark grey or black appearance to the sandstone. These bitumens plug up porosity. Location of hydrocarbons is inversely proportional to the quantity of cement. The interfingered shale layers produce common vertical permeability barriers.

4.5.2. ENVIRONMENTAL INTERPRETATION.

The 20 to 30 centimetre thick, sharp based beds of parallel-laminated coquina and bioclastic sandstone within the upper part of lithofacies E are similar in sedimentologic description to those described by Kumar and Sanders (1976) and Kreisa (1981). These beds were formed by proximal storm-generated high orbital velocity oscillatory currents. The basal lithoclastic coarse grained material is interpreted as a lag which was formed during the maximum intensity of the storm event. During this event, the coarsest material was ripped-up from the underlying stratum, and was moved on the sea bottom as traction load by high orbital velocity oscillatory currents initiated by shoaling storm-waves, the finer material being kept in suspension. The shell material was transported at the strongest velocity and shear stress. As storm currents decreased slightly in strength, the sediment supply became sandier forming parallel-laminated structures within sandstones, which overly the coquina. These sand sized grains also percolated into the coquina forming a sandstone matrix.

MacDonald (1972) has documented that below the lower shoreface bathymetric zone there is no evidence to suggest faunal mixing of skeletal remains occurs. This indicates that the most intense storm-generated oscillatory currents are located above this zone. Within the upper and lower shoreface, he documented that abundant transport of faunal skeletons occurs.

The degree of bioturbation is minimal within Lithofacies E. The burrows are large in size and robust due to the high energy levels experienced within this environment. The traces are mainly vertical, with some escape traces occurring within the sandstone beds. The traces fossil assemblage (*Teichichnus*, *Cylindrichnus* and *Planolites*) is characteristic of stressed environments (MacEachern, 1992, pers. comm.). This may be a reflection of the oxygen deficient upwelling deep, cold waters onto the continental shelf. Plates 9 and 10 show wavy-bedded sandstones and shales, representing background conditions of sedimentation. The shales contain abundant synaeresis cracks. These may indicate changing salinity conditions, possibly associated with the influx of more saline water from backbarrier areas into the immediate area via tidal inlet conduits. Background processes within this environmental zone are dominated by oscillatory currents produced by fairweather waves forming symmetrical wave ripples and ripple lamination within sandstone beds. Thus, process sedimentologic indicators suggest that this lithofacies was again deposited above fairweather wave base, in an environment of higher energy conditions than experienced in Lithofacies D, but below the effects of upper shoreface zone. This bathymetric zone is termed the lower shoreface to middle shoreface (Figure 16) (Elliott, 1986).

4.6.1. LITHOFACIES F. CROSS-BEDDED AND PARALLEL-LAMINATED SANDSTONE.

This lithofacies gradationally passes up from lithofacies E (lower shoreface) below. It may be sharply overlain by lithofacies C (offshore-transition) or D (lower shoreface). Alternatively, it commonly displays an erosional upper contact overlain by Lithofacies I or J of the Charlie Lake Formation. Average thickness of Lithofacies F is 2.2 metres (7.2 feet), with maximum thickness of 3.3 metres (10.8 feet) and minimum thickness of 1.5 metres (5 feet). Lithofacies F is composed dominantly of very-fine upper to fine upper sandstone. The sandstone is brown in colour, and may or may not be calcareous cemented to varying degrees. The grains are well-sorted to very well-sorted, and sub-rounded to well-rounded. Intergranular porosity is ubiquitous within this lithofacies, although oil staining is rare. Due to the well-sorted nature of the deposits, sedimentary structures are difficult to recognize. However, minor amounts of trough cross-bedding, ripple cross-lamination and parallel-laminations containing chert, phosphate and occasional biomold lithoclasts occur. In places, the upper part of the lithofacies is dominated by parallel-laminated convex-up biomolds in a very-fine upper to fine lower sandstone, with a sharp irregular base. These beds are repeated at closer intervals toward the top of the lithofacies. There are a few lithoclasts of beige coloured dolomite cemented shale concentrated in layers throughout the lithofacies. This lithofacies is mineralogically sub-mature, and has been described petrographically classified as sublitharenites.

Biogenic activity is rare, but can be abundant locally (up to 90%). *Skolithos* traces occur in some regions (a-083-D/94-A-16). The sandstone is very well-sorted, and consequently, in the upper regions of the lithofacies the sandstones may appear structureless (Plate 11).

4.6.2. ENVIRONMENTAL INTERPRETATION.

Sedimentological description implies that the sediments were deposited within a high energy zone affected by fairweather waves. Symmetrical ripple laminations are rare; trough cross-bedding being the most abundant sedimentary structure. This structure suggests that palaeocurrents may have been at least 65 to 70 cms/sec (Harms *et al.*, 1982) and unidirectional. The trough cross-bedding was formed by the migration of three-dimensional large ripples across the sea floor. The trough cross-bedding represents a change in the symmetrical nature of the oscillatory wave processes to an asymmetrical form, representative of the higher energy shoaling wave zone. The waves rework the sea bed to a greater degree. The amplitude and period of the waves change, so that wavelength decreases and wave height and steepness increase. As the waves progressively steepen, fine sands may be temporarily suspended, while coarser material is concentrated on the sea floor. These depositional processes and consequent sedimentary structures are characteristic of the upper shoreface bathymetric zone (Elliott, 1986) (Figure 16). Howard and Reineck (1981) recorded that modern upper and lower shoreface deposits occur between +3metres to -9metres of sea level, from the modern high energy coast of California. Similar studies conducted by the same authors from low energy coastlines of Georgia, indicate that this environmental zone (including the lower shoreface) extends down to 2 metres below mean sea level. Other detailed studies of the upper shoreface have been conducted by Clifton *et al.* (1971) and Clifton (1976).

4.7.1. LITHOFACIES G. BIODOLOMICRITE (COQUINA).

Lithofacies G has a sharp, irregular, erosional base, overlying lithofacies C (offshore-transition), D (lower shoreface), E (lower shoreface) or F (upper shoreface). In some instances the upper contact is gradational with Lithofacies H, but in most cases it is abrupt and erosional with Lithofacies I (e.g. b-045-E/94-A-16, d-046-E/94-A-16 and b-049-E/94-A-16). Thicknesses of this lithofacies vary greatly from 1.6 metres (5.1 feet) to 6.1 metres (20 feet), with average thickness of 3.3 metres (10.8 feet). The basal 20-50cms of this lithofacies is dominated by angular to sub-rounded beige to green coloured dolomite cemented shale lithoclasts (e.g. b-045-E/94-A-16) commonly 5cms (2 inches) to

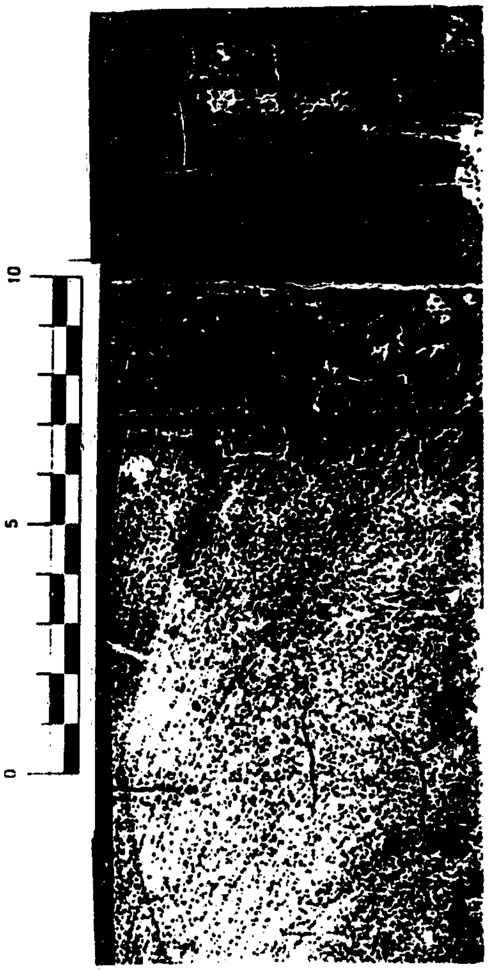

Plate 11. Structureless very fine sandstone of Lithofacies F, passing abruptly up into Lithofacies C interlaminated siltstones and shales. Well a-083-D/94-A-16, 3874 feet. (Scale in cms).

greater than 10cms (4 inches) in diameter. Some lithoclasts are tabular in shape with the longest dimension greater than the width of the core diameter (Plates 12 and 13).

Lithofacies G is characterised by up to 90% biomolds which reflect the original shell tests that have since been leached. The original bioclasts were most abundant at the base of the lithofacies, reducing in quantity and size upward, although interbedded layers of more dense and less dense bioclastic material do occur throughout the lithofacies. A sandstone matrix becomes dominant toward the top. The matrix material is very-fine lower to fine lower in grain size, brown in colour, and dolomite cemented. The biomolds are commonly very poorly-sorted, and disorientated. There are regions, however, in which a crude parallel alignment of the biomolds occurs to produce parallel-lamination. The bioclasts were orientated convex up or were imbricated (e.g. d-099-C/94-A-16).

The dominant bioclasts were originally bivalves. Bioclasts have been identified in outcrop by Pelletier (1965) and Gibson (1975) as spiriferids, terabratulids and gryphaeids. Subordinate biomolds include helical and turreted gastropods (e.g. b-074-H/94-A-15, d-060-C/94-A-16, d-99-C/94-A-16, d-100-C/94-A-16, d-061-D/94-A-16 and d-001-E/94-A-16), ammonites (d-097-H/94-A-15), possible solitary coral fragments (d-070-C/94-A-16), crinoid fragments (d-056-E/94-A-16), micritised bryozoa (d-099-C/94-A-16), and Lingulid fragments or whole disarticulated tests. Anhydrite nodules, up to 4cms in diameter, are fabric non-specific, replacing any deposits (see Chapter 6 for more detail). Throughout the entire lithofacies are scattered black, resistant, well rounded, up to 1cm in diameter, chert lithoclasts, in addition to phosphate, weathered chert, and dolomite cemented, subangular, shale and sandstone lithoclasts.

Planar and trough cross-bedding, the foresets of which dip from 5° to 23°, are common within the coquina (Plates 14 and 15). Thin olive-green shale laminae occur rarely between the foreset laminae. Biomold size varies from lower very-fine to pebble size. The biomolds may be comminuted to varying degrees, or whole and unabraded (although they are always disarticulated). Cross-bedded foresets occasionally fines upward, however, in many cases they are poorly-sorted. In some cores the biomolds display no apparent orientation or at the very best display oversteepened contorted laminae. This may be associated with soft sediment deformation produced by the dewatering (or evacuation) of

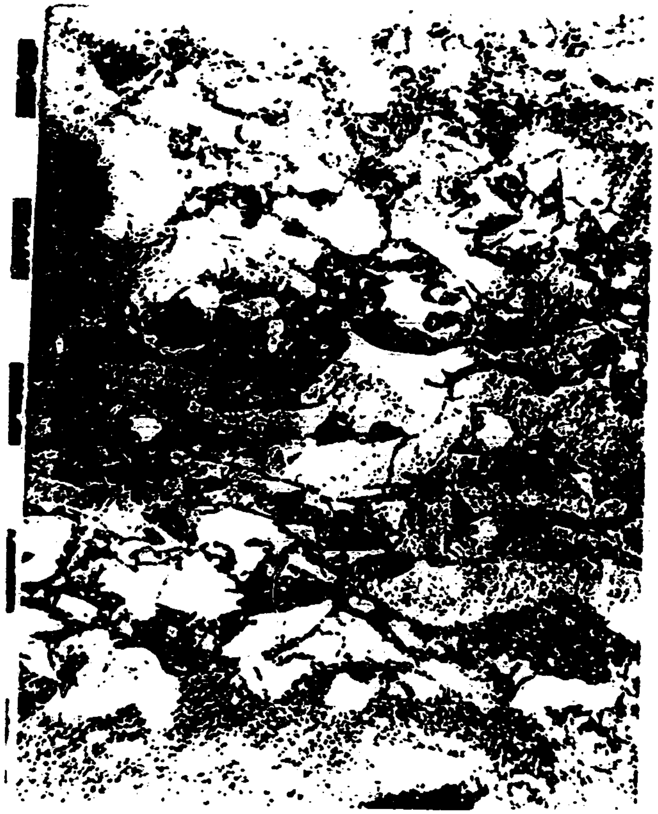

Plate 12. Sub-rounded and sub-angular shale intraclasts form a basal lag to Lithofacies G. Well d-060-C/94-A-16, 3889.1ft. (Scale in cms).

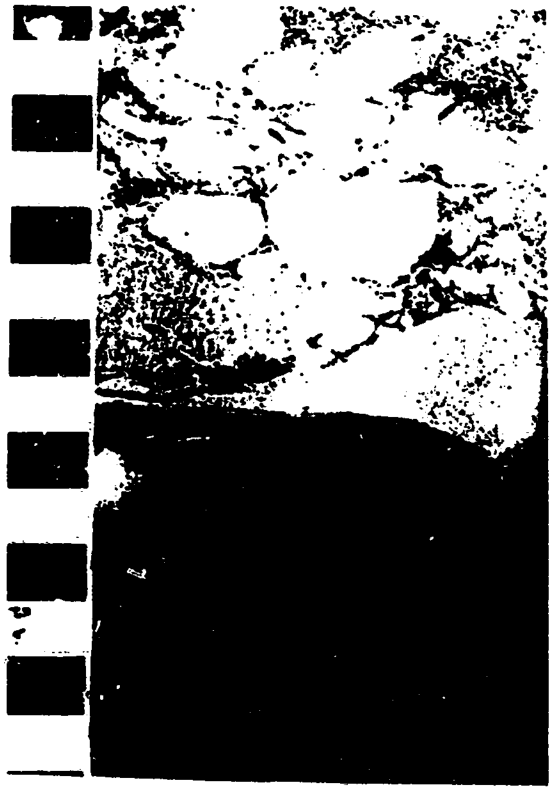

Plate 13. Basal shale intraclasts of tidal inlet deposits of Lithofacies G eroding down into Lithofacies D. Well d-033-H/94-A-15, 3903 ft. (Scale in cms).

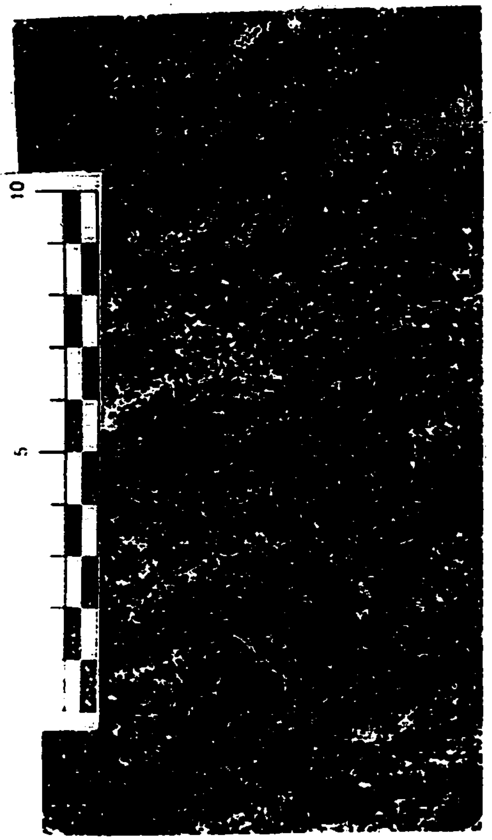

Plate 14. Cross-bedded coquina of Lithofacies G. Dolomitic cement highlights foreset laminae. Where the cement is poorly developed, biomoldic porosity is very good, the rock being stained black with bitumen. Well d-034-E/94-A-16, 3803 ft. (Scale in cms).

Plate 15. Cross-bedded and imbricated structures to the biomolds of Lithofacies G. Well b-067-E/94-A-16, 3826 feet.

(Scale in cms).

pore waters attributed to rapid rates of sedimentation. The base of the lithofacies is commonly characterized by parallel-laminated sedimentary structures.

4.7.2. ENVIRONMENTAL INTERPRETATION.

The presence of planar and trough cross-bedded structures within the biodolomicrite ('coquina') indicates that the sediments originally migrated as two- and three-dimensional large ripples, respectively (Harms *et al.*, 1982). In most cases, basal parts of the lithofacies are erosional and marked by intraclasts of beige dolomite cemented shale, probably sourced from back-barrier lagoonal areas, as well as from scouring into the underlying lower shoreface deposits.

These deposits represent the active portion of tidal inlet channels. Tidal inlet channels dissect barrier islands and link back-barrier regions to the open marine environment. The deposits of Lithofacies G are very similar to those described from modern tidal inlet channels. Modern tidal inlet channels in most instances, exhibit an erosional base with mud intraclasts and shelly lags (Van Straaten, 1965; Klein, 1963; Johnson and Friedman, 1969; Moslow and Tye, 1985). The basal channel lag deposits within Lithofacies G are between 20 and 50 centimetres (8 and 20inches) thick. This is comparable to the thickness of basal lag deposits found within recent tidal-inlet channels; at least 10cms (4 inches) (Kumar and Sanders, 1974); 30cms to 1 metre (12 to 40 inches) (Susman and Heron, 1979); 30cms to 60cms (12 to 24 inches) (Moslow and Heron, 1978).

The shell material comprising the inlet fill coquina deposits of Lithofacies G could have been derived from a back-barrier lagoonal source. As the inlet grew in size and subsequently extended its main channel into the back-barrier lagoon, an increased proportion of shell material was reworked and incorporated into the inlet channel. For example, within well d-099-C/94-A-16 (Appendix 1), high concentrations of gastropod biomolds occur in beds. It is possible that these organisms originally habited back-barrier lagoonal regions as concentrated mounds that were eventually reworked by tidal currents. Some of the biomolds, namely the ammonites, however, were derived from the open marine and subsequently washed shoreward during major storm events. The latter mechanism has been documented by Kumar and Sanders (1976).

The shell fragments are composed of comminuted and whole material. This suggests that a source for the material must have been local and continuously supplying the area. The larger biomolds are usually whole. In such a high energy environment this material would have been broken up by attrition and abrasion. The fact that some shell material appears generally unabraded would suggest that they had not been exposed to high energy events for long periods of time. The trough cross-bedding, granule grain size and parallel shell orientation in places, are attributed to high current velocities.

Taphonomical studies conducted by Henderson and Frey (1986) from within a tidal inlet channel at Sapelo Island, Georgia, have recognized admixture of faunal types, and shell size is sorted. Bivalves were commonly disarticulated. This shell material was transported seaward and landward of the tidal-inlet. They identified a greater ratio of articulate bivalves at the seaward side of the inlet, the ratio of gastropods to bivalves increased toward the landward side of the inlet; and the quantity of skeletal material increasing toward the mouth of the inlet in response to a decline in velocity of ebb-directed tidal currents. This occurred within a mesotidal ebb-dominated system. Similar studies have been conducted by Moslow and Heron (1978) and Moslow and Heron (1989) from the microtidal coastline of Core Banks, North Carolina. They state that shell fragments were sourced from backbarrier and nearshore environments. Studies by Dorjes *et al.* (1986) state that a majority of the shell material of Sapelo and Ossabaw Islands was derived from local beaches, beach related features, and the adjacent nearshore shelf.

Planar cross-bedded coquinas within this lithofacies indicate deposition from grossly asymmetrical tidal currents. Cross-bedded sedimentary structures were formed by the migration of sandwaves within the tidal inlet channel. The presence of shale laminae suggest that palaeocurrent strengths varied significantly from those enabling entrainment of shelly material, decreasing to virtual slack water periods in which mud fall-out by suspension occurred. Similar cross-bedded sedimentary structures have been observed and documented by Kumar and Sanders (1974) from the wave-dominated tidal inlet at Fire Island, New York State, and by Reddering (1983) from microtidal Keurbooms tidal inlet, South Africa. Hydrodynamic studies of the behaviour of tidal currents within modern inlets have been conducted by various researchers (Oertel, 1973; Reddering, 1983; Fitzgerald *et al.*, 1984; Hennessy and Zarillo, 1987; Sha, 1989; Sha, 1990; among others). They have identified a central deeper channel dominated by ebb-directed tidal currents and laterally adjacent shallower channels dominated by weaker flood-directed tidal currents (known as marginal flood channels). Hence, the opposing tidal currents are separated spatially into discrete channels. This indicates that unidirectional cross-bedding can be expected from a tidal inlet deposit, even though tidal processes are dominant. Since the Middle Triassic cores are not orientated, it is impossible to determine the direction of palaeocurrent flow from the cross-bedded, and hence whether ebb- or flood-directed tidal currents were responsible.

4.8.1. LITHOFACIES H. CROSS-BEDDED SUBLITHARENITE.

4.8.1.1. Sub-lithofacies H1.

This is the thickest lithofacies within the study area, and is the most productive reservoir lithofacies within the field. Average thickness of the lithofacies is 4.1 metres (13.4 feet), with maximum thickness of 11.0 metres (36.0 feet) and minimum thickness of 1.1 metres (3.6 feet). The lithofacies is largely restricted to the eastern part of the study area, although there are isolated "pockets" of this lithology located within the western part of the study area. Lithofacies H lies sharply or erosionally above lithofacies B (offshore), C (offshore-transition), D (lower shoreface) and E (lower shoreface). The base of the lithofacies is sharp and irregular, with up to 2cms of relief, occasionally lined with chert, weathered chert, phosphate, dolomitic shale and sandstone lithoclasts, all of which are granule size (Plate 16). Shell material is absent within this lithofacies except for rare calcium-phosphate Lingulid shell fragments (<3%). In some cases, the base of the lithofacies is load casted.

This sub-lithofacies is composed of very-fine lower to medium lower sand sized grains. These particles are sub-rounded to sub-angular and moderately well-sorted, dominantly composed of quartz. The sandstone is light brown to light grey, depending on whether it is hydrocarbon or water saturated, respectively.

Common sedimentary structures are small-scale low-angle to high-angle wedge- to tabular-shaped trough and planar cross-bedding (Plate 17). Cross-bedded sets vary from 2cms to 16cms (0.8 to 6.4 inches) in thickness, individual foresets being 1 to 2cms (0.4 to 0.8 inches) thick. Granule sized lithoclasts are concentrated at the base of cross-bedded sets. Foreset dips range from 5° to 22°. The tops, and in rarer cases, the bases of cross-sets commonly display ripple cross-lamination. Normal and inverse grading occur

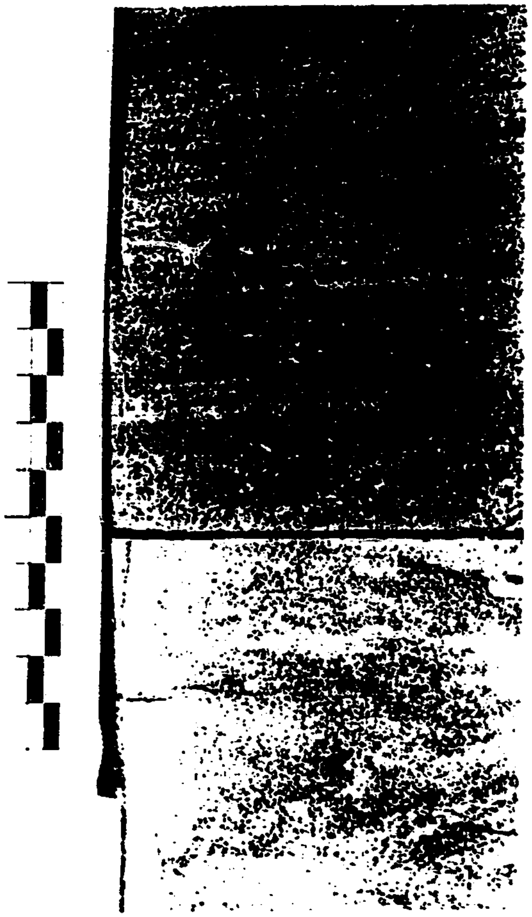

Plate 16. Concentration of lithoclasts at base of Lithofacies H, inlet deposits, eroding into Lithofacies D, Lower Shoreface deposits. The sublitharenite displays low-angle trough cross-bedding. Well a-083-D/94-A-16, 3870 ft.
(Scale in cms).

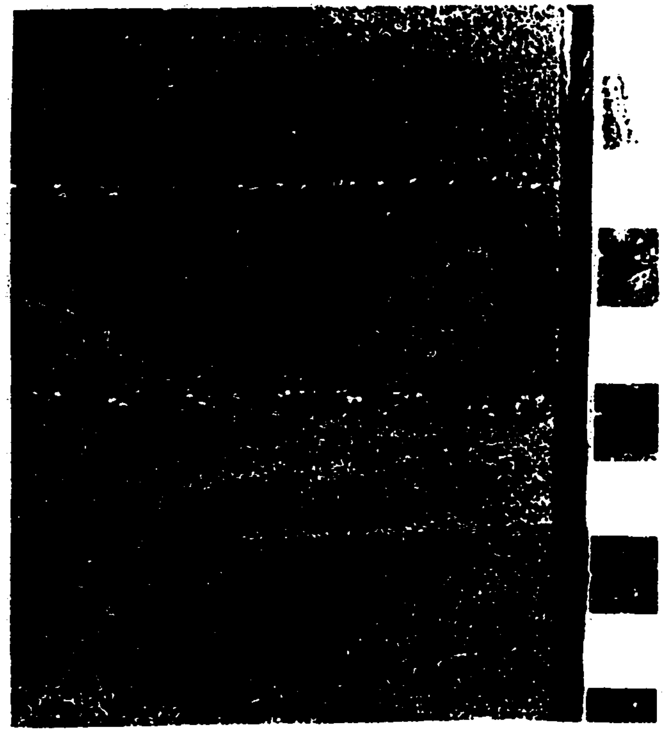

Plate 17. White chert and tripolitic granule sized lithoclasts line base of current ripple stratification and small-scale, low- to moderate-angle trough cross-beds. Close to base of Lithofacies H. Well b-038-E/94-A-16, 3860 ft.
(Scale in cms).

within individual foresets. Silty laminae may occur toward the boundaries of foreset laminae (Plate 18). Trough cross-bedding may occupy the base of the lithofacies and passes up into parallel-lamination toward the top. Rarely, depositional-stoss symmetrical climbing-ripple cross-lamination occurs above the parallel-lamination, at the top of the lithofacies. Biogenic activity and shale beds are absent within the lithofacies.

This lithofacies contains between 5 and 25% rounded granule sized lithic fragments. These include black and white unweathered to partially weathered chert grains, white powdered weathered chert grains, light brown dolomicrite, and phosphate "peloids" and ooids, the latter containing single quartz grains or phosphatic shell material as the nucleus. Petrographically determined accessory grains (2%) of rounded glauconite and sub-rounded amphibole grains occur within the sublitharenites (see Chapter 6 for more detail). Lithoclasts are common at the base of trough and planar cross-bedding structures. This basal lag truncates the foresets of the bedform below. A similar lag occurs at the base of the lithofacies. Disseminated interstitial pyrite cement is fairly common throughout the lithofacies.

The sandstone is poorly- to moderately-cemented with calcite or more commonly dolomite. Anhydrite crystals occur as poikilitic nodules that increase in size and quantity upward. These crystals may alternatively outline and accentuate cross-bedded structures (e.g. d-016-C/94-A-16). In some instances the primary intergranular porosity is lined and infilled with hydrocarbons.

4.8.1.2. Sub-lithofacies H2.

The sedimentologic description of this sub-lithofacies is similar to that of Sub-lithofacies H1, except that this sub-lithofacies is thinner and occurs ontop of Lithofacies G. Sedimentary structures vary from cross-bedding toward the base, passing up into parallel-lamination and into symmetrical ripple lamination toward the top.

4.8.2.1. ENVIRONMENTAL INTERPRETATION: SUB-LITHOFACIES H1.

The basal contact of sub-lithofacies H1 is always sharp and abrupt, with relief up to 2cms. Lithoclasts are concentrated at the base of the lithofacies in some wells. The lithoclasts are well-rounded and appear to originate from a combination of local and more distant sources. The dolomicritic lithoclasts may have been sourced from Halfway back-barrier

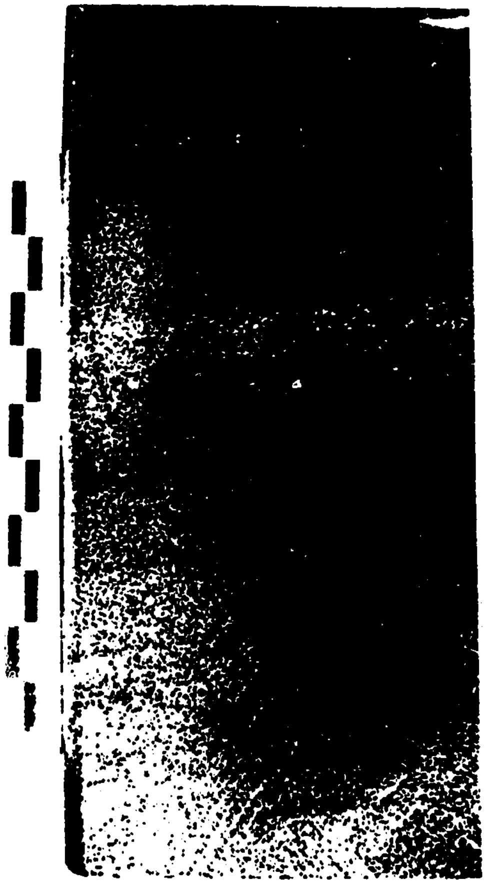

Plate 18. Normal and inverse grading within laminae of Sub-lithofacies H1. Darker laminae are silt sized deposits. Above chert lag, foreset laminae coarsen-upward. Well a-083-D/94-A-16, 3864 ft. (Scale in cms).

lagoonal regions, and were originally micrite lithoclasts. Chert and phosphate were either derived from deeper water more distal sources within the Middle Triassic marine basin, or from the exposed Permian formations, to the northeast of the study area (Gibson and Barclay, 1989). The well-rounded appearance of the chert granules implies that they have been reworked for long periods of time. Where the sublitharenites lie abruptly on dark grey shale, the lithological contact displays well formed examples of load and flame structures, loading casts extending up to 2 cms into the underlying shale. This signifies a relatively rapid rate of deposition of the sublitharenites onto a semiconsolidated, hydroplastic muddy substratum. The basal erosional contact displayed by this lithofacies, rests on offshore (Lithofacies B), offshore-transition (Lithofacies C), and lower shoreface (Lithofacies D and E) deposits. This degree of truncation displayed by Sub-lithofacies H1 can only be explained by scour and incision associated with channelisation.

Planar and trough cross-bedded structures are developed in fine lower to medium lower grained sublitharenites. These structures were produced by the unidirectional migration of two- and three-dimensional large ripples across the stratum. The normal and inverse grading within foresets bounded by siltstone laminae result from variations in the current strength on a regular periodic basis. These periodic variations in current strength may have been formed by tidal processes, which were grossly asymmetrical since cross-bedded foresets are unidirectionally orientated.

The tops, and rarer, the bases of foresets may display current ripple cross-lamination. The former may represent the waning in flow of tidal currents such that large ripples become stationary, the tops of which are reworked into small ripple forms that migrate down current. Where the small ripples occur at the base of foresets, these may have formed by reverse eddy cells forming due to separation of flow over the crest and in a leeward direction of the large ripple (Joplin, 1965b). This produces reversed ripples at the base of foresets. These are rarely preserved. The tops of some foresets pass up into parallel-laminated structures, interpreted as forming in upper flow regime conditions. This would suggest an increase in palaeocurrent velocity.

4.8.2.2. ENVIRONMENTAL INTERPRETATION: SUB-LITHOFACIES H2.

Although sedimentologic description is identical, this sub-lithfacies has been intepeted as a spit platform when located above Lithofacies G. Parallel-lamination occurs above cross-bedded structures within the lithofacies. The climbing wave rippled structures, occur above the plane beds. The absence of shale and the transition of sedimentary structures upward, indicate that current velocities gradually waned with time. However, conditions leading to the deposition of mud did not occur. These features are indicative of wave-dominated tidal inlet sedimentary fills. As the inlet channels mature with time, they may become less hydrologically efficient; in other words, sediment supply into the inlet is greater than the amount leaving the channel. This results in a shallowing and eventual plugging of the inlet at its seaward margin. This mechanism usually involves the landward migration of swash bars, due to the refraction of approaching waves (Moslow and Tye, 1985; Imperato *et al.*, 1988; Tye and Moslow, 1992). The refracted waves follow the bathymetry of ebb-tidal deltas that accumulate at the seaward extent of the inlet channel. The landward migrating swash bars may eventually plug up the mouth of the inlet channel resulting in abandonment of the inlet. This process is aided by sediment addition from lateral accretion of migrating subaerial and subaqueous spits. These spits typically form spit-platforms (subaqueous portion of the spit) in wave-dominated shorelines. The infilling of the inlet mouth by spit sands produces a shallowing of the water depth, and constitutes the abandoned phase of inlet development. Thus, any marine through-flow into the inlet channel is constricted and produces upper flow regime plane beds. Oscillatory currents rework the peritidal parts of the spit platform producing symmetrical wave ripple cross-lamination. These bedforms will aggrade as long as sediment supply is continuous and rapid. Evidence in support of these tidal inlet deposits being wave-dominated, is from the orientation of the sublitharenites along depositional strike within the study area. This geometry and spatial arrangement is due to the lateral migration of wave dominated inlets along the barrier island shoreline (see chapter 5 for more detail).

4.9.1. LITHOFACIES I-MATRIX SUPPORTED CONGLOMERATE.

This lithofacies is thin, varying between 30 and 150 cms (1 and 5 feet) in thickness, and is developed ubiquitously at the top of the Halfway Formation. It displays an erosional lower contact and gradational or sharp upper contact. Lithology of the lithoclasts may vary according to the lithology over which it is lies. Above lithofacies C, D, E, and H, it consists dominantly of lithoclasts of dolomite cemented beige to green coloured shale, and subordinate lithoclasts of chert and phosphate in a very fine upper sand sized sandstone matrix cemented with dolomite, calcite and anhydrite (Plates 19, 20 and 21).

Plate 19. Sub-angular to sub-rounded pebble grade dolomicritic, chert and phosphatic lithoclasts, and granule grade chert, phosphatic and sandstone lithoclasts in a sandstone matrix. Lithofacies I, poorly-sorted conglomerate, sits erosively on Lithofacies E, Lower Shoreface Halfway deposits. Well b-068-E/94-A-16, 3853 ft. (Scale in cms).

Plate 20. Lithofacies I sub-rounded, poorly sorted dolomicritic, and well-rounded black chert lithoclasts within a sandstone matrix, resting erosively on Lower Shoreface Halfway deposits. Well d-036-E/94-A-16, 3818.4 ft. (Scale in cms).

Plate 21. Hummocky-cross-stratified coarse siltstones of Halfway Formation, Lithofacies C offshore-transition zone, passing up into sublitharenite conglomerate of Lithofacies I, and up into dolomite cemented red siltstones of Charlie Lake Formation. Entire Halfway coarsening-upward prograding shoreface succession has been removed by Charlie Lake erosion. Well d-050-F/94-A-16, 3802.4 ft. (Scale in cms).

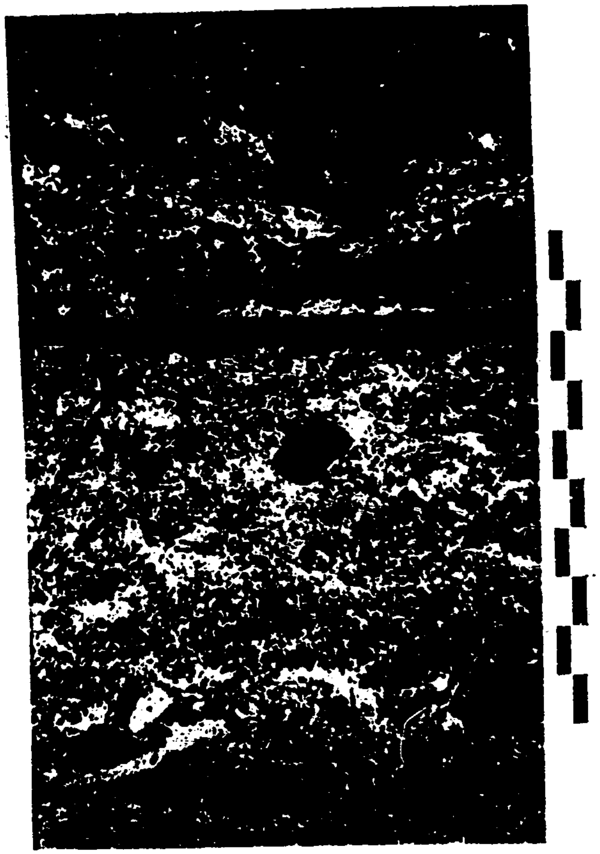

Plate 22. Lithofacies G coquinas below, with black granule to pebble grade chert lithoclasts passing up into Lithofacies I angular coquina lithoclasts within a dolomite cemented red siltstone, characteristic of the basal erosional section of the Charlie Lake Formation. Well d-034-E/94-A-16, 3796 ft. (Scale in cms).

The matrix material may grade up into a red siltstone characteristic of the Charlie Lake Formation. Nodules of pyrite occur. Shale lithoclasts are pebble grade, and angular to well-rounded (d-036-E/94-A-16). The remaining lithoclasts are coarse sand sized. Chert lithoclasts may be concentrated at the top of the lithofacies (e.g. d-084-E/94-A-16, d-100-E/94-A-16 and d-050-F/94-A-16). This lithofacies represents the erosional base of the Charlie Lake Formation.

Lithoclasts of angular lithified coquina are dominant above the coquina of Lithofacies G (Plate 22). The coquina lithoclasts display a pink colour. The pink pigment emanates from iron inclusions contained within chert, weathered chert, and peloid and oolite phosphate lithoclasts. Matrix material between the coquina lithoclasts is composed of finer bioclasts and sandstone, making the recognition of coquina lithoclasts extremely difficult in places. The matrix material may also be red coloured siltstone.

Interstitial pyrite cement is prevalent. It may also occur in discrete laminae. Within the upper sections of the lithofacies brown dolomite cemented sub-rounded sandstone, chert, and coquina lithoclasts (e.g. b-074-H/94-A-15, d-084-H/94-A-15, d-034-E/94-A-16 and a-027-L/94-A-16) and/or bioclasts are prevalent within the dolomitic siltstone.

4.9.2. Environmental Interpretation.

The poorly-sorted and angular nature of the deposits comprising Lithofacies I, the lack of sedimentary structures, and the importance of lithoclast lithology controlled by the underlying strata, suggests that subaerial exposure occurred. The iron staining may have been liberated by the chemical weathering (oxidation and hydration) of iron inclusions within chert, weathered chert, and phosphate lithoclasts, contained within the exposed coquina deposits. The prevalent dolomicritic lithoclasts may have originated from Halfway back barrier lagoonal deposits that have been reworked by the erosion event. The presence of lithified angular coquina lithoclasts suggests that the underlying coquina deposits were lithified before subaerial exposure and erosion occurred. The bioclasts within these lithoclasts had been dolomitized before exposure and subsequent erosion occurred. Cementation prior to erosion of the coquina indicates a possible hiatus event. The duration of this hiatus, however, is not known. The dolomitisation process may have taken upward of ten thousand years to occur. This evidence points to an hiatus in the stratigraphic column, resulting in the formation of an erosional lag between the Halfway and Charlie Lake formations in the study area.

The Charlie Lake erosion surface cuts down into the Halfway Formation to different degrees. In many locations it cuts down to the Halfway offshore-transition zone, thus removing almost 30 feet of Halfway deposits.

Lithofacies J, K, L and M have been assigned to the Charlie Lake Formation. They represent deposition within playa-lake and continental regions during Carnian times.

4.10.1.0. LITHOFACIES J. INTERLAMINATED SILTSTONE AND SHALE WITH INTRACLASTS.

In many cases, the lower contact of this lithofacies is abrupt and irregular, marked by a layer of pyrite. This lithofacies sits sharply on top of lithofacies C, D, E, F, G, H, I, or K. Diagenetic dolomitisation may mask the nature of lithological contacts. This lithofacies is subdivided into three sub-lithofacies. The lithology of Lithofacies J is varied, containing siltstones, shales, mudstones and anhydrite. Many areas of the lithofacies have been obscured by soft sediment deformation and dolomitisation. The lithofacies also fines-upward from dominantly siltstone at the base to shale with abundant intraclasts in the centre, to mainly shale at the top. Anhydritic nodules decrease upward in quantity, although bedded anhydrite increases in quantity upward. There are numerous discontinuities within the lithofacies, in most cases occurring at the contact between sub-lithofacies. The vertical positioning of the sub-lithofacies is complex, being repeated several times. There is, however, a crude upward-fining pattern in which sub-lithofacies J2 is dominantly positioned beneath sub-lithofacies J3. This lithofacies, including lithofacies K and L, have been deposited within a playa-lake depositional system. The regional scale and depth of the playa-lake system is unclear. The depth parameter does seem to be partially influenced by the spatial distribution of early Carnian faults, such that playa-lake deposits are thicker within local graben features (see Chapters 9 and 10).

4.10.2.1. Sub-Lithofacies J1. Interlaminated Dolomite and Anhydrite.

This sub-lithofacies displays bands of parallel-laminated, alternate dolomite and anhydrite millimetre scale laminae. They are usually horizontal and planar, but may pass gradually upward into a more undulatory geometry, with wavelengths of between 3 and 5

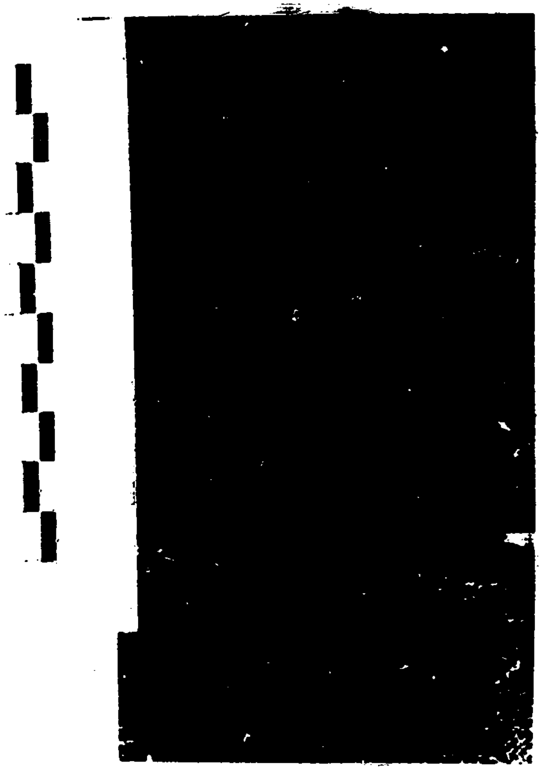

Plate 23. Parallel-laminated planar crypt-algal laminite passing up into an undulatory morphology. Composed of interlaminated anhydrite and dolomite crinkly laminae. Well d-071-D/94-A-16, 3866 ft.
(Scale in cms).

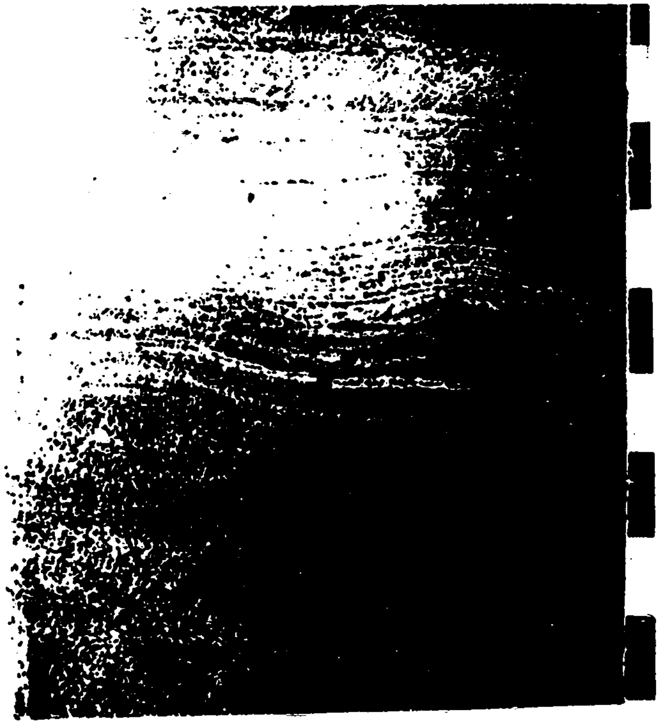

Plate 24. Parallel-laminated alternate laminae of dolomite and anhydrite, forming an undulatory morphology to the stromatolites.
Well d-068-H/94-A-15, 3845 ft.
(Scale in cms).

cms (1.2 to 2 inches) and amplitudes of 2 to 4 cms (0.8 to 1.6 inches) (Plates 23 and 24). These laminated structures may range in thickness from 3 to 10 cms (1.2 to 4 inches). They may occur singularly or as repeated layers, 20 to 30 cms (8 to 12 inches) apart. White, horizontally orientated elliptical calcite nodules may occur within these laminated structures, commonly 1.2 by 0.8 cms (0.5 to 0.3 inches) in size. Pyrite cement is commonly associated with these laminae in the form of thin layers, or discrete crystals. Anhydrite nodules are developed within the central base of the undulatory laminate forms. In places, these crypt-algal laminites have been partially or totally replaced by diagenetic anhydrite nodules. Ghost structures of the host horizontal parallel laminites are recognizable within some samples. Alternatively, the laminites gradationally pass up into, or pass down into areas containing an increased content of anhydritic nodules.

4.10.2.2. Environmental Interpretation.

The crypt-algal laminites within this sub-lithofacies have similar sedimentologic characteristics and mineralogy to modern algal mats found along the modern Trucial coastline of the Persian Gulf (Kinsman and Park, 1976), and are thus termed stromatolite structures. The algal mats of the Persian Gulf occur in mid to upper intertidal zones of sheltered lagoons, away from predators. In Sharks Bay, Australia, algal mats live in highly saline lagoonal waters (Davies, 1970). They can live within the lower intertidal areas in the latter example since predators cannot live in such saline waters. The algal mats on the Trucial coast were not found growing higher than the upper intertidal region, as extreme desiccation occurs.

Park (1976) described the internal structure of modern algal mats from the Trucial coast. He recognized a couplet, composed of a micritic lamina and an organic (originally blue-green algae) lamina (Figure 19). As burial of the blue-green algae occurred, the filamentous material decayed. High water content within the algae resulted in dehydration (a volume reduction of 70 to 80%) during compaction and burial. Thus, in the rock record, these laminae are very thin and lack internal detail. The laminae within sub-lithofacies J1 are similar to this description.

Park (1976) noticed that gypsum crystals grew beneath algal mats developing eventually into a gypsum mush that contorted the algal mat surface. Cody (1979) documented that similar gypsum crystals grew as a result of bacterial and algal decay, releasing sulphates.

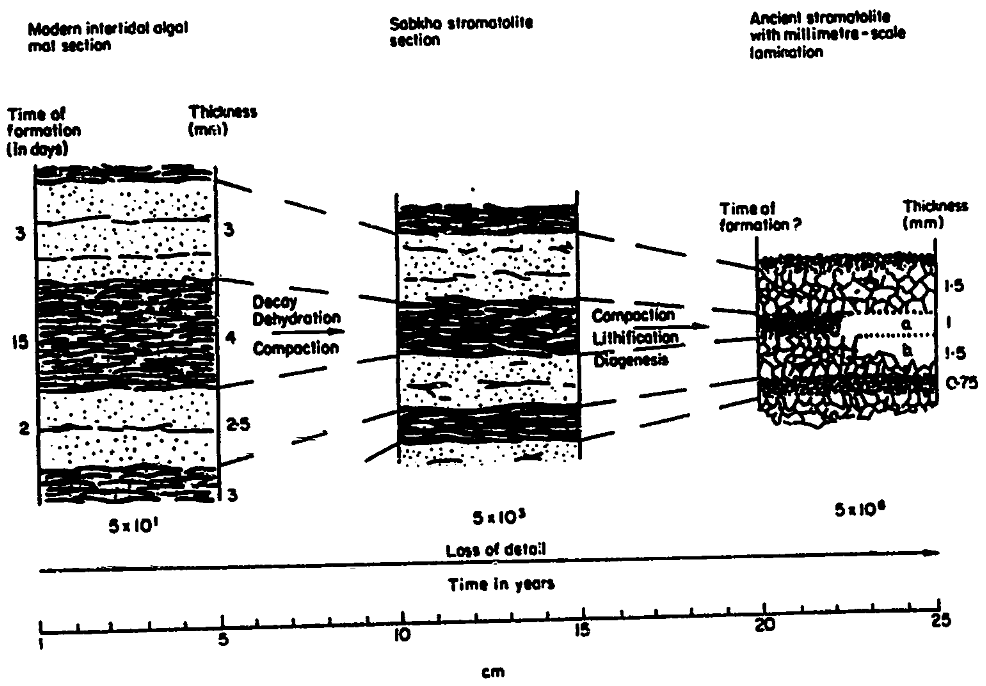

Figure 19. Diagram showing the changes occurring to algal mats upon compaction and lithification resulting in stromatolitic structures (after Park, 1976).

At high regions within the intertidal zone the gypsum crystals not only deform the overlying algal laminites but eventually slice through and destroy them, save for a few isolated rafts of material scattered throughout the gypsum mush (Kinsman, 1966; Park, 1976). Similar nodules of anhydrite have been observed beneath and between the algal laminites of sub-lithofacies J1 (Plate 25). Evidence for increase in periodic, long term excessive exposure of the algal mats, is from the gradual change in morphology from undulatory to planar shapes (Hoffman, 1976). The occurrence of ovoid calcite nodules (known as "birds-eye textures") within these sediments may also reflect the degassing of the algal material, producing gas-filled voids. These voids would later have been infilled with calcite cement before lithification proceeded. Although modern algal mats have been found and documented from the intertidal marine environment, there have been examples noted from the rock record in which algal mats were interpreted as habiting the margin of a playa-lake depositional system (Surdam and Wolfbauer, 1975). This example was recorded from the Tripton Shale Member, within the Green River Formation of Utah, Wyoming and Colorado. Various geometries of the stromatolites, ranging from domal to planar types reflected different microenvironments. Surdam and Wolfbauer (1975) speculated that the algal mats were originally located in high salinity margins of the playa-lake, since algal grazers could not survive in such extreme climatic conditions.

The presence of pyrite laminae within the stromatolites of sub-lithofacies J1 is similar to present occurrences. Cody (1979) explained the close association of pyrite to algal mats as a result of bacterial and algal decay releasing sulphates. The formation of anhydrite layers within the stromatolites may be similar to that occurring in lenticular gypsum crystals within modern sabkha settings. They form due to the decomposition of organic material (i.e., the blue-green algae).

4.10.3.1. Sub-Lithofacies J2. Red Siltstone with Shale Intraclasts.

The dolomite-anhydrite crypt-algal laminites pass up, gradationally or sharply, into beds of reddish-brown dolomite cemented silty-shale and parallel-laminated siltstone. This lithology may occur at the base of the lithofacies where the dolomite-anhydrite laminites are absent. At this location convolute and oversteepened lamination, in addition to numerous reverse microfaults are apparent, and commonly disrupt the original sedimentary layering. There are occasional preserved thin parallel-laminations of normally graded siltstone passing up into shale. The siltstone bases are loaded or erode

Plate 25. Anhydrite cement fracturing stromatolitic structures (primary feature). Well d-002-E/94-A-16, 3831 ft. (Scale in cms).

into the shale below. Tabular shaped, angular intraclasts of beige dolomite cemented shale, and tabular reddish-brown coloured dolomite cemented silty-shale are common within the brown dolomite cemented silty-shale matrix toward the base of the lithofacies (Plates 26, 27 and 28). There are occasional intraclasts of crypt-algal laminites originating from sub-lithofacies J1. The latter intraclasts display a very-fine internal parallel-laminated structure. The proportion of dolomite cemented beige coloured shale beds increases upward. Within the basal part of the sub-lithofacies asymmetrical ripple cross-lamination and subcritical climbing ripple cross-lamination occur. There are a few samples where parallel-laminated brown siltstones and beige shale laminations have been broken up *in situ* forming breccias. Sub-angular very-fine lower sand sized quartz grains are scattered throughout the sub-lithofacies.

Anhydrite displacive nodules, elliptical in shape, varying in size from 1.4 by 0.9 cms (0.6 to 0.4 inches) to 6 by 2.1 cms (2.4 to 0.8 inches) occur mainly toward the base of this sub-lithofacies. These anhydrite nodules may coalesce to form similar textures to the "chicken-wire textures" identified by Kinsman (1966) from the Trucial coast (Plate 29). Alternatively, anhydrite nodules may coalesce to form sub-horizontal contorted layers. This is similar to the enterolithic textures described by Butler (1969), Kinsman (1966) and Shearman (1966). Anhydrite nodules and pyrite crystals are closely associated; the pyrite growing as a thin layer around the anhydrite nodule, or they may occur as interlaminations, or the pyrite may form discrete euhedral crystals.

4.10.3.2. Environmental Interpretation.

The reddish-brown dolomite cemented silty-shale beds incorporating tabular intraclasts of reddish-brown dolomite cemented silty-shale and beige coloured dolomite cemented shale intraclasts are characteristic of this sub-lithofacies. The red silty lithology is parallel-laminated to chaotic in appearance. Individual silty laminae fine-up into shale drapes. Similar structures have been observed and documented by Hardie *et al.* (1978), who indicated that sheetwash flows produce flat, lenticular silty laminae capped with mud. Should these sheetwash flows enter ponded water on mudflats, turbid underflows may occur producing thin graded silty units. Hence, it is plausible that the normally graded [illegible]ne laminae within sub-lithofacies J2 were formed by sheetwash flows entering ponded water on mudflats, depositing their load.

Plate 26. Localised region of abundant beige, mud-chip tabular intraclasts within crudely recognizable interlaminated siltstone and shale. Matrix is brown (dark coloured) siltstone. Well b-067-E/94-A-16, 3815 ft.

(Scale in cms).

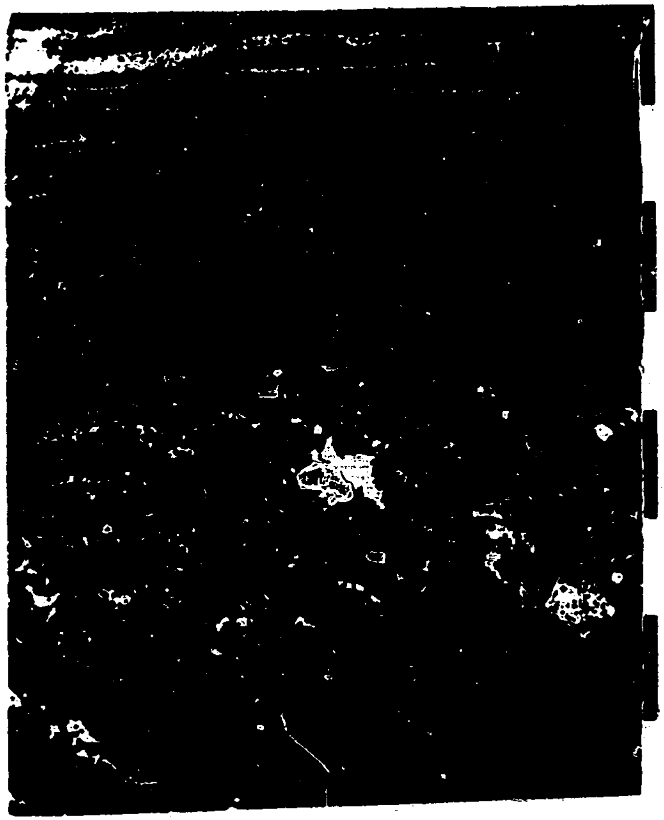

Plate 27. Chaotic appearance of beige, tabular shaped shale and red siltstone intraclasts, with occasional crypt-algal laminite intraclasts (right-hand-side), within a red silty-shale matrix.
Well d-077-H/94-A-15, 3837.6 ft.
(Scale in cms).

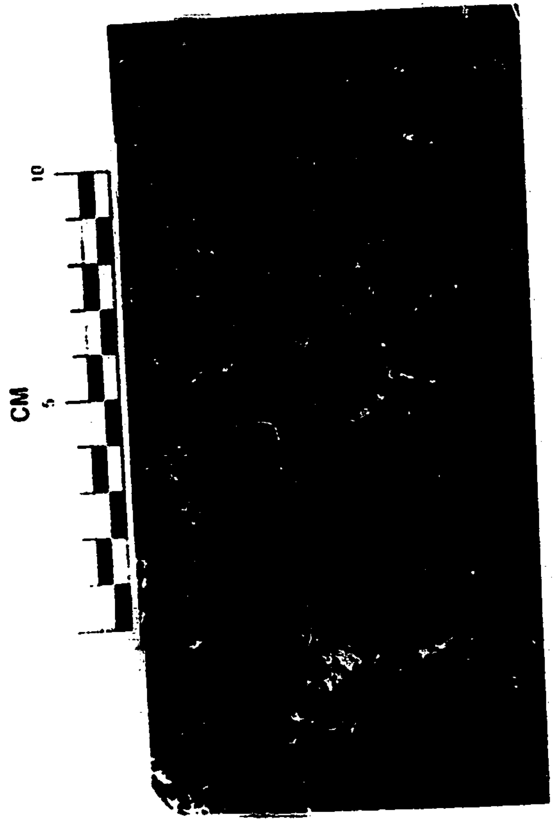

Plate 28. Chaotic fabric composed of tabular intraclasts of red siltstone and beige shale within a silty-shale matrix. Large, ovoid, inclined anhydritic replacive nodules occur at lower left-hand-side. Well a-083-D/94-A-16, 3863 ft.

(Scale in cms).

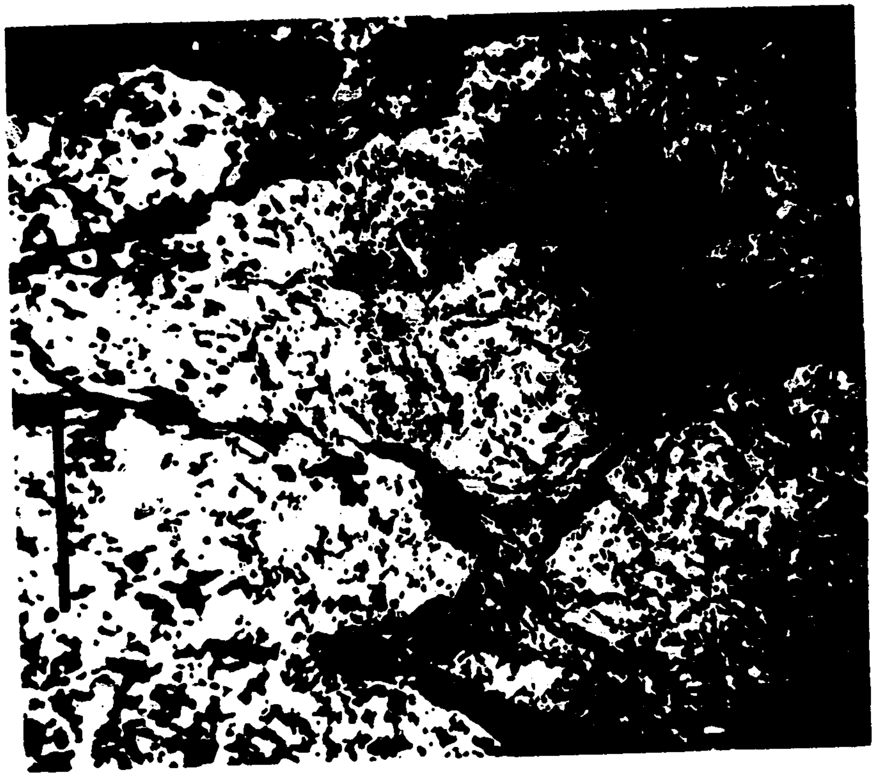

Plate 29. Petrographical micrograph of replacive anhydrite nodules forming a chicken-wire texture. Dark material is the matrix shale. Well d-068-H/94-A-15. (Scale in mm).

Stromatolitic intraclasts derived from sub-lithofacies J1 were formed by the desiccation of algal mats during dry periods when the playa-lake level lowered. These algal mats would then have been ripped up by occasional sheetwash flows, storm waves, or aeolian processes, and incorporated into the marginal mudflats.

The tabular shaped shale and silty-shale intraclasts are similar to those described by Pettijohn (1957) as "flat-pebble conglomerates" from ancient strandlines. Similar mud chips have also been documented by Handford (1982) from the modern Bristol Dry Lake playa margin mud flats, in California. These were formed by desiccation from excessive atmospheric exposure. It is believed that the intraclasts described from sub-lithofacies J2 were also produced by intense desiccation of the playa-lake margin sediments during long periods of exposure. The sediment dehydrated as pore water evaporated forming polygonal mud-cracks. Mud cracks, however, have not been identified within sub-lithofacies J2. This may be partly due to the chaotic appearance and deformation occurring in places. The mud cracks caused parts of the sediment to "peel" apart forming tabular mud chips. The intraclasts may have been removed and transported by wind deflation or sheetwash flows. Alternatively, they may have been ripped up from the lake margin by high energy storm-generated waves, forming in response to wind forcing on the water surface. Similar sequences have been documented by Eugster and Hardie (1975) within the Eocene, Wilkins Peak Member of the Green River Formation in Utah. The deposits were interpreted as playa-lake in origin. Mud-chip conglomerates were identified and interpreted as exposed and desiccated mudstones on a mudflat. The mudstone lithofacies contained finely laminated dolomitic mudstone and siltstone, strongly mud-cracked. These were interpreted as forming in an exposed playa mudflat, covered by occasional sheet floods which introduced silt and mud laminae. Other similar ancient analogues have been described by Hardie and Eugster (1971) from the Upper Miocene Solififera Series of Sicily. Periodic exposure of these mud and silt flat interpreted sediments resulted from dryer climatic periods during which lower frequency of sheetflood waters issued from upland areas. During wetter periods the lake level would have risen. The variation in lake level resulted in laterally expansive playa-lake margins. As explained earlier, modern deposits associated with playa-lakes have been described from Bristol Dry Lake, California (Handford, 1982). These deposits were described as chaotically bedded mud, halite, clay, enterolithic gypsum and anhydrite, with mud-chips scattered throughout. These deposits occurred on mudflats adjacent to the playa-lake.

Isolated quartz grains occur throughout the sub-lithofacies. These may have been transported by aeolian processes.

The presence of anhydritic nodules and enterolithic structures within the deposits of sub-lithofacies J2 may also indicate evidence for periodic exposure of the playa-lake marginal mudflats and siltflats. These nodules were formed by the rapid evaporation of pore fluids derived from sheetflood waters, resulting in high concentrations of elements responsible for the precipitation of anhydrite.

The occasional *in situ* breccias composed of parallel-laminated beige shale and brown siltstone within sub-lithofacies J2 were produced by solution collapse. This may have resulted from the diagenetic dissolution of soluble evaporitic minerals, such as halite. These soluble minerals precipitated out as a result of desiccation of marginal ephemeral ponds. These ponds formed within deflation depressions in the marginal playa-lake mudflats in response to a rise in lake level during temporary wet periods and were left isolated when lake level fell again.

4.10.4.1. Sub-Lithofacies J3. Dolomitised Interlaminated Siltstone and Shale.

The reddish-brown dolomite cemented silty-shales pass up, gradationally or abruptly, into very thinly horizontally interlaminated brown dolomite cemented to calcite cemented siltstone and beige, heavily dolomite cemented shale. These laminations are, in places, convoluted and oversteepened, and displaced by numerous reverse-microfaults (Plate 30). Primary parallel-lamination is partially or completely destroyed by either: 1.) biogenic activity mixing the sediment; 2.) diagenetic alteration (dolomitisation), compaction, and soft sediment deformation (Plate 31). It is, however, difficult to determine the process. Within this area of lithological homogenization there are isolated "rafts" or lithoclasts of undisturbed parallel-laminated siltstone and shale similar to that of sub-lithofacies J2 (Plates 30 and 32). The siltstone laminae fine-up into shale. The bases are loaded or erosional into the shale.

Pyrite nodules and disseminated crystals occur throughout these sediments. Displacive and replacive anhydrite nodules occur in laminae or isolated concentrations. Pyrite crystals occur in dense aggregates within and surrounding the anhydritic nodules. Smaller anhydrite nodules (less than 0.5 cms in diameter) occur throughout the entire sub-

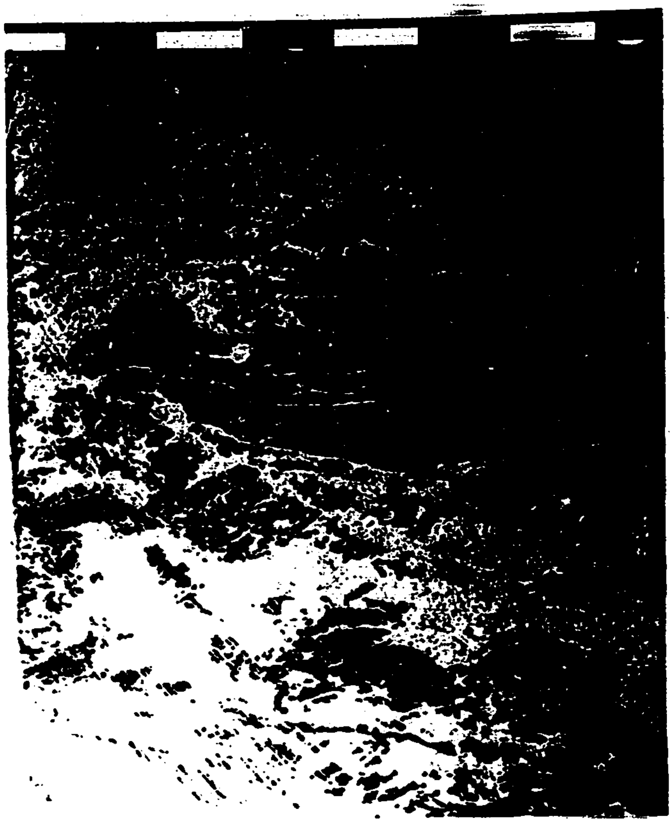

Plate 30. Area of unaffected interlaminated siltstone (dark) and shale (light). Reverse microfaults are common. Load and flame structures occur between these normally graded siltstone and shale laminae. The surrounding lithology has been dolomitised. Well d-099-C/94-A-16, 3848.2 ft.

(Scale in cms).

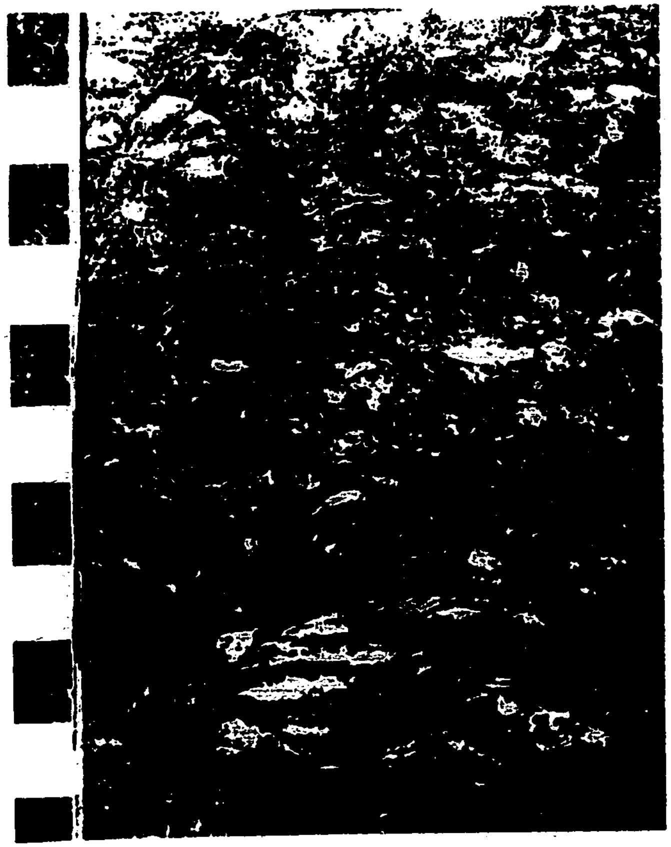

Plate 31. Mottled chaotic appearance to siltstone and shale of sub-lithofacies J2. Well d-023-E/94-A-16, 3796.2 ft.

(Scale in cms).

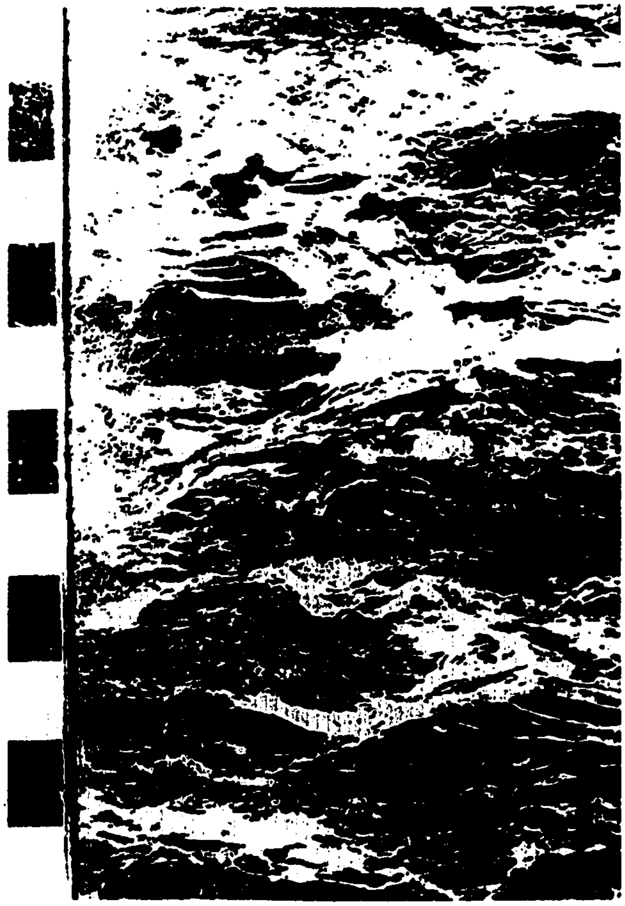

Plate 32. Areas of unaffected interlaminated siltstone and shale. Normally graded siltstones have sharp bases that are loaded into the shale. Microfaults are abundant. Well d-100-C/94-A-16, 3853.2 ft. (Scale in cms).

lithofacies. The larger anhydrite nodules form similar textures to those within sub-lithofacies J3. Anhydrite nodules are occasionally wider than the width of the core, thus giving the appearance of being primary in origin, especially when the attitude is horizontal. Some anhydrite layers are 40 to 80 cms (16 to 32 inches) thick (Plate 33). There are no ghost structures or inclusions of sediment. These are believed to be primary in formation. Stylolites are developed in the heavily dolomite cemented portions of the lithofacies. They also form at lithological contacts between sub-lithofacies (Plate 34). These stylolites are concentrated with pyrite and organic material.

4.10.4.2. Environmental Interpretation.

The dominant lithology comprising these sediments are very thinly laminated dolomite cemented brown siltstones and dolomite cemented beige shales. Under petrographical examination the siltstone laminae are sharp based and grade up into shale laminae. The siltstone laminae exhibit parallel and current ripple cross-lamination. These siltstone laminae were deposited by waning unidirectional weak currents. Similar flaser-bedded silts and muds have been reported by Handford (1982) from Bristol Dry Lake, in California, a modern continental sabkha playa. The playa-lake is located 300km from the ocean and is at an altitude of 190 metres. These flaser-bedded silts and shales were deposited on the playa mudflats by traction deposition, followed by suspension, from flood run-off during rain storms.

It is believed that the interlaminated siltstones and shales within sub-lithofacies J3 were deposited in a similar palaeoenvironmental setting reflecting similar processes. These currents flowed across the mudflats as sheetflood waters. They deposited the silts primarily under upper flow regime conditions. As these currents entered the playa-lake and marginal ephemeral ponds they decelerated depositing their load. The shale laminae were deposited by mud fall-out from suspension within the playa-lake and ponds on the mudflats. The muds were hydroplastic yielding a high water content. They subsequently dewatered as more sediment became rapidly deposited ontop, producing soft sediment deformation structures, such as contorted and oversteepened lamination. Mud-chips within this sub-lithofacies are less abundant. This is because these deposits were less frequently desiccated. The quantity of mud chips decreases upward in the sub-lithofacies. The quantity of shale contained within sub-lithofacies J3 is greater than within other sub-lithofacies, suggesting longer quiescent periods. This may reflect deposition within the

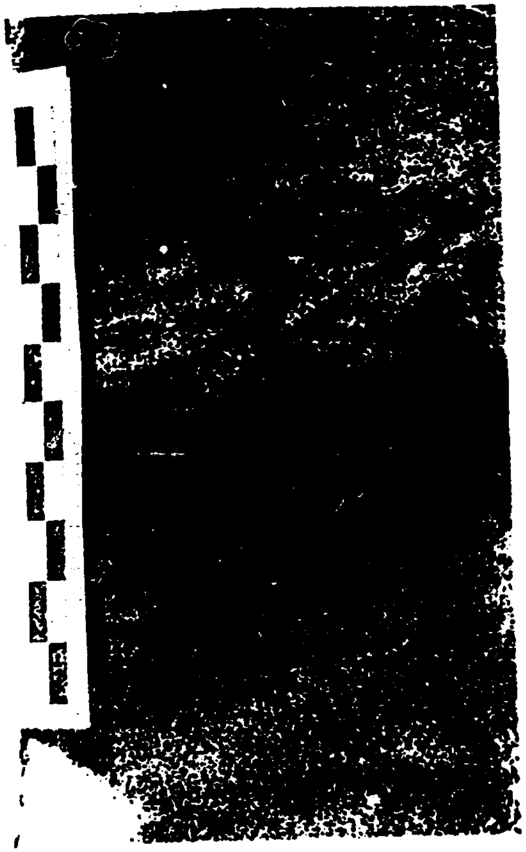

Plate 33. Primary anhydrite bed known as the "B-Marker" correlatable throughout the entire field.
Well d-024-E/94-A-16, 3717 ft.
(Scale in cms).

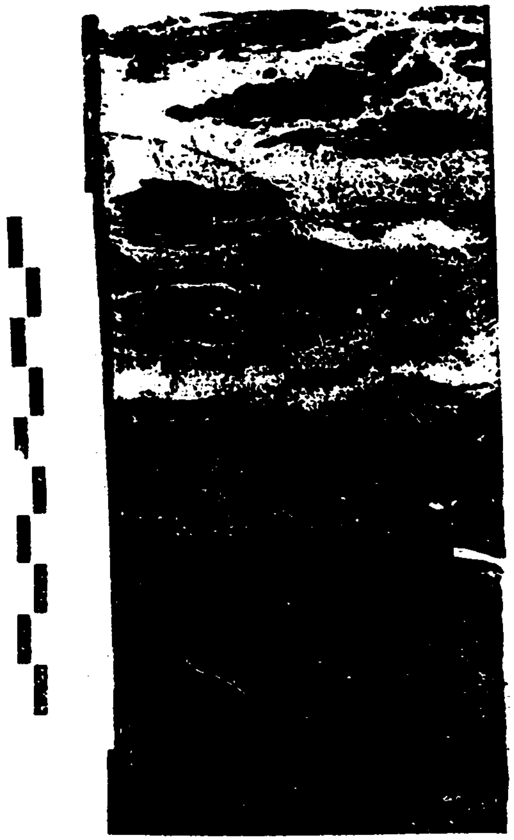

Plate 34. Pyrite lined stylolite contact between sub-lithofacies J2 (below) and J3 (above). Anhydrite nodules concentrated at base of J3. Dark regions are siltstone surrounded by dolomitised shale (light).
Well d-071-D/94-A-16, 3865 ft.
(Scale in cms).

playa-lake itself. Eugster and Hardie (1975) have interpreted thin bedded dolomitic mudstones as deposited within a playa-lake within the Eocene, Green River Formation of Utah. The limited presence of anhydritic nodules indicates that these deposits were less frequently exposed and desiccated. This may be because these sediments were located further within the playa-lake. Toward the margins of the playa-lake, however, frequency of exposure and desiccation would have been higher. It is not clear whether the playa-lake was ephemeral or not. No solution collapse breccias have been found within this lithofacies, indicating that the lake did not dry up completely and precipitate soluble minerals. Anhydritic beds do occur and represent periods when the lake level fell causing the lake size to decrease, increasing the concentration and level of salinity.

The overall vertical sequence of Lithofacies J involves an upward-fining of the sediments. This resulted from the expansion and growth of the playa-lake which transgressed marginal mudflat and siltflat deposits. Infact, the intraclasts found within sub-lithofacies J2 may reflect the transgressive nature of the playa-lake which may have reworked the marginal siltflats and mudflats.

4.11.1. LITHOFACIES K. ORANGE SHALE WITH SHALE INTRACLASTS.

This lithofacies commonly has a sharp, irregular basal contact. This contact may be stylolized and concentrated with a layer of pyrite cement (Plate 35). The dominant lithology is light orange coloured non-calcareous shale displaying a chaotic appearance. Intraclasts of orange to beige coloured shale are incorporated within the host rock. Patches or intraclasts displaying interlaminated siltstone and shale are sparsely distributed. Horizontal anhydrite nodules are greater than 5cms in length and 2cms parallel to the long axes of the core. Pyrite nodules are common within this lithofacies. They are closely associated with the anhydrite nodules.

4.11.2. ENVIRONMENTAL INTERPRETATION.

The dominant shale lithology reflects low energy conditions of deposition. The clay sized particles settled out of suspension from a non-turbid water column. These sediments were deposited within deeper parts of the playa-lake. They are similar to the playa-lake bedded mudstones described by Eugster and Hardie (1975) within the Green River Formation of Utah. Intraclasts of shale and interlaminated siltstone and shale are similar in lithological characteristics to sub-lithofacies J3. These intraclasts were ripped-up from the desiccated

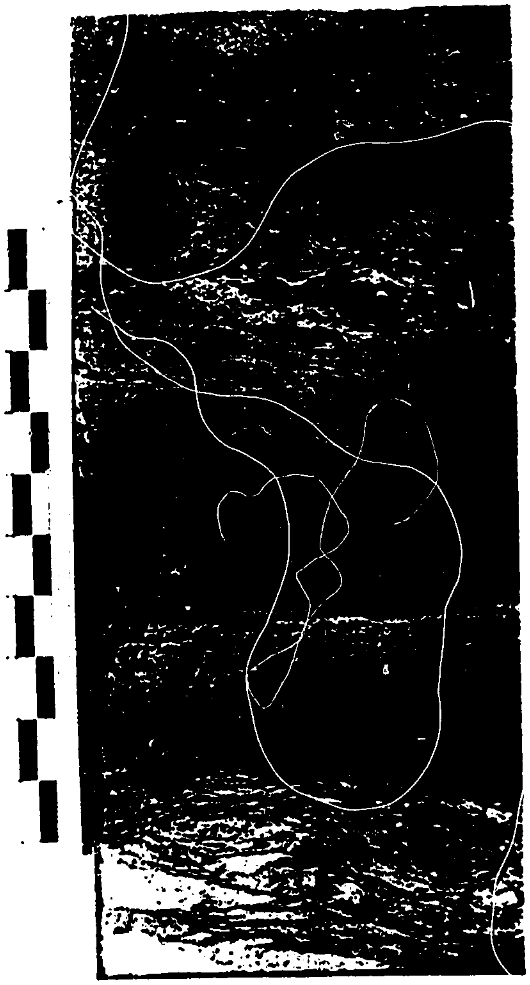

Plate 35. Stylolitic contact lined with pyrite, between Lithofacies K (above) and sub-lithofacies J3 (below). Darker patches are siltstone, lighter areas are shale, with rare lighter coloured shale intraclasts. Well a-003-E/94-A-16, 3840 ft. (Scale in cms).

mudflats and siltflats surface, located at the playa-lake margin. The sheetflood waters were responsible for erosion and transportation of these intraclasts, finally to be deposited within the playa-lake.

Anhydrite nodules are displacive and secondary in formation. They were formed a few centimetres below the sediment surface, due to the evaporation and consequent high concentration of calcium sulphate pore water chemistry. This occurred during periods of low lake level, as a result of drier climatic seasons.

The presence of stylolites within these shales were formed by diagenetic processes of lithic compaction, producing pressure solution of the sediment. It has been documented by Park and Schot (1968) that stylolites are concentrated in rocks that exhibited originally high porosity and low permeability resulting in a high water saturation. They may also be preferentially located at breaks in lithology or along bedding planes where the rock had a high original argillaceous content. The original lithology of Lithofacies K was a shale. Shales are typically characterised by high primary porosities and low permeabilities, thus conducive to the formation of stylolites.

4.12.1. LITHOFACIES L. RED SHALE.

This lithofacies is limited to the extreme east of the study area. Infact, it has been found in only three wells: d-018-B/94-A-16, d-093-D/94-A-16, and d-038-K/94-A-16. The thickness of this lithofacies is indeterminable from core, however, 7.3 metres (24 feet) has been recovered from d-018-B/94-A-16, therefore making this lithofacies is at least 7.3 metres (24 feet) thick. The base of the lithofacies is sharp and overlies Lithofacies K. Rarely, it may overly Lithofacies I (e.g. d-018-B/94-A-16). It is dominantly composed of non-calcareous shale. The shales are notably red in colour with elliptical to irregular shaped green patches. Dolomite cement is of subordinate importance occurring as late stage euhedral rhombic crystals with an internal zoned fabric. The characteristic red colour of the shale results from a coating of iron oxide around each particle. The red shale has a general chaotic appearance, but on closer inspection faint horizontal laminae are recognizable. There are a few scattered grains of silt to medium sand sized, sub-rounded to sub-angular quartz particles, plagioclase and microcline feldspar, and accessory zircon rounded grains, arranged in crude sub-horizontal laminae. White mica platy crystals are identifiable. The laminae occasionally display sharp bases and are normally graded. Red tabular shaped shale intraclasts occur within a red shale matrix making recognition of these intraclasts extremely difficult. They are found randomly throughout the lithofacies, but are orientated horizontally to sub-horizontally. These shale intraclasts are similar to the "mud-chip conglomerates" described by Kinsman (1966). There is no evidence to suggest the presence of any biogenic activity.

Toward the base of the lithofacies, anhydrite crystals form ovoid nodules that are between 1 and 2 cms (0.4 to 0.8 inches) in diameter (with the longest dimension in the horizontal plane). The nodules are secondary, replacing the shale. Where these textures are well formed, the original lithology is only present as thin laminae that border every nodule. This texture is similar to the "chicken-wire" texture described by Kinsman (1966) from the Trucial Coast.

4.12.2. ENVIRONMENTAL INTERPRETATION.

The characteristic red colour of these shales was formed by ferruginous cementation coating the particles. These red beds formed in a highly oxidising environment. The iron present is in the form of red ferric hydroxide suggesting that long periods of oxidation and subaerial exposure were experienced.

There are two theories, namely diagenetic and detrital, that explain the reddening process that occurs in red beds. T. R. Walker (1967) has discussed the reddening processes, and has inferred a diagenetic origin. The process appears to be slow acting. The reddening process is promoted by the breakdown of biotite and amphiboles into clays and immature iron oxides and hydroxides. They become washed down the weathering profile and coat the detrital grains. With time the oxides mature to haematite. Elevated temperatures and water provided by ephemeral run-off are required to produce these chemical changes. Clay-rich sediments redden more slowly than coarser grained sediments because permeabilities are much lower.

The detrital process involves the hydration of oxides to produce amorphous reddened hydroxides and oxides (Paijmans *et al*, 1971). There is no evidence petrographically, however, to indicate the presence of detrital iron present within Lithofacies L. Clays, however, have been observed, indicating support for the first theory.

The muds were originally deposited by suspension fall-out from sheetflood waters. The red shales accumulated as a continental mudflat environment. The red mud chips were formed by extreme desiccation of the shales. The formation of polygonal mud cracks weakened the mud, breaking it up into chips. Wind deflation and sheetfloods may have dislodged and transported this material a short distance before depositing it. The quartz grains were transported by aeolian or sheetflood processes.

Pools of water, resulting from run-off, slowly percolated down into the pore spaces of the muds. Evaporation of brine waters within the pores resulted in the precipitation of anhydrite crystals within the red beds. Small areas of the shale are green in colour. The red pigment disappeared as a result of reduction of ferric iron in the clay by the presence of organic material. This process occurred during burial.

This lithofacies directly overlies Lithofacies I in places, resulting from major lowering in relative base level, hence exposing and reworking the lithofacies, and depositing terrestrial sediments ontop. There is a sharp contact between lithofacies K and L. This may be due to rapid shrinkage in the lake size, or from other more catastrophic tectonic events.

5.0.0. VERTICAL LITHOFACIES ASSOCIATIONS.

The purpose of this chapter is to describe, interpret and compare the vertical lithofacies associations identified within the study area. Two broad lithofacies associations have been repeatedly recognized within the Peejay field (Table 4). Lithofacies association 1 consists of a series of upward-coarsening deposits in which grain size, bedding thickness, sand content, and scale of sedimentary structures increase upward, and biogenic activity decreases upward. This association has been interpreted as a prograding (regressive) shoreface. Lithofacies association 2 cuts into lithofacies association 1. It consists of a crude upward-fining sequence of cross-bedded and parallel-laminated sublitharenites, litharenites and arenaceous biodolomicrites (coquinas), with basal intraclastic lags. The lithofacies association has been interpreted as a tidal-inlet channel fill.

5.1.0. LITHOFACIES ASSOCIATION 1.

This lithofacies association occurs as isolated packages throughout the entire study area. It consists of an upward-coarsening series of deposits (Figure 20). It is composed of lithofacies A, B, C, D, E and F, from the lithostratigraphically defined Halfway Formation forming a prograding shoreface sequence, and lithofacies I, J, K and L forming the Charlie Lake Formation playa-lake continental deposits. The complete succession however, is rarely preserved; post-Halfway erosion being responsible for the lack of complete preservation.

The base of lithofacies association 1 is picked out at the base of Lithofacies A. These deposits are composed of lithoclasts reworked from the underlying parasequence sandstones. Shoaling waves associated with a minor transgressive pulse, were responsible for reworking the top of the underlying parasequence prior to relative increase in water depth, thus producing a ravinement surface (Nummedal and Swift, 1987). As the transgression continued sediment supply was reduced and reworking became minor resulting in deposition of black, phosphatic shale. This is associated with low sediment supply and the formation of a condensed section.

Lithofacies B to Lithofacies F form a conformable coarsening-upward cycle, interpreted as a regressive shoreline formed by the progradation of the shoreface into the marine

LITHOFACIES ASSOCIATION 1 REGRESSIVE SHOREFACE		LITHOFACIES ASSOCIATION 2 TIDAL INLET CHANNEL FILL	
LITHOFACIES	ENVIRONMENT	LITHOFACIES	ENVIRONMENT
L	Red Beds	L	Red Beds
K	Playa-Lake	K	Playa-Lake
J	Playa-Lake Margin/ Mudflats	J	Playa-Lake Margin/ Mudflats
I	Erosional Lag U/C	I	Erosional Lag U/C
F	Upper Shoreface	G/H	Active Tidal Inlet Channel
E	Lower Shoreface		
D	Lower Shoreface		
C	Offshore-Transition		
B	Offshore	MFS	
A	Transgressive Lag	RS	

Table 4. Contrast in lithofacies and environments from lithofacies associations 1 and 2 identified within the Peejay area.

Unconformity	U/C
Marine Flooding Surface	MFS
Ravinement Surface	RS

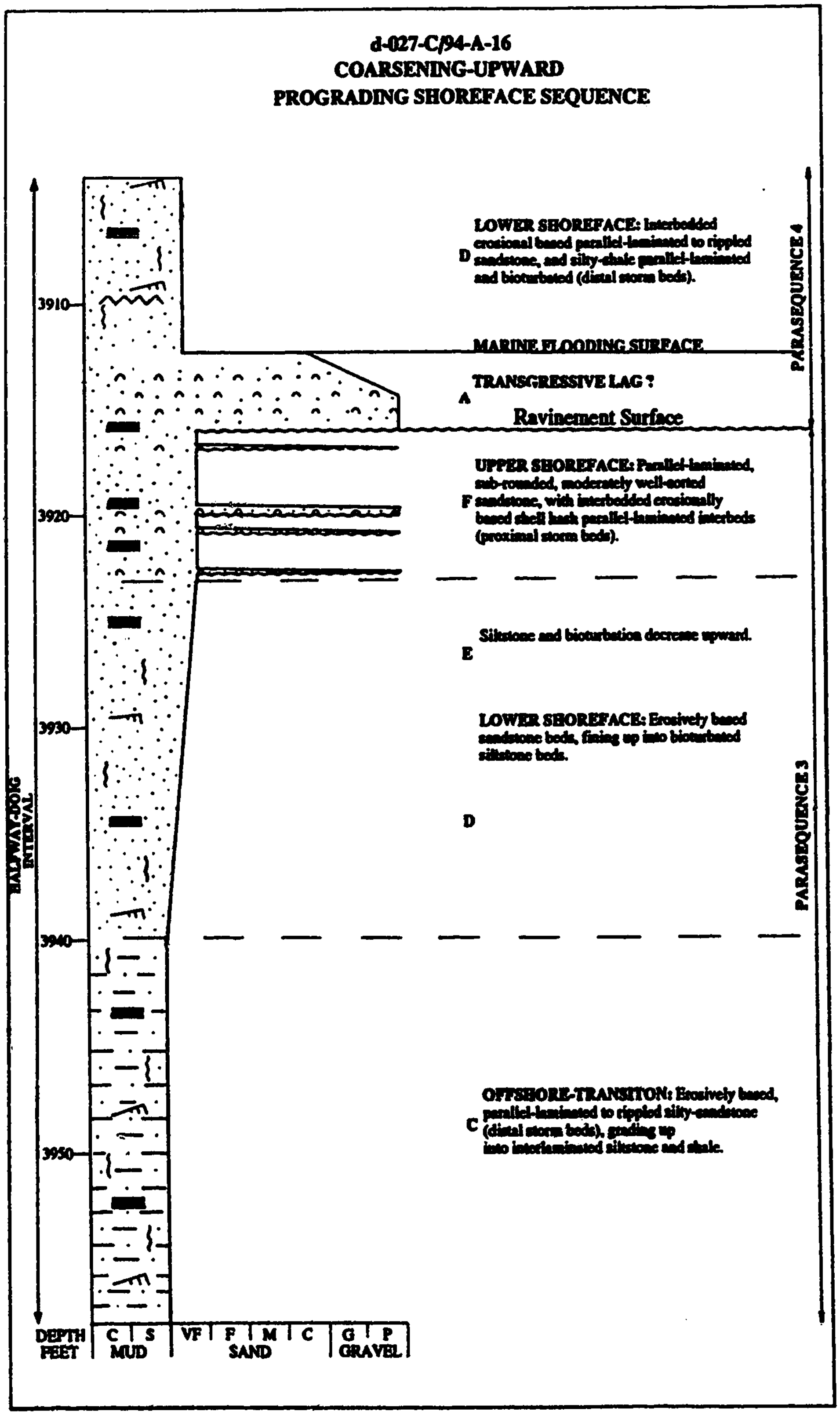

d-027-C/94-A-16
COARSENING-UPWARD
PROGRADING SHOREFACE SEQUENCE

D LOWER SHOREFACE: Interbedded erosional based parallel-laminated to rippled sandstone, and silty-shale parallel-laminated and bioturbated (distal storm beds).

MARINE FLOODING SURFACE

TRANSGRESSIVE LAG ?

A

Ravinement Surface

F UPPER SHOREFACE: Parallel-laminated, sub-rounded, moderately well-sorted sandstone, with interbedded erosionally based shell hash parallel-laminated interbeds (proximal storm beds).

Siltstone and bioturbation decrease upward.

E

LOWER SHOREFACE: Erosively based sandstone beds, fining up into bioturbated siltstone beds.

D

C OFFSHORE-TRANSITON: Erosively based, parallel-laminated to rippled silty-sandstone (distal storm beds), grading up into interlaminated siltstone and shale.

Figure 20. Lithofacies Association 1: Regressive Shoreface Sequence.

basin (Table 4). The amount of shale and siltstone decrease upward, and the grain size of the sandstone increases upward. Palaeowater depth was inferred as decreasing upward, based on the identification and interpretation of depositional and hydrodynamic processes. Dominant shale with minor sharp based, normally graded siltstone laminae of Lithofacies B were deposited below the influence of storm wave-base, within the offshore bathymetric zone. Sharp based, normally graded siltstones exhibiting hummocky-cross-stratification, and interlaminated shales of Lithofacies C are indicative of the offshore-transition zone, whereby the siltstones were formed from storm-generated high orbital velocity currents. These pass up into lithofacies D and E sharp based storm-generated sandstone beds exhibiting hummocky-cross-stratification that are intercalated with symmetrical ripple cross-laminated sandstone beds and shales, indicative of the lower shoreface. This is because the sediments had been reworked by fairweather wave-generated currents. These deposits pass up into shale-free, coarser grained, cross-bedded to parallel-laminated deposits of Lithofacies F. These are indicative of formation in the upper shoreface, due to sediment reworking by high energy fairweather wave-generated currents.

Lithofacies I rests erosively ontop of any of the previously mentioned lithofacies. It consists of a matrix supported polymict conglomerate or breccia containing lithoclasts derived from the underlying strata. This deposit has been identified as the basal part of the lithostratigraphically defined Charlie Lake Formation. The deposit was formed by subaerial exposure and subsequent erosion.

Lithofacies J, K and L sharply overly lithofacies I or H where the erosional lag is not well developed. They were deposited in a continental playa-lake depositional setting, and are not related depositionally to the prograding shoreface sequence.

The deposits comprising this vertical lithofacies association reflect a gradual shallowing of the water level indicated in part by the increased effects of fairweather wave reworking. Similar vertical sequences are formed within modern day prograding barrier-island shoreface, strandplain and wave-dominated deltaic environments (Heward, 1981).

Strandplains are sheetlike strike-elongate sand bodies developed by the successive accretion of beach ridges. Tidal-inlets are not commonly developed along a strandplain, therefore they can be ruled out as a possible environmental system for upper parasequence 4 (see Chapter 8). The lower parasequence (Pa. 3), however, contains very few, or no tidal-inlet deposits, suggesting a possible strandplain origin. If the accretion process reaches an advanced stage the strandplain can attain substantial widths, such as the Tabascan strandplain of Mexico, which is 40 km (24.5 miles) in width (Psuty, 1966). Strandplain sequences are normally less than 10 metres (33 feet) in thickness. The accretion process is attributed to storm-generated washover fans (Psuty, 1966) or to aeolian processes (Thom, 1964).

Prograding wave-dominated delta fronts have been described from Sao Francisco, Brazil, and Burdekin, Australia (Coleman and Wright, 1975). These have produced coarsening-upward sequences similar to that produced by a prograding barrier-island shoreline. Distributary channels would be expected to dissect the shoreface sequence. Channels are observed within the Peejay field. These channel fills, however, occur as isolated lenses orientated parallel to shoreline palaeostrike. Distributary channels would be oriented parallel to depositional dip and produce elongate sand ribbons. This pattern does not occur within the study area.

By process of elimination, the prograding shoreface sequence of lithofacies association 1 appears to be attributed to the regression of a barrier island shoreline. The vertical prograding barrier island sequence is similar to that described by Bernard et *al.* (1962) from Galveston Island, Texas, and Moslow (1983) from Kiawah Island, both recognized as prograding barrier island complexes. Other sedimentologic studies conducted on modern shorefaces include: the non-barred, high wave energy beachface of the Oregon coast (Clifton *et al.*, 1971) and at California (Howard and Reineck, 1981); non-barred, low wave energy shorelines at the Gulf of Gaeta in the Mediterranean sea (Reineck and Singh, 1973) and at Sapelo Island on the east coast of the United States (Howard and Reineck, 1972). Similar shoreface studies from the rock record include Hobday and Orme (1974) and Leckie *et al.* (1989).

The vertical sedimentary sequence described from the study best area fits that of low to moderate wave energy coastlines. Although storm-generated beds are frequent, background deposits are well represented throughout the sequence. The presence of symmetrical wave ripple laminated sandstones within the lower shoreface indicate that the deposits were reworked by fairweather waves representative of low to moderate energy conditions. Shale laminae within the lower shoreface, however, are suggestive of areas not reworked by fairweather waves. The presence of interlaminated sandstone and shale within the foresets of some cross-beds within the lower shoreface suggest minor tidal influences. Hence, the coastline was probably wave-dominated with respect to tidal influences. By measuring the average sediment thickness between the top of Lithofacies F (upper shoreface) and the lowest cored section of Lithofacies B (offshore) using the method outlined by Klein (1974), the minimum accommodation space of the basin was calculated at between 6.1 and 12.2 metres (20 and 40 feet). Compactional effects and erosion of the upper shoreface sediments have not been taken into account. Therefore, this is a minimum estimate.

5.2.0. LITHOFACIES ASSOCIATION 2.

The vertical lithological succession of lithofacies association 2 consists of upward-fining, cross-bedded to parallel-laminated, erosively based sublitharenites, litharenites and arenaceous biodolomicrites containing little or no shale (Figures 21 and 22). The sedimentary fill within Figure 21 is dominated by cross-bedding biodolomicrites with minor shale laminae. The deposits in Figure 22 are cross-bedded to parallel-laminated sublitharenites and litharenites. This lithofacies association has been interpreted as a tidal inlet channel fill based on the sedimentologic similarity with modern examples studied by Moslow and Heron (1978), Susman and Heron (1979), Heron *et al.* (1984), Moslow and Tye (1985) and Moslow and Heron (1989). The deposits of lithofacies association 2 occur as slightly elongate lenses (oriented parallel to depositional palaeostrike NWN-SES) cutting into and replacing the upward-coarsening prograding shoreface sequence of lithofacies association 1. This is similar to the orientation of inlet deposits observed from the aforementioned studies.

Modern tidal inlet sedimentary fills and morphologies are affected by local hydrographic regime. Modern and Halfway examples will be compared and contrasted with the aim of reconstructing the palaeohydrographical regime experienced by the Halfway shoreline within the Peejay area during Ladinian times.

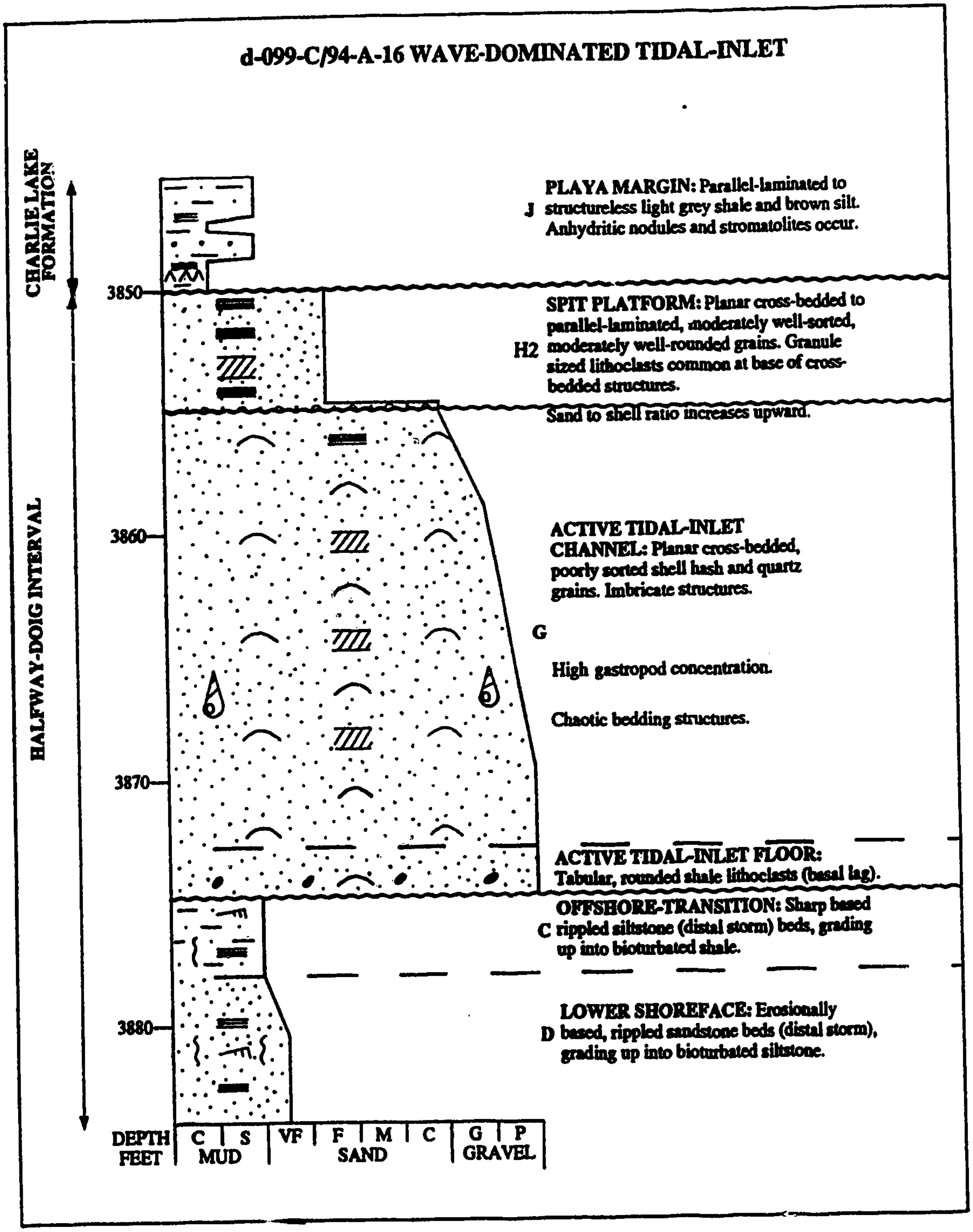

Figure 21. Lithofacies association 2 with Lithofacies G wave-dominated biodolomicrite tidal inlet channel fill deposits from the Halfway Formation, Peejay field.

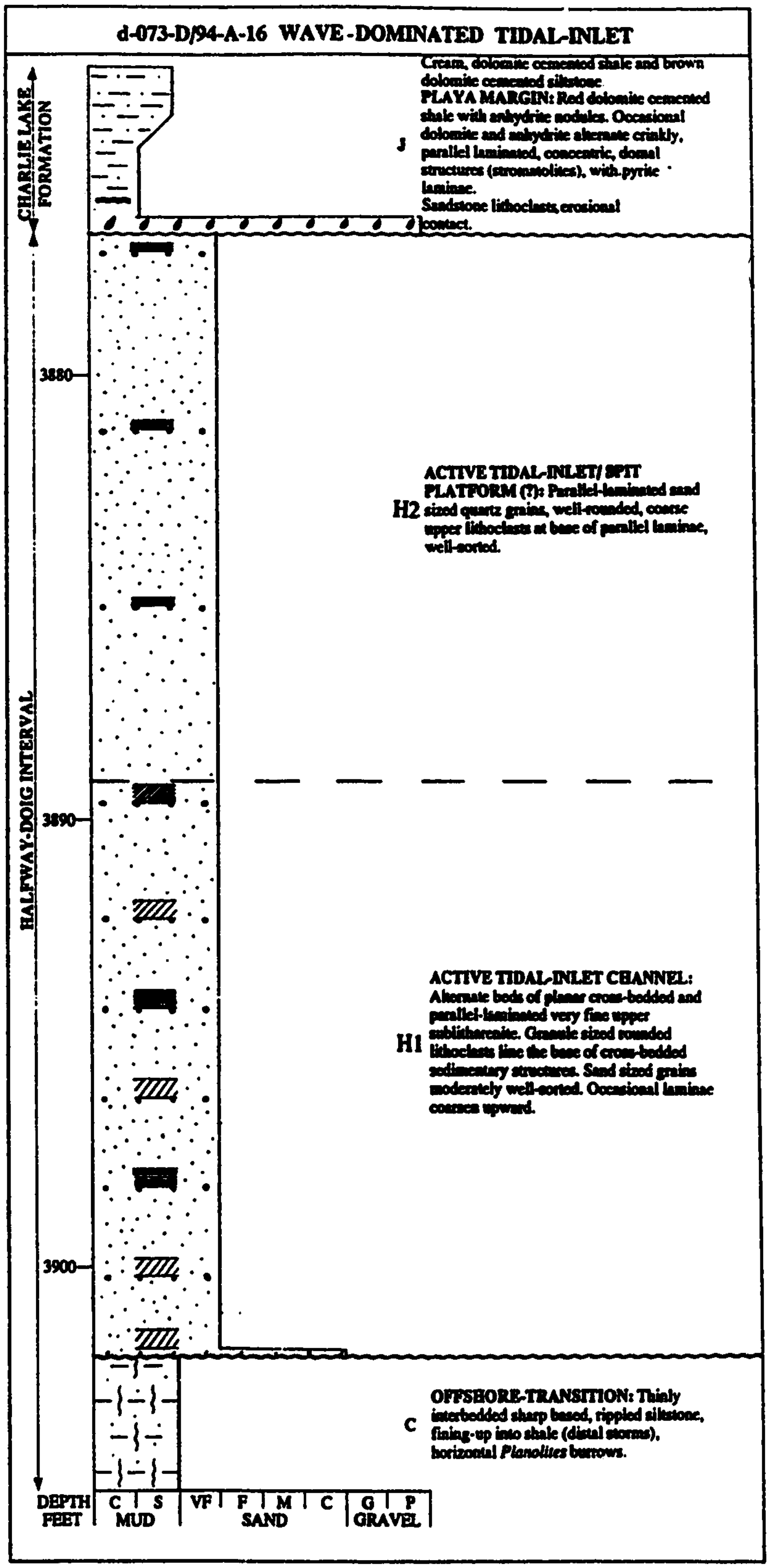

Figure 22. Lithofacies association 2 with Lithofacies H wave-dominated tidal inlet sublitharenite and litharenite channel fills from the Halfway Formation, Peejay field.

5.2.1. Variations in Tidal Inlet Sediment Fill and Morphology.

Although tidal-inlets appear to compose small regions of modern barrier-island coastlines, the corresponding inlet fills are volumetrically important in modifying the barrier island shoreline sediments. Variation in sediment fill and morphology of modern inlets have been researched from tide- and wave-dominated coastlines. Some of the documented studies are listed as follows: Kumar and Sanders (1974), Boothroyd and Hubbard (1975), Hayes and Kana (1976), Nummedal *et al.* (1977), Oertel (1977), Boothroyd (1978), Fitzgerald *et al.* (1978), Moslow and Heron (1978), Hayes (1979), Hubbard *et al.* (1979), Susman and Heron (1979), Heward (1981), Sexton (1981), Heron *et al.* (1984), Tye (1984), Moslow and Tye (1985), Moslow and Heron (1989), Tye and Moslow (1992). Results from these studies infer that wave height, tidal range, tidal prism, sediment supply and underlying strata affect the morphology and sediment fill of modern tidal inlets.

5.2.2. Tide-dominated Mesotidal Coastlines.

Tide-dominated coastlines are those where tidal action causes significant sediment transport which predominates over the effect of waves (Heward, 1981, p. 223). Mesotidal barrier island coastlines experience tidal ranges of between 2 and 4 metres. They have been documented by Hayes (1975) and Moslow and Tye (1985). The morphology of these coastlines is typically characterized by stunted, drumstick-shaped, short, wide barrier islands, separated by tidal inlets spaced about two kilometres apart (Hayes, 1975). These tidal inlets exhibit minimal amounts of lateral migration since they scour deep into the underlying strata, becoming entrenched and stable. With the additional aid from strong tidal currents, inlets migrate downcurrent less than two kilometres. Backbarrier areas are dominated by salt marsh-tidal creek environments. Ebb-oriented currents are stronger than flood-oriented currents, hence ebb-tidal deltas are more prominent than flood-tidal deltas. Alongshore currents are weak resulting in minor quantities of sediment transport parallel to the shoreline. This is also because the wave energy along these coastlines is usually low.

Tidal channel fills associated with tide-dominated shorelines are dominated by cross-bedded sand deposits, representative of the active inlet channel. These deposits pass up into mud plugs (Hayes, 1975; Moslow and Tye, 1985). The mud plug represents the abandoned phase of inlet development, associated with landward welding of swash bars;

a process know as bar by-passing. This process blocks the inlet mouth, consequently abandoning the active channel (Tye, 1984).

5.2.3. Wave-dominated Microtidal Coastlines.

Wave-dominated coastlines are "those where wave action causes significant sediment transport which predominates over the effect of tides" (Heward, 1981, p. 223). Wave-dominated coastlines are characterized by long, narrow barrier islands. These are separated by widely spaced (tens of kilometres), ephemeral, rapidly migrating inlets, that shallowly erode into the barrier island sediments (Nummedal *et al.*, 1977). These inlets migrate for large distances along the shoreline resulting in strike oriented tidal inlet fill deposits. The rate of lateral migration is dependant upon: 1.) the rates of longshore sediment transport along a wave-dominated coastline, 2.) the nature of the substrate underlying tidal inlets, 3.) the width of the barrier island (Tye and Moslow, 1992), 4.) wave climate, and 5.) possible tidal range (Hayes, 1980).

The combination of flood-oriented tidal currents and high wave energy results in the building out of lobe shaped sediment bodies landward of the main channel into back barrier lagoons. These are referred to as flood-tidal deltas. Ebb-tidal deltas developing seaward of the main inlet channel are poorly developed, as the sediment is reworked by high energy wave processes. If, however, tidal currents are more powerful than the effect of the waves (due to increased tidal prism) then ebb-tidal deltas may become exaggerated in form. Reworked ebb-tidal delta and laterally accreting spit platform sediments may become welded to the inlet mouth, reducing the tidal efficiency within the inlet and resulting in closure and abandonment (Fisher, 1962). Washover fans develop as small fan shaped accumulations of sands extending into the backbarrier lagoon. Wave built aligned beaches, recurved spits and cuspate spits are also common.

Wave-dominated tidal inlet fills contain very little shale. Typical sedimentary fills are characterized by a basal intraclastic conglomerate resulting from erosion of the underlying lithology. The conglomerate reflects the inlet floor. This passes up into cross-bedded sandstone with rare shale laminae deposited within the main active inlet channel from the migration of two- and three-dimensional bedforms. These pass up into very fine-to fine-grained spit platform sands, representing the abandoned phase of inlet development, and fine- to medium-grained overwash sands (Kumar and Sanders, 1974; Susman and Heron, 1979; Heron *et al.*, 1984; Moslow and Tye, 1985; Moslow and Heron, 1989) (Figures 23 and 24).

Lenticular to tabular shaped tidal inlet fills elongate along depositional strike are a result of the lateral migration of wave-dominated inlets along the barrier island. Rapidly migrating inlets with a high sediment supply result in thin continuous sheets of inlet fill sediments. Deeper tidal inlets will migrate at less rapid rates for shorter distances, thus producing wedge shaped cross-sections along depositional strike (Tye and Moslow, 1992) (Figure 24).

5.2.4. Halfway Tidal Inlet Fills.

Lithofacies G biodolomicritic tidal inlet fills (Figure 21) and Lithofacies H sublitharenite tidal inlet fills (Figure 22) erode into lithofacies C, D and E, all of which are grouped within the lithostratigraphically defined Halfway Formation. These are overlain by lithofacies I, J, K and L, which are part of the Charlie Lake Formation. The presence of siltstone layers between foresets within Lithofacies H cross-beds, and the presence of shale laminae between some foreset laminae of Lithofacies G, suggest that tidal processes had an important effect on the deposition of these sediments. This would rule out a fluvial origin for these channel deposits, except perhaps at a river mouth. As stated earlier, however, these channel deposits are elongate parallel to depositional strike, and not along depositional dip as would be expected by a fluvial channel. Geometrically, these deposits occur as slightly elongate but discontinuous lenses along palaeostrike. The channels had strong marine affinities as is suggested by the presence of crinoid ossicles, echinoderm fragments, bryozoan marine fauna within the coquina inlet fills. The following sedimentologic description of lithofacies association 2 displays very similar characteristics to descriptions of modern wave-dominated tidal inlet channel fills.

The characteristic vertical sedimentary sequence produced by wave-dominated tidal inlets documented at Johnson Creek, Core Banks, North Carolina (Moslow and Tye, 1985), and Beaufort Inlet, Shackleford Banks, North Carolina (Susman and Heron, 1979; Heron *et al.*, 1984) are illustrated in Figures 23 and 24. These modern fills consist of a crude fining-upward sequence of sands and shelly material. The base of the sequence is

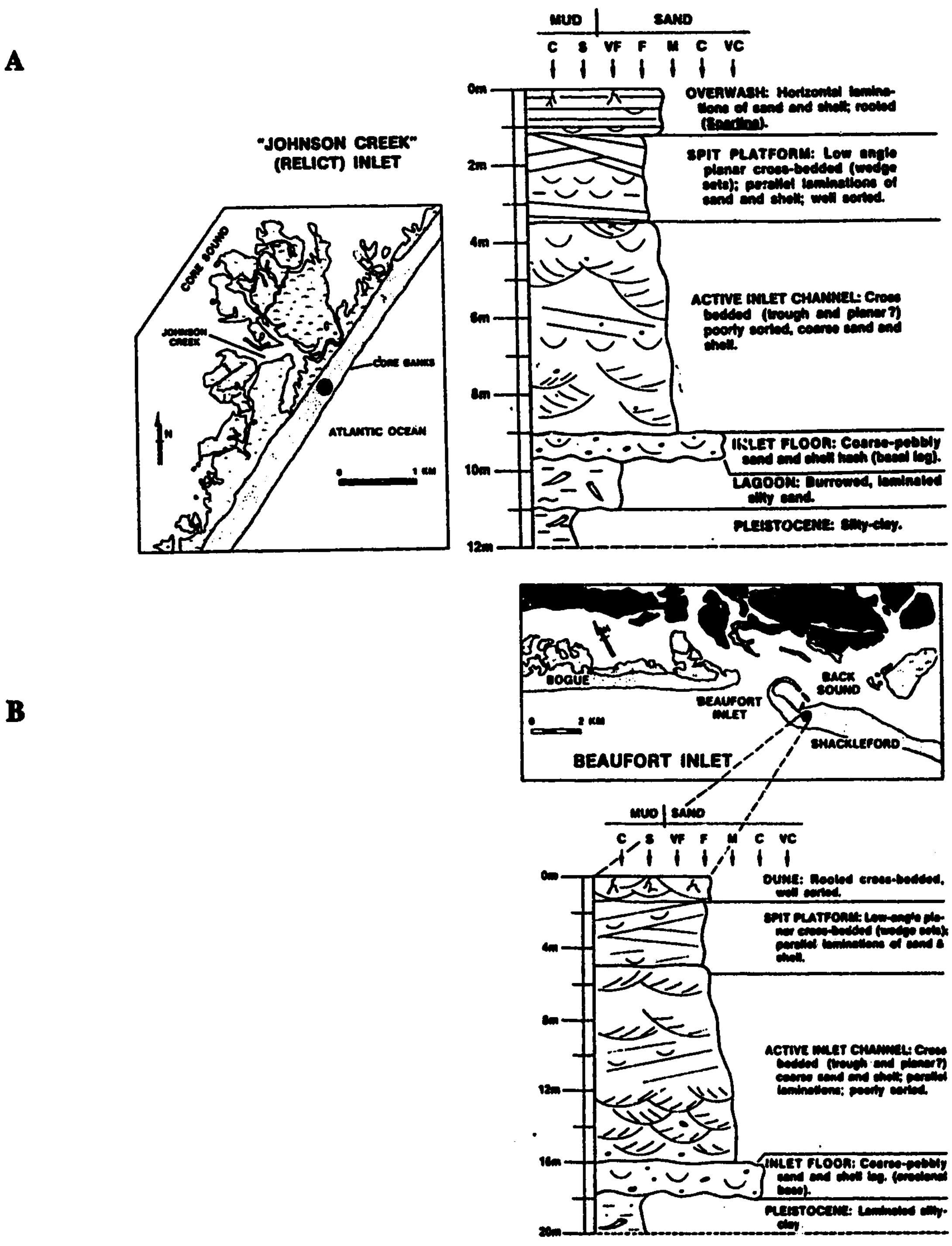

Figure 23. Recent wave-dominated tidal inlet channel fill deposits from southeastern United States. A: Johnson Creek, Core Banks, North Carolina (after Moslow and Tye, 1985) B: Beaufort Inlet, Shackleford Banks, North Carolina (after Susman and Heron, 1979; Heron *et al.*, 1984; Moslow and Tye, 1985).

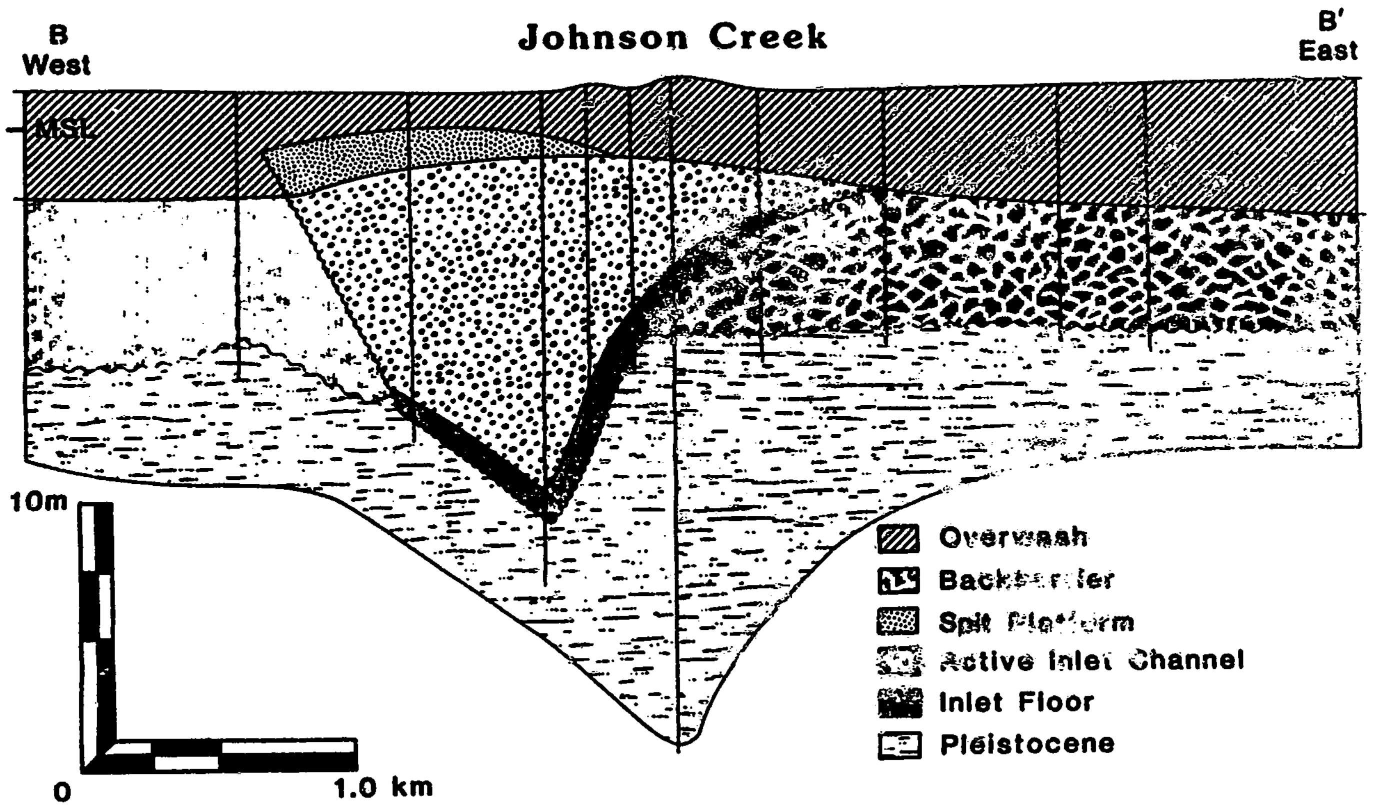

Figure 24. Cross-section (parallel to shoreline) of a wave-dominated tidal inlet fill at Johnson Creek, Core Banks, North Carolina. Note that active inlet channel sediments comprise a majority of the inlet sequence (after Moslow and Heron, 1978).

composed of 30 to 60 cms (12 to 24 inches) of coarse shell and gravel lag deposits, interpreted as the inlet floor. This material was reworked from the lithology beneath the inlet; too large to be removed from the main tidal channel by tidal currents. Shale intraclasts found at the base of Lithofacies G arenaceous biodolomicrites have been interpreted as tidal inlet floor lags (Figure 21). The inlet floor basal lag deposits are not ubiquitous within modern inlet sequences. For example, the lack of a basal lag within Captain Sam's Inlet, South Carolina (Moslow and Tye, 1985) is attributed to lack of a coarse grained source material, and from the relatively weak tidal currents occurring within the tidal inlet channel as a result of a small tidal prism. Hubbard *et al.* (1979) observed that the presence of a basal lag also depends on the position of the deepest part of the channel in relation to the shoreline. In inlets where the deepest part of the inlet is landward of the strandline, little sand enters the main channel and a lag forms. In areas where the trough is in line with, or seaward of the beach, large sand waves form. The absence of a basal lag within some Lithofacies H tidal-inlet fills are common within the Peejay field. This is attributed to the lack of shelly and coarse grained source material available from the barrier island and back barrier regions.

Moslow and Tye (1985) documented that the inlet floor gravels grade upward into trough and planar cross-bedded sandstones formed within the active tidal inlet channel at Johnson Creek (Figure 23). Cross-bedded foresets were bidirectional in places, resulting from sediment transportation by ebb- and flood-oriented tidal currents. Ripple cross-lamination occurs between cross-beds. This resulted from the migration of smaller bedforms over larger two- and three-dimensional sandwaves as a result of modification by ebb- and flood-oriented tidal-currents. Flaser-beds and clay drapes were deposited on foresets during slack water periods. This sedimentologic description is similar to that of Lithofacies G and H (Figures 21 and 22), except for the lack of mud drapes within Lithofacies H, and the lack of bidirectional foresets within both lithofacies. Infact, clay material may have settled out of suspension during slack water conditions, but was subsequently removed by the reworking effects of the next tidal current. The lack of foreset bidirectionality, as described earlier, can be attributed to the separation of flood- and ebb-dominated tidal currents into separate sub-channels, hence the limited reworking of the bedforms (Hayes, 1980; Reddering, 1983; Sha, 1990) (Figure 25). Modern wave-dominated tidal inlet sequences range in thickness from 1.5 to 10 metres (4.9 to 32.8 feet) (Kumar and Sanders, 1974; Moslow and Tye, 1985). This compares to thickness ranges within Lithofacies G and H of 1.6 to 6.1 metres (5.2 to 20.0 feet) and between 1.1 to 11.00 metres (3.6 to 36 feet), respectively. These are minimum thicknesses, however, since the Charlie Lake erosion surface has removed upper portions of the sequence. The thicknesses are however, rather similar between the ancient and modern analogues.

Very fine- to fine-grained spit platform sands and fine- to medium-grained overwash sands cap Beaufort Inlet and Johnson Creek, respectively (Figures 23 and 24). Hayes (1980) has described spit platforms as exhibiting seaward and landward directed parallel-laminated sands overlying landward and seaward oriented planar foresets. Spit platforms occupy subtidal to intertidal regions (Meistrell, 1966; Hayes 1980). The spit platforms may also form the updrift marginal flood channels which are floored with flood oriented sandwaves (Hayes, 1980). Sediment source responsible for the lateral accretion of the spit-platforms is derived from longshore-drift currents, headland beach areas, or from the tidal deltas. The continual vertical accumulation of this sediment forms a flat top on which the reworked ebb-tidal deltas and updrift recurved spits migrate onto, and ultimately infill the inlet with sand. The spit platform, therefore, represents the abandoned stage of inlet growth.

Removal of the upper part of the Halfway sequence has resulted in the preservation of only the lowest part of spit platform parallel-laminated to low-angle planar cross-bedded sandstones. In some cases Lithofacies G coquinas are overlain by Lithofacies H2 cross-bedded and parallel-laminated sublitharenites, containing subordinate quantities of shell material (Figure 21). This indicates a change in the sediment source from back barrier and offshore associated with the coquina from the active inlet channel, to one of clean sands from the depositional (updrift side) of the barrier island itself associated with the spit platform sublitharenites. Lithofacies H inlet fills are homogeneous in terms of lithology, hence it is difficult to distinguish spit platform deposits from active tidal inlet deposits (Figure 22). Wave-ripple cross-lamination and trough cross-bedding increase toward the top of sublitharenite fills. The presence of wave ripple cross-lamination indicates the reworking of sediments by oscillatory currents. This occurs within shallow regions of the spit platform where waves entering the inlet channel become refracted so that they are sub-parallel to the inlet bank. Trough cross-bedding is indicative of the lower portions of the spit platforms where lateral migration of three-dimensional large ripples across the avalanche surface of the spit platform occurred.

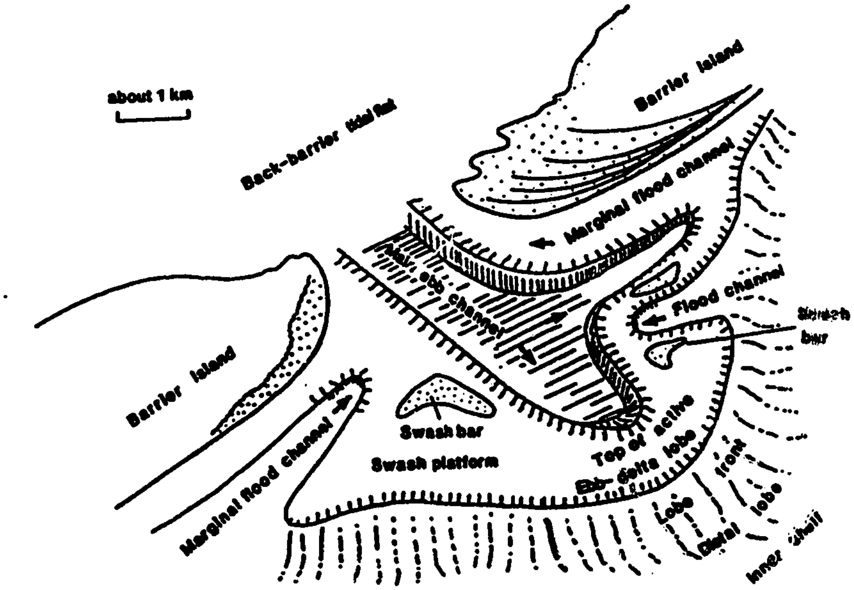

Figure 25. Spatial relationship of ebb- and flood-orientated tidal currents within a modern tidal inlet from the Frisian Islands. The main ebb channel is dominated by ebb-orientated tidal currents, whereas flood-orientated tidal currents occur within the laterally adjacent marginal flood channels (modified from Hayes, 1980; after Sha, 1990).

The description of ancient tidal inlet sequences are similar to the inlet fill deposits of lithofacies association 2. These studies include: Hobday and Orme (1974), Hobday and Horne (1977), Barwis and Makurath (1978), Uhlir *et al.* (1987) and Cheel and Leckie (1990).

5.2.5. Vertical and Lateral Relationship of Halfway Tidal Inlet Fills.

Lithofacies relationships between lithofacies G and H tidal inlet fills are important to understand in terms of depositional processes, in order to predict and model the performance of inlet reservoirs within the Peejay field.

There are a number of different vertical relationships between lithofacies G and H. The most common type of inlet sequences found within the eastern part of the study area are shown in Figures 21 and 22. Figure 21 shows the common occurrence of thick biodolomicrites indicative of an active inlet channel, overlain by sublitharenites of Lithofacies H2 interpreted as spit platform deposits. These are similar to the Holocene inlet fills of Johnson Creek, Core Banks, North Carolina (Moslow and Heron, 1978; Moslow and Tye, 1985; Moslow and Heron, 1989). Figure 22 illustrates an inlet fill dominated by sublitharenites, interpreted as forming the active inlet channel and the overlying spit platform. These fills are similar to those described by Kumar and Sanders (1974) from Fire Island, New York state. Within the western part of the field, additional lithofacies relationships have been recognized. The most common type of relationships consist of basal 1 to 2 feet thick biodolomicrites, overlain by a much thicker sequence of sublitharenites. The former have been interpreted as the inlet floor lags, whereas the latter are indicative of the active inlet channel (Kumar and Sanders, 1974; Susman and Heron, 1979; Moslow and Tye, 1985). Finally, there are thick sequences of sharp based biodolomicrites that grade up into sublitharenites. These two lithofacies are interbedded. Similar recent inlet fills have been described from Beaufort Inlet, Shackleford Banks by Susman and Heron (1979) and Heron *et al.* (1984) and from Bogue Inlet by Steel (1980) and Moslow and Heron (1989). This lithofacies relationship was formed due to the continual reworking of older inlet fills by younger inlets, resulting in the stacking nature of the deposits; the biodolomicrites representing the base of each inlet.

Temporally, these inlet fills were formed coevally since different inlet fills described above occur within the same shoreface deposits. The only reason for the variation in inlet fill is from the derivation of the source material. Where concentrated shell mounds in the back barrier regions were reworked by tidal currents, resultant inlet fills were dominated by bioclasts (Moslow and Heron, 1978; Moslow and Heron, 1989). However, in regions where source material was devoid of shell material except for calcium-phosphate Lingulid fragments (whether it was derived from a back barrier region or from reworked shoreface sediments), the resulting inlet fill was also devoid of shell material. Spit platform deposits were derived from shell-free barrier island sediments or sourced from alongshore current transportation. There has been no recognition of two or more different vertical successions composing one inlet fill within the Peejay field. Each inlet fill appears to be discrete and is not laterally correlatable.

Lithofacies H is the most wide spread reservoir lithofacies within the study area (Figure 26). It is concentrated in two north-south oriented belts in the eastern part of the study area., and occurs as north-south oriented isolated lenses within the western part of the field. Pressure and production information clearly demonstrates that the deposits are well connected in a north-south orientation. The isolation of these deposits into linear belts is associated with an early Carnian episode of faulting that removed much of the "Halfway" reservoir deposits (see Chapter 9). The north-south orientation of these deposit is a direct result of lateral migration of wave-dominated tidal inlets along the palaeoshoreline (NWN-SES). The biodolomicritic tidal inlet fill deposits are much less abundant and are thinner than the sublitharenite deposits (Figure 27).

The rate of shoreface progradation to the west-southwest occurred on a much greater time scale than the rate of lateral migration of the tidal inlets. A modern example from Kiawah Island demonstrates that the shoreface has prograded 0.5km in at least 1000 years (Moslow, 1980), whereas wave-dominated tidal inlets have been recorded as migrating at rates of 64 metres per year at Fire Island, New York (Kumar and Sanders, 1974). Lateral migration of these tidal inlets occurs geologically instantaneously. Hence, the resultant vector of tidal inlet channel fill orientation, taking inlet migration and shoreface progradation into account, would be parallel to depositional strike of the shoreline.

n and
nel fill

A

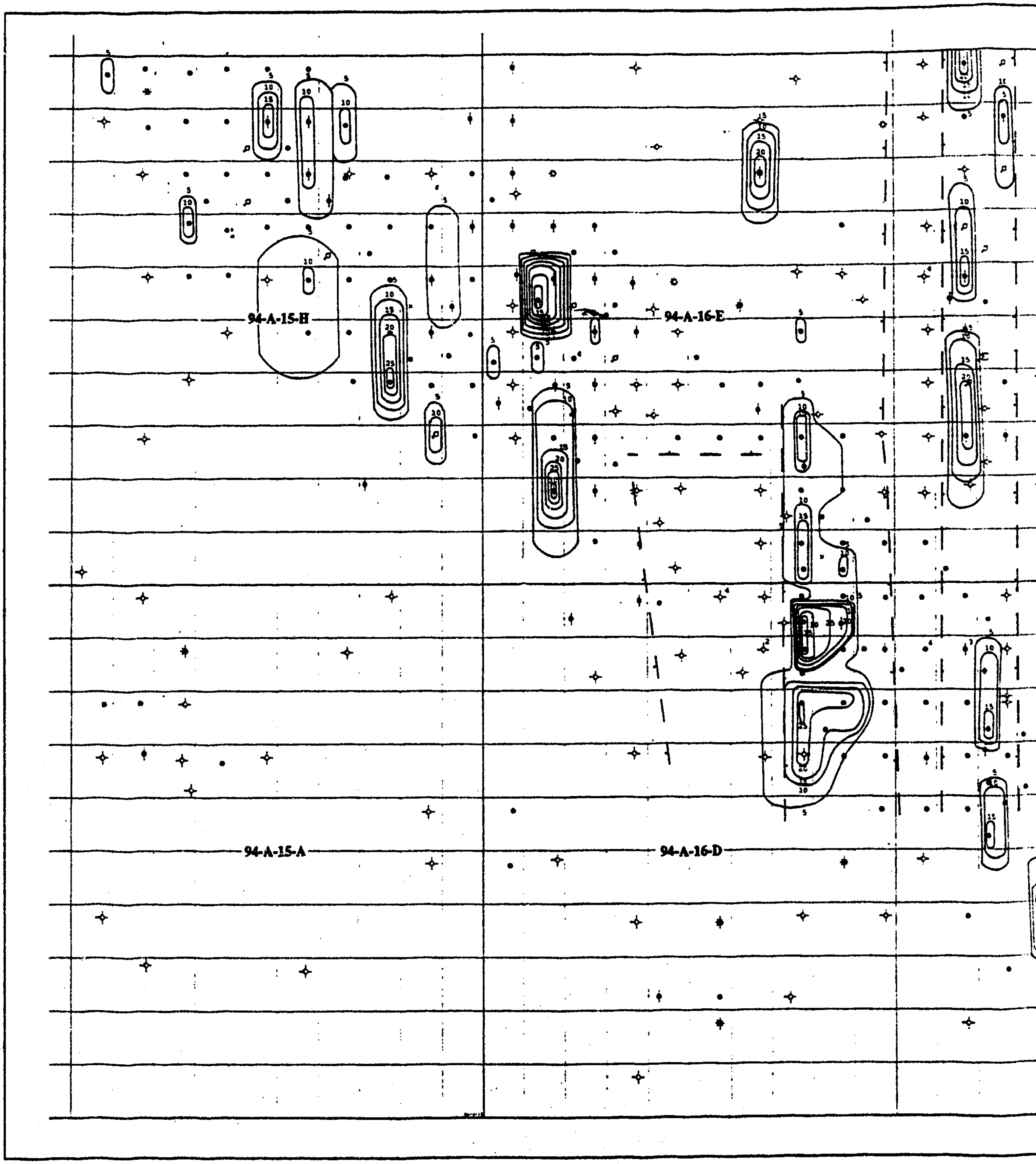

tion and
hannel fill

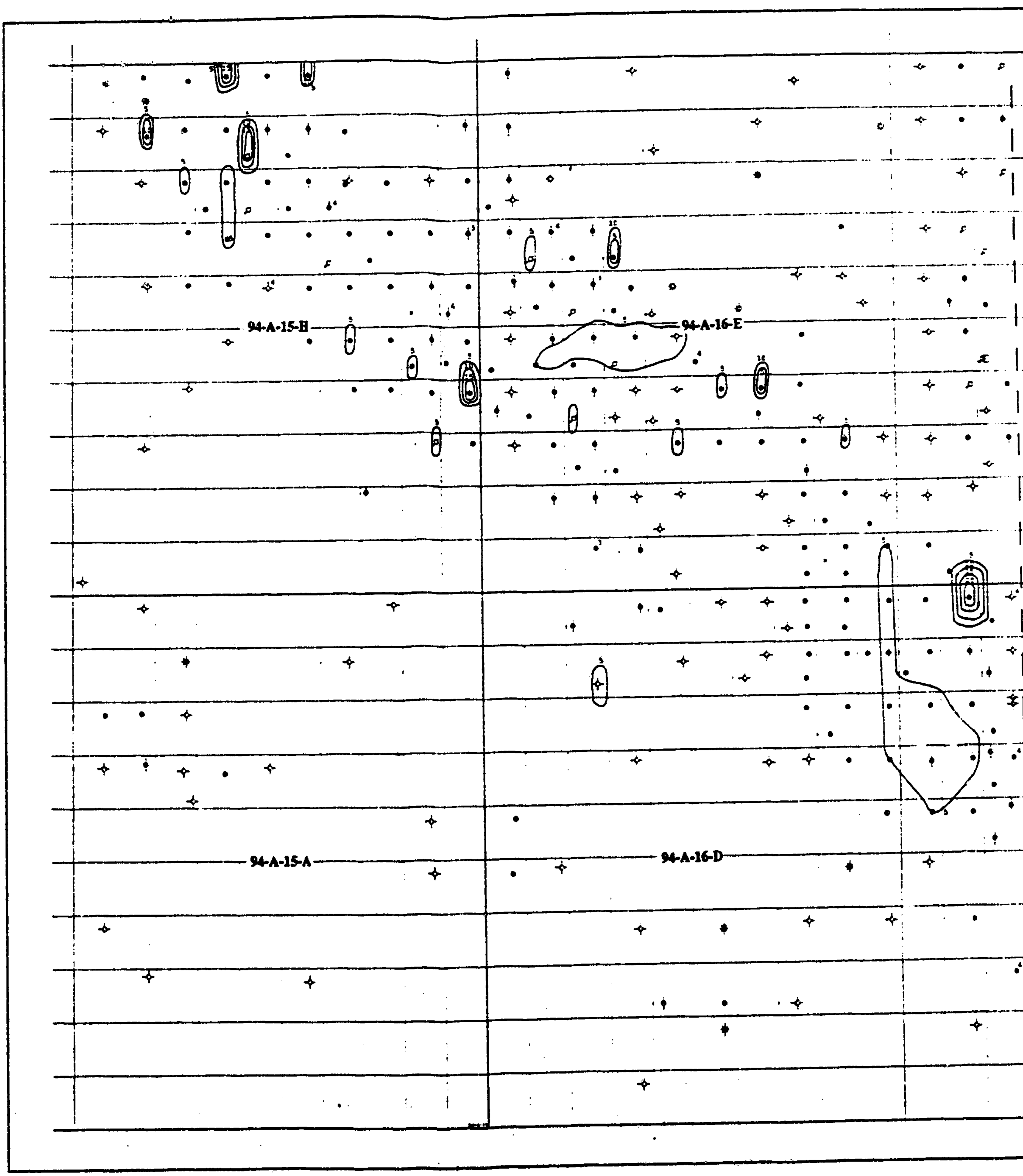

BIA
F
SITS

6.0.0. RESERVOIR QUALITY.

In order to understand and predict the gross diagenetic effects and explain the reservoir behaviour, petrographic examination of each reservoir lithofacies will be described at the micro-scale. This will not only involve the description of the texture and mineralogy, but definition and quantification of pore types, and a detailed paragenetic sequence of events terminating with the present petrophysical attributes of each reservoir lithofacies. Each reservoir lithofacies will then be studied in detail, on a bed-by-bed basis at the meso-scale, in order to observe local heterogeneities in reservoir quality with respect to subtle variations in depositional fabric. The macro-scale factors involve studying the thickness and gross diagenetic effects of the reservoir lithofacies. Pertinent to this is the accurate identification and interpretation of each reservoir lithofacies. Heterogeneities in reservoir quality between the reservoir lithofacies will also be addressed.

Permeability and porosity appear to be closely related. Both appear to increase in value at similar rates. Figure 28 illustrates the positive correlation between the two parameters for Lithofacies H, sublitharenite tidal inlet fill deposits. As primary intergranular effective porosity increases (the most abundant type of porosity within Lithofacies H), pore throat diameter also increases while pore corridor tortuosity decreases. These changes in pore morphology and connectivity tend to increase permeability values.

6.1.0. MICRO-SCALE PETROGRAPHICAL ANALYSIS.

All thin-sections were impregnated with blue epoxy resin to highlight porosity. They were also stained with Alizarin-Red-S to highlight non-ferroan calcite (red colour) and non-ferroan dolomite (white/clear colour). Potassium ferricyanide stains were added to highlight ferroan calcite (mauve colour) and ferroan dolomite (blue colour).

Three reservoir lithofacies have been identified and described within the Peejay study area. These are: Lithofacies F upper shoreface sublitharenites and tempestite biodolomicrites; Lithofacies G biodolomicrite tidal inlet fill deposits; and Lithofacies H sublitharenite and litharenite tidal inlet fill deposits and spit platforms. Thin-section samples have been described for the sublitharenite and biodolomicrite upper shoreface and tempestite deposits of Lithofacies F. Four thin-sections were studied from the biodolomicrite tidal inlet channel fills of Lithofacies G. A total of fifteen thin-sections

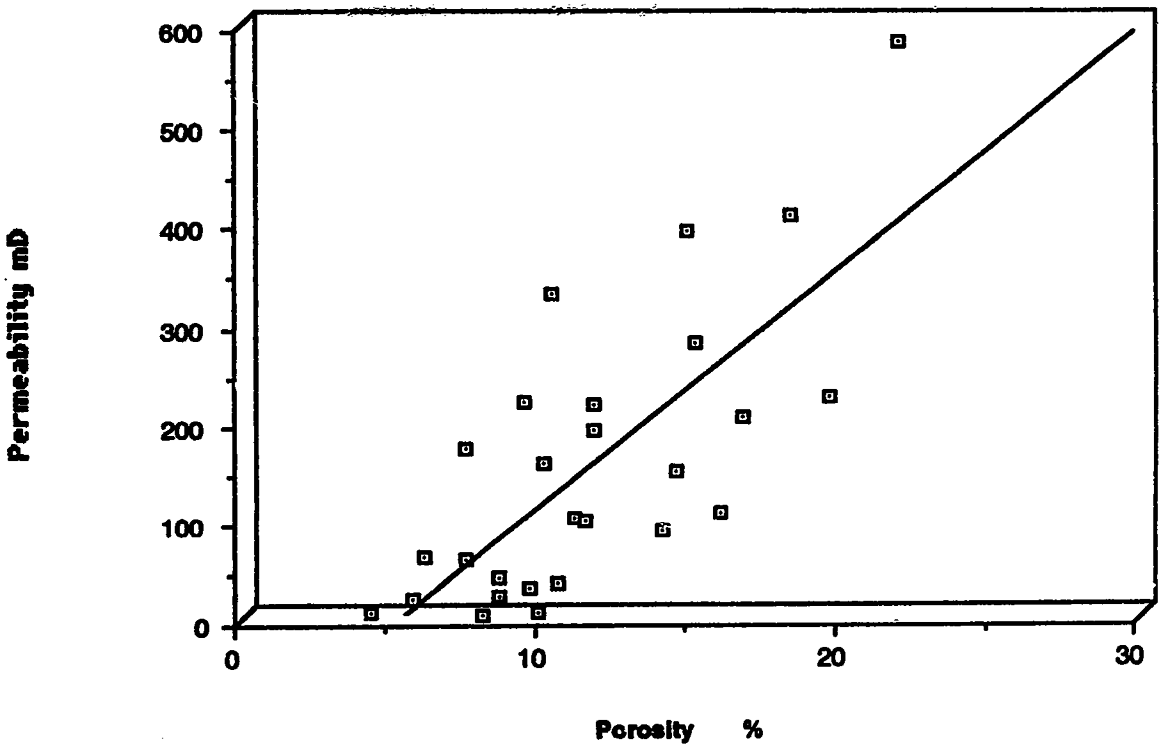

Figure 28. Graph illustrating the correlation between permeability and porosity core plug measurements for Lithofacies H, sublitharenite tidal inlet channel fill deposits from the study area.

were examined in detail from the sublitharenite and litharenite tidal inlet channel fills of Lithofacies H. Thin-section samples were taken from different spatial and areal locations, in order to observe lateral heterogeneities in reservoir quality, and to demonstrate the increase in scale of destructive effects in reservoir quality resulting from the influences of percolating brine solutions originating from the overlying Charlie Lake evaporitic deposits. This will be expanded upon in section 6.6.

6.1.1. Detrital Grains.

The detrital grains of Lithofacies H were plotted on a ternary petrographic classification diagram (Chen, 1968) (Figure 29). Lithofacies H deposits plot within the litharenite and sublitharenite category. The detrital percentage of quartz grains range from 53% to 85%, feldspar detrital grains ranging from 1% to 3.4% and lithoclasts (rock fragments) ranging from 16% to 47%. These deposits are compositionally immature. Table 5 shows the quantitative values for detrital grains and cements from lithofacies G and H. No quantitative values are available for Lithofacies F.

QUARTZ: The grain size of the quartz particles varies from very fine lower to medium lower within lithofacies G and H. Locally they are moderately- to well-sorted and are sub-rounded in Lithofacies H. They are poorly to moderately well-sorted and are sub-angular to well-rounded within Lithofacies G and very-fine lower to upper sand sized, moderately well-sorted and moderately well-rounded within Lithofacies F. Monocrystalline quartz grains rarely contain vacuoles or microlites. Polycrystalline quartz grains display sub-grains that vary in size, display sutured contacts and exhibit undulose extinction.

FELDSPAR: Average grain size is very-fine lower. Just over two-thirds of them are plagioclase feldspars displaying albite twinning. Eighty percent of the plagioclase feldspars are labradorite ($Ab_{50}An_{50}$ to $Ab_{30}An_{70}$). Labradorite is commonly derived from basic igneous rocks. Twenty percent of the plagioclase feldspars are bytownite ($Ab_{30}An_{70}$ to $Ab_{10}An_{90}$), commonly derived from basic and ultra-basic igneous rocks. The remaining one-third of the feldspars are potassium rich microclines, displaying the characteristic cross-hatch twinning. Some of these microcline feldspars have been partially to heavily weathered along their cleavage planes to form linear, thin regions of

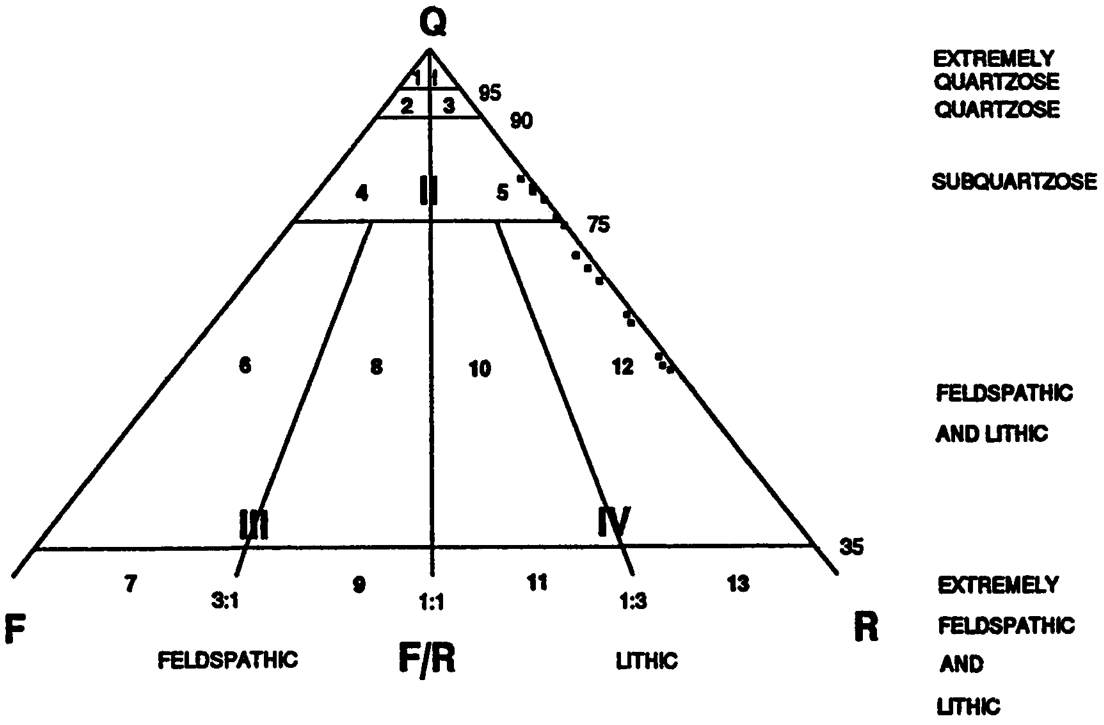

I QUARTZOSE SANDSTONE

II SUBQUARTZOSE SANDSTONE

III FELDSPATHIC SANDSTONE

IV LITHIC SANDSTONE

● Petrographical Classification

1 PURE QUARTZARENITE

2 FELDSPATHIC QUARTZARENITE

3 LITHIC QUARTZITE

4 SUBARKOSE

5 SUBLITHARENITE

6 ARKOSE

7 EXTRA-ARKOSE

8 LITHICARKOSE

9 EXTRA-LITHICARKOSE

10 FELLITHARENITE

11 EXTRA- FELLITHARENITE

12 LITHARENITE

13 EXTRA- LITHARENITE

Figure 29. Ternary petrographic classification diagram showing that Lithofacies H samples plot within the sublitharenite and litharenite sectors (after Chen, 1968).

Lithofacies Lithology Environment	G Biodolomicrite Tidal inlet channel	H Sublitharenite/ Litharenite Tidal inlet channel
Quartz		
monocrystalline	96-100	77-100
polycrystalline	0-4	0-23
non-undulose extinction	10-79	42-88
undulose extinction	21-90	12-58
Feldspar	None	Tr. La.80, By.20
Glauconite	None	Tr.
Amphibole	None	Tr.
Zircon	None	Tr.
Dolomicrite	1-2	1-8
Chert	1-3	1-14
Weathered Chert	1	1-4
Phosphate-Peloids	1-2	1-2
Phosphate-Oolites	Tr.	1-5
Phosphate-Lingulids	Tr.	1-3
Sandstone	2	Tr
Bioclasts	>50	None
Silica	1-6	5-24
Non-ferroan calcite	3	1-34
Ferroan calcite	None	1-3
Non-ferroan dolomite	63-73	1-52
Ferroan dolomite	5	1-6
Anhydrite	4	1-5
Clay	None	4-6
Pyrite	Tr.	1-10
Bitumen	2-13	1-23

Table 5. Bulk sample composition of detrital grains and cements from reservoir lithofacies G and H from the study area. (No values for Lithofacies F are available).
Tr. Trace (<1%), La. Labradorite, By. Bytownite. All values are ranges quoted in percent.

illitization, or almost total illitization in the mature stages of the process. These potassium feldspars commonly originate from low temperature, acid igneous granites and pegmatites.

TRACE MINERALS: The remaining trace minerals are very well-rounded glauconite, amphibole, and zircon. These occur within lithofacies G and H. Possible sources for the latter two trace minerals were originally acid igneous rocks.

The above detrital grains indicate two possible original sources for the sediment. One is a low temperature igneous plutonic source, such as a granite or pegmatite. This is suggested by the presence of dominantly non-undulose monocrystalline quartz grains, microcline potassium feldspar and accessory zircon minerals. Subordinate sources were from basic igneous rock, as suggested by the presence of the plagioclase feldspars and amphibole. It is possible that these grains are of second cycle formation, having been sourced from exposed sedimentary rocks to the northeast (Gibson and Barclay, 1989; Gibson and Edwards, 1990).

LITHOCLASTS: The lithoclasts are dominantly coarser grained than the quartz grains, reaching granule size within each reservoir lithofacies. They mainly occur in discrete layers. They are all very well-rounded and moderately- to well-sorted. There are six types of lithoclasts: dolomicrite, chert, weathered chert, phosphate peloids, quartz-arenite and shale.

Dolomicrite lithoclasts are composed of dolomite crystals ranging in crystal size from cryptocrystalline to microcrystalline. Dolomite preferentially replaces micrite sized crystals (<4 microns in diameter), therefore it is inferred that some dolomicrite lithoclasts were originally carbonate mud (micrite), probably sourced from a back barrier lagoonal environment. In cross-section these lithoclasts form near perfect circles or are ovoid due to lithostatic compaction. In rare cases, ghost structures can be observed in the form of shell fragments and undissolved quartz grains 'floating' within the dolomicrite. This suggests that a coquina may be another possible lithological precursor. Other dolomicrite lithoclasts appear to have partially replaced precursor phosphate lithoclasts.

There are examples whereby an original host fabric in the form of a regular grid-iron structure representing possible organic origin, occurs within dolomitised rectangular allochems. These particles are similar in appearance and shape to echinoid plates. Other dolomitised fragments are completely circular with a singular circular shaped pore at the centre that is usually occluded with cement. These rare fragments may have originally been crinoid ossicles. From the above description it may be incorrect to classify every dolomicrite allochem as a lithoclast, however, dolomitisation has commonly eradicated all precursor traces, therefore these grains are classified as lithoclasts.

Chert lithoclasts are coarse sand to granular in size (Plate 36). They are clear to brown under plane-polarized-light probably due to the presence of organic material, iron and clay inclusions. They have a microcrystalline internal fabric displaying low order whites and greys. Some chert fragments are cryptocrystalline and are black under cross-polars. They are well-rounded and do not appear to have suffered compactional effects. Closed secondary fractures infilled with chalcedony cement occur within some chert lithoclasts. Other chert lithoclasts have been partially replaced with chalcedony displaying the characteristic radiating fabric in cross-polars. The boundaries of some chert grains have embayments caused by pressure solution of these areas by more resistant quartz grains, due to lithostatic compaction. Chert could have been derived from chert beds sourced from further down in the Triassic stratigraphic section, or as is suggested by Gibson and Barclay (1989), from Permian formations exposed to the northeast. The latter is more likely as the chert grains are well-rounded having been subjected to long periods of reworking.

Weathered chert grains are coarse upper to granular well-rounded lithoclasts. These lithoclasts are brown in plane-polarized-light and appear isotropic in cross-polars. They contain clay, iron and organic inclusions. Although they can appear rounded in shape they may also be irregular or ovoid in shape due to lithostatic compactional effects. Internally they are subject to partial to almost complete removal by weathering or dissolution forming intra-constituent porosity. These grains may have high internal capillary effects, thus capturing minor amounts of irreducible water.

Phosphate grains are coarse upper to granular in size and are very well-rounded. In plane-polarised-light the phosphate is brown in colour and probably contains clay, organic and

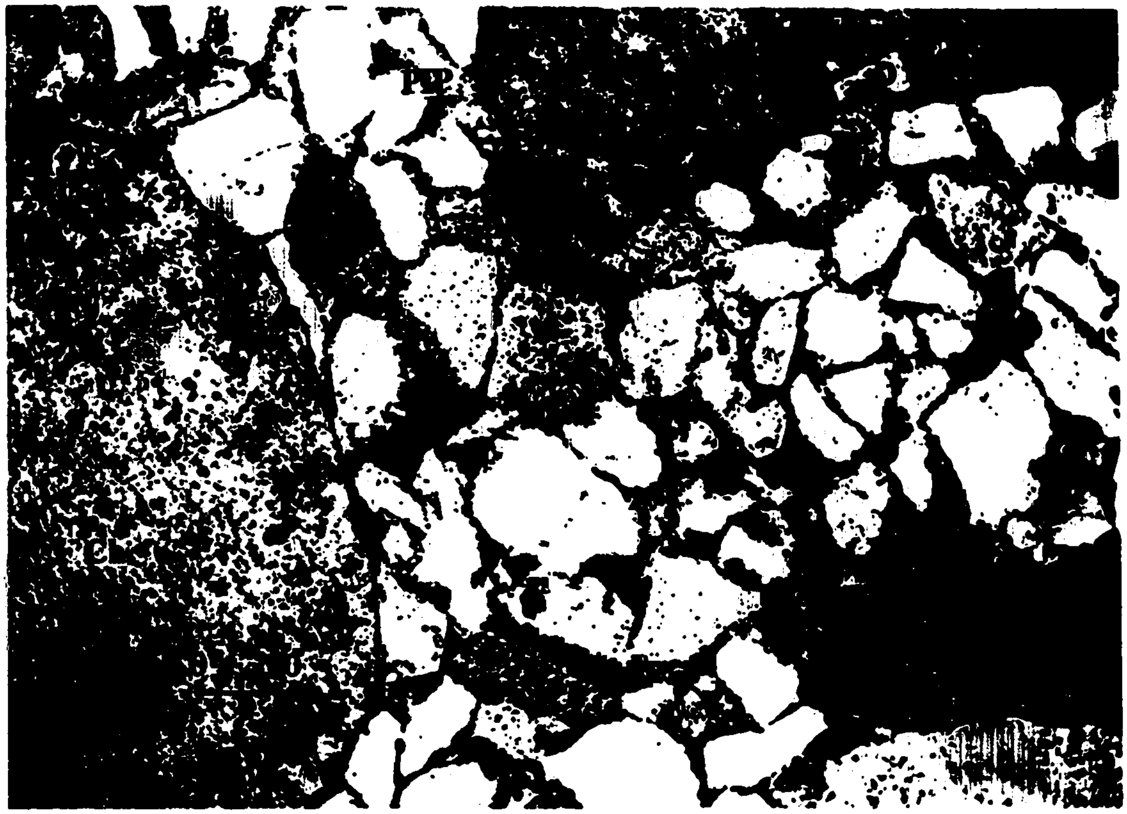

PLATE 36. d-003-E/94-A-16. PPL. x100. 3845 feet. K-max 189mD. Ø 21.1% (derived from core analysis). Lithofacies H. Left hand-side shows a granule sized, well-rounded chert lithoclast (Ch) with inclusions of organic material and pyrite. Upper-right-hand rim of chert lithoclast has been deformed by quartz indentation, resulting from mechanical compaction. Angular, mechanically deformed phosphate lithoclast (Ph) occurs at top-centre. Dolomite replacive cement (D) occurs at bottom-centre of the lithoclast. Quartz grains demonstrate little or no authigenic cement, therefore, there is little chemical and mechanical compaction. Primary intergranular porosity (PIP) is well developed. Microcrystalline dolomite crystals rim most grains reducing intergranular porosity by small amounts. (Scale in microns).

iron inclusions. It has been identified as collophane in composition, i.e. carbonate fluorapatite (Gibson, 1975). In cross-polars the phosphate appears isotropic and black. There are many different types of phosphate grains within these reservoir lithofacies. Some phosphate grains are very well-rounded and circular in shape (Plate 37). Internally they are structureless and are known as phosphatic peloids. It has been documented that similar modern phosphatic material grows by accretion at the sediment-water interface with or without a nucleus, and becomes broken up into pellets and peloids by storm action (Baturin and Bezrukov, 1979; Birch, 1980). Some phosphate lithoclasts have no internal structure, but have a nucleus composed of an agglomeration of quartz grains that have been cemented by phosphate. These lithoclasts have similar origins to those mentioned previously. They may have been transported landward by palaeo-oceanic currents or storm-generated currents.

Phosphate also occurs in forms other than lithoclasts. It can occur as phosphatic oolites (Plate 37). They have a similar internal structure and morphology to the classic carbonate oolites (Plate 38). They are well-rounded, circular in shape, and have a concentric cortex of phosphate surrounding a nucleus composed of a single or multiple quartz grains and/or calcium-phosphatic shell fragments (Plate 38). Some phosphatic oolites share the same nucleus. These oolites have suffered mechanical compaction. Shearing between the concentric laminae and along fractures radiating out perpendicularly from the centre of the oolite have resulted in fragmentation and flattening (loss of original shape) of the oolite due to reduction in internal strength (Plate 38). Clay inclusions are strikingly obvious in cross-polars since they parallel the concentric laminae of the cortex.

It has been documented by Sheldon (1981) that similar phosphatic oolites occur off the present day west African and South American coasts. There is a controversy in current literature as to whether similar modern day phosphatic ooliths are primary or secondary in origin. Cook (1976) suggested that the phosphatic oolites found off the present day coasts of West Africa and South and Central America are not primary in origin, but are the replacement of calcareous oolites. Phosphatic oolites have been found forming along the modern intertidal regimes of the South Africa coast (Birch, 1980). These were formed by authigenic precipitation a few centimetres below the water/sediment interface. Gibson (1975) has documented that phosphatic oolites were formed by phosphatisation of calcareous oolites within the Liard Formation of northeastern British Columbia.

PLATE 37. d-068-C/94-A-16. PPL. x100. 3898 feet. K-max 98mD. Ø 13.4% (derived from core analysis). Lithofacies H. The light brown coloured, well-rounded grains are phosphate (Ph). The central- and lower-left-hand-side displays grains that are composed of a nucleus and cortex, incorporating inclusions. These are termed phosphatic oolites (Ph O). The middle-left-hand grain is a phosphate lithoclast. All grains, including quartz, are surrounded by a thin rim of isopachous dolomite cement (D). This cement may originally have been a calcitic marine cement, precipitated in the eodiagenetic realm, close to the sediment surface. Primary intergranular porosity has been eradicated by glauconitic(?) cement Gl). Pyrite crystals preferentially precipitate over this cement. (Scale in microns).

PLATE 38. d-003-E/94-A-16. PPL. x100. 3848 feet. K-max 110mD. Ø 19.9% (derived from core analysis). Lithofacies H. Lower left is a phosphatic oolite with a quartz nucleus (Ph O). Right of centre is a mechanically deformed phosphatic oolite (Ph Om) with a calcium-phosphatic bioclastic fragment forming the nucleus. Fracturing occurs at right-angles to the cortex layering. Primary effective intergranular porosity is infilled with bitumen (black) (B). (Scale in microns).

Calcium-phosphatic skeletal material occurs in each reservoir lithofacies. These shell fragments are Lingulid, inarticulate brachiopods (Plate 39). These commonly occur within brackish water environments ranging from subtidal to intertidal. The internal laminae are parallel-laminated and are composed of alternate layers of calcium and more phosphatic material. These parallel laminae have been sheared off during lithostatic compaction.

Other lithoclasts of trace amounts are quartz-arenite and shale. The quartz-arenite lithoclasts are well-rounded and granule in size. They are composed of varied sized sub-grains (Plate 40).

Bioclasts originally comprised at least 50% of Lithofacies G, but have since been dolomitised. Shell material varies from whole to comminuted and ranges in size from less than a millimetre in length to more than twenty five millimetres in length. The deposit is therefore poorly-sorted. The shell material is commonly oriented in parallel-laminations, but locally may be disoriented. The shell material was originally packed close together, with shell-to-shell contacts being common (plates 41 and 42). Micritised bryozoan have also been found.

6.1.2. Diagenetic Processes.

Diagenetic processes affecting reservoir lithofacies F, G and H are mechanical compaction, chemical compaction, cementation and solution. The first three are the most important within lithofacies F and H, whereas solution and cementation are of importance within Lithofacies G.

MECHANICAL AND CHEMICAL COMPACTION: The visible effects of mechanical compaction are seen as fractures within phosphate oolites and Lingulid skeletal fragments, and as internal deformities and indentations within ductile weathered chert lithoclasts. Mechanical compaction has altered the grain fabric and reduced the primary porosity of the deposits. The grains have become packed closer together resulting in narrower pore throat corridors, and tortuosity of the pore corridors increasing within the litharenites and sublitharenites. These compactional effects are best observed at the margins of detrital grains. The thin-section analyses in Appendix B illustrate quantification of the frequency of grain-to-grain contact types. These contact types are

PLATE 39. d-063-D/94-A-16. PPL. x100. 3909 feet. K-max 153mD. Ø 20.7% (derived from core analysis). Lithofacies H. Effective primary intergranular porosity (PIP) has been well developed. Authigenic quartz cement (AuQ) is limited due to low chemical and mechanical compaction. A thin veneer of clay particles (C) rim the grains and cement. Lower-centre of the photomicrograph is a phosphate lithoclast (Ph). Centre of plate shows parallel layered calcium-phosphatic inarticulate brachiopod bioclasts (Ph Bio). Mechanical compaction has fractured this bioclast. Centre right shows poikilitic occluding anhydrite cement (A). (Scale in microns).

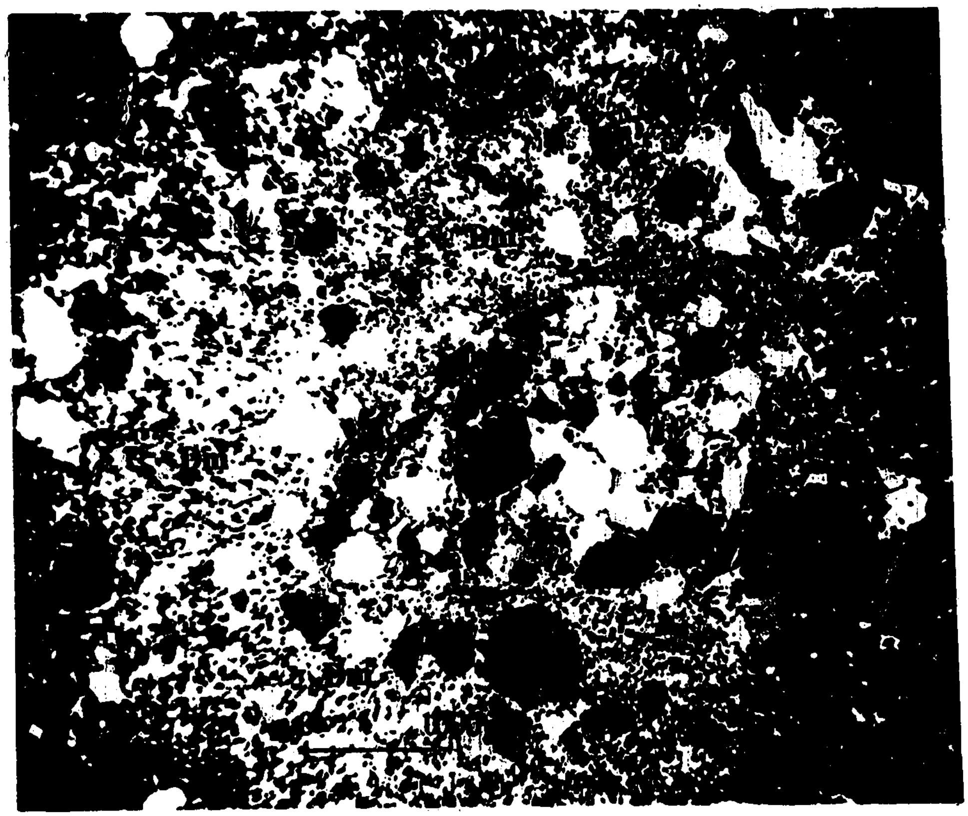

Plate 40. XPL. x25. d-099-C/94-A-16. Lithofacies G. Well-rounded quartz-arenite lithoclast within a dolomicrite cement (Dm). (Scale in microns).

PLATE 41. b-045-E/94-A-16. PPL. x100. 3802 feet. K-max 914mD. Ø 27.5%. (derived from core analysis). Lithofacies G. Ghost structures of the original bioclasts (Bcl) are clearly recognizable, packed close together. Most resultant biomolds (Bp) are only partially infilled with zoned ferroan and non-ferroan dolomite crystals (D). Matrix material has also been dolomitised (D). Biomolds are lined with a thin veneer of bitumen (B). (Scale in microns).

PLATE 42. b-045-E/94-A-16. REFLECTED LIGHT. x100. 3802 feet. K-max 914mD. Ø 27.5% (derived from core analysis). Lithofacies G. The same microphotograph taken under reflected light highlights the ghost structure of the bioclast material. Bioclasts (Bcl) were aligned parallel, with bioclast-to-bioclast contacts common. Bitumen lining is also accentuated (B). (Scale in microns).

tangential, planar, concavo-convex, and sutured in ascending order of lithostatic compaction. Most of the deposits analysed appear to be low to moderately compacted in which grain-to-grain contacts are either dominantly tangential or planar.

The amount of syntaxial silica cement appears to be proportional to the amount of compaction. This is due to the higher frequency of grain-to-grain contacts within more compacted deposits. This is known as chemical compaction (Plate 43). As lithostatic pressure increases the mineral of one or both adjacent grains will go into solution and migrate a short distance before reprecipitating in areas of low pressure as a syntaxial cement. Hence, concavo-convex contacts commonly have no syntaxial cement, however adjacent to this region the cement reprecipitates and forms a limited coating around the free part of the grain (Plate 43).

Compaction within Lithofacies G is minor resulting in poor development of authigenic silica cement. Internally open dolomitised shell tests have been broken due to compaction, however weathered chert grains have not been deformed.

CEMENTATION: Authigenic silica cement is the dominant cement type within the sublitharenites and litharenites of lithofacies G and H. The quantity of silica cementation is regulated by lithostatic compaction (see previous section). Silica cement comprises between 5% (d-088-F/94-A-16) and 24% (d-063-D/94-A-16) of the bulk sample composition. It occurs mainly in the form of an authigenic quartz syntaxial overgrowth cement (Plate 43). This cement is in optical continuity with the quartz grain on which it reprecipitates. Recognition of this cement is established by the identification of a thin veneer or coating of high birefringent material on the surface of the grain before the syntaxial cement phase occurs. The other indication is that the outer surfaces of the cements have straight edges with enfacial angles at 120°, giving the quartz grain an angular appearance. The quartz crystals are euhedral to anhedral in form. Where quartz and calcite cement are adjacent the crystal faces of the quartz cement have been modified by dissolution, becoming jagged and irregular in appearance. These authigenic crystals have the effect of reducing porosity, pore throat diameter and increasing tortuosity of the pore corridor. They do not appear to occlude porosity however, as the quartz grains are spread wide enough apart to inhibit complete cementation. This cement may occur as thin rims in Lithofacies G or may not occur at all.

PLATE 43. d-063-D/94-A-16. PPL. x100. 3909 feet. K-max 153mD. Ø 20.7%. (derived from core analysis). Lithofacies H. Photomicrograph showing good primary effective intergranular porosity (PIP). Minor amounts of authigenic quartz overgrowth cement (AuQ). The cement has straight edges demonstrating the primary formation of the porosity. (Scale in microns).

Feldspathic syntaxial overgrowth cements occur in trace amounts, reprecipitating on the feldspar grain surface.

Non-ferroan sparry calcite cement occurs mainly in trace amounts. Most calcite crystals are anhedral and poikilitic, infilling primary intergranular pores. They are limited in spatial distribution, engulfing a small area of detrital grains. The best development of calcite cement occurs in d-088-F/94-A-16, where it forms anhedral to euhedral poikilitic crystals which occlude porosity (Plate 44). These poikilitic crystals commonly corrode the outer margins of quartz grains or their overgrowth cement producing an irregular appearance to the quartz external morphology. Alternatively, calcite crystals may completely replace grains (mainly dolomicritic grains) leaving behind the trace of a ghost structure.

Calcite, non-ferroan, anhedral, sparry cement partially or totally infill biomolds, vugs and granomolds in Lithofacies G (Plates 45). Calcite cement also partially or totally infills shrinkage cracks developed within the dolomitised matrix.

Ferroan sparry calcite cement is most abundant in d-088-F/94-A-16, where it occurs in alternate zones with non-ferroan anhedral to euhedral calcite crystals. Both types of poikilitic calcite crystals tend to eradicate porosity locally, thus increasing pore corridor tortuosity. This cement does not, however, reduce the overall porosity dramatically except in d-088-F/94-A-16 where it is widespread.

Non-ferroan dolomite crystals are microcrystalline, euhedral and rhombic in shape. They occur as pore rimming cements that narrow but not completely occlude porosity within lithofacies F and H (Plate 46). They are commonly observed replacing quartz overgrowth cements.

This type of cement is very common in Lithofacies G. Dolomitisation primarily effects aragonitic or high-magnesium shell material and finer sized crystals, hence the preferential dolomitisation of the bivalve shell tests and the possible micrite matrix. The dolomite cement ubiquitously recrystallizes the shell material. Ghost structures of the original shell boundaries are still observable within the dolomite crystals (plates 41, 42 and 47). They appear as dark dusty rims within the dolomite crystals. These crystals

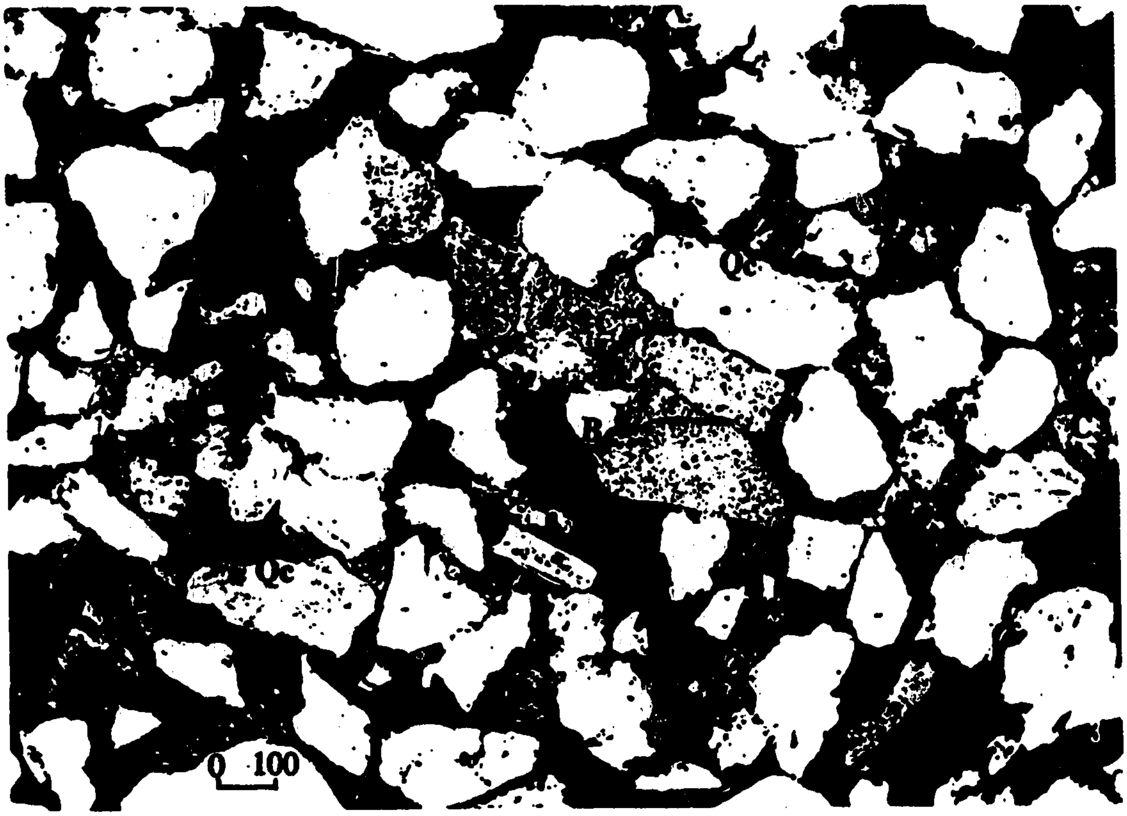

PLATE 44. d-088-F/94-A-16. PPL. x100. 3707 feet. K-max 12mD. Ø 8.4%. (derived from core analysis). Lithofacies H. Intergranular porosity has been eradicated by widespread pore occluding anhedral non-ferroan calcite cement (C). Bitumen (B) infills the remaining primary effective intergranular porosity. Boundaries of the quartz grains and cement are jagged due to corrosion (Qc). (Scale in microns).

Plate 45. d-024-E/94-A-16. PPL. x25. 3751 feet. K-max 369mD. Ø 20.6%. (derived from core analysis). Lithofacies G. Photomicrograph illustrating the occlusion of biomoldic porosity by anhedral, poikilitic non-ferroan calcite crystals (C). The biomold to the left is coarsely ribbed. Late stage pyrite crystals (P) grow over the calcite cement. Dolomicrite cement (Dm) surrounds the biomold. Intercrystalline (InX) and shrinkage porosity (S) is developed within the dolomicrite cement, and is lined with bitumen. (Scale in microns).

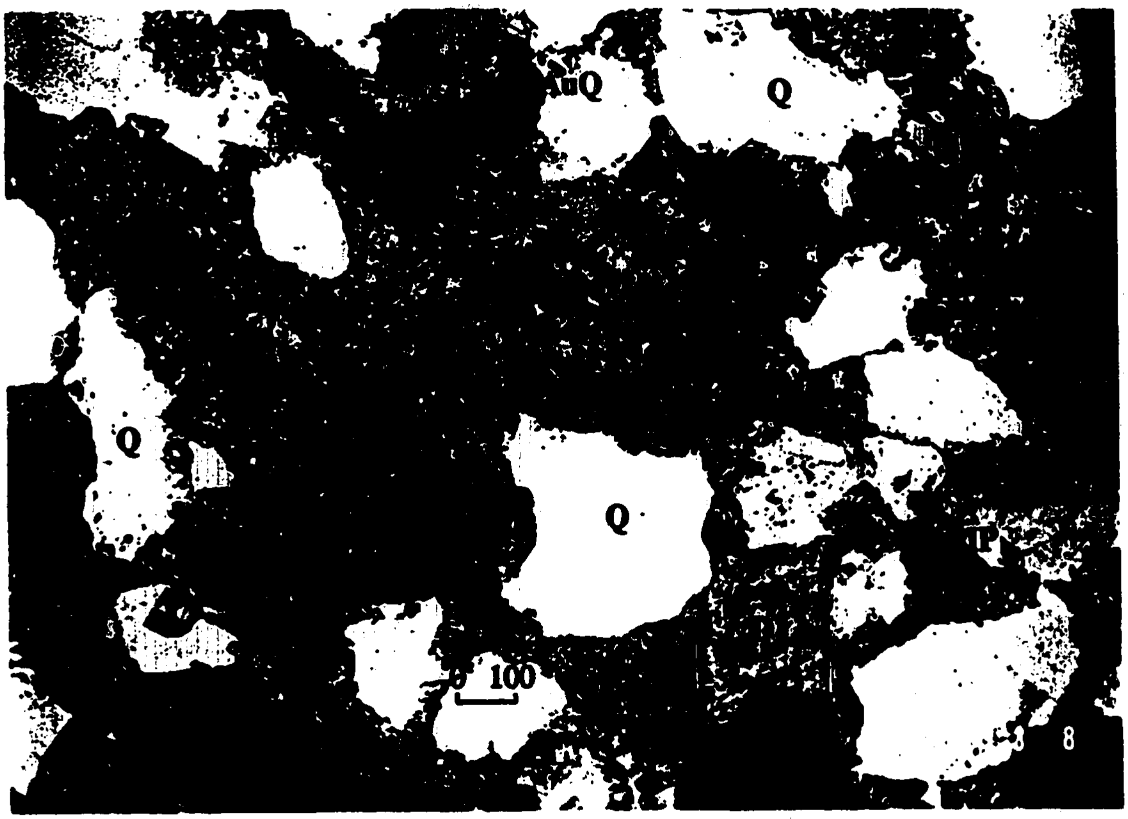

PLATE 46. b-045-E/94-A-16. PPL. x100. 3807 feet. K-max 266mD. Ø 15.9%. (derived from core analysis). Lithofacies H. Photomicrograph showing quartz grains (Q) on which authigenic quartz cement (AuQ) has been precipitated. This is rimmed with dolomite anhedral microcrystalline cement (Dim). Original primary intergranular porosity (PIP) is still recognizable between some crystals. Dolomite crystals replace authigenic quartz cement. Lower-right shows a euhedral zoned rhombic shaped dolomite crystal (D) replacing the surrounding dolomite. Left-hand-side shows the dissolution of lithic grains. Bitumen cement thinly rims all porosity types. (Scale in microns).

Plate 47. PPL. x250. Lithofacies G. Close-up illustrating the coeval nature of dolomitisation of the micritic matrix material and the molluscan tests, since the same dolomite crystal overgrows the shell margin and matrix material (arrow). Impurities (I) in the original shell material show up as a dark band outlining the original shell shape. (Scale in microns).

partially or totally infill the biomolds. Dolomite crystal size increases toward the centre of the pore. Dolomite crystallization of the matrix material is mature in its development. Sucrosic dolomite textures occur within the recrystallized matrix and shell material. The original matrix material is patchily distinguishable. It appears to be composed of micritic slightly deformed lithoclasts. Reflected light microscopy does not reveal any ghost structures of quartz grains within the recrystallized matrix suggesting three possibilities. Firstly, there were never very many quartz grains within the matrix; secondly, the quartz grains comprising the matrix material have all been dissolved and recrystallized by dolomite; thirdly, the matrix material was composed of compressed micritic lithoclasts, the boundaries of which have been destroyed during the process of compaction. Micritic lithoclasts have been observed within Lithofacies G suggesting that the third possibility is more accurate. These micritic lithoclasts could have been sourced originally from back barrier lagoons.

There are trace amounts of larger euhedral non-ferroan dolomite rhombic crystals. These tend to replace any grain or cement. Trace amounts of ferroan dolomite euhedral coarse rhombic crystals are also present. These crystals again replace any grain or cement, locally eradicating porosity. Internally they display a compositional zoning structure of non-ferroan rhombic dolomite in the core and are surrounded by ferroan dolomite, and rimmed with non-ferroan dolomite producing the final anhedral to euhedral crystal shape. Each zone appears to be slightly corroded. This may result from the chemical imbalance and subsequent reaction between the fluid chemistry and the outer rim of the previously precipitated zone until chemical equilibrium is restored. These late-stage crystals internally rim biomolds in Lithofacies G.

Anhydrite cement is recognizable in cross-polars by its high order green, pink, yellow, and blue birefringent colours and cleavage planes orientated at right-angles. It occurs as patchily distributed euhedral to anhedral poikilitic crystals which locally eradicate effective porosity. Internally they contain occasional ghost structures of original grains that have been replaced. Anhydrite cement may also occur as isolated nodules replacing and engulfing grains.

Trace amounts (0.8%) of gypsum crystals closely associated with the anhydrite occur. They display low-order grey and white colours in cross-polars. During lithostatic burial the hydrated atomic lattice of gypsum crystals was probably dehydrated, thus transforming the hydrous gypsum crystals to dehydrated anhydrite crystals. Due to the shallow depth to which the deposits have been buried this transformation process has not been complete, resulting in occasional apparently unaltered gypsum crystals closely associated with anhydrite crystals. Anhydrite and its closely related gypsum cements either partially or totally infill biomolds, or occur as poikilitic crystals infilling vuggy porosity or secondary intercrystalline porosity in Lithofacies G. They may also occur as isolated nodules.

Pyrite crystals occur as patchy framboidal crystal forms and are euhedral in shape. They commonly grow over any grain or cement, and may locally reduce effective porosity if they grow within pores. Probable microcrystalline ferruginous inclusions are also found within phosphatic, chert and weathered chert lithoclasts.

Clay particles (illite?) occur as thin pore rimming cements. The clay is light brown in colour under plane-polarised-light. It is a cement as opposed to a matrix material as it coats quartz cement surfaces as well as grains.

Bitumen occurs as a sticky tar-like substance that coats the grains and pores thus reducing porosity. In places, it completely eradicates porosity thus producing uncharacteristically low sonic log readings. Bitumen may also fill pores developed within partially weathered weathered chert lithoclasts. It also infills biomolds within Lithofacies G.

SOLUTION: Solution effects are minor within lithofacies F and H. The only visible signs of solution occur at the rims of some quartz overgrowth cement surfaces. This solution usually occurs adjacent to, or in contact with, poikilitic calcitic cement (Plate 48). The precipitation of calcite cement is from alkaline pore fluids, while quartz precipitates from acidic pore fluids. When the two minerals, or a quartz mineral and an alkaline fluid should come in contact a chemical reaction occurs between them resulting in slight dissolution of the quartz.

Dolomite rhombs are also observed at various maturity stages, replacing quartz overgrowth cement as well as lithoclasts of chert and phosphatic material.

Solution has been much more prevalent in Lithofacies G. The original shell material was predominantly bivalves with minor Lingulid fragments. The tests of Lingulids have not been altered diagenetically due to their collophane (calcium fluorapatite) chemical composition. Fragments of coarse ribbed bivalve shell material have been found displaying bilateral asymmetry characteristic of most bivalve tests. The chemical composition of these mollusc tests was originally aragonite or high-magnesium calcite. This would have been rapidly converted to low-magnesium calcite. At a later stage the shell material was dolomitised. This process involves carbonate ions being taken into solution and immediately incorporated into a new dolomite crystal lattice. Lithoclasts of weathered chert are also partially to completely removed by solution forming granomoldic and intra-constituent porosity.

6.1.3. Porosity Types.

There are two main types of pores classified according to time of formation. They are termed primary and secondary porosity. The former type is developed during deposition of the sediment, whereas the latter is produced after deposition and is attributed to diagenetic processes, namely, cementation, dehydration and solution. Table 6 quantitatively summarizes the various porosity types occurring within lithofacies G and H. Primary intergranular effective porosity occurring within the sublitharenites and litharenites of lithofacies F and H is responsible for between 50% and 100% of the augmented pores, but is of minor importance in Lithofacies G. Primary intergranular pores are spaces developed between grains during deposition. This porosity may have originally been as high as 44%, but has subsequently been reduced by diagenetic processes. Lithostatic compaction will produce a tighter fitting grain fabric. This porosity is further reduced by the development of a syntaxial overgrowth cement. Pore passages become more tortuose and pore throat diameters become narrower as cementation increases in quantity.

Secondary porosity types are of minor importance within lithofacies F and H, but are more important in Lithofacies G. Granomoldic porosity develops due to the complete solution of weathered chert and other soluble lithoclasts and grains. The resulting pores may be catenary or closed depending on whether there is a pore occluding cement surrounding the dissolved grain. The granomold may be further reduced by later mechanical compaction.

Reservoir Lithofacies	G-Biodolomicrite	H-Sublitharenite
Intergranular Porosity	None	55-100
Intercrystalline Porosity	47-96	13
Biomoldic Porosity	4-55	None
Granomoldic Porosity	9-20	7-42
Intra-constituent Porosity	18	1-9

Table 6. Quantitative comparison of porosity types between lithofacies G and H within the study area. All values are ranges of porosity expressed in percent. Note that primary effective intergranular porosity is the most abundant porosity type in Lithofacies H. Secondary intercrystalline and biomoldic porosity types are the most abundant porosity types within Lithofacies G.

Intra-constituent secondary porosity develops within partially dissolved grains or lithoclasts. This pore type commonly occurs within weathered chert lithoclasts. The internal honeycomb morphology of the porosity may develop into minor cavities if dissolution continues. Intra-constituent porosity is also developed between the cortex concentric laminae of the phosphatic oolites, and between the alternate parallel layers of calcium and phosphatic layers within Lingulid shell fragments. This occurs mainly as a result of mechanical compactional stresses.

The main type of porosity developed within Lithofacies G is secondary intercrystalline porosity. This porosity comprises between 47% and 96% of the sample. It forms by replacement of the calcite lattice on a molecule-by-molecule basis to form the dolomite crystals. This results in a reduction in bulk volume by 12 to 13% producing intercrystalline porosity. The porosity is effective and is associated with good permeabilities as interconnectivity is high between the crystals. Tortuosity of pore corridors is low. This porosity is widespread in location occurring within the matrix and biomolds. Not all dolomitised areas of the samples are characterised by intercrystalline porosity since the dolomite crystals grow resulting in reduction and eradication of pores.

Secondary biomoldic porosity is the next most abundant porosity type in Lithofacies G comprising between 4% and 54.5% of the samples. It may or may not be effective. If the dolomitised shell material is whole then the internal biomoldic porosity is ineffective, and therefore useless with respect to storing fluids. Biomoldic pore size may be further reduced by the continued occluding effects of dolomitisation which may completely occlude biomoldic porosity, or may leave small areas of secondary biomoldic porosity at the centre of the biomold (Plate 41). Within these biomolds porosity types will be a combination of secondary infilling biomoldic porosity, and toward the centre where dolomite crystals are widely spaced, intercrystalline porosity is developed.

Vuggy porosity comprises a minor part of Lithofacies G and is usually derived from dissolution of biomolds. Shrinkage porosity is also developed within the dolomitised matrix material. These microfractures have been infilled with bitumen or calcite cement (Plate 45). All pore types are lined with bitumen. Bitumen may totally eradicate the intercrystalline porosity. Biomoldic porosity may or may not be lined with bitumen. This depends on whether it is effective or ineffective, respectively. Intercrystalline pores develop within a dolomicritic matrix, and result in good connectivity and permeability between biomolds. Biomolds separated by a dense dolomite cement form an ineffective porosity, thus although porosity may be high permeability may be very poor.

6.1.4. Paragenetic Sequence.

The diagenetic regime experienced by all the reservoir lithofacies is mesodiagenetic; in other words, diagenetic processes resulted from the effects of burial. The deposits within this study area have reached the semi-mature burial diagenetic stage (Schmidt and McDonald, 1983). This is petrographically distinguished by the effects of mechanical and chemical compaction. These tend to reduce primary porosity. Chemical compaction occurs due to pressure solution of quartz grains at grain contacts. Rock volume and porosity are subsequently diminished. These samples have not reached the maximum level of chemical compaction and cementation, hence, the irreducible porosity value has not been reached. The paragenetic sequence describes the series of diagenetic events through geological time from deposition of the sediment to the present semi-mature diagenetic stage (Figure 30).

The paragenetic sequence of lithofacies F and H are similar. The first stage of diagenesis involved mechanical compaction of the detrital grains due to burial. This resulted in a lowering of primary intergranular effective porosity values, slight rotation and reorientation of the grains, and deformation of the more ductile lithoclasts, especially the weathered chert grains. Greater lithostatic stresses resulted in increased grain contact stresses. This produced pressure solution of the quartz grains resulting in the initiation of the chemical compaction process. The quartz was locally reprecipitated as quartz syntaxial overgrowth cement. This had the tendency of reducing rock volume and primary intergranular porosity. As a result pore throat diameters decreased with a subsequent increase in pore corridor tortuosity thus reducing permeability.

The next diagenetic process involved the occurrence of a thin pore lining clay cement. The source of this cement may be from the limited illitization of the feldspars, or sourced from outside the lithofacies. This further reduced primary intergranular porosity in specific areas. Secondary ineffective and effective granomoldic porosity was then produced by the dissolution of weathered chert and other unidentified lithoclasts. The pore fluids may have been slightly alkaline in order to dissolve the siliceous lithoclasts.

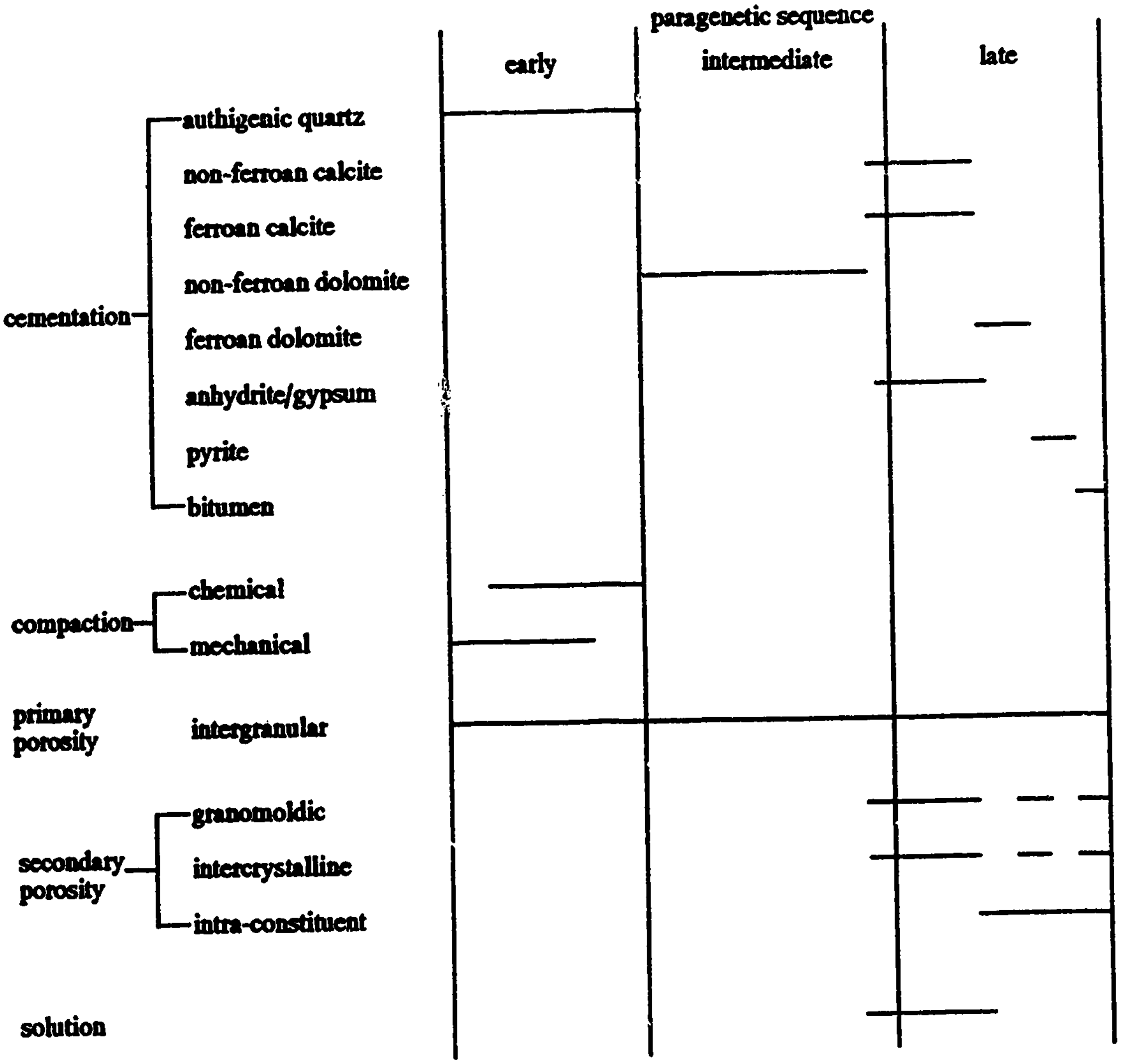

Figure 30. Diagram illustrating the paragenetic sequcnce within lithofacies F and H.

There is no widespread corrosion of the quartz cement as it still exhibits straight faces growing into the pores. The introduction of varying amounts of euhedral grain rimming, isopachous, rhombic shaped, secondary dolomite crystals occurred. In other samples the dolomite crystals were closely packed together, thus secondary or altered primary intercrystalline porosity was not developed. The source for the dolomite crystals may have been from dolomite cement and dolostone from within the Charlie Lake Formation. Alternatively, expulsion of formation water carrying elements conducive to the formation of dolomite may have been derived from 'Doig' shales below.

The next diagenetic event involved the precipitation of non-ferroan poikilitic patchy calcitic cement. This locally reduced or eradicated primary intergranular porosity. During this event the boundaries of quartz grains and cements suffered minor corrosion as a result of chemical reaction with the alkaline pore fluids. The carbonate ions may have been sourced from the dissolved shell tests within Lithofacies G. Alternatively, the carbonate may have been sourced from within the Charlie Lake Formation. Further to the north, within the Crush field, the quantity of this carbonate cement increased dramatically resulting in loss of primary intergranular porosity. Iron ions were introduced into these pore fluid. Varying iron content of the pore fluids has been displayed as zoned ferroan and non-ferroan layers within the calcite cement. It is assumed, petrographically, that the calcite cementation in both geographical regions is related paragenetically. Anhydrite (gypsum?) was precipitated as a poikilitic pore occluding patchily distributed cement on termination of calcite cementation. The Ca atoms may have originated from the continual dissolution of the remaining calcium shell material. The S atoms may have originated from the liberation of elemental sulphur by sulphate reducing bacteria. Alternately, the anhydrite may have originated from brine solutions percolating down from within the Charlie Lake Formation, above. The latter can be demonstrated by the increased frequency and quantity of anhydritic cement as the Charlie Lake contact is approached.

The next stage involved the precipitation of euhedral, isolated, zoned, rhombic shaped dolomite crystals. The internal zonation displays alternate layers of ferroan and non-ferroan dolomite. Thus pore water chemistry may have varied with respect to iron content. These pore fluids may have originated from deep sources that rose up through the stratigraphic column along faults, or by expulsion from shales. The liberation of iron from the ferroan dolomite and calcite, and sulphur from the anhydrite or sulphate reducing bacteria, may have been sources for the precipitation of framboidal patchy non-fabric selective pyrite crystals, distributed throughout the lithofacies. The final stage of diagenesis resulted in bitumen migration into the lithofacies along with lighter hydrocarbons resulting in a cessation of the diagenetic series of events since it plugged up porosity allowing no further fluids from migrating into the deposits.

Figure 31 displays the paragenetic sequence of events that affected Lithofacies G. The first stage in the paragenetic sequence involved the mechanical compression of sediments as burial increased. This resulted in the deformation of micritic lithoclasts forming a micritic matrix. There is no evidence of eodiagenetic cementation. The ensuing cementation occurred during burial of the sediments; in other words during the mesodiagenetic stage. Slight chemical compaction is evidenced by the existence of limited quartz syntaxial overgrowth cement. Initial primary porosity was probably very low. This stage was followed by widespread dolomitisation of the shell material, matrix micritic lithoclasts and echinoderm fragments. Internally, the shell material was locally left free from dolomitisation resulting in secondary effective and ineffective biomoldic porosity. The dolomitisation resulted in a volume reduction of the deposit and the consequent development of secondary intercrystalline porosity within the matrix, and to a minor extent within the biomolds. Localised vuggy porosity was developed concurrently with intercrystalline porosity due to high amounts of local matrix shrinkage.

The next stage involved the dissolution of weathered chert lithoclasts resulting in granomolds rimmed with dolomite crystals. Poikilitic non-ferroan and ferroan calcite cement later infilled biomolds, intercrystalline and vuggy pores. In other areas, or separate samples, anhydrite cement locally occluded biomoldic porosity and formed replacive nodules within the sucrosic dolomite cement. Nowhere do these two poikilitic cements occur within the same pore, therefore, it is difficult to conclude which cement type occurred first. The anhydrite cement appears to have become more abundant toward the top of the Halfway Formation, indicating that it was sourced from pore waters within the Charlie Lake Formation. Larger sized, euhedral, rhombic shaped, zoned ferroan and non-ferroan dolomite crystals occur in minor amounts as a late stage cement. They were non-fabric selective with respect to the crystallizing medium. The iron-rich pore water, responsible for the limited late stage dolomitisation, may have originated from deep seated, oxygen poor sources, rising up along fault planes. The penultimate diagenetic

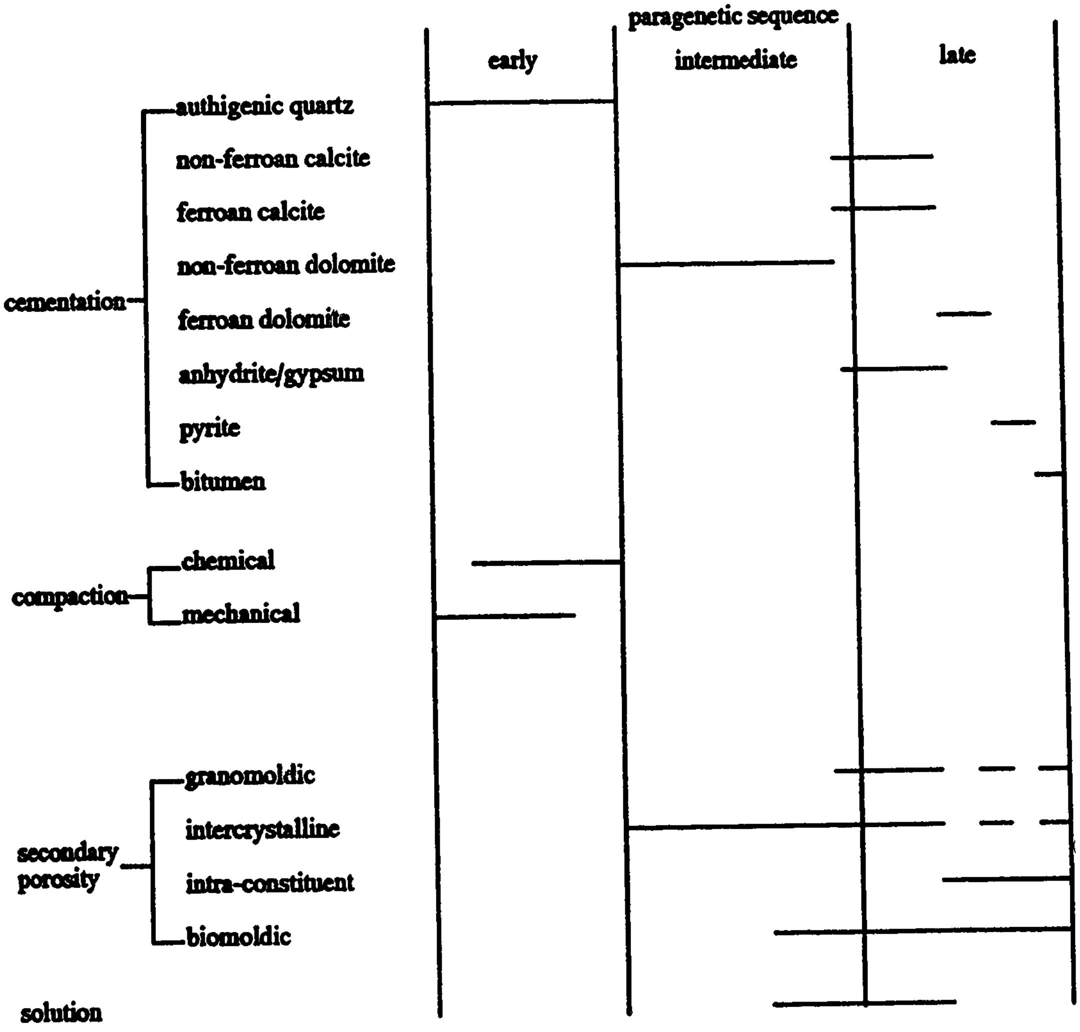

Figure 31. Diagram illustrating the paragenetic sequence within Lithofacies G.

process that occurred was the crystallization of trace amounts of euhedral pyrite, again non-fabric selective. The final process involved the migration and subsequent storage of hydrocarbons within effective pores.

6.2.0. MESO-SCALE PETROGRAPHICAL ANALYSIS.

The meso-scale factors influencing reservoir quality are governed by sedimentary structures and grain texture, in addition to diagenetic effects. There are isolated zones of higher permeability and porosity strata within particular wells. This may not only influence the migratory behaviour of hydrocarbons, but may affect the reservoir performance and productivity. Hence, it is of importance to identify the location, distribution and origin of strata exhibiting anomalously high reservoir quality.

Lithological variation is nonexistent within Lithofacies H, therefore reservoir quality is affected by other factors. It can be identified that there is a close correlation between particular sedimentary structures and reservoir quality (Figure 32). Porosity and permeability readings tend to be somewhat higher within upper flow regime plane beds than within the cross-bedded structures. This is apparent within both Lithofacies G and H. No observations were made within Lithofacies F. Grain size, and hence permeability decrease toward the top of foresets within Lithofacies H cross-beds. This is because the coarser grains migrate to the toe of the bedform. The base of these bedforms is identified by a thin basal zone of granule sized lithoclasts. Where the base of this zone truncates the low permeability sands within foresets of the bedform below, there will be a large vertical permeability difference. Fluids migrating down from the bedform above, whereupon meeting this abrupt permeability reduction, will flow laterally at a reduced rate through the basal granules thus increasing the rate of cementation within and just below the basal granules (Plate 49). Hence vertical permeability is low due to the presence of these discontinuities (Figure 33). Pore fluids also tend to flow along foreset laminae as vertical permeability is again restricted by variation of grain size between the foreset laminae (Plate 50) resulting in cementation at foreset boundaries. Horizontal permeability readings will, therefore be lower due to the constrictional and convergent nature of fluids emanating from the toe of foresets, hence, horizontal flow capacity will be lower. Anhydrite cement can commonly be traced following and emphasizing foreset laminae within cross-beds, precipitating within the coarser grained laminae (Plate 51).

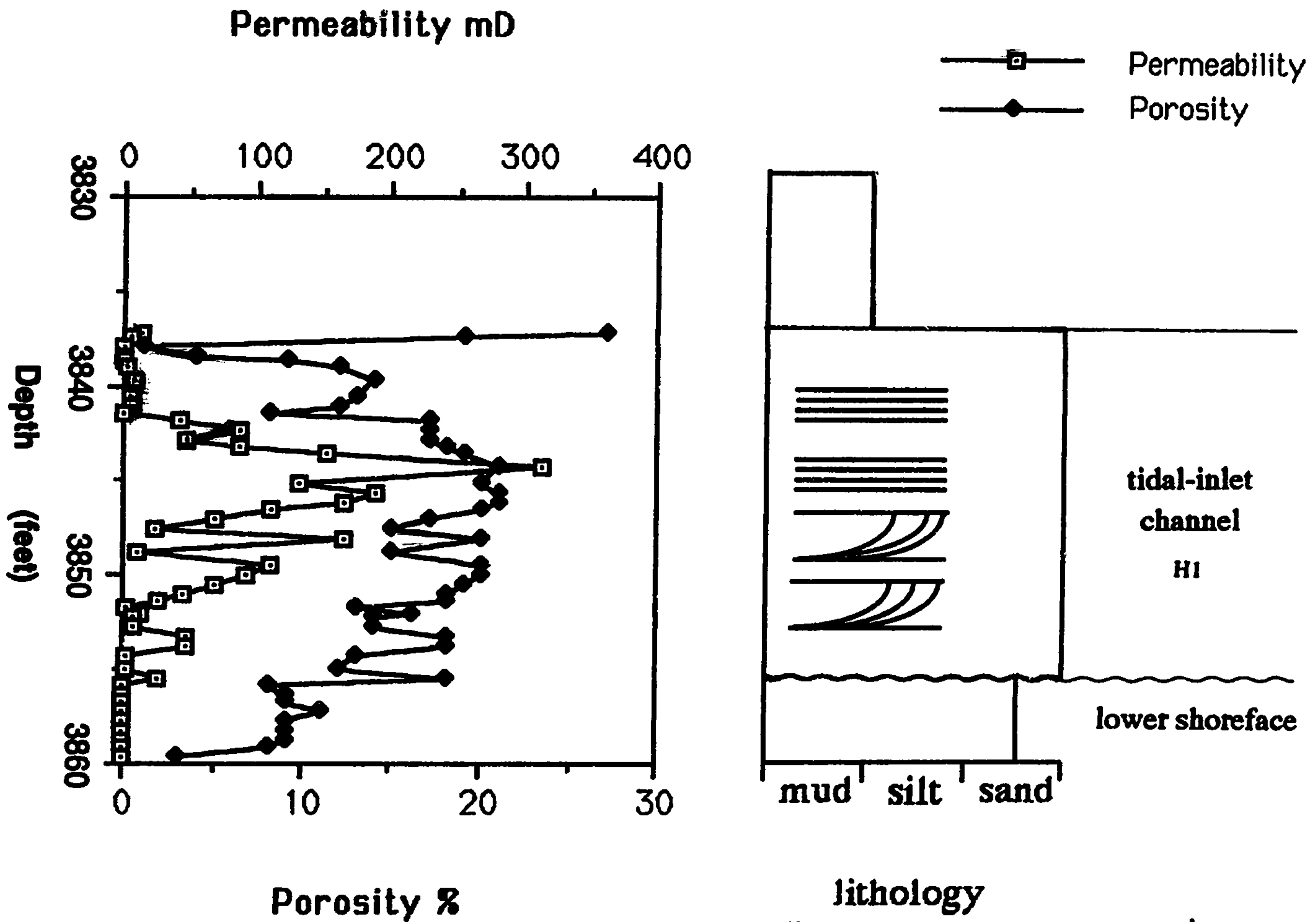

Figure 32. Diagram illustrating the effects of various sedimentary structures on reservoir quality within Lithofacies H. Average permeability and porosity values are higher within the lower part of parallel-laminated deposits. These values decrease dramatically in the lower portions of Lithofacies H since trough cross-bedded structures predominate. Reservoir quality diminishes within the upper six feet of the deposits due to diagenetic fluids, sourced from the Charlie Lake Formation, reducing porosity. Well d-003-E/94-A-16.

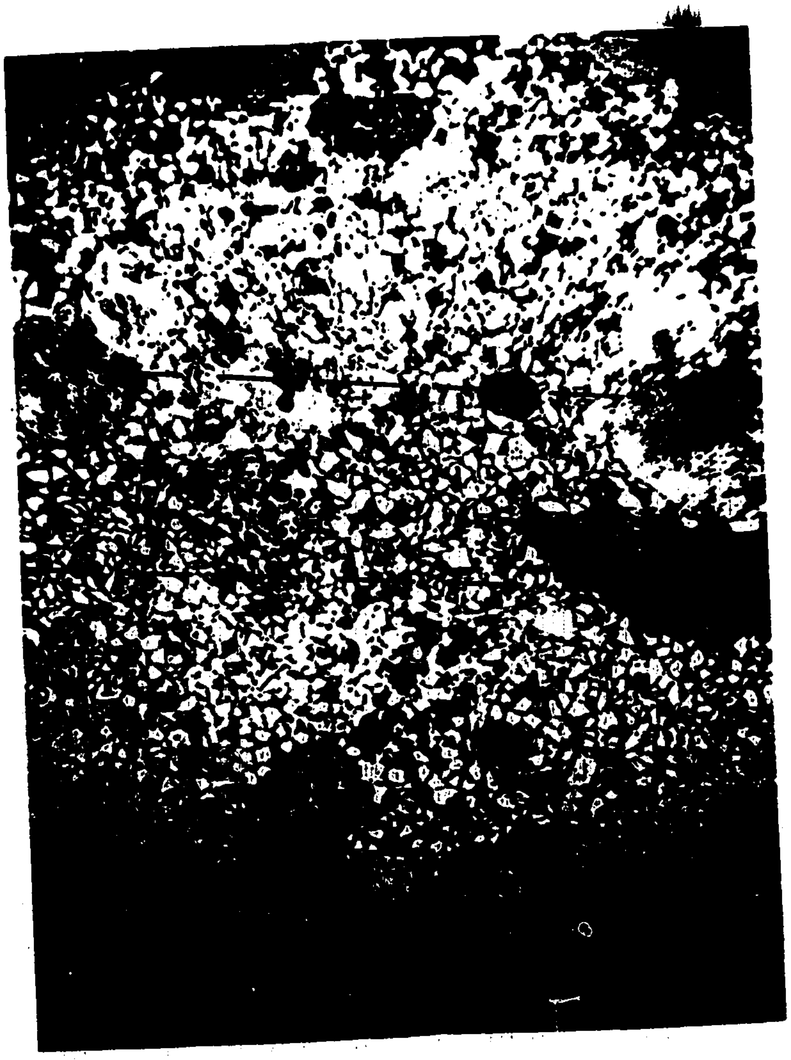

Plate 49. Coarser (C) and finer (F) grading of foreset laminae. The former contain granule sized lithoclasts and are darker in appearance due to dolomite cementation, whereas the finer grained lighter coloured laminae are poorer in cement and hence exhibit higher porosity. (Scale in microns).

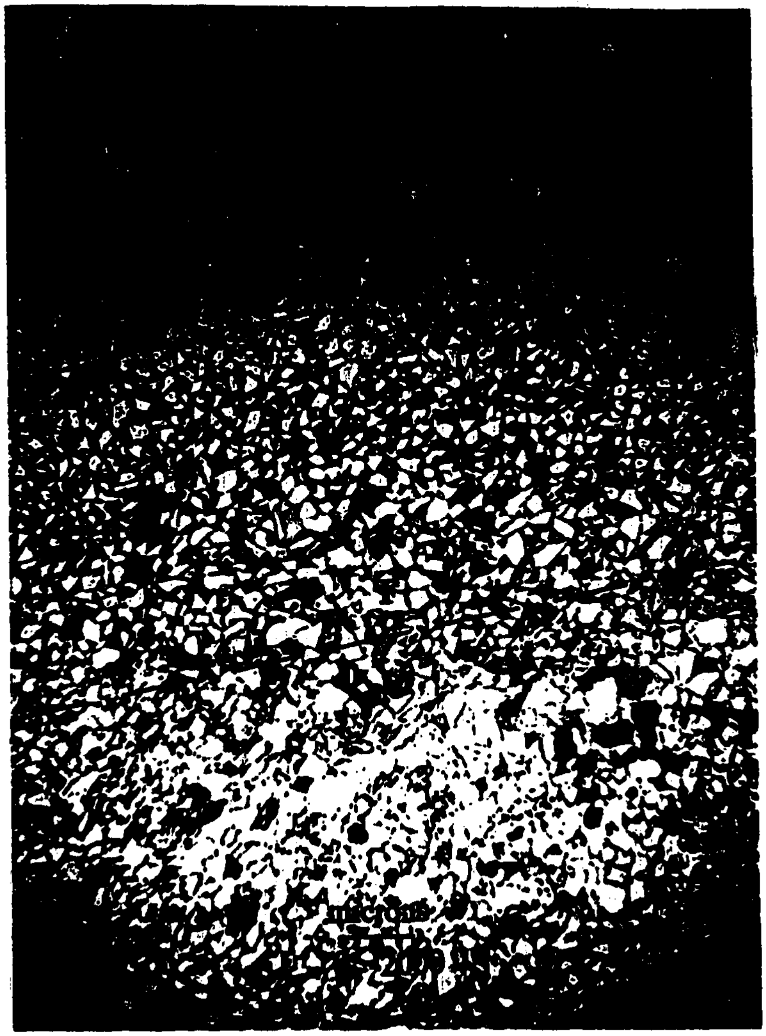

Plate 50. Close up of coarser (C) and finer (F) grading of laminae. Coarser laminae are well-cemented whereas the finer laminae are poorly-cemented (showing good primary intergranular effective porosity). (Scale in microns).

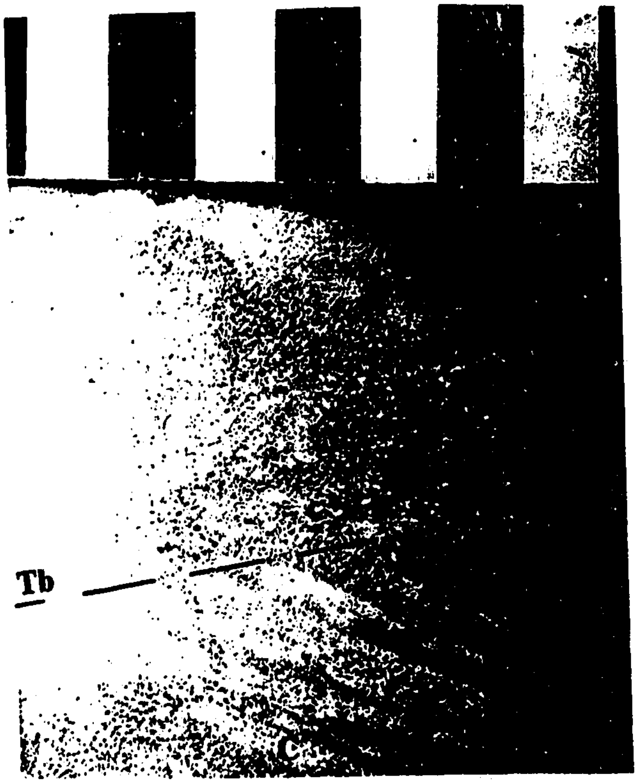

Plate 51. Cross-bedded structures. The base of the top bedform (Tb) is concentrated with granule grade lithoclasts. It is in these basal regions that horizontal fluid flow will converge, having migrated down the foreset laminae. The convergence and constriction within the basal granule zone will produce cementation and hence a vertical permeability barrier. Foresets are highlighted by calcite and anhydrite cement (C) (lighter bands). The lighter bands are low in porosity and hence permeability, whereas the darker bands are higher in porosity and permeability, therefore fluids flow along the high permeability pathways within the foreset laminae. Lithofacies H. Well d-043-E/94-A-16, 3814 ft. Lithofacies H. (Scale in cms).

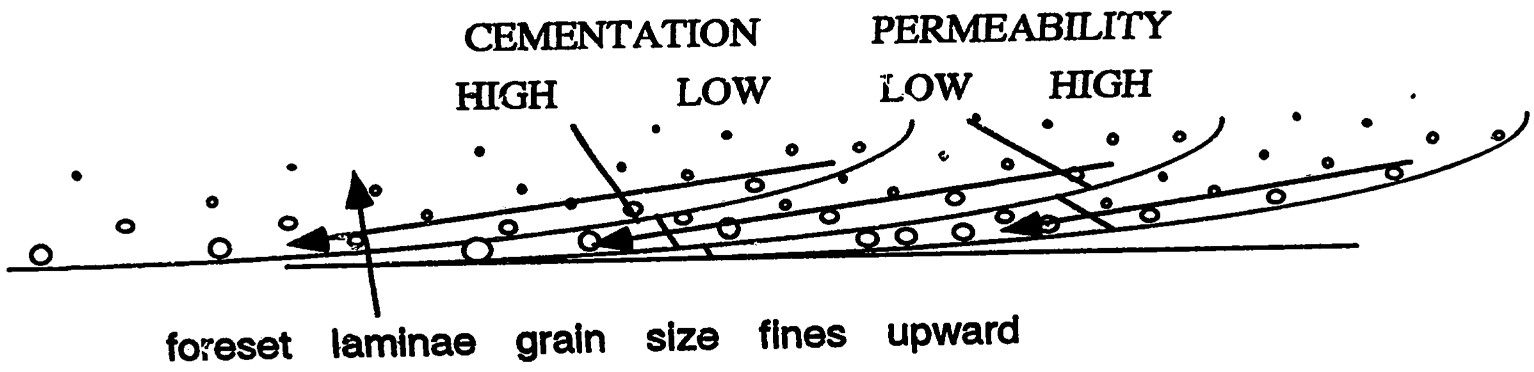

Figure 33. Diagram illustrating the fluid flow behaviour within cross-bedded arenaceous deposits. Fluids flow parallel to the foreset laminae (large arrows) converging at the toe of the cross-bed where *constriction and reduction in flow capacity results in increased cementation within the coarse basal layers*. Fluids are restricted from flowing vertically into the finer laminae below due to the finer grain size, hence permeability reduction. Horizontal permeability values are low along the basal granule zone due to constriction of fluid flow and cementation effects.

A large vertical permeability difference would not be so apparent within the plane bed structures as there are no structural discontinuities. In other words the laminae are parallel, hence pore fluids will flow parallel at different levels within these sediments as opposed to the convergence of fluids at the base of cross-bedded sedimentary structures causing increased cementation (Figure 34). Thus, the horizontal flow capacity within parallel-laminated deposits will be higher. Increased cementation occurs within the upper finer parts of the fining-upward parallel laminae and in the basal coarser grained parts of the overlying laminae, due to reduction in vertical permeability movement.

As explained above, local variations in porosity and permeability within Lithofacies G can be attributed to varying styles of sedimentary structures as well as from varying intensities in the quantity of poikilitic pore occluding cement. Cementation is also highly concentrated between foreset laminae reducing the horizontal vector of fluid flow. Instead, pore fluids flow along dip of the foresets merging at the toe in a constricting fashion, thus reducing the rate of flow of pore fluids and promoting local cementation at the base of cross-bedded bedforms (Figure 33).

The predictability of plane bed structures within the vertical cored sequence of Lithofacies H is extremely difficult. These bedforms may interfinger with each other at any scale, or may be stacked upon one another. Vertical permeability barriers may occur not only at the base of vertically stacked bedforms, but also by the truncation and stacking of individual tidal-inlet channels. The base of tidal-inlet channel is dominated by a concentration of granule sized lithoclasts (similar to those at the base of bedforms). Reservoir quality is high within the basal lag of the channel. These deposits erode down into finer grained deposits which have a lower reservoir quality, thus setting up a vertical permeability difference. This results in fluids inheriting a dominant horizontal component of flow along the basal granule zone, thus increasing the cementation occurring within this hydrologically constricted zone. This permeability restriction, however, does not seem to affect reservoir performance to a major degree.

The diagenetic effects of the fluid flow can be observed in Figure 35. The lowest eight feet of the coquina tidal-inlet channel deposits of d-034-E/94-A-16 are composed of upper flow regime parallel-laminated sedimentary structures. Within this section of the channel average permeability value is 250mD. As cross-bedding becomes more apparent

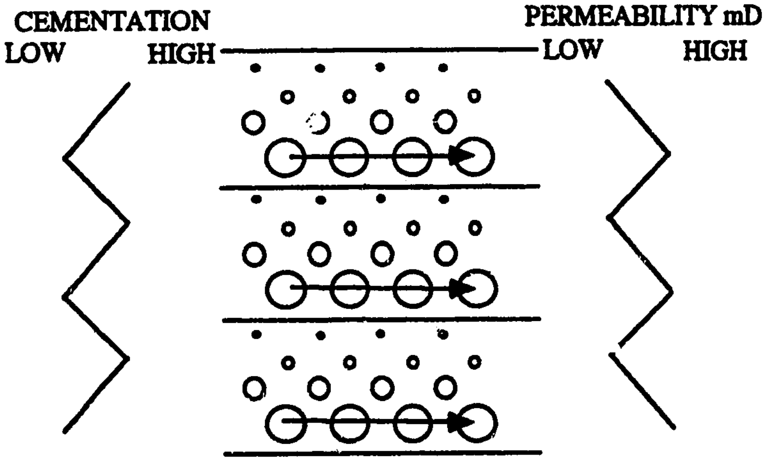

Figure 34. Illustration of unimpeded horizontal fluid flow behaviour within parallel-laminated sedimentary structures, resulting in higher horizontal permeability values. Vertical permeability values would be low due to the high cementation within the finer parts of each laminae.

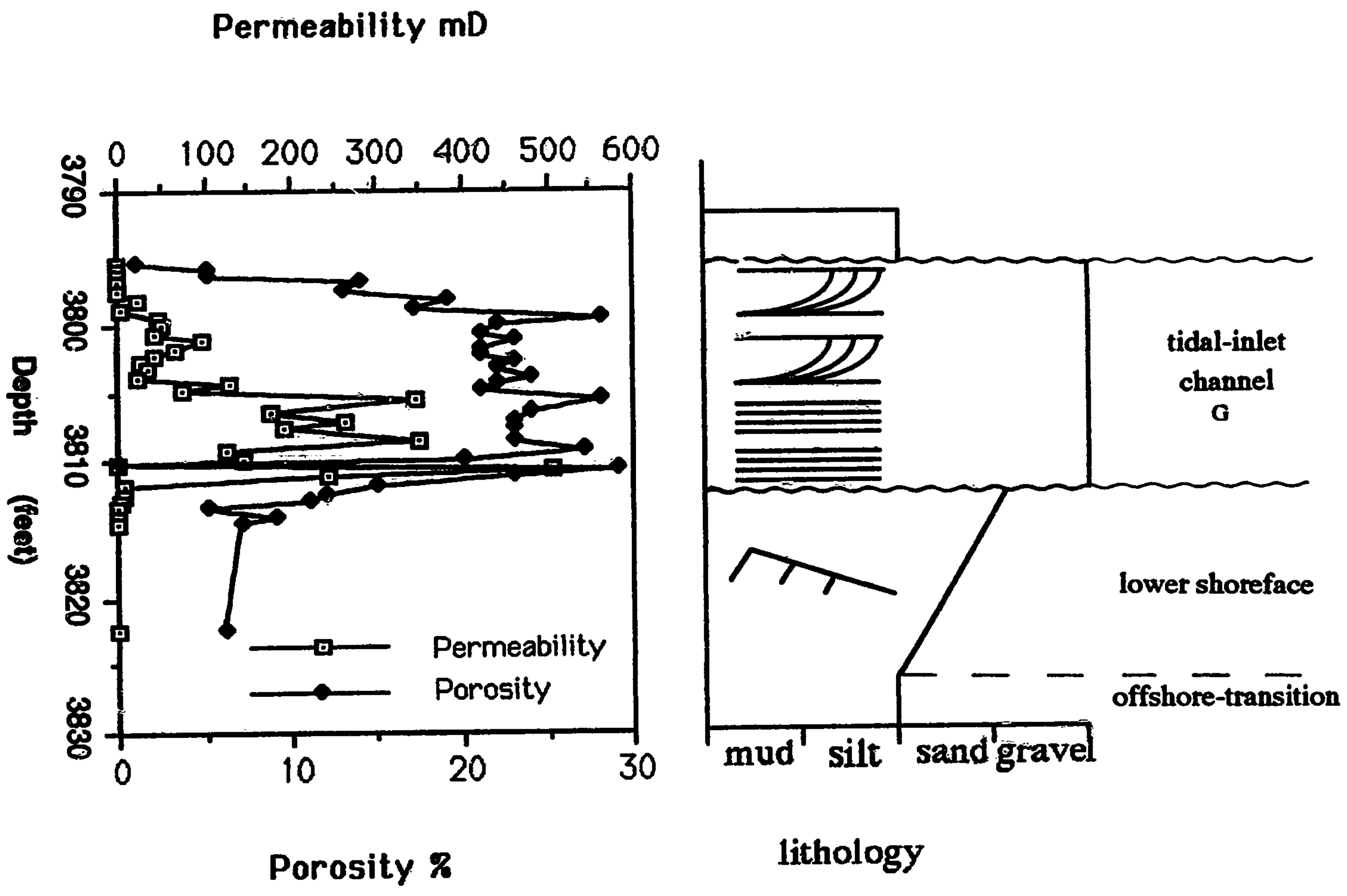

Figure 35. Permeability values within the coquina deposits (Lithofacies G) of well d-034-E/93-A-16 are closely associated with the style of sedimentary structures. Porosity, however, is not directly affected. Both petrophysical attributes, however, decrease in value between four and eight feet from the top of the Halfway deposits. Lithofacies G.within the upper section of the channel the average permeability value decreases to 60mD. This decrease in permeability may also be attributed to the destructive influences of the Charlie Lake contact.

Diagenetic processes and affects may be irregular and random in distribution exhibiting a wide variability of petrophysical readings. This is a common attribute within Lithofacies G biodolomicrites. Figure 36 illustrates the permeability and porosity for well d-099-C/94-A-16. Both attributes vary widely in range of values. At a depth of 3870 feet, both petrophysical attributes display poor reservoir quality values. By examining the core it was found that a number of low reservoir quality horizontal layers had been formed by dolomitisation. The dolomite either developed poor intercrystalline porosity, or the porosity was later occluded by another cement type. Thus, vertical permeability barriers have been developed. This diagenetic feature may extend the width of the tidal-inlet channel, or alternatively, may be an isolated patch of heavy dolomitisation. Another alternative involves the patchy distribution of heavily dolomitised areas within the channel (Plates 52 and 53). Ultimately, the dolomitisation may affect the tortuosity of the fluid pathway within this reservoir. It may also reduce the reservoir bulk porosity.

Reservoir quality may also be affected by the orientation and fabric of the biomolds within the sample. In areas where the biomolds are disoriented, there are less contacts between biomolds. This results in lower effective porosity values, assuming the dolomite cement exhibits effective porosity. Effective porosity of the biomolds is increased where the biomolds are in contact, assuming that they are not occluded with pore filling cement, and the dolomite replacement cement around the rim is not too well developed. The ultimate factor controlling the effective porosity of the biomolds, however, is the degree to which intercrystalline porosity develops within the dolomite cement. In areas where this occurs, permeability values are higher throughout the sample, even if biomolds are not located close together.

Reservoir quality between Lithofacies G and H has been compared in Figure 37. Lithofacies G occurs lower in the cored section in the form of a tidal inlet channel. Variation in petrophysical values are large. This is attributed to the patchy irregular distribution of dolomite cement with later poikilitic anhydrite and/or calcite cement reducing porosity and permeability locally. The variability is also controlled by the location of intercrystalline porosity development within the dolomite cement. In the upper part of the section deposits from Lithofacies H1 have been interpreted as another tidal inlet channel. Petrophysical attributes of this reservoir lithofacies vary less in range. This is partly because the destructive effect of dolomite cementation is volumetrically less

Plate 52. Close up of patchy dolomitisation (D) of the coquina, locally reducing reservoir quality to zero. Lithofacies G. Well d-024-E/94-A-16, 3747 ft. x50. (Scale in cms).

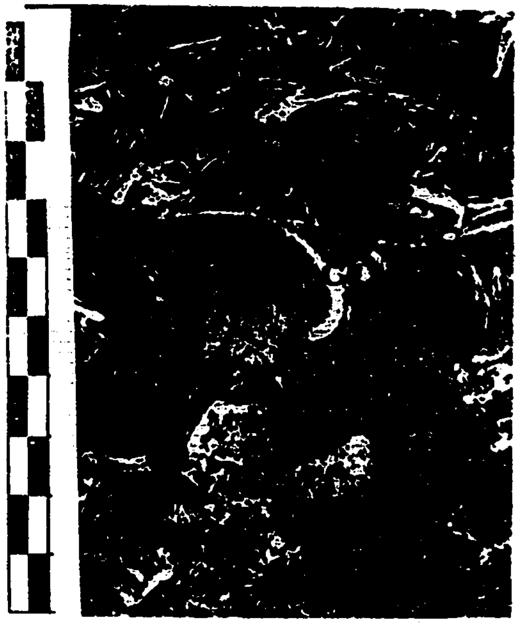

Plate 53. Biomolds infilled with anhydrite and calcite (C). Matrix has been patchily cemented with dolomite (D) consequently, forming areas of low reservoir quality. Lithofacies G. Well d-024-E/94-A-16, 3747 ft. (Scale in cms).

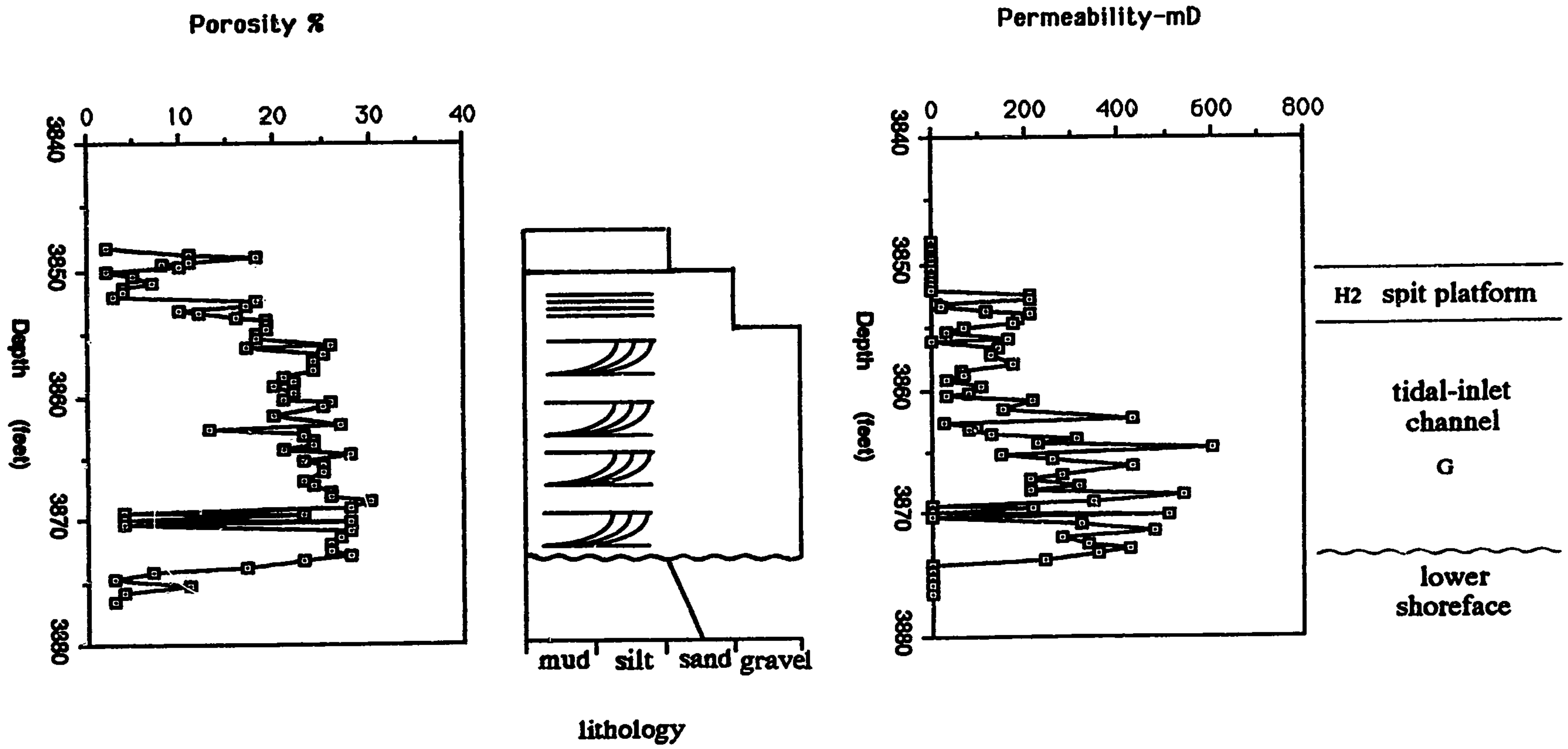

Figure 36. Local diagenetically induced variations in porosity and permeability. At depth 3870 feet dolomitisation has reduced reservoir quality locally. Poikilitic pore occluding anhydrite cement becomes more common toward the top of the channel due to the increased intensity of Charlie Lake derived pore fluids percolating down. Well d-099-C/94-A-16. Lithofacies G.

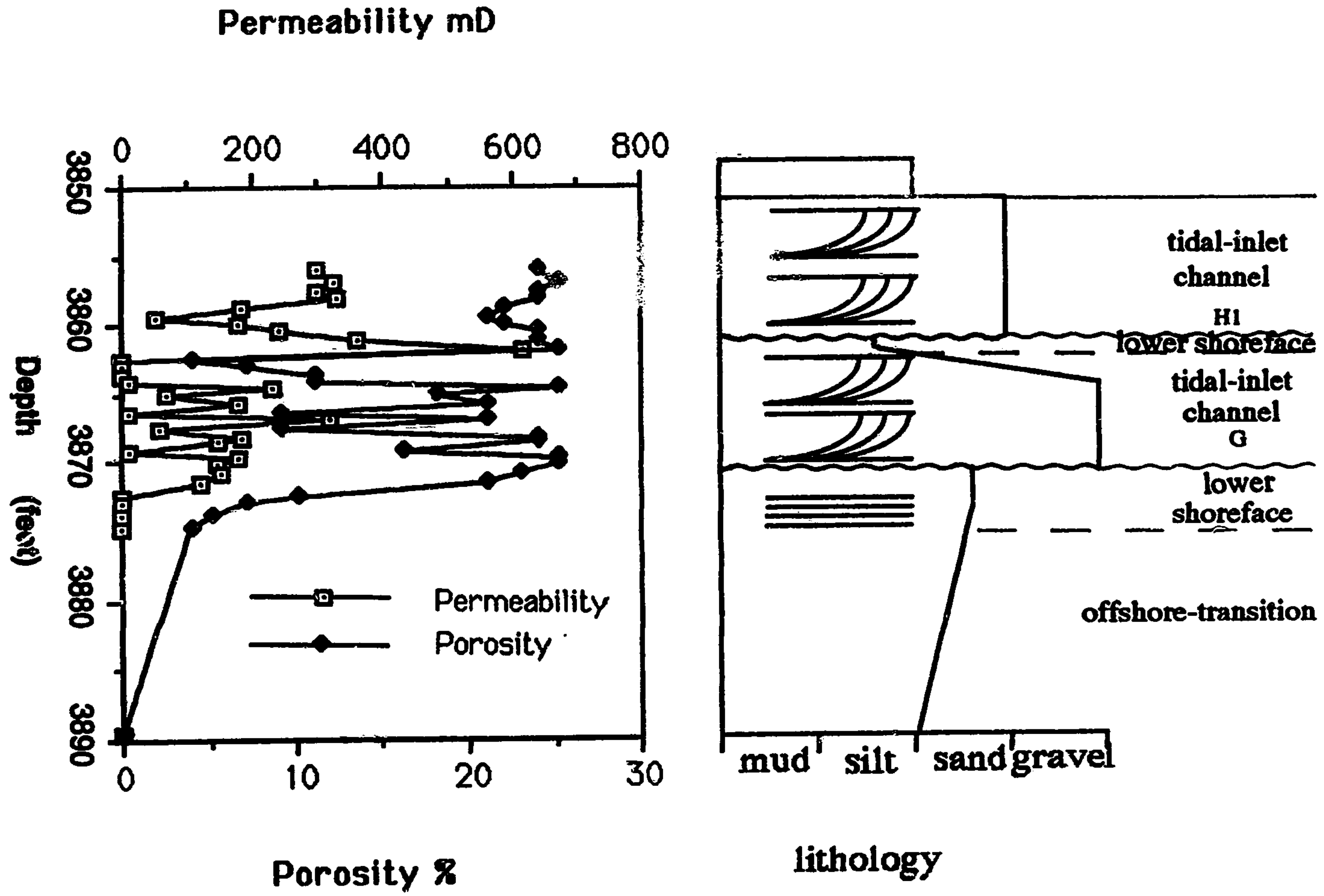

Figure 37. Diagrammatic comparison of reservoir quality between the lower tidal-inlet channel (Lithofacies G) and the upper tidal-inlet channel (Lithofacies H). The petrophysical values for the former vary greatly, whereas those of the latter are more consistent. Well b-038-E/94-A-16.

important and localised in distribution. Primary intergranular porosity is less commonly occluded by poikilitic cement. Although porosity may be higher in Lithofacies G (measured within biomolds) permeability may be low as biomolds may not be well connected. Lithofacies H may have lower porosity values but permeability and porosity are more constant due to intergranular porosity remaining free of occluding cement.

6.3.0. MACRO-SCALE ANALYSIS.

The reservoir lithofacies have been contrasted in terms of their reservoir quality attributes (Table 7). The three reservoir lithofacies of economical interest are: Lithofacies F upper shoreface and proximal storm deposits; Lithofacies G biodolomicrite (coquina) tidal inlet channel fills; and Lithofacies H sublitharenite-litharenite tidal inlet channel fills. The remaining lithofacies have not been examined petrographically since their associated reservoir quality is negligible.

Appendix B shows detailed tabulated reservoir characteristics for each of the lithofacies reservoir. As shown in Table 7, the thickness of Lithofacies H sublitharenite tidal inlet fills is greater than the other reservoir lithofacies. It also attains higher average permeability and porosity values. Maximum reservoir quality values are also higher. This reservoir lithofacies is therefore the best hydrocarbon producer within the study area. It is not affected by dolomite occluding cements to the same extent as the biodolomicritic Lithofacies G deposits, hence, fluid flow distribution and production is more uniform.

Factors affecting the reservoir quality on the macro-scale are the gross thickness variability of the reservoir, and the intensity of diagenetic affects resulting from fluids sourced within the overlying Charlie Lake Formation. The gross thickness of a reservoir lithofacies is controlled by the intensity of downcutting resulting from the intra-Charlie Lake unconformity. The gross thickness of reservoir lithofacies and the intensity of diagenetic affects are spatially unpredictable.

The biodolomicritic tidal inlet fill deposits (Lithofacies G) display lower reservoir quality attributes than Lithofacies H (Table 7). The range of values associated with the reservoir quality are greater because of the patchy distribution of dolomitisation and pore occlusion. Hence, fluid flow both laterally and vertically, is more erratic and less predictable. More permeable layers are swept with injected fluids, hence much hydrocarbon is left untouched within the other regions of the lithofacies characterized by lower permeability values. Production is slower and more continuous from this lithofacies. Injected fluids take much longer to migrate through the lithofacies due to the increased patchy dolomitisation and tortuousity of pore passages.

The vertical variability of reservoir quality is affected by the lithofacies thickness. Figures 38 and 39 show that there is a weak positive correlation between gross reservoir thickness against porosity and permeability within Lithofacies H. Thus, the gross reservoir thickness corresponds to erosional rather than depositional effects. The erosion surface has at least 9 metres (30 feet) of relief. Reservoir quality is therefore higher in thicker lithofacies, since the destructive effect of percolating Charlie Lake brines is proportionally insignificant. This can be exemplified by comparing the reservoir quality of well d-064-D/94-A-16 (gross thickness 6.8 feet) with that of d-063-D/94-A-16 (gross thickness 24 feet). The former reservoir deposit has an average porosity of 15% and average permeability of 31.99 mD compared with the latter which has an average porosity of 21% and an average permeability of 212.60 mD. Thus the porosity and permeability of the thinner reservoir is much poorer. In regions of good well control the predictability of reservoir thickness is increased as the post-Halfway erosional effects can be loosely mapped out.

Vertical variation in reservoir quality within the reservoir is less predictable in magnitude and spatial location. Reservoir quality has been compared and contrasted within the same tidal-inlet channel from two laterally adjacent wells (0.75km apart). Well d-073-D/94-A-16 has a gross thickness of 25.2 feet with an average porosity of 18.45%, and an average permeability of 16.86mD. The particulars for d-063-D/94-A-16 have been stated previously. The average permeability of d-073-D/94-A-16 is remarkably low relative to its gross thickness (Figure 40). Petrographical examination of this well reveals an increase in the quantity and size of poikilitic anhydrite pore occluding cement as the Charlie Lake contact is approached. The pore fluids responsible for the precipitation of this cement originated from dissolution of anhydrite nodules within the Charlie Lake Formation. The same magnitude of diagenetic inhibiting effects are not present within d-063-D/94-A-16 as is demonstrated by the relatively constant petrophysical values extending almost to the Charlie Lake contact (Figure 41).

Environment	Upper Shoreface	Tidal Inlet Channel	Tidal Inlet Channel
Lithology/Lithofacies	Sublitharenite-F	Biodolomicrite-G	Sublitharenite-H
Average Thickness	2.20m (7.22ft)	3.27m (10.74ft)	4.10m (13.38ft)
Maximum Thickness	3.29m (10.79ft)	6.1m (20.00ft)	10.98m (36.00ft)
Minimum Thickness	0.50m (1.64ft)	1.55m (5.10ft)	1.1m (3.60ft)
Average Permeability (mD)	70.00	97.81	141.39
Maximum Permeability (mD)	220.28	294.26	579.39
Minimum Permeability (mD)	0.11	2.40	0.52
Average Porosity (%)	15.37	12.07	12.07
Maximum Porosity (%)	20.90	21.30	29.36
Minimum Porosity (%)	5.90	6.42	4.20
Reservoir Quality	moderate-good	good	good

Table 7. Reservoir quality attributes for the lithofacies reservoirs identified within the study area. Biodolomicritic proximal storm deposits have been included within the upper shoreface deposits.

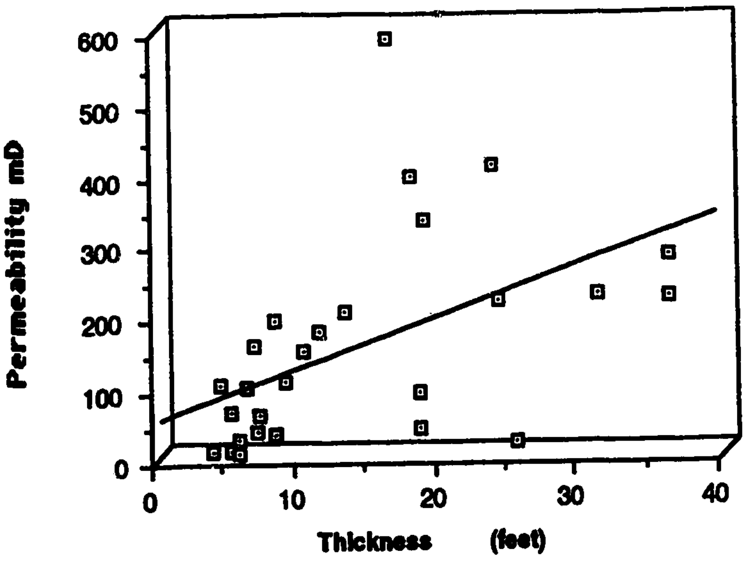

Figure 38. Correlation between permeability and thickness of Lithofacies H.

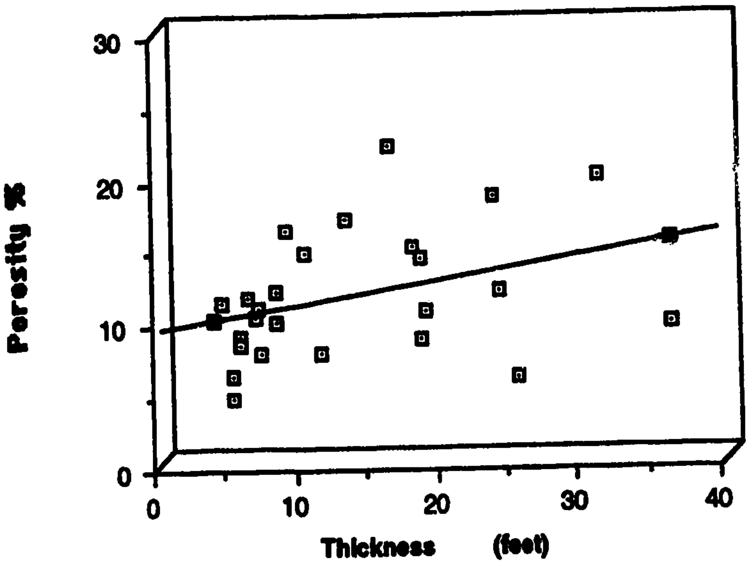

Figure 39. Correlation between porosity and thickness of Lithofacies H.

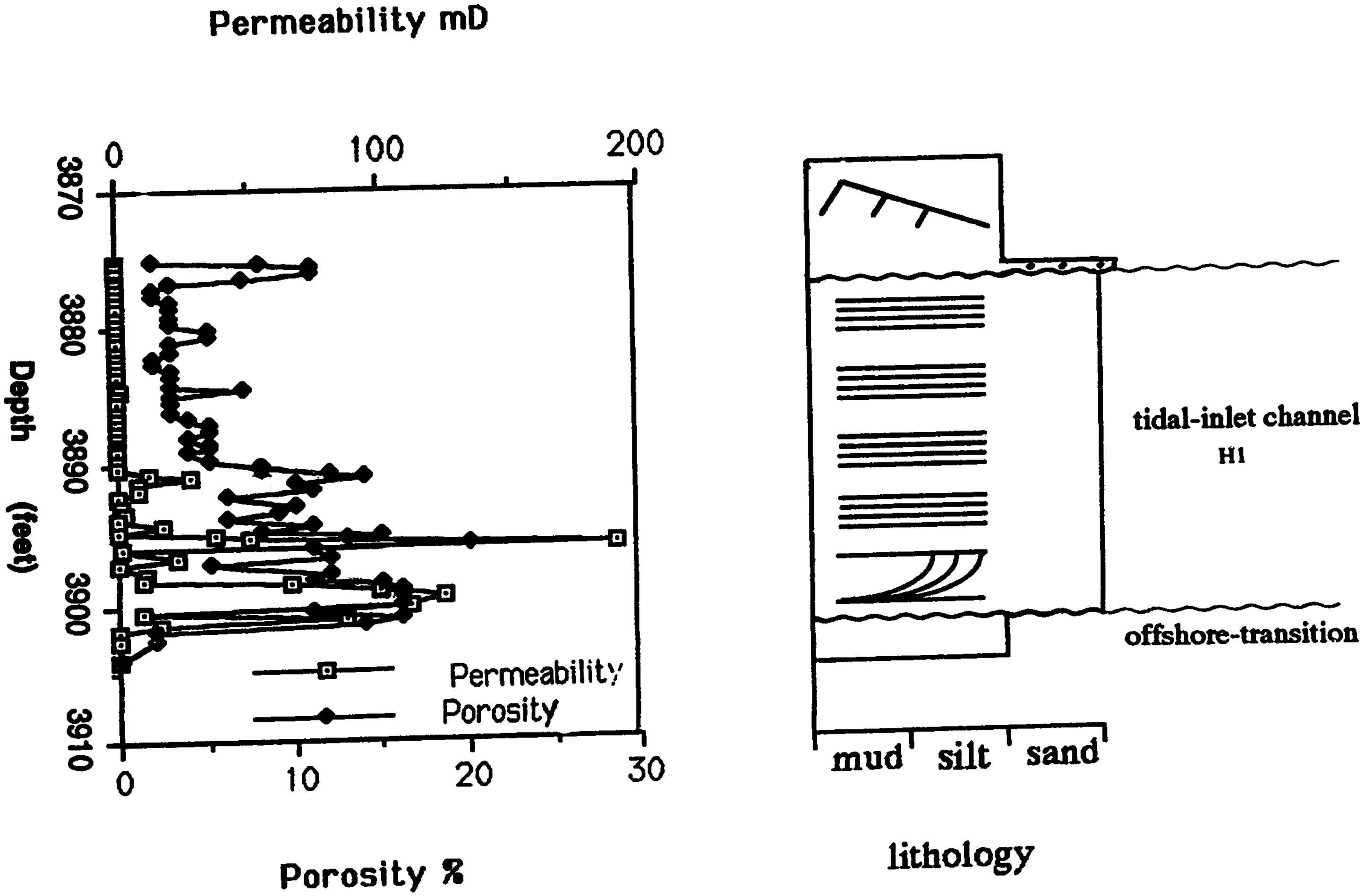

Figure 40. Reservoir quality verses depth for well d-073-D/94-A-16, Lithofacies H. The upper 14 feet of tidal inlet channel fill has reduced reservoir quality due to the destructive effects of Charlie Lake pore waters.

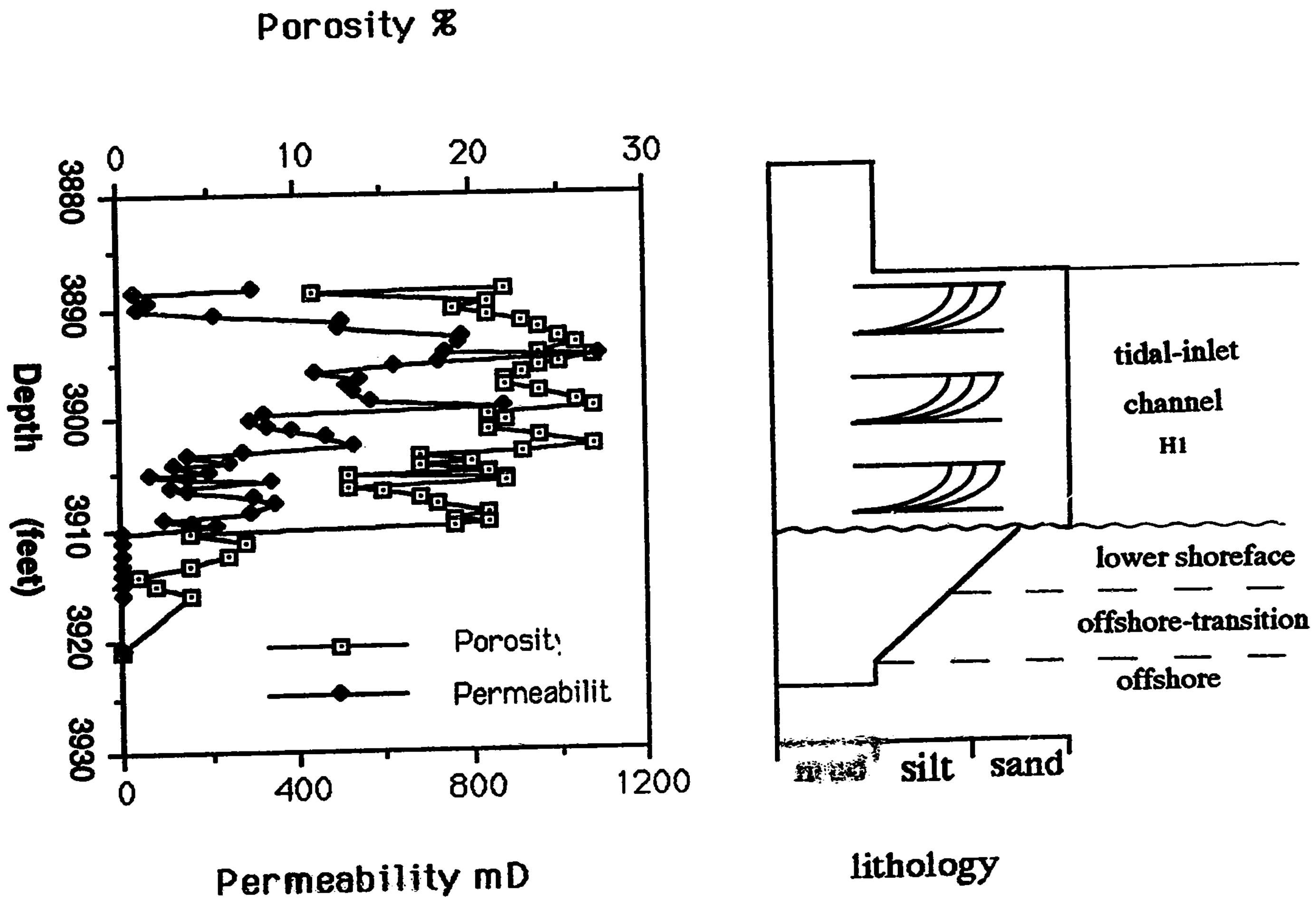

Figure 41. Reservoir quality verses depth for well d-063-D/94-A-16, Lithofacies H. Reservoir quality starts to decline four feet from the Charlie Lake contact.

It is not clear why d-073-D/94-A-16 appears to be a sink for Charlie Lake derived pore inhibiting fluids. Most other reservoirs of the same lithofacies experience a decrease in reservoir quality between two and eight feet from the Charlie Lake contact, however, d-073-D/94-A-16 experiences reservoir quality depletion over fifteen feet from the contact. It can, therefore, be visualized that the lower the gross reservoir thickness, the greater will be the proportion of poor reservoir quality rock, as has been exemplified between wells d-063-D/94-A-16 and d-064-D/94-A-16. Plate 54 shows the destructive effects of Charlie Lake derived brine pore waters which produce nodular anhydrite within the upper regions of the Halfway deposits. Anhydrite replacive nodules thus increase the tortuosity of the pore corridors. The upper 8 to 10 feet of the channel experienced a reduction in permeability, and to a lessor extent a decrease in porosity. This is due to increased tortuosity of pore corridors resulting from the introduction of pore occluding poikilitic anhydrite and/or calcite cement, locally occluding the intercrystalline porosity within the dolomite cement. The anhydrite cement may not completely infill and occlude biomoldic porosity. It will, however, reduce the pore corridor width, thus increasing the capillary action and surface tension of the grains, consequently reducing fluid migration rates.

Upper shoreface deposits of Lithofacies F are rarely preserved within the study area due to the erosive upper contact with the Charlie Lake. Figure 42 illustrates the reservoir attributes of one such well containing Lithofacies F deposits. Both porosity and permeability are very low within the upper shoreface deposits. Poikilitic anhydrite and calcite nodules have reduced the permeability to almost zero. In certain areas, higher values are attained and production does occur from these deposits, this is mainly from biodolomicrite proximal storm beds. The upper shoreface deposits are overlain by very low reservoir quality shales of the offshore-transition zone which act as a permeability barrier. In this situation the channel deposits may act as a vertical conduit for hydrocarbon fluids. Vertical permeability within Lithofacies H is low, however, through time it is feasible that vertical fluid migration can occur.

Plate 54. White nodules are poikilitic anhydrite (A) which increase in intensity and size as the Charlie Lake contact is approached. Reservoir quality consequently decreases as the contact is approached. x25. (Scale in cms).

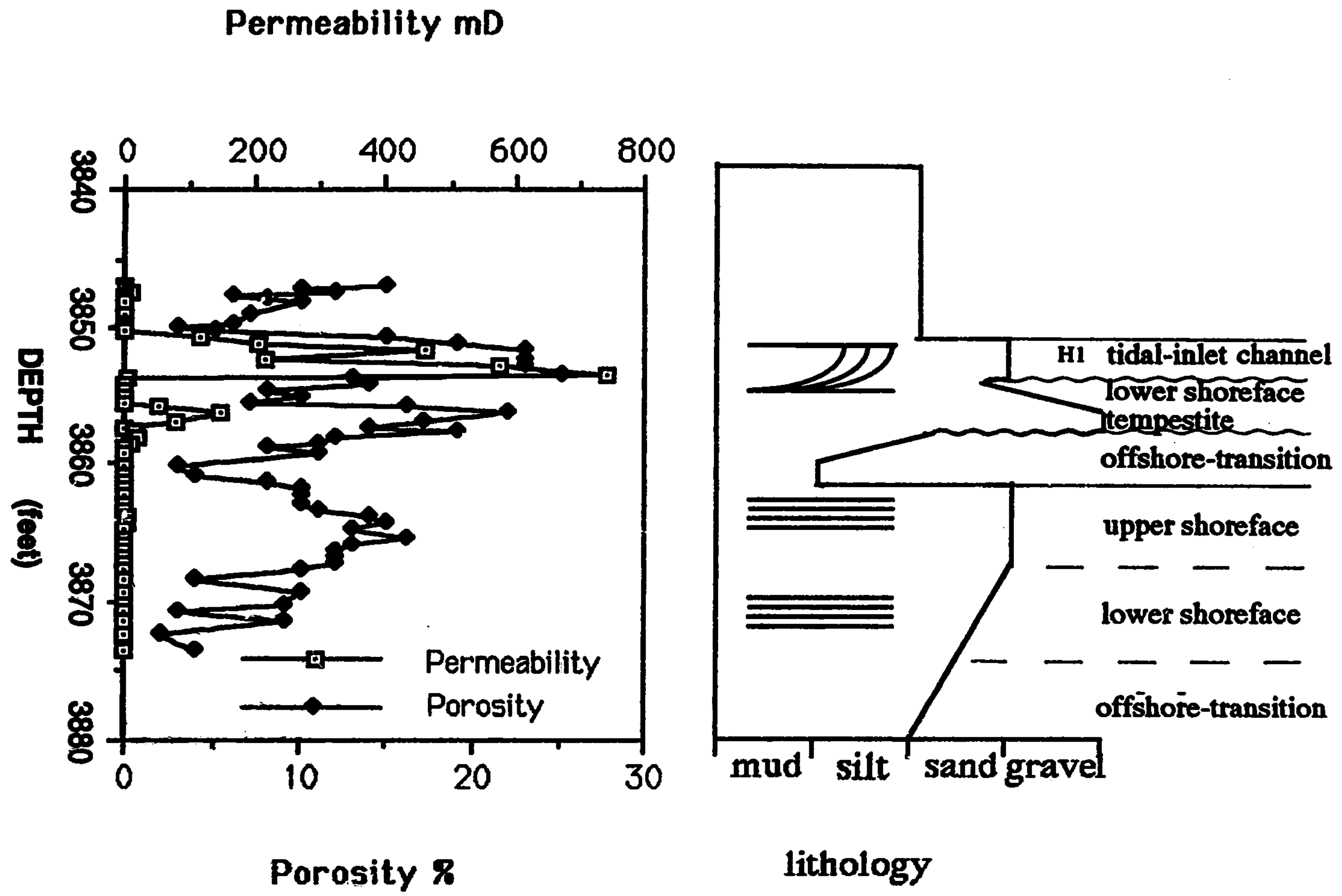

Figure 42. Petrophysical analysis of a coarsening-upward shoreface sequence. Well d-092-D/94-A-16, Lithofacies F.

7.0.0. CORE-TO-WELL-LOG CORRELATION.

This chapter describes the geophysical well-log characteristics and signatures associated with the two vertical lithofacies associations identified within the study area (see Chapter 5). Once it was certain that a particular geophysical well-log signature corresponded to a particular lithofacies association, the geophysical responses were then be used to determine the type of lithofacies association occurring within uncored or undescribed wells.

Most of the wells drilled within the field are over thirty years old, hence neutron-density, spectral gamma-ray and dipmeter logs were rarely available and therefore not used extensively in the study. The main logs incorporated in the study were gamma-ray, sonic, spontaneous-potential and resistivity logs. The gamma-ray and sonic logs were found to be the most useful in terms of lithological identification, grain size and intensity of diagenetic cementation determinations. The spontaneous-potential and resistivity logs were used to determine permeable lithology and identification of formation fluids, respectively. Combined information from the logs enabled qualitative determination of lithology, texture, diagenetic cementation and porosity development, formation fluid identification and permeability.

Before core-to-well-log cross-correlation could be undertaken it was necessary to determine the amount of missing core and to correct for such errors in the core depth. This was achieved by correlating prominent markers, such as shale beds, base of inlet channels, occasional recognizable storm beds, and anhydrite markers from the core with equivalent signatures on the gamma-ray logs. Hence, core depths were converted to gamma-ray well-log depths. No core-gamma-ray logs were available to aid this procedure, hence bore-hole gamma-rays were used. The majority of well-logs and cored intervals were measured in feet. Core depth corrections varied from 1 to 16 feet.

Gamma-ray logs record the amount of radioactivity emitted from a rock. Radioactive emissions are sourced from clays and feldspars. This is because they contain potassium, thorium and uranium radioactive elements which substitute for other elements within the atomic lattice of the mineral. Hence, a gamma-ray log can quantitatively record the amount of clay found within a lithology based on the amount of radioactive emission.

Clay content is also inversely correlated with grain size; in other words, coarser grains contain less clay material and vice versa.

Broadly speaking, it was possible to correlate the vertical lithofacies associations to the gamma-ray log responses, thus obtaining two general but characteristic and separable recurring gamma-ray log signatures. The coarsening-upward prograding shoreface sequence produced a funnel-shaped curve with high A.P.I. (American Petroleum Institute) units at the base of the sequence which gradually decreased upward. This is because the grain size not only coarsens-upward, but the clay content also decreases upward. This is dependent on the dictating depositional processes at work on the sediments. The tidal inlet channel fills produce a blocky-shaped signature with low A.P.I. values. The blocky nature of the gamma-ray log results from lithological homogeneity.

7.1.0. LITHOFACIES ASSOCIATION 1.

Two wells have been chosen to depict the signature of the log responses demonstrative of a coarsening-upward prograding shoreface sequence. However, both d-027-C/94-A-16 and d-082-D/94-A-16 reflect the progradation of two stacked shoreface sequences separated vertically by a marine-flooding surface (Figures 43 and 44). The difference between the two wells is that the former well displays medium to thick interbedded sublitharenite and biodolomicrite storm beds within the upper shoreface deposits of the lower parasequence, whereas the latter well is composed of a sublitharenite tidal inlet channel fill within the upper parasequence.

Figure 43 shows the geophysical well-log responses of two vertically stacked coarsening-upward shoreface sequences from well d-027-C/94-A-16. Two moderately to poorly formed funnel-shaped responses form the gamma-ray signature (Parasequences 3 and 4; see Chapter 8) characteristic of a prograding shoreface. From the base of the cored interval to 3948 feet the gamma-ray signature is relatively uniform and characteristic of shale values reflecting a value varying from 70 to 80 A.P.I. units. There is no indication of sand influence within this region of the section as is indicated by the continual high gamma-ray response. The shales below the cored interval, although cemented, may also contain connate water, especially coating and within the clay particles. This bound water within the shales produces a higher interval transit time on the sonic log below 3948 feet.

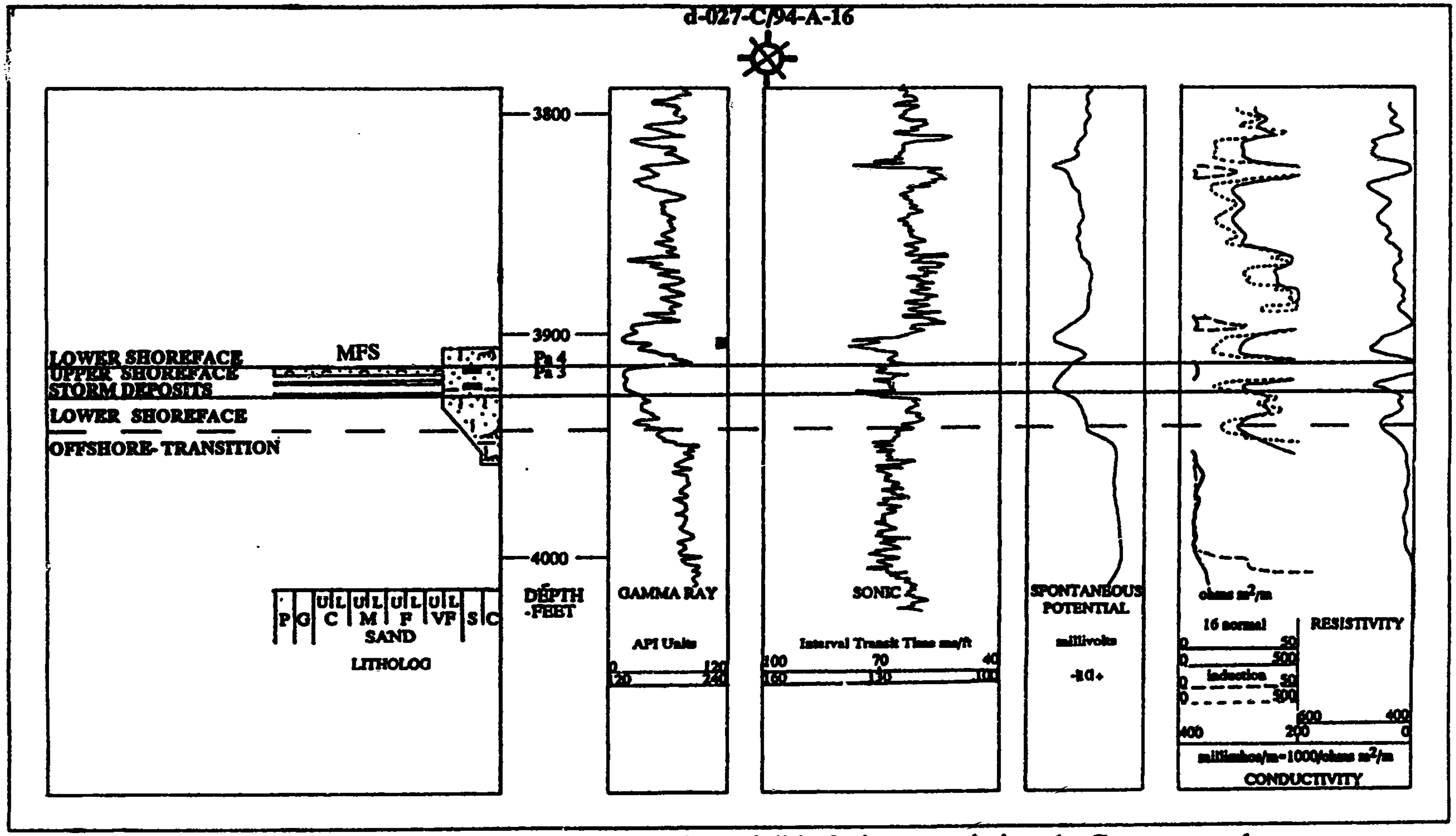

Figure 43. Core-to-well-log correlation of lithofacies association 1. Gamma-ray log displays two vertically stacked funnel-shaped signatures indicating coarsening-upward prograding shoreface cycles. Well d-027-D/94-A-16.

The gamma-ray log from 3948 to 3914 feet indicates a progressive decrease in A.P.I. value from 80 to 20 A.P.I. units. This suggests that the lithology contains less shale. This is confirmed by well-log-to-core correlation. The deposits coarsen-upward from interlaminated siltstones and shales at the base of the cored interval passing up into lower shoreface interbedded sandstones and shales. These pass up into the upper shoreface interbedded biodolomicritic and sublitharenitic beds. It is difficult to recognize individual lithofacies from the gamma-ray log signature partly because of the gradational contacts between each lithofacies and partly because the resolution of the equipment is greater than 2 feet. Individual beds cannot be easily recognized, especially within the upper shoreface. The sonic response to the coarsening-upward change in lithology is represented by a decrease in interval transit time between 3948 and 3928 feet. This occurs within the lower shoreface deposits of the lower parasequence (Pa. 3; see Chapter 8). This may be due to increased cementation of the sandstones which causes less retardation of propagating acoustic waves through the medium.

Above 3928 feet the upper shoreface deposits are indicated by higher interval transit times. This reflects an increase in porosity of the deposits. The pores may have been infilled with fluids or left open. Propagation of acoustic waves through a porous medium, whether saturated with fluids or left open, will decelerate leading to higher interval transit times on the acoustic log. The low A.P.I. readings at the same interval indicate a shale-free lithology of coarser grain size. This is confirmed by observation of the cored lithology. A gradual increase in permeability of the deposits within the lower parasequence (Pa. 3; see Chapter 8) is shown by the spontaneous-potential curve which shifts to the left in the more permeable mediums. This indirectly indicates a grain size and lithology change. The resistivity log increases in resistivity within the lower and upper shoreface deposits reflecting the possible presence of hydrocarbons.

Above the marine-flooding surface the lithology becomes more shaly. This indicates a reduction in winnowing conditions as the deposits change from upper shoreface to lower shoreface zone. This is reflected by an increase in A.P.I. units within the gamma-ray log, a slight decrease in interval transit time (reflecting a less porous medium), a noticeable shift to the right within the spontaneous-potential log (indicating less permeable strata) and lower resistivity readings due to decreased content of hydrocarbon fluids. Although the cored interval terminates before the introduction of Charlie Lake deposits, the gamma-ray response (which is similar to the upper shoreface deposits of the lower parasequence [Pa. 3; see Chapter 8]) indirectly indicates a coarsening-upward and less shale-rich trend to the lithology. This is also indicated by the increase in interval transit time (corresponding to increased porosity), a shift of the spontaneous-potential curve to the left (indicating more permeable strata), and an increase in resistivity (indicating the presence of gas). Gas was produced from this well; the reservoir rock being the lower part of the upper shoreface deposits within the upper parasequence (Pa. 4; see Chapter 8). These well-log responses are very similar to those within cored upper shoreface deposits, thus this is an example of lithological inference based on information gained from other wells.

Well d-082-D/94-A-16 (Figure 44) is composed of two parasequences. The lower parasequence (Pa. 3; see Chapter 8) consists of a coarsening-upward prograding shoreface from 3918 to 3872 feet. The cored interval displays offshore-transition deposits at its base. The gamma-ray log signature shows the base of the parasequence as a shaly unit which was probably deposited within the offshore zone. This lies abruptly ontop of sandier deposits, representing the top of a more distal parasequence (Pa. 2).

The interlaminated siltstone and shale lithofacies deposited within the offshore-transition zone of the lower parasequence (Pa. 3) is overlain sharply by lower shoreface coarser sandstones and shales, hence the abrupt decrease in A.P.I. value of the gamma-ray log and the rapid shift of the spontaneous-potential curve to the left. Acoustic velocity decreases slightly in these deposits as a result of increased porosity. There is also a continuous decrease in resistivity until the lower shoreface sands are encountered at which point it levels off. Above these deposits sit upper shoreface sublitharenites associated with no major changes in well-log response except that the gamma-ray logs indicate a continual decrease in shale.

There is an abrupt contact between the upper shoreface sandstones of the lower parasequence (Pa. 3) and the interbedded sandstones and shales of the lower shoreface deposits within the parasequence above (Pa. 4). This is represented by a marked increase in A.P.I. units at 3872 feet (due to the introduction of shale beds), with a corresponding increase in acoustic velocity (denser shale lithology), a shift to the right of the spontaneous-potential log (impermeable), and an increase in resistivity (formation water).

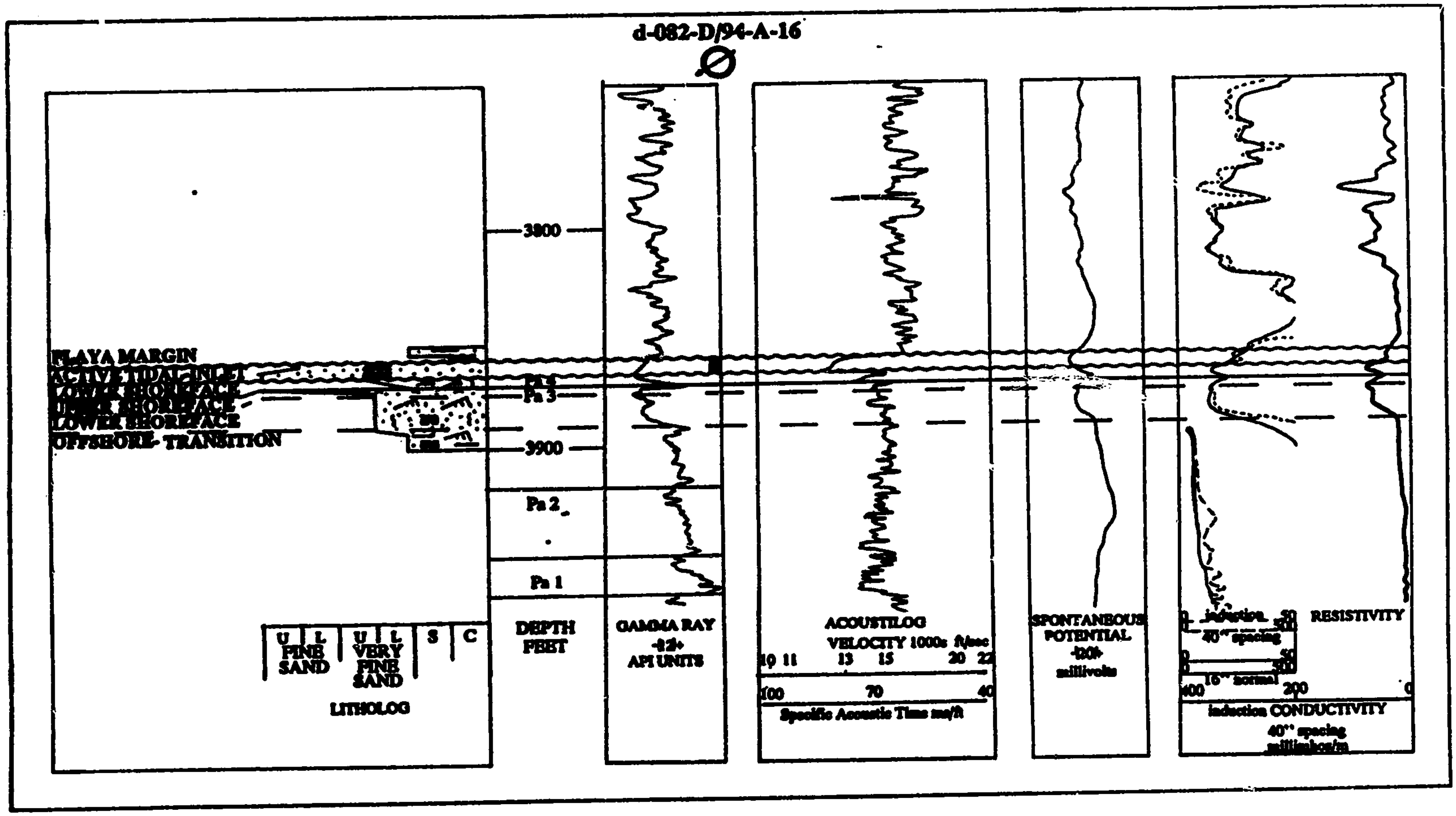

Figure 44. Core-to-well-log-log correlation displaying two coarsening-upward prograding shoreface sequences representative of lithofacies association 1. Well d-082-D/94-A-16.

The coarsening-upward lower shoreface deposits of parasequence 4 are truncated by Lithofacies H sublitharenite tidal inlet channel fill deposits. The sharp lithological contact is recognizable on the gamma-ray log as a rapid decrease in A.P.I. value and acoustic velocity which indicates a shale-free and coarser grained deposit, which is more porous, respectively. Permeability increase is signified by the leftward shift of the spontaneous-potential curve. Lower resistivity fluids are located in these deposits. These deposits are abruptly overlain by Charlie Lake evaporites, siltstones, shales and dolomites. Gamma-ray readings within these deposits increase, but are lower than readings obtained from offshore shale deposits. This is because the Charlie Lake deposits contain primary and secondary carbonates, anhydritic and other evaporitic nodules, thus reducing the A.P.I. value. Acoustic velocity is markedly higher because the density of these deposits increases as porosity decreases. Spontaneous-potential and resistivity logs indicate that the deposits are less permeable and more resistive, respectively.

The sublitharenite lithofacies was an oil producing horizon within the well, but has since been transformed to a water injection well. The upper shoreface deposits of the lower parasequence (Pa. 3) have not been perforated since sonic readings indicate low porosity. This has been confirmed by core analysis data (average porosity of 11.2% and average maximum permeability of 0.2mD).

7.2.0. LITHOFACIES ASSOCIATION 2.

The deposits characterizing lithofacies association 2 are sublitharenites, litharenites and arenaceous biodolomicrites representing the lateral migration of wave-dominated tidal inlet channels. Figures 45 and 46 show the characteristic blocky-shaped gamma-ray log signature (low A.P.I. units) of both lithological types of tidal inlet fill. Figure 45 displays the well-log responses of a sublitharenite (Lithofacies H1) tidal inlet fill from well d-019-E/94-A-16. The tidal inlet deposits rest erosively on lower shoreface deposits which rest sharply on offshore marine, black, phosphatic-rich shales. The gamma-ray readings from the shales between 3886 and 3898 feet are exceptionally high and reach values in excess of 120 A.P.I. units associated with high radioactive levels. One of the most radioactive elements is uranium. Uranium may be precipitated out of seawater in chemically reduced conditions. It becomes readily adsorped by organic matter and/or by phosphates (Rider, 1986). The reduced conditions required for the precipitation of uranium from seawater are stagnant water conditions and relatively slow rates of deposition. Thus, the absorption of

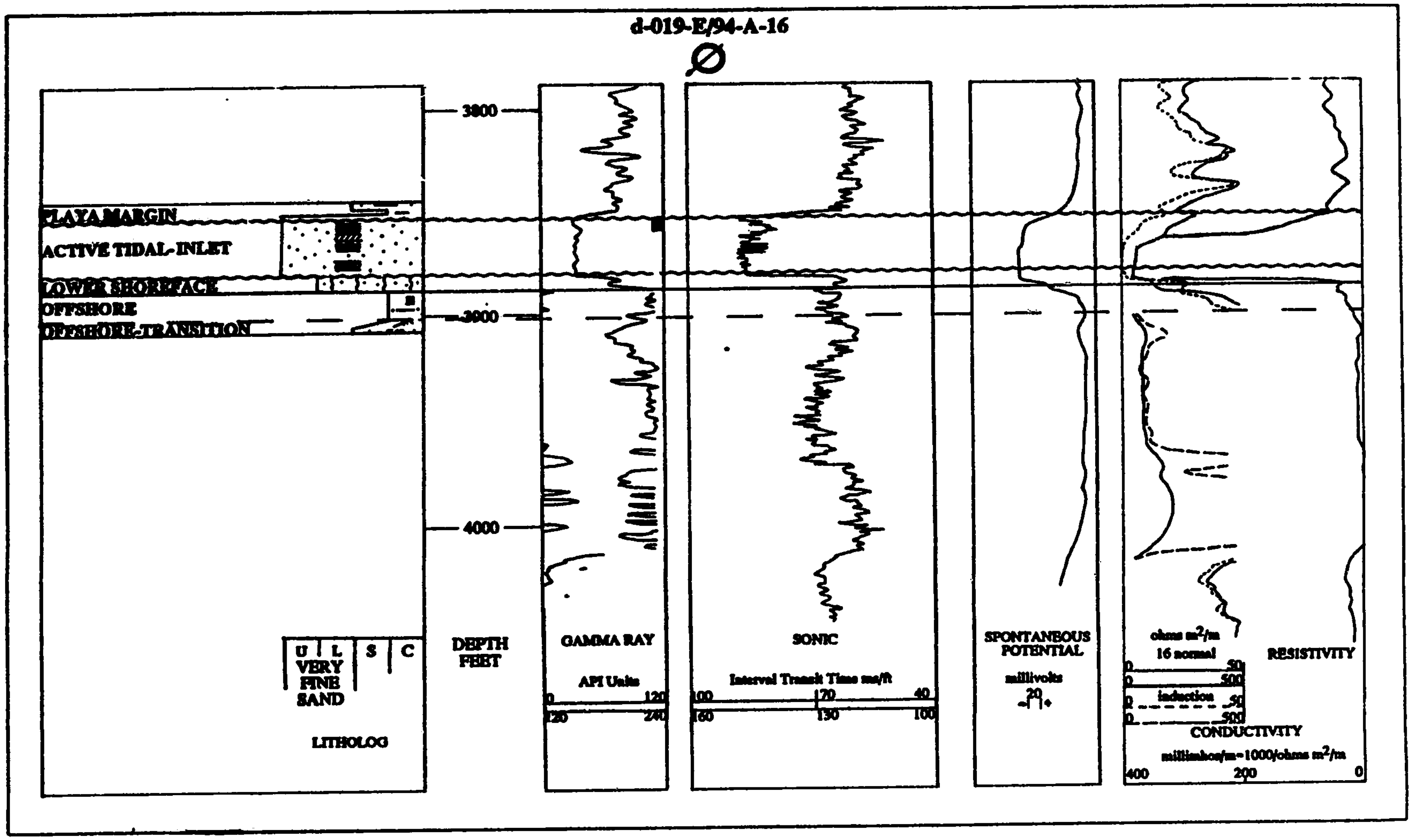

Figure 45. Core-to-well-log correlation of a sublitharenite tidal inlet channel fill (Lithofacies H1) representative of lithofacies association 2. The gamma-ray signature is blocky and displays relatively low A.P.I. values.

uranium by phosphates in an offshore euxinic environment could produce the high A.P.I. values characterized by these shales. This may also explain the high A.P.I. readings at the base of the well (between 3952 and 4014 feet). This could be verified with the aid of spectral gamma-ray well-logs since they divide up and quantify the amount of common radioactive elements found within rocks. This has been proven within similar offshore marine, black, phosphatic-rich shales within the Doig Formation, at the Wembley field in west-central Alberta (Willis, 1992).

The shales at 3898 feet have slow interval transit times because they contain much organic material and may contain bound connate water within the clay crystal lattice. The shaly-sandstone lithology below, at depths of 3904 feet has a lower interval transit time since it is probably cemented. The basal 50 to 60 feet of the well is dominate by highly radioactive and apparently dense lithology. This has been interpreted as amalgamated phosphatic- and organic rich-shale horizons that extend throughout the entire field. These have been referred to as the "Phosphatic Zone" within the basal part of the Doig Formation (Armitage, 1962).

Bioturbated shaly sandstones sharply overlie the offshore shales at 3886 feet represented by a sharp decrease in A.P.I. units to 65 on the gamma-ray log. These deposits signify a rapid progradation (due to high sediment supply) of the lower shoreface over the offshore deposits. The sandstones have been erosively overlain by sublitharenites displaying the highest reservoir quality within the field. These deposits are characterized by low A.P.I. values of 30 since the lithology is relatively compositionally mature compared to shale. Compositionally mature sandstones, however, have typical values ranging from 15-30 A.P.I. The relatively high value of 30 A.P.I. for Lithofacies H may be reflected by the concentration of phosphate material forming lags at the base of bedforms. The blocky shape of the gamma-ray log indicates homogeneity of lithology within this inlet fill. The interval transit time is very high due to the high porosity values of the lithofacies and fluid saturation of the pores. There is an isolated area toward the top of the channel deposits where interval transit time decreases. This is due to localized cementation and consequent occlusion of porosity by anhydrite. The spontaneous-potential curve indicates that permeability is very high. Resistivity is very low in the lower three-quarters of the channel fill. This may represent a salt water leg. This is confirmed from drill stem tests that recovered salty formation water from the lithofacies. The remaining upper deposits have a higher resistivity due to the presence of oil. This well produced oil for three years before becoming a water injection well. The perforated interval within this well corresponds to the limited oil leg.

The channel fill deposits pass abruptly up into Charlie Lake evaporites, dolomites, siltstones and shales. Gamma-ray readings are high and interval transit times are low, signifying that the lithology is shaly and non-porous, respectively. A low gamma-ray peak and low interval transit time occurs at 3822 feet. This is characteristic of anhydrite lithology. This unit is found throughout most of the field, and has been referred to in the past as the 'B-Marker" having been used as a correlation marker for construction of lithostratigraphic cross-sections.

Figure 46 displays the well-log signatures associated with Lithofacies G arenaceous biodolomicrite tidal inlet channel fill deposits. The gamma-ray log signature is blocky signifying the shale free nature of the lithology. The gamma-ray A.P.I. readings from Lithofacies G and Lithofacies H1 channel fill deposits are distinguishable. The difference is that the former A.P.I. values are lower (17) compared to the latter (30). This is attributed to the reduction in quantity of phosphatic lithoclasts and intraclasts within Lithofacies G, indicating a possible different sediment source. The spit-platform sublitharenite deposits (Lithofacies H2) occurring at the top of the 'coquinoid' channel fill deposits within well d-099-C/94-A-16 have higher A.P.I. readings of 25 indicating a changing sediment source. Kumar and Sanders (1974) indicated that the two sub-environments are in fact sourced from different areas. The inlet fill deposits are sourced from offshore and backbarrier areas, whereas the spit-platform sediments are sourced locally from the barrier island or from longshore-drift currents. Source supply in fact does change from offshore and backbarrier to barrier island headland, respectively. The sonic log signature of Lithofacies G has a serrated blocky shape within the channel fill deposits of well d-099-C/94-A-16, whereas the sonic signature of Lithofacies H1 deposits from well d-019-E/94-A-16 is more uniform in value. This is attributed to the formation of patchy cementation and patchy porosity distribution in the former well (see Chapter 6; Plates 52 and 53). The interval transit time decreases markedly within the spit-platform deposits. This is due to the increased size and frequency of diagenetic secondary replacive anhydritic nodules. These nodules occlude pores thus reducing porosity and result in a decrease in interval transit time. Spontaneous potential curves within

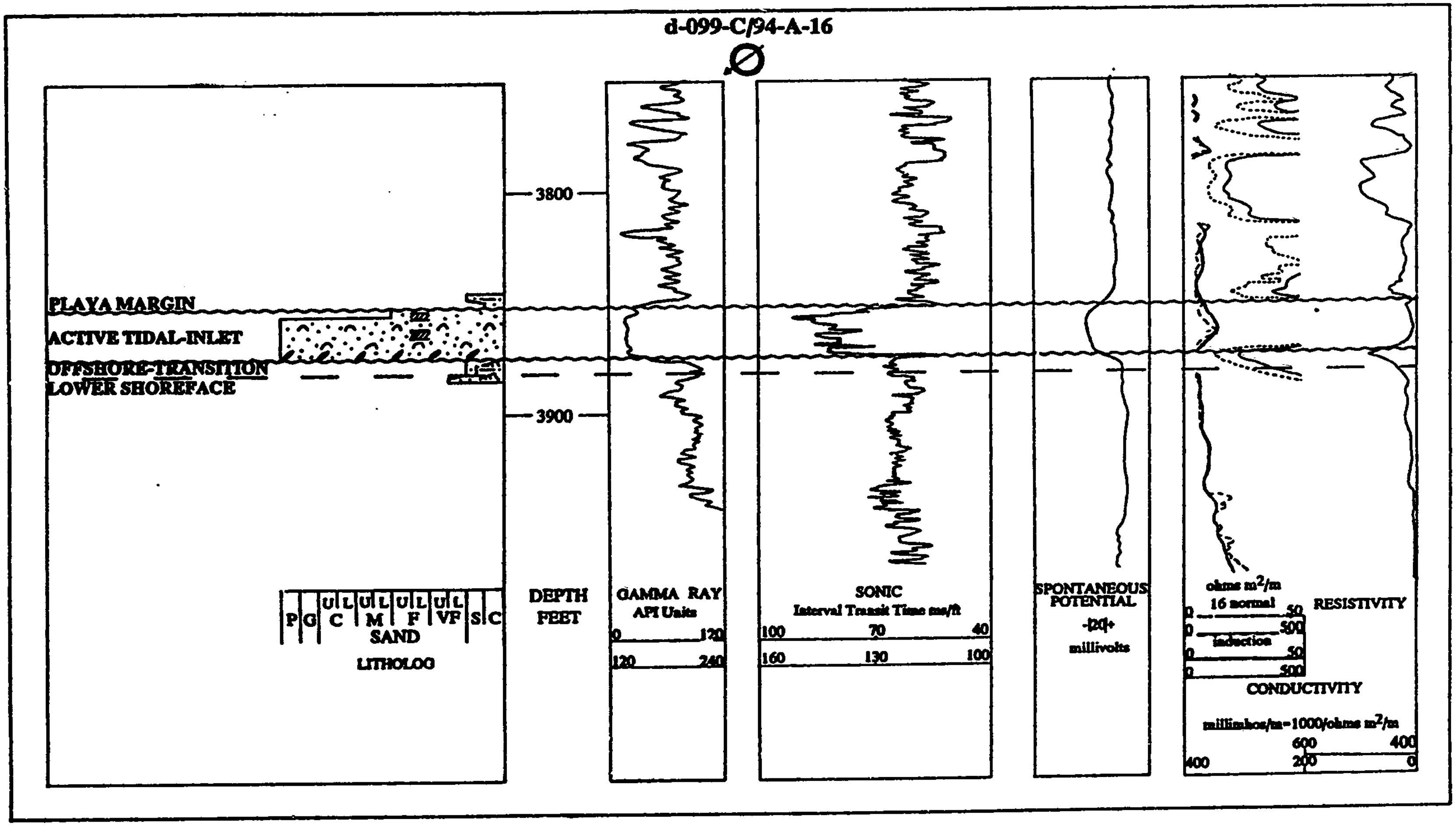

Figure 46. Core-to-well-log correlation for Lithofacies G biodolomicritic tidal inlet fill deposits representative of lithofacies association 2. Well d-099-C/94-A-16.

Lithofacies G tidal inlet channel fill deposits shift less to the left than those of Lithofacies H1 tidal inlet fill deposits because the former deposits are not as porous and permeable as the latter deposits.

In summary, the lithofacies associations occurring within the study area are contrasted by their gamma-ray well-log characteristics. Lithofacies association 1 prograding shoreface cycle is represented on gamma-ray logs as a funnel shaped signature. This reflects the coarsening-upward nature and increase in compositional maturity of the deposits. A.P.I. values decrease upward, sonic log interval transit time commonly increases upward reflecting an increase in porosity, spontaneous potential curves shift to the left indicating increased permeability, and resistivity values may increase upward with the presence of hydrocarbons within the upper shoreface lithology.

Lithofacies association 2 tidal inlet fill deposits are characterized on gamma-ray well-logs by a blocky low A.P.I. signature, reflecting a relatively shale-free lithological homogeneous fill. Gamma-ray well-log responses within Lithofacies G biodolomicritic tidal inlet fills have lower A.P.I. values than those of Lithofacies H1 sublitharenite tidal inlet fills. This is due to the decrease in phosphate lithoclasts. Interval transit times vary greatly in value within Lithofacies G due to the irregular distribution of dense dolomite cement patches.

8.0.0. SEQUENCE STRATIGRAPHIC FRAMEWORK.

A sequence stratigraphic framework was erected in the study area in order to clarify the lateral relationships between the described lithofacies associations. Cross-sections incorporating both core and well-log information were constructed in order to determine the lateral lithofacies relationships and chronostratigraphy of the study area. Gamma-ray well-logs were most useful in determining lithology and were therefore used extensively in the construction of the stratigraphic cross-sections. The sequence stratigraphic cross-sections described within this chapter covered two scales: sub-regional and local. The sub-regional sequence stratigraphic cross-section extended into the area surrounding the field in order to incorporate the Peejay field into a sub-regional sequence stratigraphic framework. The local sequence stratigraphic cross-sections were restricted to the field scale, and confined to the eastern half of the field since deep well penetration into the Doig Formation was lacking in the western part of the field. Later sections describe the vertical and lateral lithofacies relationships associated with the Peejay field.

Numerous stratigraphic cross-sections constructed by the author, had previously been hung on the top of the regionally correlatable 'A' Marker within the Charlie Lake Formation, and at the Charlie Lake-Halfway contact. This, however, produced complex results in which lateral lithofacies relationships were difficult to explain. There are two reasons for the apparent complexity related to sections hung on this marker, or indeed on any other Charlie Lake marker.

Firstly, lithology type controlled the quantity of compaction occurring within each well. The variation was partly controlled by the original primary porosity of the deposits. Clays, for example, exhibit approximately 85% primary porosity, whereas sands exhibit a maximum of 48% primary porosity (Leeder, 1982). Volume reduction of shale lithological may be over 70% that of a clean sandstone. This compactional effect produced distortions to the stratigraphic cross-sections within the study area, no matter which datum was used.

Secondly, a marked relief has been recognized at the Halfway-Charlie Lake contact due to core observations and construction of cross-sections. The relief had the effect of distorting the stratigraphy beneath the erosional surface into a complex arrangement. It was therefore inadvisable to use any marker within the Charlie Lake Formation as a datum while reconstructing the sequence stratigraphic framework for Middle Triassic deposits.

In order to preserve the original stratigraphic relationships within the Middle Triassic deposits of the study area, a regionally continuous synchronous marker within the "Phosphate Zone" of the Doig Formation was used. Many of the wells within the western part of the study area have not penetrated the "Phosphate Zone". These wells therefore lack a reliable datum to use for chronostratigraphic correlation purposes. Cross-sections were therefore restricted to the eastern part of the field where well penetration into the "Phosphatic Zone" was common.

Within the Peejay field it is not only difficult to identify the Doig sandstones in places, but when these sandstones can be seen situated below basal Halfway marine shales they display no evidence of exposure or major erosion. Results from this study agree with those proposed by Aukes and Webb (1986), enhanced by Wittenberg (1992), and successfully applied to the Wembley Field in west-central Alberta by Willis (1992).

The use of the chronostratigraphic technique has enhanced the shortcomings of the lithostratigraphic technique within the study area. The chronostratigraphic elements of correlation cut across the lithostratigraphic elements, as can be seen from the sequence stratigraphic type well of the Peejay field (Figure 47). Parasequences 1 and 2 correspond to the phosphate zone and the lower part of the Doig Formation. Parasequence 4 and the upper part of parasequence 3 correspond to the sandstones of the lithostratigraphically defined Halfway Formation. It can be demonstrated that the sandstone layer composing the Halfway Formation is composed of a number of different parasequences, and hence was diachronous in deposition. Each parasequence contains lithology originally confined to the Halfway and Doig formations. Hence, these formations are related to the same depositional package and were coevally formed.

The gamma-ray well-log of well d-093-D/94-A-16 (Figure 47) demonstrates the coarsening-upward nature associated within each parasequence. Four parasequences have been recognized within the Peejay field. The lowest coarsening-upward package of deposits within this well cannot be traced laterally within the field, and is therefore not

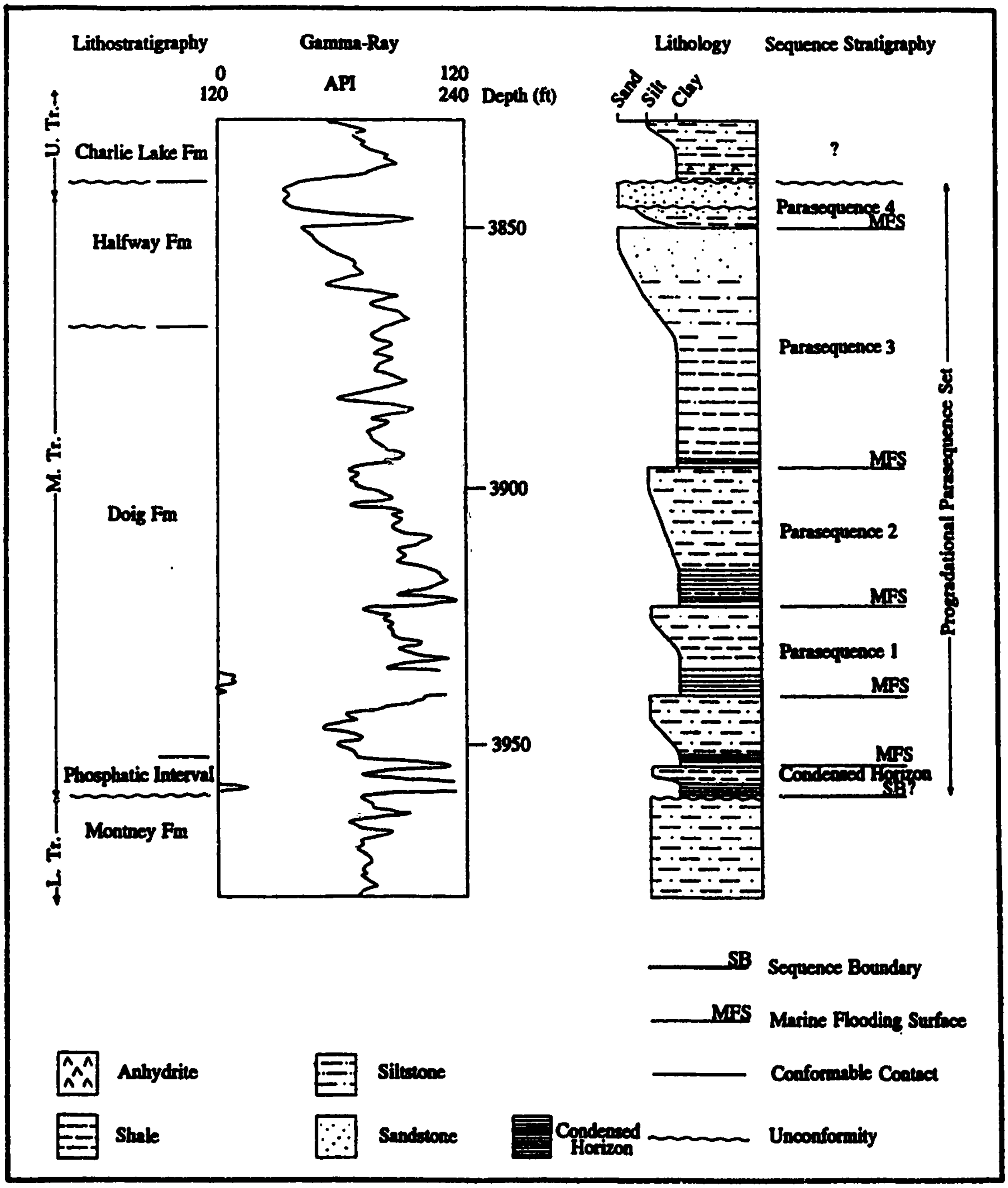

Figure 47. Sequence stratigraphic type well for the Peejay field, showing Middle Triassic lithostratigraphy and chronostratigraphy. Well d-093-D/94-A-16.

described as a parasequence. Only the most distal parts of Parasequences 1 and 2 occur within the Peejay field. The deposits coarsen-up from phosphatic-rich condensed shales into siltstones which are in turn overlain by a condensed section of phosphatic shales representing the base of the next parasequence. Each parasequence thickens and becomes coarser grained in an east-northeasterly direction, toward the palaeoshoreline. Each parasequence thins and clinoforms down to the west-southwest and amalgamates in the "Phosphate Zone". Therefore, the parasequences prograde and offlap to the west-southwest into the Middle Triassic basin. Each parasequence coarsens and thickens upward in a vertical section, such that parasequence 4 contains deposits more proximal to a palaeoshoreline than those of parasequence 3, and so on. In other words, parasequence 4 is younger and more proximal to a palaeoshoreline than parasequence 3. This vertical stacking of parasequences is termed a progradational parasequence set. Toward the west-southwest, parasequence 4 would display sedimentary structures and lithology representative of more distal locations to a palaeoshoreline. These sedimentologic features would be similar to those encountered in parasequence 3, within well d-093-D/94-A-16. To the east-northeast parasequence 3 coarsens and thickens in a palaeolandward direction becoming similar in appearance to that of parasequence 4. Each parasequence can be traced east-northeastward toward the palaeoshoreline, but they become truncated and overlain by playa-lake siltstones and shales of the Charlie Lake Formation, hence removing all traces of back barrier and coastal plain deposits.

8.1.0. SUB-REGIONAL SEQUENCE STRATIGRAPHIC FRAMEWORK.

In order to better place the Peejay field in a sub-regional sequence stratigraphic context, cross-section H-H' was constructed parallel to regional depositional dip (Figures 48, 49). The cross-section was oriented northeast-southwest, extending for a horizontal distance of 48.2 km (29.8 miles). The section was hung on a synchronous phosphate marker within the Phosphate Zone of the lower Doig Formation.

It is observable from Figure 49, that Middle Triassic deposits between the underlying Montney Formation and overlying Charlie Lake Formation, are composed of parasequences that offlap and young in a southwesterly direction into the basin. Each parasequence coarsens upward, but most are distal to a palaeostrandline and consequently do not contain proximal shoreface sandstone deposits. Further to the southwest, however, proximal shoreface sandstones as well as inlet deposits are preserved within

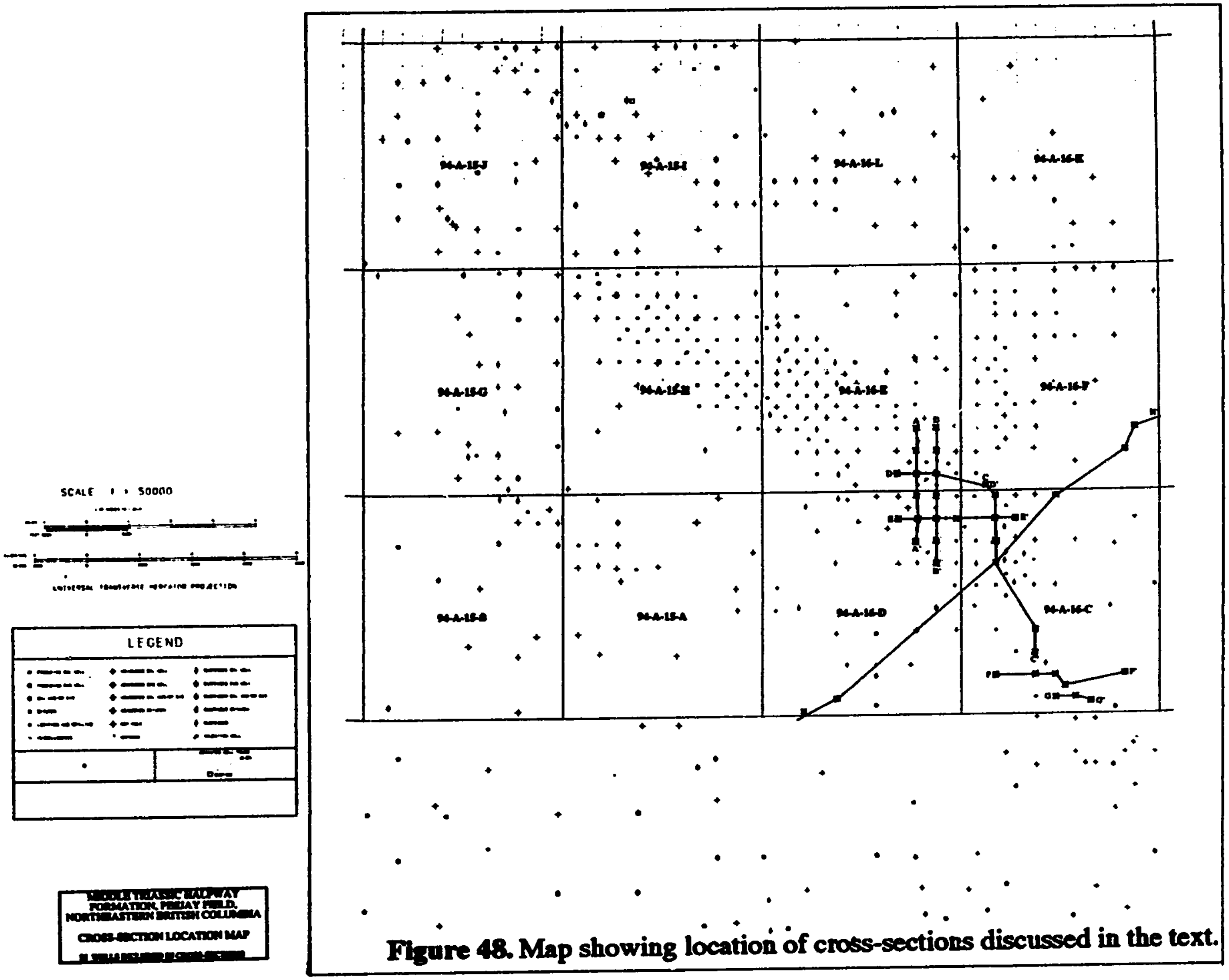

Figure 48. Map showing location of cross-sections discussed in the text.

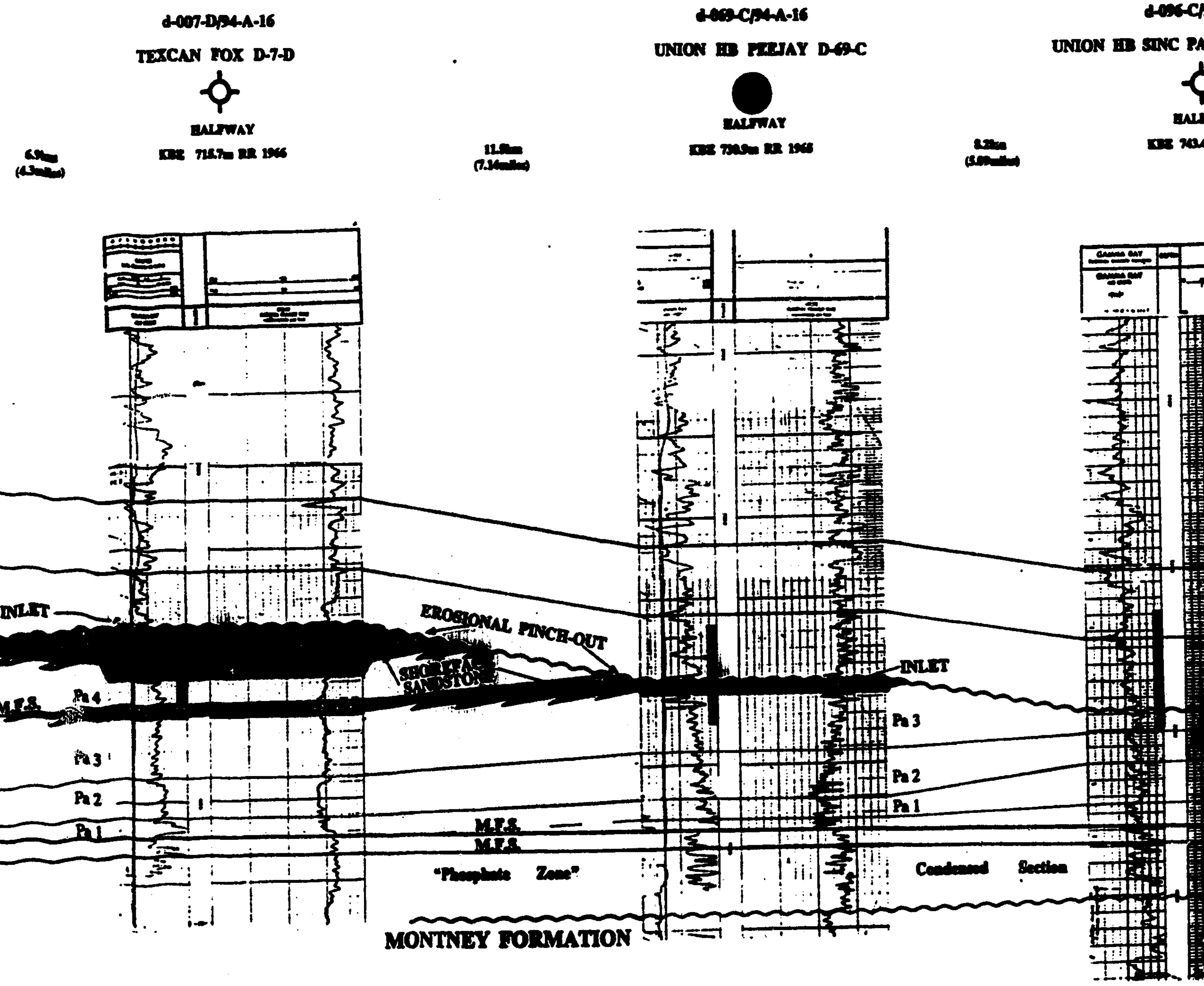

H-H' oriented southwest-northeast along
s the first phosphatic bed within the

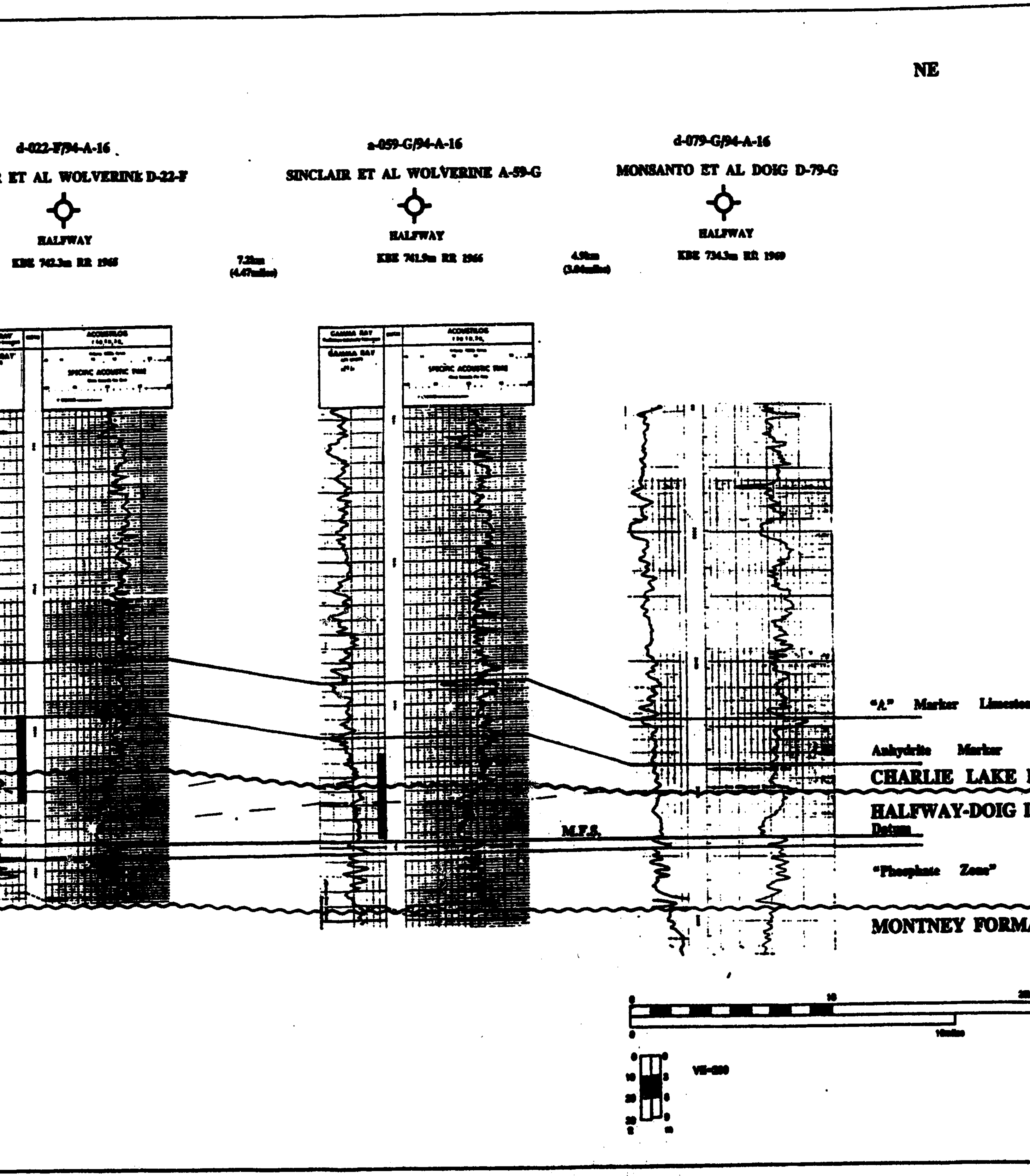
NE
d-022-F/94-A-16
ET AL WOLVERINE D-22-F
HALFWAY
KBE 742.3m RR 1965
7.2km
(4.47miles)
a-059-G/94-A-16
SINCLAIR ET AL WOLVERINE A-59-G
HALFWAY
KBE 741.9m RR 1966
4.9km
(3.04miles)
d-079-G/94-A-16
MONSANTO ET AL DOIG D-79-G
HALFWAY
KBE 734.3m RR 1969
GAMMA RAY
ACOUSTILOG
SPECIFIC ACOUSTIC TIME
"A" Marker Limesto
Anhydrite Marker
CHARLIE LAKE
HALFWAY-DOIG
M.F.S.
Datum
"Phosphate Zone"
MONTNEY FORMA
0
10
0
10miles
0
10
20
30
0
3
6
9
VE-200

parasequences. Each parasequence thickens in a northeasterly direction, and A.P.I. units on the gamma-ray log decrease to the northeast, indicating the increased influence of sandy sediment supply from a northeasterly direction. The vertical stacking nature of the parasequences within the Middle Triassic is indicative of a progradational parasequence set.

Also of interest is the nature of the Charlie Lake-Halfway contact. It can be clearly seen that the thickness of the Middle Triassic deposits between the top of the 'Halfway' Formation and the Montney Formation, or from the top of the 'Halfway' Formation to the phosphate datum within the 'Doig' Formation, reduce toward the northeast. For example, the thickness between the first 'Doig' phosphate datum and the top of the 'Halfway' in well a-063-I/94-A-10 in the southwest corner of the cross-section is 41 metres (135 feet), whereas the thickness in well d-079-G/94-A-16 in the northeast is only 8 metres (26 feet). This represents a loss of 33 metres (109 feet) of section within a horizontal distance of 48 km (30 miles). By tracing them updip (to the northeast), each parasequence becomes truncated against the Charlie Lake Formation. Coarser, more proximal deposits are found in the extreme southwestern parasequences where the least amount of erosion to the Middle Triassic deposits has occurred. Further northeast, however, the amount of truncation and erosion increases, resulting in preservation of the distal portions of parasequences to the east.

Figure 50 shows the sedimentologic relationship between Middle Triassic and Charlie Lake deposits within well d-018-B/94-A-16, located 6.2km (3.8 miles) to the east of the study area. Here, offshore laminated shales are overlain erosively by a polymict conglomerate (post-Halfway erosion surface) and are overlain by genetically unrelated continental red-beds of the Charlie Lake Formation. All traces of the Halfway prograding shoreface sequence have been removed. This, clearly indicates that there has been a significant amount of post-Halfway erosion to the northeast. The erosional edge of the lithostratigraphically defined 'Halfway' Formation is therefore adjacent to the Peejay study area (northeast).

The mechanism explaining this erosional phenomenon will be expanded upon in Chapter 9, hence will be only briefly mentioned here. The unconformable relationship between the Middle Triassic deposits and the Charlie Lake Formation was produced by the tilting

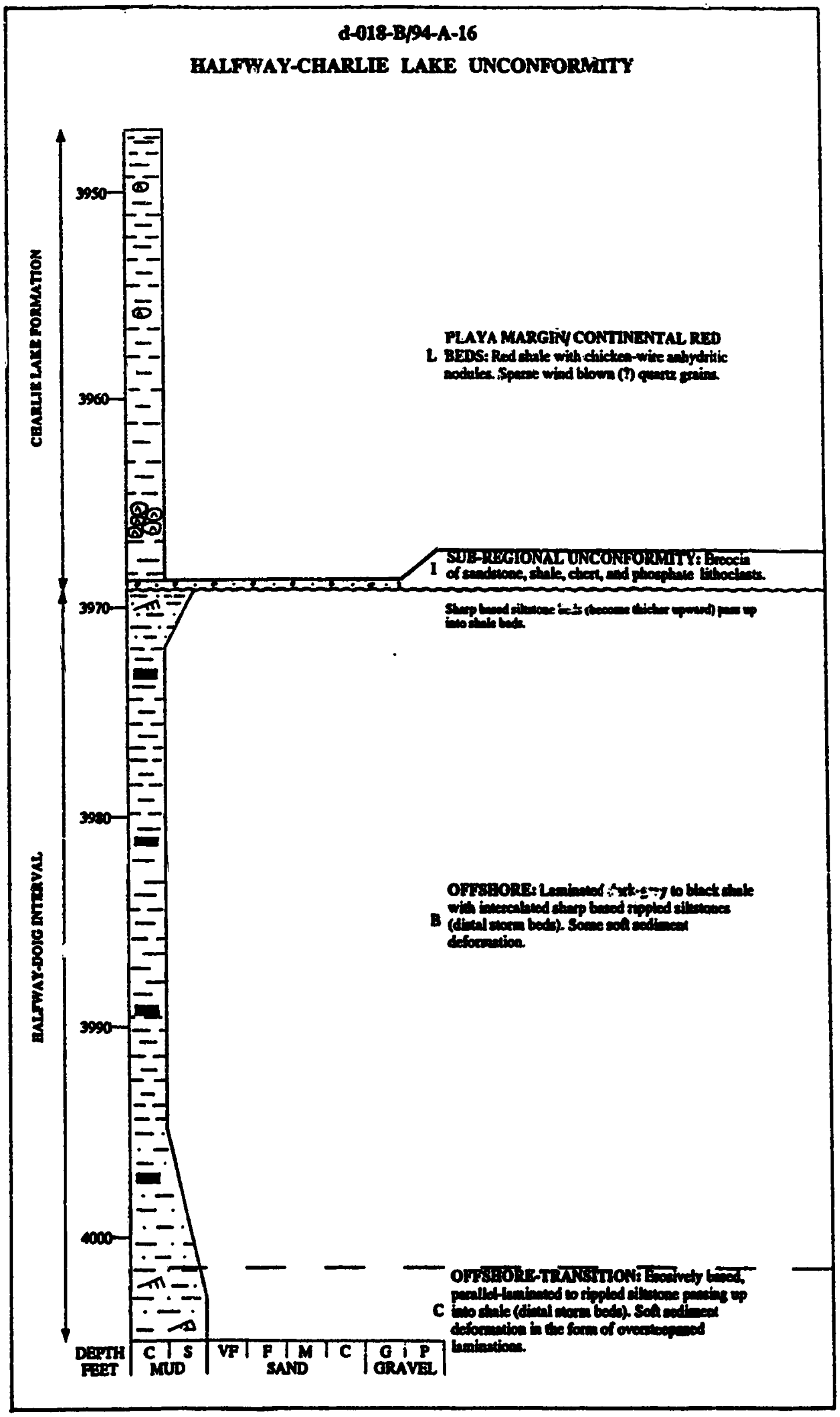

Figure 50. Well d-018-B/94-A-16 demonstrates the erosional nature of the Halfway/ Charlie Lake contact. Red beds and anhydrites of the Charlie Lake Formation rest directly on offshore marine shales of the Halfway Formation. All lower and upper shoreface and inlet deposits have been removed.

of the strata up to the northeast with coeval subsidence to the southwest, hence causing greater exposure of the Middle Triassic deposits to the northeast within northeastern British Columbia. The tilting occurred during the earliest Carnian times. Whether the erosion actually occurred at the Halfway-Charlie Lake contact, or as an intra-Charlie Lake unconformity, during Carnian times is difficult to decipher from this cross-section alone.

Increased removal of Middle Triassic deposits toward the northeast has been clearly identified within the Peejay field (Figure 51). Within 15 km (9 miles) horizontal distance in a northeasterly direction the thickness of deposits between the top of the 'Halfway' Formation and the phosphate datum within the 'Doig' Formation thins from 46 metres (150 feet) in the southwest, to 12 metres (40 feet) in the northeast, a removal of 34 metres (110 feet). There are local areas of increased sediment thickness, represented by the preservation of parasequence 4 deposits within the field. These areas of selective increased preservation potential have been attributed to the development and formation of graben structures, initiated prior to or during uplift and removal of the Middle Triassic deposits in northeastern British Columbia during early Carnian times (Figure 52) (see Chapter 9 and 10). Parasequence 4 is absent within the northeastern part of the study area, indicated by a decreased thickness of Middle Triassic deposits between the top of the 'Halfway' Formation and the phosphate marker (northeastern part of the F/94-A-16 block), as post-Halfway erosional effects become even more pronounced.

8.2.0. FIELD-SCALE SEQUENCE STRATIGRAPHIC FRAMEWORK.

Seven sequence stratigraphic cross-sections were constructed within the eastern part of the study area (Figure 48). These sections were assembled in areas where well penetration into the Phosphatic Zone of the Doig Formation allowed use of a phosphatic datum in order to establish accurate chronostratigraphic lithofacies relationships. Accurate lateral lithofacies relationships were derived from the combination of gamma-ray and sonic well-logs and cored information from wells spaced between 0.35 km (0.22 miles) and 1 km (0.62 miles) apart. The vertical scale of the well-logs is in feet. The sections were constructed in north-south and east-west trends, approximating depositional strike and dip, respectively.

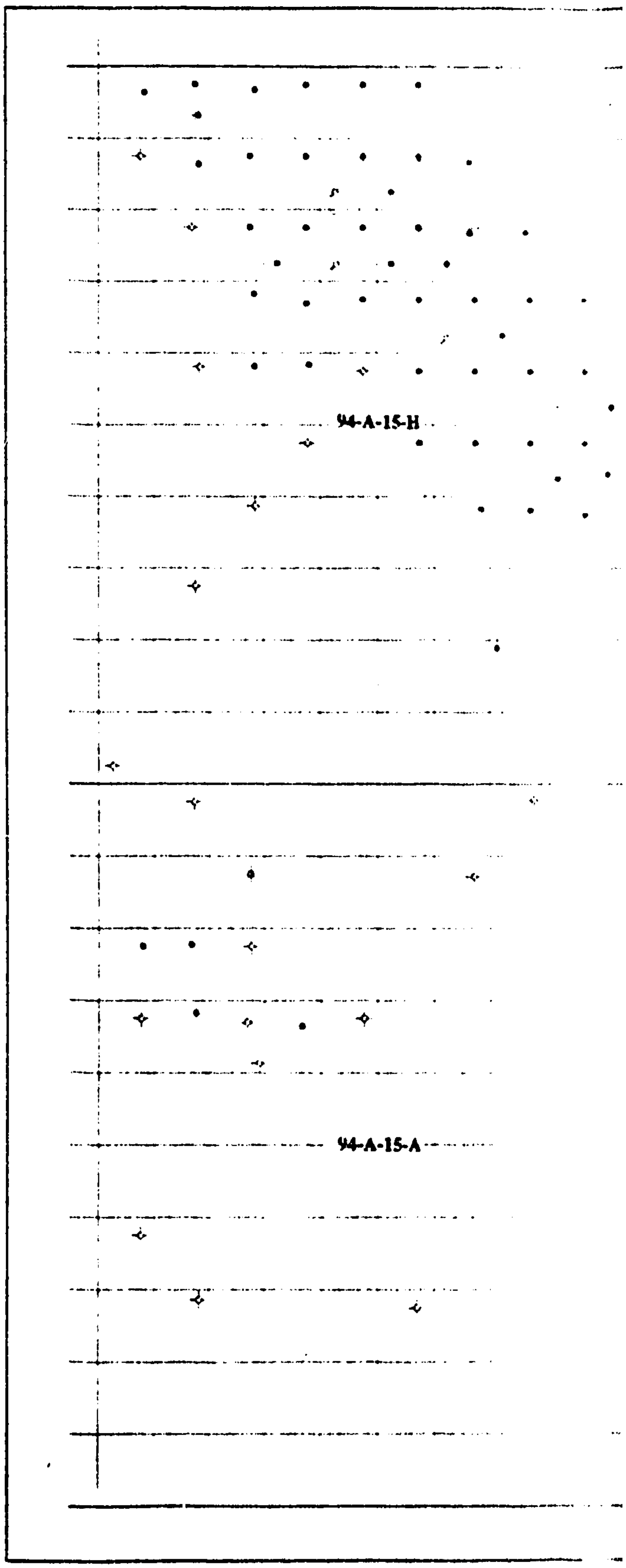

Figure 51. Isopach map between the top of the Halfway Formation and the phosphatic datum within the Doig Formation. The most obvious results are that these deposits thin to the northeast. Local thickening of these deposits, however, occurs in a north-south trend. This corresponds to sediment preservation within early Carnian activated grabons, thus dictating the preservation of the best reservoirs within the study area.

of the
atum
rious
ortheast.
ver,
ponds
hian
ervation
a.

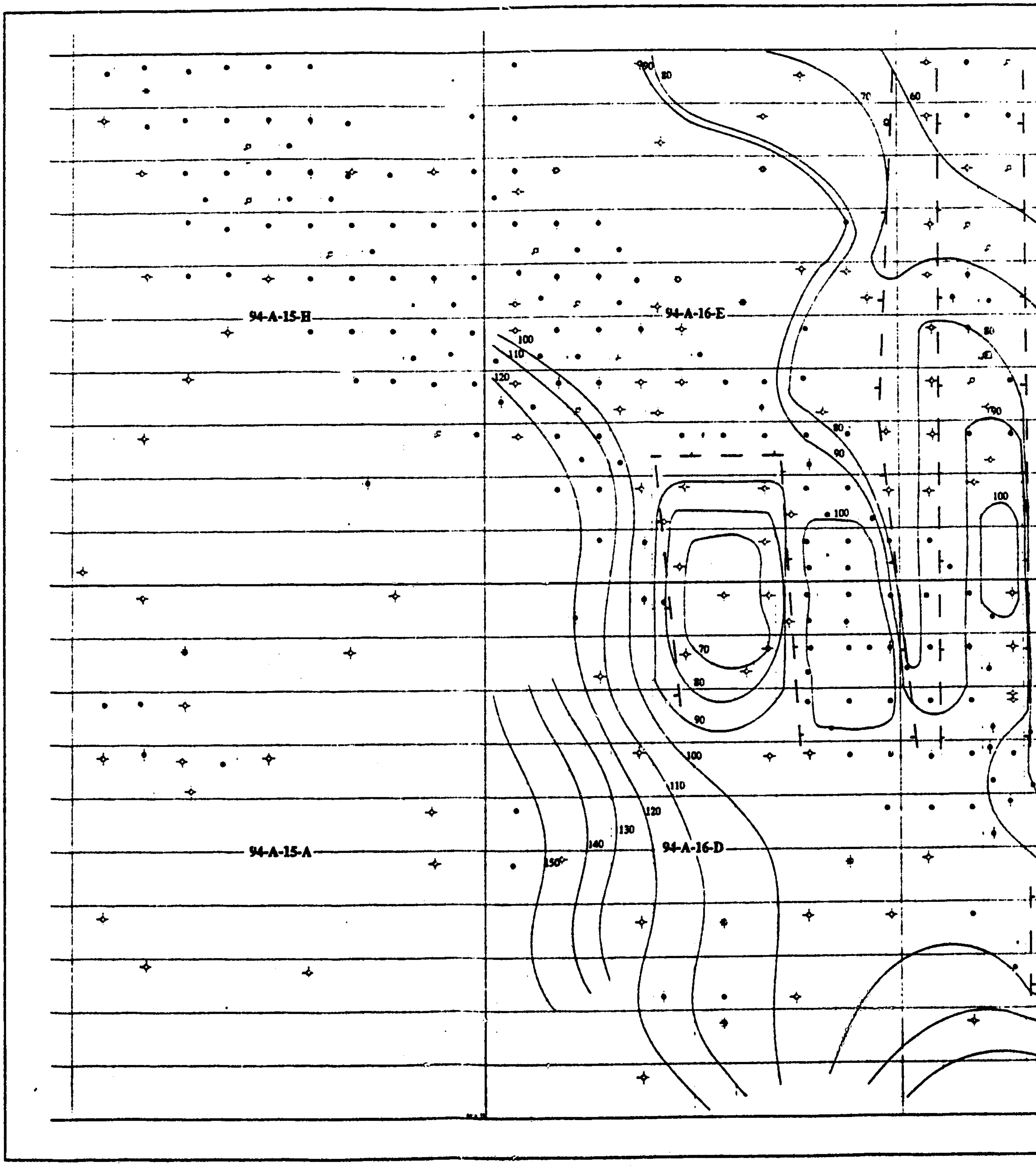

ce 4
on of

e 4
the

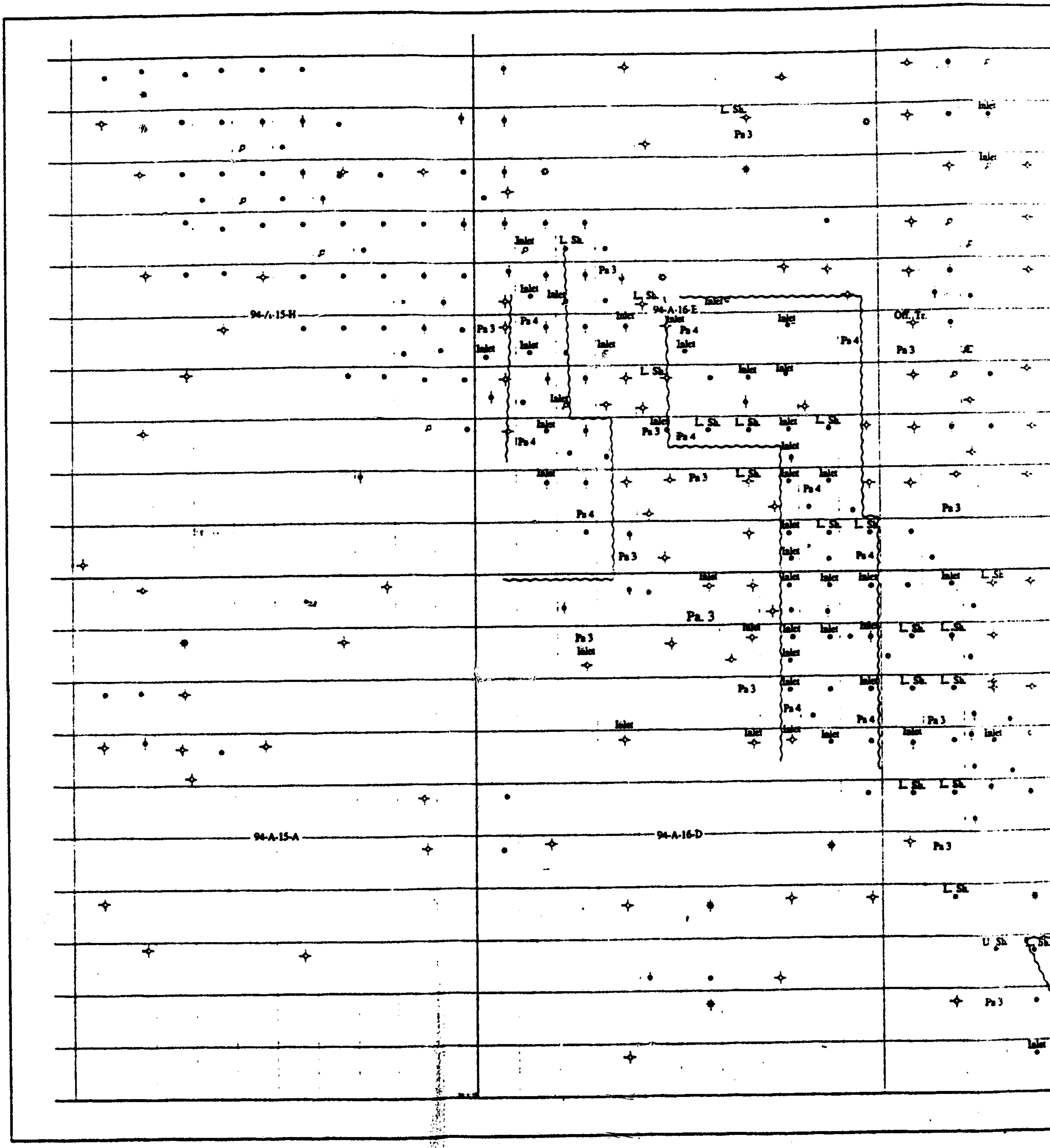

Stratigraphic cross-sections A-A', B-B' and C-C' are oriented north-south, slightly oblique to depositional strike. Evidence to support this orientation is from lateral correlation of the marine flooding surfaces. It can be seen that the marine flooding surfaces clinoform downward and converge toward the south. The deposits (parasequence) that they bind become thinner and shalier to the south and thicker and shale-free toward the north. This indicates that proximity to a palaeostrandline increased toward the north, whereas basinal influences became more prevalent toward the south. If the cross-section had been oriented parallel to depositional strike the individual thickness of parasequences would have been relatively uniform, assuming that the supply of sediment to the coastline was also uniformly distributed. The combination of north-south and east-west oriented cross-sections has led to the reconstructed palaeoshoreline in a north-northwest to south-southeast trend.

Within stratigraphic cross-section A-A' (Figure 53) the proportion of tidal inlet fill deposits is much higher than in depositional dip cross-sections. Infact, parasequence 4 shoreface deposits have been almost completely replaced with tidal inlet channel fill deposits. This is not unusual since wave-dominated tidal-inlets documented from modern barrier island wave-dominated coastlines tend to migrate rapidly along strike, reworking and replacing the underlying barrier island deposits with tidal inlet deposits (Hoyt and Henry, 1967; Moslow and Heron, 1979). Tye and Moslow (1992) document that up to 40% of deposits underlying the Holocene wave-dominated barrier island shoreline of North Carolina are of tidal-inlet origin.

Most tidal inlet deposits associated with parasequence 4 lie directly ontop of shoreface deposits of parasequence 3. This suggests that the tidal-inlets cut down deeply into, and reworked, the underlying shoreface deposits. It must be stressed, however, that the tidal inlet fill deposits shown in section A-A' (Figure 53) may represent the amalgamation of a number of different migrating inlets within the same spatial location over a period of geological time.

The thickness of some tidal-inlet channel fill deposits are greater than modern recorded thicknesses. For example, well d-083-D/94-A-16 consists of 11 metres (36 feet) of tidal inlet fill deposits. This is a minimum thickness for these deposits since material has been

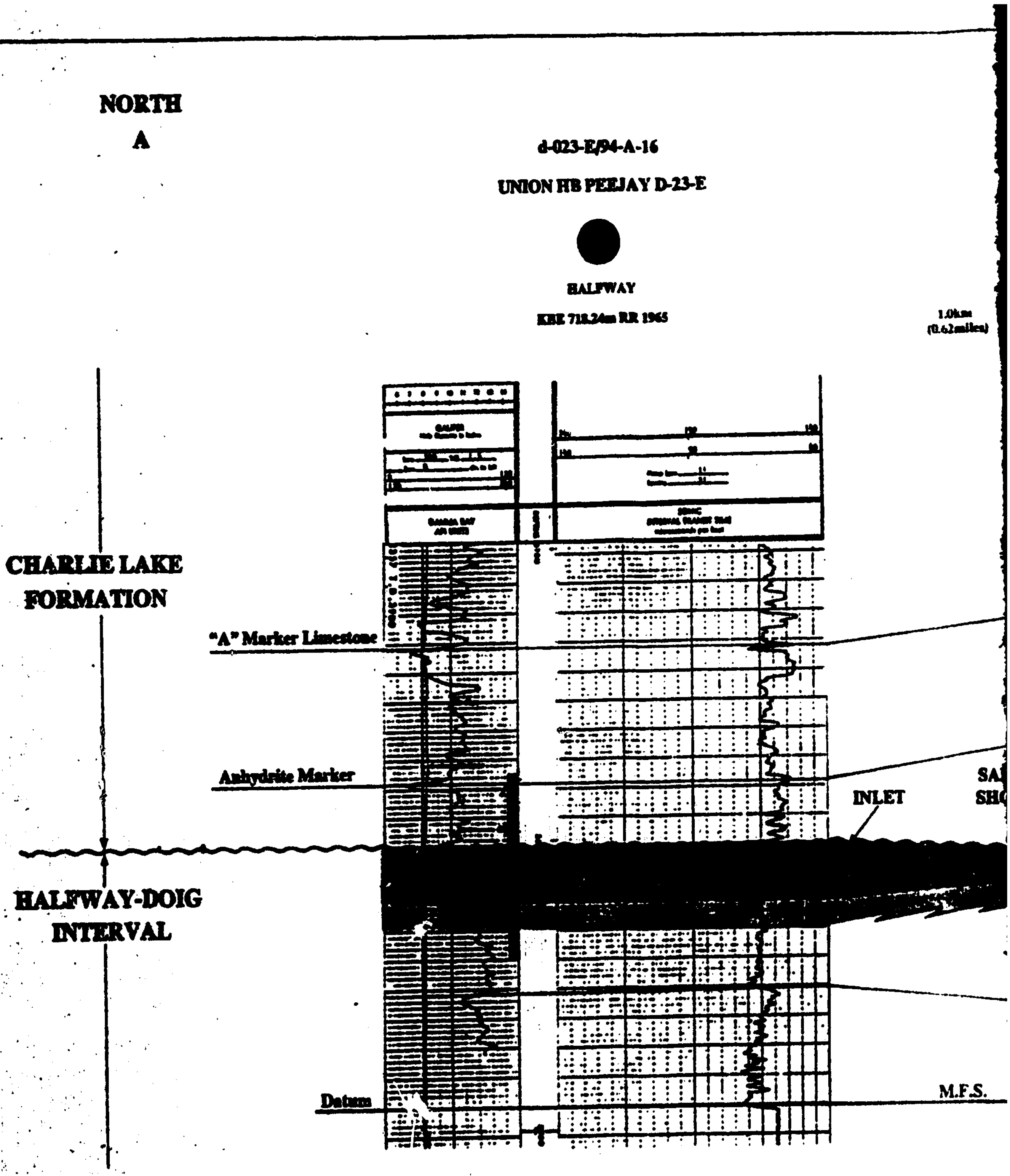

Figure 53. Sequence stratigraphic cross-section A-A' oriented north-south slightly oblique to depositional strike.

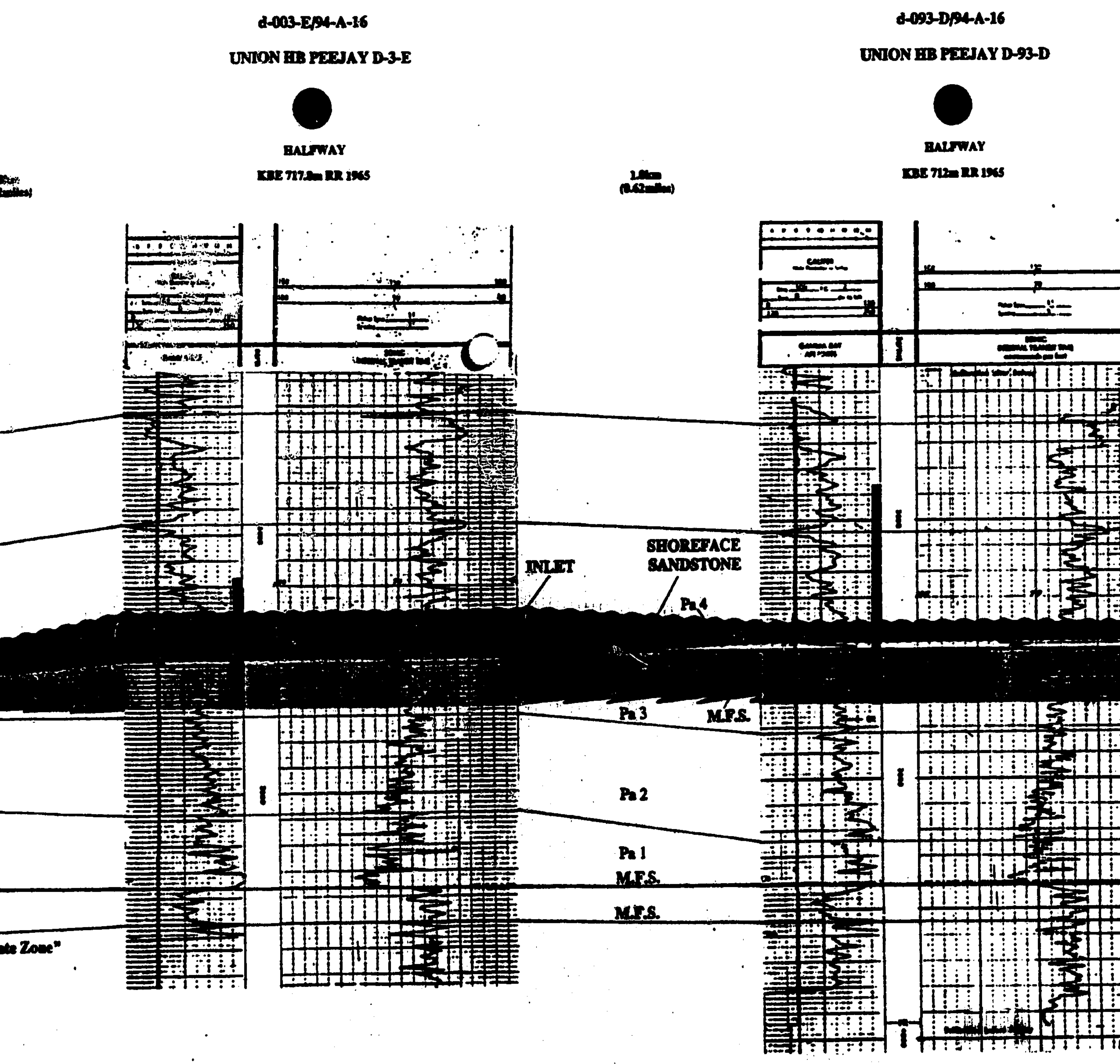
d-003-E/94-A-16
UNION HB PEEJAY D-3-E
HALFWAY
KBE 717.8m RR 1965
1.0km
(0.62miles)
d-093-D/94-A-16
UNION HB PEEJAY D-93-D
HALFWAY
KBE 712m RR 1965
INLET
SHOREFACE
SANDSTONE
Pa 4
Pa 3
M.F.S.
Pa 2
Pa 1
M.F.S.
M.F.S.
ate Zone"

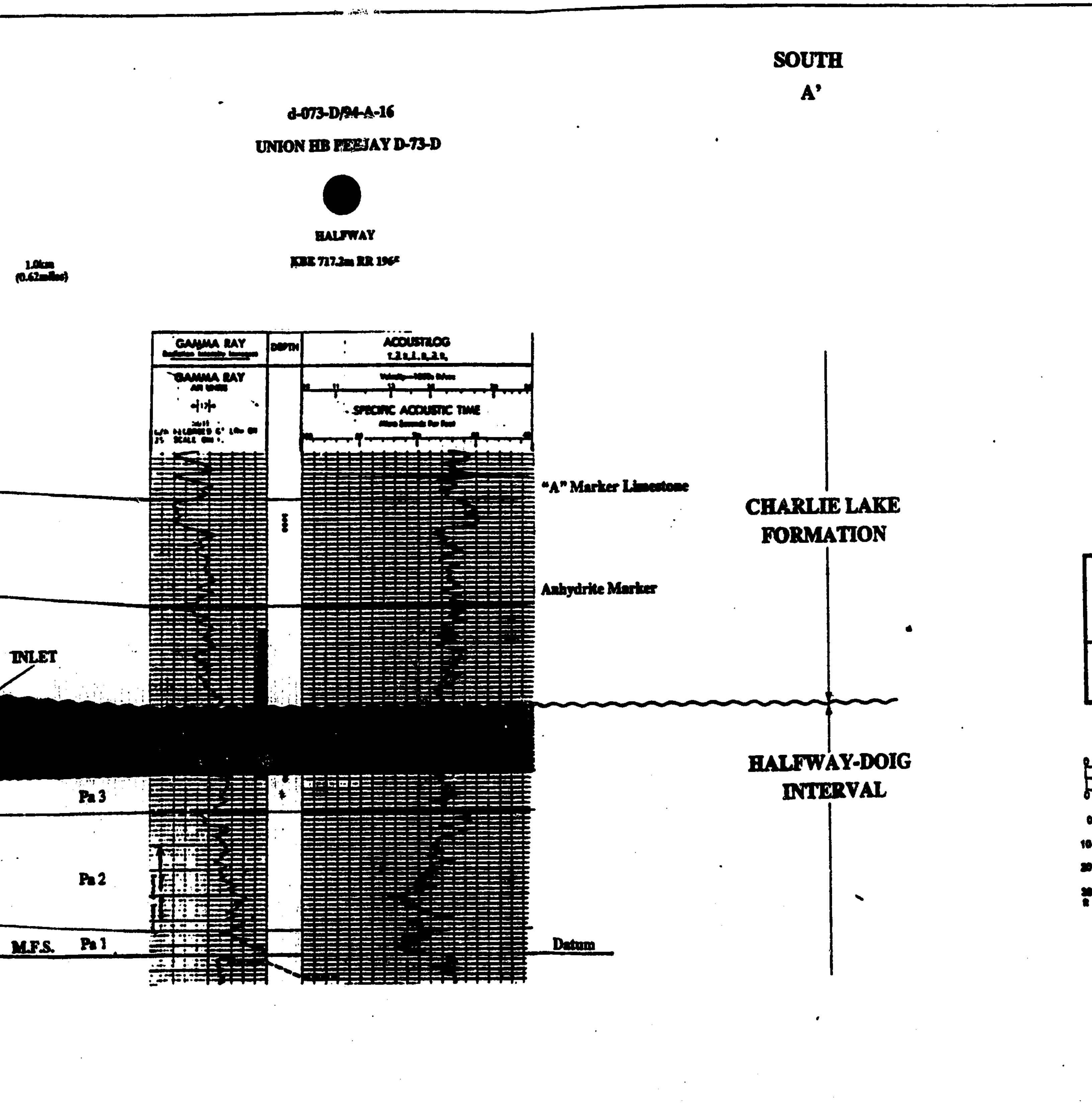
SOUTH
A'
d-073-D/94-A-16
UNION HB PEEJAY D-73-D
HALFWAY
KBE 717.2m RR 196
1.0km
(0.62miles)
GAMMA RAY
DEPTH
ACOUSTILOG
GAMMA RAY
SPECIFIC ACOUSTIC TIME
"A" Marker Limestone
CHARLIE LAKE FORMATION
Anhydrite Marker
INLET
HALFWAY-DOIG INTERVAL
Pa 3
Pa 2
M.F.S.
Pa 1
Datum

stripped off of the top of the Halfway. Modern day wave-dominated tidal inlet sequences, however, range in thickness from 1.5 to 10 metres (4.9 to 32.8 feet) (Kumar and Sanders, 1974; Moslow and Tye, 1985). Thus, it has been concluded that thick tidal inlet channel fill deposits within the cross-section were composed of at least two tidal inlet fills. The contact is sand-on-sand, and therefore difficult to recognize in core or on logs, except for a local increase in shaly and phosphate material, at the base of younger inlets.

Figure 53 also displays tidal inlet fill deposits increasing in thickness in a southerly direction. Tye and Moslow (1992) have documented that tidal inlet thickness increases in a downdrift direction. The direction of migration can therefore be derived from the three-dimensional geometry of the channel fill deposits. Hence, the downdrift lateral migration of the Middle Triassic wave-dominated tidal inlets was probably to the south-southeast.

Stratigraphic strike cross-section B-B' (Figure 54) clearly demonstrates the increased depth of scour of a tidal inlet as it matured and migrated laterally in a southerly direction. The base of these deposits appears to have eroded further down into the underlying deposits in a southerly direction until at well d-072-D/94-A-16 the basal tidal inlet deposits had eroded down into shoreface deposits of older parasequence 3, below. The deposits within well d-062-D/94-A-16 had eroded down into nearshore marine siltstones and shales of younger parasequence 4. The apparent thinning of the channel deposits in this well may indicate the initiation of a different tidal inlet channel to that associated with the inlet deposits further to the north.

Stratigraphical cross-section C-C' (Figure 55) has also been constructed slightly oblique to depositional strike. It can be clearly seen that individual parasequences thicken and become less shaly in a palaeolandward direction (toward the north). For example, parasequence 1 thickness from 5 metres (16 feet) in the south, at well d-027-C/94-A-16, to 12 metres (40 feet) in the north at well b-009-F/94-A-16. Parasequences 1 and 2 coarsen up into shaly sandstones that do not indicate good reservoir quality, hence the lack of hydrocarbon production. More proximal regions of parasequences 3 and 4, however, coarsen-upward into less shaly shoreface sandstone deposits attaining fair to good reservoir quality. These deposits were commonly reworked by laterally migrating tidal inlets, whose channel fill deposits are of good reservoir quality. Again, it can be seen that parasequence 3 contains less tidal inlet fill material than parasequence 4.

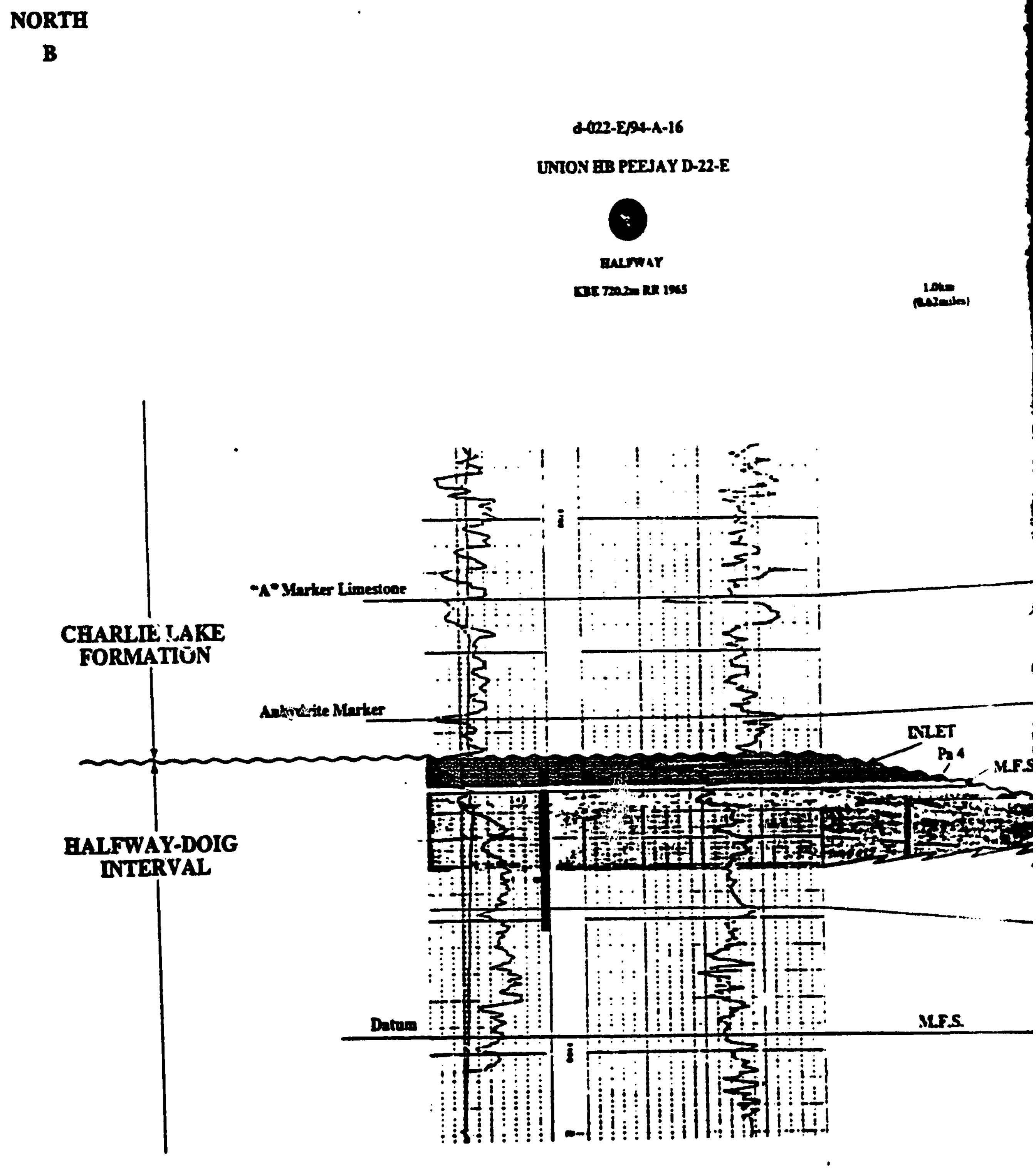

Figure 54. Sequence stratigraphic cross-section B-B' oriented north-south slightly oblique to depositional strike.

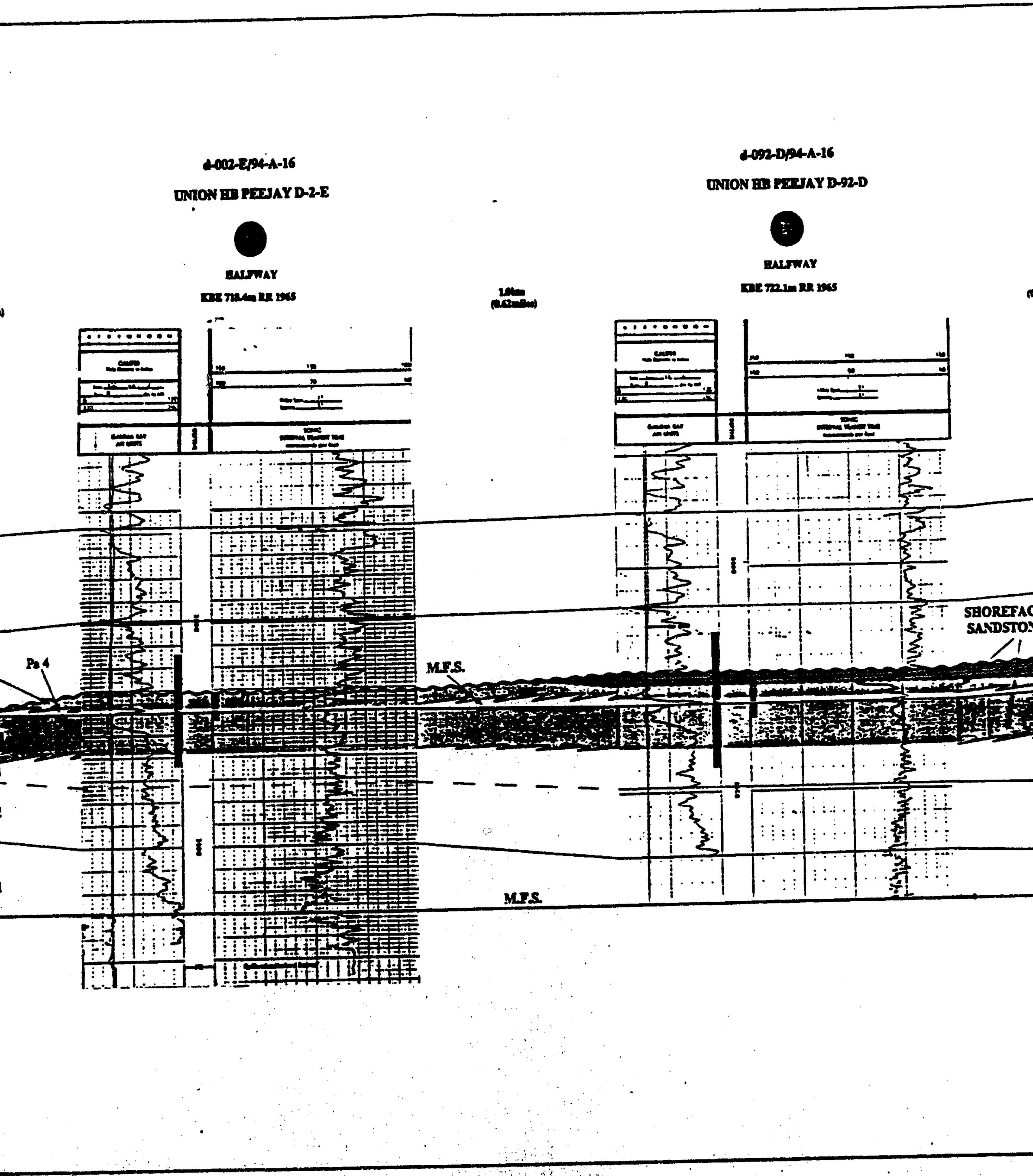
d-002-E/94-A-16
UNION HB PEEJAY D-2-E
HALFWAY
KBE 718.4m RR 1965
1.0km
(0.62miles)
d-092-D/94-A-16
UNION HB PEEJAY D-92-D
HALFWAY
KBE 722.1m RR 1965
SHOREFAC
SANDSTON
Pa 4
M.F.S.
M.F.S.

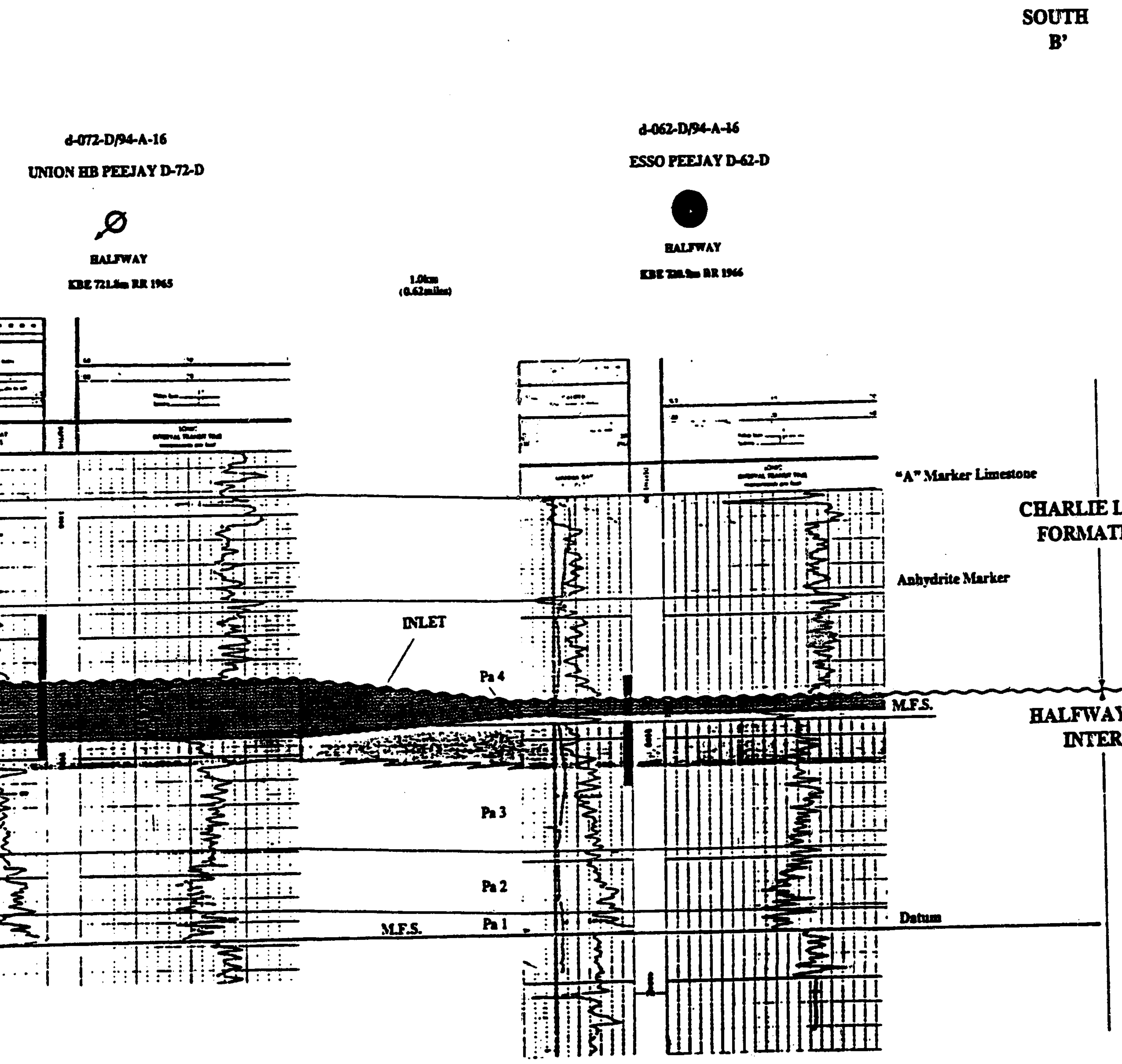
SOUTH
B'
d-072-D/94-A-16
UNION HB PEEJAY D-72-D
HALFWAY
KBE 721.8m RR 1965
1.0km
(0.62miles)
d-062-D/94-A-16
ESSO PEEJAY D-62-D
HALFWAY
KBE 720.9m RR 1966
"A" Marker Limestone
CHARLIE L
FORMATI
Anhydrite Marker
INLET
Pa 4
M.F.S.
HALFWAY
INTER
Pa 3
Pa 2
Pa 1
M.F.S.
Datum

cross-section C-C' oriented north-south slightly

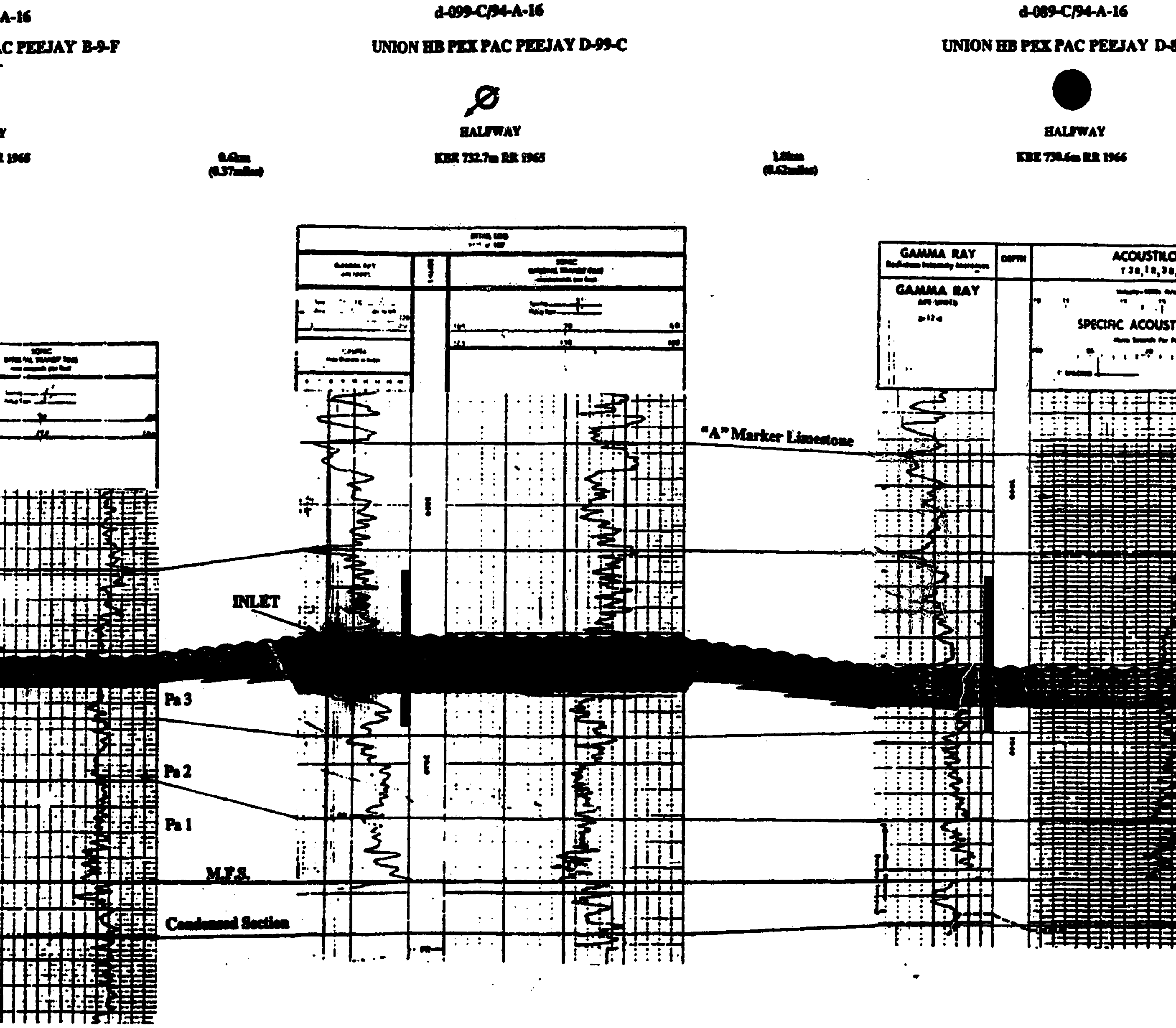

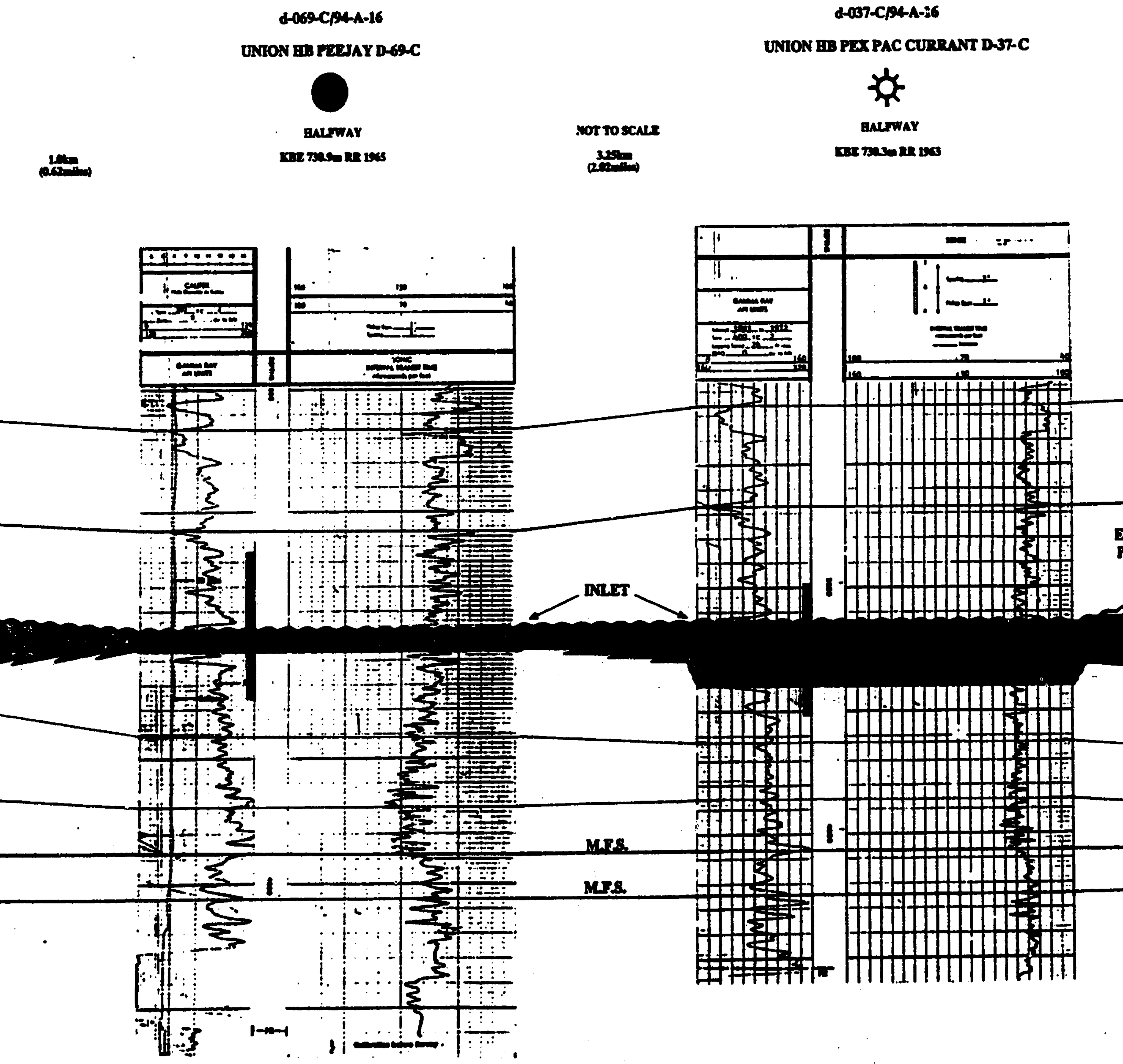
d-069-C/94-A-16
UNION HB PEEJAY D-69-C
HALFWAY
KBE 730.9m RR 1965
1.0km
(0.62miles)
NOT TO SCALE
3.25km
(2.02miles)
d-037-C/94-A-16
UNION HB PEX PAC CURRANT D-37-C
HALFWAY
KBE 730.3m RR 1963
GAMMA RAY
API UNITS
SONIC
INTERVAL TRANSIT TIME
INLET
M.F.S.
M.F.S.

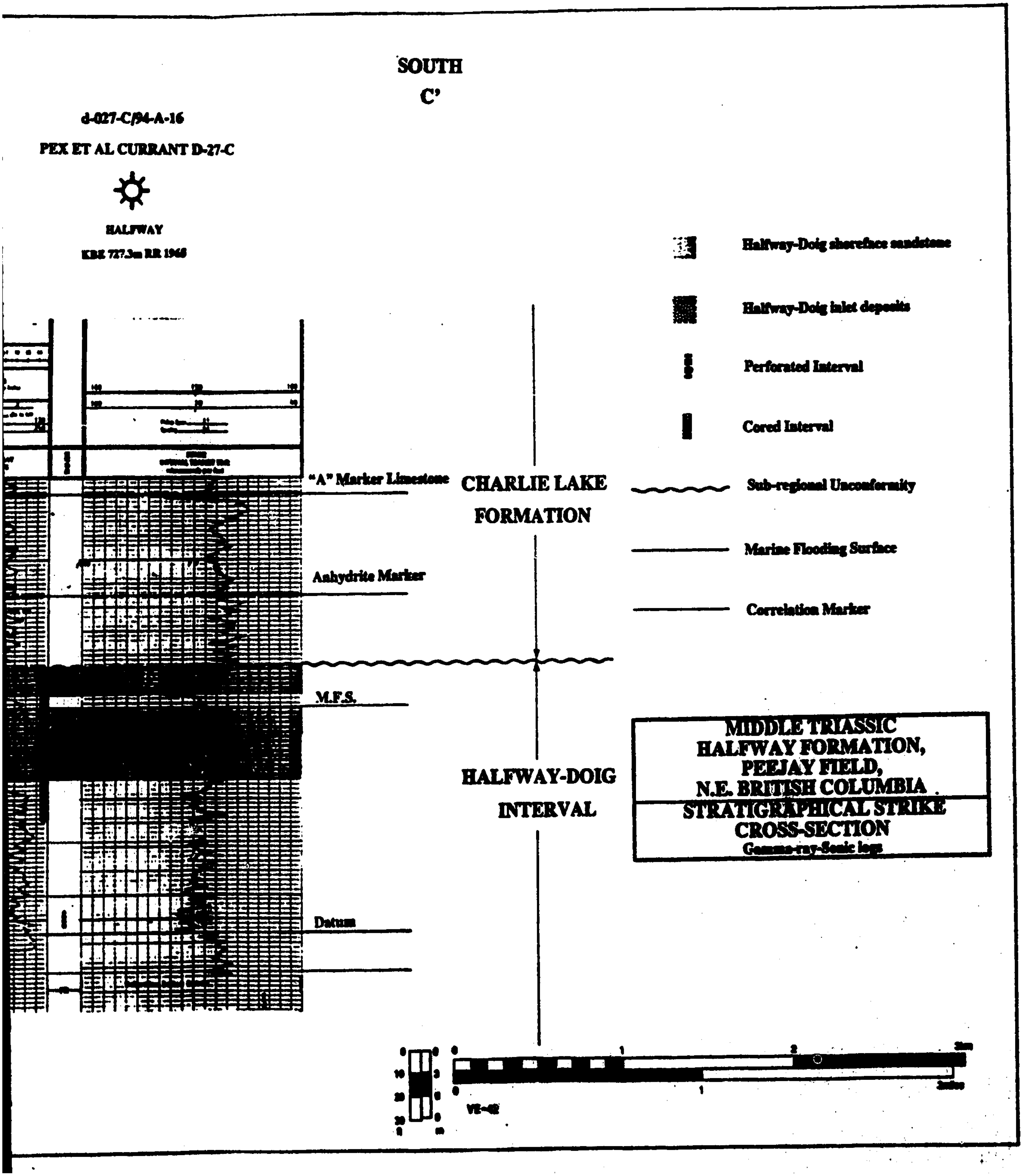
SOUTH
C'
d-027-C/94-A-16
PEX ET AL CURRANT D-27-C
HALFWAY
KBE 727.3m RR 1968
"A" Marker Limestone
Anhydrite Marker
M.F.S.
Datum
CHARLIE LAKE FORMATION
HALFWAY-DOIG INTERVAL
Halfway-Doig shoreface sandstone
Halfway-Doig inlet deposits
Perforated Interval
Cored Interval
Sub-regional Unconformity
Marine Flooding Surface
Correlation Marker
MIDDLE TRIASSIC HALFWAY FORMATION, PEEJAY FIELD, N.E. BRITISH COLUMBIA
STRATIGRAPHICAL STRIKE CROSS-SECTION
Gamma-ray-Sonic logs
0
1
2
3km
0
1
2miles
0
10
20
30
m
VE=42

Four cross-sections constructed in an east-west orientation, almost parallel to depositional dip demonstrate the effects of the Carnian erosion surface on the chronostratigraphically correlated Middle Triassic sandstone packages.

Sequence stratigraphic cross-sections D-D', E-E', F-F' and G-G' (figures 56, 57, 58 and 59) are oriented east-west, almost parallel to depositional dip. The datum on which the sections are hung is within the uppermost Doig phosphatic horizon. Each parasequence has been identified on the cross-sections by the bell-shaped signature on gamma-ray logs corresponding to the coarsening-up and increase in compositional maturity as a result of shoreface progradation. Each parasequence thins to the west and becomes more shaly thus producing a higher A.P.I. value on gamma-ray logs. Conversely, they thicken and become shale-poor to the east as shoreline proximity is approached, thus producing lower A.P.I. gamma-ray values. Each parasequence clinoforms down to the west. Successively younger parasequences are deposited ontop of and to the west of older parasequences. Thus, younger parasequences step further basinward in an offlapping arrangement.

Stratigraphic strike oriented cross section D-D' (Figure 56) illustrates the lateral variability in thickness of sandstone lithology. Well d-003-E/94-A-16 contains the thickest sandstone accumulation in the section, the tidal inlet deposits of parasequence 4 cutting down into the shoreface deposits of parasequence 3 below. Either side of the well, parasequence 4 deposits are thinner, and in well b-009-F/94-A-16 these deposits have been completely removed. Within well d-004-E/94-A-16 the entire sandstone package composing both parasequences 3 and 4 have been removed, such that good reservoir quality sandstones pass laterally to the west into continental playa-lake deposits of poor reservoir quality.

The vertical stacking of parasequences within cross-sections D-D' and E-E' (Figures 56 and 57) show that each individual stacked parasequence progressively thickens upward with respect to the former parasequence indicating the approaching proximity to a palaeostrandline (well d-082-D/94-A-16 in section E-E', Figure 57). Parasequence 3 within section E-E' (Figure 57) is composed of prograding shoreface deposits. The upper parts of this cycle have been removed by post-Halfway erosion, resulting in lack of upper shoreface preservation. The entire shoreface sandstones of parasequence 3 have been removed from well d-083-D/94-A-16 by the downcutting of later tidal inlet deposits section D-D' oriented east-west slightly oblique

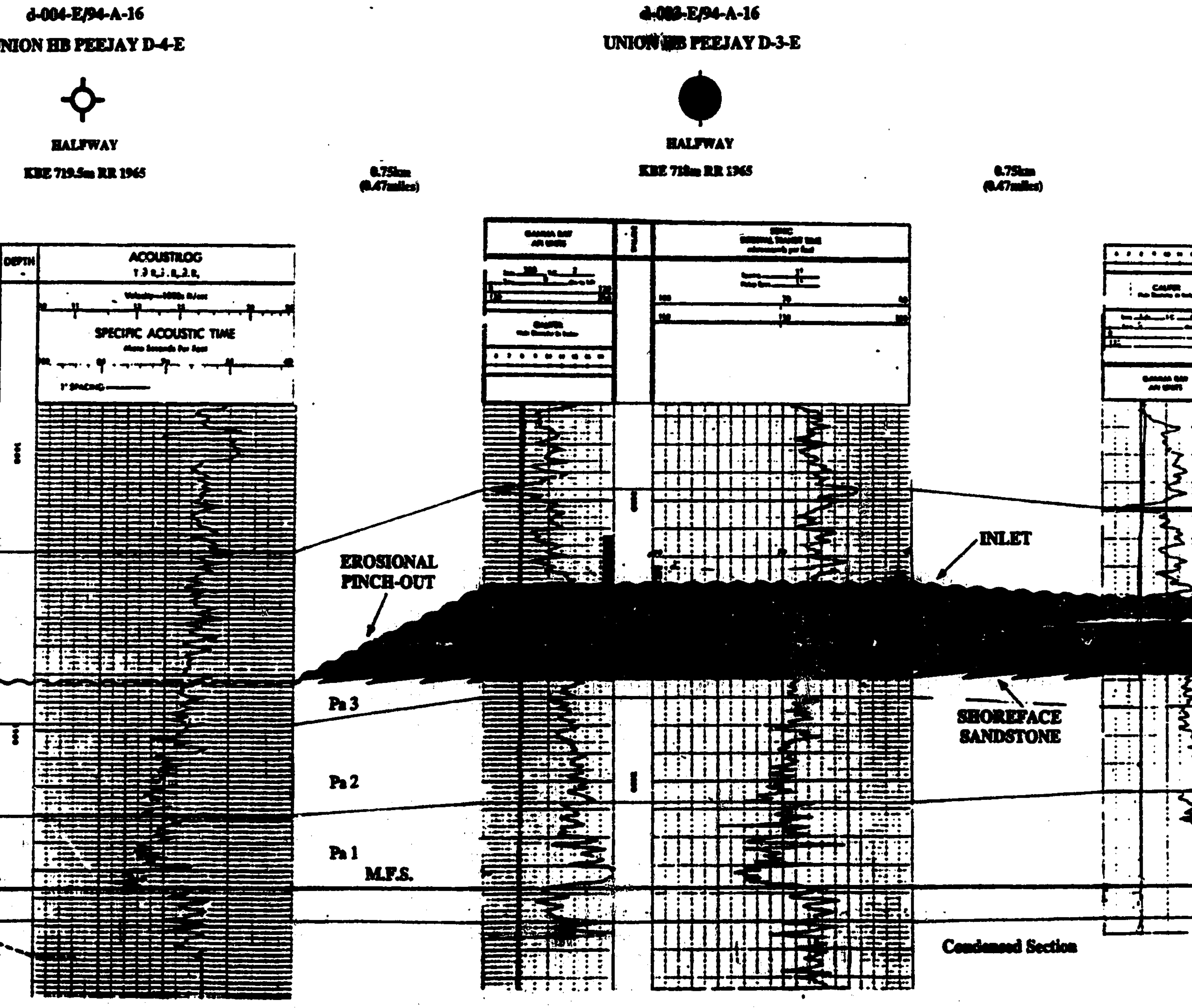

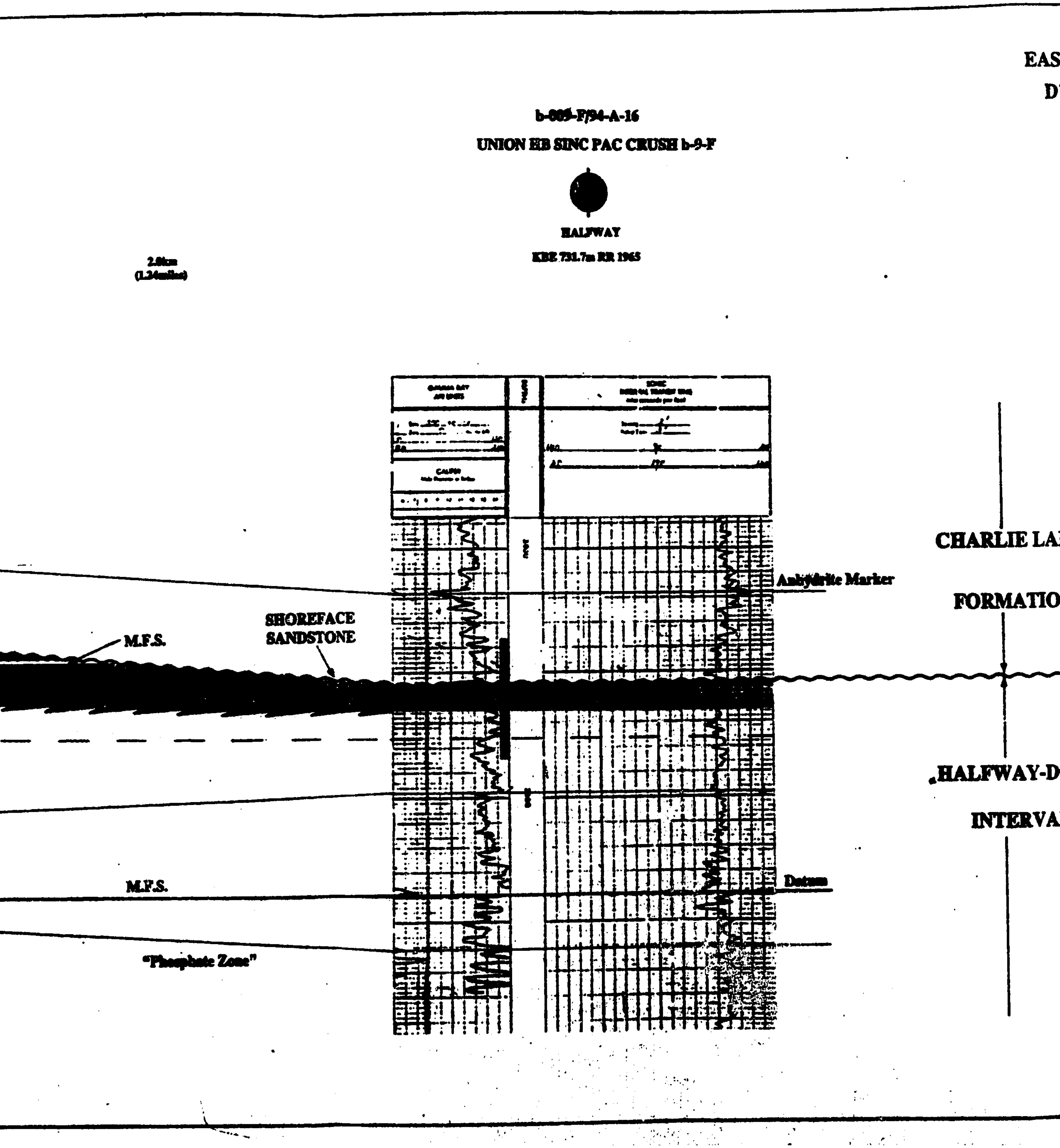

EAS
D
b-009-F/94-A-16
UNION HB SINC PAC CRUSH b-9-F
HALFWAY
KBE 731.7m RR 1965
2.0km
(1.24miles)
CHARLIE LA
FORMATIO
Anhydrite Marker
M.F.S.
SHOREFACE
SANDSTONE
HALFWAY-D
INTERVA
M.F.S.
Datum
"Phosphate Zone"

n E-E’ oriented east-west slightly oblique

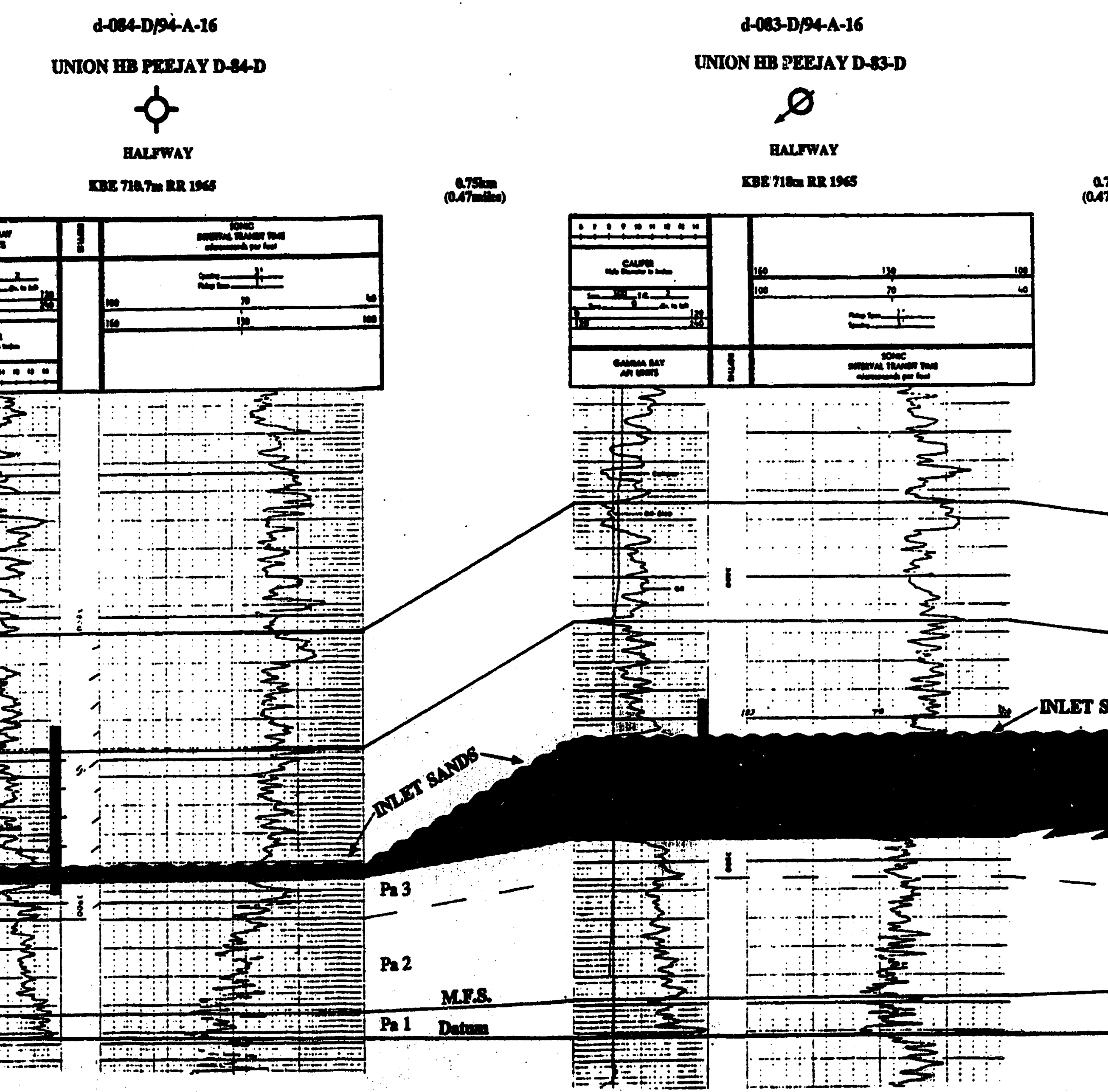

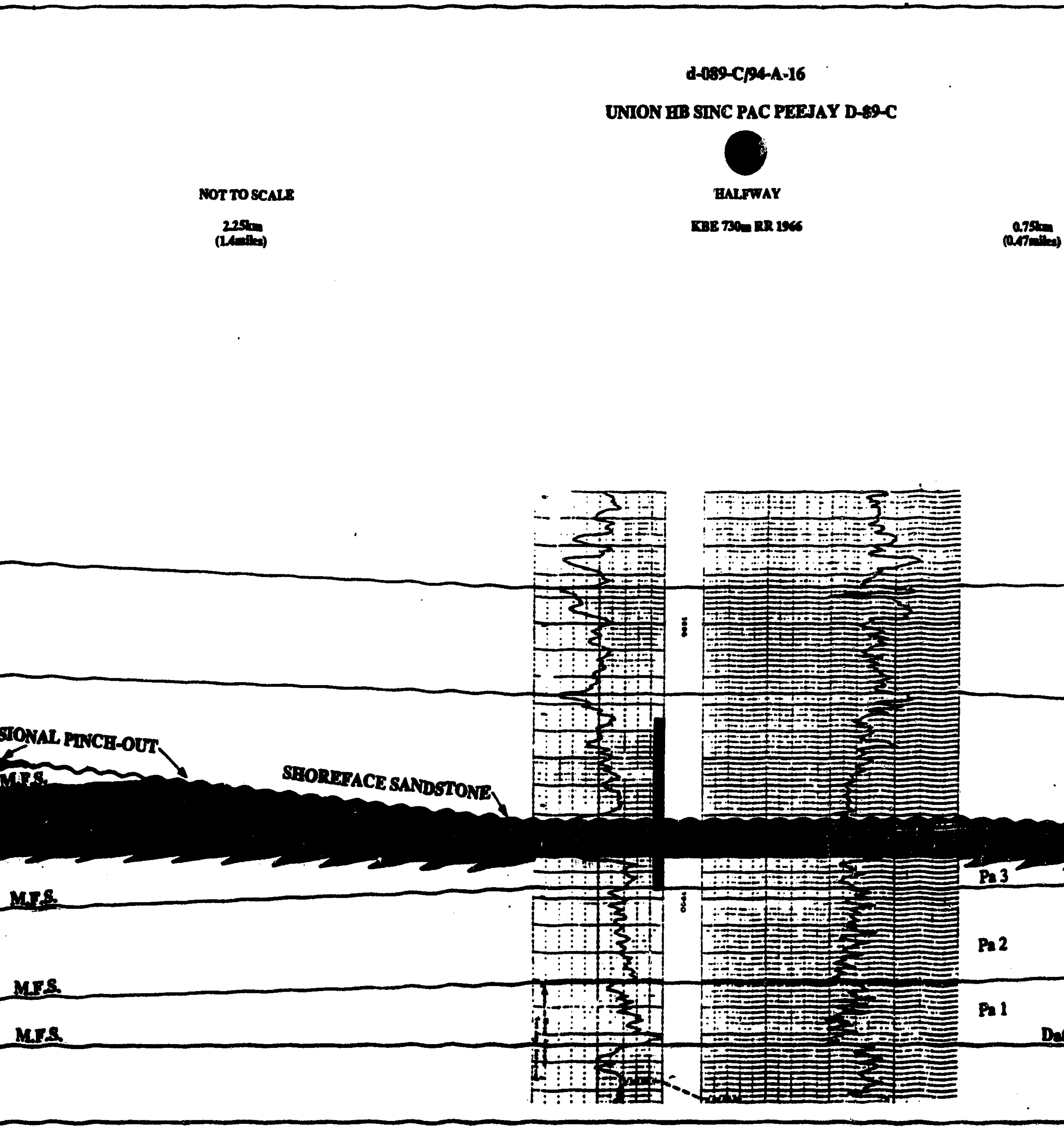
d-089-C/94-A-16
UNION HB SINC PAC PEEJAY D-89-C
NOT TO SCALE
HALFWAY
2.25km
(1.4miles)
KBE 730m RR 1966
0.75km
(0.47miles)
SIONAL PINCH-OUT
M.F.S.
SHOREFACE SANDSTONE
Pa 3
M.F.S.
Pa 2
M.F.S.
Pa 1
M.F.S.
Da

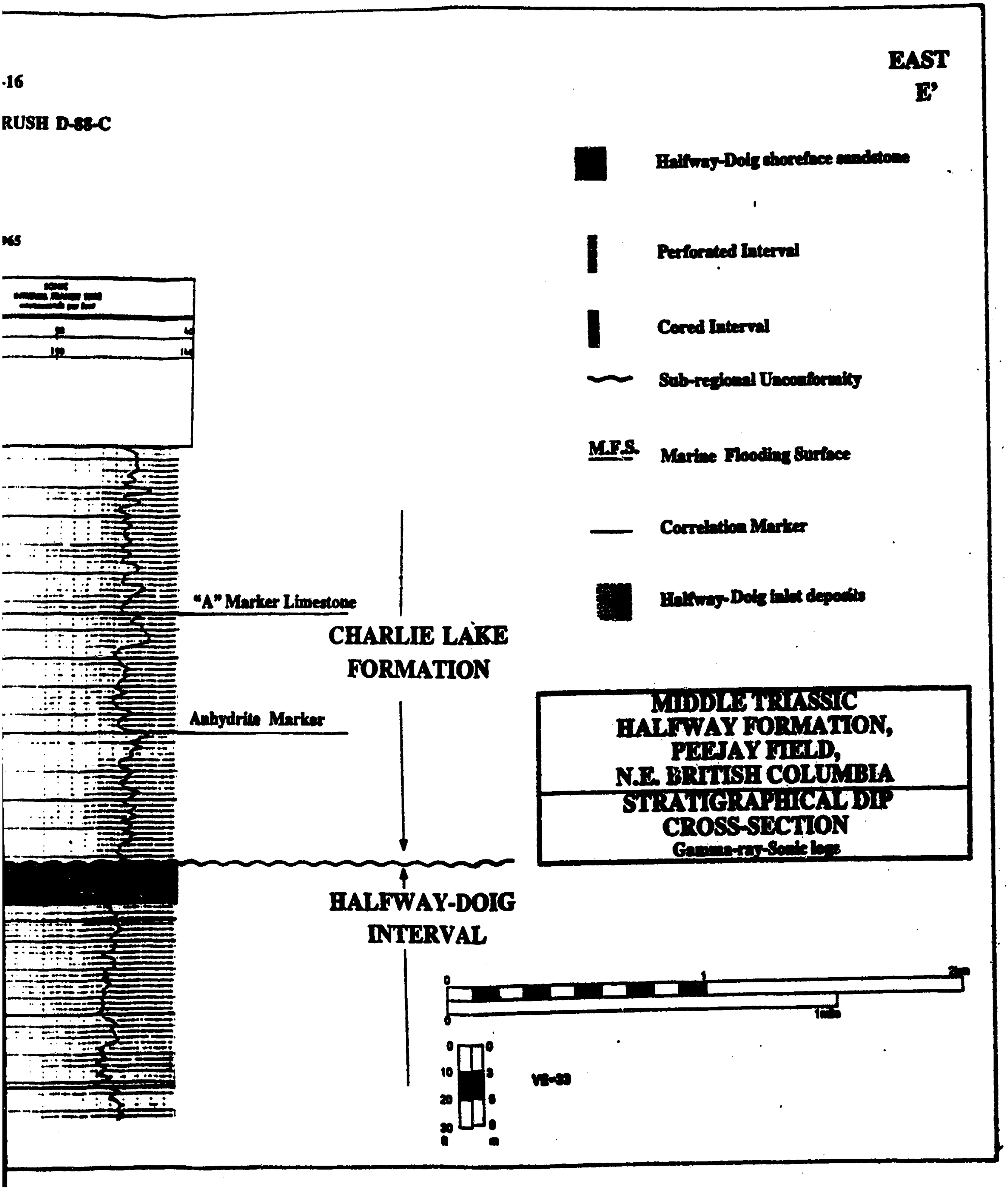
EAST
E'
-16
RUSH D-88-C
965
"A" Marker Limestone
Anhydrite Marker
CHARLIE LAKE FORMATION
HALFWAY-DOIG INTERVAL
Halfway-Doig shoreface sandstone
Perforated Interval
Cored Interval
Sub-regional Unconformity
M.F.S. Marine Flooding Surface
Correlation Marker
Halfway-Doig inlet deposits
MIDDLE TRIASSIC HALFWAY FORMATION, PEEJAY FIELD, N.E. BRITISH COLUMBIA
STRATIGRAPHICAL DIP CROSS-SECTION
Gamma-ray-Sonic logs
0
1
2km
0
1mile
0
10
20
30
ft
0
3
6
9
m
VE=33

associated with parasequence 4. Parasequence 4 shoreface deposits have been completely reworked by tidal inlet deposits. The marine flooding surface separating parasequences 3 and 4 is preserved in only one well. To the east, the surface has been removed by post-Halfway erosion (also removing the whole of parasequence 4) and to the west by tidal inlet reworking. Parasequence 3 lower and upper shoreface deposits become progressively thinner to the east in cross-section E-E' (Figure 57). This thinning is not depositional in origin, but is due to increased erosion of the Middle Triassic deposits (see section 8.1.0.; Chapter 10).

The erosional nature of the Halfway-Charlie Lake contact has stripped off all back barrier lagoonal deposits associated with the updip development of each parasequence. This has resulted in the lack of flood tidal-delta deposits being preserved in the updip (northeast) Stratigraphic section F-F' (Figure 58) shows the erosional remains of parasequence 4 as illustrated in wells d-016-C/94-A-16 and b-015-C/94-A-16, having been erosively truncated to the east and west. An isolated tidal inlet fill associated with parasequence 4 has eroded down into parasequence 3 marine shaly deposits. These deeply eroding tidal inlets can act as vertical permeability conduits between otherwise hydrologically discrete permeable sandstone packages, thus improving the distribution and connectivity of hydrocarbons parasequences. Wells d-019-C/94-A-16 and c-012-C/94-A-16 contain lower shoreface deposits of parasequence 3. Parasequence 4 deposits are not preserved. The marine flooding surface can be correlated through each well except d-016-C/94-A-16 where tidal inlet deposits of parasequence 4 have reworked the surface.

Although stratigraphic dip cross-section G-G' (Figure 59) is restricted in horizontal distance, it does however, highlight two important geological phenomena. It shows that a younger parasequence may be preserved within one isolated well along depositional dip. This style of preservation can also be traced in a north-south orientation for some distance. The preservation of parasequence 4 is again due to the formation of a graben feature with extensive erosion occurring within the laterally uplifted wells. The second point of interest is the examination of the A.P.I. values of parasequence 3 shorefacedeposits. They display an increase in value toward the west (36 in the east increasing to 72 in the west) indicating a shalier lithology, and a decrease in proximity to a palaeostrandline, thus demonstrating the prograding nature of the shoreface into the basin in a west-southwest direction.

ection F-F' oriented east-west slightly oblique

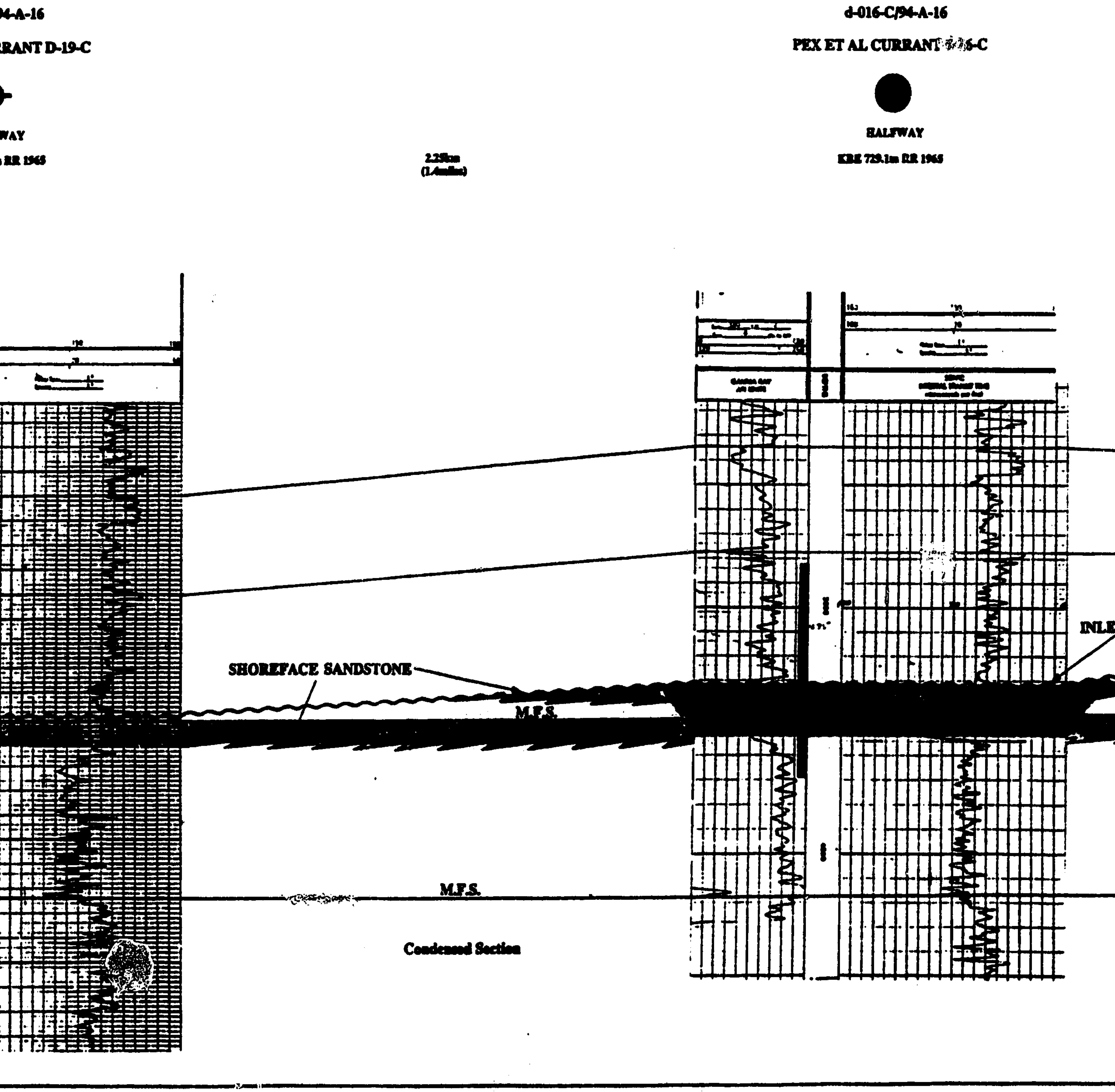

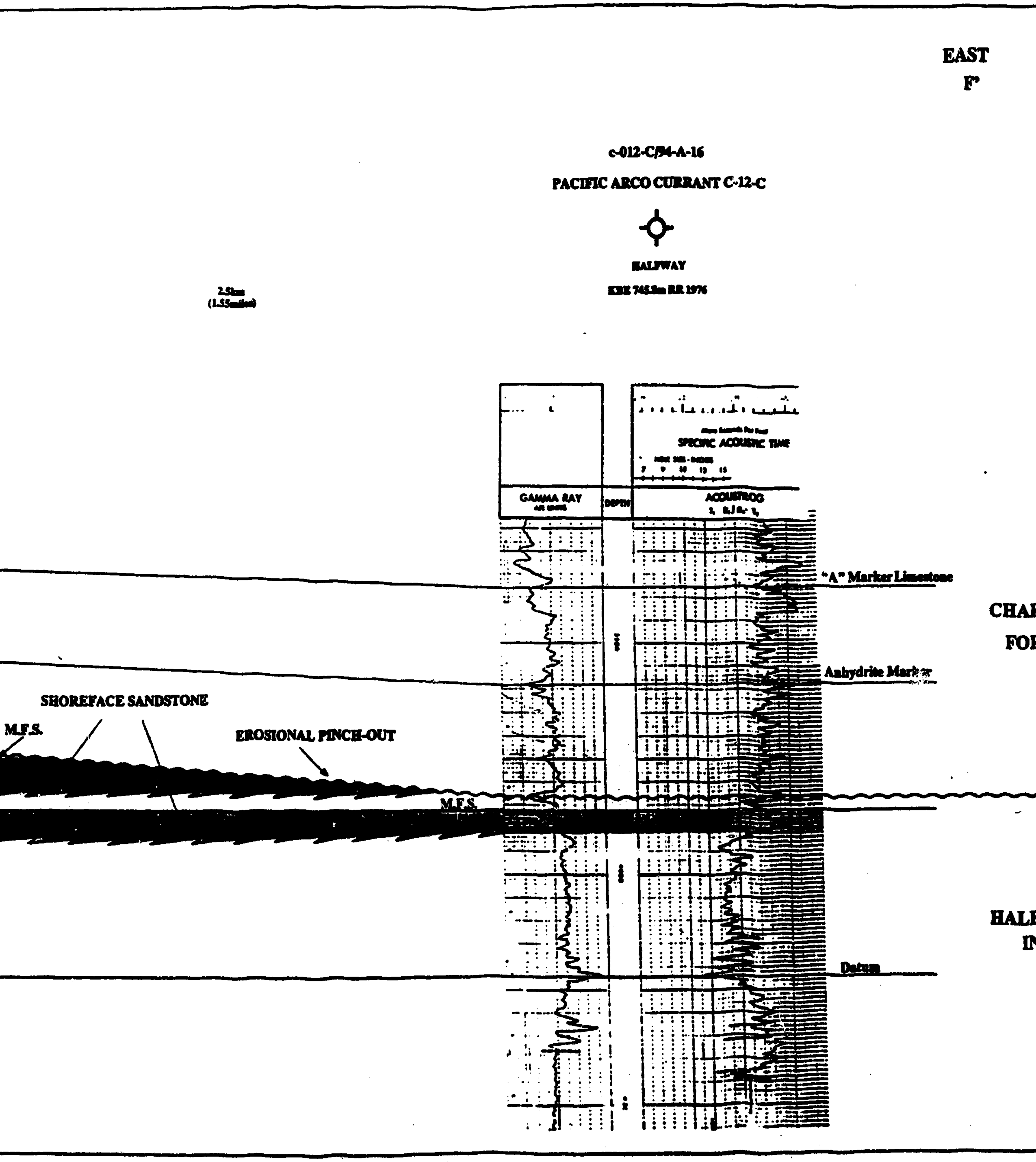
EAST
F'
c-012-C/94-A-16
PACIFIC ARCO CURRANT C-12-C
HALFWAY
KBE 745.8m RR 1976
2.5km
(1.55miles)
SPECIFIC ACOUSTIC TIME
GAMMA RAY
DEPTH
ACOUSTILOG
"A" Marker Limestone
Anhydrite Marker
SHOREFACE SANDSTONE
M.F.S.
EROSIONAL PINCH-OUT
M.F.S.
Datum

tion G-G’ oriented east-west slightly obliqu

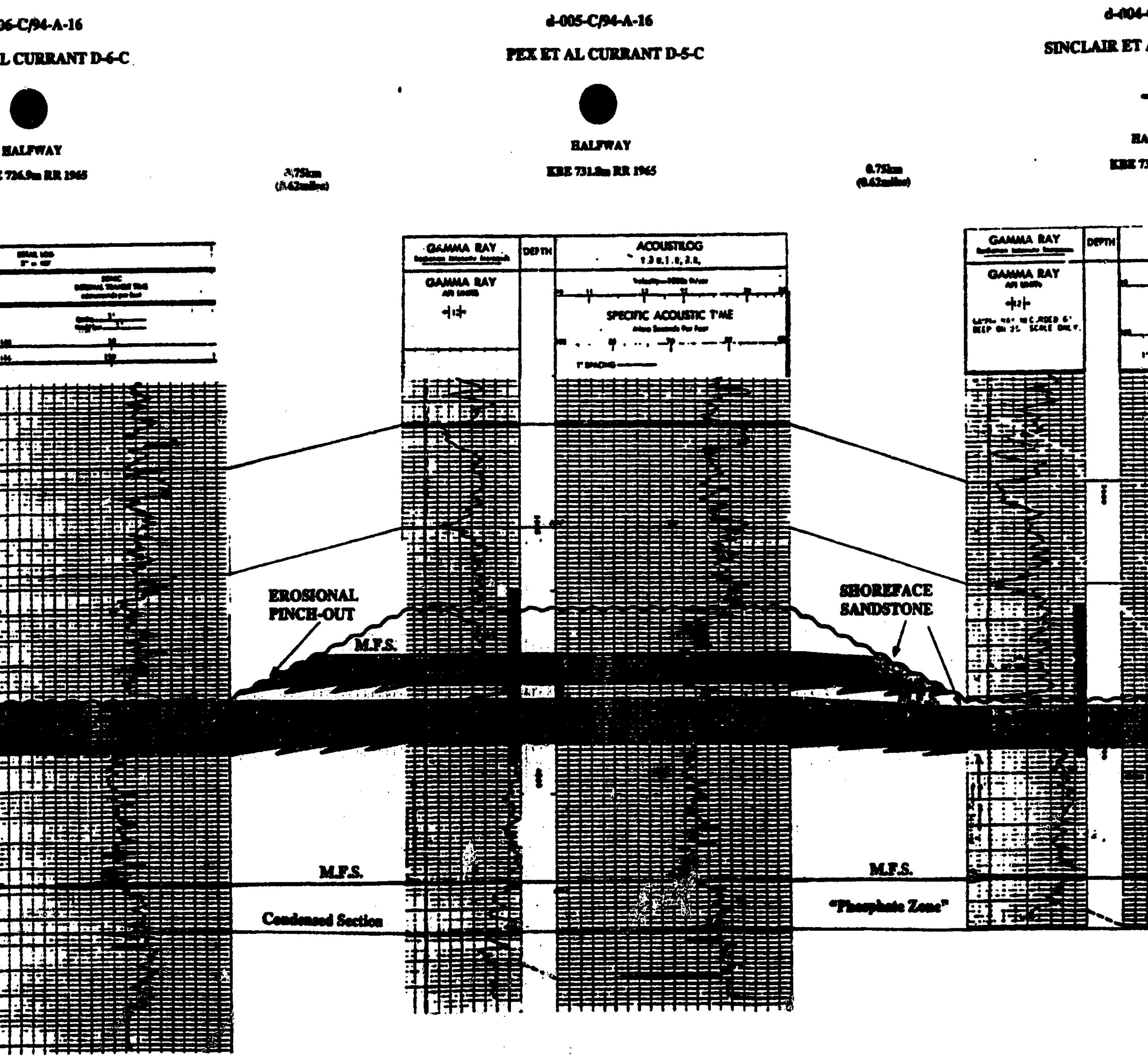

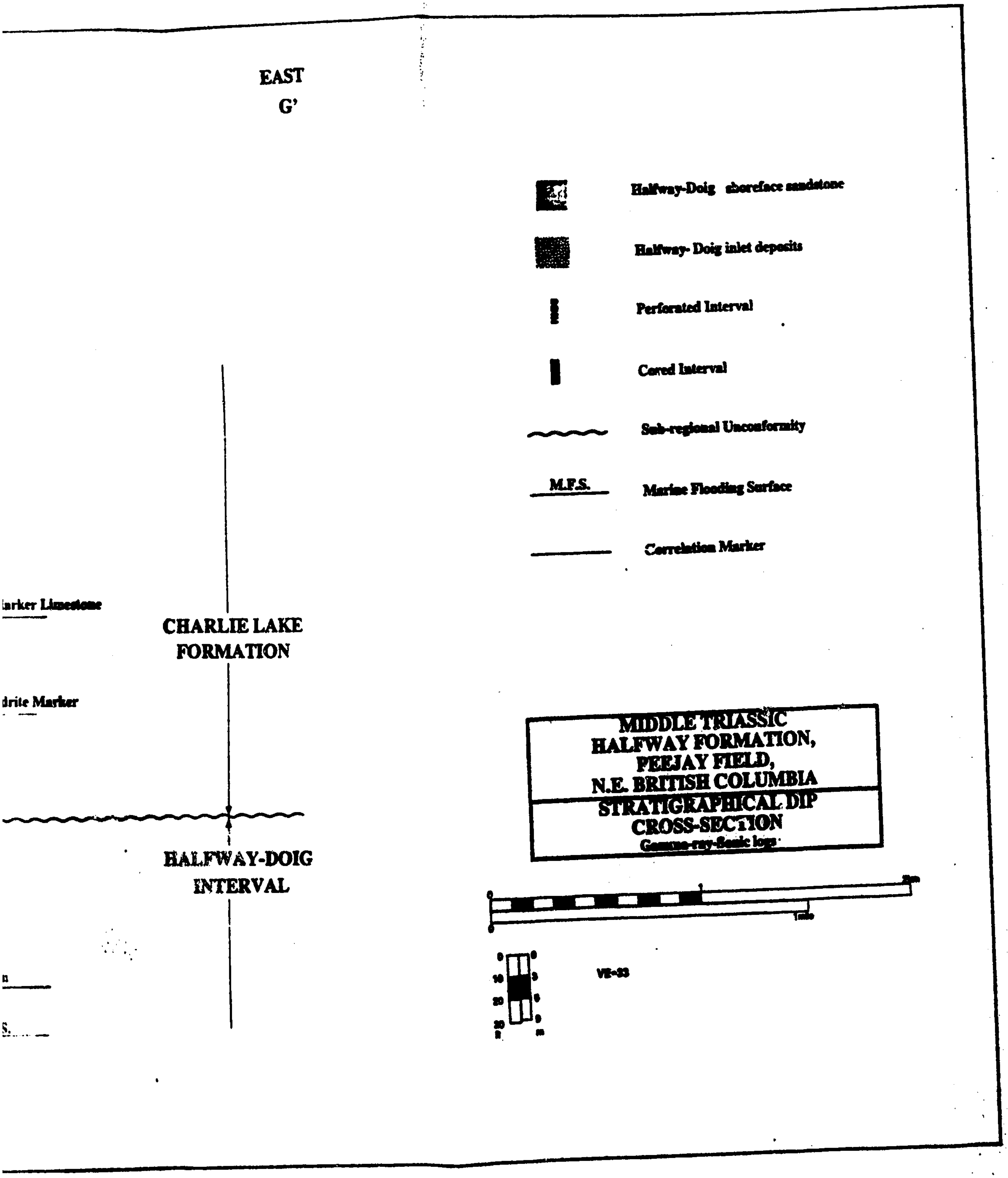

MIDDLE TRIASSIC
HALFWAY FORMATION,
PEEJAY FIELD,
N.E. BRITISH COLUMBIA
STRATIGRAPHICAL DIP
CROSS-SECTION
Gamma-ray-Sonic logs

The western part of sections D-D' and E-E', and section G-G' illustrate the removal of large quantities of deposits. Wells d-084-D/94-A-16 and d-083-D/94-A-16 from section E-E' (Figure 57) displaying this relationship are used as an example to show the mechanism of formation. This relationship is traced along a north-south trend in various parts of the study area (Figure 60a). The reservoir lithology of well d-083-D/94-A-16 forms an 11 metre (36 foot) thick tidal inlet fill associated with parasequence 4. These deposits have eroded down into the underlying offshore marine shales of parasequence 3. These inlet fill deposits can be traced westward into well d-084-D/94-A-16, however, the thickness of these deposits is only 1 metre (4 feet). They too, sit erosively on parasequence 3 offshore marine shales.

Another interesting point is noticed by comparing the thickness of deposits between the top of the 'Halfway' Formation and the datum within the 'Doig' Phosphate Zone for the same two wells. It can be clearly recognized that this thickness reduces markedly in well d-084-D/94-A-16 (Figure 60a). The 'A' Marker Limestone and 'B' Marker Anhydrite correlation markers within the overlying Charlie Lake Formation mimic the Halfway surface. There are two possible theories for the thinning of the 'Halfway' deposits and Lithofacies H1, within well d-084-D/94-A-16.

Firstly, it would appear that erosion at the onset of Charlie Lake times could have downcut into the Middle Triassic deposits, thus eroding more strata on the west than on the east to produce the present relationship. This relationship, however, is repeated in different parts of the study area in parallel aligned north-south trending patterns as is demonstrated by comparing sequence stratigraphic cross-sections D-D' (Figure 56) and E-E' (Figure 57).

This leads to the increased plausibility of the second possibility, in that regular alignment of erosional regions suggests that structural processes may have been responsible. The structural processes would have been normal faults (Figure 60b). There is no apparent repetition of strata, thus dispelling the possibility that reverse faults could have occurred. The upthrown block (i.e. well d-084-D/94-A-16) resulted in increased exposure and consequent erosion and removal of deposits. Deposits to the east within well d-083-D/94-A-16 were preserved as they were located on the downthrown block of the fault (Figure 60b and c). The fault was oriented north-south, and were active during early Carnian

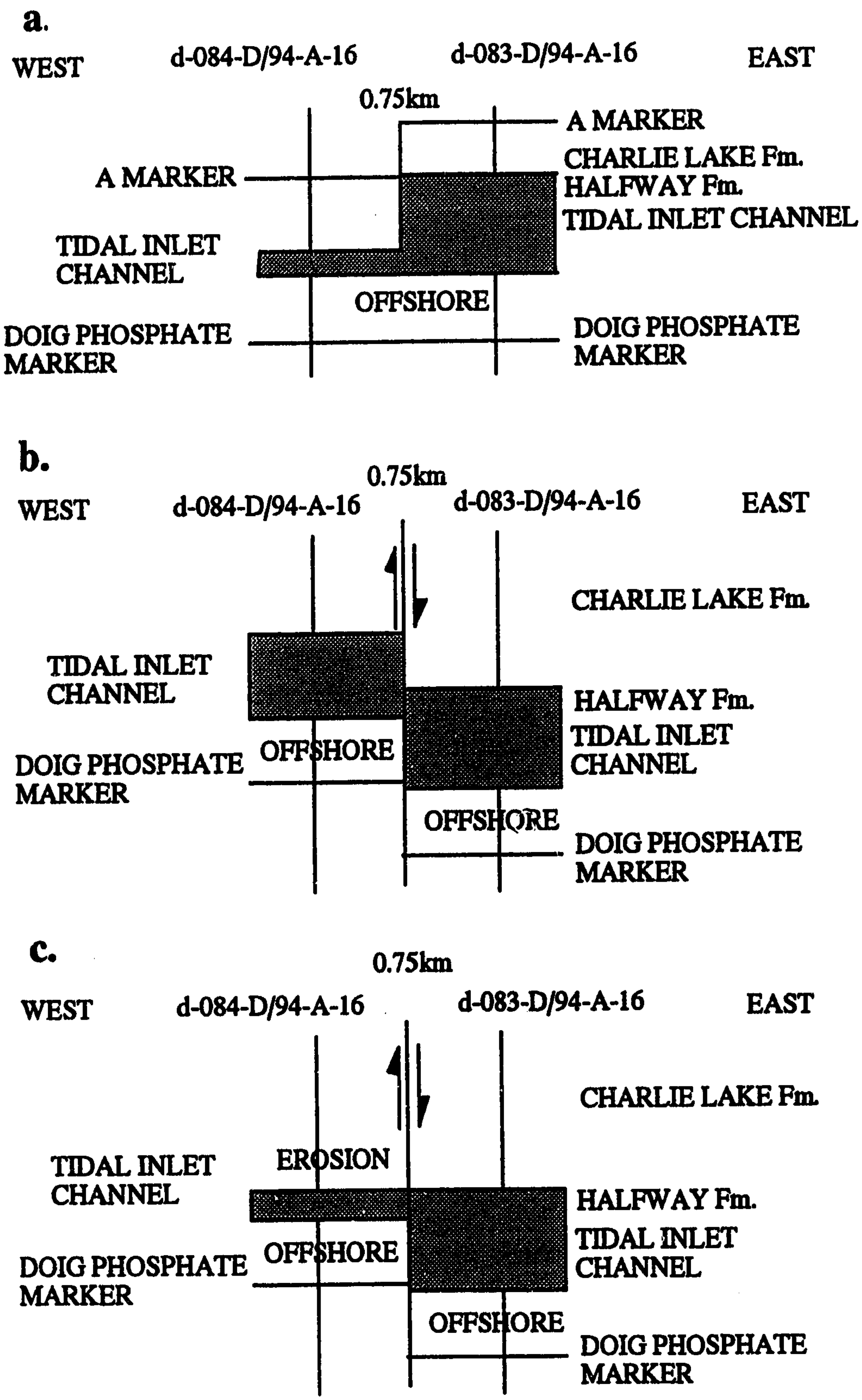
a.
WEST
d-084-D/94-A-16
d-083-D/94-A-16
EAST
0.75km
A MARKER
CHARLIE LAKE Fm.
HALFWAY Fm.
TIDAL INLET CHANNEL
A MARKER
TIDAL INLET CHANNEL
OFFSHORE
DOIG PHOSPHATE MARKER
DOIG PHOSPHATE MARKER
b.
0.75km
WEST
d-084-D/94-A-16
d-083-D/94-A-16
EAST
CHARLIE LAKE Fm.
TIDAL INLET CHANNEL
HALFWAY Fm.
TIDAL INLET CHANNEL
DOIG PHOSPHATE MARKER
OFFSHORE
OFFSHORE
DOIG PHOSPHATE MARKER
c.
0.75km
WEST
d-084-D/94-A-16
d-083-D/94-A-16
EAST
CHARLIE LAKE Fm.
TIDAL INLET CHANNEL
EROSION
HALFWAY Fm.
TIDAL INLET CHANNEL
DOIG PHOSPHATE MARKER
OFFSHORE
OFFSHORE
DOIG PHOSPHATE MARKER

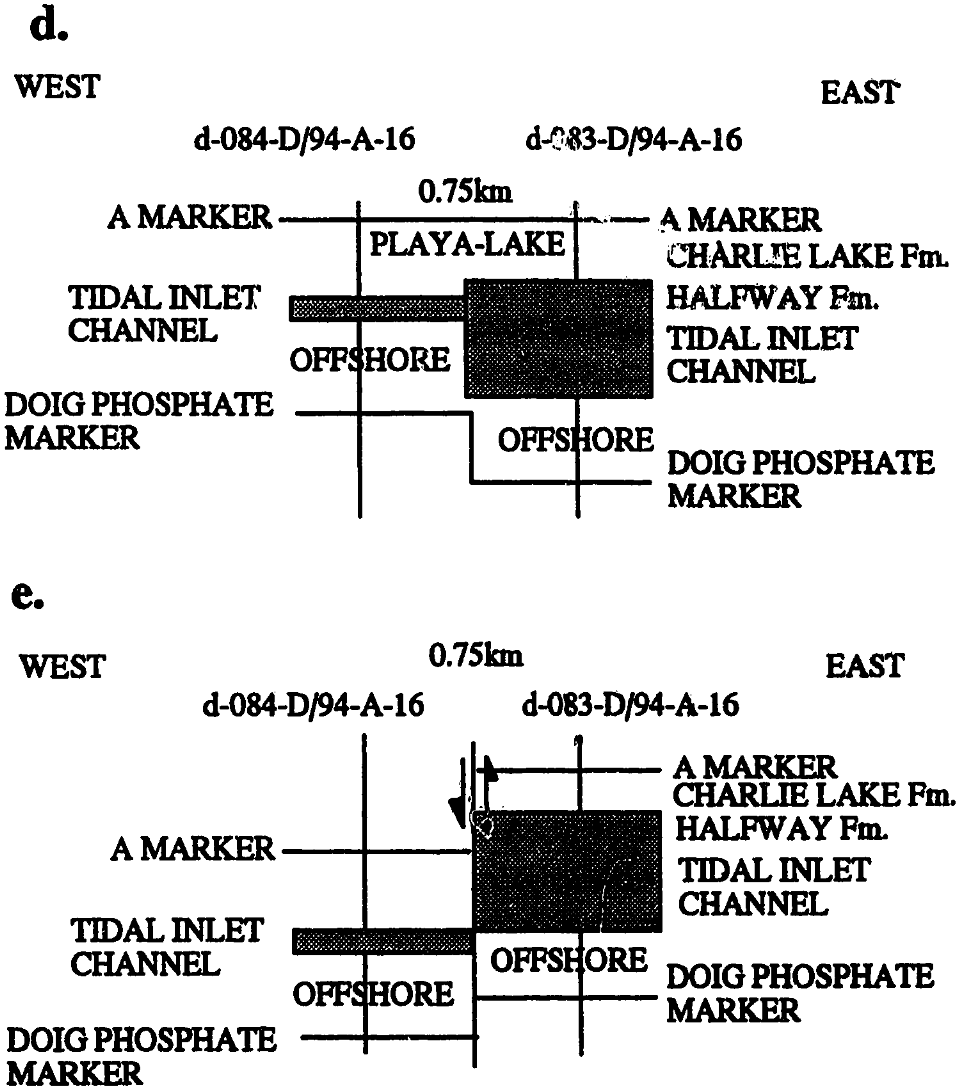

FIGURE 60. Schematic diagram showing the formation of present day hydrocarbon traps within Lithofacies H and their lithostratigraphic relationships. **a.:** Lithostratigraphic relationship of tidal inlet fills hung on the Doig phosphatic marker. The inlet deposits sit erosively on offshore marine shales. Note the thickness variations of tidal inlet deposits between the top of the Halfway Formation and the Doig phosphatic datum. **b.:** Formation of Early Carnian normal faults prior to or during Charlie Lake deposition. Vertical displacement of tidal inlet deposits occurs. **c.:** Erosion of the exposed upthrown western block, removing large quantities of the tidal inlet deposits. **d.:** Lithostratigraphic relationship of tidal inlet deposits hung on the A Marker resulting in distortion effects to lithostratigraphic correlation. Inlet deposits within d-084-D/94-A-16 sit directly on offshore marine shales and are overlain by playa lake deposits. An environmental interpretation is difficult unless faulting is invoked as a mechanism for sediment removal. **e.:** Post Early Carnian (?)reverse faulting after deposition of Charlie Lake playa-lake deposits. Well d-084-D/94-A-16 has greater thicknesses of deposits between the A Marker and the Halfway indicating synsedimentary subsidence due to reactivation of older faults. Note that displacement is opposite to faults in b and c.

times, before or during deposition of Charlie Lake deposits. Cross-sections D-D' (Figure 56) and E-E' (Figure 57) produce a misleading relationship between the wells when hung on the phosphate marker (Figure 60a). This is because the phosphate marker distorts the structural relationships somewhat, producing the effect that the downthrown side of the fault would be on the west (Figure 60a). Using the Charlie Lake 'A' Marker as the datum smooths the Halfway-Charlie Lake contact, but this distorts the underlying marine flooding surface correlation markers and the phosphatic datum bringing them up on the west side of the fault (Figure 60d). This distortion would complicate the lateral stratigraphic association and relationship of 'Halfway-Doig' deposits between wells d-084/94-A-16 and d-083-D/94-A-16, in that distal shoreface marine deposits associated with parasequence 3 would not be laterally correlatable beneath the base of the tidal inlet within well d-084-D/94-A-16. Further complications would be introduced in that a four foot thick tidal inlet fill sits directly on offshore marine shale and is directly overlain by Charlie Lake playa-lake deposits. This implies that the prograding shoreface cycle was only four feet thick! This is not feasible. The only alternative is erosion and removal of inlet fill deposits occurring within well d-084-D/94-A-16 due to an early Carnian erosional event.

From the sections described above, playa-lake deposits are seen infilling the graben features, hence producing greater thicknesses of deposits. However, in some instances, these deposits are thicker over the horst features. This suggests that faulting with displacements in the opposite direction occurred during deposition in Carnian times (Figure 60e).

8.3.0. LATERAL LITHOFACIES RELATIONSHIPS.

Lithofacies cross-sections were constructed in order to better understand the lateral relationships between vertical lithofacies association 1 and 2, and hence, the lateral distribution and arrangement of reservoir rocks throughout the study area. The palaeoenvironmental model erected for the Peejay field is a prograding strandplain overlain by a later prograding barrier island coastline (see chapters 4 and 5). The cored sequences were hung on the first (upper) phosphate marker within the Doig Formation. Sonic log responses were used where gamma-ray logs lacked sufficient penetration. Construction of a chronostratigraphic framework was restricted to areas with sufficient well penetration, hence the lack of chronostratigraphic correlation of deposits within the

H block (northwest part of the field). The cross-sections have been affected by minimal differential compaction. The location of lateral lithofacies cross-sections B-B' and E-E' are shown in Figure 48.

The lateral lithofacies relationships along depositional strike are shown in the lithofacies correlation section cross-section B-B' (Figure 61). Two coarsening-upward shoreface parasequences (Pa. 3 and 4) are shown in this cross-section. These parasequences are separated by a laterally correlatable chronostratigraphically significant marine flooding surface. Coarsening-upward shoreface deposits of the upper parasequence (Pa. 4) have been extensively reworked by migrating tidal inlets. Thicker tidal inlet fill deposits have eroded down through the marine flooding surface, and presently overly shoreface deposits of parasequence 3 below.

The offshore-transition zone and the lower shoreface deposits have been preserved within all wells. The upper shoreface deposits, however, have been eroded by shoaling waves due to shoreface erosion, associated with an increase in water depth. Upper shoreface deposits of parasequence 3 have also been dissected by the tidal inlet deposits of parasequence 4, present in wells d-012-E/94-A-16 and d-072-D/94-A-16. Factors indicating a relative deepening of water conditions from north to south suggest that the cross-section is oriented slightly oblique to depositional strike and not parallel to it. The marine-flooding surface also climbs updip to the north, partially reflecting the original bathymetry. Further north, the upper shoreface deposits beneath the marine flooding surface have been greatly reworked and were not preserved. The lack of inlet deposits associated with the lower parasequence (Pa. 3) suggests that this coastline may have been a strandplain along which tidal inlets were not formed.

The marine-flooding surface occurs with or without an associated transgressive lag within the cross-section. The lag deposits are thicker in areas where there have been greater amounts of reworking of the underlying deposits (e.g. wells d-002-E/94-A-16 and d-022-E/94-A-16). Deposits above the marine-flooding surface range from offshore shales, in the south, to offshore-transition zone interlaminated siltstones and shales, in the centre of the section, to lower shoreface interbedded sandstones and shales in the north. This is also indicative of an apparent increase water depth to the south, represented by the

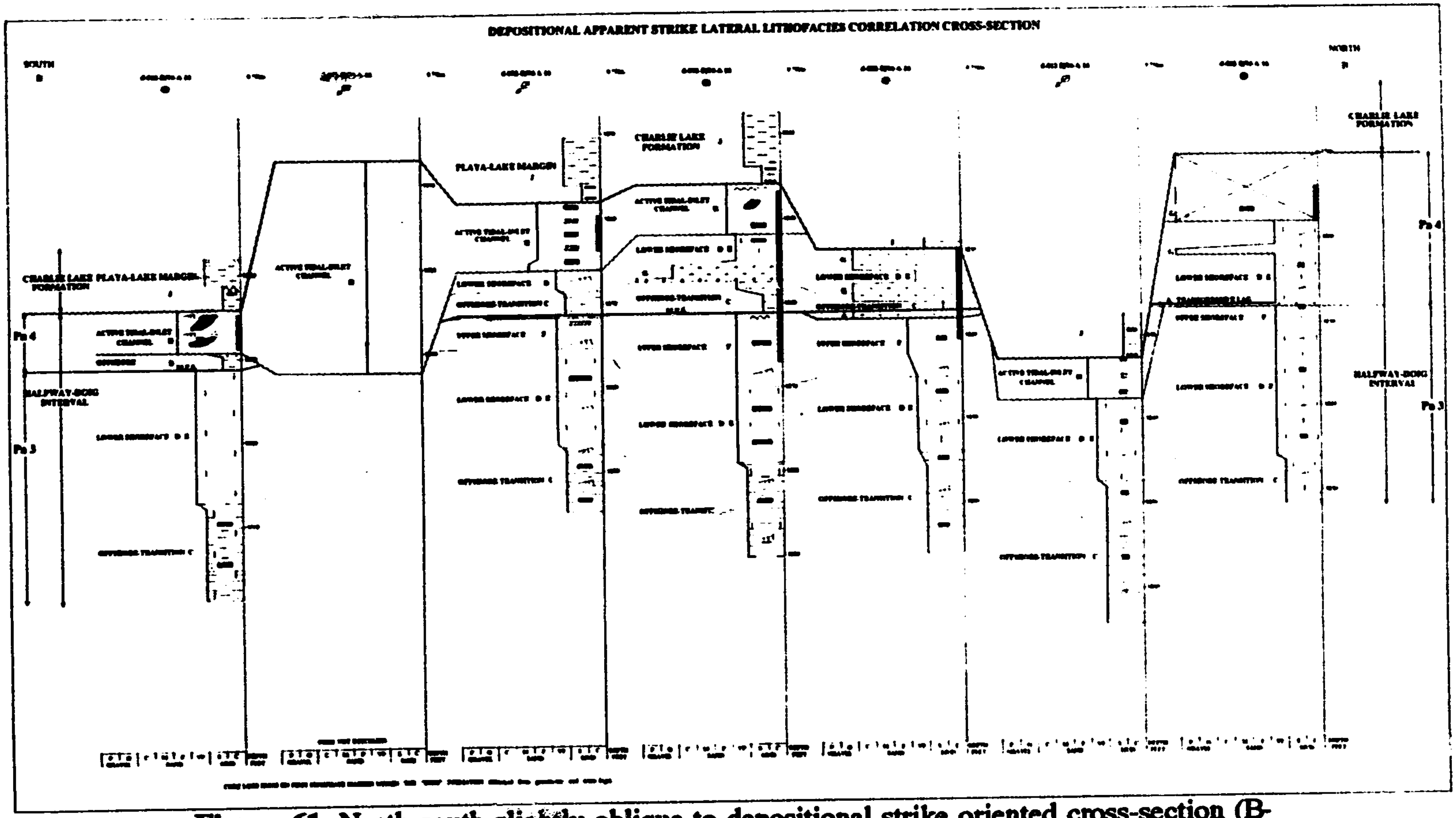

Figure 61. North-south slightly oblique to depositional strike oriented cross-section (B-B') through the Peejay field illustrating lateral lithofacies relationships. Cross-sections hung on first phosphate marker in the "Phosphate Zone".

increasingly shalier lithology and smaller scale sedimentary structures. This also suggests that the section is slightly oblique to palaeostrike. Rapid relative sea-level rise must have occurred in order to provide sufficient accommodation space responsible for the preservation of upper shoreface deposits beneath the marine-flooding surface. This may have occurred through a rise in sea-level, basinal subsidence due to sedimentary compaction, or tectonic faulting. Extensive microfaults throughout the deposits in the lower parasequence, and the location of the study area over the north flank of the Fort St. John Graben (see Chapter 9) indicate that tectonic faulting may have played a major role.

The coarsening-upward shoreface cycle within the upper parasequence (Pa. 4) has been intensely truncated and reworked by sublitharenite tidal inlet channel fill deposits. They comprise much of the remnant upper parasequence. Wells d-092-D/94-A-16, d-082-D/94-A-16, d-072-D/94-A-16 and d-062-D/94-A-16 are in pressure communication with each other. This indicates that the reservoir sandstones are in lateral connection throughout these wells. These inlet fill deposits may have been produced by a single laterally migrating tidal inlet, or alternatively, this fill may represent the amalgamation of a series of discrete inlet fill deposits over time. This, however, cannot be confirmed. The thickness of these deposits does not reflect depositional thickness of the tidal inlet, but does reflect the effects of erosion exhibited by the early Carnian erosion surface.

The lower shoreface deposits of the upper parasequence within wells d-002-E/94-A-16 and 1-012-E/94-A-16, are dominated by sharp based, fining-upward coquinoid storm beds. These deposits should thin in an offshore direction, however, the base of the tidal inlet has eroded and removed these deposits. Post-Halfway erosion has removed most of the upper parasequence leaving erosional remnants as isolated preserved pockets of good reservoir quality deposits. Thus, lateral correlation of the genetically related depositional package within this parasequence is spatially limited. Variability of palaeotopographical relief on the Charlie Lake erosion surface varies from 0.05° to 0.5°. This variability in palaeotopographical slope is less along palaeodepositional strike than along palaeodepositional dip (see later).

Lateral lithofacies cross-section E-E' (Figure 48), oriented slightly oblique to depositional dip in an east-west, trend is shown in Figure 62. The limited geographical extent of the cross-section, results from insufficient deep well penetration to a suitable datum within the Doig. The upward-coarsening shoreface deposits within the lower parasequence (Pa. 3) contain no genetically related tidal inlet channel fill deposits, hence indicating that this shoreface may have been part of a prograding palaeostrandplain. Lateral continuity of the genetically related coarsening-upward shoreface cycle along depositional dip within parasequence 3 indicates that shoreface progradation was continuous to the west-southwest depositing a diachronous blanket sand, with older deposits to the east-northeast and younger deposits to the west-southwest.

The increased truncation and consequent thickness of the tidal inlet fill deposits toward the west, within section E-E', may indicate the position of the channel thalweg (deepest part of the channel). Modern channels shallow updip and downdip of the channel thalweg (Oertel, 1973). If the sublitharenites within this cross-section were deposited by the same inlet then the width of the barrier island would have to be at least 3.1 km at any one time. This width is greater than that of any modern day barrier island. For example, the Holocene deposits off Long Island, New York (presumed to be relict tidal inlet deposits) are only 0.6 to 0.8 km wide (Sanders and Kumar, 1975a, b; Rampino and Sanders, 1981). Hence, the tidal inlet fills within the study area must be amalgamations of more than one tidal inlet channel fill, due to the process of progradation through time. No attempt has been made to divide the deposits into separate channels.

There is, however, evidence in favour of at least two vertically stacked inlet phases of reworking within well d-083-D/94-A-16 (Figure 62). The deposits within this well are at least 12 metres (38 feet) thick. Quoted thicknesses of modern wave-dominated inlet fills are less than this value (see Chapter 5), suggesting that two separate inlet phases were responsible for the formation of these thick deposits. The gamma-ray response for this well shows an increase in A.P.I. units within the middle portion of these deposits with a corresponding decrease in interval transit time, suggesting that the deposits at this zonecontain more shaly material and are less porous. This evidence suggests that a concentration of shale or phosphate lithoclasts could be present at this region occurring as a basal lag of the more recent inlet which has cut down into an older inlet. This area has been highly cemented compared to the surrounding deposits. This process has resulted in a sand-on-sand contact which in core is difficult to recognize, since granule sized lithoclasts line the base of most migrating bedforms within these deposits.

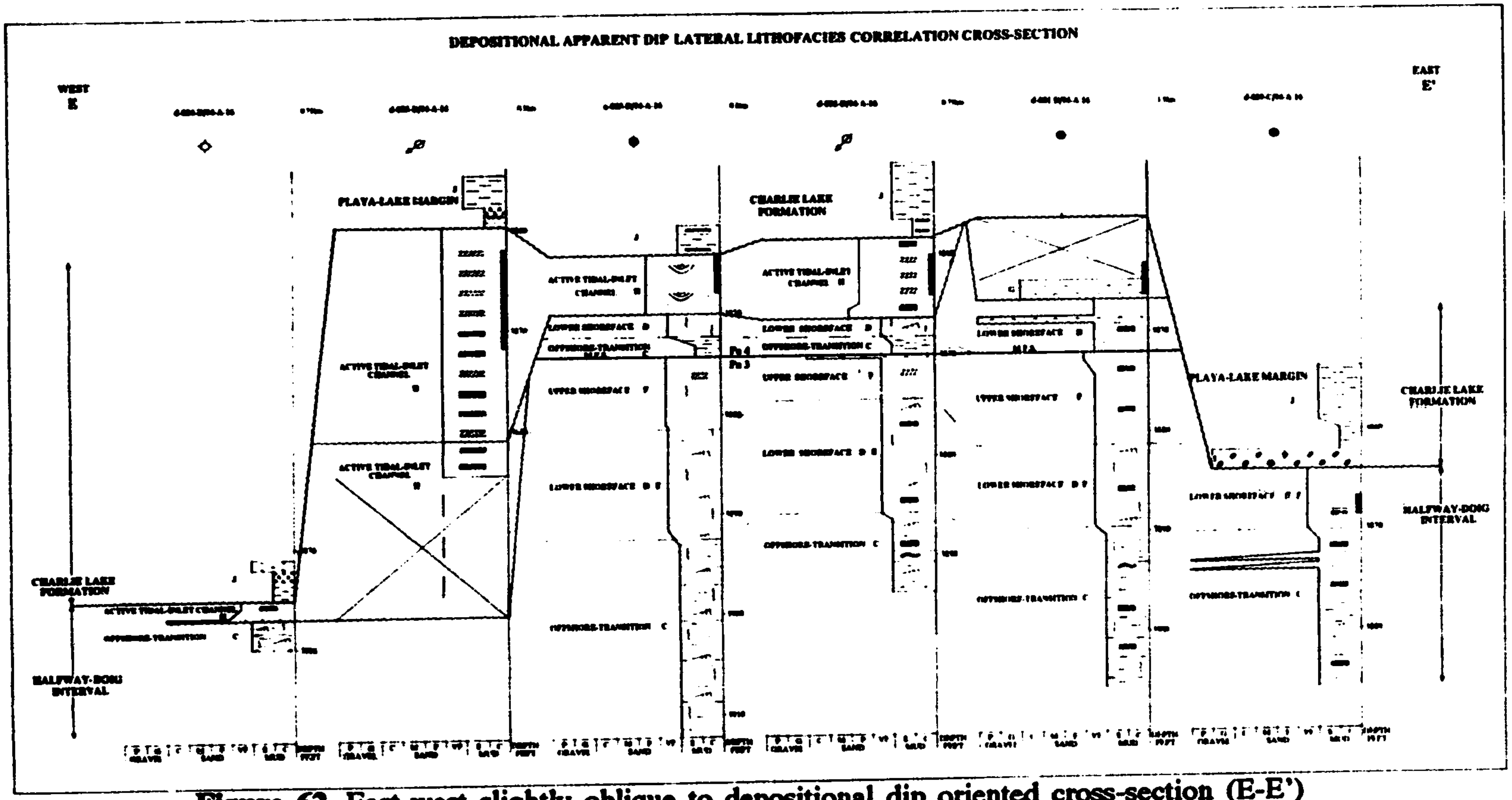

Figure 62. East-west slightly oblique to depositional dip oriented cross-section (E-E') through the Peejay field illustrating lateral lithofacies relationships. Cross-sections hung on first phosphate marker in the "Phosphate Zone".

Cross-section E-E' (Figure 62) clearly demonstrates the relief and erosional effects of the post-Halfway erosion surface. This relief is of greater magnitude than in strike oriented cross-sections. Erosional relief of some 12 metres (38 feet) has been developed by the post-Halfway erosional surface. This is demonstrated on the cross-section with palaeotopographical slopes ranging from 0.04° to 0.89° (differential compaction not accounted for). Wells d-084-D/94-A-16 and d-089-C/94-A-16 clearly show that a substantial part the vertical sequence has been removed. The former well has preserved the basal 0.8 metres (2.5 feet) of a tidal inlet channel. Sharply overlying these deposits are genetically unrelated Charlie Lake playa-lake evaporites and fine-grained siliciclastic deposits. An erosional lag was not recognized within this well. The latter well, however, contains a distinct pebble grade polymict conglomerate resting erosively on lower shoreface deposits of the lower parasequence (Pa. 3) having completely eroded the upper parasequence. Erosional remnants of the upper parasequence (Pa. 4) have been preserved within the central four wells of the cross-section. Reservoir quality is good to very good within the erosional remnants of sublitharenite tidal inlet channel deposits associated with the upper parasequence. Wherever erosional remnants of the upper parasequence occur hydrocarbon extraction is successful structurally updip of the basal water leg.

Section B-B' (Figure 61) indicates that the deposits, particularly above the marine flooding surface, fine in a southerly direction, and that the parasequences also thin in a southerly direction, hence indicating that water depth increased to the south. Section E-E' (Figure 62) indicates that the parasequences fine and thin to the west. The combined information from both cross-sections suggests that the Middle Triassic sedimentary basin deepened to the west-southwest, with palaeocoastline orientation north-northwest to south-southeast. Evidence from the slightly oblique depositional strike section, B-B' (Figure 61) indicates that lateral inlet migration was in a south-southeast direction along the barrier island trend.

9.0.0. GEOLOGIC HISTORY.

Reconstruction of geologic history can provide insights regarding the formation, preservation and distribution of reservoir rocks within the study area. The geologic history was complex within the study area, involving structural deformation, erosion and diagenetic overprinting resulting in the present distribution and reservoir quality of deposits. Six stages in the geological history are described sequentially: 1.) Formation of parasequence stratal packages within the Middle Triassic Western Canada Sedimentary Basin (earliest Anisian to earliest Carnian); 2.) Normal faulting of the Middle Triassic deposits during early Carnian times; 3.) Synsedimentary tectonism and subsequent exposure and removal of Middle Triassic deposits during early Carnian times (? associated with the early Carnian normal faulting); 4.) Deposition of Upper Triassic Charlie Lake playa-lake deposits during (?)early Carnian times; 5.) (?)Early to middle Carnian faulting; 6.) Percolation of Charlie Lake derived pore fluids down into Middle Triassic strata, reducing reservoir quality.

9.1.0. PARASEQUENCE STRATAL PACKAGES.

Chronostratigraphic reconstruction of the Middle Triassic (early Anisian to early Carnian) stratal packages has resulted in the identification of a series of genetically related sandstone packages that successively prograded westward into the Western Canada Sedimentary Basin. Each sandstone package has been termed a parasequence, as it is bounded above and below by marine flooding surfaces. The distal sections of the parasequences downlap into the "Phosphate Zone" of the lower Doig Formation as a series of amalgamated phosphatic condensed horizons (see cross-section H-H', Figure 49, section 8.1.0). Successively younger parasequences downlap into the basin, forming a progradational parasequence set. Figure 63a and b shows the formation and development of the progradational parasequence set. Each parasequence was composed of a shoreface that prograded to the southwest during regressive periods. Progradation of the shorefaces resulted from greater amounts of sediment supply than subsidence rate within the basin. The top surface of each parasequence is indicated by an apparent increase in water depth, associated with a transgressive pulse. The lithofacies correspondingly became retrogradational in nature for a short period of time, before progradation was resumed. The rapid relative increase in water depth was theresult of a decrease in the rate of sediment supply, or an increase in the subsidence rate. The reinitiation of shoreface

a.

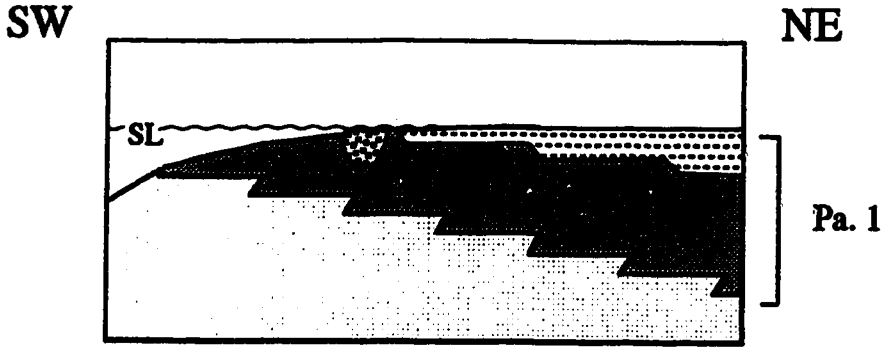

Sediment supply is greater than subsidence, hence shoreface progradation occurred. Progradation results in a basinward shift of the lithofacies.

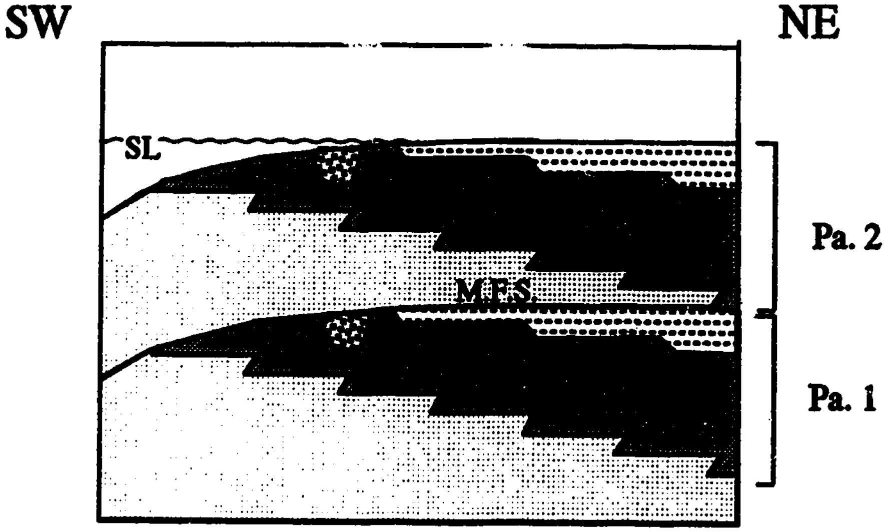

Sediment supply is less than subsidence, hence a transgressive event occurs, followed by resumption of progradation forming parasequence 2. Lithofacies shifted landward during the transgressive event.

b.

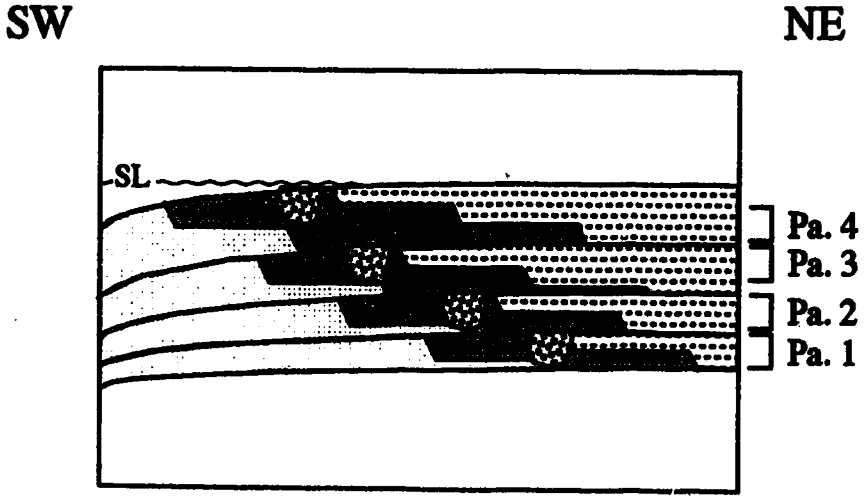

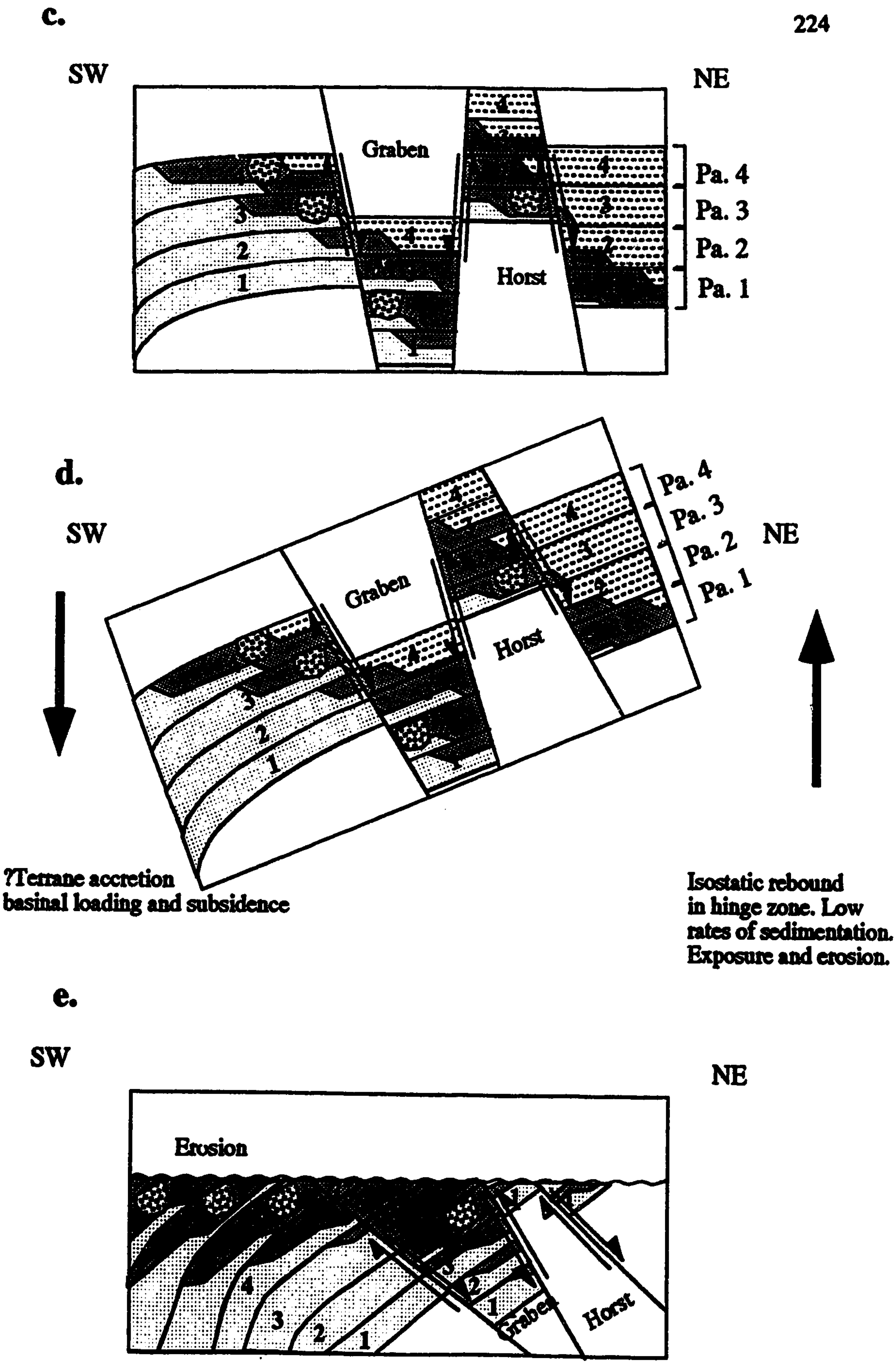

?Terrane accretion
basinal loading and subsidence

Isostatic rebound
in hinge zone. Low
rates of sedimentation.
Exposure and erosion.

f.

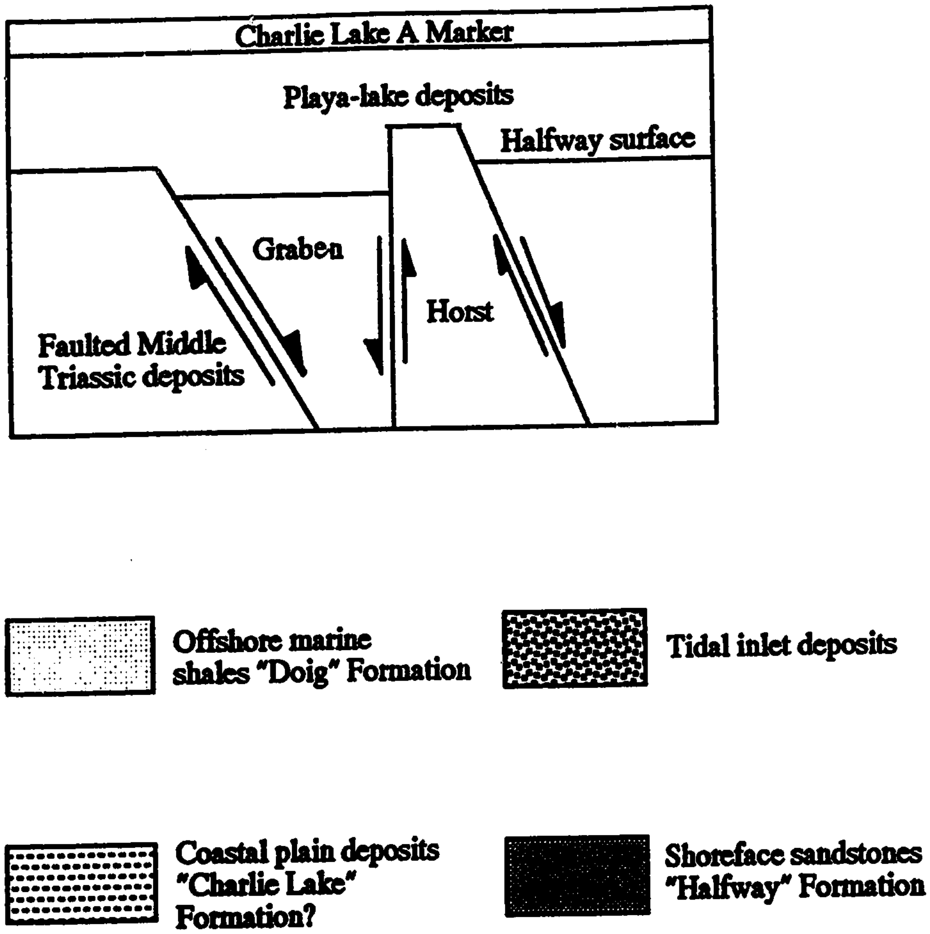

Figure 63. Geological history and evolution of the Peejay field and surrounding area. Diagrams a to e are schematic cross-sections through the study area. a.: Formation of two parasequences during Middle Triassic Anisian to Ladinian times. b.: Continuous accumulation of sediments produces a progradational parasequence set. Younger parasequences successively overstep older parasequences in a southwestward direction. c.: Development of early Carnian faults producing north-south orientated horsts and grabens associated with movement of the Fort St. John Graben. d.: Synsedimentary tilting toward the west in response to crustal loading resulting from accreted terranes to the west during early Carnian times. This caused an isostatic rebound to the east, which resulted in greater exposure and erosion of the deposits. e.: Erosion and peneplanation of the tilted strata has eroded all coastal plain deposits and much of the shoreface sandstones. This erosion may have been coeval with early Carnian faulting and tectonic tilting. Thicker accumulations of shoreface sandstone are preserved in graben features, whereas horst features tend to expose and hence result in erosion of greater amounts of sediments so that marine shales are the most dominant lithology remaining. f.: Reactivation of faults during and post Charlie Lake playa-lake deposition. Thicknesses of playa-lake deposits between the top of the Halfway and the 'A' Marker are thicker over grabens and thinner over horsts. These later faults were still active during deposition of later Charlie Lake deposits, since the 'A' Marker has also been structurally displaced. This later stage of faulting occurs along early Carnian fault traces, but displacements are in opposite directions.

progradation resulted from an increase in sediment supply or a decrease in subsidence rates. The regressive and transgressive pulses may have resulted from the loading of strata by exotic terranes accreted to the west during Triassic times (Gibson and Barclay, 1989) or due to locally induced fault movement associate with the Fort St. John Graben.

9.2.0. EARLY CARNIAN NORMAL FAULTING.

Figure 63c shows the effects of normal faulting on the Middle Triassic stratal packages of the Peejay field. The faults are oriented in a north-south direction and are spaced between one and three kilometres apart. Minor east-west fault trends have also been recognized. Vertical displacements associated with these normal faults attain maximum values of 9 metres (30 feet) (see Figure 51 and 65). These faults produced a series of graben and horst structural features. They may have been initiated before or during Charlie Lake deposition; in other words, before middle Carnian times. Dates for the erosion and faulting events were based on the Carnian aged Mahaffy Cliff fauna found in lithology of the Charlie Lake Formation by McLearn (1950). The faults may have resulted from the reactivation of older Palaeozoic faults, which had formed extensional structures within the Peace River Arch (Barclay *et al.*, 1990).

The Peejay field is positioned on the northern flanks of the Fort St. John Graben (Barclay *et al.*, 1990). This graben feature is the east to southeast oriented main graben of the Dawson Creek Graben Complex (Figure 64). The Fort St. John Graben is 50 x 110km in dimensions, internally segmented and block faulted, the faults oriented north-south and east-west (Barclay *et al.*, 1990). The graben feature was inactive by the Triassic Period except for small-scale vertical displacements associated with reactivation of Palaeozoic formed faults (O'Connell *et. al.*, 1990). The normal faults provide evidence that extensional stresses were occurring, possibly associated with the initiation of synsedimentary loading to the west within the Western Canada Sedimentary Basin (see section 9.3.0.).

9.3.0. SYNSEDIMENTARY TECTONISM.

It has been demonstrated from the construction of sub-regional stratigraphic cross-section H-H' (Figure 49, section 8.1.0.), and the isopach map between the first phosphate marker and the top of the Halfway Formation (Figure 51, section 8.1.0.), that the Middle Triassic deposits thin in a north-easterly direction. This can also be demonstrated by the thickness

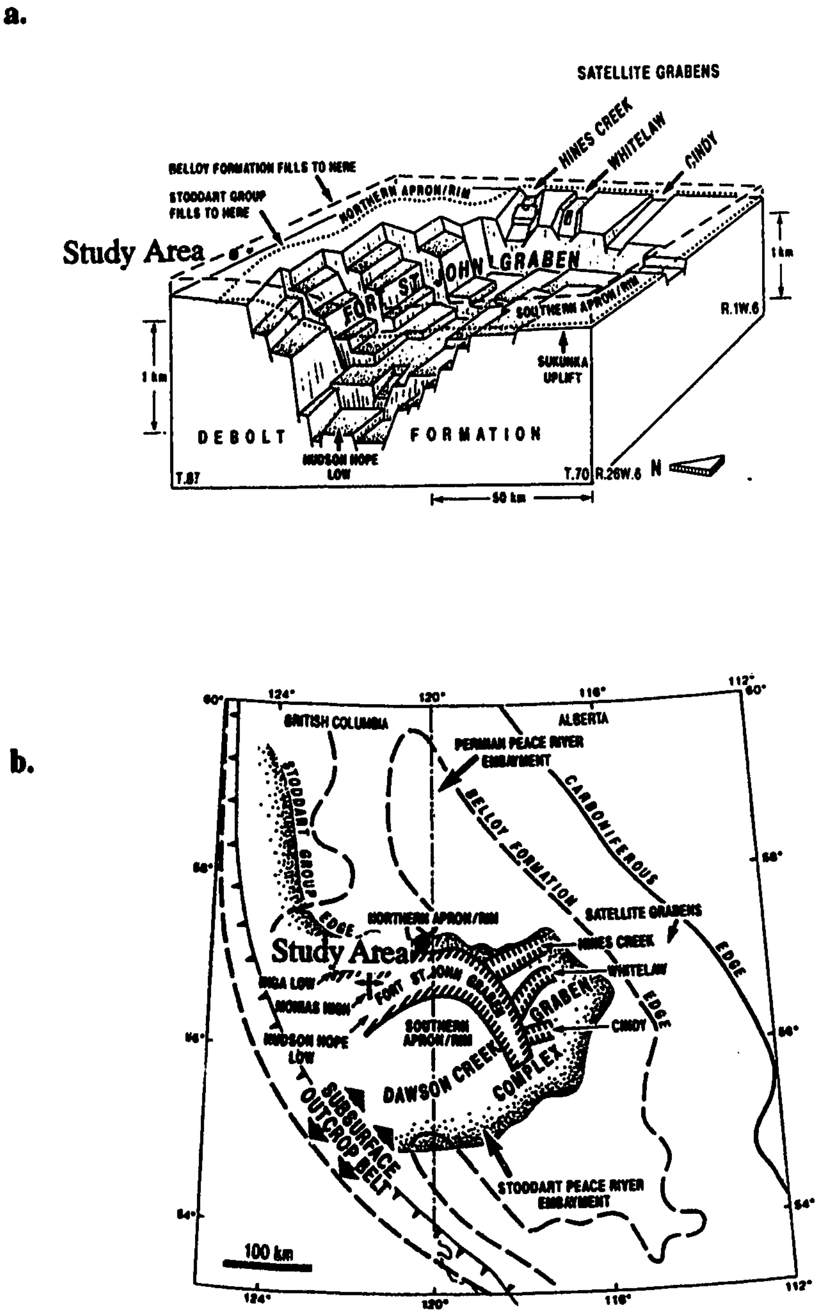

Figure 64. a. Schematic three-dimensional diagram of the Fort St. John Graben feature. The Peejay field is located on the edge of the northern flank . b. Tectonic elements of northeastern British Columbia and west-central Alberta. The study area location is included (after Barclay *et al.*, 1990).

of 'Halfway' sandstone deposits (Figure 65). These deposits thin in a northeasterly direction within the study area. Localised north-south trending thicker Halfway deposits signify the preservation of reservoir lithology within Carnian produced grabens. The lithostratigraphically defined 'Halfway' Formation has been completely removed by the Carnian erosion event, just to the northeast of the Peejay field (e.g. well d-018-B/94-A-16, Figure 50). This well shows that Charlie Lake continental red beds directly overly Halfway offshore-transition shales. The lack of coarse grained shoreface sandstones to the east and northeast of the study area, is the result of increased erosion of the Middle Triassic deposits as opposed to sedimentary thinning in an easterly direction.

As stated earlier, the Halfway-Charlie Lake contact within west-central Alberta has been interpreted as conformable by Cant (1986), Campbell and Horne (1986) and Willis (1992). However, further to the east within the Spirit River field Aukes and Webb (1986) determined that the Charlie Lake contact was erosional. The westward downwarping of the Western Canada Sedimentary Basin occurred during and after the deposition of the Doig-Halfway sandstone packages. However, the deposits to the east were coevally being uplifted, exposed and eroded (Figure 63d and e) during early Carnian times. Synsedimentary tectonism may have formed as a result of accretion of exotic terranes at the destructive plate margin, several hundred kilometres to the west. The loading of these terranes onto the continental crust resulted in tectonic subsidence and the production of increased accommodation space to the west. Abundant sediment shed from the accreted terrane may have been responsible for continual basin subsidence to the west.

It is uncertain as to whether the erosion of Middle Triassic deposits actually occurred prior to the deposition of Charlie Lake sediments, at the end of Halfway deposition, or whether the erosion surface was formed from an intra-Charlie Lake unconformity cutting further down through the deposits in an easterly direction.

The uplifted and tilted Middle Triassic deposits to the east were planed off, with increased removal of strata occurring further to the east, indicating greater amounts of uplift. Increased erosion also occurred in isolated areas, associated with early Carnian initiated horst blocks. Graben features preserved reservoir lithofacies. These deposits are associated with hydrocarbon accumulation and current production.

dstones within the study area. Basal sandstone
on gamma-ray well-logs.

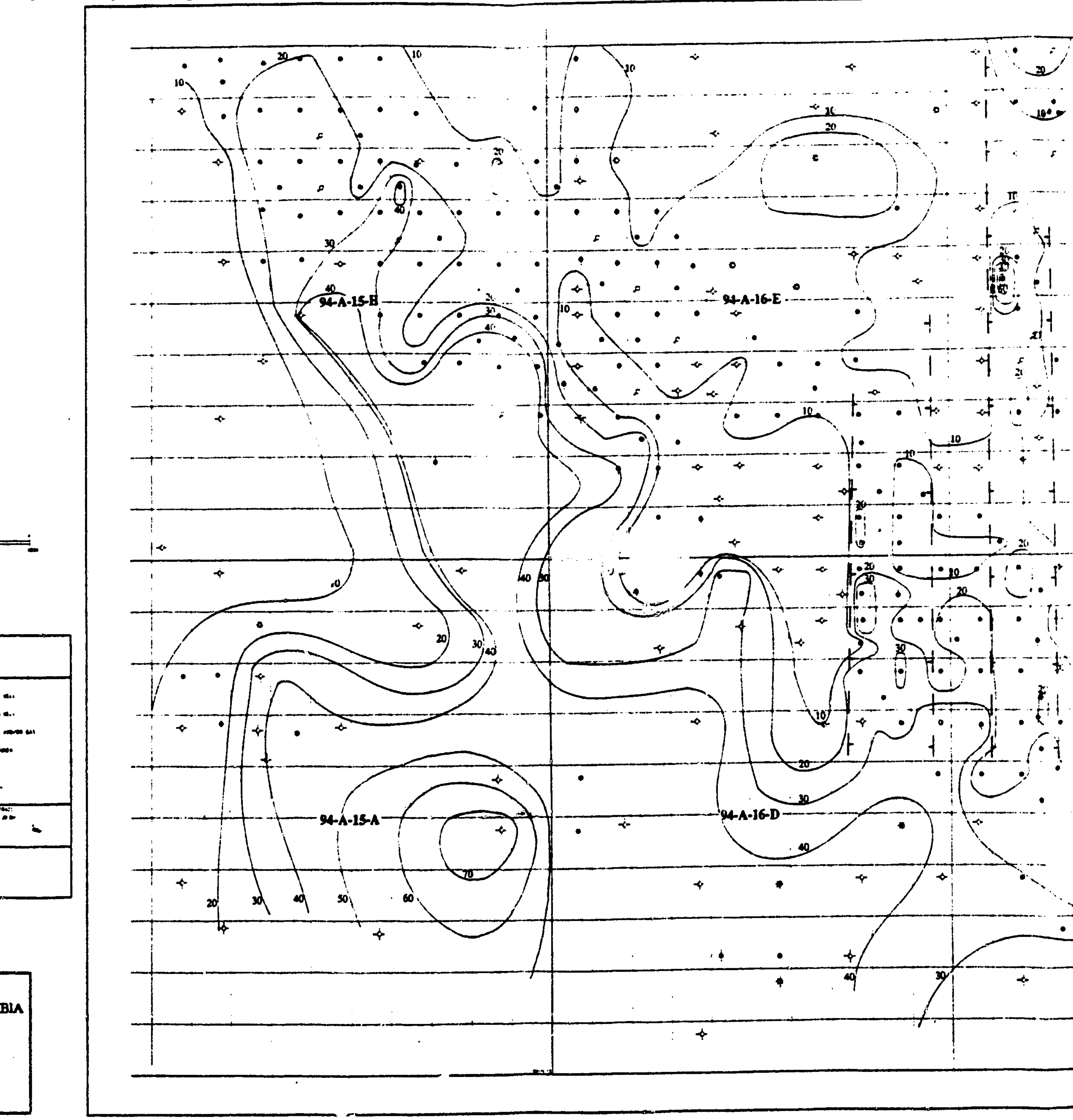

9.4.0. EARLY CARNIAN PLAYA-LAKE DEPOSITION.

Renewed sedimentation of Charlie Lake deposits occurred on the uplifted, exposed Middle Triassic surface, in the form of a continental playa-lake or lakes (Figure 63f). Pools of saline and hypersaline water became concentrated within depressions on the continent surface. These depressions may have formed in response to reactivation of earliest Carnian faults. This resulted in the production of greater thicknesses of Charlie Lake deposits over areas of local subsidence, as is demonstrated from the sequence stratigraphic cross-sections. Continental red beds are found to the northeast of the study area and occasionally overlie the playa-lake deposits. This signifies that sediment may have continued to be supplied from the east and northeast, but at much slower rates.

9.5.0. POST-EARLY CARNIAN FAULTING.

Structure contour maps of the first phosphatic horizon within the lower Doig Formation and the top of the Charlie Lake 'A' Marker (figures 66 and 67, respectively), demonstrate that these horizons have been affected by faulting that occurred after deposition of the Charlie Lake 'A' Marker limestone. The exact timing of these faults is not clear. These fault traces coincide with those of the early Carnian faults, thus suggesting that they are reactivated early Carnian faults (section 9.2.0), with fault traces oriented north-south. Maximum vertical displacement along these faults is 9 metres (30 feet). It is therefore unlikely that they would be identifiable on low resolution seismic lines. These faults have further complicated the intactness of reservoirs, in that juxtaposition of impermeable shales against permeable sandstones has occurred. These faults did not have such destructive effects on the Middle Triassic reservoir lithology compared to the early Carnian faults, that actively eroded deposits that were of potentially good reservoir quality. Figures 66 and 67 show that the fault movement contains an oblique component, since vertical displacement appears to be greater in the southern and northern regions of the study area than at the centre.

9.6.0. DIAGENETIC EFFECTS ON RESERVOIR PERFORMANCE.

The final stage in the geological history of the Middle and lowest Upper Triassic deposits affects the reservoir quality of particular lithofacies within the study area. This is due to the secondary diagenetic overprinting on the Middle Triassic rocks which has a destructive effect on the reservoir quality. Fluids rich in dissolved carbonates and sulphates percolated down into the Middle Triassic deposits during post lithification

the

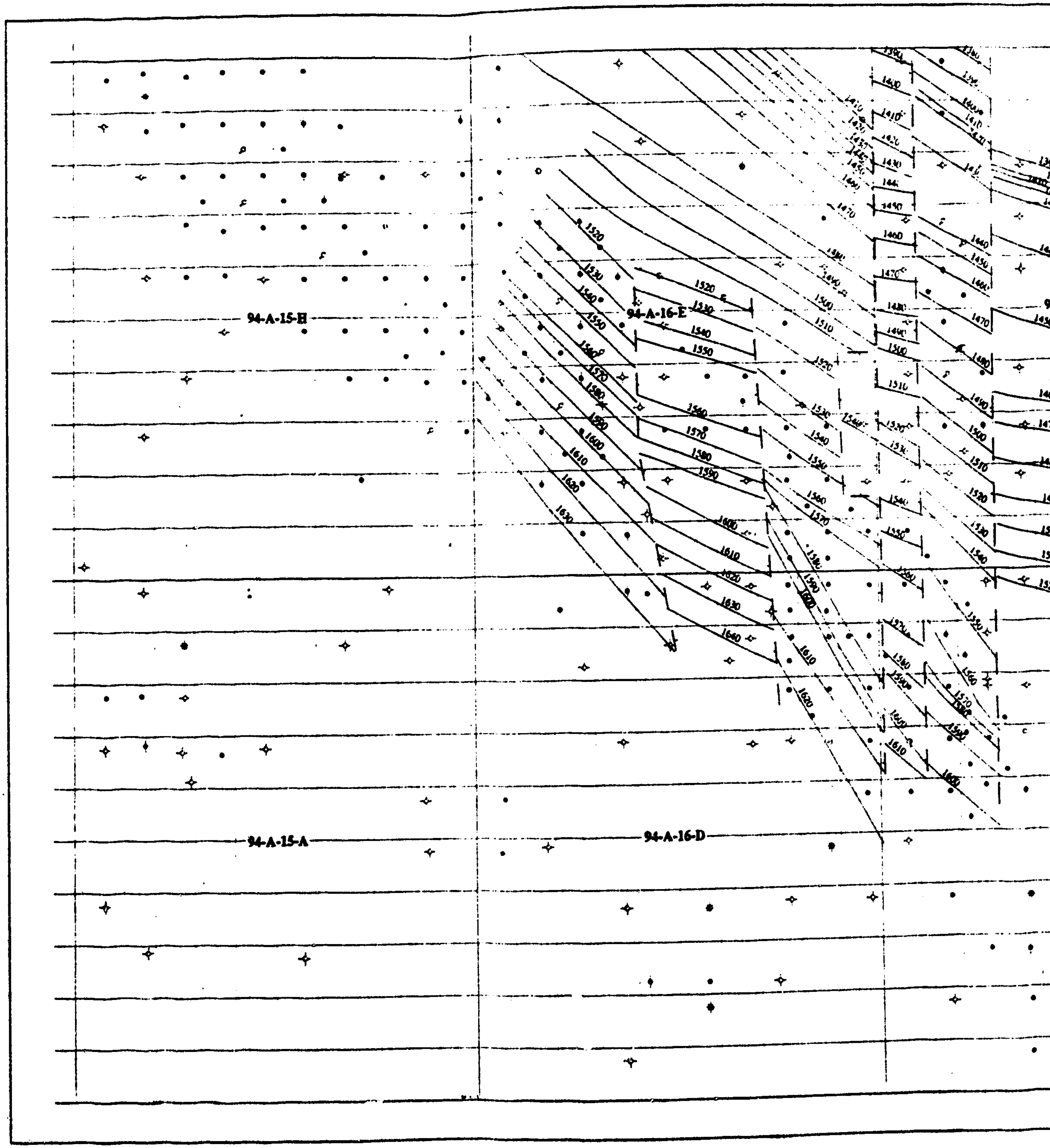
94-A-15-H
94-A-16-E
94-A-15-A
94-A-16-D
1390
1400
1410
1420
1430
1440
1450
1460
1470
1480
1490
1500
1510
1520
1530
1540
1550
1560
1570
1580
1590
1600
1610
1620
1630
1640

of the

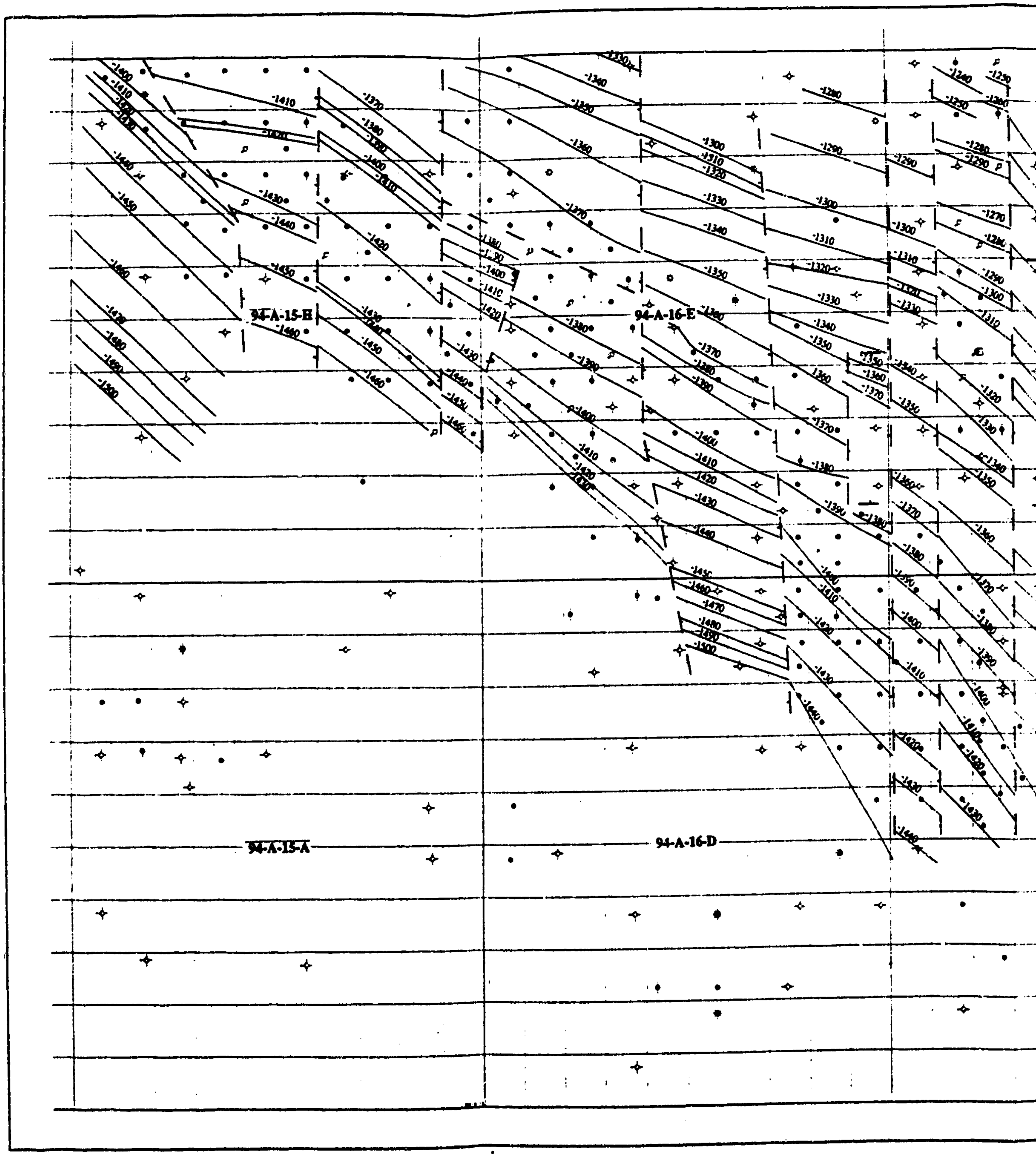

94-A-15-H
94-A-16-E
94-A-15-A
94-A-16-D
-1400
-1410
-1420
-1430
-1440
-1450
-1460
-1470
-1480
-1490
-1500
-1330
-1340
-1350
-1360
-1370
-1380
-1390
-1240
-1250
-1260
-1270
-1280
-1290
-1300
-1310
-1320

stages. The most destructive effects on reservoir quality occurred close to the Charlie Lake-Halfway contact where precipitation of calcite and anhydrite poikilitic nodules was most intense. Approaching 6 metres (20 feet) below the contact this effect becomes negligible as most of the elements within the pore water had been removed. Reservoir quality becomes poorer in an easterly direction, due in part to the thinner reservoir lithofacies associated with increased early to middle Carnian erosion, and partly to the increased intensity of cementation associated with the downward percolating pore fluids.

10.0.0. DISCUSSION.

10.1.0. DEPOSITIONAL MODEL.

The Middle Triassic deposits of the Peejay field were interpreted as "barrier beaches" by Mothersill (1968), deposited in a regressive sea. More recently, Munroe and Moslow (1990) have described and interpreted Middle Triassic Halfway cored intervals from the Peejay field, recognizing tidal inlet fill deposits characteristic of a wave-dominated barrier island shoreline. The present study is in general agreement with this interpretation. However, some refinements are suggested. The deposits within parasequence 4 from the study area have been interpreted as a prograding barrier island shoreline. This is based on the sedimentology displayed by the coarsening-upward nature of the shoreface deposits. These deposits have been truncated and reworked by laterally migrating tidal inlets, forming lenses of abrupt based, lithologically homogeneous, crude fining-upward inlet fill deposits. Critical to the identification of a barrier island shoreline sedimentary sequence are the recognition of tidal inlet channel fills. This interpretation is similar to the sedimentologic studies conducted within the Wembley Field, in west-central Alberta by Campbell and Horne (1986), Barclay and Leckie (1986), Cant (1986) and Willis (1992).

10.2.0. COMPARISONS WITH MODERN ANALOGUES.

10.2.1. Hydrographic Regime.

Sedimentologic evidence indicates that tidal inlet deposits within the study area were formed along a wave-dominated stretch of coastline. This indicates that wave processes were dominant over tidal processes. This was derived by comparing the sedimentologic nature of tidal inlet fills within the Peejay field to those of present day analogues along the eastern seaboard of the United States. Present day tidal inlet fill lithologies have been compared and contrasted within different hydrographical conditions along the coastline of the Georgia Embayment (Hayes, 1975; Nummedal *et al.*, 1977; Hubbard *et al.*, 1979; Davis and Hayes, 1984; Moslow and Tye, 1985; Tye and Moslow 1992). The preserved tidal inlet fills, within the study area, show no indication of lithological heterogeneity, both vertically and laterally. In other words, shale was absent from these deposits. These tidal inlet fills are sedimentologically very similar to those on the North Carolina coastline at Core Banks and Shakleford Banks (Moslow and Heron, 1978; Susman and Heron, 1979; Moslow and Heron, 1989). Along this coastline wave processes are dominant over tidal processes, thus characterizing this stretch of coastline as wave-dominated (Hayes, 1979). The tidal range classification, as developed by Davies (1964), has been used to compare the tidal processes between the different stretches of coastlines. It is commonly found that wave-dominated coastlines are microtidal (<2m tidal range, Davies, 1964), whereas tide-dominated coastlines are mesotidal (2-4m tidal range, Davies, 1964). This may be true in regimes of moderate wave energy (Davies and Hayes, 1984). The relative importance of these two parameters may control the coastal morphology, and hence the type of sedimentary sequences found within the rock record. Therefore, the wave-dominated Middle Triassic coastline of northeastern British Columbia may have experienced microtidal ranges.

There are, however, numerous exceptions to the rule, thus making generalizations rather precarious. Wave-dominated coastlines may experience almost any tidal range, and vice versa on tide-dominated coastlines. Parameters other than wave height and tidal range may affect the coastal morphology and hence the resultant sedimentary record. Large tidal prisms may produce tide-dominated morphologies on coastlines with microtidal ranges. For example, the Oregon and Washington coastlines of western United States experience tidal ranges of 4 metres and very high wave heights. This would be classified as a macrotidal coastline (Davies, 1964). The morphology of the coastline, however, is similar to that described by Hayes (1979) for a wave-dominated coastline. Another example is off the west peninsular of Florida along the Gulf of Mexico. Tidal range is less than 1 metre placing it in the microtidal category (Davies, 1964; and Hayes, 1979). Wave energy is also low. The general morphology, however, is similar to that described by Hayes (1975, 1979) as a high-mesotidal coast of mixed energy but with tides dominar Large ebb tidal-deltas were formed within this stretch of coastline in result to large prisms.

It has therefore been illustrated that although the tidal inlet fills within the Peejay display similar characteristics to those found along modern wave-dominated shorelin the hydrographic regime cannot be accurately qualified. Consequently, it is incorrect to state that the wave-dominated coastline, within the Peejay field, was ubiquitously microtidal. This is also indicated by the lack of abundant lateral migration of the tidal-inlets for long distances along the palaeocoastline, and the great thickness of particular inlet fills. These two factors point toward a more tide-dominated mesotidal inlet fill morphology, although sedimentologic vertical sequences suggest otherwise. Hence, the wave-dominated coastline, within the Peejay study area, may have experienced possible mesotidal ranges, but overcome by higher wave energy.

10.2.2. Percentage Tidal Inlet Fill Deposits To Shoreface Deposits.

Within the Peejay field, the youngest preserved parasequence (Pa. 4), comprising the barrier island shoreface lithosome, is composed of at least 74% tidal inlet fill deposits. This is a minimum value, since the erosional nature of the Charlie Lake sub-regional unconformity may have removed thinner tidal inlet fills. The proportion of inlet fill deposits, however, is still significantly higher than modern values of 40%, obtained along wave-dominated coastline of North Carolina (Tye and Moslow, 1992). The lower values displayed in the Holocene barrier islands are due to the evolutional and temporal immaturity of these barrier islands. The barrier islands, within the Middle Triassic Halfway Formation had prograded with geological time simultaneously to tidal inlets laterally migrating along the coastline. Hence within the study area, the tidal inlet deposits have reworked the shoreface deposits more extensively along palaeodepositional dip as well as along palaeodepositional strike. The modern day shoreface and tidal inlet lithosomes are relatively immature temporally, whereas the Halfway shoreface and tidal inlet lithosomes represent much longer periods of geological time. Hence, there has been more time for tidal inlet channels to extensively rework the shoreface lithosome within the Peejay field than within the recent analogues.

The tidal inlet fill deposits are wedge shaped along palaeodepositional strike within both the modern and the Middle Triassic barrier island lithosomes. The wedge shape of these inlet deposits, however, reflects the cumulative effect of an amalgamation of deposits formed by lateral migration of numerous tidal-inlets along the barrier island shoreline over a period of time.

The proportion of tidal inlet fill deposits within the older parasequence (Pa. 3) is only 16%. This is a significantly lower proportion than that quoted from modern analogues of wave-dominated coastlines. This indicates that the coastlines were probably continuous, rarely if ever breached and dissected by tidal inlet channels. This type of coastline was probably a strandplain. Storms may cut numerous channels through narrow barrier islands, however, most of these channels heal except within the deeper more efficient channels which are tidally maintained and form new tidal inlets (Hayes, 1967; Pierce, 1970). Strandplains are usually wide in a land-sea orientation, hence truncation and formation of channels is much more difficult to achieve than in the narrower barrier island depositional systems. Hence, this can explain the paucity of tidal inlet deposits within parasequence 3. These tidal inlets contain similar fills to those within parasequence 4, hence, they are characteristic of a wave-dominated coastline.

10.3.0. MIDDLE TRIASSIC STRATIGRAPHIC FRAMEWORK.

Middle Triassic deposits of the study area were correlated chronostratigraphically by using laterally correlatable marine flooding surfaces. The deposits, composing the identified parasequences, coarsen and thicken to the east-northeast, in a palaeolandward direction, and thin and converge into the 'Phosphatic Zone' to the west-southwest, palaeoseaward, becoming more shaly. Each younger parasequence successively oversteps the older parasequence, in a basinward direction.

Biostratigraphic data does not occur within the Peejay field, hence, it is not possible to definitively correlate the marine flooding surfaces isochronously.

Past workers identified the Doig and Halfway formations based on their lithological characteristics. The formations were correlated lithostratigraphically throughout the entire Western Canada Sedimentary Basin. The Halfway blanket sands were thought to have been deposited within a very short period of geological time. It can be seen, however, that sequence stratigraphic framework reconstruction indicates that the Halfway sandstones were indeed diachronous in formation, and are, infact, composed of a number of discrete and genetically related sandstone packages. It has been shown in this study, and those of Willis (1992) and Wittenberg (1992), that the Halfway and Doig formations are time-equivalent. The same marine flooding surface can be traced through the 'Doig' offshore marine shales and siltstones into sandstones of the Halfway shoreline to the east. The former represent the distal portions of parasequences deposited within the basin, in areas receiving low terrigenous-clastic sediments. Genetically related deposits can be traced becoming sandier and thicker to the east, and eventually form the proximal portions of parasequences within the Halfway nearshore marine sandstones.

The Charlie Lake Formation is not genetically related to the Halfway-Doig stratigraphic packages beneath, in the present study area. It is composed of continental playa-lake deposits lying erosively over the Middle Triassic marine deposits. On a field scale, the Halfway-Charlie Lake contact could be mistaken for a type 1 sequence boundary (Wagoner *et al.*, 1990). However, it has been reported in the Wembley Field by Willis (1992), that this contact is conformable, the Charlie Lake deposits being characteristic of supratidal sabkhas forming coevally behind the Halfway barrier island shorelines. Hunt and Ratcliffe (1959) recognized regional wide lateral facies changes within the Charlie Lake Formation within northeastern British Columbia. These variations recorded continental influences in the east and marine influence in the west, which corresponded to a conformable contact with the Halfway in the west and a disconformable contact in the east. The present study has also demonstrated the presence of a disconformable contact between the Halfway and Charlie Lake formations in northeastern British Columbia. These findings indicate that the term sequence boundary, separating the Middle Triassic from the Charlie Lake deposits, on a regional scale, is not correct. Within the Peejay field, this contact is clearly erosional. It is not determinable, however, whether the contact was originally conformable and has since been eroded by an intra-Charlie Lake erosional event, or whether the nature of the Halfway-Charlie Lake contact graded from a conformable contact in the southwest to an erosional contact in the northeast. If the former theory is correct, then the Charlie Lake deposits resting on the Middle Triassic deposits within the Peejay field are probably older than those within the Wembley field, in west-central Alberta. More detailed regional wide stratigraphic cross-sections may shed light on this problem.

10.4.0. HYDROCARBON TRAPPING STYLE.

The stratigraphic relationship between Middle Triassic deposits and the overlying Charlie Lake strata is a sub-regionally unconformity. Early Carnian development of horst and graben features were formed prior to, or coevally with this erosional event. Reservoir rocks within the Peejay field and surrounding area appear to have been preserved within these graben features. The trapping mechanism within the Peejay play is both stratigraphic and structural. The early Carnian erosional surface has removed the proximal updip region of all parasequences within the study area. These proximal regions have been recognized as containing very good reservoir quality lithofacies, in the form of strike oriented laterally continuous washover deposits associated with barrier island retrogradation, within the Wembley field (Willis, 1992). Overlying Charlie Lake playa-lake deposits produce an impermeable seal to the Middle Triassic reservoir rocks. This is representative of the stratigraphic hydrocarbon trapping style.

Normal faulting has formed structural traps within the Peejay field. Pre-Charlie Lake palaeotopography, produced by the early Carnian development of horst and graben structures, was consequently planed off by the ensuing, or coeval, erosional event (see Figure 63d and e). Hence, the deposits within the graben features were preserved, and those deposits of good reservoir quality have subsequently became the hydrocarbon pools. The areal and spatial geometry of these reservoir deposits was therefore controlled by the structural derived graben features, and not from depositional processes. The graben features were oriented north-south, and hence, the reservoirs have similar trends.

The combination of the sub-regional unconformity and the structural faulting produced the preservation and trapping of hydrocarbons within the present pools, in the Peejay field. The playa-lake deposits were deposited later, and produced the impermeable seal to the reservoirs.

Reactivation of later stage post-early Carnian faulting along early Carnian fault traces, aided in hydrocarbon trapping (see Figure 63f). This was achieved by the juxtaposition of an impermeable lateral seal to the pools.

10.5.0. FUTURE EXPLORATION POTENTIAL.

Close proximity to the erosional edge of the Middle Triassic deposits within northeastern British Columbia introduces increased risk associated with the areal and spatial prediction of future hydrocarbon plays. Insights into the hydrocarbon trapping mechanism within the Middle Triassic of northeastern British Columbia may reduce the risk associated with future exploration programmes. The combined result of stratigraphic erosion and structural faulting forming the reservoir pools within the Peejay area introduces difficulties when applying predictions to new play and pool locations. Three-dimensional seismic programmes may be of use in identifying thick tidal inlet channel deposits. The resolution may be poor, and hence, Triassic faulting may be difficult if not impossible to identify on the seismic lines due to the small degree of vertical displacement associated with these faults.

By tracing proximal parasequence deposits along palaeostrike, it is likely that tidal inlet fill deposits of reservoir quality will be intercepted. Whether these pools are within the water, oil or gas leg depends on the structural position of the pool on a regional scale. It must be noted, however, that structurally downdip to the south of well d-073-D/94-A-16, within the main reservoir trend of Peejay unit 2, water becomes the abundant produced fluid. North of the main reservoir trend, a gas cap is found, especially within well d-074-E/94-A-16 northward. These fluids are associated within the same parasequence. Therefore, if the proximal deposits, or tidal inlet fills of another parasequence have been preserved elsewhere in the field or surrounding area, separate oil pools may occur.

Within the Peejay field, each parasequence is separated above and below by offshore marine shales, siltstones and silty-sandstones exhibiting low reservoir quality. This produces a laterally continuous permeability barrier between each parasequence. Hence, hydrocarbon migration and accumulation will be segregated and isolated within each parasequence (Figure 68). Organic-rich phosphatic shales within the "Phosphate Zone" of the lower Doig Formation have high TOC values ranging between 9 and 11%, indicating that these are good source rocks. Source-rock-oil-to-reservoir-oil correlations by biomarker analysis have concluded that oils derived from the "Phosphate Zone" have migrated structurally updip to the northeast into Halfway traps (Riediger *et al.*, 1990). Furthermore, these oils have been identified as type II kerogens, from van Krevelen diagrams. This kerogen type is related to marine organic matter deposited in a reducing environment with medium to high sulphur content (Riediger *et al.*, 1990). These geochemical conditions were also conducive to the formation of phosphate beds within the lower Doig Formation. The hydrocarbons may well have migrated updip within each genetically related sandstone parasequence package. The only areas where hydrologic flow patterns may be permitted across parasequence sandstone packages, is where tidal inlet fill deposits are in vertical communication with porous and permeable deposits of the parasequence below. Thus, the inlet fill deposits may act as vertical conduits in localised areas. Vertical permeability values are lower than horizontal values, hence the rate of fluid migration will be greater along each parasequence, in a structural updip direction, than in a vertical direction through tidal inlet fill deposits. Had the tidal inlet deposits contained clay plugs (associated with tide-dominated shorelines), vertical communication between parasequences may have been significantly reduced.

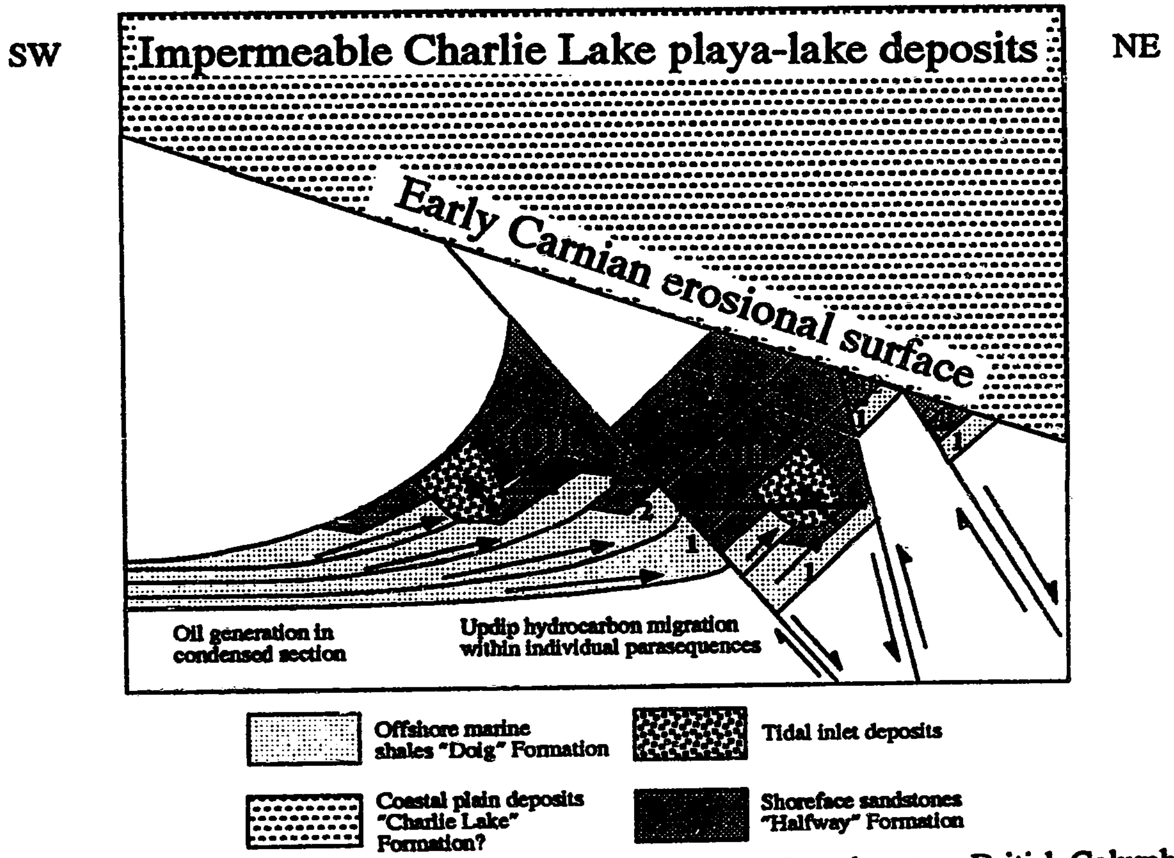

Figure 68. Hydrocarbon accumulation model for the Triassic deposits of northeastern British Columbia. The schematic diagram has been tilted so that the phosphatic horizons are horizontal, thus distorting the Carnian erosion surface. Four parasequences have been illustrated prograding to the southwest, converging within the 'Phosphate Zone'. It is from here that kerogen is generated, the hydrocarbons migrate updip (in the direction of the arrows) within each parasequence. Tidal inlet deposits act as vertical conduits for hydrocarbons, between parasequences. The majority of reservoir lithofacies are preserved within the graben features. The horst features and the early Carnian erosion surface have stripped off most of the reservoir lithofacies. Charlie Lake impermeable playa lake deposits overly the erosion surface forming a stratigraphic seal.

Further north and northeast of the study area, Middle Triassic deposits have been all but removed by the post-Halfway erosion event. Any tidal inlet fill deposits preserved will more than likely be of poor reservoir quality due to intensity of destructive diagenetic activity. This reduction in reservoir quality is attributed to the increased influence of downward percolating pore waters sourced from the Charlie Lake above. The intensity and extent of poikilitic late stage diagenetic anhydritic and calcitic pore occluding cements increases toward the north, and northeast, associated with the thinning of the Middle Triassic deposits. Reference to the sub-regional stratigraphic cross-section (see Figure 49, section 8.1.0.) indicates that inlet pools are absent northeast of the Peejay field. Reservoir quality and reservoir potential are very low within these erosively thinned deposits to the northeast.

There is a greater probability that Middle Triassic reservoir deposits will be completely preserved west and southwest of the Peejay area, since post-Halfway erosional effects are reduced in intensity. Laterally continuous, good reservoir quality washover deposits, formed due to retrogradation of the barrier island may be found in the updip portion of parasequences to the west of the Peejay field, similar to those of the Wembley field (Willis, 1992). Caution is recommended, however, since most of the Triassic deposits to the west within British Columbia are overmature with regard to hydrocarbon generation, therefore hydrocarbon exploration is areally restricted between the erosional edge to the east and the overmature region to the west (Riediger *et al.*, 1990). Increased water production may also become a more serious problem in a structurally downdip direction.

11.0.0. CONCLUSIONS.

The Middle Triassic deposits within the study area are composed of four coarsening-upward parasequences. Each parasequence prograded west-southwest into the Western Canada Sedimentary Basin. Individual parasequences thicken and become sandier to the east-northeast indicating nearness to a palaeostrandline; becoming thinner and shalier to the west-southwest, indicating more distal location to a palaeostrandline. Each parasequence successively oversteps the younger parasequence in a basinward west-southwesterly fashion, forming a progradational parasequence set.

Each parasequence cross-cuts and contains deposits assigned to the lithostratigraphically defined Doig and Halfway formations. Distal portions of parasequences are composed of basinal marine shales and siltstones typified by the Doig Formation. These coarsen to the east-northeast into shoreface sandstones and coquinas characteristic of the Halfway Formation. The deposits contained within each parasequence are coeval, hence the Halfway and Doig formations are time-equivalent.

Deposits proximal to a palaeostrandline, and backbarrier deposits within each parasequence are absent from the study area due to early Carnian synsedimentary tilting and erosion of the Middle Triassic deposits. Erosion is more pronounced to the northeast, producing a dramatic thinning of the Middle Triassic deposits. "Halfway" shoreface deposits have been completely removed to the northeast of the study area, resulting in a lack of preserved reservoir lithofacies. Reservoir quality deposits are preserved within early Carnian formed grabens. These are composed of tidal inlet sublitharenite and biodolomicrite fills. Disconformably overlying the Middle Triassic deposits are impermeable shales, siltstone and evaporites deposited within a Charlie Lake continental playa-lake depositional system. The deposits are genetically unrelated to the Middle Triassic marine deposits.

The application of sequence stratigraphy, in conjunction with biostratigraphic techniques, should be applied over lithostratigraphy in order to more accurately correlate depositional packages on both large- and small-scale projects. Besides improving the lateral correlatibility of depositional packages, these techniques can improve the predictability of hydrocarbon and other fluid migration paths within the Middle Triassic deposits.

The most proximal parasequence (Pa. 4) is composed of 74% tidal inlet channel fill deposits indicative of wave-dominated barrier island shorelines. In comparison, the paucity of tidal inlet channel fill deposits found within parasequence 3 (16%) are indicative of a palaeostrandplain shoreline.

Each parasequence is separated above and below by impermeable deposits. Each parasequence is thus hydrologically discrete, being connected vertically where tidal inlet fills erode down into the permeable shoreface deposits of the parasequence below. Hydrocarbons sourced from the "Phosphate Zone" within the lower Doig Formation, migrate slowly northeastward up structural dip into more proximal discrete shoreface reservoirs.

Reservoir quality of sublitharenite deposits is homogeneous along palaeodepositional strike and dip, but may be locally affected by sedimentary structures, thickness of the lithofacies, and pore occluding cements derived from the Charlie Lake Formation. Reservoir quality of the coquina tidal inlet fill deposits is less homogeneous due to diagenetic processes. Patchy dolomitization with late stage poikilitic calcite and anhydrite cement has locally reduced permeability.

Future hydrocarbon exploration programmes within the Middle Triassic deposits of the Western Canada Sedimentary Basin of northeastern British Columbia, will be dictated by the location of north-south oriented Carnian produced graben features, in which are preserved good reservoir quality lithofacies. The preservation of reservoir lithofacies will increase toward the west and south as early Carnian erosion is less pronounced, and middle to late stage intense diagenetic destructive processes will be less severe.

12.0.0. REFERENCES CITED.

ARMITAGE, J. H. (1962). Triassic oil and gas occurrences in northeastern British Columbia, Canada. *Journal of the Alberta Society of Petroleum Geologists*, **10**; 35-56.

ARNOTT, R. W. and SOUTHARD, J. B. (1990). Exploratory flow-duct experiments on combined-flow bed configurations, and some implications for interpreting storm-event stratification. *Journal of Sedimentary Petrology*, **60**; 211-219.

AUKES, P. G. and WEBB, T. K. (1986). Triassic Spirit River pool, northwestern Alberta. *In*: Meijer Drees, N.C. (Ed.), 1986 Core Conference, Calgary, Canadian Society of Petroleum Geology. p.3.1-3.34.

BARCLAY, J. E. (1988). Triassic, Western Canada Basin: depositional cycles, oil plays and oil potential. *Canadian Society of Petroleum Geology Reservoir*, **15** (2); 1-2.

BARCLAY, J. E., KRAUSE, F. F., CAMPBELL, R. I. and UTTING, J. (1990). Dynamic casting and growth faulting: Dawson Creek Graben Complex, Carboniferous-Permian Peace River Embayment, Western Canada, *Bulletin of Canadian Petroluem Geology*, **38A**; 115-146.

BARCLAY, J. E. and LECKIE, D. A. (1986). Tidal inlet reservoirs of the Triassic Halfway Formation, Wembley Region, Alberta. *In:* Meijer-Drees (Ed.), 1986 Core Conference, Calgary, Canadian Society of Petroleum Geology, 4.1-4.6.

BARSS, D. L., BEST, E. W. and MEYERS, N. (1964). Triassic, Chapter 9. *In:* McCrossan, R. G. and Glaister, R. P. (Eds.). *Geological History of Western Canada.* Alberta Society of Petroleum Geology, Calgary, 113-136.

BARWIS, J. H. and MAKURATH, J. H. (1978). Recognition of ancient tidal inlet sequences: an example from the Upper Silurian Keyser Limestone in Virginia. *Sedimentology*, **25**; 61-82.

BATURIN, G. N. and BEZRUKOV P. L. (1979). Phosphorites on the sea floor and their origin. *Marine Geology*, 31; 317-332.

BERELSON, W. M. and HERON, D. Jr. (1985). Correlations between Holocene flood tidal delta and barrier island inlet fill sequences: Back Sound-Shackleford Banks, North Carolina. *Sedimentology*, 32; 215-222.

BERNARD, H. A., LeBLANC, R. J. and MAJOR, C. E. (1962). Recent and Pleistocene geology of southeast Texas, *In:* Rainwater, E. H. and Zingula, R. P. (Eds.). Geology of the Gulf Coast and Central Texas and Guidebook Excursions. Houston Geological Society, Field Trip Guidebook, pp. 175-224.

BIRCH, G. F. (1980) A model of penecontemporaneous phosphatization by diagenetic and authigenic mechanisms from the western margin of Southern Africa. *Society of Economic Paleontologists and Mineralogists*, Special Paper No. 29; 79-100.

BLOME, C. D. and NESTELL, M. K. (1991). Evolution of a Permo-Triassic sedimentary melange, Grindstone terrane, east-central Oregon. *Geological Society of America Bulletin*, 103; 1280-1296.

BOOTHROYD, J. C. (1978). Mesotidal inlets and estuaries. *In:* Davis, R. A. Jr. (Ed.), *Coastal Sedimentary Environments*, 1978, Chapter 6, Springer-Verlag, 420 p.

BOOTHROYD, J. C. and HUBBARD, D. K. (1975). Genesis of bedforms in mesotidal estuaries. *In:* Cronin, L. E. (Ed.). *Estuarine Research*, Vol. II. Geology and Engineering, Academic Press, New York, 217-234pp.

BRISKIN, M. and SCHREIBER, B. C. (1978). Authigenic gypsum in marine sediments. *Marine Geology*, 28; 37-49.

BUTLER, G. P. (1969). Modern evaporite deposition and geochemistry of coexisting brines, the sabkha Trucial Coast, Arabian Gulf. *Journal of Sedimentary Petrology*, 39; 70-89.

CAMPBELL, C. V., DIXON, R. J. and FORBES, D. M. (1989). Updip erosional truncation of Halfway and Doig shoreline sequences: A new model for exploration in west central Alberta (abst.). Programs and Abstracts, Exploration Update 1989, Canadian Society of Petroleum Geology Convention, Calgary, p. 138.

CAMPBELL, C. V. and HASSLER, G. (1989). Stratigraphy and facies of the Triassic Halfway and Doig Formations in west-central Alberta (abst.). *Canadian Society of Petroleum Geology Reservoir,* **16** (2); 1-3.

CAMPBELL, C. V. and HORNE, J. C. (1986). Depositional facies of the Middle Triassic Halfway Formation, western Canada basin. *In:* Moslow, T.F. and Rhodes, E.G. (Eds.), *Modern and ancient shelf clastics:* A core workshop. Society of Economic Paleontologists and Mineralogists Core Workshop No. 9; 413-459.

CANT, D. J. (1986). Hydrocarbon trapping in the Halfway Formation (Triassic), Wembley Field, Alberta. *Bulletin of Canadian Petroleum Geology,* **34**; 329-338.

CHANG, JEN-HU. (1972). *Atmospheric Circulation Systems and Climates.* The Oriental Publishing Company. 328pp.

CHEEL, R. J. and LECKIE, D. A. (1990). A tidal inlet complex in the Cretaceous epeiric sea of North America: Virgille Member, Milk River Formation, southern Alberta, Canada, *Sedimentology,* **37**; 67-81.

CHEN, P. Y. (1968). A modification of sandstone classification. *Journal of Sedimentary Petrology,* **38**, (1); 54-60.

CHUNTA, A. (1969). The Halfway reservoir western portion, Peejay field, British Columbia (abst.). *Bulletin of Canadian Petroleum Geology,* **17**; 528.

CLARK, D. R. (1961). Primary structures of the Halfway sand in the Milligan Creek oilfield, British Columbia. *Journal of the Alberta Society of Petroleum Geologists,* **9**; 109-130.

CLIFTON, H. E. (1976). Wave-formed sedimentary structures-A conceptual model. *In:* Davis, R. A. Jr. and Ethrington, R. L. (Eds.). *Beach and Nearshore Sedimentation.* pp. 126-148. Special Pubication Society of Economic Paleontologists and Mineralogists, 24. Tulsa.

CLIFTON, H. E., HUNTER, R. E. and PHILLIPS, R. L. (1971). Depositional structures and processes in the non-barred high-energy nearshore. *Journal of Sedimentary Petrology,* 41; 651-670.

CODY, R. D. (1979). Lenticular gypsum: occurrences in nature, and experimental determinations of effects of soluble green plant material on its formation. *Journal of Sedimentary Petrology,* 49; 1015-1028.

COLEMAN, J. M. and WRIGHT. L. D. (1975). Modern river deltas: variability of processes and sand bodies. *In:* Broussard, M. L. (Ed.), *Deltas,* pp. 99-150. Houston Geological Society.

COLQUHOUN, D. J. (1960). Triassic stratigraphy of Central Western Canada, *Dissertation Abstracts,* 1522-1523.

COLQUHOUN, D. J. (1962). Triassic stratigraphy in the vicinity of Peace River Foothills, British Columbia. *Edmonton Geological Society 4th Fieldtrip Guidebook,* 57-88

COOK, P. J. (1976). Sedimentary phosphate deposits. *In:* Wolf, K. H. (Ed.). *Handbook of stratabound and stratiform ore deposits,* 7. pp. 505-535. Elsevier Publishing Company, Amsterdam.

CREANEY, S. and ALLEN, Y. (1990). Hydrocarbon generation and migration in the Western Canada Sedimentary Basin. *In:* Brooks, J. (Ed.) *Classic Petroleum Provinces,* Geological Society Special Publication no. 50 of The Geological Society of London, 189-202.

DAVIDSON-ARNOTT, R. G. D. and GREENWOOD, B. (1976). Facies relationshps on a barred coast, Kouchibouguac Bay, New Bruswick, Canada. *In: Beach and Nearshore Sedimentation,* Society of Economic Paleontologists and Mineralogists Special Publication No. 24; 149-168.

DAVIES, D. J., POWELL, E. N. and STANTON R. J. Jr. (1989). Taphonomic signature as a function of environmental process: shells and shell beds in a hurricane-influenced inlet on the Texas coast. *Paleogeography, Paleoclimatology, Paleoecology,* 72; 317-356.

DAVIES, G. A., MONGER, J. W. H. and BURCHFIEL, B. C. (1978). Mesozoic construction of the Cordilleran "collage", central British Columbia to central California. *In:* Howell, D. G. and McDougall, K. A. (Eds.) *Mesozoic Palaeogeography of the Western United States.* Society of Economic Paleontologists and Mineralogists, Pacific Section, Pacific Coast Palaeogeography Symposium 2, 1-32.

DAVIES, G. R. (1970). Algal-laminated sediments, Gladstone Embayment, Shark Bay, Western Australia. *American Association of Petroleum Geologists, Memoir 13;* 169-205.

DAVIES, J. L. (1964). A Morphogenic approach to world shorelines. Zeits. *Geomorphology,* 8; 127-142.

DAVIS, D. K., ETHRIDGE, F. G. and BERG, R. R (1971). Recognition of barrier environments. *American Association of Petroleum Geologists Bulletin,* 55; 550-565.

DAVIS, R. A. Jr. and HAYES, M. O. (1984). What is a wave-dominated coast? *Marine Geology,* 60; 313-329.

DAWSON, G. M. (1879). Preliminary report on the physical and geological features of the southern portion of the interior of British Columbia. *Geological Survey of Canada,* Report Programme 1877-1878, Report B, pp.187.

DAWSON, G. M. (1887). Vancouver Island and adjacent coasts. *Geological Natural History Survey Canada,* n. series, 2, 1886 Report B; pp. 129.

DIESTER-HAASS, L. and SCHRADER, H. J. (1979). Neogene coastal upwelling history off northwest and southwest Africa. *Marine Geology,* **29**; 39-53.

DORJES, J., FREY, R. W. and HOWARD, J. D. (1936). Origins of, and mechanisms for, mollusk shell accumulations on Georgia beaches. *Senckenbergiana marit.,* **18**; 1-43.

DUDLEY, J. S., HASKIN, H. K. and MOORE, C. H. (1989). Effects of geological heterogeneity on acidization: Halfway Formation. *In:* 1989 Core Conference, Canadian Society of Petroleum Geology, Calgary. Geology and Reservoir Heterogeneity. p. 7-1--7-18.

DUKE, W. L. (1985). Hummocky cross-stratification, tropical hurricanes, and intense winter storms. *Sedimentology,* **32**; 167-194.

DUKE, W. L. (1986). Hummocky cross-stratification, tropical hurricanes, and intense winter storms-Reply. *Sedimentology,* **34**; 344-359.

DUKE, W. L. (1990). Geostrophic circulation or shallow marine turbidity currents? The dilemma of paleoflow patterns in storm-influenced prograding shoreline systems. *Journal of Sedimentary Petrology,* **60**; 870-883.

DUKE, W. L., ARNOTT, R. W. C. and CHEEL, R. J. (1991). Shelf sandstones and hummocky cross-stratification: New insights on a stormy debate. *Geology,* **19**; 625-628.

ELLIOTT, T. (1986). Siliclastic shorelines. *In:* Reading H. G. (Ed.), *Sedimentary Environments and Facies* (2nd. Edition). Blackwell. Oxford. 155-188.

EUGSTER, H. P. and HARDIE, L. A. (1975). Sedimentation in an ancient playa-lake complex: the Wilkins Peak Member of the Green River Formation of Wyoming. *Geological Society of America Bulletin,* **86**; 319-334.

FISHER, J. J. (1962). Geomorphic expression of former inlets along the Outer Banks of N. C. Thesis, Univeristy of North Carolina Chapel Hill, North Carolina, 120pp. (unpublished).

FITZGERALD, D. M., HUBBARD, D. K. and NUMMEDAL, D. (1978). Shoreline changes associated wth tidal inlets along the South Carolina coast. *Proceedings Coastal Zone '78*, 3; 1973-1994.

FITZGERALD, D. M., PENLAND, S. and NUMMEDAL, D. (1984). Control of barrier island shape by tidal sediment bypassing: East Frisian Islands, West Germany. *Marine Geology*, **60**; 355-376.

FOLK, R. L. (1968). *Petrology of sedimentary rocks:* Hemphill's, Austin, Texas, pp 154.

FREY, R. W. and HOWARD, J. D. (1988). Beaches and beach-related facies, Holocene barrier islands of Georgia. *Geological Magazine*, **6**; 621-640.

FULTON, H. B. (1966). Triassic Halfway formation isopach Peejay-Beatton River area, northeastern British Columbia. British Columbia Department of Mines and Petroleum Resources.

GIBSON, D. W. (1970). Triassic stratigraphy, Pine Pass area, northeastern British Columbia. *In*: Bush, G. L. and J. Dooge J. (Eds.), *Peace River Pine Pass Yellowhead, Edmonton Geological Society Field Conference Guidebook*, 1970; 23-38.

GIBSON, D. W. (1975). Triassic rocks of the Rocky Mountain Foothills and Front Ranges of northeastern British Columbia and west-central Alberta. *Geological Survey of Canada Bulletin*, **247**.

GIBSON, D. W. and BARCLAY, J. E. (1989). Middle Absaroka sequence: the Triassic stable craton. *In*: Ricketts B. D. (Ed.). *Western Canada Sedimentary Basin, A Case History*, Canadian Society of Petroleum Geologists, Calgary, 1989, p.219-231.

GIBSON, D. W. and EDWARDS, D. E. (1990). An overview of Triassic stratigraphy and depositional environments in the Rocky Mountain Foothills and Western Interior Plains, Peace River Arch area, northeastern British Columbia. *Bulletin of Canadian Petroleum Geology*, **38A**, 146-158.

GIRESSE, P. (1980). Phosphorus concentrations in the unconsolidated sediments of the tropical Atlantic shelf of Africa south of the Equator-Oceanographic comments. *Society of Economic Paleontologists and Mineralogists, Special Paper* No. 29; 101-116.

GOLDRING, R. and BRIDGES, P. (1973). Sublittoral sheet sandstones. *Journal of Sedimentary Petrology,* 43; 736-747.

GRESSLY, A., (1938). Observations geologiques sur le Jura Soleurois. *Neue Denkschr. allg. schweiz. Ges. ges. Naturw.,* 2; 1-112.

HABICHT, J. K. A. (1979). Paleoclimate, Paleomagnetism, and Continental Drift. *American Association of Petroleum Geologists Studies in Geology No. 9.*

HALTON, E. (1981). Wembley Field - Facies variations in the Halfway Formation. *In:* Stoakes, F.A. (Ed.). *Environmental Analysis from core and field sample studies,* 1981 Core Conference, Calgary, Canadian Society of Petroleum Geologists, p.9.

HAMBLIN, A. P. and WALKER, R. G. (1979). Storm-dominated shallow marine deposits: the Fernie-Kootenay (Jurassic) transition, southern Rocky Mountains. *Canadian Journal of Earth Science,* 16; 1673-1690.

HANDFORD, C. R. (1982). Sedimentology and evaporite diagenesis in a Holocene continental sabkha: Bristol Dry Lake, California. *Sedimentology,* 29; 239-253.

HARDIE, L. A. and EUGSTER, H. P. (1971). The depositional environment of marine evaporites: A case study for shallow, clastic accumulation. *Sedimentology,* 16; 187-220.

HARDIE, L. A., SMOOT, J . P. and EUGSTER, H. P. (1978). Saline lakes and their deposits. In: Matter, A. and Tucker, M. E. (Eds.). *Modern and Ancient Lake Sediments.* pp. 7-42. Special Publication of International Association of Sedimentologists 2.

HARMES, J. C., SOUTHARD, J. B., SPEARING, D. R. and WALKER, R.G. (1975). Depositional environments as interpreted from primary sedimentary structures and stratification sequences. Society of Economic Paleontologists and Mineralogists, Tulsa, Short Course No. 2, 161 pp.

HARMES, J. C., SOUTHARD, J. B. and WALKER, R. G. (1982). Structures and sequences in clastic rocks. Society of Economic Paleontologists and Mineralogists Short Course No. 9. Tulsa.

HART, B. S., VANTFOORT, R. M. and PLINT, G. (1990). Is there evidence or geostrophic currents preserved in the sedimentary record of inner to middle shelf deposits?-discussion. *Journal of Sedimentary Petrology,* 60; 633-635.

HAYES, M. O. (1967). Hurricanes as geological agents, south Texas coast.- Geological Notes. *American Association of Petroleum Geologists Bulletin,* 51; 937-956.

HAYES, M. O. (1975). Morphology of sand accumulation in estuaries: an introduction to the symposium. *In:* Cronin, L. E. (Ed.),*Estuarine Research, Vol. II.* Geology and Engineering, pp. 3-22. Academic Press, London.

HAYES, M. O. (1979). Barrier island morphology as a function of tidal and wave regime. *In:* Leatherman, S.P. (Ed.), *Barrier Islands from the Gulf of St. Lawrence to the Gulf of Mexico.* Academic Press, New York, San Francisco, London, 1979, 1-27.

HAYES, M. O. (1980). General morphology and sediment patterns in tidal inlets. *Sedimentary Geology,* 26; 139-156.

HAYES, M. O. and KANA, T. W. (1976). *Terrigenous Clastic Depositional Environments-Some Modern Examples,* pp. I-131, II-184, Technical Report, II-CRD, Coastal Resources Division, University of South Carolina.

HENDERSON, S.W. and FREY, R.W. (1986). Taphonomic redistribution of mollusk shells in a tidal inlet channel, Sapelo Island, Georgia. *Palaios,* 1; 3-16.

HENNESSY, J. T. and ZARILLO, G. A. (1987). The interrelation and distinction between flood-tidal delta and washover deposits in a transgressive barrier island. *Marine Geology,* 78; 35-56.

HERON, D. S. Jr., MOSLOW, T. F., BERELSON, W. M., HERBERT, J. R., STEELE, G. A. III. and SUSMAN, K. R. (1984). Holocene sedimentation of a wave-dominated barrier-island shoreline: Cape Lookout, North Carolina. *Marine Geology,* 60; 413-434.

HEWARD, A. P. (1981). A review of wave-dominated clastic shoreline deposits. *Earth Science Reviews,* 17; 223-276.

HOBDAY, D. K. and HORNE, J. C. (1977). Tidally influenced barrier island and estuarine sedimentation in the Upper Carboniferous of southern West Virginia. *Sedimentary Geology,* 18; 97-122.

HOBDAY, D. K. and ORME, A. R. (1974). The Port Durnford Formation: A major Pleistocene barrier-island complex along the Zululand coast. *Transactions of the Geological Society of South Africa,* 77; 141-149.

HOFFMAN, P. (1976). Stromatolite morphologies in Shark Bay, Western Australia. *In:* Walter, M. R. (Ed.), *Stromatolites,* pp. 261-272, Elsevier, Amstadam.

HORNE, J. C., CAMPBELL, C. V. and ODLAND, S. K. (1985). Tidal-inlet fills as hydrocarbon reservoirs: Examples from Halfway Formation, Alberta (Abst.). *American Association of Petroleum Geologists Bulletin,* 69; 267.

HOWARD, J. D. and REINECK, H. E. (1972). Physical and biogenic sedimentary structures of the nearshore shelf. *Senckenberg Mar.,* 4; 81-123.

HOWARD, J. D. and REINECK, H. E. (1981). Depositional facies of high-energy beach-to-offshore sequence: comparison with low-energy sequence. *American Association of Petroleum Geologists Bulletin,* 65; 807-830.

HOYT, J. H. and HENRY, V. J. Jr. (1967). Influence of island migration on barrier-island sedimentation. *Geological Society of America Bulletin,* 78; 77-86.

HUBBARD, D. K., OERTEL, G. and NUMMEDAL., D. (1979). The role of wave and tidal currents in the development of tidal-inlet sedimentary structures and sand body geometry: examples from North Carolina, South Carolina, and Georgia. *Journal of Sedimentary Petrology,* 49; 1073-1092.

HUNT, A. D and RATCLIFFE, J. D. (1959). Triassic stratigraphy, Peace River area, Alberta and British Columbia, Canada. *American Association of Petroleum Geologists Bulletin,* 43; 563-589.

HUNTER, R. E. and CLIFTON, H. E. (1982). Cyclic deposits and hummocky cross-stratification of probable storm origin in Upper Cretaceous rocks of the Cape Sebastian area, southwestern Oregon. *Journal of Sedimentary Petrology,* 52; 127-143.

HUNTER, R. E., CLIFTON, H. E. and PHILLIPS, R. L. (1979). Depositional processes, sedimentary structures and predicted vertical sequences in barred nearshore systems, southern Oregon coast. *Journal of Sedimentary Petrology,* 49; 711-726.

IMPERATO, D.P., SEXTON, W. J. and HAYES, M. O. (1988). Stratigraphy and sediment characteristics of a mesotidal ebb tidal-delta, North Edisto Inlet, South Carolina, *Journal of Sedimentary Petrology,* 58; 950-958.

IRISH, E. J. W. (1968). Structure of the northern Foothills and eastern mountain ranges, Alberta and British Columbia. Geological Survey of Canada, Bulletin 168.

IRVING, E. (1977). Drift of the major continental blocks since the Devonian. *Nature,* 270; 304-309.

IRVING, E., WOODSWORTH, G. J., WYNNE, P. J. and MORRISON, A. (1985). Paleomagnetic evidence for displacement from the south of the Coast Plutonic Complex, British Columbia. *Canadian Journal of Earth Sciences,* 22; 584-598.

JOHNSON, K. G. and FRIEDMAN, G. M. (1969). The Tully clastic correlatives (Upper Devonian) of New York state: a model for recognition of alluvial, dune(?), tidal, nearshore (bar and lagoon), and offshore sedimentary envirnoments in a tectonic delta complex. *Journal of Sedimentary Petrology,* 39; 451-485.

JOPLING, A. V. (1965b). Hydraulic factors and the shape of laminae. *Journal of Sedimentary Petrology,* 35; 777-791.

KINDLE, E. D. (1944). Geological reconnaissance along Fort Nelson, Liard and Beaver Rivers, northeastern British Columbia and southeastern Yukon. *Geological Survey of Canada Paper* 44-16.

KINSMAN, D. J. J. (1966). Gypsum and anhydrite of Recent age, Trucial Coast, Persian Gulf. *In:* Rau, J. L. (Ed.). *Second Symposium on Salt.I.* pp. 302-326.Northern Ohio Geological Society, Cleveland, Ohio.

KINSMAN, D. J. J. and PARK, R. K. (1976). Algal belt and coastal sabkha evolution, Trucial coast, Persian Gulf. *In:* Walter, M. R. (Ed.). *Interpreting Stromatolites.* pp. 421-433, Elsevier, Amstadam.

KLEIN, G. DE V. (1963). Bay of Fundy intertidal zone sediments. *Journal of Sedimentary Petrology,* 33; 844-854.

KLEIN, G. DE V. (1974). Estimating water depths from analysis of barrier island and deltaic sedimentary sequences. *Geology,* 409-412.

KREISA, R. D. (1981). Storm-generated sedimentary structures in subtidal marine facies with examples from the Middle and Upper Ordovician of southwestern Virginia. *Journal of Sedimentary Petrology,* 51; 823-848.

KRISTAN-TOLLMANN, VON E. and TOLLMANN, A. (1981). Die Stellung der Tethys in der Trias und die Herkunft ihrer Fauna. *Mitteilungen der Osterreichischen Geologische Gesellschaft,* 74/75; 129-135.

KUMAR, N. and SANDERS, J. E. (1974). Inlet sequences: a vertical succession of sedimentary structures and texture created by the lateral migration of tidal inlets. *Sedimentology,* **21**; 491-532.

KUMAR, N. and SANDERS, J. E. (1976). Characteristics of shoreface storm deposits: modern and ancient examples. *Journal of Sedimentary Petrology,* **46**; 145-162.

LECKIE, D. A., CHEEL, R. J. and ROSENTHAL, L. (1989). Sedimentology of the Upper Virgille Member (Upper Cretaceous Milk River Formation), Writing-on-Stone Provincial Park, Alberta. Field trip guide to the second international research symposium on tidal clastic deposits. Canadian Society of Petroleum Geologists, Calgary, Alberta.

LECKIE, D. A. and ROSENTHAL, L. (1987). Sedimentology of sandstone reservoirs. Canadian Society of Petroleum Geologists. *Geological Survey of Canada Contribution #* **22487.** 34-41.

LECKIE, D. A. and WALKER, R. G. (1982). Storm- and tide-dominated shorelines in Cretaceous Moosebar-Lower Gates interval-outcrop equivalents of deep basin gas trap in western Canada. *American Association of Petroleum Geologists Bulletin,* **66**; 138-157.

LEEDER, M.R. (1982). *Sedimentology.* George Allen and Unwin, London. 344p.

LYNCHE-BLOSSE, M. A. and KUMAR, N. (1976). Evolution of downdrift-offset tidal inlets: a model based on the Brigantine inlet system of New Jersey. *Journal of Sedimentary Petrology,* **84**; 165-178.

McCONNELL, R. G. (1891). Report on a portion of the District of Athabasca comprising the country between Peace River and Athabasca River North of Lesser Slave Lake. *Geological Survey of Canada Annual Report,* **5**; part I, part D.

McLEARN, F. H. (1921). Mesozoic of Upper Peace River, B.C. *Geological Survey of Canada Summary Report,* 1920, Part B; 1-6

McLEARN, F. H. (1940). Notes on the geography and geology of the Peace River Foothills. *Transaction Royal Society of Canada,* 3rd series, 34; 63-74.

McLEARN, F. H. (1946a). Middle Triassic (Anisian) Fauna in Halfway, Sikanni Chief and Tetsa Valleys, Northeastern British Columbia. *Geological Survey of Canada Paper* 46-1.

McLEARN, F. H. (1953). Correlation of the Triassic formations of Canada. *Geological Society of America Bulletin,* 64; 1205-1228.

McLEARN, F. H. (1960). Ammonoid faunas of the Upper Triassic Pardonet Formation; Peace River Foothills, British Columbia. Geological Survey of Canada, Memoir 311.

McLEARN, F. H. and KINDLE, E. D. (1950). Geology of northeastern British Columbia. *Geological Survey of Canada Memoir* 259. 34-66.

MEISRALL, F. L. (1966). The Spit-Platform concept: Labortory observation of spit development, 46pp. Unpublished Master's Thesis, University of Alberta, Edmonton, Alberta.

MIALL, A. D. (1976). The Triassic sediments of Sturgeon Lake south and surrounding areas. *In:* Lerand, M.M. (Ed.), *The sedimentology of selected clastic oil and gas reservoirs in Alberta.* Canadian Society of Petroleum Geologists, Calgary, 25-43.

MONGER, J. W. H. and IRVING, E. (1980). Northward displacement of north-central British Columbia. *Nature,* 285; 289-294.

MONGER, J. W. H., PRICE, R. A., and TEMPELMAN-KLUIT, D. J. (1982). Tectonic accretion and the origin of the two metamorphic and plutonic welts in the Canadian Cordillera. *Geology,* 10; 70-75

MORTIMER, N. (1986). Late Triassic, arc-related, potassic igneous rocks in the North American Cordillera, *Geology;* 14; 1035-1038.

MORTON, R. A. (1982). Formation of storm deposits by storm-forced currents in the Gulf of Mexico and the North Sea. *In:* Nio, S. D., Shuttenhelm, T. E. and van Weering, Tj. C. E., (Eds.). *Holocene Marine Sedimentation in the North Sea Basin.* Special Publication International Association of Sedimentologists, 5; 385-396. Blackwell Scientific Publications. Oxford, 524 p.

MOSLOW, T. F. (1980). Stratigraphy of mesotidal barrier islands. Unpublished Ph.D. Thesis, University of South Carolina, South Carolina, USA. 265 p.

MOSLOW, T. F. (1983). Depositional mdels of shelf and shoreline sandstones. *Continuing Education Course Notes Series #27,* American Society of Petroleum Geology.

MOSLOW, T. F. and HERON, S. D. Jr. (1978). Relict inlets: preservation and occurrence in the Holocene stratigraphy of southern Core Banks, North Carolina. *Journal of Sedimentary Petrology,* 48; 1275-1286.

MOSLOW, T. F. and HERON, S. D. Jr. (1989). Outer Banks Depositional Systems, North Carolina. Field Trip Guidebook T171, 28th International Geological Congress.

MOSLOW, T. F. and TYE, R. S. (1985). Recognition and characterization of Holocene tidal inlet sequences. *Marine Geology,* 63; 129-151.

MOTHERSILL, J. S. (1968). Environments of deposition of the Halfway Formation, Milligan Creek area, British Columbia. *Bulletin of Canadian Petroleum Geology,* 16; 180-199.

MOUNT, J. F. (1982). Storm-surge-ebb origin of hummocky cross-stratified units of the Andrews Mountain Member, Campito Formation (Lower Cambrian), White-Inyo Mountains, Eastern California. *Journal of Sedimentary Petrology,* 52; 941-958.

MUNROE, H. D. (1991). Depositional models for the Doig Formation of northeastern British Columbia (abstract). *Bulletin of Canadian Petroleum Geology,* 39; 220.

MUNROE, H. D. and MOSLOW, T. F. (1990). Reservoir quality and architecture of tidal inlet sandstones, Halfway Formation, northeastern British Columbia. Abstracts, Canadian Society of Petroleum Geologists Convention, Calgary, Alberta, 1990. *Bulletin of Canadian Petroleum Geology,* 38; 174.

MUZA, J. P. and WISE, S. W. (1983). An authigenic gypsum, pyrite and glauconite association in a Miocene deep sea biogenic ooze from the Falkland Plateau, southwest Atlantic Ocea. *Initial Reports of the Deep Sea Drilling Project, 71 (Pt. 1).* Washington (U.S. Government Printing Office). 361-375.

NUMMEDAL, D., OERTEL, G. F., HUBBARD, D. K. and HINE, A. C. (1977). Tidal inlet variability-Cape Hatteras to Cape Canaveral. *Proc. Conf. on Coastal Sediments '77,* A.S.C.E., Charleston, South Carolina, pp. 543-562.

NUMMEDAL, D. and SWIFT, D. J. P. (1987). Transgressive stratigraphy at sequence-bounding unconformities: some principles derived from Holocene and Cretaceous examples. In: Nummedal, D., Pilkey, O. H., and Howard, J. D. (Eds.), *Sea Level fluctuations and coastal evolution.* Society of Economic Paleontologists and Mineralogists Special Publication No. 41. p. 241-260.

O'CONNELL, S. C., DIX, G. R. and BARCLAY, J. E. (1990). The origin, history, and regional structural development of the Peace River Arch, Western Canada. *Bulletin of Canadian Petroleum Geology,* 38A, 4-25.

OERTEL, G. F. (1973). Examination of textures and structures of mud in layered sediments at the entrance of a Georgia tidal inlet. *Journal of Sedimentary Petrology,* 43; 33-41.

OERTEL, G. F. (1977). Geomorphic cycles in ebb deltas and related patterns of shore erosion and accretion. *Journal of Sedimentary Petrology,* 47; 1121-1131.

OERTEL, G. F. (1985). The barrier island system. *Marine Geology,* 63; 1-18.

PAIJMANS, K, BLAKE, D. H., BLEEKER, P. and McALPINE, J. R. (1971). Land resources of the Marchead-Kiunga area, Territory of Papua New Guinea. *CSIRP Australia Land Resource Series*, **29**, 124pp.

PARK, R. (1976). A note on the significance of lamination in stromatolites. *Sedimentology*, **23**; 379-393.

PARK, W. C. and SCHOT, E. H. (1968). Stylolites: Their nature and origin. *Journal of Sedimentary Petrology*, **38**; 175-191.

PELLETIER, B. R. (1962). Triassic stratigraphy of the Rocky Mountains and Foothills, Peace River District, British Columbia. *Geological Survey of Canada Paper* **62-26**.

PELLETIER, B. R. (1965). Paleocurrents in the Triassic of northeastern British Columbia. *In:* Middleton, G.V. (Ed.). *Primary sedimentary structures and their hydrodynamic interpretation.* Society of Economic Paleontologists and Mineralogists Special Publication No. 12. 233-245.

PETTIJOHN, F. J. (1957). "Harper Row, New York, N. Y. 2nd. ed., 718pp.

PIERCE, J. W. (1970). Tidal inlets and washover fans. *Journal of Geology*, **78**; 230-234.

PODRUSKI, J. A., BARCLAY, J. E., HAMBLIN, A. P., LEE, P. J., OSADETZ, K. G., PROCTER, R. M. and TAYLOR, G. C. (1988). Conventional oil resources of Western Canada (light and medium). *Geological Survey of Canada Paper 87-26.*

POSTMA, H., (1967). Sediment transport and sedimentation in the estuarine environment. *In:* Lauff, G. H., (Ed.), *Estuaries*. American Association of Advanced Scientific Publications, 83; 158-179.

POWERS, M. C. and KINSMAN, B. (1953). Shell accummulations in underwater sediments and their relation to the thickness of the traction zone. *Journal of Sedimentary Petrology*, **23**; 229-234.

PSUTY, N. P. (1966). The geomorphology of beach ridges in Tabasco, Mexico. Coastal Studies Institute, Louisiana State University, Technical Report, 30.

RAMPINO, M. R. and SANDERS, J. E. (1981). Evolution of barrier islands of southern Long Island, New York. *Sedimentology,* **28**; 37-48.

REDDERING, J. S. V. (1983). An inlet sequence produced by migration of a small microtidal inlet against longshore drift: the Keurbooms Inlet, South Africa. *Sedimentology,* **30**; 201-218.

REINECK, H. E. and SINGH, I. B. (1972). Genesis of laminated sand and graded rhythmites in storm-sand layers of shelf mud. *Sedimentology,* **18**; 123-128.

REINECK, H. E. and SINGH, I. B. (1973). *Depositional Sedimentary Environments-with Reference to Terrigenous Clastics,* 439 pp. Springer-Verlag, Berlin.

RIDER, M. H. (1986). *The geological interpretation of well logs.* Blackie, London. 175pp.

RIEDIGER, C. L., BROOKS, P. W., FOWLER, M. G. and SNOWDON, L. R. (1990). Lower and Middle Triassic source rocks, thermal maturation, and oil-source rock correlations in the Peace River Embayment area, Alberta and British Columbia. *Bulletin of Canadian Petroleum Geology,* **38A**; 218-236.

ROGAN, A. D. and SMITH, B. R. (1965). Waterflood Pressure Maintenance of the Peejay Field-British Columbia. *The Journal of Canadian Petroleum Geology,* **4**; 36-41.

SANDERS, J. E. and KUMAR, N. (1975a). Evidence of shoreline retreat and in-place "drowning" during Holocene submergence of barriers, Shelf off Fire Island, New York. *Geological Society of America Bulletin,* **86**; 65-76.

SANDERS, J. E. and KUMAR, N. (1975b). Holocene shoestring sand on inner continental shelf off Long Island, New York. *American Association of Petroleum Geologists Bulletin,* **59**; 997-1009.

SCHMIDT, V. and McDONALD, (1983). *Secondary Reservoir Porosity in the Course of Sandstone Diagenesis.* American Association of Petroleum Geologists Education Course Note Series No. 12. 125p.

SELWYN, A. R. C. (1871). Journal and report of preliminary explorations in British Columbia, Geological Survey of Canada, Report Programme for 1871-72, 16-72.

SEXTON, W. J. and MOSLOW, T. F. (1981). Effects of hurricane David, 1979, on the beaches of Seabrook Island, South Carolina. *Northeastern Geology,* 3; 297-305.

SHA, L. P. (1989). Variation in ebb-delta morphologies along the west and east Frisian Islands, The Netherlands and Germany. *Marine Geology,* 89; 11-28.

SHA, L. P. (1989). Holocene-Pleistocene inteface and three-dimensional geometry of the ebb-delta complex, Texel Inlet, The Netherlands. *Marine Geology,* 89; 207-228.

SHA, L. P. (1990). Surface sediments and sequence models in the ebb-tidal delta of Texel Inlet, Wadden Sea, The Netherlands. *Sedimentary Geology,* 68; 125-141.

SHARMA, G. D. (1969). Paragenetic evolution in Peejay Field, British Columbia, Canada. *Mineral. Deposita (Berl.),* 4; 346-354.

SHEARMAN, D. J. (1966). Origin of marine evaporites by diagenesis. *Transactions Institute of Mining and Metalurgy,* 75; 208-215

SHELDON, P. (1980). Episodicity of phosphate deposition and deep ocean circulation-a hypothesis. *In:* Bentor, Y. K. (Ed.). *Marine Phosphorites,* pp. 239-247. Special Publication Society of Economic Paleontologists and Mineralogists, 29, Tulsa.

SHEPARD, F. P. (1960). Gulf coast barriers. *In:* Shepard, F. P., Phleger, F. B. and van Andel, Tj. H. (Eds.). *Recent Sediments, Northwest Gulf of Mexico.* pp. 197-220. American Association of Petroleum Geologists, Tulsa.

SIEMERS, C. T. and TILLMAN, R. W. (1981). Recommendations for the proper handling of cores and sedimentological analysis of core sequences. *In:* Siemers, C. T., Tillman, R. W. and Williamson, C. R. (Eds.). *Deep-water clastic sediments:* A core workshop: Society of Paleontologists and Mineralogists Core Workshop No. 2, 1981, 20-44.

SIESSER, W. G. and ROGERS, J. (1976). Authigenic pyrite and gypsum in South West African continental slope sediments. *Sedimentology,* **23**; 567-577.

SNEDDEN, J. W., NUMMEDAL, D. and AMOS, A. F. (1988). Storm- and fair-weather combined flow on the central Texas continental shelf. *Journal of Sedimentary Petrology,* **58**; 580-595.

SOUTHARD, J. B., LAMBIE, J. M., FEDERICO, D. C., PILE, H. T. and WEIDMAN, C. R. (1990). Experiments on bed configurations in fine sands under bidirectional purely oscillatory flow, and the origin of hummocky cross-stratification. *Journal of Sedimentary Petrology,* **60**, 1-17.

STEELE, G. A. (1980). Stratigraphy and depositional history of Bogue Banks, North Carolina. M. Sc. Thesis, Duke University, Durham, N. C., 201p.

SURDAM, R. C. and WOLFBAUER, C. A. (1975). Green River Formation, Wyoming: A playa-lake complex. *Geological Society of America Bulletin,* **86**; 335-345.

SUSMAN, K. R. and HERON, S. D. Jr. (1979). Evolution of a barrier island, Shackleford Banks, Carteret County, North Carolina, *Geological Society of America Bulletin,* **90**; 205-215.

SWIFT, D. J. P., FIGUEIREDO, A. G. Jr., FREELAND, G. L. and OERTEL, G.F. (1983). Hummocky cross-stratification and megaripples: A geological double standard? *Journal of Sedimentary Petrology,* **53**; 1295-1317.

SWIFT, D. J. P. and NUMMEDAL, D. (1987). Hummocky cross-stratification, tropical hurricanes, and intense winter storms-Discussion. *Sedimentology*, **34**; 338-344.

THOM, B. G. (1964). Origin of sand beach ridges. *Australian Journal of Science*, **26**; 351.

TORRIE, J. E. (1973). Northeastern British Columbia. *In:* McCrossan, R. G. (Ed.), *The Future Petroleum Provinces of Canada.* Canadian Society of Petroleum Geologists Memoir 1, 151-186.

TOZER, E. T. (1961). The sequence of marine Triassic faunas in western Canada. *Geological Survey of Canada* Paper **61-6**; 1-20.

TOZER, E. T. (1967). A standard for Triassic time. *Geological Survey of Canada Bulletin* **156**.

TOZER, E. T. (1982). Marine Triassic faunas of North America: Their significance for assessing plate and terrane movements.*Geologische Rundschau*, **71** (3); 1077-1104.

TUCKER, M. E. (1991). *Sedimentary Petrology.* Blackwell Scientific Publications. 260 pp.

TYE, R. S. (1984). Geomorphic evolution and stratigraphy of Price and Capers Inlets, South Carolina. *Sedimentology*, **31**; 655-674.

TYE, R. S. and MOSLOW, T. F. (*In Press*, 1992). Chapter 4. Tidal inlet reservoirs: insights from modern examples. *In:* Rhodes, E. G. and Moslow, T. F. (Eds.). *Marine Clastic Reservoirs: Examples and Analogues.* Springer-Verlag, New York.

UHLIR, D. M., AKERS A. and VONDRA, C. F. (1987). Tidal inlet sequence, Sundance Formation (Upper Jurssic), north-central Wyoming. *Sedimentology*, **35**; 739-752.

Van STRAATEN, L. M. J. U. (1965). Composition of shell beds formed in tidal flat environment in The Netherlands and in the Bay of Arcachon (France). *Geologie en Mijnbouw*, **18**; 209-226.

Van WAGONER, J. C., MITCHUM, R. M. CAMPION, K. M. and RAHMANIAN, V. D. (1990). Siliciclastic sequence stratigraphy in well logs, cores, and outcrops. *American Association of Petroleum Geologists Methods in Exploration Series,* No. 7. Tulsa, Oklahoma, 55p.

WALKER, R. G. (1979). Shallow Marine Sands. *In:* Walker, H. G. (Ed.). *Facies Models.* Geoscience Canada, Reprint Series 1. pp 75-89. Kitchener, Ontario, Ainsworth Press.

WALKER, R. G., DUKE, W. L. and LECKIE, D. A. (1983). Hummocky stratification: significance of its variable bedding sequences: discussion. *Geological Society of America Bulletin,* **94**; 1245-1249.

WALKER, T.R. (1967). Formation of red beds in ancient and modern deserts. *Geological Society of America Bulletin,* **78**; 353-368.

WARREN, J. K. (1982). The hydrological significance of Holocene teepees, stromatolites and boxwork limestones in coastal salinas in South Australia*Journal of Sedimentary Petrology,* **52**; 1`171-1201.

WHITTEN, D. G. A. and BROOKS, R. V. (1985). *Dictionary of Geology.* Penguin Reference Books, 495p.

WILLIS, A. J. (1992). Sedimentology and stratigraphic framework of the Middle Triassic Halfway Formation, Wembley oilfield, Alberta. Unpublished M. Sc. Thesis, University of Alberta, Edmonton, Canada. 219p.

WITTENBERG, J. (1992). Origin and stratigraphic significance of anomalouly thick sandstone trends in the Middle Triassic Doig Formation of west-central Alberta. Unpublished M. Sc. Thesis, University of Alberta, Edmonton, Canada. 290p.

WITTENBERG, J and MOSLOW, T. F. (1991). Origin and facies variability of overthickened sandstones in the Middle Triassic Doig Formation, west-central Alberta (abstract). *Bulletin of Canadian Petroleum Geology,* **39**; 228.

APPENDIX

APPENDIX A.

Appendix A contains Middle Triassic Halfway cores described from the study area.

WELL NAME: SINCLAIR PACIFIC LYNX
FORMATION: HALFWAY-CHARLIE LAKE
DATE: 2/08/90
LOCATION: d-066-A/94-A-15
CORE INTERVAL:
KB: 2382.5ft

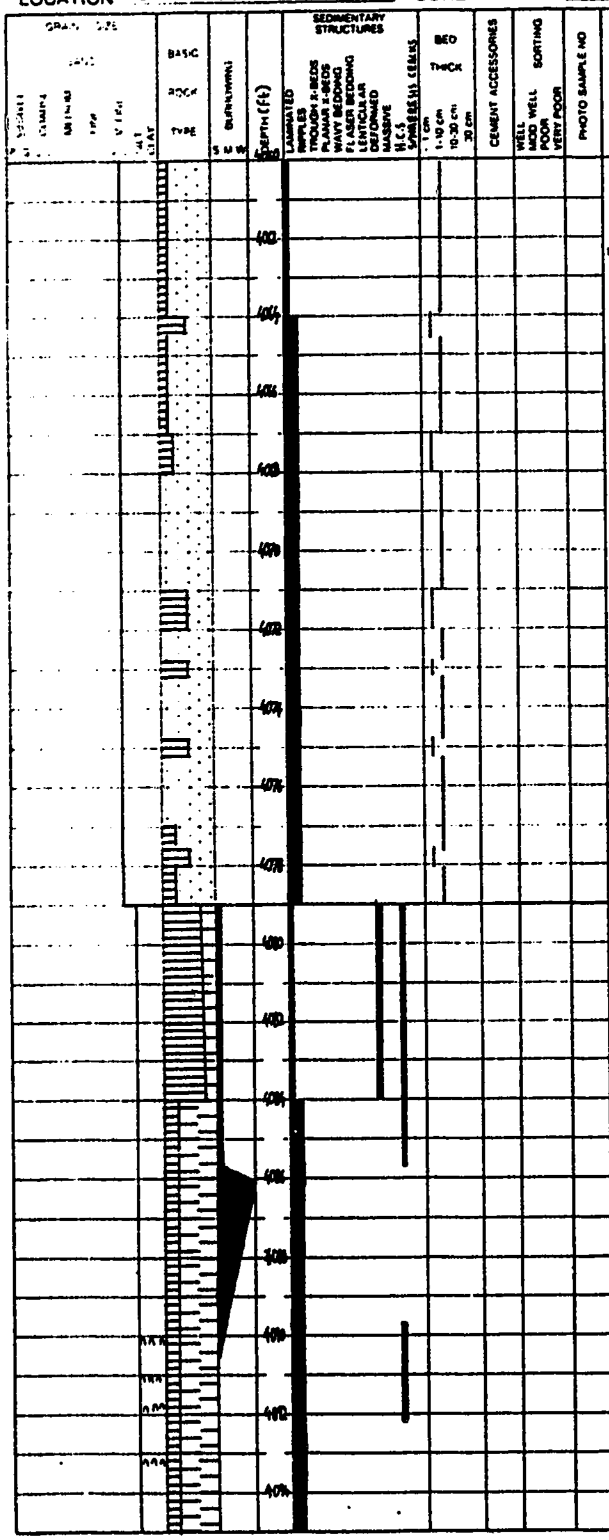

COMMENTS

lam. disrupted by some vertical burrows.

well-sorted, sub-angular oil-stained and good intergranular φ. pyrite & dol. cem.

beige-brown dol-cem. sh & dol. cem. brown sst, loaded. Shale is Planolites burrowed wavy-laminated

slst. lam. have abrupt bases loaded & have convolute lam. passing up into parallel-lam. slst. & sh. → sh.

Planolites burrows appear as shells disappear

H.C.S. in slst.
shells in layers have calc. rods projecting up above surface, punctate brachiopods.
shells are delicate & abraded, but commonly ribbed.
sh. is dk. grey to blk

FACIES/DEP. ENVIRONMENT

F1 LOWER SHOREFACE

C OFFSHORE-TRANSITION

WELL NAME: SINCLAIR PACIFIC LYNX
FORMATION: HALFWAY-CHARLIE LAKE
DATE: 2/08/90
LOCATION: d-066-A/94-A-15
CORE INTERVAL:
KB: 2382.5ft

GRAIN SIZE SAND GRAVEL, COARSE, MEDIUM, FINE, V FINE, SILT CLAY P G U L U L U L U L	BASIC ROCK TYPE	BURROWING S M W	DEPTH (ft)	SEDIMENTARY STRUCTURES LAMINATED RIPPLED TROUGH X-BEDS PLANAR X-BEDS WAVY BEDDING FLASER BEDDING LENTICULAR DEFORMED MASSIVE	BED THICK < 1 cm 1-10 cm 10-30 cm 30 cm	CEMENT/ACCESSORIES	SORTING WELL MOD WELL POOR VERY POOR	PHOTO/SAMPLE NO	COMMENTS	FACIES DEP ENVIRONMENT
									dol. cem. beige sh & dol. cem. brown slt pyrite & anhydrite nods	33
			1056							
									layer of pyrite overlies stromatolites	31
			1058							32
										31

PLAYA LAKE MARGINAL MUDFLATS

WELL NAME: PACIFIC SINCLAIR NANCY FORMATION: HALFWAY-CHARLIE LAKE DATE: 14/08/90

LOCATION: d-A84-A/94-A-15 CORE INTERVAL: KB: 2394.3ft

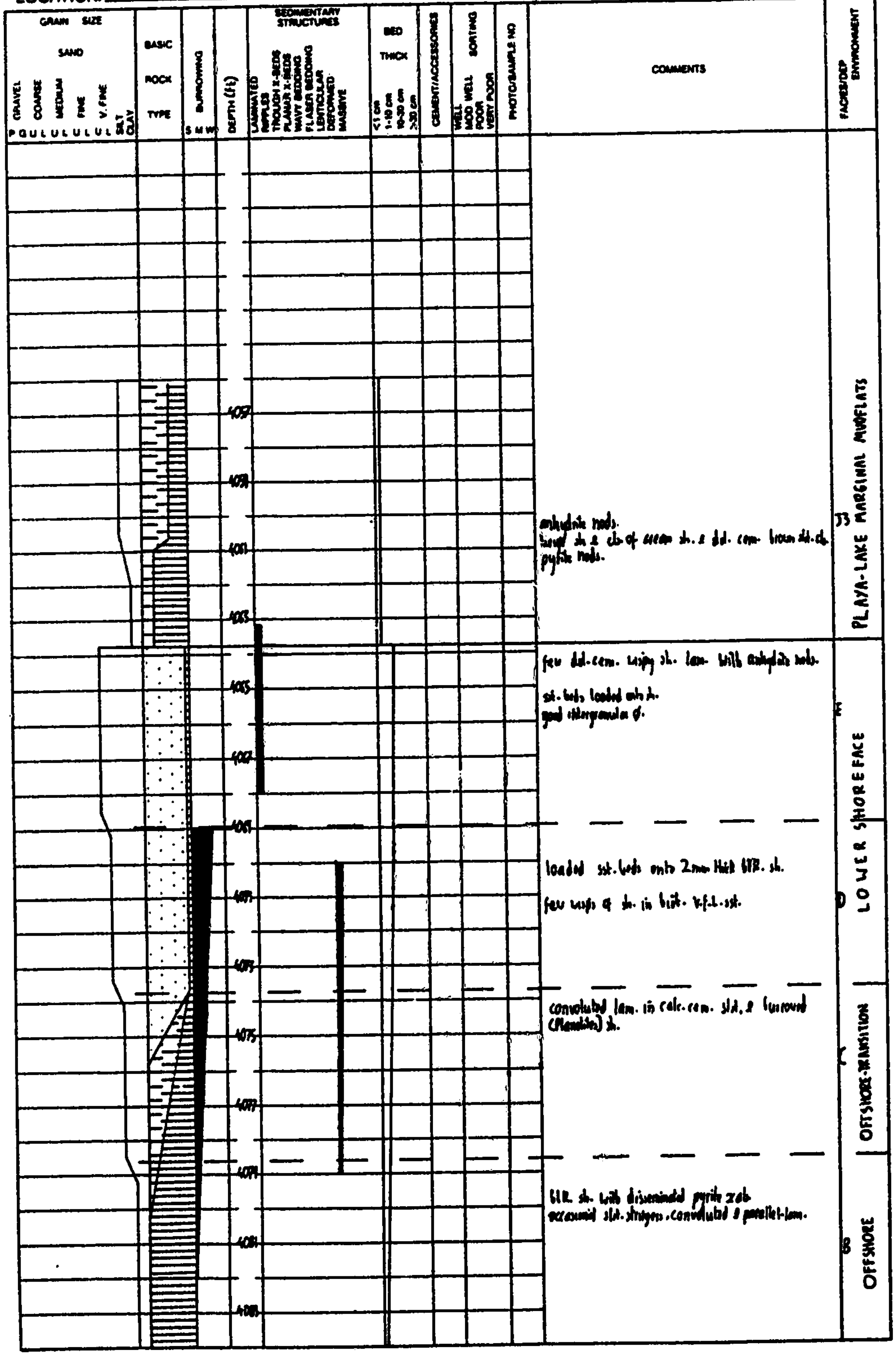

anhydrite nods.
[illegible] sh. & cls of green sh. & dol. cem. brown slt.-st.
pyrite nods.

few dol.-cem. wispy sh. lam. with anhydrite nods.

sst. beds loaded onto sh.
good intergranular ϕ.

loaded sst. beds onto 2mm thick blk. sh.

few wisps of sh. in biot. v.f.-l. sst.

convoluted lam. in calc.-cem. sltst. & burrowed (Planolites) sh.

blk. sh. with disseminated pyrite xals.
occasional slt. stringers. convoluted & parallel-lam.

WELL NAME: SINCLAIR PACIFIC MINK

FORMATION: HALFWAY-CHARLIE LAKE

DATE: 1/08/90

LOCATION: d-088-A/94-A-15

CORE INTERVAL:

KB: 2372 G.L.

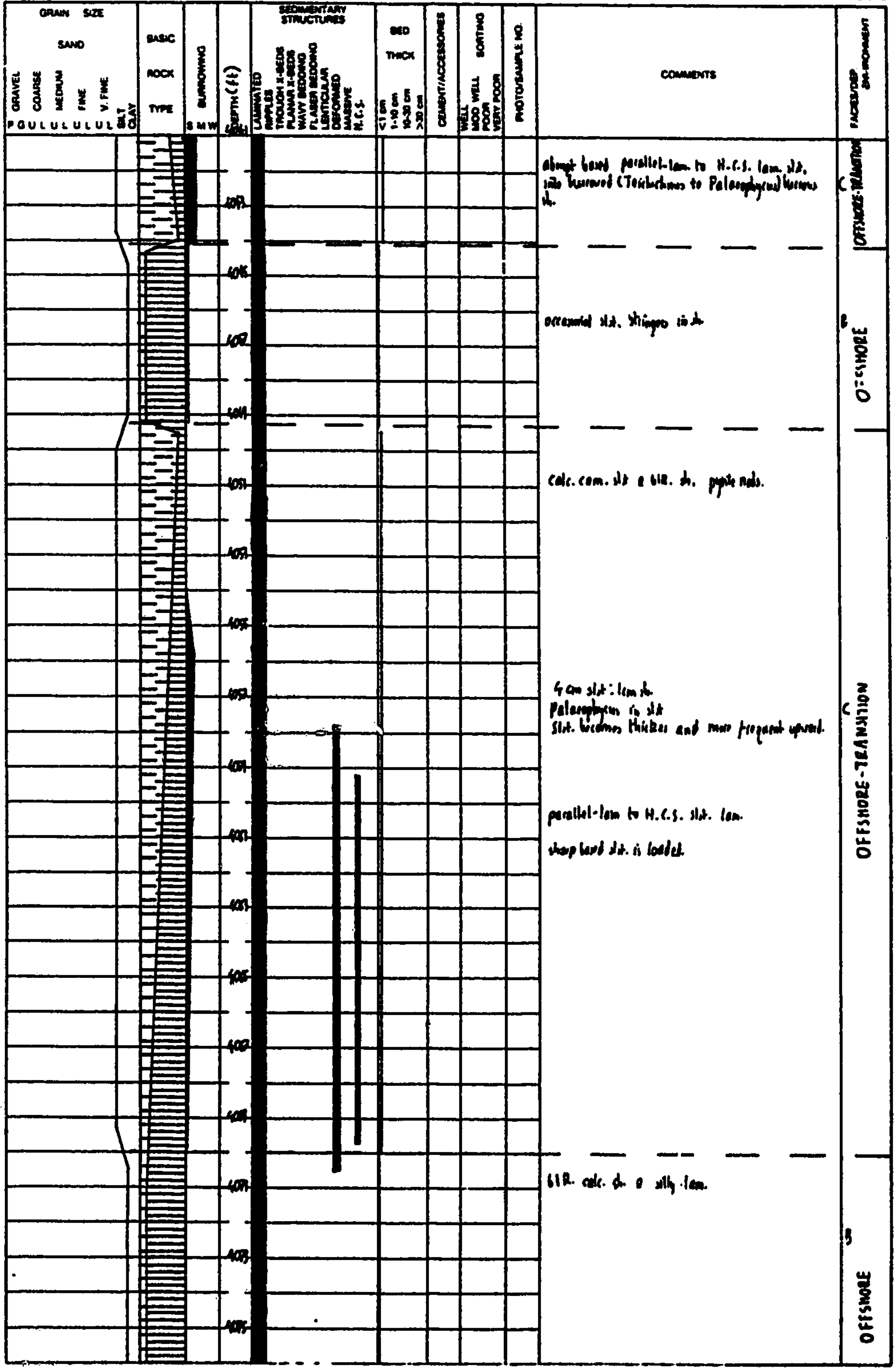

abrupt base parallel-lam. to H.C.S. lam. slt. sdo burrowed (Teichichnus to Palaeophycus) burrows sh.

occasional slt. stringers in sh.

calc. cem. slt & blk. sh. pyrite nods.

4 cm slt : lam sh.
Palaeophycus in slt
Slt. becomes thicker and more frequent upward.

parallel-lam to H.C.S. slt. lam.

sharp base slt. is loaded.

blk. calc. sh. & silty lam.

WELL NAME: SINCLAIR PACIFIC MINK FORMATION: HALFWAY-CHARLIE LAKE DATE: [illegible]/08/90

LOCATION: d-088-A/94-A-16 CORE INTERVAL: [illegible] 61 23724

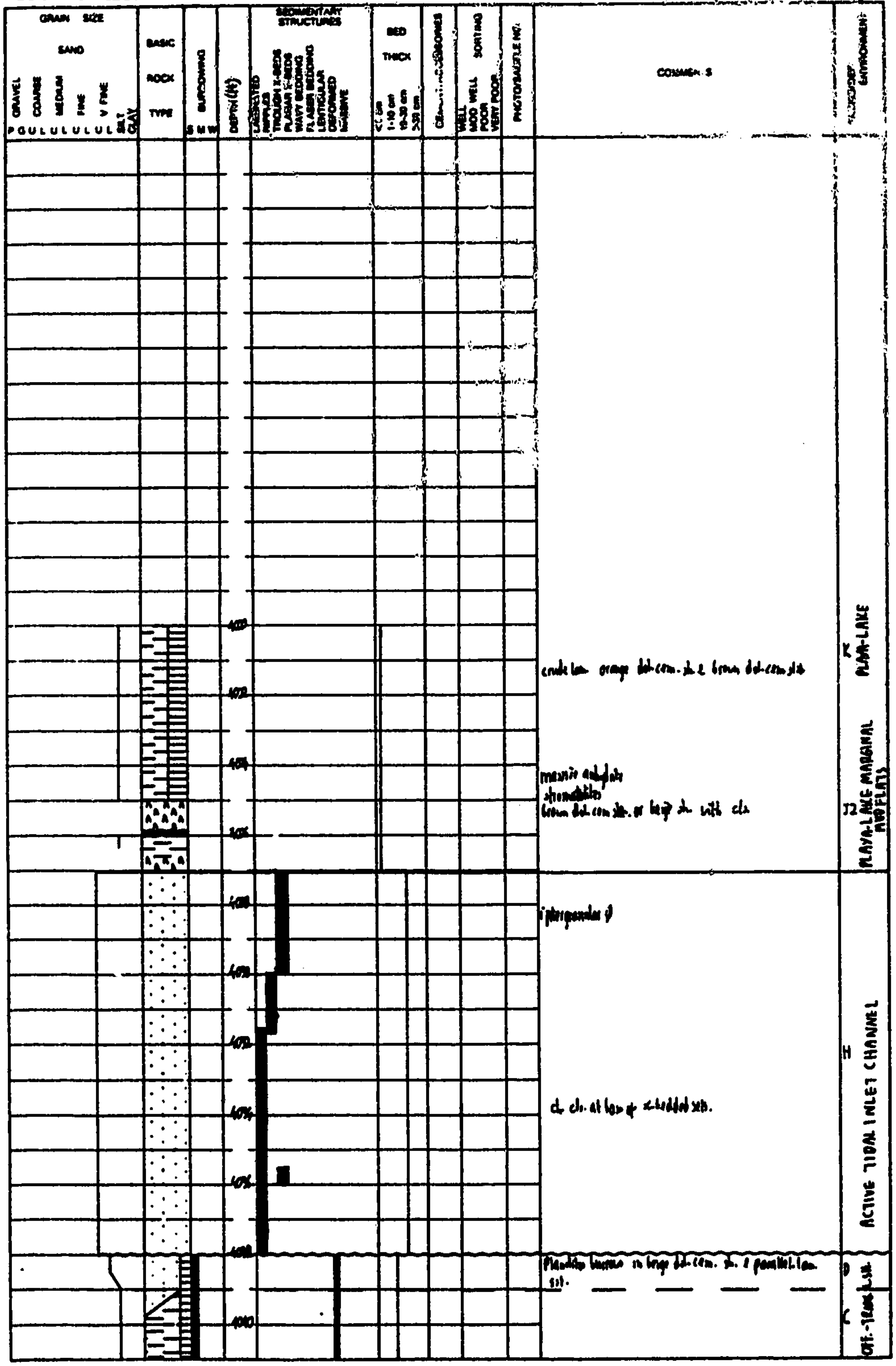

crude lam. orange dol-cem. sh. & brown dol-cem. sh.

massive anhydrite
stromatolites
brown dol.cem. sh. or large sh. with cls

[illegible]

cl. cls. at base of [illegible] sst.

Planolites burrows in large dol.-cem. sh. & parallel lam. sst.

WELL NAME: PACIFIC SINCLAIR PEEJAY d-22-H
FORMATION: HALFWAY-CHARLIE LAKE
DATE: 8/08/90
LOCATION: d-022-H/94-A-15
CORE INTERVAL:
KB: 2370ft

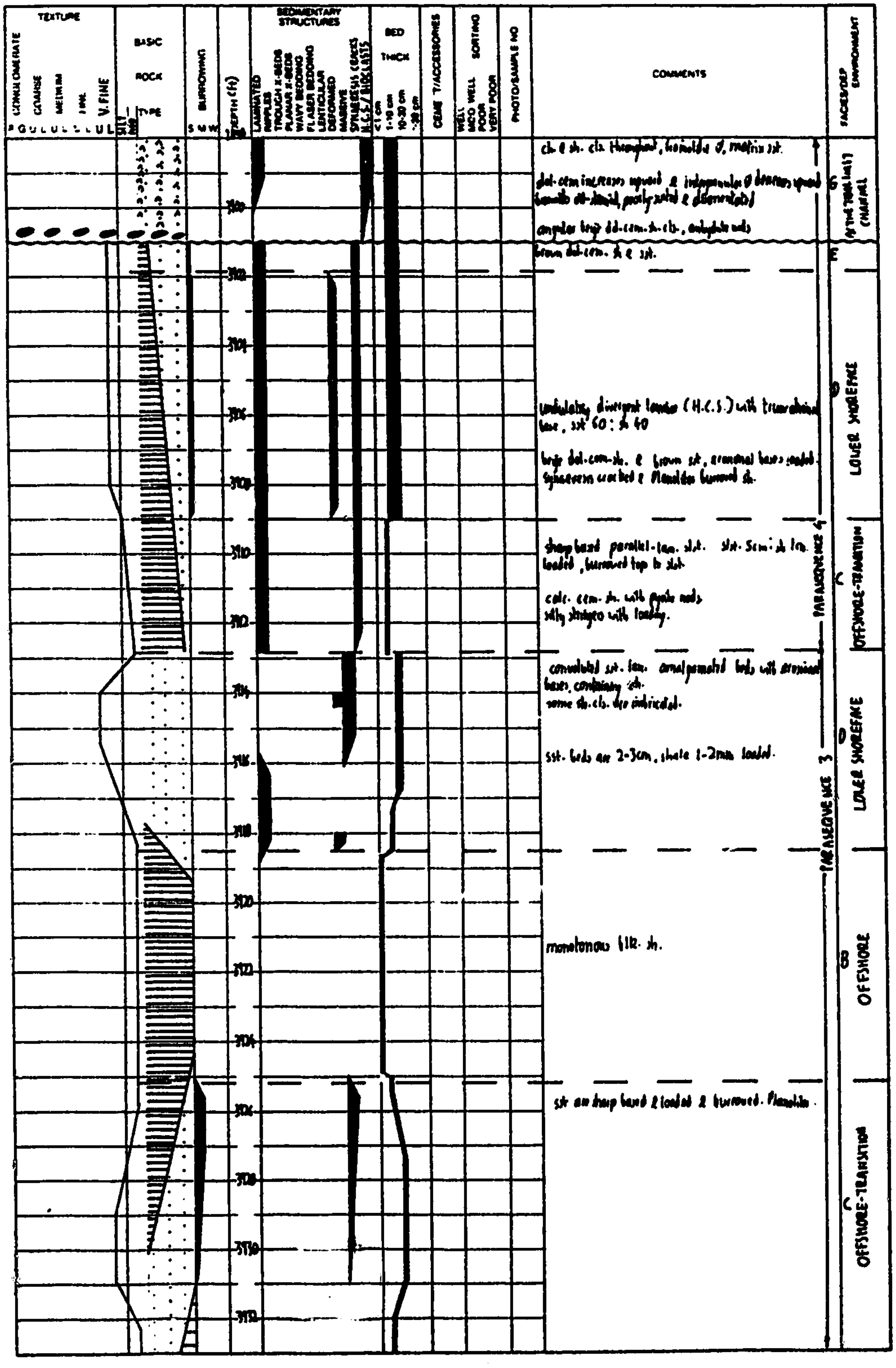

ch. & sh. cls. throughout, homolds of, matrix sst.

dol-cem increases upward & intergranular ..., upward (... poorly sorted & disoriented)

angular large dol-cem. sh. cls., anhydrite nods

brown dol-cem. sh. & sst.

undulating divergent laminae (H.C.S.) with truncational base, sst 60 : sh 40

large dol-cem-sh. & brown sst, erosional bases, graded. Syneresis cracked & Planolites burrowed sh.

sharp based parallel-lam. sst. sst. 5cm : sh 1cm. loaded, burrowed top to sst.

calc. cem. sh. with pyrite nods
silty stringers with loading.

convoluted sst. lam. amalgamated beds with erosional bases, containing sh.
some sh. cls. are imbricated.

sst. beds are 2-3cm, shale 1-2mm loaded.

monotonous blk. sh.

sst are sharp based & loaded & burrowed. Planolites.

WELL NAME: PACIFIC SINCLAIR PEEJAY d-22-H

FORMATION: HALFWAY-CHARLIE LAKE

DATE: 8/08/90

LOCATION: d-022-H/94-A-15

CORE INTERVAL:

KB: 2370.7ft

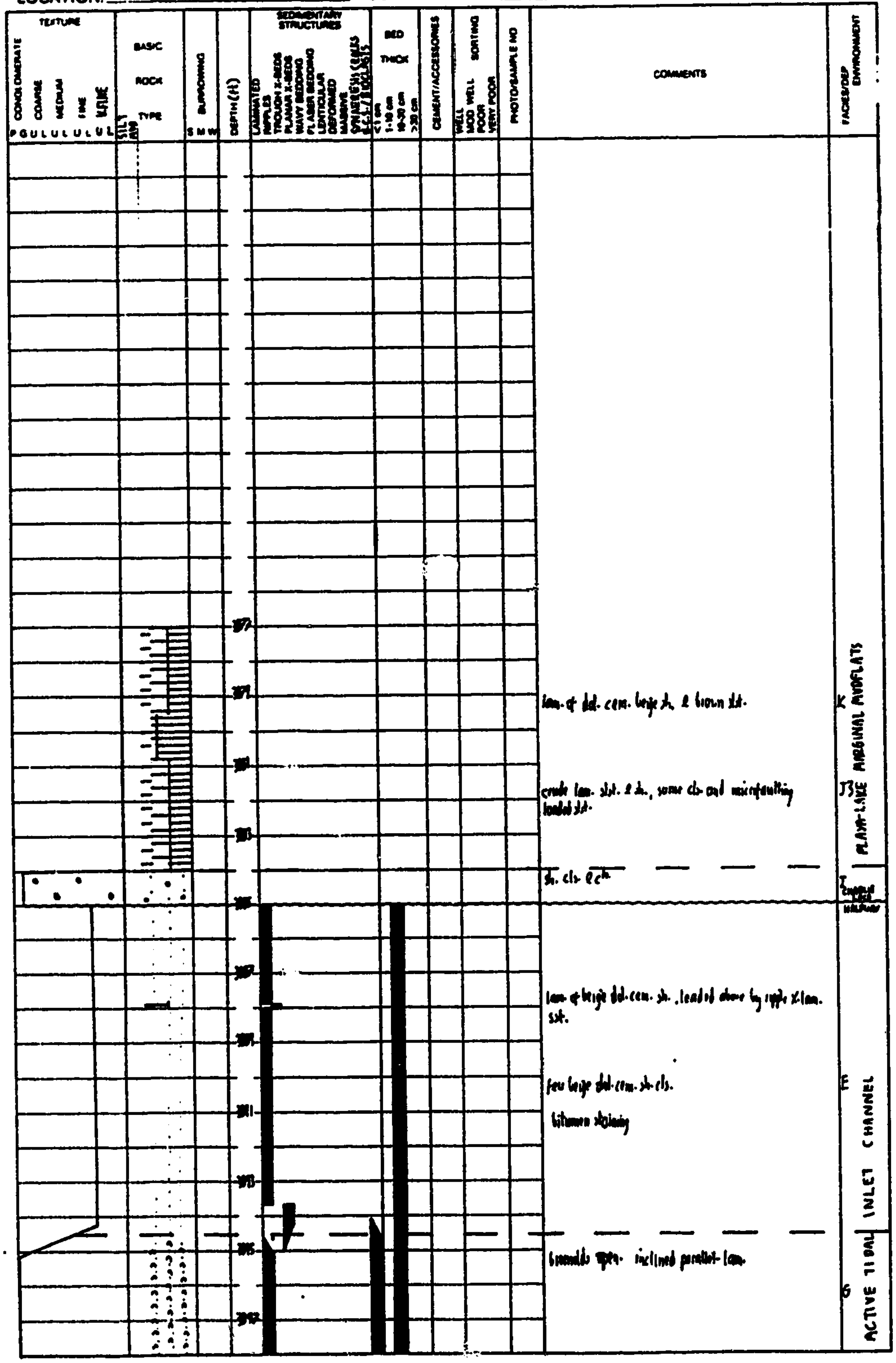

lam. of dol. cem. beige sh. & brown slt.

crude lam. slt. & sh., some cls. and microfaulting loaded slt.

sh. cls. @ c^ts

lam. of beige dol. cem. sh., loaded above by ripple X-lam. sst.

few beige dol. cem. sh. cls.

bitumen staining

bimodal spr. inclined parallel-lam.

WELL NAME: PACIFIC SINCLAIR NANCY d-31-H

FORMATION: HALFWAY-CHARLIE LAKE

DATE: 29/06/90

LOCATION: d-031-H/94-A-15

CORE INTERVAL:

KB: 2372.3ft

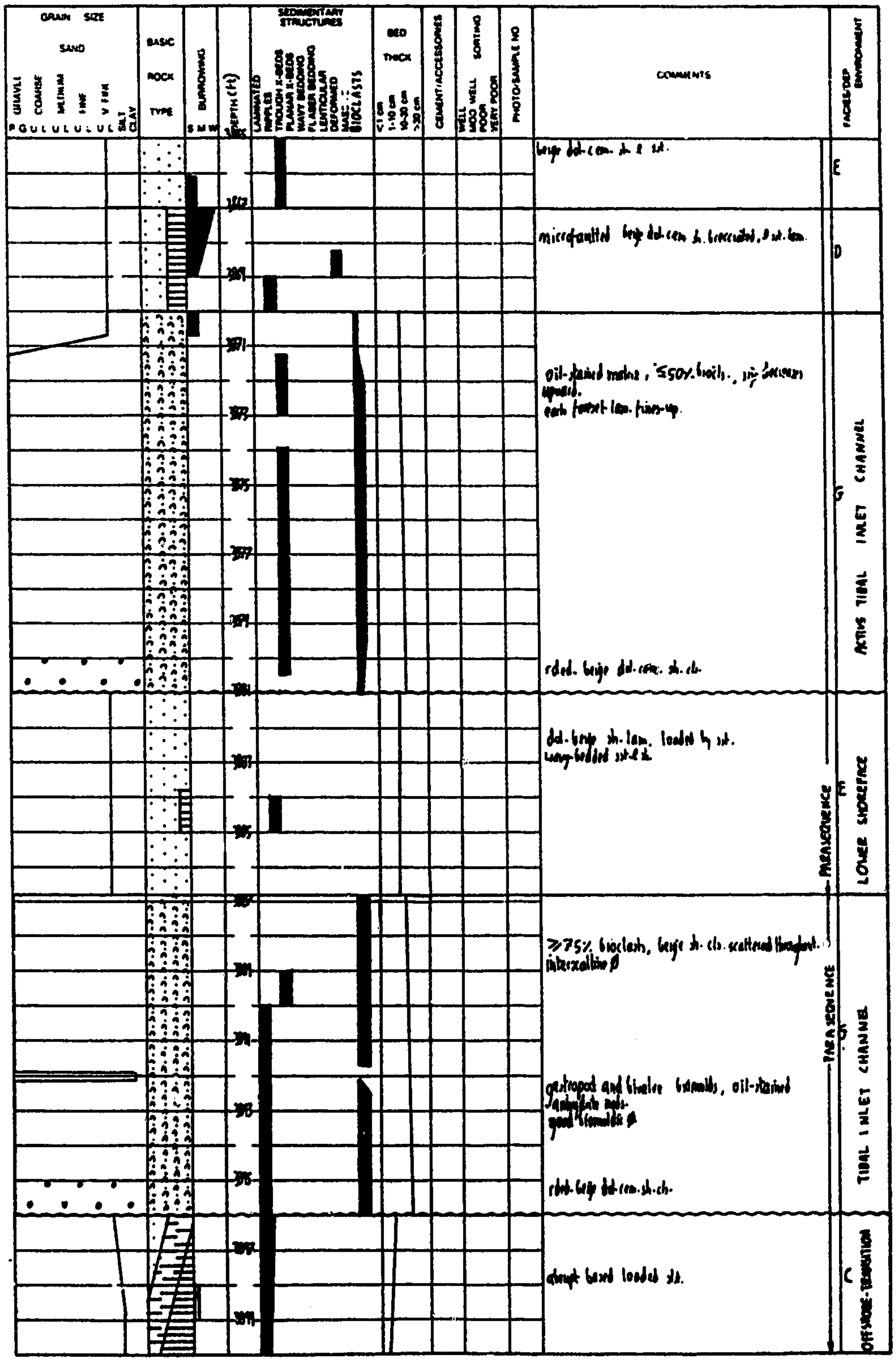

beige dol-cem. sh. & slt.

microfaulted beige dol-cem sh. brecciated, & slt. lam.

oil-stained matrix, ≤50% bioclasts., size decreases upward.
each foreset lam. fines-up.

rdd. beige dol-cem. sh. cl.

dol. beige sh. lam. loaded by slt.
wavy-bedded slt & sh.

≥75% bioclasts, beige sh. cls. scattered throughout.
intercrystalline ∅

gastropod and bivalve biomolds, oil-stained
[illegible] mod-
good biomoldic ∅

rdd. beige dol-cem. sh. ch.

abrupt base loaded slt.

WELL NAME: PACIFIC SINCLAIR NANCY d-31-H FORMATION: HALFWAY-CHARLIE LAKE DATE: 29/06/90

LOCATION: d-031-H/94-A-15 CORE INTERVAL: KB: 2372.3ft

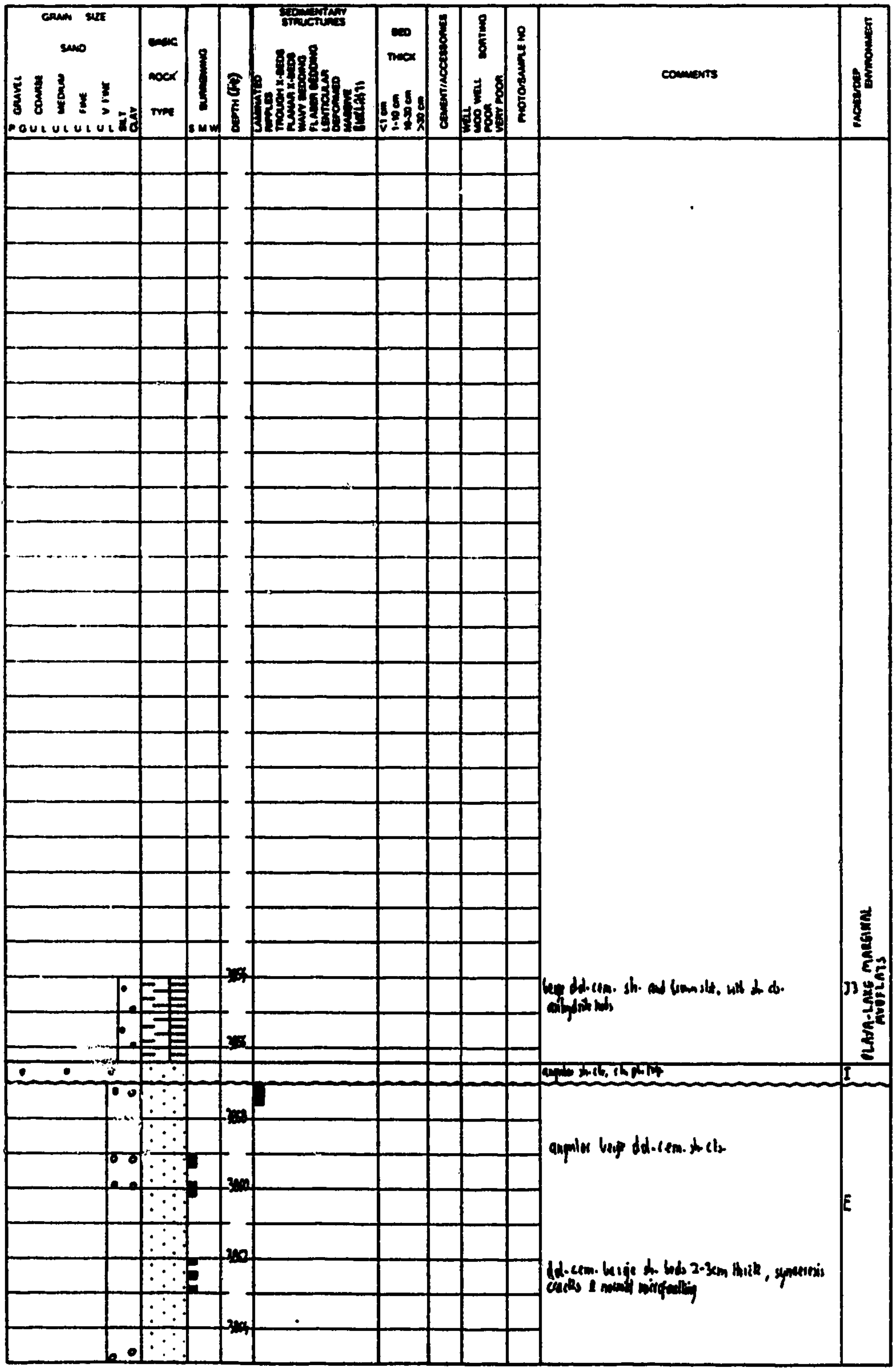

beige dol.-cem. sh. and limeslt. with sh. cls. anhydrite beds

J3 PLAYA-LAKE MARGINAL MUDFLATS

angular sh. cls., ch. pb. lag

I

angular beige dol.-cem. sh. cls.

E

dol.-cem. beige sh. beds 2-3cm thick, syneresis cracks & normal microfaulting

WELL NAME: PACIFIC SINCLAIR NANCY d-33-H FORMATION: HALFWAY-CHARLIE LAKE DATE: 20/07/90

LOCATION: d-033-H/94-A-15 CORE INTERVAL: KB: 2366ft

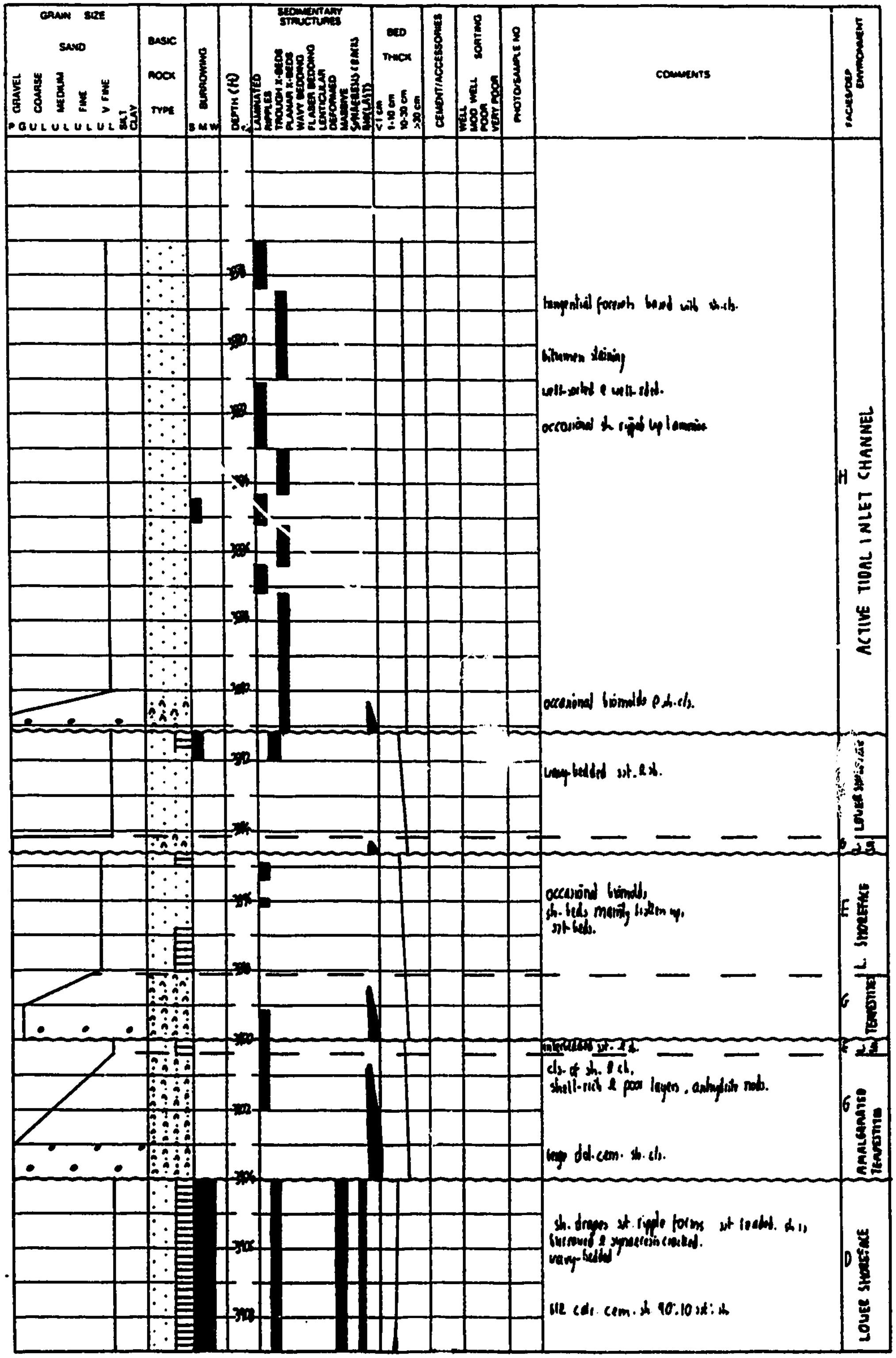

tangential forsets bound with sh.cls.

bitumen staining

well-sorted & well-rdd.

occasional sh. rippled up laminae

occasional bimodal & sh.cls.

wavy-bedded sst. & sh.

occasional bimodal
sh. beds mainly broken up.
sst. beds.

interbedded sst. & sh.

cls. of sh. & cl.
shell-rich & poor layers, anhydrite nods.

large dol.-cem. sh. cls.

sh. drapes sst. ripple forms sst. loaded. sh.
burrowed & synaeresis cracked.
wavy-bedded

[illegible] cem. sh 90:10 sst: sh

WELL NAME PACIFIC SINCLAIR NANCY d-41-H FORMATION: HALFWAY-CHARLIE LAKE DATE: i/02/91

LOCATION: d-041-H/94-A-15 CORE INTERVAL: KB: 2372ft

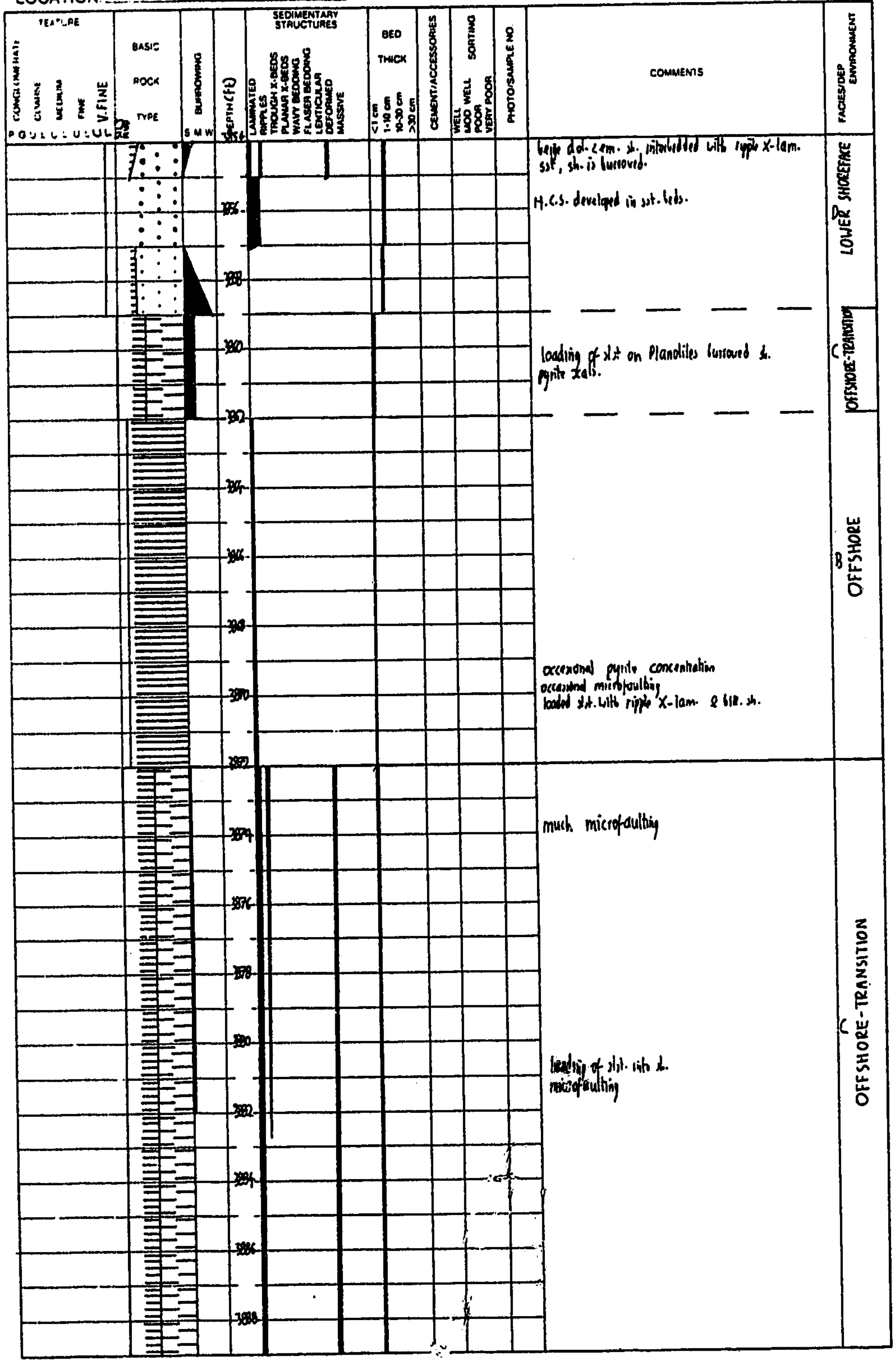

beige dol. cem. sh. interbedded with ripple X-lam. sst, sh. is burrowed.

H.C.S. developed in sst. beds.

loading of slst on Planolites burrowed sh. pyrite xals.

occasional pyrite concentration
occasional microfaulting
loaded slst. with ripple X-lam. & blk. sh.

much microfaulting

loading of slst. into sh.
microfaulting

WELL NAME: PACIFIC SINCLAIR NANCY d-41-H FORMATION: HALFWAY-CHARLIE LAKE DATE: 1/02/91

LOCATION: d-041-H/94-A-15 CORE INTERVAL: KB: 2372 ft

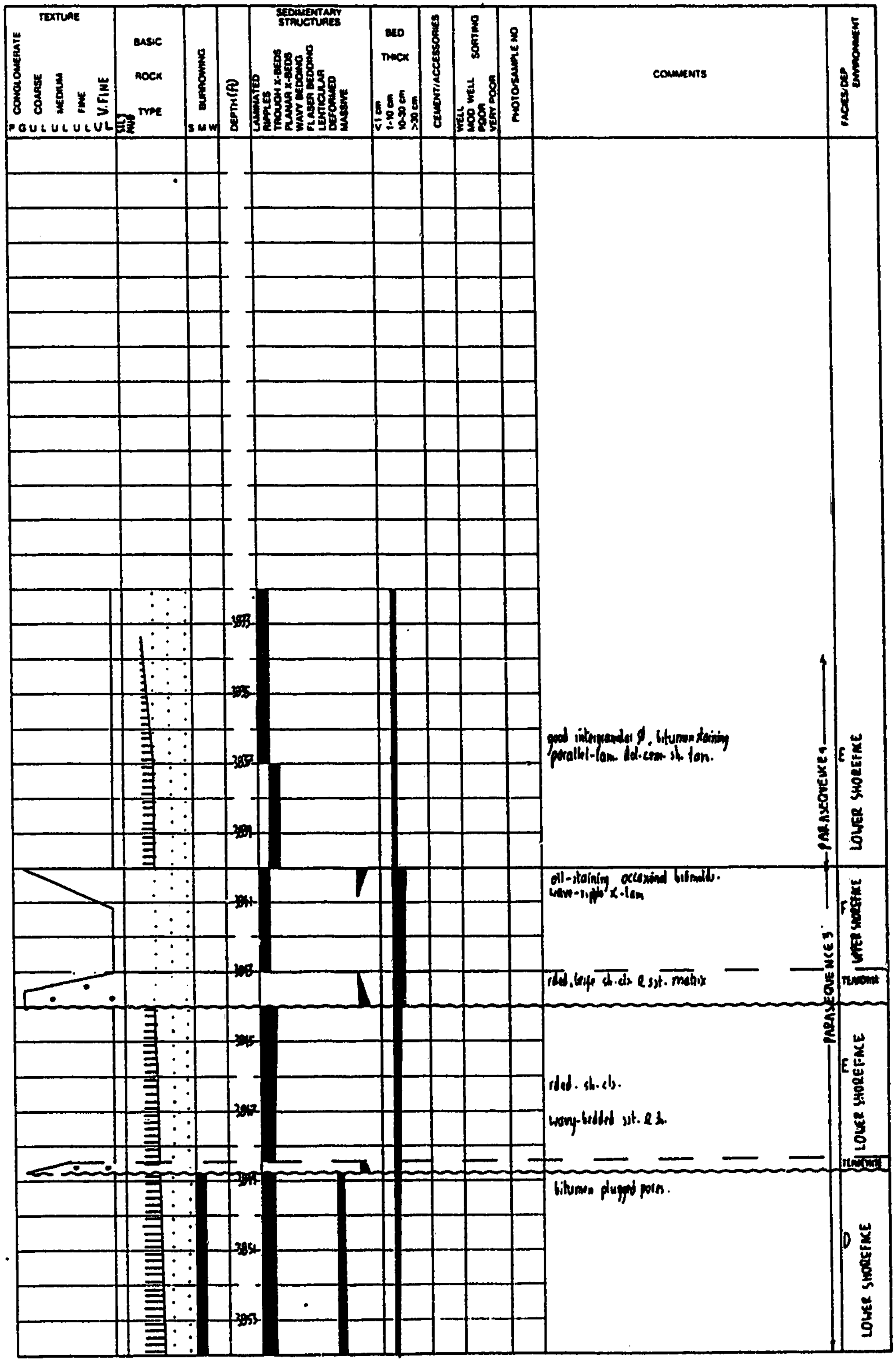

good intergranular ∅, bitumen staining parallel-lam. dol-cem. sh. lam.

oil-staining occasional biomolds. wave-ripple x-lam

rded. large sh. cls & sst. matrix

rded. sh. cls.

wavy-bedded sst. & sh.

bitumen plugged pores.

WELL NAME: PACIFIC SINCLAIR PEEJAY

FORMATION: HALFWAY-CHARLIE LAKE

DATE: 29/06/90

LOCATION: b-042-H/94-A-15

CORE INTERVAL:

KB: 2364ft

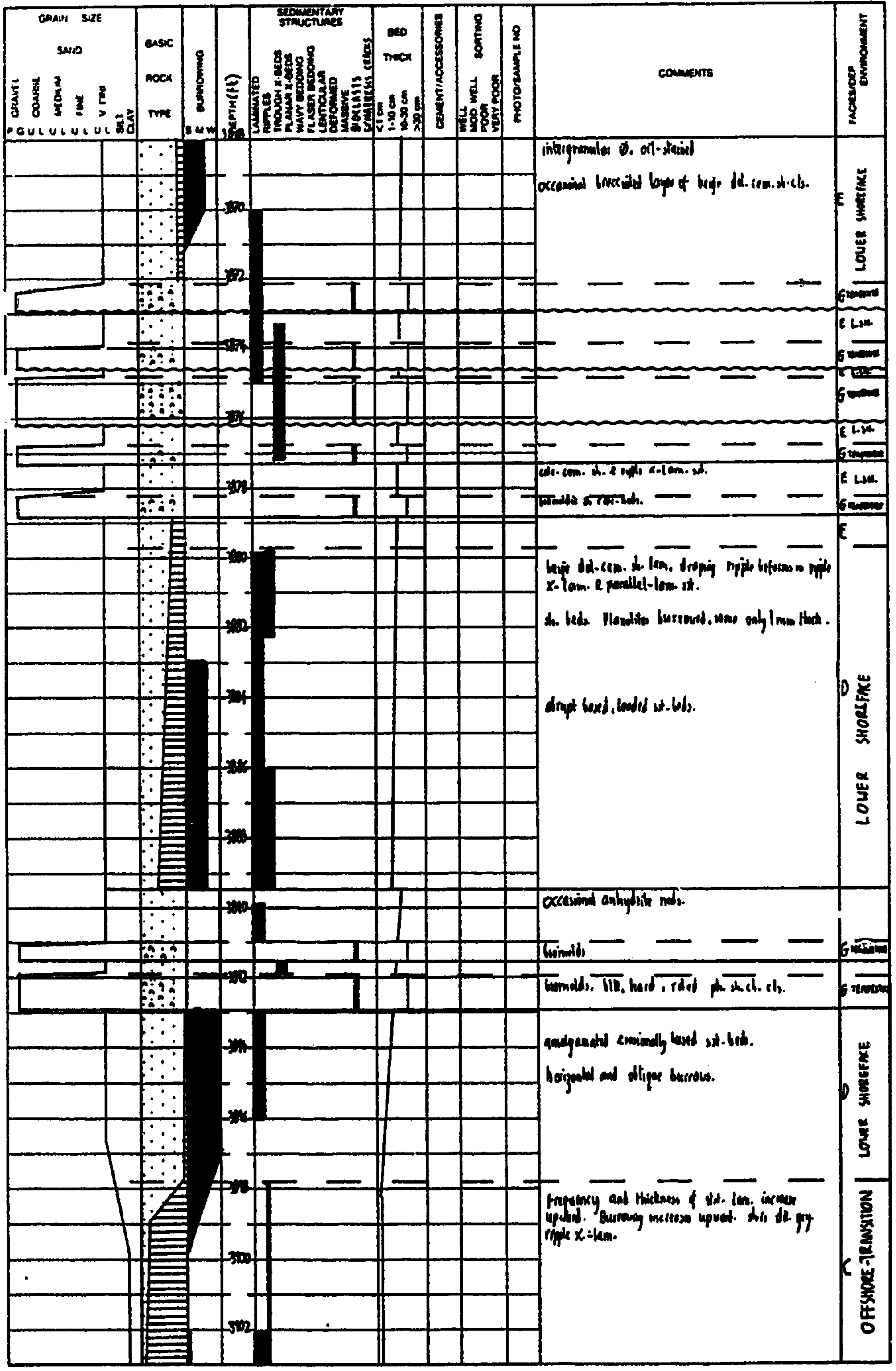

intergranular Ø. oil-stained

occasional brecciated layer of beige dol.cem.sh.cls.

calc-cem. sh. & ripple x-lam. sst.

possible sh. cast-beds.

beige dol-cem. sh. lam, draping ripple bedforms or ripple x-lam. & parallel-lam. sst.

sh. beds. Planolites burrowed, some only 1mm thick.

abrupt based, loaded sst.-beds.

occasional anhydrite nods.

biomolds

biomolds, blk, hard, rdd ph. sh.cl. cls.

amalgamated erosionally based sst.-beds.

horizontal and oblique burrows.

Frequency and thickness of sst. lam. increase upward. Burrowing increase upward. this dk. gry ripple x-lam.

WELL NAME: PACIFIC SINCLAIR PEEJAY FORMATION: HALFWAY-CHARLIE LAKE DATE: 29/06/90

LOCATION: b-042-H/94-A-15 CORE INTERVAL: KB: 2364ft

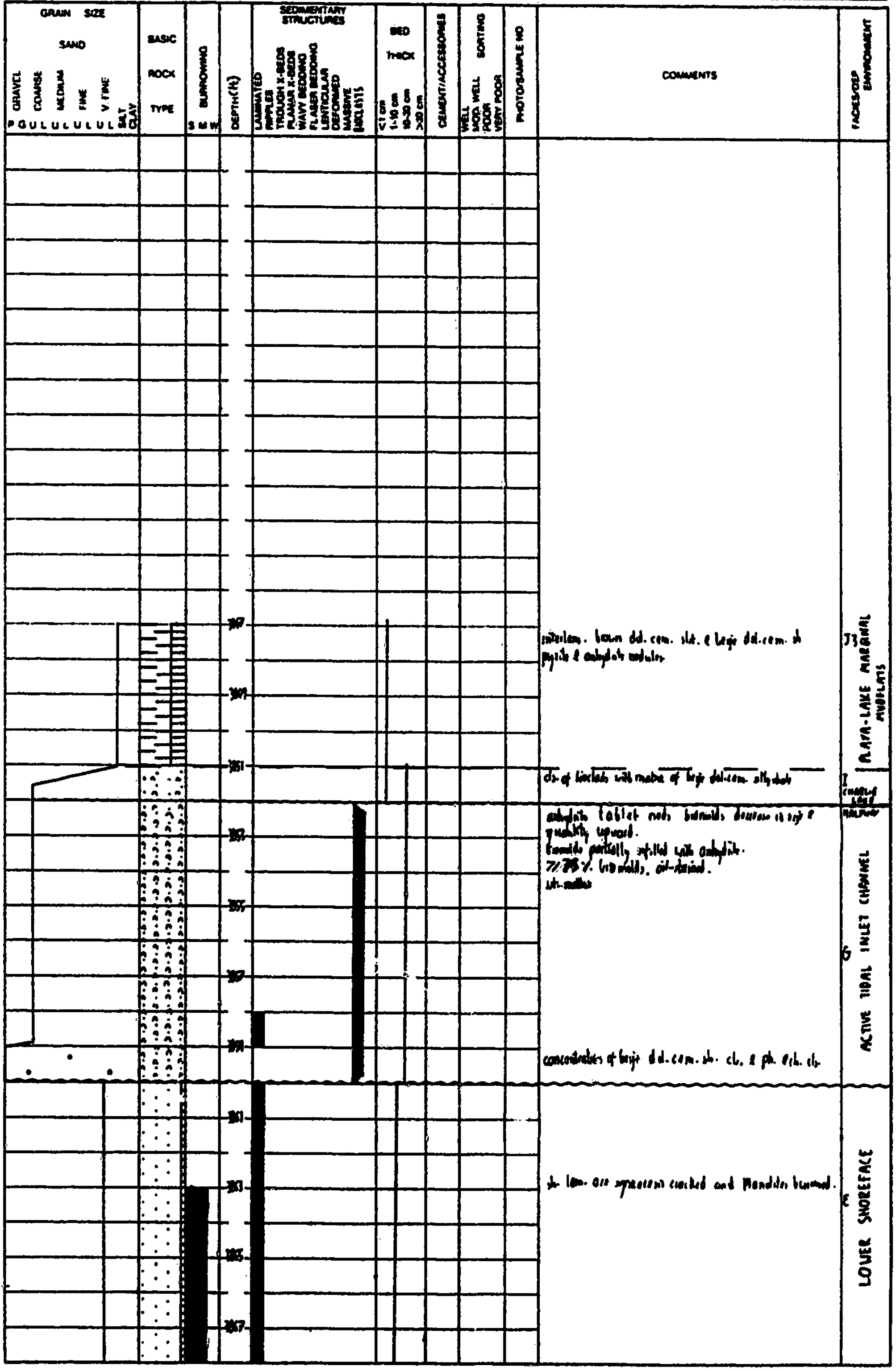

interlam. brown dol.cem. slt. & large dol.cem. sh pyrite & anhydrite nodules

J3 PLAYA-LAKE MARGINAL MUDFLATS

cls. of laminated with matrix of large dol.cem. sltst.

I CHARLIE LAKE

HALFWAY

anhydrite tablet molds burrowed, decrease in size & quantity upward.
Burrows partially infilled with anhydrite.
7/75% (?) moldic, oil-stained.
wh-mottles

concentrations of large dol.cem. sh. cls. & ph. [illegible] cls.

G ACTIVE TIDAL INLET CHANNEL

sh. lam. [illegible] [illegible] cracked and Planolites burrowed.

E LOWER SHOREFACE

WELL NAME: PACIFIC SINCLAIR NANCY
FORMATION: HALFWAY-CHARLIE LAKE
DATE: 28/06/90
LOCATION: d-043-H/94-A-15
CORE INTERVAL:
KB: 2362 ft

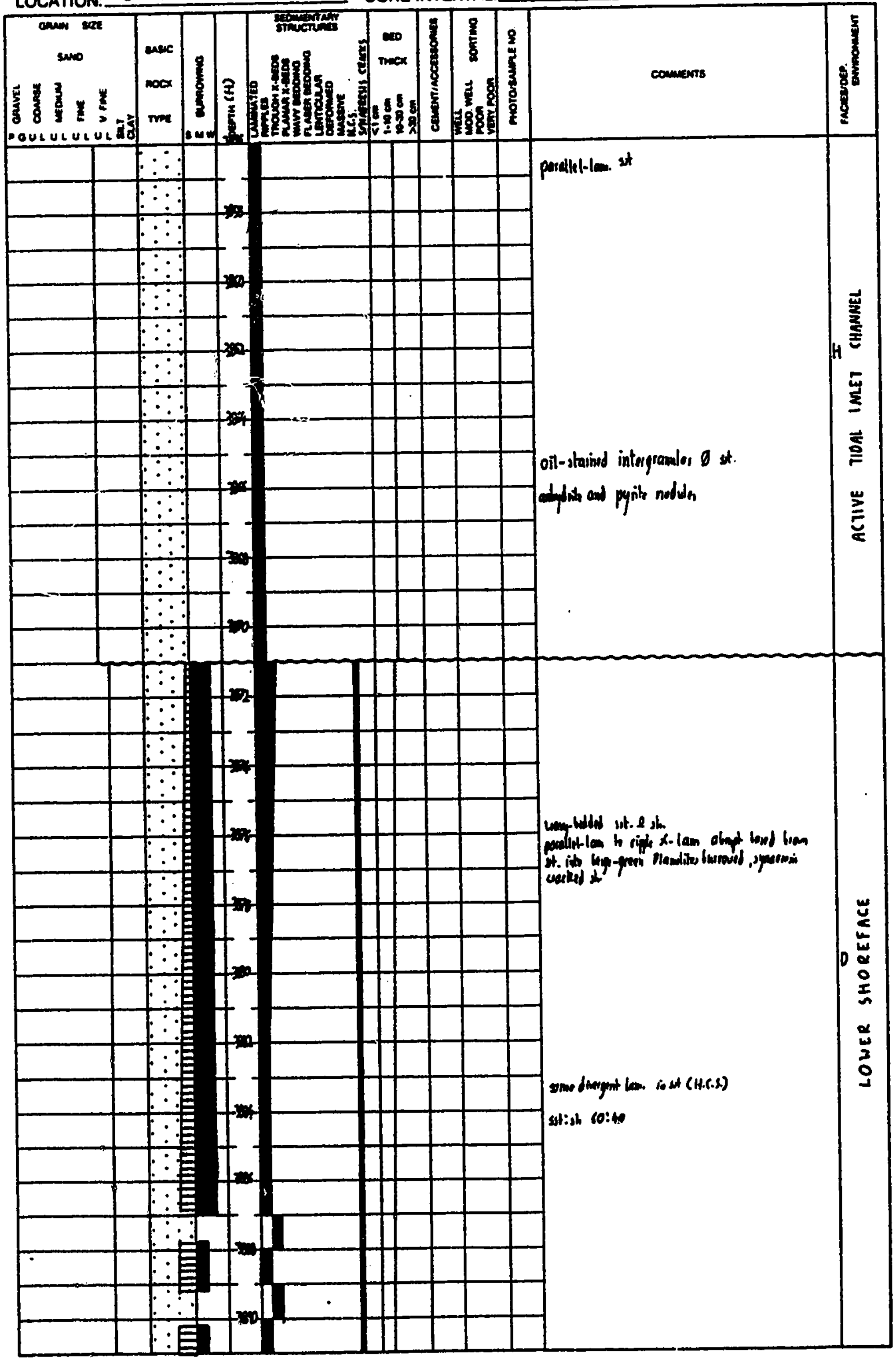

parallel-lam. sst

oil-stained intergranular Ø st.
anhydrite and pyrite nodules

wavy-bedded sst. & sh.
parallel-lam to ripple X-lam abrupt bases from
st. into beige-green Planolites burrowed, synaeresis
cracked sh.

some divergent lam. in st (H.C.S.)
sst:sh 60:40

WELL NAME: PACIFIC SINCLAIR NANCY

FORMATION: HALFWAY-CHARLIE LAKE

DATE: 28/06/90

LOCATION: d-043-H/94-A-15

CORE INTERVAL:

KB: 2362 ft

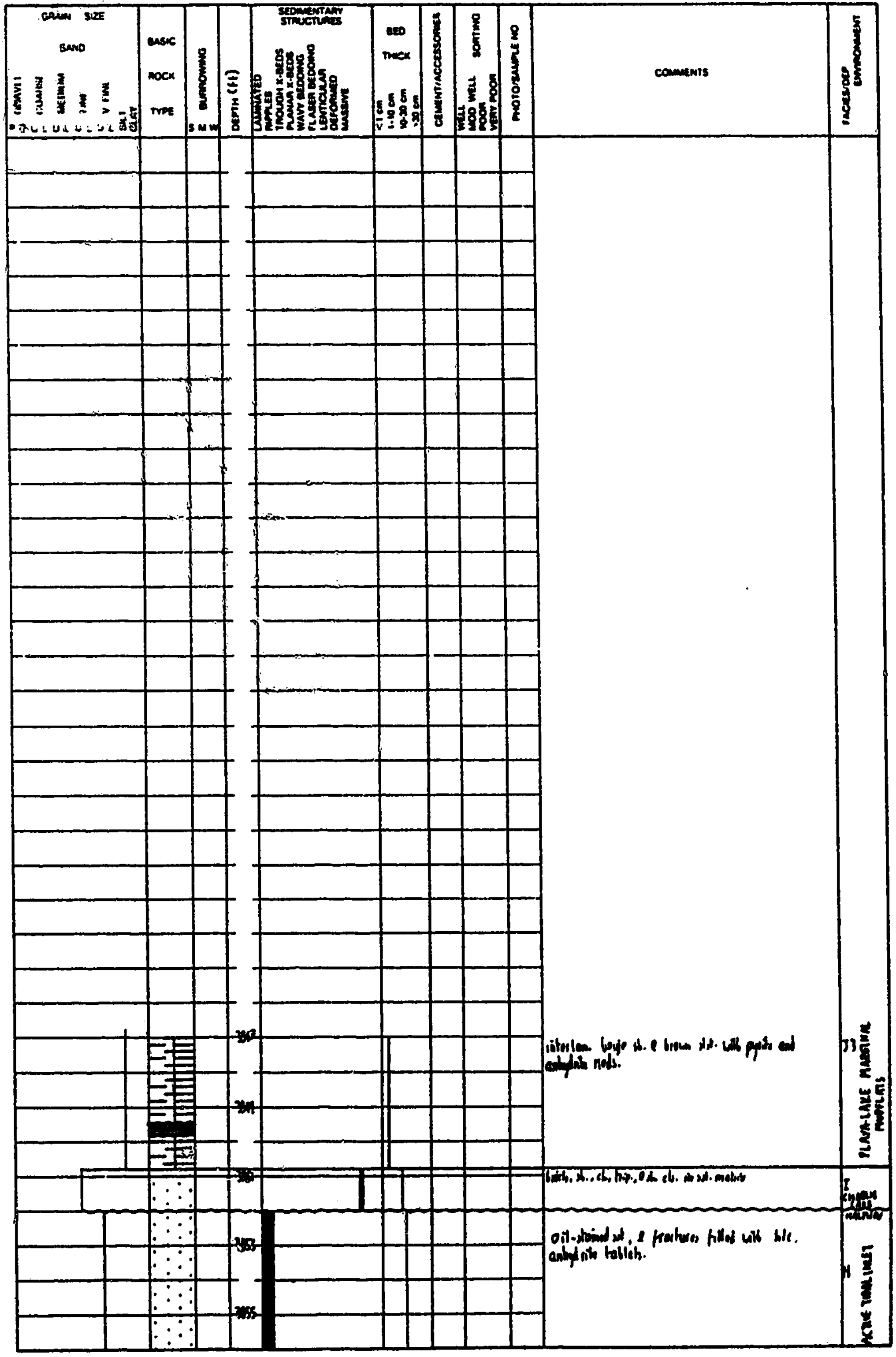

interlam. beige sh. & brown slt. with pyrite and anhydrite nods.

brecc., sh., cl., lrp., & ch. cl. in sd. matrix

Oil-stained sst, & fractures filled with blk. anhydrite bitumen.

WELL NAME: CANDEL SR NANCY
FORMATION: HALFWAY-CHARLIE LAKE
DATE: 28/06/90
LOCATION: d-044-H/94-A-15
CORE INTERVAL:
KB: 2360ft

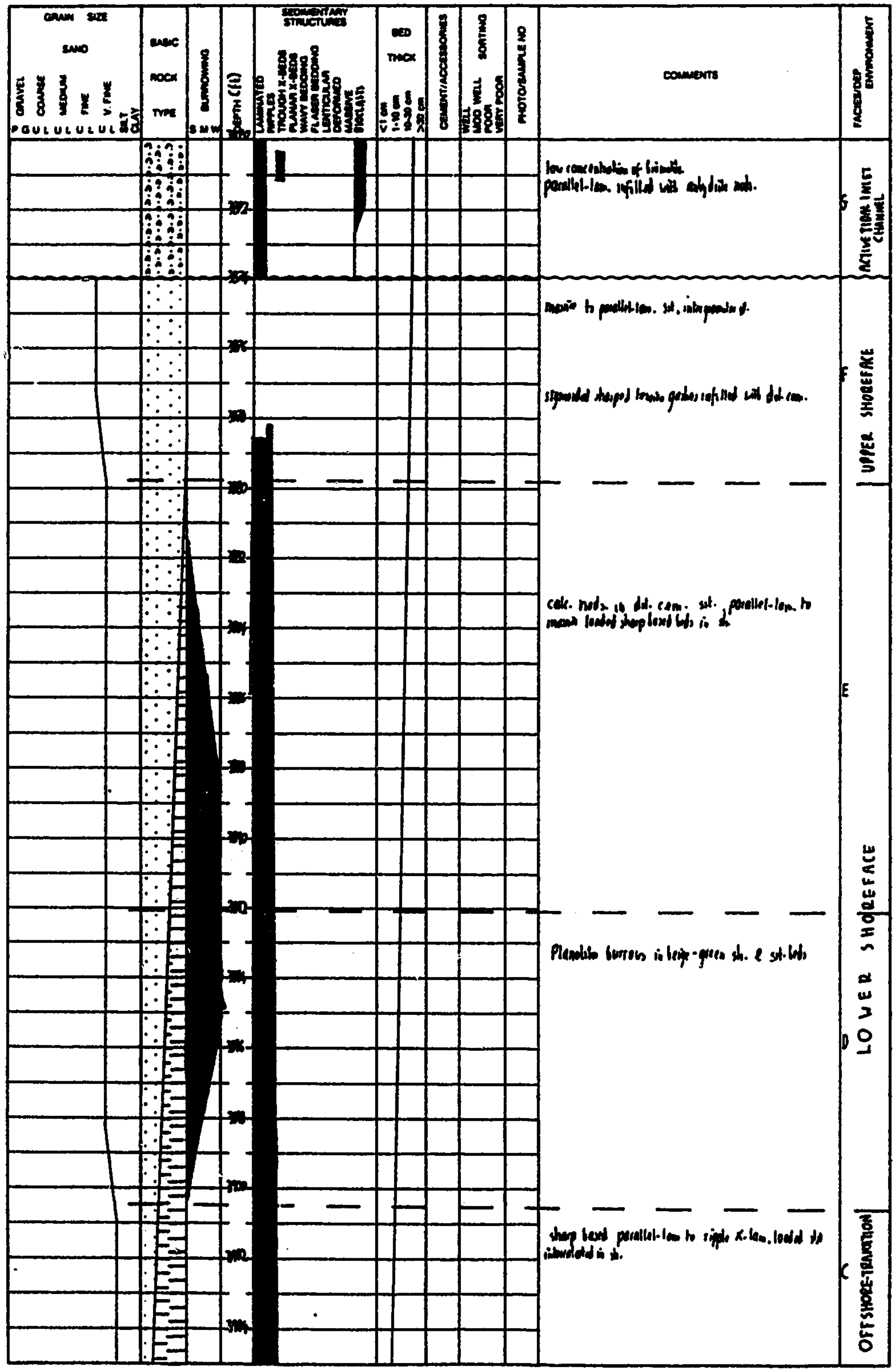

low concentration of bivalve.
parallel-lam. infilled with anhydrite nods.

massive to parallel-lam. sst. interspersing g.

sigmoidal shaped burrow galleries infilled with dol. cem.

calc. nods. in dol. cem. sst. parallel-lam. to massive loaded sharp based beds in sh.

Planolites burrows in beige-green sh. & sst. beds

sharp based parallel-lam to ripple X-lam. loaded sst interbedded in sh.

WELL NAME: CANDEL SR NANCY FORMATION: HALFWAY-CHARLIE LAKE DATE: 28/06/90

LOCATION: d-044-H/94-A-15 CORE INTERVAL: KB: 2360ft

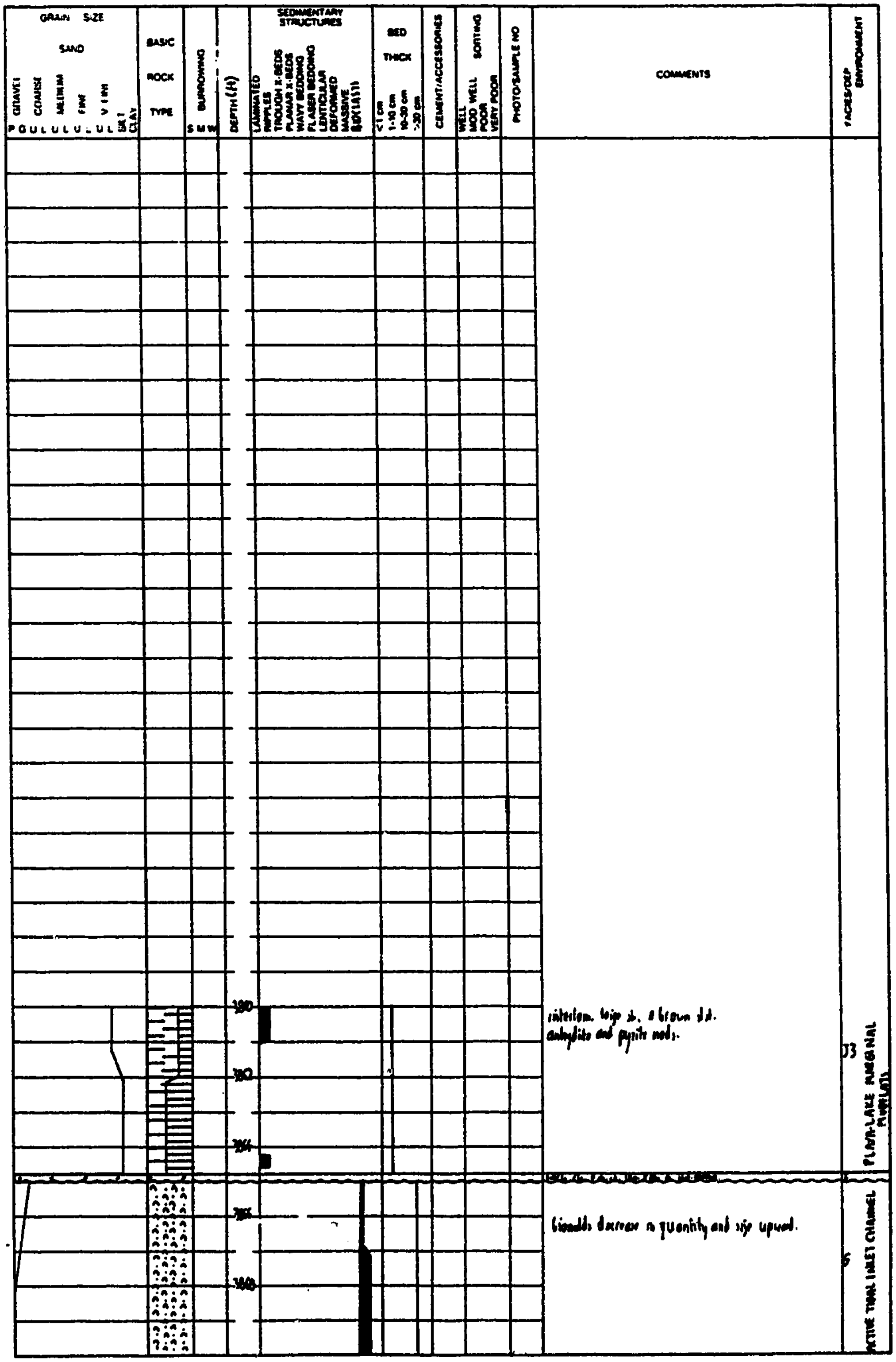

siltstone, beige st., & brown d.d. anhydrite and pyrite nods.

[illegible]

bioclasts decrease in quantity and size upward.

WELL NAME: CANDEL SR NANCY FORMATION: HALFWAY-CHARLIE LAKE DATE: 27/06/90

LOCATION: d-045-H/94-A-15 CORE INTERVAL: KB: 2364ft

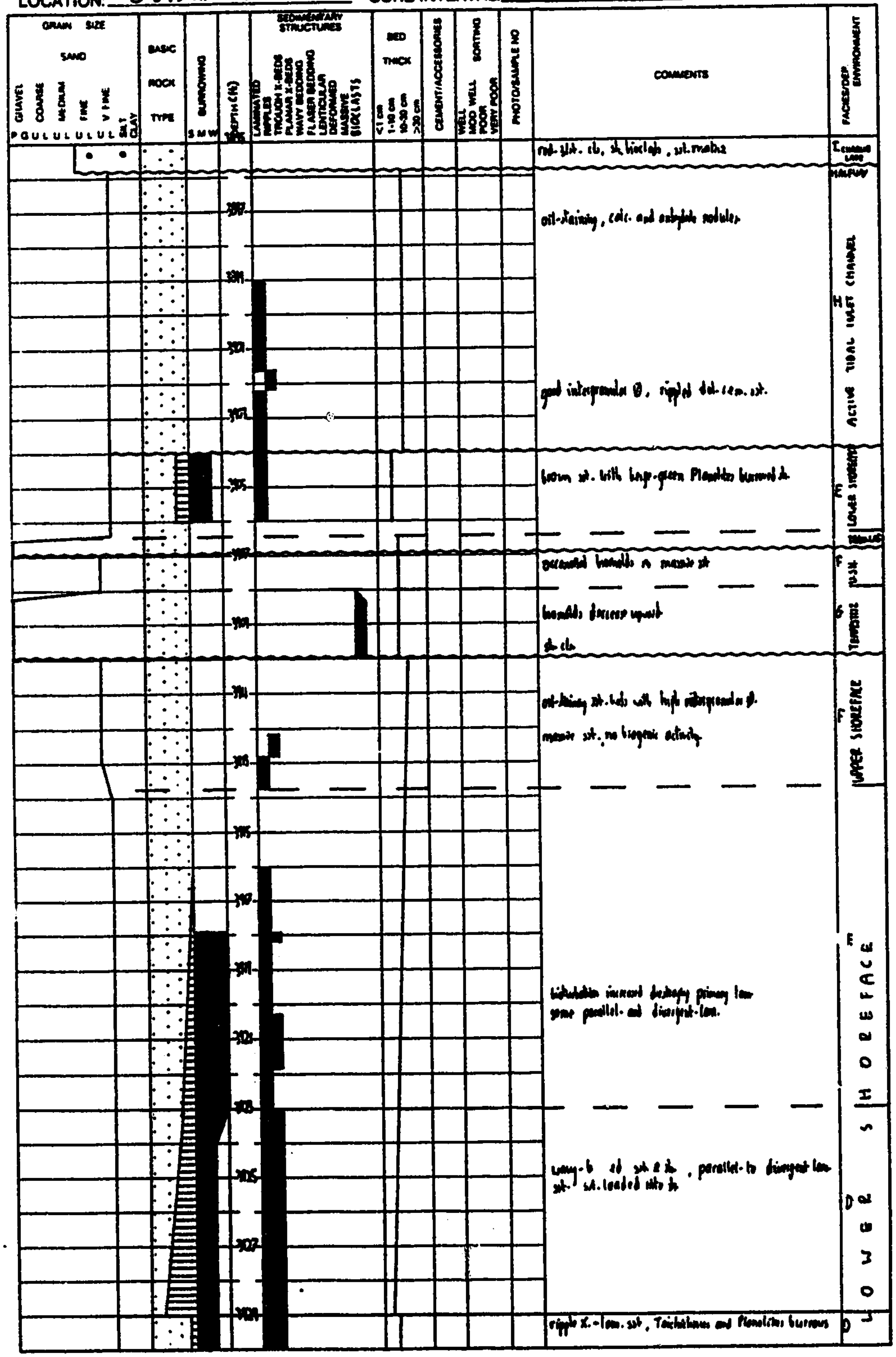

red-slst. cb, sh. bioclasts, slt. matrix

oil-staining, calc. and anhydrite nodules

good intergranular Ø, rippled dol.-cem. sst.

brown sst. with large-green Planolites burrowed sh.

occasional bioclasts in massive sst

bioclasts decrease upward

sh. cls.

oil-staining sst. beds with high intergranular Ø.

massive sst., no biogenic activity.

bioturbation increased destroying primary lam.
some parallel- and divergent-lam.

wavy-b [illegible] sst. & sh., parallel- to divergent lam.
sst. sst. loaded into sh.

ripple X.-lam. sst, Teichichnus and Planolites burrows

WELL NAME: CANDEL SR NANCY
FORMATION: HALFWAY-CHARLIE LAKE
DATE: 27/06/90
LOCATION: d-045-H/94-A-15
CORE INTERVAL:
KB: 2364 ft

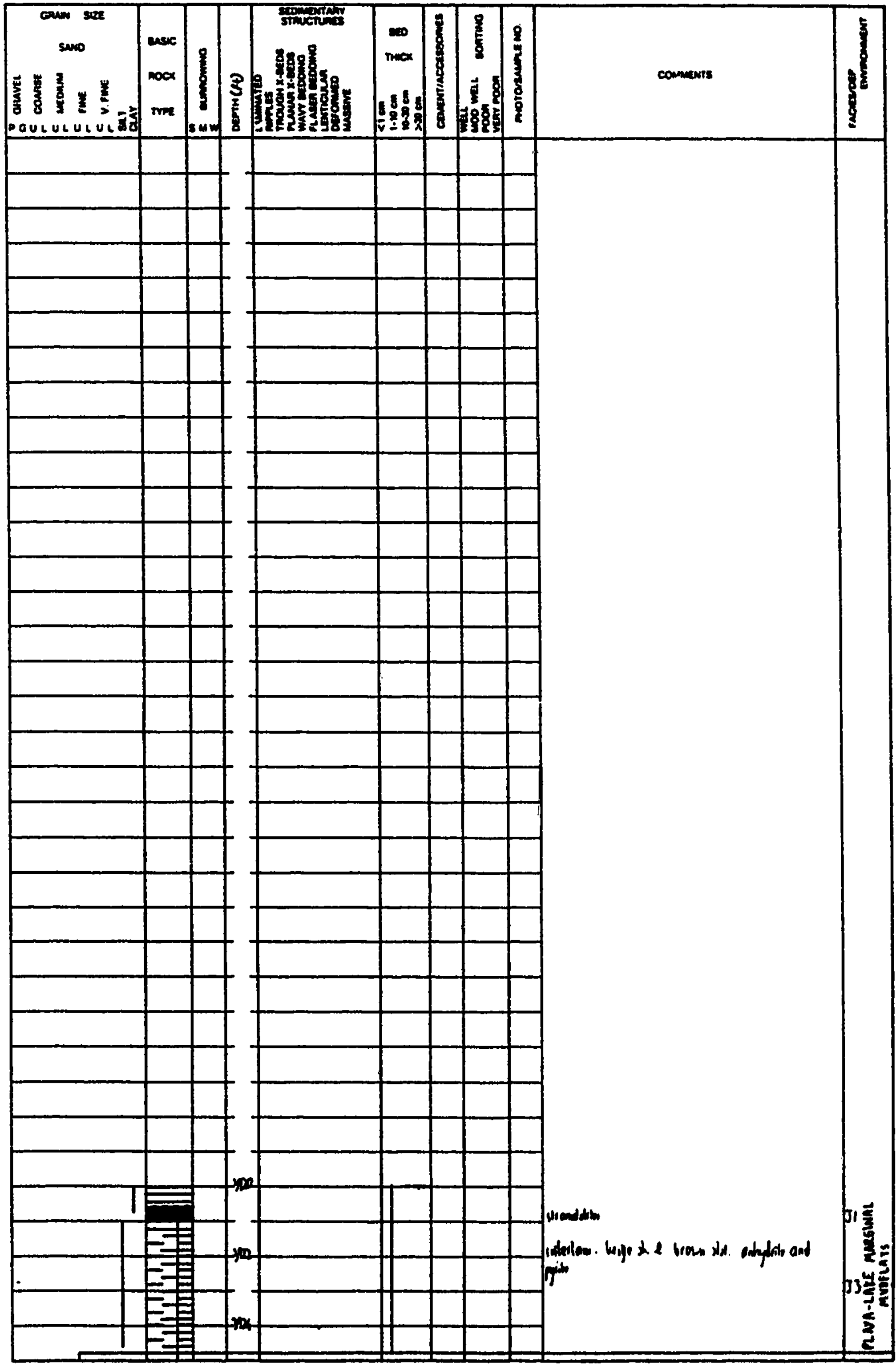

WELL NAME: PCI ET AL PEEJAY 6-51-H FORMATION: HALFWAY-CHARLIE LAKE DATE: 25/01/91

LOCATION: 6-051-H/94-A-15 CORE INTERVAL: KB: 723.25m

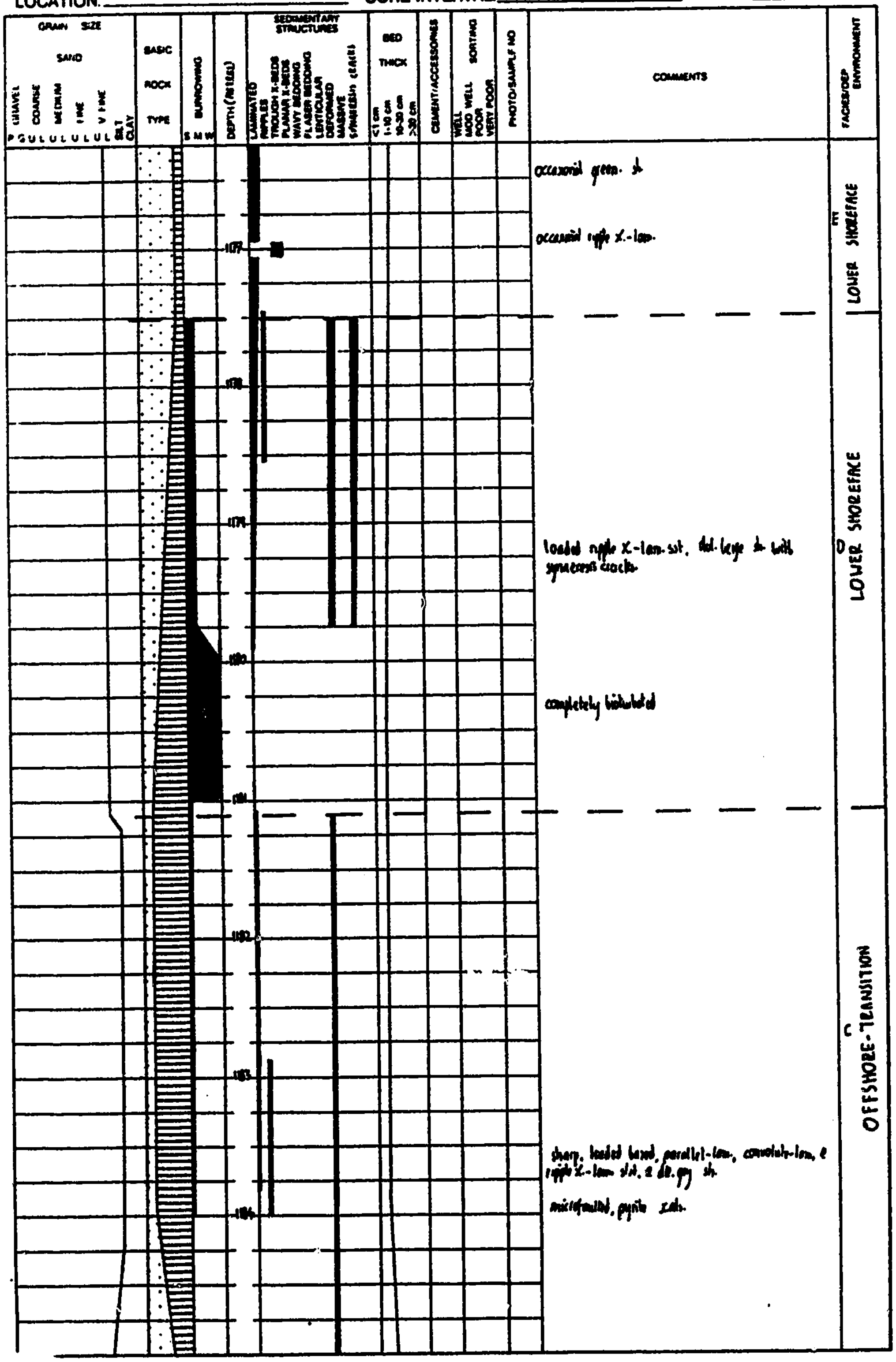

occasional green. sh

occasional ripple X.-lam.

loaded ripple X-lam. sst, dol. beige sh with synaeresis cracks.

completely bioturbated

sharp, loaded based, parallel-lam., convolute-lam, & ripple X.-lam. slt, & dk. gry sh.

microfaulted, pyrite xals.

WELL NAME: PCI ET AL PEEJAY 6-51-H FORMATION: HALFWAY-CHARLIE LAKE DATE: 25/01/91

LOCATION: 6-051-H/94-A-15 CORE INTERVAL: KB: 723.25m

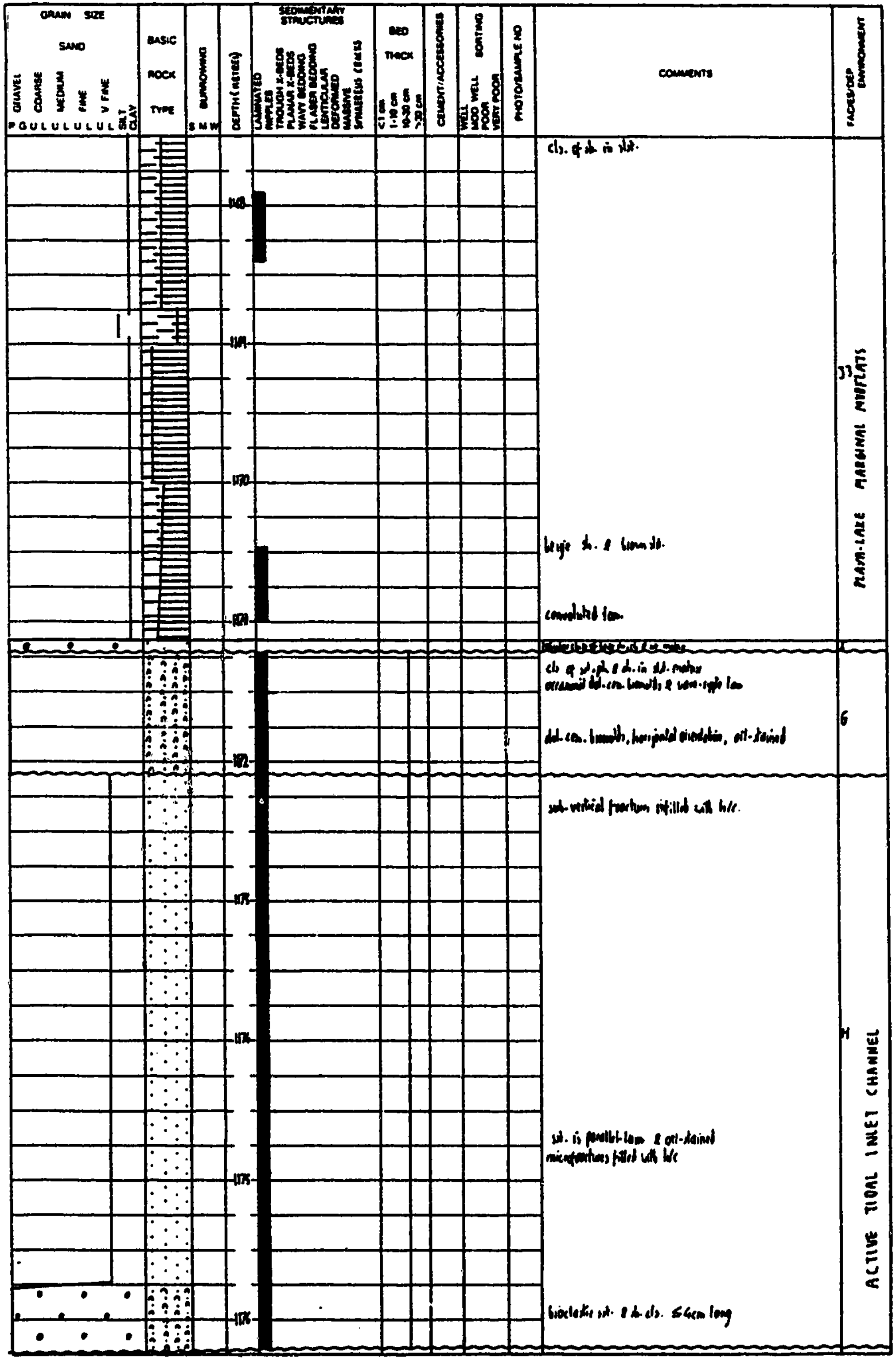

cls. of sh. in slst.

beige sh. & brown slt.

convoluted lam.

[illegible]

cls of slt., ph. & sh. in sst. matrix
occasional dol.-cem. burrows & wave-ripple lam

dol.-cem. burrows, horizontal orientation, oil-stained

sub-vertical fracture infilled with h/c.

sst. is parallel-lam & oil-stained
microfractures filled with h/c

bioclastic sst. & sh. cls. ≤4cm long

WELL NAME: CANDEL SR NANCY d-51-H FORMATION: HALFWAY-CHARLIE LAKE DATE: 26/07/90

LOCATION: d-051-H/94-A-15 CORE INTERVAL: KB: 2370ft

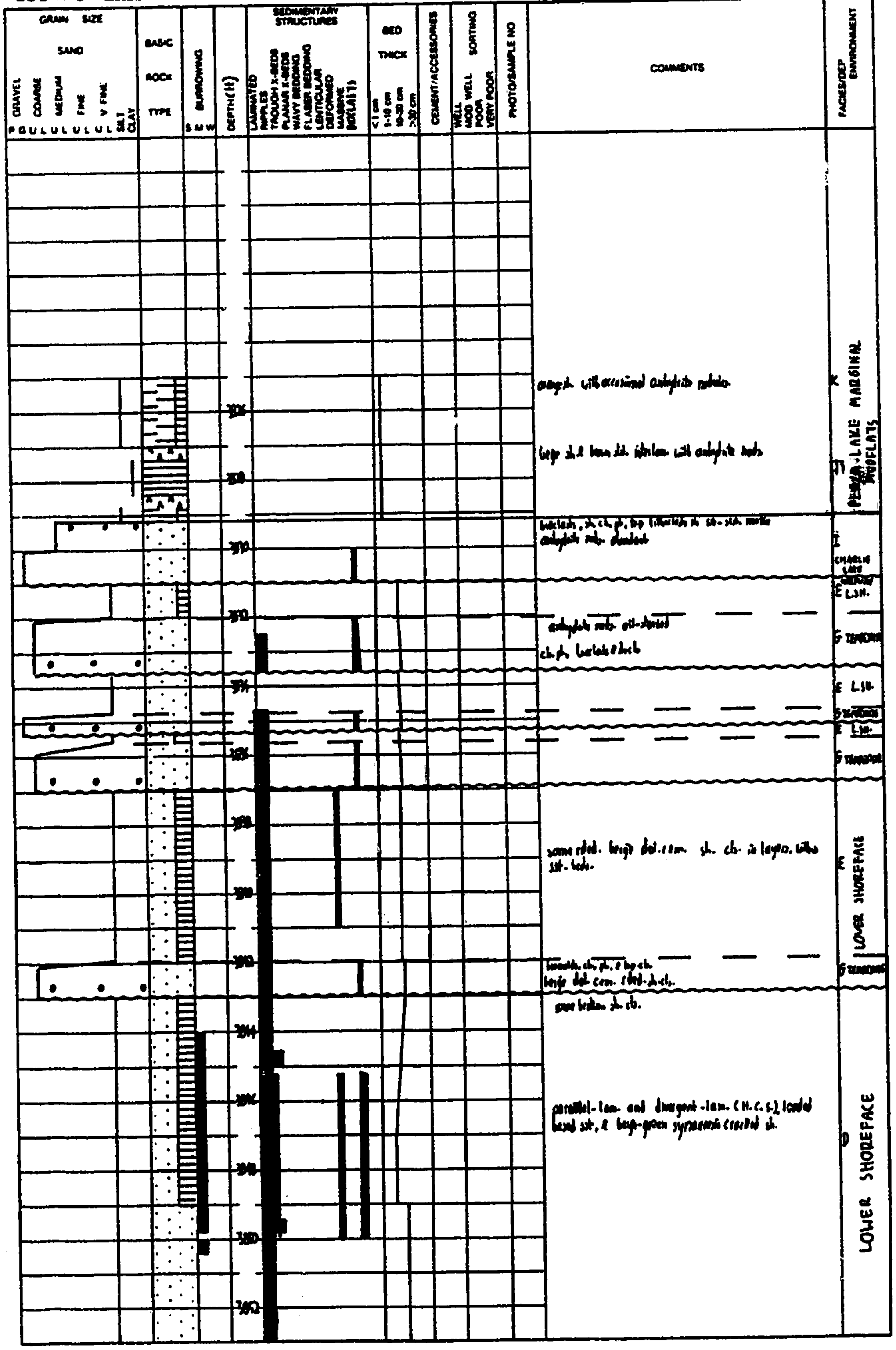

mrg. sh. with occasional anhydrite nodules.

beige sh. & brown dol. siltstone with anhydrite nods.

bioclasts, sh. cl., ph., top lithoclasts in ss.-slst. matrix anhydrite nods. abundant

anhydrite nods. oil-stained

ch. ph. bioclasts & lcls.

some rbd. beige dol.-cem. sh. cls. in layers, with sst. beds.

bioclasts, cls, ph. & top cls. beige dol. cem. rbd.-sh.cls.

some broken sh. cls.

parallel-lam. and divergent-lam. (H.C.S.) loaded based sst, & beige-green syneresis cracked sh.

WELL NAME: CANDEL SR NANCY d-52-H FORMATION: HALFWAY-CHARLIE LAKE DATE: 24/07/90

LOCATION: d-052-H/94-A-15 CORE INTERVAL: KB: 2370ft

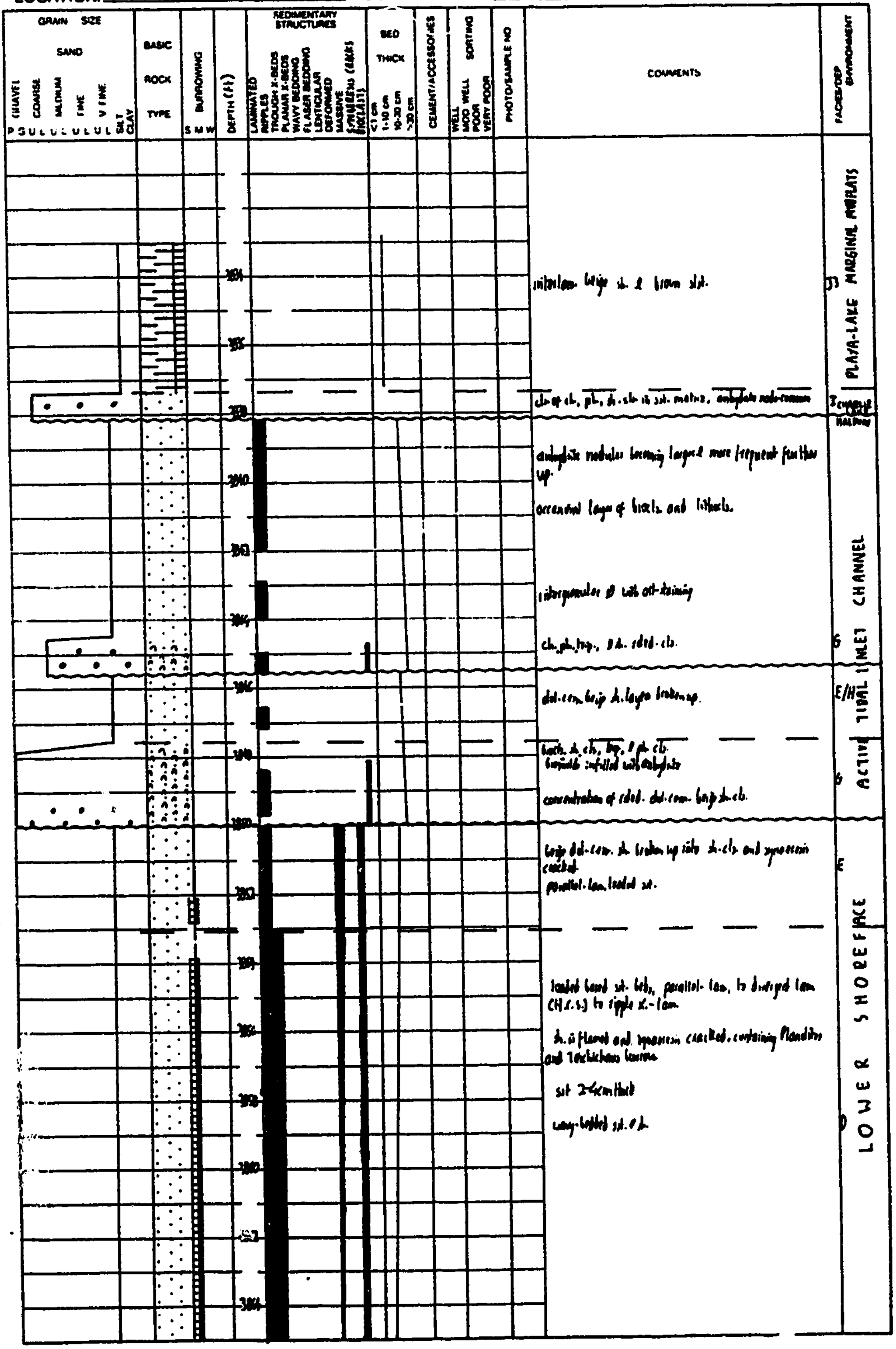

interlam. beige sh. & brown slst.

clasts of ch., ph., sh. clasts in sst. matrix, anhydrite nodes common

anhydrite nodules becoming larger & more frequent further up.

occasional layers of bioclasts and lithoclasts.

intergranular ø with oil-staining

ch., ph., frg., sh. sdst.-cls.

dol.-cem. beige sh. layers broken up.

bioclasts, sh. cls., frg., & ph. cls.
burrows infilled with anhydrite

concentration of sdst. dol.-cem. beige sh. cls.

beige dol.-cem. sh. broken up into sh.-cls and synaeresis cracked.
parallel-lam. loaded sst.

loaded based sst. beds, parallel-lam., to draped lam (H.C.S.) to ripple x.-lam.

sh. is flamed and synaeresis cracked, containing Planolites and Teichichnus burrows

sst 2-4cm thick

wavy-bedded sst. & sh.

WELL NAME: PACIFIC CAN-DEL SR PEEJAY d-55-H FORMATION: HALFWAY-CHARLIE LAKE DATE: 18/07/90

LOCATION: d-055-H/94-A-15 CORE INTERVAL: KB: 2356ft

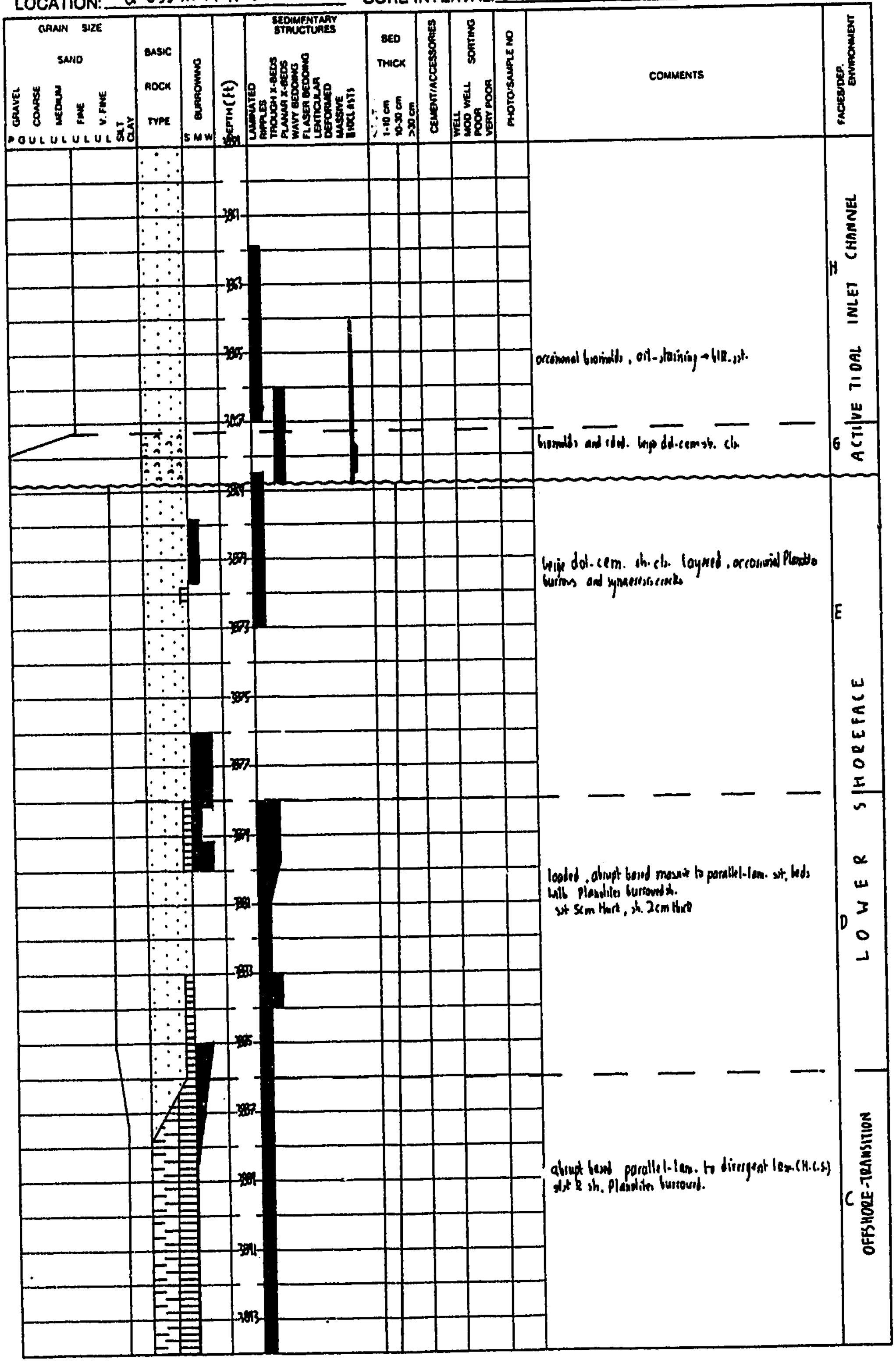

occasional bioclasts, oil-staining → bik. sst.

bioclasts and rded. beige dol-cem. sh. cls.

beige dol-cem. sh. cls. layered, occasional Planolites burrows and synaeresis cracks

loaded, abrupt based massive to parallel-lam. sst. beds with Planolites burrowed sh.
sst 5cm thick, sh. 2cm thick

abrupt based parallel-lam. to divergent lam. (H.C.S) slst & sh. Planolites burrowed.

WELL NAME: PACIFIC CAN-DEL SR PEEJAY d-55-H

FORMATION: HALFWAY-CHARLIE LAKE

DATE: 18/07/90

LOCATION: d-055-H/94-A-16

CORE INTERVAL:

KB: 2356ft

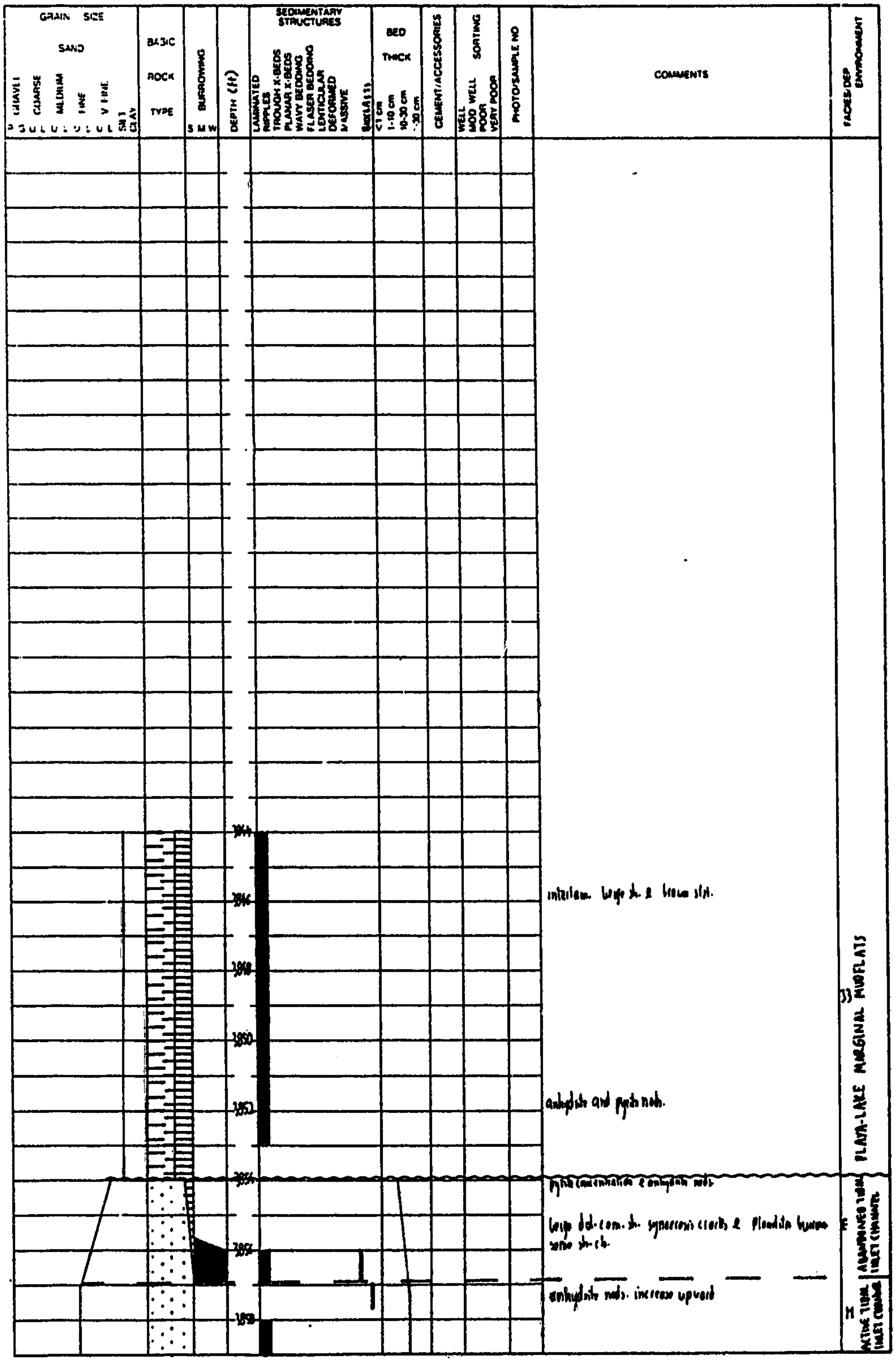

interlam. beige sh. & brown slst.

anhydrite and pyrite nods.

pyrite concentration & anhydrite nods.

beige dol-cem. sh. synaeresis cracks & Planolites burrows some sh. cl.

anhydrite nods. increase upward

33 PLAYA-LAKE MARGINAL MUDFLATS

E ABANDONED TIDAL INLET CHANNEL

H ACTIVE TIDAL INLET CHANNEL

WELL NAME: PACIFIC SINCLAIR CANDEL NANCY d-56-H FORMATION: HALFWAY- CHARLIE LAKE DATE: 26/06/90

LOCATION: d-056-H/94-A-15 CORE INTERVAL: KB: 2349.8ft

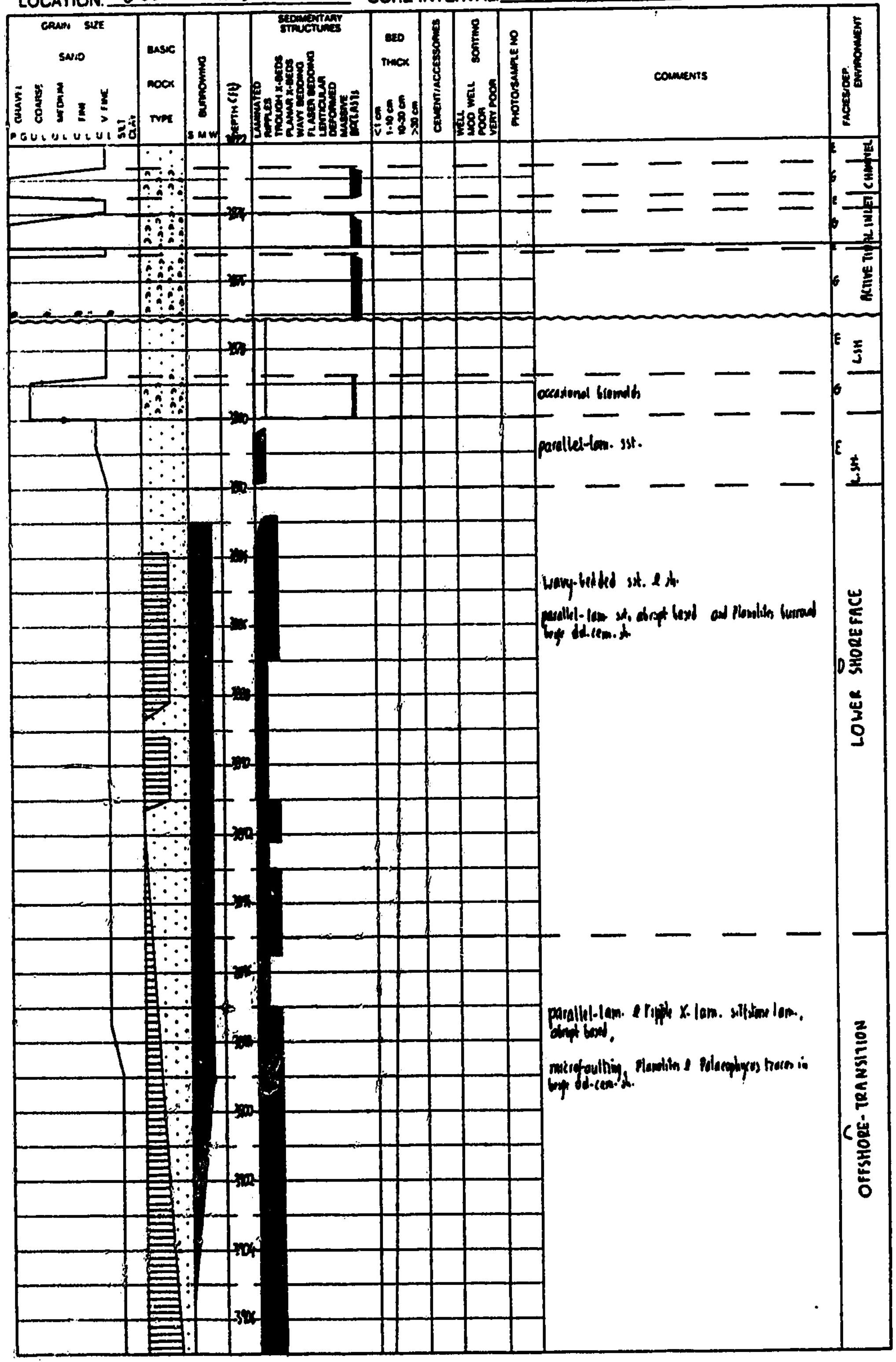

occasional bioroclasts

parallel-lam. sst.

wavy-bedded sst. & sh.

parallel-lam sst, abrupt based and Planolites burrowed large dd.-cem. sh.

parallel-lam. & ripple X-lam. siltstone lam., abrupt based,

microfaulting, Planolites & Palaeophycus traces in large dd-cem. sh.

WELL NAME: PACIFIC SINCLAIR CANDEL NANCY d-56-H FORMATION: HALFWAY-CHARLIE LAKE DATE: 26/06/90

LOCATION: d-056-H/94-A-15 CORE INTERVAL: KB: 2349.8ft

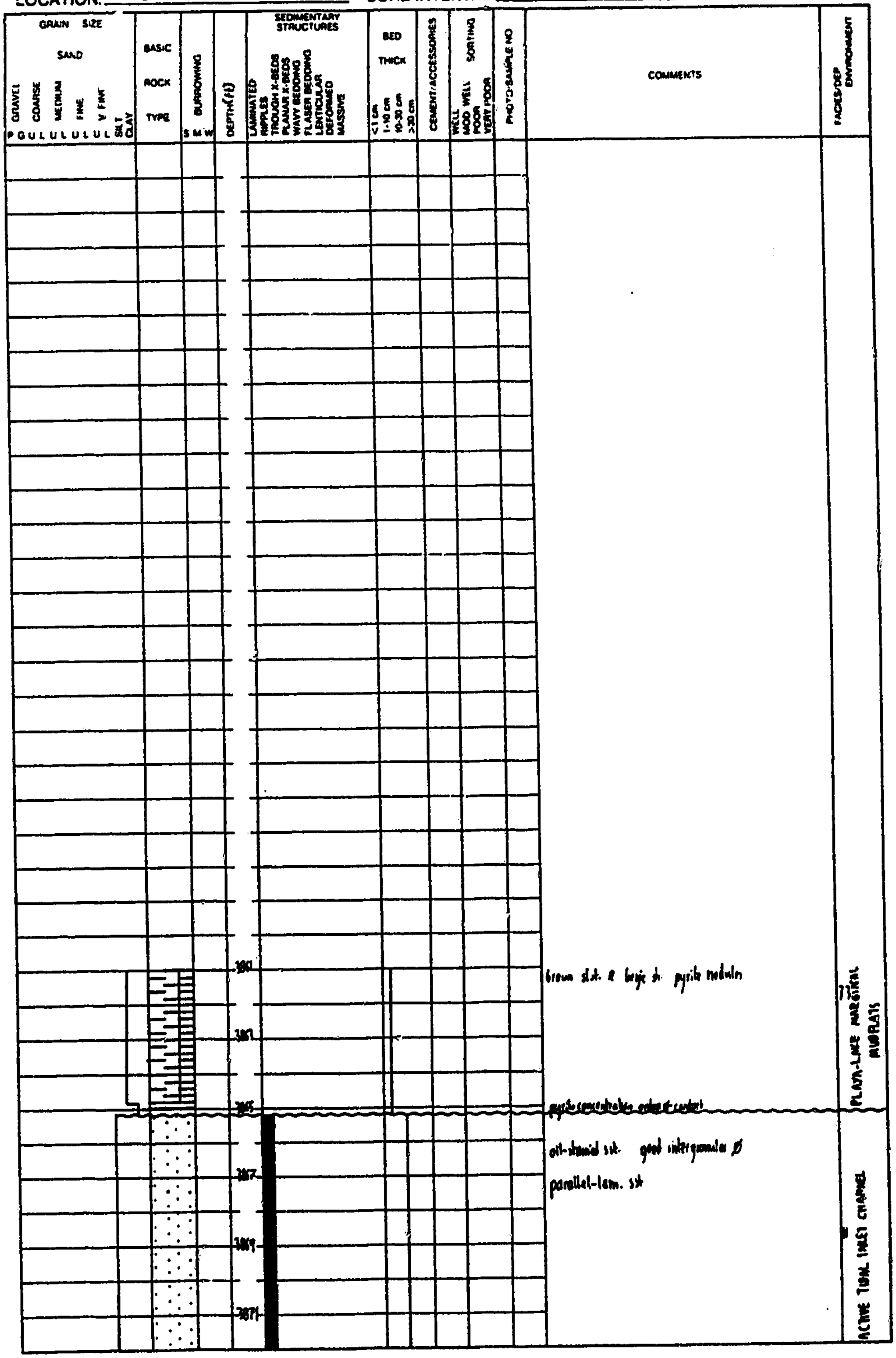

brown slst. & beige sh. pyrite nodules

pyrite concentration erosional contact

oil-stained sst. good intergranular ∅

parallel-lam. sst

WELL NAME: MEDALLION ASHLAND PEEJAY d-61-H

FORMATION: HALFWAY-CHARLIE LAKE

DATE: 5/02/91

LOCATION: d-061-H/94-A-15

CORE INTERVAL:

KB: 2374 ft

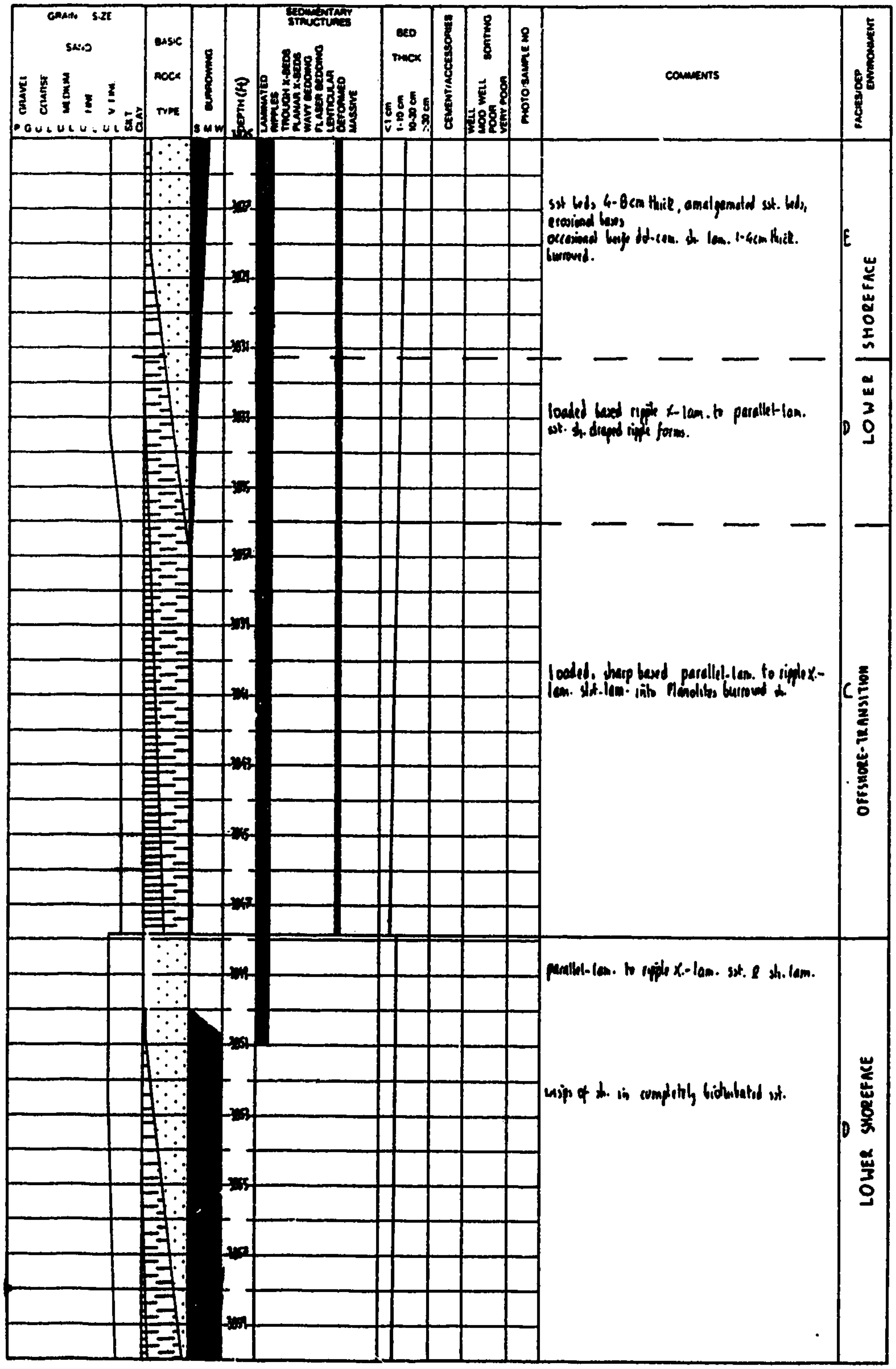

sst beds 4-8cm thick, amalgamated sst. beds, erosional bases
occasional burrowed sh. lam. 1-4cm thick.
burrowed.

E — LOWER SHOREFACE

loaded based ripple X-lam. to parallel-lam. sst. sh. draped ripple forms.

D

loaded, sharp based parallel-lam. to ripple X-lam. slst-lam. into Planolites burrowed sh.

C — OFFSHORE-TRANSITION

parallel-lam. to ripple X.-lam. sst. & sh. lam.

wisps of sh. in completely bioturbated sst.

D — LOWER SHOREFACE

WELL NAME: MEDALLION ASHLAND PEEJAY d-61-H FORMATION: HALFWAY-CHARLIE LAKE DATE: 5/02/91

LOCATION: d-061-H/94-A-15 CORE INTERVAL: KB: 2374 ft

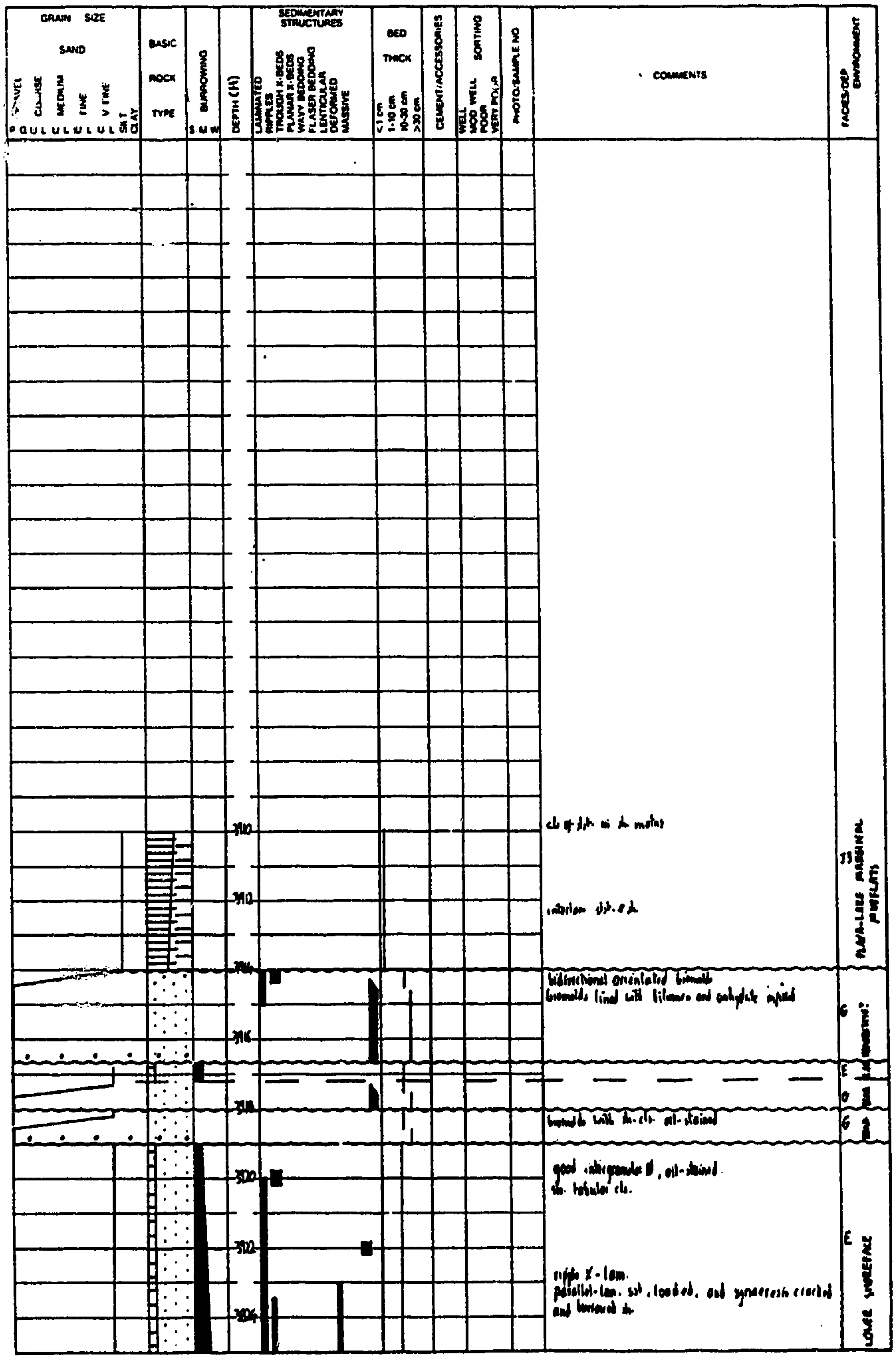

cls of dol. in sh. matrix

interlam. dol. & sh.

bidirectional orientated biomolds
biomolds lined with [illegible] and anhydrite infilled

biomolds with sh. cls. oil-stained

good intergranular ϕ, oil-stained.
sh. tabular cls.

ripple X-lam.
parallel-lam. sst. loaded, and syneresis cracked and burrowed sh.

WELL NAME: CAN DEL SR PEEJAY d-62-H
FORMATION: HALFWAY-CHARLIE LAKE
DATE: 24/07/90
LOCATION: d-062-H/94-A-15
CORE INTERVAL:
KB: 2365.6ft

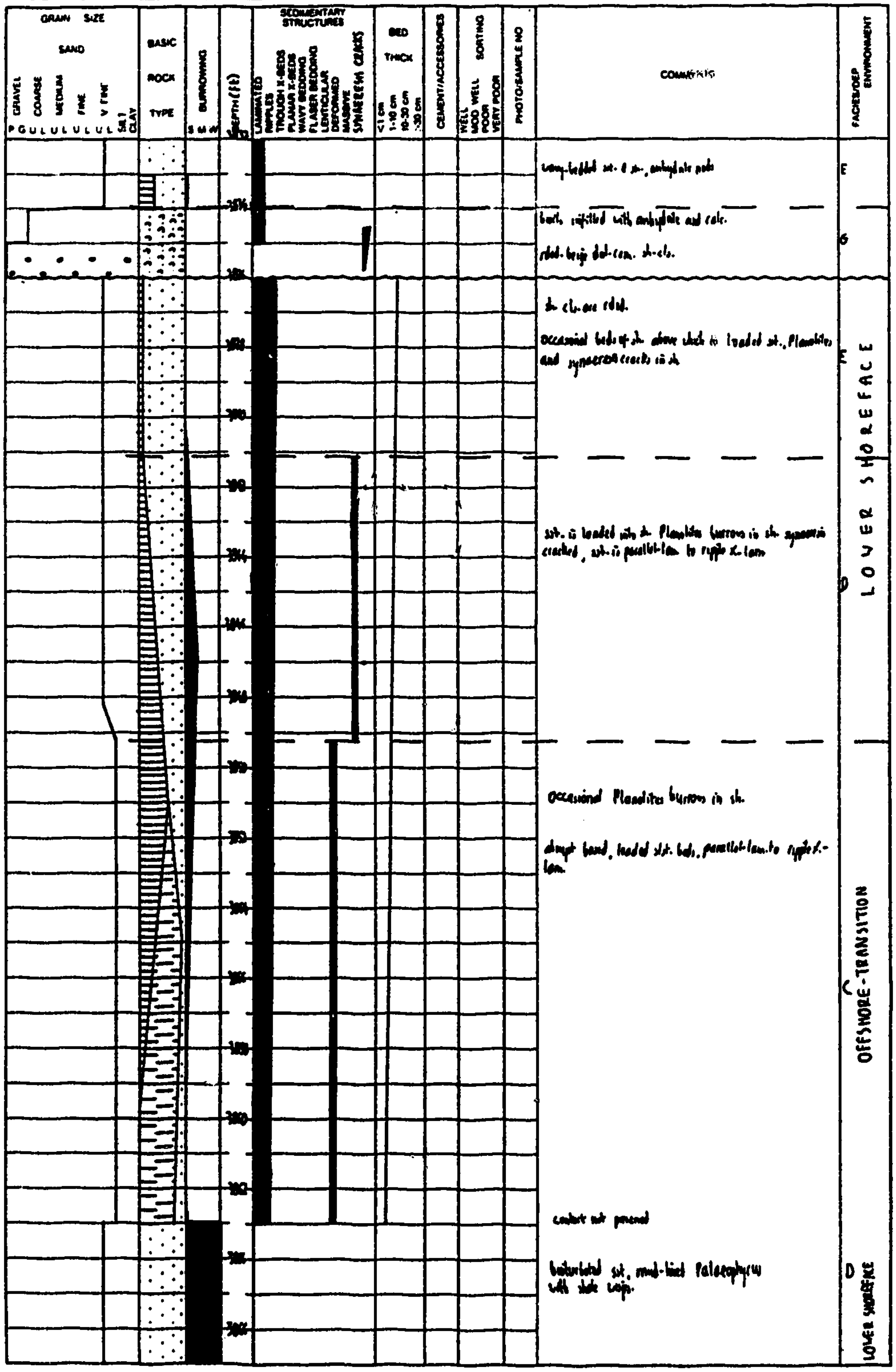

wavy-bedded slt. & sh., anhydrite nods

burr. infilled with anhydrite and calc.

rded. large dol-cem. sh-clts.

sh. cl. are rded.

Occasional beds of sh. above which is loaded st., Planolites and synaeresis cracks in sh.

slt. is loaded into sh. Planolites burrows in sh. synaeresis cracked, slt. is parallel-lam. to ripple X-lam

Occasional Planolites burrows in sh.

abrupt based, loaded slt. beds, parallel-lam. to ripple X-lam.

contact not preserved

bioturbated sst, mud-lined Palaeophycus with shale wisps.

WELL NAME: CAN DEL SR PEEJAY d-62-H FORMATION: HALFWAY-CHARLIE LAKE DATE: 24/07/90

LOCATION: d-062-H/94-A-15 CORE INTERVAL: KB: 2365 ft

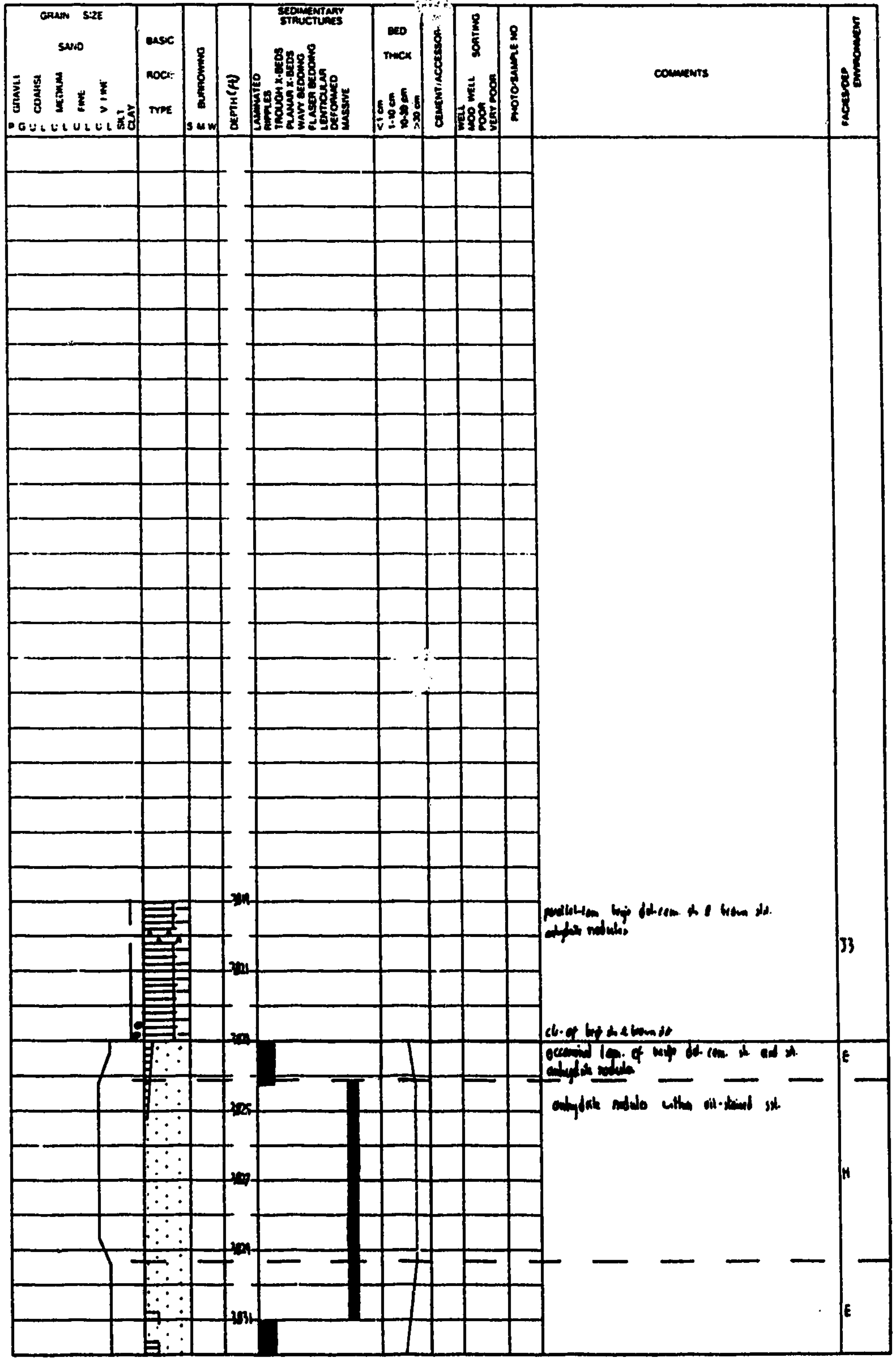

parallel-lam. beige dol-cem. sh & brown sltst. anhydrite nodules

cls. of beige sh & brown sl

occasional lam. of beige dol-cem. sh and sl. anhydrite nodules

anhydrite nodules within oil-stained sst.

WELL NAME: CANDEL SR. NANCY d-63-H FORMATION: HALFWAY-CHARLIE LAKE DATE: 25/07/90

LOCATION: d-063-H/94-A-15 CORE INTERVAL:________ KB: 2365ft

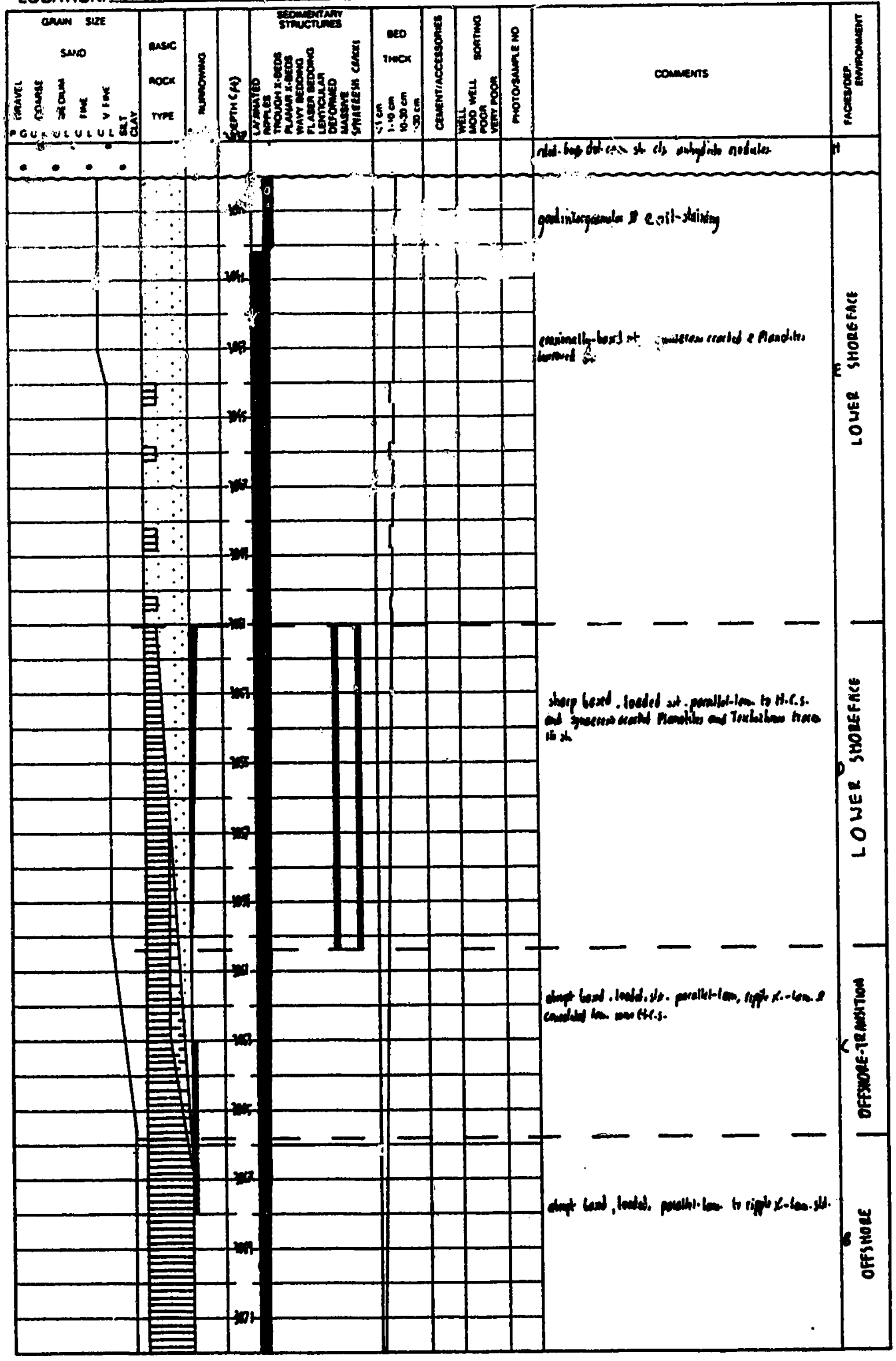

rlat-bag dol cas sh cls anhydrite nodules

good intergranular Ø & oil-staining

occasionally-bored st. scattered & Planolites burrowed

sharp based . loaded sst . parallel-lam. to H.C.S. and sparsely scattered Planolites and Teichichnus traces in sh.

sharp based . loaded. slt. parallel-lam, ripple X.-lam. & convoluted lam. rare H.C.S.

sharp based , loaded. parallel-lam. to ripple X-lam. slt.

WELL NAME: CANDEL SR NANCY d-33-H FORMATION: HALFWAY-CHARLIE LAKE DATE: 25/07/90

LOCATION: d-063-H/94-A-15 CORE INTERVAL: KB: 2365ft

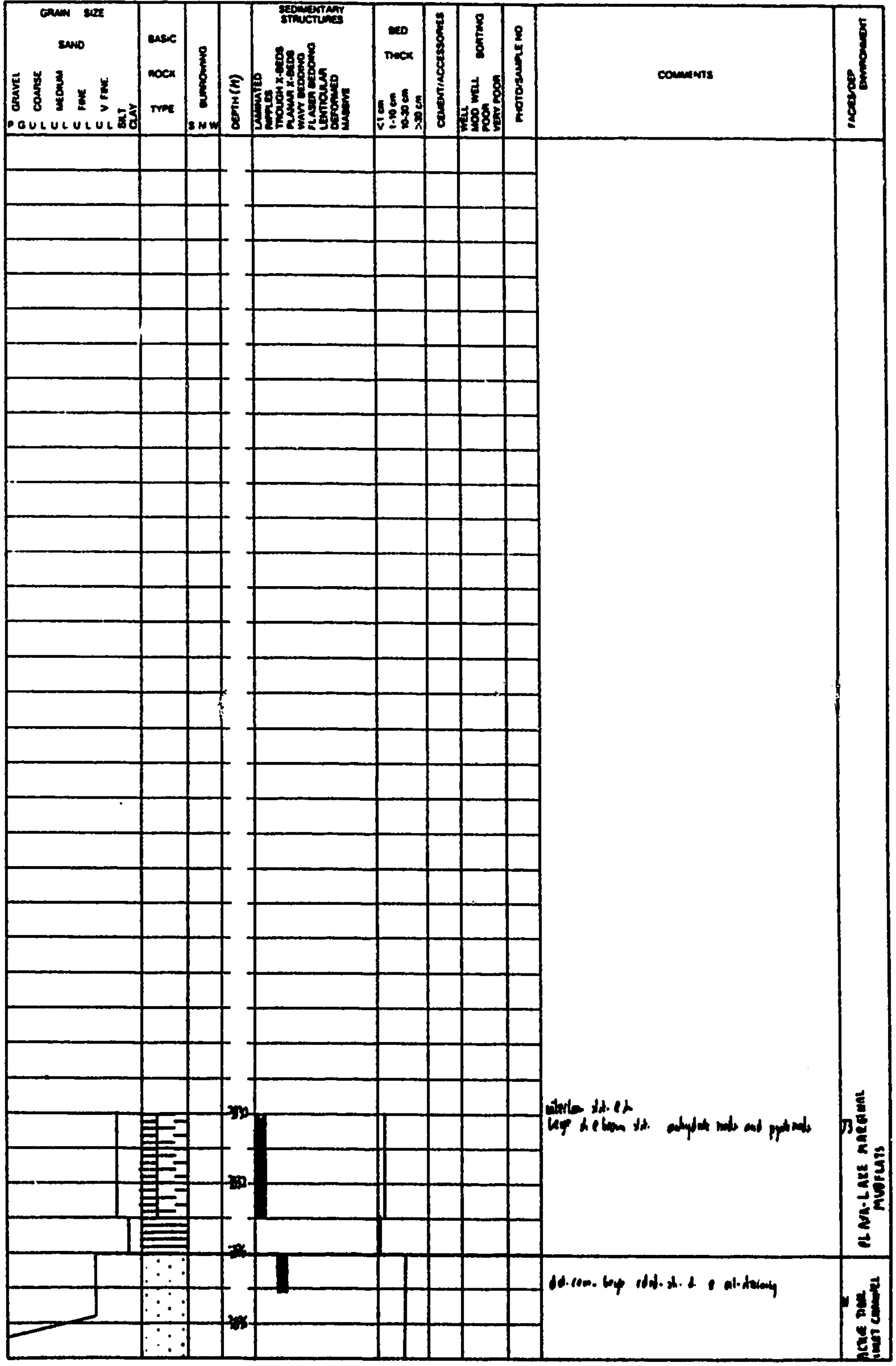

WELL NAME: PACIFIC ET AL PEEJAY 6-64-H FORMATION: HALFWAY-CHARLIE LAKE DATE: 18/07/90

LOCATION: 6-064-H/94-A-15 CORE INTERVAL: KB: 2359ft

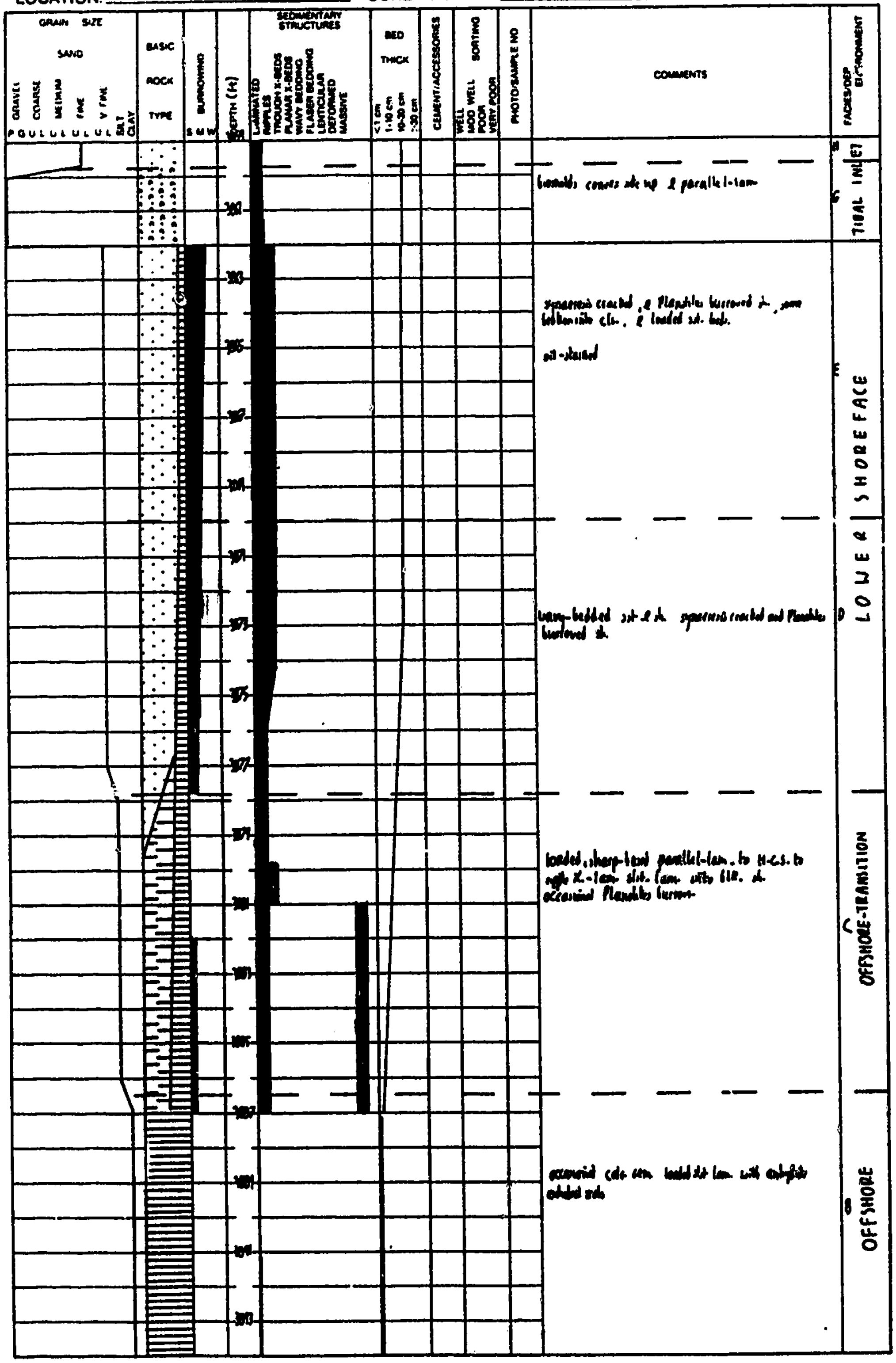

[illegible] coarse [illegible] & parallel-lam.

syneresis cracked, & Planolites burrowed sh., some bentonitic cls., & loaded st. beds.

oil-stained

wavy-bedded sst. & sh. syneresis cracked and Planolites burrowed sh.

loaded, sharp-based parallel-lam. to H.C.S. to ripple X-lam. slst. lam. with [illegible] sh. occasional Planolites burrows

occasional calc. cem. loaded slt lam. with anhydrite [illegible]

WELL NAME: PACIFIC ET AL PEEJAY 6-64-H FORMATION: HALFWAY-CHARLIE LAKE DATE: 18/07/90

LOCATION: 6-064-H/94-A-15 CORE INTERVAL: KB: 2359ft

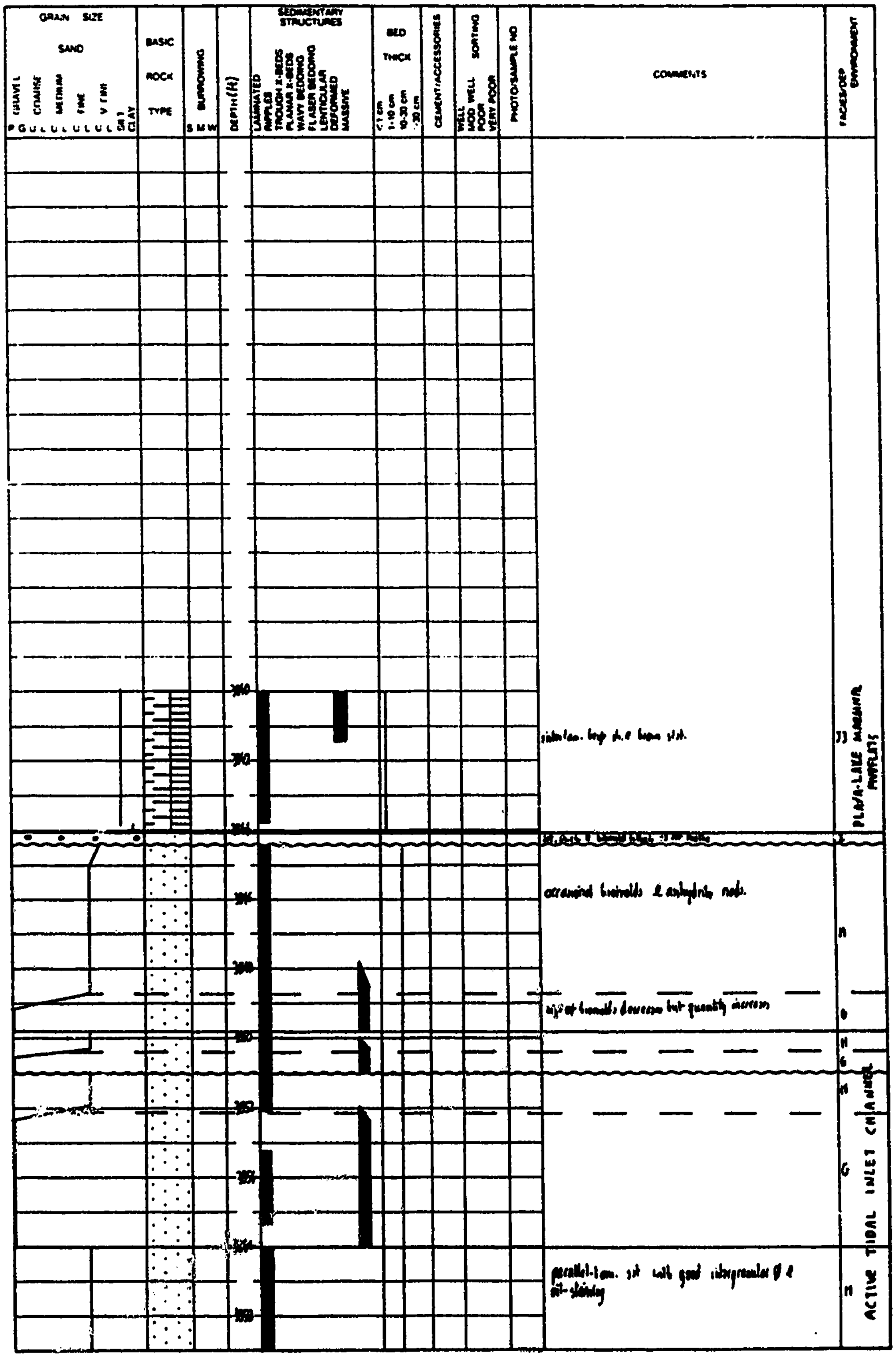

sub-lam. [illegible] brown slst.

[illegible]

occasional bioturb. & anhydrite nods.

size of bioturb. decrease but quantity increase

parallel-lam. sst with good intergranular ϕ & oil-staining

WELL NAME: PACIFIC SR CANDEL NANCY d-67H
FORMATION: HALFWAY-CHARLIE LAKE
DATE: 26/06/90
LOCATION: d-067-H/94-A-15
CORE INTERVAL:
KB: .2351ft

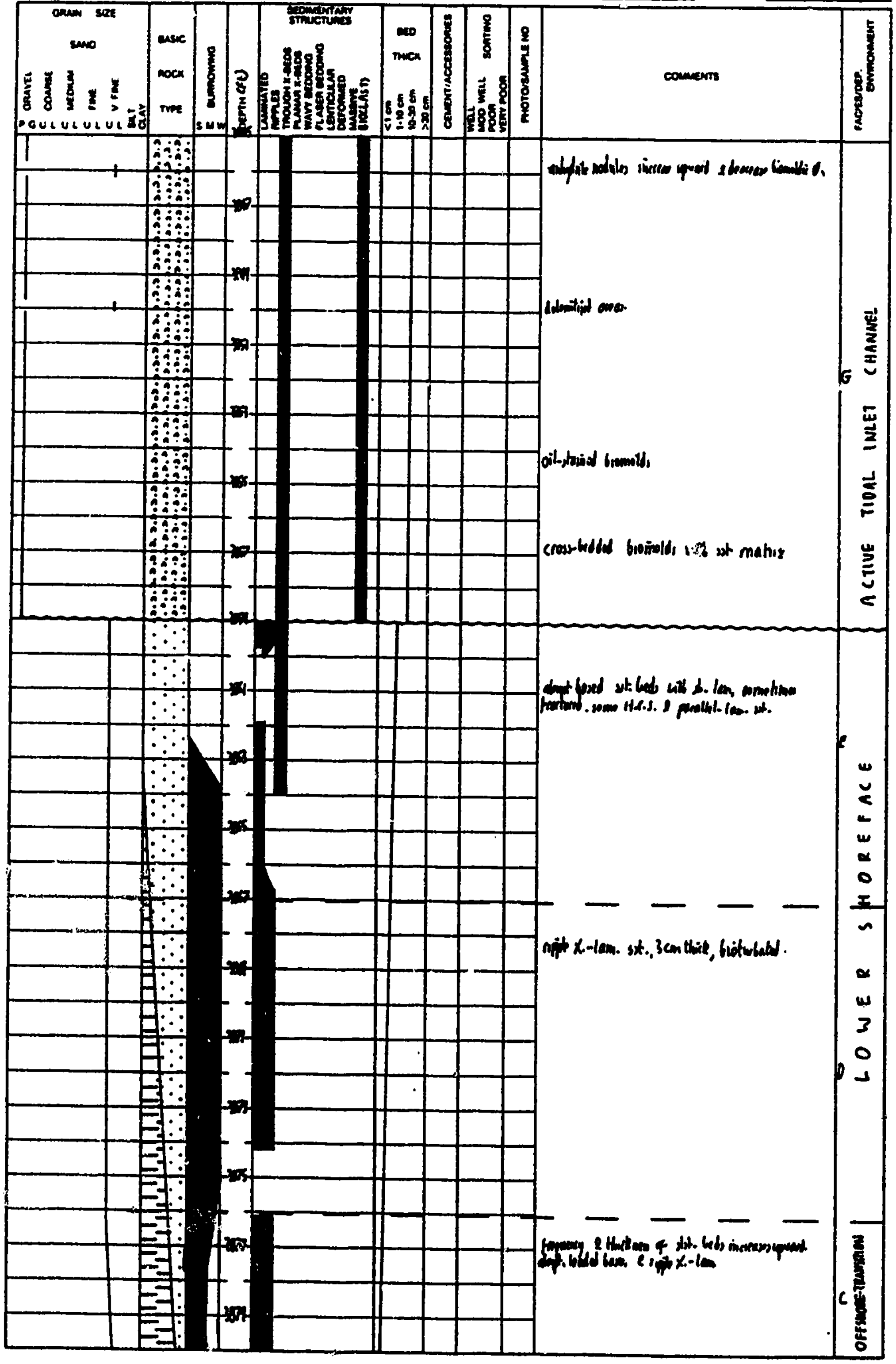

anhydrite nodules increase upward & decrease biomoldic ø.

dolomitized ooze.

oil-stained biomolds

cross-bedded biomolds with slt matrix

sharp based slt. beds with lt. lam, sometimes fractured. some H.C.S. & parallel-lam. slt.

ripple X-lam. slt., 3cm thick, bioturbated.

frequency & thickness of slt. beds increases upward. dispt. bedded lam. & ripple X-lam

WELL NAME: PACIFIC SR CANDEL NANCY d-67-H

FORMATION: HALFWAY-CHARLIE LAKE

DATE: 26/06/90

LOCATION: d-067-H/94-A-15

CORE INTERVAL:

KB: 2351ft

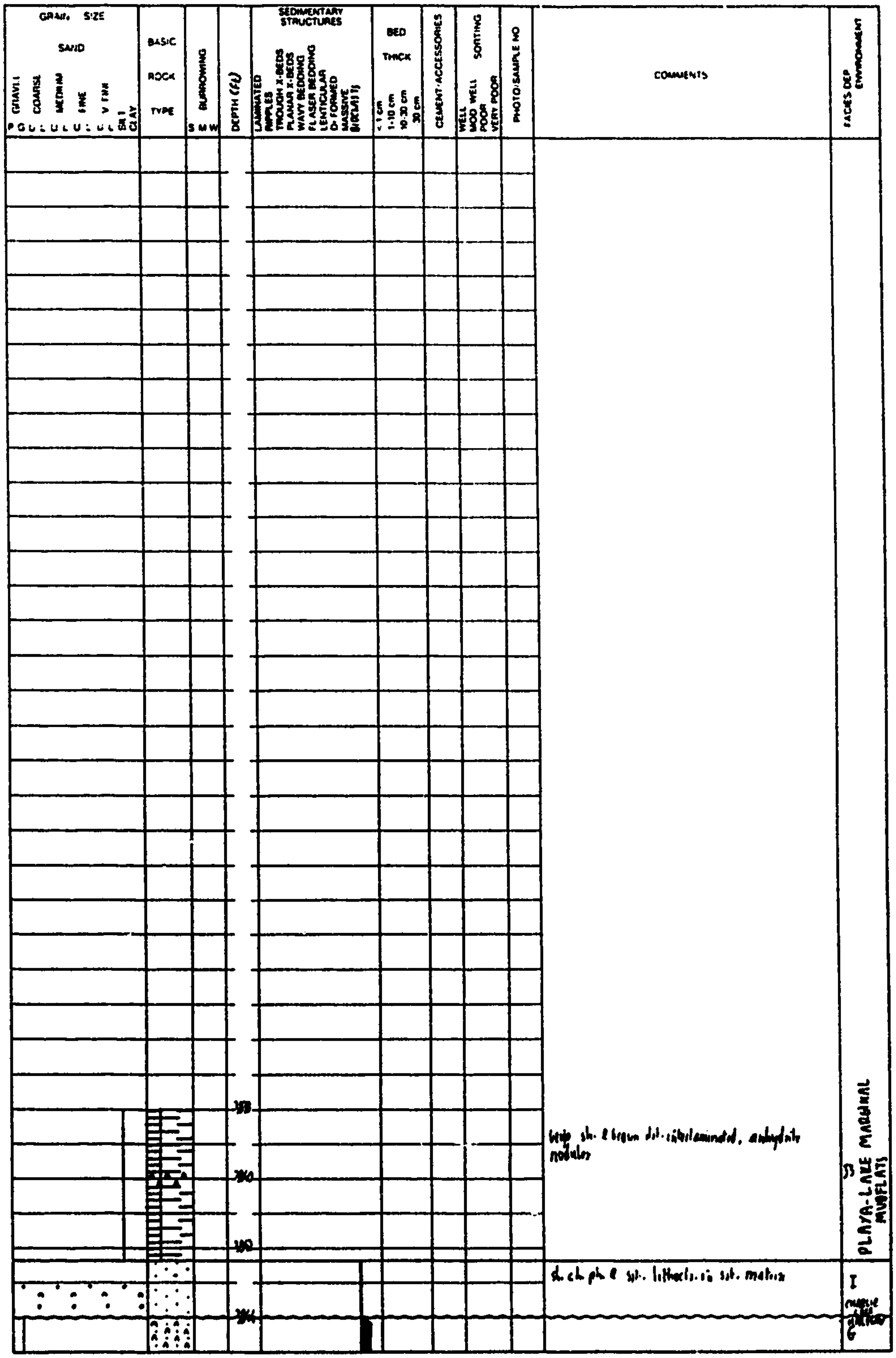

beige sh. & brown dol. siltlaminated, anhydrite nodules

33 PLAYA-LAKE MARGINAL MUDFLATS

sh. cl. ph. & sst. lithoclasts in sst. matrix

I massive

6

WELL NAME: PACIFIC SR CANDEL NANCY d-68-H
FORMATION: HALFWAY-CHARLIE LAKE
DATE: 10/07/90
LOCATION: d-068-H/94-A-15
CORE INTERVAL:
KB: 2353ft

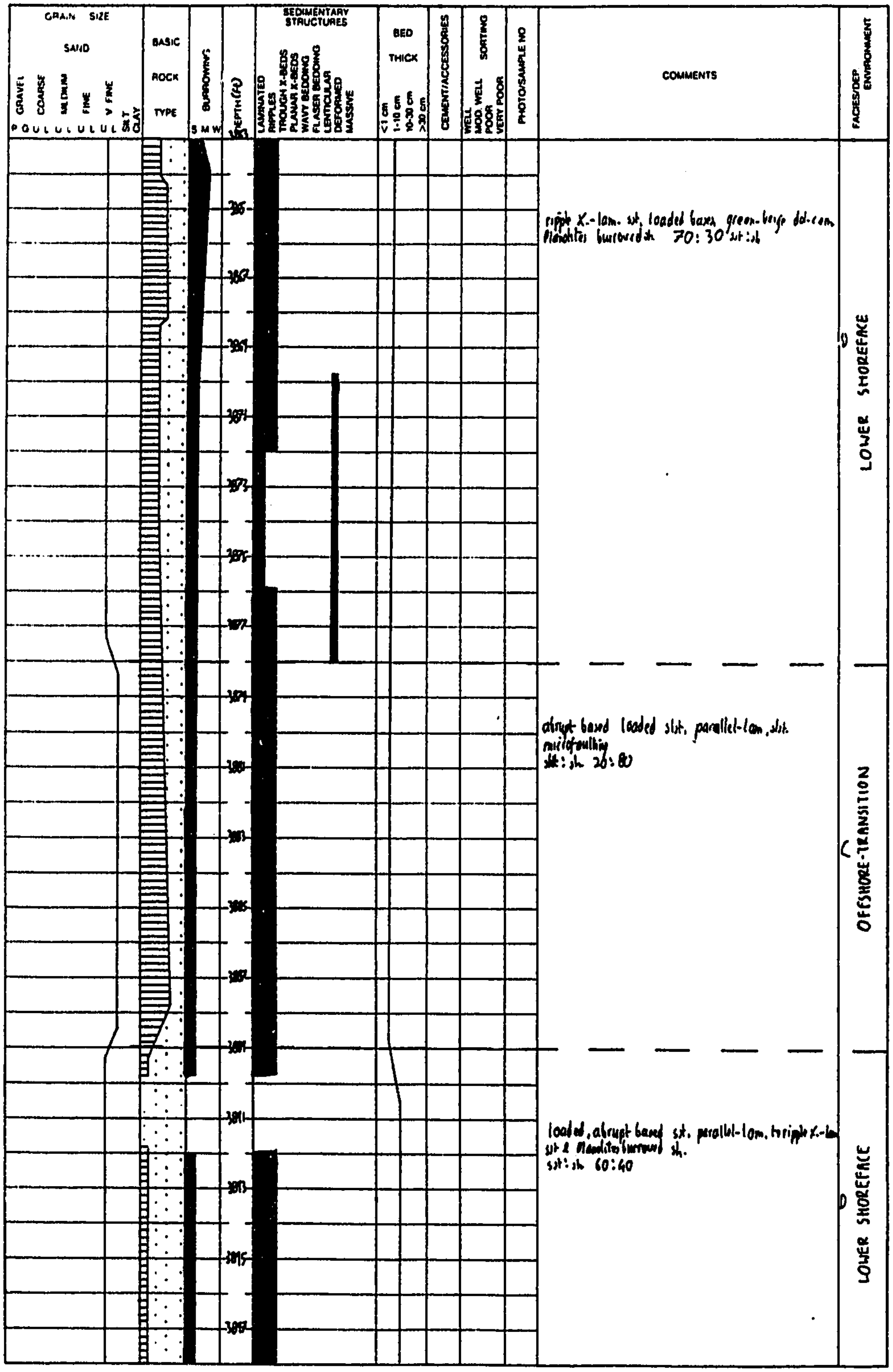

ripple X.-lam. slt, loaded bases green-beige dol-cem.
Planolites burrowed sh. 70:30 slt:sh

abrupt based loaded slt, parallel-lam, slt.
microfaulting
slt:sh 20:80

loaded, abrupt based slt, parallel-lam, ripple X.-lam
slt & Planolites burrowed sh.
slt:sh 60:40

WELL NAME: PACIFIC SR CANDEL NANCY d-68-H FORMATION: HALFWAY- CHARLIE LAKE DATE: 10/07/90

LOCATION: d-068-H/94-A-15 CORE INTERVAL: KB: 2353ft

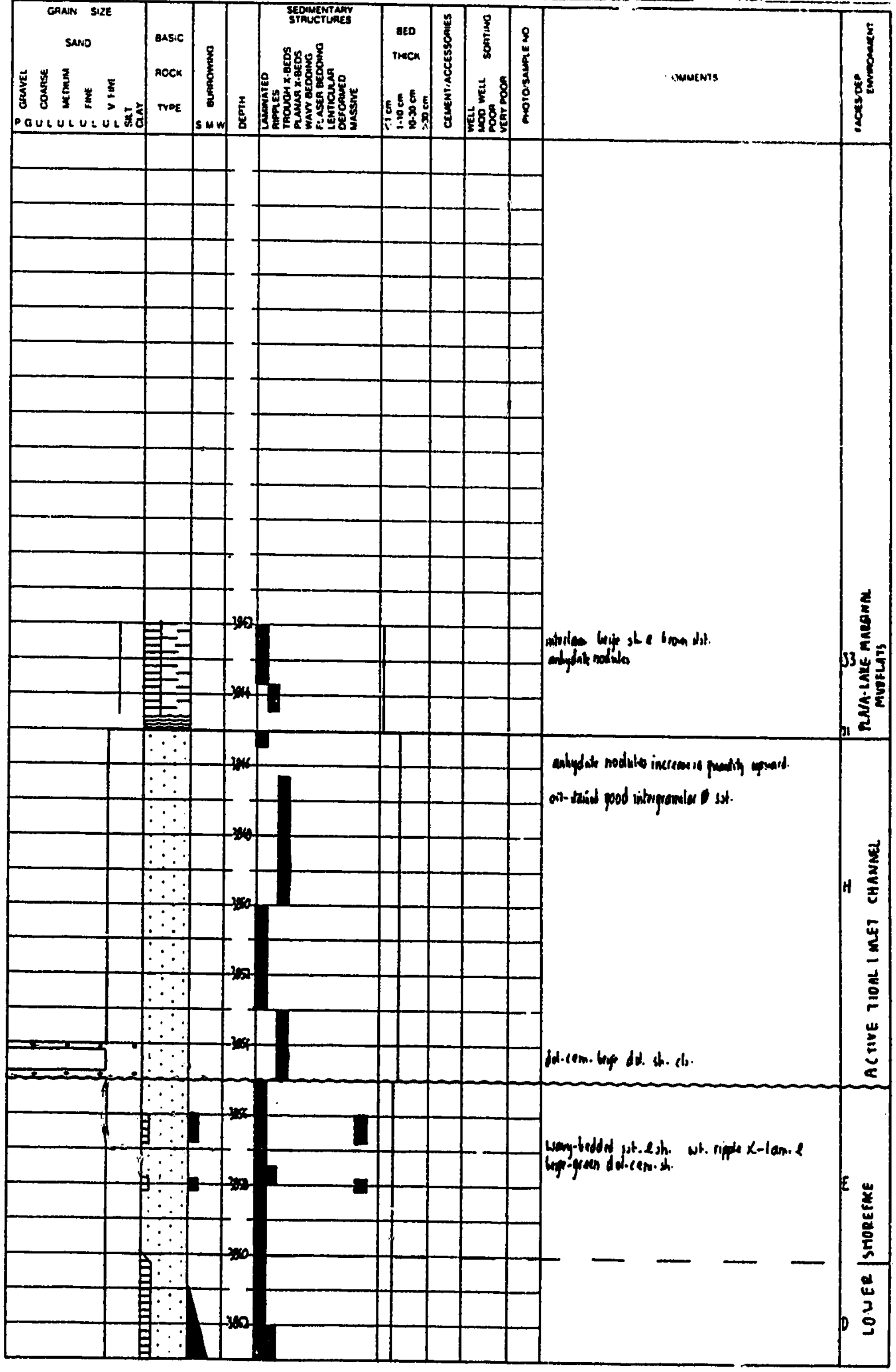

interlam. beige sh. & brown dol.
anhydrite nodules

anhydrite nodules increase in quantity upward.

oil-stained good intergranular Ø sst.

dol-cem. beige dol. sh. cl.

wavy-bedded sst. & sh. wt. ripple X-lam. & beige-green dol-cem. sh.

WELL NAME: PACIFIC SR CANDEL PEEJAY
FORMATION: HALFWAY-CHARLIE LAKE
DATE: 7/08/90
LOCATION: d-071-H/94-A-15
CORE INTERVAL:
KB: 2369.4ft

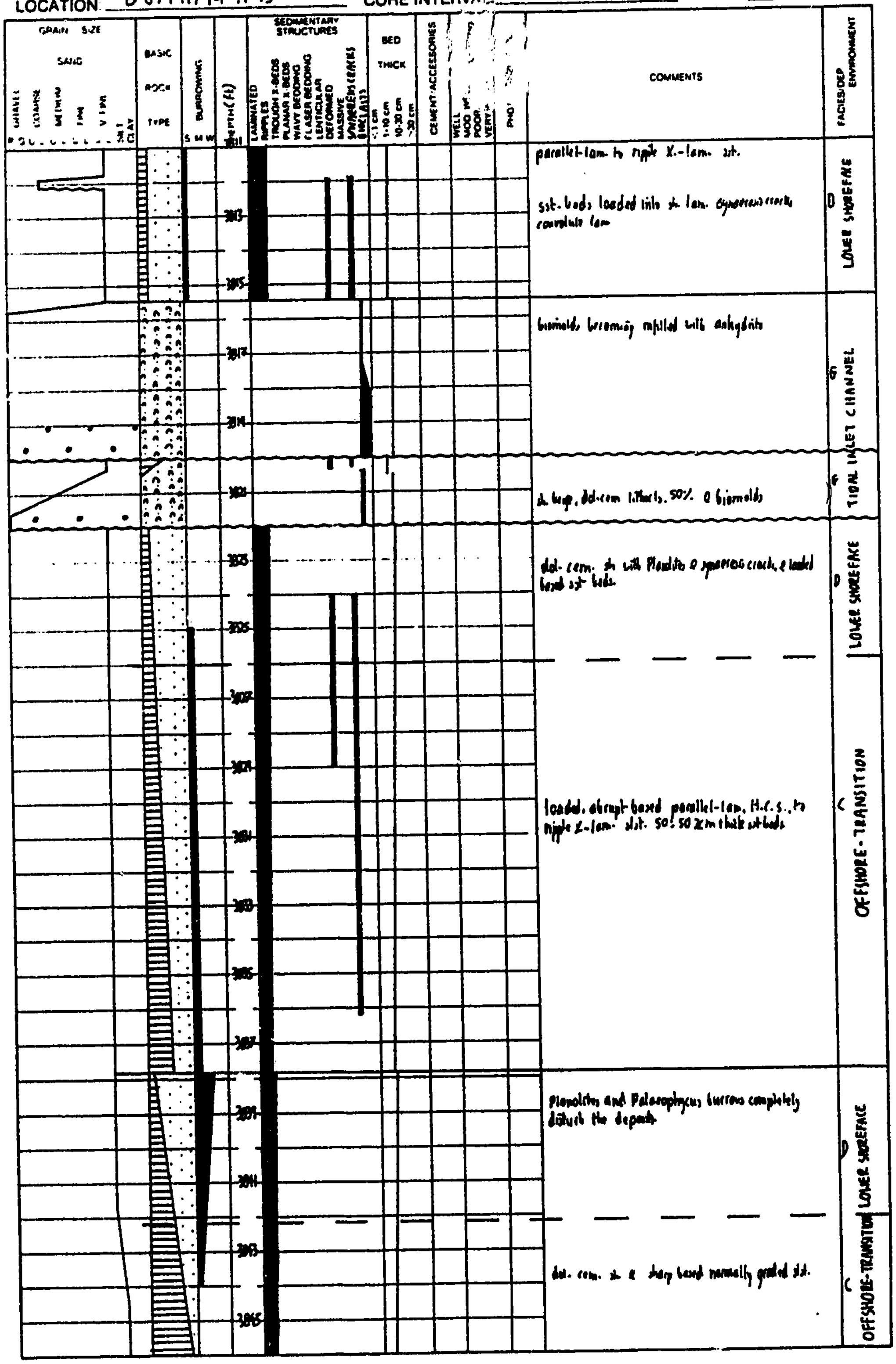

parallel-lam. to ripple X.-lam. slt.

sst. beds loaded into sh. lam. synaeresis cracks, convolute lam

D LOWER SHOREFACE

biomolds becoming infilled with anhydrite

G TIDAL INLET CHANNEL

sh. rip., dol.-cem. lithcls. 50% 0 biomolds

F

dol.-cem. sh with Planolites & synaeresis cracks, & loaded based sst beds.

D LOWER SHOREFACE

loaded, abrupt-based parallel-lam., H.C.S., to ripple X-lam. slst. 50:50 cm thick sst beds

C OFFSHORE-TRANSITION

Planolites and Palaeophycus burrows completely disturb the deposit

D LOWER SHOREFACE

dol. cem. sh. & sharp based normally graded slt.

C OFFSHORE-TRANSITION

WELL NAME: PACIFIC SR CANDEL PEEJAY
FORMATION: HALFWAY-CHARLIE LAKE
DATE: 7/08/90
LOCATION: d-07i-H/94-A-15
CORE INTERVAL:
KB: 2369.4ft

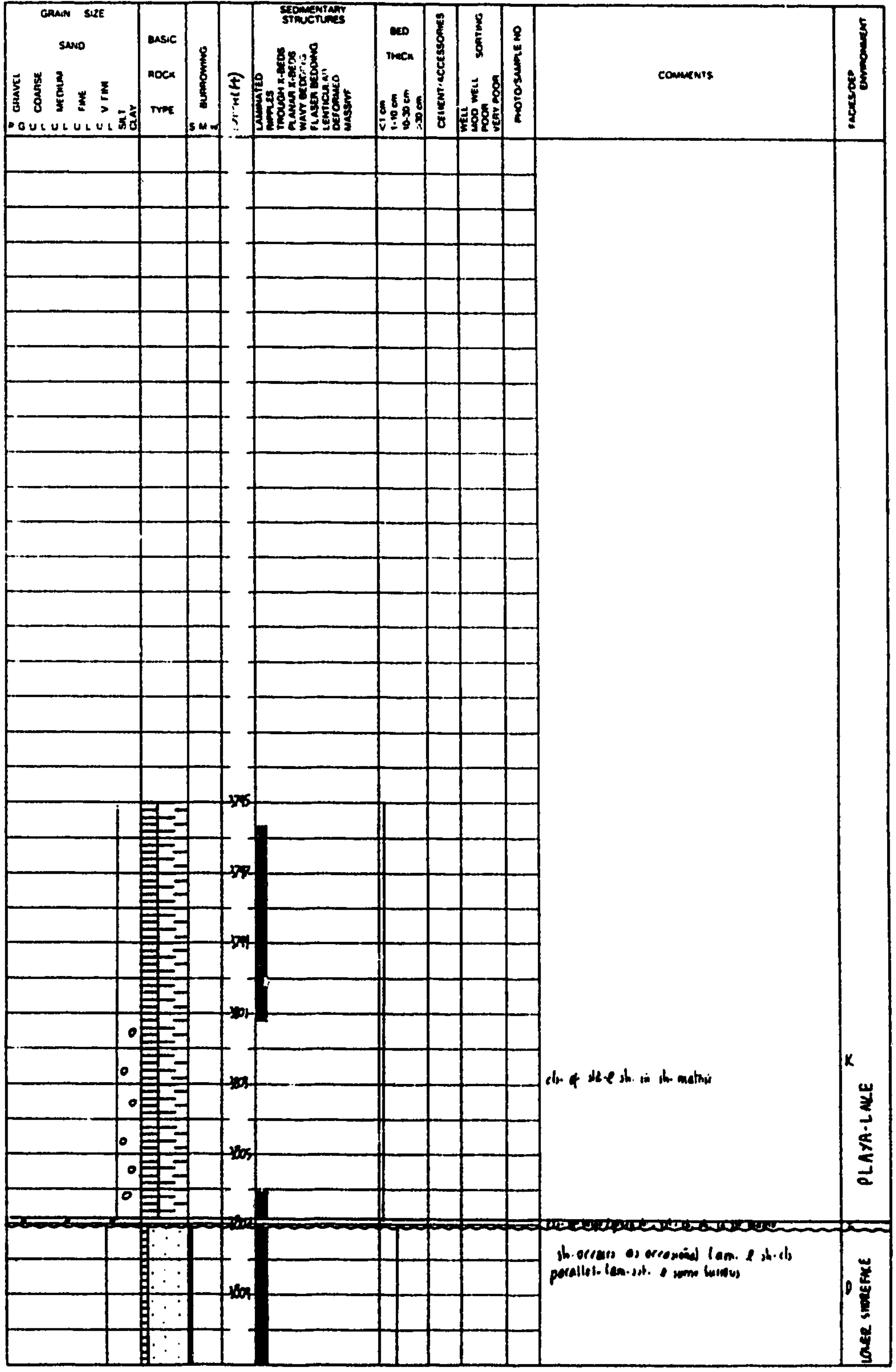

cls. of red & gr sh. in sh. matrix

[illegible]

sh. occurs as occasional lam. & sh. cls parallel lam. sst. & some burrows

K PLAYA-LAKE

D LOWER SHOREFACE

WELL NAME: PACIFIC ET AL PEEJAY 6-74-H
FORMATION: HALFWAY-CHARLIE LAKE
DATE: 20/07/90
LOCATION: 6-074-H/94-A-15
CORE INTERVAL:
KB: 2366.15ft

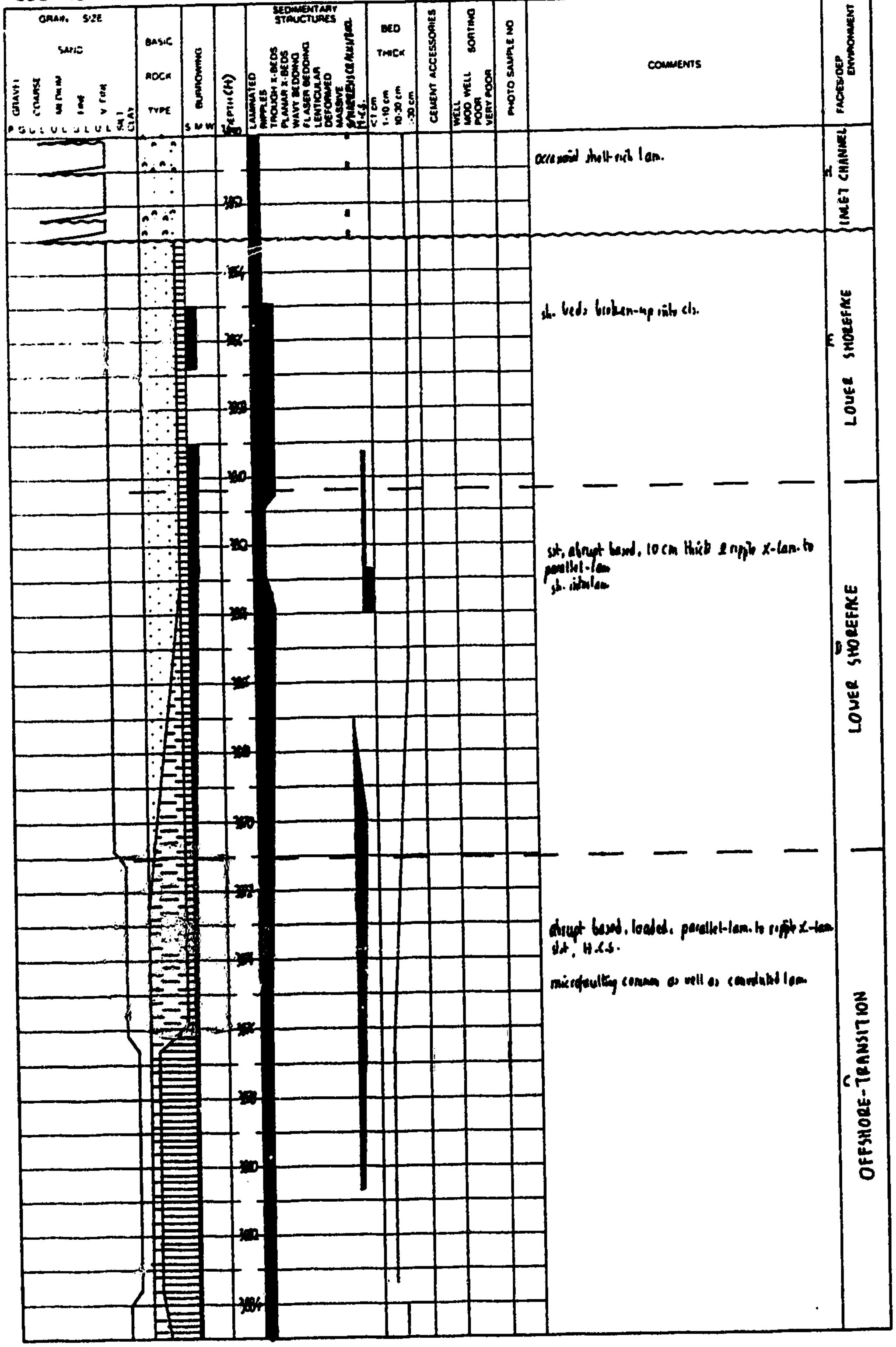

occasional shell-rich lam.

sh. beds broken-up into cls.

sst, abrupt based, 10 cm thick & ripple X-lam. to parallel-lam
sh. interlam

abrupt based, loaded, parallel-lam. to ripple X-lam sst, H.C.S.

microfaulting common as well as convoluted lam.

WELL NAME: PACIFIC ET AL PEEJAY 6-74-H FORMATION: HALFWAY-CHARLIE LAKE DATE: 20/07/90

LOCATION: 6-074-H/94-A-15 CORE INTERVAL: KB: 2366.15ft

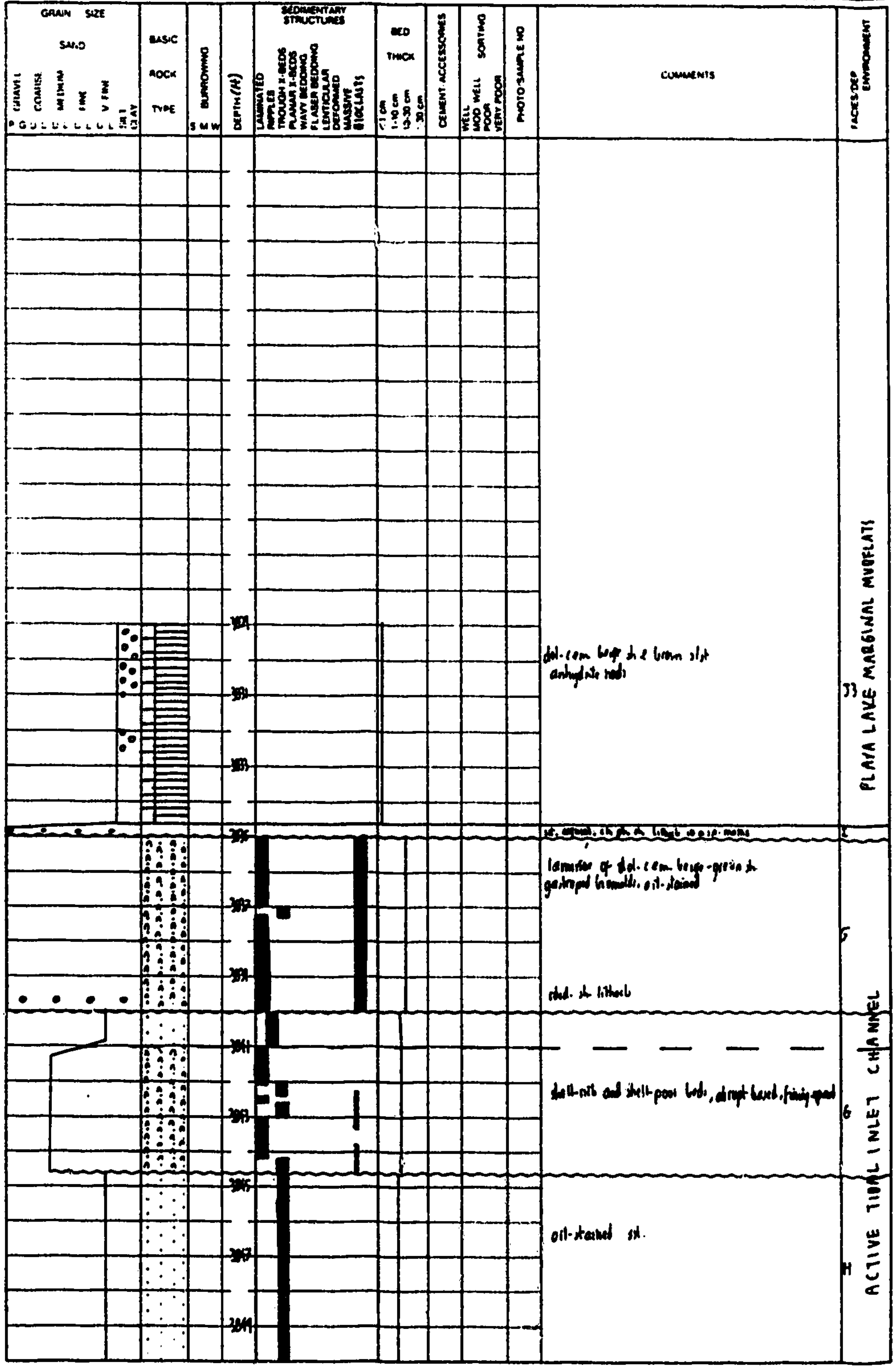

dol-cem beige sh & brown slst
anhydrite nods

st, [illegible], ch [illegible] lithocl [illegible]

laminae of dol. cem. beige-green sh
gastropod bimoulds, oil-stained

rded. sh lithocl

shell-rich and shell-poor beds, abrupt based, fining upward

oil-stained st.

WELL NAME: PACIFIC ET AL PEEJAY 6-75-H FORMATION: HALFWAY-CHARLIE LAKE DATE: 29/01/91

LOCATION: 6-075-H/94-A-15 CORE INTERVAL: KB: 2357ft

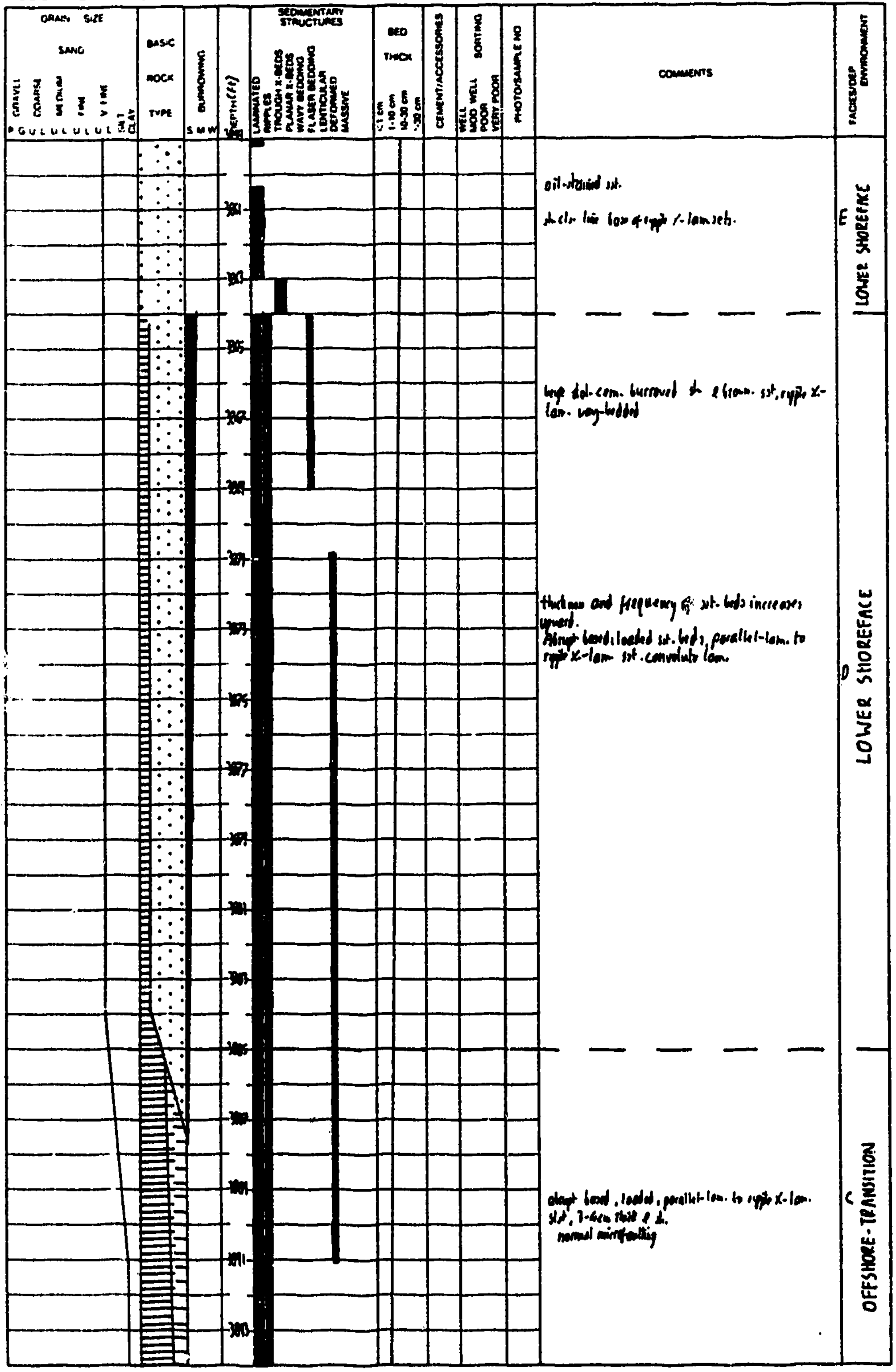

oil-stained sst.

sh. clr. lim. box of ripple X-lam. sst.

large dol-cem. burrowed sh. & brown. sst, ripple X-lam. wavy-bedded

thickness and frequency of sst. beds increases upward.
Abrupt based, loaded sst. beds, parallel-lam. to ripple X-lam sst. convolute lam.

abrupt based, loaded, parallel-lam. to ripple X-lam. slst, 1-4cm thick & sh.
normal microfaulting

WELL NAME: PACIFIC ET AL PEEJAY 6-75-H FORMATION: HALFWAY-CHARLIE LAKE DATE: 29/01/91

LOCATION: 6-075-H/94-A-15 CORE INTERVAL: KB: 2357ft

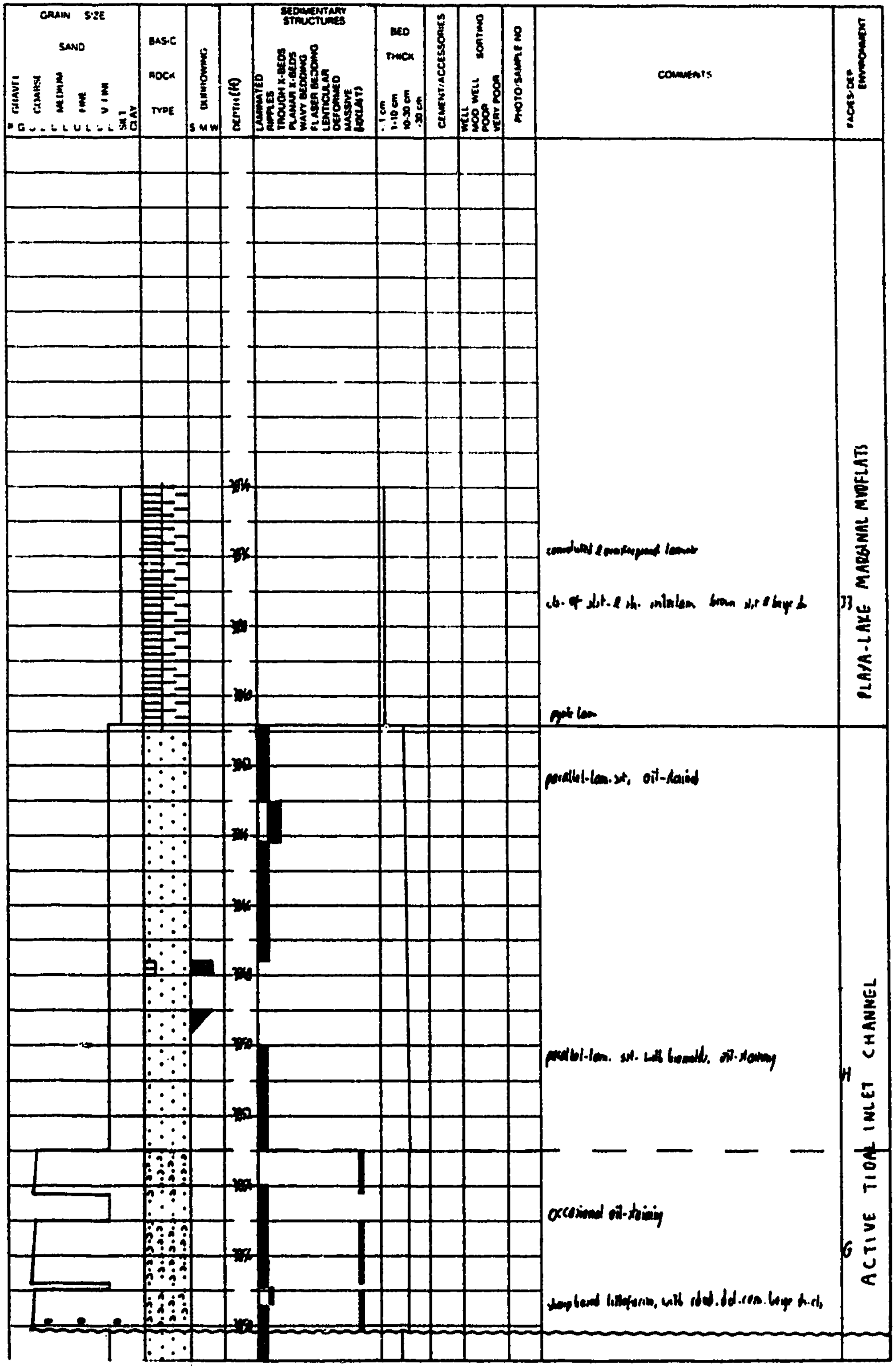

WELL NAME: PACIFIC SR CANDEL NANCY d-75-H FORMATION: HALFWAY-CHARLIE-LAKE DATE: 23/07/90

LOCATION: d-075-H/94-A-15 CORE INTERVAL: KB: 2360.6ft

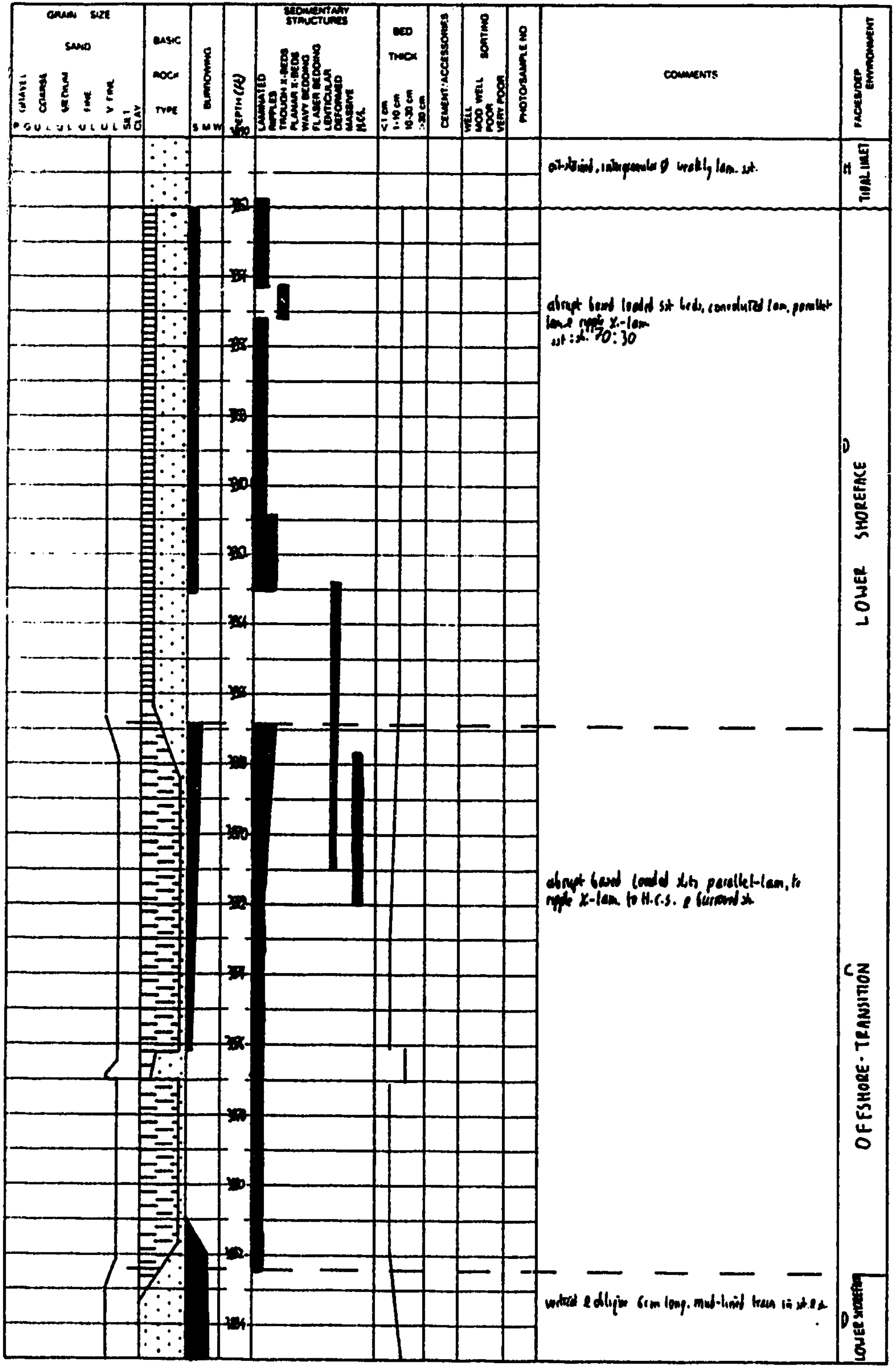

oil-stained, intergranular Ø weakly lam. sst.

abrupt based loaded sst beds, convoluted lam, parallel lam. & ripple X-lam.
sst:sh. 70:30

abrupt based loaded slts parallel-lam, to ripple X-lam. to H.C.S. & burrowed sh.

vertical & oblique 6cm long. mud-lined traces in sst.

WELL NAME: PACIFIC SR CANDEL NANCY

FORMATION: HALFWAY-CHARLIE LAKE

DATE: 23/07/90

LOCATION: d-075-H/94-A-15

CORE INTERVAL:

KB: 2360.6ft

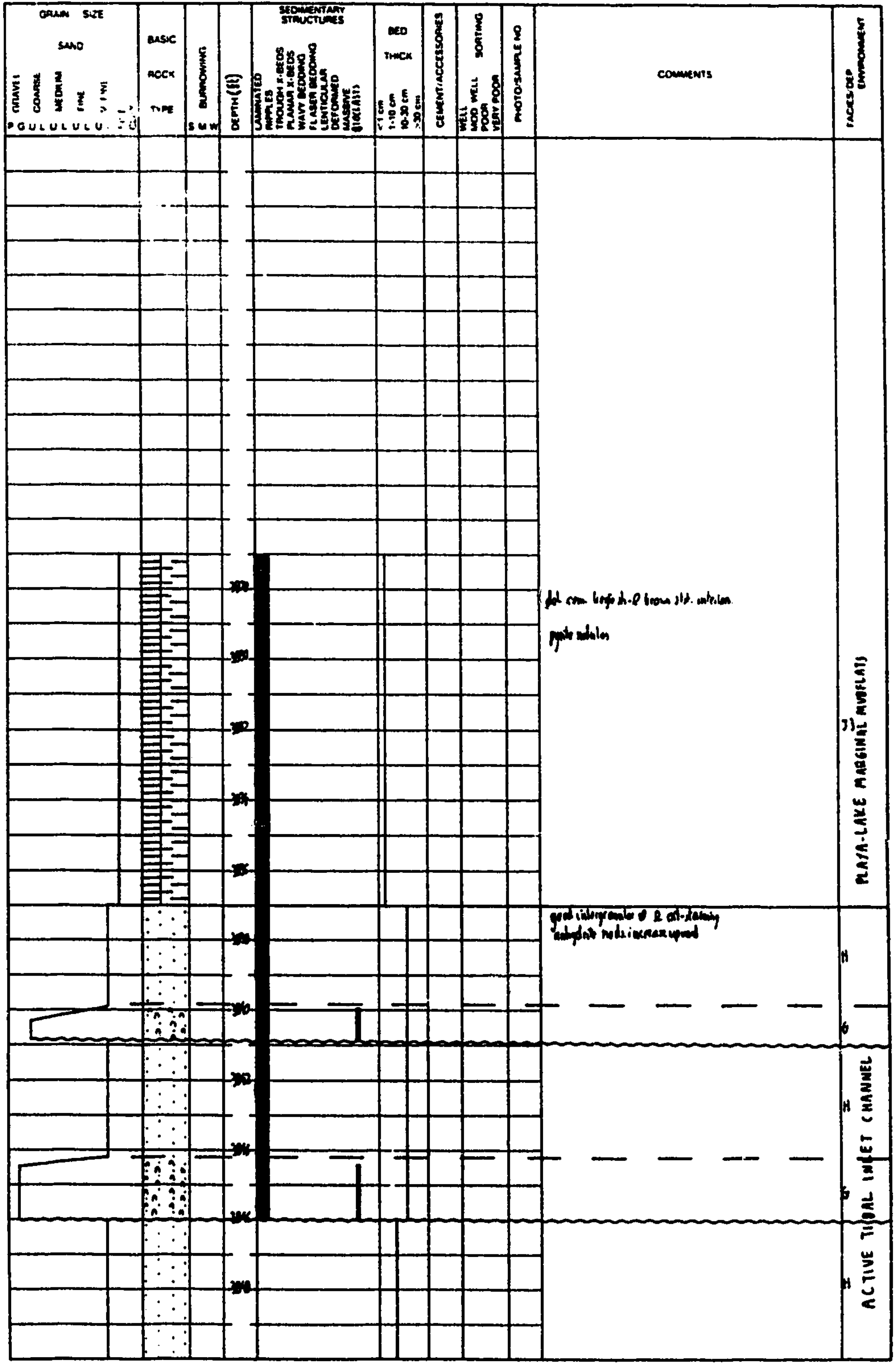

dol. cem. [illegible] brown slt. intclasts.

pyrite nodules

good intergranular ø & oil-staining

anhydrite nodules increase upward

WELL NAME: JENN NANCY A d-77-H

FORMATION: HALFWAY-CHARLIE LAKE

DATE: 10/07/90

LOCATION: d-077-H/94-A-15

CORE INTERVAL:

KB: 2353.9ft

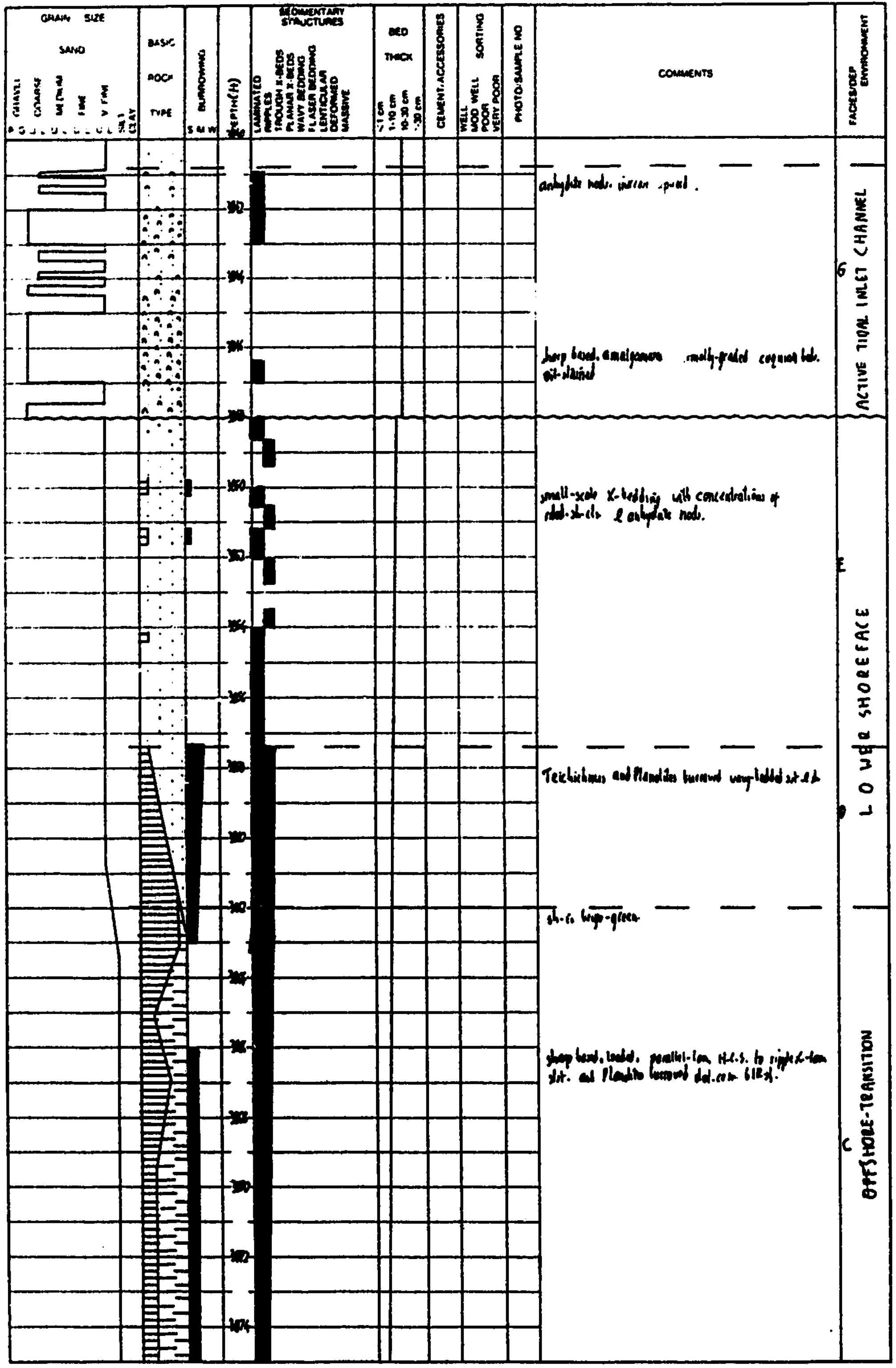

anhydrite nods. [illegible] .pvd.

sharp based, amalgamated crudely-graded coquina bds. oil-stained

small-scale X-bedding with concentration of shell-debris & anhydrite nods.

Teichichnus and Planolites burrowed wavy-bedded sst & sh.

sh.-cl. beige-green

sharp based, loaded, parallel-lam. H.C.S. to ripple X-lam slst. and Planolites burrowed dol.-cem. [illegible].

WELL NAME: TENN NANCY A d-77-H FORMATION: HALFWAY-CHARLIE LAKE DATE: 10/07/90

LOCATION: d-077-H/94-A-15 CORE INTERVAL: KB: 2353 ft

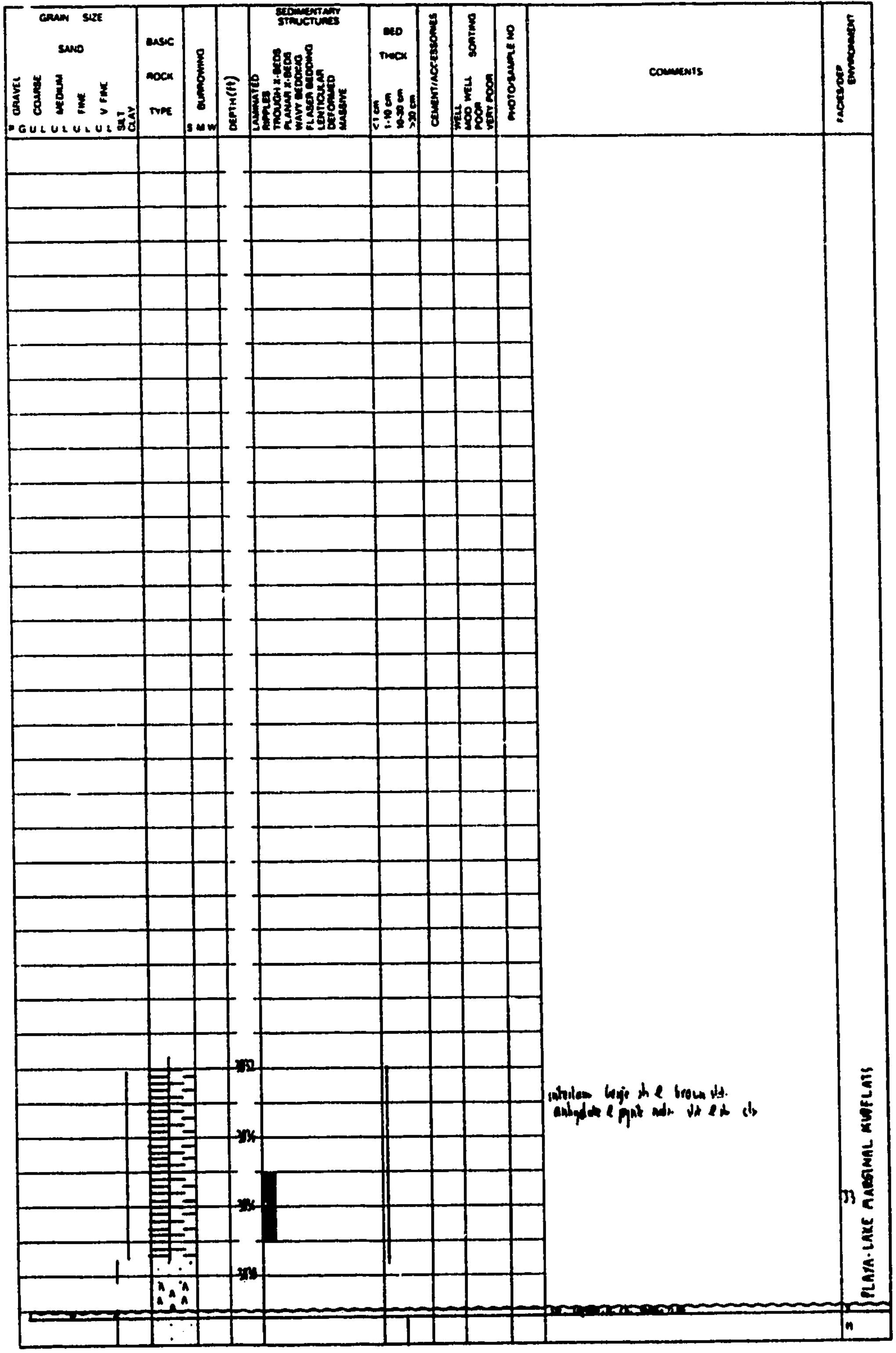

interlam beige sh & brown slt.
anhydrite & pink nod. slt & sh clr

WELL NAME: TENN NANCY d-78-H FORMATION: HALFWAY-CHARLIE LAKE DATE: 22/06/90

LOCATION: d-078-H/94-A-15 CORE INTERVAL: KB: 2353.1ft

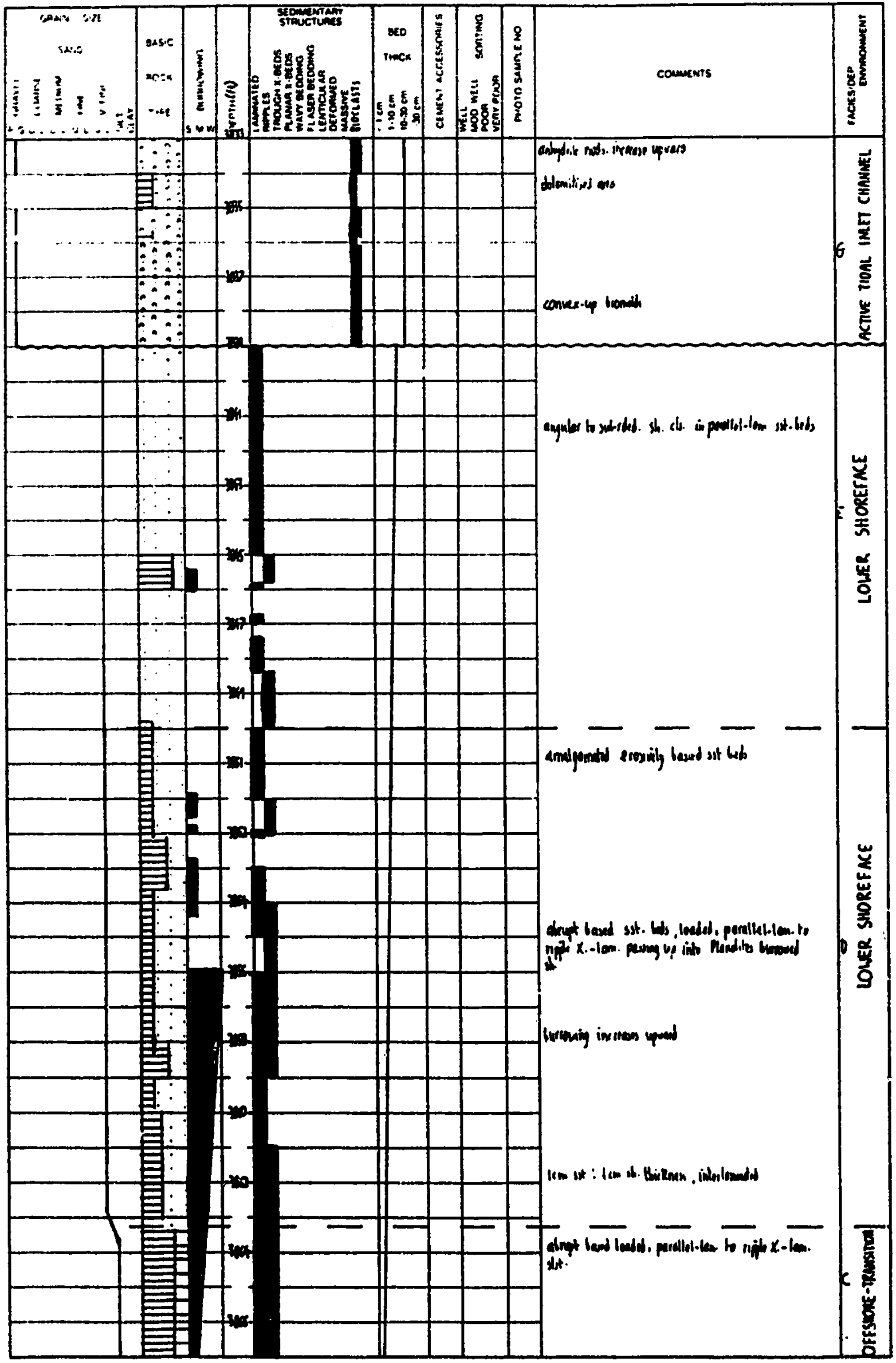

anhydrite nods. increase upwards

dolomitized ooids

convex-up bioclasts

angular to sub-rded. sh. cls. in parallel-lam. sst. beds

amalgamated erosively based sst beds

abrupt based sst. beds, loaded, parallel-lam. to ripple X.-lam. passing up into Planolites burrowed sh.

burrowing increases upward

1cm sst : 1cm sh. thickness, interlaminated

abrupt based loaded, parallel-lam. to ripple X.-lam. sst.

WELL NAME: TENN NANCY d-78-H FORMATION: HALFWAY-CHARLIE LAKE DATE: 22/06/90

LOCATION: d-078-H/94-A-15 CORE INTERVAL: KB: 2353.1ft

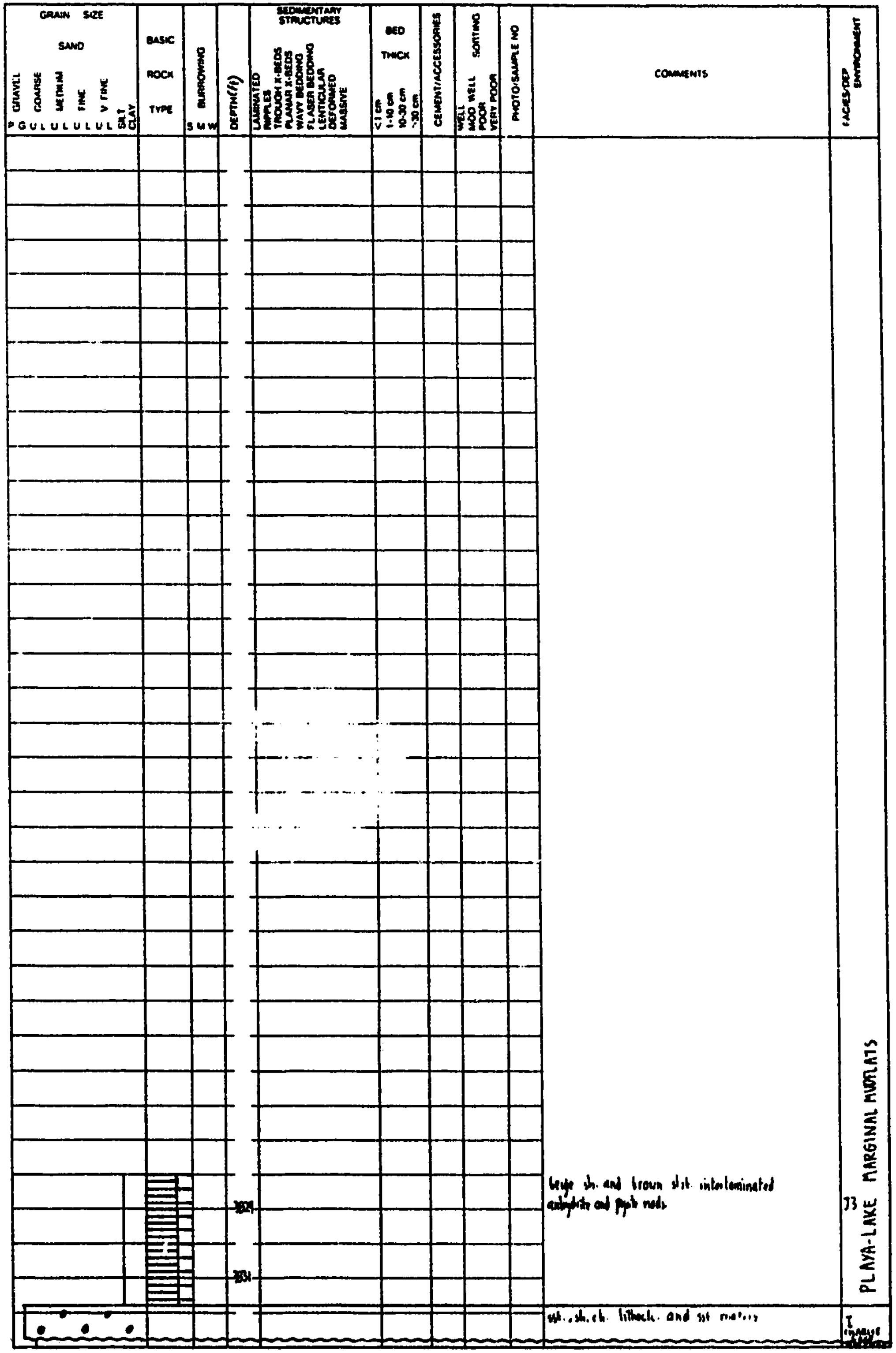

beige sh. and brown slst. interlaminated anhydrite and gypsum nods

sst., sh., ch. lithocl. and sst matrix

WELL NAME: PACIFIC SR CAN DEL PEEJAY d-81-H FORMATION: HALFWA/ CHARLIE LAKE DATE: 28/01/91

LOCATION: d-081-H/94-A-15 CORE INTERVAL: KB: 2371ft

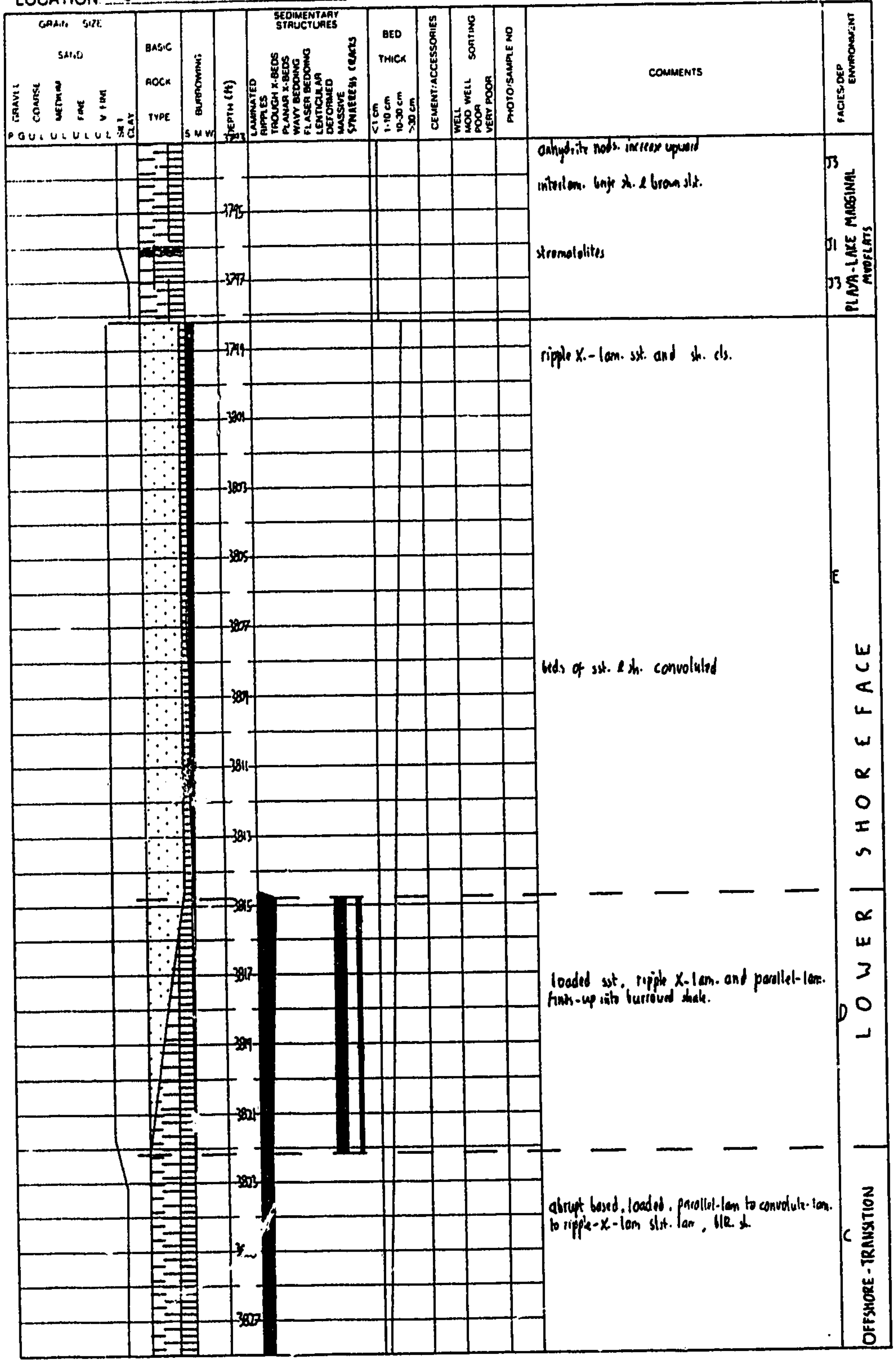

anhydrite nods. increase upward

interlam. beige sh. & brown slt.

stromatolites

ripple X.-lam. sst. and sh. cls.

beds of sst. & sh. convoluted

loaded sst, ripple X-lam. and parallel-lam. fines-up into burrowed shale.

abrupt based, loaded, parallel-lam to convolute-lam. to ripple-X-lam slst. lam, blk. sh.

WELL NAME: PACIFIC SR SINCLAIR PEEJAY FORMATION: HALFWAY-CHARLIE LAKE DATE 6/02/91

LOCATION d-084-H/94-A-15 CORE INTERVAL: KB 2360ft.

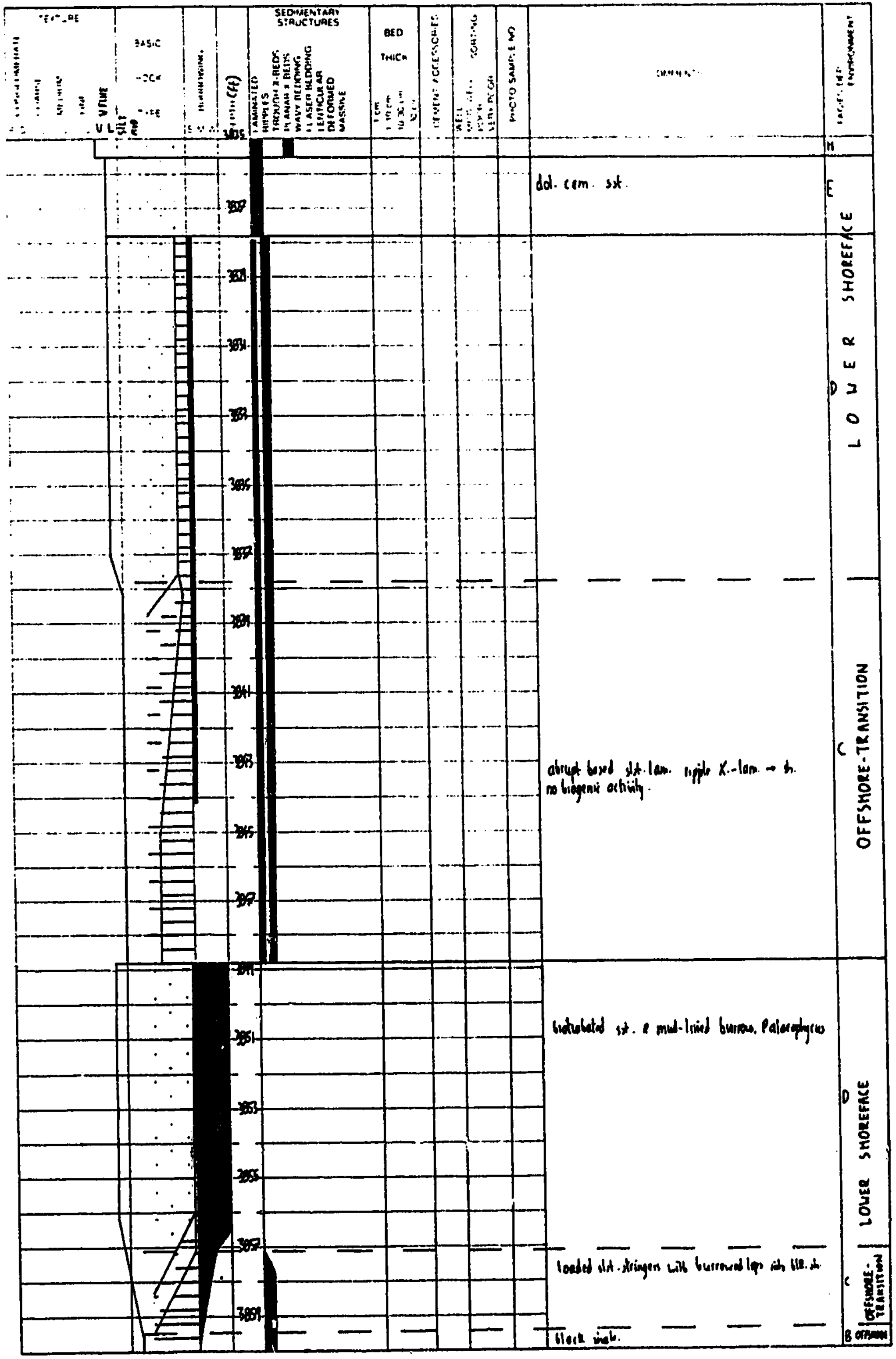

dol. cem. sst.

abrupt based slt.-lam. ripple X.-lam. → sh.
no biogenic activity.

bioturbated sst. c mud-lined burrows. Paleophycus

loaded slt. stringers with burrowed tops into sh.

black shale.

WELL NAME PACIFIC SR SINCLAIR PEEJAY FORMATION: HALFWAY-CHARLIE LAKE DATE: 6/02/91

LOCATION d-084-H/94-A-15 CORE INTERVAL: KB: 2360ft

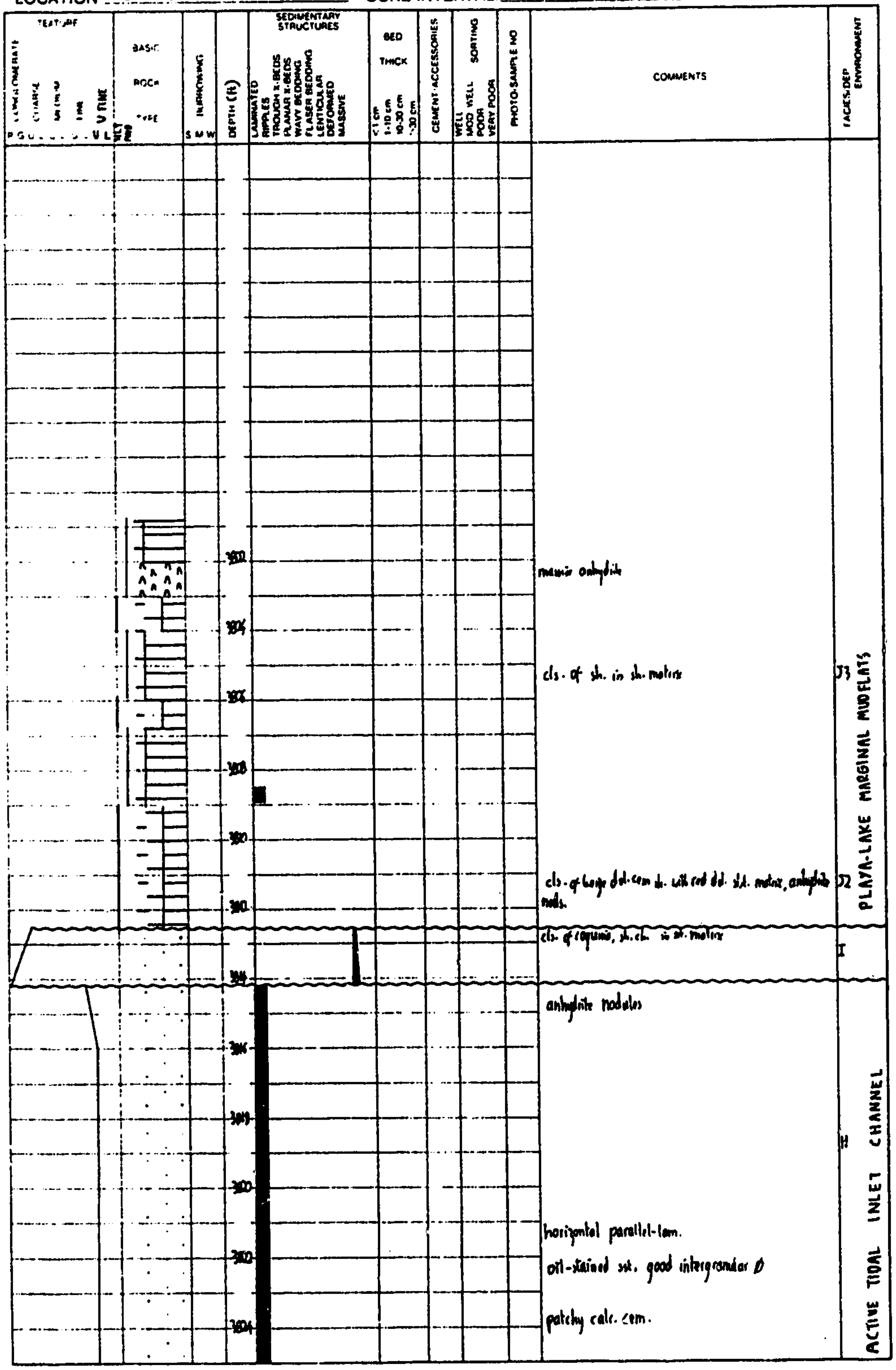

massive anhydrite

cls. of sh. in sh. matrix

J3

cls. of large dol.-cem. sh. with red dol. slt. matrix, anhydrite nods.

J2

PLAYA-LAKE MARGINAL MUDFLATS

cls. of coquina, sh.cl. in sst. matrix

I

anhydrite nodules

horizontal parallel-lam.

oil-stained sst. good intergranular ϕ

patchy calc. cem.

H

ACTIVE TIDAL INLET CHANNEL

WELL NAME PACIFIC SR CAN DEL NANCY d-85-H FORMATION: HALFWAY-CHARLIE LAKE DATE 12/07/90

LOCATION: d-085-H/94-A-15 CORE INTERVAL: KB 2357ft

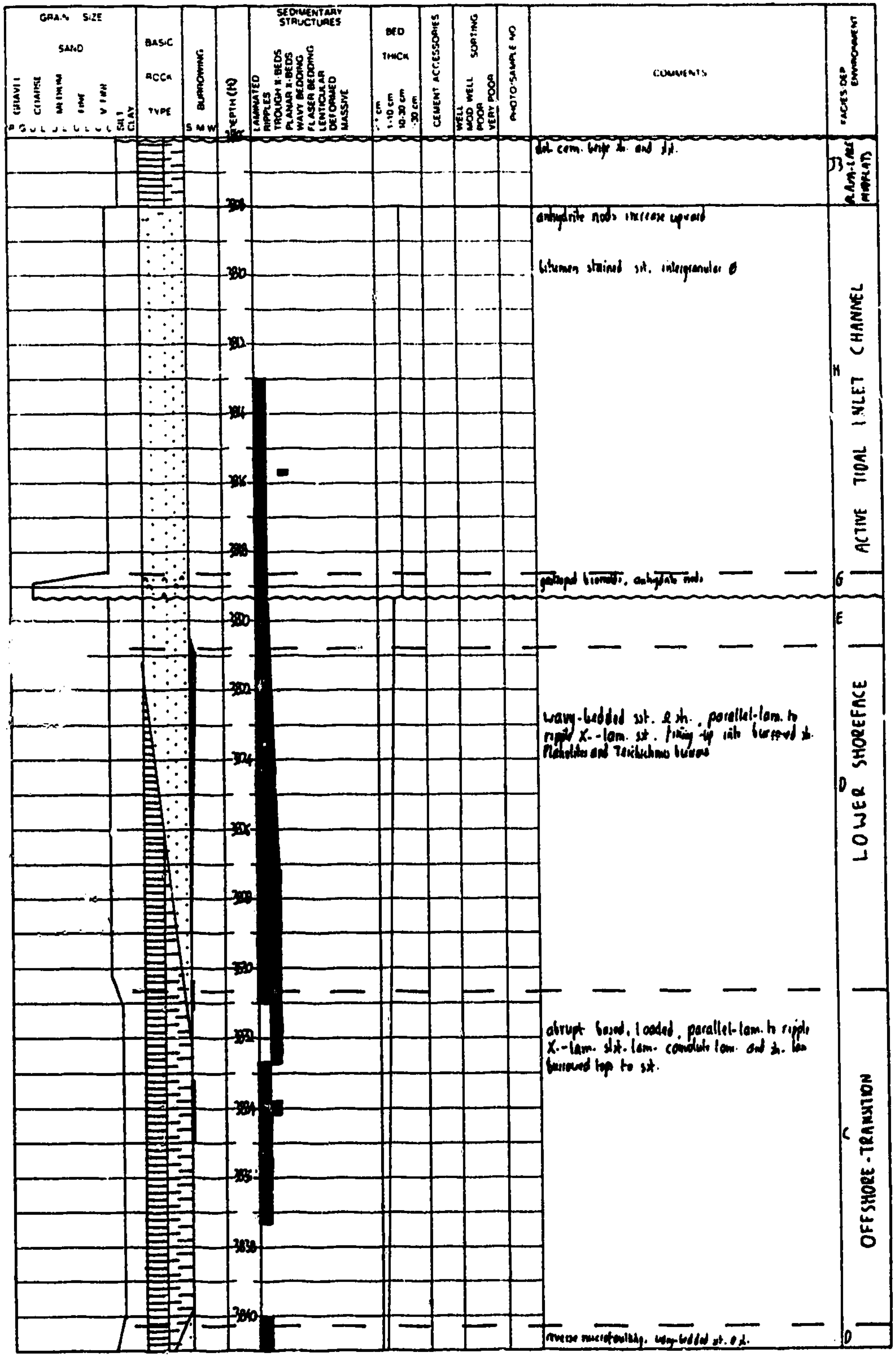

dol. cem. brgz sh. and slt.

anhydrite nods increase upward

bitumen stained slt. intergranular ø

garlanded biomolds, anhydrite nods

wavy-bedded slt. & sh., parallel-lam. to ripple X.-lam. slt. fining-up into burrowed sh. Planolites and Teichichnus burrows

abrupt based, loaded, parallel-lam. to ripple X.-lam. slst.-lam. convolute lam. and sh. lam burrowed top to slt.

massive microfaulting, wavy-bedded slt. & sh.

WELL NAME TENN PEEJAY 6-86-H FORMATION: HALFWAY-CHARLIE LAKE DATE: 11/07/90

LOCATION b-086-H/94-A-15 CORE INTERVAL: KB: 2353ft

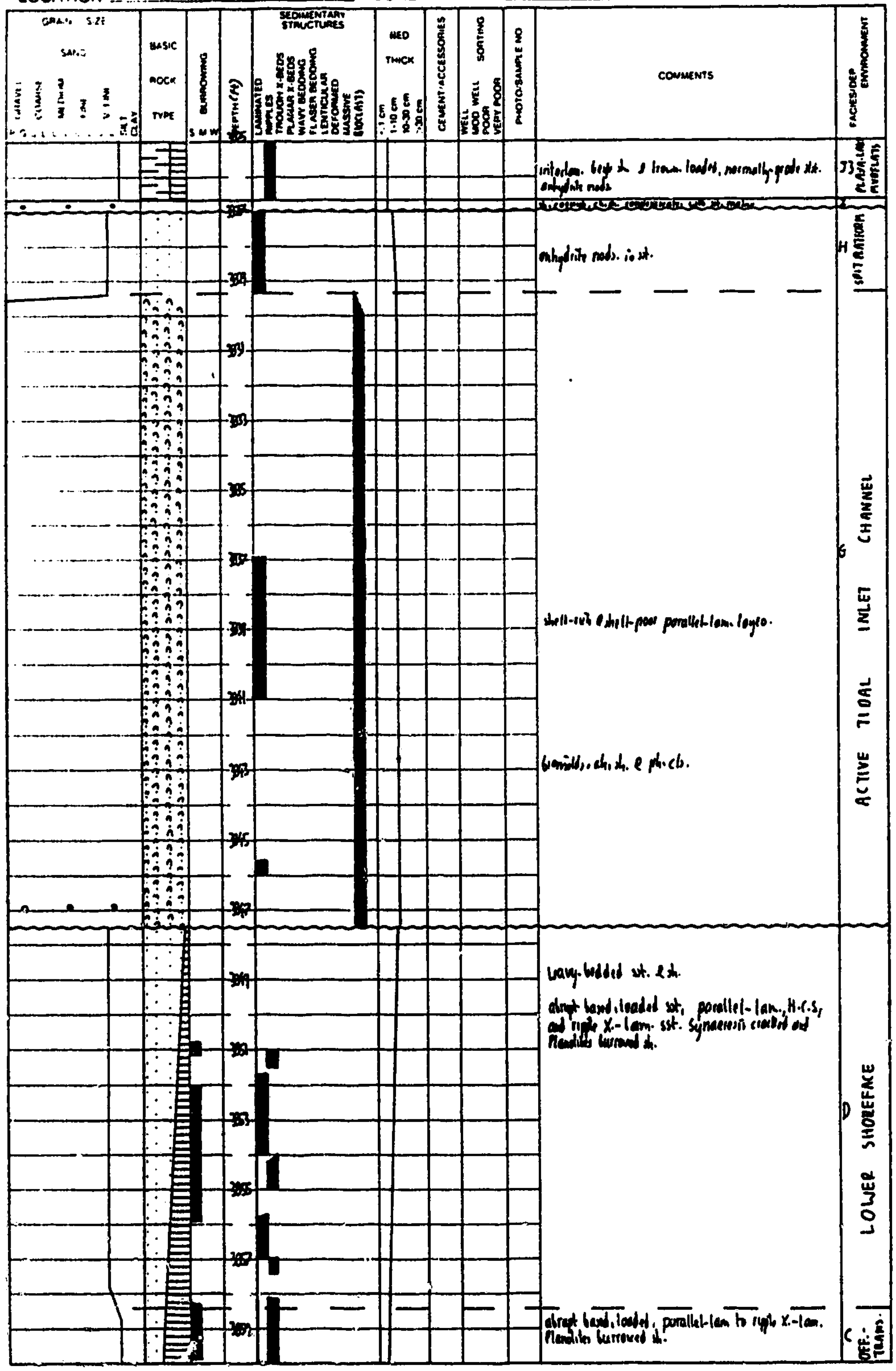

interlam. burr. sh. & lam. loaded, normally-grade sst. anhydrite nods

[illegible] conglomerate [illegible]

anhydrite nods. in st.

shell-rich & shell-poor parallel-lam. layers.

bimodal, ch. sh. & ph. cb.

wavy-bedded slt. & sh.

abrupt based, loaded slt, parallel-lam., H.C.S, and ripple X.-lam. sst. Synaeresis cracked and Planolites burrowed sh.

abrupt based, loaded, parallel-lam to ripple X.-lam. Planolites burrowed sh.

WELL NAME: TENN PEEJAY 6-86-H FORMATION: HALFWAY-CHARLIE LAKE DATE 11/07/90

LOCATION: 6-086-H/94-A-15 CORE INTERVAL: KB: 2353ft

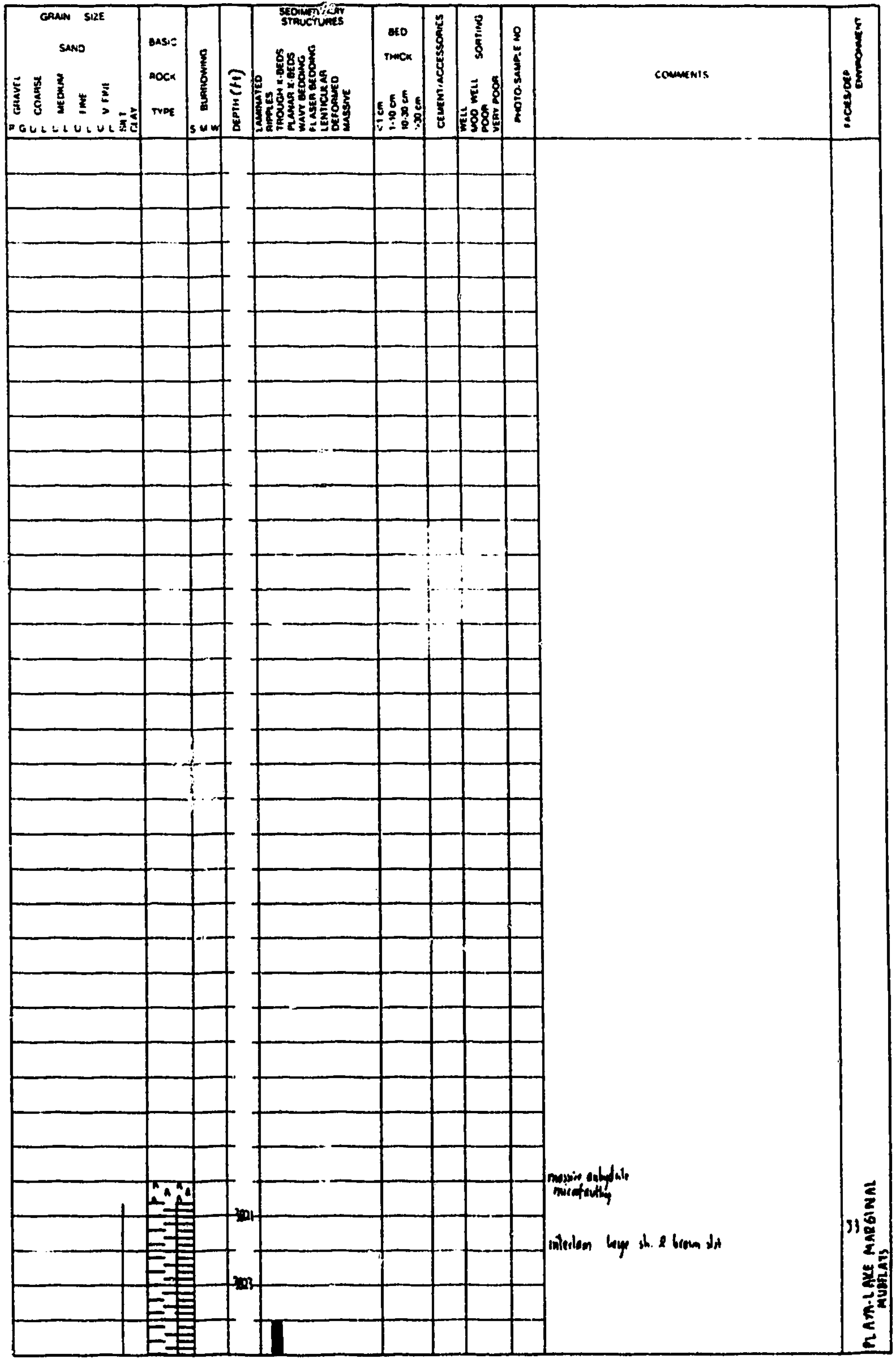

massive anhydrite microfaulting

interlam beige sh. & brown slst

WELL NAME TENN NANCY d-86-H FORMATION: HALFWAY-CHARLIE LAKE DATE: 23/07/90

LOCATION d-086-H/94-A-15 CORE INTERVAL: KB: 2360.75ft

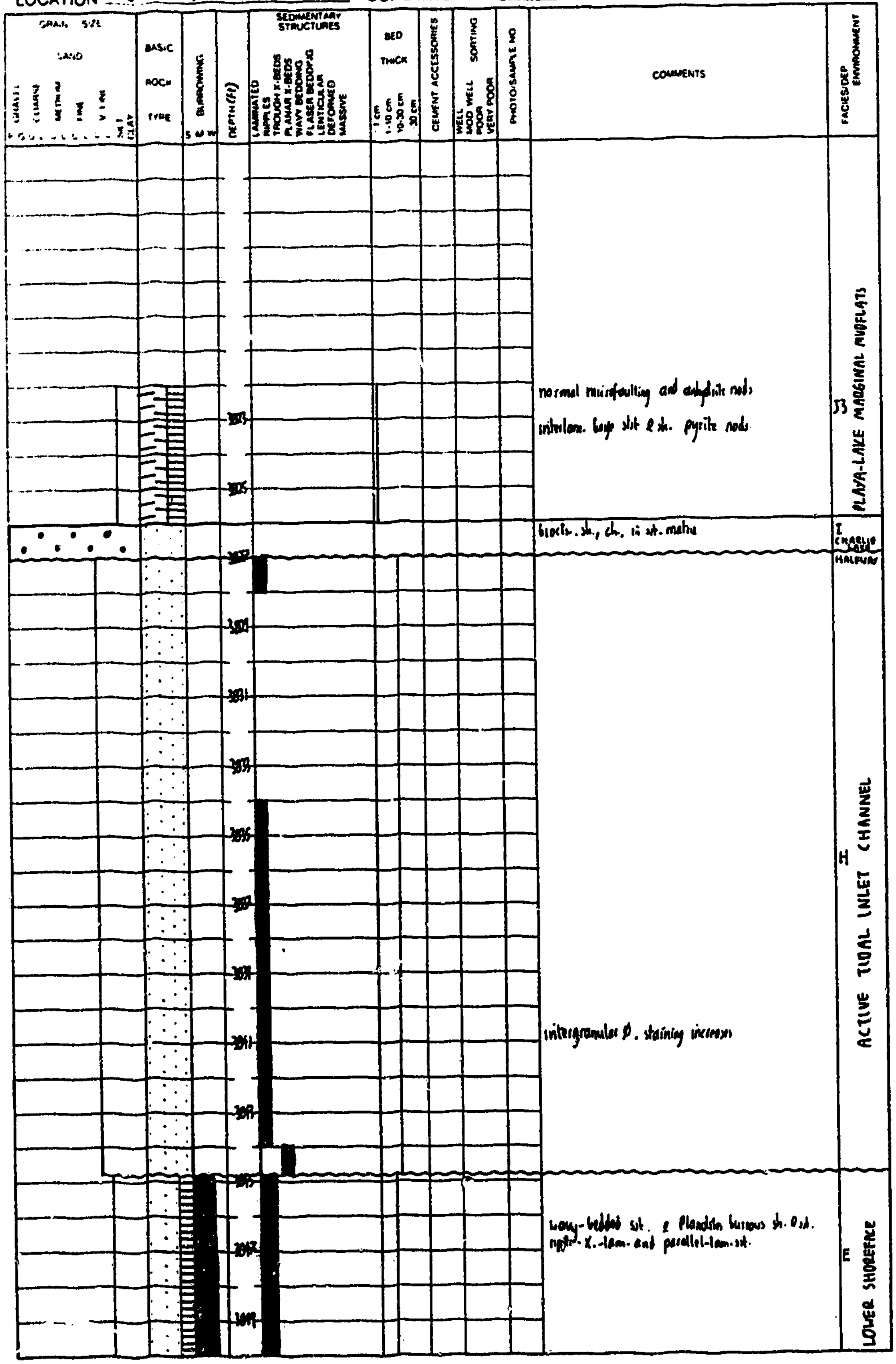

normal microfaulting and anhydrite nods

interlam. beige slt & sh. pyrite nods

breccia. sh., ch., in slt. matrix

intergranular ∅. staining increases

wavy-bedded slt. & Planolites burrows sh. & sd.
ripple-X.-lam- and parallel-lam.-slt.

WELL NAME: SILVERTON PEEJAY d-89-H FORMATION: HALFWAY-CHARLIE LAKE DATE: 25/06/90

LOCATION: d-089-H/94-A-16 CORE INTERVAL: KB: 716.09m

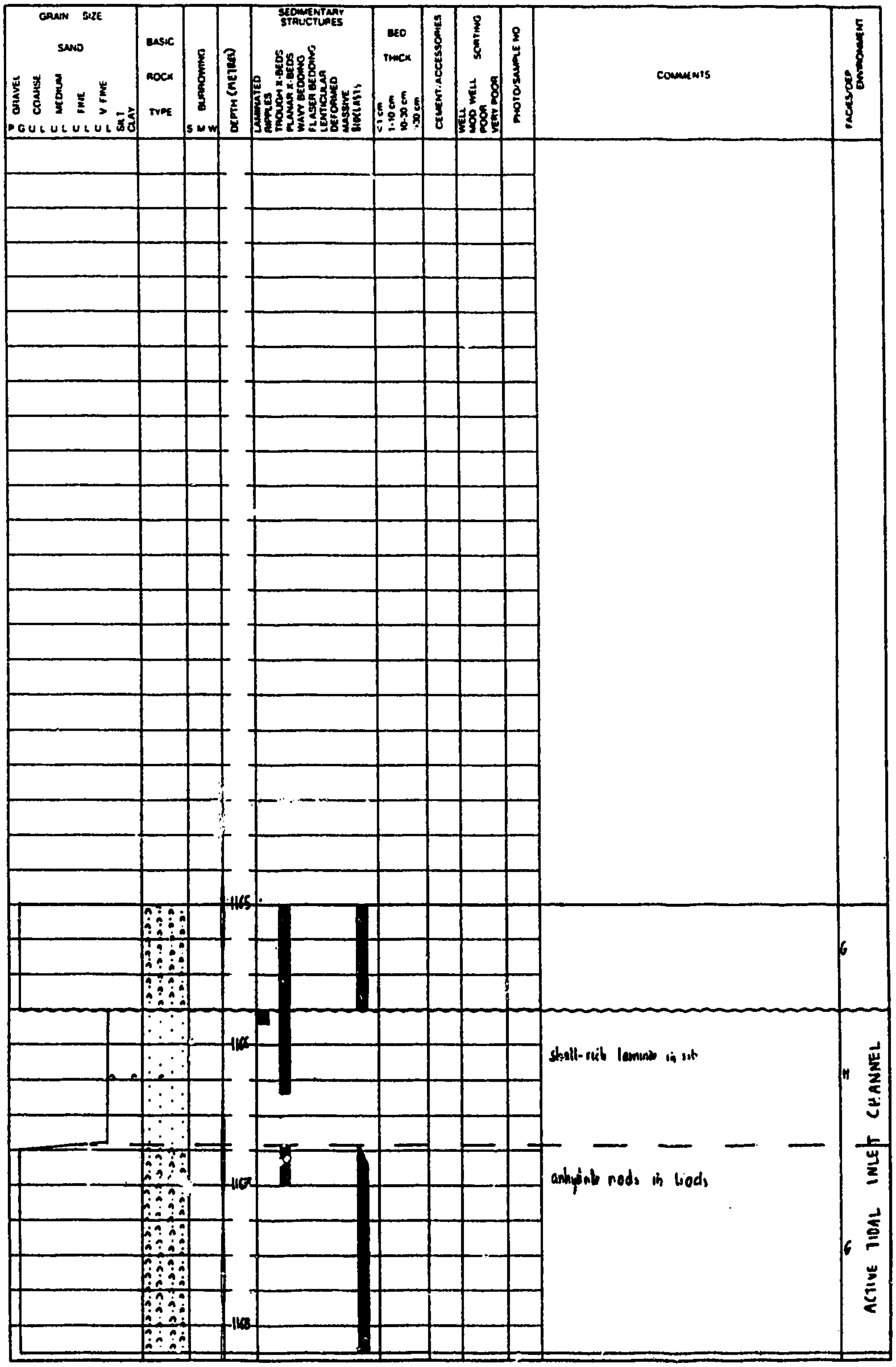

shell-rich laminae in silt

anhydrite nods in beds

WELL NAME: PEE JAY SR CAN DEL NANCY d-95-H FORMATION: HALFWAY-CHARLIE LAKE DATE: 13/07/90

LOCATION: d-095-H/94-A-15 CORE INTERVAL: KB: 2353ft

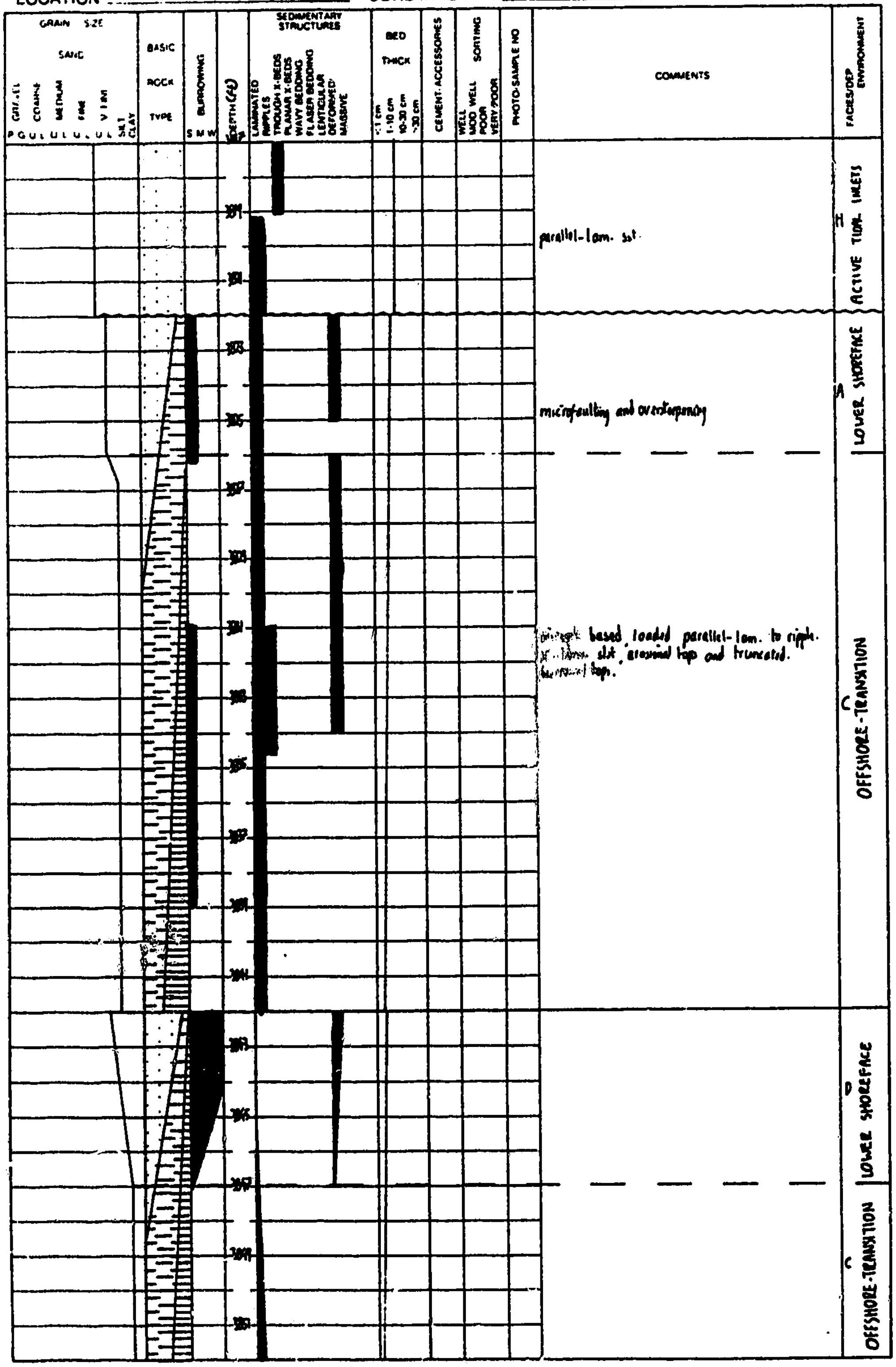

parallel-lam. sst

microfaulting and oversteepening

[illegible] based loaded parallel-lam. to ripple x-lam. slst, erosional top and truncated. burrowed top.

WELL NAME: PEEJAY SR CAN DEL NANCY d-95-H FORMATION: HALFWAY-CHARLIE LAKE DATE: 13/07/90

LOCATION: d-095-H/94-A-15 CORE INTERVAL: KB: 2353ft

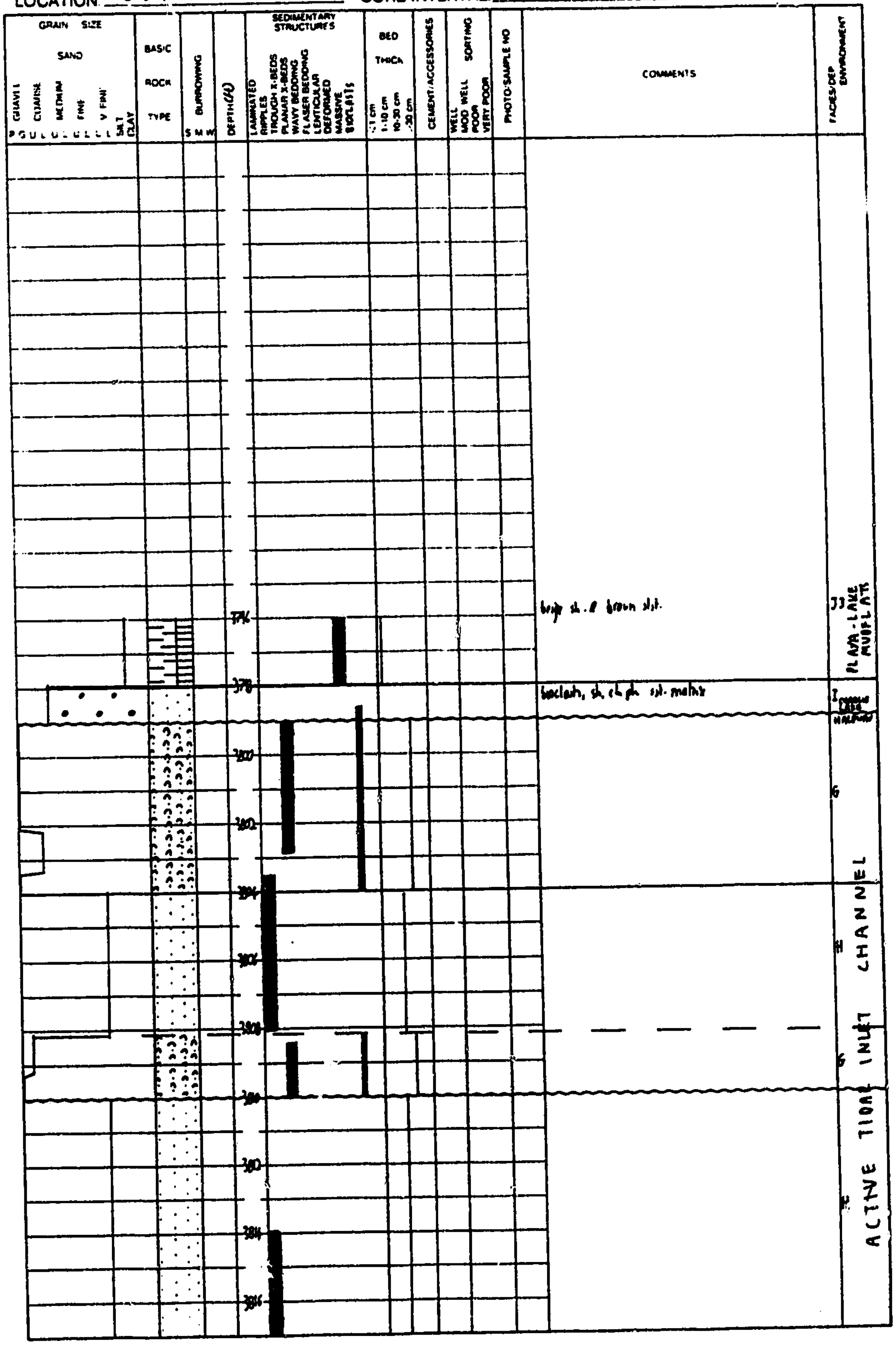

WELL NAME BAYSEL SR NANCY d-97-H FORMATION: HALFWAY-CHARLIE LAKE DATE: 9/07/90

LOCATION d-097-H/94-A-15 CORE INTERVAL: KB: 2360ft

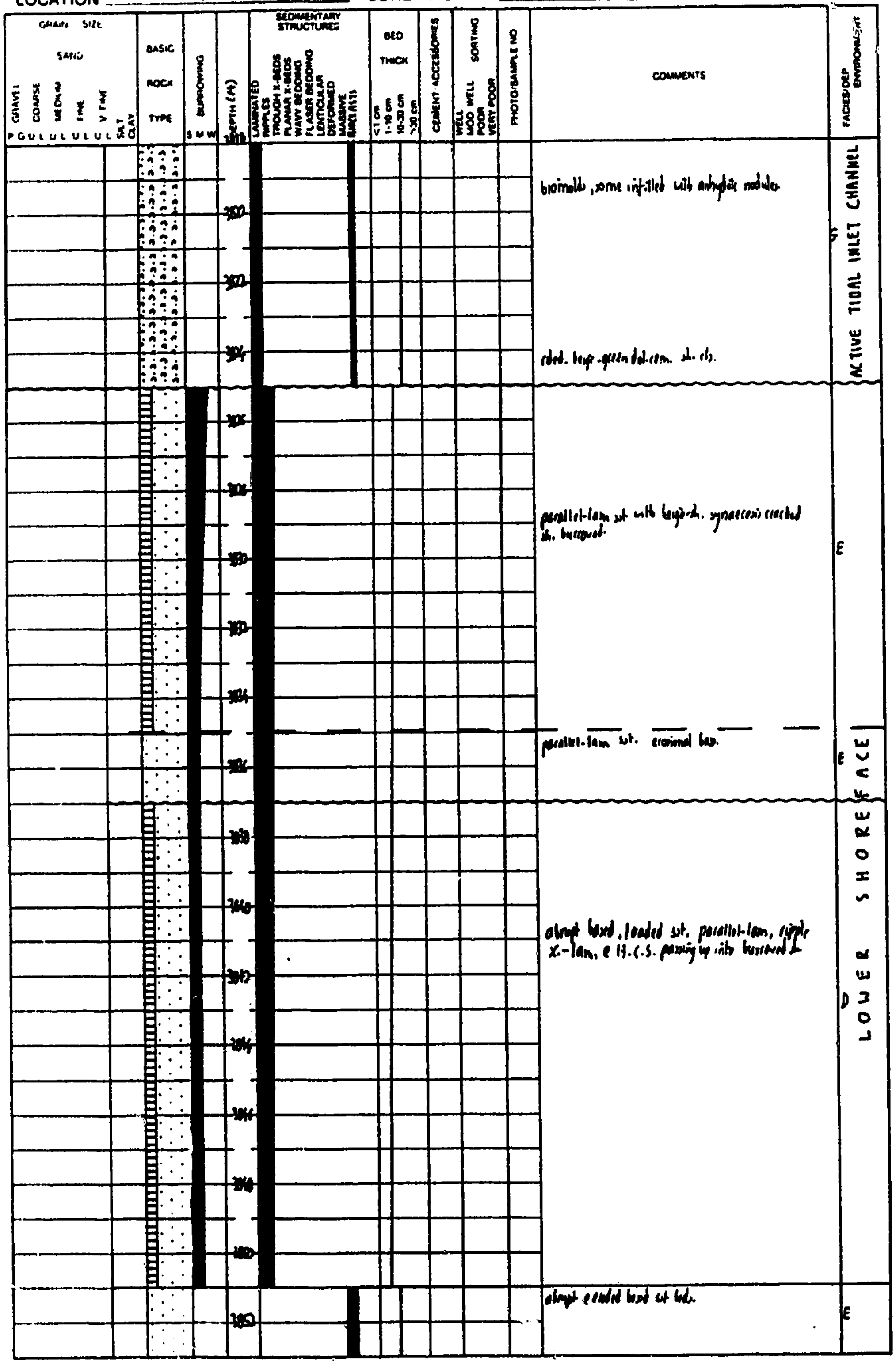

biomolds, some infilled with anhydrite nodules

rded. brp.-green dol.-cem. sh. cls.

G ACTIVE TIDAL INLET CHANNEL

parallel-lam slt with long-sh. synaeresis cracked sh. burrowed.

E

parallel-lam slt. erosional base.

E

abrupt based, loaded slt. parallel-lam, ripple X.-lam, & H.C.S. passing up into burrowed sh.

D LOWER SHOREFACE

abrupt graded based slt beds.

E

WELL NAME BAY SEL SR NANCY d-97-H FORMATION: HALFUAY-CHARLIE LAKE DATE 9/07/90

LOCATION d-097-H/94-A-15 CORE INTERVAL: KB 2360ft

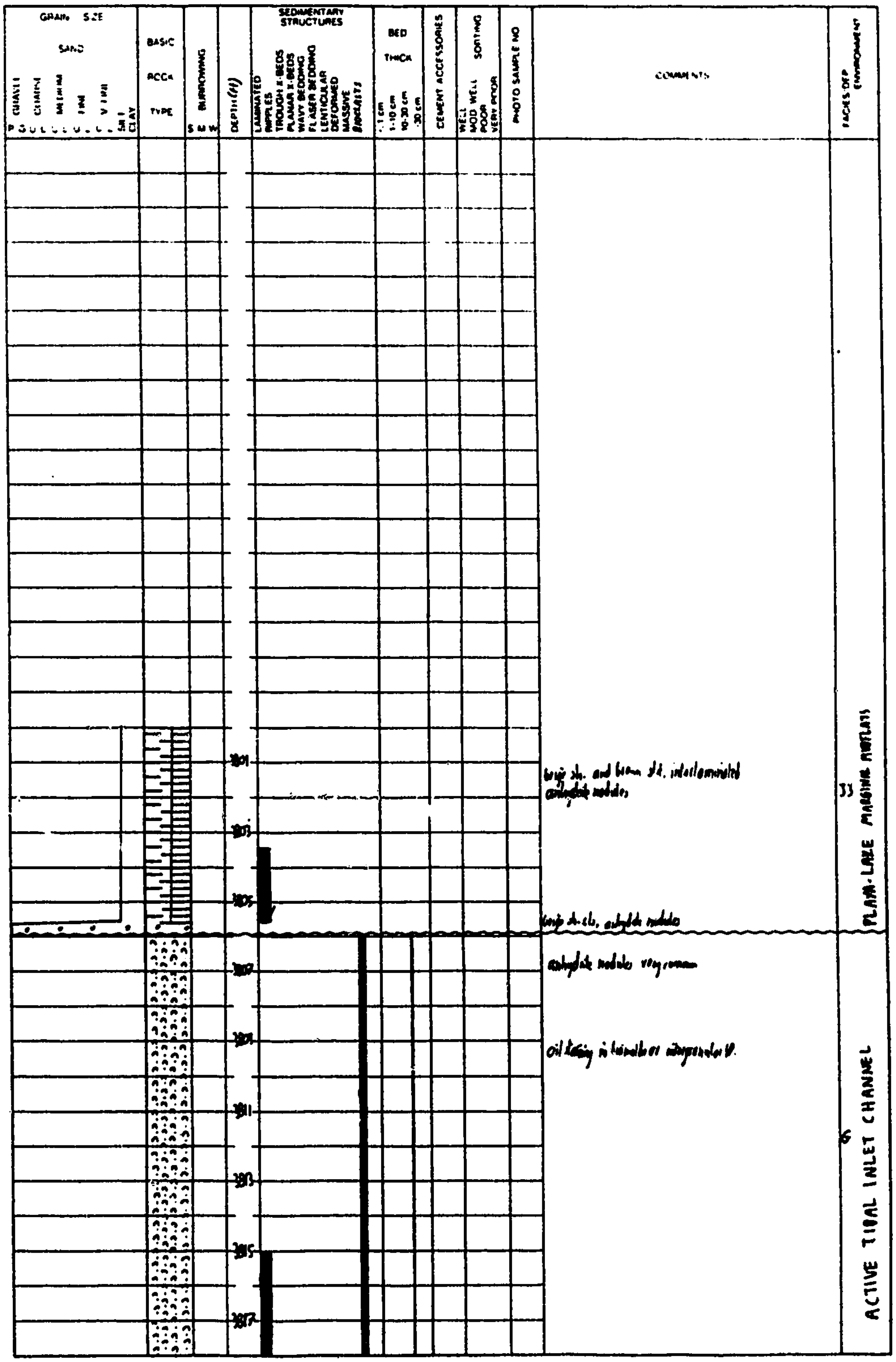

beige sh. and brown sl. interlaminated anhydrite nodules

beige sh.-cl., anhydrite nodules

anhydrite nodules very common

oil staining in horizontal or subperpendicular V.

PLAIN-LAKE MARGINE MUDFLATS

ACTIVE TIDAL INLET CHANNEL

WELL NAME SILVERTON PEEJAY d-100-H FORMATION: HALFWAY-CHARLIE LAKE DATE: 25/06/90

LOCATION d-100-H/94-A-15 CORE INTERVAL: KB: 710.6m

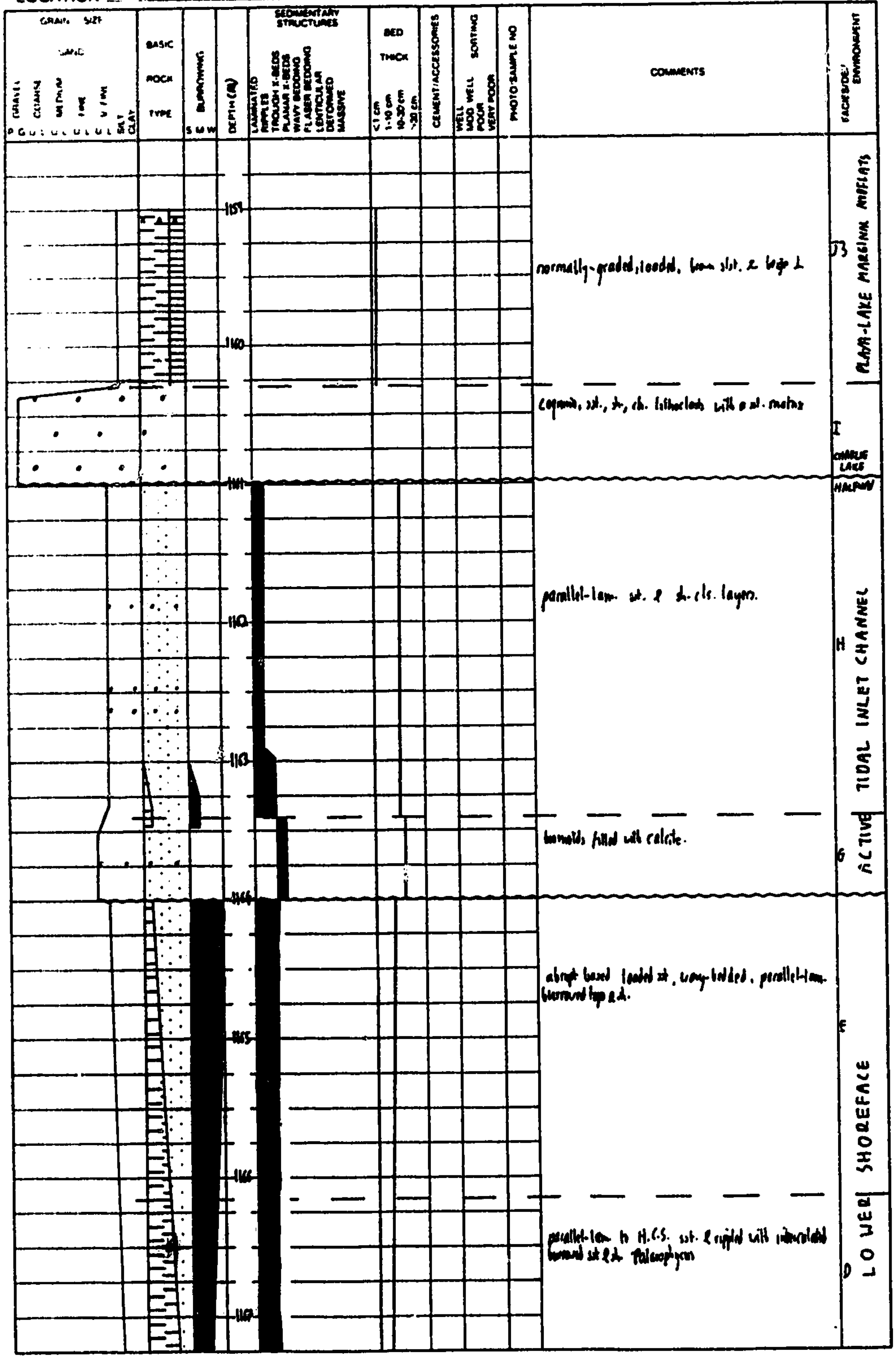

normally-graded, loaded, brown silt. & beige L

conglom., slt., sh., ch. lithoclasts with a sl. matrix

parallel-lam. st. & sh.-cls. layers.

biomolds filled with calcite.

abrupt based loaded st, wavy-bedded, parallel-lam. burrowed top a.d.

parallel-lam. to H.C.S. sst. & rippled with interbedded burrowed sst & sh. Palaeophycus

J3 PLAYA-LAKE MARGINAL MUDFLATS

I

H TIDAL INLET CHANNEL

G ACTIVE

E SHOREFACE

D LOWER

WELL NAME: PACIFIC SR WEST CDN PEEJAY d-33-I FORMATION: HALFWAY-CHARLIE LAKE DATE 17/07/90

LOCATION: d-033-I/94-A-15 CORE INTERVAL: KB 2338.9ft

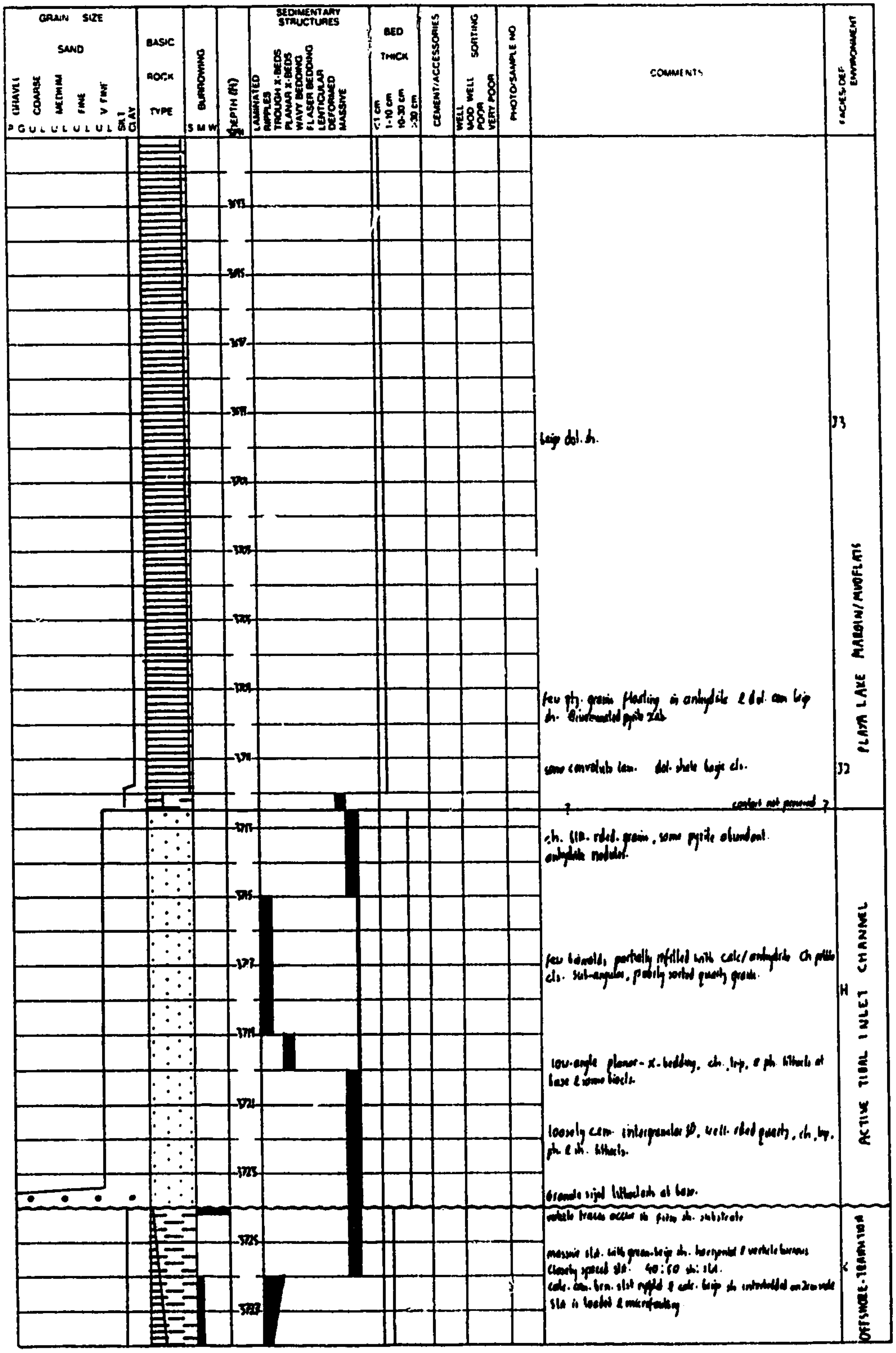

beige dol. sh.

few gy. grain floating in anhydrite & dol. cm beige sh. disseminated pyrite xals

some convolute lam. dol. shale beige cls.

? contact not preserved ?

ch. sub- rdd. grain, some pyrite abundant anhydrite nodules.

few bioclasts, partially infilled with calc/anhydrite Ch pebble cls. sub-angular, poorly sorted quartz grain.

low-angle planar-x-bedding. ch., trp. & ph. lithcls at base & some biocls.

loosely cem. intergranular Φ, well-rdd quartz, ch, trp. ph. & sh. lithcls.

granule sized lithoclasts at base.

vertical traces occur in firm sh. substrate

massive slt. with green-beige sh. horizontal & vertical burrows closely spaced slt. 40:60 sh: slt.

calc. cem. brn. slst rippled & calc. beige sh interbedded on 2cm scale slt is loaded & microfaulting

WELL NAME: TENECO OSPREY d-13-J FORMATION: HALFWAY DATE: 30/01/91

LOCATION: d-013-J/94-A-15 CORE INTERVAL: KB: 2251.3ft

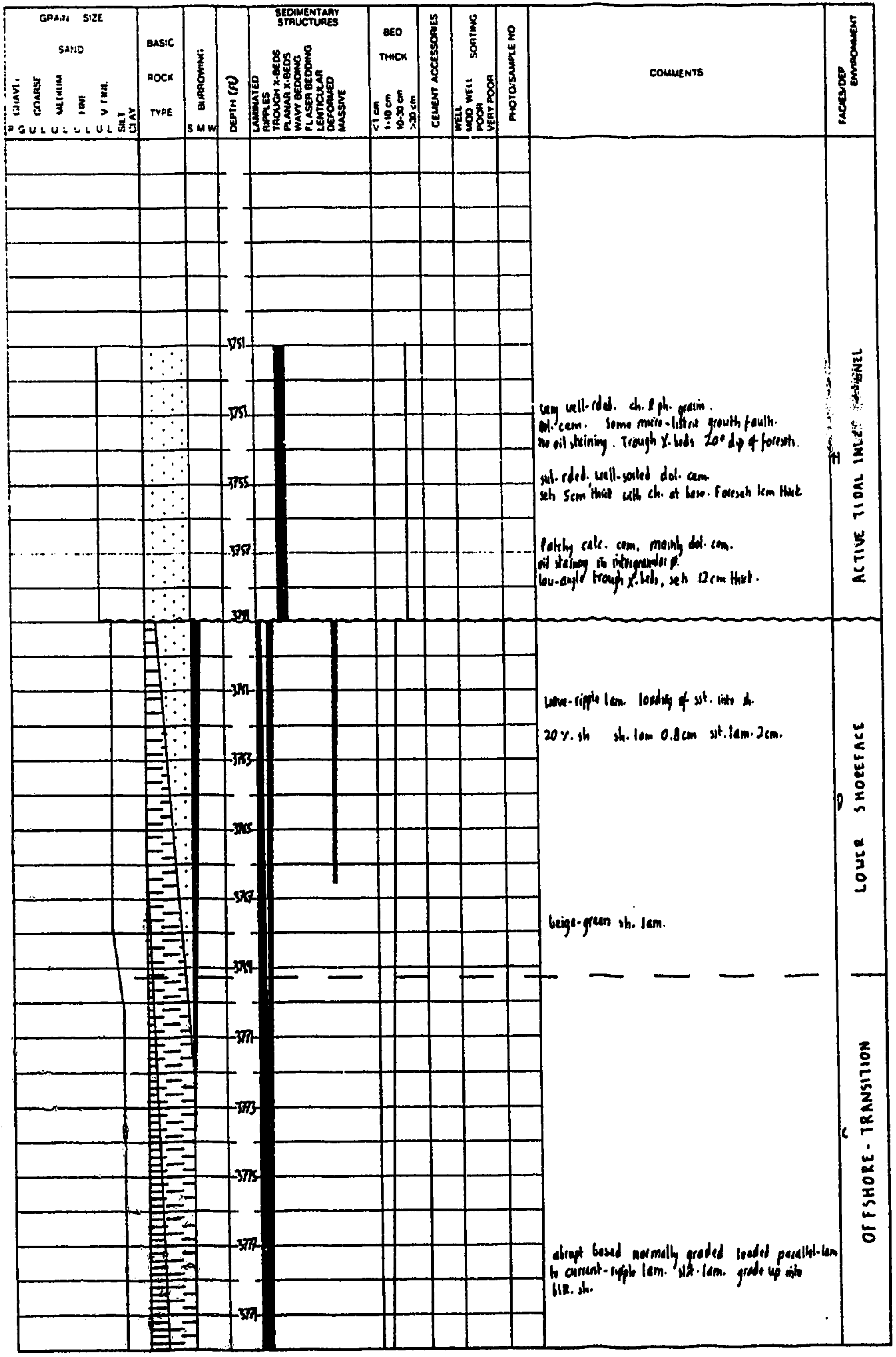

very well-rded. ch. & ph. grain.
dol. cem. Some micro-listric growth faults.
no oil staining. Trough X-beds 20° dip of foresets.

sub-rded. well-sorted dol. cem.
sets 5cm thick with ch. at base. Foresets 1cm thick

Patchy calc. cem. mainly dol. cem.
oil staining in intergranular φ.
low-angle trough X-beds, sets 12cm thick.

wave-ripple lam. loading of sst. into sh.

20%. sh sh. lam 0.8cm sst. lam. 3cm.

beige-green sh. lam.

abrupt based normally graded loaded parallel-lam
to current-ripple lam. slt. lam. grade up into
blk. sh.

WELL NAME: SINCLAIR ET AL CURRENT d-18-B

FORMATION: DOIG?/HALFWAY?/CHARLIE LAKE

DATE: 4/02/91

LOCATION: d-018-B/94-A-16

CORE INTERVAL:

KB: G.L. 2458 ft

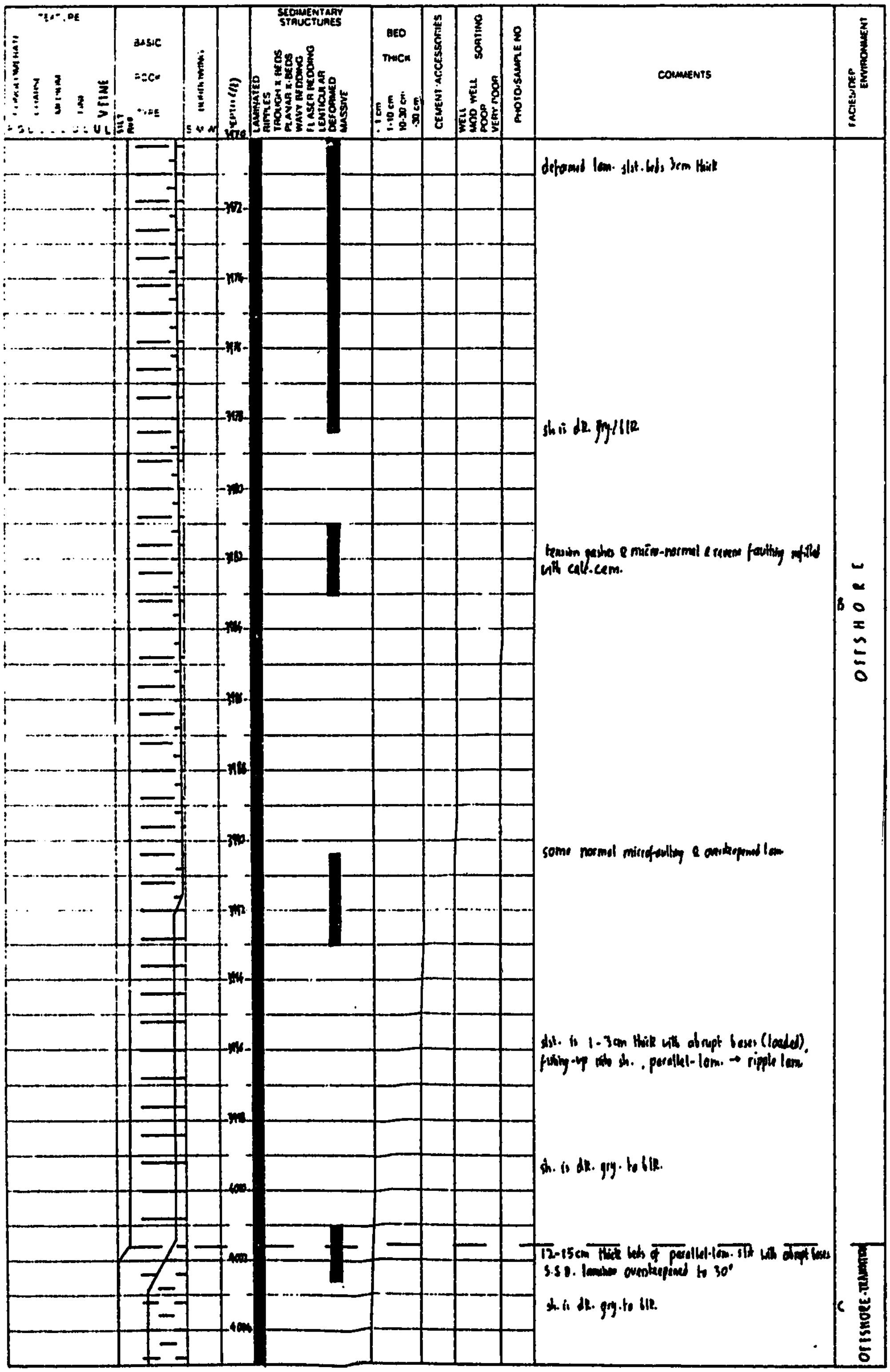

deformed lam. slst. beds 3cm thick

sh. is dk. gry/blk

tension gashes & micro-normal & reverse faulting infilled with calc.cem.

some normal microfaulting & oversteepened lam.

slst. is 1-3cm thick with abrupt bases (loaded), fining-up into sh., parallel-lam. → ripple lam.

sh. is dk. gry. to blk.

12-15cm thick beds of parallel-lam. slt with abrupt bases S.S.D. laminae oversteepened to 30°

sh. is dk. gry. to blk.

WELL NAME: SINCLAIR ET AL PEEJAY d-18-B

FORMATION: DOIG?/HALFWAY?/CHARLIE LAKE

DATE 4/03/91

LOCATION: d-018-B/94-A-16

CORE INTERVAL:

KB: 6.L 2458ft

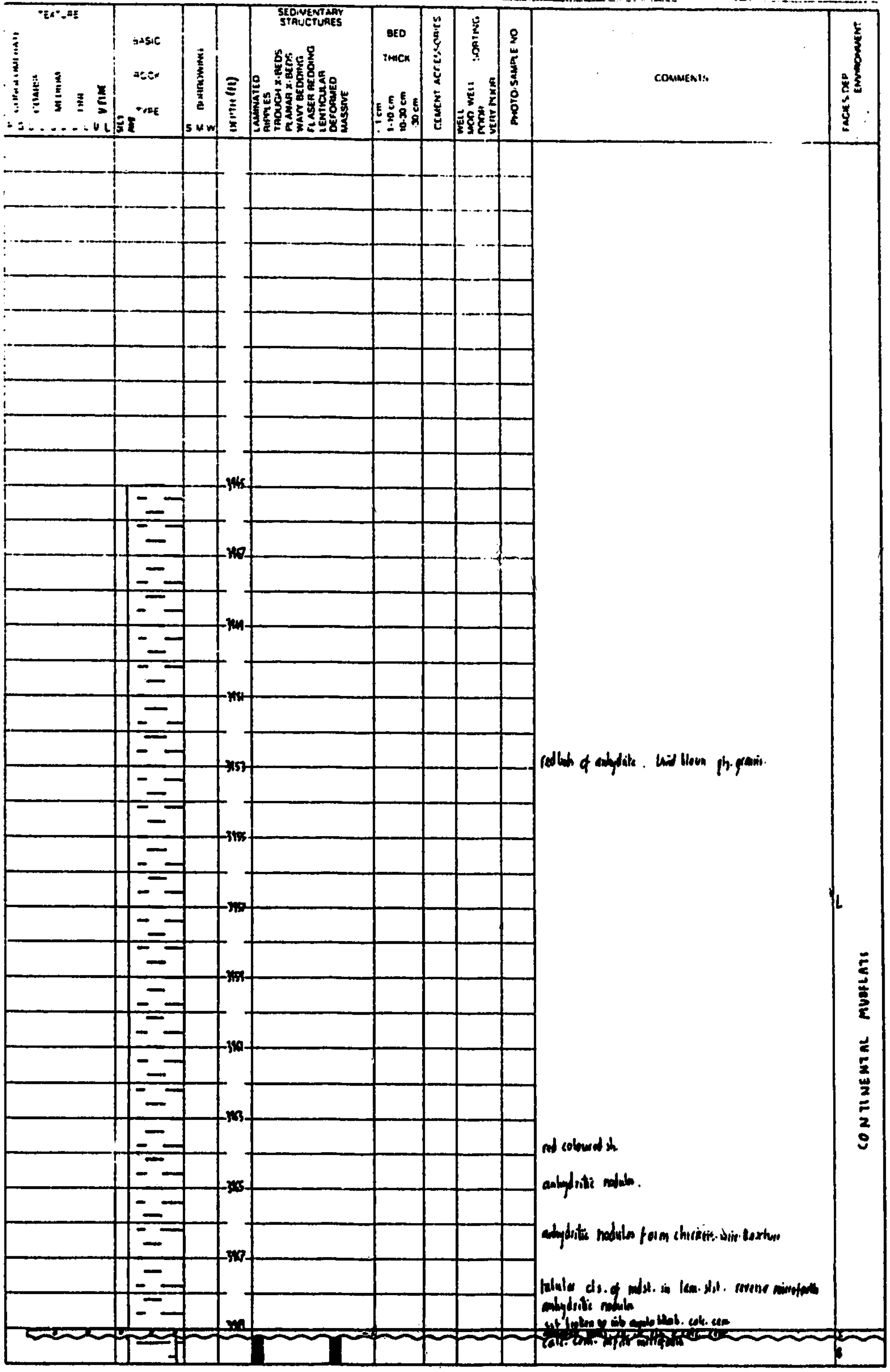

[illegible] of anhydrite. Wind blown [illegible] grains.

red coloured sh.

anhydritic nodules.

anhydritic nodules form chicken-wire texture

tabular cls. of mdst. in lam. slst. reverse microfaults

anhydritic nodules

sst [illegible] sub angular [illegible]. calc. cem

calc. cem. [illegible]

WELL NAME SINCLAIR ET AL CURRENT 0-5-C
FORMATION: HALFWAY/CHARLIE LAKE
DATE: 23/01/91
LOCATION: d-005-C/94-A-16
CORE INTERVAL:
KB: 2401.01ft

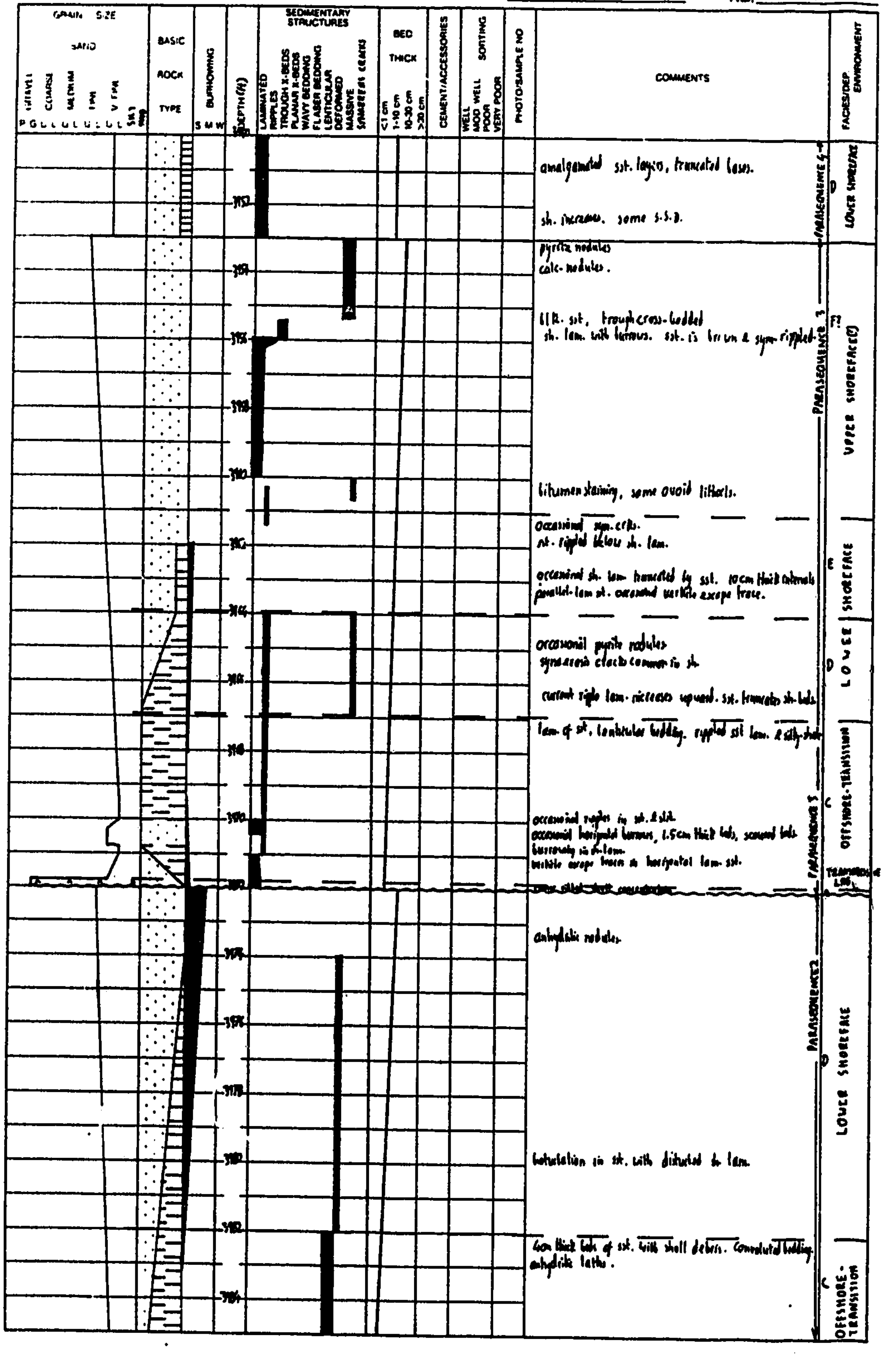

amalgamated sst. layers, truncated bases.

sh. increases. some s.s.d.

pyrite nodules
calc-nodules.

llk. sst, trough cross-bedded
sh. lam. with burrows. sst. is brown & sym-rippled.

bitumen staining, some ovoid lithics.

occasional syn. cracks.
sst. rippled below sh. lam.

occasional sh. lam. truncated by sst. 10cm thick intervals
parallel-lam sst. occasional vertical escape trace.

occasional pyrite nodules
synaeresis cracks common in sh.

current ripple lam. increases upward. sst. truncates sh. beds

lam. of sst, lenticular bedding. rippled sst lam. & silty shale

occasional ripples in sh. & slt.
occasional horizontal burrows, 1.5cm thick beds, scoured beds
burrowing in sh. lam.
invisible except traces in horizontal lam. sst.

chert pebble-shell concentration

anhydritic nodules.

bioturbation in sst. with disturbed sh. lam.

4cm thick beds of sst. with shell debris. Convoluted bedding.
anhydritic laths.

WELL NAME: SINCLAIR ET AL CURRENT 0-5-C

FORMATION: HALFWAY/CHARLIE LAKE

DATE: 23/01/91

LOCATION: d-005-C/94-A-16

CORE INTERVAL:

KB: 2401ft

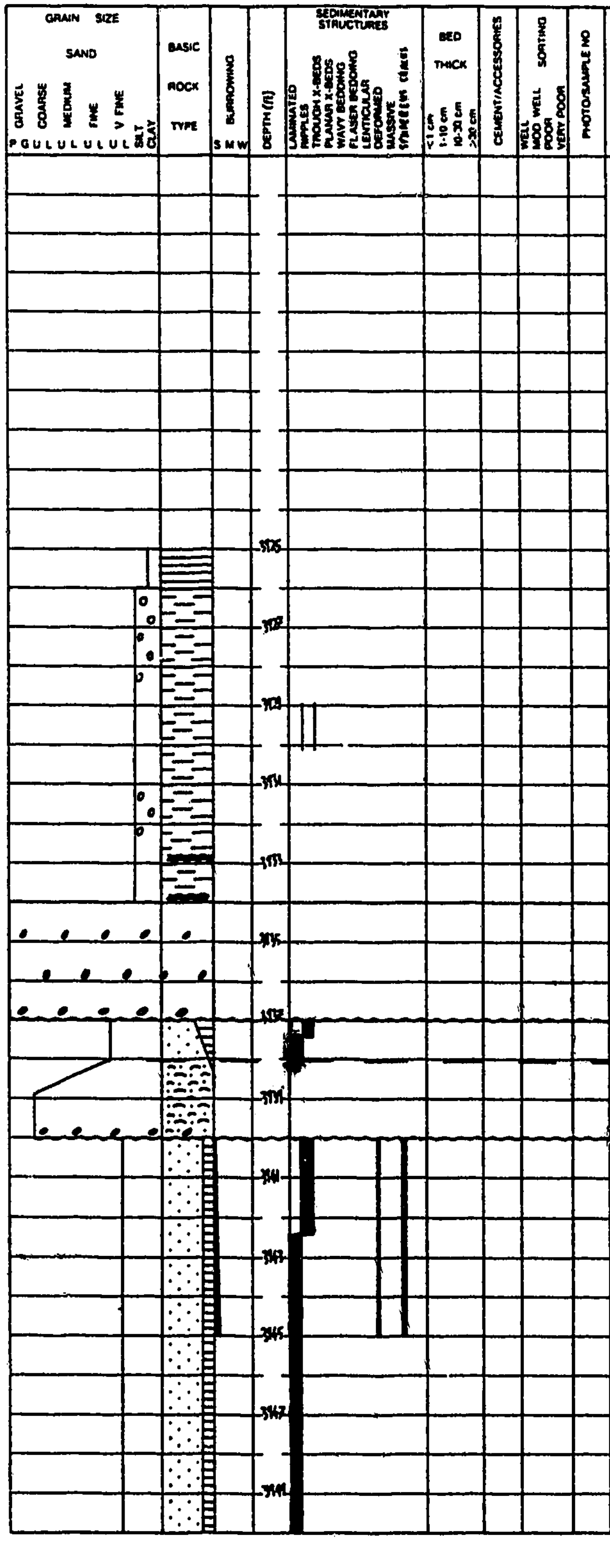

COMMENTS

dol brgy sh.

anhydritic nodules

lithoclasts of slst. & sh. in slst. matrix, anhydritic nodules

current ripple lam.

large cls of sh. in slst. matrix, anhydritic nods.

anhydrite nodules & stromatolites

anhydrite nodules, cls of sh. ph. [illegible]

dol. [illegible] infilled with anhydrite. Red [illegible] to sst.
[illegible]
cls. of sh. [illegible]

current ripple lam.

coarse [illegible] [illegible] [illegible] ([illegible]), 20% [illegible] infilled with anhydrite. dol. brgy is common.
cls of sh.

current ripple lam.

syn-cracks in sh.

occasional lam. of sh. truncated & loaded.

parallel lam, 5° inclined sst. occasional sh. cls.

FACIES/DEP ENVIRONMENT

K PLAYA LAKE

J3 PLAYA LAKE MARGIN/[illegible] FLATS

J2

J1

J2

J1

[illegible] HALFWAY/[illegible]

E [illegible]

G TEMPESTITE

D LOWER SHOREFACE

WELL NAME: PACIFIC ET AL CURRENT D-7-C FORMATION: HALFWAY-CHARLIE LAKE DATE: 24/01/91

LOCATION: d-007-C/94-A-16 CORE INTERVAL: KB: 2370ft

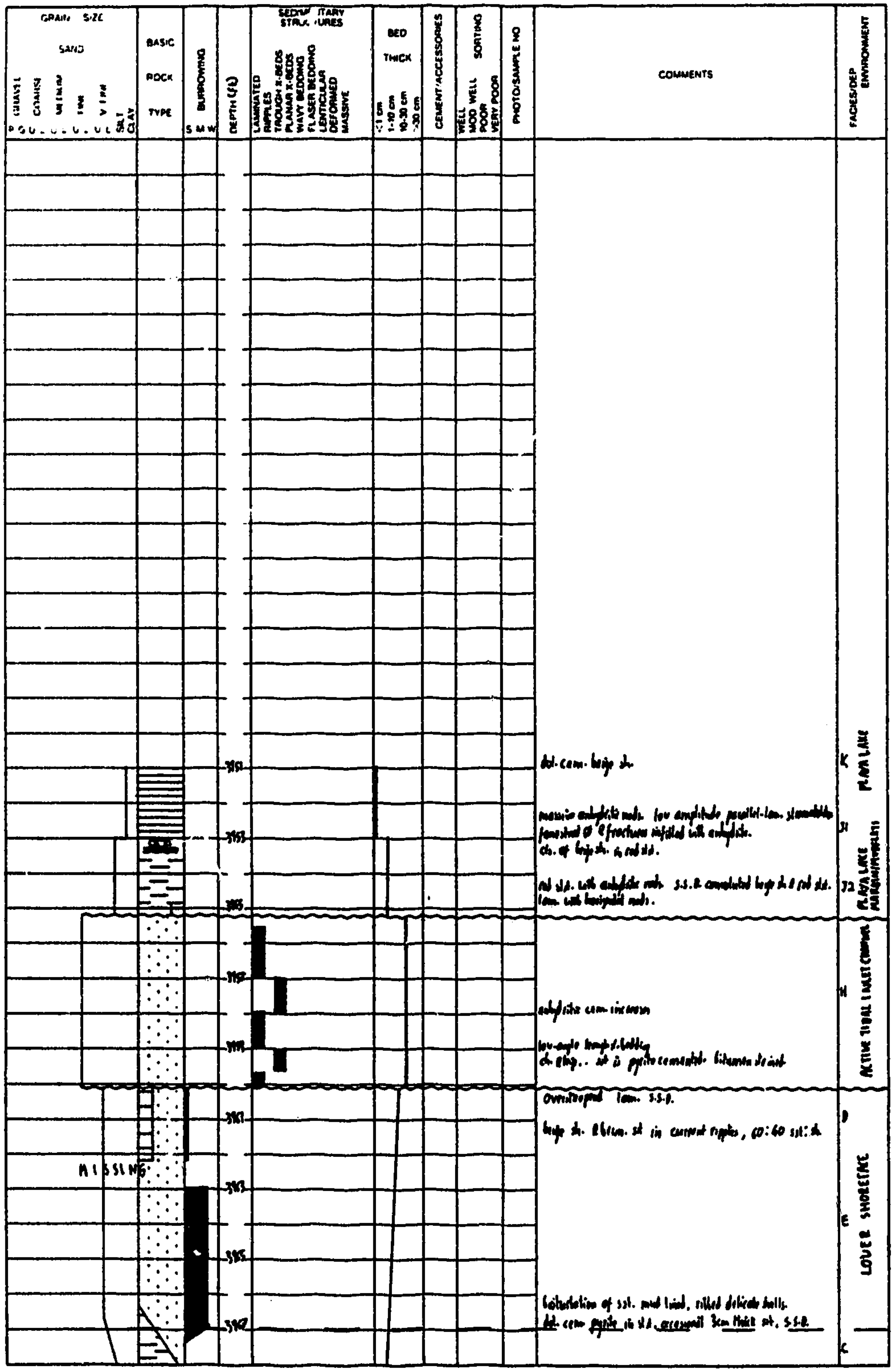

dol.-cem. beige sh.

massive anhydrite nods. low amplitude parallel-lam. stromatolites fenestral ∅ & fractures infilled with anhydrite.
ch. of beige sh. & red slt.

red slt. with anhydrite nods. s.s. & convoluted beige sh. & red slt. lam. with [illegible] nods.

anhydrite cem. increase

low-angle trough x-bedding
ch. clasts.. at & pyrite cemented. bitumen stained

Oversteepened lam. s.s.?

beige sh. & brown. st in current ripples, 60:40 sst:sh

bioturbation of sst. and [illegible], [illegible] delicate trails.
dol. cem. pyrite in sst. occasional 3cm thick sh. s.s.?

WELL NAME: SINCLAIR ET AL CURRENT D-16-C

FORMATION: HALFWAY / CHARLIE LAKE

DATE: 23/01/91

LOCATION: d-016-C/94-A-16

CORE INTERVAL:

KB: 61 2379.5 ft

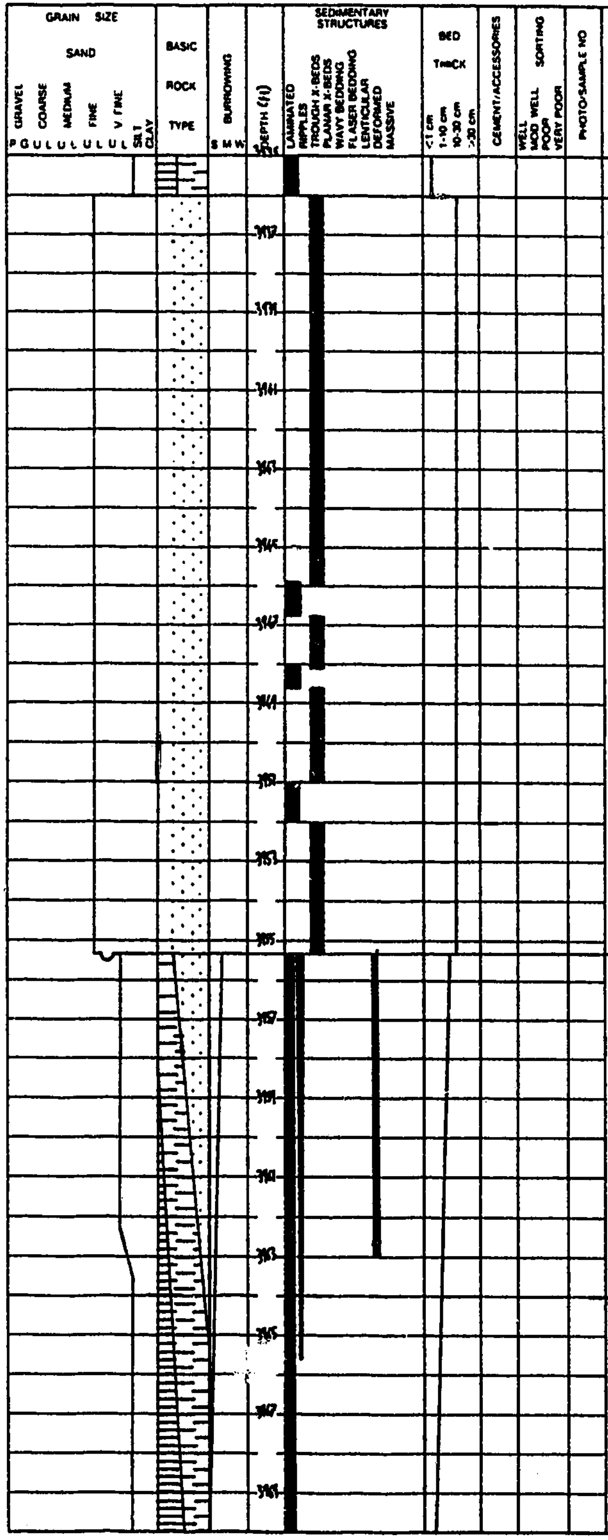

COMMENTS

slt. & sh. cl. - s.l.b. in red slt.

anhydrite cem. plugs Ø.

fining upward foresets

poorly cemented

beds patchy in appearance due to patchy dissolution of anhydrite

current ripple lam. above trough x-bedding, basal lithoclastic granule lam.

anhydrite nodules
reverse ripple climbing x-beds (?)
basal concentrated [illegible] by . ch. & ph. lithcls.
foreset dip 23°
sets 12cm thick . Foresets 1-3cm thick.

anhydrite nodules & siltly beneath . dol. cem. patchily located producing a mottling appearance.

occasional anhydrite crystals & nodules

burrowing in beige sh. slt. in red. bedded bur.
wave-ripple lam.

slt. lam. in dk.gry. sh.
occasional burrows

FACIES/DEP ENVIRONMENT

22

H

ACTIVE TIDAL INLET CHANNEL

D

LOWER SHOREFACE

C

OFFSHORE-TRANSITION

WELL NAME SINCLAIR ET AL CURRENT D-16-C
FORMATION: HALFWAY- CHARLIE LAKE
DATE: 23/01/91
LOCATION d-016-C/94-A-16
CORE INTERVAL:
KB: G.L. 2379.5ft

GRAIN SIZE SAND GRAVEL COARSE MEDIUM FINE V FINE SILT CLAY G U L U L U L U L	BASIC ROCK TYPE	BURROWING S M W	DEPTH (ft)	SEDIMENTARY STRUCTURES LAMINATED RIPPLES TROUGH X-BEDS PLANAR X-BEDS WAVY BEDDING FLASER BEDDING LENTICULAR DEFORMED MASSIVE	BED THICK <1 cm 1-10 cm 10-30 cm >30 cm	CEMENT ACCESSORIES	SORTING WELL MOD WELL POOR VERY POOR	PHOTO/SAMPLE NO	COMMENTS	FACIES/DEP ENVIRONMENT
00			[illegible] [illegible] [illegible] [illegible] 3936						ch-ip red sh in brown slt. anhydrite nods. disrupt lam. red siltstone & beige sh. mudcracking ? [illegible] anhydrite [illegible] nodules. red slt. & beige sh. & anhydrite nodules + chip lam. [illegible] (31) angular chip.	32 PLAYA LAKE MARGIN/MUDFLATS

WELL NAME SINCLAIR ET AL CURRANT d-27-C FORMATION: HALFWAY - CHARLIE LAKE DATE 22/01/91

LOCATION: d-027-C/94-A-16 CORE INTERVAL: KB: 2385 8ft

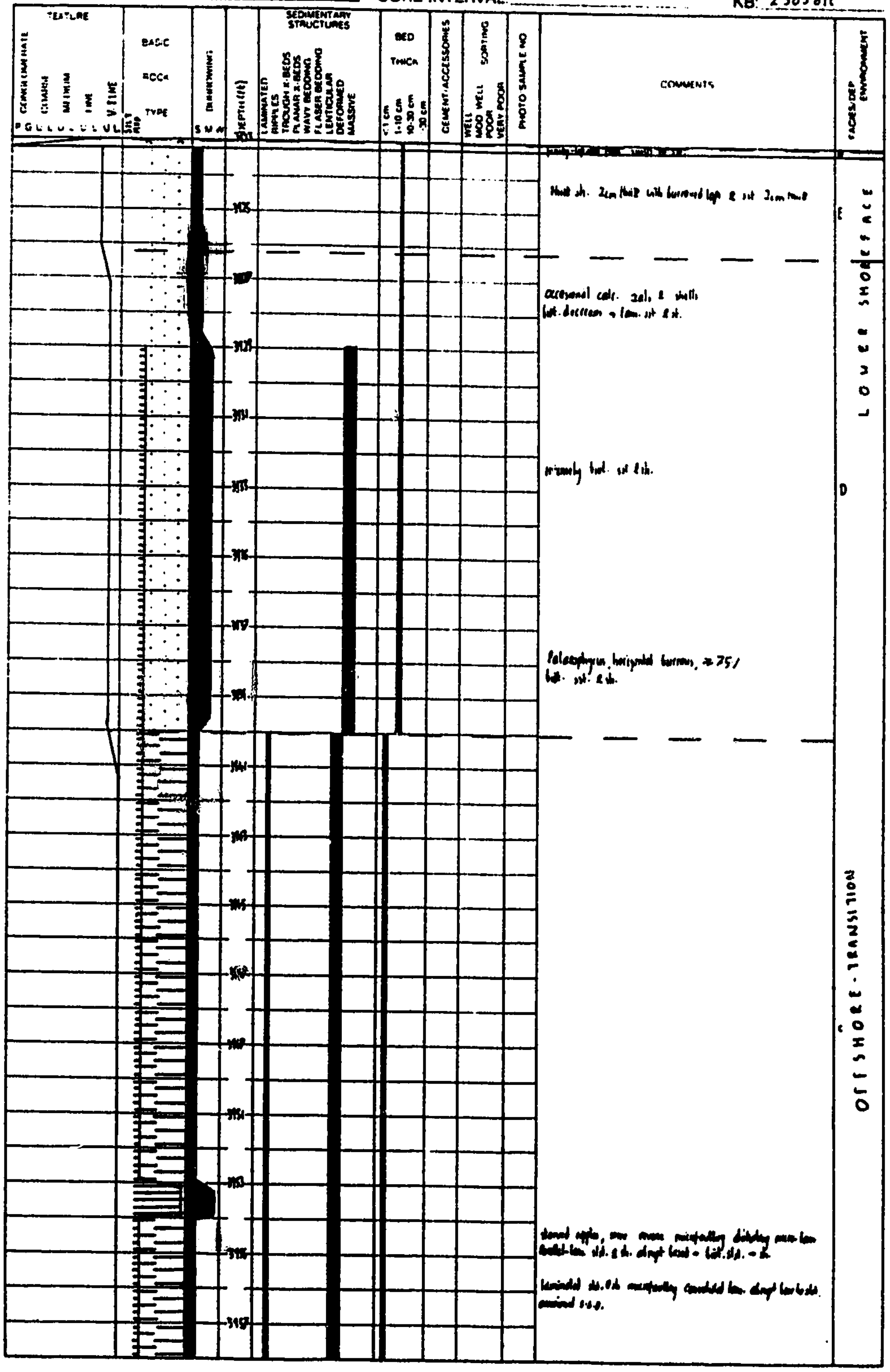

Black sh. 2cm thick with burrowed top & sst 3cm thick

occasional calc. sol. & shells
bot. decrease in lam. sst & sh.

primarily biot. sst & sh.

Palaeophycus, horizontal burrows, ≈ 75%
biot. sst. & sh.

[illegible]

[illegible]

WELL NAME: SINCLAIR ET AL CURRANT d-27-C
FORMATION: HALFWAY- CHARLIE LAKE
DATE: 22/01/91
LOCATION: d-027-C/94-A-16
CORE INTERVAL:
KB: 2385 BH

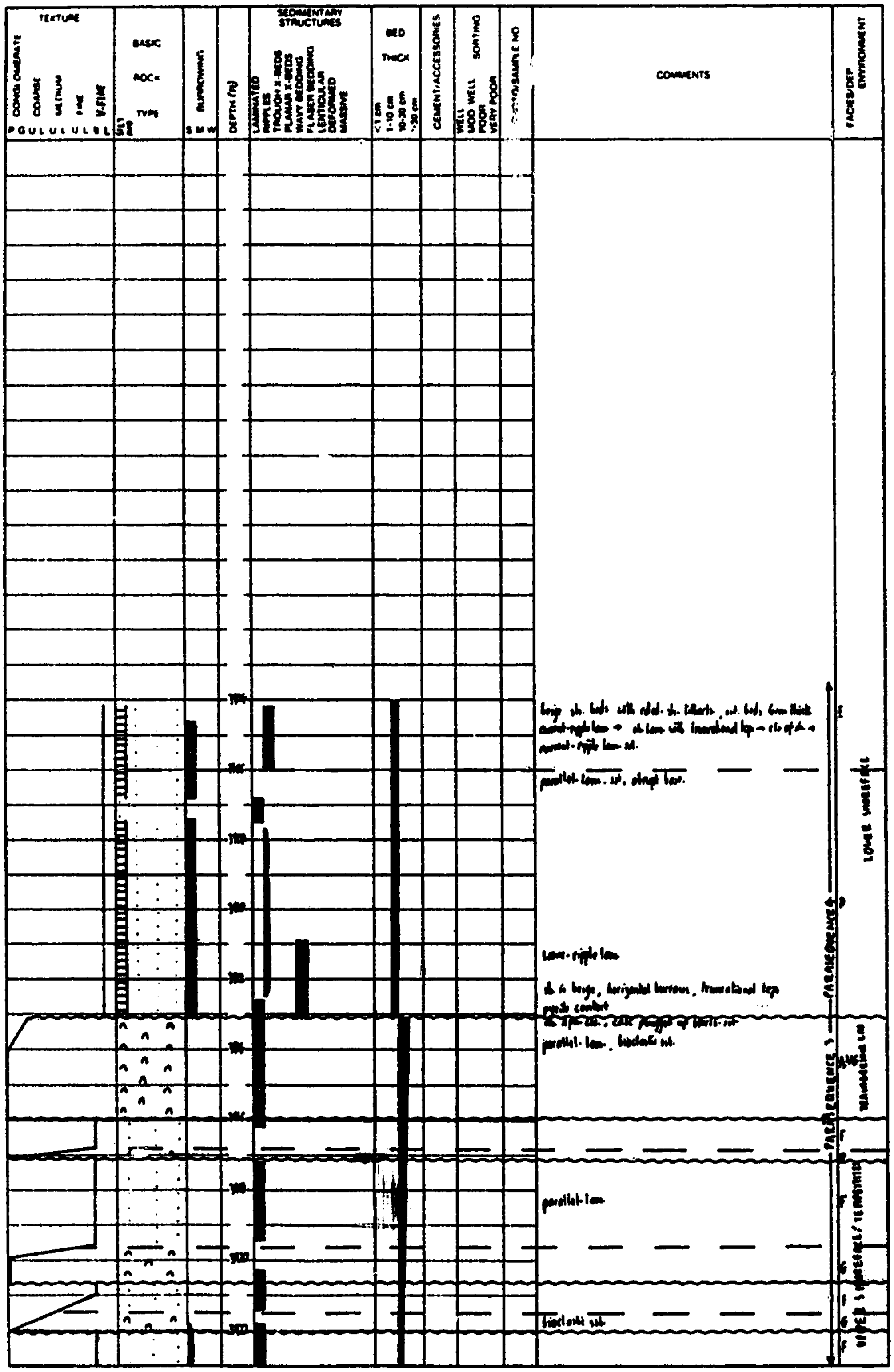

beige sh. beds with [illegible] sh. laminae, sst. beds from thick current-ripple lam. → sh. lam. with transitional top — [illegible] current-ripple lam. sst.

parallel-lam. sst., abrupt base.

wave-ripple lam.

sh. to beige, horizontal burrows, transitional top [illegible] contact

[illegible]

parallel-lam., bioclastic sst.

parallel-lam.

bioclastic sst.

WELL NAME: UNION H.B. CURRANT d-28-C

FORMATION: HALFWAY-CHARLIE LAKE

DATE: 31/01/91

LOCATION: d-028-C/94-A-16

CORE INTERVAL:

KB: 2375 ft

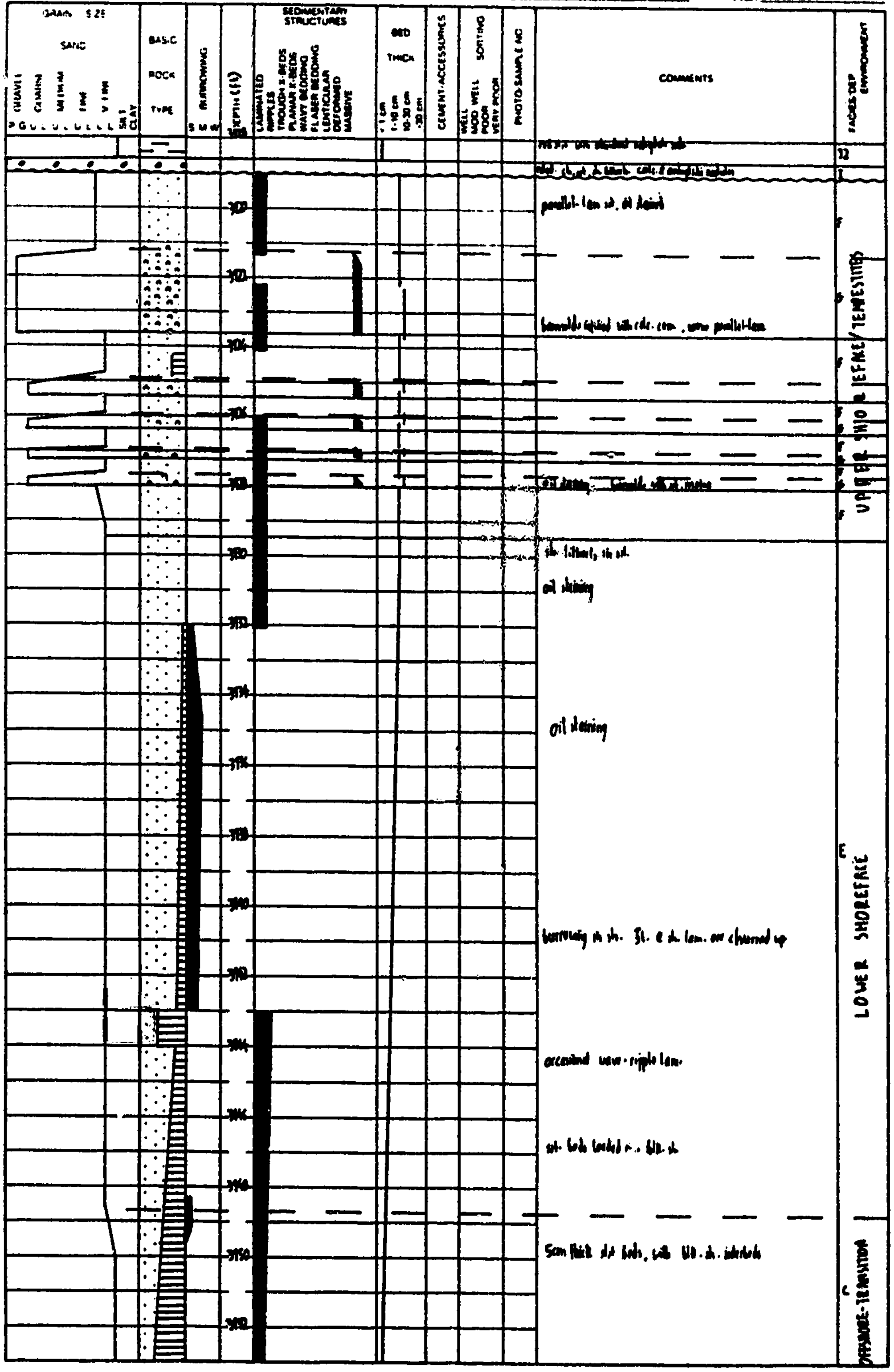

WELL NAME: UNION H B CURRANT d-28-C
FORMATION: HALFWAY-CHARLIE LAKE
DATE: 31/01/91
LOCATION: d-028-C/94-A-16
CORE INTERVAL:
KB: 2375 ft

GRAIN SIZE SAND GRAVEL COARSE MEDIUM FINE V FINE SILT CLAY	BASIC ROCK TYPE	BURROWING S M W	DEPTH (ft)	SEDIMENTARY STRUCTURES LAMINATED RIPPLES TROUGH X-BEDS PLANAR X-BEDS WAVY BEDDING FLASER BEDDING LENTICULAR DEFORMED MASSIVE	BED THICK <1 cm 1-10 cm 10-30 cm >30 cm	CEMENT. ACCESSORIES	SORTING WELL MOD WELL POOR VERY POOR	PHOTO/SAMPLE NO	COMMENTS	FACIES/DEP ENVIRONMENT
	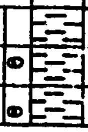		3115						sh. dol. in brown sltd. anhydritic nodules.	J3E PLAYA-LAKE MARGIN MUDFLATS
θ										
θ			3118	I					enterolithic anhydrite replacing dol. sh.	

WELL NAME: UNION HB SINC PAC CURRANT
FORMATION: HALFWAY-CHARLIE LAKE
DATE: 24/01/91
LOCATION: d-039-C/94-A-16
CORE INTERVAL:
KB: 2371.8ft

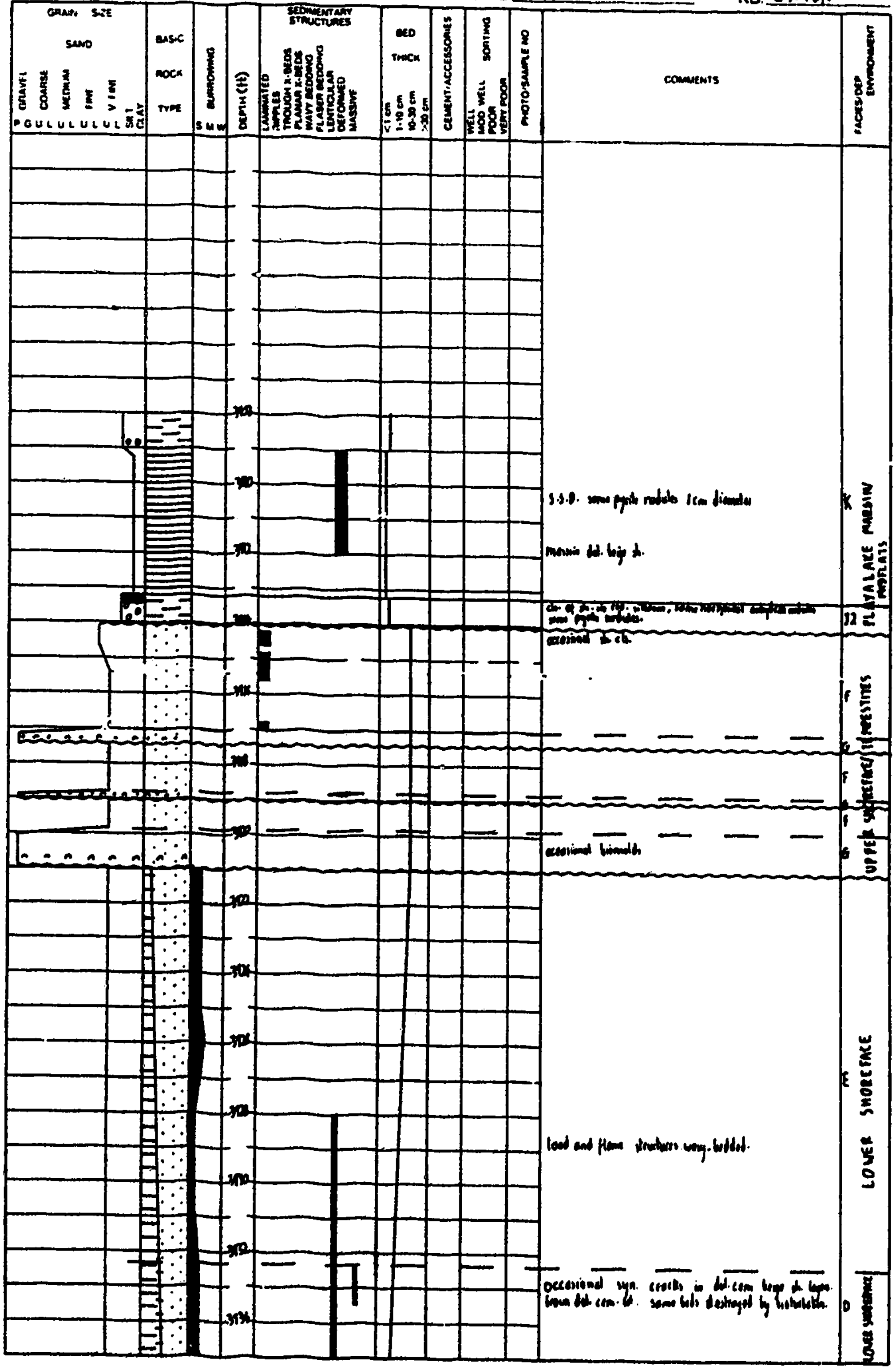

s.s.d. some pyrite nodules 1cm diameter

massive dol. beige sh.

[illegible] some pyrite nodules.

occasional sh. cl.

occasional bioturb.

load and flame structures wavy-bedded.

occasional syn. cracks in dol.-cem. beige sh. lam. brown dol. cem. sl. some beds destroyed by bioturbation

WELL NAME: UNION H B. PEEJAY d-59-C FORMATION: HALFWAY-CHARLIE LAKE DATE: 21/01/91

LOCATION: d-059-C/94-A-16 CORE INTERVAL: KB: 2394ft

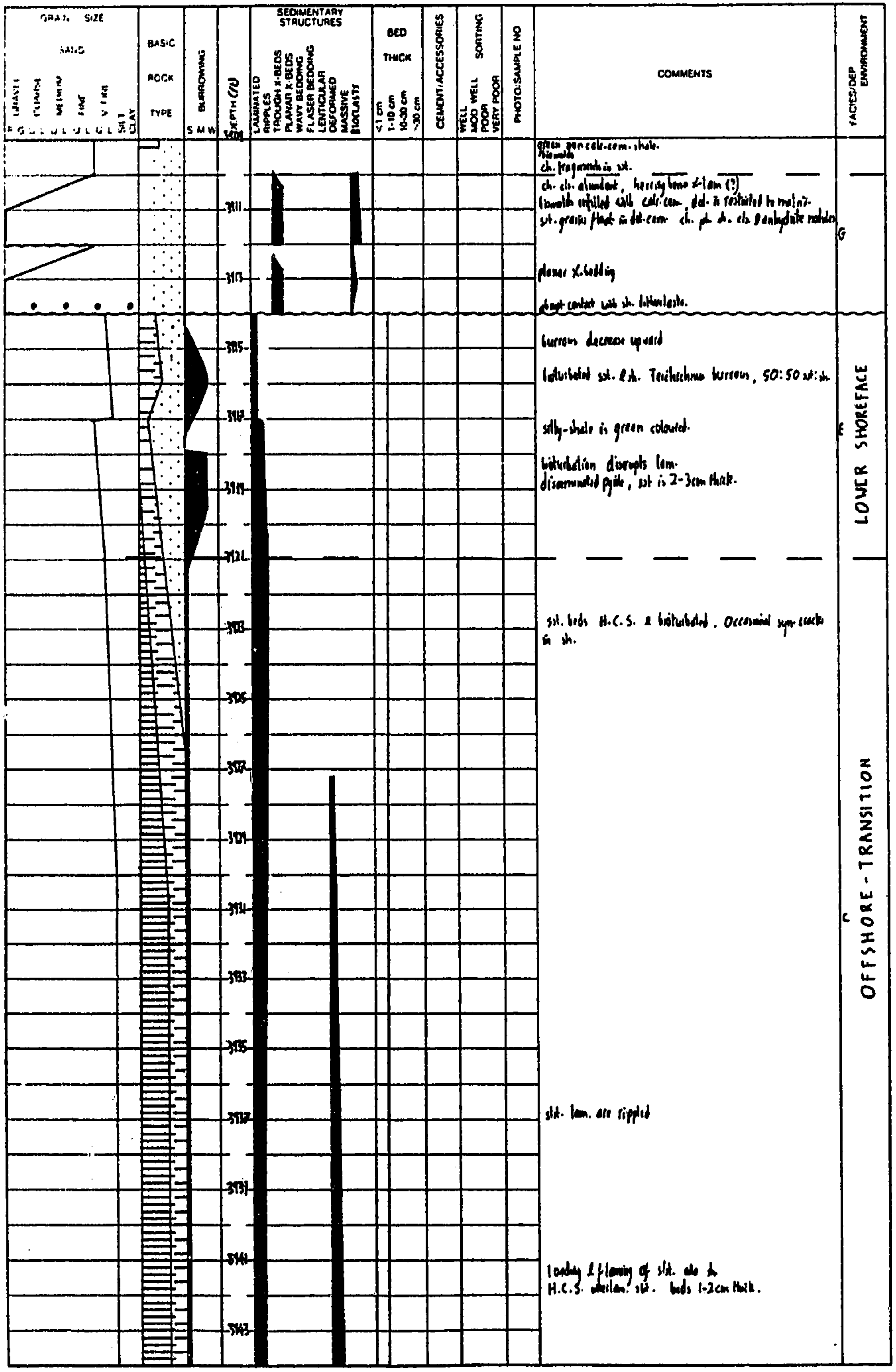

green non calc.cem. shale.
[illegible]
ch. fragments in sst.

ch. cls. abundant, herring bone x-lam (?)
burrows infilled with calc.cem., dol. is restricted to matrix-
sst. grains float in dol-cem ch. pb. sh. cls. Anhydrite nodules

planar X-bedding

sharp contact with sh. lithoclasts.

burrows decrease upward

bioturbated sst. & sh. Teichichnus burrows, 50:50 sst:sh.

silty-shale is green coloured.

bioturbation disrupts lam.
disseminated pyrite, sst is 2-3cm thick.

slt. beds H.C.S. & bioturbated. Occasional syn-cracks in sh.

slt. lam. are rippled

loading & flaming of slt. into sh.
H.C.S. within slt. beds 1-2cm thick.

WELL NAME: UNION H & PEEJAY d-59-C

FORMATION: HALFWAY- CHARLIE LAKE

DATE: 21/01/91

LOCATION: d-059-C/94-A-16

CORE INTERVAL:

KB: 2394ft

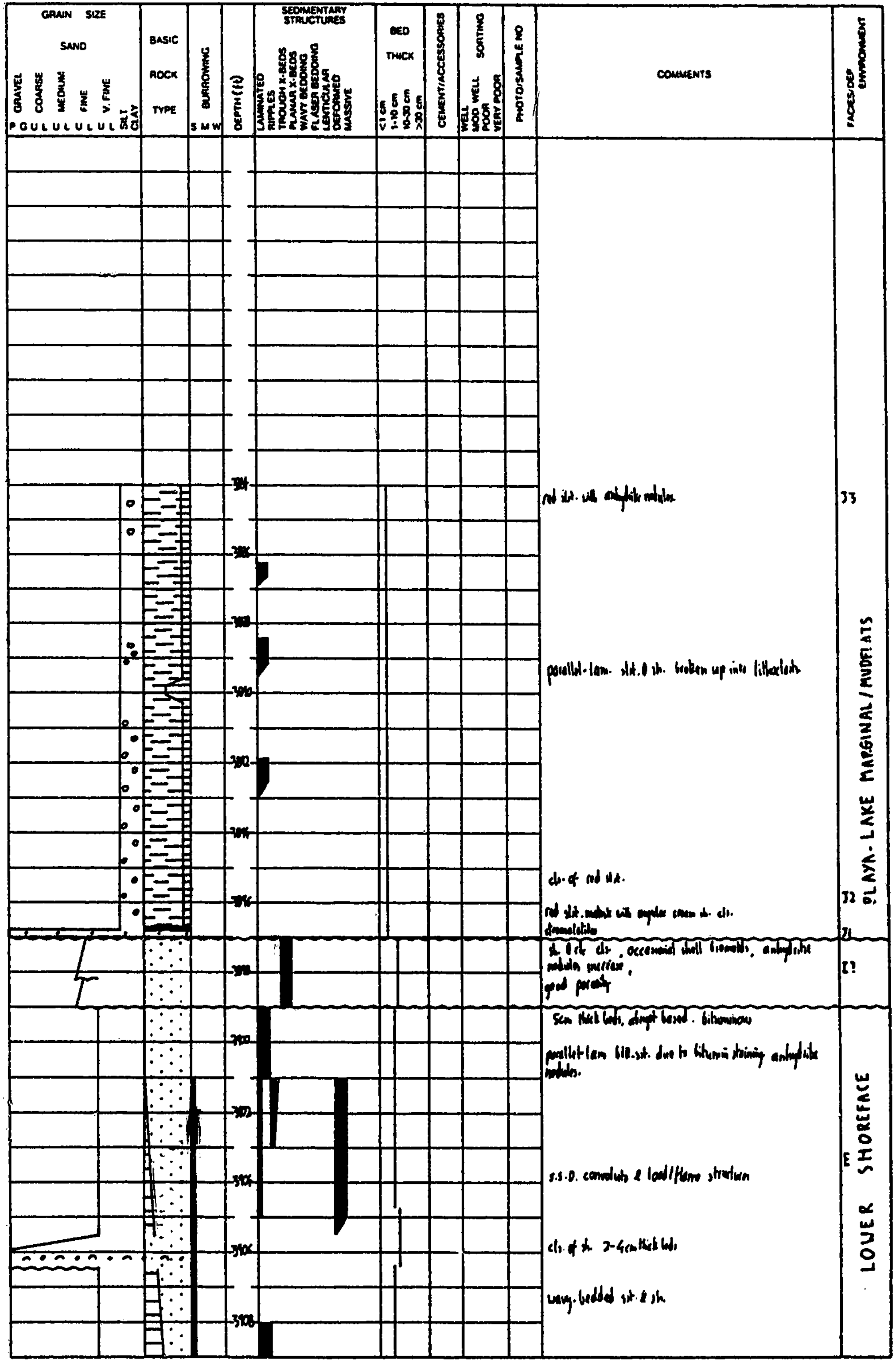

red slt. with anhydrite nodules

parallel-lam. slt. & sh. broken up into lithoclasts

cls. of red slt.

red slt. matrix with angular cream sh. cls.
stromatolite

sh. & slt. cls. , occasional shell fragments, anhydrite
nodules surface ,
good porosity

5cm thick beds, abrupt based. bituminous

parallel-lam blk.-sst. due to bitumen staining anhydrite
nodules.

s.s.D. convolute & load/flame structure

cls. of sh. 2-4cm thick beds

wavy-bedded sst. & sh.

WELL NAME: TEXCAN TEXACO PEESAY
FORMATION: HALFWAY-CHARLIE LAKE
DATE: 6/07/90
LOCATION: d-060-C/94-A-16
CORE INTERVAL:
KB: 2375ft

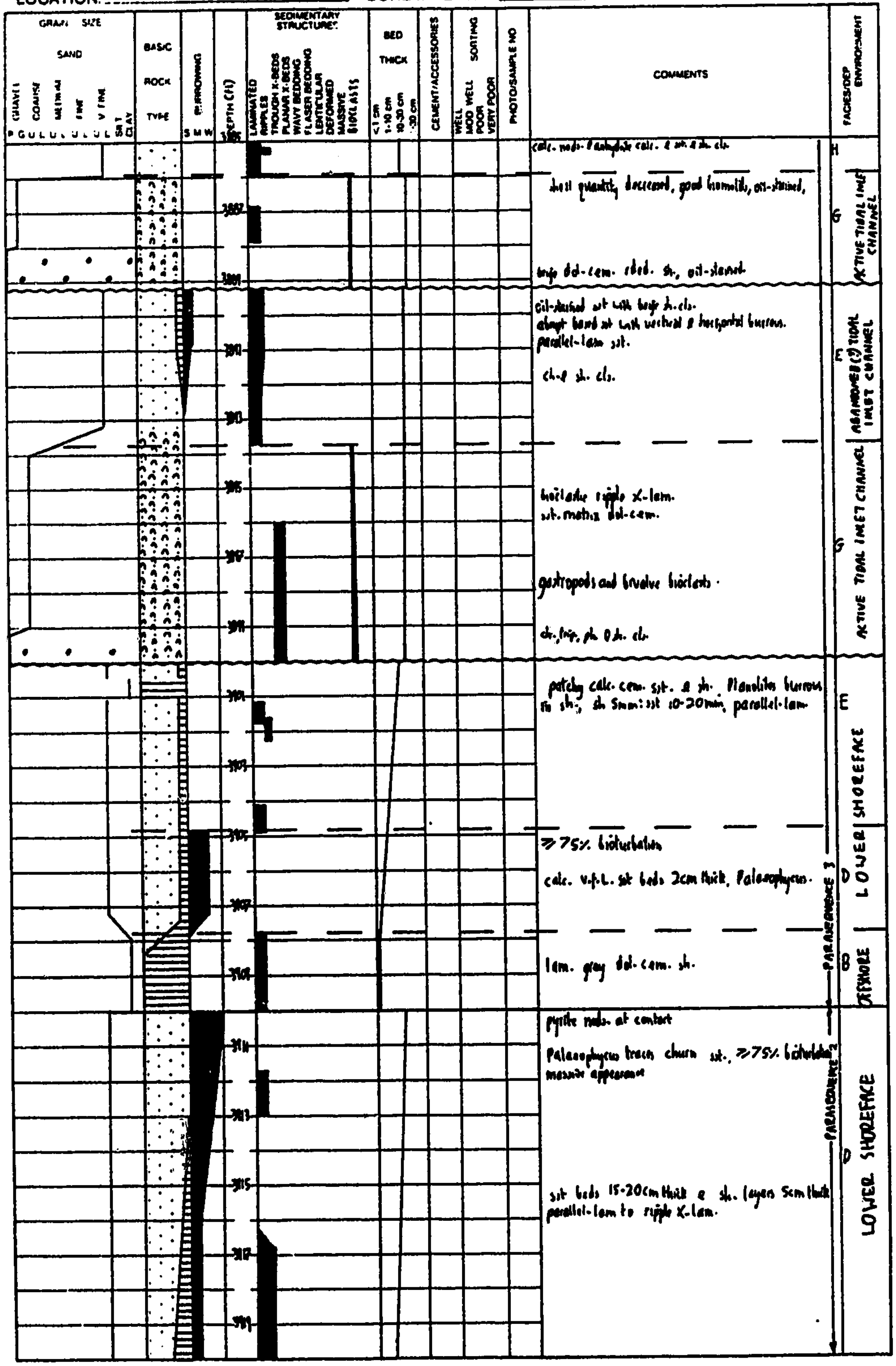

calc. nods. & ankylosite calc. & slt. & sh. cls.

shell quantity decreased, good bioclasts, oil-stained,

large dol-cem. rbd. sh., oil-stained

oil-stained slt with large sh. cls.
abrupt band slt with vertical & horizontal burrows.
parallel-lam slt.

ch.-& sh. cls.

bioclastic ripple X-lam.
slt. matrix dol-cem.

gastropods and bivalve bioclasts.

ch., frag., ph & sh. cls.

patchy calc. cem. slt. & sh. Planolites burrows in sh.; sh 5mm: slt 10-20mm, parallel-lam

≥75% bioturbation

calc. v.f.L. slt beds 2cm thick, Palaeophycus.

lam. gray dol-cem. sh.

pyrite nods. at contact

Palaeophycus traces churn slt., ≥75% bioturbation, massive appearance

slt beds 15-20cm thick & sh. layers 5cm thick parallel-lam to ripple X-lam.

WELL NAME: TEXCAN TEXACO PEEJAY FORMATION: HALFWAY-CHARLIE LAKE DATE: 6/07/90

LOCATION: d-060-C/94-A-16 CORE INTERVAL: KB: 2375ft

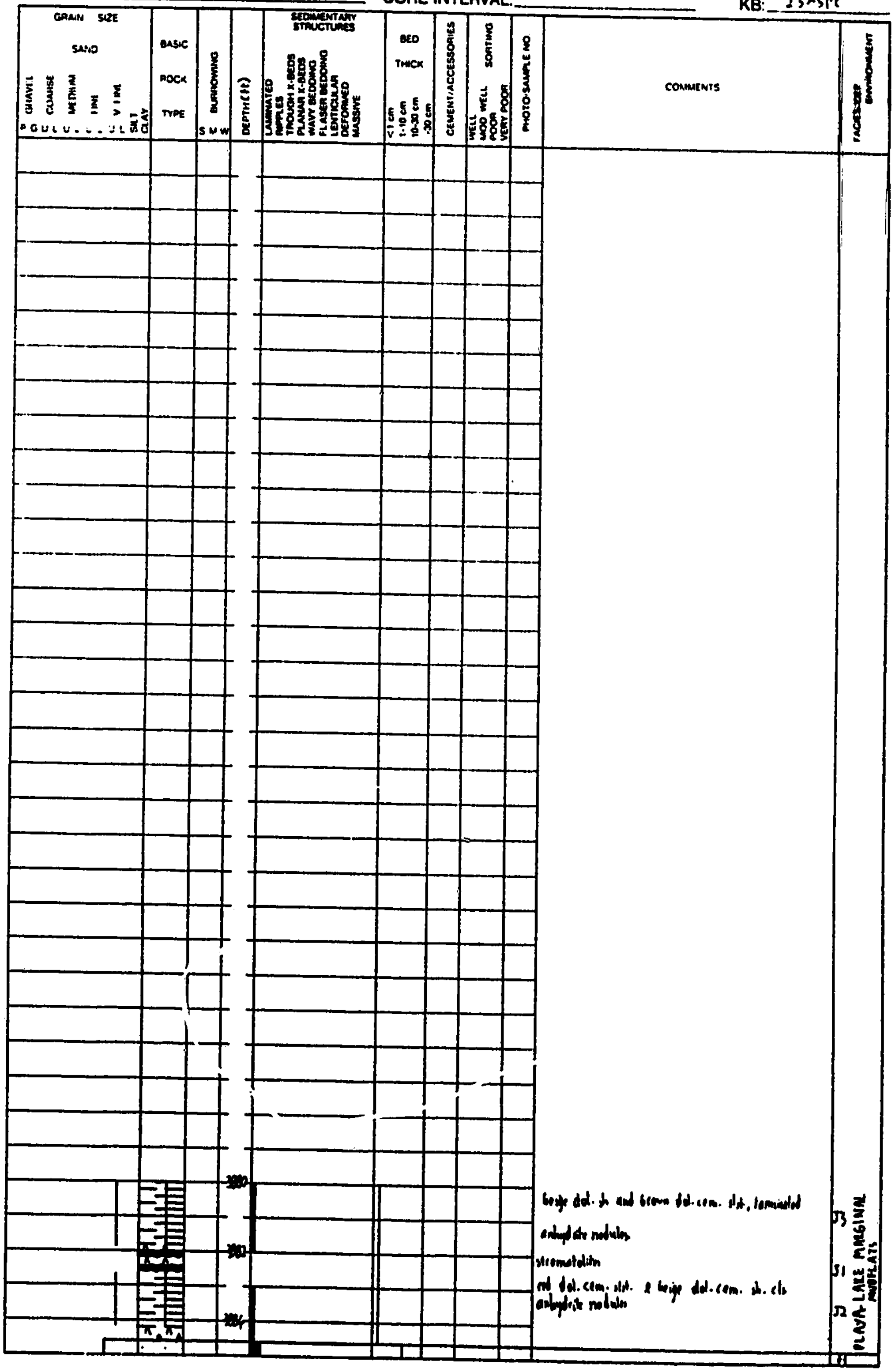

beige dol. sh and brown dol.-cem. slt, laminated

anhydrite nodules

stromatolites

red dol.cem. slt. & beige dol.-cem. sh. cls

anhydrite nodules

WELL NAME: UNION ET AL PEEJAY C-68-C FORMATION: HALFWAY- CHARLIE LAKE DATE: 3/07/91

LOCATION: C-068-C/94-A-16 CORE INTERVAL: KB: 734.3m

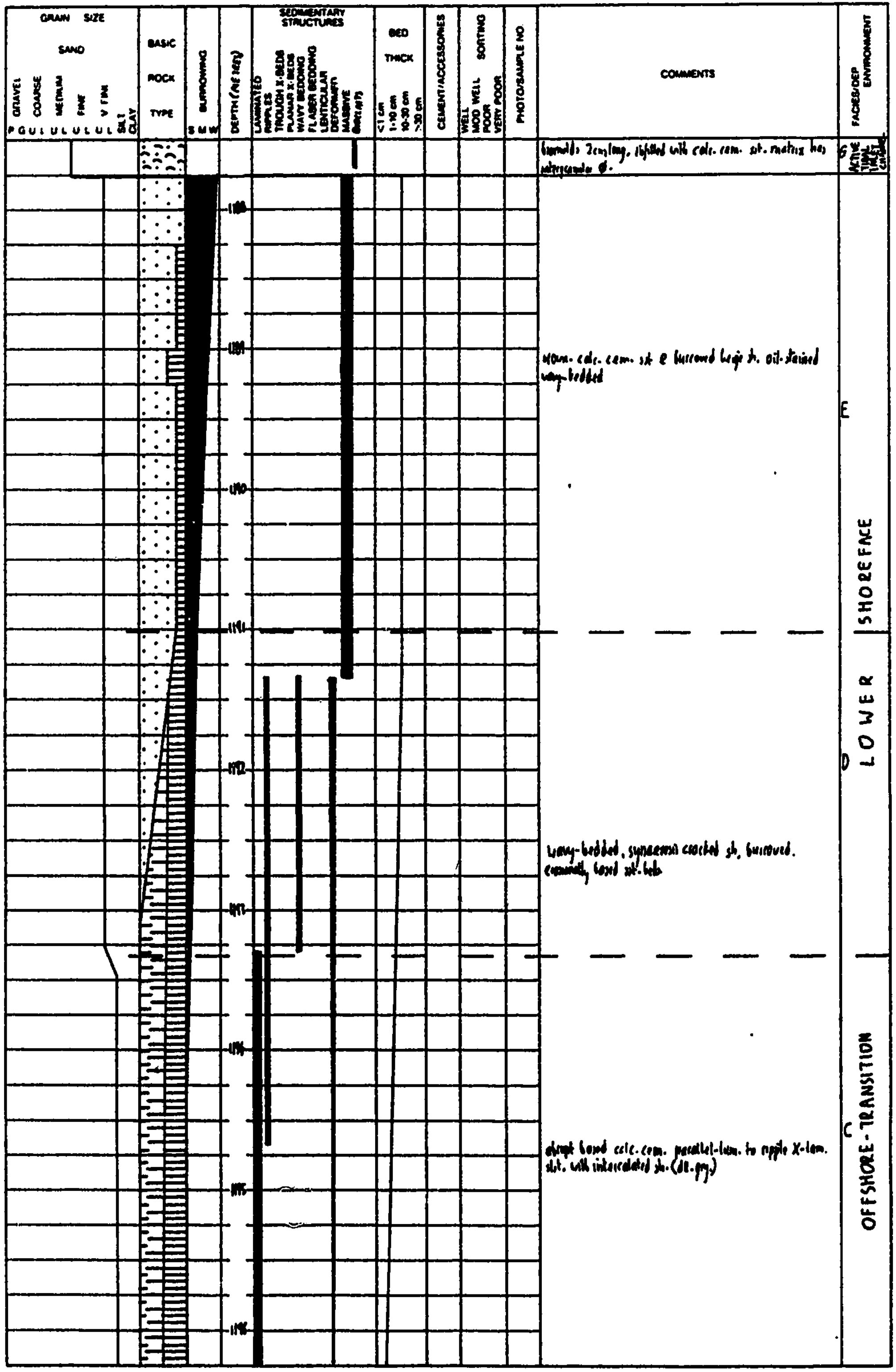

burrows 2cm long, infilled with calc. cem. slt. matrix has intergranular ϕ.

Hom. calc. cem. slt e burrowed large sh. oil-stained wavy-bedded

wavy-bedded, synaeresis cracked sh, burrowed. commonly based slt. beds

abrupt based calc. cem. parallel-lam. to ripple X-lam. slt. with intercalated sh. (dk. gry.)

WELL NAME: UNION ET AL PEEJAY C-68-C FORMATION: HALFWAY-CHARLIE LAKE DATE: 31/07/91

LOCATION: C-068-C/94-A-16 CORE INTERVAL: KB: 734.3m

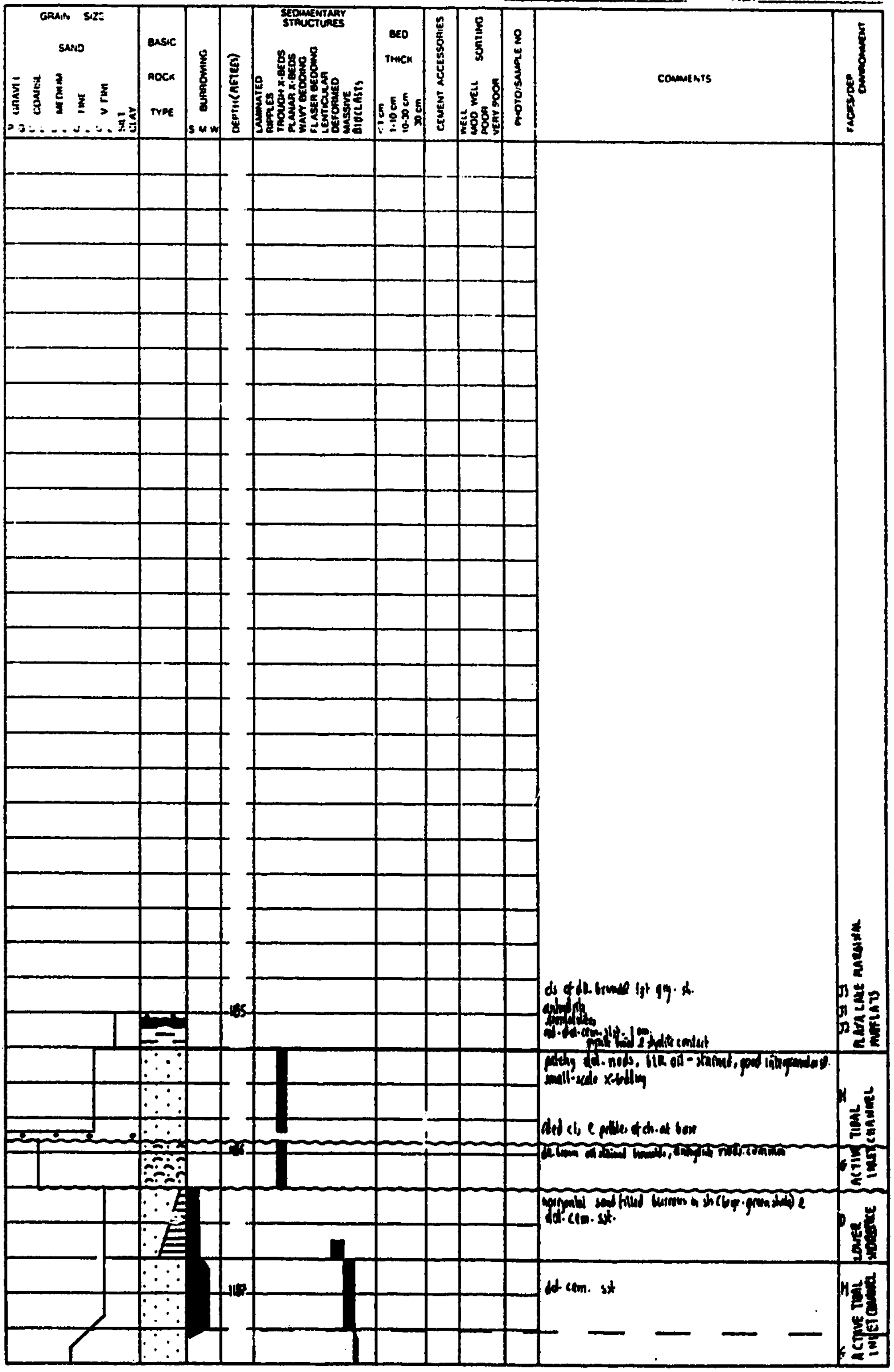

cls of dk. brown & lgt gry. sh.
anhydrite
dolomitization
oil-dol-cem.-slst. 1 cm.
gentle load & dolomite contact

patchy dol. nods., blk oil-stained, good intergranular φ.
small-scale X-bedding

rded cls, & pebbles of ch. at base

dk. brown oil stained burrows, anhydrite nods. common

horizontal sand filled burrows in sh (bge-green shale) & dol. cem. sst.

dol. cem. sst

WELL NAME: UNION H B PEEJAY d-68-C
FORMATION: HALFWAY-CHARLIE LAKE
DATE: 4/07/91
LOCATION: d-068-C/94-A-16
CORE INTERVAL:
KB: 2415ft

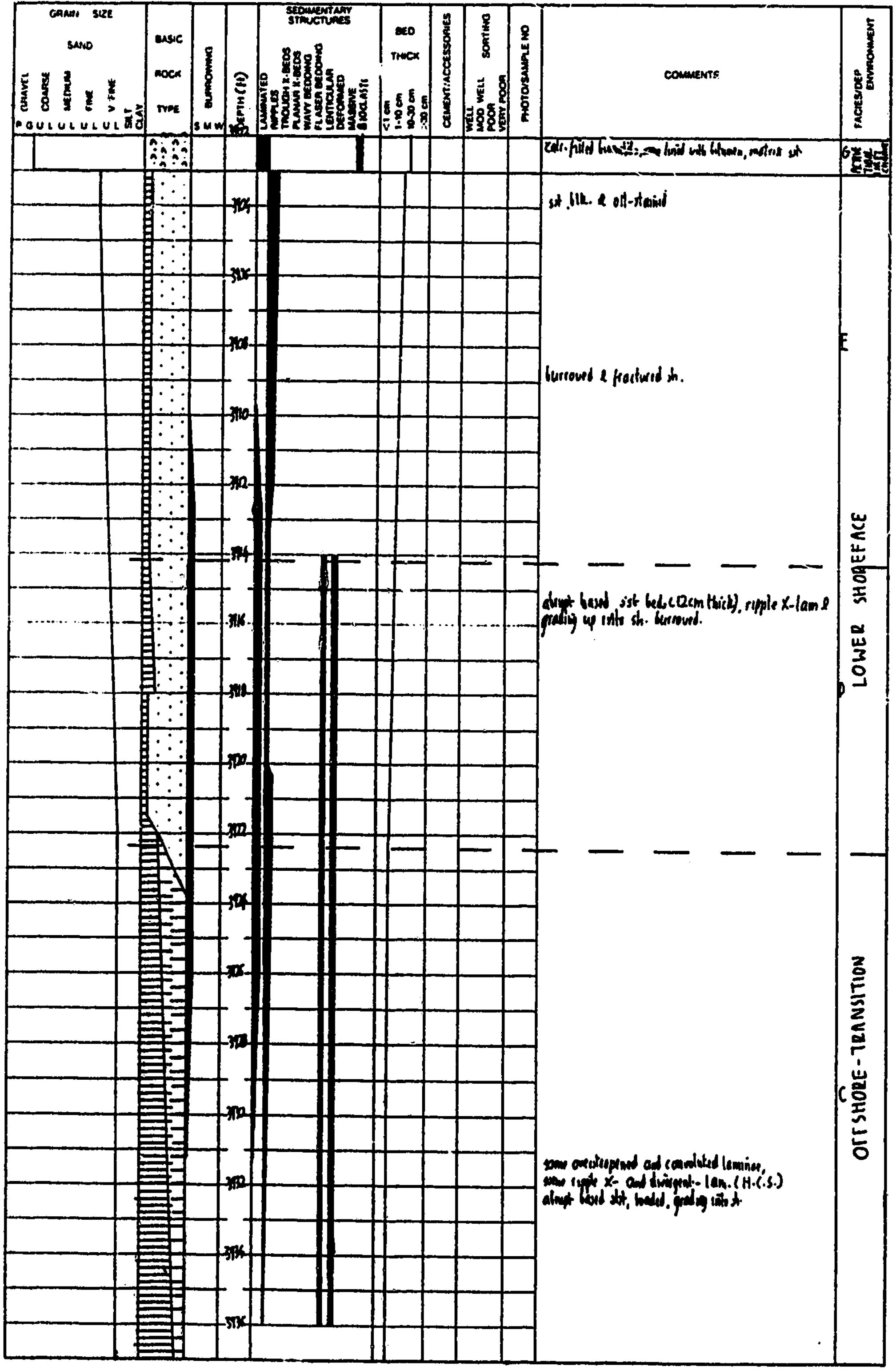

Calc.-filled burrows; some lined with bitumen, matrix sh

sh, blk. & oil-stained

burrowed & fractured sh.

abrupt based sst bed (<2cm thick), ripple X-lam & grading up into sh. burrowed.

some oversteepened and convoluted laminae,
some ripple X- and divergent- lam. (H.C.S.)
abrupt based sltst, loaded, grading into sh.

WELL NAME: UNION HB PEEJAY d-68-C
FORMATION: HALFWAY-CHARLIE LAKE
DATE: 4/07/91
LOCATION: d-068-C/94-A-16
CORE INTERVAL:
KB: 2415ft

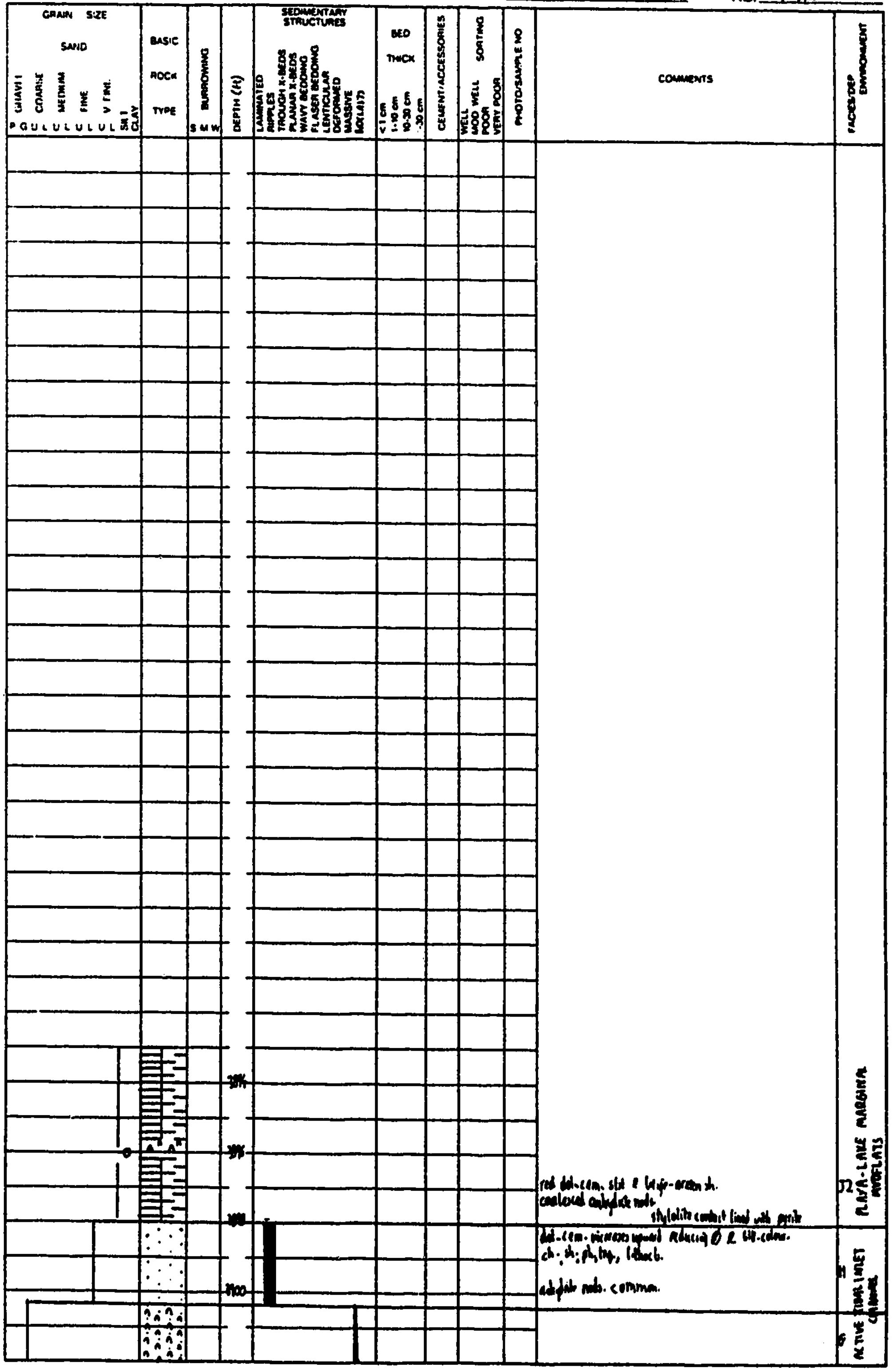

red dol.-cem. slst & lt.gr-green sh.
coalesced anhydrite nods.
stylolite contact lined with pyrite

dol.-cem. micro-x upward reducing Ø & lt.-colour.
ch., sh., pl., bg., lithocl.

anhydrite nods. common.

J2 PLAYA-LAKE MARGINAL MUDFLATS

H

G ACTIVE TIDAL INLET CHANNEL

WELL NAME ... HB CRUSH

FORMATION: HALFWAY-CHARLIE LAKE

DATE: 3/08/90

LOCATION: d-069-C/94-A-16

CORE INTERVAL:

KB: 2398 ft

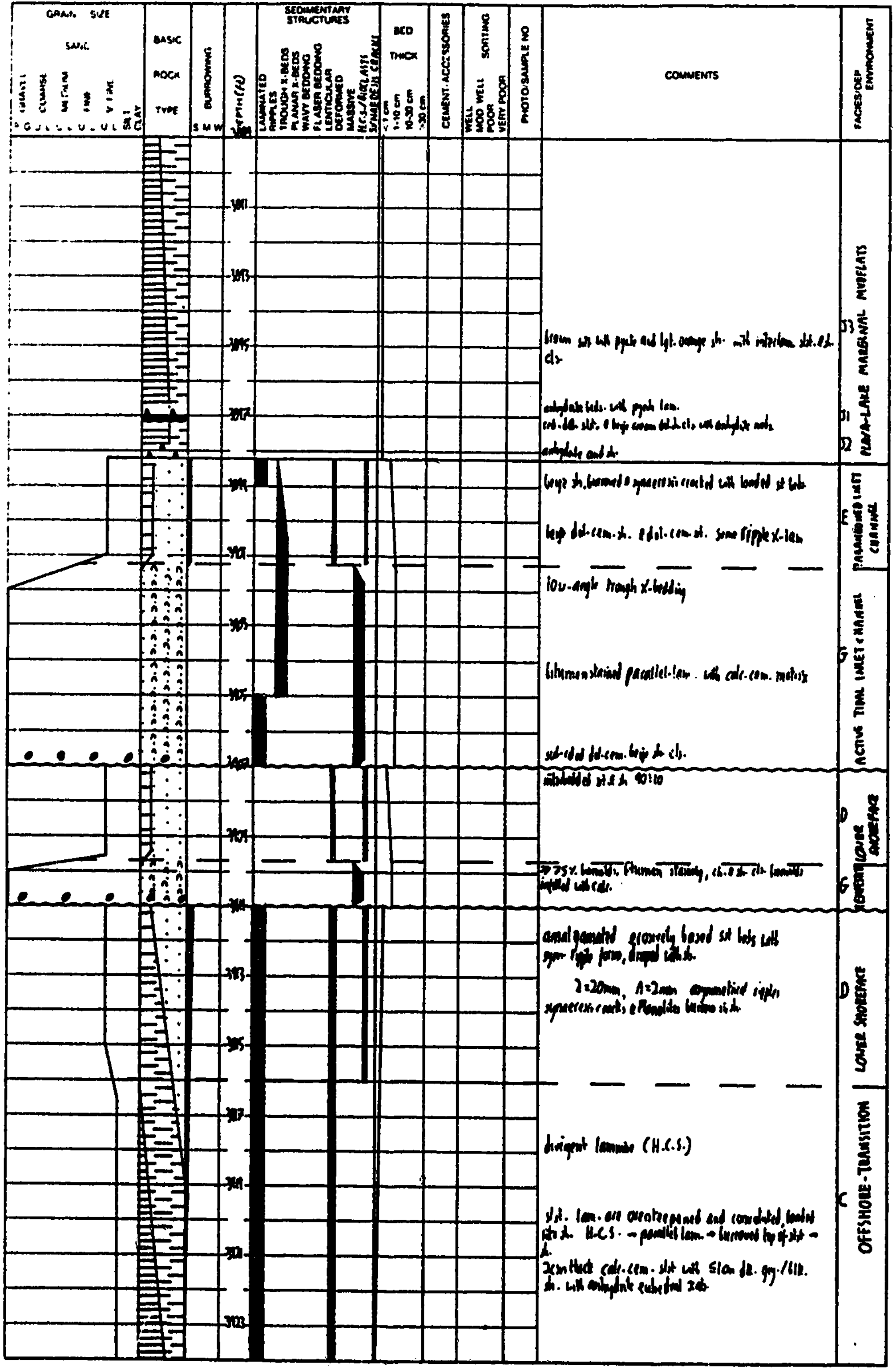

brown slt with pyrite and lgt. orange sh. with interlam. slt. & sh. cls. — D3

anhydrite beds. with pyrite lam. — D1

red-brown slt. & large cream dol. sh. cls. with anhydrite nods. — D2

anhydrite and sh.

PLAYA-LAKE MARGINAL MUDFLATS

large sh. burrowed & synaeresis cracked with loaded st beds

large dol-cem.-sh. & dol.-cem.-st. some ripple X-lam — E

ABANDONED INLET CHANNEL

low-angle trough X-bedding

bitumen stained parallel-lam. with calc-cem. matrix — G

sub-rded dol-cem. large sh. cls.

ACTIVE TIDAL INLET CHANNEL

interbedded st & sh. 90:10 — D

LOWER SHOREFACE

75% bioturb. Bitumen staining, cl. & sh. cls. bioturb. infilled with calc. — G

amalgamated graded based st beds with sym- ripple form, draped with sh.

λ=20mm, A=2mm asymmetrical ripples synaeresis cracks & Planolites burrows in sh. — D

LOWER SHOREFACE

divergent laminae (H.C.S.)

slt. lam. are overstepped and convoluted, loaded into sh. H.C.S. → parallel lam. → burrowed top of slt → sh. — C

2cm thick calc.cem. slt with 5cm dk. gry./blk. sh. with anhydrite cubes and [illegible]

OFFSHORE-TRANSITION

WELL NAME: TEXCAN TEXACO PEEJAY FORMATION: HALFWAY-CHARLIE LAKE DATE: 21/08/90

LOCATION: d-070-C/94-A-16 CORE INTERVAL: KB: 2384.04ft

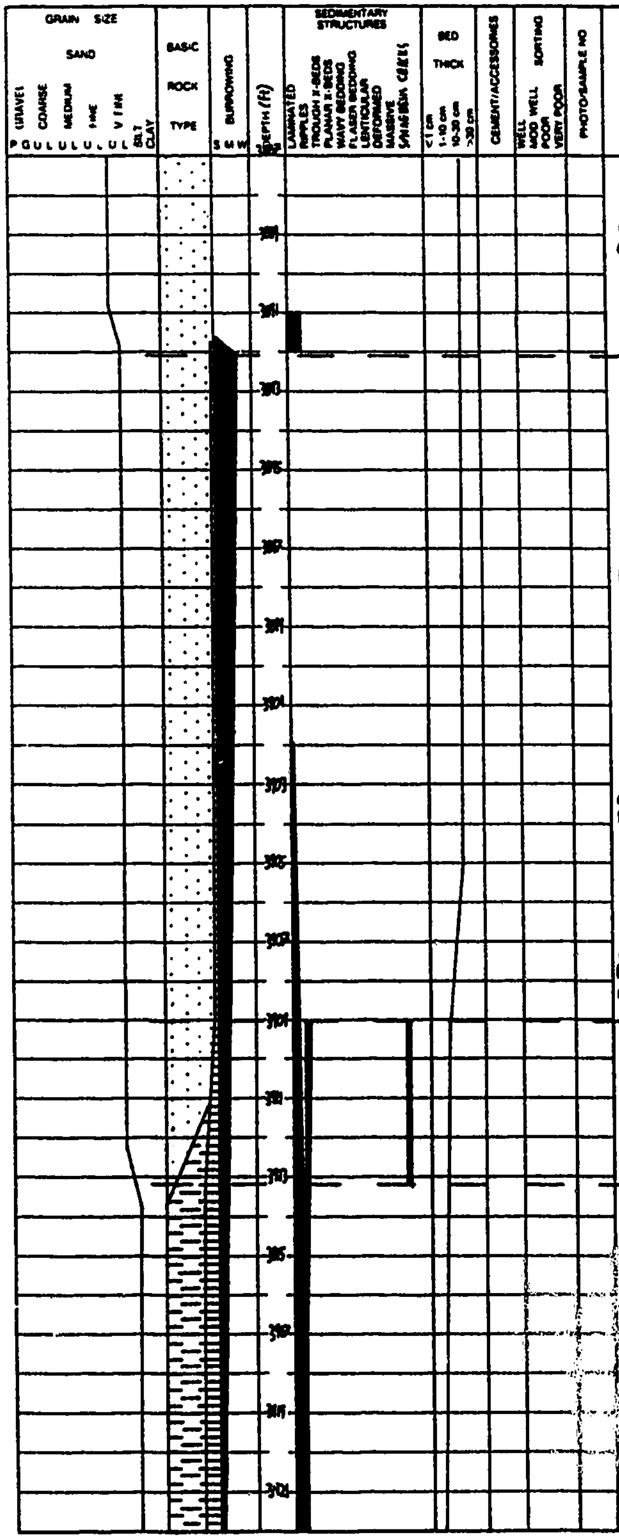

COMMENTS

cls. of sh. & top. cls. & burrows, dol. cem. calc. nod.

sh. cls. in layers

bioturbation Teichichnus.

beige sh. and massive st.

dol. cem. v.f.L. st. with parallel-lam, massive, and ripple X-lam. & thin laminae of sh. burrowed with burrows

85 st : 15 sh. st 25-35cm thick st & 2cm sh. burrowed & synaeresis cracked. st. is parallel-lam & ripple X-lam

sh. draped on st. which is asymmetrical ripples st. is dol. cem. brown. sh. is beige & synaeresis cracks & Planolites, st. is sharp based.

[illegible] cement concentrated in st.-lam. dark bed [illegible] with parallel- and ripple X-lam burrowing [illegible] 60:40 st.:sh.
[illegible] brown-gray sh.

FACIES/DEP ENVIRONMENT

F UPPER SHOREFACE

E LOWER SHOREFACE

D

C OFFSHORE-TRANSITION

WELL NAME TEXCAN TEXACO PEEJAY FORMATION: HALFWAY-CHARLIE LAKE DATE: 21/08/90

LOCATION d-070-C/94-A-16 CORE INTERVAL: KB: 2384.04ft

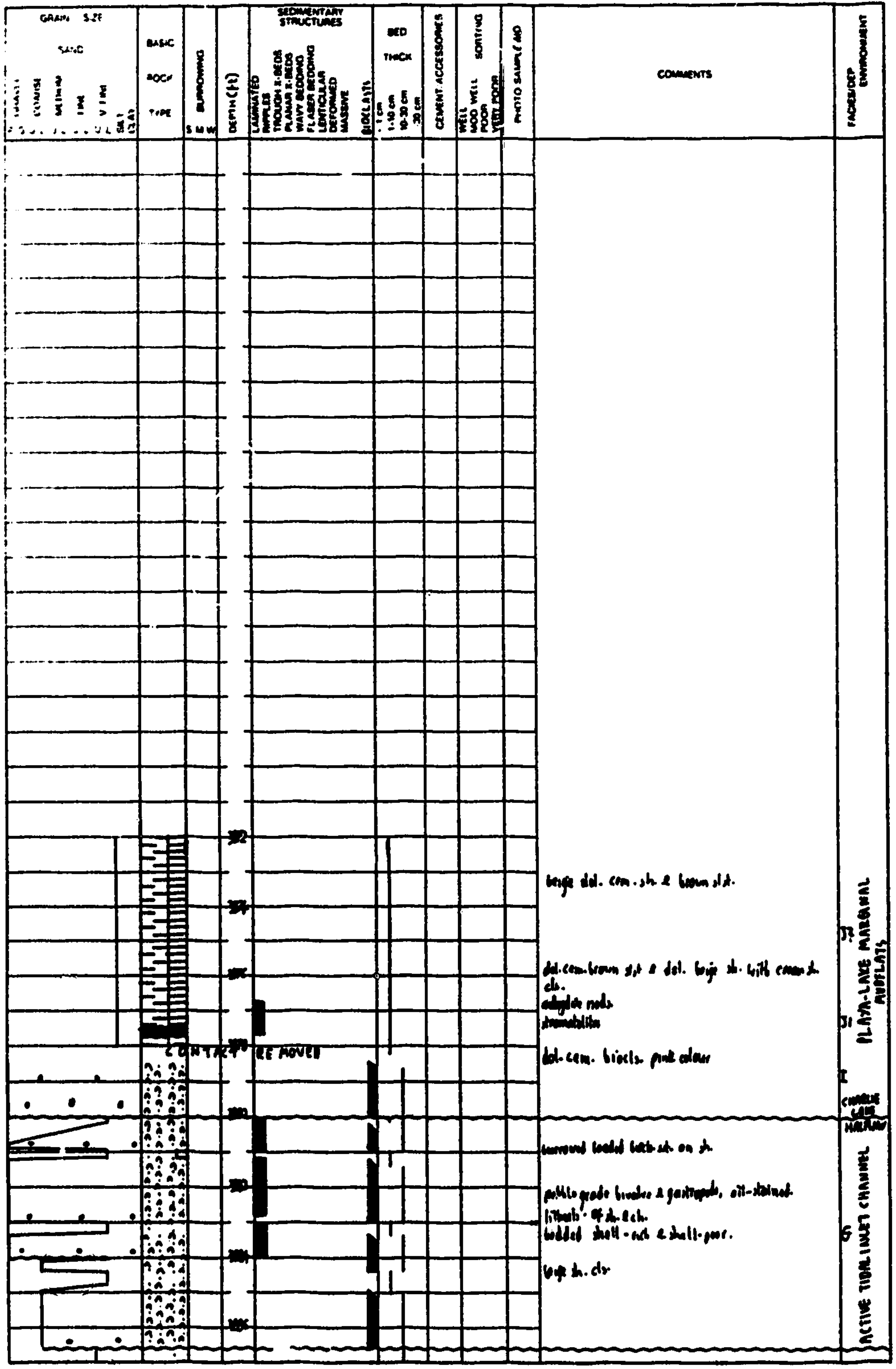

beige dol. cem. sh. & brown slt.

dol. cem. brown slt & dol. beige sh. with cream sh. cls.
anhydrite nods
stromatolites

dol. cem. bioclst. pink colour

burrowed loaded bioclst. sst. on sh.

pebble grade bivalves & gastropods, oil-stained.
lithoclasts of sh. & ch.
bedded shell-rich & shell-poor.

beige sh. cls.

WELL NAME: UNION HB SINCLAIR PACIFIC CRUSH FORMATION: HALFWAY-CHARLIE LAKE DATE: 21/08/90

LOCATION: d-079-C/94-A-16 CORE INTERVAL: KB: 2393.5ft

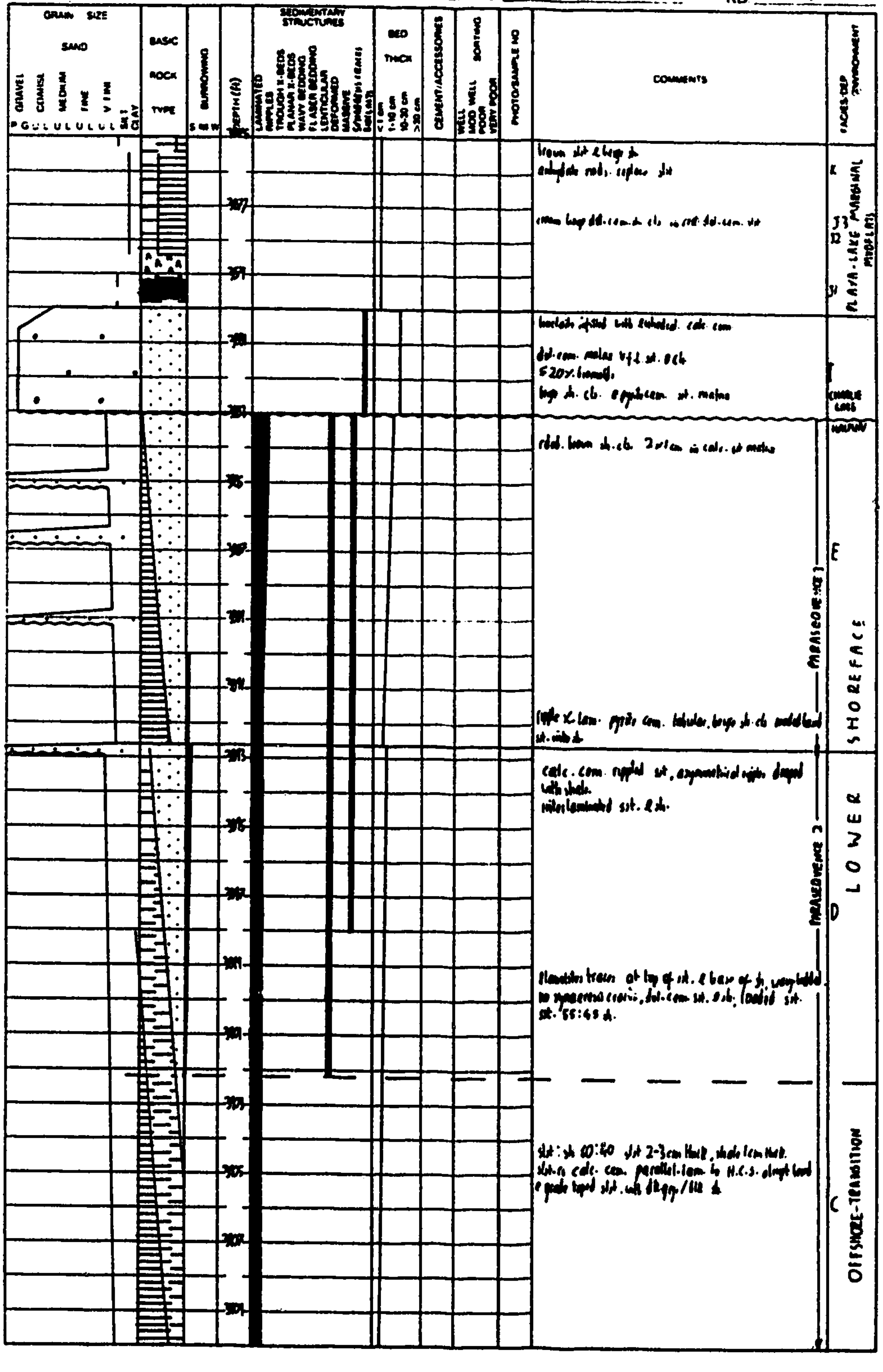

brown slt & [illegible] sh.
[illegible] rods. [illegible] slt

[illegible] dol-cem. [illegible] dol-cem. slt

[illegible] with [illegible] calc cem

dol-cem. [illegible] vfL st. [illegible]
≤20% [illegible]
[illegible] sh. cl. [illegible] st. [illegible]

[illegible] brown sh. cl. 2-x/cm in calc. st [illegible]

[illegible] X-lam. [illegible] cem. tabular, [illegible] sh. cl. [illegible]
st. [illegible] sh.

calc. cem. rippled st, asymmetrical ripples draped with shale.
interlaminated slt. & sh.

[illegible] traces at top of st. & base of sh. [illegible] to symmetrical [illegible], dol-cem. st. [illegible] loaded slt.
slt. 55:45 sh.

slt : sh 60:40 slt 2-3cm thick, shale 1cm thick.
slt-ss calc. cem. parallel-lam. to H.C.S. [illegible]
& grade [illegible] slt. with [illegible] sh.

WELL NAME TEXCAN BUCKTHORN FORMATION: HALFWAY-CHARLIE LAKE DATE: 3/08/90

LOCATION d-080-C/94-A-16 CORE INTERVAL: KB: 2382.2ft

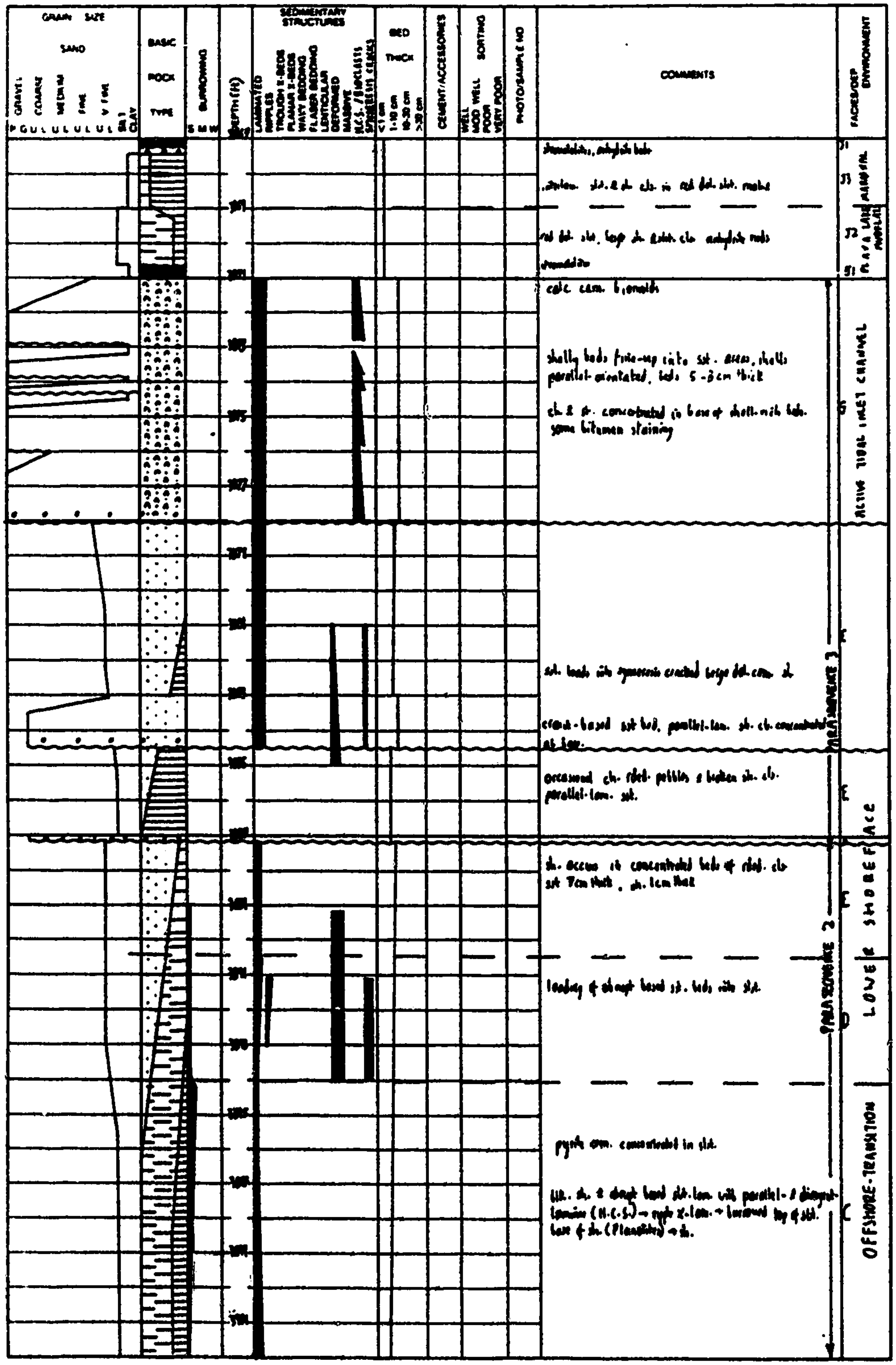

[illegible], anhydrite beds

[illegible] sst. & sh. clo. in red dol. slst. matrix

red dol. slst. large sh. [illegible] clo. anhydrite nodules

[illegible]

calc cem. [illegible]

shelly beds fine-up into sst. [illegible], shells parallel-orientated, beds 5-8cm thick

ch. & sh. concentrated in base of shell-rich beds. some bitumen staining

sst. beds with [illegible] cracked large dol.-cem. sh.

erosion-based sst bed, parallel-lam. sh. clo. concentrated at base.

occasional ch. [illegible] pebbles & broken sh. clo. parallel-lam. sst.

sh. occurs in concentrated beds of [illegible] clo. sst 7cm thick, sh. 1cm thick

loading of abrupt based sst. beds into slst.

pyrite cem. concentrated in slst.

[illegible] sh. & abrupt based slst.-lam. with parallel- & divergent-laminae (H.C.S.) → ripple x-lam. → burrowed top of slst. base of sh. (Planolites) → sh.

WELL NAME: UNION SINCLAIR PAC CRUSH d-89-C

FORMATION: HALFWAY-CHARLIE LAKE

DATE 31/01/91

LOCATION: d-089-C/94-A-16

CORE INTERVAL:

KB: 2395 8ft

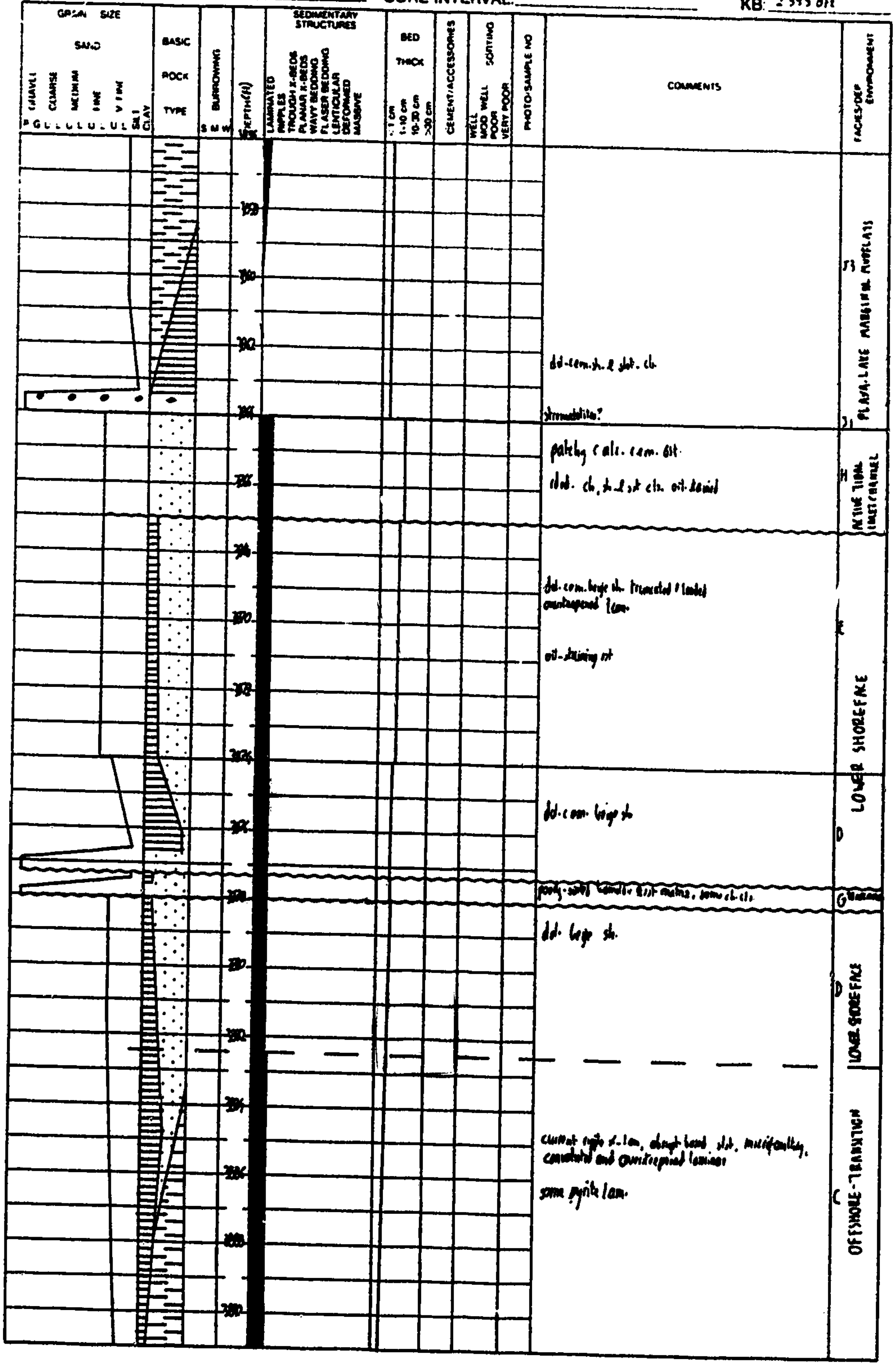

dd-com.sh.& slot. cl.

stromatolites?

patchy calc. cem. sst.

clast. cl., sh.-l, sst cls. oil-stained

dd-com. large sh. truncated / lenticular
countergraded lam.

oil-staining sst

dd-com. large sh.

poorly-sorted sandy silt matrix, some cl. cls.

dd- large sh.

current ripple x-lam., abrupt based sst., multifaceted,
convoluted and countergraded laminae

some pyrite lam.

WELL NAME: TEXCAN BUCKTHORN d-90-C

FORMATION: HALFWAY-CHARLIE LAKE

DATE: 22/01/91

LOCATION: d-090-C/94-A-16

CORE INTERVAL:

KB: 2389ft

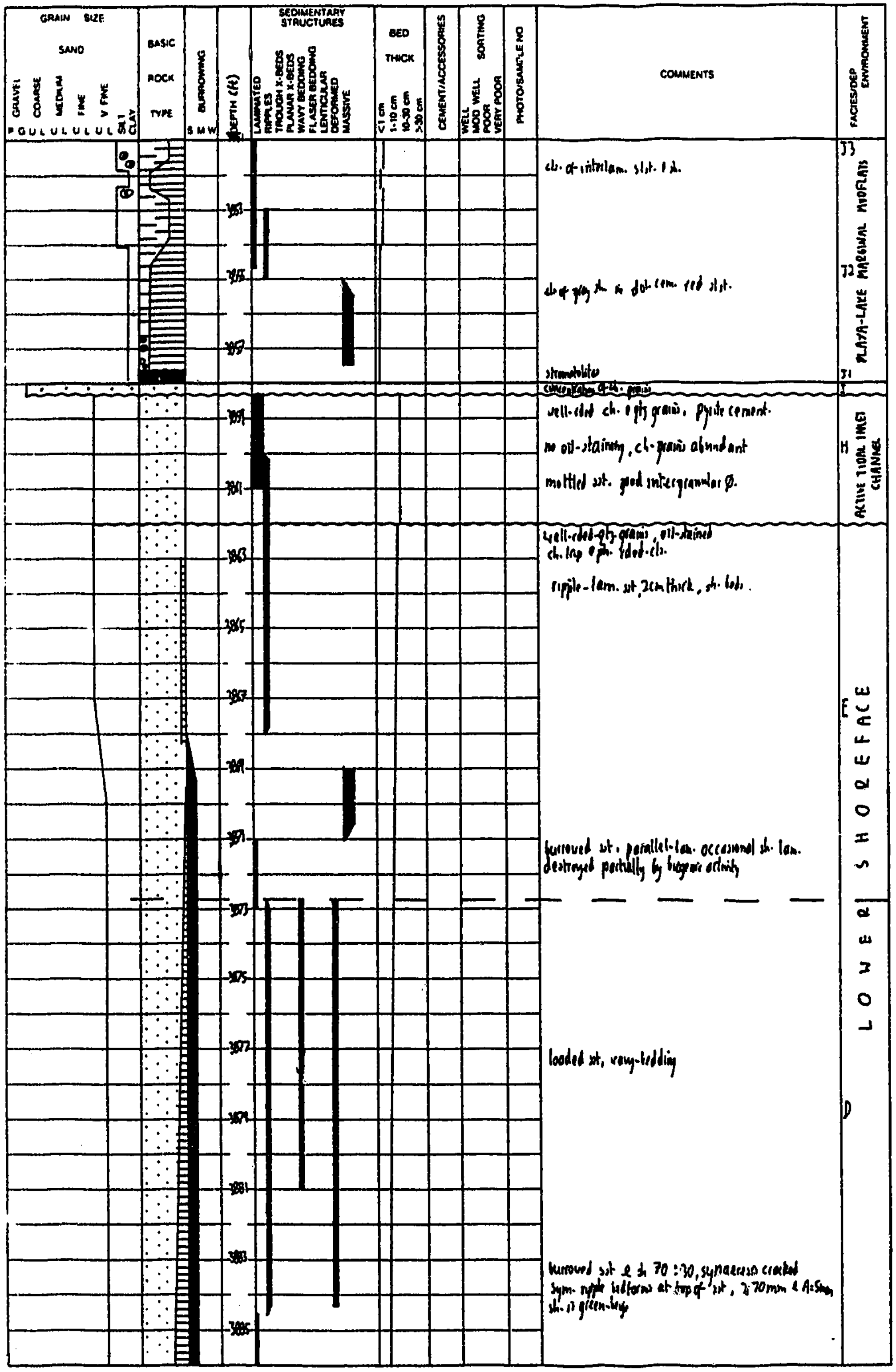

cl. of intrlam. slst. & sh.

cl. of gry sh. in dol-cem. red slst.

stromatolites

concentration of cl. grains

well-rdd cl. & qtz grains, pyrite cement.

no oil-staining, cl-grains abundant

mottled sst. good intergranular Ø.

well-rdd-qtz-grains, oil-stained

cl. lag & ph. rdd-cls.

ripple-lam. sst, 2cm thick, sh. lobs.

burrowed sst. parallel-lam. occasional sh. lam.
destroyed partially by biogenic activity

loaded sst, wavy-bedding

burrowed sst & sh 70:30, synaeresis cracked
sym. ripple bedforms at top of sst, 2:70mm & A:Sm
sh. is green-gry

WELL NAME: TEXCAN BUCKTHORN d-90-C FORMATION: HALFWAY-CHARLIE LAKE DATE: 22/01/91

LOCATION: d-090-C/94-A-16 CORE INTERVAL: KB: 2389ft

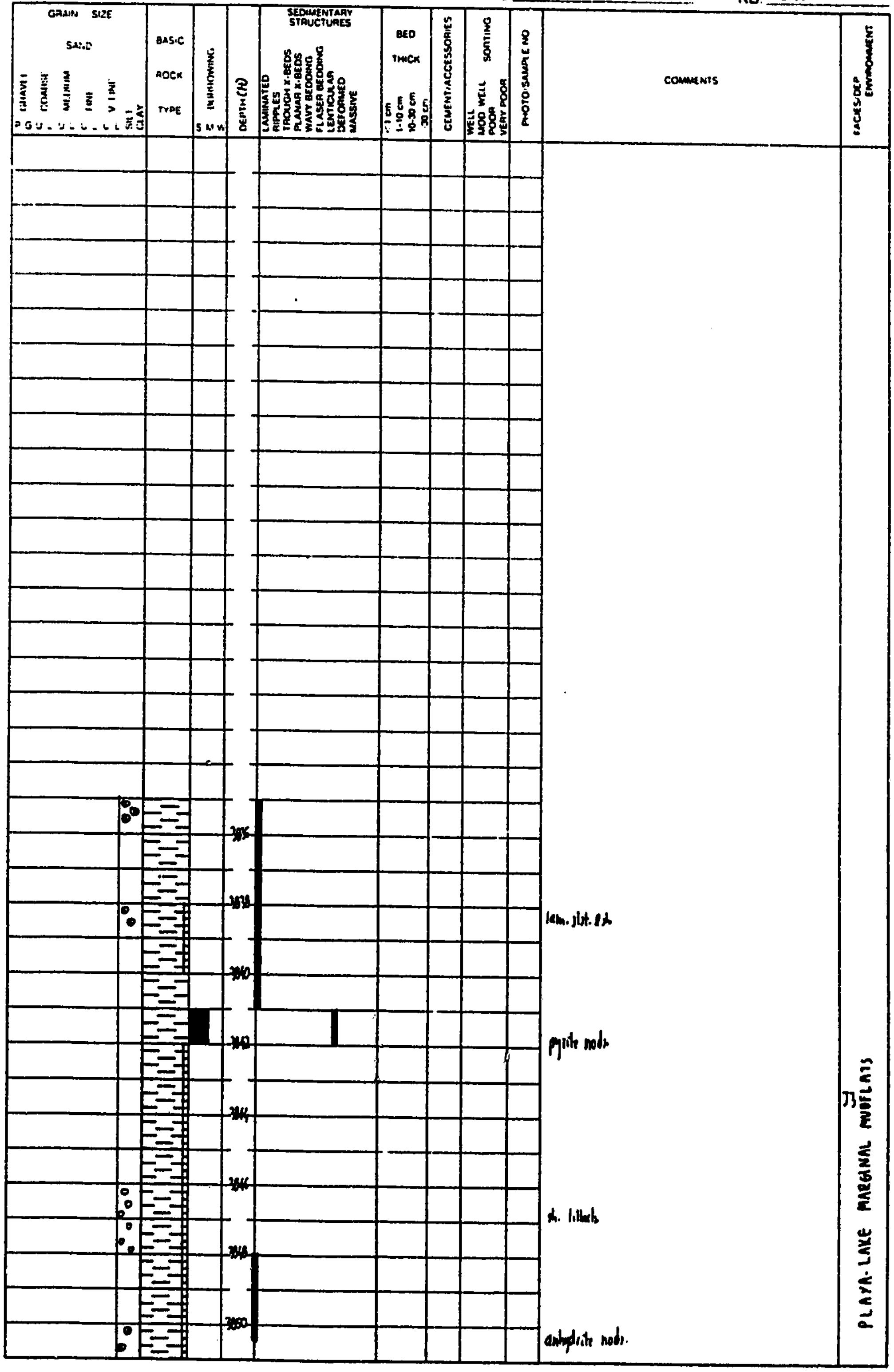

WELL NAME: UNION HB SINC. PAC. CIGOL CRUSH FORMATION: HALFWAY-CHARLIE LAKE DATE: 22/08/90

LOCATION: d-098-C/94-A-16 CORE INTERVAL: KB: 2408ft

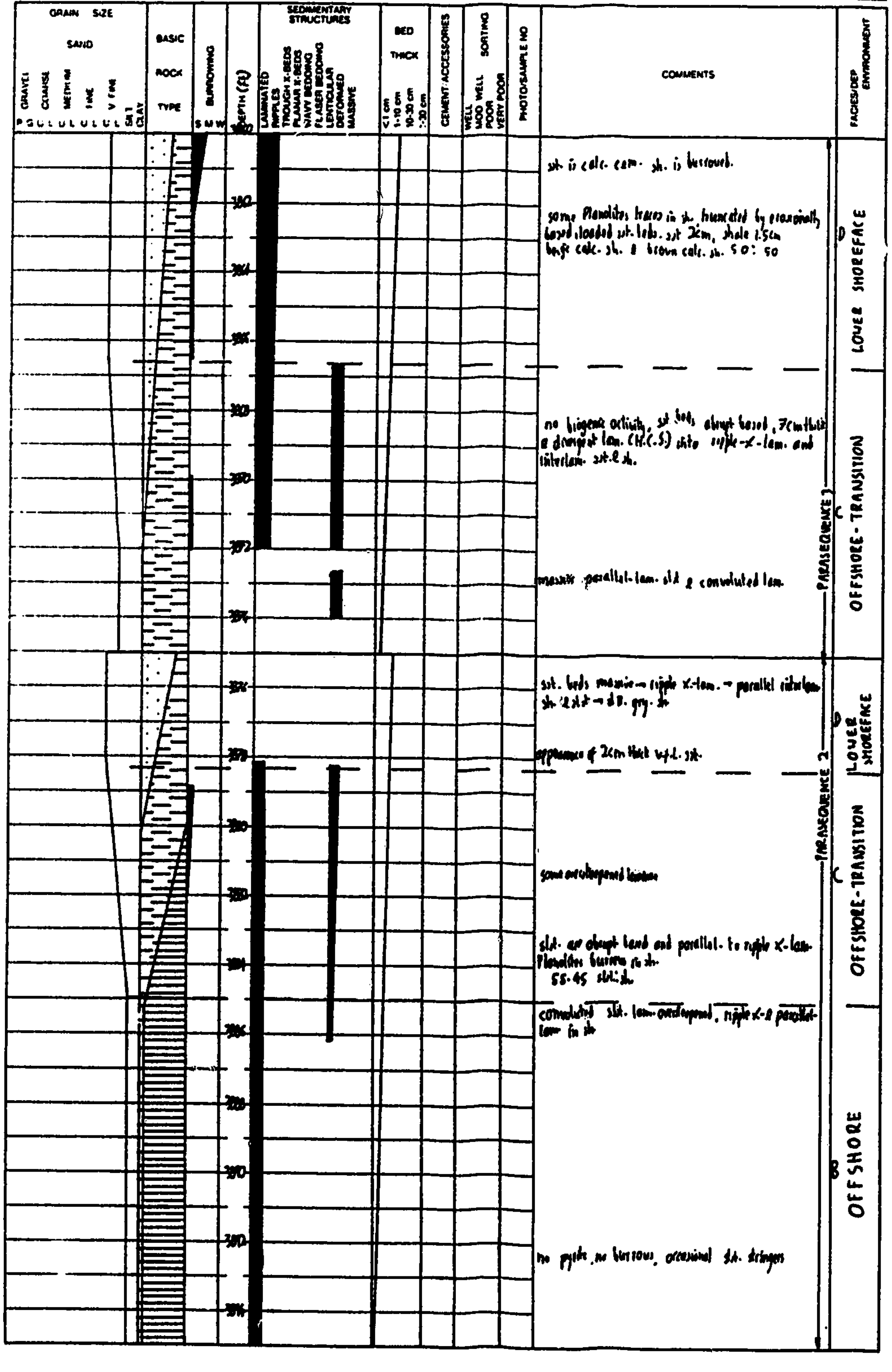

slt. is calc. cem. sh. is burrowed.

some Planolites traces in sh. truncated by erosionally based, loaded slt. beds. slt 2cm, shale 1.5cm beige calc. sh. & brown calc. sh. 50: 50

no biogenic activity, slt beds abrupt based, 7cm thick & divergent lam. (H.C.S.) into ripple-x-lam. and interlam. slt. & sh.

massive parallel-lam. slt & convoluted lam.

slt. beds massive → ripple x-lam. → parallel interlam. sh. & slt → dk. gry. sh.

appearance of 2cm thick v.f.-L. slt.

some oversteepened laminae

slt. are abrupt based and parallel- to ripple x-lam. Planolites burrows in sh.
55:45 slt:sh.

convoluted slt. lam. oversteepened, ripple x- & parallel-lam. in sh.

no pyrite, no burrows, occasional slt. stringers

WELL NAME: UNION HB SINC PAC. CIGOL CRUSH
FORMATION: HALFWAY-CHARLIE LAKE
DATE: 22/08/90
LOCATION: d-098-C/94-A-16
CORE INTERVAL:
KB: 2408H

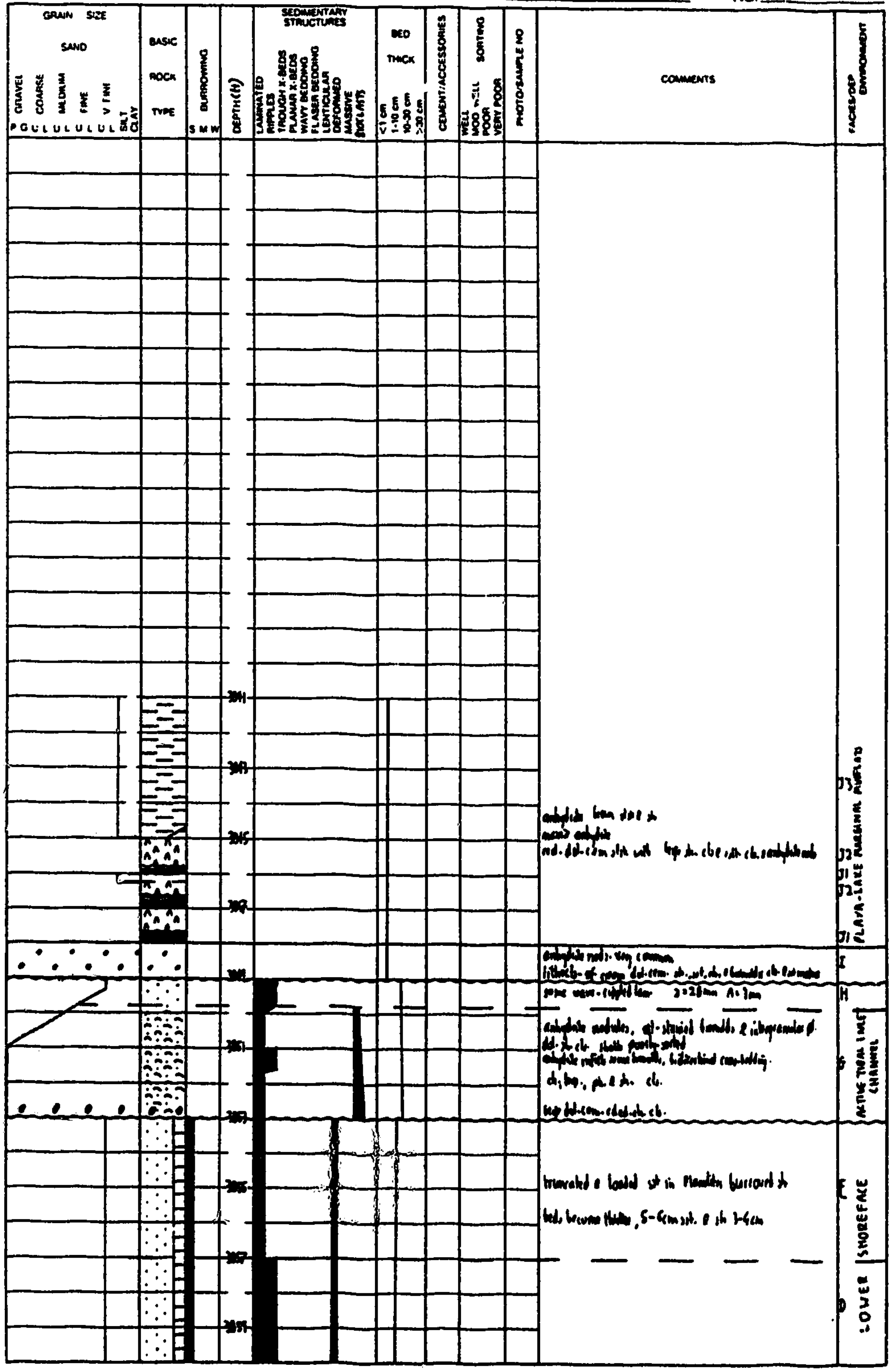

anhydrite bands [illegible] sh
[illegible] anhydrite
red. dol-c.crn. slst. with [illegible] sh. [illegible] ch. anhydrite [illegible]

anhydrite nods. very common
lithoclasts of [illegible] dol-crm. sh., slt, cb., [illegible] cb. [illegible]
some wave-rippled lam. [illegible]=28mm A=1mm

anhydrite nodules, oil-stained [illegible] & [illegible]
dol. sh. cl. shells poorly-sorted
anhydrite [illegible], bidirectional cross-bedding.
cl., bop., ps. & sh. cl.
top dol-crm. clast. sh. cl.

truncated & loaded st in [illegible] burrowed sh
beds become thicker, 5-6cm slt. & sh 3-4cm

WELL NAME UNION HB SINCLAIR PACIFIC C160L CRUSH FORMATION: HALFWAY-CHARLIE LAKE DATE: 21/06/90

LOCATION d-099-C/94-A-16 CORE INTERVAL: KB: 2403.5ft

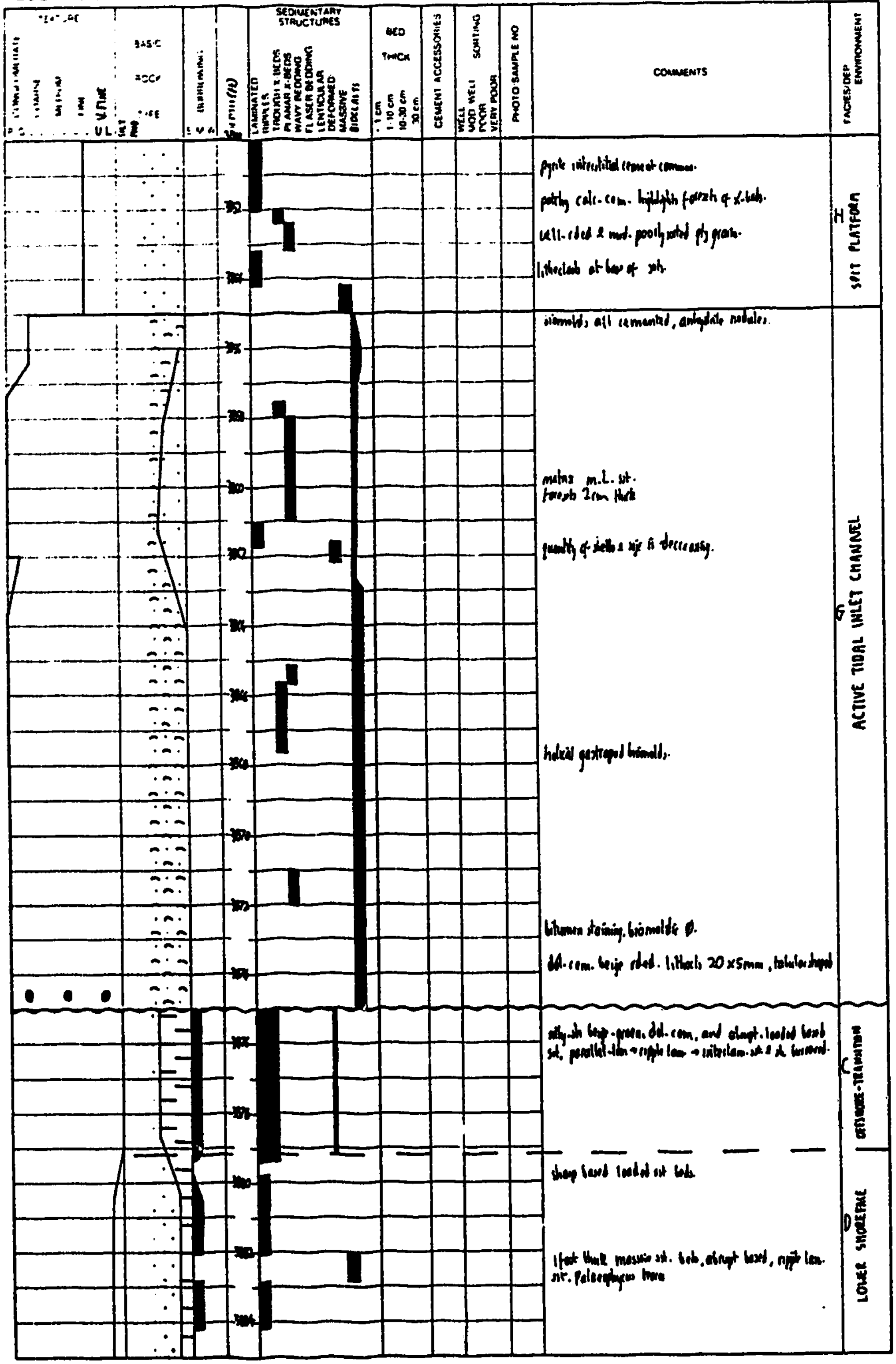

pyrite interstitial cement common.

patchy calc-cem. highlights foresets of x-beds.

well-rded & mod. poorly sorted qtz grains.

lithoclasts at base of set.

biomolds, all cemented, anhydrite nodules.

mainly m.L. sst.
foresets 2cm thick

quantity of shells & size is decreasing.

helical gastropod biomolds.

bitumen staining, biomoldic ϕ.

dol-cem. beige rded. lithocls 20 x 5mm, tabular shaped

silty-sh beige-green, dol-cem, and abrupt. loaded based sst, parallel-lam + ripple lam → interlam. sst & sh. burrowed.

sharp based loaded sst beds.

1 foot thick massive sst. beds, abrupt based, ripple lam. sst. Palaeophycus trace

WELL NAME: UNION HB SINCLAIR PACIFIC CIGOL CRUSH FORMATION: HALFWAY-CHARLIE LAKE DATE: 21/06/90

LOCATION: d-099-C/94-A-16 CORE INTERVAL: KB: 2403 5ft

TEXTURE CONGLOMERATE COARSE MEDIUM FINE	BASIC ROCK TYPE	BURROWING S M W	DEPTH (ft)	SEDIMENTARY STRUCTURES LAMINATED RIPPLES TROUGH X-BEDS PLANAR X-BEDS WAVY BEDDING FLASER BEDDING LENTICULAR DEFORMED MASSIVE	BED THICK <1 cm 1-10 cm 10-30 cm >30 cm	CEMENT/ACCESSORIES	SORTING WELL MOD WELL POOR VERY POOR	PHOTO/SAMPLE NO	COMMENTS	FACIES/DEP ENVIRONMENT
			3846	■					interlam. green/grey dol.-cem sh. & brown dol.-cem st. common microfaulting	J3
			3848	■					algal-laminites anhydrite nodules	J1
									[illegible] lines contact	J2

PLAYA-LAKE MARGINAL MUDFLATS

WELL NAME: CIGOL PEEJAY d-100-C FORMATION: HALFWAY-CHARLIE LAKE DATE: 15/08/90

LOCATION: d-100-C/94-A-16 CORE INTERVAL: KB: 2394ft

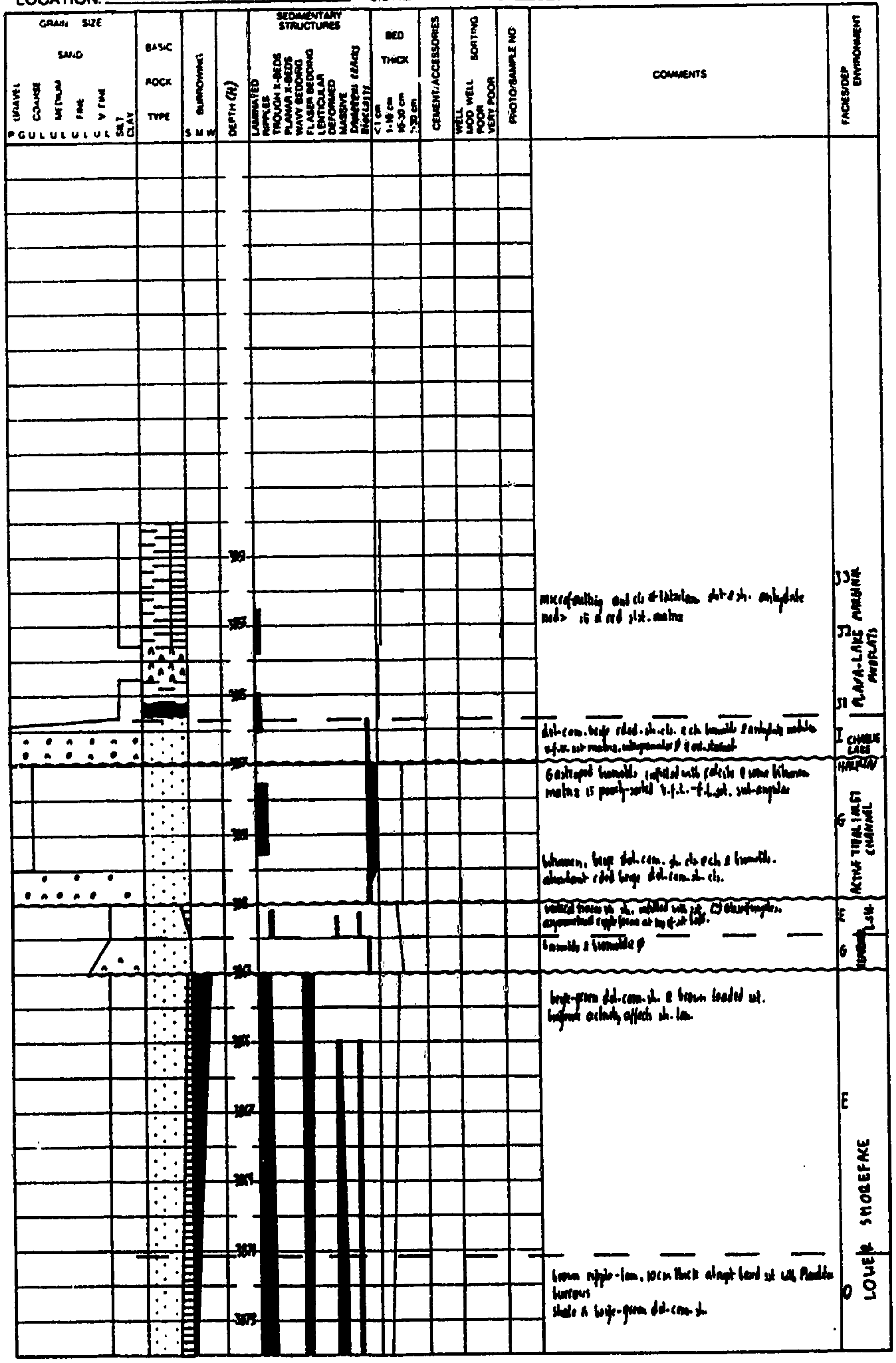

microfaulting and cls of laminated silt & sh. anhydrite nod> 15 & red slt. matrix

dol-cem. beige clast. sh.-cls. & ch. bioclasts & anhydrite nodules v.f.-m. sst matrix, subangular & sub-rounded

Gastropod bioclasts infilled with calcite & some bitumen matrix is poorly-sorted v.f.L.-f.L.sst. sub-angular

bitumen, beige dol.cem. sh. cls & ch & bioclasts. abundant clast beige dol.-cem. sh. cls.

vertical traces in sh. infilled with ss. (?) Ophiomorpha. asymmetrical ripple forms at top of ss bed.

bioclasts & bioclastic ?

beige-green dol.-cem. sh. & brown loaded sst. burrow activity affects sh. lam.

brown ripple-lam., 10cm thick abrupt based sst with Planolites burrows
shale & beige-green dol.-cem. sh.

WELL NAME: PACIFIC PROV FOX
FORMATION: HALFWAY-CHARLIE LAKE
DATE: 16/08/90
LOCATION: d-060-B/94-A-16
CORE INTERVAL:
KB: 2373ft

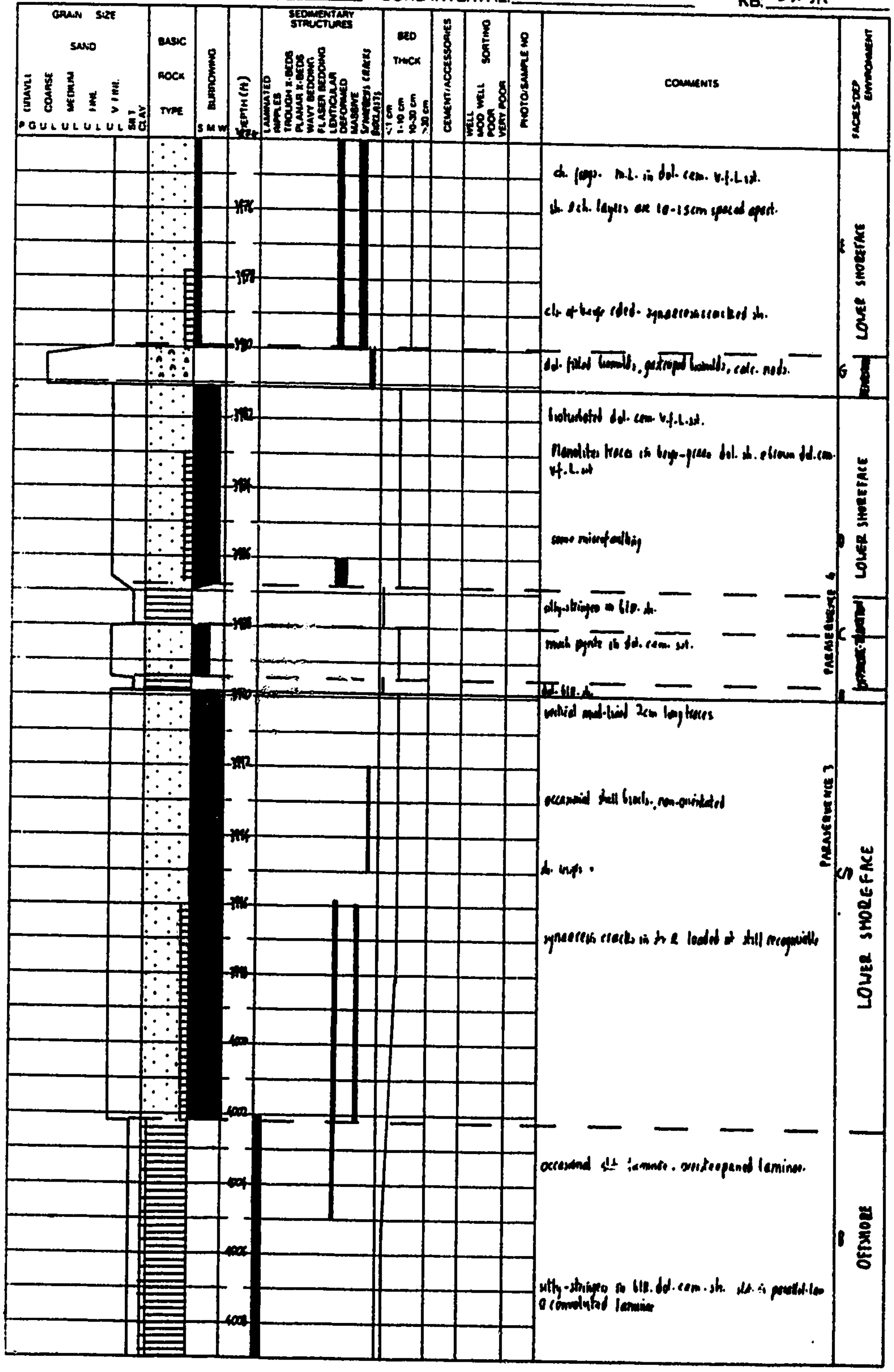

sh. laps. m.L. in dol. cem. v.f.L.st.

sh. sch. layers are 10-15cm spaced apart.

cls of beige cdcd. synaeresiscracked sh.

dol. filled burrows, gastropod burrows, calc. nods.

bioturbated dol. cem. v.f.L.st.

Planolites traces in beige-green dol. sh. & brown dol. cem. v.f.L.st

some microfaulting

silty-stringers in blk. sh.

much pyrite in dol. cem. st.

dol. blk. sh.

vertical mud-lined 2cm long traces

occasional shell beds, non-orientated

sh. rips.

synaeresis cracks in sh & loaded at still recognizable

occasional slt laminae. overdeepened laminae.

silty-stringers in blk. dol. cem. sh. slt is parallel-lam & convoluted laminae

WELL NAME: PACIFIC PROV FOX

FORMATION: HALFWAY-CHARLIE LAKE

DATE: [illegible] 08/90

LOCATION: d-060-D/94-A-16

CORE INTERVAL:

2373ft

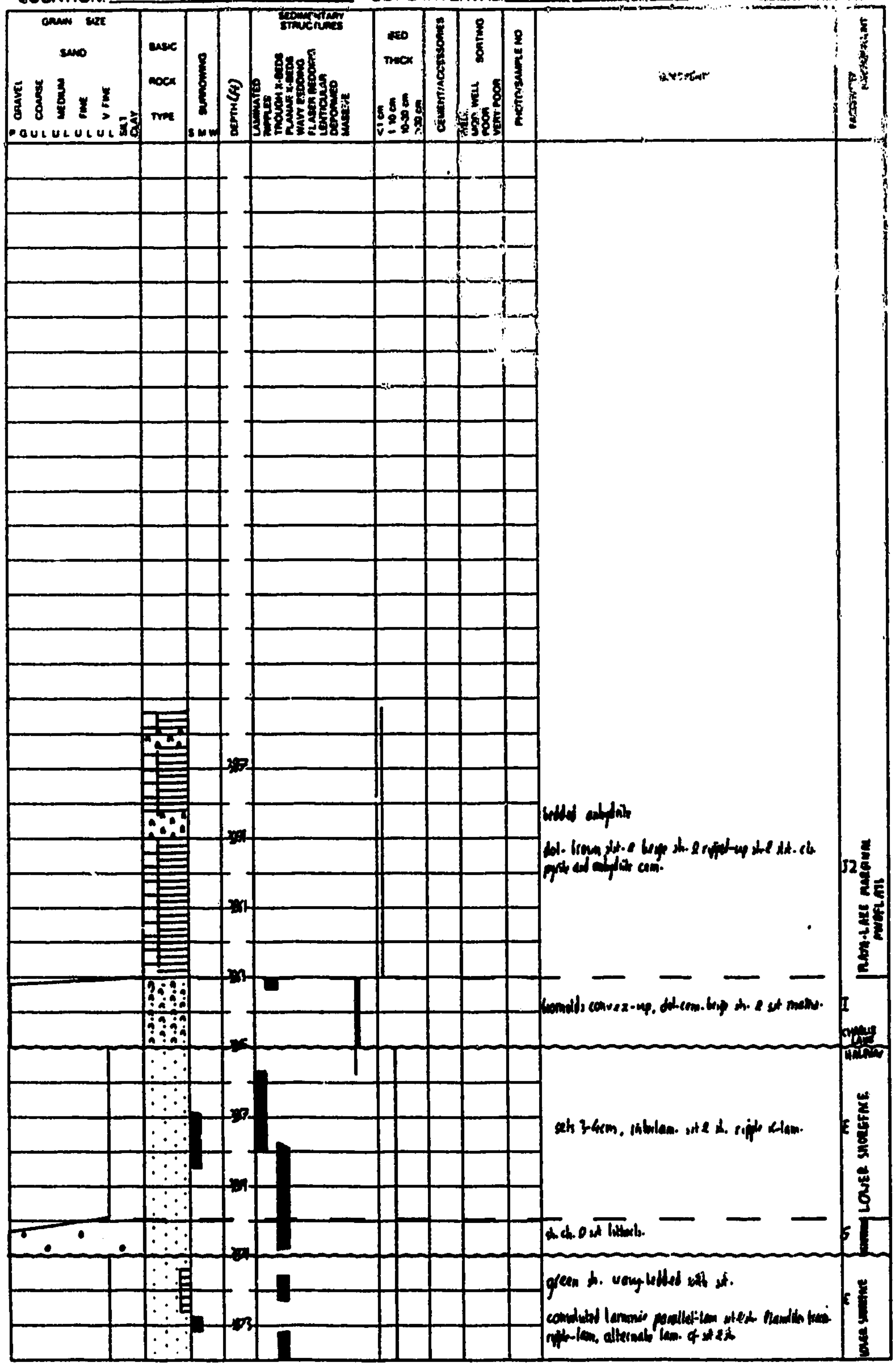

bedded anhydrite

dol. brown silt. & beige sh. & ripped-up shell det. cl. pyrite and anhydrite cem.

bioturbated convex-up, dol-cem. beige sh. & silt matrix.

sets 3-6cm, tabular lam. silt & sh. ripple x-lam.

sh. ch. & silt lithocl.

green sh. wavy-bedded with st.

convoluted laminae parallel-lam silt & sh. flaser/lenticular ripple-lam. alternate lam. of st & sh.

WELL NAME: TEXCAN TEXACO BUCKTHORN FORMATION: HALFWAY-CHARLIE LAKE DATE: 6/07/90

LOCATION: d-061-D/94-A-16 CORE INTERVAL: KB: 2370ft

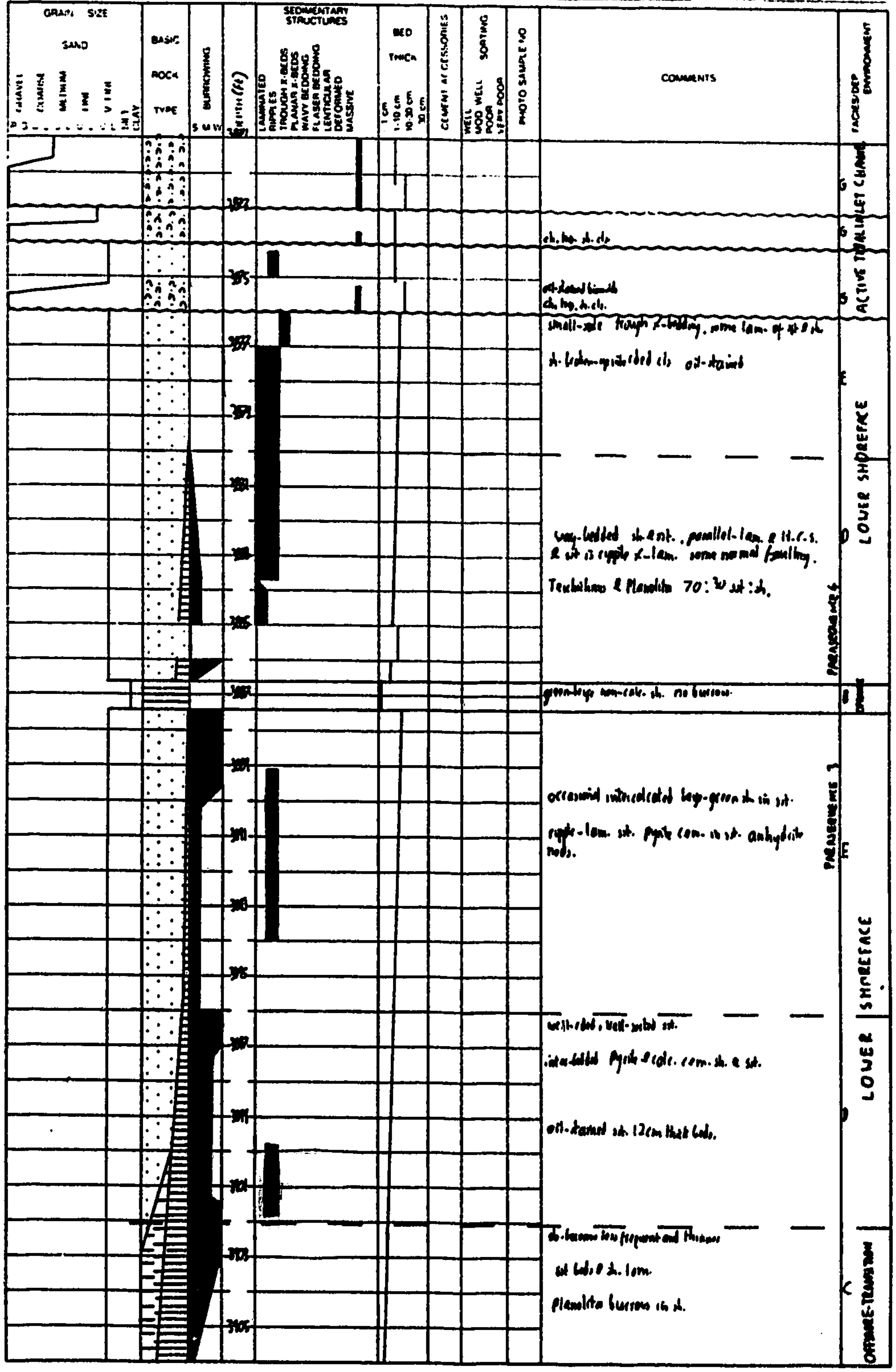

ch. lag. sh. cls

oil-stained bioturb.
ch. lag. sh. cls.

small-scale trough x-bedding, some lam. of st & sh.

sh. [illegible] cls oil-stained

wavy-bedded sh. & sst., parallel-lam. & H.C.S. & sst is ripple x-lam. some normal faulting.

Teichichnus & Planolites 70:30 sst:sh.

green-beige non-calc. sh. no burrows.

occasional intercalated beige-green sh. in sst. ripple-lam. sst. Pyrite conc. in sst. anhydrite nods.

well-sorted, well-rounded sst.

interbedded Pyrite & calc. cem. sh. & sst.

oil-stained sst. 12cm thick beds.

sh. becomes less frequent and thinner

sst beds & sh. lam.

Planolites burrows in sh.

WELL NAME: TEXCAN TEXACO BUCKTHORN
FORMATION: HALFWAY-CHARLIE LAKE
DATE: 6/07/90
LOCATION: d-061-D/94-A-16
CORE INTERVAL:
KB: 2370ft

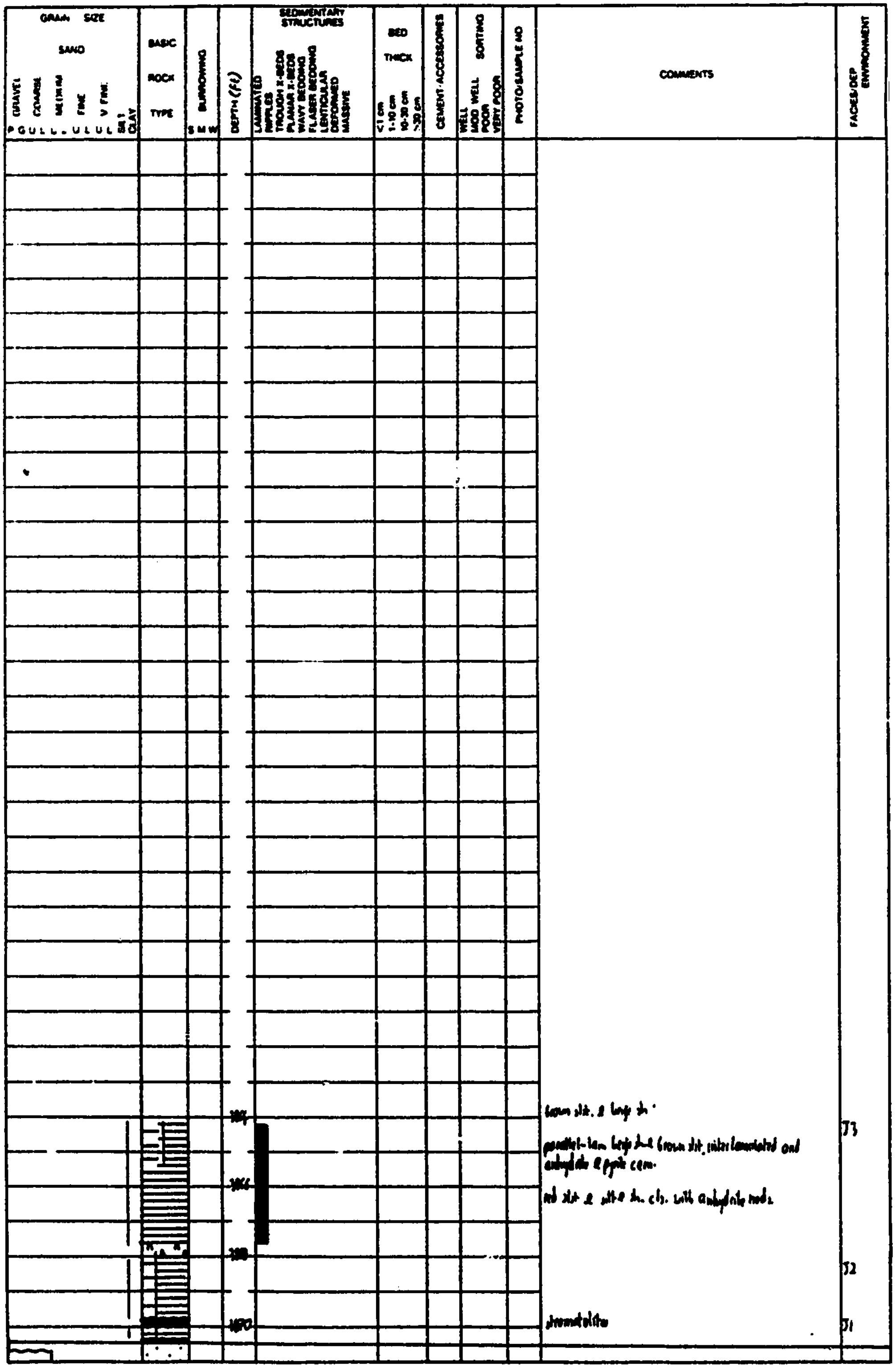

brown slt. & lmy sh.

parallel-lam lmy sh. & brown slt. interlaminated and anhydrite & pyrite cem.

red slt & silty sh. cly. with anhydrite nods.

stromatolite

WELL NAME TEXCAN TEXACO BUCKTHORN FORMATION: HALFWAY-CHARLIE LAKE DATE 3/07/91

LOCATION d-062-D/94-A-16 CORE INTERVAL: KB 2365ft

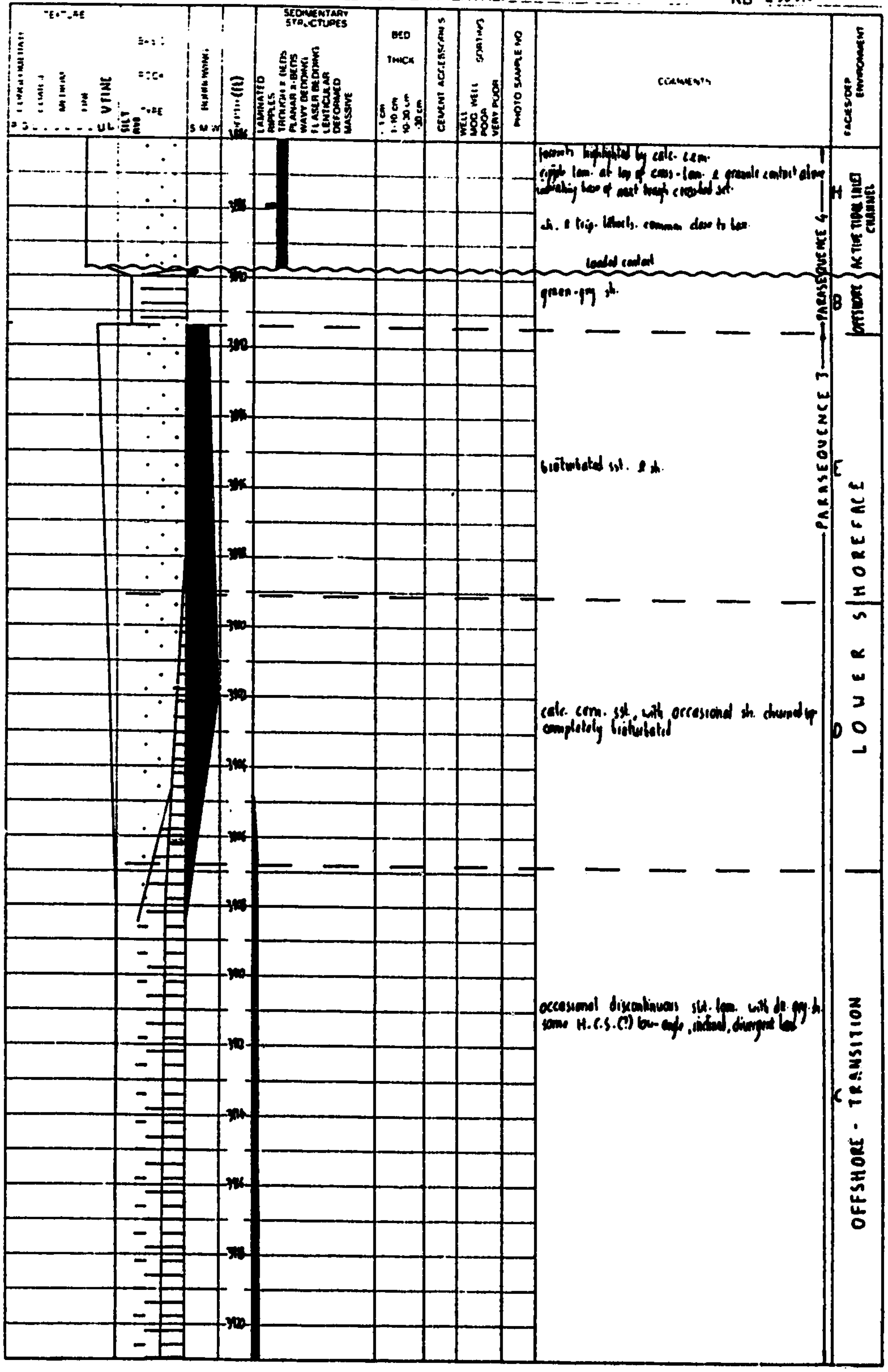

WELL NAME TEXCAN TEXACO BUCKTHORN FORMATION: HALFWAY-CHARLIE LAKE DATE: 3/07/91

LOCATION: d-062-D/94-A-16 CORE INTERVAL: KB: 2365ft

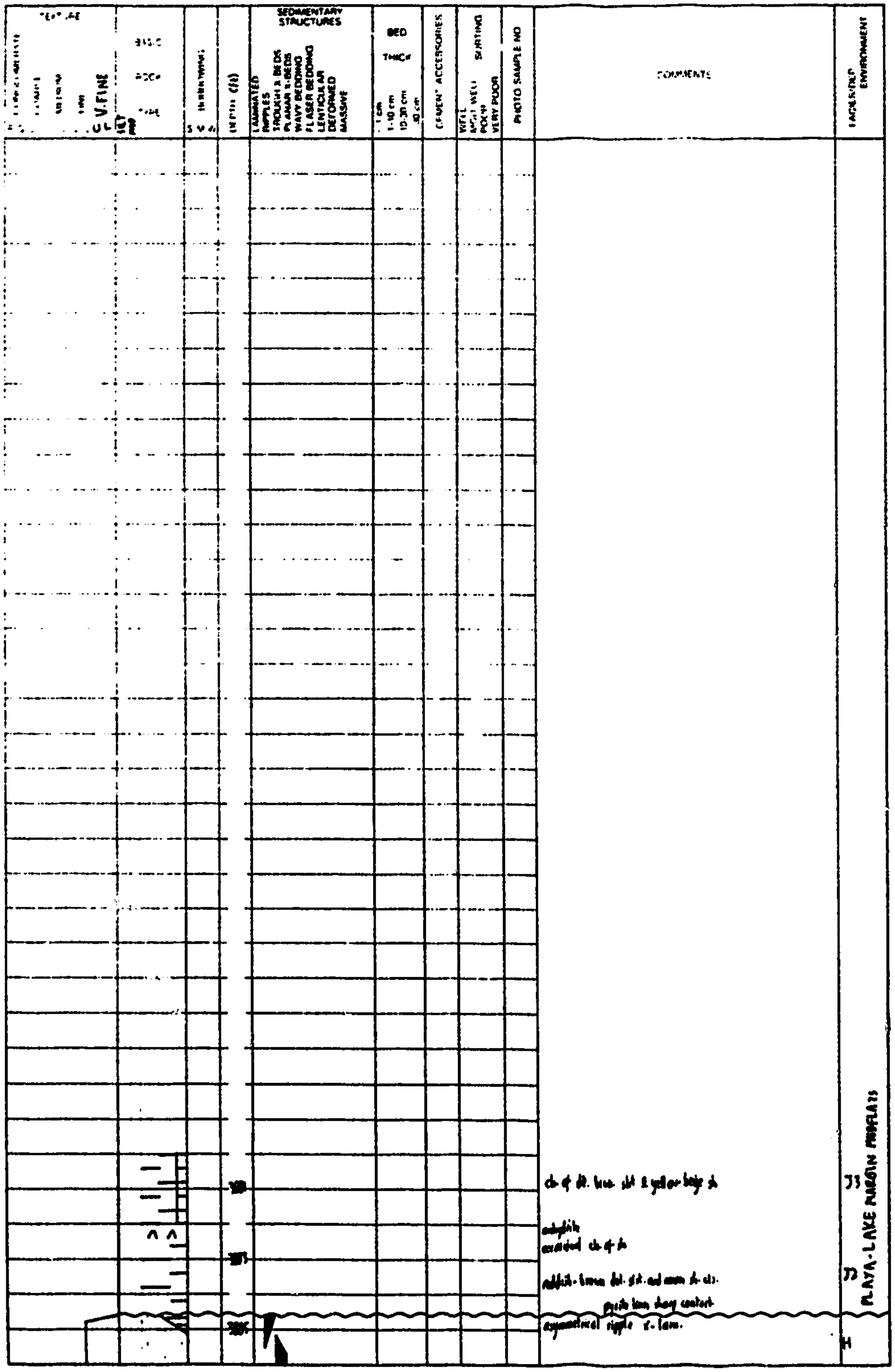

cln of dk. brn. slt & yellow beige sh

anhydrite
scattered cln of sh

reddish-brown dol. slt. and anom sh. cls.

pyrite lam. sharp contact

asymmetrical ripple x-lam.

WELL NAME: TEXCAN TEXACO PEEJAY d-63-D
FORMATION: HALFWAY-CHARLIE LAKE
DATE 2/07/91
LOCATION: d-063-D/94-A-16
CORE INTERVAL:
KB. 2366 3ft

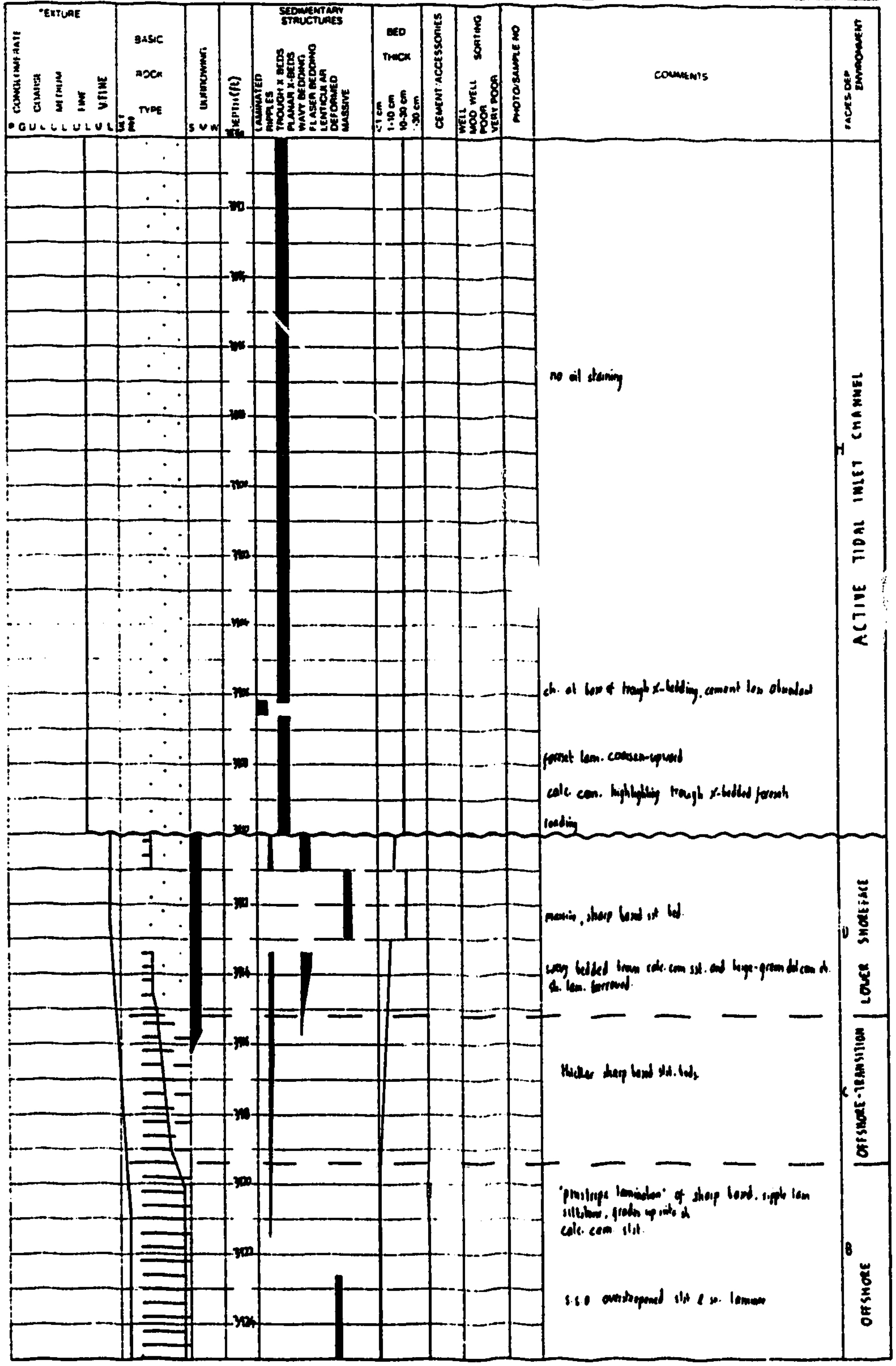

no oil staining

ch. at base of trough x-bedding, cement less abundant

foreset lam. coarsen-upward

calc. cem. highlighting trough x-bedded foresets

loading

massive, sharp based sst bed.

wavy bedded brown calc. cem sst. and large-grained calc. cem. sh.
sh. lam. burrowed

thicker sharp based sst. beds

'pinstripe lamination' of sharp based, ripple lam
siltstone, grades up into sh
calc. cem slst.

s.s.a. overstepped slst & sh. lamina

WELL NAME: TEXCAN TEXACO PEEJAY d-63-D
FORMATION: HALFWAY- CHARLIE LAKE
DATE: 2/07/92
LOCATION: d-063-D/94-A-16
CORE INTERVAL:
KB: 2366.3ft

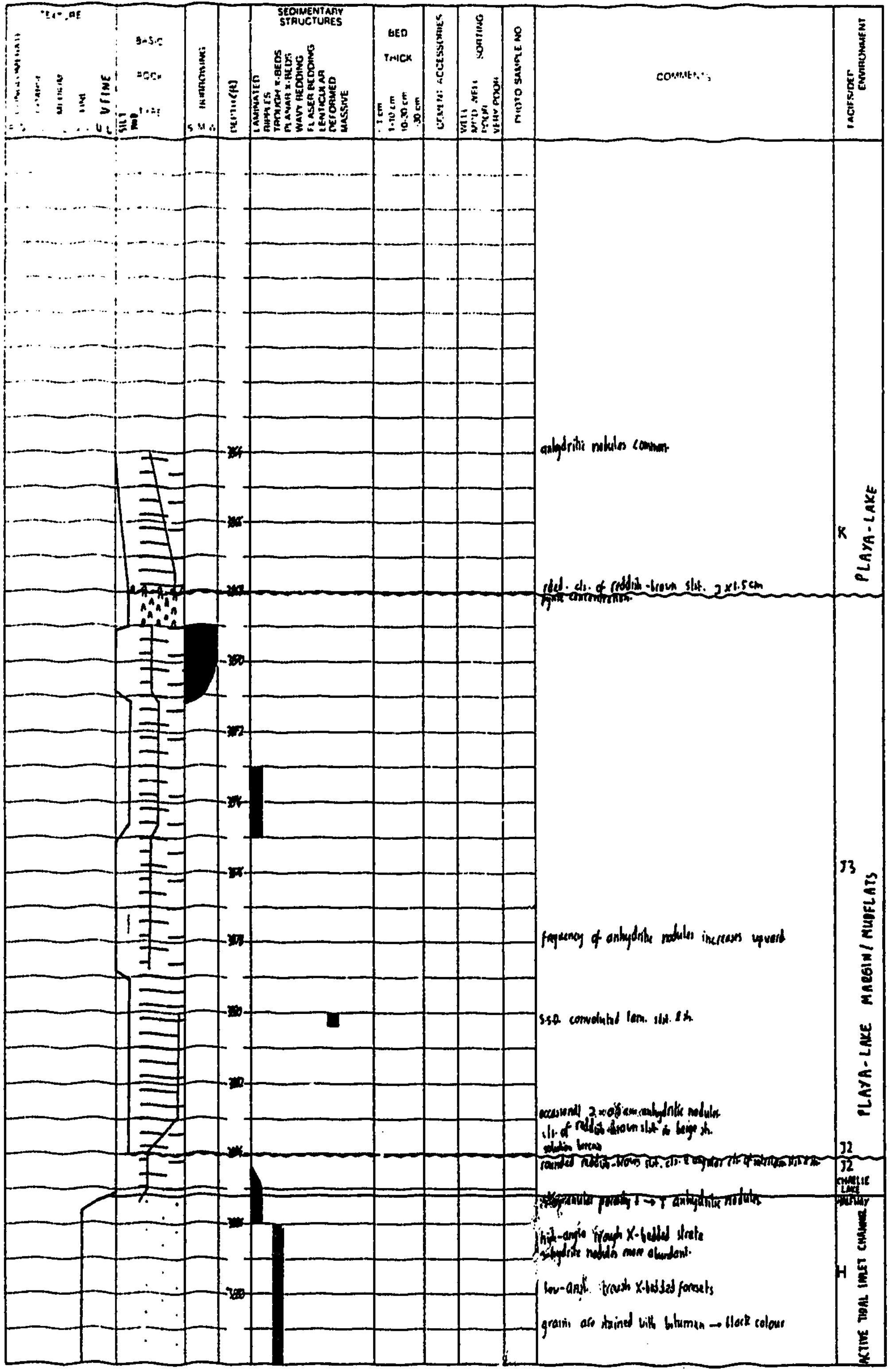

anhydritic nodules common

rdd. cl. of reddish-brown slst. 2x1.5cm
pyrite concentration

frequency of anhydrite nodules increases upward

s.s.a. convoluted lam. slst. & sh.

occasional 2x0.5cm anhydritic nodules
cl. of reddish brown slst in beige sh.
solution breccia

rounded reddish-brown slst. cl. & angular cl. of [illegible]

[illegible] granular porosity ↓ → ↑ anhydritic nodules

high-angle trough X-bedded strata
anhydrite nodules more abundant.

low-angl. trough X-bedded foresets

grains are stained with bitumen → black colour

WELL NAME: UNION HB BUCKTHORN d-64-D

FORMATION: HALFWAY-CHARLIE LAKE

DATE: 16/08/90

LOCATION: d-064-D/94-A-16

CORE INTERVAL:

KB: 2364 ft

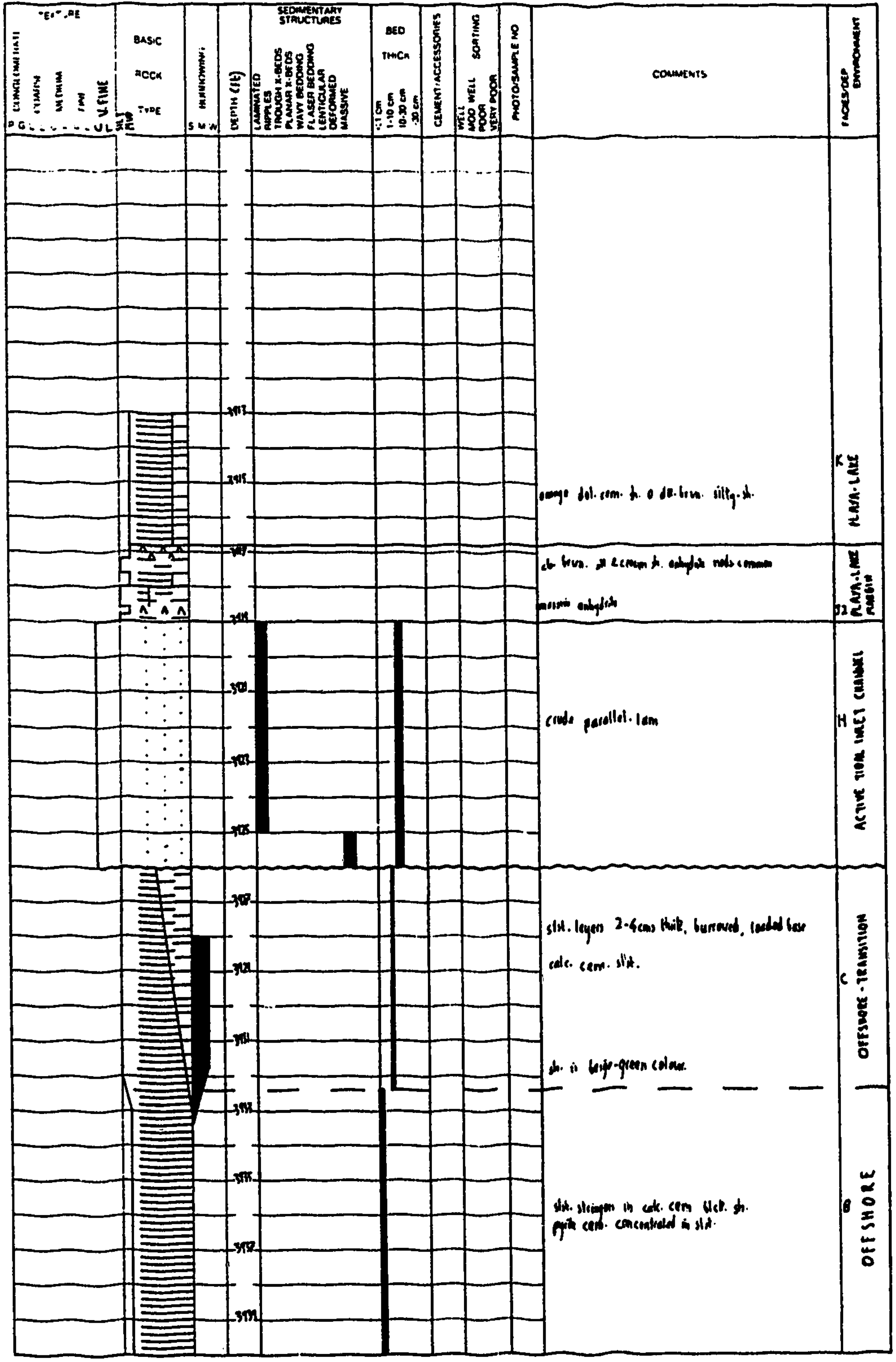

COMMENTS

orange dol. cem. sh. & dk. brn. silty. sh.

dk. brn. sh. & cream sh. anhydrite nodules common
massive anhydrite

crude parallel. lam

slt. layers 2-4cms thick, burrowed, loaded base
calc. cem. slt.

sh. is beige-green colour.

slt. stringers in calc. cem. blck. sh.
pyrite cem. concentrated in slt.

FACIES/DEP ENVIRONMENT

K PLAYA-LAKE

J2 PLAYA-LAKE MARGIN

H ACTIVE TIDAL INLET CHANNEL

C OFFSHORE-TRANSITION

B OFFSHORE

WELL NAME: 10E FOX d-67-D FORMATION: HALFWAY-CHARLIE LAKE DATE: 29/01/91

LOCATION: d-067-D/94-A-16 CORE INTERVAL: KB: 2353ft

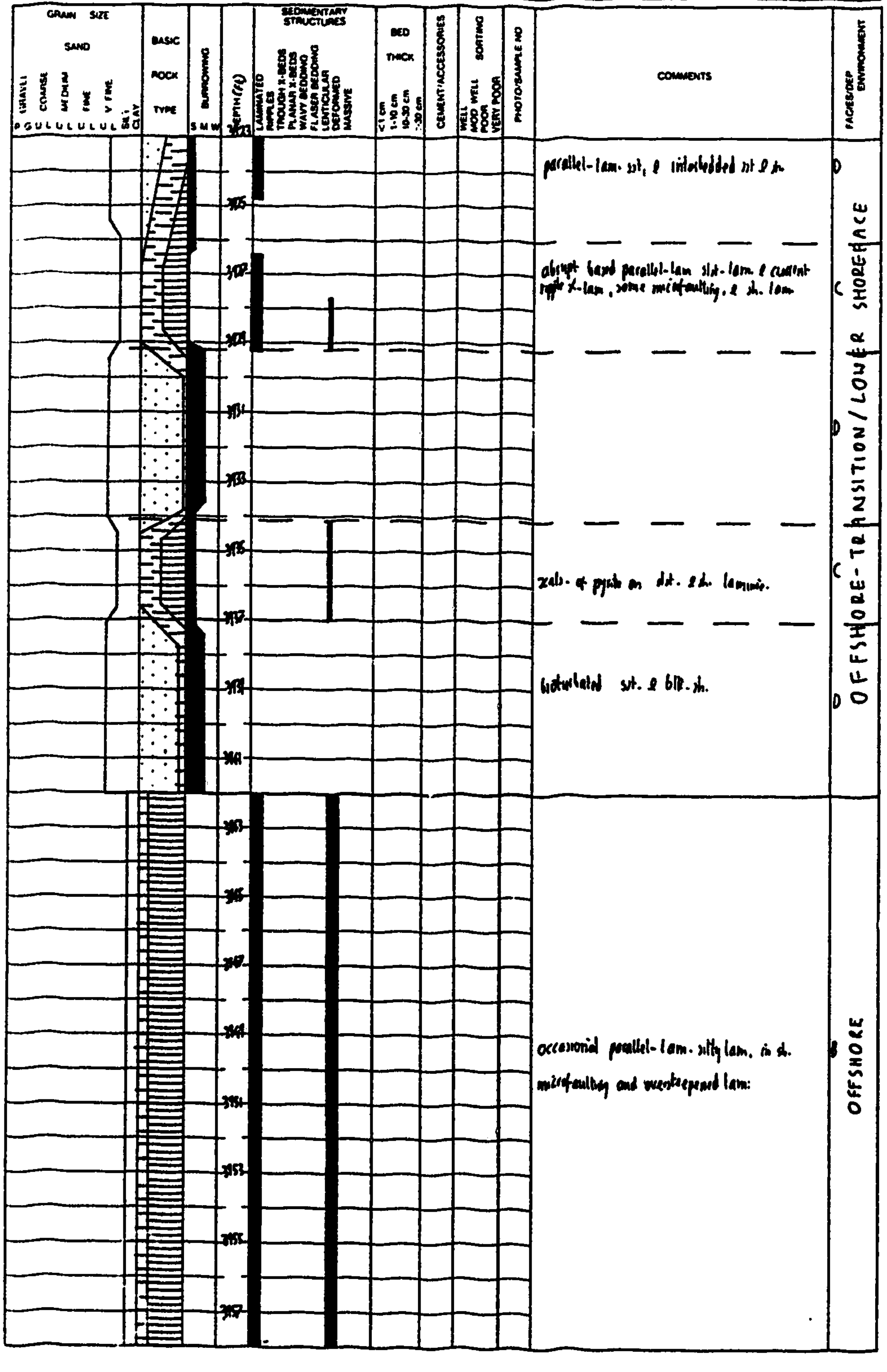

parallel-lam. sst. & interbedded sst & sh.

abrupt based parallel-lam slst-lam. & current ripple X-lam, some microfaulting, & sh. lam.

xals. of pyrite on slst. & sh. laminae.

bioturbated sst. & blk. sh.

occasional parallel-lam. silty lam. in sh. microfaulting and oversteepened lam:

WELL NAME: IOE FOX d-67-D

FORMATION: HALFWAY-CHARLIE LAKE

DATE: 29/01/91

LOCATION: d-067-D/94-A-16

CORE INTERVAL:

KB: 2353ft

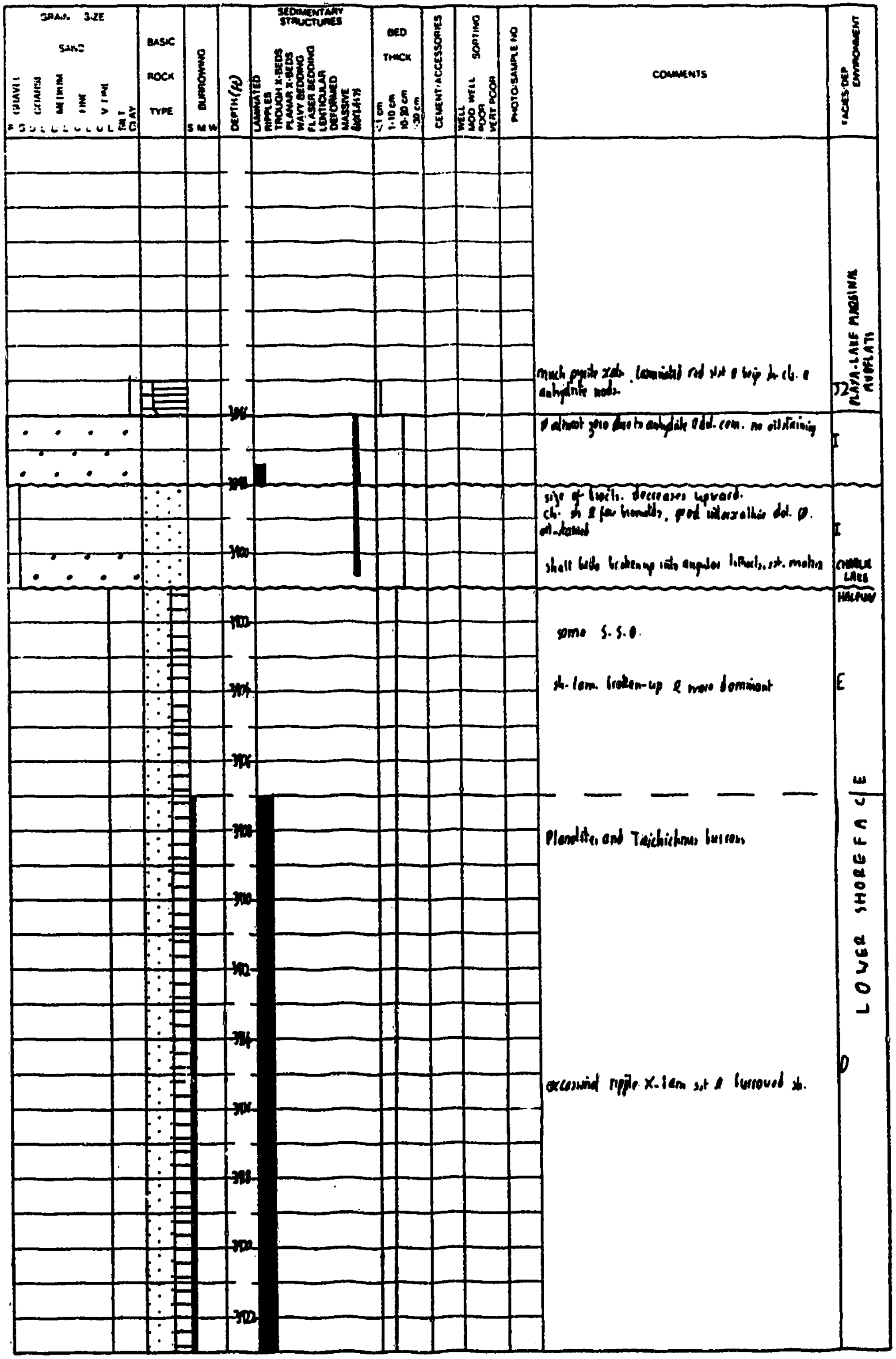

much pyrite xals. laminated red slt & bkg dr. cly. & anhydrite nods.

ϕ almost zero due to anhydrite & dol. cem. no oil staining

size of lithcls. decreases upward.
ch. sh & few brachiopds, good intercrystalline dol. ϕ.
oil-stained

shell beds broken up into angular lithcls., st. mottled

some S.S.B.

sh. lam. broken-up & more dominant

Planolites and Teichichnus burrows

occasional ripple X-lam. slt & burrowed sh.

WELL NAME: TEXCAN BUCKTHORN d-71-D

FORMATION: HALFWAY-CHARLIE LAKE

DATE: 2/07/?

LOCATION: d-071-D/94-A-16

CORE INTERVAL:

KB: 2373ft

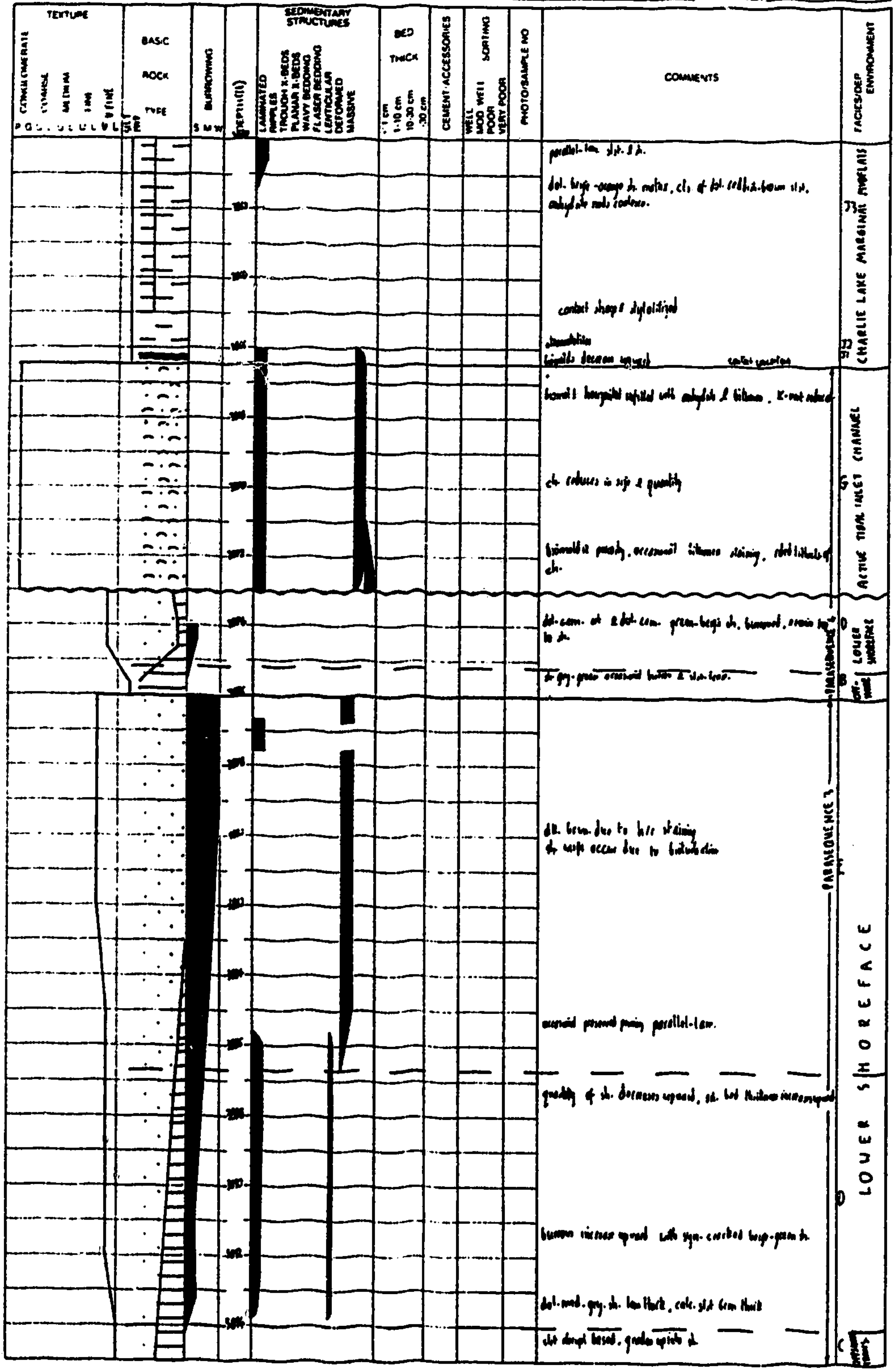

parallel-lam. slst. & sh.

dol. beige-orange sh. matrix, cls of dol. reddish-brown slst., anhydrite nodules common.

contact sharp & dolomitized

[illegible]

[illegible] decrease upward [illegible]

burrows [illegible] infilled with anhydrite & bitumen. [illegible]

sh. reduces in size & quantity

bioturbated partly, occasional bitumen staining, [illegible] sh.

dol-cem. ss & dol-cem. green-beige sh., burrowed, grain [illegible] to sh.

dk gry-green occasional burrow & [illegible]

dk. brown due to bit staining
sh. wisps occur due to bioturbation

occasional preserved planar parallel-lam.

quantity of sh. decreases upward, ss. bed thickness increases upward

burrows increase upward with syn-[illegible] beige-green sh.

dol.-mod. gry. sh. [illegible], calc. slst [illegible]

[illegible] sharp based, grades upward sh.

WELL NAME: UNION HB EAST PEEJAY D-73-D FORMATION: HALFWAY-CHARLIE LAKE DATE 5/07/90

LOCATION: d-073-D/94-A-16 CORE INTERVAL: KB 2351 ft

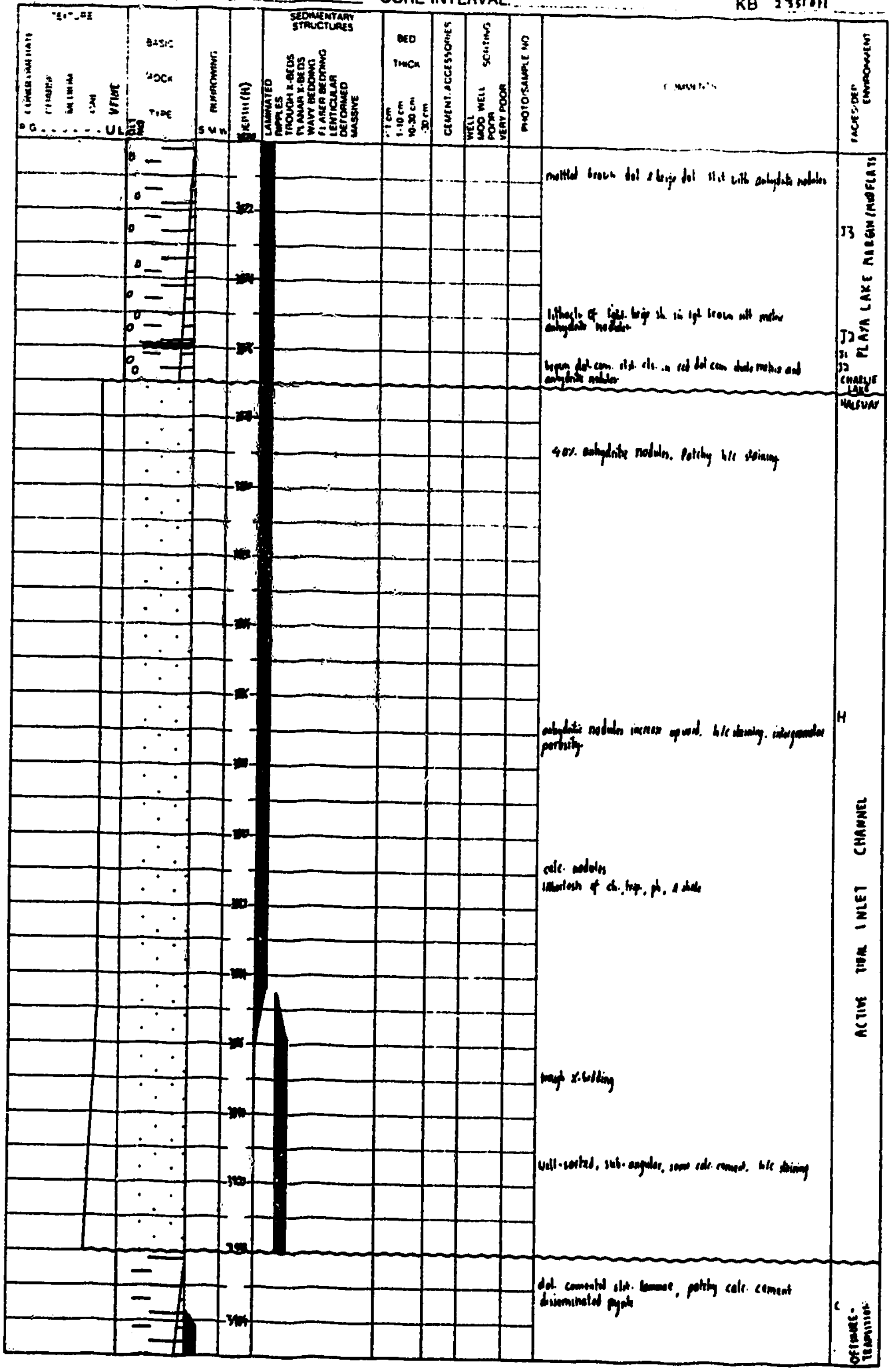

mottled brown dol & beige dol silt with anhydrite nodules

lithoclasts of lgt. beige sh. in lgt brown silt matrix anhydrite nodules

brown dol-cem. slst. clst. in red dol cem shale matrix and anhydrite nodules

40% anhydrite nodules. Patchy h/c staining

anhydrite nodules increase upward. h/c staining. intergranular porosity

calc. nodules
lithoclasts of ch., frags., ph., & shale

trough X-bedding

well-sorted, sub-angular, some calc. cement. h/c staining

dol. cemented slst. laminae, patchy calc. cement
disseminated pyrite

WELL NAME: TEXCAN BUCKTHORN FORMATION: HALFWAY-CHARLIE LAKE DATE: 31/07/90

LOCATION: d-081-D/94-A-16 CORE INTERVAL: KB: 2384ft

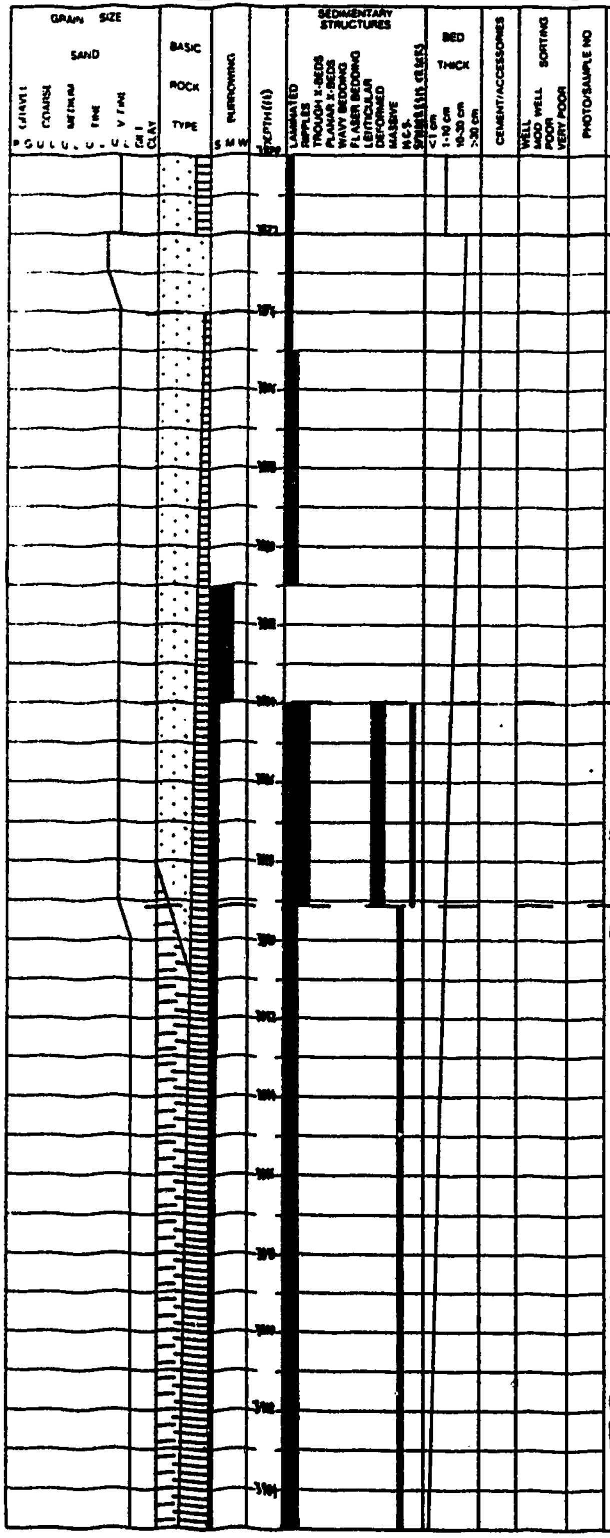

COMMENTS	FACIES/DEP ENVIRONMENT
load & flaming, Planolites, brown dol. cem. sh. & brown dol. cem. sst.	E LOWER SHOREFACE
intergranular ϕ, loose dol. cem.	F UPPER SHOREFACE
occasional parallel lam. of dol. beige sh. & brown sst. loaded bases.	E LOWER SHOREFACE
brown dol. cem. sst & grey dol. cem. sh. with burrows Planolites, destroying laminae. 90:10 sst : sh	
dol. cem. beige-green sh. and brown dol. cem. sst. Flame and loaded bases. Planolites. synaeresis cracks. Sst. is ripple x-lam.	D
burrowing increases upward & slt. increases.	C OFFSHORE-TRANSITION
few Planolites burrows on top of sh.	
blk. sh. & lgt. grey slt. both calc. cem. Slt. is parallel-lam. to domed laminae (H.C.S.). Slt. has transitional base.	

PARASEQUENCE 4

PARASEQUENCE 3

WELL NAME: TEXCAN BUCKTHORN FORMATION: HALFWAY-CHARLIE LAKE DATE: 31/07/90

LOCATION: d-081-D/94-A-16 CORE INTERVAL: KB: 2384ft

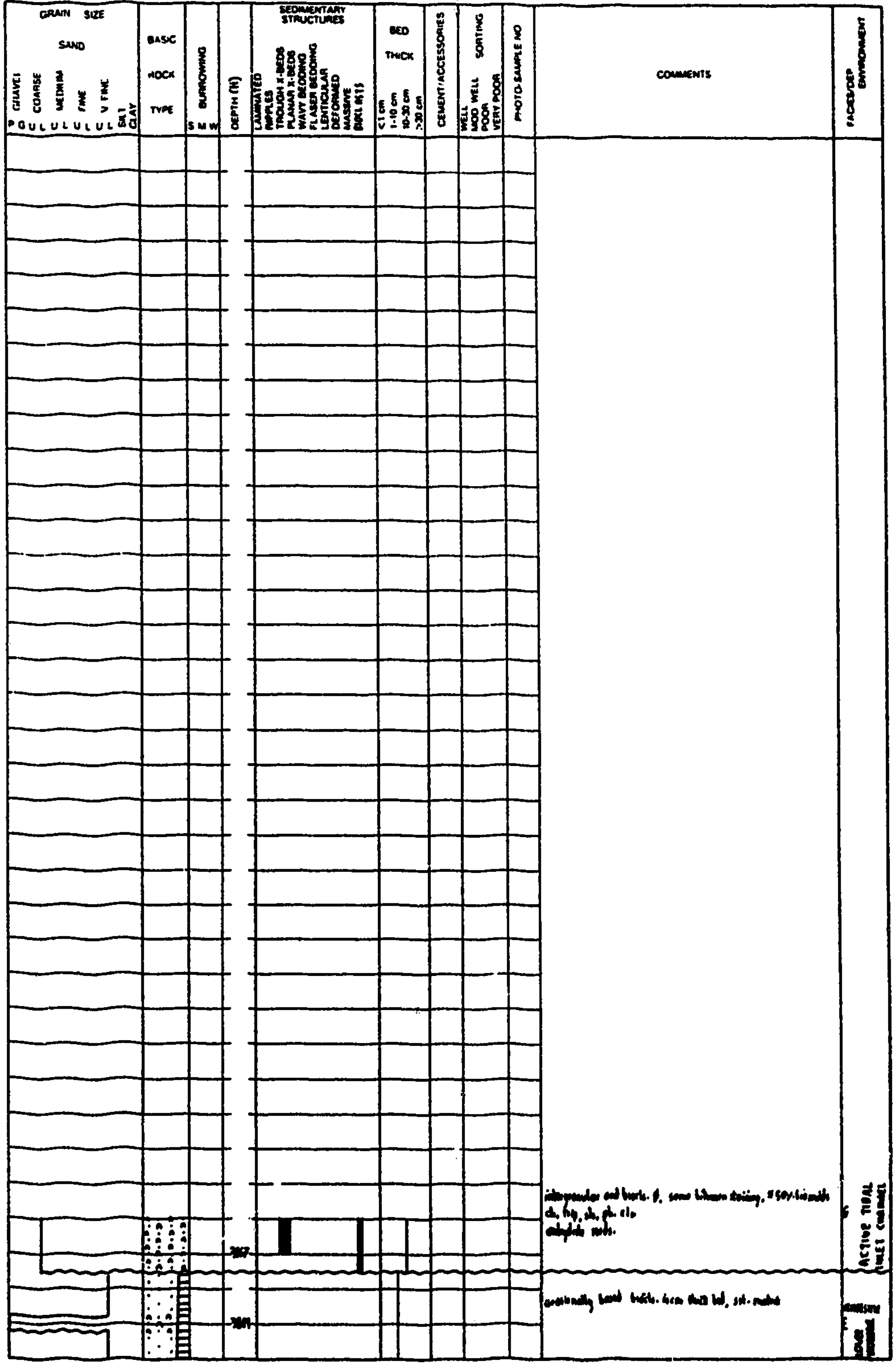

intergranular and [illegible] φ, some bitumen staining, [illegible]
[illegible]
[illegible]

occasionally [illegible]

WELL NAME: UNION HB EAST PEEJAY No D-82-D FORMATION: HALFWAY-CHARLIE LAKE DATE: 28/01/91

LOCATION: d-082-D/94-A-16 CORE INTERVAL: KB: 2371.5ft

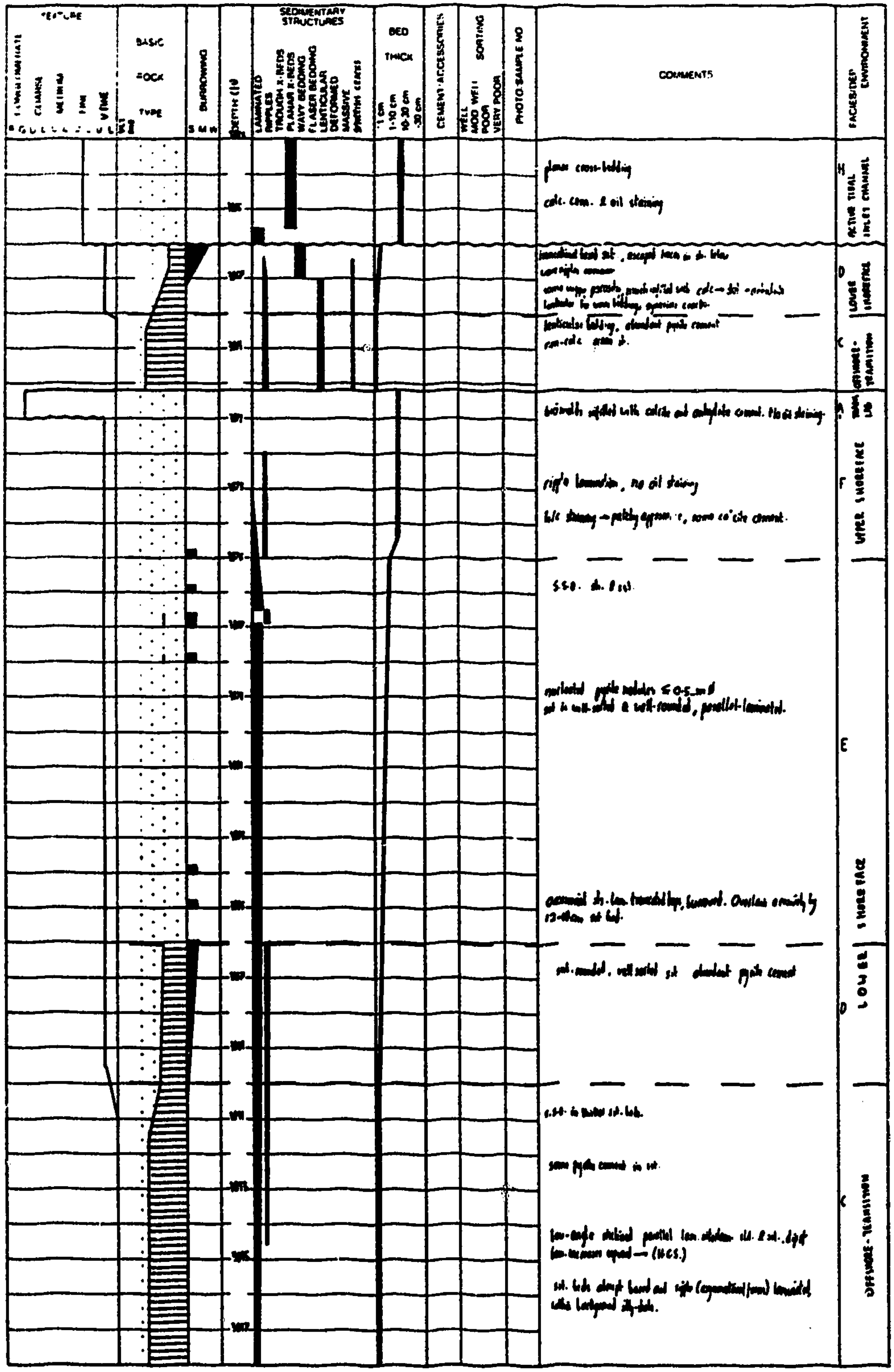

WELL NAME: UNION HB EAST FEETAY NO D 82-D

FORMATION: HALFWAY - CHARLIE LAKE

DATE: 28/01/91

LOCATION: d-082-D/94-A-16

CORE INTERVAL:

KB: 2371.5 ft

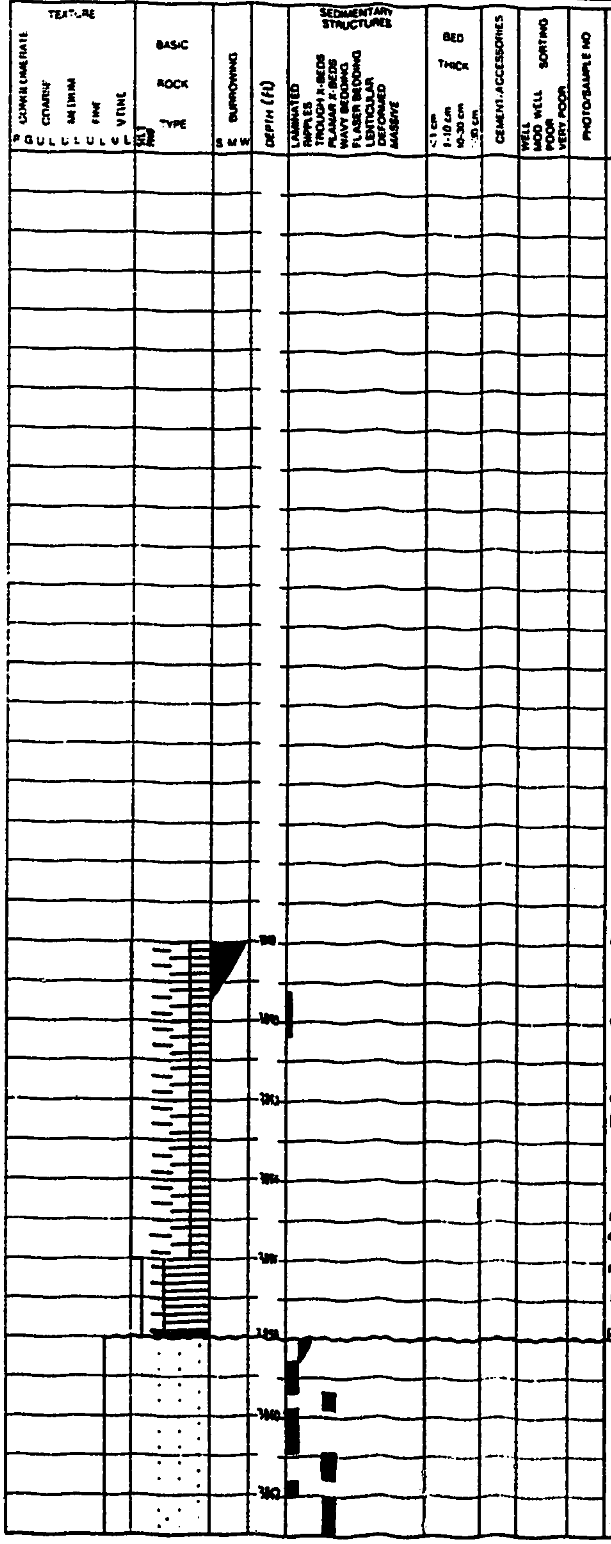

COMMENTS

clr. of laminated slt. & sh. anhydrite nodules common, sabkha

vertical fractures infilled with anhydrite cement

clr. of sh. & slt. in sh. matrix, few grains of v.f.L. sd. few anhydrite nodules

fractures - vertical in attitude, infilled with anhydrite anhydrite nodules.

massive anhydrite

sh. & siltstone clr. in large sh. matrix, some large anhydrite nodules.

fractured & infilled with calc. [illegible]

wave ripple lamination

patchy calc. cmt. com. oil staining

FACIES/DEP. ENVIRONMENT

PLAYA-LAKE MARGIN/MUDFLATS

EXPOSURE SURFACE

ACTIVE TIDAL INLET CHANNEL

WELL NAME: UNION ET AL PEEJAY a-83-D

FORMATION: HALFWAY-CHARLIE LAKE

DATE: 2/07/91

LOCATION: a-083-D/94-A-16

CORE INTERVAL:

KB: 23492ft

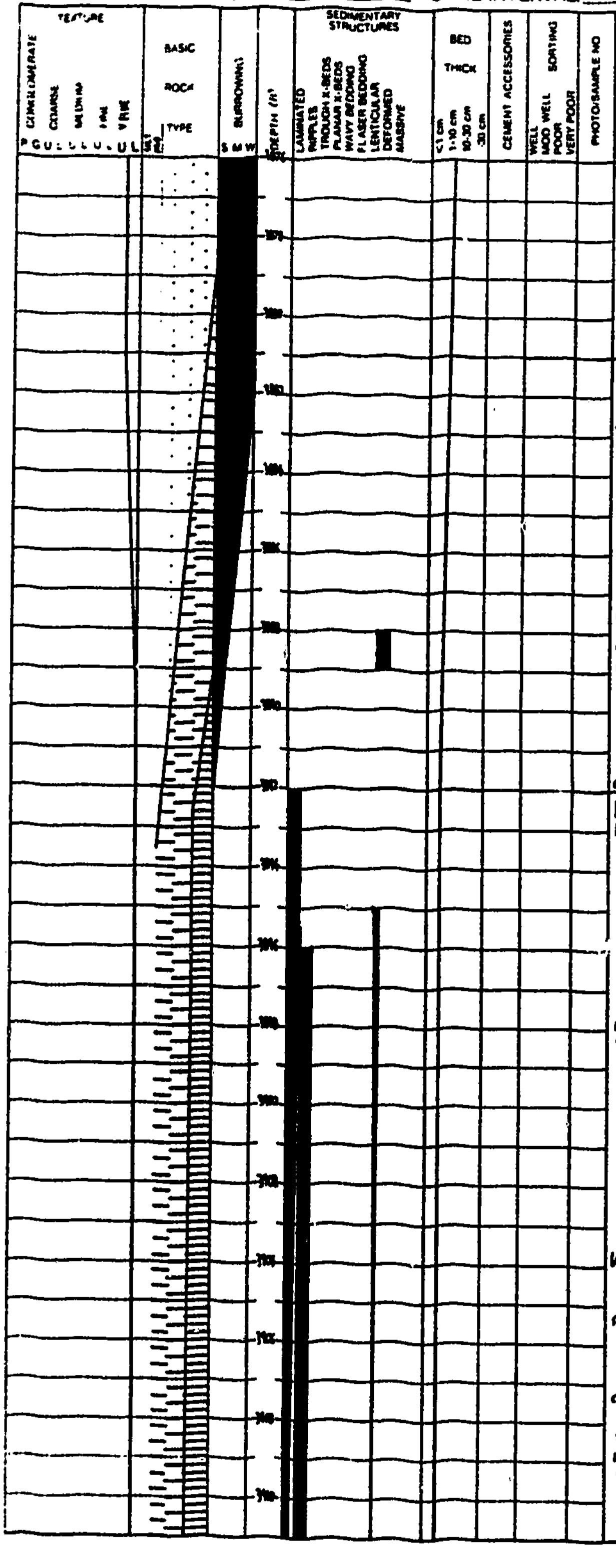

COMMENTS

completely bioturbated.

calc. cem. slt bedding varies from 5-15cm

burrowing increases → churned up slt. and sh. Thicker slt. beds are not completely bioturbated. Burrows are horizontal, sand filled and no mud lining, Planolites.

sharp based slt beds, scour into sh. 2 : [illegible] [illegible]. Parallel lam. → plane, biogenic activity destroys most physical sed. structures.

patchy calc. cem., dol. cement increases in green-beige sh.

interbedded [illegible] of slt. & sh., burrowing increases, partly destroying lam.

occasional burrowing of silt, some beige-green calc. cem. sh.
parallel-laminated sharp based slt.
ripple lam.

rare syneresis cracks in top of sh. lam., infilled with slt.
slt. more calcite than slt. sh.

bed of slt. increase in frequency and thickness upward

some minor fluid escape structures and microfaulting in slt.

calcite cemented sltstone and black shale
slt : sh 70:30
sharp base to silt, loaded. Parallel-laminated at base of slt. → asymmetrical ripple lam. → interlaminated slt. and sh. Slt beds 1.5-2cm thick. (Distal Storm Beds/Geostrophic Current)

FACIES/DEP ENVIRONMENT

?) UPPER SHOREFACE

D LOWER SHOREFACE

C OFFSHORE - TRANSITION

WELL NAME: UNION ET AL PEEJAY a-83-D
FORMATION: HALFWAY-CHARLIE LAKE
DATE: 2/07/91
LOCATION: a-083-D/94-A-16
CORE INTERVAL:
KB: 2349?ft

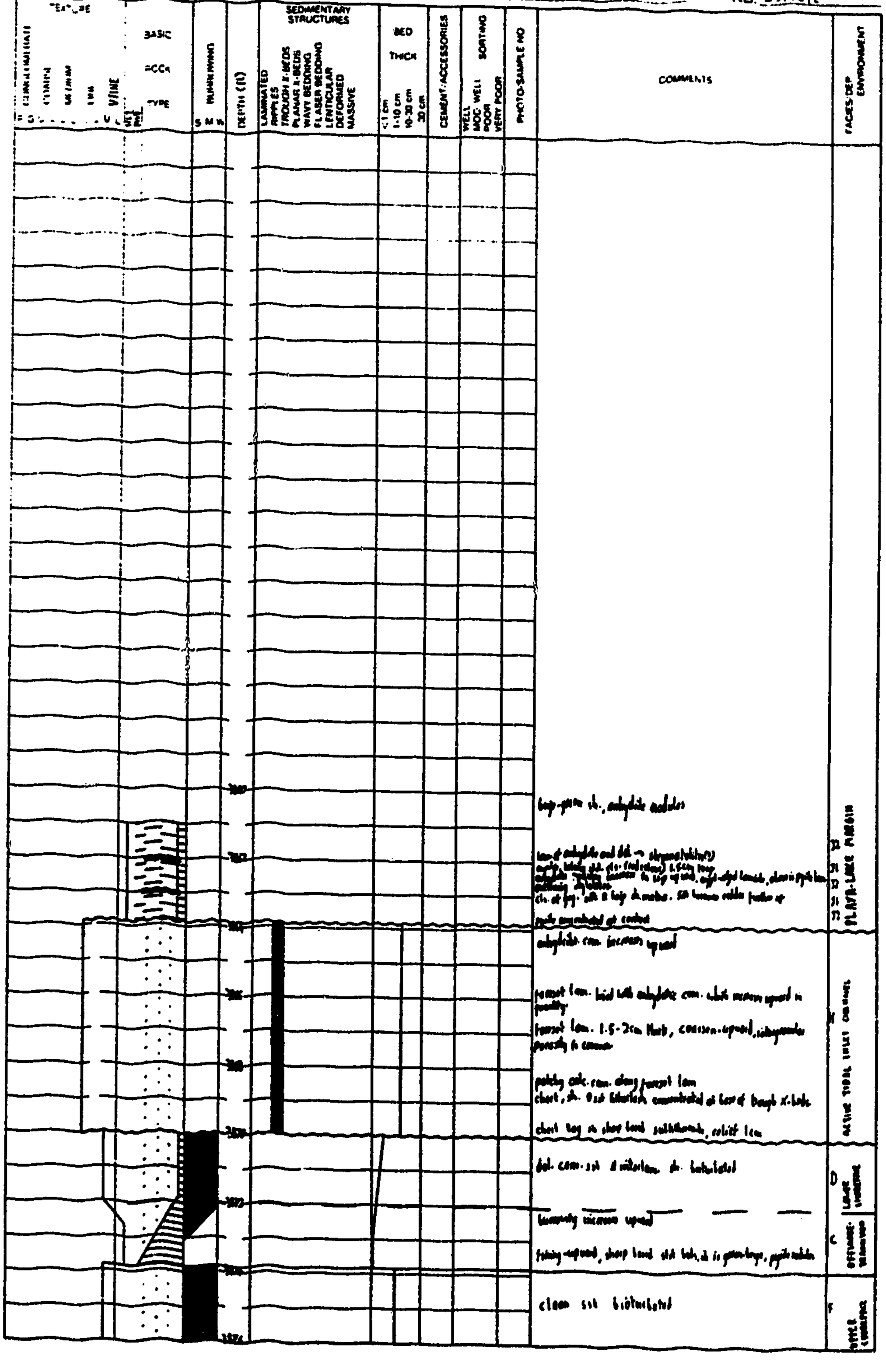

beige-green sh., anhydrite nodules

laminated anhydrite and dol. → stromatolite(?)
[illegible]
[illegible]
[illegible]
[illegible]
pyrite concentrated at contact

anhydrite cem. increases upward

foreset lam. lined with anhydrite cem. which increases upward in quantity

foreset lam. 1.5-2cm thick, coarsen-upward, intergranular porosity is common

patchy calc. cem. along foreset lam
chert, sh. and dol lithoclasts concentrated at base of trough X-beds

chert lag on sharp base subhorizontal, oolitic lam

dol. cem. sst & interlam. sh. bioturbated

burrowing increases upward

fining-upward, sharp based sst beds, sh is green-beige, pyrite nodules

clean sst bioturbated

WELL NAME: UNION HB EAST PEEJAY d-83-D FORMATION: HALFWAY-CHARLIE LAKE DATE: 5/02/91

LOCATION: d-083-D/94-A-16 CORE INTERVAL: KB: 2356 ft

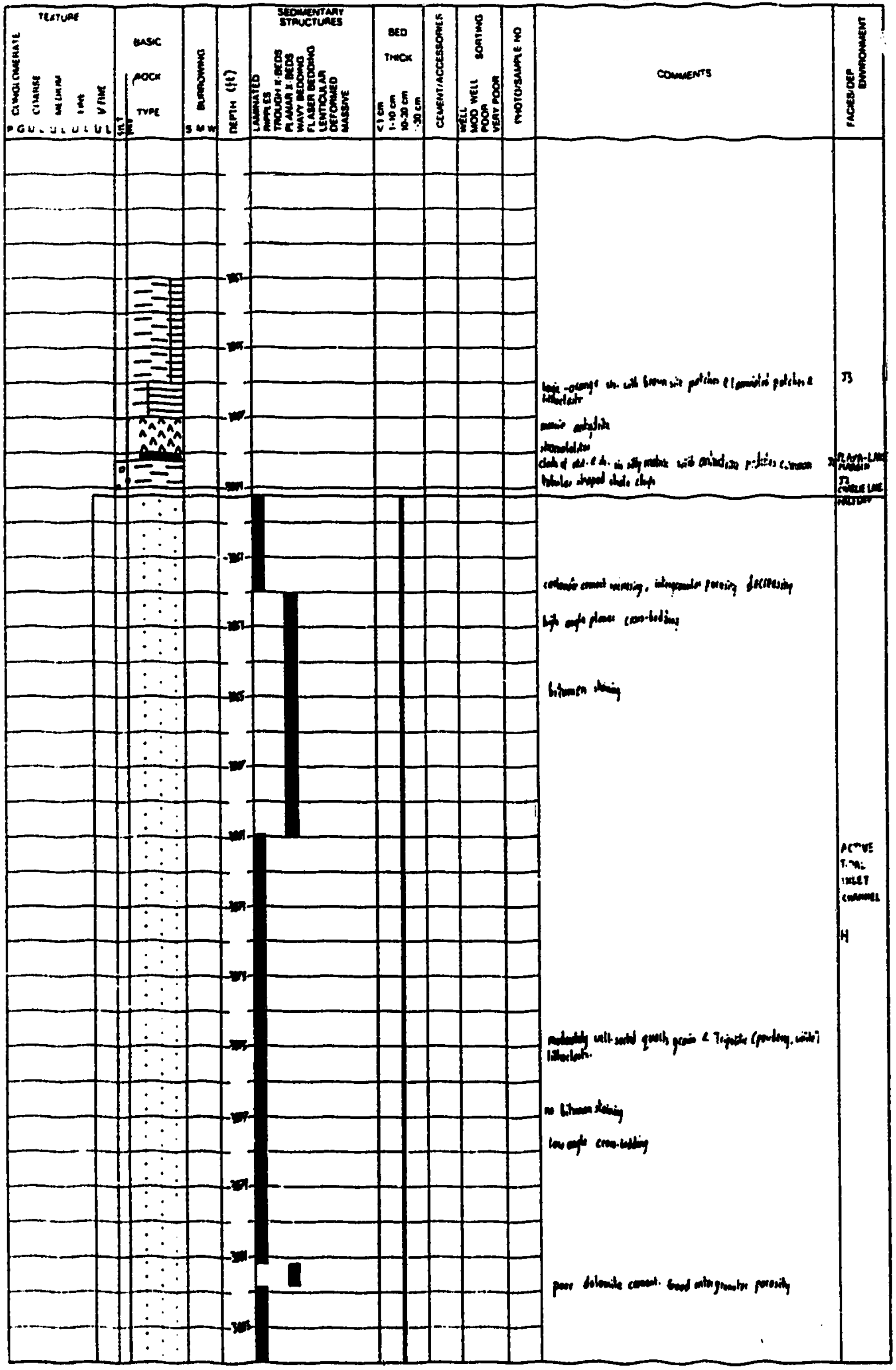

beige-orange ss. with brown ss. patches & [illegible] patches & lithoclasts

massive anhydrite

stromatolites

clasts of ss. & ds. in silty matrix with anhydrite pebbles common tubular shaped shale chips

carbonate cement increasing, intergranular porosity decreasing

high angle planar cross-bedding

bitumen staining

moderately well-sorted quartz grains & Triassic (porcelaneous, white) lithoclasts.

no bitumen staining

low angle cross-bedding

poor dolomite cement. Good intergranular porosity

WELL NAME UNION H B EAST PEEJAY d-84-D FORMATION: HALFWAY-CHARLIE LAKE DATE: 5/07/90

LOCATION: d-084-D/94-A-16 CORE INTERVAL: KB 2331 ft

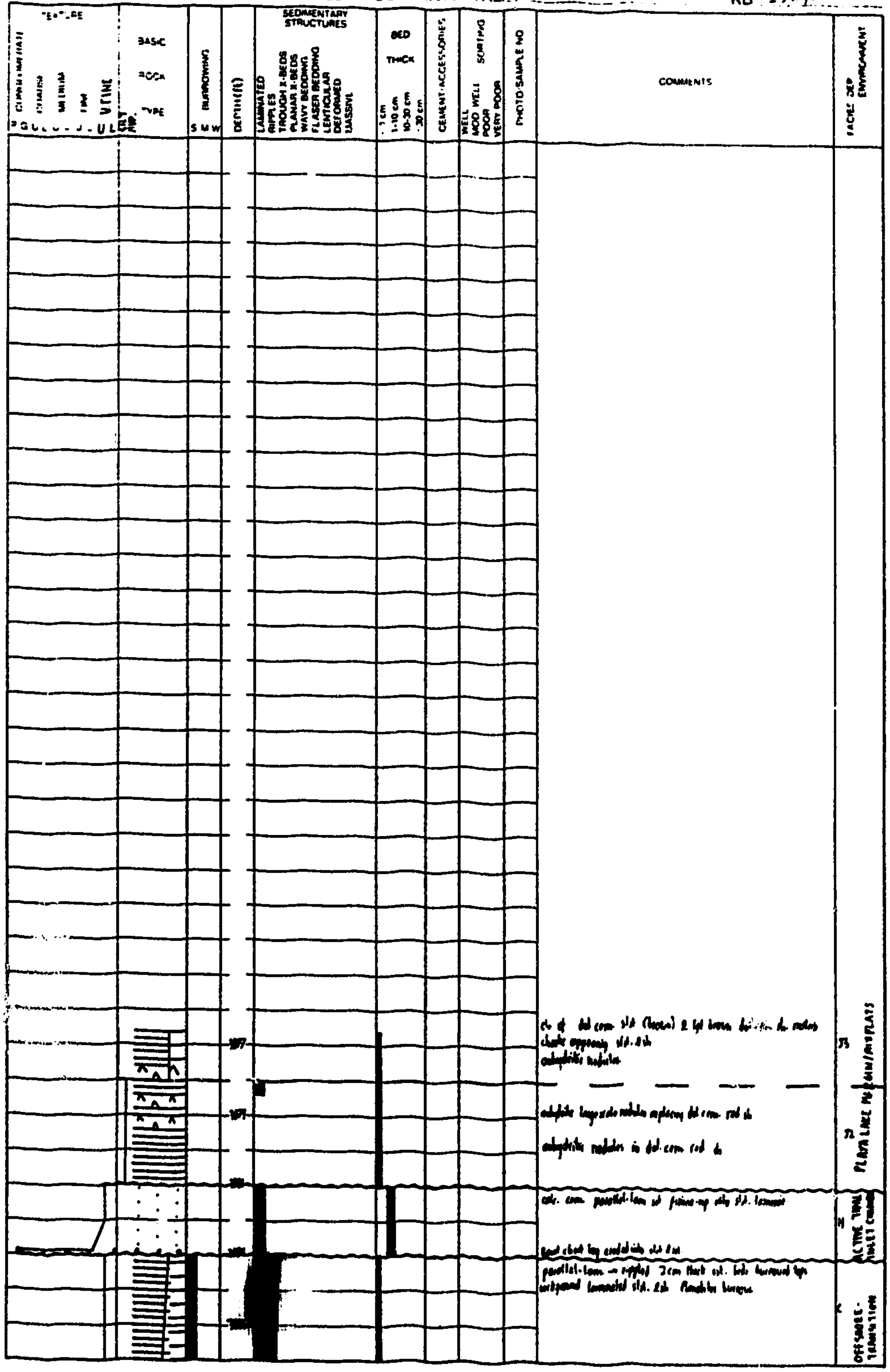

[illegible] dol-com sltst (brown) & lgt brown dol-stn [illegible] nodes
chalk appearing sltst-sh
anhydrite nodules

anhydrite large nodules replacing dol-com sed sh

anhydrite nodules in dol-com sed sh

calc. com. parallel-lam w/ fining-up silty sst. laminae

[illegible] chert lag [illegible]

parallel-lam — rippled 3cm thick sst. beds burrowed tops
interspersed laminated slt. sh Planolites burrows

WELL NAME: HUBER AMERADA FOX FORMATION: HALFWAY- CHARLIE LAKE DATE: 13/08/90

LOCATION: a-088-D/94-A-16 CORE INTERVAL: KB: 2342 ft

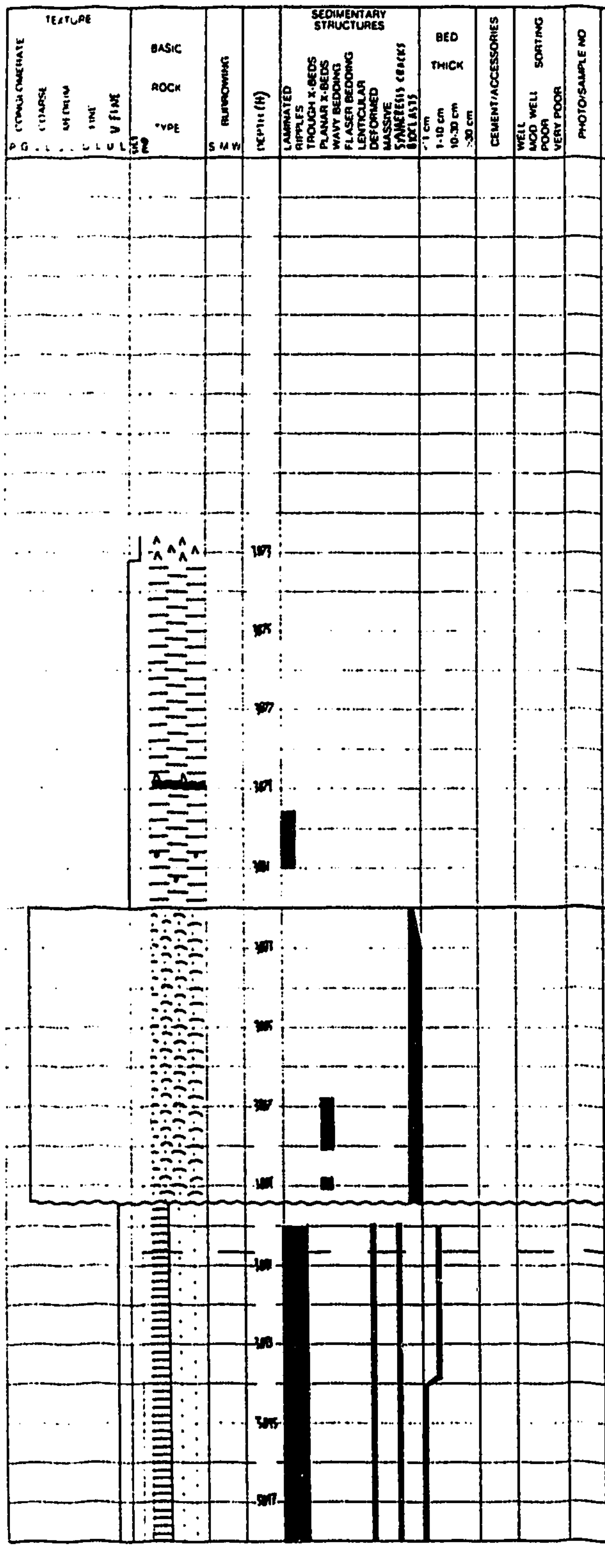

COMMENTS

much microfaulting of beige & brown slst.

nodular anhydrite
dis. of beige & brown slt.

anhydrite nods become more common upward.

interlaminated beige sh. & brown slt. anhydrite nods common. pyrite discontinuous laminae.

red dol. & beige dol. sh. clr. anhydrite nods. & pyrite.

anhydrite coalesced nods common burrows infilled with anhydrite, remainder oil stained. Lithology is pink coloured. bioclastic frags common.
anhydrite nods. increase in quantity & size upward. decreasing in burrow quantity & size upward.

shell. dol. sh. lam. lithoclasts
occasional sh. frags oil staining of burrows common.

some sh. lam. ripped up & shl. Load flame bars. sst is organic rippled beige-green dol. sh. lam

sst. 10cm: sh. 1cm.
some beige dol. cem. sh. interbedded with dol. cem. sst.
pyrite nodules common. Load & flame structures. Nautilus rare.

FACIES/DEP ENVIRONMENT

J3
J2
CHARLIE LAKE MARGINAL MUDFLATS

G
ACTIVE TIDAL INLET CHANNEL

E
D
LOWER SHOREFACIE

WELL NAME: CIGOL CRUSH d-91-D

FORMATION: HALFWAY-CHARLIE LAKE

DATE: 2/07/91

LOCATION: d-091-D/94-A-16

CORE INTERVAL:

KB: 2389ft

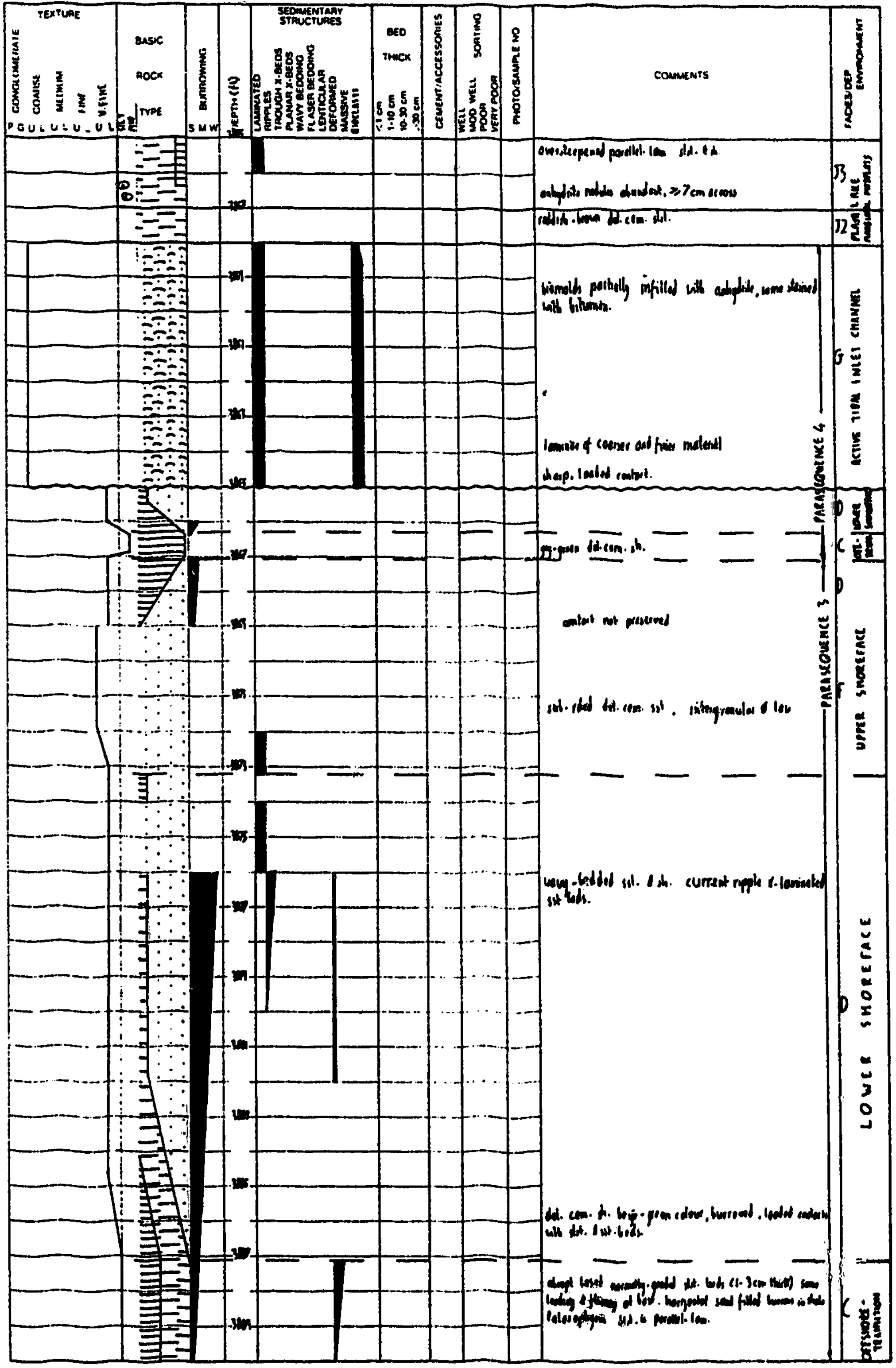

oversteepened parallel lam. sld. & sh.

anhydrite nodules abundant, ≥7cm across

reddish-brown dol. cem. sltst.

biomolds partially infilled with anhydrite, some stained with bitumen.

laminae of coarser and finer material

sharp, loaded contact.

grey-green dol-cem. sh.

contact not preserved

sub-rded dol. cem. sst, intergranular ϕ low

wavy-bedded sst. & sh. current ripple x-laminated sst beds.

dol. cem. sh. beige-green colour, burrowed, loaded contacts with dol. & sst. beds.

abrupt based normally-graded slt. beds (1-3cm thick) some loading & flaming at base. horizontal sand filled burrows in shale Palaeophycus sld. & parallel lam.

WELL NAME: UNION H.B EAST PEEJAY FORMATION: HALFWAY-CHARLIE LAKE DATE: 20/08/90

LOCATION: d-092-D/94-A-16 CORE INTERVAL: KB: 2369ft

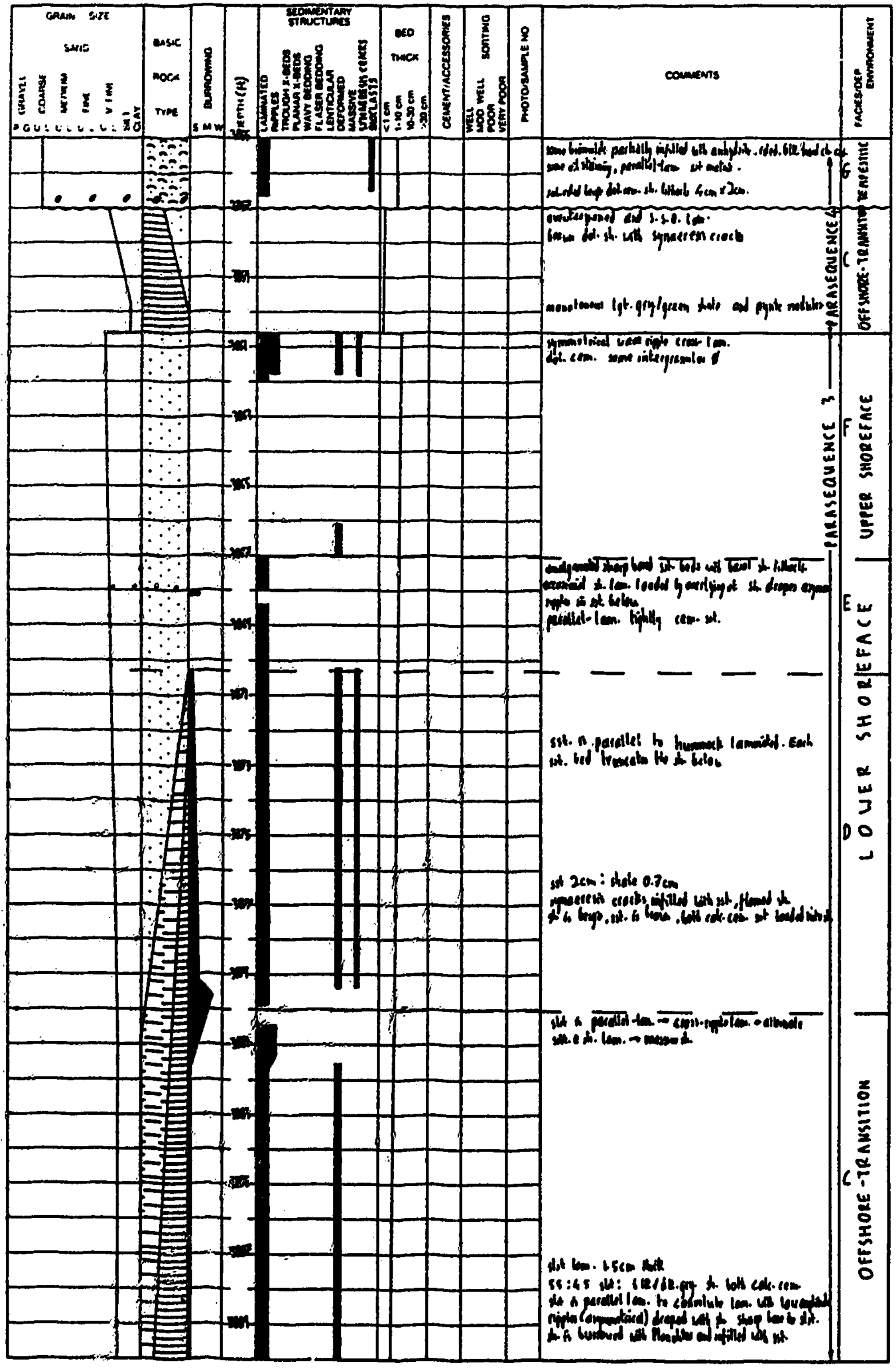

some burrows partially infilled with anhydrite. rdol. blk' bed ch. cl.
some oil staining, parallel-lam. sst matrix.
sub-rdd large dol.-cem. sh. lithcls 4cm x 2cm.

overlapped and s.s.d. lam.
brown dol. sh. with syneresis cracks

monotonous lgt. grey/green shale and pyrite nodules

symmetrical wave ripple cross-lam.
dol. cem. some intergranular ϕ

amalgamated sharp based sst. beds with basal sh. lithcls.
occasional sh. lam. loaded by overlying sst. sh. drapes on some
ripple in sst. below
parallel-lam. tightly cem. sst.

sst. in parallel to hummock laminated. Each
sst. bed truncates the sh. below

sst 2cm : shale 0.7cm
syneresis cracks infilled with sst., flamed sh.
sh. in burrows, sst. to laminae, both calc-cem. sst loaded into sh.

sst. in parallel-lam. → cross-ripple lam. → alternate
sst. & sh. lam. → massive sh.

sst lam. 1.5cm thick
55:45 sst: lt.gr./dk.grey sh. both calc.-cem.
sst. in parallel lam. to convolute lam. with few asymmetric
ripples (asymmetrical) draped with sh. sharp base to sst.
sh. is burrowed with Planolites and infilled with sst.

WELL NAME: UNION H-8. EAST PEEJAY FORMATION: HALFWAY- CHARLIE LAKE DATE: 20/08/90

LOCATION: d-092-D/94-A-16 CORE INTERVAL: ______ KB: 2369 ft

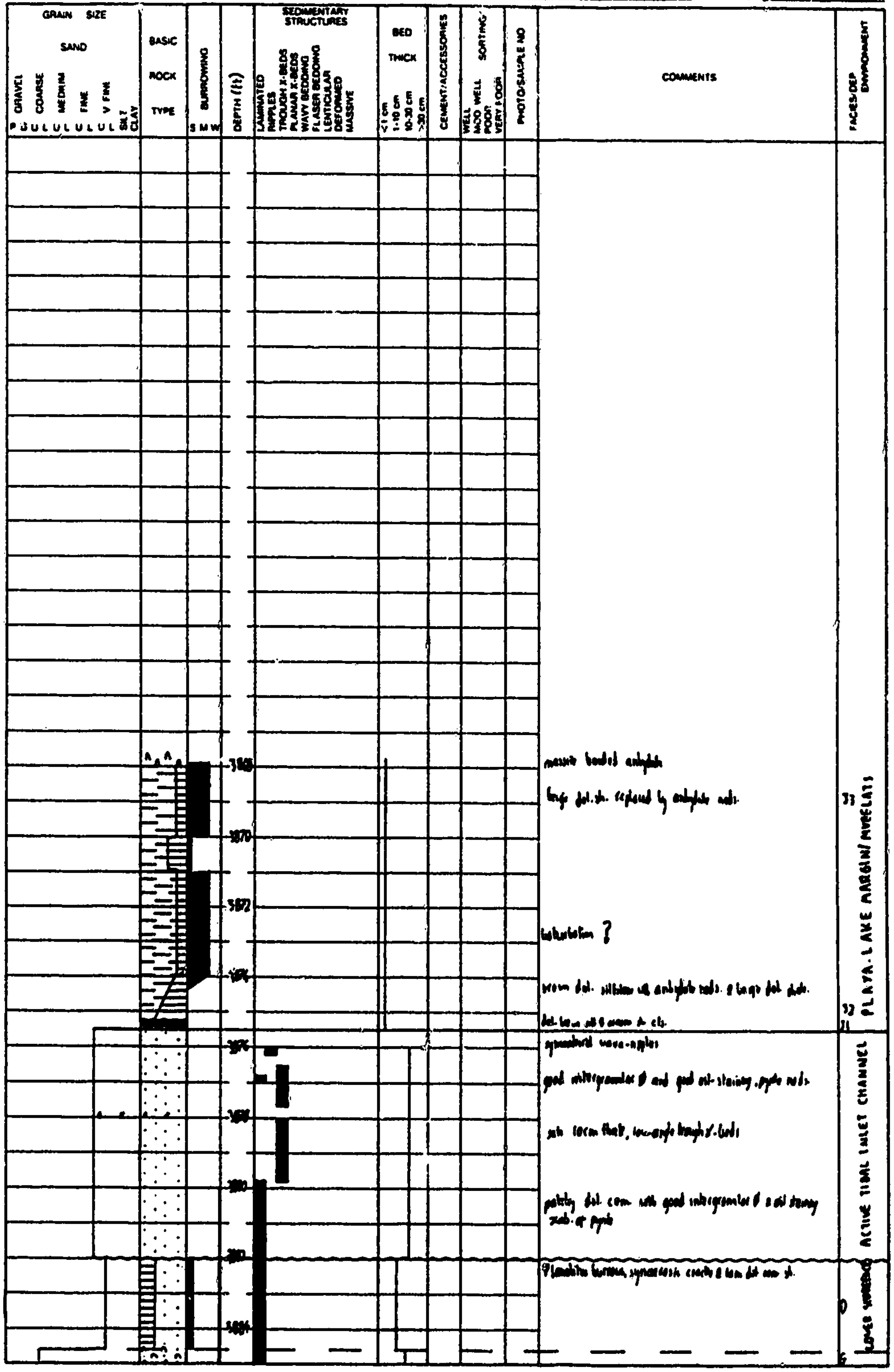

massive banded anhydrite

large dol. sh. replaced by anhydrite nods.

bioturbation ?

brown dol. siltstone w/ anhydrite nods. & large dol. clasts.

dol. brown silt & [illegible] cls.

symmetrical wave-ripples

good intergranular ϕ and good oil-staining, pyrite nods.

sets 10cm thick, low-angle trough X-beds

patchy dol. cem. with good intergranular ϕ & oil staining sub. of pyrite

Planolites burrows, syneresis cracks & brn dol. [illegible] sh.

WELL NAME: UNION HB E PEEJAY d-93-D

FORMATION: HALFWAY-CHARLIE LAKE

DATE: 28/01/91

LOCATION: d-093-D/94-A-16

CORE INTERVAL:

KB: 2336 ft

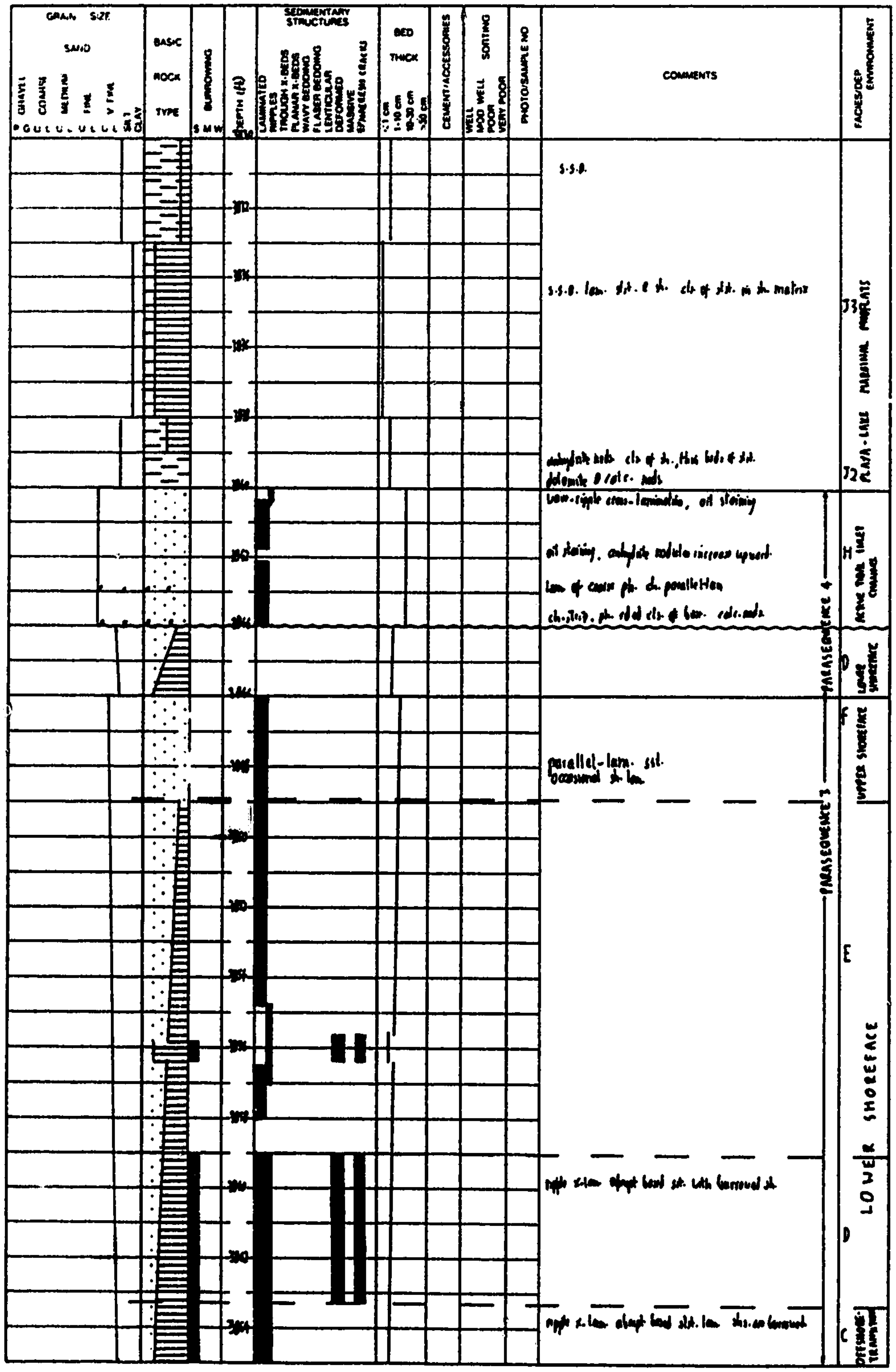

s.s.a.

s.s.a. lam. slt. & sh. cls of slt. in sh. matrix

anhydrite nods cls of sh., thin beds of slt.
dolomite & calc. nods

low-ripple cross-lamination, oil staining

oil staining, anhydrite nodules increase upward

lam. of coarse gr. sh. parallel-lam.

ch., lit., gr. rdd cls. of bur. calc. nods.

parallel-lam. sst.
occasional sh. lam.

ripple x-lam. abrupt bed sst. with burrowed sh.

ripple x-lam. abrupt bed slt. lam. shs. are burrowed

WELL NAME: UNION HB PEEJAY d-95-D
FORMATION: HALFWAY-CHARLIE LAKE
DATE: 5/07/90
LOCATION: d-095-D/94-A-16
CORE INTERVAL:
KB: 2278 BH

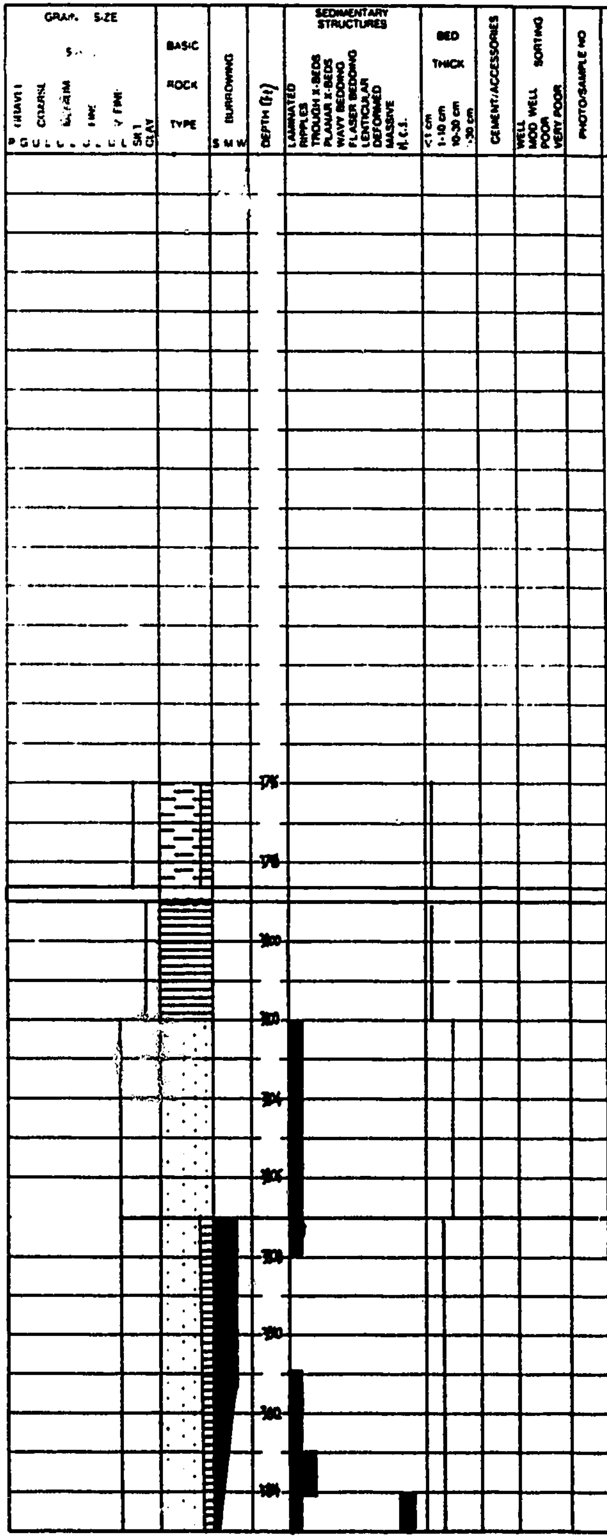

COMMENTS

[illegible] 6-10cm [illegible], some oil-staining & pyrite nodu

reddish-brown red silty-sh. with sts. clr. pyrite nodules

[illegible], anhydrite clasts-rich to laminated, oil-stained

dol. cem. red shale, anhydrite nodules
silty lam.

contact not preserved

parallel-lam.
well-sorted, well-rounded, calc. cem.
oil-stained in places

bioturbation destroyed primary structures

burrows in sh. wavy-bedded calc cem. [illegible]
brown sst.

divergent lam. (H.C.S.)

FACIES-DEP ENVIRONMENT

J1
J2
MARGINAL FLATS
J1
J2
PLAYA-LAKE
CHARLIE LAKE
HALFWAY
TIDAL INLET CHANNEL
LOWER SHOREFACE

WELL NAME: CIGOL PEEJAY d.001-E

FORMATION: HALFWAY-CHARLIE LAKE

DATE: 6/02/91

LOCATION: d-001-E/94-A-16

CORE INTERVAL:

KB: 2373ft

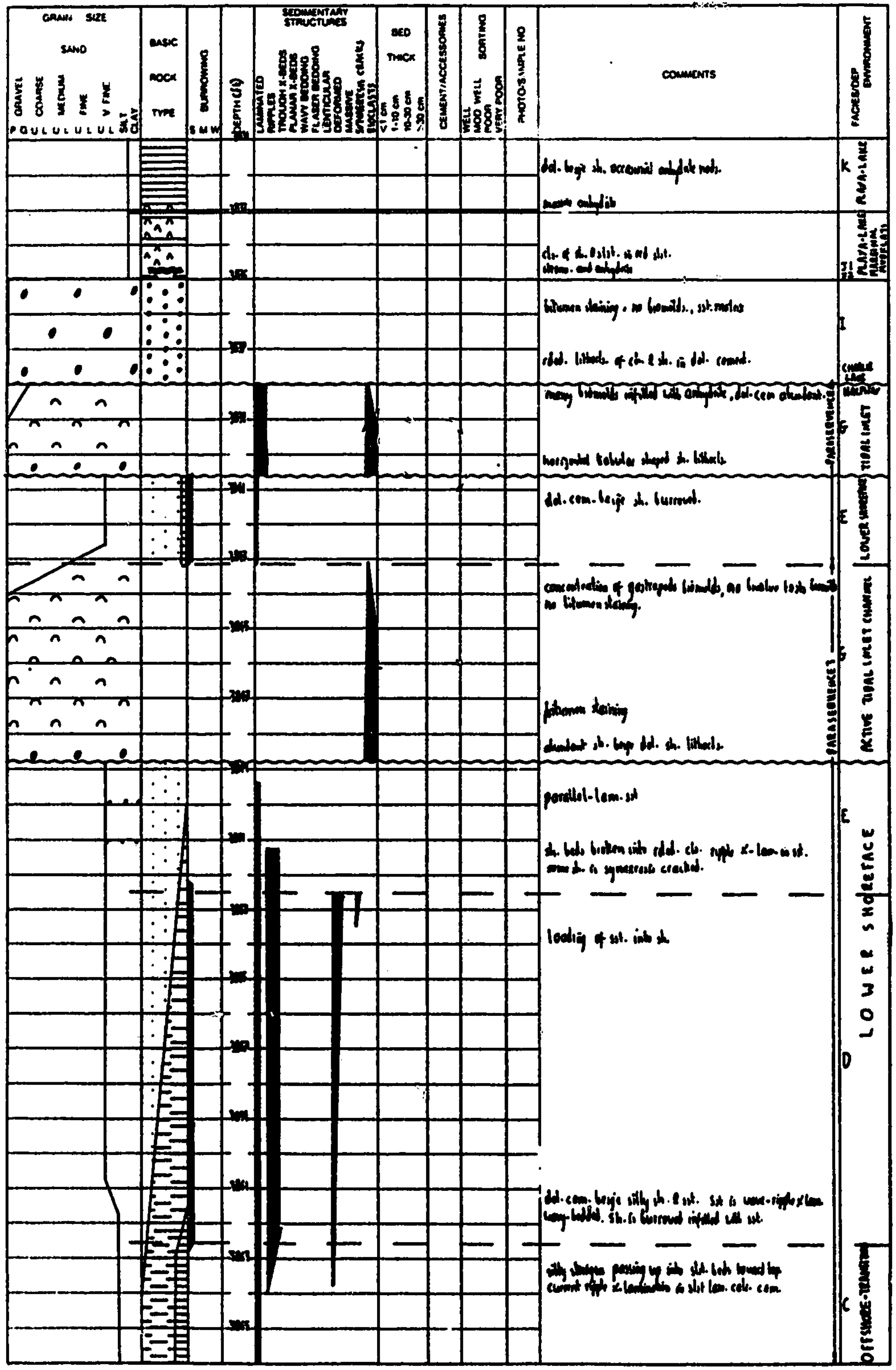

dol. beige sh. occasional anhydrite nods.

massive anhydrite

cls. of sh. & slst. in red slst.
[illegible] and anhydrite

bitumen staining, no biomolds., sst. matrix

rdd. lithcls. of cl. & sh. in dol. cement.

many biomolds infilled with anhydrite, dol-cem abundant.

horizontal tabular shaped sh. lithcls.

dol. cem. beige sh. burrowed.

concentration of gastropods biomolds, no bivalve tests biomolds
no bitumen staining.

bitumen staining

abundant sh. beige dol. sh. lithcls.

parallel-lam. sst

sh. beds broken into rdd. cls. ripple x-lam. in st.
some sh. is syneresis cracked.

loading of sst. into sh.

dol. cem. beige silty sh. & sst. Sst is wave-ripple x lam.
wavy-bedded. Sh. is burrowed infilled with sst.

silty sltstone passing up into slst. beds toward top.
Current ripple x-lamination & slst lam. calc. cem.

WELL NAME: UNION HB E PEEJAY d-2-E FORMATION: HALFWAY-CHARLIE LAKE DATE: 4/07/91

LOCATION: d-002-E/94-A-16 CORE INTERVAL: KB: 2356 ft

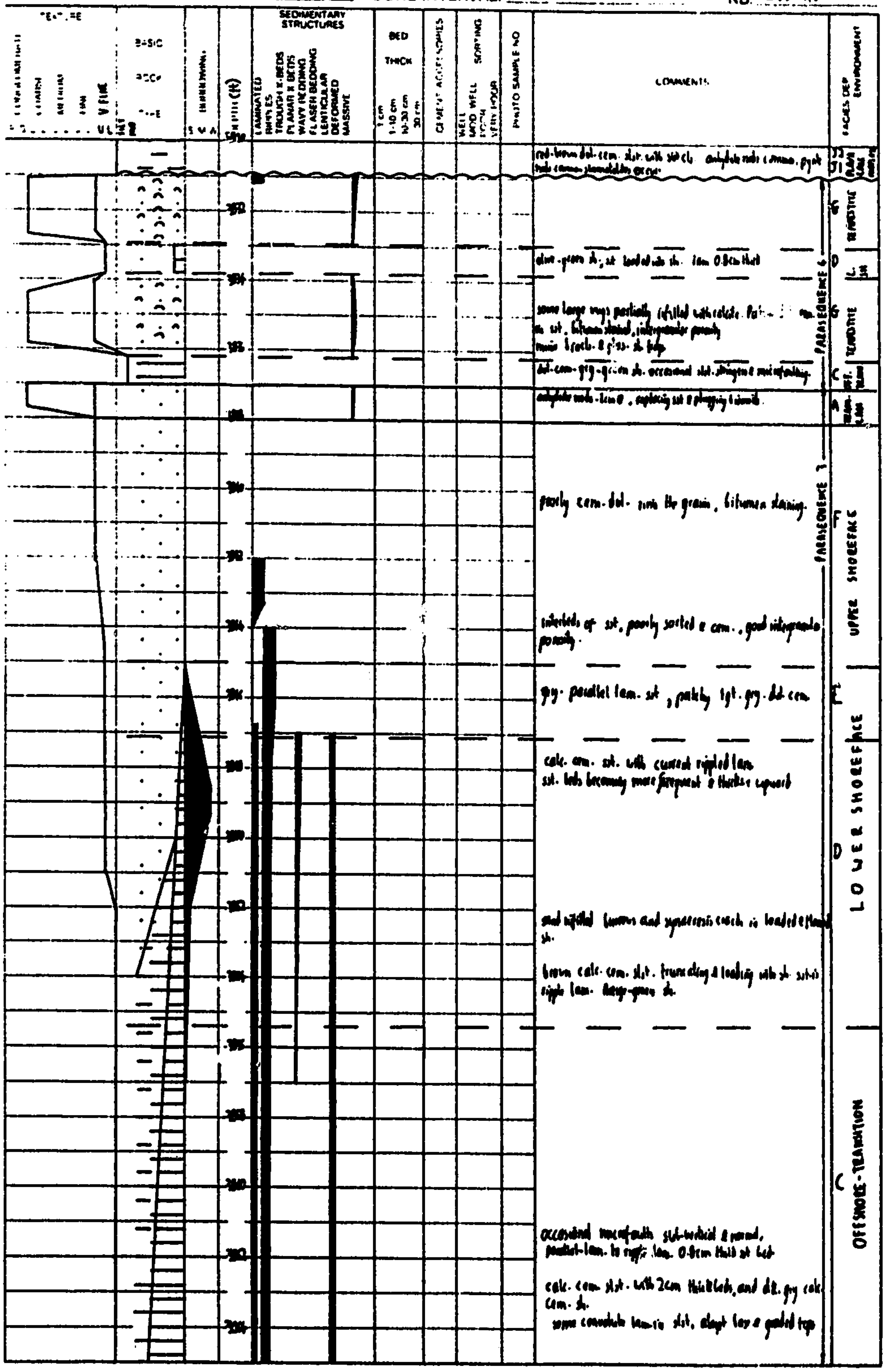

red-brown dol-cem. slst. with sh cl. anhydrite nods common, pyrite nods common, stromatolites occur.

olive-green sh., slt. loaded into sh. lam 0.8cm thick

some large vugs partially infilled with calcite. Pat- [illegible] in slt. bitumen stained, intergranular porosity
minor brach. & glss. sh. frag.

dol-cem-gry-green sh. occasional slst. stringers & microfaulting.

anhydrite nods-lens, replacing sst & plugging bioturb.

poorly cem. dol. sst. fine grain, bitumen staining.

interbeds of sst, poorly sorted & cem., good intergranular porosity.

gry. parallel lam. sst, patchy lgt. gry. dol cem.

calc. cem. sst. with current rippled lam.
sst. beds becoming more frequent & thicker upward

sand infilled burrows and synaeresis cracks in loaded & flamed sh.

brown calc. cem. slst. truncating & loading into sh. sst. in ripple lam. dark-green sh.

occasional microfaults, slst-infilled & normal, parallel-lam. to ripple lam. 0.8cm thick at bed

calc. cem. slst. with 2cm thick beds, and dk. gry calc. cem. sh.
some convolute lam. in slst, always have a graded top

WELL NAME: UNION HB PEEJAY a-003-E FORMATION: HALFWAY-CHARLIE LAKE DATE: 4/07/91

LOCATION: a-003-E/94-A-16 CORE INTERVAL: KB: 2351ft

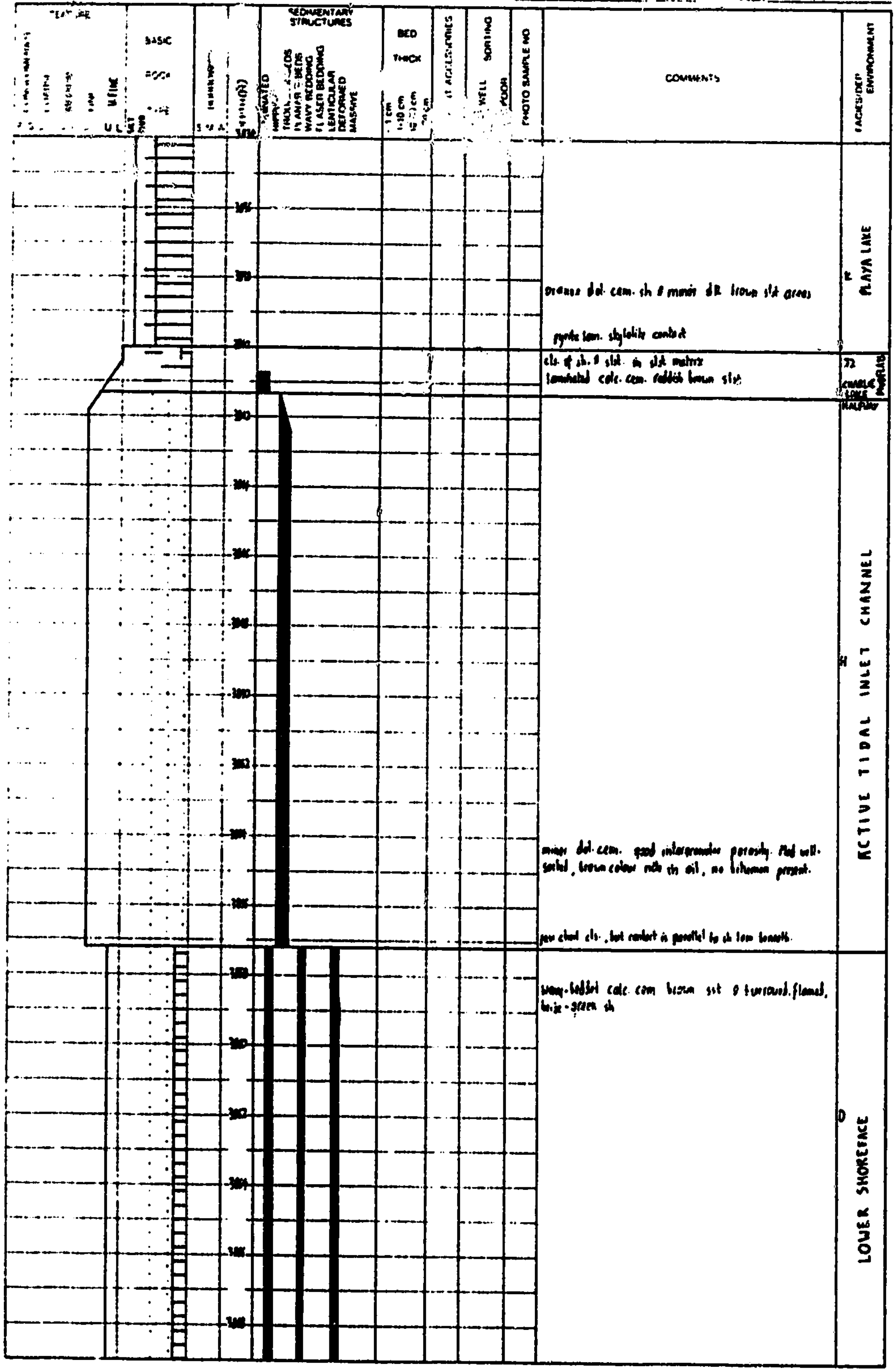

[illegible] dol. cem. sh & minor dk brown slt areas

pyrite lam. stylolite contact

cls. of sh. & slst. in slst matrix
laminated calc. cem. reddish brown slst

minor dol. cem. good intergranular porosity. Md well-sorted, brown colour rich in oil, no bitumen present.

few clast cls., but contact is parallel to sh lam beneath.

wavy-bedded calc. cem. brown sst & burrowed, flamed, beige-green sh

P PLAYA LAKE

72 CHARLIE LAKE
HALFWAY

H ACTIVE TIDAL INLET CHANNEL

D LOWER SHOREFACE

WELL NAME: UNION HB EAST PEEJAY D-3-E

FORMATION: HALFWAY-CHARLIE LAKE

DATE 31/07/90

LOCATION: d-003-E/94-A-16

CORE INTERVAL:

KB: 2355.3ft

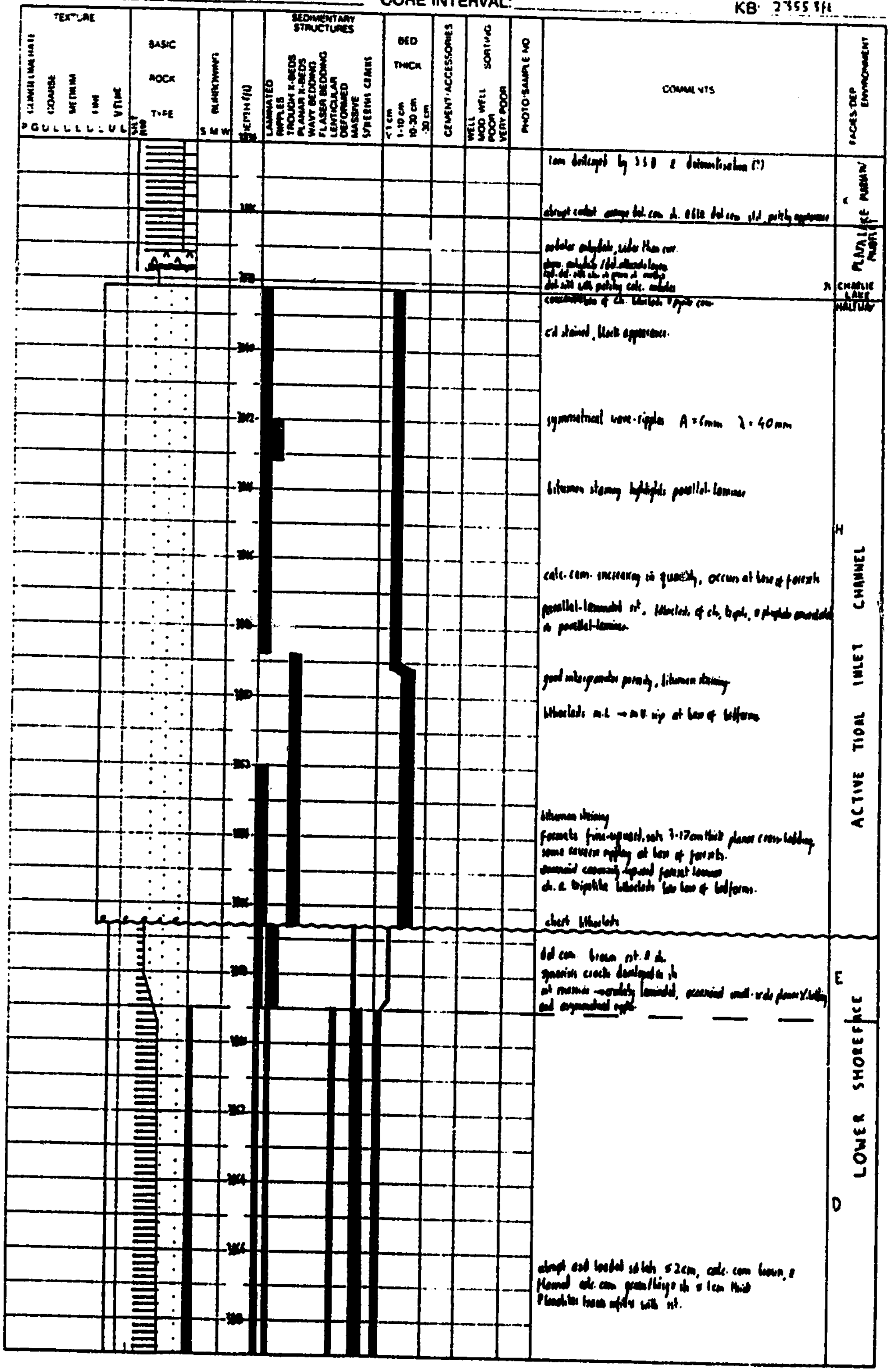

lam. disrupted by SSD & dolomitization (?)

abrupt contact, orange dol. cem. & [illegible] dol cem. sltst, patchy appearance

nodular anhydrite, wider than core.
dom. nodules / dol. alternate layers
[illegible]
dol. silt with patchy calc. nodules

concentration of ch. lithoclasts & pyrite cem.

cd stained, black appearance.

symmetrical wave-ripples A = 6mm λ = 40mm

bitumen staining highlights parallel-laminae

calc. cem. increasing in quantity, occurs at base of foresets

parallel-laminated sst. lithoclasts of ch, bnpl., & phosphate concentrated in parallel-laminae.

good intergranular porosity, bitumen staining

lithoclasts m.L → m.U. sized at base of bedforms

bitumen staining
foresets fining-upward, sets 7-17cm thick planar cross-bedding.
some reverse grading at base of foresets.
occasional coarsening-upward foreset laminae
ch. & bioplastic lithoclasts line base of bedforms.

chert lithoclasts

dol. cem. brown sst. & sh.
synaeresis cracks developed in sh.
sst moderate-variably laminated, occasional small-scale planar X-bedding
and asymmetrical ripples

abrupt and loaded siltstones ≤2cm, calc. cem. brown, &
flasered calc. cem. grey/beige sh ≤ 1cm thick
Planolites burrows infilled with sst.

WELL NAME: PACIFIC SINCLAIR PEEJAY d-8-E

FORMATION: HALFWAY-CHARLIE LAKE

DATE: 9/08/90

LOCATION: d-008-E/94-A-16

CORE INTERVAL:

KB: 2356ft

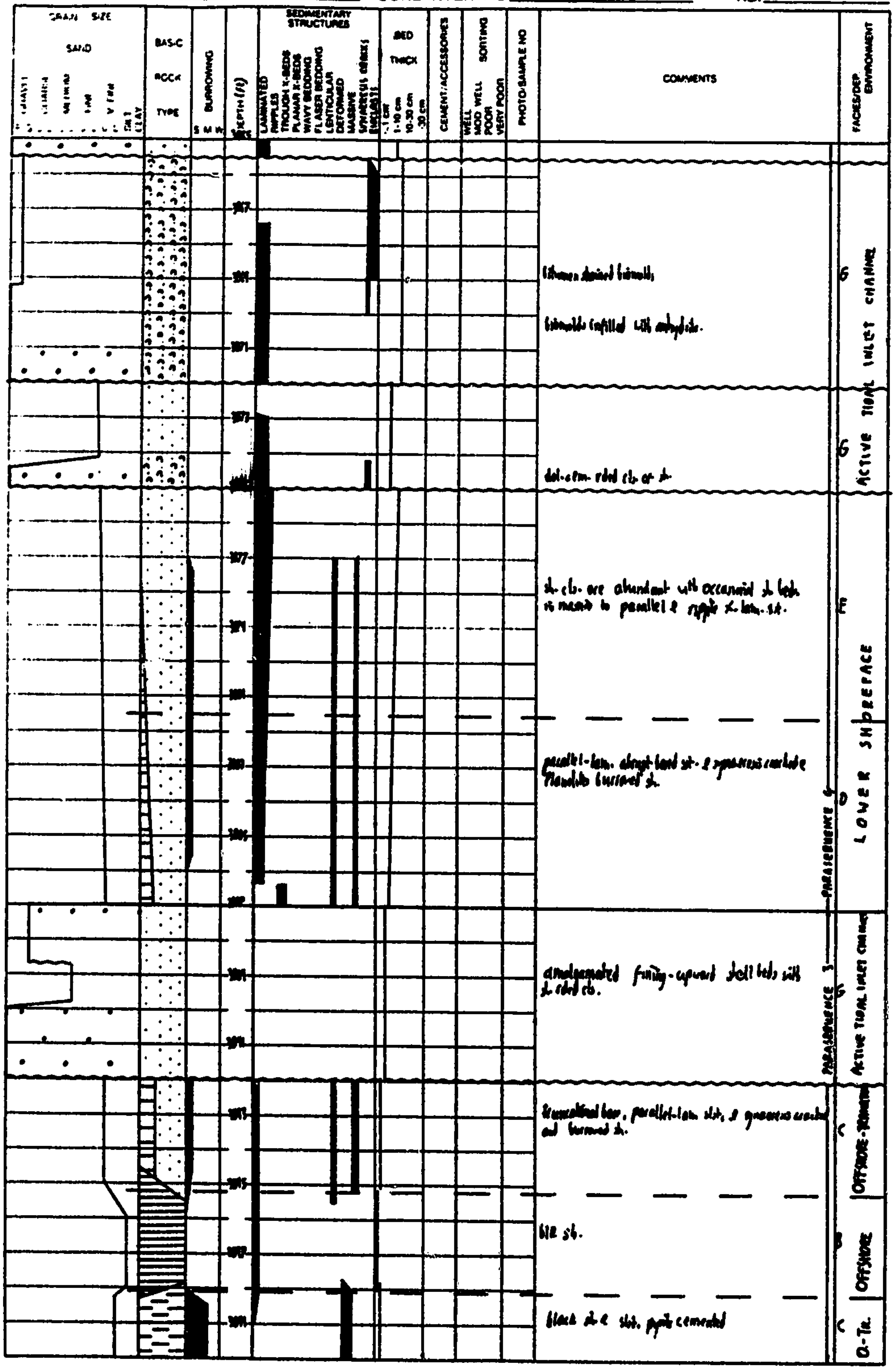

[illegible] burrows

burrows infilled with anhydrite.

dol.-cem. rdd cl. of sh.

sh. cl. are abundant with occasional sh. beds. ss massive to parallel & ripple x-lam. ss.

parallel-lam. abrupt-based st. & synaeresis cracks Planolites burrowed sh.

amalgamated fining-upward shell beds with sh. rdd cls.

[illegible], parallel-lam. slst. & synaeresis cracked and burrowed sh.

blk sh.

black sh. & slst. pyrite cemented

WELL NAME: PACIFIC SINCLAIR PEEJAY d-8E

FORMATION: HALFWAY-CHARLIE LAKE

DATE: 9/08/90

LOCATION: d-008-E/94-A-16

CORE INTERVAL:

KB: 2356ft

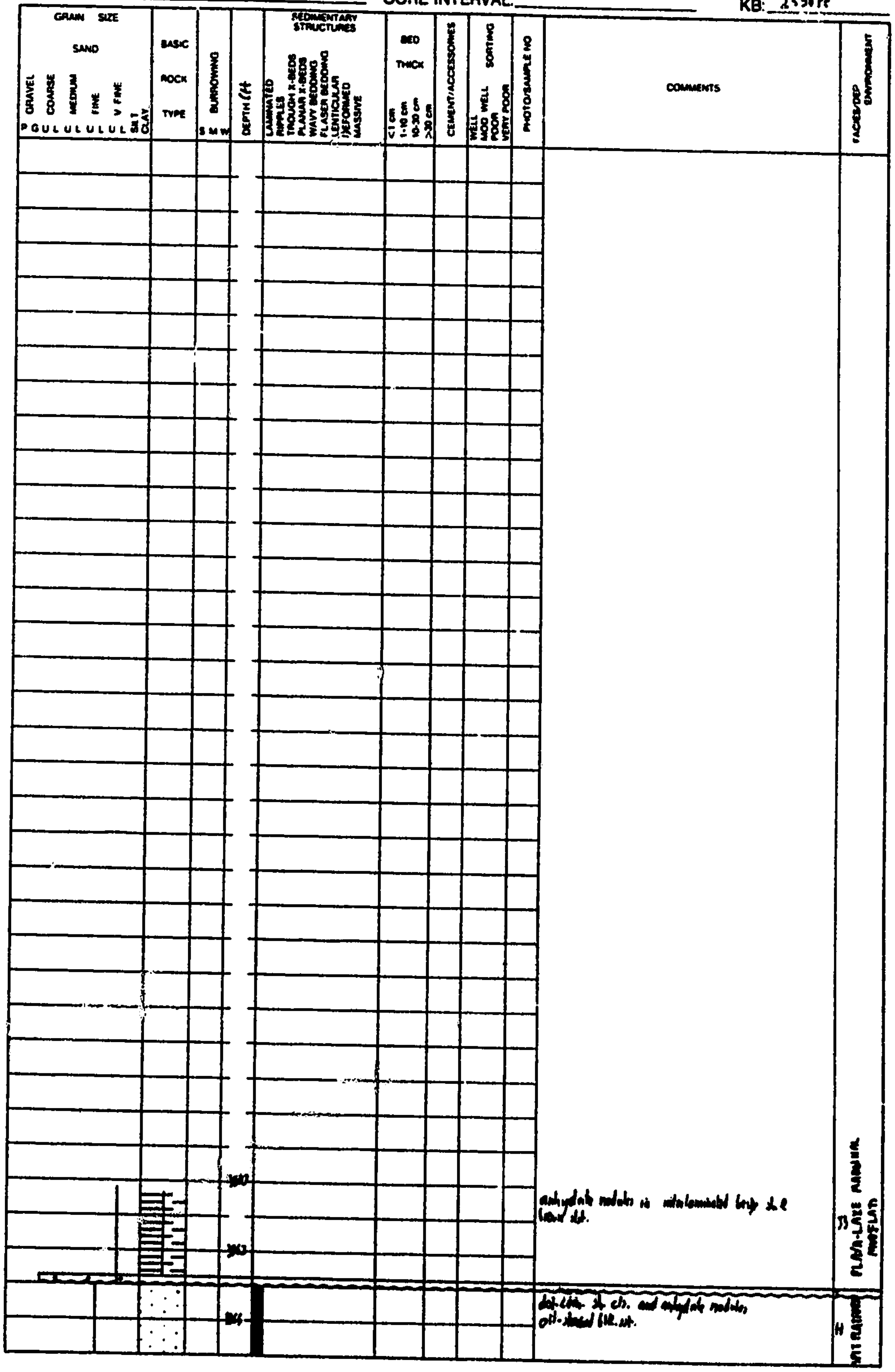

anhydrite nodules in mm-laminated [illegible] sh & [illegible] slt.

J3 PLAYA-LAKE MARGINAL MUDFLAT

dol. lith. [illegible] cls. and anhydrite nodules, oil-stained [illegible]

H [illegible] FLATS

WELL NAME: CIGOL PEEJAY d-11-E

FORMATION: HALFWAY-CHARLIE LAKE

DATE: 20/6/90

LOCATION: d-011-E/94-A-16

CORE INTERVAL:

KB: 2366ft

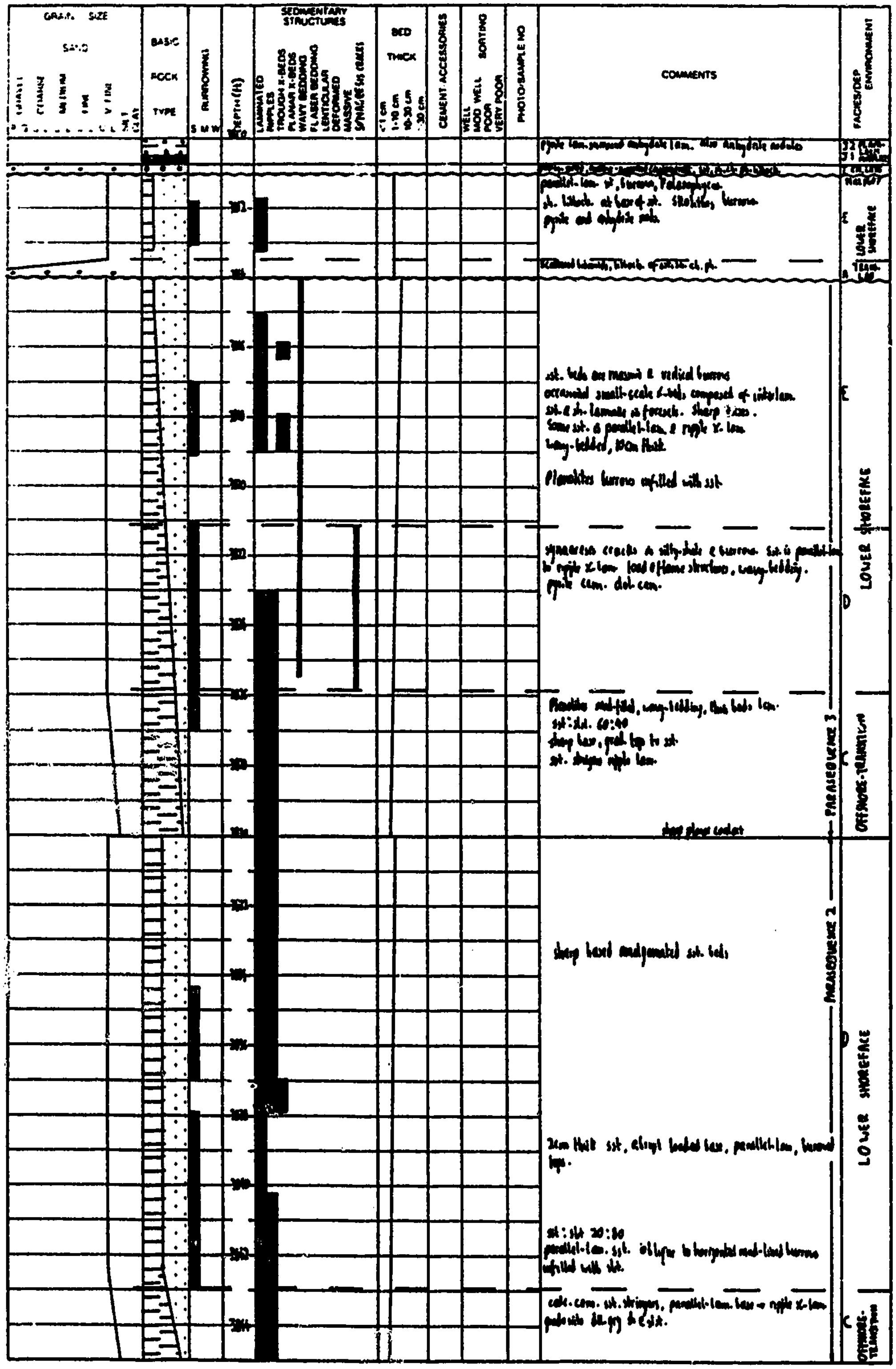

Pyrite lam. [illegible] anhydrite lam. Also Anhydrite nodules

[illegible]

parallel-lam. st., burrows, Palaeophycus.
sh. lithocl. at base of st. Skolithos burrows
pyrite and anhydrite nods.

Scattered bioclasts, lithocl. of [illegible] ch. ph.

sst. beds are massive & vertical burrows
occasional small-scale X-beds composed of siltst. lam.
sst. & sh. laminae in foresets. Sharp bases.
Some sst. & parallel-lam. & ripple X-lam.
wavy-bedded, 10cm thick.

Planolites burrows infilled with sst.

syneresis cracks in silty-shale & burrows. sst. is parallel-lam to ripple X-lam. load & flame structures, wavy-bedding.
pyrite cem. dol. cem.

Planolites sand-filled, wavy-bedding, thin beds lam.
sst:sld. 60:40
sharp base, grad. top to sst.
st. stringers ripple lam.

sharp planar contact

sharp based amalgamated sst. beds

3cm thick sst., abrupt loaded base, parallel-lam., burrowed top.

sst : slt 20:80
parallel-lam. sst. oblique to horizontal mud-lined burrows infilled with slt.

calc. cem. sst. stringers, parallel-lam. base → ripple X-lam. [illegible] dk. gry sh & slt.

WELL NAME: UNION H B EAST PEEJAY D-12-E

FORMATION: HALFWAY - CHARLIE LAKE

DATE: 4/02/91

LOCATION: d-012-E/94-A-16

CORE INTERVAL:

KB: 2370ft

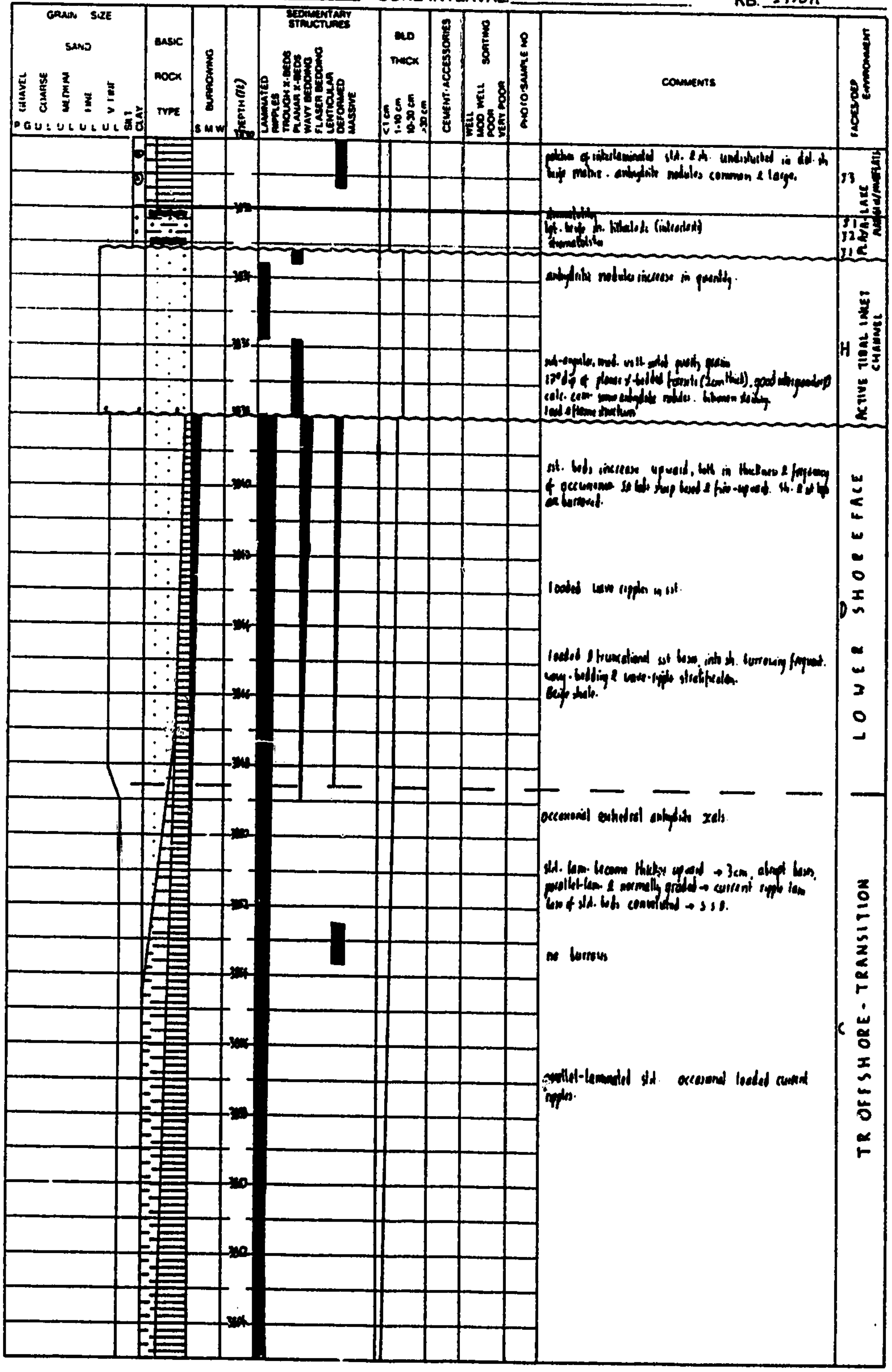

patches of interlaminated sld. & sh. undisturbed in dol. sh. beige matrix. anhydrite nodules common & large.

stromatolites
lgt. beige sh. lithoclasts (intraclasts)
stromatolites

anhydrite nodules increase in quantity.

sub-angular, mod. well sorted quartz grain
17° dip of planar x-bedded foresets (2cm thick), good intergranular φ
calc. cem. some anhydrite nodules. bitumen staining.
load & flame structure

slt. beds increase upward, both in thickness & frequency of occurrence. St beds sharp based & fine-upward. [illegible] are burrowed.

loaded wave ripples in slt.

loaded & truncational slt base, into sh. burrowing frequent. wavy-bedding & wave-ripple stratification. Beige shale.

occasional euhedral anhydrite xals.

sld. lam. become thicker upward → 3cm, abrupt base, parallel-lam. & normally graded → current ripple lam. base of sld. beds convoluted → s.s.d.

no burrows

parallel-laminated sld. occasional loaded current ripples.

WELL NAME: UNION ET AL PEEJAY
FORMATION: HALFWAY-CHARLIE LAKE
DATE: 3/07/91
LOCATION: 6-013-E/94-A-16
CORE INTERVAL:
KB: 720 METRES

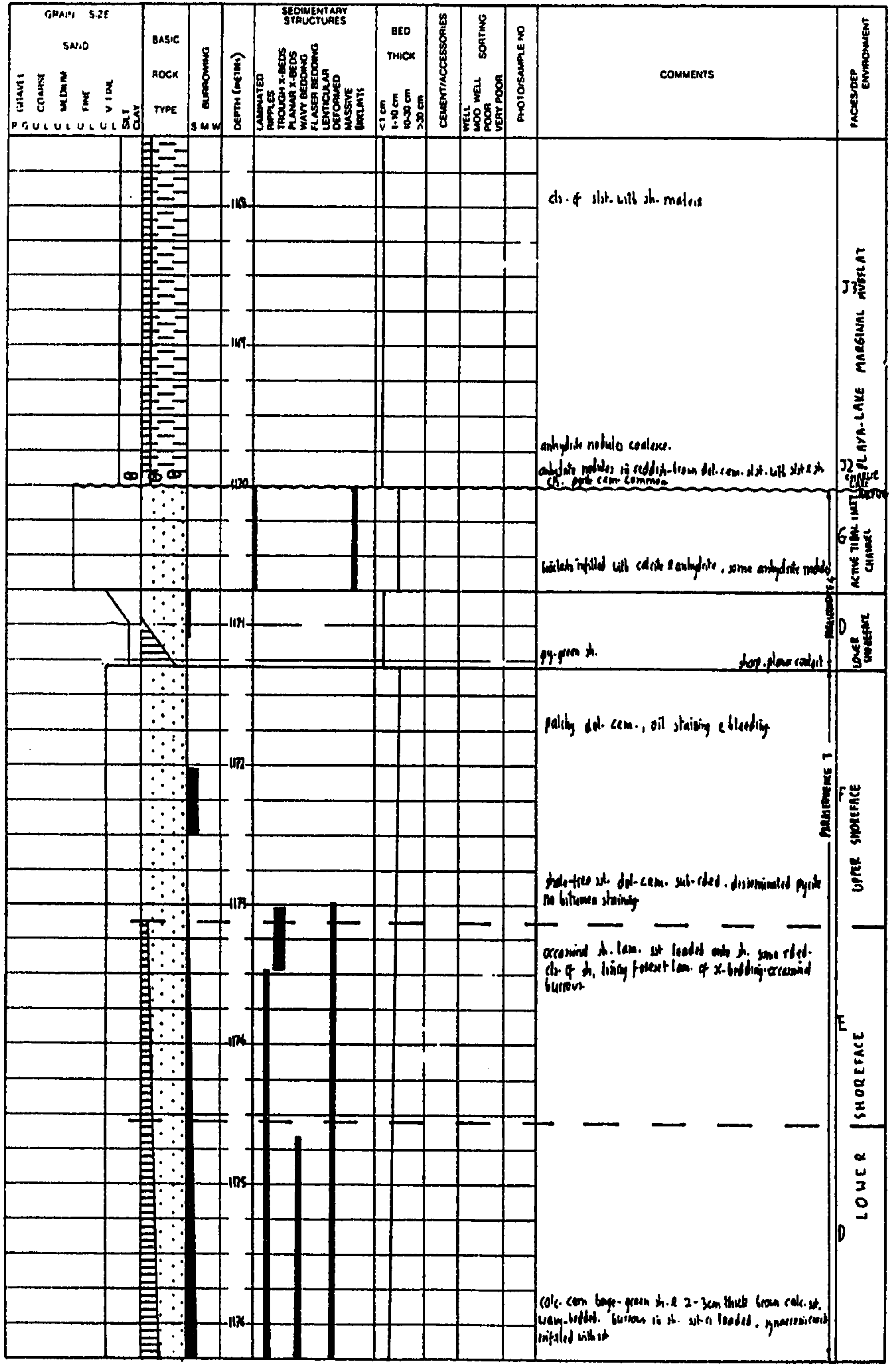

cl. & slst. with sh. matrix

anhydrite nodules coalesce.

anhydrite nodules in reddish-brown dol.-cem. slst. with slst & sh. Cl. pyrite cem. common

burrows infilled with calcite & anhydrite, some anhydrite nodules

gy-green sh.

sharp, planar contact

patchy dol. cem., oil staining & bleeding

shale-free sst. dol-cem. sub-rded. disseminated pyrite no bitumen staining

occasional sh. lam. sst loaded onto sh. some rded. cls. of sh. lining foreset lam. of x-bedding. occasional burrows

calc. cem. beige-green sh. & 2-3cm thick brown calc. sst. wavy-bedded. burrows in sh. sst. is loaded. synaeresis cracks infilled with sst

WELL NAME: UNION H B EAST PEEJAY d-13-E FORMATION: HALFWAY-CHARLIE LAKE DATE: 4/07/91

LOCATION: d-013-E/94-A-16 CORE INTERVAL: KB: 2367 ft

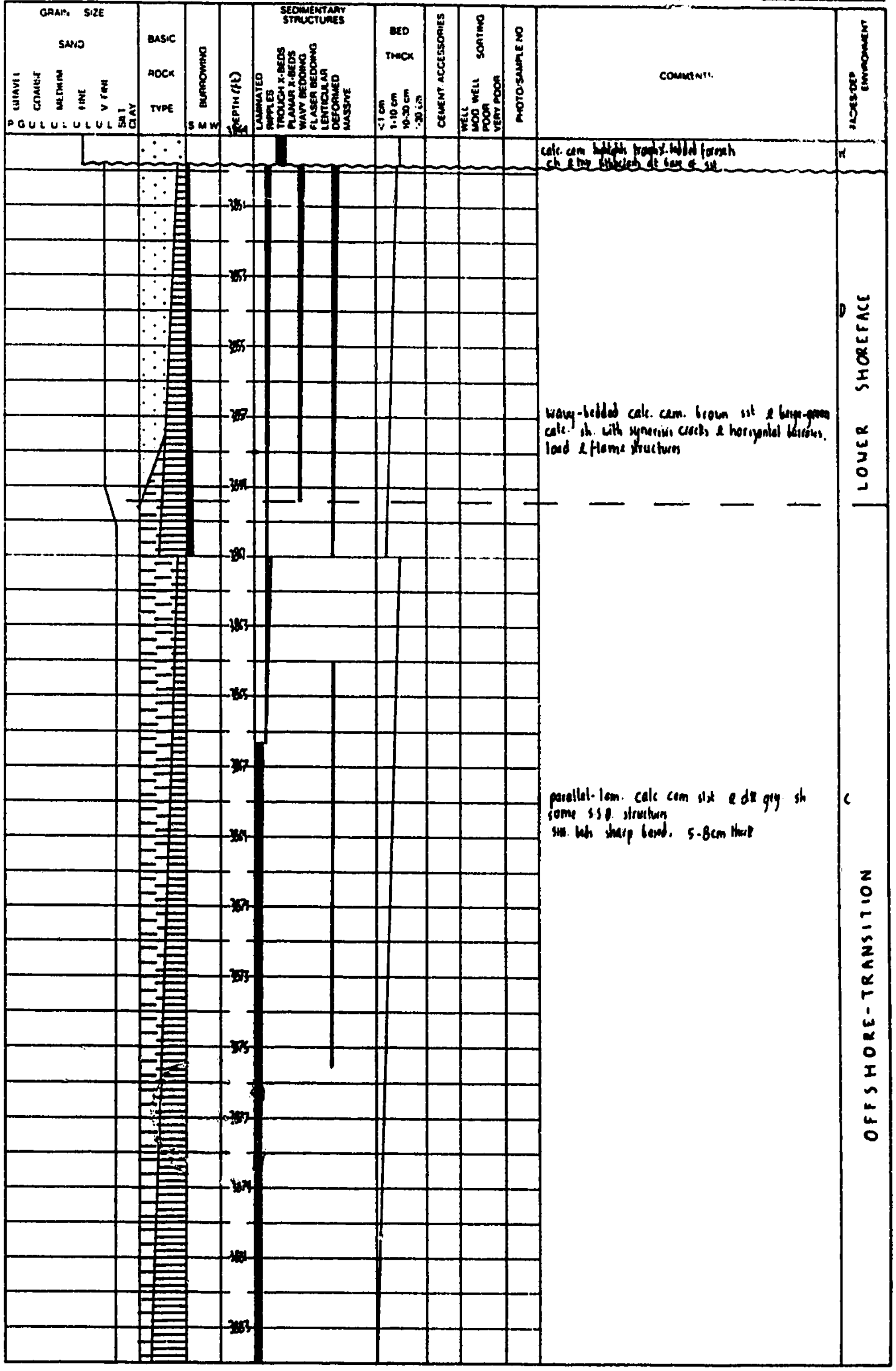

calc. cem bubbly trough-bedded foresh
ch & tiny lithoclasts at base of sst

wavy-bedded calc. cem. brown sst & beige-green calc. sh. with syneresis cracks & horizontal burrows. load & flame structures

parallel-lam. calc cem slst & dk gry sh
some SSD. structures
sst. beds sharp based. 5-8cm thick

WELL NAME: UNION H B EAST PEEJAY d-13-E FORMATION: HALFWAY-CHARLIE LAKE DATE: 4/07/8

LOCATION: d-013-E/94 A-16 CORE INTERVAL: KB:

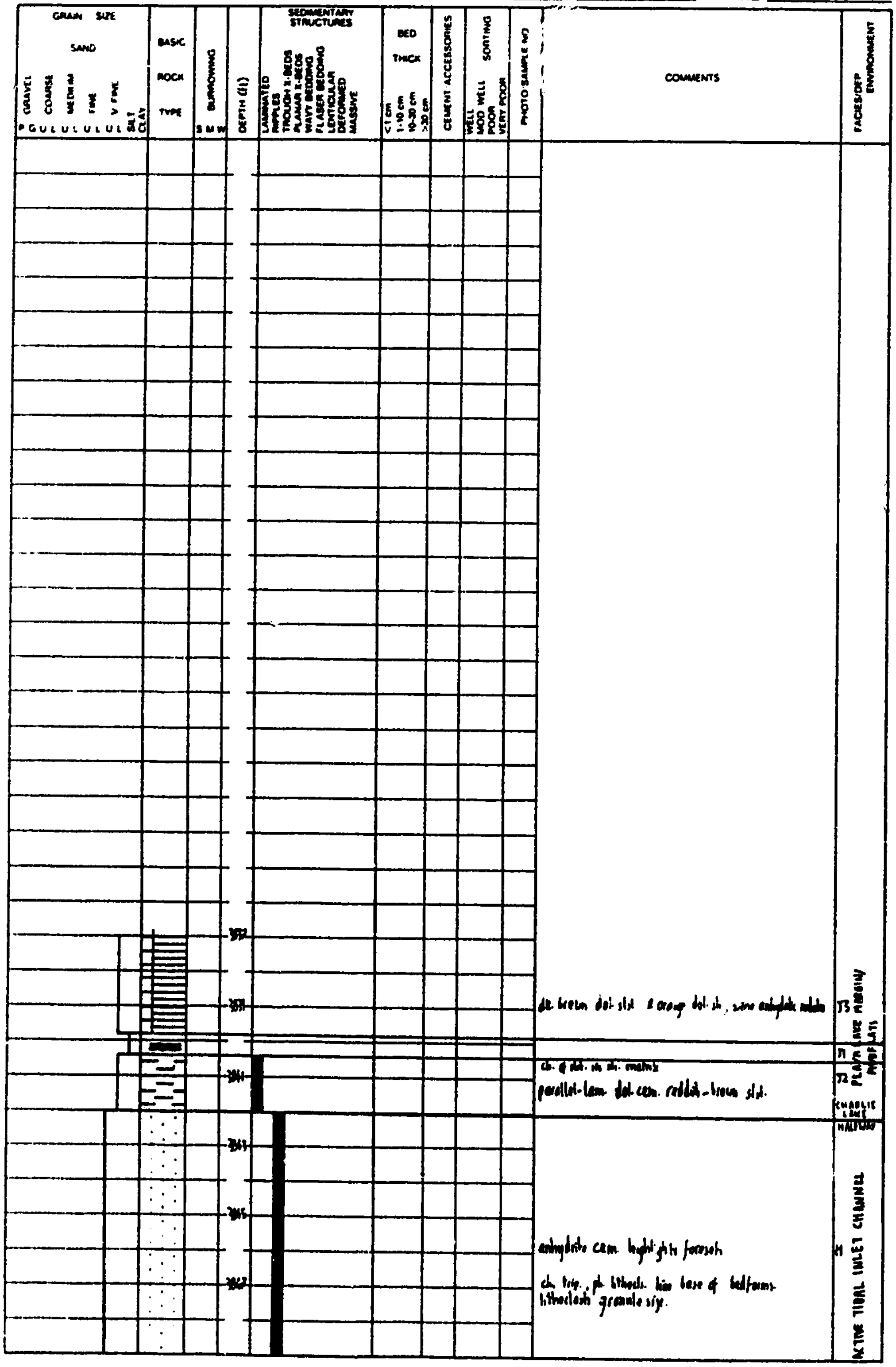

dk. brown dol. slst. & orang dol. sh., some anhydrite nodules

ch. of dol. in sh. matrix

parallel-lam. dol. cem. reddish-brown slst.

anhydrite cem. highlights foresets

ch. trip., pb. lithocls. line base of bedforms. lithoclasts granule size.

WELL NAME: UNION H & EAST PEEJAY

FORMATION: HALFWAY- CHARLIE LAKE

DATE: 30/07/90

LOCATION: a-014-E/94-A-16

CORE INTERVAL:

KB: 2359 ft

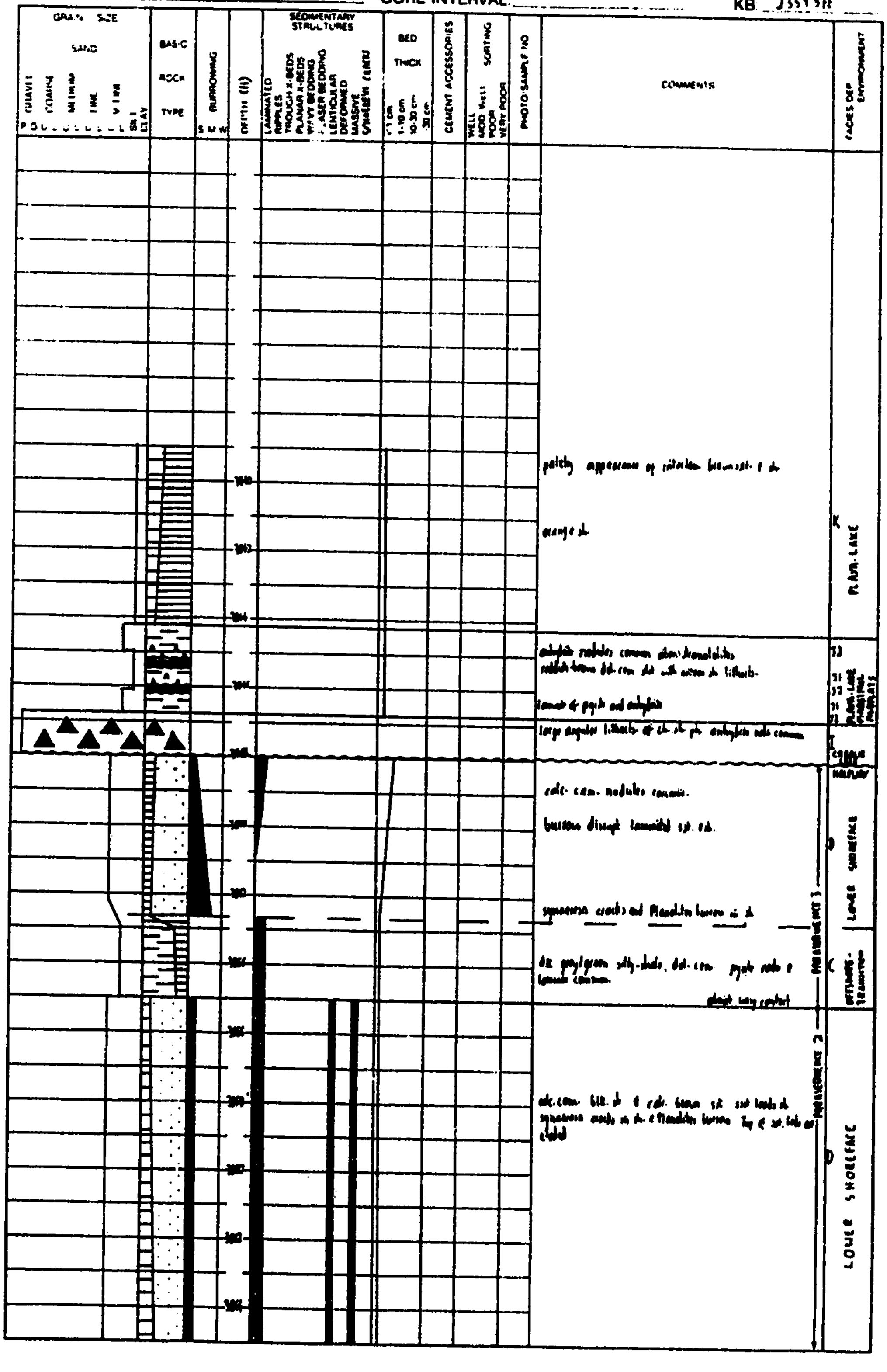

patchy appearance of reddish brown silt. & sh.

orange sh.

anhydrite nodules common above brecciated...
reddish brown dol.-cem. slst. with common sh. lithoclasts.

laminae of pyrite and anhydrite

large angular lithoclasts of ch. sh. grn. anhydrite nods common

calc. cem. nodules common.

burrows disrupt laminated ss. ch.

synaeresis cracks and Planolites burrows in sh.

dk. grey/green silty-shale, dol.-cem. pyrite nods & laminae common.

sharp wavy contact

calc.cem. blk. sh. & calc. brown slt. and lenses sh. synaeresis cracks in sh. & Planolites burrows top of ss. beds are calcified

WELL NAME SINCLAIR ETAL PEEJAY D-19-E FORMATION: HALFWAY-CHARLIE LAKE DATE: 29/01/91

LOCATION d-019-E/94-A-16 CORE INTERVAL: KB: G.L. 2347.96 ft.

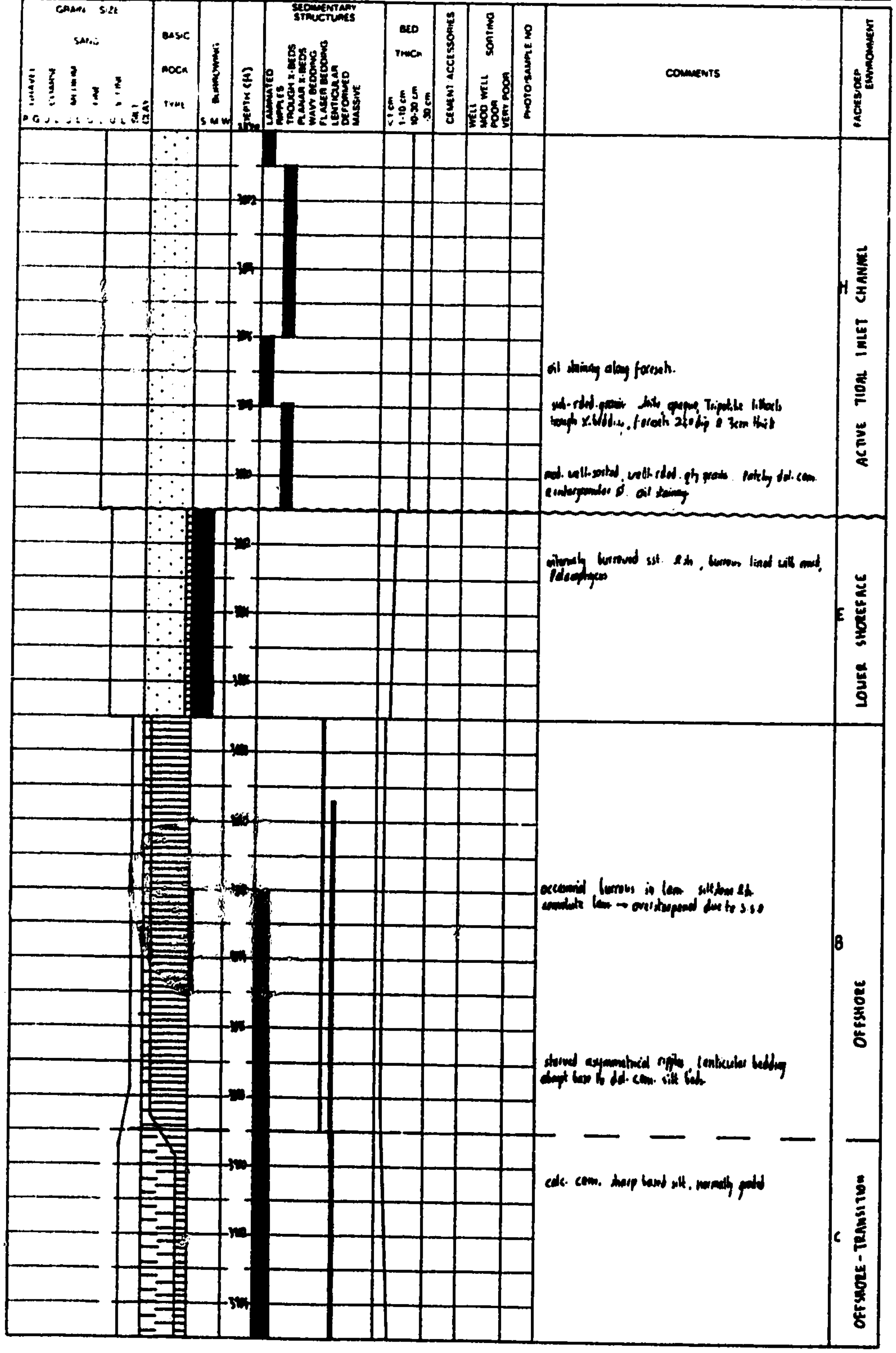

oil staining along foresets.

sub-rdd. grains, [illegible] opaque, Tripolite lithoclasts, trough X-bedding, foresets 25° dip & 3cm thick

mod. well-sorted, well-rdd. qtz grains. Patchy dol. cem. & intergranular Ø. oil staining

intensely burrowed sst. [illegible], burrows lined with mud, Palaeophycus

occasional burrows in lam. siltstone & sh. convolute lam. → oversteepened due to s.s.d

starved asymmetrical ripples, lenticular bedding abrupt base to dol. cem. silt beds

calc. cem. sharp based silt, normally graded

WELL NAME SINCLAIR ET AL PEEJAY D-19-E

FORMATION HALFWAY- CHARLIE LAKE

DATE 29/01/91

LOCATION d-019-E/94-A-16

CORE INTERVAL:

KB: 6 L 2347.95 ft

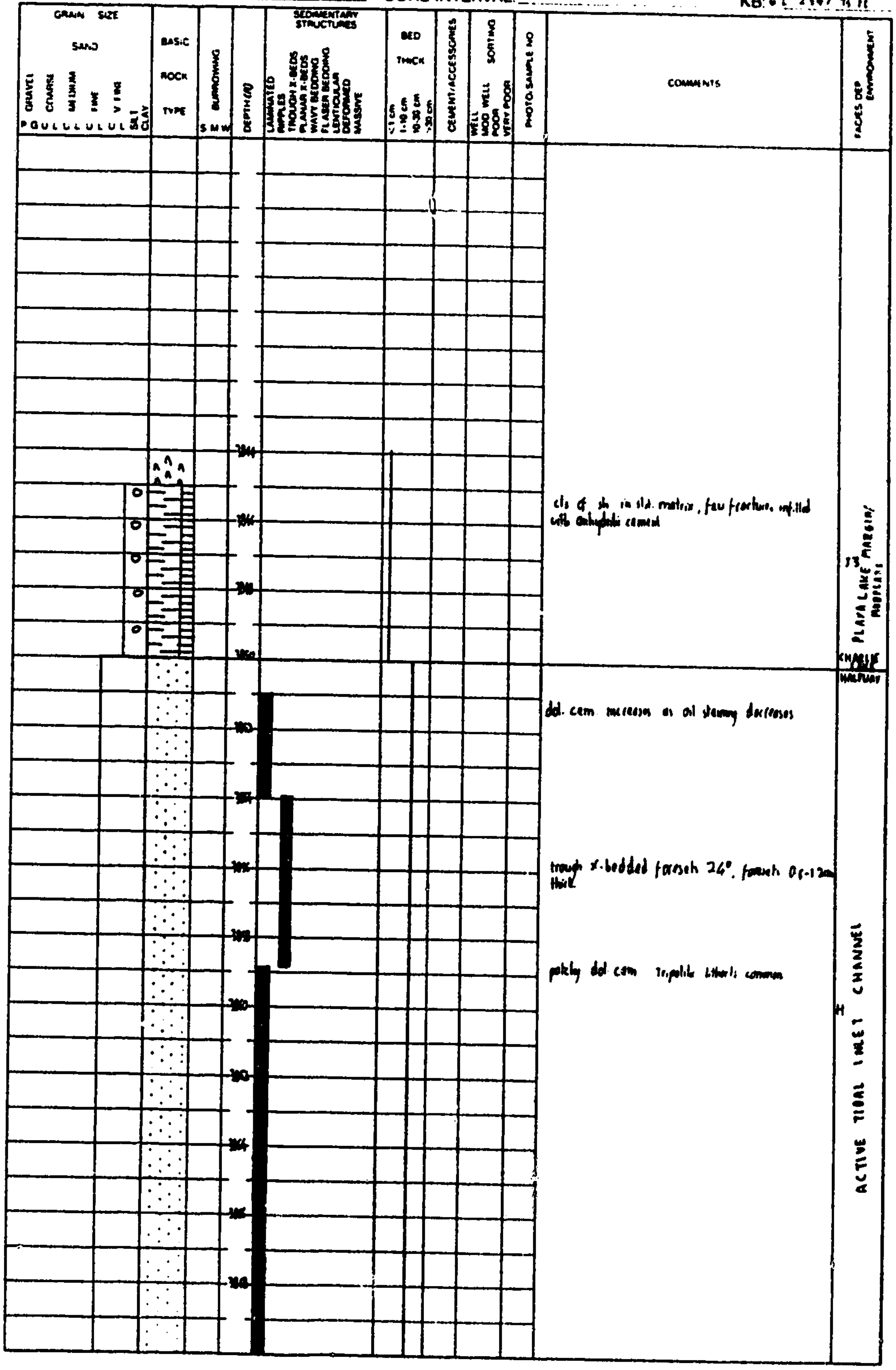

cls of sh in sld. matrix, few fracture, infilled with anhydrite cement

dol. cem. increases as oil staining decreases

trough x-bedded foreset 24°, foreset 0.5-1.2cm thick

patchy dol cem. Tripolite litharls common

WELL NAME UNION HB EAST PEEJAY FORMATION: HALFWAY-CHARLIE LAKE DATE: 19/01/90

LOCATION d-022-E/94-A-16 CORE INTERVAL: KB: 2363ft

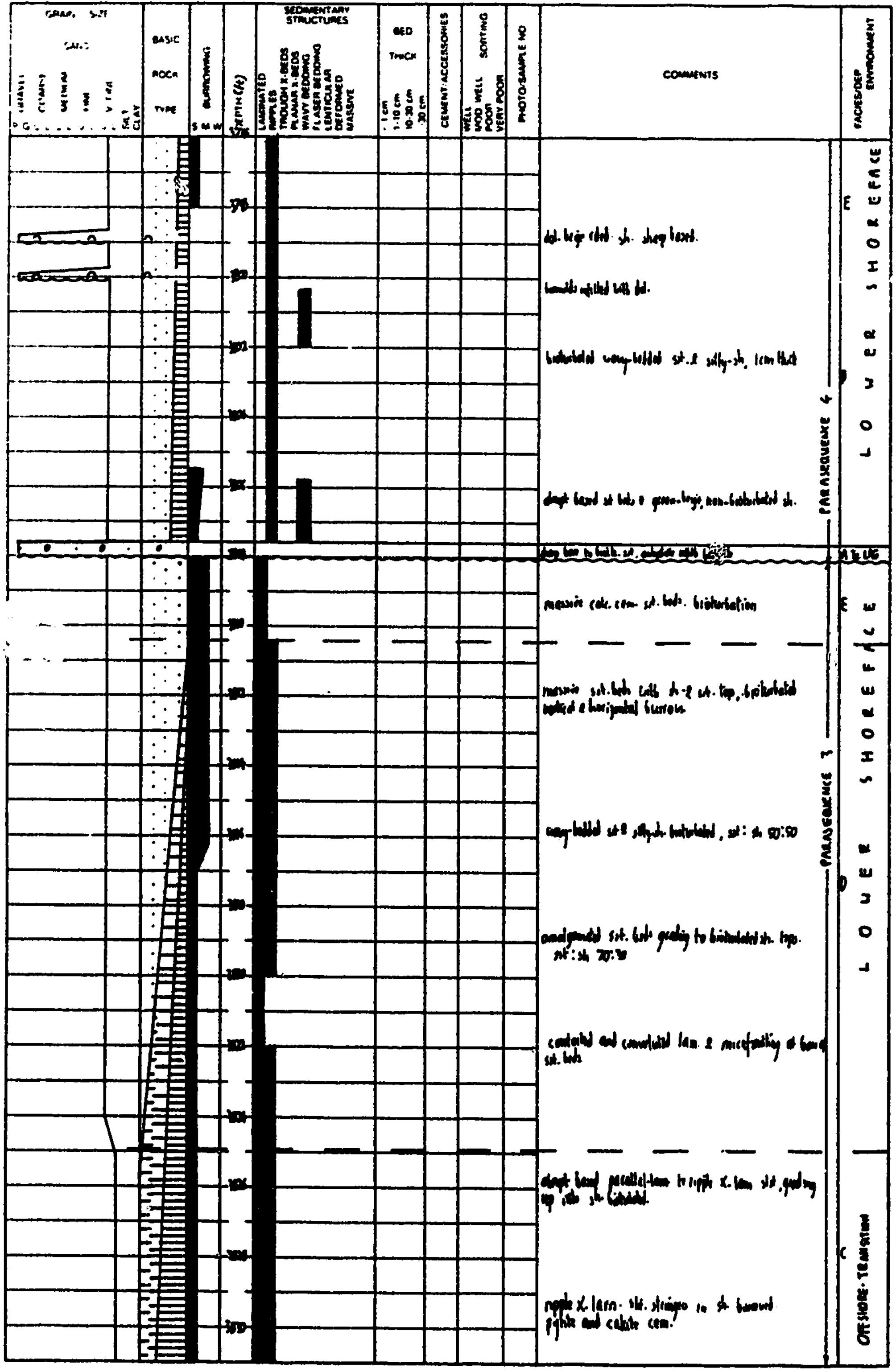

dol. beige clrd. sh. sharp based.

burrows infilled with dol.

bioturbated wavy-bedded st. & silty-sh, 1cm thick

sharp based st. beds & green-beige, non-bioturbated sh.

sharp base to biocl. st., [illegible]

massive calc. cem. st. beds. bioturbation

massive sst. beds with sh. & st. top, bioturbated vertical & horizontal burrows

wavy-bedded st & silty-sh bioturbated, st : sh 50:50

amalgamated sst. beds grading to bioturbated sh. tops. sst : sh 70:30

contorted and convoluted lam. & microfaulting at base of sst. beds

sharp based parallel-lam to ripple X-lam slt, grading up into sh. bioturbated.

ripple X-lam. slt. stringers in sh. burrowed pyrite and calcite cem.

WELL NAME: UNION HB EAST PEEJAY FORMATION: HALFWAY- CHARLIE LAKE DATE 19/06/90

LOCATION: d-022-E/94-A-16 CORE INTERVAL: KB 2363 ft

GRAIN SIZE SAND GRAVEL COARSE MEDIUM FINE V FINE SILT CLAY P G U L U L U L U L	BASIC ROCK TYPE	BURROWING S M W	DEPTH (ft)	SEDIMENTARY STRUCTURES LAMINATED RIPPLES TROUGH X-BEDS PLANAR X-BEDS WAVY BEDDING FLASER BEDDING LENTICULAR DEFORMED MASSIVE	BED THICK < 1 cm 1-10 cm 10-30 cm >30 cm	CEMENT ACCESSORIES	SORTING WELL MOD WELL POOR VERY POOR	PHOTO SAMPLE NO	COMMENTS	FACIES-DEP ENVIRONMENT
			[illegible]						[illegible]	[illegible]

WELL NAME UNION H.B. FEE JAY a-23-E FORMATION HALFWAY-CHARLIE LAKE DATE 4/07/91

LOCATION a-23-E/94-A-16 CORE INTERVAL KB 2363ft

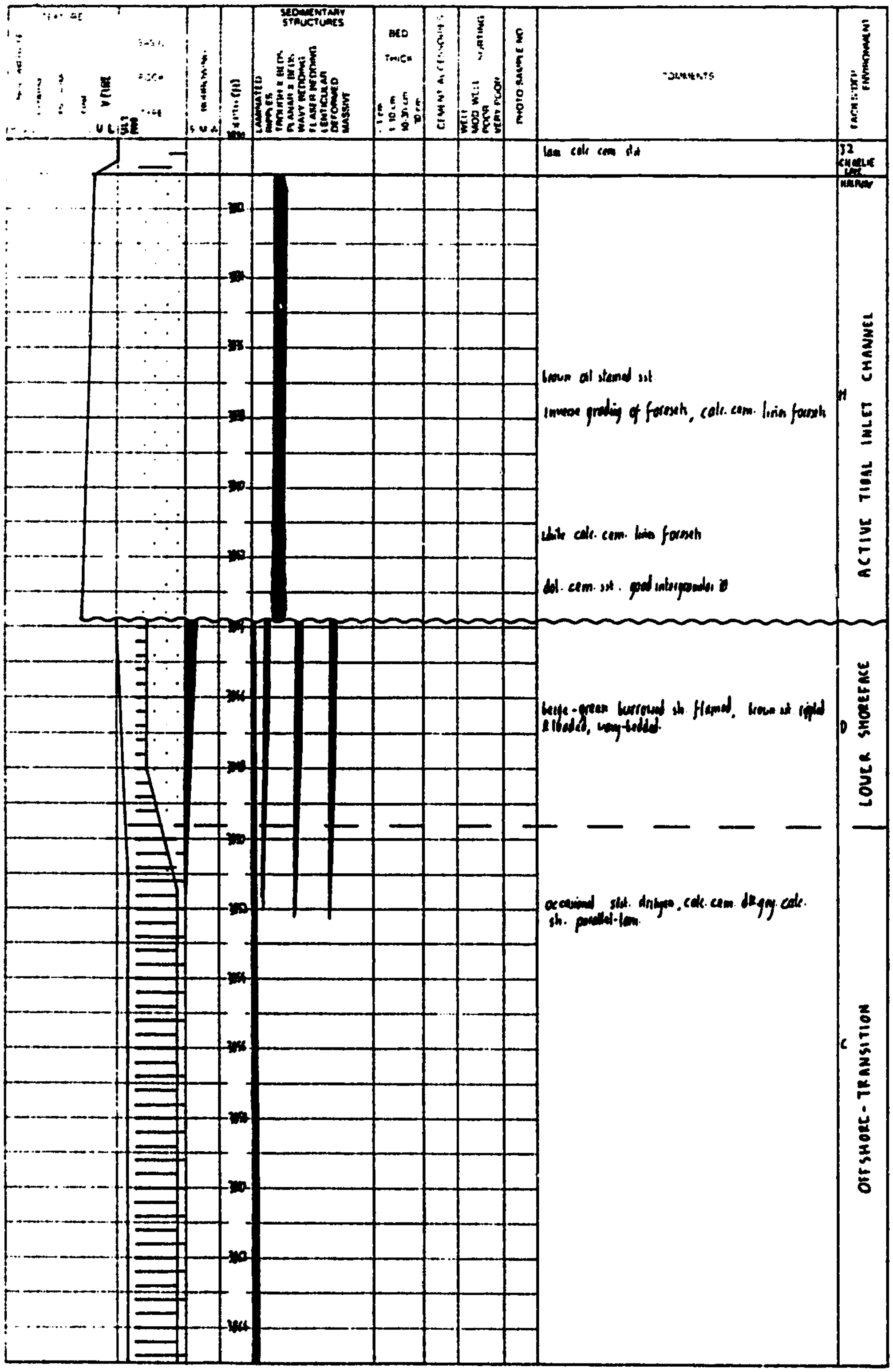

lam. calc. cem. sts

brown oil stained sst.

inverse grading of forsets, calc. cem. lmin forsets

white calc. cem. lmin forsets

dol. cem. sst. good intergranular Ø

beige-green burrowed sh. flamed, brown st. rippled & bedded, wavy-bedded.

occasional slst. dringen, calc. cem. dk gry calc. sh. parallel-lam.

WELL NAME UNION H B PEEJAY a-23-E FORMATION HALFWAY-CHARLIE LAKE DATE 4/07/91

LOCATION a-23-E/94-A-16 CORE INTERVAL KB 2363ft

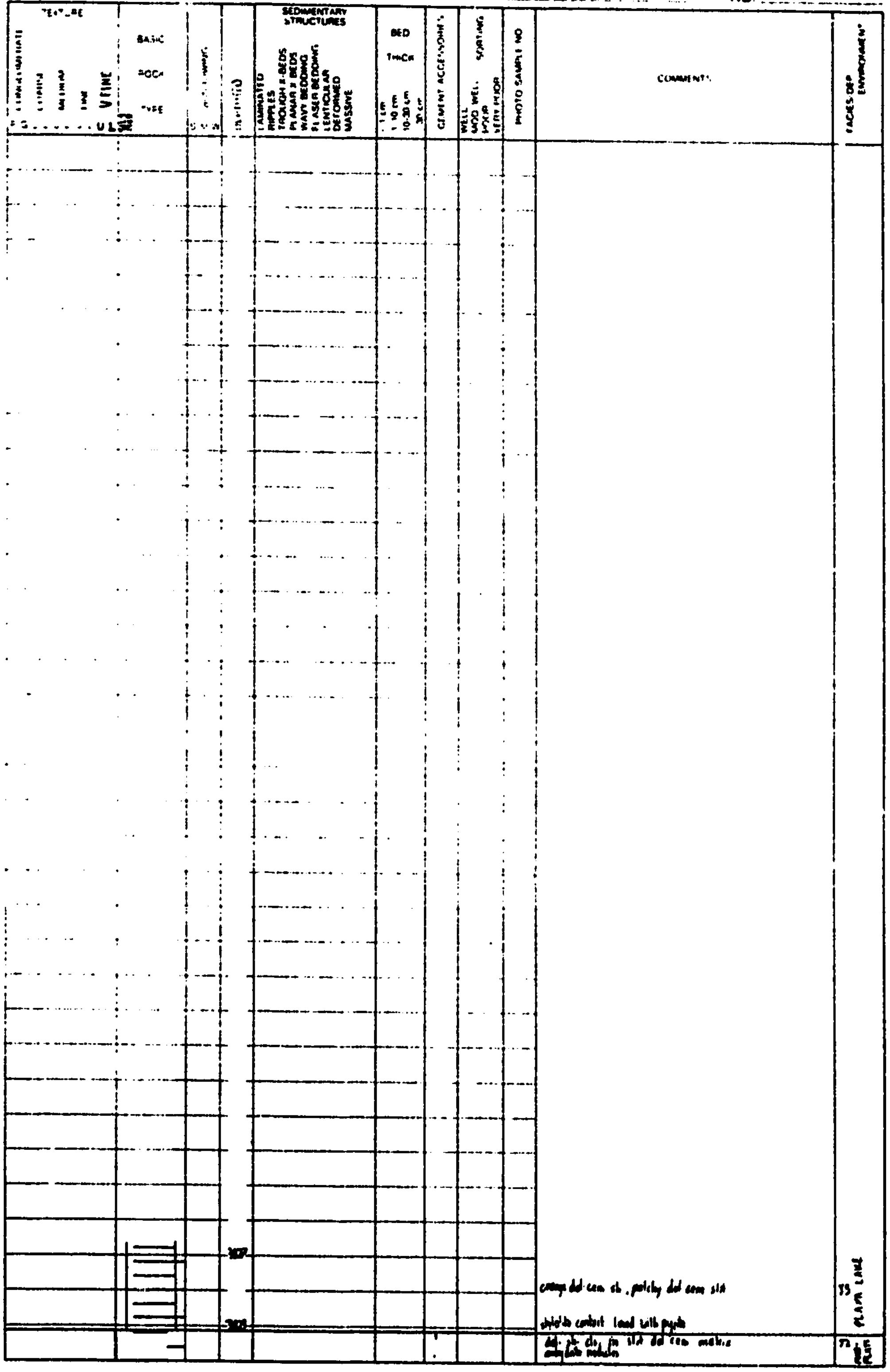

conglo dol cem sh , patchy dol cem slst

sh/slst contact lined with pyrite

dol. sh. cls, fn slst dol cem matrix
anhydrite nodules

33 PLAYA LAKE

72 [illegible] FLAT

WELL NAME: UNION H B EAST PEEJAY d-23-E FORMATION: HALFWAY-CHARLIE LAKE DATE: 17/08/90

LOCATION: d-023-E/94-A-16 CORE INTERVAL: KB: 2357ft

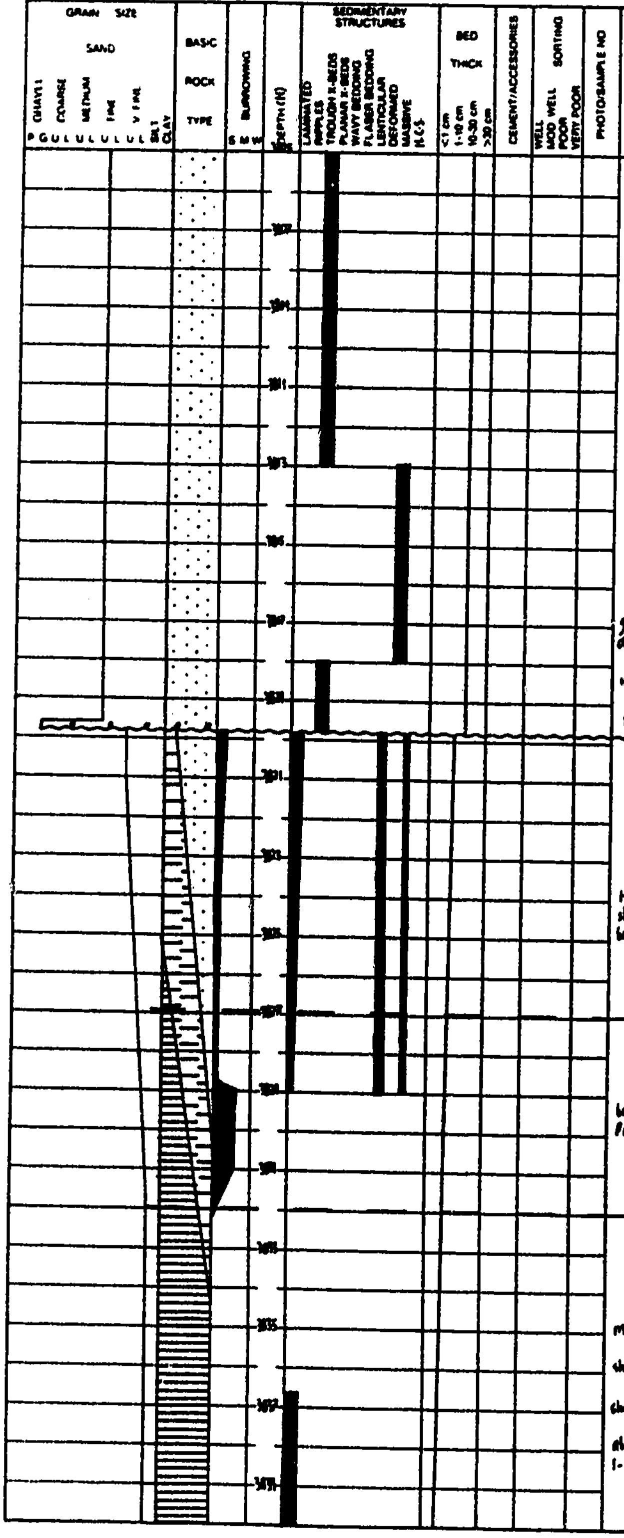

COMMENT:

excellent intergranular ø, oil staining

good intergranular ø, scattered pyrite nodules & calc nodules
oil stained, sub-rded dol. cem. brown

low-angle trough X-bedding

[illegible] of sh. & ch. [illegible]

sst. becomes thinner, sh. thicker more bioturbation

H.C.S. alternation of sst. & sh. lam., load & flame
structures at base of sst. no syneresis cracks
beige sh. dol. cem. & burrowed

beige lam. sh. and coarse brown slt, disrupted by
Palaeophycus & Planolites burrows

microfaulting

shale with slst. 'pinstripe' stringers

shale is dk. gry.

abrupt based, parallel-lam., normally graded slt bds,
1-2cm thick, spaced 12cm apart

FACIES/DEP ENVIRONMENT

H ACTIVE TIDAL INLET CHANNEL

D LOWER SHOREFACE

C OFFSHORE-TRANSITION

B OFFSHORE

WELL NAME: Union H 3 East Feejay d-23-E
FORMATION: Halfway-Charlie Lake
DATE: 17/08/90
LOCATION: d-023-E/94-A-16
CORE INTERVAL:
KB: 2357ft

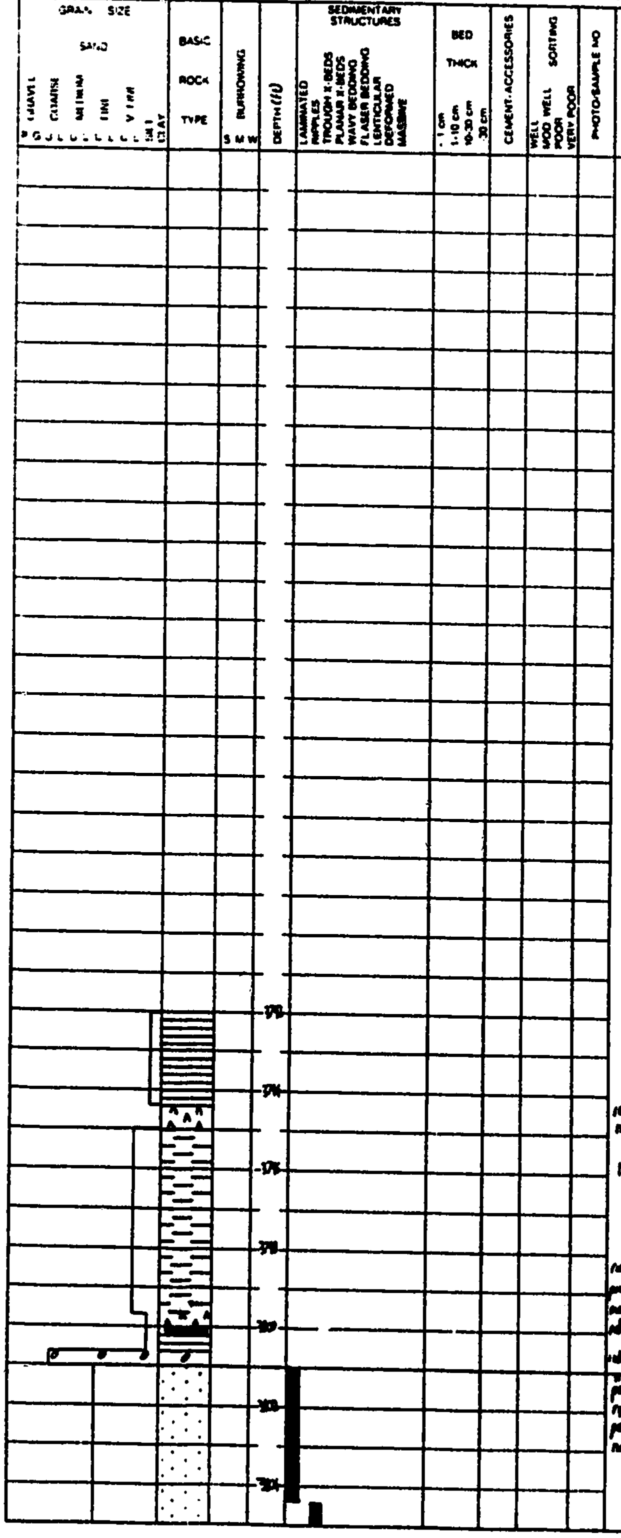

COMMENTS

red dol. silty-shale, anhydrite nodules, & sh. beige (cream) cls & much pyrite - massive anhydrite

tabular rip-up cls. of slst. & sh, red & beige, [illegible]

red dol. silt with anhydrite nodules, [illegible] lam
parallel-lam. red silt & beige sh. with cls. & anhydrite nodules
massive anhydrite with clearly associated pyrite
red dol. com. sh. with anhydrite nodules

red-dol. slst. cls in green-beige sh. anhydrite nodules
[illegible]
parallel-lam. [illegible] grading up to C.L. scale ripples truncated by parallel-lam.
parallel-lam with lithoclasts of slt. & sh
no oil staining, good intergranular ∅

FACIES/DEP ENVIRONMENT

PLAYA LAKE MARGIN/MUDFLATS

T2

CHARLIE LAKE

HALFWAY

d

WELL NAME: UNION H & E PEEJAY d.24.E

FORMATION: HALFWAY-CHARLIE LAKE

DATE: 4/07/91

LOCATION: d-024-E/94-A-16

CORE INTERVAL:

KB: 2282.1 ft

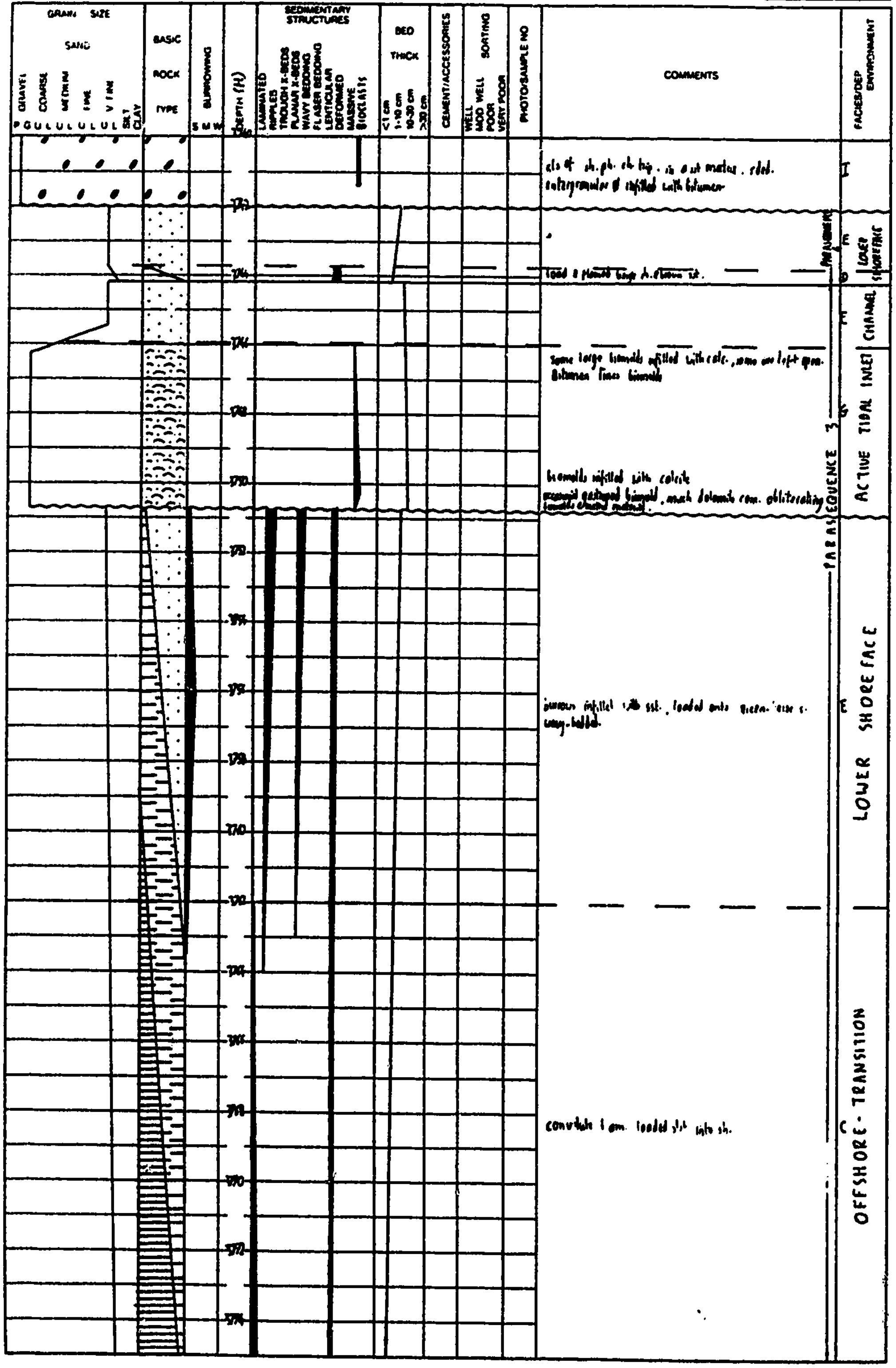

cls of sh. pb. ch tip. in a ut matrix. rdd. intergranular Ø infilled with bitumen

Load & flamed [illegible] st.

Some large biomolds infilled with calc., some are left open. Bitumen lines biomolds

biomolds infilled with calcite
[illegible] [illegible] biomold, much dolomite cem. obliterating biomolds [illegible] material.

burrows infilled with sst., loaded onto [illegible] s. wavy-bedded.

convolute lam. loaded silt into sh.

WELL NAME: UNION HB E PEEJAY d-24-E FORMATION: HALFWAY-CHARLIE LAKE DATE: 4/07/91

LOCATION: d-024-E/94-A-16 CORE INTERVAL: KB: 2282 ft

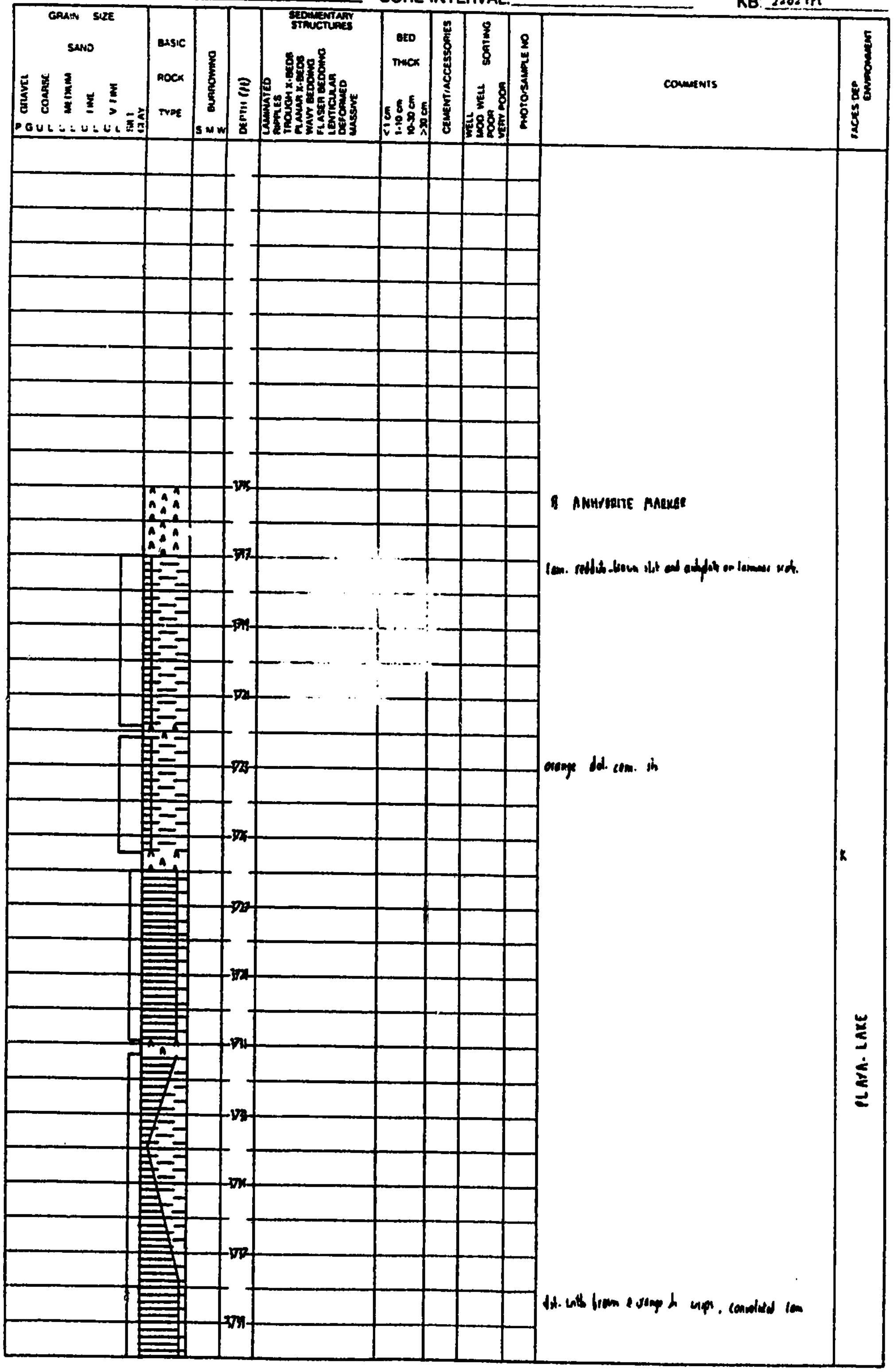

B ANHYDRITE MARKER

lam. reddish-brown silt and anhydrite or laminae sch.

orange dol. com. sh

dol. with brown & orange [illegible] ups, convoluted lam

WELL NAME: UNION HB E PEEJAY d-25-E

FORMATION: HALFWAY-CHARLIE LAKE

DATE: 4/07/91

LOCATION: d-025-E/94-A-16

CORE INTERVAL:

KB: 2358.9ft

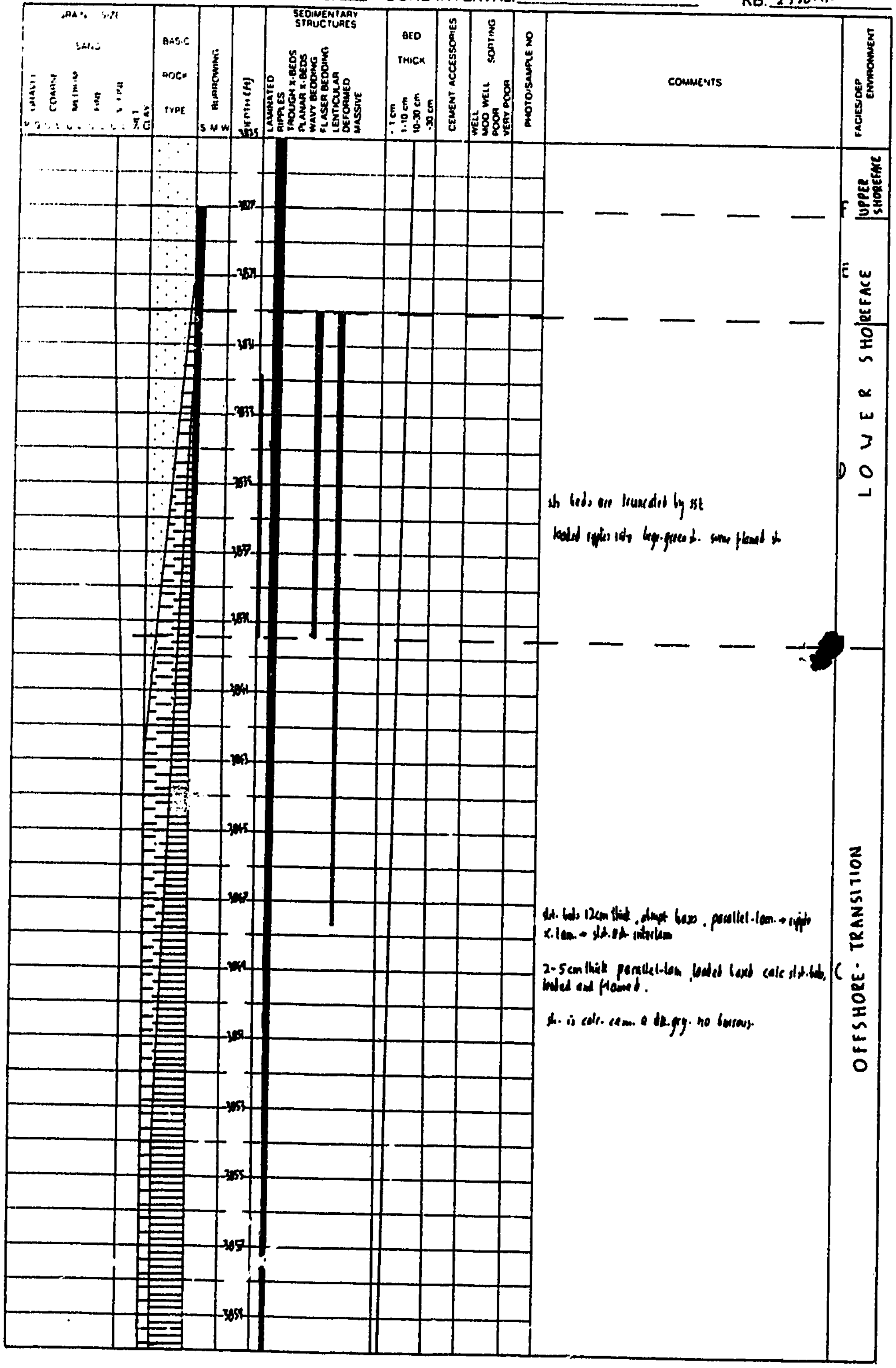

sh beds are truncated by sst

loaded ripples into lrg-grained sh. some flamed sh

slt. beds 12cm thick, abrupt bases, parallel-lam. + ripple x-lam. + slt.sh interlam

2-5cm thick parallel-lam, loaded based calc slst.beds, loaded and flamed.

sh. is calc. cem. & dk.gry. no burrows.

WELL NAME: UNION HB E PEEJAY d-25-E

FORMATION HALFWAY-CHARLIE LAKE

DATE 4/07/91

LOCATION: d-025-E/94-A-16

CORE INTERVAL

KB: 2358.9ft

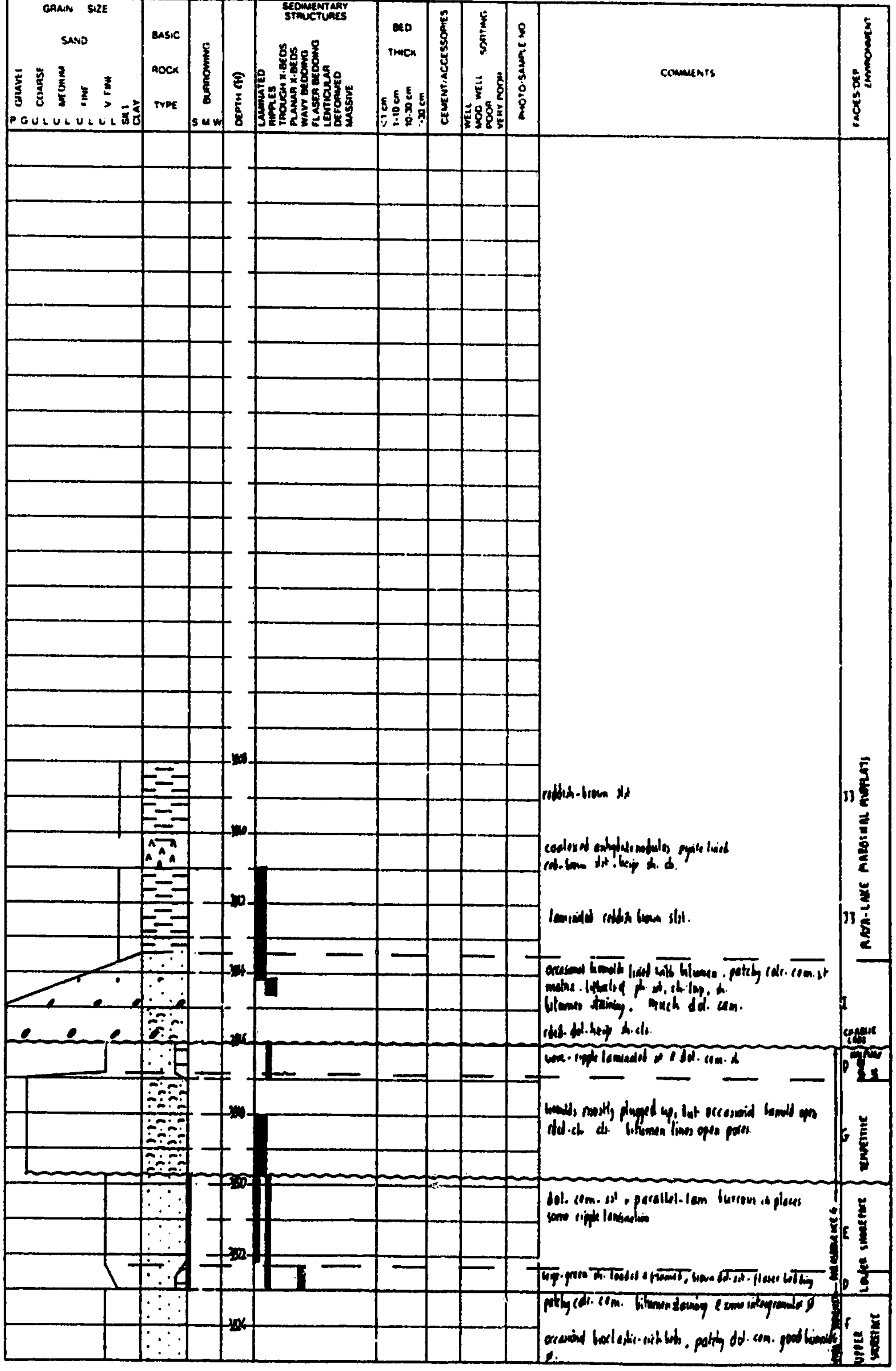

reddish-brown slt

coalesced anhydrite nodules, pyrite lined
red-brown slt. brecc sh. cls.

laminated reddish brown slst.

occasional burrows lined with bitumen. patchy calc. cem. st
matrix. lithoclast ph. st, sh-lmp, sh.
bitumen staining. much dol. cem.

reddish dol. brecc sh. cls.

wave-ripple laminated vf f dol. cem. ss

burrows mostly plugged up, but occasional burrow open
rdel-ch cls. bitumen lines open pores

dol. cem. sst. parallel-lam burrows in places
some ripple lamination

large green sh. loaded & flamed, brown dol. sst. flaser bedding

patchy calc. cem. bitumen staining & some intergranular ø

occasional bioclastic-rich beds, patchy dol. cem. good bioclastic
ø.

WELL NAME CIGOL MOBIL PEEJAY

FORMATION: HALFWAY- CHARLIE LAKE

DATE: 30/07/90

LOCATION d-026-E/94-A-16

CORE INTERVAL:

KB: 2354ft

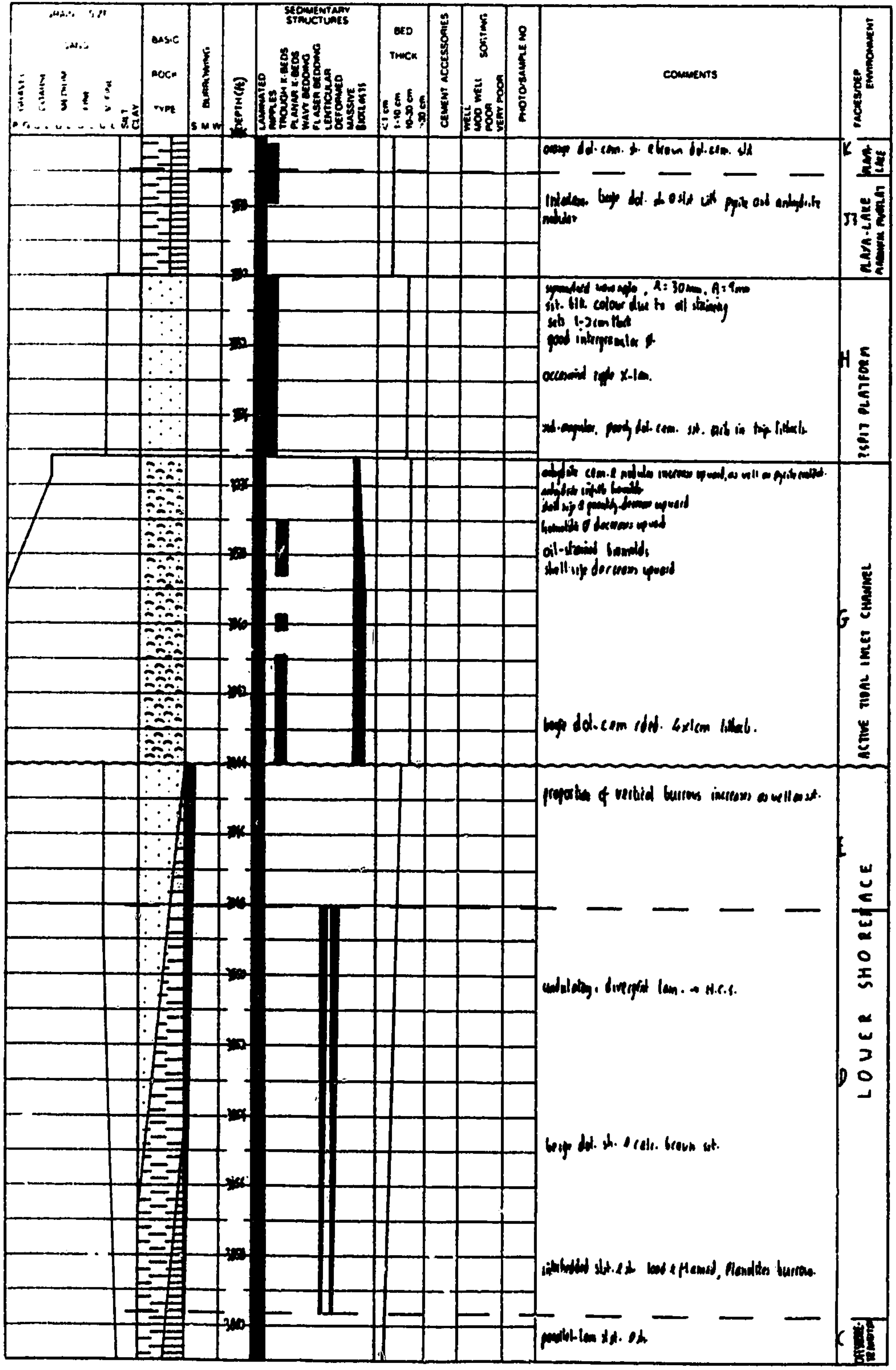

orange dol-cem. sh. & brown dol-cem. slt

Interlam. beige dol. sh. & slt with pyrite and anhydrite nodules

symmetrical wave ripple, A: 30mm, A: 9mm
slt. blk. colour due to oil staining
sets 1-2cm thick
good intergranular ϕ

occasional ripple X-lam.

sub-angular, poorly dol-cem. slt. rich in rip-up lithocl.

anhydrite cem. & nodules increase upward, as well as pyrite nodules.
anhydrite infills burrows
shell rip & peloids decrease upward
bioclasts & decrease upward
oil-stained bioclasts
shell rip decrease upward

beige dol.cem rdd. 4x1cm lithocl.

proportion of vertical burrows increases as well as st.

undulating, divergent lam. → H.C.S.

beige dol. sh. & calc. brown slt.

interbedded slt. & sh. load & flamed, Planolites burrows.

parallel-lam slt. & sh.

WELL NAME: F.P.C WHITEHALL PEEJAY 6-27-E FORMATION: HALFWAY-CHARLIE LAKE DATE: 7.07.90

LOCATION: c-027-E/94-A-16 CORE INTERVAL: KB 2357ft

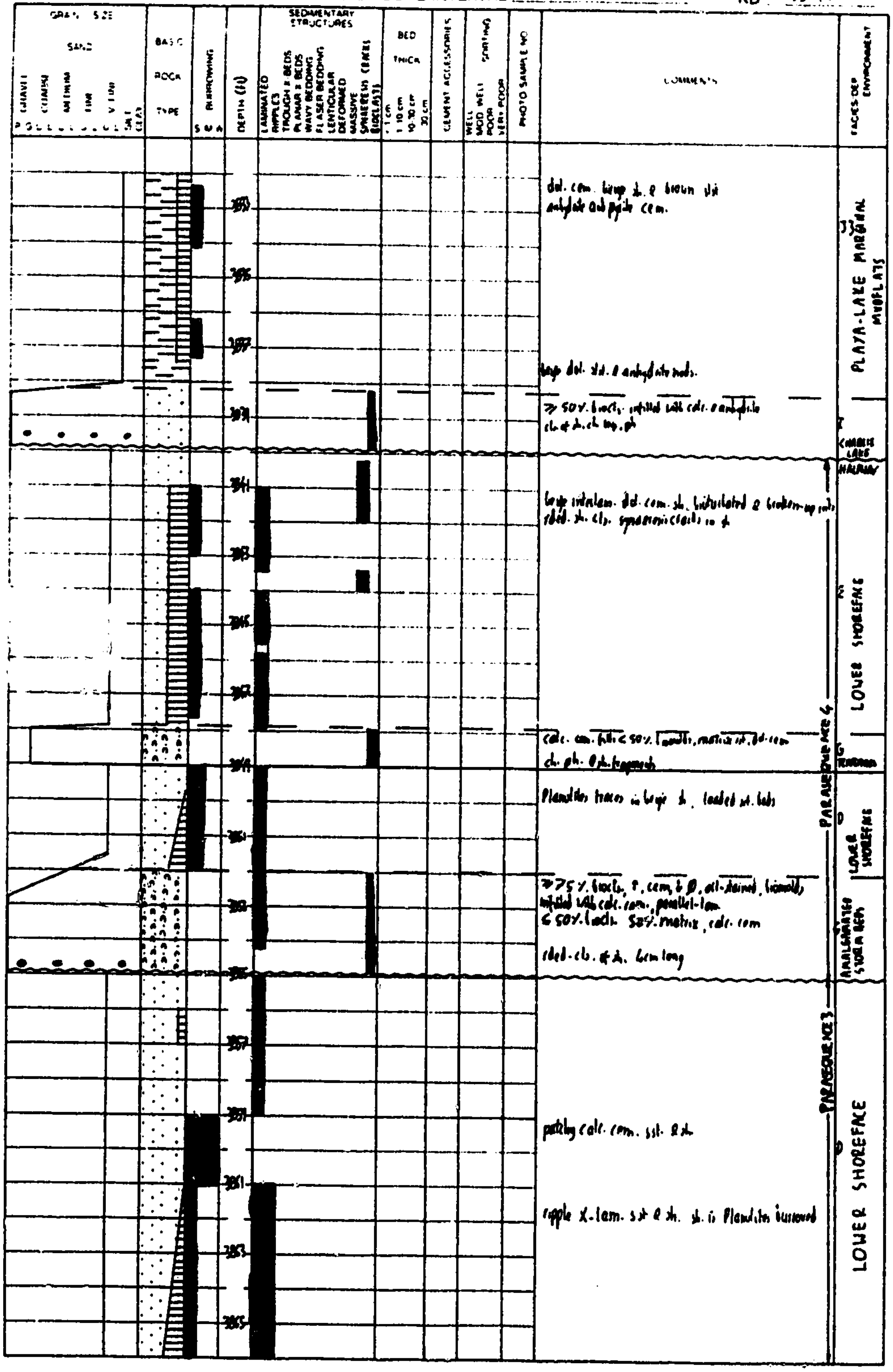

WELL NAME: SINCLAIR ET AL PEEJAY d-29-E
FORMATION: HALFWAY-CHARLIE LAKE
DATE: 4/07/90
LOCATION: d-029-E/94-A-16
CORE INTERVAL:
KB: 2356ft

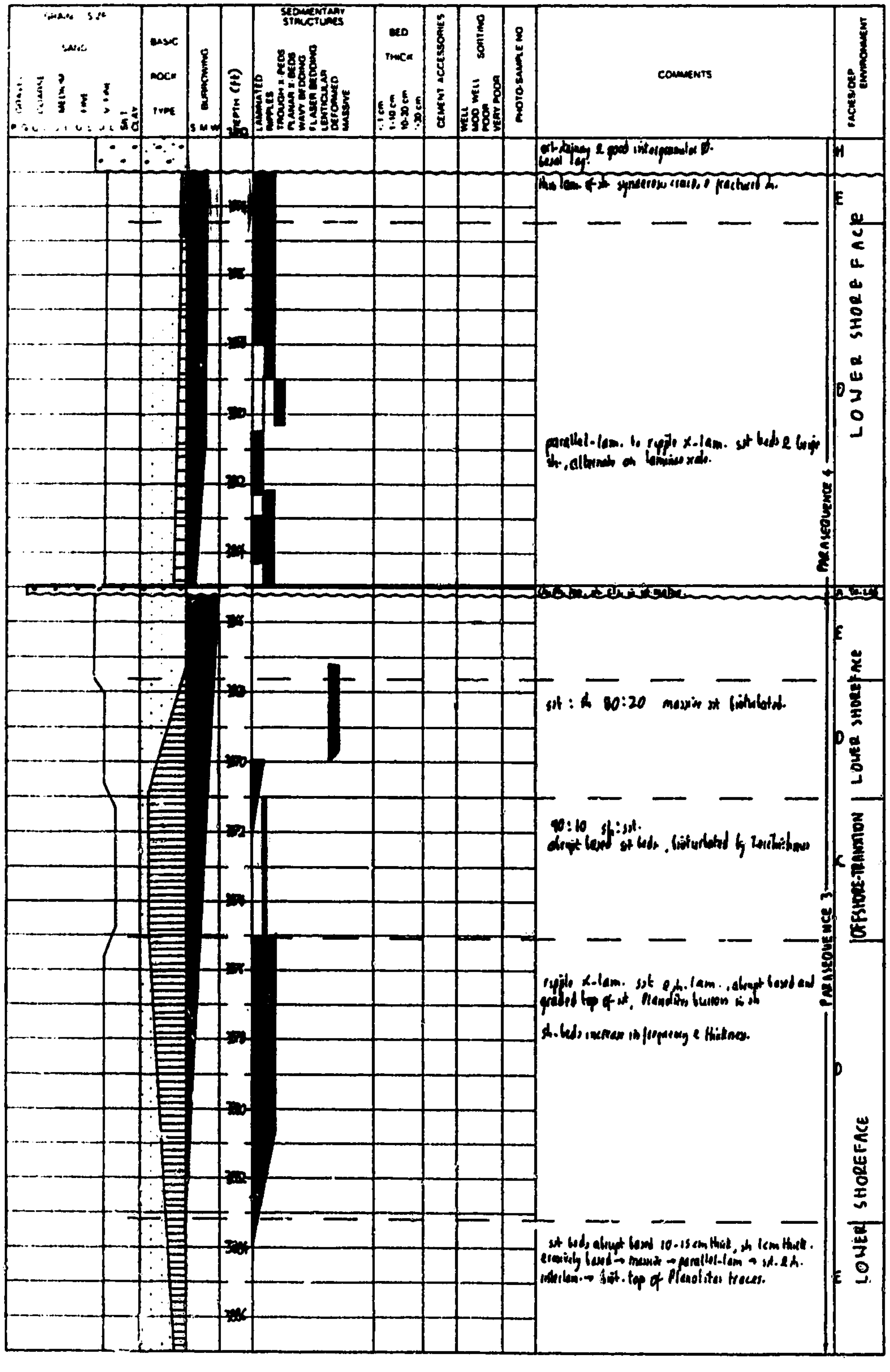

oil-staining & good intergranular Ø. based log.

thin lam. of sh. syneresis crack, & fractured sh.

parallel-lam. to ripple x-lam. slt beds & large sh., alternate on laminae scale.

[illegible]

slt : sh 80:20 massive slt bioturbated.

90:10 sh:slt.
abrupt based slt beds, bioturbated by Teichichnus

ripple x-lam. slt & sh. lam., abrupt based and graded top of slt, Planolites burrows in sh

sh. beds increase in frequency & thickness.

slt beds abrupt based 10-15 cm thick, sh 1cm thick. erosively based → massive → parallel-lam → slt. & sh. interlam. → biot. top of Planolites traces.

WELL NAME SINCLAIR ET AL PEESAY d-29-E

FORMATION HALFWAY-CHARLIE LAKE

DATE 4/07/90

LOCATION d-029-E/94-A-16

CORE INTERVAL

KB 2356ft

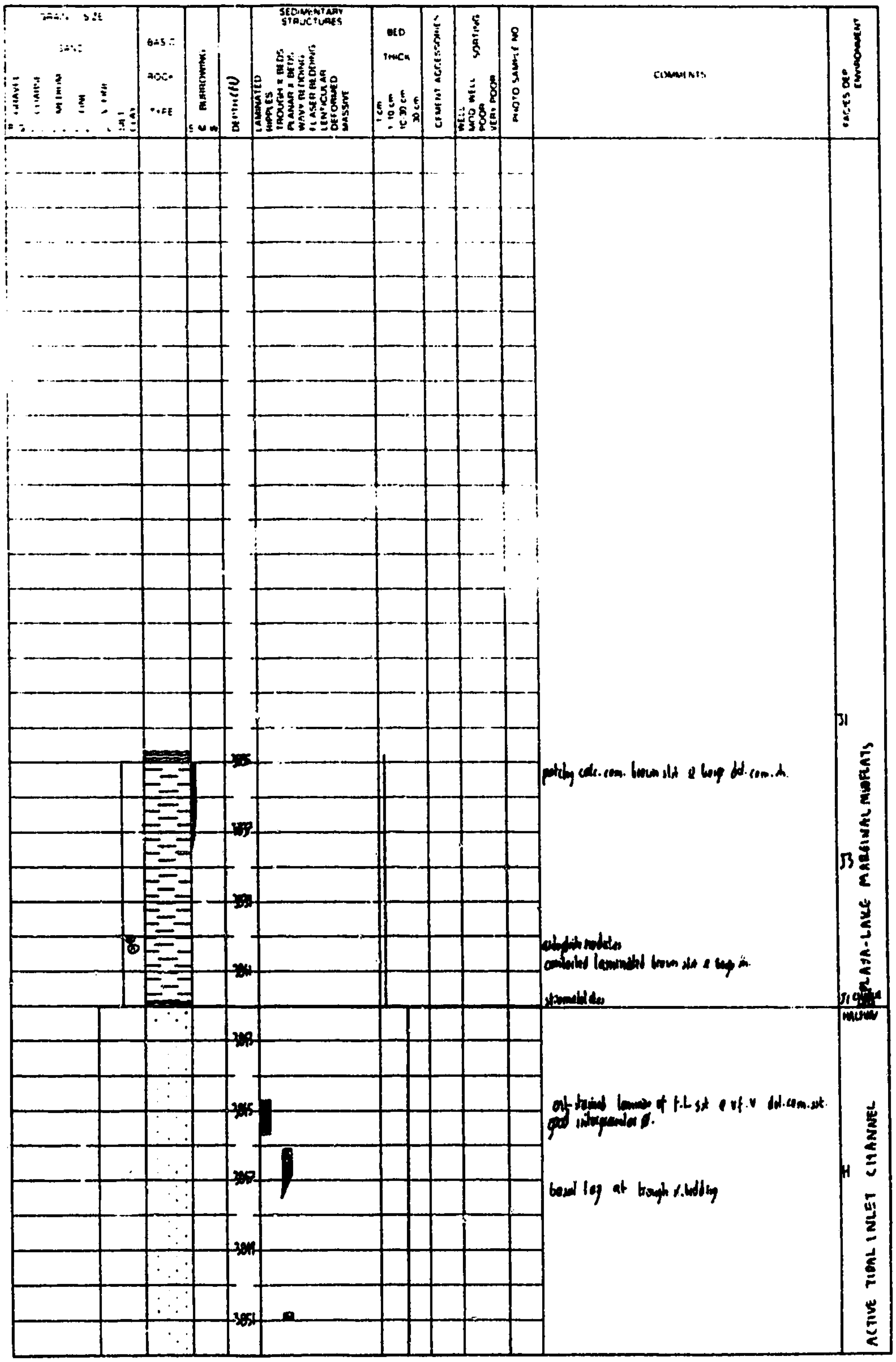

patchy calc.cem. brown slst & beige dol.cem.sh.

anhydrite nodules

contorted laminated brown slst & beige sh.

stromatolites

oil-stained laminae of f.-L. sst & vf.-v. dol.cem.sst. good intergranular ø.

basal lag at trough x.bedding

WELL NAME PATHFINDER E PEEJAY FORMATION: HALFWAY-CHARLIE LAKE DATE: 19/06/90

LOCATION d-033-E/94-A-16 CORE INTERVAL: KB: 2353ft

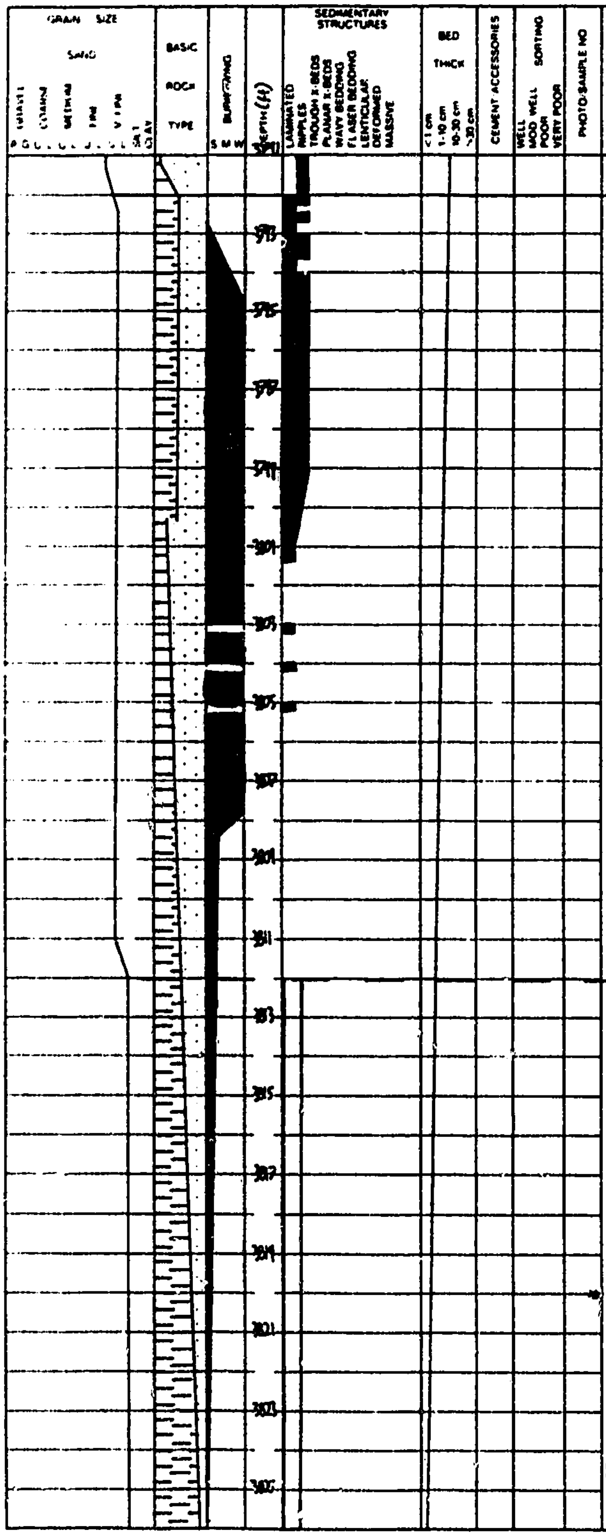

COMMENTS

FACIES/DEP ENVIRONMENT

E

7cm thick abrupt based at parallel-lam.

wavy-bedded burrowed sh. & parallel-lam to ripple x-ripple lam. st.

D LOWER SHOREFACE

sst: slst 70:30

sharp based at 1cm thick, - microfaulting and contorted bedding.

Planolites burrow sandfilled.

sst: slst 10:90 sst ≤1cm thick & 10cm apart horizontal burrows in shale. abrupt based & normally graded.
microfaulting.

C OFFSHORE-TRANSITION

WELL NAME: PATHFINDER E PEEJAY
FORMATION: HALFWAY-CHARLIE LAKE
DATE: 19/06/90
LOCATION: d-033-E/94-A-16
CORE INTERVAL:
KB: 2353ft

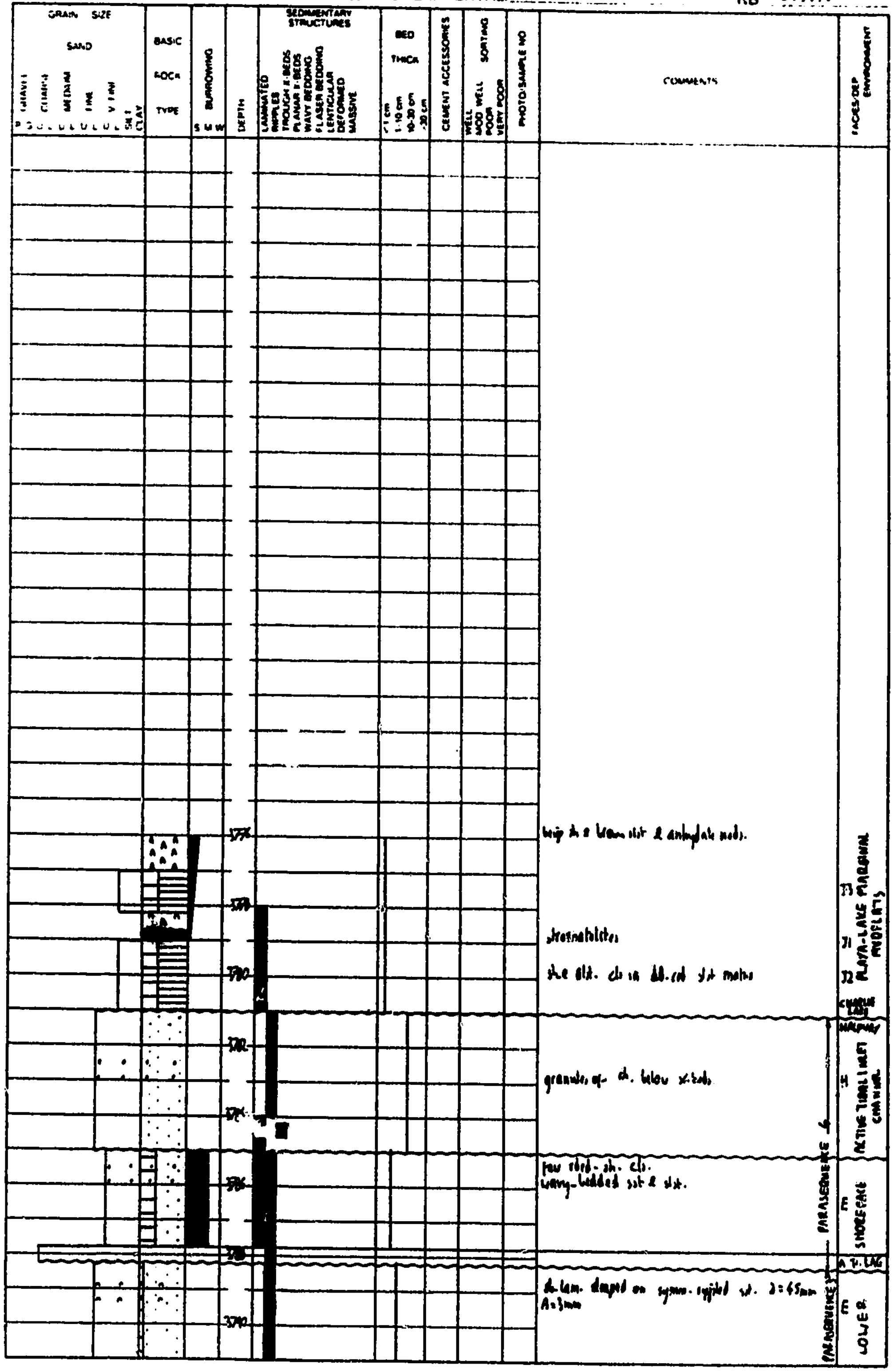

beige to a brown silt & anhydrite nods.

stromatolites

sh. clst. cl. in bl.-red slt matrix

granules of ch. below x-beds

few rbrd.-sh. cls.
wavy-bedded sst & slt.

sh. lam. draped on symm.-rippled sst. λ=65mm
A=3mm

WELL NAME CIGOL MOBIL E PEEJAY d-34-E FORMATION: HALFWAY-CHARLIE LAKE DATE: 5/07/91

LOCATION: d-034-E/94-A-16 CORE INTERVAL: ______ KB: 2367ft

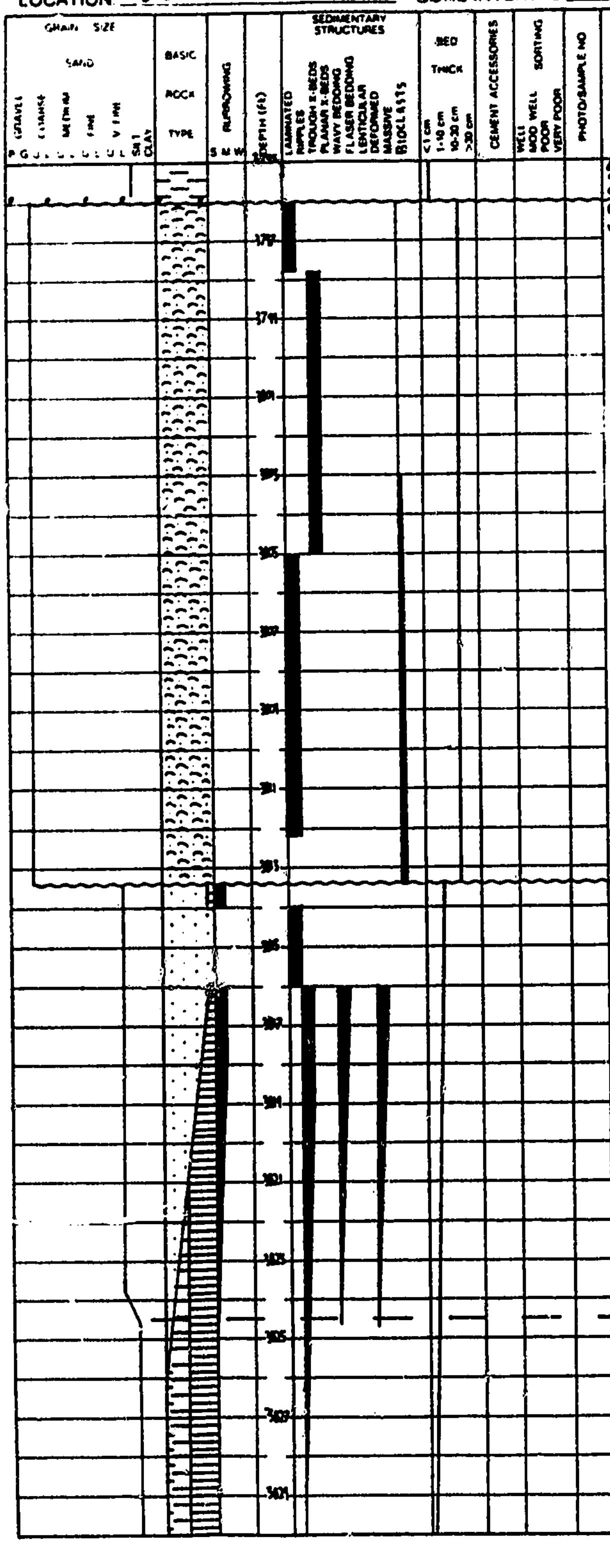

COMMENTS

dol. cem. slst. with replacive anhydrite nodules
[illegible] of exposure with open burrows, closed due to anhydrite cem. & bitumen lined
cls. angular - sub-angular bioclasts set in dol. [illegible] [illegible]

[illegible] is low, cem complete, anhydrite replacive nodules common
very abundant dol. cem. Abundant cl. gravel, angular & fractured.

some burrows infilled with anhydrite
does. [illegible] represent [illegible] dol. [illegible] bed with bitumen.

rdd. ch. cls. pebble/granule sized.

stylolites [illegible] dol. cem. & some open vertical
microfractures [illegible], some infilled with calc. cem.
patchy [illegible] replaces everything. Some burrows infilled
with calc. [illegible] filled with bitumen.
some vuggy [illegible] develop in calc. nodules

H.C.S.

laminae warped upward due to dewatering

syneresis cracks in sh.

beige-green dol. cem. burrowed sh. infilled with sst.
loading of brown sst. beds into sh.

some S.S.D. in form of convolution of laminae
Sharp based slst. parallel-lam. & rippled.

FACIES/DEP ENVIRONMENT

CHARLIE LAKE

HALFWAY

WELL NAME: CIGOL MOBIL E PEEJAY d-34-E
FORMATION: HALFWAY-CHARLIE LAKE
DATE 5/07/91
LOCATION: d-034-E/94-A-16
CORE INTERVAL:
KB. 2367ft

GRAIN SIZE SAND GRAVEL COARSE MEDIUM FINE V FINE SILT CLAY P G U L U L U L U L U L	BASIC ROCK TYPE	BURROWING S M W	DEPTH (ft)	SEDIMENTARY STRUCTURES LAMINATED RIPPLES TROUGH X-BEDS PLANAR X-BEDS WAVY BEDDING FLASER BEDDING LENTICULAR DEFORMED MASSIVE	BED THICK <1 cm 1-10 cm 10-30 cm >30 cm	CEMENT/ACCESSORIES	SORTING WELL MOD WELL POOR VERY POOR	PHOTO/SAMPLE NO	COMMENTS	FACIES/DEP ENVIRONMENT
									laminated dk. brown slst, irregular orange	
			3792							
									coalesced anhydrite nodules orange-yellow sh abundant, dk. brown slst irregular mottled appearance.	K PLAYA LAKE
			3794							
			3796							

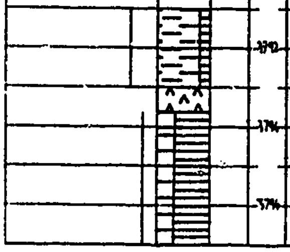

WELL NAME CIGOL MOBIL PEEJAY d-35-E

FORMATION: HALFWAY-CHARLIE LAKE

DATE: 1/08/90

LOCATION d-035-E/94-A-16

CORE INTERVAL:

KB: 2368ft

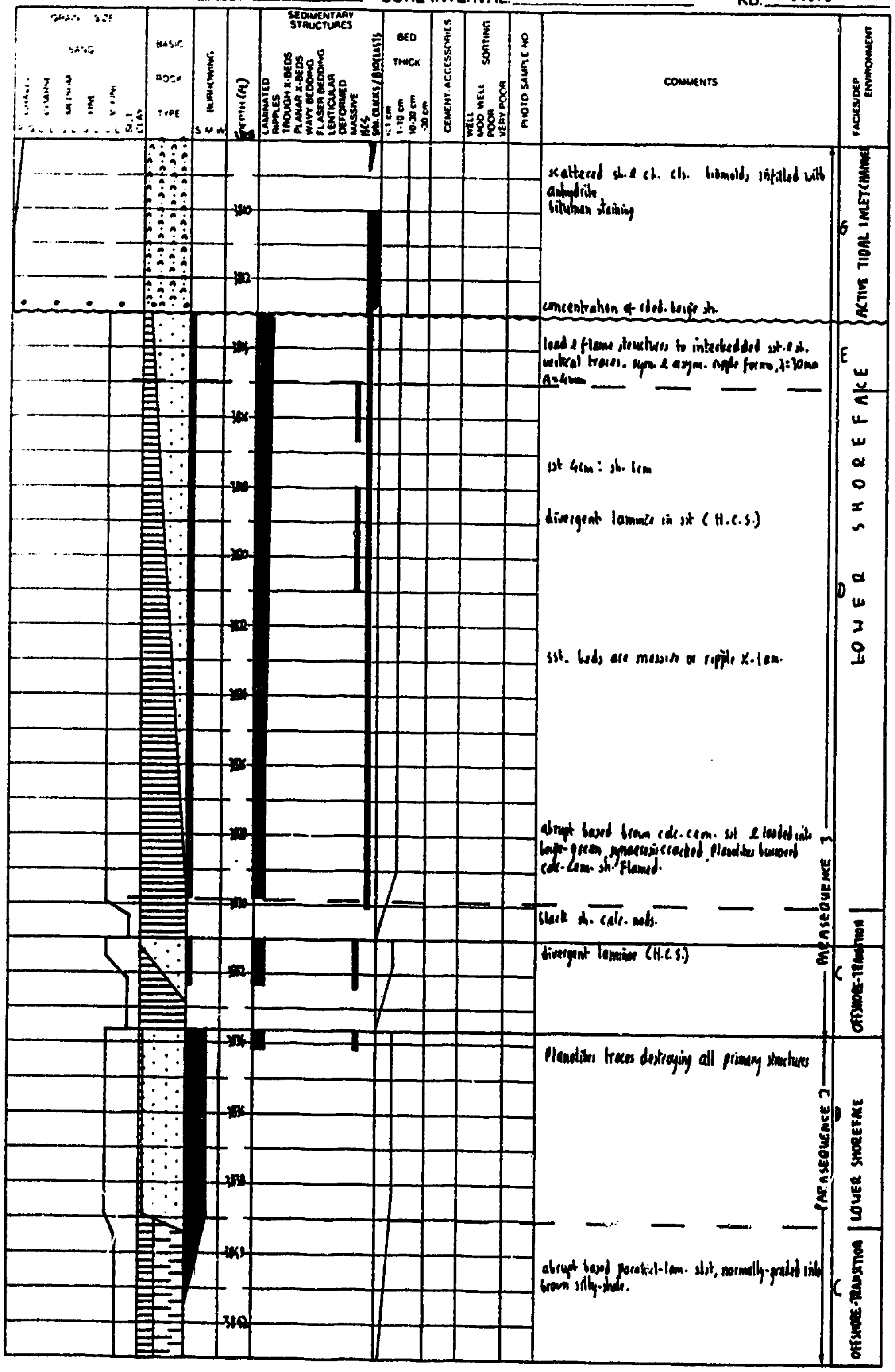

scattered sh. & cl. cls. biomolds infilled with anhydrite
bitumen staining

concentration of rlod. beige sh.

load & flame structures to interbedded sst. & sh.
vertical traces. sym. & asym. ripple forms, λ=30mm A=4mm

sst 4cm : sh. 1cm

divergent laminae in sst (H.C.S.)

sst. beds are massive or ripple X-lam.

abrupt based brown calc. cem. sst & loaded into beige-green syneresis cracked Planolites burrowed calc. cem. sh. Flamed.

black sh. calc. nods.

divergent laminae (H.C.S.)

Planolites traces destroying all primary structures

abrupt based parallel-lam. slst, normally-graded into brown silty-shale.

WELL NAME: CIGOL MOBIL PEEJAY d-35-E
FORMATION: HALFWAY-CHARLIE LAKE
DATE: 1/08/90
LOCATION: d-035-E/94-A-16
CORE INTERVAL:
KB: 2368ft

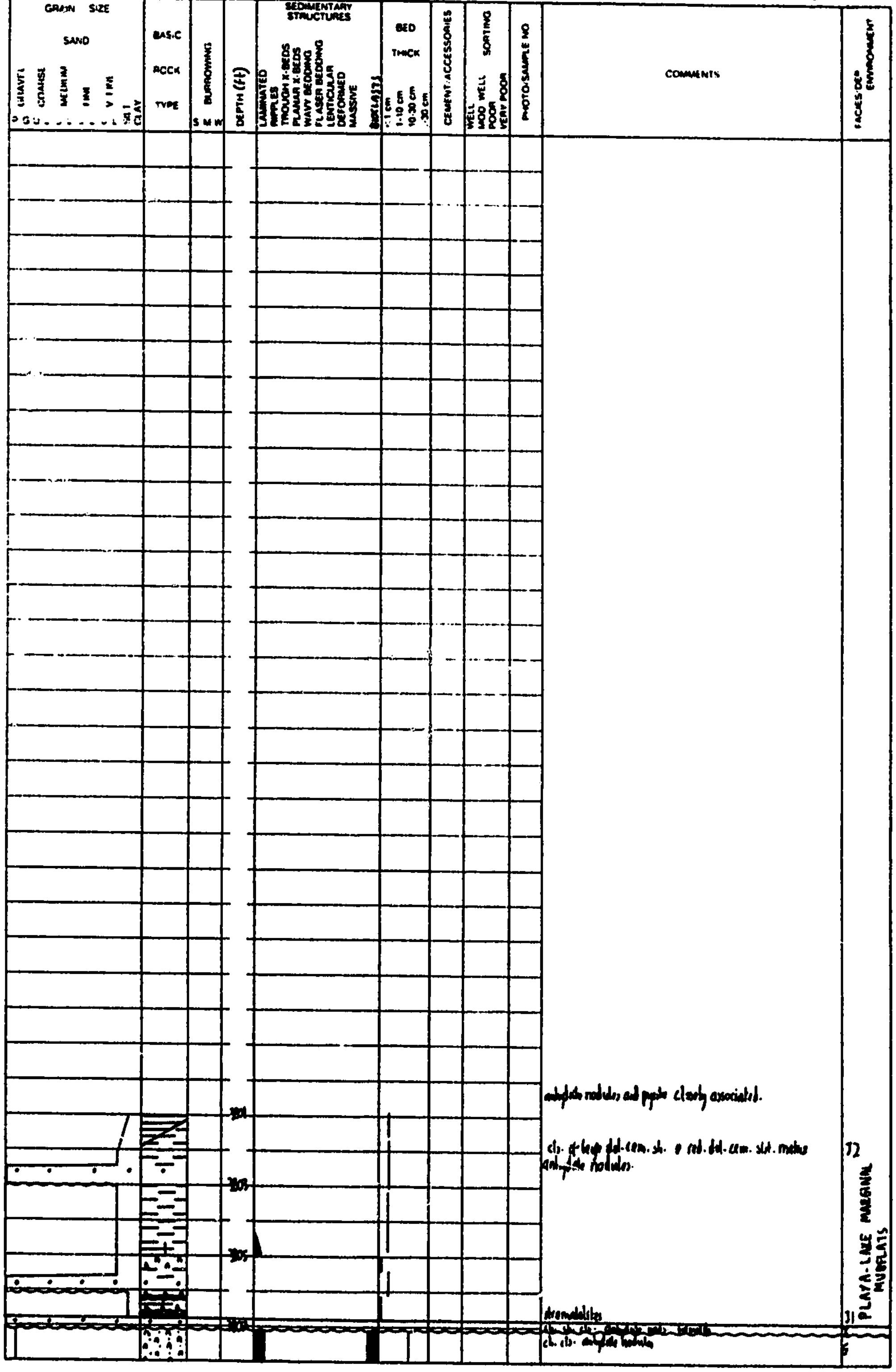

anhydrite nodules and pyrite clearly associated.

cl3. of large dol-cem. sh. & red. dol-cem. slt. matrix anhydrite nodules.

[illegible]

cl3. sh. cl3. anhydrite pods. [illegible]

cl. cl3. anhydrite nodules

32

31 PLAYA-LAKE MARGINAL MUDFLATS

6

WELL NAME: CIGOL MOBIL PEEJAY d-36-E
FORMATION: HALFWAY - CHARLIE LAKE
DATE: 30/07/90
LOCATION: d-036-E/94-A-16
CORE INTERVAL:
KB: 2367ft

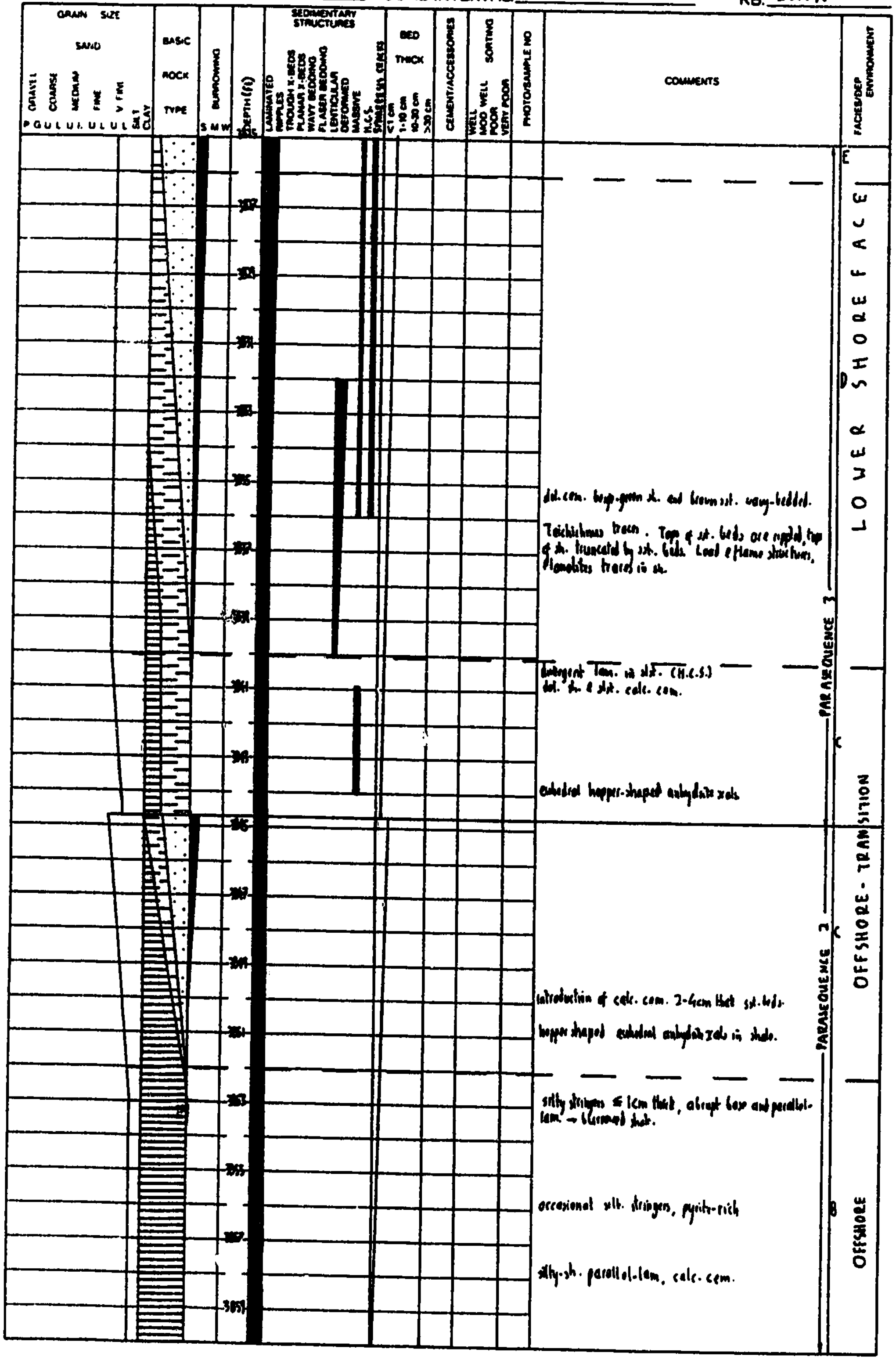

dol.cem. beige-green sh. and brown slt. wavy-bedded.

Teichichnus traces. Tops of slt. beds are rippled, tops of sh. truncated by slt. beds. Load & flame structures, Planolites traces in sh.

divergent lam. in slt. (H.C.S.)
dol. sh. & slt. calc. cem.

euhedral hopper-shaped anhydrite xals

introduction of calc. cem. 2-4cm thick slt. beds.

hopper shaped euhedral anhydrite xals in shale.

silty stringers ≤ 1cm thick, abrupt base and parallel-lam. → bioturbated shale.

occasional slt. stringers, pyrite-rich

silty-sh. parallel-lam, calc. cem.

WELL NAME: CIGOL MOBIL PEEJAY d-36-E FORMATION: HALFWAY-CHARLIE LAKE DATE: 30/07/90

LOCATION: d-036-E/94-A-16 CORE INTERVAL: KB: 2367ft

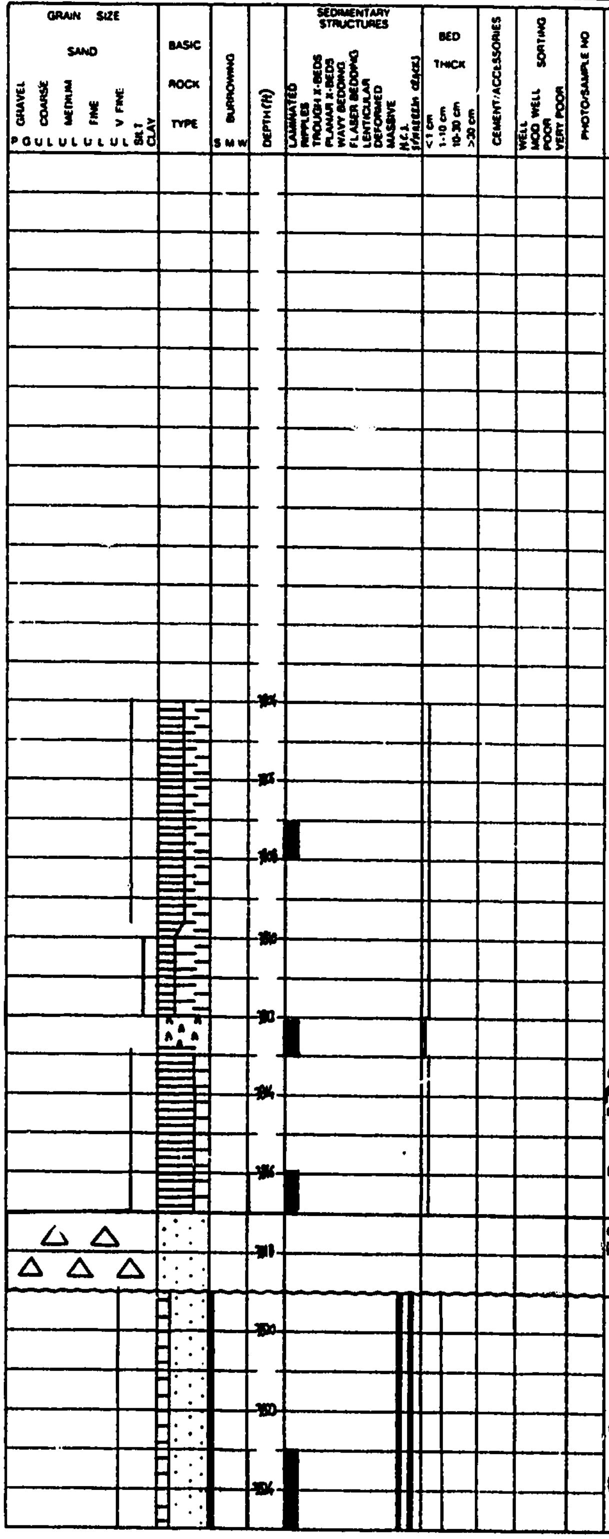

COMMENTS

interlam. slt. & sh., some broken up into cls

slt lam. loaded into sh.
anhydrite cem.

lam. destroyed

dol.-cem. brown slt & orange sh. with anhydrite nods
pyrite cem. in both.
much normal microfaulting
slumping & overstepped lam. sh. cls

red dol.-cem. slst. & sh. cls

angular frags of dol.-cem. beige sh. with calc. cem. in matrix. Ch. big. pl. [illegible], & breccia. Calc. cem. nodules coalesced.

dol. cem. beige sh. contains burrows & syneresis cracks and are truncated by st. beds. Sh. is massive with calcite nodules common & increase upward.

wk. parallel-lam. to massive.

burrowed beige-brown dol. cem. sst. & burrowed (Planolites) syneresis cracked shale.

FACIES/DEP. ENVIRONMENT

J3

PLAYA-LAKE MARGINAL MUDFLATS

J2

I

CHARLIE LAKE

E

LOWER SHOREFACE

WELL NAME: PACIFIC ET AL PEEJAY 6-38-E FORMATION: HALFWAY-CHARLIE LAKE DATE: 17/08/90

LOCATION: 6-038-E/94-A-16 CORE INTERVAL: KB: 2388.7ft

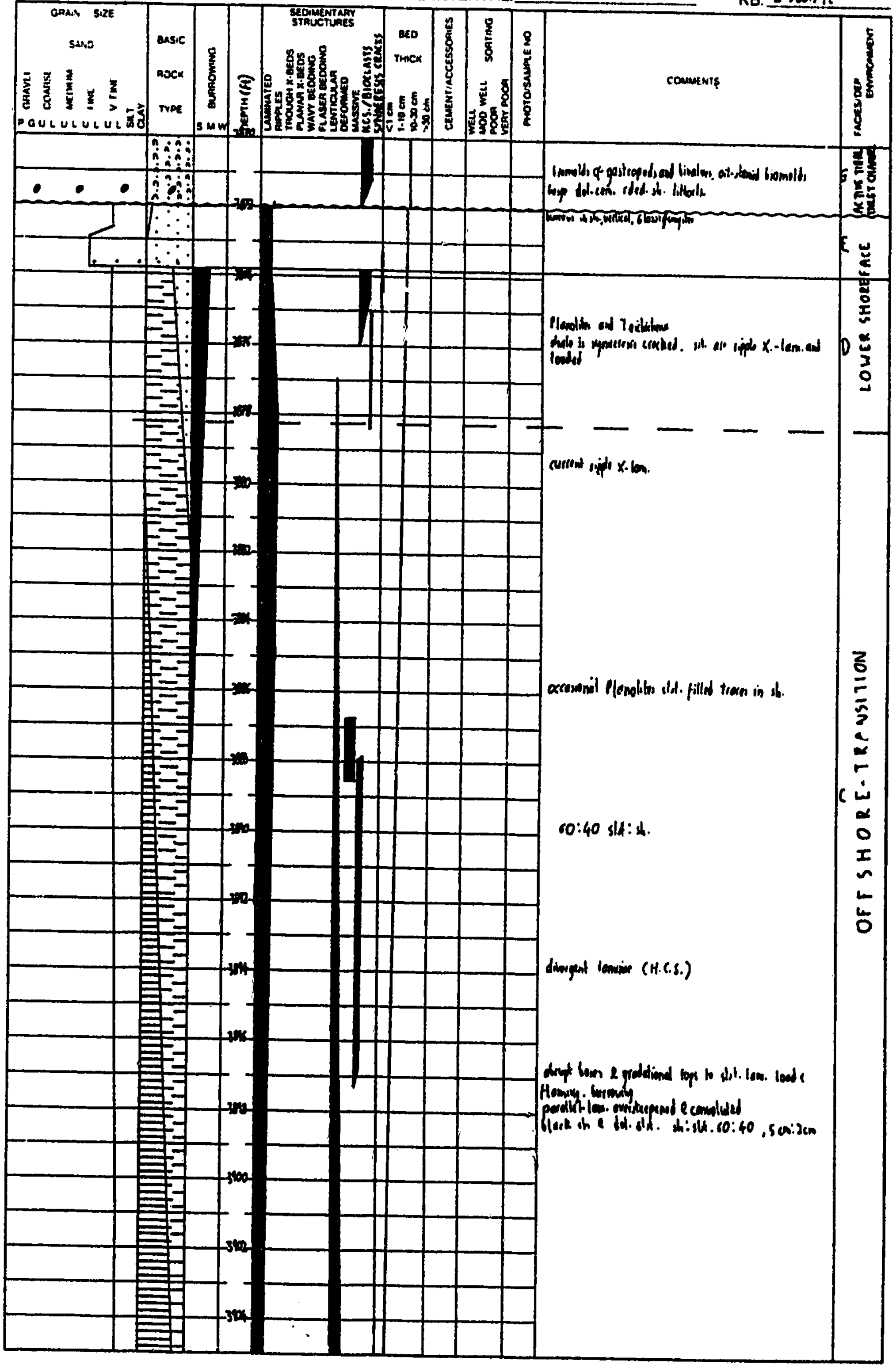

COMMENTS

Biomolds of gastropods and bivalves, oil-stained biomolds

bioturbated dol.-cem. rdcd. sh. lithcls.

burrows in sh., vertical, Glossifungites

Planolites and Teichichnus

shale is syneresis cracked. slt. are ripple X.-lam. and loaded

current ripple X.-lam.

occasional Planolites slt.-filled traces in sh.

60:40 slt.: sh.

divergent laminae (H.C.S.)

abrupt bases & gradational tops to slt. lam. load & flaming. burrowing

parallel-lam. oversteepened & convoluted

black sh & dol. slt. sh.:slt. 60:40, 5cm:2cm

WELL NAME: PACIFIC ET AL PEEJAY 6-38-E FORMATION: HALFWAY-CHARLIE LAKE DATE: 17/08/90

LOCATION: 6-038-E/94-A-16 CORE INTERVAL: KB: 2388.7ft

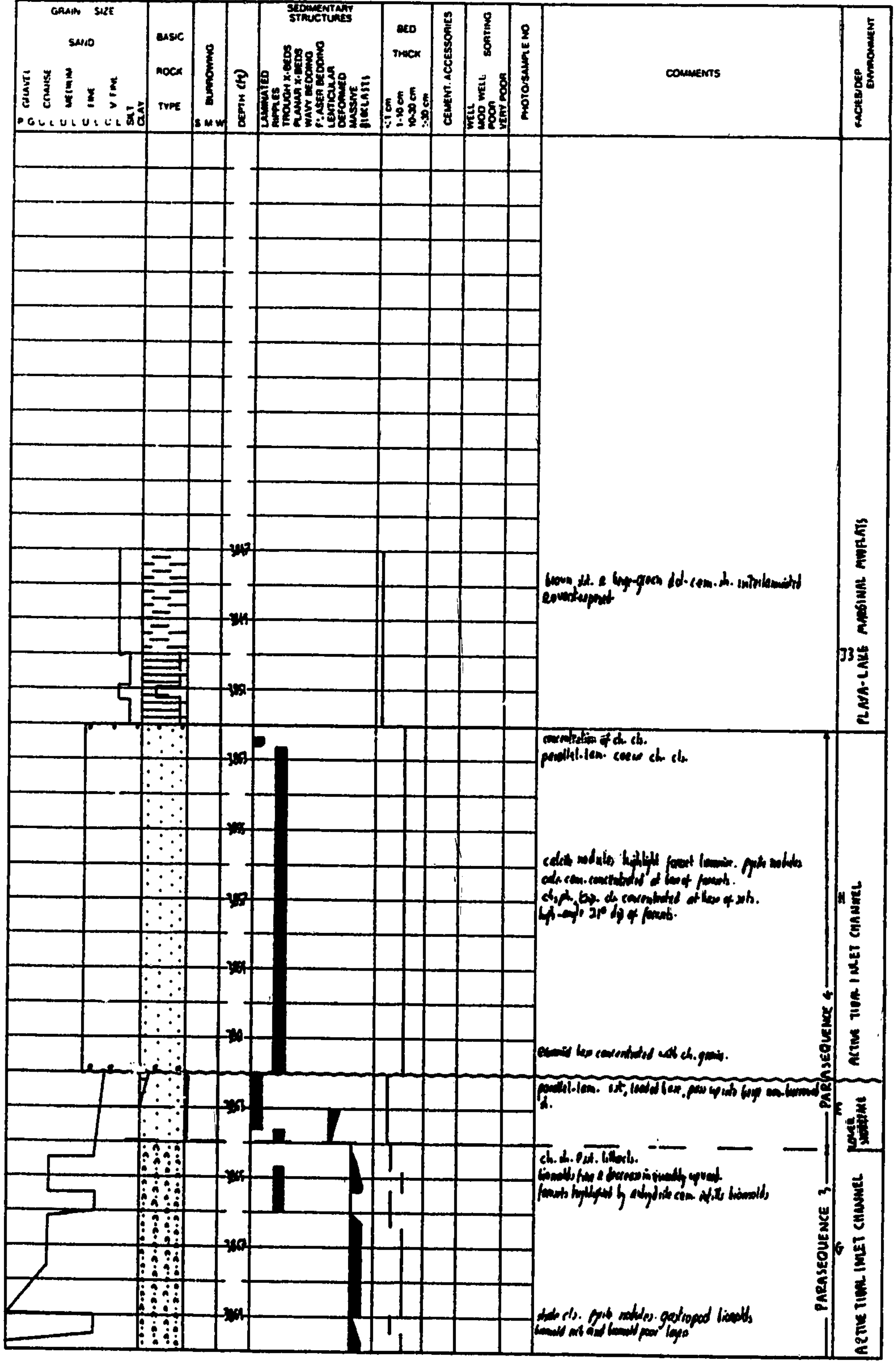

brown slt. & lt. grey-green dol-cem. sh. interlaminated ~~overlapping~~

concentration of ch. cls.
parallel-lam. coarse ch. cls.

calcite nodules highlight foreset laminae. pyrite nodules
calc. cem. concentrated at base of foresets.
ch. pb. lag. cls. concentrated at base of sets.
high-angle 21° dip of foresets.

channel base concentrated with ch. grains.

parallel-lam. sst, loaded base, pass up into large non-burrowed sl.

ch. sl. 8 sst. lithocls.
bioclasts fine & decrease in quantity upward.
foresets highlighted by anhydrite cem. infills bioclasts

shale cls. pyrite nodules. gastropod bioclasts
bioclasts not and bioclast poor layers

WELL NAME: PACIFIC ET AL PEEJAY 6-40-E
FORMATION: HALFWAY-CHARLIE LAKE
DATE: 3/07/90
LOCATION: 6-040-E/94-A-16
CORE INTERVAL:
KB: 2385.6ft

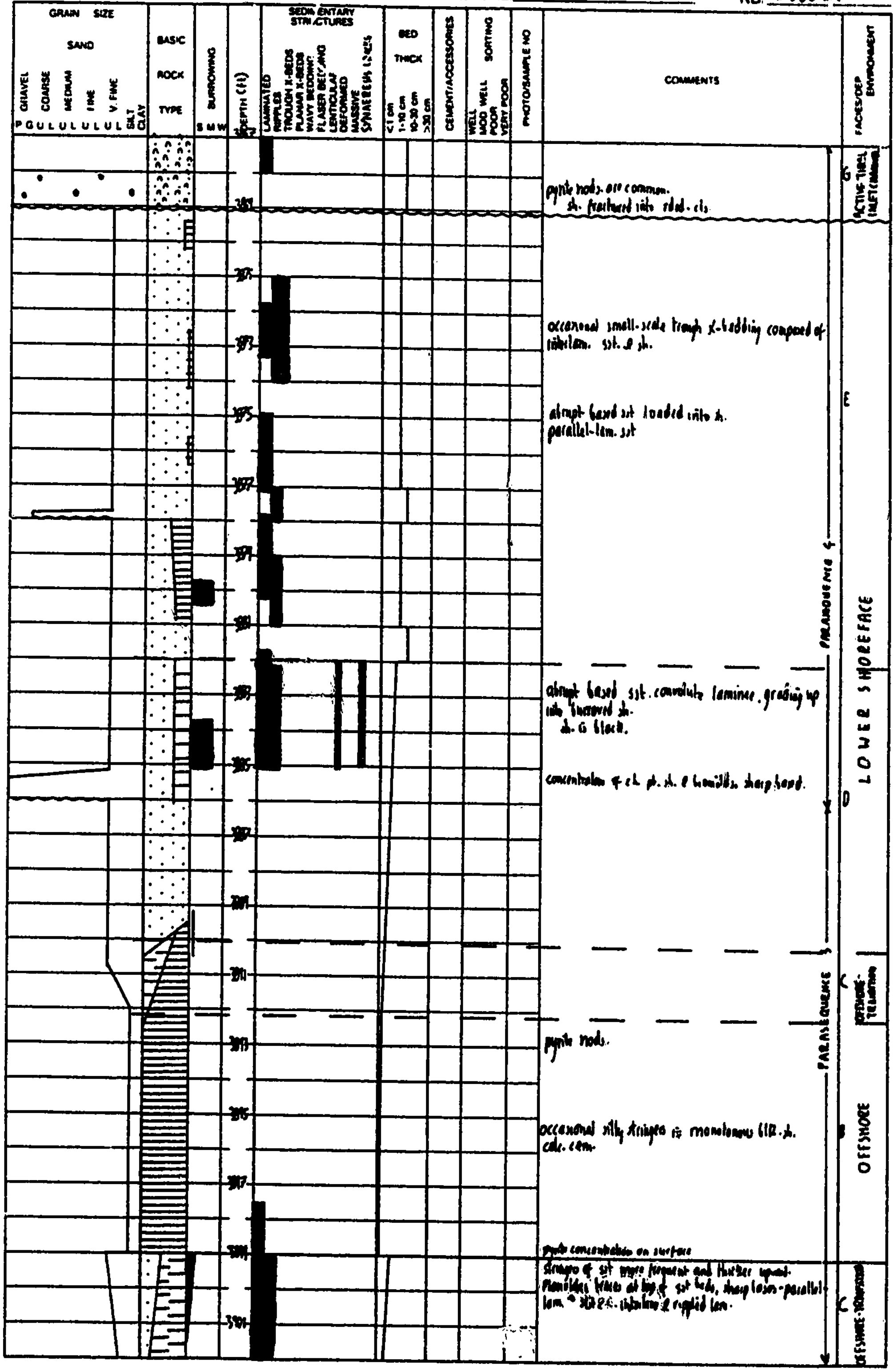

pyrite nods. are common.
sh. fractured into rdd. cls.

occasional small-scale trough X-bedding composed of interlam. sst. & sh.

abrupt based sst loaded into sh.
parallel-lam. sst

abrupt based sst. convolute laminae, grading up into burrowed sh.
sh. G black.

concentration of cl. pb. sh. & bivalves, sharp based.

pyrite nods.

occasional silty stringers in monotonous blk. sh.
calc. cem.

pyrite concentration on surface

Stringers of sst more frequent and thicker upward.
Planolites traces at top of sst beds, sharp bases-parallel lam. & 3D P.C. interlam & rippled lam.

WELL NAME: PACIFIC ET AL PEEJAY 6-40-E FORMATION: HALFWAY-CHARLIE LAKE DATE: 3/07/90

LOCATION: 6-040-E/94-A-16 CORE INTERVAL: KB: 2385.6 ft

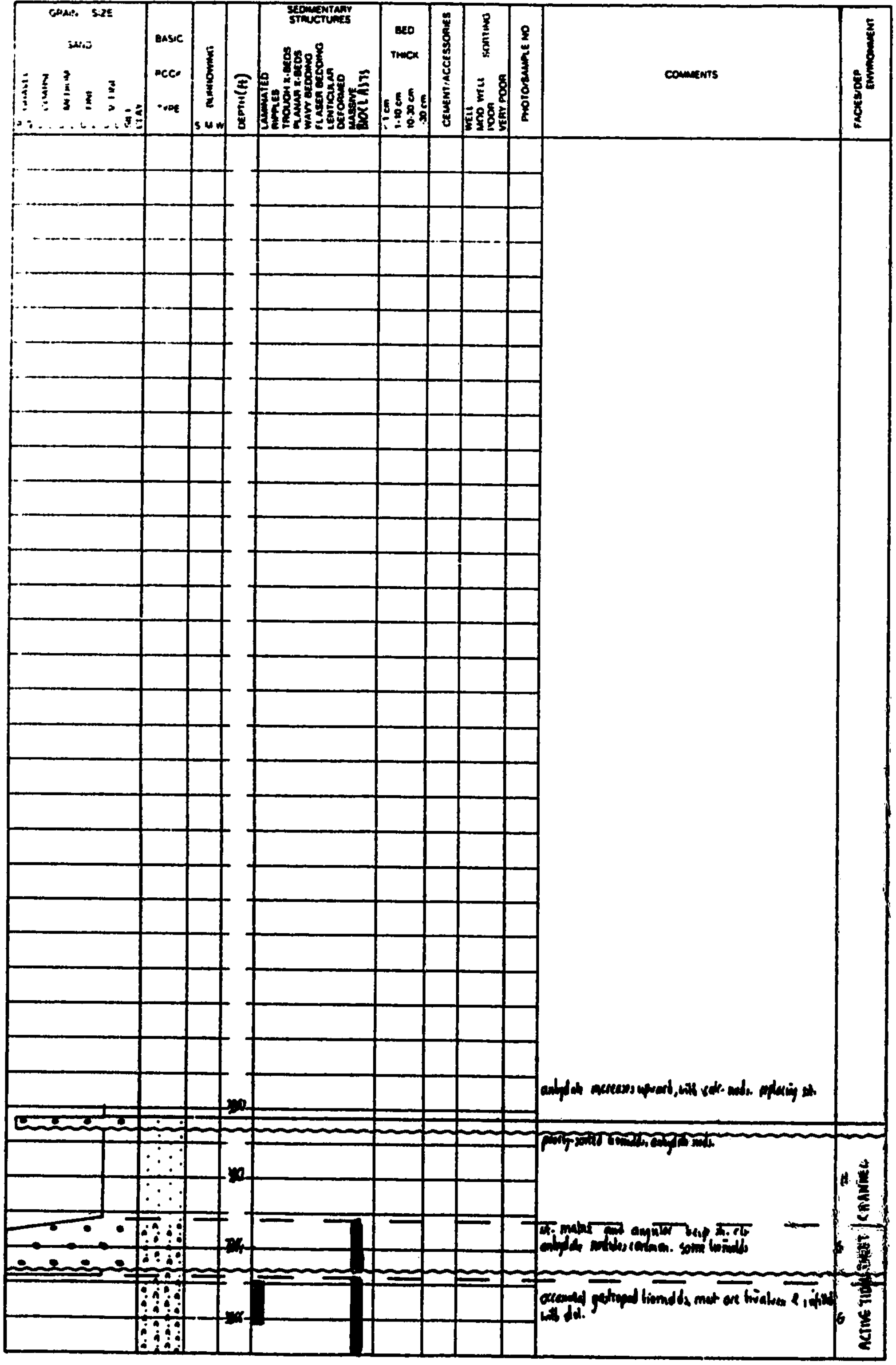

anhydrite increases upward, with calc. nods. replacing sh.

poorly sorted bivalves, anhydrite nods.

sh. matrix and angular [illegible] sh. cls
anhydrite nodules common. some bivalves

occasional gastropod bioclasts, most are bivalves & infilled with dol.

WELL NAME: PATHFINDER E PEEJAY d-43-E FORMATION: HALFWAY-CHARLIE LAKE DATE: 18/06/90

LOCATION: d-043-E/94-A-16 CORE INTERVAL: KB: 2373ft

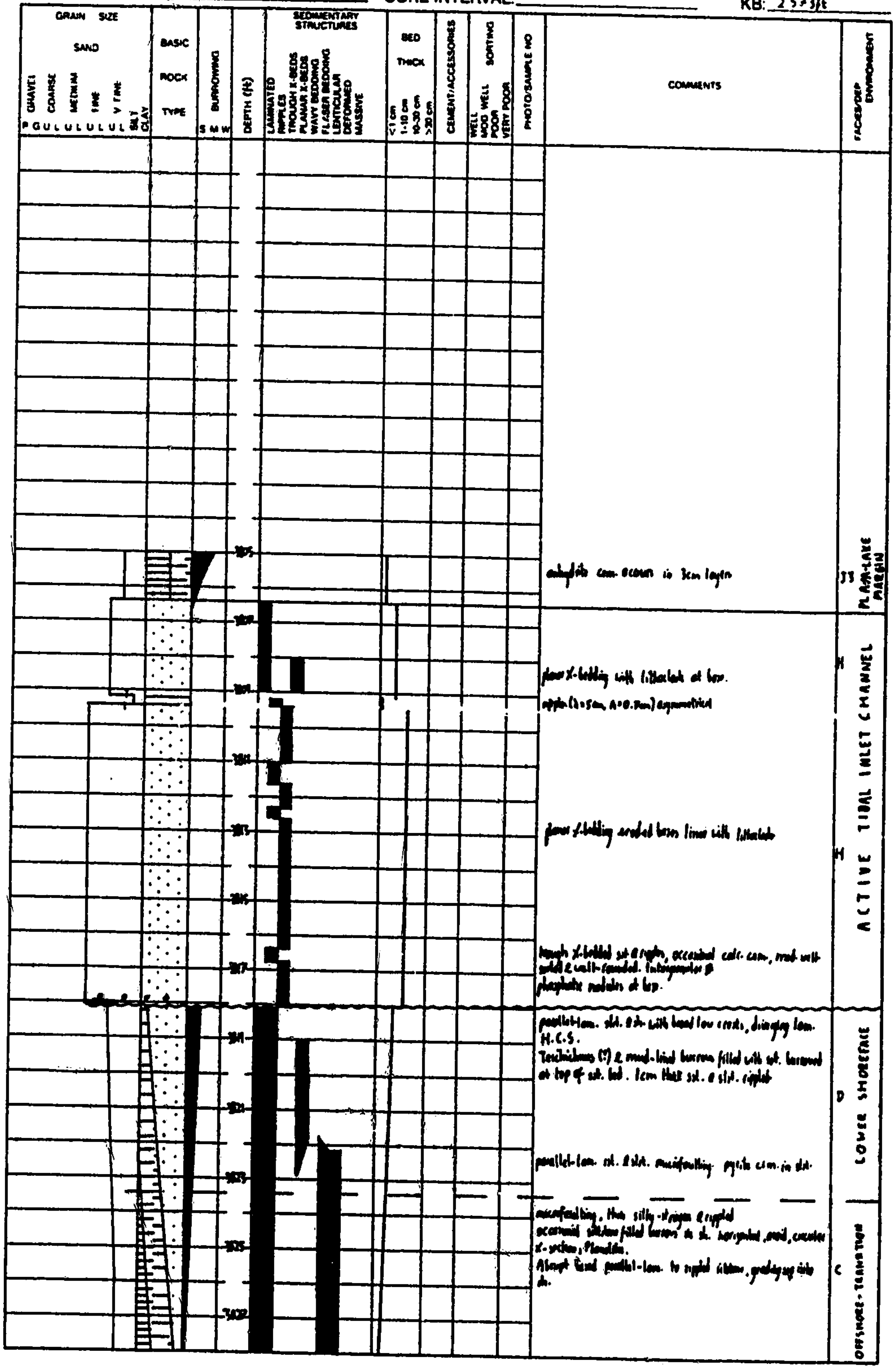

anhydrite cem. occurs in 3cm layer

planar X-bedding with lithoclasts at base.

ripples (λ=5cm, A=0.7cm) asymmetrical

planar X-bedding eroded bases lined with lithoclasts

trough X-bedded sst & ripples, occasional calc. cem., mod. well sorted & well-rounded. Intergranular ϕ phosphate nodules at top.

parallel-lam. slt. & sh. with broad low crests, diverging lam. H.C.S.

Teichichnus (?) & mud-lined burrows filled with sst. burrowed at top of sst. bed. 1cm thick sst. & slst. ripples

parallel-lam. sst. & slst. microfaulting pyrite cem. in slst.

microfaulting, thin silty stringers & rippled

occasional siltstone filled burrows in sh. horizontal, oval, circular X-section, Planolites.

Abrupt based parallel-lam. to rippled siltstone, grading up into sh.

WELL NAME: CIGOL MOBIL PEEJAY 6-45-E FORMATION: HALFWAY-CHARLIE LAKE DATE: 3/07/91

LOCATION: 6-045-E/94-A-16 CORE INTERVAL: KB: 2372 ft

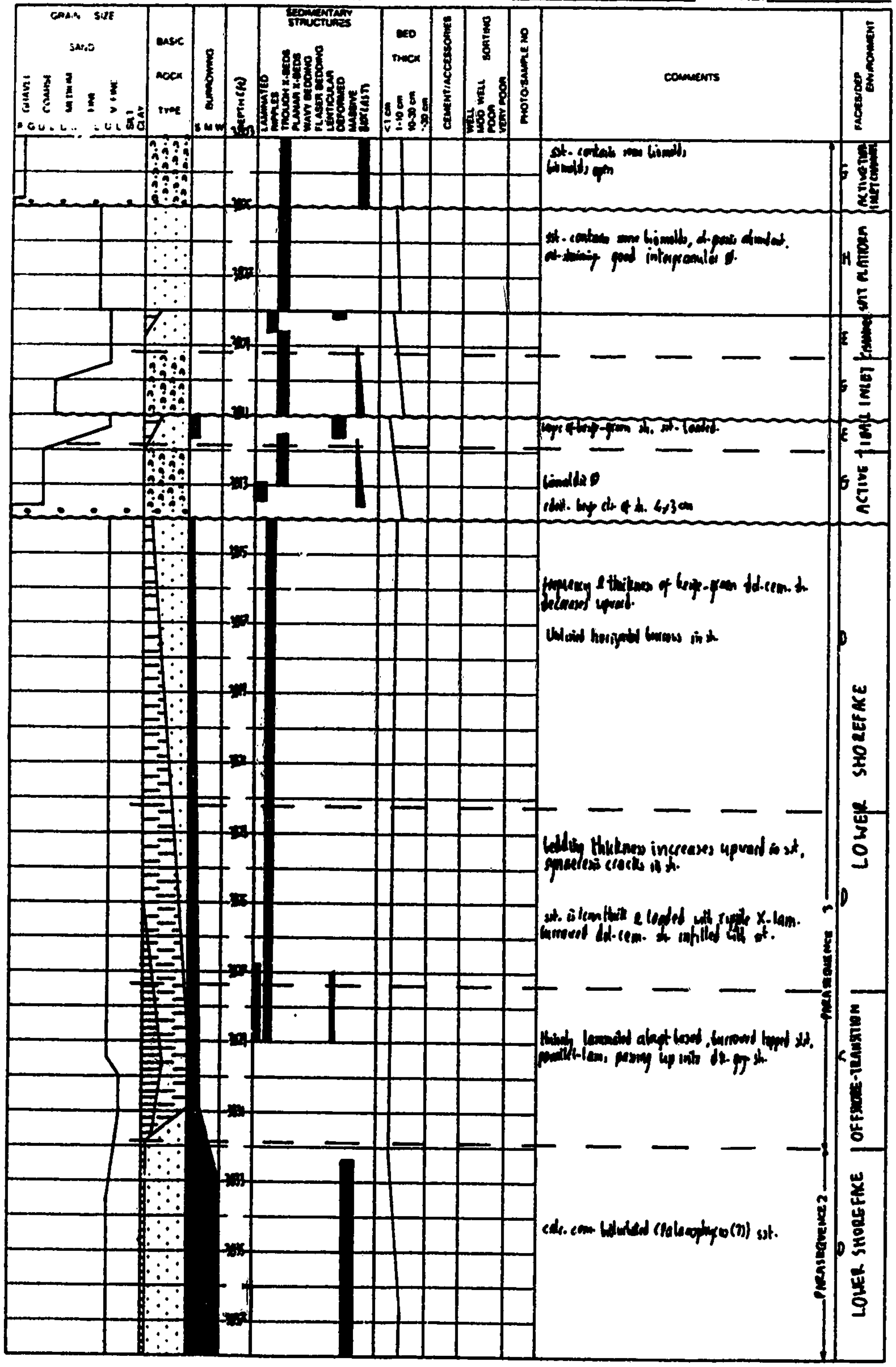

sst. contains some bivalves bivalves open

sst. contains some bivalves, ol-pods abundant. oil-staining good intergranular ϕ.

layer of large-grain sh., sst.-loaded.

bivalves ϕ

dolt. lag cls & sh. 4×3cm

frequency & thickness of large-grain dol-cem. sh. decreases upward.

Unlined horizontal burrows in sh.

bedding thickness increases upward in sst, syneresis cracks in sh.

sst. is 1cm thick & loaded with ripple X-lam. burrowed dol-cem. sh. infilled with st.

thinly laminated along base, burrowed topped slt, parallel-lam, passing up into dk-gy sh.

calc. cem. bioturbated (Palaeophycus(?)) sst.

WELL NAME: CIGOL MOBIL PEEJAY 6-45-E
FORMATION: HALFWAY-CHARLIE LAKE
DATE: 3/07/91
LOCATION: 6-045-E/94-A-16
CORE INTERVAL:
KB: 2372ft

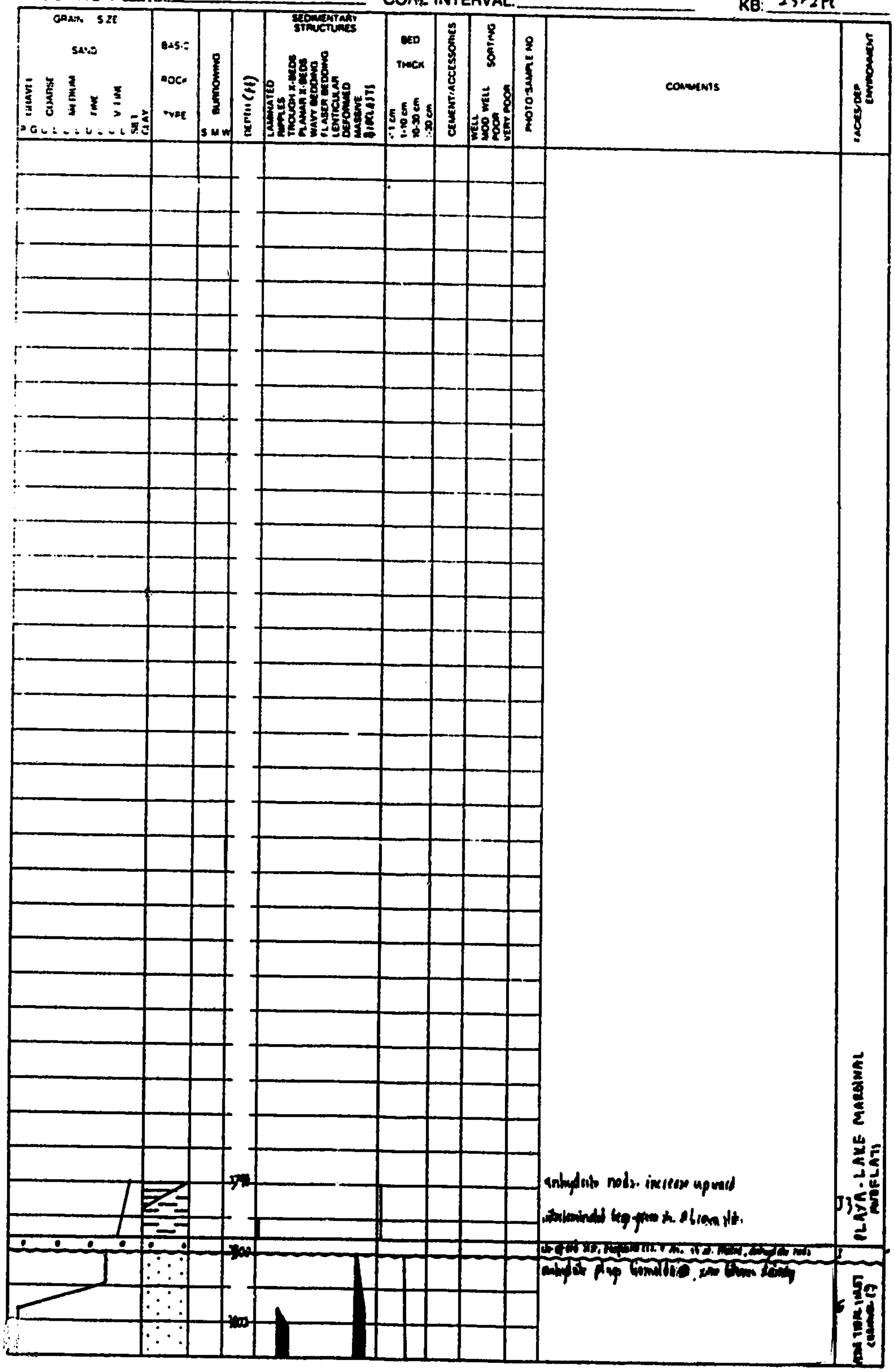

anhydrite nods. increase upward
interlaminated beige-green sh. & brown slt.
[illegible]
anhydrite plug [illegible], some brown staining

J3 PLAYA-LAKE MARGINAL (MUDFLAT)

6 [illegible]

WELL NAME: MEDALLION MOBIL PEEJAY d-46-E FORMATION: HALFWAY-CHARLIE LAKE DATE: 5/07/91

LOCATION: d-046-E/94-A-16 CORE INTERVAL: KB: 2378.9ft

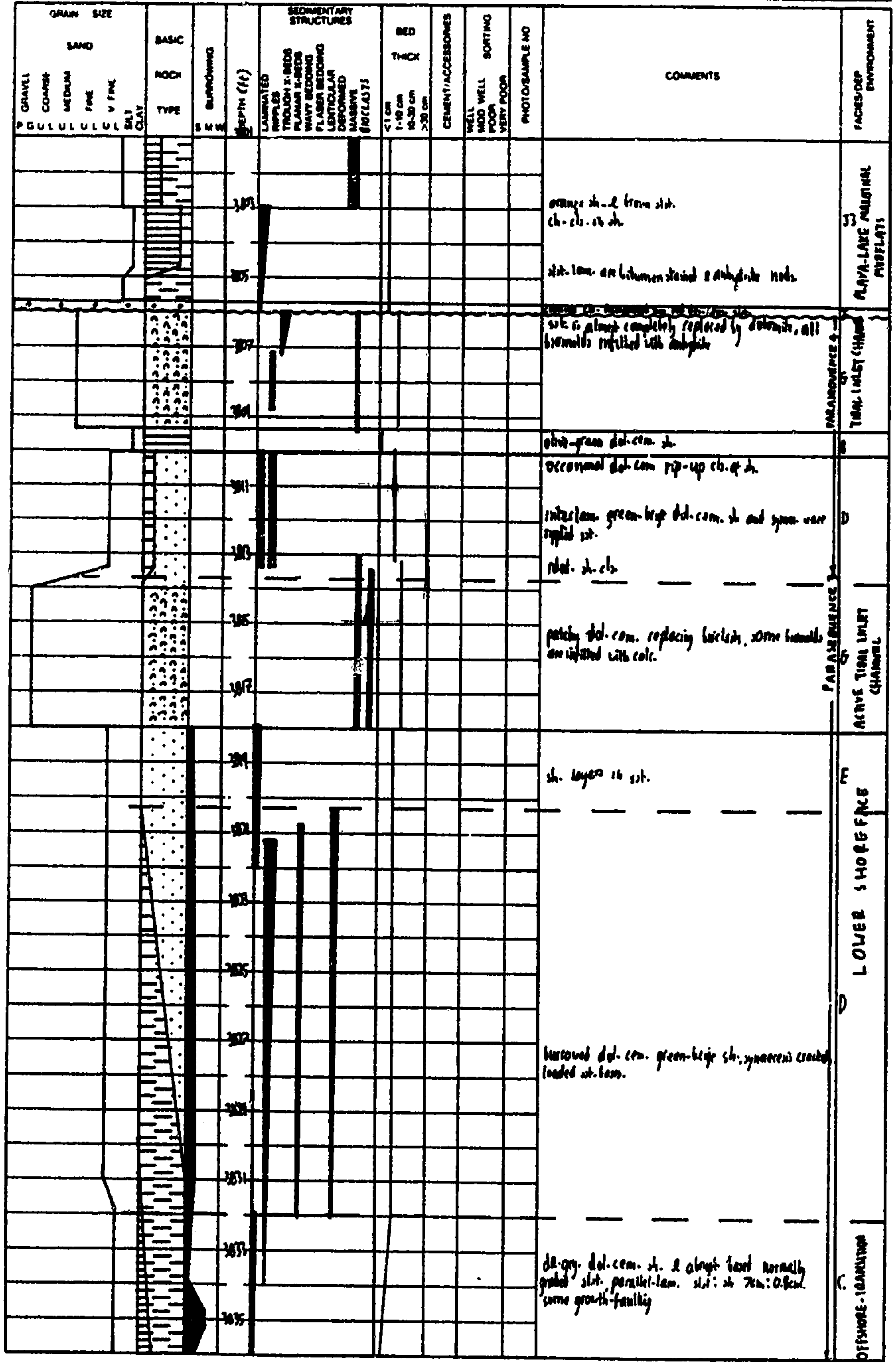

orange sh. & brown slst.
ch.-cls. in sh.

slst.-lam. are bitumen stained & anhydrite nods.

sst. is almost completely replaced by dolomite, all biomolds infilled with anhydrite

olive-green dol.-cem. sh.

occasional dol.-cem. rip-up cls. of sh.

interlam. green-beige dol.-cem. sh. and green-wave rippled sst.

dol. sh. cls.

patchy dol.-cem. replacing bioclasts, some biomolds are infilled with calc.

sh. layers in sst.

burrowed dol.-cem. green-beige sh., synaeresis cracks, loaded sst. base.

dk.-gry. dol.-cem. sh. & abrupt based normally graded slst. parallel-lam. slst : sh 7cm : 0.8cm.
some growth-faulting

WELL NAME: PAC!FIC ET AL PEEJAY 6-47E

FORMATION: HALFWAY- CHARLIE LAKE

DATE: 27/07/90

LOCATION: 6-047-E/94-A-16

CORE INTERVAL:

KB: 2386 3ft

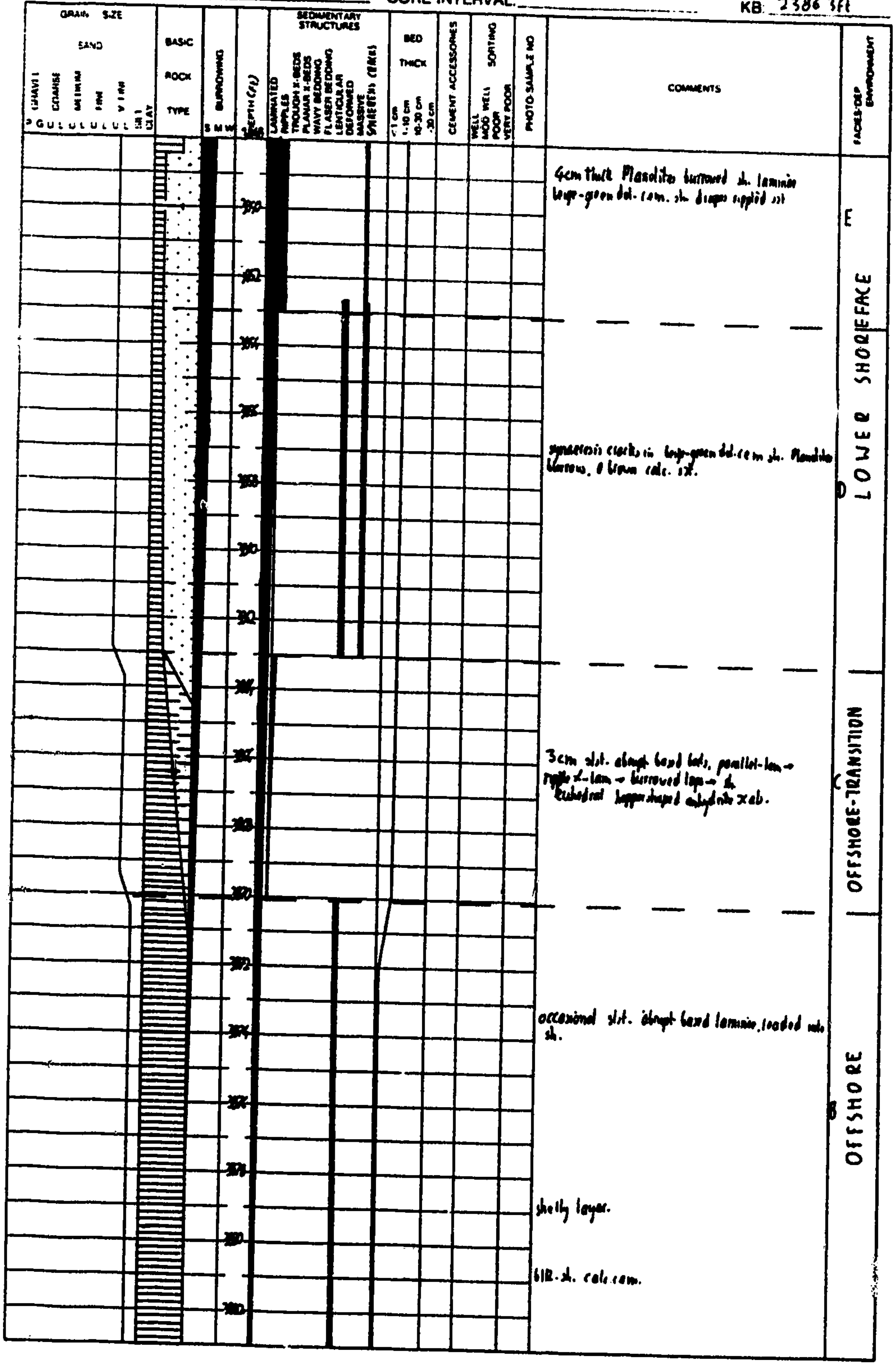

4cm thick Planolites burrowed sh. laminae beige-green dol. cem. sh. drapes rippled sst

synaeresis cracks in beige-green dol. cem sh. Planolites burrows, & brown calc. sst.

3cm sltst. abrupt based beds, parallel-lam → ripple x-lam → burrowed top → sh.
Euhedral hopper-shaped anhydrite xals.

occasional sltst. abrupt based laminae, loaded into sh.

shelly layer.

6IR-sh. calc. cem.

WELL NAME: PACIFIC ET AL PEEJAY 6-47E
FORMATION: HALFWAY-CHARLIE LAKE
DATE: 27/07/90
LOCATION: 6-047-E/94-A-16
CORE INTERVAL:
KB: 2386.3ft

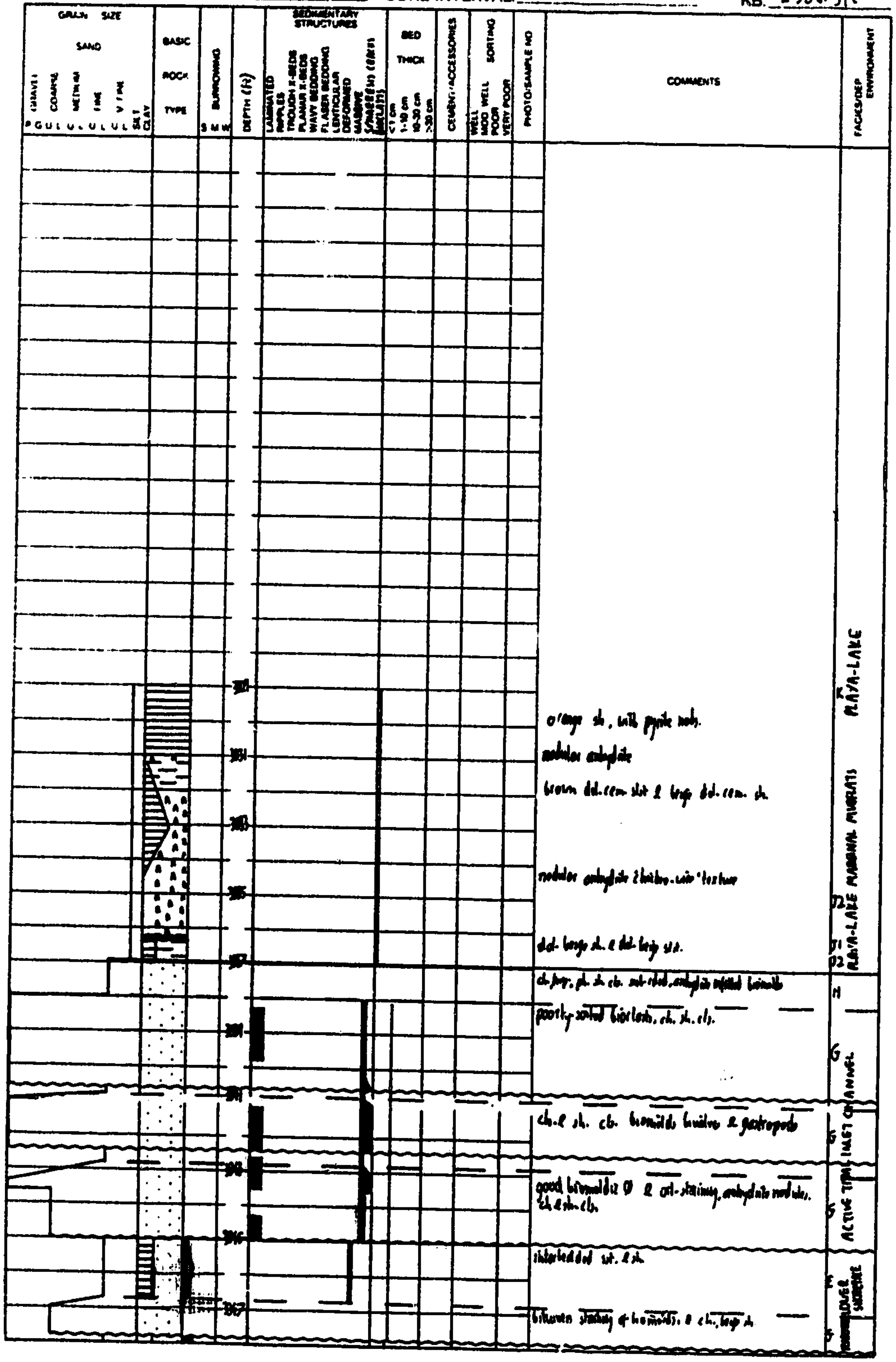

orange sh., with pyrite nods.

nodular anhydrite

brown dol.-cem. slt & lmy dol.-cem. sh.

nodular anhydrite 'chicken-wire' texture

dol. lmy sh. & dol. lmy slt.

ch. frag., pl. sh. cl. sub-rdd., anhydrite infilled burrows

poorly sorted bioclasts, ch. sh. cls.

ch. & sh. cl. biomolds bivalves & gastropods

good biomoldic Ø & oil-staining, anhydrite nodules, ch. & sh. cl.

interbedded slt. & sh.

bitumen staining of biomolds, & ch., lmy sh.

K PLAYA-LAKE
MARGINAL MUDFLATS
J2 PLAYA-LAKE
J1
J2
H
G ACTIVE TIDAL INLET CHANNEL
G
G
F LOWER SHOREFACE
F

WELL NAME: SINCLAIR ET AL PEEJAY d-47-E
FORMATION: HALFWAY-CHARLIE LAKE
DATE: 4/02/91
LOCATION: d-047-E/94-A-16
CORE INTERVAL:
KB: GL 2369ft

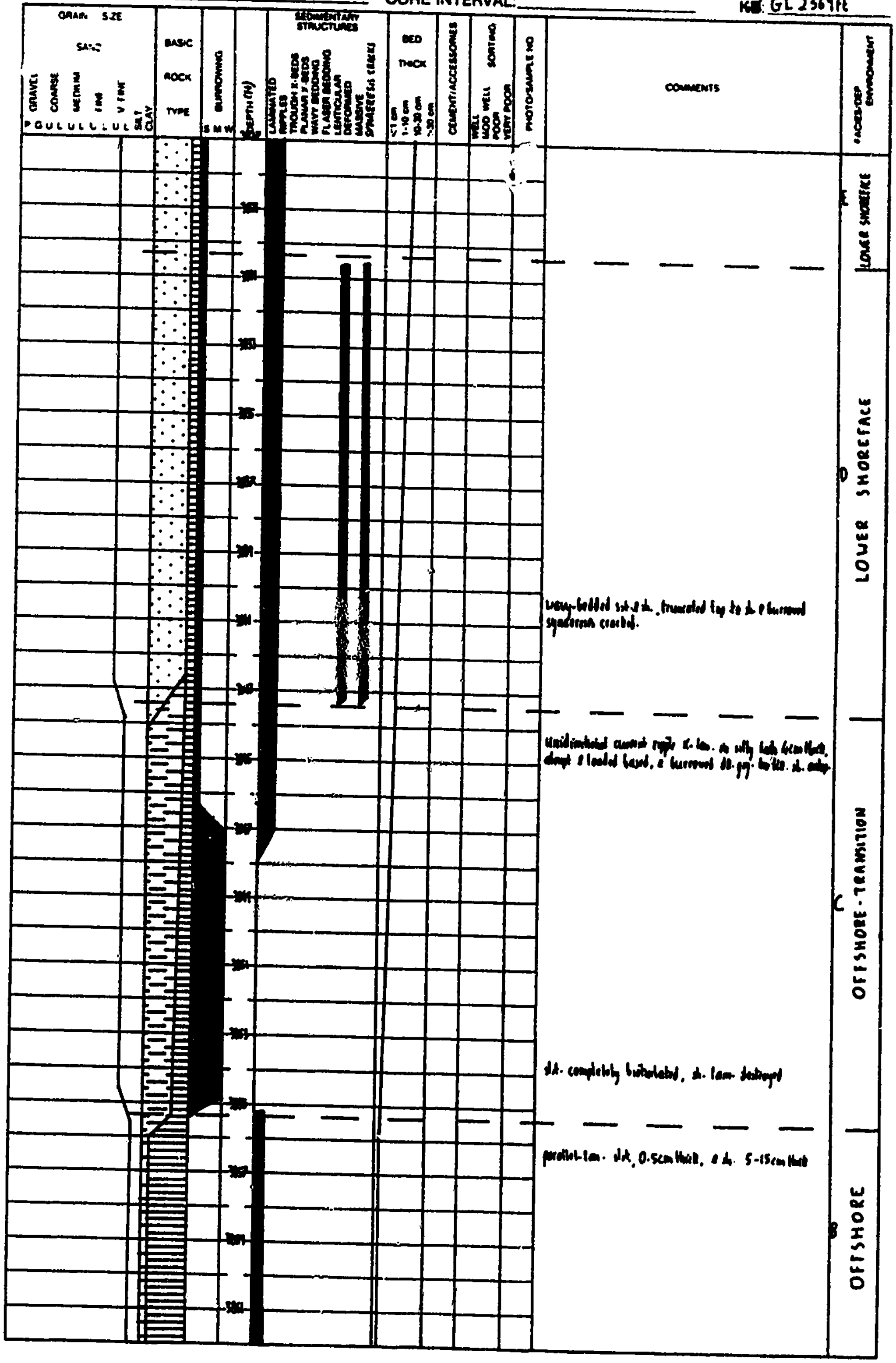

wavy-bedded sst. & sh., truncated top to sh. & burrowed syneresis cracked.

Unidirectional current ripple x-lam. in silty beds 6cm thick, sharp & loaded based, & burrowed [illegible] [illegible] [illegible]. sh. [illegible]

sltst. completely bioturbated, sh. lam. destroyed

parallel-lam. sltst. 0.5cm thick, & sh. 5-15cm thick

WELL NAME: SINCLAIR ET AL PEEJAY d-47-E
FORMATION: HALFWAY- CHARLIE LAKE
DATE: 4/02/91

LOCATION: d-047-E/94-A-16
CORE INTERVAL:
KB: 6L 2369ft

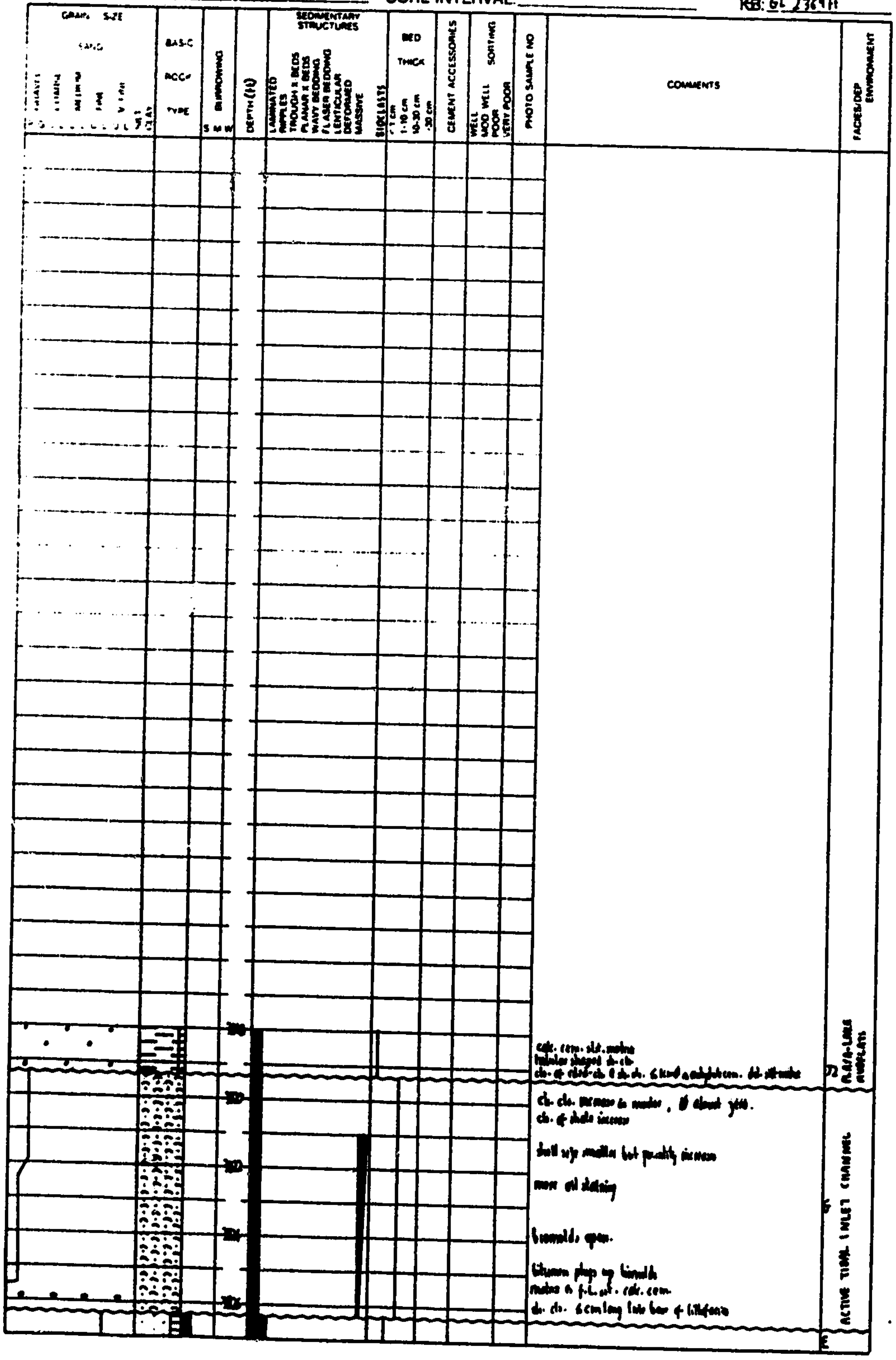

calc. cem. slst. matrix
tabular shaped cl.-cls.
cl. of [illegible] [illegible] [illegible]

cl. cls. increase in number, & about [illegible].
cl. of shale increase

shell w/p smaller but possibly increase

more oil staining

biomolds open.

bitumen plugs up biomolds
matrix is f.L. sst. calc. cem.
cl. cls. 6cm long into base of lithofacies

WELL NAME: PACIFIC ET AL PEEJAY 6-48-E

FORMATION: HALFWAY-CHARLIE LAKE

DATE: 26/07/90

LOCATION: 6-048-E/94-A-16

CORE INTERVAL:

KB: 2390 ft

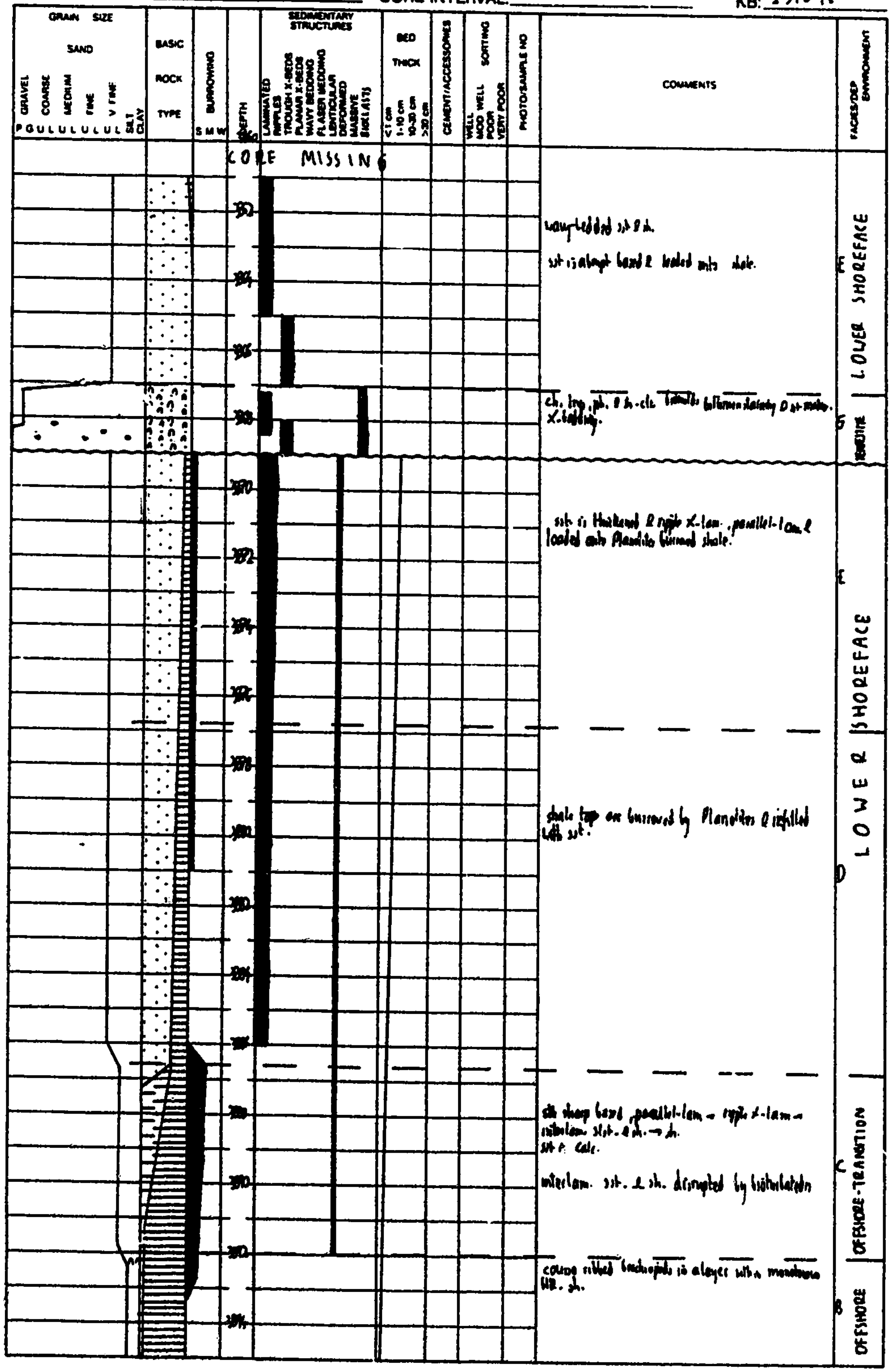

wavy-bedded sst & sh.

sst is abrupt based & loaded into shale.

ch. lrg. pb. & sh.-cls. [illegible] bituminous [illegible] & sst matrix. X-bedding.

sst is thickened & ripple X-lam. parallel-lam. & loaded onto Planolites burrowed shale.

shale tops are burrowed by Planolites & infilled with sst.

sh. sharp based, parallel-lam. → ripple X-lam. → interlam. slst. & sh. → sh.
sst. calc.

interlam. sst. & sh. disrupted by bioturbation

coarse ribbed brachiopods in a layer with a mudstone
blk. sh.

WELL NAME: PACIFIC ET AL PEEJAY 6-48-E FORMATION: HALFWAY-CHARLIE LAKE DATE: 26/07/90

LOCATION: 6-048-E/94-A-16 CORE INTERVAL: KB: 2390ft

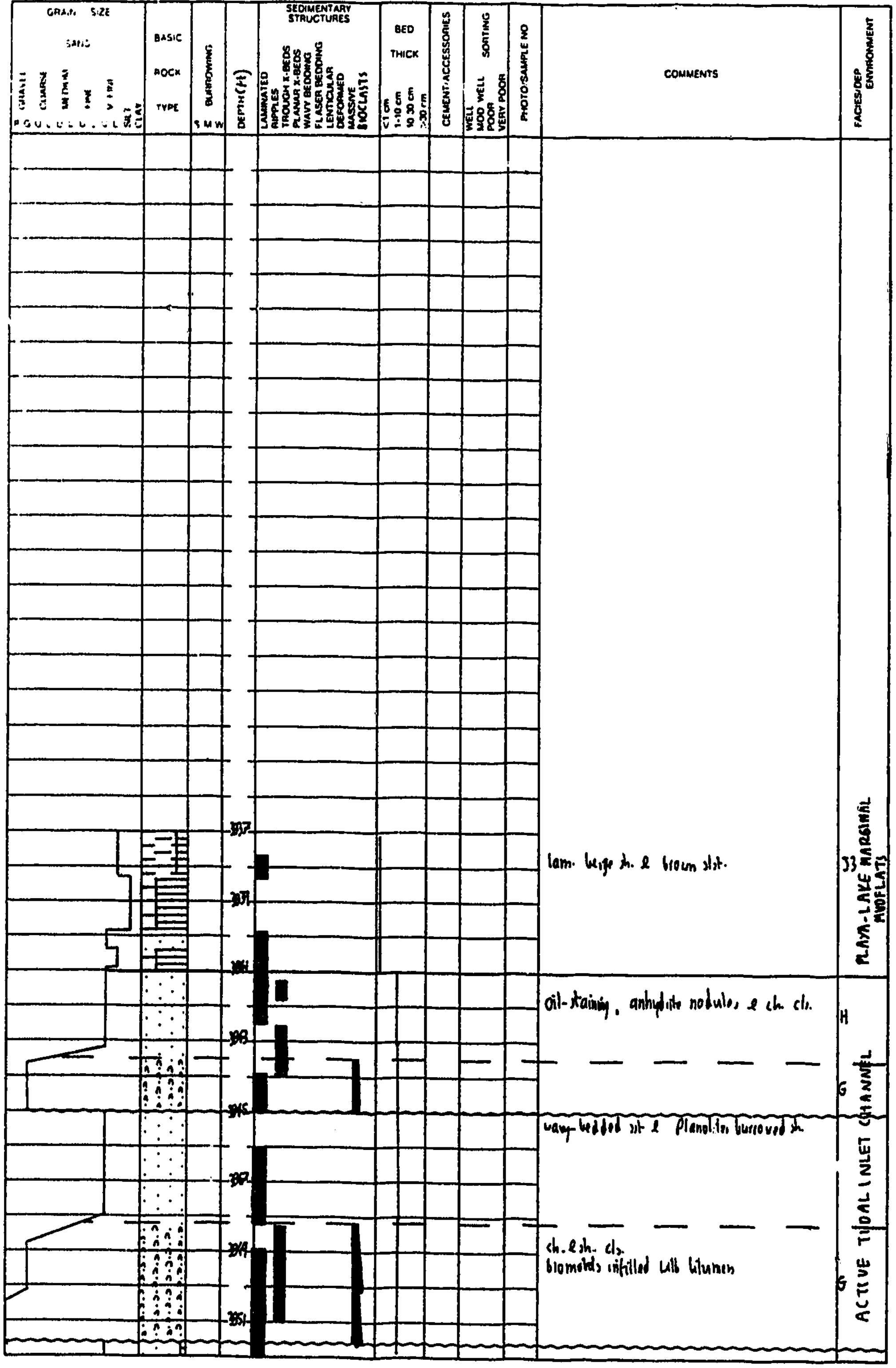

lam. beige sh. & brown slst.

oil-staining, anhydrite nodules & ch. cls.

wavy-bedded slt & Planolites burrowed sh.

ch. & sh. cls.
biomolds infilled with bitumen

WELL NAME: SINCLAIR ET AL PEEJAY

FORMATION: HALFWAY-CHARLIE LAKE

DATE: 6/02/91

LOCATION: d-048-E/94-A-16

CORE INTERVAL:

KB: GL: 2374 7ft

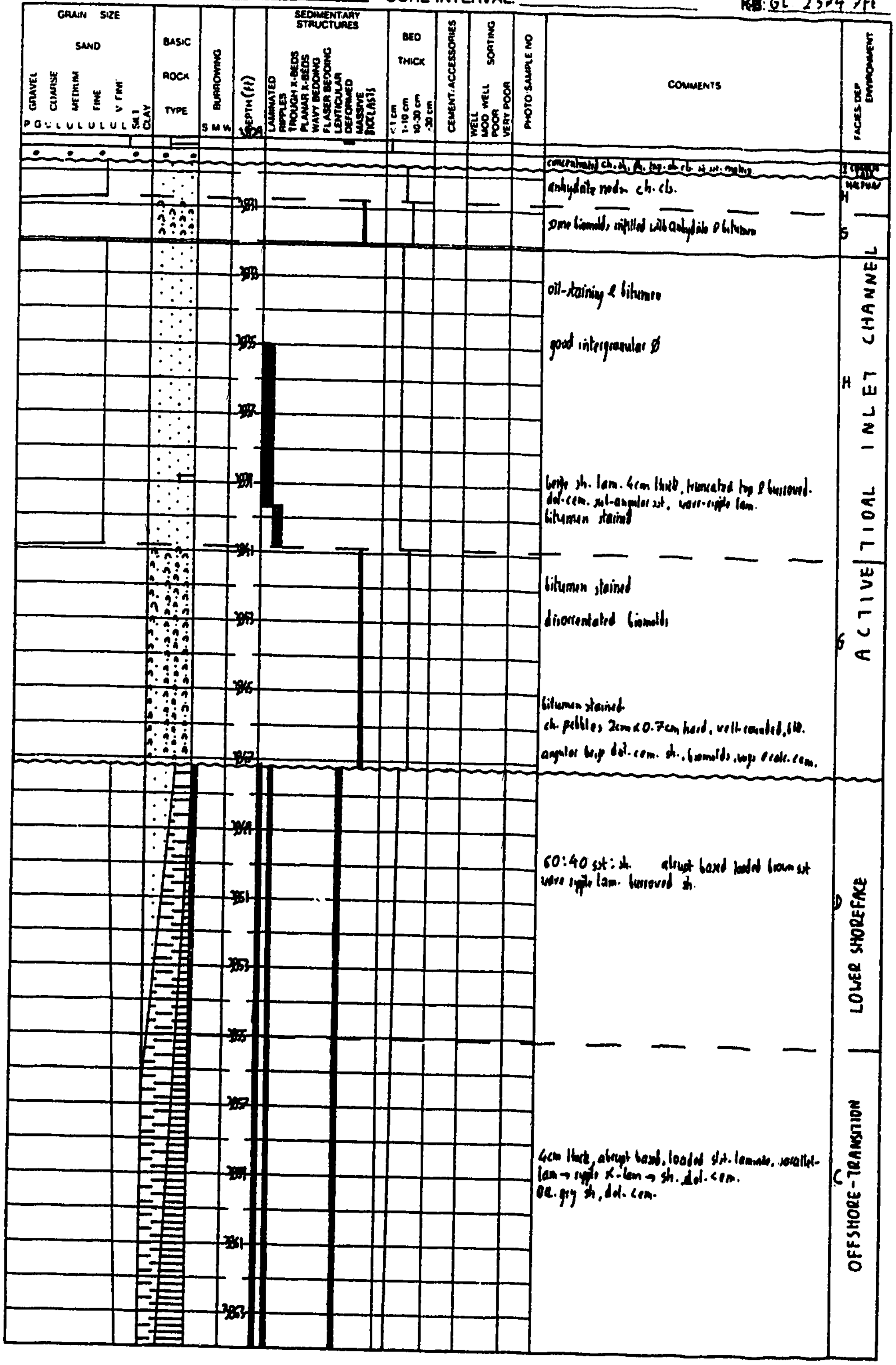

concentrated ch. cl., ph. frag. ch. cl. of art. angular

anhydrite nodu. ch. cl.

some biomolds, infilled with anhydrite & bitumen

oil-staining & bitumen

good intergranular Ø

beige sh. lam. 4cm thick, truncated top & burrowed.
dol.-cem. sub-angular sst., wave-ripple lam.
bitumen stained

bitumen stained

disorientated biomolds

bitumen stained.
ch. pebbles 2cm x 0.7cm hard, well-rounded, ltt.
angular beige dol.-cem. sh., biomolds, wisps calc.-cem.

60:40 sst : sh. abrupt based loaded brown sst
wave ripple lam. burrowed sh.

4cm thick, abrupt based, loaded sst. laminae, parallel-
lam → ripple X-lam → sh. dol.-cem.
dk. gry sh., dol. cem.

WELL NAME: SINCLAIR ET AL PEEJAY FORMATION: HALFWAY-CHARLIE LAKE DATE: 6/02/91

LOCATION. d-048-E/94-A-16 CORE INTERVAL: ~~KB~~: GL: 2374.7ft

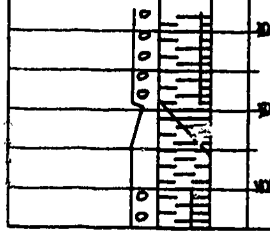

GRAIN SIZE SAND GRAVEL P G · COARSE U L · MEDIUM U L · FINE U L · V FINE U L · SILT · CLAY	BASIC ROCK TYPE	BURROWING S M W	DEPTH (ft)	SEDIMENTARY STRUCTURES LAMINATED · RIPPLES · TROUGH X-BEDS · PLANAR X-BEDS · WAVY BEDDING · FLASER BEDDING · LENTICULAR · DEFORMED · MASSIVE	BED THICK <1 cm · 1-10 cm · 10-30 cm · >30 cm	CEMENT/ACCESSORIES	SORTING WELL · MOD WELL · POOR · VERY POOR	PHOTO/SAMPLE NO	COMMENTS	FACIES/DEP ENVIRONMENT
			104						lam. slt. & sh. angular cls in orange sh. matrix	33 PLAYA-LAKE MARGINAL MUDFLATS
			106							
									cls. of lam. slt. & sh. in orange sh. matrix with [illegible]	
			108						cls. of sh. & slt. in slt matrix, oversteepened laminae.	33

WELL NAME: PACIFIC ET AL PEEJAY 6-49-E

FORMATION: HALFWAY-CHARLIE LAKE

DATE: 30/01/91

LOCATION: 6-049-E/94-A-16

CORE INTERVAL:

KB: 2391 7ft

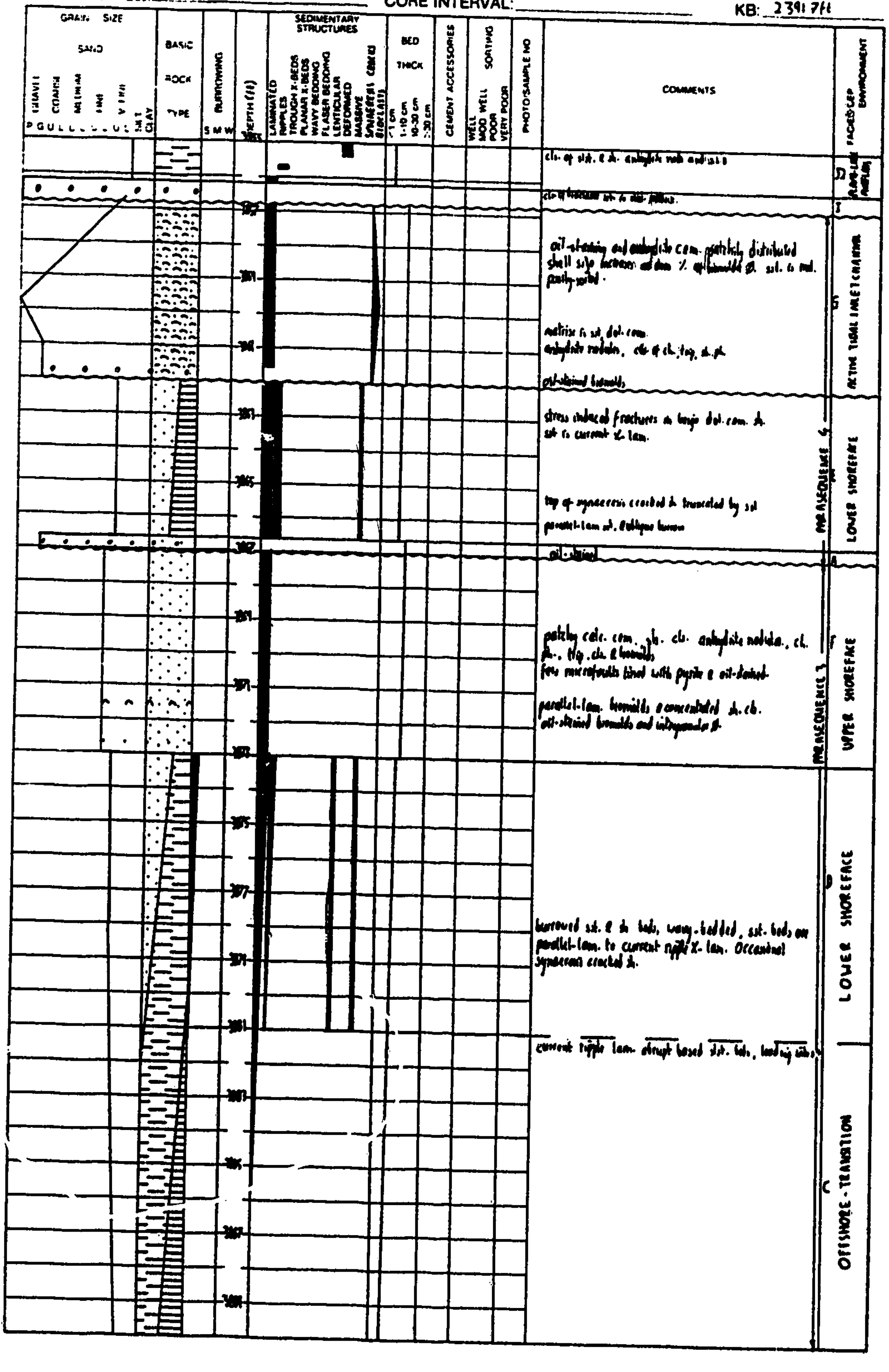

cls. of slt. & sh. anhydrite nodule and [illegible]

cls of [illegible] [illegible] pebbles.

oil-staining and anhydrite cem. patchily distributed shell size increases and then % of bivalve fr. sst. to med. poorly-sorted.

matrix is sst. dol. cem.
anhydrite nodules, cls of sh., frag. sh. pb.

oil-stained bivalves

stress induced fractures in large dol. cem. sh.
sst is current X-lam.

top of syneresis cracked sh. truncated by sst
parallel-lam. w/. oblique burrow

oil-stained

patchy calc. cem., sh. cls. anhydrite nodule., cl. sh., frag. cls. & bivalves
few microfaults lined with pyrite & oil-stained.

parallel-lam. bivalves & concentrated sh. cls.
oil-stained bivalves and intergranular fr.

burrowed sst. & sh. beds, wavy-bedded, sst. beds are parallel-lam. to current ripple X-lam. Occasional syneresis cracked sh.

current ripple lam. abrupt based sst. beds, loading [illegible]

WELL NAME: PACIFIC SINCLAIR PEEJAY FORMATION: HALFWAY-CHARLIE LAKE DATE: 11/06/90

LOCATION: 6-050-E/94-A-16 CORE INTERVAL: KB: 2371ft

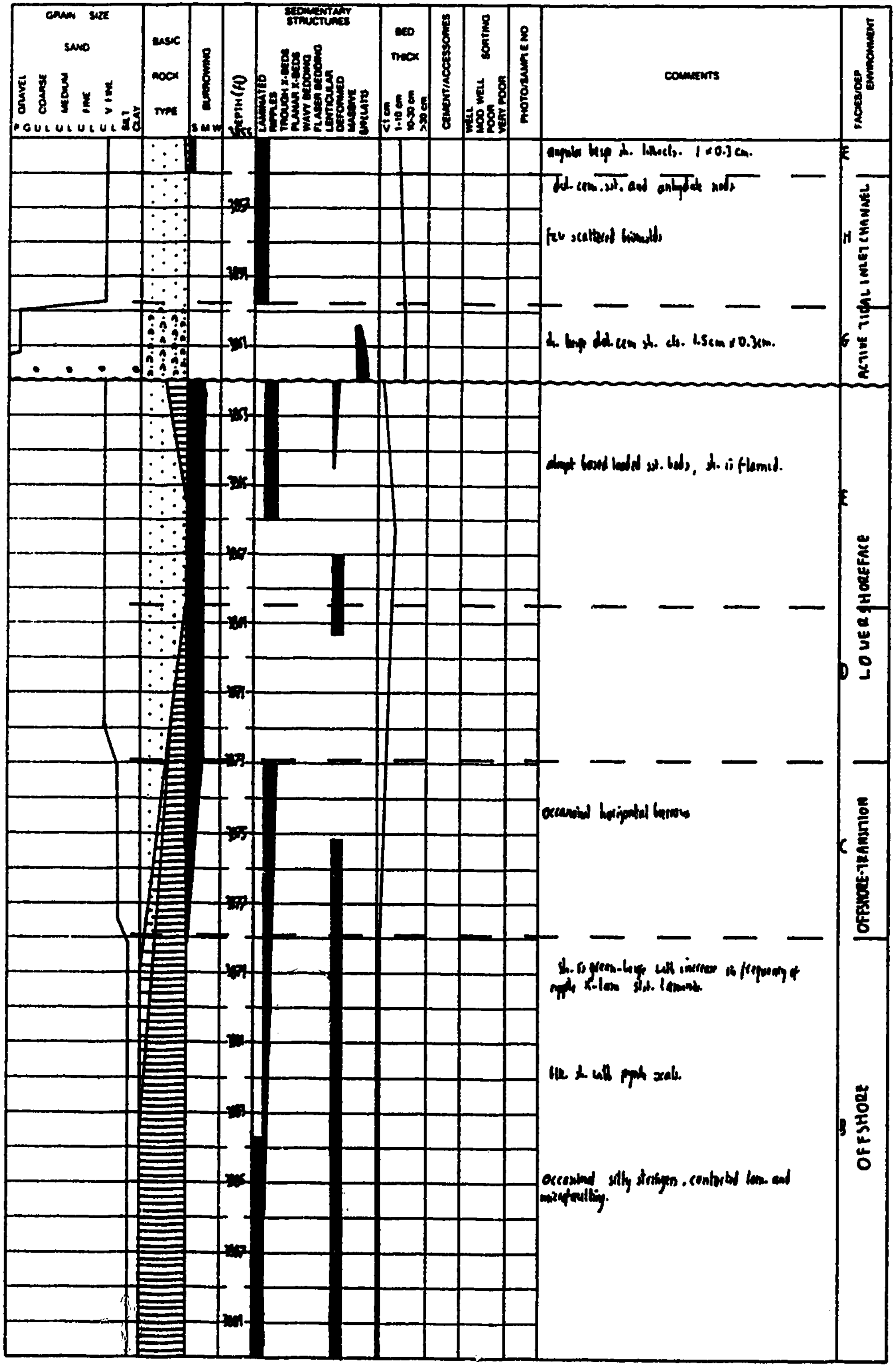

angular large sh. lithocls. 1 × 0.3 cm.

dol.-cem. sst. and anhydrite nods

few scattered biomolds

sh. large dol.-cem sh. cls. 1.5cm × 0.3cm.

abrupt based loaded sst. beds, sh. is flamed.

occasional horizontal burrows

sh. is green-beige with increase in frequency of ripple X-lam silt. laminae.

blk. sh. with pyrite xals.

Occasional silty stringers, contorted lam. and microfaulting.

WELL NAME: PACIFIC SINCLAIR PEEJAY
FORMATION: HALFWAY- CHARLIE LAKE
DATE: 11/06/90
LOCATION: 6-050-E/94-A-16
CORE INTERVAL:
KB: 2371ft

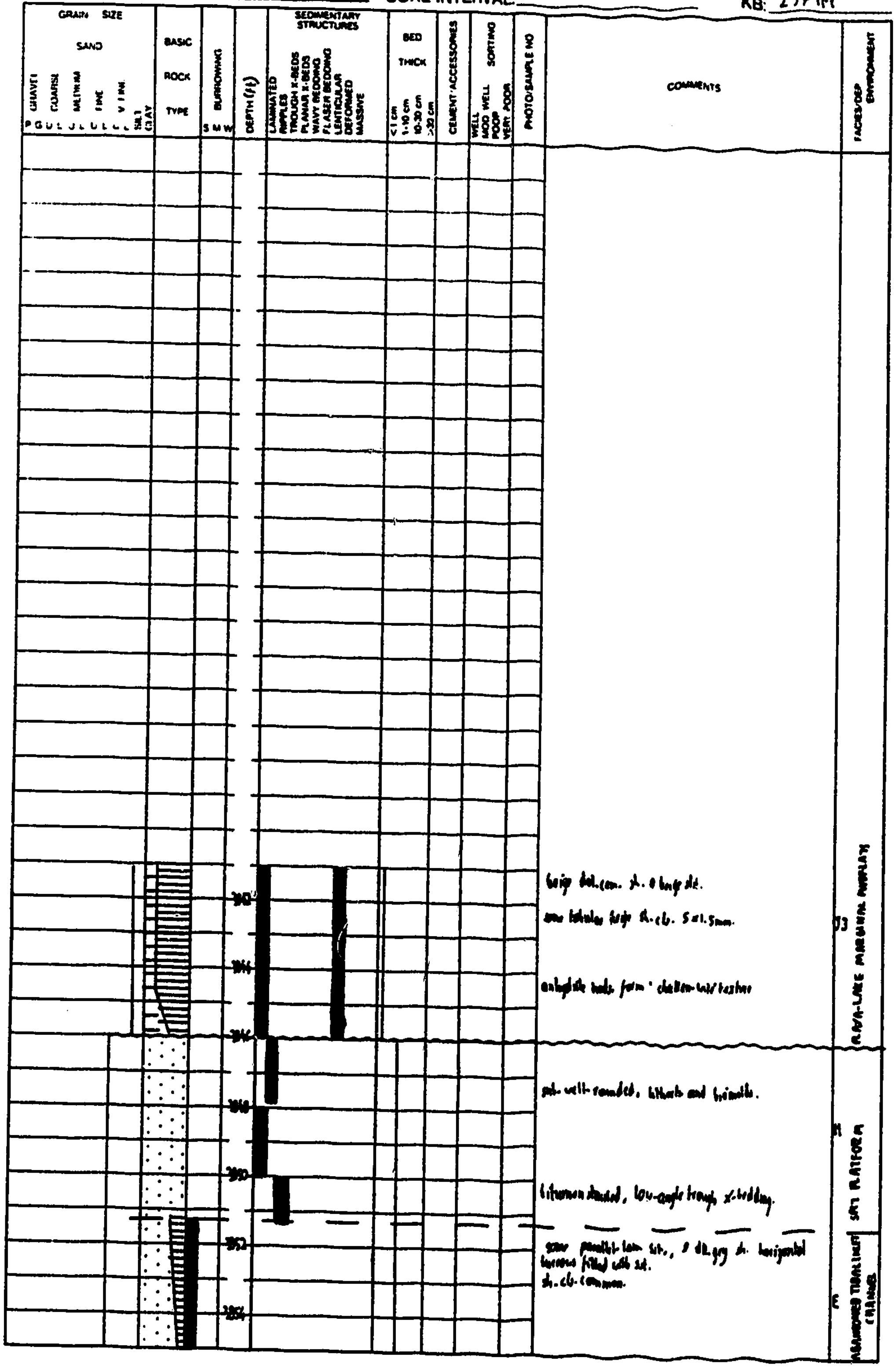

beige dol.com. sh. & beige slt.

some tabular beige sh.cl. 5×1.5mm.

anhydrite nodules form "chicken-wire" texture

sub-well-rounded, lithoclasts and bioclasts.

bitumen stained, low-angle trough x-bedding.

some parallel-lam. slt., & dk.grey sh. horizontal burrows filled with slt.
sh.cl. common.

J3 PLAYA-LAKE MARGINAL MUDFLATS

H SAND PLATFORM

E ABANDONED TIDAL INLET CHANNEL

WELL NAME: UNION H.B. E PEEJAY 6-54-E FORMATION: HALFWAY-CHARLIE LAKE DATE: 18/06/90

LOCATION: 6-054-E/94-A-16 CORE INTERVAL: KB: 2380ft

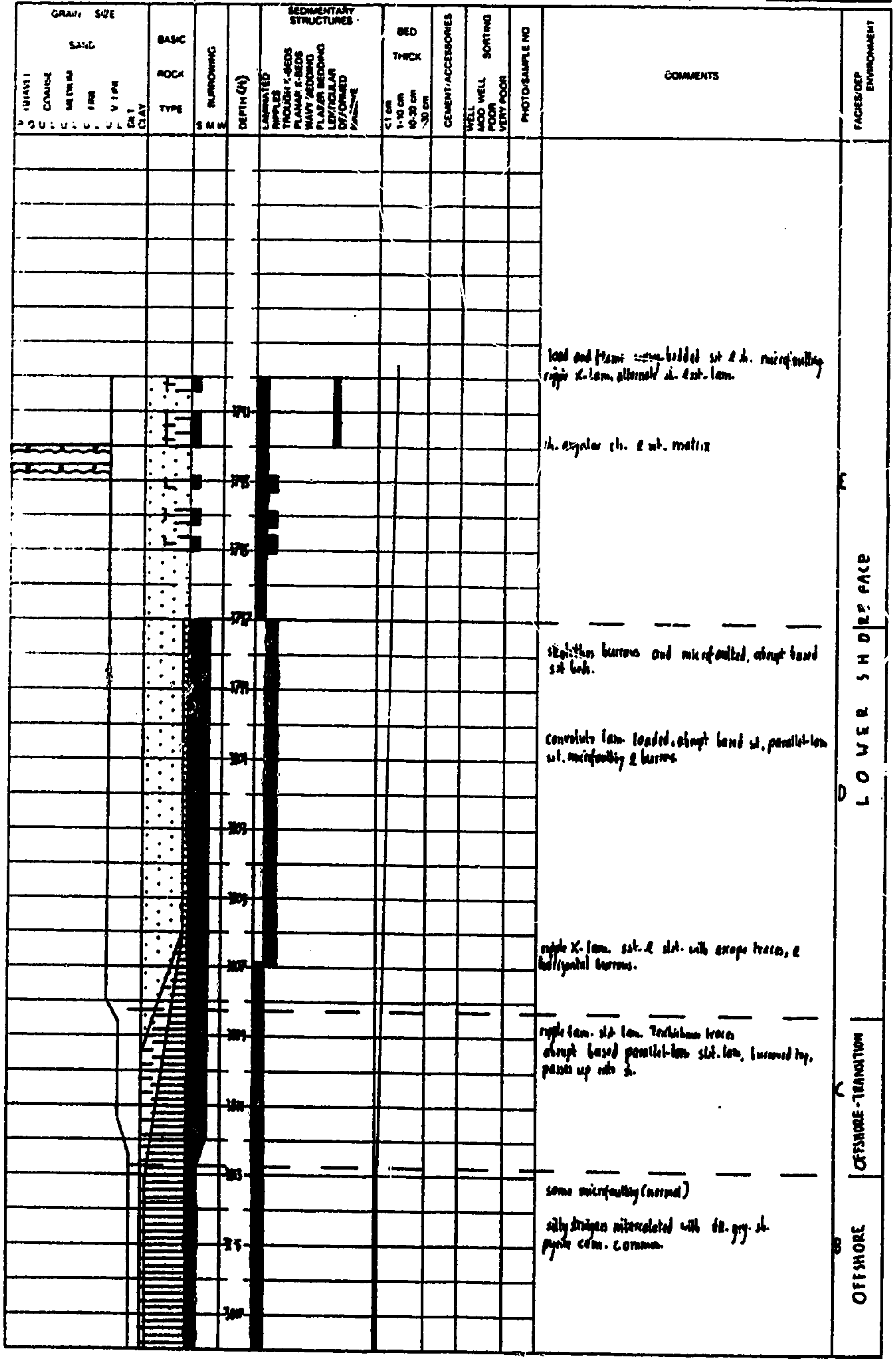

load and flame ~~[illegible]~~-bedded st & sh. microfaulting ripple X-lam. alternated sh. & st. lam.

sh. angular cl. & st. matrix

skolithos burrows and microfaulted, abrupt based sst beds.

convolute lam. loaded, abrupt based st, parallel-lam. st. microfaulting & burrows.

ripple X-lam. sst. & slst. with arenicolites traces, & helicoidal burrows.

ripple lam. slt lam. Teichichnus traces
abrupt based parallel-lam slst. lam., burrowed top, passes up into s.

some microfaulting (normal)

silty stringers intercalated with dk. gry. sh.
pyrite cem. common.

WELL NAME: CIGOL MOBIL PEEJAY
FORMATION: HALFWAY-CHARLIE LAKE
DATE: 13/08/90
LOCATIC: 6-056-E/94-A-16
CORE INTERVAL:
KB: 2397ft

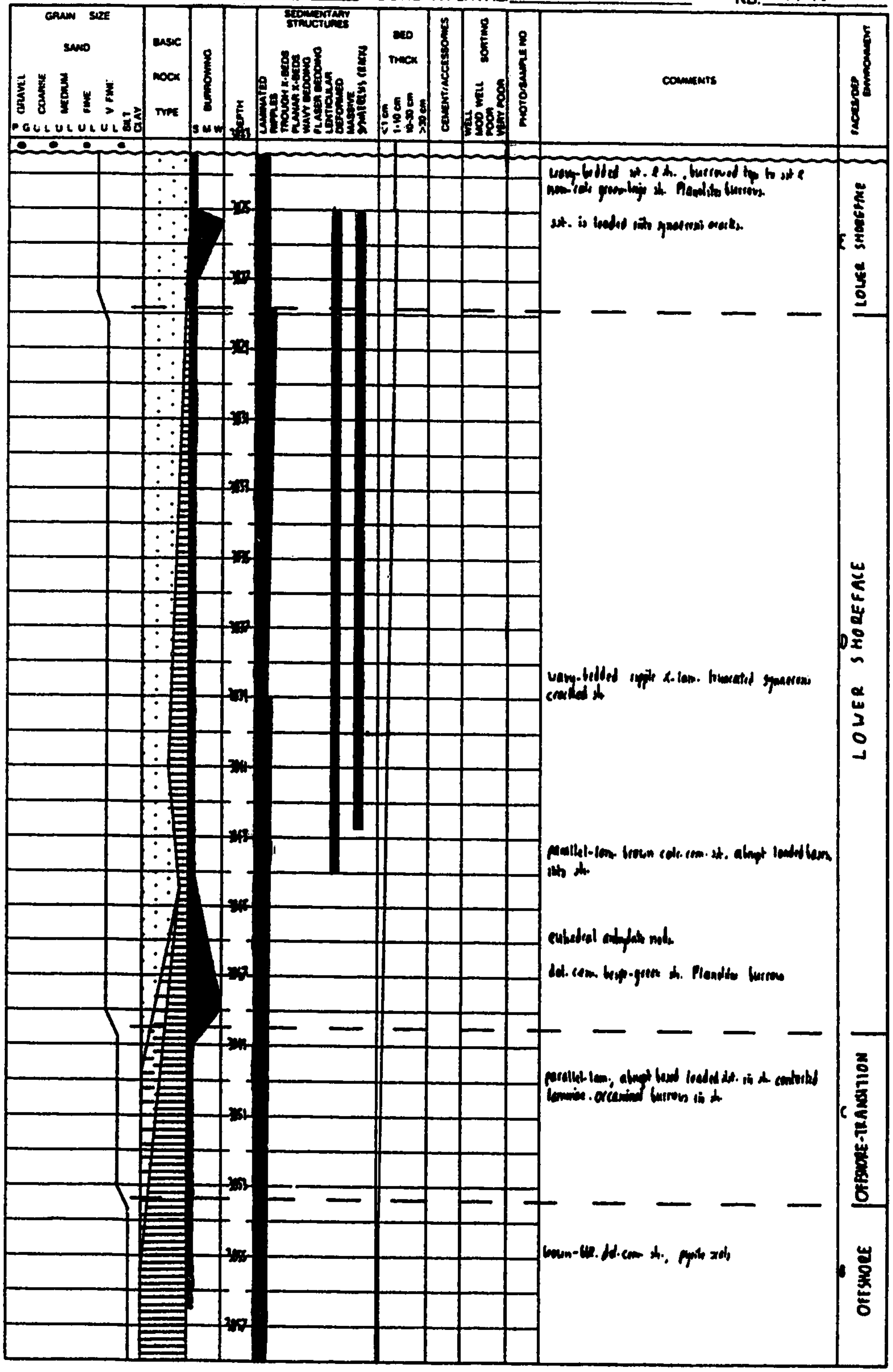

wavy-bedded sst. & sh., burrowed top to sst & non-calc green-beige sh. Planolites burrows.

sst. is loaded into synaeresis cracks.

wavy-bedded ripple x-lam. truncated synaeresis cracked sh.

parallel-lam. brown calc. cem. sst., abrupt loaded base, silty sh.

euhedral anhydrite nod.

dol. cem. beige-green sh. Planolites burrows

parallel-lam., abrupt based loaded sst. in sh. contorted laminae. occasional burrows in sh.

brown-blk. dol. cem. sh., pyrite nod.

WELL NAME CIGOL MOBIL PEEJAY

FORMATION: HALFWAY-CHARLIE LAKE

DATE: 13/08/90

LOCATION: 6-056-E/94-A-16

CORE INTERVAL:

KB: 2397ft

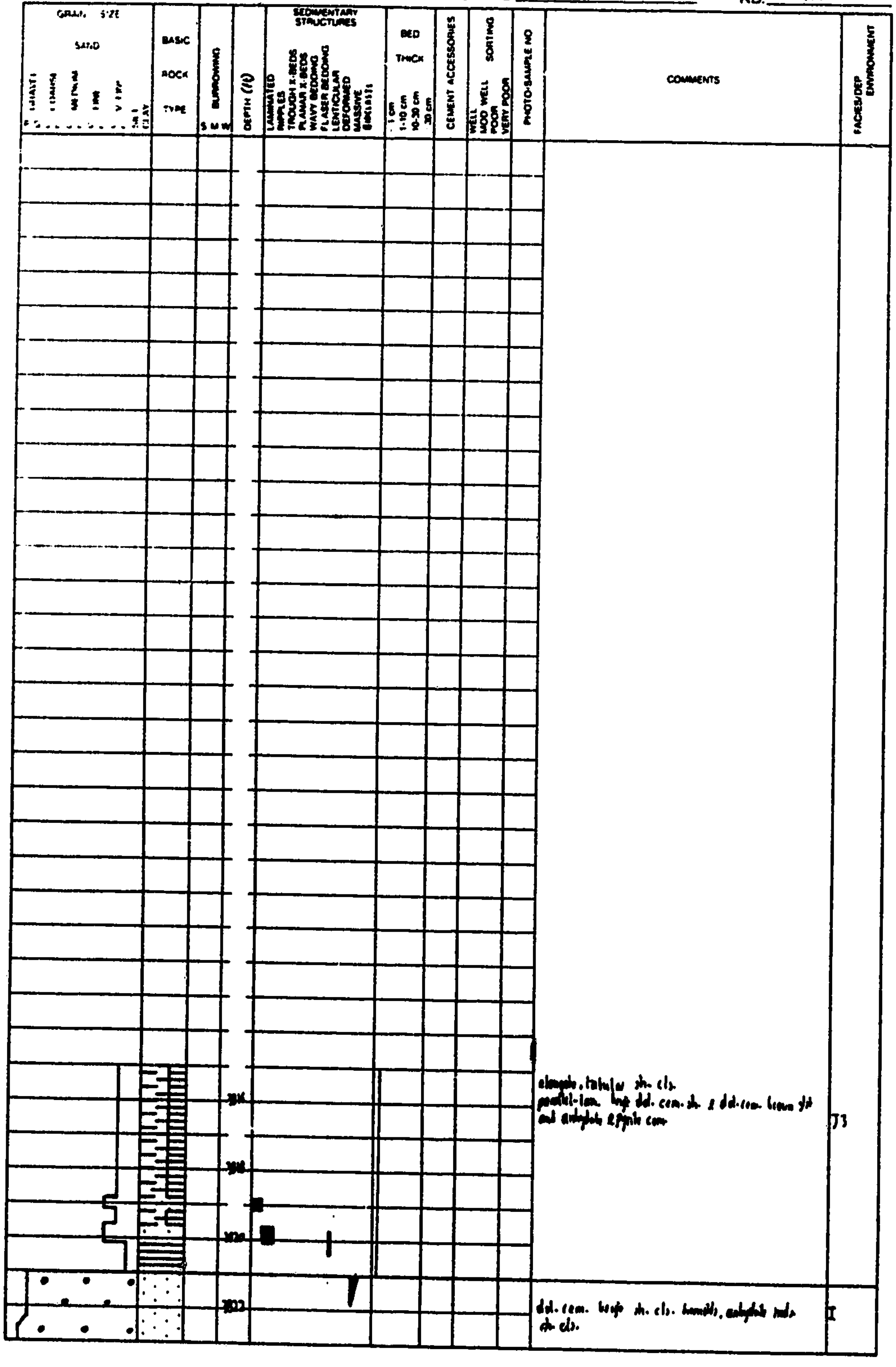

elongate, tabular sh. cls.
parallel-lam. burp dol. cem. sh. & dol-cem. brown slt and anhydrite & pyrite cem.

J3

dol. cem. burp sh. cls. burrowed, anhydrite nod. sh. cls.

I

WELL NAME: CIGOL MOBIL PEEJAY

FORMATION: HALFWAY-CHARLIE LAKE

DATE: 14/06/90

LOCATION: d-056-E/94-A-16

CORE INTERVAL:

KB: 2389ft

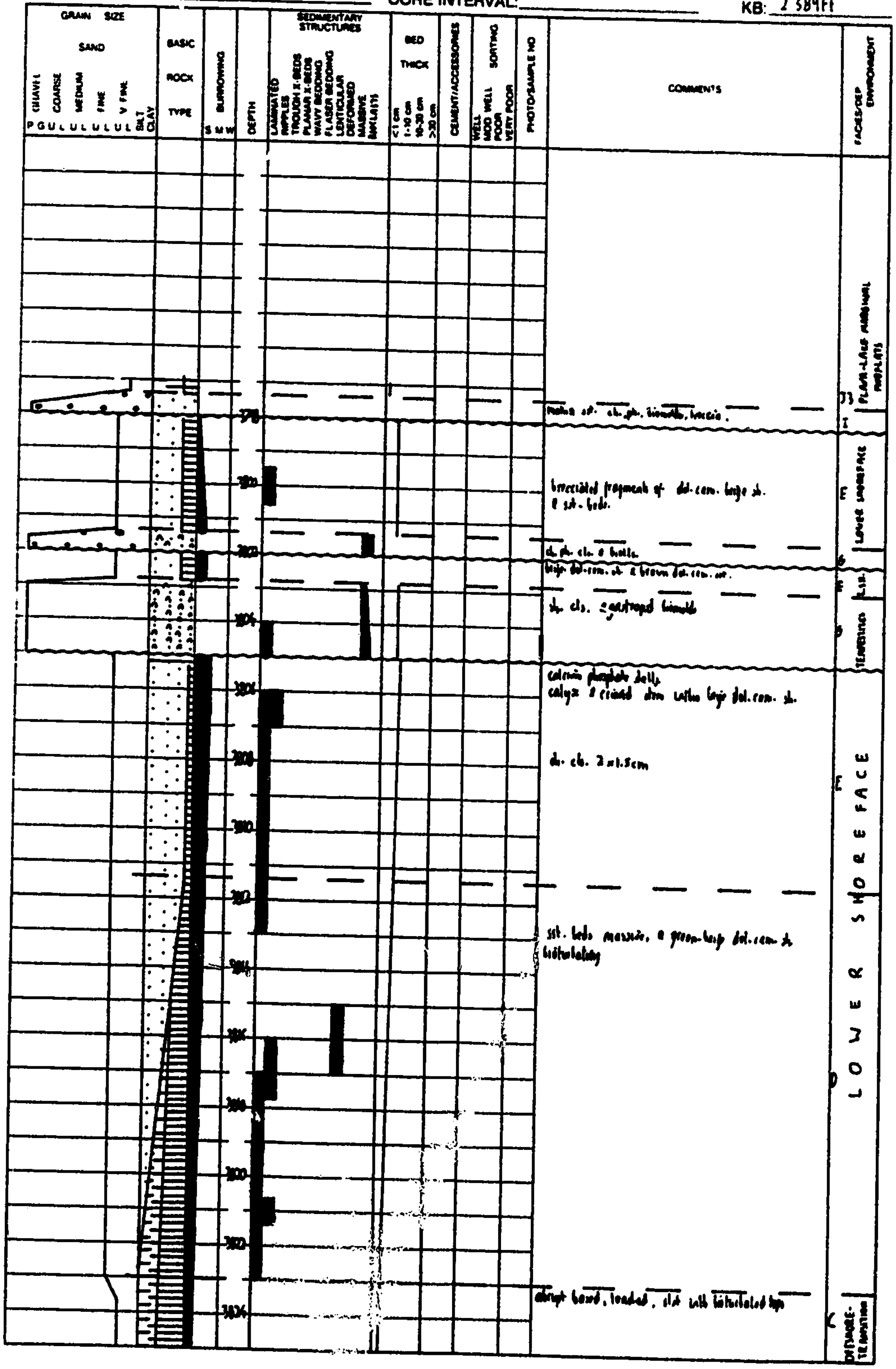

matrix sst. cl. ph. bioclasts, breccia.

brecciated fragments of dol.-cem. beige sh. & sst. beds.

ch. ph. cls. & [illegible]

beige dol.-cem. sh. & brown dol.-cem. sst.

sh. cls. gastropod bivalve

calcium phosphate balls

calyx & crinoid stem within beige dol.-cem. sh.

sh. cls. 2×1.5cm

sst. beds massive, & green-beige dol.-cem. sh. bioturbating

abrupt based, loaded, sst. with bioturbated top

WELL NAME SINCLAIR ET AL PEEJAY d-58-E FORMATION: HALFWAY-CHARLIE LAKE DATE: 6/02/91

LOCATION d-058-E/94-A-16 CORE INTERVAL: KB: 2393.4ft

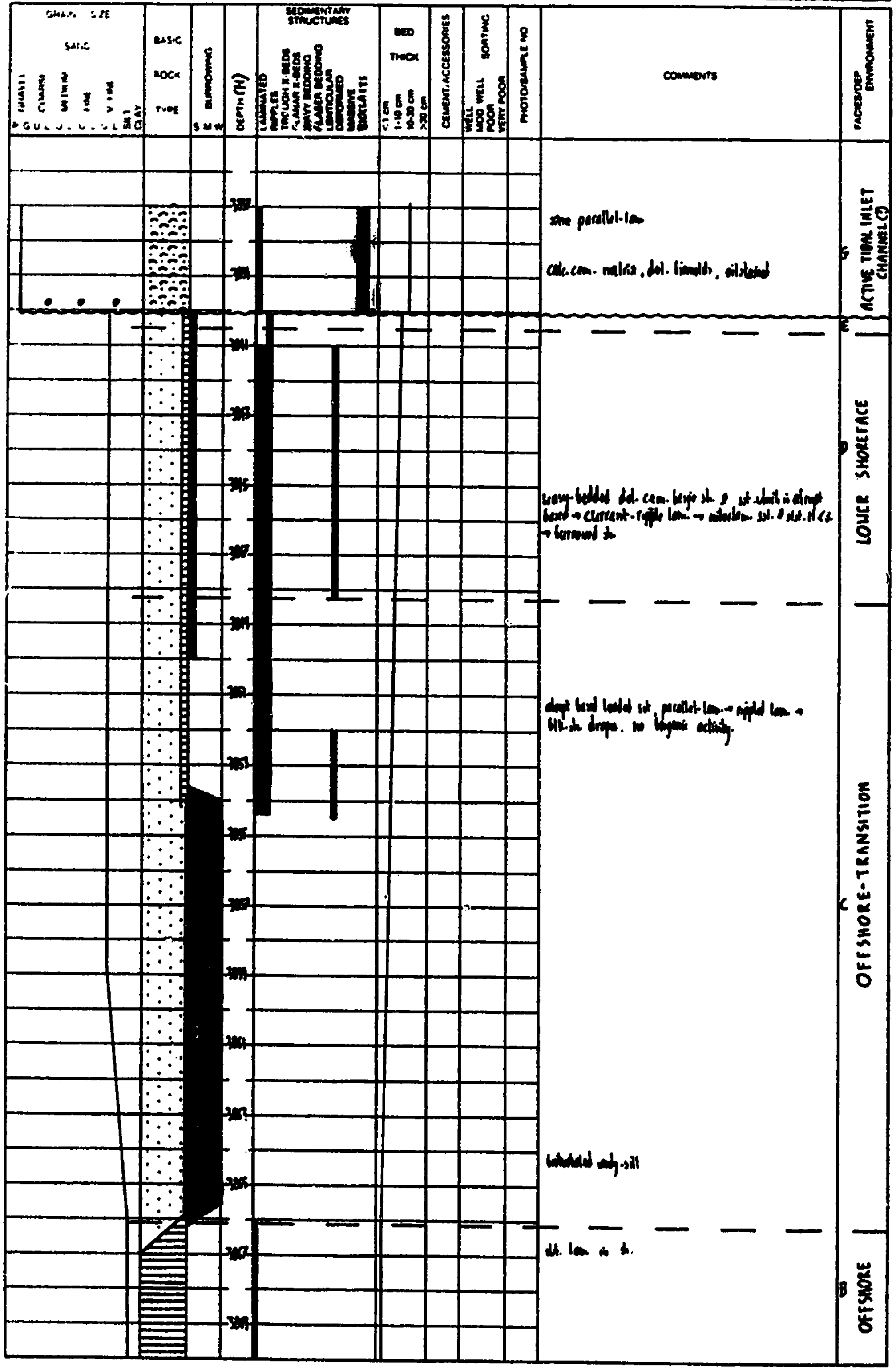

sme parallel-lam

calc.cem. matrix, dol. lithcls, oilstained

wavy-bedded dol.-cem. beige sh. & slt. which is abrupt based → current-ripple lam. → interlam. sst. & slt. HCS → burrowed sh.

abrupt based bedded sst. parallel-lam. → rippled lam. → blk.sh. drapes. no biogenic activity.

interbedded sndy-silt

dk. lam. sh.

WELL NAME: PACIFIC ET AL PEEJAY 6-59-E FORMATION: HALFWAY-CHARLIE LAKE DATE: 25/07/90

LOCATION: 6-059-E/94-A-16 CORE INTERVAL: KB: 2394 ft

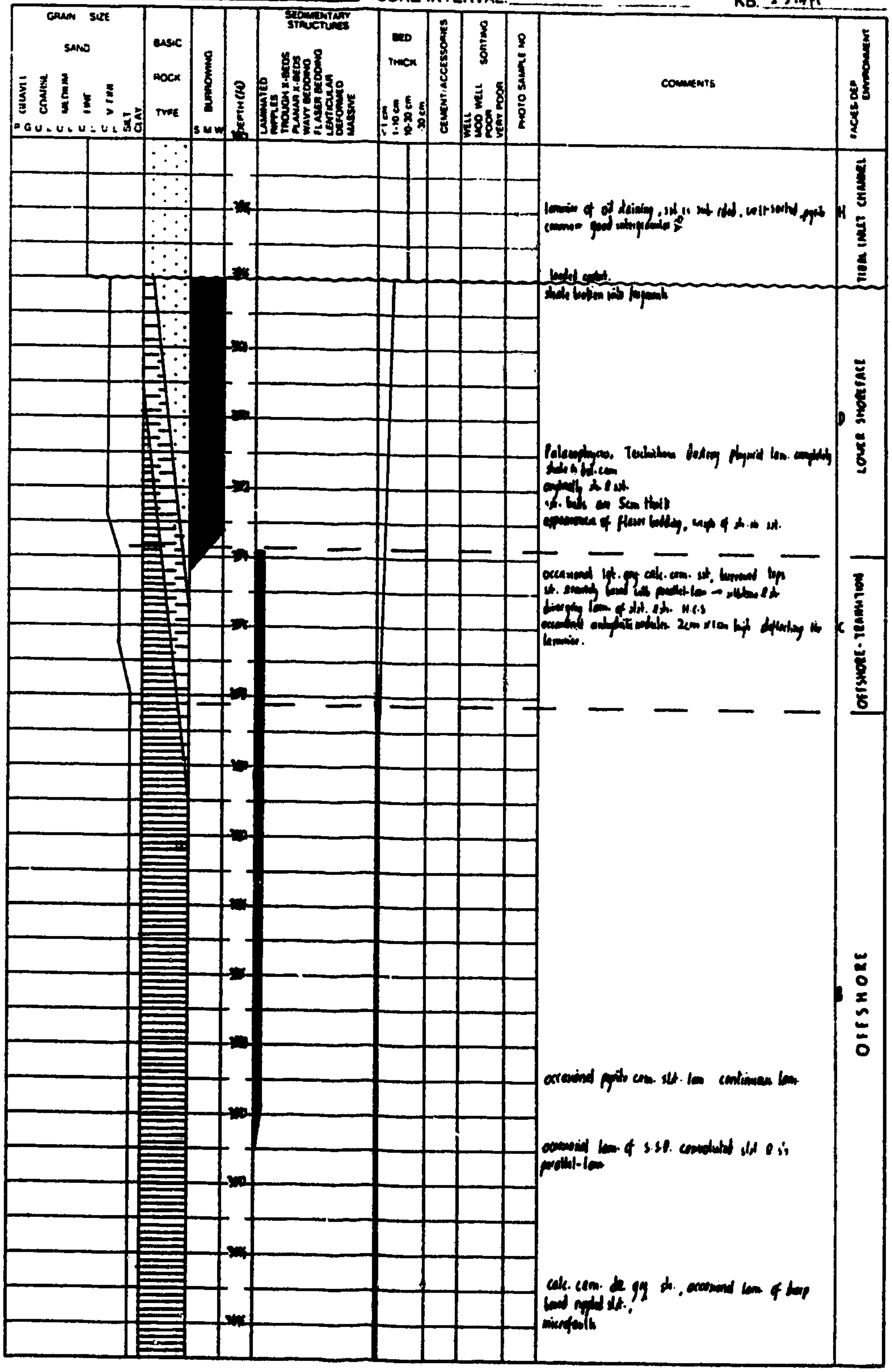

lamina of oil staining, sd. is sub rdd. well-sorted, pyrite
common good interparticle ϕ

loaded contact.
shale broken into fragments

Palaeophycus, Teichichnus destroying physical lam. completely
shale to bd.com
originally sh & slt.
sd. beds are 5cm thick
appearance of flaser bedding, wisps of sh. in slt.

occasional lt. gry calc. cem. slt, burrowed tops
slt. strongly bound with parallel-lam → siltstone & sh.
diverging lam. of slt. & sh. H.C.S
occasional anhydrite nodules. 2cm x 1cm high deflecting the
laminae.

occasional pyrite cem. slt. lam continuous lam.

occasional lam. of s.s.t. convoluted slt & sh
parallel-lam

calc. cem. dk. gry sh., occasional lam. of [illegible]
band rippled slt.,
microfossils

WELL NAME PACIFIC ETAL PEEJAY 6-59-E

FORMATION: HALFWAY-CHARLIE LAKE

DATE: 25/07/90

LOCATION: 6-059-E/94-A-16

CORE INTERVAL:

KB: 2394 ft

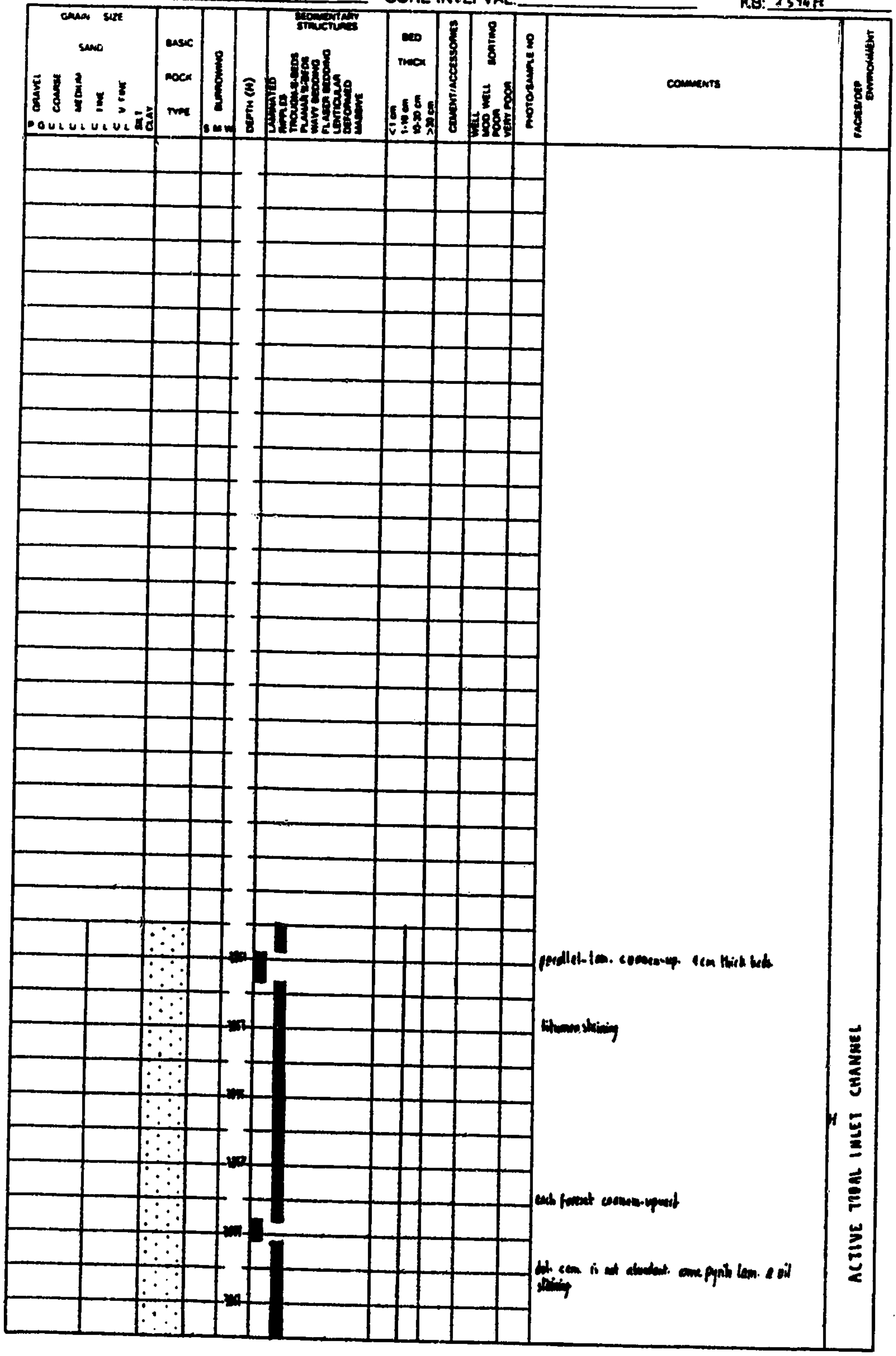

parallel-lam. coarsen-up. 4cm thick beds

bitumen staining

each foreset coarsen-upward

bi. com. is not abundant. some pyrite lam. & oil staining

ACTIVE TIDAL INLET CHANNEL

WELL NAME: PACIFIC SR CANDEL PEEJAY

FORMATION: HALFWAY-CHARLIE LAKE

DATE 13/06/90

LOCATION: 6-067-E/94-A-16

CORE INTERVAL:

KB: 2399ft

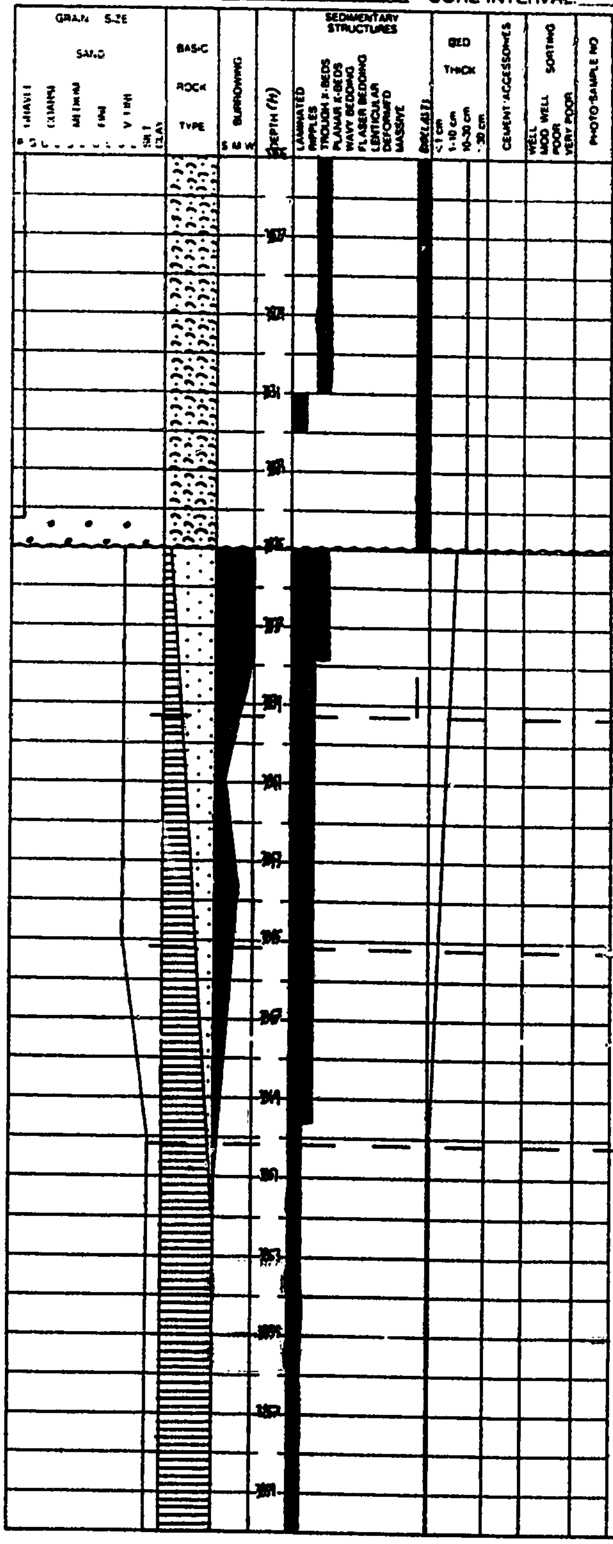

COMMENTS

ooidal O, some bioclasts, infilled with calcite

foreset laminae 5°, each laminae f.-U. & cement increases upward.
shells parallel to bedding, some imbrication,

ostracods up to 3cm long & calcite filled.
matrix m. to f.L.

large dol.-sh. basal conglomerate.

large scale ripple X-lam. some vertical escape traces & Teichichnus · Ch. frag. mottles.

wavy-bedded ss. & sh. ss is calc. cem. massive with ripple X-lam. & interbedded with mudstone oxidized sh. Oblique & horizontal burrows (Teichichnus)

silty lam. & biogenic activity increases upward
sd. lam. current & ripple lam. abrupt bases, 3mm thick, grad-top with burrowed, blk., sh.

blk. mudstones sh. pyrite cemented

FACIES/DEP ENVIRONMENT

F ACTIVE TIDAL INLET CHANNEL

E

D LOWER SHOREFACE

C OFFSHORE-TRANSITION

B OFFSHORE

WELL NAME: PACIFIC SR CANDEL PEEJAY
FORMATION: HALFWAY- CHARLIE LAKE
DATE: 13/06/90
LOCATION: 6-067-E/94-A-16
CORE INTERVAL:
KB: 2399ft

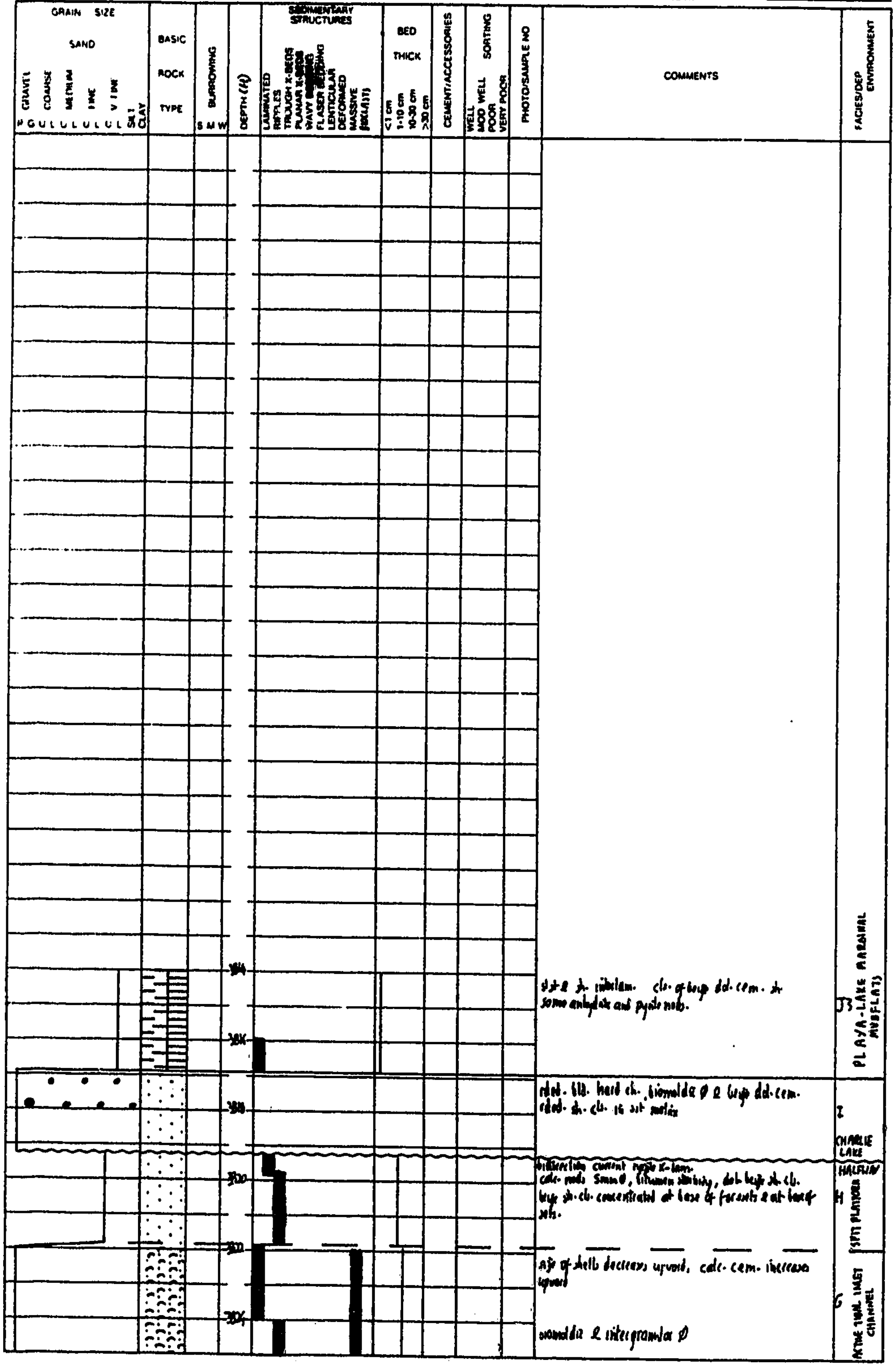

slt & sh. interlam. cls. of brgp dd. cem. sh. some anhydrite and pyrite nods.

J3 PLAYA-LAKE MARGINAL (MUDFLATS)

rdd. bld. hard cl. biomolds ∅ & brgp dd. cem. rdd. sh. cls. in ssl matrix

I

CHARLIE LAKE

HALFWAY

bidirectional current ripple x-lam. calc. moldc Sand ∅, bitumen staining, dol. brgp sh. cls. brgp sh. cls. concentrated at base of forsets & at base of sets.

H SPIT PLATFORM

size of shells decreases upward, calc. cem. increases upward

moldic & intergranular ∅

G ACTIVE TIDAL INLET CHANNEL

WELL NAME: MEDALLION ASHLAND PEEJAY
FORMATION: HALFWAY - CHARLIE LAKE
DATE: 9/08/90
LOCATION. 6-068-E/94-A-16
CORE INTERVAL:
KB: 2407ft

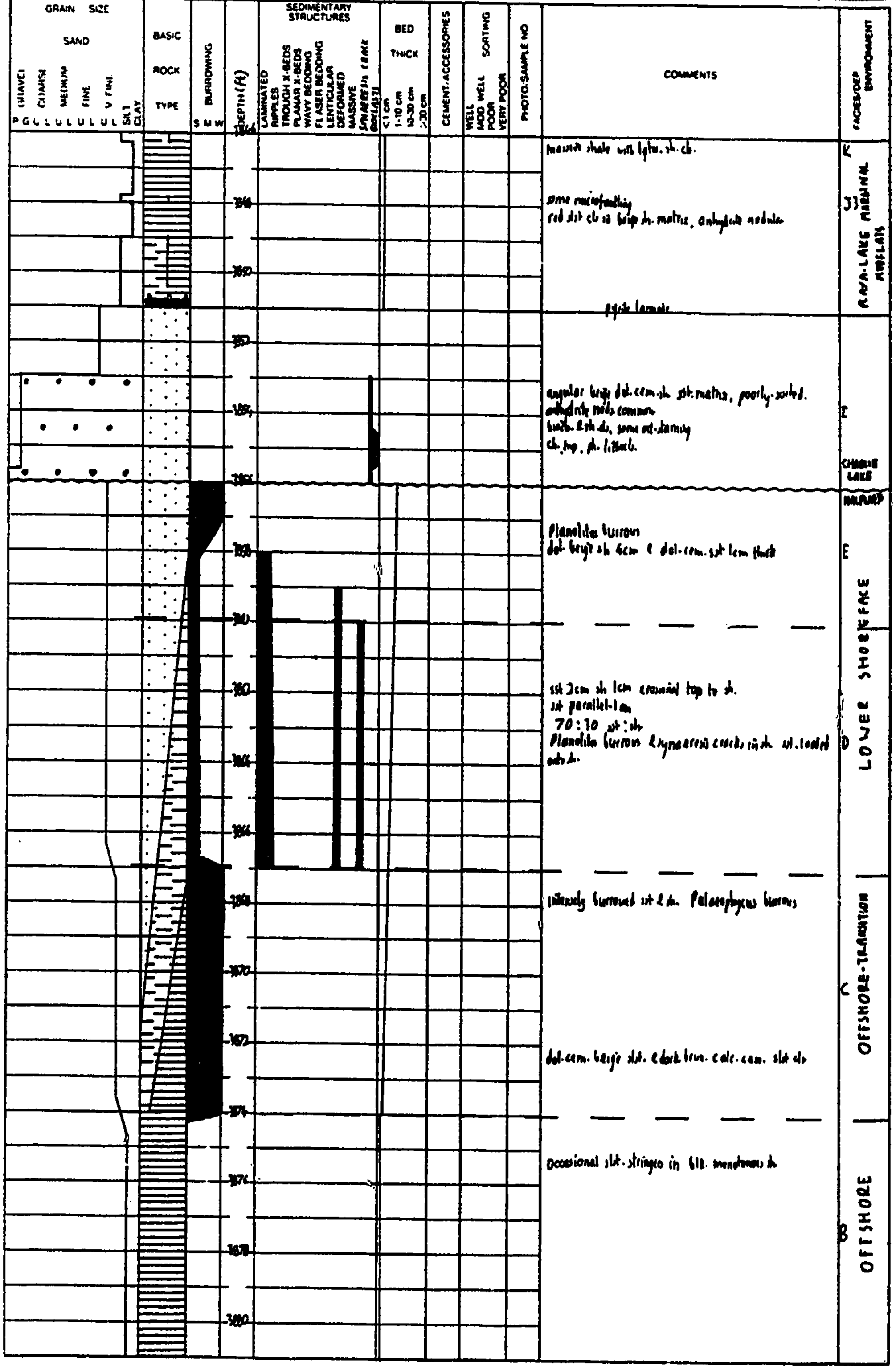

massive shale with lgtn. sh. cb.

some microfaulting
red slst cls in beige sh. matrix, anhydrite nodules

pyrite laminae

angular beige dol.cem. sh. sst. matrix, poorly-sorted.
anhydrite nods common
burro. & sh. cls, some sol.-damaging
ch. imp. ph. lithcl.

Planolites burrows
dol. beige sh 4cm & dol.-cem. sst 1cm thick

sst 3cm sh 1cm erosional top to sh.
sst parallel-lam
70:30 sst : sh
Planolites burrows & syneresis cracks in sh. wl. loaded onto sh.

intensely burrowed sst & sh. Palaeophycus burrows

dol.-cem. beige slst. & dark brn. calc.-cem. slst cls

occasional slst. stringers in blk. monotonous sh.

WELL NAME: PACIFIC ET AL PEEJAY 6-69-E

FORMATION: HALFWAY-CHARLIE LAKE

DATE: 1/02/91

LOCATION: 6-069-E/94-A-16

CORE INTERVAL:

KB: 2396ft

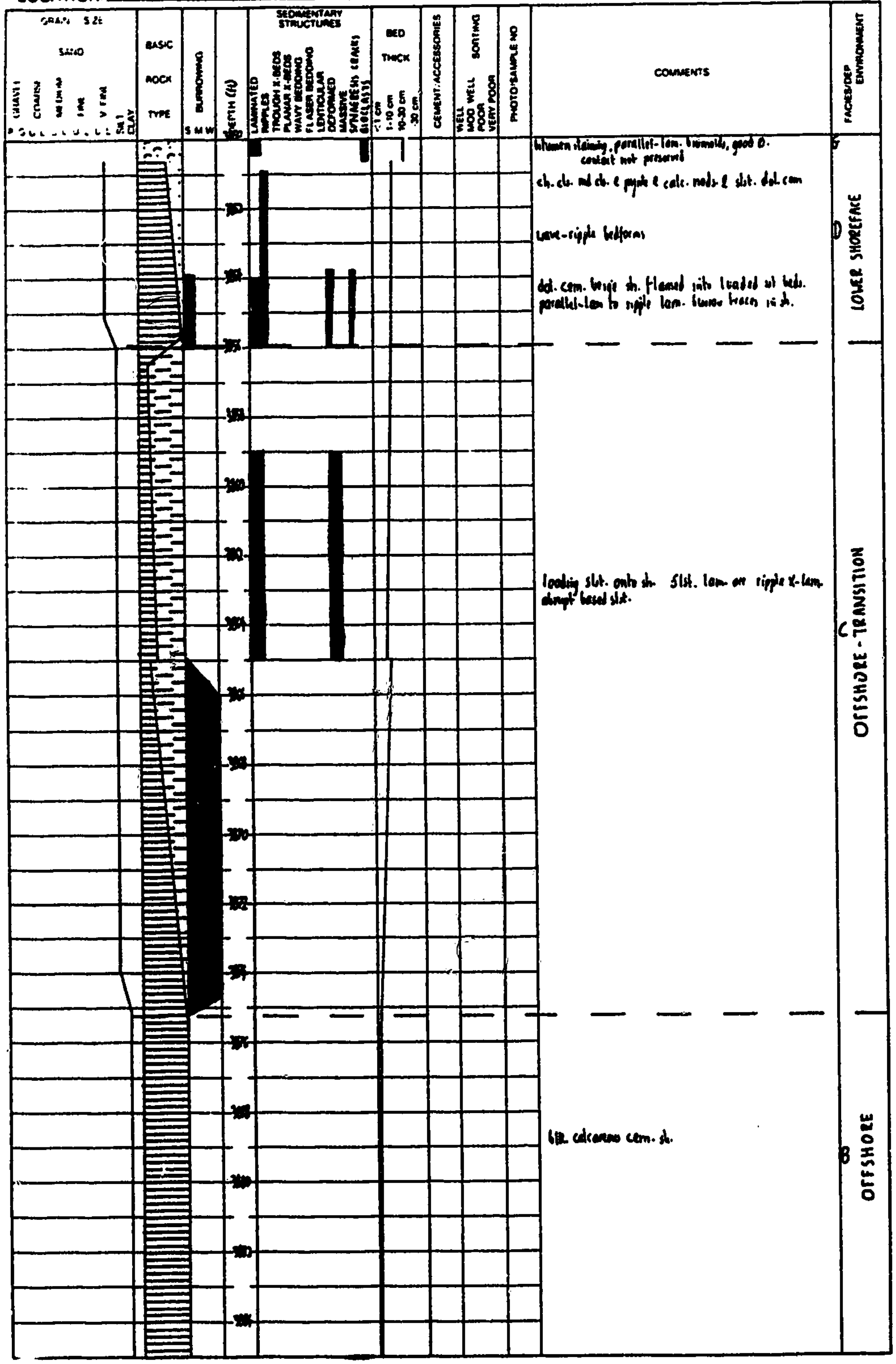

bitumen staining, parallel-lam. bivalves, good Ø.
contact not preserved

ch. cls. md cls. c pyrite c calc. nods. c slst. dol. cem

wave-ripple bedforms

dol. cem. beige sh. flasered silts loaded at beds.
parallel-lam to ripple lam. burrow traces in sh.

loading slt. onto sh. Slst. lam. or ripple X-lam.
abrupt based slt.

blk. calcareous cem. sh.

WELL NAME: PACIFIC ET AL PEEJAY 6-69-E FORMATION: HALFWAY- CHARLIE LAKE DATE: 1/02/91

LOCATION: 6-069-E/94-A-16 CORE INTERVAL: KB: 2396 ft

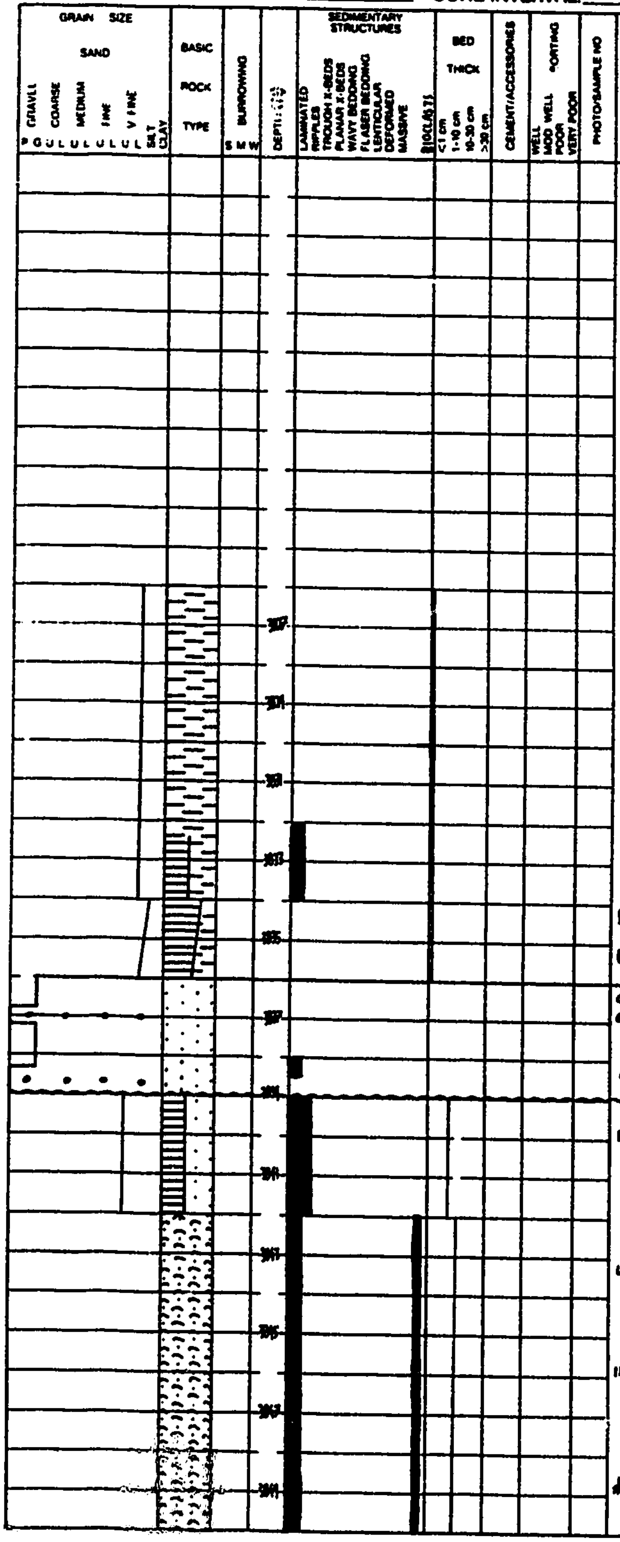

COMMENTS

cb. of sh.

lam. red slt. & beige sh.

beige dol-cem. sh & red slt. with sh. cb.

cb. of angular to sub-rounded dol. cem. sh., slt matrix and anhydrite nods.

cb. of red dol. sh. with slt. matrix

dol. cem. slt, parallel-lam. → wave ripple lam. → shale

contact not preserved

bitumen plugging biomolds. Shell quantity decreases upward.

bitumen occurs in layers

increase in anhydrite nods. plugging up Gastropod biomolds

shells, parallel-lam.

FACIES/DEP ENVIRONMENT

J2

J3

PLAIN-LAKE MARGINAL MUDFLATS

I

CHARLIE LAKE

HALFWAY

E

G

ACTIVE TIDAL INLET CHANNEL

WELL NAME: MEDALLION ASHLAND PEEJAY d-69-E
FORMATION: HALFWAY-CHARLIE LAKE
DATE: 12/06/90
LOCATION: d-069-E/94-A-16
CORE INTERVAL:
KB: 2396 ft

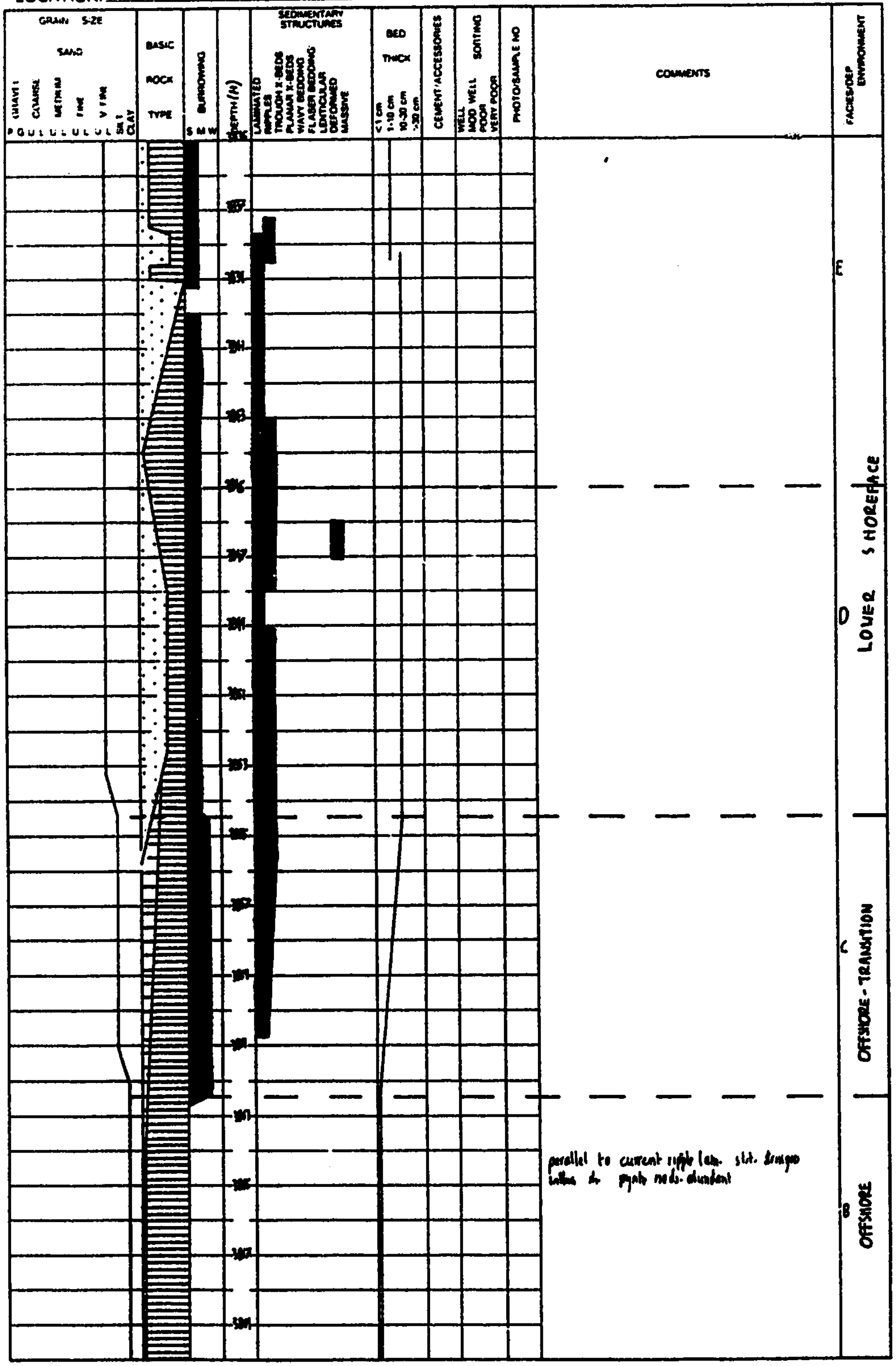

parallel to current ripple lam. slt. [illegible]
[illegible] [illegible] pyrite nods. abundant

WELL NAME: MEDALLION ASHLAND PEEJAY d-69-E FORMATION: HALFWAY-CHARLIE LAKE DATE: 12/06/90

LOCATION: d-069-E/94-A-16 CORE INTERVAL: KB: 2396ft

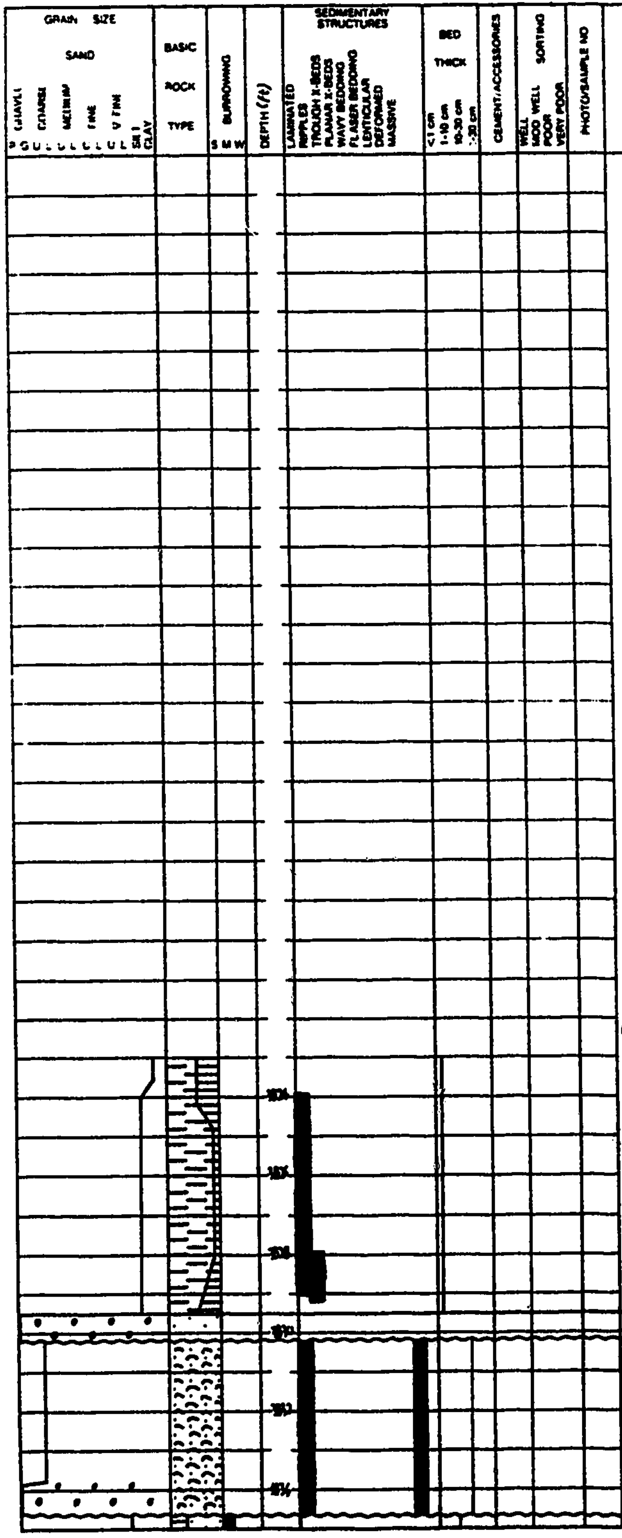

COMMENTS	FACIES/DEP ENVIRONMENT
massive anhydrite replaces red sh. red sh. anhydrite nods. coalesced, e.d.-cls. anhydrite & pyrite nods. common interlam. dol. & sh.	7 2 PLAYA-LAKE MARGINAL MUDFLATS
dol. cem. long. [illegible]	1
anhydrite nods. scatter upward ooids decrease in size & quantity [illegible] cl. top, ph & sh fragments scattered in lithofacies bimodal coarsen-up	6 ACTIVE TIDAL INLET CHANNEL

WELL NAME: UNION HB SPRUCE d-74-E
FORMATION: HALFWAY-CHARLIE LAKE
DATE: 15/08/90
LOCATION: d-074-E/94-A-16
CORE INTERVAL:
KB: 2400ft

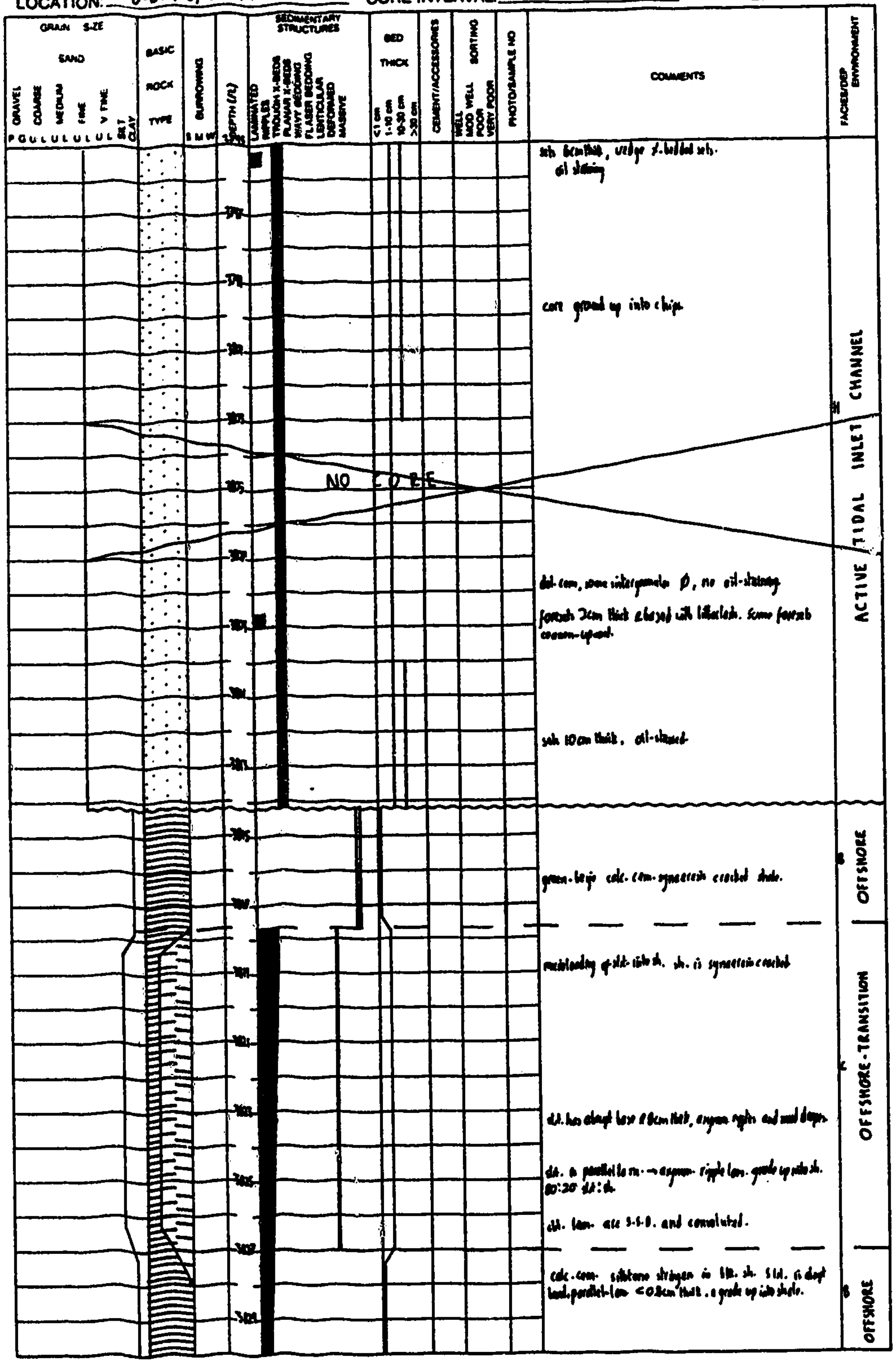

sst. 6cm thick, wedge x-bedded sst.
oil staining

core ground up into chips.

dol. cem., some intergranular ϕ, no oil-staining.

forset 3cm thick draped with lithoclasts. some forset coarsen-upward.

sst. 10cm thick. oil-stained.

green-beige calc. cem. syneresis cracked shale.

mudcloading of slt. into sh. sh. is syneresis cracked

slt. has abrupt base 8cm thick, asymm. ripples and mud drapes.

slt. a parallel lam. → asymm. ripple lam. grade up into sh. 80:20 slt:sh.

slt. lam. are S-S-D. and convoluted.

calc. cem. siltstone stringers in blk. sh. Slt. is abrupt based, parallel-lam <0.8cm thick, & grade up into shale.

WELL NAME: UNION H B SPRUCE d-074-E FORMATION: HALFWAY-CHARLIE LAKE DATE: 15/08/90

LOCATION: d-074-E/94-A-16 CORE INTERVAL: KB: 2400ft

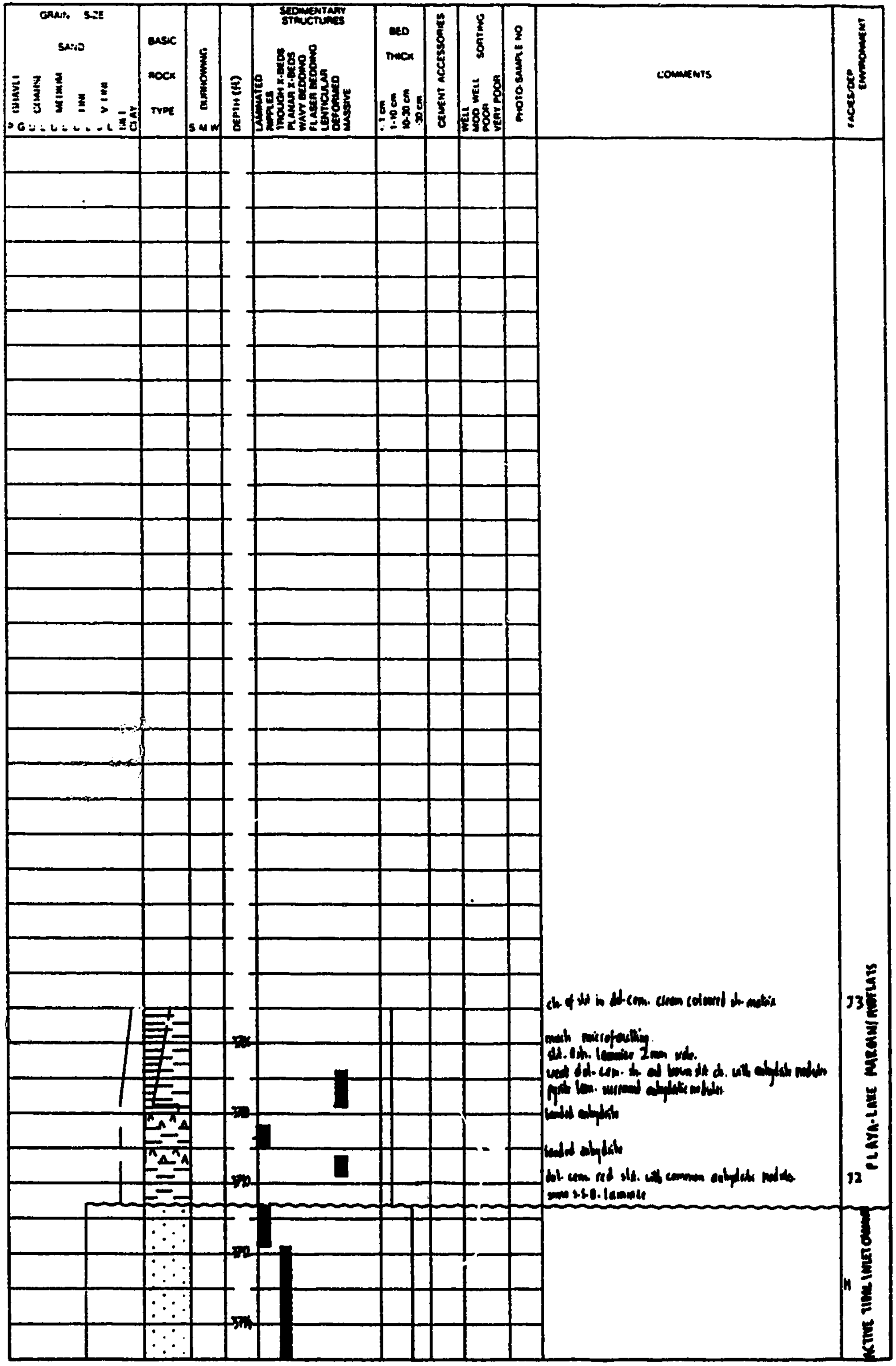

cls. of slt in dol-cem. cream coloured sh. matrix

much microfaulting.

sld. f.lh. laminae 2mm wide.

weak dol-cem. sh. and brown slt cl. with anhydrite nodules

pyrite lam. surround anhydrite nodules.

banded anhydrite

banded anhydrite

dol-cem. red slt. with common anhydrite nodules

some s-s-B. laminae

WELL NAME: UNION H B SPRUCE d-084-E

FORMATION: HALFWAY- CHARLIE LAKE

DATE: 14/08/90

LOCATION: d-084-E/94-A-16

CORE INTERVAL:

KB: 2411ft

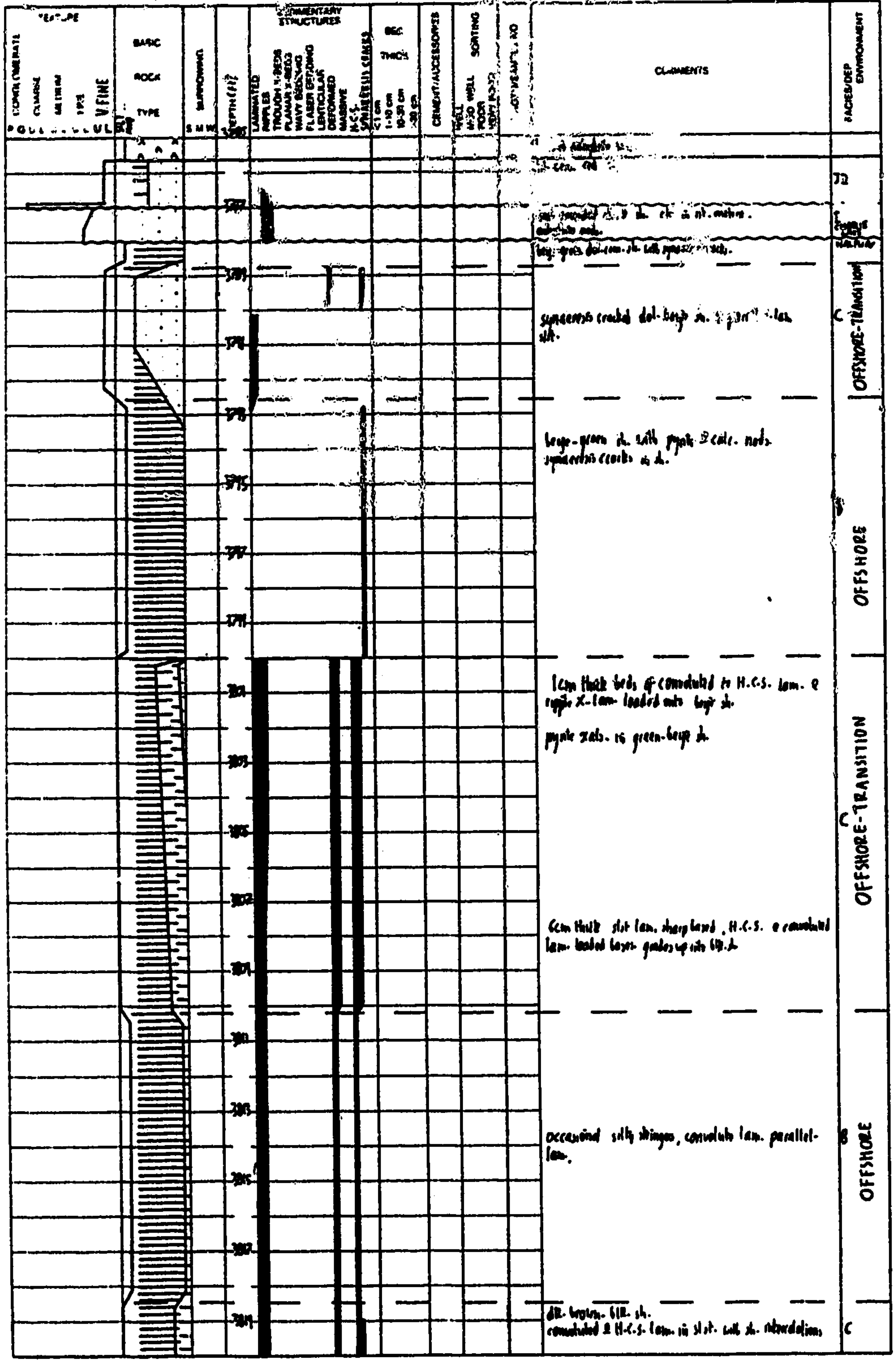

[illegible] anhydrite [illegible]
[illegible] cem. [illegible]

[illegible] rounded cl., & sh. clr in slt. matrix.
anhydrite nod.

beige-grey dol-cem. sh. with synaeresis cracks.

synaeresis cracks dol-beige sh. & green [illegible] lam. silt.

beige-green sh. with pyrite & calc. nods.
synaeresis cracks in sh.

1cm thick beds of convoluted to H.C.S. lam. & ripple X-lam. loaded into beige sh.

pyrite nods. in green-beige sh.

6cm thick slst lam. sharp based, H.C.S. & convoluted lam. loaded bases grades up into blk. sh.

occasional silty stringers, convolute lam. parallel-lam.

dk. brown. blk. sh.
convoluted & H.C.S. lam. in slst. with sh. [illegible]

WELL NAME: UNION HB SPRUCE d-084-E FORMATION: HALFWAY-CHARLIE LAKE DATE: 14/08/90

LOCATION: d-084-E/94-A-16 CORE INTERVAL: KB: 2411ft

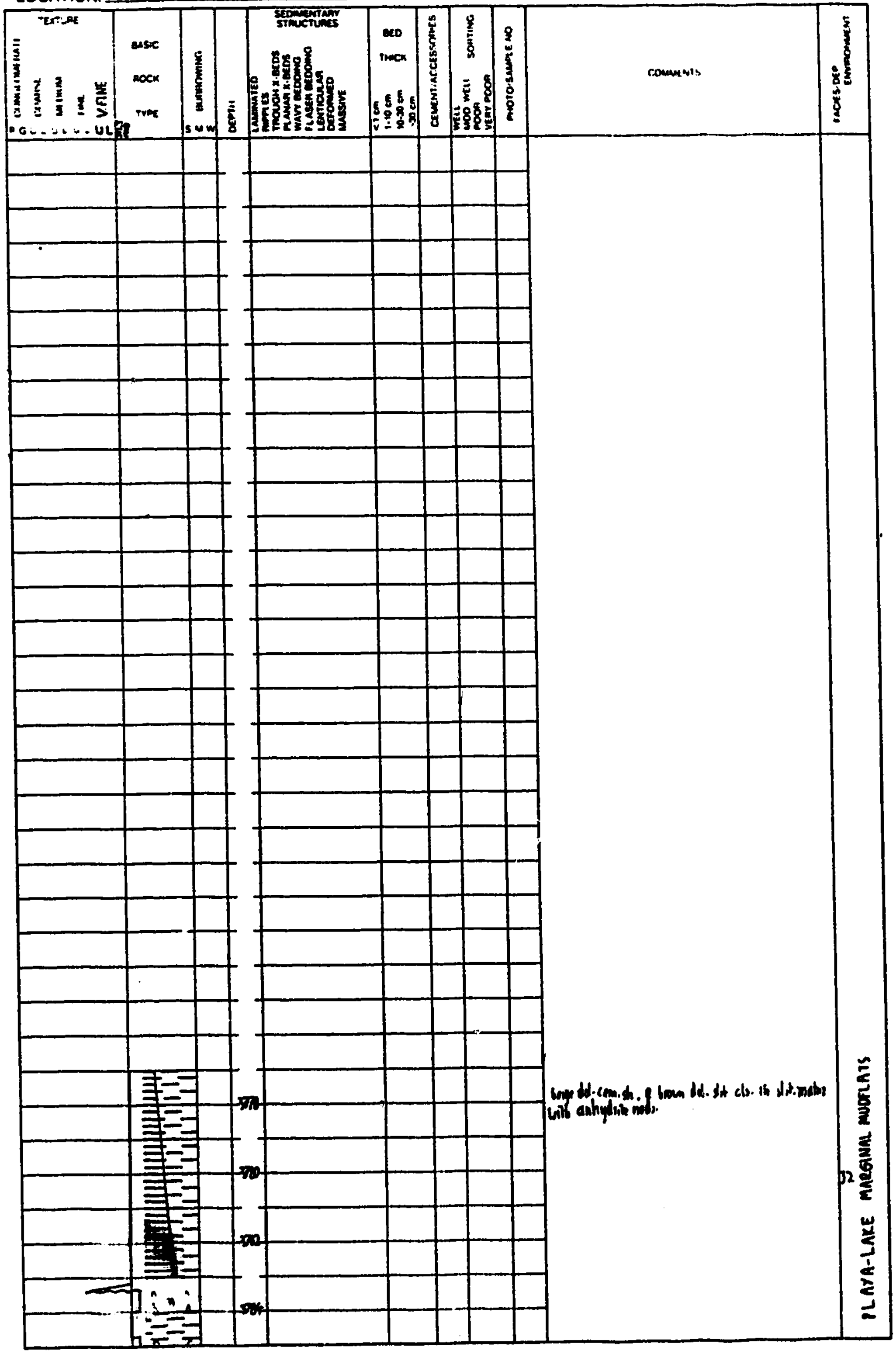

beige dol-cem. sh. & brown dol. slt clst. in slst. matrix with anhydrite nods.

PLAYA-LAKE MARGINAL MUDFLATS

WELL NAME: PACIFIC SR CAM DEL PEEJAY d-100-E FORMATION: HALFWAY-CHARLIE LAKE DATE: 7/08/90

LOCATION: d-100-E/94-A-16 CORE INTERVAL: KB: 2377ft

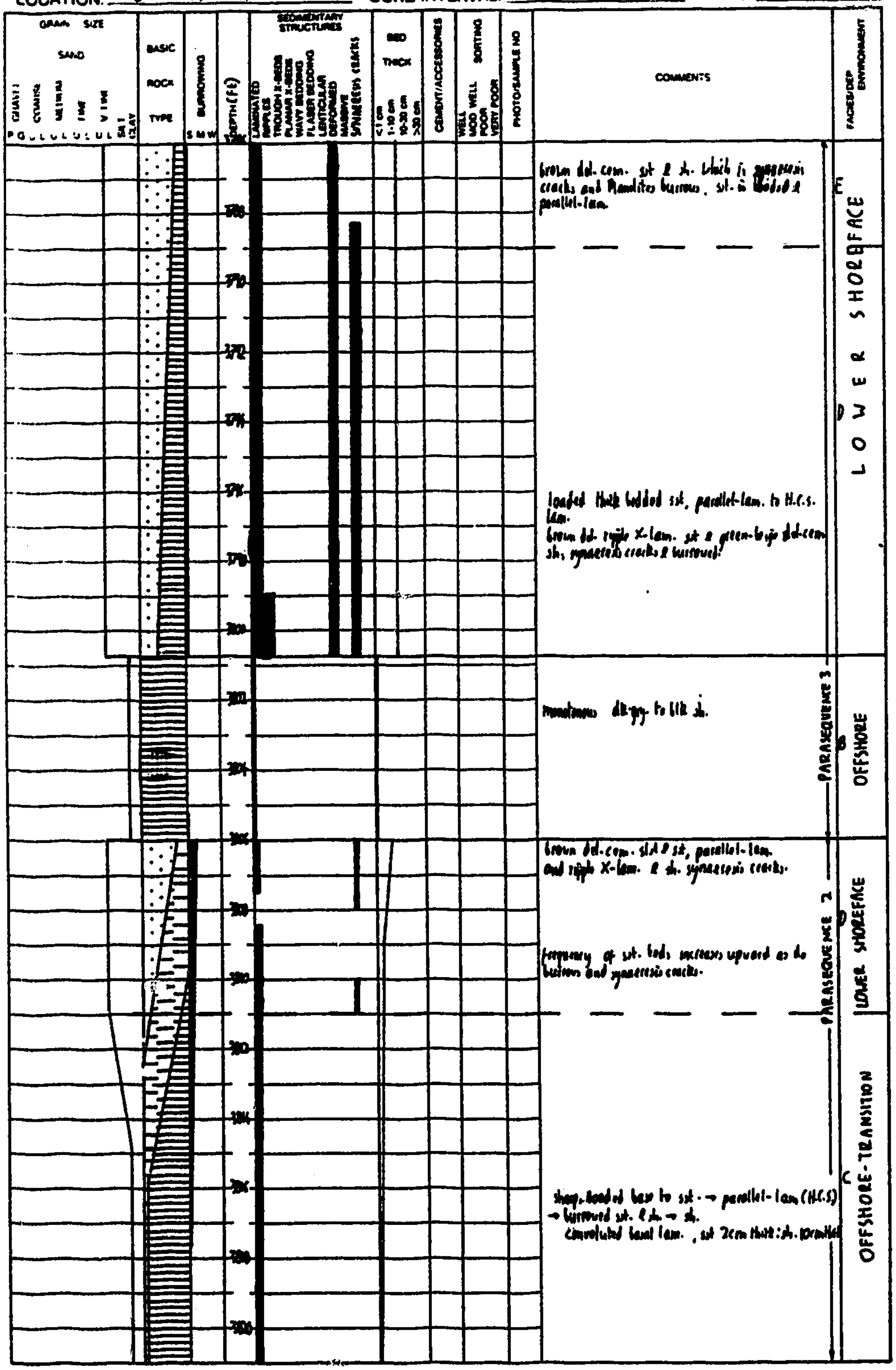

brown dol.-cem. slt & sh. which is synaeresis cracks and Planolites burrows, slt. is ~~[illegible]~~ [illegible] & parallel-lam.

loaded thick bedded sst, parallel-lam. to H.C.S. lam.
brown dol. ripple X-lam. slt & green-beige dol-cem sh, synaeresis cracks & burrowed.

monotonous dk-gy. to blk sh.

brown dol.-cem. slt & sst, parallel-lam. and ripple X-lam. & sh. synaeresis cracks.

frequency of slt. beds increases upward as do burrows and synaeresis cracks.

sharp, loaded base to sst. → parallel-lam (H.C.S) → burrowed slt. & sh. → sh.
Convoluted basal lam., sst 2cm thick: sh. parallel

WELL NAME: PACIFIC SR CAM DEL PEEJAY d-100-E FORMATION: HALFWAY-CHARLIE LAKE DATE: 7/08/90

LOCATION: d-100-E/94-A-16 CORE INTERVAL: KB: 2377ft

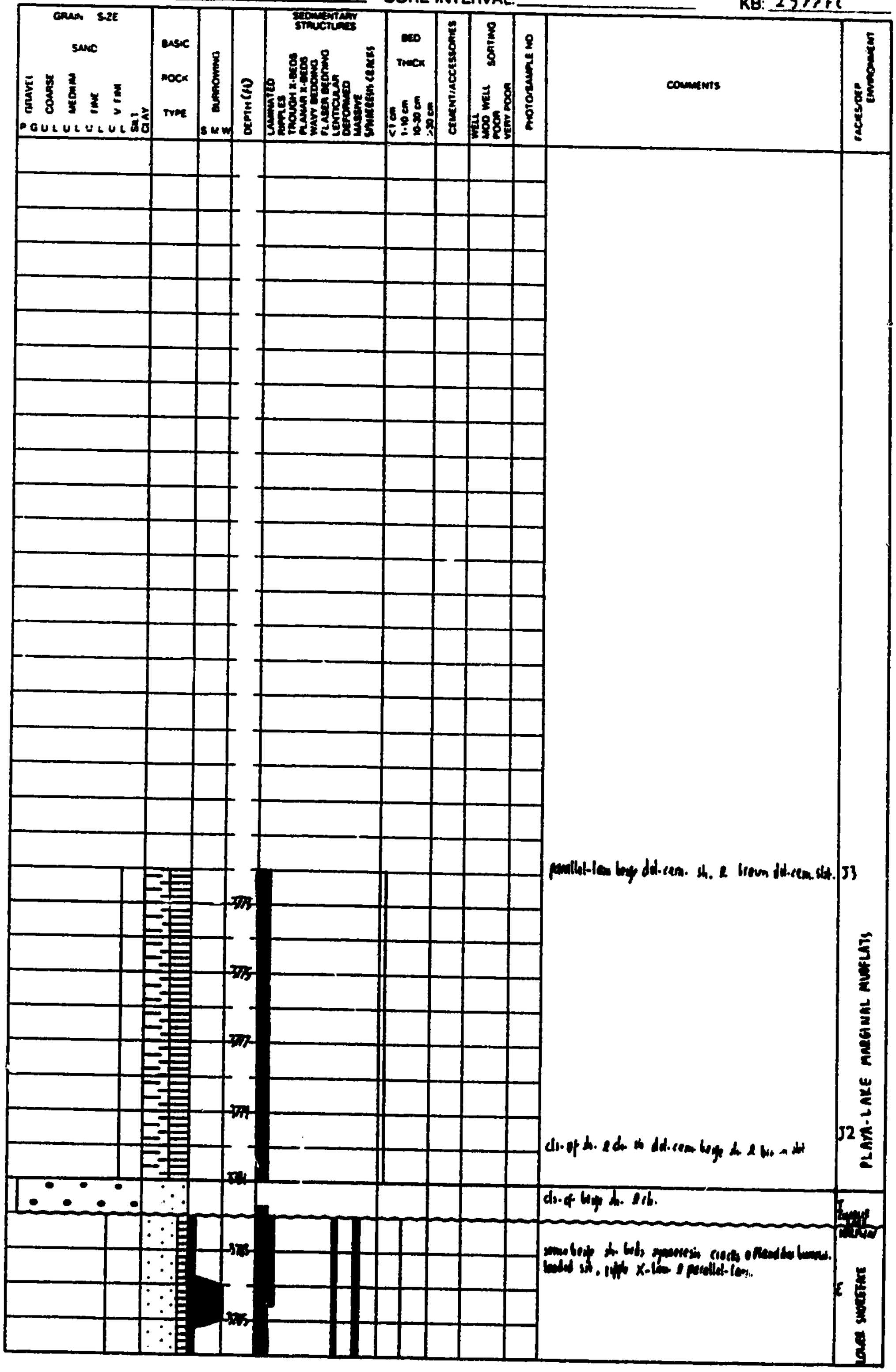

parallel-lam. beige dol.-cem. sh. & brown dol.-cem. slst. J3

cls.-of sh. & cls. in dol.-cem. beige sh. & brown slst. J2

cls.-of beige sh. [illegible] I

some beige sh. beds, syneresis cracks & Planolites burrows. banded slt., ripple X-lam. & parallel-lam. K

WELL NAME: CIGOL CRUSH FORMATION: HALFWAY-CHARLIE LAKE DATE: 20/06/90

LOCATION: d-010-F/94-A-16 CORE INTERVAL: KB: 2394 ft

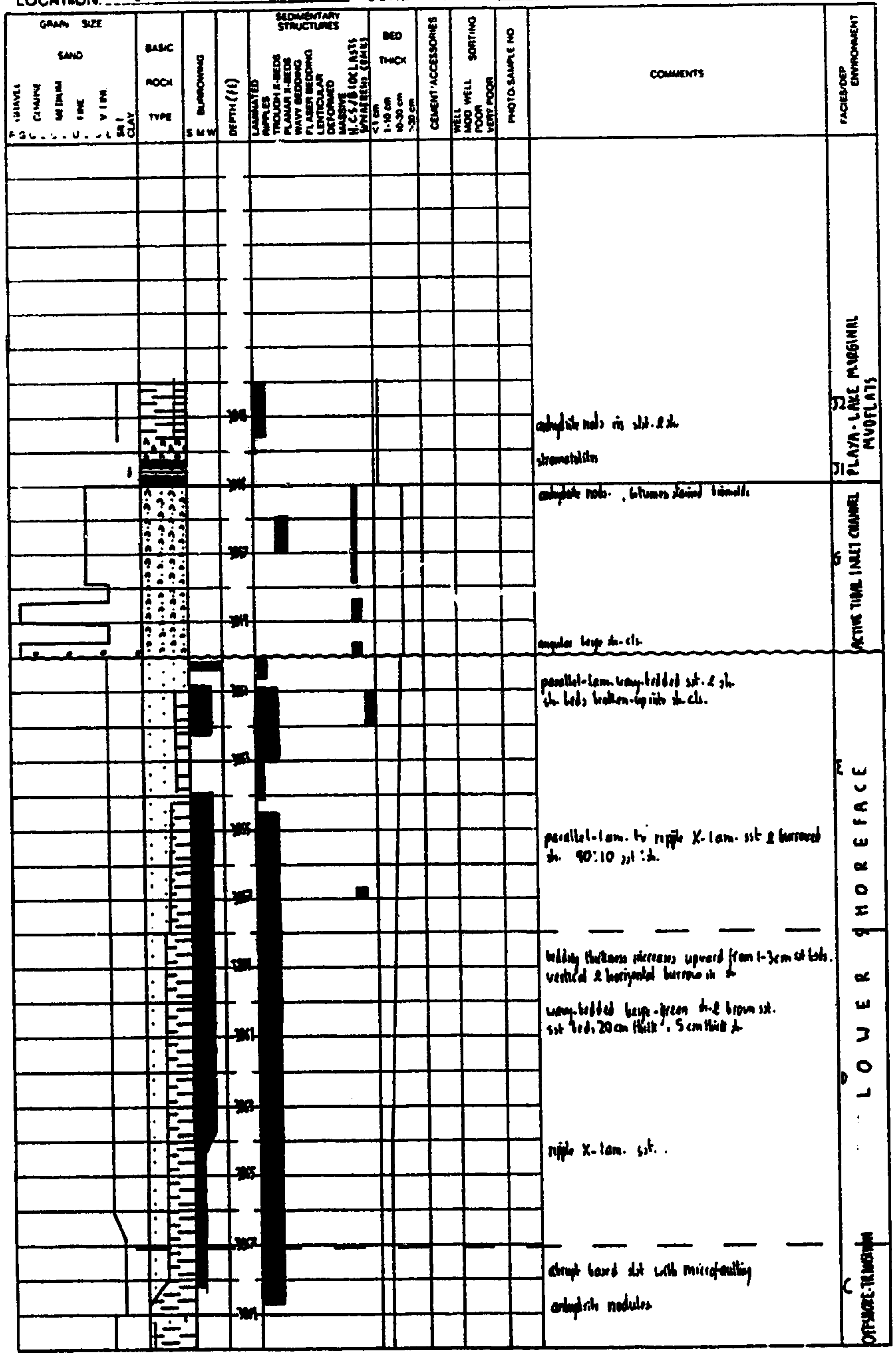

anhydrite nods in slt. & sh.

stromatolites

anhydrite nods. , bitumen stained bimodal

angular beige sh. cls.

parallel-lam. wavy-bedded sst. & sh.
sh. beds broken-up into sh. cls.

parallel-lam. to ripple X-lam. sst & burrowed sh. 90:10 sst : sh.

bedding thickness increases upward from 1-3cm at btm.
vertical & horizontal burrows in sh.

wavy-bedded beige-green sh. & brown sst.
sst beds 20cm thick, 5cm thick sh.

ripple X-lam. sst. .

abrupt based slt with microfaulting

anhydrite nodules

WELL NAME: UNION ET AL CRUSH
FORMATION: HALFWAY-CHARLIE LAKE
DATE: 20/08/90
LOCATION: d-019-F/94-A-16
CORE INTERVAL:
KB: 739lft

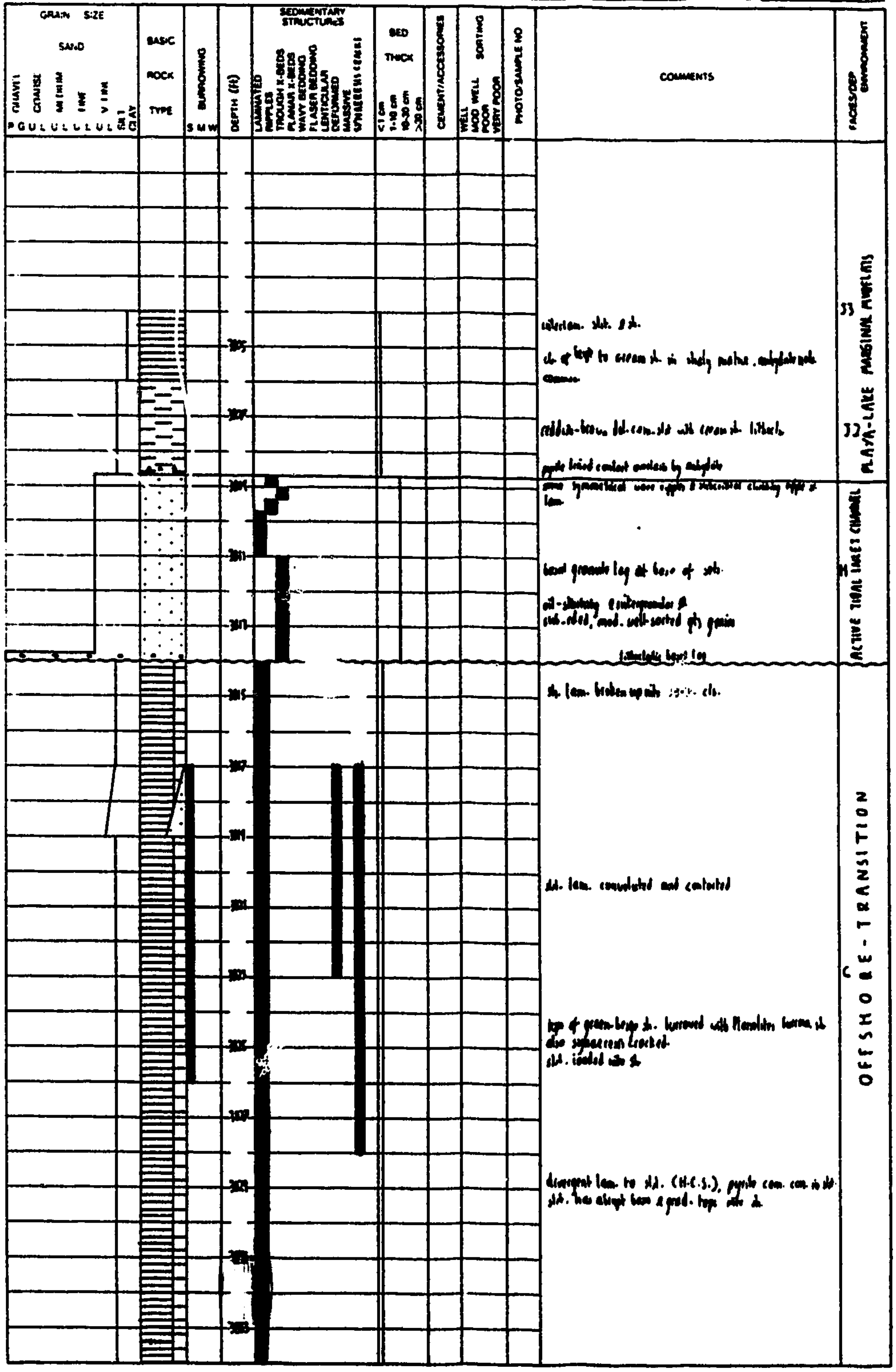

interlam. sltst. & sh.

sh. of [illegible] to green sh. in shaly matrix. anhydrite nodules common.

reddish-brown dol.-cem. slt with green sh. lithocl.

pyrite lined contact overlain by anhydrite

some symmetrical wave ripples & subcritical climbing ripple x-lam.

basal granule lag at base of sds.

oil-staining & [illegible]
sub-rded, mod. well-sorted qtz grains

lithoclastic basal lag

sh. lam. broken up with [illegible] cls.

sltst. lam. convoluted and contorted

top of green-beige sh. burrowed with Planolites burrows, sh. also syneresis cracked.
sltst. loaded into sh.

divergent lam. to sltst. (H.C.S.), pyrite com. con. in sltst.
sltst. has abrupt base & grad. tops into sh.

WELL NAME: CIGOL CRUSH d-50-F

FORMATION: DOG/HALFWAY/CHARLIE LAKE

DATE: 5/02/91

LOCATION: d-050-F/94-A-16

CORE INTERVAL:

KB: 2388ft

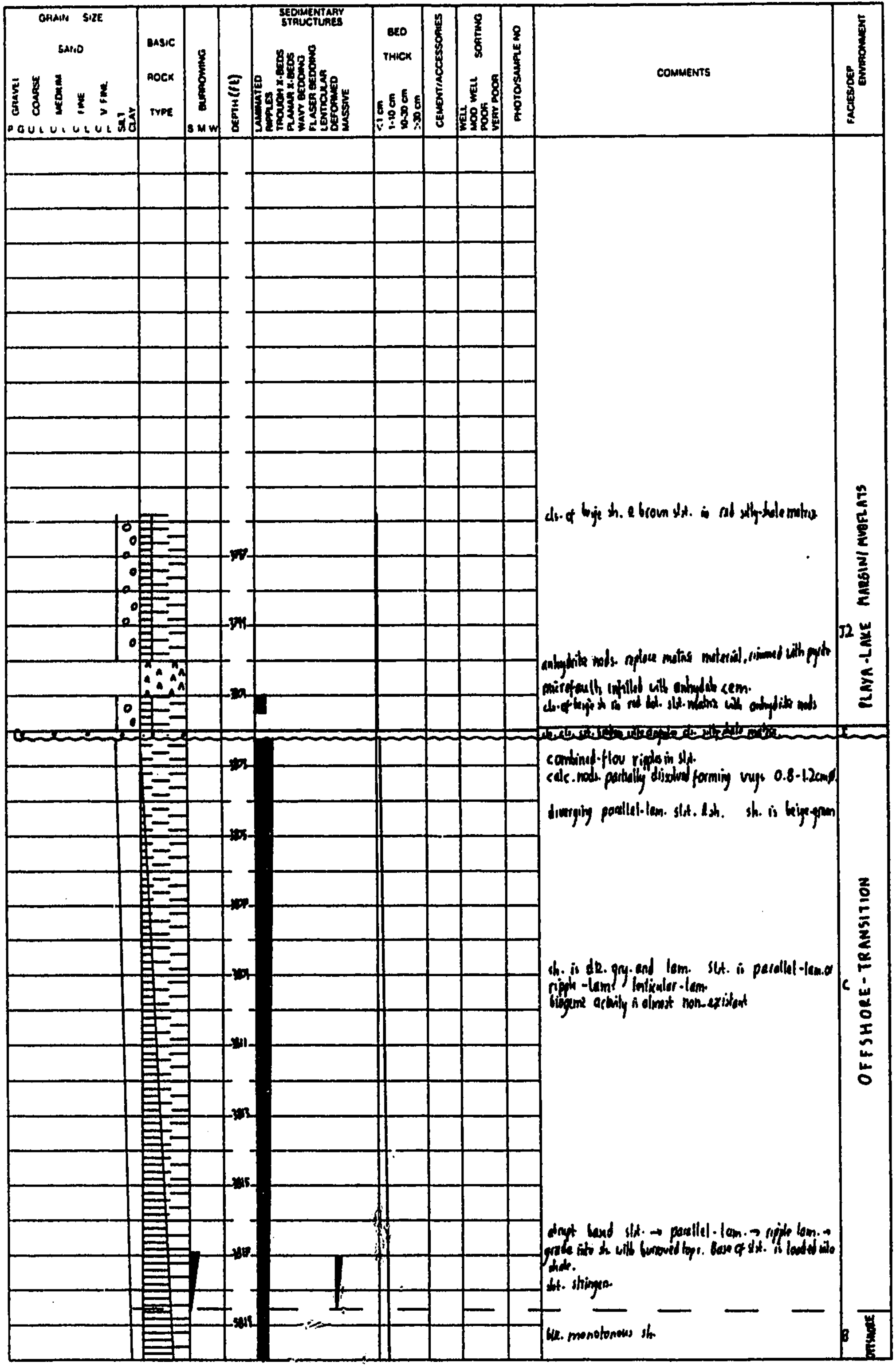

cls. of beige sh. & brown slt. in red silty-shale matrix

anhydrite nods. replace matrix material, rimmed with pyrite

microfaults infilled with anhydrite cem.

cls. of beige sh. in red dol. slt. matrix with anhydrite nods

sh. cls. slt. [illegible] cls. silty shale matrix.

combined-flow ripples in slt.

calc. nods. partially dissolved forming vugs 0.8-1.2cm⌀

diverging parallel-lam. slt. & sh. sh. is beige-green

sh. is dk. gry. and lam. slt. is parallel-lam. or ripple-lam. / lenticular-lam.

biogenic activity is almost non-existent

abrupt based slt. → parallel-lam. → ripple lam. → grade into sh. with burrowed tops. Base of slt. is loaded into shale.

slt. stringers

blk. monotonous sh.

WELL NAME: UNION H B CRUSH d-59-F

FORMATION: HALFWAY- CHARLIE LAKE

DATE: 5/02/91

LOCATION: d-059-F/94-A-16

CORE INTERVAL:

KB: 2373.8 ft

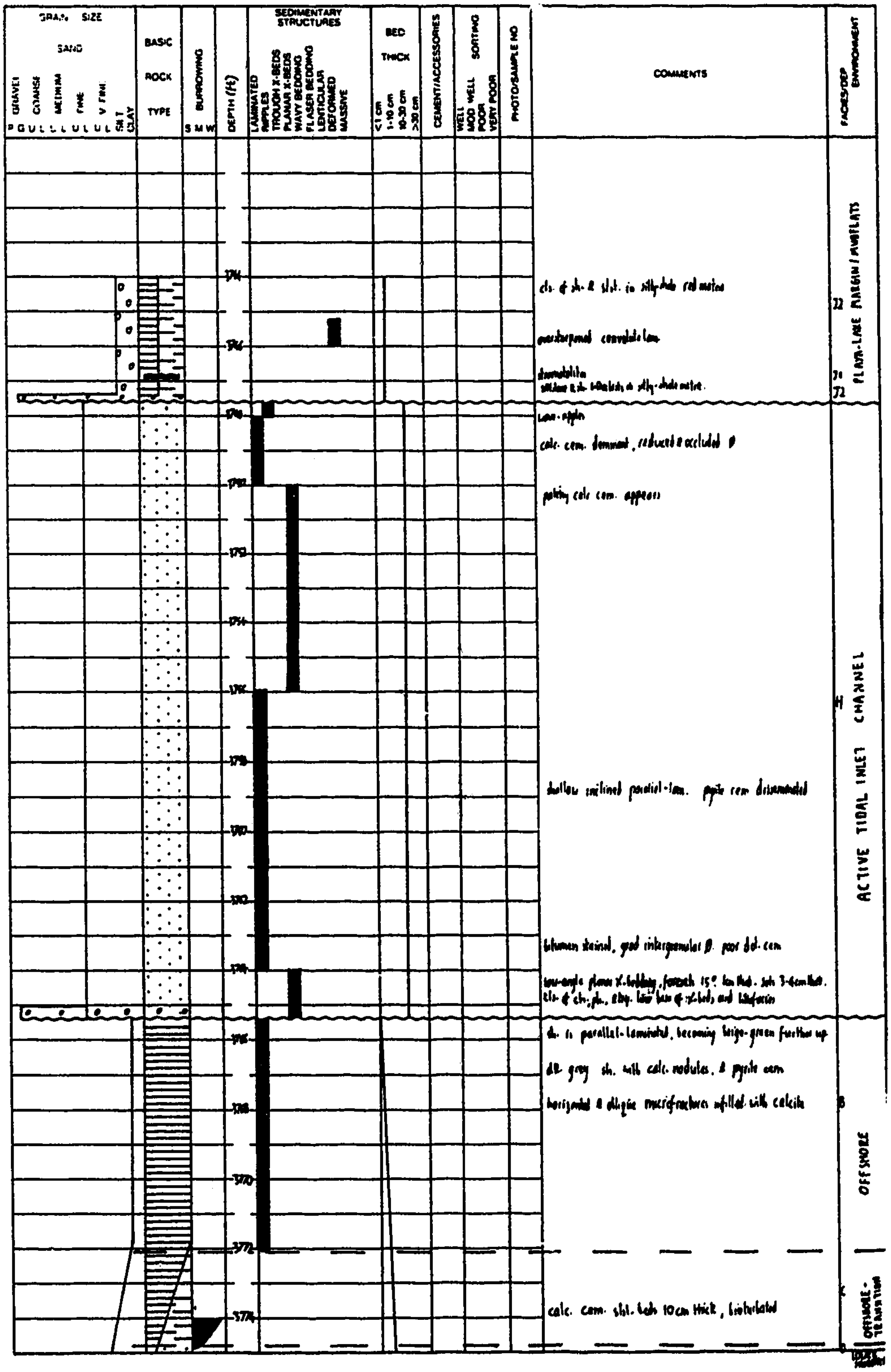

cls. of sh. & slst. in silty-shale red matrix

overturned convolute lam.

[illegible]
siltstone & sh. intraclasts in silty-shale matrix.

lam.-ripples

calc. cem. dominant, reduced & occluded Ø

poikilitic calc. cem. appears

shallow inclined parallel-lam. pyrite cem disseminated

bitumen stained, good intergranular Ø. poor dol. cem

low-angle planar X-bedding, foresets 15°, [illegible] thick. sets 3-4cm thick. cls. of ch., ph., esp. low base of X-beds and [illegible]

sh. is parallel-laminated, becoming beige-green further up

dk grey sh. with calc. nodules, & pyrite cem

horizontal & oblique microfractures infilled with calcite

calc. cem. slst. beds 10cm thick, bioturbated

WELL NAME: UNION HB CRUSH FORMATION: HALFWAY-CHARLIE LAKE DATE: 10/08/90

LOCATION: d-060-F/94-A-16 CORE INTERVAL: KB: 2368ft

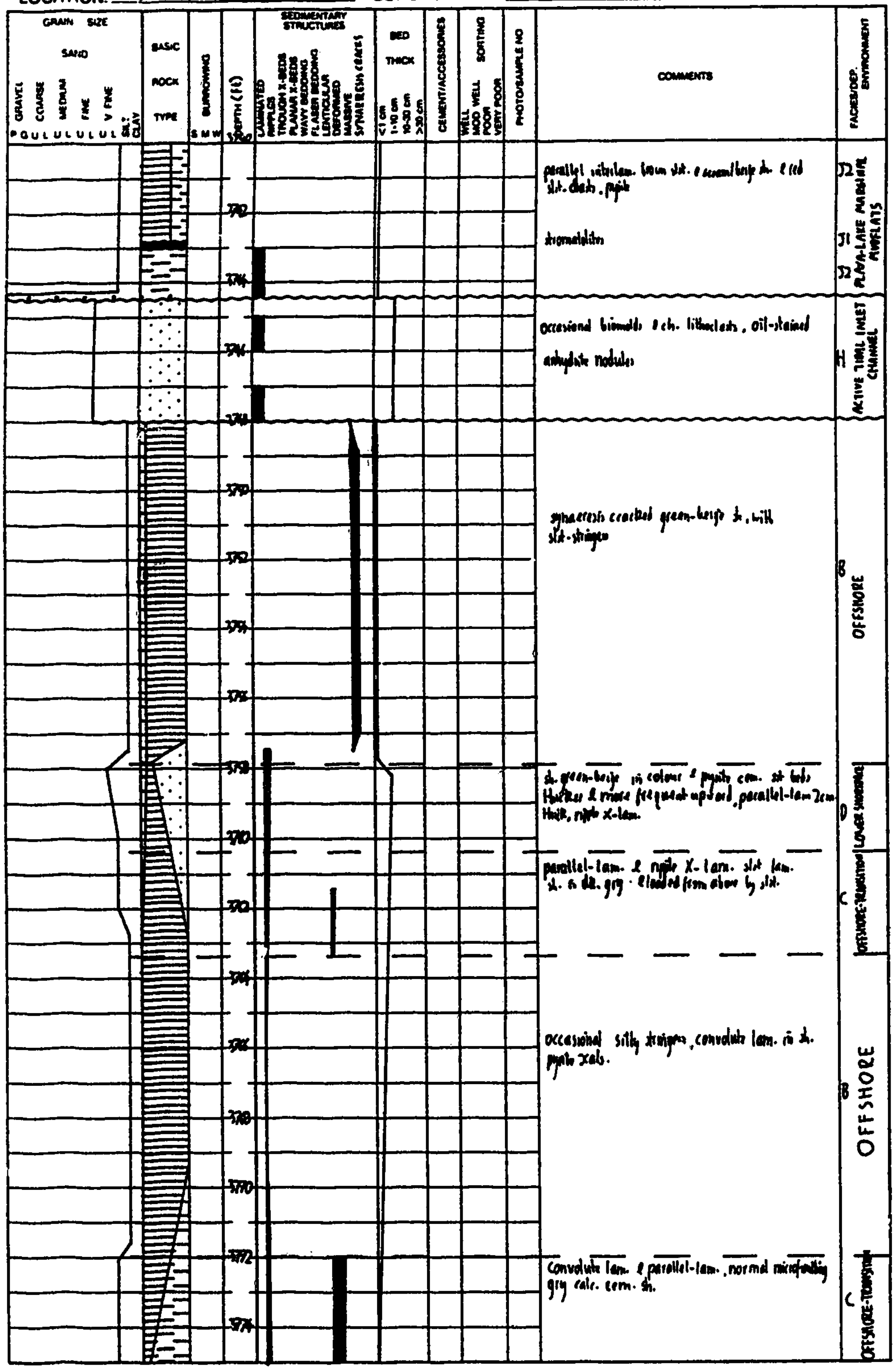

parallel interlam. brown slt. & cream/beige sh. & red slt. clasts, pyrite

stromatolites

occasional bivalves & ch. lithoclasts, oil-stained anhydrite nodules

synaeresis cracked green-beige sh. with slt-stringers

sh. green-beige in colour & pyrite com. slt beds thicker & more frequent upward, parallel-lam 2cm thick, ripple X-lam.

parallel-lam. & ripple X-lam. slt lam. sh. is dk. grey. loaded from above by slt.

occasional silty stringers, convolute lam. in sh. pyrite xals.

Convolute lam. & parallel-lam., normal microfaulting gry calc. cem. sh.

WELL NAME: UNION HB CRUSH
FORMATION: HALFWAY-CHARLIE LAKE
DATE: 10/08/90
LOCATION: d-060-F/94-A-16
CORE INTERVAL:
KB: 2368ft

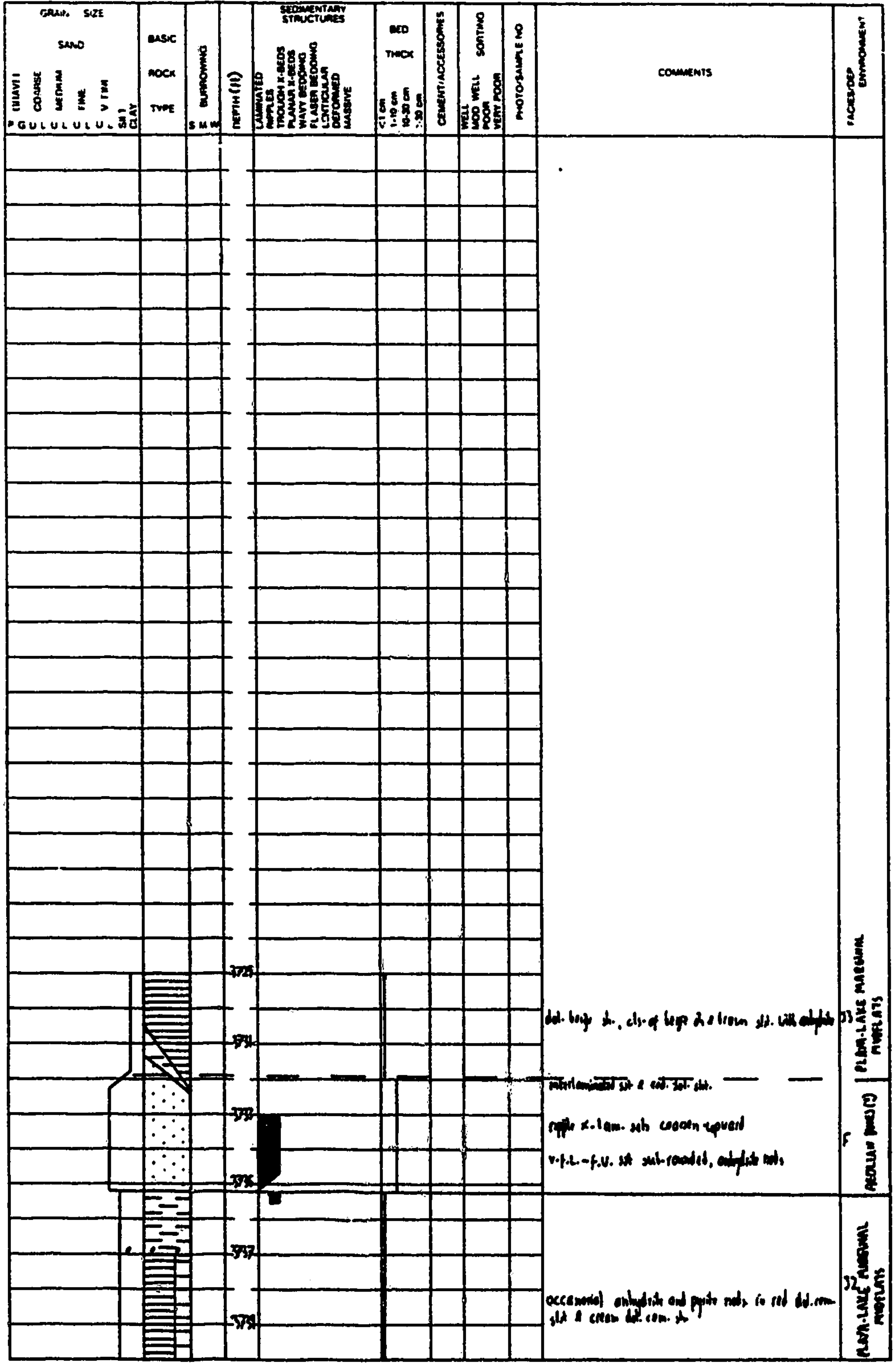

dol. beige sh., clst. of beige & a brown slt. with anhydrite

interlaminated slt & dol. sst. sh.

ripple x-lam. sets coarsen upward

v.f.L.-f.U. sst sub-rounded, anhydrite nods

occasional anhydrite and pyrite nods in red dol.-cem. slt & green dol. cem. sh.

WELL NAME: UNION HB SINCLAIR ET AL BULRUSH
FORMATION: HALFWAY-CHARLIE LAKE
DATE: 21/08/90
LOCATION: d-078-F/94-A-16
CORE INTERVAL:
KB: 2362 ft.

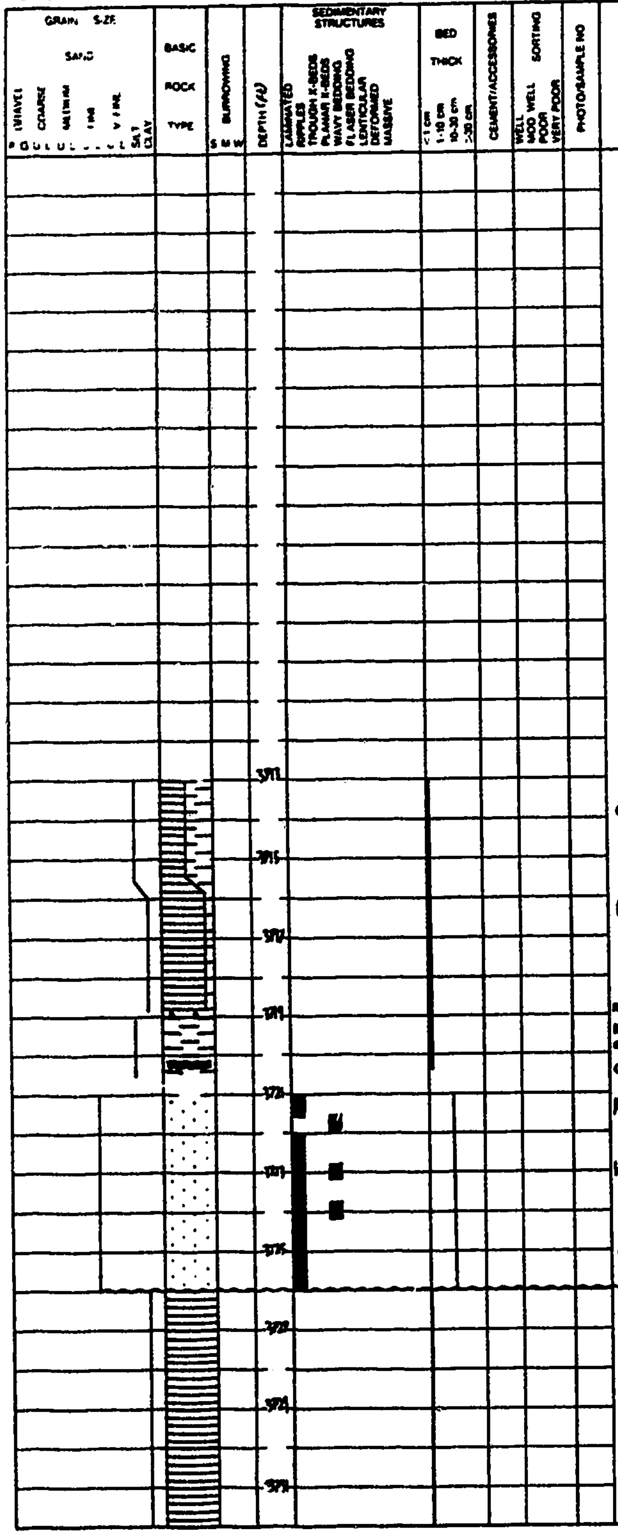

COMMENTS

cl. of parallel-lam. slt. & sh. in beige sh. matrix

brown slt. & beige sh. with anhydrite nodules

massive anhydrite
nods. of anhydrite replacing brown dol.-cem. slt & ch. of sh.
alternate lam. of brown dol.-cem. slt & anhydrite → [illegible]
content not preserved

φ decreases upward as anhydrite cem. increases. lithcls. of slt, ph., & ch. etc. Pyrite nodules common. parallel-lam. common upward intergranular φ high-angle planes ⊥ bedding.

parallel-lam. well-rounded sst, calc. cem., well-sorted.

silty calc. cem. laminae, parallel-lam. & microfaults. sh. is grey-green & calc. cem.

FACIES/DEP. ENVIRONMENT

J3
J1
PLAYA-LAKE MARGIN/MUDFLATS

H
ACTIVE TIDAL INLET CHANNEL

B
OFFSHORE

WELL NAME: UNION HB SINC PAC BULRUSH d-88-F FORMATION: HALFWAY-CHARLIE LAKE DATE: 5/07/91

LOCATION: d-088-F/94-A-16 CORE INTERVAL: KB: 2374 ft

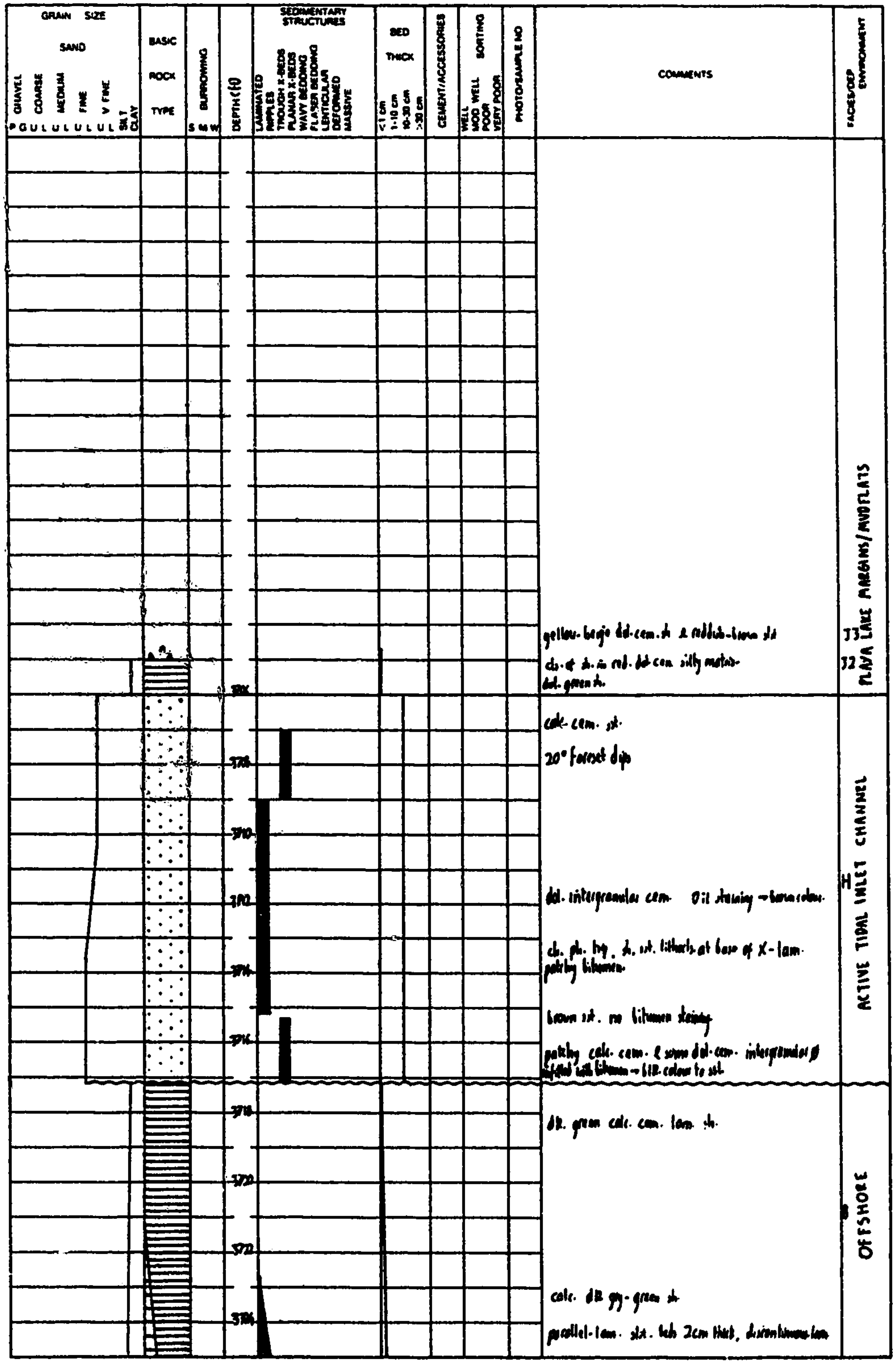

yellow-beige dol-cem. sh & reddish-brown sh

cls. of sh. in red. dol-cem silty mottled-dol. green sh.

calc-cem. sst.

20° foreset dips

dol. intergranular cem. Oil staining → brown colour.

cls. ph. bg. sh. sst. lithoclasts at base of X-lam. patchy bitumen.

brown sst. no bitumen staining

patchy calc. cem. & some dol-cem. intergranular infilled with bitumen → blk. colour to sst.

dk. green calc. cem. lam. sh.

calc. dk gy-green sh

parallel-lam. sst. beds 2cm thick, discontinuous lam

WELL NAME: UNION HB MOOSE d-38-K

FORMATION: HALFWAY- CHARLIE LAKE

DATE: 2/08/90

LOCATION: d-038-K/94-A-16

CORE INTERVAL:

KB: 2396 ft

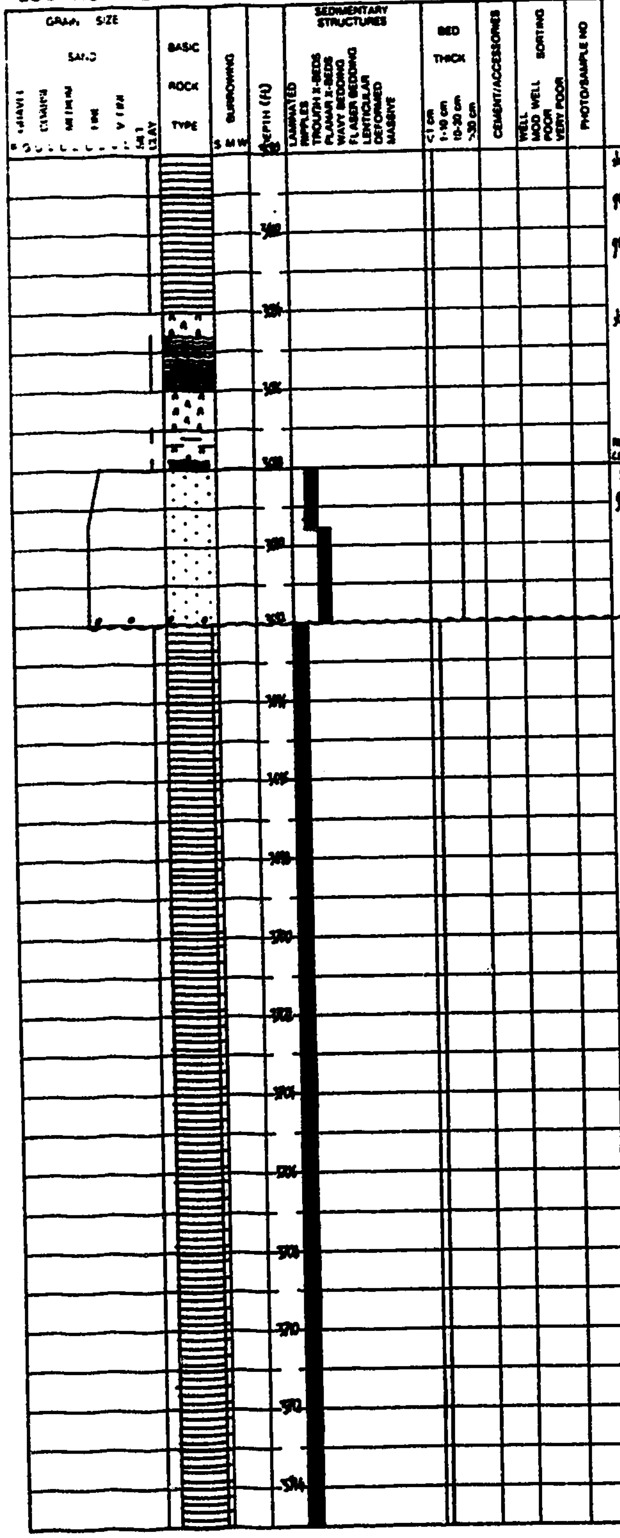

COMMENTS

shale becomes red and anhydrite nodules

green sh. & pyrite nodules

green-grey sh. with pyrite nods. & anhydrite nodules.

stromatolite

massive anhydrite
crinkly lam. dol. & anhydrite laminae with pyrite → stromatolite

symmetrical wave-ripple lam. A=3mm λ=30mm
good intergranular ∅ & oil staining. Sets 5-15cm thick.
ch. frag. pb. at base of trough x-beds

grey-green silty-shale, calc. nodules and pyrite.

grey-green calc. cem. silty-shale.

calc. nods. liberally distributed

monotonous dol-cem. dk.brn.-green & grey silty-shale, no pyrite.

FACIES/DEP ENVIRONMENT

L CONTINENTAL RED BED MUDFLATS

J1 PLAYA LAKE MARGIN MUDFLATS

J1

H ACTIVE TIDAL INLET CHANNEL

B OFFSHORE

WELL NAME: CHAUT DUNBAR BEAVERDAM a-27-L FORMATION: HALFWAY- CHARLIE LAKE DATE: 8/08/90

LOCATION: a-027-L/94-A-16 CORE INTERVAL: KB:

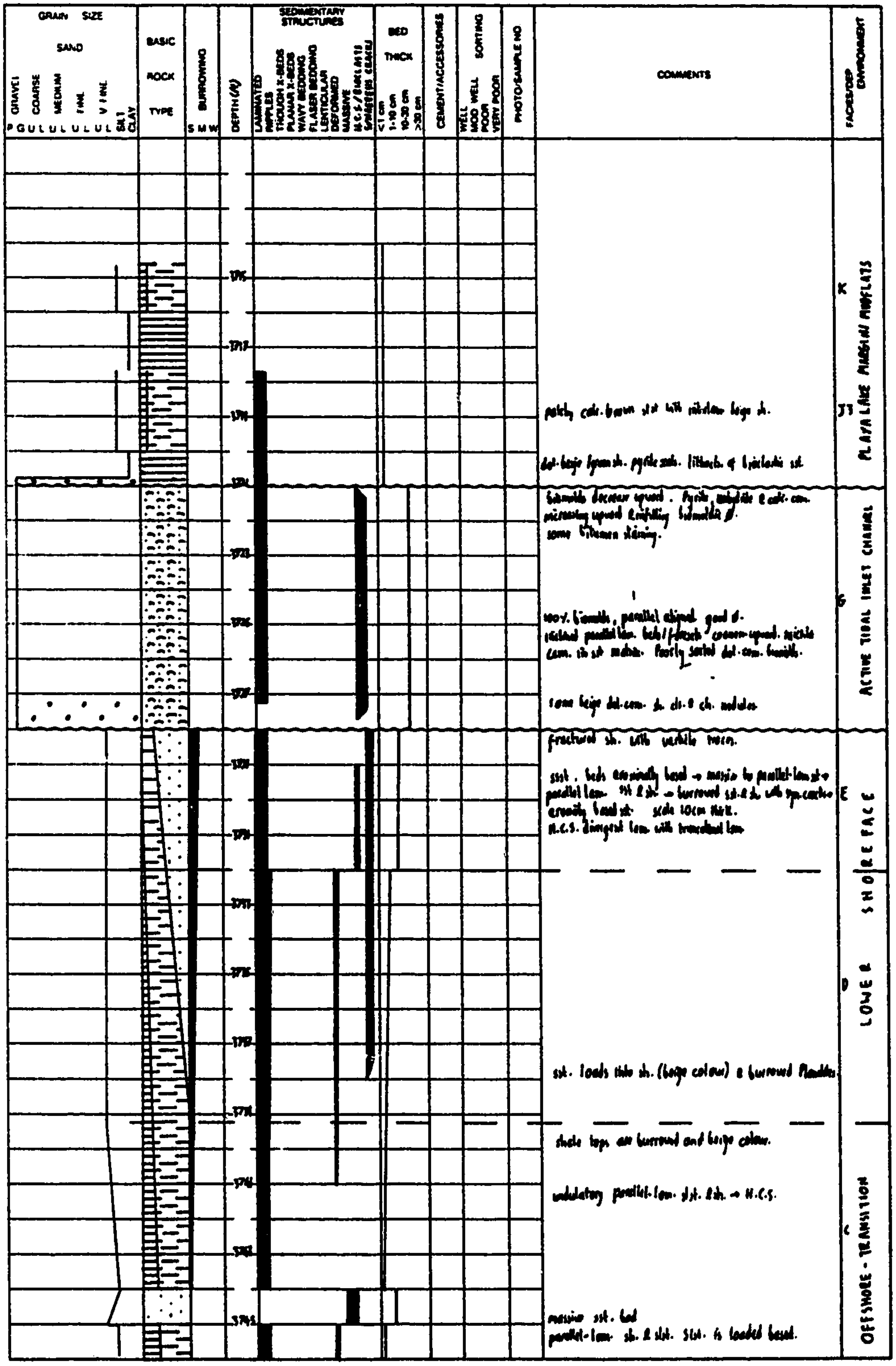

patchy calc. brown slst with nodular beige sh.

dol. beige gypsum sh. pyrite nods. lithocl. & brecciated sst

bimodal decrease upward. Pyrite, anhydrite & calc. cem. increasing upward & infilling bimodal ø.
some bitumen staining.

100% bimodal, parallel aligned good ø.
isolated parallel lam. beds/foresets coarsen upward. [illegible]
cem. in sst matrix. Poorly sorted dol. cem. bimodal.

some beige dol. cem. sh. clst & ch. nodules

fractured sh. with vertical frac.

ssst. beds erosionally based → massive to parallel-lam. sst →
parallel lam. sst & sh. → burrowed sst & sh. with sp. carbon.
erosionally based sst. scale 10cm thick.
H.C.S. divergent lam. with truncated lam.

sst. loads into sh. (beige colour) & burrowed Planolites.

shale tops are burrowed and beige colour.

undulatory parallel-lam. slst. & sh. → H.C.S.

massive sst. bed
parallel-lam. sh. & slst. Sst. is loaded based.

APPENDIX B

Appendix B provides a detailed database of the reservoir quality of reservoir lithofacies F, G and H taken from individual wells.

WELL LOCATION	GROSS THICKNESS (feet)	GROSS PAY (feet)	K-MAX mD	K-MIN mD	K-AVERAGE mD	QUALITY OF RESERVOIR ROCK
d-005-C/94-A-16	7.10	7.10	122.00	3.00	20.66	MODERATE
d-039-C/94-A-16	6.00	6.00	56.00	2.90	18.71	MODERATE
d-081-D/94-A-16	9.10	8.91	4.40	0.25	0.44	VERY POOR
d-082-D/94-A-16	5.00	5.00	4.00	0.10	0.41	VERY POOR
a-083-D/94-A-16	7.62	7.62	0.50	0.11	0.25	VERY POOR
d-091-D/94-A-16	5.41	5.41	16.00	0.17	4.82	POOR
d-092-D/94-A-16	6.63	6.63	6.30	0.10	0.59	VERY POOR
d-093-D/94-A-16	10.79	10.79	0.35	0.10	0.11	VERY POOR
d-002-E/94-A-16	6.89	6.89	37.00	0.41	2.25	POOR
d-025-E/94-A-16	7.62	6.74	194.00	0.13	7.54	POOR
WELL LOCATION			Ø-MAX %	Ø-MIN %	Ø-AVERAGE %	QUALITY OF RESERVOIR ROCK
d-005-C/94-A-16			18.90	10.30	14.60	GOOD
d-039-C/94-A-16			17.90	13.30	15.60	VERY GOOD
d-081-D/94-A-16			12.90	8.30	10.60	GOOD
d-082-D/94-A-16			15.70	10.00	12.85	GOOD
a-083-D/94-A-16			9.30	8.00	8.65	MODERATE
d-091-D/94-A-16			12.60	9.30	10.95	GOOD
d-092-D/94-A-16			14.60	10.00	12.30	GOOD
d-093-D/94-A-16			11.60	8.60	10.10	GOOD
d-002-E/94-A-16			13.30	10.40	11.85	GOOD
d-025-E/94-A-16			17.30	8.40	12.85	GOOD

Spreadsheet A displaying reservoir quality parameters of Lithofacies F upper shoreface deposits. Gross thickness refers to the total thickness of the lithofacies. Gross pay is the thickness of the reservoir with porosity values of at least 8% and permeability of at least 0.1mD.

WELL LOCATION	GROSS	GROSS PAY (feet)	K-MAX mD	K-MIN mD	K-AVERAGE mD	QUALITY OF
	THICKNESS (feet)					RESERVOIR ROCK
d-031-H/94-A-15	20.00	20.00	796.00	11.00	220.95	GOOD
b-042-H/94-A-15	9.10	7.88	1276.00	0.10	182.62	GOOD
d-044-H/94-A-15	9.00	9.00	49.00	3.40	19.87	MODERATE
d-067-H/94-A-15	14.10	12.39	926.00	0.82	191.77	GOOD
b-074-H/94-A-15	5.10	2.71	107.00	2.20	18.78	MODERATE
b-086-H/94-A-15	17.40	12.86	473.00	1.10	96.44	GOOD
d-097-H/94-A-15	19.20	16.74	1170.00	16.00	294.26	VERY GOOD
d-069-C/94-A-16	6.50	5.16	28.00	0.13	2.40	POOR
d-099-C/94-A-16	20.00	19.51	600.00	10.00	97.24	GOOD
d-071-D/94-A-16	7.20	7.20	66.00	1.80	14.81	POOR
d-091-D/94-A-16	7.10	7.10	109.00	1.50	14.84	POOR
d-024-E/94-A-16	5.10	5.10	547.00	7.70	106.58	GOOD
d-026-E/94-A-16	8.10	8.10	180.00	5.40	51.08	GOOD
d-034-E/94-A-16	17.70	17.70	505.00	3.40	75.61	GOOD
b-038-E/94-A-16	8.30	8.30	321.00	8.00	75.07	GOOD
d-047-E/94-A-16	7.10	7.10	224.00	3.60	45.92	MODERATE
d-048-E/94-A-16	6.60	6.60	462.00	52.00	185.06	GOOD
b-049-E/94-A-16	5.60	5.60	128.00	1.00	28.55	MODERATE
b-067-E/94-A-16	13.10	13.10	481.00	30.00	75.87	GOOD
b-069-E/94-A-16	8.40	8.40	1843.00	0.10	158.51	GOOD

WELL LOCATION			Ø-MAX %	Ø-MIN %	Ø-AVERAGE %	QUALITY OF RESERVOIR ROCK
d-031-H/94-A-15			27.10	12.40	20.60	EXCELLENT
b-042-H/94-A-15			29.00	8.40	11.59	GOOD
d-044-H/94-A-15			16.30	9.70	12.43	GOOD
d-067-H/94-A-15			30.60	8.60	14.69	GOOD
b-074-H/94-A-15			18.00	11.60	14.80	GOOD
b-086-H/94-A-15			24.00	8.60	9.50	MODERATE
d-097-H/94-A-15			27.70	12.40	21.30	EXCELLENT
d-069-C/94-A-16			19.40	7.20	12.20	GOOD
d-099-C/94-A-16			28.40	10.10	14.70	GOOD
d-071-D/94-A-16			24.00	8.20	11.54	GOOD
d-091-D/94-A-16			25.50	9.70	12.20	GOOD
d-024-E/94-A-16			25.20	10.20	16.20	VERY GOOD
d-026-E/94-A-16			29.40	9.40	13.38	GOOD
d-034-E/94-A-16			28.90	11.10	12.97	GOOD
b-038-E/94-A-16			25.20	8.80	10.93	GOOD
d-047-E/94-A-16			24.70	8.00	11.88	GOOD
d-048-E/94-A-16			22.10	15.20	16.70	VERY GOOD
b-049-E/94-A-16			23.80	11.00	18.56	VERY GOOD
b-067-E/94-A-16			26.30	14.30	21.70	EXCELLENT
b-069-E/94-A-16			26.20	9.80	10.32	MODERATE

Spreadsheet B displaying reservoir quality parameters of Lithofacies G tidal-inlet channels. Gross thickness refers to the total thickness of the lithofacies. Gross pay is the thickness of the reservoir with porosity values of at least 8% and permeability of at least 0.1mD

WELL LOCATION	GROSS THICKNESS (feet)	GROSS PAY (feet)	K-MAX mD	K-MIN mD	K-AVERAGE mD	QUALITY OF RESERVOIR ROCK
d-007-C/94-A-16	5.00	2.43	26.00	0.14	2.95	POOR
d-016-C/94-A-16	18.30	16.75	511.00	2.90	84.00	GOOD
d-062-D/94-A-16	5.00	4.12	143.00	15.00	29.36	GOOD
d-063-D/94-A-16	24.00	24.00	1094.00	31.00	212.60	GOOD
d-064-D/94-A-16	6.80	4.83	119.00	2.90	31.99	MODERATE
d-073-D/94-A-16	25.20	10.54	60.75	0.10	16.86	MODERATE
d-082-D/94-A-16	8.00	8.00	718.00	18.00	186.18	GOOD
a-083-D/94-A-16	6.00	6.00	228.00	42.00	93.40	GOOD
d-083-D/94-A-16	36.00	>33.8	1523.00	1.50	215.94	GOOD
d-092-D/94-A-16	6.60	3.67	740.00	0.12	152.34	GOOD
d-093-D/94-A-16	4.20	4.20	303.00	67.00	98.03	GOOD
a-003-E/94-A-16	16.00	16.00	1250.00	230.00	579.39	VERY GOOD
d-003-E/94-A-16	18.30	17.77	314.00	0.41	35.51	MODERATE
d-012-E/94-A-16	5.00	5.00	254.00	72.00	57.26	GOOD
d-013-E/94-A-16	7.00	7.00	255.00	17.00	55.34	GOOD
d-019-E/94-A-16	31.00	26.70	970.00	6.80	219.48	GOOD
a-023-E/94-A-16	13.00	13.00	358.00	46.00	198.52	GOOD
d-023-E/94-A-16	18.60	18.60	1605.00	0.79	323.70	VERY GOOD
b-038-E/94-A-16	10.00	8.79	617.00	18.00	144.37	GOOD
d-043-E/94-A-16	8.80	7.98	216.00	27.00	102.22	GOOD
b-049-E/94-A-16	8.10	8.10	84.00	4.40	25.92	MODERATE
b-059-E/94-A-16	36.00	>16.0	1112.00	78.00	276.40	VERY GOOD
d-074-E/94-A-16	23.60	23.60	1530.00	[illegible]	404.39	VERY GOOD
d-019-F/94-A-16	5.50	4.58	2.00	0.16	0.52	VERY POOR
d-059-F/94-A-16	17.80	16.92	1721.00	56.00	386.48	VERY GOOD
d-060-F/94-A-16	3.60	1.02	3.27	3.27	3.26	POOR
d-078-F/94-A-16	5.50	3.90	32.00	13.00	18.30	MODERATE
d-088-F/94-A-16	11.10	9.20	1453.00	1.50	168.96	GOOD

WELL LOCATION			Ø-MAX %	Ø-MIN %	Ø-AVERAGE %	QUALITY OF RESERVOIR ROCK
d-007-C/94-A-16			12.80	3.70	10.95	GOOD
d-016-C/94-A-16			26.30	7.50	22.55	EXCELLENT
d-062-D/94-A-16			17.40	10.20	12.30	GOOD
[illegible]63-D/94-A-16			26.90	11.10	21.35	EXCELLENT
d-064-D/94-A-16			19.60	10.00	14.60	GOOD
d-073-D/94-A-16			19.70	2.50	18.45	VERY GOOD
d-082-D/94-A-16			28.70	16.40	20.50	EXCELLENT
a-083-D/94-A-16			20.30	9.00	15.80	VERY GOOD
d-083-D/94-A-16			29.60	10.00	24.60	EXCELLENT
d-092-D/94-A-16			25.00	9.70	20.15	VERY GOOD
d-093-D/94-A-16			29.60	13.10	23.05	EXCELLENT
a-003-E/94-A-16			25.90	18.30	16.75	VERY GOOD
d-003-E/94-A-16			21.10	7.90	17.15	VERY GOOD
d-012-E/94-A-16			20.60	14.70	13.25	GOOD
d-013-E/94-A-16			19.10	12.60	12.80	GOOD
d-019-E/94-A-16			26.90	10.70	21.55	EXCELLENT
a-023-E/94-A-16			22.50	12.50	16.25	VERY GOOD
d-023-E/94-A-16			28.50	12.70	22.15	EXCELLENT
b-038-E/94-A-16			25.30	10.20	20.20	EXCELLENT
d-043-E/94-A-16			19.70	13.80	12.80	GOOD
b-049-E/94-A-16			20.50	10.70	15.15	VERY GOOD
b-059-E/94-A-16			28.70	15.50	20.95	EXCELLENT
d-074-E/94-A-16			28.50	18.30	19.35	VERY GOOD

WELL LOCATION			Ø-MAX %	Ø-MIN %	Ø-AVERAGE %	QUALITY OF RESERVOIR ROCK
d-019-F/94-A-16			18.30	11.00	12.80	GOOD
d-059-F/94-A-16			28.30	11.10	22.75	EXCELLENT
d-060-F/94-A-16			9.60	9.60	4.80	POOR
d-078-F/94-A-16			13.40	11.30	7.75	MODERATE
d-088-F/94-A-16			25.60	13.30	18.95	VERY GOOD

Spreadsheet C displaying reservoir quality parameters of Lithofacies H tidal-inlet channel fills. Gross thickness refers to the total thickness of the lithofacies. Gross pay is the thickness of the reservoir with porosity values of at least 8% and permeability of at least 0.1mD.

APPENDIX C

Appendix C contains Kelly Bushing elevations of each well providing sub-sea depths of particular markers, in order to construct structural maps. All values are in feet. The tops of parasequences (at the marine flooding surface) have been identified and laterally correlated in order to produce structural and isopach maps. The depth of the top of the Halfway Formation has also been recorded in order for isopach maps to be constructed. The base of the "Halfway" sands have also been recorded in order to produce a "Halfway" sand isopach map. This attempts to show the decrease in thickness of these sandstones to the northeast.

	A	B	C	D	E
1	WELL ID.	KB	TOP HAL	S.S. TOP	TOP MON
2		(ft)	(ft)	HAL (ft)	(ft)
3	b-010-A/94-A-15	2722.70	NO VALUE	NO VALUE	NO VALUE
4	d-025-A/94-A-15	2412.00	4142.00	-1730.00	NO VALUE
5	d-029-A/94-A-15	2417.60	4211.50	-1793.90	4366.70
6	d-040-A/94-A-15	2402.80	4182.00	-1779.20	NO VALUE
7	d-042-A/94-A-15	2420.90	4066.60	-1645.70	NO VALUE
8	d-052-A/94-A-15	2418.60	4044.20	-1625.60	NO VALUE
9	d-066-A/94-A-15	2392.50	4064.00	-1671.50	4209.90
10	d-067-A/94-A-15	2416.70	4094.80	-1678.10	NO VALUE
11	a-068-A/94-A-15	2397.90	NO VALUE	NO VALUE	4248.00
12	d-068-A/94-A-15	2378.60	4093.50	-1714.90	NO VALUE
13	d-069-A/94-A-15	2405.10	4103.20	-1698.10	NO VALUE
14	d-070-A/94-A-15	2397.90	4109.90	-1712.00	NO VALUE
15	d-078-A/94-A-15	2377.90	4028.00	-1650.10	NO VALUE
16	d-079-A/94-A-15	2403.50	4080.30	-1676.80	NO VALUE
17	d-080-A/94-A-15	2392.00	4078.70	-1686.70	NO VALUE
18	d-A84-A/94-A-15	2394.30	4054.00	-1659.70	NO VALUE
19	d-088-A/94-A-15	2372.00	4023.90	-1651.90	NO VALUE
20	d-093-A/94-A-15	2382.80	3962.20	-1579.40	NO VALUE
21	d-099-A/94-A-15	2381.80	4031.00	-1649.20	NO VALUE
22					
23	b-010-H/94-A-15	2372.00	4026.00	-1654.00	NO VALUE
24	c-013-H/94-A-15	NO VALUE	NO VALUE	NO VALUE	NO VALUE
25	d-021-H/94-A-15	2374.60	3881.50	-1506.90	NO VALUE
26	d-022-H/94-A-15	2370.70	3890.00	-1519.30	NO VALUE
27	d-029-H/94-A-15	2357.90	3954.00	-1596.10	NO VALUE
28	d-031-H/94-A-15	2372.30	3856.00	-1483.70	NO VALUE
29	d-032-H/94-A-15	2368.10	3864.00	-1495.90	NO VALUE
30	d-033-H/94-A-15	2366.00	3869.00	-1503.00	NO VALUE
31	d-034-H/94-A-15	2362.80	3885.00	-1522.20	NO VALUE
32	d-038-H/94-A-15	2294.60	3949.30	-1654.70	NO VALUE
33	b-041-H/94-A-15	2367.10	3854.00	-1486.90	NO VALUE
34	d-041-H/94-A-15	2372.00	3840.00	-1468.00	NO VALUE
35	b-042-H/94-A-15	2364.00	3861.00	-1497.00	NO VALUE
36	d-042-H/94-A-15	2365.10	3854.00	-1488.90	NO VALUE
37	d-043-H/94-A-15	2362.00	3856.00	-1494.00	NO VALUE
38	d-044-H/94-A-15	2360.00	3868.10	-150[illegible].10	NO VALUE
39	d-045-H/94-A-15	2364.00	3896.00	-1532.00	NO VALUE
40	d-047-H/94-A-15	2358.20	3889.00	-1530.80	NO VALUE
41	b-051-H/94-A-15	2373.00	3840.90	-1467.90	NO VALUE

	A	B	C	D	E
1	WELL ID.	KB	TOP HAL	S.S. TOP	TOP MON
2		(ft)	(ft)	HAL (ft)	(ft)
42	d-051-H/94-A-15	2370.00	3832.00	-1462.00	NO VALUE
43	b-052-H/94-A-15	2370.00	3848.00	-1478.00	NO VALUE
44	d-052-H/94-A-15	2370.00	3838.00	-1468.00	NO VALUE
45	d-053-H/94-A-15	2362.80	3846.80	-1484.00	NO VALUE
46	d-054-H/94-A-15	2354.00	3846.00	-1492.00	NO VALUE
47	d-055-H/94-A-15	2356.00	3856.00	-1500.00	NO VALUE
48	d-056-H/94-A-15	2349.80	3868.10	-1518.30	NO VALUE
49	d-057-H/94-A-15	2341.80	3856.00	-1514.20	NO VALUE
50	d-058-H/94-A-15	2336.90	3860.00	-1523.10	NO VALUE
51	d-059-H/94-A-15	2347.10	3900.00	-1552.90	NO VALUE
52	d-061-H/94-A-15	2374.00	3818.00	-1444.00	NO VALUE
53	d-062-H/94-A-15	2365.60	3825.00	-1459.40	NO VALUE
54	b-063-H/94-A-15	2362.80	3841.80	-1479.00	NO VALUE
55	d-063-H/94-A-15	2365.00	3838.00	-1473.00	NO VALUE
56	b-064-H/94-A-15	2359.00	3848.10	-1489.10	NO VALUE
57	d-064-H/94-A-15	2359.90	3836.00	-1476.10	NO VALUE
58	d-065-H/94-A-15	2361.80	3848.00	-1486.20	NO VALUE
59	d-066-H/94-A-15	2356.00	3856.00	-1500.00	NO VALUE
60	d-067-H/94-A-15	2351.00	3850.00	-1499.00	NO VALUE
61	d-068-H/94-A-15	2353.00	3849.60	-1496.60	NO VALUE
62	d-071-H/94-A-15	2369.40	3808.00	-1438.60	NO VALUE
63	d-072-H/94-A-15	2362.80	3810.00	-1447.20	NO VALUE
64	d-073-H/94-A-15	2361.80	3820.00	-1458.20	NO VALUE
65	b-074-H/94-A-15	2366.15	3839.00	-1472.85	NO VALUE
66	d-074-H/94-A-15	2362.80	3818.00	-1455.20	NO VALUE
67	d-A74-H/94-A-15	2363.80	3828.00	-1464.20	NO VALUE
68	b-075-H/94-A-15	2357.00	3836.00	-1479.00	NO VALUE
69	d-075-H/94-A-15	2360.60	3840.00	-1479.40	NO VALUE
70	b-076-H/94-A-15	2350.00	3848.00	-1498.00	NO VALUE
71	d-076-H/94-A-15	2354.00	3830.00	-1476.00	NO VALUE
72	b-077-H/94-A-15	2356.90	3848.00	-1491.10	NO VALUE
73	d-077-H/94-A-15	2353.90	3840.00	-1486.10	NO VALUE
74	d-078-H/94-A-15	2353.10	3836.00	-1482.90	NO VALUE
75	d-079-H/94-A-15	2350.00	3846.00	-1496.00	NO VALUE
76	d-081-H/94-A-15	2371.00	3798.00	-1427.00	NO VALUE
77	d-084-H/94-A-15	2360.00	3814.00	-1454.00	NO VALUE
78	b-085-H/94-A-15	2356.90	3835.90	-1479.00	NO VALUE
79	d-085-H/94-A-15	2357.00	3817.00	-1460.00	NO VALUE
80	b-086-H/94-A-15	2354.90	3832.00	-1477.10	NO VALUE

	A	B	C	D	E
1	WELL ID.	KB	TOP HAL	S.S. TOP	TOP MON
2		(ft)	(ft)	HAL (ft)	(ft)
81	d-086-H/94-A-15	2360.75	3828.00	-1467.25	NO VALUE
82	d-087-H/94-A-15	2359.90	3822.00	-1462.10	NO VALUE
83	d-088-H/94-A-15	2358.90	3830.10	-1471.20	NO VALUE
84	d-089-H/94-A-15	2348.40	3821.20	-1472.80	NO VALUE
85	d-090-H/94-A-15	2332.00	3856.00	-1524.00	NO VALUE
86	d-095-H/94-A-15	2353.00	3804.00	-1451.00	NO VALUE
87	d-096-H/94-A-15	2362.80	3824.30	-1461.50	NO VALUE
88	d-097-H/94-A-15	2360.00	3801.00	-1441.00	NO VALUE
89	d-098-H/94-A-15	2350.00	3810.00	-1460.00	NO VALUE
90	a-099-H/94-A-15	2361.20	3824.50	-1463.30	NO VALUE
91	d-099-H/94-A-15	2347.10	3815.00	-1467.90	NO VALUE
92	d-100-H/94-A-15	2332.00	3809.70	-1477.70	NO VALUE
93					
94	d-033-I/94-A-15	NO VALUE	3712.50	NO VALUE	NO VALUE
95					
96	d-013-J/94-A-15	2259.30	2259.30	NO VALUE	NO VALUE
97					
98	d-018-B/94-A-16	2458.00	3969.00	-1511.00	NO VALUE
99					
100	a-003-C/94-A-16	2441.90	3982.00	-1540.10	NO VALUE
101	d-004-C/94-A-16	2416.30	3984.00	-1567.70	NO VALUE
102	d-005-C/94-A-16	2401.00	3932.00	-1531.00	NO VALUE
103	d-006-C/94-A-16	2373.00	3964.00	-1591.00	NO VALUE
104	d-007-C/94-A-16	2370.00	3961.00	-1591.00	NO VALUE
105	c-012-C/94-A-16	2446.80	3968.00	-1521.20	NO VALUE
106	b-015-C/94-A-16	2383.00	3930.30	-1547.30	NO VALUE
107	d-016-C/94-A-16	2379.50	3928.00	-1548.50	NO VALUE
108	d-017-C/94-A-16	2358.90	3937.00	-1578.10	NO VALUE
109	d-019-C/94-A-16	2356.90	3950.00	-1593.10	NO VALUE
110	b-026-C/94-A-16	2375.00	3932.00	-1557.00	NO VALUE
111	d-027-C/94-A-16	2385.80	3896.00	-1510.20	NO VALUE
112	d-028-C/94-A-16	2375.60	3915.00	-1539.40	NO VALUE
113	d-037-C/94-A-16	2395.90	3912.00	-1516.10	NO VALUE
114	d-039-C/94-A-16	2371.80	3913.00	-1541.20	NO VALUE
115	d-043-C/94-A-16	2452.00	3945.00	-1493.00	4108.00
116	d-050-C/94-A-16	2374.00	3908.10	-1534.10	NO VALUE
117	d-051-C/94-A-16	2479.90	3936.00	-1456.10	NO VALUE
118	d-056-C/94-A-16	2398.90	3921.90	-1523.00	NO VALUE
119	d-057-C/94-A-16	2423.20	3908.80	-1485.60	NO VALUE

	A	B	C	D	E
1	WELL ID.	KB	TOP HAL	S.S. TOP	TOP MON
2		(ft)	(ft)	HAL (ft)	(ft)
120	b-058-C/94-A-16	2396.90	3890.00	-1493.10	NO VALUE
121	d-058-C/94-A-16	2409.70	3901.90	-1492.20	NO VALUE
122	d-059-C/94-A-16	2394.00	3900.00	-1506.00	NO VALUE
123	d-060-C/94-A-16	2375.00	3881.80	-1506.80	NO VALUE
124	b-067-C/94-A-16	2426.50	3906.50	-1480.00	NO VALUE
125	d-067-C/94-A-16	2421.50	NO VALUE	NO VALUE	NO VALUE
126	b-068-C/94-A-16	2410.10	3916.00	-1505.90	NO VALUE
127	c-068-C/94-A-16	2408.50	3886.80	-1478.30	NO VALUE
128	d-068-C/94-A-16	2415.00	3896.00	-1481.00	NO VALUE
129	d-069-C/94-A-16	2398.10	3896.00	-1497.90	NO VALUE
130	d-070-C/94-A-16	2384.00	3876.00	-1492.00	NO VALUE
131	d-073-C/94-A-16	2480.60	3919.60	-1439.00	NO VALUE
132	d-075-C/94-A-16	2454.00	3920.00	-1466.00	NO VALUE
133	b-077-C/94-A-16	2424.20	3896.60	-1472.40	NO VALUE
134	d-077-C/94-A-16	2433.00	3903.20	-1470.20	NO VALUE
135	b-078-C/94-A-16	2409.10	3883.50	-1474.40	NO VALUE
136	d-078-C/94-A-16	2393.50	3881.00	-1487.50	NO VALUE
137	d-078-C/94-A-16	2419.60	3886.80	-1467.20	NO VALUE
138	d-079-C/94-A-16	2393.50	3880.00	-1486.50	NO VALUE
139	d-080-C/94-A-16	2382.20	3874.00	-1491.80	NO VALUE
140	d-082-C/94-A-16	2481.90	3898.00	-1416.10	NO VALUE
141	b-088-C/94-A-16	2410.70	3867.10	-1456.40	NO VALUE
142	d-088-C/94-A-16	2415.00	3872.00	-1457.00	NO VALUE
143	d-089-C/94-A-16	2395.80	3873.00	-1477.20	NO VALUE
144	b-090-C/94-A-16	2382.20	3866.10	-1483.90	NO VALUE
145	d-090-C/94-A-16	2389.00	3866.00	-1477.00	NO VALUE
146	d-096-C/94-A-16	2438.90	3890.00	-1451.10	4038.00
147	d-097-C/94-A-16	2425.10	3870.00	-1444.90	NO VALUE
148	b-098-C/94-A-16	2401.90	3858.00	-1456.10	NO VALUE
149	d-098-C/94-A-16	2408.00	3846.10	-1438.10	NO VALUE
150	d-099-C/94-A-16	2403.50	3850.00	-1446.50	NO VALUE
151	D-100-C/94-A-16	2394.00	3858.00	-1464.00	NO VALUE
152					
153	d-007-D/94-A-16	2348.00	3993.00	-1645.00	NO VALUE
154	d-015-D/94-A-16	2369.00	3959.00	-1590.00	NO VALUE
155	b-023-D/94-A-16	2360.80	3936.00	-1575.20	NO VALUE
156	a-025-D/94-A-16	2367.70	3947.50	-1579.80	NO VALUE
157	b-026-D/94-A-16	2359.90	3956.00	-1596.10	NO VALUE
158	d-031-D/94-A-16	2368.10	3920.00	-1551.90	NO VALUE

	A	B	C	D	E
1	WELL ID.	KB	TOP HAL	S.S. TOP	TOP MON
2		(ft)	(ft)	HAL (ft)	(ft)
159	d-033-D/94-A-16	2365.10	3906.00	-1540.90	NO VALUE
160	d-035-D/94-A-16	2375.00	3935.30	-1560.30	NO VALUE
161	d-037-D/94-A-16	2362.20	3942.60	-1580.40	NO VALUE
162	d-042-D/94-A-16	2372.00	3903.00	-1531.00	NO VALUE
163	d-049-D/94-A-16	2368.10	3930.10	-1562.00	NO VALUE
164	d-050-D/94-A-16	2387.10	3984.90	-1597.80	NO VALUE
165	d-051-D/94-A-16	2371.00	3881.00	-1510.00	NO VALUE
166	d-060-D/94-A-16	2373.00	3964.80	-1591.80	NO VALUE
167	d-061-D/94-A-16	2370.00	3874.00	-1504.00	NO VALUE
168	d-062-D/94-A-16	2365.00	3884.00	-1519.00	NO VALUE
169	d-063-D/94-A-16	2364.00	3888.10	-1524.10	NO VALUE
170	d-064-D/94-A-16	2364.00	3912.00	-1548.00	NO VALUE
171	d-067-D/94-A-16	2353.00	3899.90	-1546.90	NO VALUE
172	d-071-D/94-A-16	2373.00	3873.00	-1500.00	NO VALUE
173	b-072-D/94-A-16	2359.90	3886.70	-1526.80	NO VALUE
174	d-072-D/94-A-16	2368.10	3868.00	-1499.90	NO VALUE
175	d-073-D/94-A-16	2351.80	3878.00	-1526.20	NO VALUE
176	c-081-D/94-A-16	2379.90	3868.00	-1488.10	NO VALUE
177	d-081-D/94-A-16	2384.00	3865.00	-1481.00	NO VALUE
178	d-082-D/94-A-16	2371.50	3858.00	-1486.50	NO VALUE
179	a-083-D/94-A-16	2349.00	3864.00	-1515.00	NO VALUE
180	d-083-D/94-A-16	2356.00	3856.00	-1500.00	NO VALUE
181	b-084-D/94-A-16	2335.90	3893.40	-1557.50	NO VALUE
182	d-084-D/94-A-16	2331.00	3896.00	-1565.00	NO VALUE
183	d-086-D/94-A-16	2339.20	3877.90	-1538.70	NO VALUE
184	a-088-D/94-A-16	2342.00	3880.00	-1538.00	NO VALUE
185	d-091-D/94-A-16	2389.00	3859.00	-1470.00	NO VALUE
186	a-092-D/94-A-16	2371.00	3854.00	-1483.00	NO VALUE
187	d-092-D/94-A-16	2369.00	3845.00	-1476.00	NO VALUE
188	a-093-D/94-A-16	2333.90	3834.00	-1500.10	NO VALUE
189	b-093-D/94-A-16	2332.00	3872.00	-1540.00	NO VALUE
190	d-093-D/94-A-16	2336.00	3844.00	-1508.00	NO VALUE
191	d-094-D/94-A-16	2339.80	3870.40	-1530.60	NO VALUE
192	d-095-D/94-A-16	2278.80	NO VALUE	NO VALUE	NO VALUE
193	c-096-D/94-A-16	2354.00	3862.20	-1508.20	NO VALUE
194	d-097-D/94-A-16	2358.90	3863.80	-1504.90	NO VALUE
195	d-097-D/94-A-16	2358.90	3867.10	-1508.20	NO VALUE
196	b-098-D/94-A-16	2349.00	3860.60	-1511.60	NO VALUE
197					

	A	B	C	D	E
1	WELL ID.	KB	TOP HAL	S.S. TOP	TOP MON
2		(ft)	(ft)	HAL (ft)	(ft)
198	d-001-E/94-A-16	2373.00	3832.00	-1459.00	NO VALUE
199	a-002-E/94-A-16	2357.90	3826.00	-1468.10	NO VALUE
200	b-002-E/94-A-16	2352.00	3838.00	-1486.00	NO VALUE
201	d-002-E/94-A-16	2357.00	3830.00	-1473.00	NO VALUE
202	a-003-E/94-A-16	2351.00	3839.80	-1488.80	NO VALUE
203	d-003-E/94-A-16	2355.30	3830.00	-1474.70	NO VALUE
204	d-004-E/94-A-16	2359.90	3884.00	-1524.10	NO VALUE
205	a-006-E/94-A-16	2351.00	3886.80	-1535.80	NO VALUE
206	d-007-E/94-A-16	2356.90	3876.90	-1520.00	NO VALUE
207	d-008-E/94-A-16	2356.00	3869.00	-1513.00	NO VALUE
208	b-011-E/94-A-16	2359.90	3810.00	-1450.10	NO VALUE
209	d-011-E/94-A-16	2366.00	3812.00	-1446.00	NO VALUE
210	b-012-E/94-A-16	2359.20	3832.70	-1473.50	NO VALUE
211	d-012-E/94-A-16	2370.00	3838.00	-1468.00	NO VALUE
212	b-013-E/94-A-16	2362.20	3837.00	-1474.80	NO VALUE
213	d-013-E/94-A-16	2367.00	3836.90	-1469.90	NO VALUE
214	d-014-E/94-A-16	2359.50	3850.00	-1490.50	NO VALUE
215	b-016-E/94-A-16	2355.90	3844.10	-1488.20	NO VALUE
216	d-016-E/94-A-16	2347.10	3864.00	-1516.90	NO VALUE
217	d-017-E/94-A-16	2353.00	3850.00	-1497.00	NO VALUE
218	d-018-E/94-A-16	2355.90	3844.00	-1488.10	NO VALUE
219	d-019-E/94-A-16	2352.00	3850.00	-1498.00	4012.00
220	d-021-E/94-A-16	2374.00	3836.00	-1462.00	NO VALUE
221	d-022-E/94-A-16	2363.00	3789.00	-1426.00	NO VALUE
222	a-023-E/94-A-16	2363.00	3826.10	-1463.10	NO VALUE
223	d-023-E/94-A-16	2357.00	3800.00	-1443.00	NO VALUE
224	d-024-E/94-A-16	2282.00	3734.00	-1452.00	NO VALUE
225	d-025-E/94-A-16	2359.00	3819.00	-1460.00	NO VALUE
226	d-026-E/94-A-16	2359.00	3824.00	-1465.00	NO VALUE
227	b-027-E/94-A-16	2357.00	3838.00	-1481.00	NO VALUE
228	b-028-E/94-A-16	2372.00	3856.00	-1484.00	NO VALUE
229	d-028-E/94-A-16	2360.80	3834.00	-1473.20	NO VALUE
230	d-029-E/94-A-16	2367.10	3853.00	-1485.90	NO VALUE
231	d-030-E/94-A-16	2370.00	3876.00	-1506.00	NO VALUE
232	b-033-E/94-A-16	2354.00	3786.00	-1432.00	NO VALUE
233	d-033-E/94-A-16	2353.00	3782.00	-1429.00	NO VALUE
234	a-034-E/94-A-16	2370.00	3818.00	-1448.00	NO VALUE
235	d-034-E/94-A-16	2367.10	3796.00	-1428.90	NO VALUE
236	d-035-E/94-A-16	2368.00	3803.00	-1435.00	NO VALUE

	A	B	C	D	E
1	WELL ID.	KB	TOP HAL	S.S. TOP	TOP MON
2		(ft)	(ft)	HAL (ft)	(ft)
237	b-036-E/94-A-16	2360.80	3830.00	-1469.20	NO VALUE
238	d-036-E/94-A-16	2367.00	3818.00	-1451.00	NO VALUE
239	b-037-E/94-A-16	2378.90	3834.00	-1455.10	NO VALUE
240	d-037-E/94-A-16	2369.00	3825.00	-1456.00	NO VALUE
241	b-038-E/94-A-16	2388.70	3854.40	-1465.70	NO VALUE
242	d-038-E/94-A-16	2374.30	3826.00	-1451.70	NO VALUE
243	b-039-E/94-A-16	2389.10	3862.00	-1472.90	NO VALUE
244	d-039-E/94-A-16	2380.90	3842.00	-1461.10	NO VALUE
245	b-040-E/94-A-16	2385.60	3867.00	-1481.40	NO VALUE
246	d-040-E/94-A-16	2375.90	3860.00	-1484.10	NO VALUE
247	d-043-E/94-A-16	2373.00	3810.00	-1437.00	NO VALUE
248	b-045-E/94-A-16	2372.00	3800.40	-1428.40	NO VALUE
249	d-046-E/94-A-16	2379.00	3810.30	-1431.30	3962.00
250	b-047-E/94-A-16	2386.30	3835.90	-1449.60	NO VALUE
251	d-047-E/94-A-16	2379.90	3817.40	-1437.50	NO VALUE
252	b-048-E/94-A-16	2390.00	3838.00	-1448.00	NO VALUE
253	d-048-E/94-A-16	2385.80	3833.00	-1447.20	NO VALUE
254	b-049-E/94-A-16	2391.70	3850.00	-1458.30	NO VALUE
255	d-049-E/94-A-16	2386.10	3830.00	-1443.90	NO VALUE
256	b-050-E/94-A-16	2371.00	3859.90	-1488.90	NO VALUE
257	d-050-E/94-A-16	2382.80	NO VALUE	NO VALUE	NO VALUE
258	b-051-E/94-A-16	2290.00	3704.00	-1414.00	NO VALUE
259	d-052-E/94-A-16	2377.90	3757.00	-1379.10	NO VALUE
260	d-053-E/94-A-16	2390.40	3780.20	-1389.80	NO VALUE
261	b-054-E/94-A-16	2380.00	3788.00	-1408.00	NO VALUE
262	b-056-E/94-A-16	2397.00	3817.00	-1420.00	NO VALUE
263	d-056-E/94-A-16	2389.00	3800.00	-1411.00	NO VALUE
264	b-057-E/94-A-16	2400.90	3832.00	-1431.10	NO VALUE
265	d-057-E/94-A-16	2392.00	3824.00	-1432.00	3971.00
266	b-058-E/94-A-16	2401.90	3846.10	-1444.20	NO VALUE
267	d-058-E/94-A-16	2393.40	3828.00	-1434.60	NO VALUE
268	b-059-E/94-A-16	2394.00	3832.00	-1438.00	NO VALUE
269	d-059-E/94-A-16	2392.00	3843.00	-1451.00	NO VALUE
270	a-060-E/94-A-16	2395.60	3862.20	-1466.60	NO VALUE
271	d-060-E/94-A-16	2381.80	3832.00	-1450.20	NO VALUE
272	d-062-E/94-A-16	2387.10	3770.00	-1382.90	NO VALUE
273	b-067-E/94-A-16	2399.00	3818.80	-1419.80	NO VALUE
274	b-068-E/94-A-16	2405.00	3854.00	-1449.00	NO VALUE
275	d-068-E/94-A-16	2399.90	3832.00	-1432.10	NO VALUE

	A	B	C	D	E
1	WELL ID.	KB	TOP HAL	S.S. TOP	TOP MON
2		(ft)	(ft)	HAL (ft)	(ft)
276	b-069-E/94-A-16	2396.00	3830.60	-1434.60	NO VALUE
277	d-069-E/94-A-16	2393.00	3836.00	-1443.00	NO VALUE
278	d-070-E/94-A-16	2378.90	3821.00	-1442.10	NO VALUE
279	d-074-E/94-A-16	2400.00	3787.00	-1387.00	NO VALUE
280	d-079-E/94-A-16	2384.80	3806.00	-1421.20	NO VALUE
281	a-080-E/94-A-16	2387.10	3812.00	-1424.90	NO VALUE
282	b-080-E/94-A-16	2383.80	3826.00	-1442.20	NO VALUE
283	d-080-E/94-A-16	2365.10	3800.00	-1434.90	NO VALUE
284	d-081-E/94-A-16	2402.80	3749.00	-1346.20	NO VALUE
285	d-084-E/94-A-16	2411.00	3792.00	-1381.00	NO VALUE
286	b-086-E/94-A-16	2409.10	3810.00	-1400.90	3934.00
287	d-090-E/94-A-16	2376.90	3800.80	-1423.90	NO VALUE
288	d-093-E-94-A-16	2408.10	3794.90	-1386.80	NO VALUE
289	d-097-E/94-A-16	2395.90	3790.00	-1394.10	NO VALUE
290	d-100-E/94-A-16	2377.00	3784.00	-1407.00	NO VALUE
291					
292	b-009-F/94-A-16	2399.90	3854.00	-1454.10	3990.00
293	d-010-F/94-A-16	2394.00	3845.10	-1451.10	NO VALUE
294	c-012-F/94-A-16	2458.90	3854.00	-1395.10	4014.70
295	a-015-F/94-A-16	2430.10			NO VALUE
296	d-017-F/94-A-16	2411.00	3834.30	-1423.30	NO VALUE
297	d-019-F/94-A-16	2391.00	3810.00	-1419.00	NO VALUE
298	d-020-F/94-A-16	2382.80	3811.00	-1428.20	NO VALUE
299	d-022-F/94-A-16	2435.00	3814.00	-1379.00	NO VALUE
300	b-027-F/94-A-16	2409.10	3832.00	-1422.90	NO VALUE
301	b-028-F/94-A-16	2398.90	3810.00	-1411.10	NO VALUE
302	d-028-F/94-A-16	2404.80	3810.00	-1405.20	NO VALUE
303	d-029-F/94-A-16	2383.80	3796.00	-1412.20	NO VALUE
304	d-030-F/94-A-16	2370.00	3809.00	-1439.00	NO VALUE
305	d-035-F/94-A-16	2421.90	3808.00	-1386.10	NO VALUE
306	d-037-F/94-A-16	2408.10	3803.00	-1394.90	NO VALUE
307	b-038-F/94-A-16	2395.00	3810.00	-1415.00	NO VALUE
308	d-038-F/94-A-16	2398.90	3796.00	-1397.10	NO VALUE
309	b-039-F/94-A-16	2389.00	3864.00	-1475.00	NO VALUE
310	d-040-F/94-A-16	2388.10	3812.00	-1423.90	NO VALUE
311	d-044-F/94-A-16	2418.30	3811.40	-1393.10	NO VALUE
312	d-046-F/94-A-16	2409.10	3788.40	-1379.30	NO VALUE
313	b-048-F/94-A-16	2389.10	3808.00	-1418.90	NO VALUE
314	d-049-F/94-A-16	2383.80	3770.00	-1386.20	NO VALUE

	A	B	C	D	E
1	WELL ID.	KB	TOP HAL	S.S. TOP	TOP MON
2		(ft)	(ft)	HAL (ft)	(ft)
315	d-050-F/94-A-16	2388.00	3800.00	-1412.00	NO VALUE
316	d-057-F/94-A-16	2389.10	3768.00	-1378.90	NO VALUE
317	b-058-F/94-A-16	2380.90	3767.00	-1386.10	NO VALUE
318	b-059-F/94-A-16	2389.40	3758.80	-1369.40	NO VALUE
319	d-059-F/94-A-16	2373.80	3750.00	-1376.20	NO VALUE
320	d-060-F/94-A-16	2368.00	3750.90	-1382.90	NO VALUE
321	d-063-F/94-A-16	2397.90	3742.10	-1344.20	NO VALUE
322	d-065-F/94-A-16	2350.00	3700.10	-1350.10	NO VALUE
323	d-066-F/94-A-16	2361.80	3674.10	-1312.30	NO VALUE
324	d-067-F/94-A-16	2377.90	3741.20	-1363.30	NO VALUE
325	b-068-F/94-A-16	2374.00	3748.00	-1374.00	NO VALUE
326	d-069-F/94-A-16	2329.00	3687.00	-1358.00	NO VALUE
327	d-070-F/94-A-16	2388.40	3750.40	-1362.00	NO VALUE
328	d-076-F/94-A-17	2320.80	3650.00	-1329.20	NO VALUE
329	d-077-F/94-A-16	2352.00	3688.00	-1336.00	NO VALUE
330	d-078-F/94-A-16	2362.80	3720.10	-1357.30	NO VALUE
331	d-079-F/94-A-16	2379.50	3742.00	-1362.50	NO VALUE
332	d-081-F/94-A-16	2354.90	3647.40	-1292.50	NO VALUE
333	d-083-F/94-A-16	2296.90	3598.00	-1301.10	NO VALUE
334	d-086-F/94-A-16	2354.90	3660.10	-1305.20	NO VALUE
335	d-088-F/94-A-16	2374.00	3704.00	-1330.00	NO VALUE
336	d-089-F/94-A-16	2394.00	3732.00	-1338.00	NO VALUE
337	d-090-F/94-A-16	2398.90	3751.90	-1353.00	NO VALUE
338	d-093-F/94-A-16	2381.80	3640.00	-1258.20	NO VALUE
339	d-094-F/94-A-16	2379.90	3670.90	-1291.00	NO VALUE
340	d-095-F/94-A-16	2398.90	3690.00	-1291.10	NO VALUE
341	d-096-F/94-A-16	2368.70	3683.40	-1314.70	NO VALUE
342	d-098-F/94-A-16	2389.10	3702.00	-1312.90	NO VALUE
343	d-099-F/94-A-16	2395.90	3714.00	-1318.10	NO VALUE
344	D-100-F/94-A-16	2397.90	3746.00	-1348.10	NO VALUE
345					
346	d-038-K/94-A-16	2396.00	3682.00	-1286.00	NO VALUE
347					
348	a-027-L/94-A-16	2385.00	3719.00	-1334.00	NO VALUE

	F	G	H	I	J
1	S.S. TOP	TOP 'A'	S.S. T 'A'	ISOPACH	T PHOSPHATE
2	MON (ft)	MARKER (ft)	MARKER (ft)	THAL TO 'A' (ft)	DATUM (ft)
3	NO VALUE	NO VALUE	NO VALUE	NO VALUE	NO VALUE
4	NO VALUE	4052.00	-1640.00	90.00	NO VALUE
5	-1949.10	4126.20	-1708.60	85.30	4320.00
6	NO VALUE	4092.00	-1689.20	90.00	NO VALUE
7	NO VALUE	3978.00	-1557.10	88.60	NO VALUE
8	NO VALUE	3962.20	-1543.60	82.00	NO VALUE
9	-1817.40	3974.00	-1581.50	90.00	4170.00
10	NO VALUE	4004.90	-1588.20	89.90	NO VALUE
11	-1850.10	NO VALUE	NO VALUE	NO VALUE	NO VALUE
12	NO VALUE	4006.50	-1627.90	87.00	NO VALUE
13	NO VALUE	4014.70	-1609.60	88.50	NO VALUE
14	NO VALUE	4017.00	-1619.10	92.90	NO VALUE
15	NO VALUE	NO VALUE	NO VALUE	NO VALUE	NO VALUE
16	NO VALUE	4054.10	-1650.60	26.20	NO VALUE
17	NO VALUE	3988.50	-1596.50	90.20	NO VALUE
18	NO VALUE	3965.00	-1570.70	89.00	NO VALUE
19	NO VALUE	NO VALUE	NO VALUE	NO VALUE	4140.00
20	NO VALUE	3886.80	-1504.00	75.40	NO VALUE
21	NO VALUE	3936.00	-1554.20	95.00	NO VALUE
22					
23	NO VALUE	3932.70	-1560.70	93.30	NO VALUE
24	NO VALUE	NO VALUE	NO VALUE	NO VALUE	NO VALUE
25	NO VALUE	3832.00	-1457.40	49.50	NO VALUE
26	NO VALUE	3835.00	-1464.30	55.00	NO VALUE
27	NO VALUE	3860.00	-1502.10	94.00	NO VALUE
28	NO VALUE	3804.00	-1431.70	52.00	NO VALUE
29	NO VALUE	3808.00	-1439.90	56.00	NO VALUE
30	NO VALUE	3804.00	-1438.00	65.00	NO VALUE
31	NO VALUE	3824.00	-1461.20	61.00	NO VALUE
32	NO VALUE	3855.60	-1561.00	93.70	NO VALUE
33	NO VALUE	3806.00	-1438.90	48.00	NO VALUE
34	NO VALUE	3785.00	-1413.00	55.00	NO VALUE
35	NO VALUE	3804.00	-1440.00	57.00	NO VALUE
36	NO VALUE	3789.00	-1423.90	65.00	NO VALUE
37	NO VALUE	3788.00	-1426.00	68.00	NO VALUE
38	NO VALUE	3809.00	-1449.00	59.10	NO VALUE
39	NO VALUE	3822.00	-1458.00	74.00	NO VALUE
40	NO VALUE	3814.60	-1456.40	74.40	NO VALUE
41	NO VALUE	3795.00	-1422.00	45.90	NO VALUE

	F	G	H	I	J
1	S.S. TOP	TOP 'A'	S.S. T 'A'	ISOPACH	T PHOSPHATE
2	MON (ft)	MARKER (ft)	MARKER (ft)	THAL TO 'A' (ft)	DATUM (ft)
42	NO VALUE	3778.00	-1408.00	54.00	NO VALUE
43	NO VALUE	3796.00	-1426.00	52.00	NO VALUE
44	NO VALUE	3782.00	-1412.00	56.00	NO VALUE
45	NO VALUE	3791.00	-1428.20	55.80	NO VALUE
46	NO VALUE	3779.00	-1425.00	67.00	NO VALUE
47	NO VALUE	3796.00	-1440.00	60.00	NO VALUE
48	NO VALUE	3808.00	-1458.20	60.10	NO VALUE
49	NO VALUE	3784.00	-1442.20	72.00	NO VALUE
50	NO VALUE	3780.00	-1443.10	80.00	NO VALUE
51	NO VALUE	3804.00	-1456.90	96.00	NO VALUE
52	NO VALUE	3753.00	-1379.00	65.00	NO VALUE
53	NO VALUE	3768.00	-1402.40	57.00	NO VALUE
54	NO VALUE	3784.00	-1421.20	57.80	NO VALUE
55	NO VALUE	3779.00	-1414.00	59.00	NO VALUE
56	NO VALUE	3792.00	-1433.00	56.10	NO VALUE
57	NO VALUE	3780.00	-1420.10	56.00	NO VALUE
58	NO VALUE	3792.00	-1430.20	56.00	NO VALUE
59	NO VALUE	3798.00	-1442.00	58.00	NO VALUE
60	NO VALUE	3788.00	-1437.00	62.00	NO VALUE
61	NO VALUE	3774.00	-1421.00	75.60	NO VALUE
62	NO VALUE	3744.00	-1374.60	64.00	NO VALUE
63	NO VALUE	3741.00	-1378.20	69.00	NO VALUE
64	NO VALUE	3762.00	-1400.20	58.00	NO VALUE
65	NO VALUE	3785.00	-1418.85	54.00	NO VALUE
66	NO VALUE	3752.00	-1389.20	66.00	NO VALUE
67	NO VALUE	3764.00	-1400.20	64.00	NO VALUE
68	NO VALUE	3778.00	-1421.00	58.00	NO VALUE
69	NO VALUE	3783.00	-1422.40	57.00	NO VALUE
70	NO VALUE	3784.00	-1434.00	64.00	NO VALUE
71	NO VALUE	3784.00	-1430.00	46.00	NO VALUE
72	NO VALUE	3787.00	-1430.10	61.00	NO VALUE
73	NO VALUE	3778.00	-1424.10	62.00	NO VALUE
74	NO VALUE	3778.00	-1424.90	58.00	NO VALUE
75	NO VALUE	3773.00	-1423.00	73.00	NO VALUE
76	NO VALUE	3733.00	-1362.00	65.00	NO VALUE
77	NO VALUE	3758.00	-1398.00	56.00	NO VALUE
78	NO VALUE	3778.00	-1421.10	57.90	NO VALUE
79	NO VALUE	3760.00	-1403.00	57.00	NO VALUE
80	NO VALUE	3776.00	-1421.10	56.00	NO VALUE

	F	G	H	I	J
1	S.S. TOP	TOP 'A'	S.S. T 'A'	ISOPACH	T PHOSPHATE
2	MON (ft)	MARKER (ft)	MARKER (ft)	THAL TO 'A' (ft)	DATUM (ft)
81	NO VALUE	3775.00	-1414.25	33.00	NO VALUE
82	NO VALUE	3764.00	-1404.10	58.00	NO VALUE
83	NO VALUE	3766.00	-1407.10	64.10	NO VALUE
84	NO VALUE	3765.40	-1417.00	55.80	NO VALUE
85	NO VALUE	3768.00	-1436.00	88.00	NO VALUE
86	NO VALUE	3746.00	-1393.00	58.00	NO VALUE
87	NO VALUE	3748.00	-1385.20	76.30	NO VALUE
88	NO VALUE	3748.00	-1388.00	53.00	NO VALUE
89	NO VALUE	3754.00	-1404.00	56.00	NO VALUE
90	NO VALUE	3758.90	-1397.70	65.60	NO VALUE
91	NO VALUE	3741.00	-1393.90	74.00	NO VALUE
92	NO VALUE	3739.20	-1407.20	70.50	NO VALUE
93					
94	NO VALUE	NO VALUE	NO VALUE	NO VALUE	NO VALUE
95					
96	NO VALUE	NO VALUE	NO VALUE	NO VALUE	NO VALUE
97					
98	NO VALUE	3884.00	-1426.00	85.00	NO VALUE
99					
100	NO VALUE	3894.00	-1452.10	88.00	NO VALUE
101	NO VALUE	3896.00	-1479.70	88.00	4032.00
102	NO VALUE	3849.00	-1448.00	83.00	4040.00
103	NO VALUE	3876.00	-1503.00	88.00	4036.00
104	NO VALUE	3874.00	-1504.00	87.00	NO VALUE
105	NO VALUE	NO VALUE	NO VALUE	NO VALUE	4044.00
106	NO VALUE	3852.00	-1469.00	78.30	NO VALUE
107	NO VALUE	3834.00	-1454.50	94.00	4020.00
108	NO VALUE	3850.00	-1491.10	87.00	NO VALUE
109	NO VALUE	NO VALUE	NO VALUE	NO VALUE	4024.00
110	NO VALUE	3842.00	-1467.00	90.00	4012.00
111	NO VALUE	3822.00	-1436.20	74.00	4020.00
112	NO VALUE	3836.00	-1460.40	79.00	4008.00
113	NO VALUE	3822.00	-1426.10	90.00	NO VALUE
114	NO VALUE	3826.00	-1454.20	87.00	4008.00
115	-1656.00	3857.00	-1405.00	88.00	4006.00
116	NO VALUE	3814.00	-1440.00	94.10	NO VALUE
117	NO VALUE	3848.00	-1368.10	88.00	NO VALUE
118	NO VALUE	3837.00	-1438.10	84.90	NO VALUE
119	NO VALUE	3821.20	-1398.00	87.60	4005.00

	F	G	H	I	J
1	S.S. TOP	TOP 'A'	S.S. T 'A'	ISOPACH	T PHOSPHATE
2	MON (ft)	MARKER (ft)	MARKER (ft)	THAL TO 'A' (ft)	DATUM (ft)
120	NO VALUE	3814.60	-1417.70	75.40	NO VALUE
121	NO VALUE	3827.80	-1418.10	74.10	NO VALUE
122	NO VALUE	3822.00	-1428.00	78.00	3996.00
123	NO VALUE	3805.00	-1430.00	76.80	NO VALUE
124	NO VALUE	3827.80	-1401.30	78.70	NO VALUE
125	NO VALUE	NO VALUE	NO VALUE	NO VALUE	NO VALUE
126	NO VALUE	NO VALUE	NO VALUE	NO VALUE	NO VALUE
127	NO VALUE	3814.60	-1406.10	72.20	NO VALUE
128	NO VALUE	3821.00	-1406.00	75.00	3980.00
129	NO VALUE	3817.00	-1418.90	79.00	3968.00
130	NO VALUE	3802.00	-1418.00	74.00	NO VALUE
131	NO VALUE	3834.30	-1353.70	85.30	NO VALUE
132	NO VALUE	3838.00	-1384.00	82.00	NO VALUE
133	NO VALUE	3817.90	-1393.70	78.70	3988.00
134	NO VALUE	3814.60	-1381.60	88.60	NO VALUE
135	NO VALUE	3811.40	-1402.30	72.10	NO VALUE
136	NO VALUE	3804.80	-1411.30	76.20	3954.00
137	NO VALUE	3804.80	-1385.20	82.00	NO VALUE
138	NO VALUE	3800.00	-1406.50	80.00	3954.00
139	NO VALUE	3795.00	-1412.80	79.00	NO VALUE
140	NO VALUE	3820.00	-1338.10	78.00	NO VALUE
141	NO VALUE	3790.00	-1379.30	77.10	NO VALUE
142	NO VALUE	3788.00	-1373.00	84.00	3956.00
143	NO VALUE	3786.00	-1390.20	87.00	3954.00
144	NO VALUE	3791.70	-1409.50	74.40	NO VALUE
145	NO VALUE	3791.00	-1402.00	75.00	NO VALUE
146	-1599.10	3802.00	-1363.10	88.00	NO VALUE
147	NO VALUE	3778.60	-1353.50	91.40	3949.00
148	NO VALUE	3775.00	-1373.10	83.00	NO VALUE
149	NO VALUE	3772.00	-1364.00	74.10	NO VALUE
150	NO VALUE	3776.00	-1372.50	74.00	3946.00
151	NO VALUE	3782.00	-1388.00	76.00	NO VALUE
152					
153	NO VALUE	3920.00	-1572.00	73.00	4120.00
154	NO VALUE	3899.90	-1530.90	59.10	NO VALUE
155	NO VALUE	NO VALUE	NO VALUE	NO VALUE	NO VALUE
156	NO VALUE	3880.20	-1512.50	67.30	NO VALUE
157	NO VALUE	3900.00	-1540.10	56.00	NO VALUE
158	NO VALUE	3830.00	-1461.90	90.00	NO VALUE

	F	G	H	I	J
1	S.S. TOP	TOP 'A'	S.S. T 'A'	ISOPACH	T PHOSPHATE
2	MON (ft)	MARKER (ft)	MARKER (ft)	THAL TO 'A' (ft)	DATUM (ft)
159	NO VALUE	3836.00	-1470.90	70.00	NO VALUE
160	NO VALUE	3863.80	-1488.80	71.50	NO VALUE
161	NO VALUE	3883.50	-1521.30	59.10	NO VALUE
162	NO VALUE	3818.00	-1446.00	85.00	NO VALUE
163	NO VALUE	3876.00	-1507.90	54.10	4078.00
164	NO VALUE	3908.00	-1520.90	76.90	NO VALUE
165	NO VALUE	3800.00	-1429.00	81.00	NO VALUE
166	NO VALUE	3906.00	-1533.00	58.80	NO VALUE
167	NO VALUE	3802.00	-1432.00	72.00	NO VALUE
168	NO VALUE	3802.00	-1437.00	82.00	3978.00
169	NO VALUE	3800.00	-1436.00	88.10	NO VALUE
170	NO VALUE	3830.00	-1466.00	82.00	3993.00
171	NO VALUE	3829.00	-1476.00	70.90	3944.00
172	NO VALUE	3800.00	-1427.00	73.00	3970.00
173	NO VALUE	3795.00	-1435.10	91.70	NO VALUE
174	NO VALUE	3792.00	-1423.90	76.00	3976.00
175	NO VALUE	3792.00	-1440.20	86.00	3974.00
176	NO VALUE	3794.00	-1414.10	74.00	3963.00
177	NO VALUE	3788.00	-1404.00	77.00	3960.00
178	NO VALUE	3786.00	-1414.50	72.00	3966.00
179	NO VALUE	3780.00	-1431.00	84.00	NO VALUE
180	NO VALUE	3774.00	-1418.00	82.00	3964.00
181	NO VALUE	3838.10	-1502.20	55.30	NO VALUE
182	NO VALUE	3802.00	-1471.00	94.00	3966.00
183	NO VALUE	3790.00	-1450.80	87.90	NO VALUE
184	NO VALUE	3822.00	-1480.00	58.00	NO VALUE
185	NO VALUE	3786.00	-1397.00	73.00	NO VALUE
186	NO VALUE	3783.00	-1412.00	71.00	NO VALUE
187	NO VALUE	3756.00	-1387.00	89.00	3960.00
188	NO VALUE	3756.00	-1422.10	78.00	NO VALUE
189	NO VALUE	3786.00	-1454.00	86.00	NO VALUE
190	NO VALUE	NO VALUE	NO VALUE	NO VALUE	3942.00
191	NO VALUE	3785.10	-1445.30	85.30	NO VALUE
192	NO VALUE	NO VALUE	NO VALUE	NO VALUE	NO VALUE
193	NO VALUE	3781.80	-1427.80	80.40	NO VALUE
194	NO VALUE	3788.40	-1429.50	75.40	NO VALUE
195	NO VALUE	3788.40	-1429.50	78.70	NO VALUE
196	NO VALUE	3804.80	-1455.80	55.80	NO VALUE
197					

	F	G	H	I	J
1	S.S. TOP	TOP 'A'	S.S. T 'A'	ISOPACH	T PHOSPHATE
2	MON (ft)	MARKER (ft)	MARKER (ft)	THAL TO 'A' (ft)	DATUM (ft)
198	NO VALUE	3762.00	-1389.00	70.00	NO VALUE
199	NO VALUE	3752.00	-1394.10	74.00	NO VALUE
200	NO VALUE	3764.00	-1412.00	74.00	NO VALUE
201	NO VALUE	3756.00	-1399.00	74.00	3942.00
202	NO VALUE	3754.00	-1403.00	85.80	NO VALUE
203	NO VALUE	3753.00	-1397.70	77.00	3936.00
204	NO VALUE	3794.00	-1434.10	90.00	3958.00
205	NO VALUE	3798.20	-1447.20	88.60	NO VALUE
206	NO VALUE	3788.40	-1431.50	88.50	NO VALUE
207	NO VALUE	3794.00	-1438.00	75.00	NO VALUE
208	NO VALUE	3737.00	-1377.10	73.00	NO VALUE
209	NO VALUE	3740.00	-1374.00	72.00	NO VALUE
210	NO VALUE	3752.30	-1393.10	80.40	NO VALUE
211	NO VALUE	3754.00	-1384.00	84.00	NO VALUE
212	NO VALUE	3752.30	-1390.10	84.70	NO VALUE
213	NO VALUE	3752.00	-1385.00	84.90	3924.00
214	NO VALUE	3764.00	-1404.50	86.00	NO VALUE
215	NO VALUE	3772.00	-1416.10	72.10	NO VALUE
216	NO VALUE	3775.00	-1427.90	89.00	NO VALUE
217	NO VALUE	NO VALUE	NO VALUE	NO VALUE	NO VALUE
218	NO VALUE	3768.00	-1412.10	76.00	NO VALUE
219	-1660.00	NO VALUE	NO VALUE	NO VALUE	3974.00
220	NO VALUE	3750.00	-1376.00	86.00	NO VALUE
221	NO VALUE	3730.00	-1367.00	59.00	NO VALUE
222	NO VALUE	3738.00	-1375.00	88.10	NO VALUE
223	NO VALUE	3732.00	-1375.00	68.00	NO VALUE
224	NO VALUE	3674.00	-1392.00	60.00	NO VALUE
225	NO VALUE	3754.00	-1395.00	65.00	3922.00
226	NO VALUE	3760.00	-1401.00	64.00	NO VALUE
227	NO VALUE	3766.00	-1409.00	72.00	NO VALUE
228	NO VALUE	3779.00	-1407.00	77.00	NO VALUE
229	NO VALUE	3765.00	-1404.20	69.00	NO VALUE
230	NO VALUE	3778.00	-1410.90	75.00	NO VALUE
231	NO VALUE	3814.00	-1444.00	62.00	NO VALUE
232	NO VALUE	3712.00	-1358.00	74.00	NO VALUE
233	NO VALUE	3718.00	-1365.00	64.00	NO VALUE
234	NO VALUE	3754.00	-1384.00	64.00	NO VALUE
235	NO VALUE	3736.00	-1368.90	60.00	NO VALUE
236	NO VALUE	3744.00	-1376.00	59.00	NO VALUE

	F	G	H	I	J
1	S.S. TOP	TOP 'A'	S.S. T 'A'	ISOPACH	T PHOSPHATE
2	MON (ft)	MARKER (ft)	MARKER (ft)	THAL TO 'A' (ft)	DATUM (ft)
237	NO VALUE	3761.00	-1400.20	69.00	NO VALUE
238	NO VALUE	3758.00	-1391.00	60.00	NO VALUE
239	NO VALUE	3775.00	-1396.10	59.00	NO VALUE
240	NO VALUE	3761.00	-1392.00	64.00	3926.00
241	NO VALUE	3787.00	-1398.30	67.40	NO VALUE
242	NO VALUE	3768.00	-1393.70	58.00	NO VALUE
243	NO VALUE	3803.00	-1413.90	59.00	NO VALUE
244	NO VALUE	3780.00	-1399.10	62.00	NO VALUE
245	NO VALUE	3811.00	-1425.40	56.00	NO VALUE
246	NO VALUE	3784.00	-1408.10	76.00	NO VALUE
247	NO VALUE	3718.00	-1345.00	92.00	NO VALUE
248	NO VALUE	3742.00	-1370.00	58.40	NO VALUE
249	-1583.00	3752.00	-1373.00	58.30	3932.00
250	NO VALUE	3778.00	-1391.70	57.90	NO VALUE
251	NO VALUE	3754.00	-1374.10	63.40	NO VALUE
252	NO VALUE	3778.00	-1388.00	60.00	NO VALUE
253	NO VALUE	3762.00	-1376.20	71.00	NO VALUE
254	NO VALUE	3782.00	-1390.30	68.00	NO VALUE
255	NO VALUE	3775.00	-1388.90	55.00	NO VALUE
256	NO VALUE	3788.00	-1417.00	71.90	NO VALUE
257	NO VALUE	3778.00	-1395.20	NO VALUE	NO VALUE
258	NO VALUE	3615.00	-1325.00	89.00	NO VALUE
259	NO VALUE	3697.00	-1319.10	60.00	NO VALUE
260	NO VALUE	3710.00	-1319.60	70.20	NO VALUE
261	NO VALUE	3732.00	-1352.00	56.00	3906.00
262	NO VALUE	3752.00	-1355.00	65.00	NO VALUE
263	NO VALUE	3740.00	-1351.00	60.00	NO VALUE
264	NO VALUE	3774.00	-1373.10	58.00	NO VALUE
265	-1579.00	3767.00	-1375.00	57.00	3920.00
266	NO VALUE	3787.00	-1385.10	59.10	NO VALUE
267	NO VALUE	3763.00	-1369.60	65.00	NO VALUE
268	NO VALUE	3772.00	-1378.00	60.00	NO VALUE
269	NO VALUE	3762.00	-1370.00	81.00	NO VALUE
270	NO VALUE	3775.30	-1379.70	86.90	NO VALUE
271	NO VALUE	3774.00	-1392.20	58.00	NO VALUE
272	NO VALUE	3690.00	-1302.90	80.00	NO VALUE
273	NO VALUE	3764.00	-1365.00	54.80	NO VALUE
274	NO VALUE	3778.00	-1373.00	76.00	NO VALUE
275	NO VALUE	3758.00	-1358.10	74.00	NO VALUE

	F	G	H	I	J
1	S.S. TOP	TOP 'A'	S.S. T 'A'	ISOPACH	T PHOSPHATE
2	MON (ft)	MARKER (ft)	MARKER (ft)	THAL TO 'A' (ft)	DATUM (ft)
276	NO VALUE	3772.00	-1376.00	58.60	NO VALUE
277	NO VALUE	3771.00	-1378.00	65.00	NO VALUE
278	NO VALUE	3769.00	-1390.10	52.00	NO VALUE
279	NO VALUE	3700.00	-1300.00	87.00	3882.00
280	NO VALUE	3754.00	-1369.20	52.00	NO VALUE
281	NO VALUE	3760.00	-1372.90	52.00	NO VALUE
282	NO VALUE	3751.00	-1367.20	75.00	NO VALUE
283	NO VALUE	3742.00	-1376.90	58.00	NO VALUE
284	NO VALUE	3683.40	-1280.60	65.60	3821.00
285	NO VALUE	3714.00	-1303.00	78.00	NO VALUE
286	-1524.90	3727.00	-1317.90	83.00	3900.00
287	NO VALUE	3743.00	-1366.10	57.80	NO VALUE
288	NO VALUE	3717.00	-1308.90	77.90	NO VALUE
289	NO VALUE	3716.00	-1320.10	74.00	3876.00
290	NO VALUE	3716.00	-1339.00	68.00	NO VALUE
291					
292	-1590.10	NO VALUE	NO VALUE	NO VALUE	3940.00
293	NO VALUE	3771.00	-1377.00	74.10	NO VALUE
294	-1555.80	3772.00	-1313.10	[illegible]2.00	NO VALUE
295	NO VALUE	3770.00	-1339.90	-3770.00	NO VALUE
296	NO VALUE	3752.30	-1341.30	82.00	NO VALUE
297	NO VALUE	3742.00	-1351.00	68.00	NO VALUE
298	NO VALUE	3738.00	-1355.20	73.00	NO VALUE
299	NO VALUE	3752.00	-1317.00	62.00	3892.00
300	NO VALUE	3749.00	-1339.90	83.00	NO VALUE
301	NO VALUE	3737.00	-1338.10	73.00	NO VALUE
302	NO VALUE	3732.00	-1327.20	78.00	NO VALUE
303	NO VALUE	3717.00	-1333.20	79.00	NO VALUE
304	NO VALUE	3722.00	-1352.00	87.00	NO VALUE
305	NO VALUE	3727.00	-1305.10	81.00	NO VALUE
306	NO VALUE	3717.90	-1309.80	85.10	NO VALUE
307	NO VALUE	3724.00	-1329.00	86.00	NO VALUE
308	NO VALUE	3713.00	-1314.10	83.00	3888.00
309	NO VALUE	3704.00	-1315.00	160.00	NO VALUE
310	NO VALUE	3726.00	-1337.90	86.00	NO VALUE
311	NO VALUE	3734.30	-1316.00	77.10	NO VALUE
312	NO VALUE	3704.80	-1295.70	83.60	NO VALUE
313	NO VALUE	3719.00	-1329.90	89.00	NO VALUE
314	NO VALUE	3700.00	-1316.20	70.00	3874.00

	F	G	H	I	J
1	S.S. TOP	TOP 'A'	S.S. T 'A'	ISOPACH	T PHOSPHATE
2	MON (ft)	MARKER (ft)	MARKER (ft)	THAL TO 'A' (ft)	DATUM (ft)
315	NO VALUE	3724.00	-1336.00	76.00	NO VALUE
316	NO VALUE	3679.00	-1289.90	89.00	NO VALUE
317	NO VALUE	3683.00	-1302.10	84.00	3854.00
318	NO VALUE	NO VALUE	NO VALUE	NO VALUE	NO VALUE
319	NO VALUE	3666.00	-1292.20	84.00	NO VALUE
320	NO VALUE	3672.00	-1304.00	78.90	NO VALUE
321	NO VALUE	3665.00	-1267.10	77.10	NO VALUE
322	NO VALUE	3634.00	-1284.00	66.10	NO VALUE
323	NO VALUE	3627.00	-1265.20	47.10	NO VALUE
324	NO VALUE	3663.80	-1285.90	77.40	NO VALUE
325	NO VALUE	3661.00	-1287.00	87.00	3834.00
326	NO VALUE	3602.00	-1273.00	85.00	NO VALUE
327	NO VALUE	3673.60	-1285.20	76.80	NO VALUE
328	NO VALUE	3600.00	-1279.20	50.00	NO VALUE
329	NO VALUE	3616.00	-1264.00	72.00	3754.00
330	NO VALUE	3648.00	-1285.20	72.10	NO VALUE
331	NO VALUE	3672.00	-1292.50	70.00	NO VALUE
332	NO VALUE	3570.30	-1215.40	77.10	NO VALUE
333	NO VALUE	3520.00	-1223.10	78.00	3642.00
334	NO VALUE	NO VALUE	NO VALUE	NO VALUE	NO VALUE
335	NO VALUE	3632.00	-1258.00	72.00	NO VALUE
336	NO VALUE	3648.00	-1254.00	84.00	3810.00
337	NO VALUE	3676.00	-1277.10	75.90	NO VALUE
338	NO VALUE	3567.00	-1185.20	73.00	NO VALUE
339	NO VALUE	3596.00	-1216.10	74.90	NO VALUE
340	NO VALUE	3625.00	-1226.10	65.00	NO VALUE
341	NO VALUE	3611.30	-1242.60	72.10	NO VALUE
342	NO VALUE	3636.00	-1246.90	66.00	3772.00
343	NO VALUE	3629.00	-1233.10	85.00	3794.00
344	NO VALUE	3672.00	-1274.10	74.00	3792.00
345					
346	NO VALUE	3621.00	-1225.00	61.00	NO VALUE
347					
348	NO VALUE	3672.00	-1287.00	47.00	NO VALUE

	K	L	M
1	S.S. T PHOSPHATE	ISO T PHOSPHATE	BASE HAL SAND
2	DATUM (ft)	TO THAL (ft)	65A.P.I. (ft)
3	NO VALUE	NO VALUE	NO VALUE
4	NO VALUE	NO VALUE	4198.00
5	-1902.40	108.50	4231.00
6	NO VALUE	NO VALUE	4200.00
7	NO VALUE	NO VALUE	4147.00
8	NO VALUE	NO VALUE	4098.00
9	-1777.50	106.00	4107.00
10	NO VALUE	NO VALUE	4106.00
11	NO VALUE	NO VALUE	NO VALUE
12	NO VALUE	NO VALUE	4133.00
13	NO VALUE	NO VALUE	4115.00
14	NO VALUE	NO VALUE	NO VALUE
15	NO VALUE	NO VALUE	4064.00
16	NO VALUE	NO VALUE	4097.00
17	NO VALUE	NO VALUE	4093.00
18	NO VALUE	NO VALUE	4068.00
19	-1768.00	116.10	4038.00
20	NO VALUE	NO VALUE	3998.00
21	NO VALUE	NO VALUE	4035.00
22			
23	NO VALUE	NO VALUE	4008.00
24	NO VALUE	NO VALUE	NO VALUE
25	NO VALUE	NO VALUE	3910.00
26	NO VALUE	NO VALUE	3906.00
27	NO VALUE	NO VALUE	3957.00
28	NO VALUE	NO VALUE	3895.00
29	NO VALUE	NO VALUE	3905.00
30	NO VALUE	NO VALUE	3906.00
31	NO VALUE	NO VALUE	3910.00
32	NO VALUE	NO VALUE	3949.00
33	NO VALUE	NO VALUE	3890.00
34	NO VALUE	NO VALUE	3876.00
35	NO VALUE	NO VALUE	3906.00
36	NO VALUE	NO VALUE	NO VALUE
37	NO VALUE	NO VALUE	3888.00
38	NO VALUE	NO VALUE	3914.00
39	NO VALUE	NO VALUE	3924.00
40	NO VALUE	NO VALUE	3923.00
41	NO VALUE	NO VALUE	3861.00

	K	L	M
1	S.S. T PHOSPHATE	ISO T PHOSPHATE	BASE THAL SAND
2	DATUM (ft)	TO THAL (ft)	65A.P.I. (ft)
42	NO VALUE	NO VALUE	3860.00
43	NO VALUE	NO VALUE	3872.00
44	NO VALUE	NO VALUE	3854.00
45	NO VALUE	NO VALUE	3864.00
46	NO VALUE	NO VALUE	3876.00
47	NO VALUE	NO VALUE	3886.00
48	NO VALUE	NO VALUE	3901.00
49	NO VALUE	NO VALUE	3882.00
50	NO VALUE	NO VALUE	3880.00
51	NO VALUE	NO VALUE	3898.00
52	NO VALUE	NO VALUE	NO VALUE
53	NO VALUE	NO VALUE	3840.00
54	NO VALUE	NO VALUE	3874.00
55	NO VALUE	NO VALUE	3854.00
56	NO VALUE	NO VALUE	3880.00
57	NO VALUE	NO VALUE	3860.00
58	NO VALUE	NO VALUE	3874.00
59	NO VALUE	NO VALUE	3880.00
60	NO VALUE	NO VALUE	3872.00
61	NO VALUE	NO VALUE	3872.00
62	NO VALUE	NO VALUE	NO VALUE
63	NO VALUE	NO VALUE	3830.00
64	NO VALUE	NO VALUE	3834.00
65	NO VALUE	NO VALUE	3878.00
66	NO VALUE	NO VALUE	3846.00
67	NO VALUE	NO VALUE	3842.00
68	NO VALUE	NO VALUE	3854.00
69	NO VALUE	NO VALUE	3853.00
70	NO VALUE	NO VALUE	3866.00
71	NO VALUE	NO VALUE	3857.00
72	NO VALUE	NO VALUE	3872.00
73	NO VALUE	NO VALUE	3861.00
74	NO VALUE	NO VALUE	3862.00
75	NO VALUE	NO VALUE	3858.00
76	NO VALUE	NO VALUE	NO VALUE
77	NO VALUE	NO VALUE	3830.00
78	NO VALUE	NO VALUE	3856.00
79	NO VALUE	NO VALUE	3829.00
80	NO VALUE	NO VALUE	3860.00

	K	L	M
1	S.S. T PHOSPHATE	ISO T PHOSPHATE	BASE HAL SAND
2	DATUM (ft)	TO THAL (ft)	65A.P.I. (ft)
81	NO VALUE	NO VALUE	3850.00
82	NO VALUE	NO VALUE	3845.00
83	NO VALUE	NO VALUE	3850.00
84	NO VALUE	NO VALUE	3838.00
85	NO VALUE	NO VALUE	3861.00
86	NO VALUE	NO VALUE	3824.00
87	NO VALUE	NO VALUE	3842.00
88	NO VALUE	NO VALUE	3822.00
89	NO VALUE	NO VALUE	3824.00
90	NO VALUE	NO VALUE	3841.00
91	NO VALUE	NO VALUE	3830.00
92	NO VALUE	NO VALUE	3824.00
93			
94	NO VALUE	NO VALUE	NO VALUE
95			
96	NO VALUE	NO VALUE	NO VALUE
97			
98	NO VALUE	NO VALUE	NO VALUE
99			
100	NO VALUE	NO VALUE	4002.00
101	-1634.00	48.00	3990.00
102	-1639.00	108.00	3975.00
103	-1663.00	76.00	3967.00
104	NO VALUE	NO VALUE	3976.00
105	-1597.20	76.00	3982.00
106	NO VALUE	NO VALUE	3973.00
107	-1640.50	92.00	3956.00
108	NO VALUE	NO VALUE	3950.00
109	-1667.10	74.00	3962.00
110	-1637.00	80.00	3947.00
111	-1634.20	124.00	3948.00
112	-1632.40	93.00	3950.00
113	NO VALUE	NO VALUE	3940.00
114	-1636.20	95.00	3943.00
115	-1554.00	61.00	3946.00
116	NO VALUE	NO VALUE	3936.00
117	NO VALUE	NO VALUE	3936.00
118	NO VALUE	NO VALUE	3931.00
119	-1581.80	96.20	NO VALUE

	K	L	M
1	S.S. T PHOSPHATE	ISO T PHOSPHATE	BASE HAL SAND
2	DATUM (ft)	TO THAL (ft)	65A.P.I. (ft)
120	NO VALUE	NO VALUE	3916.00
121	NO VALUE	NO VALUE	3916.00
122	-1602.00	96.00	3925.00
123	NO VALUE	NO VALUE	3904.00
124	NO VALUE	NO VALUE	3920.00
125	NO VALUE	NO VALUE	NO VALUE
126	NO VALUE	NO VALUE	3926.00
127	NO VALUE	NO VALUE	3907.00
128	-1565.00	84.00	3915.00
129	-1569.90	72.00	3912.00
130	NO VALUE	NO VALUE	3906.00
131	NO VALUE	NO VALUE	3923.00
132	NO VALUE	NO VALUE	3924.00
133	-1563.80	91.40	3913.00
134	NO VALUE	NO VALUE	3913.00
135	NO VALUE	NO VALUE	3905.00
136	-1560.50	73.00	3896.00
137	NO VALUE	NO VALUE	3897.00
138	-1560.50	74.00	3894.00
139	NO VALUE	NO VALUE	3893.00
140	NO VALUE	NO VALUE	3905.00
141	NO VALUE	NO VALUE	3887.00
142	-1541.00	84.00	3876.00
143	-1558.20	81.00	3886.00
144	NO VALUE	NO VALUE	3893.00
145	NO VALUE	NO VALUE	NO VALUE
146	NO VALUE	NO VALUE	3891.00
147	-1523.90	79.00	3871.00
148	NO VALUE	NO VALUE	3870.00
149	NO VALUE	NO VALUE	3855.00
150	-1542.50	96.00	3878.00
151	NO VALUE	NO VALUE	3865.00
152			
153	-1772.00	127.00	4028.00
154	NO VALUE	NO VALUE	3992.00
155	NO VALUE	NO VALUE	NO VALUE
156	NO VALUE	NO VALUE	3969.00
157	NO VALUE	NO VALUE	3992.00
158	NO VALUE	NO VALUE	NO VALUE

	K	L	M
1	S.S. T PHOSPHATE	ISO T PHOSPHATE	BASE HAL SAND
2	DATUM (ft)	TO THAL (ft)	65A.P.I. (ft)
159	NO VALUE	NO VALUE	3948.00
160	NO VALUE	NO VALUE	3969.00
161	NO VALUE	NO VALUE	3975.00
162	NO VALUE	NO VALUE	3950.00
163	-1709.90	147.90	3980.00
164	NO VALUE	NO VALUE	4016.00
165	NO VALUE	NO VALUE	3916.00
166	NO VALUE	NO VALUE	NO VALUE
167	NO VALUE	NO VALUE	3912.00
168	-1613.00	94.00	3909.00
169	NO VALUE	NO VALUE	3916.00
170	-1629.00	81.00	3924.00
171	-1591.00	44.10	3944.00
172	-1597.00	97.00	3894.00
173	NO VALUE	NO VALUE	3907.00
174	-1607.90	108.00	3906.00
175	-1622.20	96.00	3902.00
176	-1583.10	95.00	3890.00
177	-1576.00	95.00	3889.00
178	-1594.50	108.00	3888.00
179	NO VALUE	NO VALUE	3880.00
180	-1608.00	108.00	3893.00
181	NO VALUE	NO VALUE	3905.00
182	-1635.00	70.00	3896.00
183	NO VALUE	NO VALUE	3913.00
184	NO VALUE	NO VALUE	3940.00
185	NO VALUE	NO VALUE	3878.00
186	NO VALUE	NO VALUE	3882.00
187	-1591.00	115.00	3870.00
188	NO VALUE	NO VALUE	3874.00
189	NO VALUE	NO VALUE	3873.00
190	-1606.00	98.00	3864.00
191	NO VALUE	NO VALUE	3870.00
192	NO VALUE	NO VALUE	NO VALUE
193	NO VALUE	NO VALUE	3903.00
194	NO VALUE	NO VALUE	3878.00
195	NO VALUE	NO VALUE	NO VALUE
196	NO VALUE	NO VALUE	3874.00
197			

	K	L	M
1	S.S. T PHOSPHATE	ISO T PHOSPHATE	BASE HAL SAND
2	DATUM (ft)	TO THAL (ft)	65A.P.I. (ft)
198	NO VALUE	NO VALUE	3850.00
199	NO VALUE	NO VALUE	3850.00
200	NO VALUE	NO VALUE	3860.00
201	-1585.00	112.00	3850.00
202	NO VALUE	NO VALUE	3860.00
203	-1580.70	106.00	3852.00
204	-1598.10	74.00	3884.00
205	NO VALUE	NO VALUE	3893.00
206	NO VALUE	NO VALUE	3897.00
207	NO VALUE	NO VALUE	3880.00
208	NO VALUE	NO VALUE	3823.00
209	NO VALUE	NO VALUE	3847.00
210	NO VALUE	NO VALUE	3847.00
211	NO VALUE	NO VALUE	3843.00
212	NO VALUE	NO VALUE	3847.00
213	-1557.00	87.10	3846.00
214	NO VALUE	NO VALUE	3860.00
215	NO VALUE	NO VALUE	3874.00
216	NO VALUE	NO VALUE	NO VALUE
217	NO VALUE	NO VALUE	NO VALUE
218	NO VALUE	NO VALUE	3860.00
219	-1622.00	124.00	3883.00
220	NO VALUE	NO VALUE	3838.00
221	NO VALUE	NO VALUE	3810.00
222	NO VALUE	NO VALUE	3840.00
223	NO VALUE	NO VALUE	3820.00
224	NO VALUE	NO VALUE	3752.00
225	-1563.00	103.00	3836.00
226	NO VALUE	NO VALUE	3840.00
227	NO VALUE	NO VALUE	3847.00
228	NO VALUE	NO VALUE	3882.00
229	NO VALUE	NO VALUE	3860.00
230	NO VALUE	NO VALUE	3864.00
231	NO VALUE	NO VALUE	3894.00
232	NO VALUE	NO VALUE	NO VALUE
233	NO VALUE	NO VALUE	3794.00
234	NO VALUE	NO VALUE	3834.00
235	NO VALUE	NO VALUE	3814.00
236	NO VALUE	NO VALUE	3815.00

	K	L	M
1	S.S. T PHOSPHATE	ISO T PHOSPHATE	BASE HAL SAND
2	DATUM (ft)	TO THAL (ft)	65A.P.I. (ft)
237	NO VALUE	NO VALUE	3842.00
238	NO VALUE	NO VALUE	3831.00
239	NO VALUE	NO VALUE	3856.00
240	-1557.00	101.00	3840.00
241	NO VALUE	NO VALUE	3876.00
242	NO VALUE	NO VALUE	3850.00
243	NO VALUE	NO VALUE	3895.00
244	NO VALUE	NO VALUE	NO VALUE
245	NO VALUE	NO VALUE	3882.00
246	NO VALUE	NO VALUE	NO VALUE
247	NO VALUE	NO VALUE	3824.00
248	NO VALUE	NO VALUE	3817.00
249	-1553.00	121.70	3824.00
250	NO VALUE	NO VALUE	3852.00
251	NO VALUE	NO VALUE	3827.00
252	NO VALUE	NO VALUE	3864.00
253	NO VALUE	NO VALUE	3854.00
254	NO VALUE	NO VALUE	3870.00
255	NO VALUE	NO VALUE	3854.00
256	NO VALUE	NO VALUE	3890.00
257	NO VALUE	NO VALUE	NO VALUE
258	NO VALUE	NO VALUE	3710.00
259	NO VALUE	NO VALUE	3762.00
260	NO VALUE	NO VALUE	3788.00
261	-1526.00	118.00	3798.00
262	NO VALUE	NO VALUE	3822.00
263	NO VALUE	NO VALUE	3817.00
264	NO VALUE	NO VALUE	3850.00
265	-1528.00	96.00	3840.00
266	NO VALUE	NO VALUE	3870.00
267	NO VALUE	NO VALUE	3845.00
268	NO VALUE	NO VALUE	3872.00
269	NO VALUE	NO VALUE	3879.00
270	NO VALUE	NO VALUE	3864.00
271	NO VALUE	NO VALUE	3850.00
272	NO VALUE	NO VALUE	3786.00
273	NO VALUE	NO VALUE	3840.00
274	NO VALUE	NO VALUE	3868.00
275	NO VALUE	NO VALUE	3838.00

	K	L	M
1	S.S. T PHOSPHATE	ISO T PHOSPHATE	BASE HAL SAND
2	DATUM (ft)	TO THAL (ft)	65A.P.I. (ft)
276	NO VALUE	NO VALUE	3850.00
277	NO VALUE	NO VALUE	3850.00
278	NO VALUE	NO VALUE	3840.00
279	-1482.00	95.00	3814.00
280	NO VALUE	NO VALUE	3815.00
281	NO VALUE	NO VALUE	3831.00
282	NO VALUE	NO VALUE	3832.00
283	NO VALUE	NO VALUE	3818.00
284	-1418.20	72.00	3756.00
285	NO VALUE	NO VALUE	3798.00
286	-1490.90	90.00	3811.00
287	NO VALUE	NO VALUE	3820.00
288	NO VALUE	NO VALUE	3798.00
289	-1480.10	86.00	3792.00
290	NO VALUE	NO VALUE	3792.00
291			
292	-1540.10	86.00	3862.00
293	NO VALUE	NO VALUE	3864.00
294	NO VALUE	NO VALUE	3857.00
295	NO VALUE	NO VALUE	NO VALUE
296	NO VALUE	NO VALUE	3841.00
297	NO VALUE	NO VALUE	3820.00
298	NO VALUE	NO VALUE	3824.00
299	-1457.00	78.00	3844.00
300	NO VALUE	NO VALUE	3836.00
301	NO VALUE	NO VALUE	3817.00
302	NO VALUE	NO VALUE	3816.00
303	NO VALUE	NO VALUE	3816.00
304	NO VALUE	NO VALUE	3811.00
305	NO VALUE	NO VALUE	3812.00
306	NO VALUE	NO VALUE	3802.00
307	NO VALUE	NO VALUE	3827.00
308	-1489.10	92.00	3802.00
309	NO VALUE	NO VALUE	3802.00
310	NO VALUE	NO VALUE	3812.00
311	NO VALUE	NO VALUE	3818.00
312	NO VALUE	NO VALUE	3794.00
313	NO VALUE	NO VALUE	3820.00
314	-1490.20	104.00	3789.00

	K	L	M
1	S.S. T PHOSPHATE	ISO T PHOSPHATE	BASE HAL SAND
2	DATUM (ft)	TO THAL (ft)	65A.P.I. (ft)
315	NO VALUE	NO VALUE	3805.00
316	NO VALUE	NO VALUE	3778.00
317	-1473.10	87.00	3780.00
318	NO VALUE	NO VALUE	3811.00
319	NO VALUE	NO VALUE	3766.00
320	NO VALUE	NO VALUE	3755.00
321	NO VALUE	NO VALUE	3747.00
322	NO VALUE	NO VALUE	3705.00
323	NO VALUE	NO VALUE	3688.00
324	NO VALUE	NO VALUE	3748.00
325	-1460.00	86.00	3745.00
326	NO VALUE	NO VALUE	3696.00
327	NO VALUE	NO VALUE	3756.00
328	NO VALUE	NO VALUE	3674.00
329	-1402.00	66.00	3696.00
330	NO VALUE	NO VALUE	3728.00
331	NO VALUE	NO VALUE	3748.00
332	NO VALUE	NO VALUE	3657.00
333	-1345.10	44.00	3599.00
334	NO VALUE	NO VALUE	3666.00
335	NO VALUE	NO VALUE	3715.00
336	-1416.00	78.00	3740.00
337	NO VALUE	NO VALUE	3758.00
338	NO VALUE	NO VALUE	3628.00
339	NO VALUE	NO VALUE	3684.00
340	NO VALUE	NO VALUE	3697.00
341	NO VALUE	NO VALUE	3690.00
342	-1382.90	70.00	3728.00
343	-1398.10	80.00	3734.00
344	-1394.10	46.00	3747.00
345			
346	NO VALUE	NO VALUE	NO VALUE
347			
348	NO VALUE	NO VALUE	NO VALUE

	N	O	P	Q
1	ISO BASE HAL SAND	S.S. BASE HAL SAND	TOP Pa. 3	S.S. TOP
2	65 A.P.I. (ft)	65 A.P.I. (ft)		Pa. 3
3	NO VALUE	NO VALUE	NO VALUE	NO VALUE
4	52.00	-1786.00	NO VALUE	NO VALUE
5	20.00	-1813.40	NO VALUE	NO VALUE
6	17.00	-1797.20	NO VALUE	NO VALUE
7	74.00	-1726.10	NO VALUE	NO VALUE
8	56.00	-1679.40	NO VALUE	NO VALUE
9	42.00	-1714.50	NO VALUE	NO VALUE
10	42.00	-1689.30	NO VALUE	NO VALUE
11	NO VALUE	NO VALUE	NO VALUE	NO VALUE
12	39.00	-1754.40	NO VALUE	NO VALUE
13	12.00	-1709.90	NO VALUE	NO VALUE
14	NO VALUE	NO VALUE	NO VALUE	NO VALUE
15	36.00	-1686.10	NO VALUE	NO VALUE
16	16.00	-1693.50	NO VALUE	NO VALUE
17	13.00	-1701.00	NO VALUE	NO VALUE
18	14.00	-1673.70	NO VALUE	NO VALUE
19	14.00	-1666.00	NO VALUE	NO VALUE
20	36.00	-1615.20	NO VALUE	NO VALUE
21	4.00	-1653.20	NO VALUE	NO VALUE
22				
23	4.00	-1636.00	NO VALUE	NO VALUE
24	NO VALUE	NO VALUE	NO VALUE	NO VALUE
25	30.00	-1535.40	3918.00	-1543.40
26	16.00	-1535.30	3916.00	-1545.30
27	4.00	-1599.10	NO VALUE	NO VALUE
28	39.00	-1522.70	3884.00	-1511.70
29	41.00	-1536.90	3892.00	-1523.90
30	49.00	-1540.00	NO VALUE	NO VALUE
31	25.00	-1547.20	NO VALUE	NO VALUE
32	4.00	-1654.40	NO VALUE	NO VALUE
33	36.00	-1522.90	NO VALUE	NO VALUE
34	24.00	-1504.00	3864.00	-1492.00
35	40.00	-1542.00	3898.00	-1534.00
36	NO VALUE	NO VALUE	NO VALUE	NO VALUE
37	25.00	-1526.00	NO VALUE	NO VALUE
38	18.00	-1554.00	NO VALUE	NO VALUE
39	30.00	-1560.00	NO VALUE	NO VALUE
40	31.00	-1564.80	NO VALUE	NO VALUE
41	20.00	-1488.00	NO VALUE	NO VALUE

	N	O	P	Q
1	ISO BASE HAL SAND	S.S. BASE HAL SAND	TOP Pa. 3	S.S. TOP
2	65 A.P.I. (ft)	65 A.P.I. (ft)		Pa. 3
42	24.00	-1490.00	NO VALUE	NO VALUE
43	24.00	-1502.00	NO VALUE	NO VALUE
44	16.00	-1484.00	NO VALUE	NO VALUE
45	18.00	-1501.20	NO VALUE	NO VALUE
46	24.00	-1522.00	NO VALUE	NO VALUE
47	30.00	-1530.00	NO VALUE	NO VALUE
48	32.00	-1551.20	NO VALUE	NO VALUE
49	26.00	-1540.20	NO VALUE	NO VALUE
50	18.00	-1543.10	NO VALUE	NO VALUE
51	3.00	-1550.90	NO VALUE	NO VALUE
52	NO VALUE	NO VALUE	NO VALUE	NO VALUE
53	18.00	-1474.40	NO VALUE	NO VALUE
54	30.00	-1511.20	NO VALUE	NO VALUE
55	16.00	-1489.00	NO VALUE	NO VALUE
56	30.00	-1521.00	NO VALUE	NO VALUE
57	26.00	-1500.10	NO VALUE	NO VALUE
58	28.00	-1512.20	NO VALUE	NO VALUE
59	26.00	-1524.00	NO VALUE	NO VALUE
60	24.00	-1521.00	NO VALUE	NO VALUE
61	20.00	-1519.00	NO VALUE	NO VALUE
62	NO VALUE	NO VALUE	NO VALUE	NO VALUE
63	20.00	-1467.20	NO VALUE	NO VALUE
64	10.00	-1472.20	NO VALUE	NO VALUE
65	40.00	-1511.85	NO VALUE	NO VALUE
66	18.00	-1483.20	NO VALUE	NO VALUE
67	14.00	-1478.20	NO VALUE	NO VALUE
68	18.00	-1497.00	NO VALUE	NO VALUE
69	14.00	-1492.40	NO VALUE	NO VALUE
70	22.00	-1516.00	NO VALUE	NO VALUE
71	26.00	-1503.00	NO VALUE	NO VALUE
72	24.00	-1515.10	NO VALUE	NO VALUE
73	22.00	-1507.10	NO VALUE	NO VALUE
74	24.00	-1508.90	NO VALUE	NO VALUE
75	4.00	-1508.00	NO VALUE	NO VALUE
76	NO VALUE	NO VALUE	NO VALUE	NO VALUE
77	16.00	-1470.00	NO VALUE	NO VALUE
78	19.00	-1499.10	NO VALUE	NO VALUE
79	12.00	-1472.00	NO VALUE	NO VALUE
80	28.00	-1505.10	NO VALUE	NO VALUE

	N	O	P	Q
1	ISO BASE HAL SAND	S.S. BASE HAL SAND	TOP Pa. 3	S.S. TOP
2	65 A.P.I. (ft)	65 A.P.I. (ft)		Pa. 3
81	20.00	-1489.25	NO VALUE	NO VALUE
82	24.00	-1485.10	NO VALUE	NO VALUE
83	22.00	-1491.10	NO VALUE	NO VALUE
84	18.00	-1489.60	NO VALUE	NO VALUE
85	4.00	-1529.00	NO VALUE	NO VALUE
86	20.00	-1471.00	NO VALUE	NO VALUE
87	18.00	-1479.20	NO VALUE	NO VALUE
88	20.00	-1462.00	NO VALUE	NO VALUE
89	16.00	-1474.00	NO VALUE	NO VALUE
90	15.00	-1479.80	NO VALUE	NO VALUE
91	16.00	-1482.90	NO VALUE	NO VALUE
92	13.00	-1492.00	NO VALUE	NO VALUE
93				
94	NO VALUE	NO VALUE	NO VALUE	NO VALUE
95				
96	NO VALUE	NO VALUE	NO VALUE	NO VALUE
97				
98	NO VALUE	NO VALUE	NO VALUE	NO VALUE
99				
100	24.00	-1560.10	NO VALUE	NO VALUE
[illegible]	10.00	-1573.70	NO VALUE	NO VALUE
[illegible]	6.00	-1574.00	3950.00	-1549.00
103	2.00	-1594.00	NO VALUE	NO VALUE
104	6.00	-1606.00	NO VALUE	NO VALUE
105	10.00	-1535.20	NO VALUE	NO VALUE
106	16.00	-1590.00	3930.00	-1547.00
107	20.00	-1576.50	NO VALUE	NO VALUE
108	18.00	-1591.10	NO VALUE	NO VALUE
109	14.00	-1605.10	NO VALUE	NO VALUE
110	20.00	-1572.00	NO VALUE	NO VALUE
111	34.00	-1562.20	3912.00	-1526.20
112	32.00	-1574.40	NO VALUE	NO VALUE
113	28.00	-1544.10	NO VALUE	NO VALUE
114	30.00	-1571.20	NO VALUE	NO VALUE
115	6.00	-1494.00	NO VALUE	NO VALUE
116	26.00	-1562.00	NO VALUE	NO VALUE
117	4.00	-1456.10	3948.00	-1468.10
118	10.00	-1532.10	NO VALUE	NO VALUE
119	NO VALUE	NO VALUE	NO VALUE	NO VALUE

	N	O	P	Q
1	ISO BASE HAL SAND	S.S. BASE HAL SAND	TOP Pa. 3	S.S. TOP
2	65 A.P.I. (ft)	65 A.P.I. (ft)		Pa. 3
120	26.00	-1519.10	NO VALUE	NO VALUE
121	21.00	-1506.30	NO VALUE	NO VALUE
122	19.00	-1531.00	3904.00	-1510.00
123	16.00	-1529.00	NO VALUE	NO VALUE
124	15.00	-1493.50	NO VALUE	NO VALUE
125	NO VALUE	NO VALUE	NO VALUE	NO VALUE
126	23.00	-1515.90	3916.00	-1505.90
127	20.00	-1498.50	3893.00	-1484.50
128	15.00	-1500.00	NO VALUE	NO VALUE
129	10.00	-1513.90	NO VALUE	NO VALUE
130	32.00	-1522.00	NO VALUE	NO VALUE
131	4.00	-1442.40	NO VALUE	NO VALUE
132	4.00	-1470.00	NO VALUE	NO VALUE
133	13.00	-1488.80	NO VALUE	NO VALUE
134	7.00	-1480.00	NO VALUE	NO VALUE
135	20.00	-1495.90	NO VALUE	NO VALUE
136	14.00	-1502.50	NO VALUE	NO VALUE
137	10.00	-1477.40	NO VALUE	NO VALUE
138	14.00	-1500.50	NO VALUE	NO VALUE
139	22.00	-1510.80	NO VALUE	NO VALUE
140	4.00	-1423.10	NO VALUE	NO VALUE
141	13.00	-1476.30	NO VALUE	NO VALUE
142	4.00	-1461.00	NO VALUE	NO VALUE
143	14.00	-1490.20	NO VALUE	NO VALUE
144	26.00	-1510.80	3877.00	-1494.80
145	NO VALUE	NO VALUE	NO VALUE	NO VALUE
146	4.00	-1452.10	NO VALUE	NO VALUE
147	4.00	-1445.90	NO VALUE	NO VALUE
148	16.00	-1468.10	NO VALUE	NO VALUE
149	10.00	-1447.00	NO VALUE	NO VALUE
150	28.00	-1474.50	NO VALUE	NO VALUE
151	10.00	-1471.00	NO VALUE	NO VALUE
152				
153	35.00	-1680.00	4042.00	-1694.00
154	36.00	-1623.00	NO VALUE	NO VALUE
155	NO VALUE	NO VALUE	NO VALUE	NO VALUE
156	20.00	-1601.30	NO VALUE	NO VALUE
157	36.00	-1632.10	4000.00	-1640.10
158	NO VALUE	NO VALUE	NO VALUE	NO VALUE

	N	O	P	Q
1	ISO BASE HAL SAND	S.S. BASE HAL SAND	TOP Pa. 3	S.S. TOP
2	65 A.P.I. (ft)	65 A.P.I. (ft)		Pa. 3
159	42.00	-1582.90	NO VALUE	NO VALUE
160	33.00	-1594.00	NO VALUE	NO VALUE
161	36.00	-1612.80	NO VALUE	NO VALUE
162	44.00	-1578.00	NO VALUE	NO VALUE
163	44.00	-1611.90	3964.00	-1595.90
164	32.00	-1628.90	3998.00	-1610.90
165	34.00	-1545.00	3906.00	-1535.00
166	NO VALUE	NO VALUE	3991.00	-1618.00
167	38.00	-1542.00	3892.00	-1522.00
168	28.00	-1544.00	3892.00	-1527.00
169	28.00	-1552.00	NO VALUE	NO VALUE
170	10.00	-1560.00	NO VALUE	NO VALUE
171	44.00	-1591.00	NO VALUE	NO VALUE
172	10.00	-1521.00	3884.00	-1511.00
173	20.00	-1547.10	NO VALUE	NO VALUE
174	36.00	-1537.90	NO VALUE	NO VALUE
175	24.00	-1550.20	NO VALUE	NO VALUE
176	12.00	-1510.10	3880.00	-1500.10
177	24.00	-1505.00	3872.00	-1488.00
178	16.00	-1516.50	3872.00	-1500.50
179	8.00	-1531.00	3872.00	-1523.00
180	37.00	-1537.00	NO VALUE	NO VALUE
181	11.00	-1569.10	3906.00	-1570.10
182	4.00	-1565.00	NO VALUE	NO VALUE
183	30.00	-1573.80	3906.00	-1566.80
184	28.00	-1598.00	3912.00	-1570.00
185	8.00	-1489.00	3868.00	-1479.00
186	28.00	-1511.00	NO VALUE	NO VALUE
187	8.00	-1501.00	3860.00	-1491.00
188	38.00	-1540.10	NO VALUE	NO VALUE
189	3.00	-1541.00	NO VALUE	NO VALUE
190	14.00	-1528.00	3850.00	-1514.00
191	3.00	-1530.20	NO VALUE	NO VALUE
192	NO VALUE	NO VALUE	NO VALUE	NO VALUE
193	36.00	-1549.00	NO VALUE	NO VALUE
194	13.00	-1519.10	NO VALUE	NO VALUE
195	NO VALUE	NO VALUE	3888.00	-1529.10
196	16.00	-1525.00	3886.80	-1537.80
197				

	N	O	P	Q
1	ISO BASE HAL SAND	S.S. BASE HAL SAND	TOP Pa. 3	S.S. TOP
2	65 A.P.I. (ft)	65 A.P.I. (ft)		Pa. 3
198	16.00	-1477.00	NO VALUE	NO VALUE
199	8.00	-1492.10	3840.00	-1482.10
200	12.00	-1508.00	3850.00	-1498.00
201	8.00	-1493.00	3840.00	-1483.00
202	20.00	-1509.00	NO VALUE	NO VALUE
203	22.00	-1496.70	NO VALUE	NO VALUE
204	4.00	-1524.10	NO VALUE	NO VALUE
205	4.00	-1542.00	NO VALUE	NO VALUE
206	10.00	-1540.10	NO VALUE	NO VALUE
207	12.00	-1524.00	3894.00	-1538.00
208	5.00	-1463.10	NO VALUE	NO VALUE
209	13.00	-1481.00	NO VALUE	NO VALUE
210	13.00	-1487.80	NO VALUE	NO VALUE
211	4.00	-1473.00	NO VALUE	NO VALUE
212	11.00	-1484.80	3837.60	-1475.40
213	9.00	-1479.00	NO VALUE	NO VALUE
214	4.00	-1500.50	NO VALUE	NO VALUE
215	3.00	-1518.10	NO VALUE	NO VALUE
216	NO VALUE	NO VALUE	NO VALUE	NO VALUE
217	NO VALUE	NO VALUE	NO VALUE	NO VALUE
218	16.00	-1504.10	NO VALUE	NO VALUE
219	30.00	-1531.00	NO VALUE	NO VALUE
220	3.00	-1464.00	NO VALUE	NO VALUE
221	22.00	-1447.00	3804.00	-1441.00
222	14.00	-1477.00	NO VALUE	NO VALUE
223	24.00	-1463.00	NO VALUE	NO VALUE
224	8.00	-1470.00	3744.00	-1462.00
225	20.00	-1477.00	3829.00	-1470.00
226	18.00	-1481.00	NO VALUE	NO VALUE
227	10.00	-1490.00	3856.00	-1499.00
228	22.00	-1510.00	3873.00	-1501.00
229	10.00	-1499.20	NO VALUE	NO VALUE
230	10.00	-1496.90	3870.00	-1502.90
231	20.00	-1524.00	3900.00	-1530.00
232	NO VALUE	NO VALUE	NO VALUE	NO VALUE
233	8.00	-1441.00	3788.00	-1435.00
234	18.00	-1464.00	NO VALUE	NO VALUE
235	12.00	-1446.90	NO VALUE	NO VALUE
236	12.00	-1447.00	NO VALUE	NO VALUE

	N	O	P	Q
1	ISO BASE HAL SAND	S.S. BASE HAL SAND	TOP Pa. 3	S.S. TOP
2	65 A.P.I. (ft)	65 A.P.I. (ft)		Pa. 3
237	8.00	-1481.20	NO VALUE	NO VALUE
238	10.00	-1464.00	NO VALUE	NO VALUE
239	22.00	-1477.10	NO VALUE	NO VALUE
240	12.00	-1471.00	3826.00	-1457.00
241	8.00	-1487.30	3868.00	-1479.30
242	24.00	-1475.70	NO VALUE	NO VALUE
243	10.00	-1505.90	NO VALUE	NO VALUE
244	NO VALUE	NO VALUE	NO VALUE	NO VALUE
245	14.00	-1496.40	3888.00	-1502.40
246	NO VALUE	NO VALUE	NO VALUE	NO VALUE
247	14.00	-1451.00	NO VALUE	NO VALUE
248	18.00	-1445.00	NO VALUE	NO VALUE
249	9.00	-1445.00	3816.00	-1437.00
250	14.00	-1465.70	NO VALUE	NO VALUE
251	12.00	-1447.10	NO VALUE	NO VALUE
252	19.00	-1474.00	NO VALUE	NO VALUE
253	20.00	-1468.20	NO VALUE	NO VALUE
254	8.00	-1478.30	3862.00	-1470.30
255	22.00	-1467.90	NO VALUE	NO VALUE
256	10.00	-1519.00	NO VALUE	NO VALUE
257	NO VALUE	NO VALUE	NO VALUE	NO VALUE
258	4.00	-1420.00	NO VALUE	NO VALUE
259	6.00	-1384.10	NO VALUE	NO VALUE
260	11.00	-1397.60	NO VALUE	NO VALUE
261	8.00	-1418.00	NO VALUE	NO VALUE
262	4.00	-1425.00	NO VALUE	NO VALUE
263	12.00	-1428.00	NO VALUE	NO VALUE
264	18.00	-1449.10	NO VALUE	NO VALUE
265	16.00	-1448.00	NO VALUE	NO VALUE
266	22.00	-1468.10	NO VALUE	NO VALUE
267	18.00	-1451.60	NO VALUE	NO VALUE
268	30.00	-1478.00	NO VALUE	NO VALUE
269	26.00	-1487.00	NO VALUE	NO VALUE
270	4.00	-1468.40	NO VALUE	NO VALUE
271	12.00	-1468.20	NO VALUE	NO VALUE
272	18.00	-1398.90	NO VALUE	NO VALUE
273	21.00	-1441.00	NO VALUE	NO VALUE
274	8.00	-1463.00	NO VALUE	NO VALUE
275	8.00	-1438.10	NO VALUE	NO VALUE

	N	O	P	Q
1	ISO BASE HAL SAND	S.S. BASE HAL SAND	TOP Pa. 3	S.S. TOP
2	65 A.P.I. (ft)	65 A.P.I. (ft)		Pa. 3
276	20.00	-1454.00	NO VALUE	NO VALUE
277	16.00	-1457.00	NO VALUE	NO VALUE
278	18.00	-1461.10	NO VALUE	NO VALUE
279	28.00	-1414.00	NO VALUE	NO VALUE
280	8.00	-1430.20	NO VALUE	NO VALUE
281	18.00	-1443.90	NO VALUE	NO VALUE
282	5.00	-1448.20	NO VALUE	NO VALUE
283	18.00	-1452.90	NO VALUE	NO VALUE
284	4.00	-1353.20	NO VALUE	NO VALUE
285	4.00	-1387.00	NO VALUE	NO VALUE
286	4.00	-1401.90	NO VALUE	NO VALUE
287	20.00	-1443.10	NO VALUE	NO VALUE
288	4.00	-1389.90	NO VALUE	NO VALUE
289	4.00	-1396.10	NO VALUE	NO VALUE
290	12.00	-1415.00	NO VALUE	NO VALUE
291				
292	8.00	-1462.10	NO VALUE	NO VALUE
293	14.00	-1470.00	NO VALUE	NO VALUE
294	3.00	-1398.10	NO VALUE	NO VALUE
295	NO VALUE	NO VALUE	NO VALUE	NO VALUE
296	4.00	-1430.00	NO VALUE	NO VALUE
297	10.00	-1429.00	NO VALUE	NO VALUE
298	14.00	-1441.20	NO VALUE	NO VALUE
299	2.00	-1409.00	NO VALUE	NO VALUE
300	4.00	-1426.90	NO VALUE	NO VALUE
301	4.00	-1418.10	NO VALUE	NO VALUE
302	6.00	-1411.20	NO VALUE	NO VALUE
303	26.00	-1432.20	NO VALUE	NO VALUE
304	4.00	-1441.00	NO VALUE	NO VALUE
305	4.00	-1390.10	NO VALUE	NO VALUE
306	4.00	-1393.90	NO VALUE	NO VALUE
307	16.00	-1432.00	NO VALUE	NO VALUE
308	6.00	-1403.10	NO VALUE	NO VALUE
309	18.00	-1413.00	NO VALUE	NO VALUE
310	4.00	-1423.90	NO VALUE	NO VALUE
311	4.00	-1399.70	NO VALUE	NO VALUE
312	8.00	-1384.90	NO VALUE	NO VALUE
313	12.00	-1430.90	NO VALUE	NO VALUE
314	20.00	-1405.20	NO VALUE	NO VALUE

	N	O	P	Q
1	ISO BASE HAL SAND	S.S. BASE HAL SAND	TOP Pa. 3	S.S. TOP
2	65 A.P.I. (ft)	65 A.P.I. (ft)		Pa. 3
315	4.00	-1417.00	NO VALUE	NO VALUE
316	10.00	-1388.90	NO VALUE	NO VALUE
317	8.00	-1399.10	NO VALUE	NO VALUE
318	52.00	-1421.60	NO VALUE	NO VALUE
319	18.00	-1392.20	NO VALUE	NO VALUE
320	4.00	-1387.00	NO VALUE	NO VALUE
321	4.00	-1349.10	NO VALUE	NO VALUE
322	4.00	-1355.00	NO VALUE	NO VALUE
323	12.00	-1326.20	NO VALUE	NO VALUE
324	10.00	-1370.10	NO VALUE	NO VALUE
325	10.00	-1371.00	NO VALUE	NO VALUE
326	10.00	-1367.00	NO VALUE	NO VALUE
327	4.00	-1367.60	NO VALUE	NO VALUE
328	24.00	-1353.20	NO VALUE	NO VALUE
329	6.00	-1344.00	NO VALUE	NO VALUE
330	7.00	-1365.20	NO VALUE	NO VALUE
331	5.00	-1368.50	NO VALUE	NO VALUE
332	10.00	-1302.10	NO VALUE	NO VALUE
333	4.00	-1302.10	NO VALUE	NO VALUE
334	6.00	-1311.10	NO VALUE	NO VALUE
335	12.00	-1341.00	NO VALUE	NO VALUE
336	12.00	-1346.00	NO VALUE	NO VALUE
337	5.00	-1359.10	NO VALUE	NO VALUE
338	8.00	-1246.20	NO VALUE	NO VALUE
339	7.00	-1304.10	NO VALUE	NO VALUE
340	4.00	-1298.10	NO VALUE	NO VALUE
341	4.00	-1321.30	NO VALUE	NO VALUE
342	20.00	-1338.90	NO VALUE	NO VALUE
343	22.00	-1338.10	NO VALUE	NO VALUE
344	4.00	-1349.10	NO VALUE	NO VALUE
345				
346	NO VALUE	NO VALUE	NO VALUE	NO VALUE
347				
348	NO VALUE	NO VALUE	NO VALUE	NO VALUE

	R	S	T	U
1	TOP Pa. 2	S.S. TOP	TOP Pa. 1	S.S. TOP
2		Pa. 2		Pa. 1
3	NO VALUE	NO VALUE	NO VALUE	NO VALUE
4	NO VALUE	NO VALUE	NO VALUE	NO VALUE
5	NO VALUE	NO VALUE	NO VALUE	NO VALUE
6	NO VALUE	NO VALUE	NO VALUE	NO VALUE
7	NO VALUE	NO VALUE	NO VALUE	NO VALUE
8	NO VALUE	NO VALUE	NO VALUE	NO VALUE
9	NO VALUE	NO VALUE	NO VALUE	NO VALUE
10	NO VALUE	NO VALUE	NO VALUE	NO VALUE
11	NO VALUE	NO VALUE	NO VALUE	NO VALUE
12	NO VALUE	NO VALUE	NO VALUE	NO VALUE
13	NO VALUE	NO VALUE	NO VALUE	NO VALUE
14	NO VALUE	NO VALUE	NO VALUE	NO VALUE
15	NO VALUE	NO VALUE	NO VALUE	NO VALUE
16	NO VALUE	NO VALUE	NO VALUE	NO VALUE
17	NO VALUE	NO VALUE	NO VALUE	NO VALUE
18	NO VALUE	NO VALUE	NO VALUE	NO VALUE
19	NO VALUE	NO VALUE	NO VALUE	NO VALUE
20	NO VALUE	NO VALUE	NO VALUE	NO VALUE
21	NO VALUE	NO VALUE	NO VALUE	NO VALUE
22				
23	NO VALUE	NO VALUE	NO VALUE	NO VALUE
24	NO VALUE	NO VALUE	NO VALUE	NO VALUE
25	NO VALUE	NO VALUE	NO VALUE	NO VALUE
26	3930.00	-1559.30	NO VALUE	NO VALUE
27	NO VALUE	NO VALUE	NO VALUE	NO VALUE
28	NO VALUE	NO VALUE	NO VALUE	NO VALUE
29	NO VALUE	NO VALUE	NO VALUE	NO VALUE
30	NO VALUE	NO VALUE	NO VALUE	NO VALUE
31	NO VALUE	NO VALUE	NO VALUE	NO VALUE
32	NO VALUE	NO VALUE	NO VALUE	NO VALUE
33	NO VALUE	NO VALUE	NO VALUE	NO VALUE
34	3886.00	-1514.00	NO VALUE	NO VALUE
35	3920.00	-1556.00	NO VALUE	NO VALUE
36	NO VALUE	NO VALUE	NO VALUE	NO VALUE
37	NO VALUE	NO VALUE	NO VALUE	NO VALUE
38	NO VALUE	NO VALUE	NO VALUE	NO VALUE
39	NO VALUE	NO VALUE	NO VALUE	NO VALUE
40	NO VALUE	NO VALUE	NO VALUE	NO VALUE
41	NO VALUE	NO VALUE	NO VALUE	NO VALUE

	R	S	T	U
1	TOP Pa. 2	S.S. TOP	TOP Pa. 1	S.S. TOP
2		Pa. 2		Pa. 1
42	NO VALUE	NO VALUE	NO VALUE	NO VALUE
43	NO VALUE	NO VALUE	NO VALUE	NO VALUE
44	NO VALUE	NO VALUE	NO VALUE	NO VALUE
45	NO VALUE	NO VALUE	NO VALUE	NO VALUE
46	NO VALUE	NO VALUE	NO VALUE	NO VALUE
47	NO VALUE	NO VALUE	NO VALUE	NO VALUE
48	NO VALUE	NO VALUE	NO VALUE	NO VALUE
49	NO VALUE	NO VALUE	NO VALUE	NO VALUE
50	NO VALUE	NO VALUE	NO VALUE	NO VALUE
51	NO VALUE	NO VALUE	NO VALUE	NO VALUE
52	NO VALUE	NO VALUE	NO VALUE	NO VALUE
53	NO VALUE	NO VALUE	3862.00	-1496.40
54	NO VALUE	NO VALUE	NO VALUE	NO VALUE
55	NO VALUE	NO VALUE	3876.00	-1511.00
56	NO VALUE	NO VALUE	NO VALUE	NO VALUE
57	NO VALUE	NO VALUE	NO VALUE	NO VALUE
58	NO VALUE	NO VALUE	NO VALUE	NO VALUE
59	NO VALUE	NO VALUE	NO VALUE	NO VALUE
60	NO VALUE	NO VALUE	NO VALUE	NO VALUE
61	NO VALUE	NO VALUE	NO VALUE	NO VALUE
62	NO VALUE	NO VALUE	3838.00	-1468.60
63	NO VALUE	NO VALUE	3838.00	-1475.20
64	NO VALUE	NO VALUE	3852.00	-1490.20
65	NO VALUE	NO VALUE	3890.00	-1523.85
66	NO VALUE	NO VALUE	3855.00	-1492.20
67	NO VALUE	NO VALUE	NO VALUE	NO VALUE
68	NO VALUE	NO VALUE	3880.00	-1523.00
69	NO VALUE	NO VALUE	3872.00	-1511.40
70	NO VALUE	NO VALUE	NO VALUE	NO VALUE
71	NO VALUE	NO VALUE	NO VALUE	NO VALUE
72	NO VALUE	NO VALUE	NO VALUE	NO VALUE
73	NO VALUE	NO VALUE	NO VALUE	NO VALUE
74	NO VALUE	NO VALUE	NO VALUE	NO VALUE
75	NO VALUE	NO VALUE	NO VALUE	NO VALUE
76	3830.00	-1459.00	NO VALUE	NO VALUE
77	NO VALUE	NO VALUE	3850.00	-1490.00
78	NO VALUE	NO VALUE	3878.00	-1521.10
79	NO VALUE	NO VALUE	3850.00	-1493.00
80	NO VALUE	NO VALUE	NO VALUE	NO VALUE

	R	S	T	U
1	TOP Pa. 2	S.S. TOP	TOP Pa. 1	S.S. TOP
2		Pa. 2		Pa. 1
81	NO VALUE	NO VALUE	NO VALUE	NO VALUE
82	NO VALUE	NO VALUE	NO VALUE	NO VALUE
83	NO VALUE	NO VALUE	NO VALUE	NO VALUE
84	NO VALUE	NO VALUE	NO VALUE	NO VALUE
85	NO VALUE	NO VALUE	NO VALUE	NO VALUE
86	NO VALUE	NO VALUE	NO VALUE	NO VALUE
87	NO VALUE	NO VALUE	NO VALUE	NO VALUE
88	NO VALUE	NO VALUE	NO VALUE	NO VALUE
89	NO VALUE	NO VALUE	NO VALUE	NO VALUE
90	NO VALUE	NO VALUE	NO VALUE	NO VALUE
91	NO VALUE	NO VALUE	NO VALUE	NO VALUE
92	NO VALUE	NO VALUE	NO VALUE	NO VALUE
93				
94	NO VALUE	NO VALUE	NO VALUE	NO VALUE
95				
96	NO VALUE	NO VALUE	NO VALUE	NO VALUE
97				
98	NO VALUE	NO VALUE	NO VALUE	NO VALUE
99				
100	NO VALUE	NO VALUE	4032.00	-1590.10
101	3985.00	-1568.70	4014.00	-1597.70
102	3968.00	-1567.00	4000.00	-1599.00
103	3966.00	-1593.00	4010.00	-1637.00
104	3972.00	-1602.00	NO VALUE	NO VALUE
105	3970.00	-1523.20	4020.00	-1573.20
106	3955.00	-1572.00	NO VALUE	NO VALUE
107	NO VALUE	NO VALUE	NO VALUE	NO VALUE
108	NO VALUE	NO VALUE	NO VALUE	NO VALUE
109	3950.00	-1593.10	3990.00	-1633.10
110	NO VALUE	NO VALUE	3975.00	-1600.00
111	3968.00	-1582.20	3990.00	-1604.20
112	3966.00	-1590.40	3984.00	-1608.40
113	3962.00	-1566.10	3988.00	-1592.10
114	3952.00	-1580.20	3980.00	-1608.20
115	3962.00	-1510.00	3984.00	-1532.00
116	NO VALUE	NO VALUE	NO VALUE	NO VALUE
117	3948.00	-1468.10	NO VALUE	NO VALUE
118	NO VALUE	NO VALUE	NO VALUE	NO VALUE
119	NO VALUE	NO VALUE	NO VALUE	NO VALUE

	R	S	T	U
1	TOP Pa. 2	S.S. TOP	TOP Pa. 1	S.S. TOP
2		Pa. 2		Pa. 1
120	NO VALUE	NO VALUE	NO VALUE	NO VALUE
121	NO VALUE	NO VALUE	NO VALUE	NO VALUE
122	3948.00	-1554.00	3974.00	-1580.00
123	3911.00	-1536.00	NO VALUE	NO VALUE
124	NO VALUE	NO VALUE	NO VALUE	NO VALUE
125	NO VALUE	NO VALUE	NO VALUE	NO VALUE
126	NO VALUE	NO VALUE	NO VALUE	NO VALUE
127	NO VALUE	NO VALUE	NO VALUE	NO VALUE
128	3943.00	-1528.00	3972.00	-1557.00
129	3942.00	-1543.90	3970.00	-1571.90
130	NO VALUE	NO VALUE	NO VALUE	NO VALUE
131	NO VALUE	NO VALUE	NO VALUE	NO VALUE
132	NO VALUE	NO VALUE	NO VALUE	NO VALUE
133	NO VALUE	NO VALUE	NO VALUE	NO VALUE
134	NO VALUE	NO VALUE	NO VALUE	NO VALUE
135	NO VALUE	NO VALUE	NO VALUE	NO VALUE
136	3902.00	-1508.50	3924.00	-1530.50
137	NO VALUE	NO VALUE	NO VALUE	NO VALUE
138	3896.00	-1502.50	3954.00	-1560.50
139	3891.00	-1508.80	NO VALUE	NO VALUE
140	NO VALUE	NO VALUE	NO VALUE	NO VALUE
141	NO VALUE	NO VALUE	NO VALUE	NO VALUE
142	3888.00	-1473.00	3926.00	-1511.00
143	3898.00	-1502.20	3930.00	-1534.20
144	NO VALUE	NO VALUE	NO VALUE	NO VALUE
145	NO VALUE	NO VALUE	NO VALUE	NO VALUE
146	NO VALUE	NO VALUE	NO VALUE	NO VALUE
147	NO VALUE	NO VALUE	NO VALUE	NO VALUE
148	NO VALUE	NO VALUE	NO VALUE	NO VALUE
149	3868.00	-1460.00	3902.00	-1494.00
150	3880.00	-1476.50	3919.00	-1515.50
151	NO VALUE	NO VALUE	NO VALUE	NO VALUE
152				
153	NO VALUE	NO VALUE	NO VALUE	NO VALUE
154	NO VALUE	NO VALUE	NO VALUE	NO VALUE
155	NO VALUE	NO VALUE	NO VALUE	NO VALUE
156	NO VALUE	NO VALUE	NO VALUE	NO VALUE
157	4033.00	-1673.10	4060.00	-1700.10
158	NO VALUE	NO VALUE	NO VALUE	NO VALUE

	R	S	T	U
1	TOP Pa. 2	S.S. TOP	TOP Pa. 1	S.S. TOP
2		Pa. 2		Pa. 1
159	NO VALUE	NO VALUE	NO VALUE	NO VALUE
160	NO VALUE	NO VALUE	NO VALUE	NO VALUE
161	NO VALUE	NO VALUE	NO VALUE	NO VALUE
162	NO VALUE	NO VALUE	NO VALUE	NO VALUE
163	4001.00	-1632.90	4052.00	-1683.90
164	NO VALUE	NO VALUE	NO VALUE	NO VALUE
165	NO VALUE	NO VALUE	NO VALUE	NO VALUE
166	NO VALUE	NO VALUE	NO VALUE	NO VALUE
167	NO VALUE	NO VALUE	NO VALUE	NO VALUE
168	3944.00	-1579.00	3970.00	-1605.00
169	NO VALUE	NO VALUE	NO VALUE	NO VALUE
170	3946.00	-1582.00	3980.00	-1616.00
171	NO VALUE	NO VALUE	NO VALUE	NO VALUE
172	NO VALUE	NO VALUE	NO VALUE	NO VALUE
173	NO VALUE	NO VALUE	NO VALUE	NO VALUE
174	3938.00	-1569.90	3964.00	-1595.90
175	3918.00	-1566.20	3964.00	-1612.20
176	NO VALUE	NO VALUE	NO VALUE	NO VALUE
177	NO VALUE	NO VALUE	NO VALUE	NO VALUE
178	3914.00	-1542.50	3946.00	-1574.50
179	NO VALUE	NO VALUE	NO VALUE	NO VALUE
180	3906.00	-1550.00	3948.00	-1592.00
181	NO VALUE	NO VALUE	NO VALUE	NO VALUE
182	3906.00	-1575.00	3940.00	-1609.00
183	NO VALUE	NO VALUE	NO VALUE	NO VALUE
184	NO VALUE	NO VALUE	NO VALUE	NO VALUE
185	3892.00	-1503.00	NO VALUE	NO VALUE
186	3902.00	-1531.00	NO VALUE	NO VALUE
187	3898.00	-1529.00	3926.00	-1557.00
188	NO VALUE	NO VALUE	NO VALUE	NO VALUE
189	NO VALUE	NO VALUE	NO VALUE	NO VALUE
190	3896.00	-1560.00	3924.00	-1588.00
191	NO VALUE	NO VALUE	NO VALUE	NO VALUE
192	NO VALUE	NO VALUE	3900.00	-1621.20
193	NO VALUE	NO VALUE	NO VALUE	NO VALUE
194	NO VALUE	NO VALUE	NO VALUE	NO VALUE
195	NO VALUE	NO VALUE	NO VALUE	NO VALUE
196	NO VALUE	NO VALUE	NO VALUE	NO VALUE
197				

	R	S	T	U
1	TOP Pa. 2	S.S. TOP	TOP Pa. 1	S.S. TOP
2		Pa. 2		Pa. 1
198	NO VALUE	NO VALUE	NO VALUE	NO VALUE
199	NO VALUE	NO VALUE	NO VALUE	NO VALUE
200	NO VALUE	NO VALUE	NO VALUE	NO VALUE
201	3864.00	-1507.00	3900.00	-1543.00
202	NO VALUE	NO VALUE	NO VALUE	NO VALUE
203	3874.00	-1518.70	3907.00	-1551.70
204	3902.00	-1542.10	3932.00	-1572.10
205	NO VALUE	NO VALUE	NO VALUE	NO VALUE
206	NO VALUE	NO VALUE	NO VALUE	NO VALUE
207	NO VALUE	NO VALUE	NO VALUE	NO VALUE
208	NO VALUE	NO VALUE	NO VALUE	NO VALUE
209	3830.00	-1464.00	NO VALUE	NO VALUE
210	NO VALUE	NO VALUE	NO VALUE	NO VALUE
211	3858.00	-1488.00	3880.00	-1510.00
212	3858.00	-1495.80	NO VALUE	NO VALUE
213	3858.00	-1491.00	3888.00	-1521.00
214	3856.00	-1496.50	3912.00	-1552.50
215	NO VALUE	NO VALUE	NO VALUE	NO VALUE
216	NO VALUE	NO VALUE	NO VALUE	NO VALUE
217	NO VALUE	NO VALUE	NO VALUE	NO VALUE
218	NO VALUE	NO VALUE	NO VALUE	NO VALUE
219	3927.00	-1575.00	3966.00	-1614.00
220	NO VALUE	NO VALUE	3850.00	-1476.00
221	3817.00	-1454.00	3844.00	-1481.00
222	NO VALUE	NO VALUE	NO VALUE	NO VALUE
223	3926.00	-1569.00	3950.00	-1593.00
224	3766.00	-1484.00	3800.00	-1518.00
225	3848.00	-1489.00	3888.00	-1529.00
226	NO VALUE	NO VALUE	NO VALUE	NO VALUE
227	NO VALUE	NO VALUE	NO VALUE	NO VALUE
228	3916.00	-1544.00	NO VALUE	NO VALUE
229	NO VALUE	NO VALUE	NO VALUE	NO VALUE
230	3890.00	-1522.90	NO VALUE	NO VALUE
231	3928.00	-1558.00	NO VALUE	NO VALUE
232	NO VALUE	NO VALUE	NO VALUE	NO VALUE
233	NO VALUE	NO VALUE	NO VALUE	NO VALUE
234	NO VALUE	NO VALUE	NO VALUE	NO VALUE
235	NO VALUE	NO VALUE	NO VALUE	NO VALUE
236	3834.00	-1466.00	NO VALUE	NO VALUE

	R	S	T	U
1	TOP Pa. 2	S.S. TOP	TOP Pa. 1	S.S. TOP
2		Pa. 2		Pa. 1
237	NO VALUE	NO VALUE	NO VALUE	NO VALUE
238	3846.00	-1479.00	NO VALUE	NO VALUE
239	NO VALUE	NO VALUE	NO VALUE	NO VALUE
240	3855.00	-1486.00	3888.00	-1519.00
241	NO VALUE	NO VALUE	NO VALUE	NO VALUE
242	NO VALUE	NO VALUE	NO VALUE	NO VALUE
243	NO VALUE	NO VALUE	NO VALUE	NO VALUE
244	NO VALUE	NO VALUE	NO VALUE	NO VALUE
245	3910.00	-1524.40	NO VALUE	NO VALUE
246	NO VALUE	NO VALUE	NO VALUE	NO VALUE
247	NO VALUE	NO VALUE	3833.00	-1460.00
248	3830.00	-1458.00	NO VALUE	NO VALUE
249	3838.00	-1459.00	3865.00	-1486.00
250	3873.00	-1486.70	NO VALUE	NO VALUE
251	3842.00	-1462.10	3876.00	-1496.10
252	3878.00	-1488.00	NO VALUE	NO VALUE
253	NO VALUE	NO VALUE	NO VALUE	NO VALUE
254	3880.00	-1488.30	NO VALUE	NO VALUE
255	NO VALUE	NO VALUE	NO VALUE	NO VALUE
256	NO VALUE	NO VALUE	NO VALUE	NO VALUE
257	NO VALUE	NO VALUE	NO VALUE	NO VALUE
258	NO VALUE	NO VALUE	3734.00	-1444.00
259	NO VALUE	NO VALUE	3790.00	-1412.10
260	NO VALUE	NO VALUE	NO VALUE	NO VALUE
261	NO VALUE	NO VALUE	3830.00	-1450.00
262	NO VALUE	NO VALUE	NO VALUE	NO VALUE
263	NO VALUE	NO VALUE	3842.00	-1453.00
264	NO VALUE	NO VALUE	3862.00	-1461.10
265	NO VALUE	NO VALUE	3866.00	-1474.00
266	NO VALUE	NO VALUE	3884.00	-1482.10
267	3856.00	-1462.60	NO VALUE	NO VALUE
268	NO VALUE	NO VALUE	NO VALUE	NO VALUE
269	NO VALUE	NO VALUE	NO VALUE	NO VALUE
270	NO VALUE	NO VALUE	NO VALUE	NO VALUE
271	NO VALUE	NO VALUE	NO VALUE	NO VALUE
272	3801.00	-1413.90	NO VALUE	NO VALUE
273	NO VALUE	NO VALUE	3864.00	-1465.00
274	NO VALUE	NO VALUE	3880.00	-1475.00
275	NO VALUE	NO VALUE	NO VALUE	NO VALUE

	R	S	T	U
1	TOP Pa. 2	S.S. TOP	TOP Pa. 1	S.S. TOP
2		Pa. 2		Pa. 1
276	NO VALUE	NO VALUE	3862.00	-1466.00
277	NO VALUE	NO VALUE	3862.00	-1469.00
278	NO VALUE	NO VALUE	NO VALUE	NO VALUE
279	3818.00	-1418.00	NO VALUE	NO VALUE
280	NO VALUE	NO VALUE	NO VALUE	NO VALUE
281	NO VALUE	NO VALUE	NO VALUE	NO VALUE
282	NO VALUE	NO VALUE	NO VALUE	NO VALUE
283	3830.00	-1464.90	NO VALUE	NO VALUE
284	NO VALUE	NO VALUE	NO VALUE	NO VALUE
285	3813.00	-1402.00	NO VALUE	NO VALUE
286	NO VALUE	NO VALUE	3852.00	-1442.90
287	NO VALUE	NO VALUE	NO VALUE	NO VALUE
288	NO VALUE	NO VALUE	NO VALUE	NO VALUE
289	NO VALUE	NO VALUE	3820.00	-1424.10
290	3808.00	-1431.00	NO VALUE	NO VALUE
291				
292	3874.00	-1474.10	3900.00	-1500.10
293	NO VALUE	NO VALUE	NO VALUE	NO VALUE
294	NO VALUE	NO VALUE	3890.00	-1431.10
295	NO VALUE	NO VALUE	NO VALUE	NO VALUE
296	NO VALUE	NO VALUE	3850.70	-1439.70
297	3836.00	-1445.00	NO VALUE	NO VALUE
298	NO VALUE	NO VALUE	NO VALUE	NO VALUE
299	NO VALUE	NO VALUE	3842.00	-1407.00
300	NO VALUE	NO VALUE	3860.00	-1450.90
301	NO VALUE	NO VALUE	NO VALUE	NO VALUE
302	NO VALUE	NO VALUE	3830.00	-1425.20
303	NO VALUE	NO VALUE	NO VALUE	NO VALUE
304	NO VALUE	NO VALUE	3820.00	-1450.00
305	NO VALUE	NO VALUE	NO VALUE	NO VALUE
306	NO VALUE	NO VALUE	NO VALUE	NO VALUE
307	NO VALUE	NO VALUE	NO VALUE	NO VALUE
308	NO VALUE	NO VALUE	3832.00	-1433.10
309	NO VALUE	NO VALUE	3828.00	-1439.00
310	NO VALUE	NO VALUE	NO VALUE	NO VALUE
311	NO VALUE	NO VALUE	NO VALUE	NO VALUE
312	NO VALUE	NO VALUE	NO VALUE	NO VALUE
313	NO VALUE	NO VALUE	3830.00	-1440.90
314	NO VALUE	NO VALUE	3800.00	-1416.20

	R	S	T	U
1	TOP Pa. 2	S.S. TOP	TOP Pa. 1	S.S. TOP
2		Pa. 2		Pa. 1
315	NO VALUE	NO VALUE	NO VALUE	NO VALUE
316	NO VALUE	NO VALUE	NO VALUE	NO VALUE
317	NO VALUE	NO VALUE	3784.00	-1403.10
318	NO VALUE	NO VALUE	3818.00	-1428.60
319	NO VALUE	NO VALUE	3774.00	-1400.20
320	NO VALUE	NO VALUE	3778.00	-1410.00
321	NO VALUE	NO VALUE	3752.00	-1354.10
322	NO VALUE	NO VALUE	3712.00	-1362.00
323	NO VALUE	NO VALUE	NO VALUE	NO VALUE
324	NO VALUE	NO VALUE	NO VALUE	NO VALUE
325	NO VALUE	NO VALUE	3760.00	-1386.00
326	NO VALUE	NO VALUE	3706.00	-1377.00
327	NO VALUE	NO VALUE	NO VALUE	NO VALUE
328	NO VALUE	NO VALUE	NO VALUE	NO VALUE
329	NO VALUE	NO VALUE	3720.00	-1368.00
330	NO VALUE	NO VALUE	NO VALUE	NO VALUE
331	NO VALUE	NO VALUE	NO VALUE	NO VALUE
332	NO VALUE	NO VALUE	NO VALUE	NO VALUE
333	NO VALUE	NO VALUE	3604.00	-1307.10
334	NO VALUE	NO VALUE	NO VALUE	NO VALUE
335	NO VALUE	NO VALUE	NO VALUE	NO VALUE
336	NO VALUE	NO VALUE	NO VALUE	NO VALUE
337	NO VALUE	NO VALUE	NO VALUE	NO VALUE
338	NO VALUE	NO VALUE	NO VALUE	NO VALUE
339	NO VALUE	NO VALUE	NO VALUE	NO VALUE
340	NO VALUE	NO VALUE	NO VALUE	NO VALUE
341	NO VALUE	NO VALUE	NO VALUE	NO VALUE
342	NO VALUE	NO VALUE	3728.00	-1338.90
343	NO VALUE	NO VALUE	3734.00	-1338.10
344	NO VALUE	NO VALUE	3753.00	-1355.10
345				
346	NO VALUE	NO VALUE	NO VALUE	NO VALUE
347				
348	NO VALUE	NO VALUE	NO VALUE	NO VALUE